MOLECULAR MECHANISMS AND SIGNALING IN ENDOTHELIAL CELL BIOLOGY AND VASCULAR HETEROGENEITY

EDITED BY: Bin Ren, Xiaofeng Yang and Ramani Ramchandran

PUBLISHED IN: Frontiers in Cell and Developmental Biology

frontiers Research Topics

Frontiers eBook Copyright Statement

The copyright in the text of individual articles in this eBook is the property of their respective authors or their respective institutions or funders. The copyright in graphics and images within each article may be subject to copyright of other parties. In both cases this is subject to a license granted to Frontiers.

The compilation of articles constituting this eBook is the property of Frontiers.

Each article within this eBook, and the eBook itself, are published under the most recent version of the Creative Commons CC-BY licence. The version current at the date of publication of this eBook is CC-BY 4.0. If the CC-BY licence is updated, the licence granted by Frontiers is automatically updated to the new version.

When exercising any right under the CC-BY licence, Frontiers must be attributed as the original publisher of the article or eBook, as applicable.

Authors have the responsibility of ensuring that any graphics or other materials which are the property of others may be included in the CC-BY licence, but this should be checked before relying on the CC-BY licence to reproduce those materials. Any copyright notices relating to those materials must be complied with.

Copyright and source acknowledgement notices may not be removed and must be displayed in any copy, derivative work or partial copy which includes the elements in question.

All copyright, and all rights therein, are protected by national and international copyright laws. The above represents a summary only. For further information please read Frontiers' Conditions for Website Use and Copyright Statement, and the applicable CC-BY licence.

ISSN 1664-8714
ISBN 978-2-88974-252-3
DOI 10.3389/978-2-88974-252-3

About Frontiers

Frontiers is more than just an open-access publisher of scholarly articles: it is a pioneering approach to the world of academia, radically improving the way scholarly research is managed. The grand vision of Frontiers is a world where all people have an equal opportunity to seek, share and generate knowledge. Frontiers provides immediate and permanent online open access to all its publications, but this alone is not enough to realize our grand goals.

Frontiers Journal Series

The Frontiers Journal Series is a multi-tier and interdisciplinary set of open-access, online journals, promising a paradigm shift from the current review, selection and dissemination processes in academic publishing. All Frontiers journals are driven by researchers for researchers; therefore, they constitute a service to the scholarly community. At the same time, the Frontiers Journal Series operates on a revolutionary invention, the tiered publishing system, initially addressing specific communities of scholars, and gradually climbing up to broader public understanding, thus serving the interests of the lay society, too.

Dedication to Quality

Each Frontiers article is a landmark of the highest quality, thanks to genuinely collaborative interactions between authors and review editors, who include some of the world's best academicians. Research must be certified by peers before entering a stream of knowledge that may eventually reach the public - and shape society; therefore, Frontiers only applies the most rigorous and unbiased reviews.
Frontiers revolutionizes research publishing by freely delivering the most outstanding research, evaluated with no bias from both the academic and social point of view. By applying the most advanced information technologies, Frontiers is catapulting scholarly publishing into a new generation.

What are Frontiers Research Topics?

Frontiers Research Topics are very popular trademarks of the Frontiers Journals Series: they are collections of at least ten articles, all centered on a particular subject. With their unique mix of varied contributions from Original Research to Review Articles, Frontiers Research Topics unify the most influential researchers, the latest key findings and historical advances in a hot research area! Find out more on how to host your own Frontiers Research Topic or contribute to one as an author by contacting the Frontiers Editorial Office: frontiersin.org/about/contact

MOLECULAR MECHANISMS AND SIGNALING IN ENDOTHELIAL CELL BIOLOGY AND VASCULAR HETEROGENEITY

Topic Editors:
Bin Ren, University of Alabama at Birmingham, United States
Xiaofeng Yang, Temple University, United States
Ramani Ramchandran, Medical College of Wisconsin, United States

Citation: Ren, B., Yang, X., Ramchandran, R., eds. (2022). Molecular Mechanisms and Signaling in Endothelial Cell Biology and Vascular Heterogeneity. Lausanne: Frontiers Media SA. doi: 10.3389/978-2-88974-252-3

Table of Contents

05 ***Editorial: Molecular Mechanisms and Signaling in Endothelial Cell Biology and Vascular Heterogeneity***
Bin Ren, Ramani Ramchandran and Xiaofeng Yang

11 ***Molecular Bases of VEGFR-2-Mediated Physiological Function and Pathological Role***
Xinrong Wang, Alfredo Maria Bove, Giuseppe Simone and Binyun Ma

23 ***Endocytic Adaptors in Cardiovascular Disease***
Kui Cui, Yunzhou Dong, Beibei Wang, Douglas B. Cowan, Siu-Lung Chan, John Shyy and Hong Chen

32 ***Molecular Mechanisms Controlling Lymphatic Endothelial Junction Integrity***
Pieter R. Norden and Tsutomu Kume

42 ***TGF-β-Induced Endothelial to Mesenchymal Transition Is Determined by a Balance Between SNAIL and ID Factors***
Jin Ma, Gerard van der Zon, Manuel A. F. V. Gonçalves, Maarten van Dinther, Midory Thorikay, Gonzalo Sanchez-Duffhues and Peter ten Dijke

62 ***Notch Signaling in Vascular Endothelial Cells, Angiogenesis, and Tumor Progression: An Update and Prospective***
Abdellah Akil, Ana K. Gutiérrez-García, Rachael Guenter, J. Bart Rose, Adam W. Beck, Herbert Chen and Bin Ren

78 ***Chronic Inhibition of mROS Protects Against Coronary Endothelial Dysfunction in Mice With Diabetes***
Hang Xing, Zhiqi Zhang, Guangbin Shi, Yixin He, Yi Song, Yuhong Liu, Elizabeth O. Harrington, Frank W. Sellke and Jun Feng

88 ***Mitogen-Inducible Gene 6 Inhibits Angiogenesis by Binding to SHC1 and Suppressing Its Phosphorylation***
Lixian Liu, Liying Xing, Rongyuan Chen, Jianing Zhang, Yuye Huang, Lijuan Huang, Bingbing Xie, Xiangrong Ren, Shasha Wang, Haiqing Kuang, Xianchai Lin, Anil Kumar, Jong Kyong Kim, Chunsik Lee and Xuri Li

100 ***Reconciling VEGF With VPF: The Importance of Increased Vascular Permeability for Stroma Formation in Tumors, Healing Wounds, and Chronic Inflammation***
Harold F. Dvorak

108 ***Endothelial Cell Behavior Is Determined by Receptor Clustering Induced by Thrombospondin-1***
Verônica Morandi, Jim Petrik and Jack Lawler

119 ***The Role of Histone Protein Acetylation in Regulating Endothelial Function***
Zhi Fang, Xiang Wang, Xiaoran Sun, Wenquan Hu and Qing R. Miao

139 **FOXC2** ***Autoregulates Its Expression in the Pulmonary Endothelium After Endotoxin Stimulation in a Histone Acetylation-Dependent Manner***
Sheng Xia, Wei Yu, Heather Menden, Scott T. Younger and Venkatesh Sampath

150 ***Loss of Primary Cilia Protein IFT20 Dysregulates Lymphatic Vessel Patterning in Development and Inflammation***
Delayna Paulson, Rebecca Harms, Cody Ward, Mackenzie Latterell, Gregory J. Pazour and Darci M. Fink

166 ***Single-Cell Transcriptomics Reveals Endothelial Plasticity During Diabetic Atherogenesis***
Guizhen Zhao, Haocheng Lu, Yuhao Liu, Yang Zhao, Tianqing Zhu, Minerva T. Garcia-Barrio, Y. Eugene Chen and Jifeng Zhang

180 ***Sinner or Saint?: Nck Adaptor Proteins in Vascular Biology***
Mabruka Alfaidi, Matthew L. Scott and Anthony Wayne Orr

198 ***AMPK and Pulmonary Hypertension: Crossroads Between Vasoconstriction and Vascular Remodeling***
Qiang Zhao, Ping Song and Ming-Hui Zou

212 ***Endothelial Aryl Hydrocarbon Receptor Nuclear Translocator Mediates the Angiogenic Response to Peripheral Ischemia in Mice With Type 2 Diabetes Mellitus***
Tu Nguyen, Mei Zheng, Maura Knapp, Nikola Sladojevic, Qin Zhang, Lizhuo Ai, Devin Harrison, Anna Chen, Albert Sitikov, Le Shen, Frank J. Gonzalez, Qiong Zhao, Yun Fang, James J. K. Liao and Rongxue Wu

224 ***Distinct Signaling Functions of Rap1 Isoforms in NO Release From Endothelium***
Ramoji Kosuru, Bandana Singh, Sribalaji Lakshmikanthan, Yoshinori Nishijima, Jeannette Vasquez-Vivar, David X. Zhang and Magdalena Chrzanowska

232 ***Corrigendum: Distinct Signaling Functions of Rap1 Isoforms in NO Release From Endothelium***
Ramoji Kosuru, Bandana Singh, Sribalaji Lakshmikanthan, Yoshinori Nishijima, Jeannette Vasquez-Vivar, David X. Zhang and Magdalena Chrzanowska

233 ***The Role of BMP Signaling in Endothelial Heterogeneity***
Orjin Han, Boryeong Pak and Suk-Won Jin

241 ***Developmental Perspectives on Arterial Fate Specification***
Dongying Chen, Martin A. Schwartz and Michael Simons

253 ***Endothelial-Myocardial Angiocrine Signaling in Heart Development***
Hyeonyu Kim, Mingqiang Wang and David T. Paik

261 ***Insights Into the Mechanisms of Brain Endothelial Erythrophagocytosis***
Jiahong Sun, Prema Vyas, Samar Mann, Annlia Paganini-Hill, Ane C. F. Nunes, Wei Ling Lau, David H. Cribbs, Mark J. Fisher and Rachita K. Sumbria

275 ***New Technologies With Increased Precision Improve Understanding of Endothelial Cell Heterogeneity in Cardiovascular Health and Disease***
Ashley Dawson, Yidan Wang, Yanming Li, Scott A. LeMaire and Ying H. Shen

287 ***Obesity Inhibits Angiogenesis Through TWIST1-SLIT2 Signaling***
Tendai Hunyenyiwa, Kathryn Hendee, Kienna Matus, Priscilla Kyi, Tadanori Mammoto and Akiko Mammoto

301 ***Regulation of Partial and Reversible Endothelial-to-Mesenchymal Transition in Angiogenesis***
Jennifer S. Fang, Nan W. Hultgren and Christopher C. W. Hughes

315 ***Mechanism-Based Cardiac Regeneration Strategies in Mammals***
Nawazish Naqvi, Siiri E. Iismaa, Robert M. Graham and Ahsan Husain

frontiers in Cell and Developmental Biology

EDITORIAL
published: 17 December 2021
doi: 10.3389/fcell.2021.821100

Editorial: Molecular Mechanisms and Signaling in Endothelial Cell Biology and Vascular Heterogeneity

Bin Ren[1], Ramani Ramchandran[2] and Xiaofeng Yang[3]*

[1]Department of Surgery, O'Neal Comprehensive Cancer Center, and Comprehensive Cardiovascular Center, Heersink School of Medicine, University of Alabama at Birmingham, Birmingham, AL, United States, [2]Department of Pediatrics and Children's Research Institute, Medical College of Wisconsin, Milwaukee, WI, United States, [3]Department of Cardiovascular Sciences, Centers for Cardiovascular Research and Metabolic Disease Research, Lewis Katz School of Medicine at Temple University, Philadelphia, PA, United States

Keywords: endothelial cells, angiogenesis, arterial, lymphangiogenesis, signaling, differentiation

OPEN ACCESS

Edited and reviewed by:
Ana Cuenda,
Spanish National Research Council (CSIC), Spain

****Correspondence:***
Bin Ren
bren@uabmc.edu

Specialty section:
This article was submitted to Signaling, a section of the journal Frontiers in Cell and Developmental Biology

Received: *23 November 2021*
Accepted: *25 November 2021*
Published: *17 December 2021*

Citation:
Ren B, Ramchandran R and Yang X (2021) Editorial: Molecular Mechanisms and Signaling in Endothelial Cell Biology and Vascular Heterogeneity. Front. Cell Dev. Biol. 9:821100. doi: 10.3389/fcell.2021.821100

Editorial on the Research Topic

Heterogeneity of Endothelial Cells and Vascular Networks: Beyond Scope of Angiogenesis and Lymphangiogenesis

Early in 1865, the Swiss anatomist Wihelm His introduced a new concept of *endothelium* in a programmatic assay and first defined the endothelium as the lining of the vasculature and the lymphatic system (Aird, 2007). Endothelium was considered as a cover and barrier facing a hollow face. The blood and lymphatic vessels are always filled with blood, different types of cells and other substances. Endothelial cells (ECs) may actually mediate communications between biological substances in the circulation system and other tissues. Later in 1958, Hibbs et al. (1958) noted that there was some variation in the structure of capillaries and arterioles from one organ to another, and even among blood vessels of the same organ . It is reasonable to speculate that the heterogeneity of vascular ECs may contribute to this difference in the structure and functional variations.

Nevertheless, with the first successful isolation and primary culture of human ECs from umbilical veins independently by Jaffe et al. (1973a) and Jaffe et al. (1973b) and Gimbrone et al. (1974), extensive studies on EC biology and growth of new blood vessels have started at molecular and cellular levels and by using animal models and human patient samples. Along with the discovery of tools for the culture of vascular and lymphatic ECs and other new models and technologies, the concept of the heterogeneity of ECs and blood and lymphatic vessels is getting increased recognition as an important feature of vascular biology by several researchers and scientists in various disciplines of biomedical research (Aird, 2006; Kang et al., 2010; Yuan et al., 2016; Mojiri et al., 2019; Ren et al., 2019; Takeda et al., 2019; Turgeon et al., 2020; Xiang et al., 2020; Sibler et al., 2021). It is known that ECs can interact with the blood constituents such as RBCs and can also interact with cells in a tissue that they reside in to influence functions (Cao et al., 2017; Kumar et al., 2019; Akil et al.; Jiang et al., 2021). Despite immense progress in our understanding of the molecular mechanisms and signaling that regulate EC patterning, the organ-specific function of ECs and the underlying mechanisms that dictate organ-specific function is poorly understood. In this special topic of "*Molecular Mechanisms and Signaling in Endothelial Cell Biology and Vascular Heterogeneity*," researchers from a variety of institutions have submitted manuscripts that report EC function in various tissue beds, which influence vascular development process in health and disease. We received two hypothesis articles, ten original research articles and thirteen review articles for a total of 25 original contributions to this research topic. These articles cover many areas including EC heterogeneity, mechanisms underlying EC heterogeneity, novel ligands and receptor signaling pathways in vascular biology, angiogenesis,

and lymphangiogenesis in health and disease. We will discuss these aspects and hope to provide insights into EC and vascular biology in this editorial.

LIGANDS, RECEPTOR AND INTRACELLULAR SIGNALING IN ECs

We begin with vascular endothelial growth factor (VEGF), also known as vascular permeability factor (VPF), one of the most important growth factor in EC and vascular biology. This important proangiogenic molecule was discovered over 3 decades ago by the Dvorak Laboratory at Harvard Medical School (Senger et al., 1983) and was first isolated and cloned by Napoleone Ferrara and his colleagues at Genentech 1989 (Leung et al., 1989). In an hypothesis article (Dvorak), Dr. Dvorak describes that VEGF is widely believed to induce angiogenesis by its direct mitogenic and motogenic actions on vascular ECs. However, he emphasizes the role of VEGF in vascular permeability, the role of delayed hypersensitivity in pathological stroma generation, particularly extravascular fibrin deposition and clotting within the tumor microenvironment (TME). Based upon his prior work where he concludes that tumors are "wounds that do not heal," he now proposes that tumors are wounds that continually exhibit elements of local healing but do damage the host (patients) whereas the healing process actually facilitates tumor survival and growth. Moreover, solid tumors, and healing wounds feature enlarged feeder arteries, draining veins, and several other abnormal vessel types in addition to new angiogenic blood vessels. He also proposes that that VPF/VEGF induces stroma formation primarily by way of its potent "VPF" function. Much remains to be explored about the signaling and functions of VEGF in wound healing, tumor progression and chronic inflammatory diseases.

VEGF generally signals through interaction with its receptors. An article reviewed key advances in our understanding of VEGF signaling via VEGF receptor 2 (VEGFR-2) (Simons et al., 2016), a predominant receptor that mediates angiogenesis and arteriolar differentiation. In this special topic, Wang et al. describe the basics of VEGF/VEGFR-2 signaling and provide an update on VEGFR-2 signaling-mediated physiological and pathological functions as well as potential treatment strategies. Potent VEGF signaling also promotes angiogenesis and dictates arterial fate but inhibits venous specification, and this may depend on Notch signaling status (Lanner et al., 2007; CasieChetty et al., 2017). Akil et al. provide a comprehensive overview and update about Notch signaling in EC functions and angiogenesis. They emphasize the critical role and mechanisms by which Notch signaling promotes tumor progression via stimulating tumor angiogenesis, inducing phenotypes of cancer stem cells (CSCs) and thus conferring therapeutic resistance. They also discuss the Notch signaling crosstalk between CSCs and vascular ECs within the TME. They believe that therapeutic approaches could be developed by targeting the essential role of Notch pathway in CSCs and development of the arteriolar niche that promotes the self-renewal of CSCs (Jiang et al., 2021).

External stimuli induce a specific intracellular signaling pathway that can often come from multiple ligands. To integrate these multiple signaling pathways, adaptor proteins can ensure the temporal and spatial regulation of cellular signaling and contribute significantly to the signaling specificity. Cui et al. (2021) provide an excellent and focused review on endocytic adaptors epsins and Dab2 in the context of cardiovascular disease. Additionally, Alfaidi et al. emphasize the role of Nck1/2 adaptor proteins in vascular biology, vascular permeability and angiogenesis, and discuss their therapeutic potential. A study on an adaptor protein widely expressed in vascular ECs by Liu et al. demonstrates that the mitogen-inducible gene 6 acts as a potent anti-angiogenic factor in the regulation of physiological and pathological angiogenesis. In terms of anti-angiogenesis, thrombospondin-1 (TSP-1) is one of the first discovered endogenous angiogenesis inhibitor, and negatively regulates EC functions (Jiménez et al., 2000; Ren et al., 2006; Ren et al., 2009). Morandi et al. describe about new mechanisms by which the presence of TSP-1 at the plasma membrane affects EC signal transduction and angiogenesis via induction of receptor clustering. Additionally, small GTPase Rap1 is essential for the maintenance of EC homeostasis by promoting NO release. Rap1A and Rap1B are closely related Rap1 isoforms and regulate vascular homeostasis (Chrzanowska-Wodnicka, 2017). Kosuru et al. show that Rap1B directly and positively regulates eNOS activation whereas Rap1A prevents negative regulation of eNOS, thereby converging NO release, which may be important in the regulation of hypertension.

EC FUNCTION IN DEVELOPMENT AND DISEASE

EC function is intimately associated with developmental processes and dysfunction of ECs is associated with several disease states. For example, arterial specification of vascular ECs is essential for arteriogenesis. Chen et al. discuss the arterial fate specification from a developmental perspective (Chen et al.). Although VEGF-activation of Notch signaling is known as the key to arterial specification, they have performed carefully analysis in the settings of *de novo* vasculogenesis of the dorsal aorta during early embryogenesis and vasculature development in the neonatal mouse retina and described novel signaling mechanisms and a new understanding of this subject. They also emphasize the role of shear stress in the maintenance of arterial identity after blood circulation is established, as shear-induced Notch signaling activation and cell cycle arrest may contribute to A/V specification process (Fang et al., 2017). However, much remains to be investigated as for how arteriolar networks are involved under pathological ischemic conditions. In this regard, Nguyen et al. demonstrate that the deficiency of endothelial aryl hydrocarbon receptor nuclear translocator may exacerbate impaired angiogenic potential under peripheral ischemic conditions in mice with type 2 diabetes, which may be associated with defective angiogenic activity of ECs due to oxidative stress. As persistent oxidative stress during diabetes contributes to coronary endothelial

dysfunction, and reactive oxygen species (ROS) mainly originates from the mitochondria in diabetes, a study from Xing et al. (2021) demonstrates that chronic inhibition of mitochondrial ROS may improve coronary endothelial function/dilation and SK channel activity in an animal model of diabetes. Furthermore, Zhao et al. describe the paradox of adenosine monophosphate-activated protein kinase (AMPK), a heterotrimeric serine-threonine kinase, in the involvement of vascular remodeling and the development of pulmonary hypertension. They emphasize the differential effects of AMPK on pulmonary vasoconstriction and pulmonary vascular remodeling, which may also be involved in the regulation of pathological microvascular remodeling and angiogenesis under obese conditions (Dong et al., 2017).

EC HETEROGENEITY

EC heterogeneity is emerging as an important area in vascular biology. It is well known that ECs show tissue- and organ-specificity, and significantly contribute to the formation of different types of blood and lymphatic vessels. They serve as an important cell type in the development of vasculogenesis, angiogenesis, venogenesis and arteriogenesis under physiological and pathological conditions. As newly classified innate immune cells (Drummer et al., 2021; Shao et al., 2020; Mai et al., 2013), ECs are essential for normal tissue homeostasis and various pathologies (Aird, 2006; Ren et al., 2019; Marcu et al., 2018; Miyasaka, 2021) including contribution to the pathogenesis of COVID-19 (Shao et al., 2021). Majority of articles in this topic focus on EC heterogeneity and biology in health and disease. Dawson et al. review the heterogeneity of EC types, states, and phenotypes based upon the findings from ECs in multiple different experiments and among several tissue types and disease states and by using new techniques in transcriptome analysis, particularly single cell RNA-sequencing (also see single Cell Portal at https://singlecell.broadinstitute.org/single_cell). They functionally classify ECs as quiescent ECs involved in maintaining homeostasis, proliferative ECs, inflammatory ECs, remodeling ECs, ECs involved in EndMT, and ECs involved in angiogenesis. This classification may well explain two new connected processes such as inflammatory angiogenesis and non-inflammatory regenerative angiogenesis dissected in hind-limb ischemia-triggered angiogenesis (Fu et al., 2020). Dawson et al. also provide an update on innate contributions to EC heterogeneity, effects of biomechanical and biochemical stress on ECs and EC phenotypes in cardiovascular disease. Interestingly, Zhao et al. characterize the phenotypic and metabolic heterogeneity of ECs in diabetes-associated atherogenesis at the single-cell level by performing single-cell RNA sequencing study using EC-enriched single cells from mouse heart and aorta. Their study provides critical insight into EC biology and EC-related cardiovascular diseases. Whereas, Kim et al. provide an overview on the angiocrine role of heterogeneous subsets of cardiac ECs during cardiac development, shedding lights on the heterogenic nature of angiocrine signaling within the cardiac arterial, venous, and lymphatic ECs. In addition, Han et al. update the bone morphogenetic protein signaling functions in the regulation of EC heterogeneity and the underlying molecular mechanisms. Furthermore, Fang et al. present a comprehensive overview about regulation of endothelial functions by acetylation of histone proteins, a fundamental process that regulates gene expression epigenetically. They also discuss the roles of histone acetylation in ECs under physiological and pathophysiological conditions including vascular tone, inflammation, oxidative stress, angiogenesis, barrier function, thrombosis, and coagulation. An interesting study (Xia et al.) shows that lipopolysaccharide induces transcriptional activation of forkhead box protein C2 and promotes itself expression in a histone acetylation manner using lung ECs and a sterile sepsis model in neonatal mice.

NOVEL MECHANISMS UNDERLYING SPROUTING ANGIOGENESIS AND LYMPHANGIOGENESIS

In the field of angiogenesis, the endothelial-to-mesenchymal transition (EndoMT/EndMT) and partial epithelial-to-mesenchymal transition (EMT)/EndoMT have been extensively reported. EndoMT is a process whereby an EC undergoes a series of molecular events that lead to a change in phenotype toward a mesenchymal cell. In a hypothesis and theory article, Fang et al. propose that an EndoMT program is partially and reversibly activated event in angiogenic ECs to support acquisition of the subset of mesenchymal characteristics, which is necessary to develop sprouting angiogenesis. They also discuss the potential signaling and regulatory mechanisms that may control the EndoMT program as well as potential therapeutic approaches in cancers. EndoMT is known to be regulated by transforming growth factor-β (TGF-β) family. Ma et al. report that TGF-β2 may be essential for this process by regulation of the balance between transcription factor SNAIL and ID factors (Ma et al.) and this may also regulate angiogenesis (Akil et al.; Fang et al.). Additionally, a study by Hunyenyiwa et al. shows that obesity inhibits angiogenesis via TWIST1-SLIT2 signaling, similar to an angiogenic phenotype occurred in tumor angiogenesis under diet-induced obesity conditions (Dong et al., 2017). It should be noted that Twist 1 is known as a master transcription factor of EndoMT. The study thus suggests that obesity may determine the angiogenic fate via regulation of the EndoMT. Interestingly, Sun et al. reveal that ROS and RBC phosphatidylserine exposure can mediate brain endothelial erythrophagocytosis, implicating in cerebral microhemorrhage-like lesions independent of disruption of the microvasculature.

In addition to new sprouting from blood vessels, the sprouting of lymphatic vessels, lymphangiogenesis, is actively involved in many pathological processes including tissue inflammation and tumor dissemination but is insufficient in patients suffering from lymphedema. Cilia, a microtubule-based organelle expressed on the apical surface of blood ECs is thought to function as a blood flow sensor. Paulson et al. show that primary cilia exists in lymphatic vasculature, and surprisingly is expressed on the abluminal surface of the lymphatic vessel. They also present evidence that lymphatic vessel patterning is regulated by a

primary cilium protein IFT20 in lymphatic ECs during development and inflammation, which could lead to a new paradigm in the field of lymphangiogenesis. Last but not the least, Norden and Kume provide an elegant review about current status and the mechanisms by which lymphatic permeability and function are regulated in a tissue- and organ-specific manner, including lacteals of the small intestine. Disrupted lymphatic EC junctions are associated with various diseases, including lymphatic leakage present in chylothorax and lymphedema, metabolic syndrome, and impaired immune surveillance. They also describe key signaling pathways and factors that control lymphatic EC junctional integrity including VEGF, S1P, LPA signaling molecules and FOXC1 and FOXC2 transcription factors as well as RhoA/ROCK and Ephrinb2-Ephb4 pathways.

SUMMARY AND PROSPECTIVE

Heterogeneous endothelium and vasculature play a pivotal role in the regulation of tissue and organ homeostasis in human health and disease progression. This topic only covers the tip of iceberg in the field of EC and vascular biology, and significant studies are urgently needed to move the field forward. One emerging area is the immunological properties of ECs and their role in angiogenesis and lymphangiogenesis. ECs show distinguished immunological functions and have innate and trained immunity (Shao et al., 2020; Drummer et al., 2021; McCoy et al., 2021). McCoy et al. recently demonstrate that ECs facilitate proangiogenic immune cell recruitment and contribute to tumor angiogenesis *via* toll-like receptor 2 signaling (McCoy et al., 2021). Secondly, angiogenesis is regulated by paracrine and autocrine mechanism, including regulation by VEGF and hypoxia-inducible factor 1α (HIF1-α) whereas HIF-α directly regulates VEGF under ischemic conditions, thereby leading to angiogenesis and arteriogenesis in ischemic diseases and cancers (Semenza, 2007; Fong, 2009; Ren et al., 2010; Ho et al., 2012; Ren, 2016; Simons et al., 2016). The resulted neovascularization may improve ischemic conditions or promote tumor progression via provision of CSCs with a favorable vascular microenvironment (Jiang et al., 2021). Thirdly, the studies on EC differentiation and transdifferentiation are emerging as an important area, and they contribute significantly to capillary arterialization or *de novo* arteriogenesis, particularly under pathological conditions (Mac Gabhann and Peirce, 2010; Ren et al., 2010; Moraes et al., 2013; Ren et al., 2016a; Ren et al., 2016b; Ren et al.; Jiang et al., 2021). Furthermore, venous ECs may contribute to the generation of arterial ECs and expansion of arteriolar networks (Lee et al., 2021). Key pathways and gene signature may be conserved in certain types of ECs (Ren et al., 2011; Coppiello et al., 2015; Ren et al., 2016a; Jiang et al., 2021) but it would be of significance to study EC biology and angiogenic and lymphangiogenic processes using heterogeneous types of ECs, animal models and human patient samples before novel findings and concepts can be effectively translated into clinic settings.

AUTHOR CONTRIBUTIONS

BR wrote the editorial. RR and XY made substantial contribution to the writing of this editorial. The authors have approved it for publication.

FUNDING

BR's work has been supported by the National Institute of Health (HL136423), the American Cancer Society (86-004-26; Institution Fund to BR, Medical College of Wisconsin), the American Heart Association (13SDG14800019), the Ann's Hope Foundation (FP00011709), and the University of Alabama at Birmingham Heersink School of Medicine.

ACKNOWLEDGMENTS

We appreciate all the authors for their dedication to contribute quality manuscripts and all reviewers for their insightful comments on manuscripts in this Research Topic. We also appreciate Dr. Arie Horowitz from Université de Rouen, France for his editing of the manuscript from the Ren Laboratory of Molecular and Vascular Pathobiology at UAB Heersink School of Medicine.

REFERENCES

Aird, W. C. (2007). *Endothelial Biomedicine*. Cambridge, United Kingdom: Cambridge University Press, 5–19. doi:10.1017/CBO9780511546198

Aird, W. C. (2006). Mechanisms of Endothelial Cell Heterogeneity in Health and Disease. *Circ. Res.* 98, 159–162. doi:10.1161/01.res.0000204553.32549.a7

Cao, Z., Scandura, J. M., Inghirami, G. G., Shido, K., Ding, B.-S., and Rafii, S. (2017). Molecular Checkpoint Decisions Made by Subverted Vascular Niche Transform Indolent Tumor Cells into Chemoresistant Cancer Stem Cells. *Cancer Cell* 31, 110–126. doi:10.1016/j.ccell.2016.11.010

Casie Chetty, S., Rost, M. S., Enriquez, J. R., Schumacher, J. A., Baltrunaite, K., Rossi, A., et al. (2017). Vegf Signaling Promotes Vascular Endothelial Differentiation by Modulating Etv2 Expression. *Developmental Biol.* 424, 147–161. doi:10.1016/j.ydbio.2017.03.005

Chrzanowska-Wodnicka, M. (2017). Rap1 in Endothelial Biology. *Curr. Opin. Hematol.* 24, 248–255. doi:10.1097/moh.0000000000000332

Coppiello, G., Collantes, M., Sirerol-Piquer, M. S., Vandenwijngaert, S., Schoors, S., Swinnen, M., et al. (2015). Meox2/Tcf15 Heterodimers Program the Heart Capillary Endothelium for Cardiac Fatty Acid Uptake. *Circulation* 131, 815–826. doi:10.1161/circulationaha.114.013721

Cui, K., Movahedi, M., Bombardier, C., and Kuriya, B. (2021). Cardiovascular Risk Factors Are Negatively Associated with Rheumatoid Arthritis Disease Outcomes. *Ther. Adv. Musculoskelet. Dis.* 13, 1759720X20981217. doi:10.1177/1759720X20981217

Dong, L., Yuan, Y., Opansky, C., Chen, Y., Aguilera-Barrantes, I., Wu, S., et al. (2017). Diet-induced Obesity Links to ER Positive Breast Cancer Progression via LPA/PKD-1-CD36 Signaling-Mediated Microvascular Remodeling. *Oncotarget* 8, 22550–22562. doi:10.18632/oncotarget.15123

Drummer, C., Saaoud, F., Shao, Y., Sun, Y., Xu, K., Lu, Y., et al. (2021). Trained Immunity and Reactivity of Macrophages and Endothelial Cells. *Arterioscler Thromb. Vasc. Biol.* 41, 1032–1046. doi:10.1161/atvbaha.120.315452

Fang, J. S., Coon, B. G., Gillis, N., Chen, Z., Qiu, J., Chittenden, T. W., et al. (2017). Shear-induced Notch-Cx37-P27 axis Arrests Endothelial Cell Cycle to Enable Arterial Specification. *Nat. Commun.* 8, 2149. doi:10.1038/s41467-017-01742-7

Fong, G.-H. (2009). Regulation of Angiogenesis by Oxygen Sensing Mechanisms. *J. Mol. Med.* 87, 549–560. doi:10.1007/s00109-009-0458-z

Fu, H., Sun, Y., Shao, Y., Saredy, J., Cueto, R., Liu, L., et al. (2020). Interleukin 35 Delays Hindlimb Ischemia-Induced Angiogenesis through Regulating ROS-Extracellular Matrix but Spares Later Regenerative Angiogenesis. *Front. Immunol.* 11, 595813. doi:10.3389/fimmu.2020.595813

Gimbrone, M. A., Jr., Cotran, R. S., and Folkman, J. (1974). Human Vascular Endothelial Cells in Culture. *J. Cell Biol* 60, 673–684. doi:10.1083/jcb.60.3.673

Hibbs, R. G., Burch, G. E., and Phillips, J. H. (1958). The fine Structure of the Small Blood Vessels of normal Human Dermis and Subcutis. *Am. Heart J.* 56, 662–670. doi:10.1016/0002-8703(58)90209-6

Ho, V. C., Duan, L.-J., Cronin, C., Liang, B. T., and Fong, G.-H. (2012). Elevated Vascular Endothelial Growth Factor Receptor-2 Abundance Contributes to Increased Angiogenesis in Vascular Endothelial Growth Factor Receptor-1-Deficient Mice. *Circulation* 126, 741–752. doi:10.1161/circulationaha.112.091603

Jaffe, E. A., Hoyer, L. W., and Nachman, R. L. (1973). Synthesis of Antihemophilic Factor Antigen by Cultured Human Endothelial Cells. *J. Clin. Invest.* 52, 2757–2764. doi:10.1172/jci107471

Jaffe, E. A., Nachman, R. L., Becker, C. G., and Minick, C. R. (1973). Culture of Human Endothelial Cells Derived from Umbilical Veins. Identification by Morphologic and Immunologic Criteria. *J. Clin. Invest.* 52, 2745–2756. doi:10.1172/jci107470

Jiang, Y., Guo, Y., Hao, J., Guenter, R., Lathia, J., Beck, A. W., et al. (2021). Development of an Arteriolar Niche and Self-Renewal of Breast Cancer Stem Cells by Lysophosphatidic Acid/protein Kinase D Signaling. *Commun. Biol.* 4, 780. doi:10.1038/s42003-021-02308-6

Jiménez, B., Volpert, O. V., Crawford, S. E., Febbraio, M., Silverstein, R. L., and Bouck, N. (2000). Signals Leading to Apoptosis-dependent Inhibition of Neovascularization by Thrombospondin-1. *Nat. Med.* 6, 41–48. doi:10.1038/71517

Kang, J., Yoo, J., Lee, S., Tang, W., Aguilar, B., Ramu, S., et al. (2010). An Exquisite Cross-Control Mechanism Among Endothelial Cell Fate Regulators Directs the Plasticity and Heterogeneity of Lymphatic Endothelial Cells. *Blood* 116, 140–150. doi:10.1182/blood-2009-11-252270

Kumar, S., Sharife, H., Kreisel, T., Mogilevsky, M., Bar-Lev, L., Grunewald, M., et al. (2019). Intra-Tumoral Metabolic Zonation and Resultant Phenotypic Diversification Are Dictated by Blood Vessel Proximity. *Cell Metab.* 30, 201–211. doi:10.1016/j.cmet.2019.04.003

Lanner, F., Sohl, M., and Farnebo, F. (2007). Functional Arterial and Venous Fate Is Determined by Graded VEGF Signaling and Notch Status during Embryonic Stem Cell Differentiation. *Arterioscler Thromb. Vasc. Biol.* 27, 487–493. doi:10.1161/01.atv.0000255990.91805.6d

Lee, H. W., Xu, Y., He, L., Choi, W., Gonzalez, D., Jin, S. W., et al. (2021). The Role of Venous Endothelial Cells in Developmental and Pathologic Angiogenesis. *Circulation* 144 (16), 1308–1322. doi:10.1161/CIRCULATIONAHA.121.054071

Leung, D. W., Cachianes, G., Kuang, W.-J., Goeddel, D. V., and Ferrara, N. (1989). Vascular Endothelial Growth Factor Is a Secreted Angiogenic Mitogen. *Science* 246, 1306–1309. doi:10.1126/science.2479986

Liu, L., Xing, L., Chen, R., Zhang, J., Huang, Y., Huang, L., et al. (2021). Mitogen-Inducible Gene 6 Inhibits Angiogenesis by Binding to SHC1 and Suppressing its Phosphorylation. *Front. Cell Dev. Biol.* 9, 634242. doi:10.3389/fcell.2021.634242

Mac Gabhann, F., and Peirce, S. M. (2010). Collateral Capillary Arterialization Following Arteriolar Ligation in Murine Skeletal Muscle. *Microcirculation* 17, 333–347. doi:10.1111/j.1549-8719.2010.00034.x

Mai, J., Virtue, A., Shen, J., Wang, H., and Yang, X.-F. (2013). An Evolving New Paradigm: Endothelial Cells - Conditional Innate Immune Cells. *J. Hematol. Oncol.* 6, 61. doi:10.1186/1756-8722-6-61

Marcu, R., Choi, Y. J., Xue, J., Fortin, C. L., Wang, Y., Nagao, R. J., et al. (2018). Human Organ-specific Endothelial Cell Heterogeneity. *iScience* 4, 20–35. doi:10.1016/j.isci.2018.05.003

McCoy, M. G., Nascimento, D. W., Veleeparambil, M., Murtazina, R., Gao, D., Tkachenko, S., et al. (2021). Endothelial TLR2 Promotes Proangiogenic Immune Cell Recruitment and Tumor Angiogenesis. *Sci. Signal.* 14, eabc5371. doi:10.1126/scisignal.abc5371

Miyasaka, M. (2021). A Short Review on Lymphatic Endothelial Cell Heterogeneity. *Inflamm. Regener* 41, 32. doi:10.1186/s41232-021-00183-6

Mojiri, A., Alavi, P., Lorenzana Carrillo, M. A., Nakhaei-Nejad, M., Sergi, C. M., Thebaud, B., et al. (2019). Endothelial cells of different organs exhibit heterogeneity in von Willebrand factor expression in response to hypoxia. *Atherosclerosis* 282, 1–10. doi:10.1016/j.atherosclerosis.2019.01.002

Moraes, F., Paye, J., Mac Gabhann, F., Zhuang, Z. W., Zhang, J., Lanahan, A. A., et al. (2013). Endothelial Cell-dependent Regulation of Arteriogenesis. *Circ. Res.* 113, 1076–1086. doi:10.1161/circresaha.113.301340

Ren, B., Best, B., Weihrauch, D., Jones, D. W., Dong, L., Opansky, C., et al. (2016). Abstract 15673: LPA/PKD-1-FoxO1-CD36 Signaling Axis Regulates Capillary Arterialization in Ischemic Conditions. *Circulation* 134, A15673. doi:10.1161/circ.134.suppl_1.15673

Ren, B., Rose, J. B., Liu, Y., Jaskular-Sztul, R., Contreras, C., Beck, A., et al. (2019). Heterogeneity of Vascular Endothelial Cells, De Novo Arteriogenesis and Therapeutic Implications in Pancreatic Neuroendocrine Tumors. *J. Clin. Med.* 8. doi:10.3390/jcm8111980

Ren, B., Best, B., Ramakrishnan, D. P., Walcott, B. P., Storz, P., and Silverstein, R. L. (2016). LPA/PKD-1-FoxO1 Signaling Axis Mediates Endothelial Cell CD36 Transcriptional Repression and Proangiogenic and Proarteriogenic Reprogramming. *Arterioscler Thromb. Vasc. Biol.* 36, 1197–1208. doi:10.1161/atvbaha.116.307421

Ren, B., Deng, Y., Mukhopadhyay, A., Lanahan, A. A., Zhuang, Z. W., Moodie, K. L., et al. (2010). ERK1/2-Akt1 Crosstalk Regulates Arteriogenesis in Mice and Zebrafish. *J. Clin. Invest.* 120, 1217–1228. doi:10.1172/jci39837

Ren, B., Hale, J., Srikanthan, S., and Silverstein, R. L. (2011). Lysophosphatidic Acid Suppresses Endothelial Cell CD36 Expression and Promotes Angiogenesis via a PKD-1-dependent Signaling Pathway. *Blood* 117, 6036–6045. doi:10.1182/blood-2010-12-326017

Ren, B. (2016). Protein Kinase D1 Signaling in Angiogenic Gene Expression and VEGF-Mediated Angiogenesis. *Front. Cell Dev. Biol.* 4, 37. doi:10.3389/fcell.2016.00037

Ren, B., Song, K., Parangi, S., Jin, T., Ye, M., Humphreys, R., et al. (2009). A Double Hit to Kill Tumor and Endothelial Cells by TRAIL and Antiangiogenic 3TSR. *Cancer Res.* 69, 3856–3865. doi:10.1158/0008-5472.can-08-2940

Ren, B., Yee, K. O., Lawler, J., and Khosravi-Far, R. (2006). Regulation of Tumor Angiogenesis by Thrombospondin-1. *Biochim. Biophys. Acta (Bba) - Rev. Cancer* 1765, 178–188. doi:10.1016/j.bbcan.2005.11.002

Semenza, G. L. (2007). Vasculogenesis, Angiogenesis, and Arteriogenesis: Mechanisms of Blood Vessel Formation and Remodeling. *J. Cell. Biochem.* 102, 840–847. doi:10.1002/jcb.21523

Senger, D. R., Galli, S. J., Dvorak, A. M., Perruzzi, C. A., Harvey, V. S., and Dvorak, H. F. (1983). Tumor Cells Secrete a Vascular Permeability Factor that Promotes Accumulation of Ascites Fluid. *Science* 219, 983–985. doi:10.1126/science.6823562

Shao, Y., Saredy, J., Yang, W. Y., Sun, Y., Lu, Y., Saaoud, F., et al. (2020). Vascular Endothelial Cells and Innate Immunity. *Arterioscler Thromb. Vasc. Biol.* 40, e138–e152. doi:10.1161/ATVBAHA.120.314330

Shao, Y., Saredy, J., Xu, K., Sun, Y., Saaoud, F., Drummer, C., et al. (2021). Endothelial Immunity Trained by Coronavirus Infections, DAMP Stimulations and Regulated by Anti-oxidant NRF2 May Contribute to Inflammations, Myelopoiesis, COVID-19 Cytokine Storms and Thromboembolism. *Front. Immunol.* 12, 653110. doi:10.3389/fimmu.2021.653110

Sibler, E., He, Y., Ducoli, L., Keller, N., Fujimoto, N., Dieterich, L. C., et al. (2021). Single-Cell Transcriptional Heterogeneity of Lymphatic Endothelial Cells in Normal and Inflamed Murine Lymph Nodes. *Cells* 10, 1371. doi:10.3390/cells10061371

Simons, M., Gordon, E., and Claesson-Welsh, L. (2016). Mechanisms and Regulation of Endothelial VEGF Receptor Signalling. *Nat. Rev. Mol. Cell Biol* 17, 611–625. doi:10.1038/nrm.2016.87

Takeda, A., Hollmén, M., Dermadi, D., Pan, J., Brulois, K. F., Kaukonen, R., et al. (2019). Single-Cell Survey of Human Lymphatics Unveils Marked Endothelial Cell Heterogeneity and Mechanisms of Homing for Neutrophils. *Immunity* 51, 561–572. doi:10.1016/j.immuni.2019.06.027

Turgeon, P. J., Chan, G. C., Chen, L., Jamal, A. N., Yan, M. S., Ho, J. J. D., et al. (2020). Epigenetic Heterogeneity and Mitotic Heritability Prime Endothelial Cell Gene Induction. *J. Immunol.* 204, 1173–1187. doi:10.4049/jimmunol.1900744

Xiang, M., Grosso, R. A., Takeda, A., Pan, J., Bekkhus, T., Brulois, K., et al. (2020). A Single-Cell Transcriptional Roadmap of the Mouse and Human Lymph Node Lymphatic Vasculature. *Front. Cardiovasc. Med.* 7, 52. doi:10.3389/fcvm.2020.00052

Xing, H., Zhang, Z., Shi, G., He, Y., Song, Y., Liu, Y., et al. (2021). Chronic Inhibition of mROS Protects against Coronary Endothelial Dysfunction in Mice with Diabetes. *Front Cell Dev Biol* 9, 643810. doi:10.3389/fcell.2021.643810

Yuan, L., Chan, G. C., Beeler, D., Janes, L., Spokes, K. C., Dharaneeswaran, H., et al. (2016). A Role of Stochastic Phenotype Switching in Generating Mosaic Endothelial Cell Heterogeneity. *Nat. Commun.* 7, 10160. doi:10.1038/ncomms10160

Conflict of Interest: The authors declare that the research was conducted in the absence of any commercial or financial relationships that could be construed as a potential conflict of interest.

Publisher's Note: All claims expressed in this article are solely those of the authors and do not necessarily represent those of their affiliated organizations, or those of the publisher, the editors, and the reviewers. Any product that may be evaluated in this article, or claim that may be made by its manufacturer, is not guaranteed or endorsed by the publisher.

Copyright © 2021 Ren, Ramchandran and Yang. This is an open-access article distributed under the terms of the Creative Commons Attribution License (CC BY). The use, distribution or reproduction in other forums is permitted, provided the original author(s) and the copyright owner(s) are credited and that the original publication in this journal is cited, in accordance with accepted academic practice. No use, distribution or reproduction is permitted which does not comply with these terms.

frontiers in Cell and Developmental Biology

REVIEW
published: 16 November 2020
doi: 10.3389/fcell.2020.599281

Molecular Bases of VEGFR-2-Mediated Physiological Function and Pathological Role

Xinrong Wang[1], Alfredo Maria Bove[2], Giuseppe Simone[2] and Binyun Ma[3]**

[1] College of Animal Science and Technology, Gansu Agricultural University, Lanzhou, China, [2] Regina Elena National Cancer Institute, Rome, Italy, [3] Department of Medicine/Hematology, Keck School of Medicine of the University of Southern California, Los Angeles, CA, United States

The vascular endothelial growth factors (VEGFs) and their receptors (VEGFRs) play crucial roles in vasculogenesis and angiogenesis. Angiogenesis is an important mechanism in many physiological and pathological processes, and is involved in endothelial cell proliferation, migration, and survival, then leads to further tubulogenesis, and finally promotes formation of vessels. This series of signaling cascade pathways are precisely mediated by VEGF/VEGFR-2 system. The VEGF binding to the IgD2 and IgD3 of VEGFR-2 induces the dimerization of the receptor, subsequently the activation and trans-autophosphorylation of the tyrosine kinase, and then the initiation of the intracellular signaling cascades. Finally the VEGF-activated VEGFR-2 stimulates and mediates variety of signaling transduction, biological responses, and pathological processes in angiogenesis. Several crucial phosphorylated sites Tyr801, Try951, Try1175, and Try1214 in the VEGFR-2 intracellular domains mediate several key signaling processes including PLCγ-PKC, TSAd-Src-PI3K-Akt, SHB-FAK-paxillin, SHB-PI3K-Akt, and NCK-p38-MAPKAPK2/3 pathways. Based on the molecular structure and signaling pathways of VEGFR-2, the strategy of the VEGFR-2-targeted therapy should be considered to employ in the treatment of the VEGF/VEGFR-2-associated diseases by blocking the VEGF/VEGFR-2 signaling pathway, inhibiting VEGF and VEGFR-2 gene expression, blocking the binding of VEGF and VEGFR-2, and preventing the proliferation, migration, and survival of vascular endothelial cells expressing VEGFR-2.

Keywords: VEGF, VEGFR-2, structure, function and role, vasculogenesis, angiogenesis

OPEN ACCESS

Edited by:
Xiaofeng Yang,
Temple University, United States

Reviewed by:
Qian Yang,
Fourth Military Medical University, China
Adam Odell,
York St John University, United Kingdom

****Correspondence:***
Binyun Ma
binyunma@usc.edu
Xinrong Wang
wangxr@gsau.edu.cn

Specialty section:
This article was submitted to Signaling, a section of the journal Frontiers in Cell and Developmental Biology

Received: *26 August 2020*
Accepted: *21 October 2020*
Published: *16 November 2020*

Citation:
Wang X, Bove AM, Simone G and Ma B (2020) Molecular Bases of VEGFR-2-Mediated Physiological Function and Pathological Role. Front. Cell Dev. Biol. 8:599281. doi: 10.3389/fcell.2020.599281

INTRODUCTION

In organism, various physiological and pathological processes are involved in vasculogenesis, angiogenesis, and formation and maintenance of new blood vessel structures, including embryonic development (Vallon et al., 2014), tissue growth and wound healing (Ivkovic et al., 2003), tumorigenesis (Yehya et al., 2018), rheumatoid arthritis (Marrelli et al., 2011), diabetic retinopathy (Crawford et al., 2009; Cheng and Ma, 2015), axon growth (Klagsbrun and Eichmann, 2005), cancer (Hanahan and Folkman, 1996; Rajabi and Mousa, 2017; Li et al., 2020), and inflammation (Alkim et al., 2015), which are stimulated by a variety of factors, including basic fibroblast growth factor (bFGF) (Iwasaki et al., 2004), vascular endothelial growth factor (VEGF) (Hoeben et al., 2004;

Nilsson and Heymach, 2006), platelet-derived growth Factor (PDGF) (Lindahl et al., 1999), ephrin-Eph receptors (Zhang and Hughes, 2006), angiopoietin-1 (Yin et al., 2020), hepatocyte growth factor (HGF) (Kaga et al., 2012), transforming growth factor-β (TGF-β) (Ferrari et al., 2009), and interleukin 6 (IL-6) (Gopinathan et al., 2015), etc. VEGFs and their receptors (VEGFRs) are currently the most important and specific factors to stimulate endothelial cell proliferation, regulate both the development of blood vessels from precursor cells during early embryogenesis and the formation of blood vessels from pre-existing vessels at a later stage, and increase vascular permeability and chemotaxis of vascular endothelial cells (Ferrara and Kerbel, 2005; Benedito et al., 2012; Chen et al., 2013). The VEGF and its receptor VEGFR have been reported to play crucial roles not only in physiological but in most pathological angiogenesis.

Vascular endothelial growth factors are important signaling molecules involved in both vasculogenesis and angiogenesis that are the two distinct processes by which new vascular network are formed during embryonic development (Drake et al., 2000). The vasculogenesis is a fundamental process of blood vessel system formation in the embryo, occurring by a *De novo* synthesis and differentiation of endothelial precursor cells into endothelial cells, and it is the first stage of the formation of the vascular network. The angiogenesis is a vital physiological process of growth of new capillaries through which the pre-existing vasculatures formed in the earlier stage of the vasculogenesis continue to grow, sprout, split, and grow (Drake et al., 2000). VEGF is crucial to ensure normal vascular morphogenesis, especial to increase the number of capillaries in angiogenesis. The embryos lacking a single VEGF allele exhibit abnormal vascular development and lethality (Carmeliet et al., 1996; Ferrara et al., 1996). The VEGF and its receptor VEGFR have been shown to play important roles in many angiogenic processes not only in normal physiological conditions but in most pathological conditions, such as embryonic development, axon growth, cancer, and inflammation (Hanahan and Folkman, 1996; Risau, 1997; Bellon et al., 2010). VEGF is a sub-family of the cystine-knot growth factor PDGF supergene family. All members of the VEGF family can stimulate cellular responses by binding to their tyrosine kinase receptors (VEGFRs) on the cell surface.

Currently, the human VEGF/VEGFR system is composed of VEGF-A (also VEGF), VEGF-B, VEGF-C, VEGF-D, and PGF (placental growth factor), three main VEGF receptors VEGFR-1 (Flt-1), VEGFR-2 (KDR), VEGFR-3 (Flt-4), and two non-protein kinase co-receptors neuropilin-1 and neuropilin-2 (NRP-1 and -2) (Rahimi, 2006; Shibuya, 2011). The VEGFR-1 and VEGFR-2 regulate angiogenesis and vascular permeability, and the VEGFR-3 mainly regulates lymphangiogenesis (Alitalo and Carmeliet, 2002). Among them, VEGFR-2 is mainly distributed in vascular endothelial cells and acts as major signal transducer for angiogenesis by PLCγ-PKC-MAPK, PLCγ-PKC-eNOS-NO, TSAd-Src-PI3K-Akt, SHB-FAK-paxillin, SHB-PI3K-Akt, and NCK-p38-MAPKAPK2/3 pathways (Wong and Jin, 2005; Shibuya, 2011). The VEGF/VEGFR system is an important target for anti-angiogenic therapy in cancer and for pro-angiogenic therapy in neuronal degeneration and ischemic diseases (Yang et al., 2018). Here, the molecular structures, physiological functions, and pathological roles of VEGFR-2 and its regulation mechanisms of signal transduction have been analyzed and reviewed.

VEGFR-2 STRUCTURAL CHARACTERISTICS AND FUNCTION

Vascular endothelial growth factors are main regulators in vasculogenesis and angiogenesis and play their roles by binding to VEGFRs on cell surface and activating subsequently the signaling pathways of angiogenesis. The VEGFR-2 is the major receptor of VEGF, expresses in vascular endothelial cells, and plays a major role in angiogenesis (Bellon et al., 2010; Leppanen et al., 2010).

VEGFR-2 Molecular Characteristics

Human VEGFR-2, a kinase insert domain containing receptor (KDR) gene, is located at chromosome locus 4q11-12 and encodes 1356 amino acids of the full-length receptor (Park et al., 2018). Mature VEGFR-2 is a transmembrane glycoprotein with a molecular weight of 230 kD (**Figure 1**; Takahashi and Shibuya, 1997). The other two forms of VEGFR-2 are the non-glycosylated form with a molecular weight of 150 kD and the intermediate form with a molecular weight of 200 kD (Shen et al., 1998). Only the mature glycosylated form of VEGFR-2 (KDR) can achieve intracellular signal transduction (Shibuya, 2013). Mouse VEGFR-2 is also called fetal liver kinase 1 (Flk-1), which is composed of 1367 amino acids and has 83% homology with human KDR, and has three forms, molecular weight of 180, 200, and 220 kD, respectively.

VEGFR-2 is mainly distributed in vascular endothelial cells, lymphatic endothelial cells, and embryonic precursor cells, and can bind to VEGF-A, VEGF-C, and VEGF-D. By binding and activating VEGFR-2, VEGF mediates endothelial cell proliferation, invasion and migration, and survival, and increases vascular permeability and neovascularization (Holmes et al., 2007).

VEGFR-2 Molecular Structure

The full-length VEGFR-2 is composed of 1356 amino acids including a signal peptide (1∼19 aa) and a mature protein (20∼1356 aa). As a mature transmembrane protein, the VEGFR-2 is divided into extracellular domain (ECD, 20∼764 aa), transmembrane domain (TMD, 765∼789 aa), juxtamembrane domain (JMD, 790∼833 aa), catalytic tyrosine kinas domain (TKD, 834∼1162 aa) including ATP binding domain (TKD1, 834∼930 aa), kinase insert domain (KID, 931∼998 aa) and phosphotransferase domain (TKD2, 999∼1162 aa), and a flexible C-terminal domain (CTD, 1163∼1356 aa) (**Table 1** and **Figure 1**).

The ECD is composed of 7 immunoglobulin-like subdomains, IgD1 (46∼110 aa), IgD2 (141∼207 aa), IgD3 (224∼320 aa), IgD4 (328∼414 aa), IgD5 (421∼548 aa), IgD6 (551∼660 aa), and IgD7 (667∼753 aa) (**Figure 1A**; Fuh et al., 1998). Investigation have showed that the IgD1 is involved in regulating the binding of receptors to ligands; while the IgD2 and IgD3 are required for tight binding to the dimeric VEGF and VEGF-induced VEGFR-2 dimerization and activation; the IgD2 and IgD4 can affect the

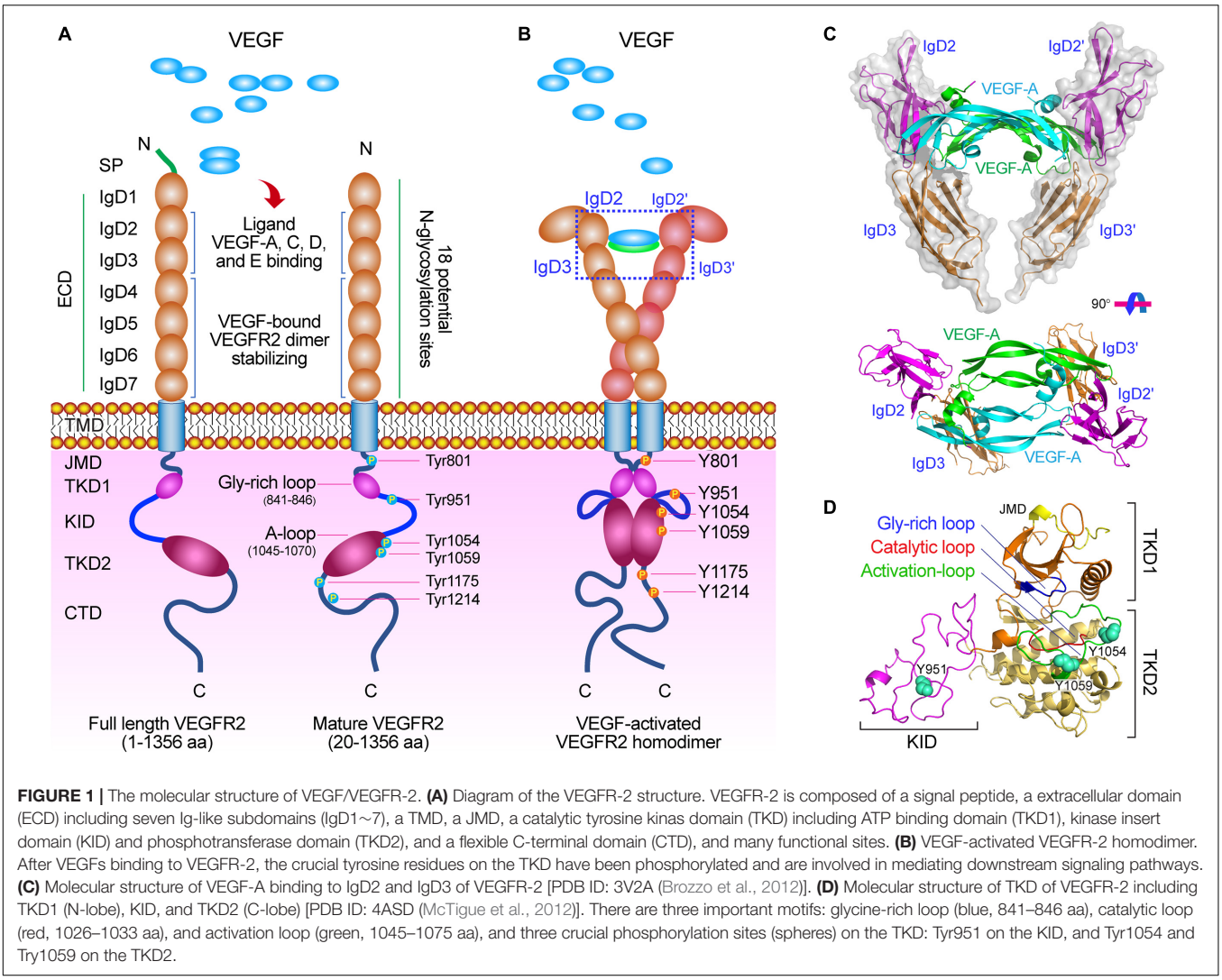

FIGURE 1 | The molecular structure of VEGF/VEGFR-2. **(A)** Diagram of the VEGFR-2 structure. VEGFR-2 is composed of a signal peptide, a extracellular domain (ECD) including seven Ig-like subdomains (IgD1∼7), a TMD, a JMD, a catalytic tyrosine kinas domain (TKD) including ATP binding domain (TKD1), kinase insert domain (KID) and phosphotransferase domain (TKD2), and a flexible C-terminal domain (CTD), and many functional sites. **(B)** VEGF-activated VEGFR-2 homodimer. After VEGFs binding to VEGFR-2, the crucial tyrosine residues on the TKD have been phosphorylated and are involved in mediating downstream signaling pathways. **(C)** Molecular structure of VEGF-A binding to IgD2 and IgD3 of VEGFR-2 [PDB ID: 3V2A (Brozzo et al., 2012)]. **(D)** Molecular structure of TKD of VEGFR-2 including TKD1 (N-lobe), KID, and TKD2 (C-lobe) [PDB ID: 4ASD (McTigue et al., 2012)]. There are three important motifs: glycine-rich loop (blue, 841–846 aa), catalytic loop (red, 1026–1033 aa), and activation loop (green, 1045–1075 aa), and three crucial phosphorylation sites (spheres) on the TKD: Tyr951 on the KID, and Tyr1054 and Try1059 on the TKD2.

binding rate of the ligand; the IgD5 and IgD6 may be involved in affect the receptor molecules unbinding from the ligands; and the IgD7 plays a crucial role in receptor dimerization and regulation (**Figures 1B,C**; Shinkai et al., 1998; Di Stasi et al., 2019).

The TKD is the most conserved region among VEGFRs (Park et al., 2018). This protein kinase core of the VEGFR-2 has a two-lobed spatial structure that forms the active center between the both lobes. At the N-terminus of the intracellular tyrosine kinas domain, there is a hydrophobic pocket containing a glycine-rich (GXGXXG, 841∼846 aa) ATP phosphate binding loop in the β-sheet structures. At the TKD C-terminal, there are several α-helical structures, including a catalytic loop (HRDLAARN, 1026∼1033 aa), and activation loop (A-loop, 1045∼1075 aa), which play important roles for VEGFR-2 catalytic properties (**Tables 1**, **2** and **Figures 1A,D**).

In the human VEGFR-2, there are 18 N-linked glycosylation sites, 15 phosphorylation sites, and many ATP binding sites and substrate binding sites, which play important roles in post-translational modifications of VEGFR-2, protein folding, protein activation, and cellular attachment, and can further modulate the function of VEGFR-2 (Croci et al., 2014; Chandler et al., 2019; Chung et al., 2019).

Mechanism of VEGFR-2 Activation

VEGFR-2 is activated by VEGF-A, -C, and -D binding to its Ig-like domains 2 and 3 (**Figure 1C**). Similar to other receptor tyrosine kinases (RTKs), cellular signaling mediated by VEGFR-2 is stimulated and initiated upon binding of its ligand dimer to the extracellular receptor Ig-like domains 2 and 3 (Ruch et al., 2007). This ligand-receptor interaction causes VEGFR-2 homo- and hetero-dimerization followed by phosphorylation of specific tyrosine residues located in the intracellular region including juxtamembrane domain, tyrosine kinas domain, and the carboxy-terminal domain. Subsequently, a variety of signaling molecules are recruited to VEGFR-2 dimers that activate downstream signaling pathways, and ultimately affect the physiological characteristics of endothelial cells and the entire vascular environment (**Figure 2A**; Fuh et al., 1998; Ruch et al., 2007; Ma et al., 2011).

TABLE 1 | The structures and functions of the VEGFR-2 domains.

Domains	Structure characteristic	Functions and roles
ECD	20∼764 aa	Plays a central role in VEGF binding, trafficking, stabilizing, and pro-angiogenic signaling in physiological and pathological condition by the IgD2 and IgD3, and the *N*-glycosylation sites.
	The extracellular domain including 7 Ig-like subdomains (IgD1∼7) connected by the linkers, and 18 potential *N*-glycosylation sites	
TMD	765∼789 aa	Regulates VEGFR-2 kinase activity, specific orientation of the intracellular kinase domains in active VEGFR-2 dimers, and dimerization of the receptor monomers with specific orientations.
	A single transmembrane α-helical	
JMD	790∼833 aa	Plays a crucial role for the autophosphorylation rate of VEGFR-2. Unphosphorylated JMD autoinhibits kinase activity by the site Y801 interacting with the activation loop in the kinase domain.
	A flexible intracellular regulatory region including the first phosphorylation site Y801 of VEGFR-2	
TKD	834∼1162 aa	Contains the catalytic site of VEGFR-2 and is involved in VEGFR-2 activation and signaling by its multiple phosphorylation sites and VEGFR-2-mediate cellular signaling, and regulation of endothelial cell survival, proliferation, cell migration, and the vascular tube formation.
	The catalytic tyrosine kinas domain contains three subdomains: • TKD1 (834∼930aa), an ATP binding domain including a hydrophobic pocket with a glycine-rich motif • KID (931∼998aa), a kinase insert domain including a phosphorylation site Y951 • TKD2 (999∼1162aa), a phosphotransferase domain including two sites Y1054 and Y1059, a catalytic loop and an activation loop	
CTD	1163∼1356 aa	Is critical for VEGFR-2 activation and signaling and is involved in VEGFR-2-mediate cellular signaling and endothelial cell survival, proliferation, cell migration, and permeability of vascular endothelial cells.
	The carboxyl terminus domain including two important autophosphorylation sites Y1175 and Y1214	

The ECD Is Required for VEGFR-2 Dimerization

The extracellular domain (ECD) of VEGFR-2 consists of several Ig-like subdomains, the linkers connecting these subdomains, and multiple N-linked glycosylation sites, which play important roles in formation of VEGF/VEGFR-2 system, in receptor dimerization after with ligand binding, and in maintain of the monomeric VEGFR-2 in the absence of ligand (**Table 1**). Each VEGF monomer is composed of two α-helix and five β-sheets that forms a central antiparallel beta sheet. In VEGF-A, a canonical cysteine knot formed by three intramolecular disulfide bridges Cys263-Cys308, Cys267-Cys310, and Cys232-Cys274, and two receptor binding sites and dimerization interface sites are critical for VEGF binding to VEGFR-2 and subsequently VEGFR-2 dimerization (**Figure 2B**).

In the ECD of VEGFRs, the ability to bind to its ligand is best studied at the biochemical and the structural level. For VEGFR-2, the ligands binding to VEGFR-2 required two Ig-like subdomains 2 and 3 (IgD2 and IgD3), and the stabilization of VEGF-bound VEGFR-2 dimers and VEGF-mediated VEGFR activity required Ig-like subdomains 4∼7 (IgD4∼7) (Li et al., 2000; Yang et al., 2010). As a *N*-glycosylated RTK, VEGFR-2 has 18 potential *N*-glycosylation sites in the seven Ig-like subdomains, which play a central role in RTK ligand binding, trafficking, stabilizing, and pro-angiogenic signaling in physiological and pathological contexts, including cancer (**Table 2** and **Figure 1**; Croci et al., 2014; Chandler et al., 2017, 2019).

The TMD and JMD Is Crucial for Regulating VEGFR-2 Activity

The transmembrane domain (TMD) and juxtamembrane domain (JMD) of VEGFR-2 have been shown to play pivotal roles in regulating VEGFR-2 kinase activity (Solowiej et al., 2009; Koch and Claesson-Welsh, 2012; **Table 1**).

Investigations on the role of the TMD in VEGFR-2 signaling showed that the activation of VEGFR-2 may depend on specific orientation of the receptor monomers in an active dimer resulting from VEGF-induced ECD rearrangement, and the TMD is involved in dimerization of the receptor monomers with specific orientations (Moriki et al., 2001; Bennasroune et al., 2004; Holmes et al., 2007; Manni et al., 2014b). The JMD of VEGFR-2 has the first phosphorylation site Y801, which is crucial for the autophosphorylation rate of VEGFR-2 (Solowiej et al., 2009). The unphosphorylated JMD autoinhibits kinase activity by interacting with the activation loop (A-loop) in the kinase domain 2 (TKD2). Therefore, the phosphorylated JMD at specific tyrosine residue Y801 may disrupt this interaction with the A-loop, promote reorientation of the activation loop, and induce an enzymatically active conformation (**Table 2** and

TABLE 2 | Functional sites and motifs in VEGFR2.

Sites and motifs	Location	Function
N-linked glycosylation sites:		
Asn46, 66, 96, 143, 158, 245, 318, 374, 395, 511, 523, 580, 613, 619, 631, 675, 704, and 721	ECD	These sites play a central role in RTK ligand binding, trafficking, stabilizing, and pro-angiogenic signaling in physiological and pathological contexts.
Phosphorylation sites:		
Tyr801	JMD	Y801 is crucial for the autophosphorylation rate of VEGFR-2, and phosphorylated Y801 disrupts the interaction of JMD with the A-loop, promotes reorientation of the activation loop, and induces an enzymatically active conformation.
Tyr951	KID	Y951 is phosphorylated on VEGFA stimulation, and phosphorylated Y951 at the TKD of VEGFR-2 can bind TSAd, activate formation of TSAd and Src complex, subsequently regulate cell migration and mediate cell survival and permeability.
Tyr1054	TKD2	Y1054 and Y1059 sites are located in the TKD2 A-loop and play crucial role in kinase activity, and phosphorylated Y1054 and Y1059 increase the VEGFR-2 kinase activity.
Tyr1059		
Tyr1175	CTD	Y1175 and Y1214 are critical for VEGFR-2 activation and signaling and are involved in VEGFR-2-mediate cellular signaling, and phosphorylated Y1175 mediates the binding of VEGFR-2 with PLCγ, PI3K, and adapter proteins SHB and SCK and phosphorylated Y1214 mediates the binding of VEGFR-2 with adapter protein NCK, and the both of pY1175 and pY1214 finally directly activate VEGFR-2 to promote the proliferation, migration, and permeability of vascular endothelial cells.
Tyr1214		
Others phosphorylation sites:		
Ser982, Ser984, and Tyr996	KID	They are potential phosphorylation sites and may be involved in VEGFR-2 activation and signaling.
Ser1231, Ser1235, and Thr1238	CTD	
Tyr1305, Tyr1309, and Tyr1319	CTD	
Functional motifs:		
Glycine-rich (G^{841}XGXXG) (841∼846 aa)	TKD1	The glycine-rich forms a functionally important ATP phosphate binding loop, which is a flexible segment whose position differs among kinase structures in various activated and liganded states.
Catalytic loop (H^{1026}RDLAARN) (1026∼1033 aa)	TKD2	The catalytic loop contains an invariant aspartic acid residue (D1028) that is essential for catalysis of the phosphotransferase reaction. The catalytic loop is highly conserved among protein tyrosine kinases.
Activation loop (A-loop) (1045∼1075 aa)	TKD2	The activation loop is a large flexible loop in protein kinases and contains two tyrosines Y1054 and Y1059, whose conformation is postulated to regulate kinase activity.

Figures 1A,B; Wybenga-Groot et al., 2001; Walter et al., 2007; Solowiej et al., 2009).

The TKD Mediates VEGFR-2 Cellular Signaling

The activation of VEGFR-2 upon its VEGFs-mediated dimerization allows the TKD transphosphorylation, and then mediates cellular signaling, and regulates endothelial cell survival, proliferation, cell migration, and the vascular tube formation (Koch et al., 2011; **Table 1**). The VEGFR-2 TKD contains three subdomains, TKD1, an ATP binding domain, KID, the kinase insert domain, and TKD2, a phosphotransferase domain. The TKD is involved in VEGFR-2 activation and signaling by its multiple phosphorylation sites (**Figures 1B,D**).

In VEGFR-2 TKD, there are several major phosphorylation sites involved in cellular signaling mediated by TKD, including Tyr951 (Y951) in the KID and Try1054 (Y1054) and Try1059 (Y1059) in the TKD2, which is phosphorylated for the kinase activation (Takahashi et al., 2001; Matsumoto et al., 2005; **Table 2**). The Y951 site is phosphorylated on VEGFA stimulation, and the phosphorylated Y951 is indispensable for downstream signaling by the activated kinase (Matsumoto et al., 2005). The Y1054 and Y1059 sites are located in the TKD2 A-loop and play crucial role in kinase activity, whose autophosphorylation resulted by autophosphorylation at Y801 site increases the VEGFR-2 kinase activity (**Figures 1B,D**; Kendall et al., 1999; Solowiej et al., 2009).

The CTD Is Critical for VEGFR-2 Activation and Signaling

The carboxyl terminus domain (CTD) is critical for VEGFR-2 activation and signaling. In VEGFR-2 CTD, there are two important autophosphorylation sites Try1175 (Y1175) and Try1214 (Y1214) (**Table 1** and **Figures 1B,D**). After VEGF-A binding to VEGFR-2, activation of VEGFR-2 phosphorylates the Y1175 and Y1214 (Sase et al., 2009; **Table 2**). Then, the VEGF-activated VEGFR-2 bind to several signaling molecules such as PLCγ (Takahashi et al., 2001), PI3K (Kim et al., 2019), and adapter proteins SHB and SCK (Warner et al., 2000; Holmqvist et al., 2004) by the phosphorylated Try1175 site (pY1175), and adapter protein NCK (Lamalice et al., 2006) by the phosphorylated Try1214 site (pY1214), which directly

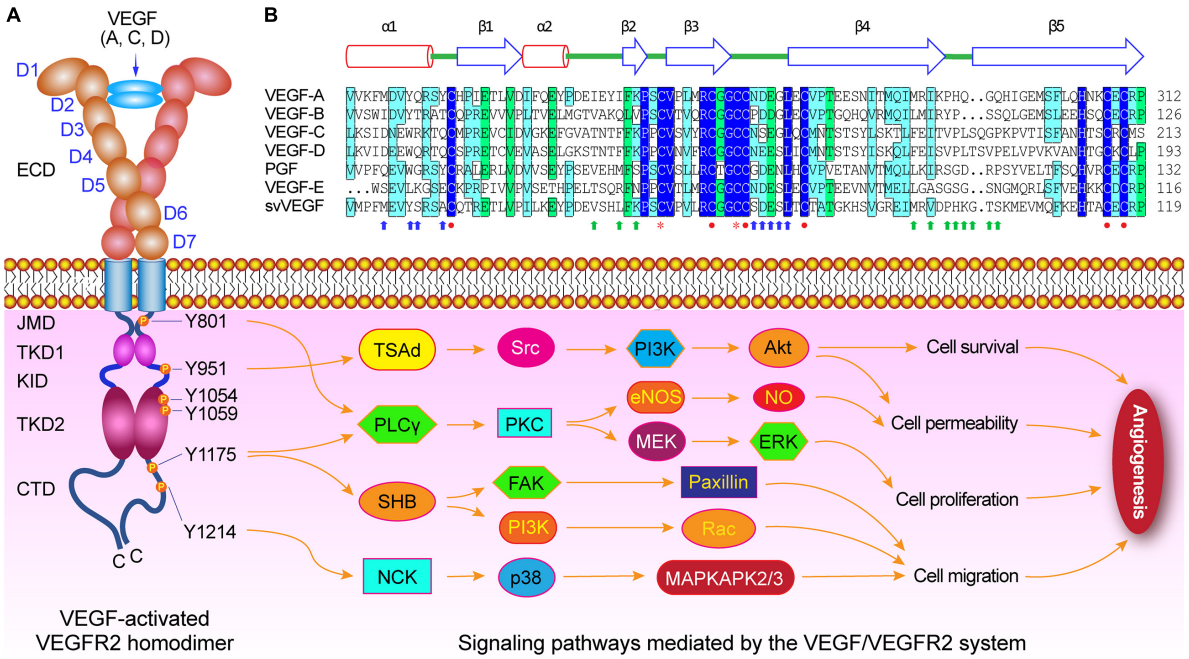

FIGURE 2 | VEGF/VEGFR-2 mediated signaling pathways during angiogenesis. **(A)** Diagram of VEGF-activated VEGFR-2 homodimer. Several crucial tyrosine residues have been phosphorylated after VEGFs binding to VEGFR-2. The Try801 on JMD is involved in cell permeability and proliferation by mediating the PLCγ-PKC, then eNOS-NO or MEK-ERK, respectively. The Try951 on KID mediates the cell survival and permeability via the TSAd-Src-PI3K-Akt pathway. The Try1054 and Try1059 on TKD2 can increase VEGFR-2 kinase activity. The Try1175 is involved in cell permeability, proliferation, and migration by regulating PLCγ-PKC, SHB-FAK-paxillin, and SHB-PI3K-Rac pathways. The Try1214 mediates cell migration through NCK-p38-MAPKAPK2/3 pathway. **(B)** Structure-based sequence alignment of PDGF-derived regions of the VEGF family members, includes human VEGF-A (NP_003367), human VEGF-B (NP_003368), human VEGF-C (NP_005420), human VEGF-D (NP_004460), human PGF (placental growth factor) (NP_002623), *Orf virus* orfVEGF (VEGF-E) (ABA00650), and *Snake venom* svVEGF (BAD38844), which are composed of two α-helix and five β-sheets. There are functional sites, including receptor binding site 1 (blue arrow) and site 2 (green arrows), cysteine knot motifs (red closed circles) that form three disulfide bridges including Cys263-Cys308, Cys267-Cys310, and Cys232-Cys274 in VEGF-A, and dimerization interface sites (orange stars).

activate VEGFR-2 to promote the proliferation, migration, and permeability of vascular endothelial cells (**Figure 2A**; Koch and Claesson-Welsh, 2012; Manni et al., 2014a).

VEGFR-2 MEDIATED CELLULAR SIGNALING

The VEGF/VEGFR-2 signaling is essential for the development and maintenance of the organ-specific vascular systems and physiological function of many tissues and plays important roles in the pathogenesis of diseases such as cardiovascular disease and cancer. The VEGFR-2 has been proved to mediate various VEGF-stimulated cellular signal transduction including endothelial cell survival, proliferation, migration, and to enhance vascular permeability (Holmes et al., 2007; Siveen et al., 2017).

VEGFR-2 Is Involved in Regulating the Survival of Endothelial Cells

The VEGFR-2 plays crucial roles in vascular endothelial cell survival and blood vessel formation *in vivo* (Sase et al., 2009). VEGFR-2 regulates endothelial cell survival mainly by the activation of TSAd-Src-PI3K-PKB/AKT signaling pathway (**Figure 2**). Depending on VEGFR-2 and subsequent activated PI3K, VEGF-A regulates the survival of human umbilical vein endothelial cells. The PI3K can catalyze creation of PIP3 from PIP2, and then phosphorylate and activate protein kinase B (PKB) and Akt pathway (PKB/Akt pathway) (Downward, 2004). The Akt directly phosphorylates two types of apoptosis proteins: Bcl-2 associated death promoter (BAD) and caspase 9, and then inhibits their apoptotic activity to ensure cell survival (Lee et al., 2014).

VEGFR-2 Is Required for Mediating the Proliferation of Endothelial Cells

VEGFR-2 plays a critical role in endothelial cell proliferation during angiogenesis. Through the VEGFR-2 on the cell membrane, the VEGF-A, a mitogen of many endothelial cells, can transmit extracellular signals to the cytoplasm and activate a series of downstream signaling pathways, and regulate the proliferation of endothelial cells. VEGFR-2 is mainly through the PLCγ-PKC-Raf-MEK-MAPK signaling pathway, and transmits the VEGF signal to the nucleus to activate DNA synthesis and promote the proliferation of endothelial cells (Takahashi et al., 1999; **Figure 2**). The VEGFR-2 can bind and activate phospholipase C-γ (PLCγ) by phosphorylation of the C-terminal

Y1175 of VEGFR-2, and then phosphorylate the PLCγ and enhance its catalytic activity (Takahashi et al., 2001; Sase et al., 2009). The activated PLCγ hydrolyzes phosphatidylinositol (4, 5)-bisphosphate (PIP2) and then produces diacylglycerol (DAG) and inositol 1, 4, 5-trisphosphate (IP3), in which IP3 can increase the intracellular Ca^{2+} concentration, and DAG is a physiological activator of PKC. The ERK in the PKC-Raf-MEK-ERK signaling cascade is activated by the VEGF-activated VEGFR-2, enters the nucleus, and then binds to transcription factors that induce gene expression in response to extracellular stimuli. Finally, VEGFR-2 is involved in the endothelial cell proliferation (Holmes et al., 2007; Rask-Madsen and King, 2008).

VEGFR-2 Is Closely Related to the Migration of Endothelial Cells

The migration of endothelial cells is crucial for angiogenesis. A variety of signal pathways mediated by VEGFR-2 are related to the migration of endothelial cells. VEGFR-2 has been proved to regulate cell migration by activating SHB, NCK, and PI3K mediated pathway via the both phosphorylation sites Y1175 and Y1214 on VEGFR-2 CTD (Laramee et al., 2007; Graupera et al., 2008). The phosphorylated Tyr1175 (pY1175) site at the CTD of VEGFR-2 can bind the Src homology domain-2 (SH2) of the adaptor protein SHB and regulate cell migration caused by VEGF (Holmqvist et al., 2004; **Figure 2**). The downregulated expression of SHB can prevent VEGF/VEGFR-2-mediated cell scaffold reorganization, migration, and PI3K activation (Masoumi Moghaddam et al., 2012; Park et al., 2018). The phosphorylated Tyr951 (pY951) site at the TKD of VEGFR-2 can bind T-cell-specific adapter (TSAd) in the vascular endothelial cells of tumor tissue (Matsumoto et al., 2005), activate formation of TSAd and Src complex, and subsequently regulate cell migration. Site-directed mutation of Tyr951 on VEGFR-2 can inhibit VEGF-mediated cytoskeletal reorganization and migration (Cebe-Suarez et al., 2006). While the phosphorylated Tyr1214 (pY1214) site at the C-terminus domain of VEGFR-2 is involved in the remodeling of actin by VEGFR-2 mediated NCK/Src-p21/Cdc42-SAPK2/p38-MAPK pathway (Lamalice et al., 2004, 2006).

VEGFR-2 Enhances Vascular Permeability

The VEGF-A acts as a vascular permeability factor and its signal can activate endothelial nitric oxide synthase (eNOS) to create NO, and then change vascular permeability (Holmes et al., 2007). VEGF-activated VEGFR-2 can stimulate vascular endothelial cells to release NO, in which the phosphorylation of the Try801 (pY801) residue at the JMD of VEGFR-2 is necessary for the release of NO induced by VEGF, and the pY801 activates eNOS mainly by the PKC-PI3K/Akt pathway (Blanes et al., 2007; **Figure 2**). VEGFR-2 mediated signals can promote eNOS binding to its molecular chaperone heat shock protein 90 (Hsp90), and then enhance the release of NO by endothelial cells (Duval et al., 2007). VEGFR-2 can also mediate effect of lowering blood pressure via increased permeability of blood vessels and relaxed of blood vessels caused by VEGF-A (Gliki et al., 2001).

VEGFR-2 PHYSIOLOGICAL FUNCTIONS AND PATHOLOGICAL ROLES

In organism, many angiogenic proteins are involved in the stimulation of angiogenesis including EphrinB2/EphB4 (Groppa et al., 2018), fibroblast growth factors (FGFs) (Maddaluno et al., 2017), VEGFs/VEGFR-2 (Basagiannis et al., 2016), angiopoietin/Tie receptors (Zhang et al., 2019), and platelet-derived growth factors (PDGFs/PDGFRs) (Zhang et al., 2009; Manzat Saplacan et al., 2017). Among the angiogenic proteins, VEGFs/VEGFR-2 is a crucial regulator of physiological vasculogenesis and angiogenesis in early embryonic and adult stages and pathological angiogenesis in tumorigenesis.

Physiological Functions of VEGFR-2

VEGFR-2 mediates the main physiological functions of VEGF. VEGF, the vascular permeability factor (VPF), is an essential and crucial growth factor for vascular endothelial cells, and plays various roles in cardiovascular system (Wang et al., 2019), central nervous system (Bellon et al., 2010; Luck et al., 2019), hematopoiesis (Hooper et al., 2009), development (Karaman et al., 2018), and tumorigenesis (Volz et al., 2020; Zhong et al., 2020). Despite having so many physiological functions, the main physiological functions of VEGF on endothelial cells are almost all achieved by activating VEGFR-2, including stimulating endothelial cell proliferation, increasing vascular permeability, and chemotaxis to endothelial cells, etc. Investigations showed that VEGFR-2 is the main receptor to mediate the increase in vascular permeability by VEGF (Koch and Claesson-Welsh, 2012; Smith et al., 2020). VEGFR-2 is required for VEGF-mediated signaling and regulating. The phosphorylation of VEGFR-2 can be found on the surface of whole cell. Several important phosphorylation sites, Try951, Try1054, Try1059, and Try1175 had been proved to be involved in this process by binding SHB (Holmqvist et al., 2004; Smith et al., 2020), SCK (Warner et al., 2000), PLCγ (Takahashi et al., 2001), PI3K (Blanes et al., 2007), and TASD (Matsumoto et al., 2005) and activating their respective signal pathway.

VEGFR-2 plays a very important role in embryonic development. VEGF-activated VEGFR-2 stimulates endothelial cell proliferation and is crucial to the development of the embryonic vascular system and hematopoietic system (Hooper et al., 2009; Han et al., 2018). During embryonic development, the VEGFR-2 signaling pathway is involved in the proliferation, growth, and migration of hematopoietic and early endothelial cells (angioblasts) (Dias et al., 2000; LeCouter et al., 2004). Several studies showed that the VEGF/VEGFR-2 signaling directly regulates the development and function of neurons, e.g., increased axon branching (Luck et al., 2019).

Pathological Rroles of VEGF-Activated VEGFR-2

Though the VEGF/VEGFR-2 system plays important functions in normal physiological condition, de-regulation of the VEGF/VEGFR-2 implicates directly in various diseases, and dysfunctional VEGFR-2 can cause developmental disorders of

the vascular system and hematopoietic system during embryonic development (Shibuya, 2001; Zeng et al., 2001).

VEGF-activated VEGFR-2 plays important roles in mediating the formation of new blood vessels under various pathological conditions and processes, including wound healing, rheumatoid arthritis (RA), diabetic retinopathy (DR), Alzheimer's disease (AD), small vessel disease, coronary heart disease (CHD), and cancer owing to its complicated molecular and structural characteristics. The VEGFA/VEGFR-2 signal transduction leads to endothelial cell proliferation, migration, survival and new vessel formation involved in angiogenesis, and has been implicated in pathogenesis of several diseases, e.g., inflammation, cancers, ophthalmic diseases, and neurological diseases (Louveau et al., 2015; Ferrara and Adamis, 2016; Ma et al., 2017).

VEGFR-2 is required for cardiovascular system diseases. Investigations showed that VEGFR-2-deficient mice die in early embryo for an early defect in the development of hematopoietic and endothelial cells (Shalaby et al., 1995; Carmeliet et al., 1996; Ferrara et al., 1996). VEGFR-2 is also involved in tumor angiogenesis and lymphatic development via recruiting endothelial cells (Dumont et al., 1998; Rafii et al., 2002). Studies have reported that the expression of Ets-1 and Flk-1 (mouse VEGFR-2) are highly correlated in angiogenesis and tumor angiogenesis, and are involved in stem cell leukemia (Elvert et al., 2003).

VEGFR-2 is an important target of anti-tumor angiogenesis. VEGF secreted by tumor cells activates its receptor VEGFR-2, and they subsequently promote vascular growth and supply the oxygen and nutrition into the hypoxic areas of tumor tissues (Lugano et al., 2020). VEGF-activated VEGFR-2 mediate the phosphorylation of many proteins in the downstream signaling pathways, e.g., Akt (protein kinase B), mTOR (mammalian target of rapamycin), Erk1/2 (extracellular signal-regulated kinase 1/2), FAK (focal adhesion kinase), and p70S6K (ribosomal protein S6 kinase), and promotes tumor angiogenesis (Karar and Maity, 2011; Lechertier and Hodivala-Dilke, 2012; Ji et al., 2018). Therefore, VEGFR-2 functions as an important target for anti-tumor therapy (Weis and Cheresh, 2011; Fallah et al., 2019).

CONCLUSION AND PERSPECTIVES

Vascular endothelial growth factors, as the key regulators, are involved in vasculogenesis, angiogenesis, and hematopoiesis during development. Thay play their roles by binding to and activating their tyrosine kinase receptors (VEGFRs) on the cell surface. In VEGF/VEGFR-2 system, the VEGF binding to the Ig-like subdomains 2 and 3 (IgD2 and IgD3) of VEGFR-2 induces the dimerization of the receptor, the activation and trans-autophosphorylation of the tyrosine kinase, and then the initiation of the intracellular signaling cascades, finally is involved in proliferation, survival, migration, and permeability of vascular endothelial cells.

The interaction of VEGF and VEGFR-2 is crucial for the dimerization of VEGFR-2. In endothelial cell, the signaling by VEGFR-2 requires VEGF-mediated dimerization with precise positioning of VEGFR-2 subunits in active dimers. In VEGF-A, there are a canonical cysteine knot that consists of three intramolecular disulfide bridges Cys263-Cys308, Cys267-Cys310, and Cys232-Cys274, and two receptor binding sites that bind to each VEGFR-2 of the dimer and dimerization interface sites, which are critical for the ligand binding to VEGFR-2. In VGEFR2 Ig-like subdomains, the IgD2 and IgD3 are involved in the VEGF binding to its receptor. The dimeric VEGF/VEGFR-2 complexes subsequently induce the dimerization of the receptor.

The dimerization of VEGFAR-2 is required for activation of VEGFR-2. The dimeric VEGF ligands binding to diffusing monomeric VEGFR-2 promotes dimerization of the later, and then stimulates the activation of VEGFR-2. It is reported that ligand-induced VEGFR-2 phosphorylation is increased as much as 10-fold compared to the phosphorylation in the absence of ligand (Sarabipour et al., 2016). In the active homotypic VEGFR-2-VEGFR-2, the IgD4∼7 were proved to be critical for efficient phosphorylation of the VEGFR-2 in the presence of VEGF, and the TMD dimer upon ligand binding increases VEGFR-2 phosphorylation and stabilizes the VEGFR-2 dimers, indicating that VEGF binding and VEGFR-2 dimerization are required for its activation.

The VEGFR-2-mediated intracellular signaling are involved in cell survival, proliferation, migration, and vascular permeability. VEGFR-2 is the primary mediator of the physiological effects of VEGF in angiogenesis. The VEGF binding to VEGFR-2 induces autophosphorylation of specific tyrosine residues in the cytoplasmic domain of VEGFR-2, including the Try801 on JMD involved in cell permeability and proliferation by mediating the PLCγ-PKC, then eNOS-NO or MEK-ERK, respectively, the Try951 on KID mediating the cell survival and permeability via the TSAd-Src-PI3K-Akt pathway, the Try1054 and Try1059 on TKD2 increasing VEGFR-2 kinase activity, the Try1175 involved in cell permeability, proliferation, and migration by regulating PLCγ-PKC, SHB-FAK-paxillin, and SHB-PI3K-Rac pathways, and the Try1214 mediates cell migration through NCK-p38-MAPKAPK2/3 pathway. These signaling networks mediated by VEGF/VEGFR-2 are involved in regulating the process of angiogenesis, and controlling endothelial cell survival, proliferation and motility, and vascular fenestration and permeabilization.

The VEGFR-2-targeted therapy strategies will contribution to clinical treatment of disease. So far, the in-depth study of the structure and signal transduction of VEGFR-2 has made the mechanism of related pathogenesis further elucidated and effectively treated. VEGFR-2-targeted therapy strategies have been widely explored and applied clinically in cancer treatment. VEGF/VEGFR-2 signal transduction pathway is used in anti-tumor angiogenesis. VEGF/VEGFR-2 system is involved in various pathological conditions and processes, especially in tumorigenesis, owing to its complicated molecular structure and signal transduction, indicating these diseases can be considered to employ the strategy of the VEGFR-2-targeted therapy. The tumor microenvironment stimulates the specific expression of VEGF and VEGFR-2 in tumor cells and endothelial cells around the tumor, making the expression of VEGF and VEGFR-2 significantly higher than in normal tissues, indicating that inhibiting tumor angiogenesis by blocking the VEGF/VEGFR-2

signaling pathway may be an effective anti-cancer treatment strategy, including (a) inhibiting VEGF and VEGFR-2 gene expression level by antisense oligonucleotides (ASOs), RNA interference (RNAi), and ribozyme (Rz) (Marchand et al., 2002); (b) blocking the binding of VEGF and VEGFR-2 in protein level through neutralizing antibodies (nAbs), soluble VEGFR-2 (sVEGFR-2), and small molecule inhibitor VEGF/VEGFR-2 tyrosine kinase signaling pathway (Jain et al., 2006); and (c) destroying vascular endothelial cells through directed therapy by VEGF combined with small molecule toxic substances or VEGFR-2 monoclonal antibody (mAb) cross-linked with drugs and killing or inhibiting the growth of vascular endothelial cells expressing VEGFR-2 (Stopeck et al., 2002).

AUTHOR CONTRIBUTIONS

XW, AMB, GS, and BM contributed to manuscript writing and language improving. BM and XW designed and made the figures and wrote and edited the review. All authors contributed to the article and approved the submitted version.

FUNDING

The study was funded by Discipline Construction Fund Project of Gansu Agricultural University (GAU-XKJS-2018-037)

REFERENCES

Alitalo, K., and Carmeliet, P. (2002). Molecular mechanisms of lymphangiogenesis in health and disease. *Cancer Cell* 1, 219–227. doi: 10.1016/s1535-6108(02)00051-x

Alkim, C., Alkim, H., Koksal, A. R., Boga, S., and Sen, I. (2015). Angiogenesis in Inflammatory Bowel Disease. *Int. J. Inflam.* 2015:970890.

Basagiannis, D., Zografou, S., Murphy, C., Fotsis, T., Morbidelli, L., Ziche, M., et al. (2016). VEGF induces signalling and angiogenesis by directing VEGFR2 internalisation through macropinocytosis. *J. Cell Sci.* 129, 4091–4104.

Bellon, A., Luchino, J., Haigh, K., Rougon, G., Haigh, J., Chauvet, S., et al. (2010). VEGFR2 (KDR/Flk1) signaling mediates axon growth in response to semaphorin 3E in the developing brain. *Neuron* 66, 205–219. doi: 10.1016/j.neuron.2010.04.006

Benedito, R., Rocha, S. F., Woeste, M., Zamykal, M., Radtke, F., Casanovas, O., et al. (2012). Notch-dependent VEGFR3 upregulation allows angiogenesis without VEGF-VEGFR2 signalling. *Nature* 484, 110–114. doi: 10.1038/nature10908

Bennasroune, A., Fickova, M., Gardin, A., Dirrig-Grosch, S., Aunis, D., Cremel, G., et al. (2004). Transmembrane peptides as inhibitors of ErbB receptor signaling. *Mol. Biol. Cell* 15, 3464–3474. doi: 10.1091/mbc.e03-10-0753

Blanes, M. G., Oubaha, M., Rautureau, Y., and Gratton, J. P. (2007). Phosphorylation of tyrosine 801 of vascular endothelial growth factor receptor-2 is necessary for Akt-dependent endothelial nitric-oxide synthase activation and nitric oxide release from endothelial cells. *J. Biol. Chem.* 282, 10660–10669. doi: 10.1074/jbc.m609048200

Brozzo, M. S., Bjelic, S., Kisko, K., Schleier, T., Leppanen, V. M., Alitalo, K., et al. (2012). Thermodynamic and structural description of allosterically regulated VEGFR-2 dimerization. *Blood* 119, 1781–1788. doi: 10.1182/blood-2011-11-390922

Carmeliet, P., Ferreira, V., Breier, G., Pollefeyt, S., Kieckens, L., Gertsenstein, M., et al. (1996). Abnormal blood vessel development and lethality in embryos lacking a single VEGF allele. *Nature* 380, 435–439. doi: 10.1038/380435a0

Cebe-Suarez, S., Zehnder-Fjallman, A., and Ballmer-Hofer, K. (2006). The role of VEGF receptors in angiogenesis; complex partnerships. *Cell Mol. Life Sci.* 63, 601–615. doi: 10.1007/s00018-005-5426-3

Chandler, K. B., Leon, D. R., Kuang, J., Meyer, R. D., Rahimi, N., and Costello, C. E. (2019). N-Glycosylation regulates ligand-dependent activation and signaling of vascular endothelial growth factor receptor 2 (VEGFR2). *J. Biol. Chem.* 294, 13117–13130. doi: 10.1074/jbc.ra119.008643

Chandler, K. B., Leon, D. R., Meyer, R. D., Rahimi, N., and Costello, C. E. (2017). Site-Specific N-glycosylation of endothelial cell receptor tyrosine kinase VEGFR-2. *J Proteome Res* 16, 677–688. doi: 10.1021/acs.jproteome.6b00738

Chen, X., Yang, G., Song, J. H., Xu, H., Li, D., Goldsmith, J., et al. (2013). Probiotic yeast inhibits VEGFR signaling and angiogenesis in intestinal inflammation. *PLoS One* 8:e64227. doi: 10.1371/journal.pone.0064227

Cheng, R., and Ma, J. X. (2015). Angiogenesis in diabetes and obesity. *Rev. Endocr. Metab. Disord.* 16, 67–75.

Chung, T. W., Kim, E. Y., Choi, H. J., Han, C. W., Jang, S. B., Kim, K. J., et al. (2019). 6'-Sialylgalactose inhibits vascular endothelial growth factor receptor 2-mediated angiogenesis. *Exp. Mol. Med.* 51, 1–13. doi: 10.1038/s12276-019-0311-6

Crawford, T. N., Alfaro, D. V. III, Kerrison, J. B., and Jablon, E. P. (2009). Diabetic retinopathy and angiogenesis. *Curr. Diabetes Rev.* 5, 8–13.

Croci, D. O., Cerliani, J. P., Dalotto-Moreno, T., Mendez-Huergo, S. P., Mascanfroni, I. D., Dergan-Dylon, S., et al. (2014). Glycosylation-dependent lectin-receptor interactions preserve angiogenesis in anti-VEGF refractory tumors. *Cell* 156, 744–758. doi: 10.1016/j.cell.2014.01.043

Di Stasi, R., Diana, D., De Rosa, L., Fattorusso, R., and D'Andrea, L. D. (2019). Biochemical and conformational characterization of recombinant VEGFR2 domain 7. *Mol. Biotechnol.* 61, 860–872. doi: 10.1007/s12033-019-00211-4

Dias, S., Hattori, K., Zhu, Z., Heissig, B., Choy, M., Lane, W., et al. (2000). Autocrine stimulation of VEGFR-2 activates human leukemic cell growth and migration. *J. Clin. Invest.* 106, 511–521. doi: 10.1172/jci8978

Downward, J. (2004). PI 3-kinase. Akt and cell survival. *Semin. Cell Dev. Biol.* 15, 177–182. doi: 10.1016/j.semcdb.2004.01.002

Drake, C. J., LaRue, A., Ferrara, N., and Little, C. D. (2000). VEGF regulates cell behavior during vasculogenesis. *Dev. Biol.* 224, 178–188. doi: 10.1006/dbio.2000.9744

Dumont, D. J., Jussila, L., Taipale, J., Lymboussaki, A., Mustonen, T., Pajusola, K., et al. (1998). Cardiovascular failure in mouse embryos deficient in VEGF receptor-3. *Science* 282, 946–949. doi: 10.1126/science.282.5390.946

Duval, M., Le Boeuf, F., Huot, J., and Gratton, J. P. (2007). Src-mediated phosphorylation of Hsp90 in response to vascular endothelial growth factor (VEGF) is required for VEGF receptor-2 signaling to endothelial NO synthase. *Mol. Biol. Cell* 18, 4659–4668. doi: 10.1091/mbc.e07-05-0467

Elvert, G., Kappel, A., Heidenreich, R., Englmeier, U., Lanz, S., Acker, T., et al. (2003). Cooperative interaction of hypoxia-inducible factor-2alpha (HIF-2alpha) and Ets-1 in the transcriptional activation of vascular endothelial growth factor receptor-2 (Flk-1). *J. Biol. Chem.* 278, 7520–7530. doi: 10.1074/jbc.m211298200

Fallah, A., Sadeghinia, A., Kahroba, H., Samadi, A., Heidari, H. R., Bradaran, B., et al. (2019). Therapeutic targeting of angiogenesis molecular pathways in angiogenesis-dependent diseases. *Biomed. Pharmacother.* 110, 775–785. doi: 10.1016/j.biopha.2018.12.022

Ferrara, N., and Adamis, A. P. (2016). Ten years of anti-vascular endothelial growth factor therapy. *Nat. Rev. Drug Discov.* 15, 385–403. doi: 10.1038/nrd.2015.17

Ferrara, N., Carver-Moore, K., Chen, H., Dowd, M., Lu, L., O'Shea, K. S., et al. (1996). Heterozygous embryonic lethality induced by targeted inactivation of the VEGF gene. *Nature* 380, 439–442. doi: 10.1038/380439a0

Ferrara, N., and Kerbel, R. S. (2005). Angiogenesis as a therapeutic target. *Nature* 438, 967–974.

Ferrari, G., Cook, B. D., Terushkin, V., Pintucci, G., and Mignatti, P. (2009). Transforming growth factor-beta 1 (TGF-beta1) induces angiogenesis through vascular endothelial growth factor (VEGF)-mediated apoptosis. *J. Cell Physiol.* 219, 449–458. doi: 10.1002/jcp.21706

Fuh, G., Li, B., Crowley, C., Cunningham, B., and Wells, J. A. (1998). Requirements for binding and signaling of the kinase domain receptor for vascular endothelial growth factor. *J. Biol. Chem.* 273, 11197–11204. doi: 10.1074/jbc.273.18.11197

Gliki, G., Abu-Ghazaleh, R., Jezequel, S., Wheeler-Jones, C., and Zachary, I. (2001). Vascular endothelial growth factor-induced prostacyclin production is mediated by a protein kinase C (PKC)-dependent activation of extracellular signal-regulated protein kinases 1 and 2 involving PKC-delta and by mobilization of intracellular Ca2+. *Biochem. J.* 353, 503–512. doi: 10.1042/0264-6021:3530503

Gopinathan, G., Milagre, C., Pearce, O. M., Reynolds, L. E., Hodivala-Dilke, K., Leinster, D. A., et al. (2015). Interleukin-6 stimulates defective angiogenesis. *Cancer Res.* 75, 3098–3107. doi: 10.1158/0008-5472.can-15-1227

Graupera, M., Guillermet-Guibert, J., Foukas, L. C., Phng, L. K., Cain, R. J., Salpekar, A., et al. (2008). Angiogenesis selectively requires the p110alpha isoform of PI3K to control endothelial cell migration. *Nature* 453, 662–666. doi: 10.1038/nature06892

Groppa, E., Brkic, S., Uccelli, A., Wirth, G., Korpisalo-Pirinen, P., Filippova, M., et al. (2018). EphrinB2/EphB4 signaling regulates non-sprouting angiogenesis by VEGF. *EMBO Rep.* 19:e45054.

Han, S., Tan, C., Ding, J., Wang, J., Ma'ayan, A., and Gouon-Evans, V. (2018). Endothelial cells instruct liver specification of embryonic stem cell-derived endoderm through endothelial VEGFR2 signaling and endoderm epigenetic modifications. *Stem. Cell Res.* 30, 163–170. doi: 10.1016/j.scr.2018.06.004

Hanahan, D., and Folkman, J. (1996). Patterns and emerging mechanisms of the angiogenic switch during tumorigenesis. *Cell* 86, 353–364. doi: 10.1016/s0092-8674(00)80108-7

Hoeben, A., Landuyt, B., Highley, M. S., Wildiers, H., Van Oosterom, A. T., and De Bruijn, E. A. (2004). Vascular endothelial growth factor and angiogenesis. *Pharmacol. Rev.* 56, 549–580.

Holmes, K., Roberts, O. L., Thomas, A. M., and Cross, M. J. (2007). Vascular endothelial growth factor receptor-2: structure, function, intracellular signalling and therapeutic inhibition. *Cell Signal.* 19, 2003–2012. doi: 10.1016/j.cellsig.2007.05.013

Holmqvist, K., Cross, M. J., Rolny, C., Hagerkvist, R., Rahimi, N., Matsumoto, T., et al. (2004). The adaptor protein shb binds to tyrosine 1175 in vascular endothelial growth factor (VEGF) receptor-2 and regulates VEGF-dependent cellular migration. *J. Biol. Chem.* 279, 22267–22275. doi: 10.1074/jbc.m312729200

Hooper, A. T., Butler, J. M., Nolan, D. J., Kranz, A., Iida, K., Kobayashi, M., et al. (2009). Engraftment and reconstitution of hematopoiesis is dependent on VEGFR2-mediated regeneration of sinusoidal endothelial cells. *Cell Stem. Cell* 4, 263–274. doi: 10.1016/j.stem.2009.01.006

Ivkovic, S., Yoon, B. S., Popoff, S. N., Safadi, F. F., Libuda, D. E., Stephenson, R. C., et al. (2003). Connective tissue growth factor coordinates chondrogenesis and angiogenesis during skeletal development. *Development* 130, 2779–2791. doi: 10.1242/dev.00505

Iwasaki, A., Kuwahara, M., Yoshinaga, Y., and Shirakusa, T. (2004). Basic fibroblast growth factor (bFGF) and vascular endothelial growth factor (VEGF) levels, as prognostic indicators in NSCLC. *Eur. J. Cardiothorac. Surg.* 25, 443–448. doi: 10.1016/j.ejcts.2003.11.031

Jain, R. K., Duda, D. G., Clark, J. W., and Loeffler, J. S. (2006). Lessons from phase III clinical trials on anti-VEGF therapy for cancer. *Nat. Clin. Pract. Oncol.* 3, 24–40. doi: 10.1038/ncponc0403

Ji, L., Wu, M., and Li, Z. (2018). Rutacecarpine inhibits angiogenesis by targeting the VEGFR2 and VEGFR2-Mediated Akt/mTOR/p70s6k Signaling Pathway. *Molecules* 23:2047. doi: 10.3390/molecules23082047

Kaga, T., Kawano, H., Sakaguchi, M., Nakazawa, T., Taniyama, Y., and Morishita, R. (2012). Hepatocyte growth factor stimulated angiogenesis without inflammation: differential actions between hepatocyte growth factor, vascular endothelial growth factor and basic fibroblast growth factor. *Vascul. Pharmacol.* 57, 3–9. doi: 10.1016/j.vph.2012.02.002

Karaman, S., Leppanen, V. M., and Alitalo, K. (2018). Vascular endothelial growth factor signaling in development and disease. *Development* 145:dev151019. doi: 10.1242/dev.151019

Karar, J., and Maity, A. (2011). PI3K/AKT/mTOR Pathway in Angiogenesis. *Front. Mol. Neurosci.* 4:51. doi: 10.3389/fnmol.2011.00051

Kendall, R. L., Rutledge, R. Z., Mao, X., Tebben, A. J., Hungate, R. W., and Thomas, K. A. (1999). Vascular endothelial growth factor receptor KDR tyrosine kinase activity is increased by autophosphorylation of two activation loop tyrosine residues. *J. Biol. Chem.* 274, 6453–6460. doi: 10.1074/jbc.274.10.6453

Kim, D. Y., Park, J. A., Kim, Y., Noh, M., Park, S., Lie, E., et al. (2019). SALM4 regulates angiogenic functions in endothelial cells through VEGFR2 phosphorylation at Tyr1175. *FASEB J.* 33, 9842–9857. doi: 10.1096/fj.201802516rr

Klagsbrun, M., and Eichmann, A. (2005). A role for axon guidance receptors and ligands in blood vessel development and tumor angiogenesis. *Cytokine Growth Factor. Rev.* 16, 535–548. doi: 10.1016/j.cytogfr.2005.05.002

Koch, S., and Claesson-Welsh, L. (2012). Signal transduction by vascular endothelial growth factor receptors. *Cold Spring Harb. Perspect. Med.* 2:a006502. doi: 10.1101/cshperspect.a006502

Koch, S., Tugues, S., Li, X., Gualandi, L., and Claesson-Welsh, L. (2011). Signal transduction by vascular endothelial growth factor receptors. *Biochem. J.* 437, 169–183. doi: 10.1042/bj20110301

Lamalice, L., Houle, F., and Huot, J. (2006). Phosphorylation of Tyr1214 within VEGFR-2 triggers the recruitment of Nck and activation of Fyn leading to SAPK2/p38 activation and endothelial cell migration in response to VEGF. *J. Biol. Chem.* 281, 34009–34020. doi: 10.1074/jbc.m603928200

Lamalice, L., Houle, F., Jourdan, G., and Huot, J. (2004). Phosphorylation of tyrosine 1214 on VEGFR2 is required for VEGF-induced activation of Cdc42 upstream of SAPK2/p38. *Oncogene* 23, 434–445. doi: 10.1038/sj.onc.1207034

Laramee, M., Chabot, C., Cloutier, M., Stenne, R., Holgado-Madruga, M., Wong, A. J., et al. (2007). The scaffolding adapter Gab1 mediates vascular endothelial growth factor signaling and is required for endothelial cell migration and capillary formation. *J. Biol. Chem.* 282, 7758–7769. doi: 10.1074/jbc.m611327200

Lechertier, T., and Hodivala-Dilke, K. (2012). Focal adhesion kinase and tumour angiogenesis. *J. Pathol.* 226, 404–412. doi: 10.1002/path.3018

LeCouter, J., Zlot, C., Tejada, M., Peale, F., and Ferrara, N. (2004). Bv8 and endocrine gland-derived vascular endothelial growth factor stimulate hematopoiesis and hematopoietic cell mobilization. *Proc. Natl. Acad. Sci. U.S.A.* 101, 16813–16818. doi: 10.1073/pnas.0407697101

Lee, M. Y., Luciano, A. K., Ackah, E., Rodriguez-Vita, J., Bancroft, T. A., Eichmann, A., et al. (2014). Endothelial Akt1 mediates angiogenesis by phosphorylating multiple angiogenic substrates. *Proc. Natl. Acad. Sci. U.S.A.* 111, 12865–12870. doi: 10.1073/pnas.1408472111

Leppanen, V. M., Prota, A. E., Jeltsch, M., Anisimov, A., Kalkkinen, N., Strandin, T., et al. (2010). Structural determinants of growth factor binding and specificity by VEGF receptor 2. *Proc. Natl. Acad. Sci. U.S.A.* 107, 2425–2430. doi: 10.1073/pnas.0914318107

Li, B., Fuh, G., Meng, G., Xin, X., Gerritsen, M. E., Cunningham, B., et al. (2000). Receptor-selective variants of human vascular endothelial growth factor. *Generation and characterization. J. Biol. Chem.* 275, 29823–29828. doi: 10.1074/jbc.m002015200

Li, X., He, S., and Ma, B. (2020). Autophagy and autophagy-related proteins in cancer. *Mol. Cancer* 19:12.

Lindahl, P., Bostrom, H., Karlsson, L., Hellstrom, M., Kalen, M., and Betsholtz, C. (1999). Role of platelet-derived growth factors in angiogenesis and alveogenesis. *Curr. Top. Pathol.* 93, 27–33. doi: 10.1007/978-3-642-58456-5_4

Louveau, A., Smirnov, I., Keyes, T. J., Eccles, J. D., Rouhani, S. J., Peske, J. D., et al. (2015). Structural and functional features of central nervous system lymphatic vessels. *Nature* 523, 337. doi: 10.1038/nature14432

Luck, R., Urban, S., Karakatsani, A., Harde, E., Sambandan, S., Nicholson, L., et al. (2019). VEGF/VEGFR2 signaling regulates hippocampal axon branching during development. *eLife* 8:e49818.

Lugano, R., Ramachandran, M., and Dimberg, A. (2020). Tumor angiogenesis: causes, consequences, challenges and opportunities. *Cell Mol. Life Sci.* 77, 1745–1770. doi: 10.1007/s00018-019-03351-7

Ma, B., Xiang, Y., and An, L. (2011). Structural bases of physiological functions and roles of the vacuolar H(+)-ATPase. *Cell Signal* 23, 1244–1256. doi: 10.1016/j.cellsig.2011.03.003

Ma, Q. L., Ineichen, B. V., Detmar, M., and Proulx, S. T. (2017). Outflow of cerebrospinal fluid is predominantly through lymphatic vessels and is reduced in aged mice. *Nat. Commun.* 8:1434.

Maddaluno, L., Urwyler, C., and Werner, S. (2017). Fibroblast growth factors: key players in regeneration and tissue repair. *Development* 144, 4047–4060. doi: 10.1242/dev.152587

Manni, S., Kisko, K., Schleier, T., Missimer, J., and Ballmer-Hofer, K. (2014a). Functional and structural characterization of the kinase insert and the carboxy

terminal domain in VEGF receptor 2 activation. *FASEB J.* 28, 4914–4923. doi: 10.1096/fj.14-256206

Manni, S., Mineev, K. S., Usmanova, D., Lyukmanova, E. N., Shulepko, M. A., Kirpichnikov, M. P., et al. (2014b). Structural and functional characterization of alternative transmembrane domain conformations in VEGF receptor 2 activation. *Structure* 22, 1077–1089. doi: 10.1016/j.str.2014.05.010

Manzat Saplacan, R. M., Balacescu, L., Gherman, C., Chira, R. I., Craiu, A., Mircea, P. A., et al. (2017). The role of PDGFs and PDGFRs in colorectal cancer. *Mediat. Inflamm.* 2017, 4708076.

Marchand, G. S., Noiseux, N., Tanguay, J. F., and Sirois, M. G. (2002). Blockade of in vivo VEGF-mediated angiogenesis by antisense gene therapy: role of Flk-1 and Flt-1 receptors. *Am. J. Physiol. Heart Circ. Physiol.* 282, H194–H204.

Marrelli, A., Cipriani, P., Liakouli, V., Carubbi, F., Perricone, C., Perricone, R., et al. (2011). Angiogenesis in rheumatoid arthritis: a disease specific process or a common response to chronic inflammation? *Autoimmun. Rev.* 10, 595–598. doi: 10.1016/j.autrev.2011.04.020

Masoumi Moghaddam, S., Amini, A., Morris, D. L., and Pourgholami, M. H. (2012). Significance of vascular endothelial growth factor in growth and peritoneal dissemination of ovarian cancer. *Cancer Metastasis Rev.* 31, 143–162. doi: 10.1007/s10555-011-9337-5

Matsumoto, T., Bohman, S., Dixelius, J., Berge, T., Dimberg, A., Magnusson, P., et al. (2005). VEGF receptor-2 Y951 signaling and a role for the adapter molecule TSAd in tumor angiogenesis. *EMBO J.* 24, 2342–2353. doi: 10.1038/sj.emboj.7600709

McTigue, M., Murray, B. W., Chen, J. H., Deng, Y. L., Solowiej, J., and Kania, R. S. (2012). Molecular conformations, interactions, and properties associated with drug efficiency and clinical performance among VEGFR TK inhibitors. *Proc. Natl. Acad. Sci. U.S.A.* 109, 18281–18289. doi: 10.1073/pnas.1207759109

Moriki, T., Maruyama, H., and Maruyama, I. N. (2001). Activation of preformed EGF receptor dimers by ligand-induced rotation of the transmembrane domain. *J. Mol. Biol.* 311, 1011–1026. doi: 10.1006/jmbi.2001.4923

Nilsson, M., and Heymach, J. V. (2006). Vascular endothelial growth factor (VEGF) pathway. *J. Thorac. Oncol.* 1, 768–770. doi: 10.1097/01243894-200610000-00003

Park, S. A., Jeong, M. S., Ha, K. T., and Jang, S. B. (2018). Structure and function of vascular endothelial growth factor and its receptor system. *BMB Rep.* 51, 73–78. doi: 10.5483/bmbrep.2018.51.2.233

Rafii, S., Meeus, S., Dias, S., Hattori, K., Heissig, B., Shmelkov, S., et al. (2002). Contribution of marrow-derived progenitors to vascular and cardiac regeneration. *Semin. Cell Dev. Biol.* 13, 61–67. doi: 10.1006/scdb.2001.0285

Rahimi, N. (2006). VEGFR-1 and VEGFR-2: two non-identical twins with a unique physiognomy. *Front. Biosci.* 11:818–829. doi: 10.2741/1839

Rajabi, M., and Mousa, S. A. (2017). The role of angiogenesis in cancer treatment. *Biomedicines* 5:34. doi: 10.3390/biomedicines5020034

Rask-Madsen, C., and King, G. L. (2008). Differential regulation of VEGF signaling by PKC-alpha and PKC-epsilon in endothelial cells. *Arterioscler. Thromb. Vasc. Biol.* 28, 919–924. doi: 10.1161/atvbaha.108.162842

Risau, W. (1997). Mechanisms of angiogenesis. *Nature* 386, 671–674.

Ruch, C., Skiniotis, G., Steinmetz, M. O., Walz, T., and Ballmer-Hofer, K. (2007). Structure of a VEGF-VEGF receptor complex determined by electron microscopy. *Nat. Struct. Mol. Biol.* 14, 249–250. doi: 10.1038/nsmb1202

Sarabipour, S., Ballmer-Hofer, K., and Hristova, K. (2016). VEGFR-2 conformational switch in response to ligand binding. *eLife* 5:e13876.

Sase, H., Watabe, T., Kawasaki, K., Miyazono, K., and Miyazawa, K. (2009). VEGFR2-PLCgamma1 axis is essential for endothelial specification of VEGFR2+ vascular progenitor cells. *J. Cell Sci.* 122, 3303–3311. doi: 10.1242/jcs.049908

Shalaby, F., Rossant, J., Yamaguchi, T. P., Gertsenstein, M., Wu, X. F., Breitman, M. L., et al. (1995). Failure of blood-island formation and vasculogenesis in Flk-1-deficient mice. *Nature* 376, 62–66. doi: 10.1038/376062a0

Shen, B. Q., Lee, D. Y., Gerber, H. P., Keyt, B. A., Ferrara, N., and Zioncheck, T. F. (1998). Homologous up-regulation of KDR/Flk-1 receptor expression by vascular endothelial growth factor in vitro. *J. Biol. Chem.* 273, 29979–29985. doi: 10.1074/jbc.273.45.29979

Shibuya, M. (2001). Structure and function of VEGF/VEGF-receptor system involved in angiogenesis. *Cell Struct. Funct.* 26, 25–35. doi: 10.1247/csf.26.25

Shibuya, M. (2011). Vascular endothelial growth factor (VEGF) and its receptor (VEGFR) signaling in angiogenesis: a crucial target for anti- and pro-angiogenic therapies. *Genes Cancer* 2, 1097–1105. doi: 10.1177/1947601911423031

Shibuya, M. (2013). VEGFR and type-V RTK activation and signaling. *Cold Spring Harb. Perspect. Biol.* 5, a009092. doi: 10.1101/cshperspect.a009092

Shinkai, A., Ito, M., Anazawa, H., Yamaguchi, S., Shitara, K., and Shibuya, M. (1998). Mapping of the sites involved in ligand association and dissociation at the extracellular domain of the kinase insert domain-containing receptor for vascular endothelial growth factor. *J. Biol. Chem.* 273, 31283–31288. doi: 10.1074/jbc.273.47.31283

Siveen, K. S., Prabhu, K., Krishnankutty, R., Kuttikrishnan, S., Tsakou, M., Alali, F. Q., et al. (2017). Vascular endothelial growth factor (VEGF) signaling in tumour vascularization: potential and challenges. *Curr. Vasc. Pharmacol.* 15, 339–351.

Smith, R. O., Ninchoji, T., Gordon, E., Andre, H., Dejana, E., Vestweber, D., et al. (2020). Vascular permeability in retinopathy is regulated by VEGFR2 Y949 signaling to VE-cadherin. *eLife* 9:e54056.

Solowiej, J., Bergqvist, S., McTigue, M. A., Marrone, T., Quenzer, T., Cobbs, M., et al. (2009). Characterizing the effects of the juxtamembrane domain on vascular endothelial growth factor receptor-2 enzymatic activity, autophosphorylation, and inhibition by axitinib. *Biochemistry* 48, 7019–7031. doi: 10.1021/bi900522y

Stopeck, A., Sheldon, M., Vahedian, M., Cropp, G., Gosalia, R., and Hannah, A. (2002). Results of a Phase I dose-escalating study of the antiangiogenic agent, SU5416, in patients with advanced malignancies. *Clin. Cancer Res.* 8, 2798–2805.

Takahashi, T., and Shibuya, M. (1997). The 230 kDa mature form of KDR/Flk-1 (VEGF receptor-2) activates the PLC-gamma pathway and partially induces mitotic signals in NIH3T3 fibroblasts. *Oncogene* 14, 2079–2089. doi: 10.1038/sj.onc.1201047

Takahashi, T., Ueno, H., and Shibuya, M. (1999). VEGF activates protein kinase C-dependent, but Ras-independent Raf-MEK-MAP kinase pathway for DNA synthesis in primary endothelial cells. *Oncogene* 18, 2221–2230. doi: 10.1038/sj.onc.1202527

Takahashi, T., Yamaguchi, S., Chida, K., and Shibuya, M. (2001). A single autophosphorylation site on KDR/Flk-1 is essential for VEGF-A-dependent activation of PLC-gamma and DNA synthesis in vascular endothelial cells. *EMBO J.* 20, 2768–2778. doi: 10.1093/emboj/20.11.2768

Vallon, M., Chang, J., Zhang, H., and Kuo, C. J. (2014). Developmental and pathological angiogenesis in the central nervous system. *Cell Mol. Life Sci.* 71, 3489–3506. doi: 10.1007/s00018-014-1625-0

Volz, C., Breid, S., Selenz, C., Zaplatina, A., Golfmann, K., Meder, L., et al. (2020). Inhibition of tumor VEGFR2 induces serine 897 EphA2-dependent tumor cell invasion and metastasis in NSCLC. *Cell Rep.* 31:107568. doi: 10.1016/j.celrep.2020.107568

Walter, M., Lucet, I. S., Patel, O., Broughton, S. E., Bamert, R., Williams, N. K., et al. (2007). The 2.7 A crystal structure of the autoinhibited human c-Fms kinase domain. *J. Mol. Biol.* 367, 839–847.

Wang, L., Ge, H., Peng, L., and Wang, B. (2019). A meta-analysis of the relationship between VEGFR2 polymorphisms and atherosclerotic cardiovascular diseases. *Clin. Cardiol.* 42, 860–865. doi: 10.1002/clc.23233

Warner, A. J., Lopez-Dee, J., Knight, E. L., Feramisco, J. R., and Prigent, S. A. (2000). The Shc-related adaptor protein, Sck, forms a complex with the vascular-endothelial-growth-factor receptor KDR in transfected cells. *Biochem. J.* 347, 501–509. doi: 10.1042/0264-6021:3470501

Weis, S. M., and Cheresh, D. A. (2011). Tumor angiogenesis: molecular pathways and therapeutic targets. *Nat. Med.* 17, 1359–1370. doi: 10.1038/nm.2537

Wong, C., and Jin, Z. G. (2005). Protein kinase C-dependent protein kinase D activation modulates ERK signal pathway and endothelial cell proliferation by vascular endothelial growth factor. *J. Biol. Chem.* 280, 33262–33269. doi: 10.1074/jbc.m503198200

Wybenga-Groot, L. E., Baskin, B., Ong, S. H., Tong, J., Pawson, T., and Sicheri, F. (2001). Structural basis for autoinhibition of the Ephb2 receptor tyrosine kinase by the unphosphorylated juxtamembrane region. *Cell* 106, 745–757. doi: 10.1016/s0092-8674(01)00496-2

Yang, J., Yan, J., and Liu, B. (2018). Targeting VEGF/VEGFR to modulate antitumor immunity. *Front. Immunol.* 9:978.

Yang, Y., Xie, P., Opatowsky, Y., and Schlessinger, J. (2010). Direct contacts between extracellular membrane-proximal domains are required for VEGF receptor activation and cell signaling. *Proc. Natl. Acad. Sci. U.S.A.* 107, 1906–1911. doi: 10.1073/pnas.0914052107

Yehya, A. H. S., Asif, M., Petersen, S. H., Subramaniam, A. V., Kono, K., Majid, A., et al. (2018). Angiogenesis: managing the culprits behind tumorigenesis and metastasis. *Medicina* 54:8. doi: 10.3390/medicina54010008

Yin, Z., Gong, G., Zhu, C., Wang, B., Sun, C., Liu, X., et al. (2020). Angiopoietin-1 protects neurons by inhibiting autophagy after neuronal oxygen-glucose deprivation/recovery injury. *Neuroreport* 31, 825–832.

Zeng, H., Dvorak, H. F., and Mukhopadhyay, D. (2001). Vascular permeability factor (VPF)/vascular endothelial growth factor (VEGF) peceptor-1 down-modulates VPF/VEGF receptor-2-mediated endothelial cell proliferation, but not migration, through phosphatidylinositol 3-kinase-dependent pathways. *J. Biol. Chem.* 276, 26969–26979. doi: 10.1074/jbc.m103213200

Zhang, J., Cao, R., Zhang, Y., Jia, T., Cao, Y., and Wahlberg, E. (2009). Differential roles of PDGFR-alpha and PDGFR-beta in angiogenesis and vessel stability. *FASEB J.* 23, 153–163. doi: 10.1096/fj.08-113860

Zhang, J., and Hughes, S. (2006). Role of the ephrin and Eph receptor tyrosine kinase families in angiogenesis and development of the cardiovascular system. *J. Pathol.* 208, 453–461. doi: 10.1002/path.1937

Zhang, Y., Kontos, C. D., Annex, B. H., and Popel, A. S. (2019). Angiopoietin-tie signaling pathway in endothelial cells: a computational model. *iScience* 20, 497–511. doi: 10.1016/j.isci.2019.10.006

Zhong, M., Li, N., Qiu, X., Ye, Y., Chen, H., Hua, J., et al. (2020). TIPE regulates VEGFR2 expression and promotes angiogenesis in colorectal cancer. *Int. J. Biol. Sci.* 16, 272–283. doi: 10.7150/ijbs.37906

Conflict of Interest: The authors declare that the research was conducted in the absence of any commercial or financial relationships that could be construed as a potential conflict of interest.

Copyright © 2020 Wang, Bove, Simone and Ma. This is an open-access article distributed under the terms of the Creative Commons Attribution License (CC BY). The use, distribution or reproduction in other forums is permitted, provided the original author(s) and the copyright owner(s) are credited and that the original publication in this journal is cited, in accordance with accepted academic practice. No use, distribution or reproduction is permitted which does not comply with these terms.

frontiers in Cell and Developmental Biology

MINI REVIEW
published: 11 December 2020
doi: 10.3389/fcell.2020.624159

Endocytic Adaptors in Cardiovascular Disease

*Kui Cui[1,2], Yunzhou Dong[1,2], Beibei Wang[1,2], Douglas B. Cowan[1,2,3], Siu-Lung Chan[1,2], John Shyy[4] and Hong Chen[1,2]**

[1] Vascular Biology Program, Boston Children's Hospital, Boston, MA, United States, [2] Department of Surgery, Harvard Medical School, Boston, MA, United States, [3] Department of Cardiology, Boston Children's Hospital, Boston, MA, United States, [4] Division of Cardiology, Department of Medicine, University of California, San Diego, San Diego, CA, United States

Endocytosis is the process of actively transporting materials into a cell by membrane engulfment. Traditionally, endocytosis was divided into three forms: phagocytosis (cell eating), pinocytosis (cell drinking), and the more selective receptor-mediated endocytosis (clathrin-mediated endocytosis); however, other important endocytic pathways (e.g., caveolin-dependent endocytosis) contribute to the uptake of extracellular substances. In each, the plasma membrane changes shape to allow the ingestion and internalization of materials, resulting in the formation of an intracellular vesicle. While receptor-mediated endocytosis remains the best understood pathway, mammalian cells utilize each form of endocytosis to respond to their environment. Receptor-mediated endocytosis permits the internalization of cell surface receptors and their ligands through a complex membrane invagination process that is facilitated by clathrin and adaptor proteins. Internalized vesicles containing these receptor-ligand cargoes fuse with early endosomes, which can then be recycled back to the plasma membrane, delivered to other cellular compartments, or destined for degradation by fusing with lysosomes. These intracellular fates are largely determined by the interaction of specific cargoes with adaptor proteins, such as the epsins, disabled-homolog 2 (Dab2), the stonin proteins, epidermal growth factor receptor substrate 15, and adaptor protein 2 (AP-2). In this review, we focus on the role of epsins and Dab2 in controlling these sorting processes in the context of cardiovascular disease. In particular, we will focus on the function of epsins and Dab2 in inflammation, cholesterol metabolism, and their fundamental contribution to atherogenicity.

Keywords: epsin, disabled-homolog 2, endocytic adaptor proteins, atherosclerosis, diabetes, inflammation, receptor-mediated endocytosis, clathrin

OPEN ACCESS

Edited by:
Xiaofeng Yang,
Temple University, United States

Reviewed by:
Jun Yu,
Temple University, United States
Tohru Fukai,
Augusta University, United States

Correspondence:
Hong Chen
hong.chen@childrens.harvard.edu

Specialty section:
This article was submitted to Signaling, a section of the journal Frontiers in Cell and Developmental Biology

Received: *30 October 2020*
Accepted: *23 November 2020*
Published: *11 December 2020*

Citation:
Cui K, Dong Y, Wang B, Cowan DB, Chan S-L, Shyy J and Chen H (2020) Endocytic Adaptors in Cardiovascular Disease. Front. Cell Dev. Biol. 8:624159. doi: 10.3389/fcell.2020.624159

Endocytosis is the method that cells utilize to uptake material from outside of the membrane to inside of the cells. There are three major forms of endocytosis, phagocytosis, pinocytosis, and clathrin-mediated endocytosis, each involving its own specific cell machinery.

CLATHRIN-MEDIATED ENDOCYTOSIS

Receptor-mediated endocytosis (i.e., clathrin-mediated endocytosis) is a process by which cells internalize metabolites, hormones, and proteins to allow them to respond to their local environment. This form of endocytosis typically consists of the following steps: (1) extracellular ligand binding to cell surface receptors, (2) the formation of a clathrin cage around the

receptor-ligand complex resulting from the interaction with a multitude of molecules and proteins, such as phosphatidylinositol 4,5-bisphosphate (PIP_2), adaptor protein 2 (AP-2), clathrin-coat assembly protein 180 (AP180), and epsin proteins, (3) lipid bilayer invagination with the aid of membrane curvature promoting proteins, such as members of the epsin family, (4) vesicle formation and release from the plasma membrane, and (5) sorting of the vesicle and receptor-ligand cargo within the cell (**Figure 1**). Each of these steps requires a variety of endocytic adaptor proteins that include the epsins, epidermal growth factor receptor substrate 15 (Eps15), disabled homolog 2 (Dab2), AP-2, and PIP_2 (Eberhard et al., 1990; Chen et al., 1998; Pearse et al., 2000; Ford et al., 2002; Polo et al., 2002; Maurer and Cooper, 2005; Bhattacharjee et al., 2020). In this review we focus on the epsin and Dab2 proteins, which play crucial roles in clathrin-mediated endocytosis and are implicated as important modulators of cardiovascular diseases.

PHAGOCYTOSIS

Phagocytosis, also called "cell eating," is used by the cells, such as neutrophils, macrophages and other white blood cells, to engulf debris, bacteria, or other solid objects through the produced pseudopodia (Jaggi et al., 2020; Joffe et al., 2020; Reine et al., 2020; Smirnov et al., 2020). The invagination of cell membrane produces phagosomes, which later fuse with lysosomes containing enzymes. Materials in the phagosome are broken down into simpler substance by these enzymes and degraded.

PINOCYTOSIS

Pinocytosis is called "cell drinking" that cells, such as hepatocytes, kidney cells and epithelial cells, engulf extracellular fluid, including various solutes, such as sugars, ions, amino acids, and proteins. The cell membrane folds inward to form invagination, which takes up the extracellular fluid and releases it inside the cells. Kidney cell can utilize pinocytosis to separate nutrients and fluid from the urine (Bode et al., 1975). Capillary epithelial cells can use pinocytosis to engulf the liquid part of blood at its surface (Orlov, 1988).

EPSINS

Epsins are a family of adaptor proteins associated with clathrin-coated pits that support lipid bilayer curvature and coordinate the recruitment of ubiquitinated cargo proteins (Ko et al., 2010). The first member of this family to be isolated was epsin 1, which was identified through its interaction with the clathrin-associated protein Eps15 (Chen et al., 1998). Subsequent investigations established that there are three classic members of this family (epsins 1, 2, and 3) in addition to a non-classic isoform named either epsin 4 or epsin R, which is now more commonly referred to as clathrin interactor 1 (CLINT1). In mammals, epsins 1 and 2 are ubiquitously expressed and particularly enriched in the brain (Rosenthal et al., 1999). While epsins 1 and 2 are functionally redundant, epsin 3 is predominantly expressed in the gastric parietal cells of the stomach (Spradling et al., 2001).

Epsins 1, 2, and 3 share a structure termed the Epsin N-terminal Homology (ENTH) domain, which interacts with PIP_2 at the plasma membrane (Chen et al., 1999; De Camilli et al., 2002; Chen and De Camilli, 2005). Ubiquitin-interacting motifs (UIMs) that recognize and recruit ubiquitinated surface receptors to clathrin-coated pits for internalization are situated next to the ENTH domain (Oldham et al., 2002; Sakamoto et al., 2004; Chen and De Camilli, 2005). An adjacent region, characterized by DPW (Asp-Pro-Trp)-rich amino acid motifs flanked by a clathrin-binding domain, is responsible for binding to AP-2

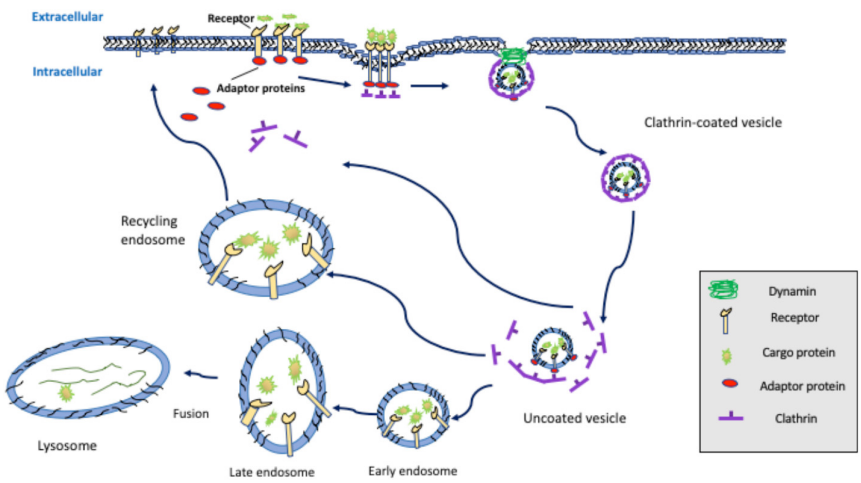

FIGURE 1 | Clathrin-mediated endocytosis. Extracellular ligands binding to cell surface receptors triggers the recruitment of the adaptor proteins, such as AP-2, Dab2, and/or members of the epsin family, which induces plasma membrane invagination and formation of clathrin-coated pits that are subsequently released via dynamin-mediated scission. Clathrin-coated vesicles undergo de-coating and sorting through fusion with early endosomes, late endosomes, and ultimately, lysosomes, leading to receptor degradation, or sorting back to the cell surface by recycling endosomes.

and clathrin, respectively (**Figure 2**). In the COOH-terminal region, NPF (Asn-Pro-Phe) motifs function to bind Eps15-homology (EH) domain-containing proteins, such as Eps15 and the BTB/POZ domain-containing protein POB1 (Salcini et al., 1999; De Camilli et al., 2002).

DISABLED HOMOLOG 2 (Dab2)

Dab2 is another clathrin- and cargo-binding endocytic adaptor protein that was first isolated as a mitogen-responsive phosphoprotein called p96 (Xu et al., 1995). Although the messenger RNA transcript encoding this protein was initially named *DOC2* (for Differentially expressed in Ovarian Cancer) because it was differentially expressed in ovarian cancer, the protein is now referred to as Disabled homolog-2 or Dab2 as it is transcribed from an ortholog of the *Drosophila Dab* gene (Gertler et al., 1989). At the same time, a neuronal-specific isoform named Dab1 represents an additional protein produced from a mammalian ortholog of this *Drosophila* gene (Howell et al., 1997). Interestingly, several spliced isoforms of Dab2 have been identified, including p96 and p67 (Xu et al., 1995; Sheng et al., 2000, 2001) and mammalian Dab2 is expressed in a wide variety of cells and tissues including macrophages, kidney, white adipose tissues, the placenta, and the adrenal gland (Xu et al., 1995; Fazili et al., 1999; Moore R. et al., 2013; Hocevar, 2019). Aside from Dab1, Dab2 shares sequence similarity to other endocytic adaptors, such as Numb, Numbl, and Arh.

Dab2, Numb, Numblike, and Arh are similar in structure and share an N-terminal phosphotyrosine-binding domain (PTB) or phosphotyrosine-interacting domain (PID) for cargo recognition (Bork and Margolis, 1995; Howell et al., 1999). The PID/PTB domain of Dab2 can interact with transmembrane proteins, such as the LDL and EGF receptors as well as integrins through a NPXY (Asn-Pro-x-Tyr) motif (Morris and Cooper, 2001; Tao et al., 2016a). The interaction between Dab2 and the endocytic proteins clathrin and α-adaptin is mediated by the middle and C-terminal portions of this motif (Traub, 2003). The C-terminus also binds to the motor protein myosin IV (Inoue et al., 2002; Morris et al., 2002a), which facilitates its role in clathrin-mediated endocytosis and trafficking (**Figure 3**).

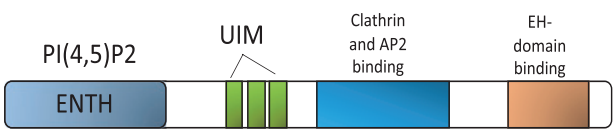

FIGURE 2 | Epsin domain structure. Epsin interacting regions for binding partners. PIP_2, phosphatidylinositol-4,5-bisphosphate; ENTH, epsin N-terminal homology; UIM, Ubiquitin-interacting motifs; AP-2, Adaptor protein 2; EH, Eps 15 homology domain.

EPSIN-DEFICIENT ANIMAL MODELS

Epsins 1 and 2 are expressed in most vertebrates, contribute to clathrin-mediated endocytosis, and are located near the plasma membrane. Given their ubiquitous expression, their function is strictly cell-type and tissue dependent. Epsins 1 and 2 are widely expressed (Rosenthal et al., 1999), whereas epsin 3 is predominantly expressed in the gastric parietal cells of the stomach (Spradling et al., 2001). As discussed above, epsins are multi-functional proteins that act as endocytic adapters and sort ubiquitinated cargoes. Several studies show that epsins sort ubiquitinated proteins, such as vascular endothelial growth factor receptor-2 (VEGFR2) (Pasula et al., 2012; Dong et al., 2015, 2017), the linear ubiquitin chain assembly complex (LUBAC) (Song et al., 2020), the receptor tyrosine-protein kinase ErbB3 (Szymanska et al., 2016), Notch ligands (Tian et al., 2004; Wang and Struhl, 2004; Chen et al., 2009; Xie et al., 2012; Langridge and Struhl, 2017), and low-density lipoprotein receptor-related protein 1 (LRP1) (Brophy et al., 2019), in addition to playing a role in establishing cell polarity (Li L.et al., 2016). Because epsins are involved in the Notch signaling pathway, which is essential for normal embryonic development, the deficiency of both epsins 1 and 2 results in embryonic lethality. As a result, the study of these proteins in adulthood has relied on inducible knock-out models (Chen and De Camilli, 2005; Chen et al., 2009).

Inducible deficiency of epsins 1 and 2 in endothelial cells in a tumor angiogenesis mouse model revealed the regulatory role of these proteins in vascular development (Song et al.,

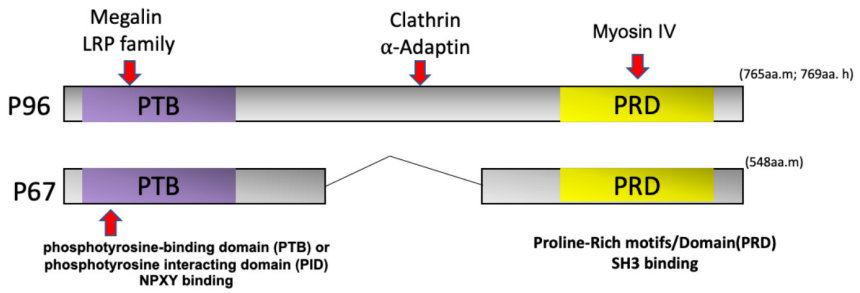

FIGURE 3 | Dab2 domain structure and isoforms. Dab2 has two splice variants called p96 and p67. The NH2-terminal phosphotyrosine-binding domain (PTB) or phosphotyrosine-interacting domain (PID) interacts with receptors, such as the LDL receptor or LDL receptor-related protein (LRP) via the NPXY (Asn-Pro-x-Tyr) motif. The middle region of p96 interacts with endocytic proteins clathrin and α-Adaptin. The COOH-terminal of Dab2 contains a Proline-Rich Domain (PRD) that can bind to Src homology 3 (SH3)-containing proteins. The Dab2 COOH-terminus can also bind myosin VI to mediate endocytic trafficking.

2017; Dong et al., 2018). More recent studies showed that epsins are involved in regulating Notch signaling to modulate murine embryonic stem cells exit from pluripotency (Cardano et al., 2019). In addition, epsin-mediated Notch signaling has also been reported in another study where the lethality of epsins 1 and 2 double knockout mice die at embryonic day 9.5–10 (E9.5-10), owing to defects in organogenesis, which included failure of blood vessel and heart tube formation and insufficient yolk sac circulation (Chen et al., 2009). Using cell-type and tissue-specific epsin mutant mouse models, the regulatory role of these proteins in development (Chen et al., 2009), tumor angiogenesis (Pasula et al., 2012; Dong et al., 2015), developmental and physiological angiogenesis (Tessneer et al., 2014; Rahman et al., 2016), lymph angiogenesis (Liu et al., 2014; Wu et al., 2018), atherosclerosis (Brophy et al., 2019; Dong et al., 2020), diabetes (Wu et al., 2018), and cancer progression (Pasula et al., 2012; Tessneer et al., 2013a,b; Chang et al., 2015; Dong et al., 2015; Song et al., 2017) have become better understood.

EPSINS IN CARDIOVASCULAR DISEASE

Atherosclerosis, a leading cause of morbidity and mortality in cardiovascular diseases, is a multi-factorial and chronic inflammatory disease (Lusis, 2000; Falk, 2006; Yin et al., 2013; Fang et al., 2014). It is characterized by low-density lipoprotein (LDL) cholesterol deposition and macrophage accumulation in the arterial wall (Charo and Taubman, 2004; Zhang et al., 2012; Hilgendorf et al., 2015; Bobryshev et al., 2016). Excessive oxidized LDL (oxLDL) and cholesterol esterification result in the formation of foam cells, which subsequently generate atheromatous plaques (Moore K. J. et al., 2013; Yu et al., 2013; Chistiakov et al., 2016). These plaques can rupture and hemorrhage, which leads to severe conditions including myocardial infarction, peripheral artery disease, stroke, and kidney dysfunction (Swirski and Nahrendorf, 2013). Further, this complex process involves the interaction of pathological mediators (e.g., oxLDL) with arterial wall constituents, such as endothelial cells (Mai et al., 2013; Yin et al., 2015; Li X. et al., 2016; Xi et al., 2016; Li et al., 2017, 2018a; Shao et al., 2020), monocyte-derived macrophages, immune cells (including T cells) (Pastrana et al., 2012; Li et al., 2018b), and vascular smooth muscle cells (Galkina and Ley, 2009). Consequently, atherosclerosis has been defined as a metabolic and immune disease that involves multiple cell types (Paoletti et al., 2006; Galkina and Ley, 2009; Sun et al., 2020; Zhong et al., 2020), as well as the liver (Liu and Czaja, 2013; Fargion et al., 2014; Palmal et al., 2014).

Numerous studies indicate that macrophages are crucial for the development of atherosclerotic lesions because they participate in all stages of plaque formation and progression (Yang et al., 2014; Bories and Leitinger, 2017; Groh et al., 2018). In the early stages, circulating monocytes migrate from the blood stream to the arterial intima. Locally polarized macrophage subsets engulf accumulated oxidized lipids, and become foam cells, which accumulate at the lesion sites and, eventually, cause the failure of plaque resolution. Therefore, monocytes/macrophages are central to lesion formation and the progression of atherosclerosis (Shapiro and Fazio, 2017).

Genome wide-association studies have reported several genes related to cancer biology that are also associated with cardiovascular diseases—suggesting the involvement of epsins in both cancer and atherosclerosis (Holdt and Teupser, 2012). In addition, it has been reported that epsin 1 binds to LDLR to facilitate LDLR internalization through an FxNPxY-independent mechanism in *Caenorhabditis elegans* (Kang et al., 2013). Studies from our laboratory show that epsins are upregulated in lesional macrophages. Using engineered myeloid cell-specific epsin 1 and 2 knock-out mice (LysM-DKO) on an ApoE$^{-/-}$ background and fed a "Western Diet," these mice display a dramatic reduction in atherosclerotic plaque size and lesion number as well as decreased immune cell infiltration in the aorta and reduced necrotic core formation with an increase in smooth muscle cell number in the aortic root (Brophy et al., 2019). *In vitro* studies demonstrate the absence of epsins inhibited foam cell formation and reduced M1 phenotype macrophages, but increased M2 phenotype macrophages. We also observed a pro-atherogeneic role for myeloid-specific epsins that was resulted from a downregulation of LRP-1. LRP-1 is known to have anti-atherosclerotic and anti-inflammatory functions, which is mediated by the interaction of the epsin UIM domain with LRP-1. With the treatment of oxLDL, the ubiquitination of LRP-1 was markedly increased, resulting in the enhanced interaction between LRP-1 and epsins 1/2. Genetic reduction of LRP-1 in ApoE$^{-/-}$/LysM-DKO-LRP1$^{fl/+}$ mice restored atherosclerosis and confirmed the interaction between LRP1 and epsins in atherosclerosis (Brophy et al., 2019). These findings suggest that myeloid-epsin-mediated LRP-1 downregulation plays a vital role in promoting atherogenesis.

In another study, we found that the inducible deletion of epsins 1 and 2 in endothelial cells significantly attenuated atherosclerosis (Dong et al., 2020). Using cultured aortic endothelial cells from double knock-out (DKO) mice treated with atherogenic cholesterol, we discovered that epsins interact with ubiquitinated inositol 1,4,5-trisphosphate receptor type 1 (IP3R1) to promote the degradation of this calcium release channel (Dong et al., 2020). Furthermore, we confirmed that the binding of epsin to IP3R1 in atherogenic conditions occurred through the UIM and N-terminal suppressor domain (SD) of these proteins, respectively. These findings established the role of epsins in endothelial cell dysfunction and the initiation and progression of atherosclerosis.

Dab2-DEFICIENT ANIMAL MODELS

Dab2 is a multi-functional adaptor protein and plays roles in many cell functions, including endocytosis (Morris and Cooper, 2001), cell signaling (Drahos et al., 2009; Schutte-Nutgen et al., 2019), lipid uptake (Morris and Cooper, 2001), cholesterol homeostasis (Eden et al., 2007), and cell adhesion (Rosenbauer et al., 2002). Dab2 is also important in embryonic development as deletion of the *Dab2* gene in mice leads to early embryonic lethality prior to gastrulation (Morris

et al., 2002b). Interestingly, conditional deletion of Dab2 in embryonic stem cells did not affect the development of embryos, but showed reduced clathrin-coated pits, decreased transport mediated by the lipoprotein receptor in kidney proximal tubule, and increased serum cholesterol levels, which suggest a regulatory role for Dab2 in embryonic development and lipoprotein receptor trafficking (Morris et al., 2002b). In addition, the endocytosis of megalin (also known as low density lipoprotein-related protein 2) is mediated by Dab2 by binding to NPXY motifs on the receptor (Maurer and Cooper, 2005). Studies showing the rescue of embryonic viability also indicates that Dab2-mediated endocytosis is critical for embryonic development (Maurer and Cooper, 2005).

Dab2 IN INFLAMMATION AND CHOLESTEROL METABOLISM

Recent studies from Norbert Leitinger's laboratory found that the expression of Dab2 was increased in M2 macrophages and suppressed in M1 macrophages in both mice and humans (Adamson et al., 2016). Deletion of Dab2 results in a pro-inflammatory M1 phenotype, which suggests that Dab2 regulates macrophage phenotypic polarization and inflammatory signaling by inhibiting the NF-κB pathway by binding to TNF receptor associated factor (TRAF) 6 (Adamson et al., 2016). In other studies, analysis of Dab2-deficient bone marrow revealed increased systemic inflammation and cytokine expression, which led to liver injury; however, the effect of Dab2 deletion in atherosclerosis has yet to be determined (Adamson et al., 2018). Moreover, whether the decreased serum lipids as a result of liver injury could counter the elevated inflammation resulted in pro-inflammatory macrophage accumulation in atherogenesis and whether atherosclerotic lesion formation is impacted because of a myeloid deficiency in Dab2 are poorly understood. Consistent with its role in regulating inflammation, Dab2 was also markedly reduced by toll like receptor (TLR) ligands in a TRIF- and MyD88-dependent manner, resulting in a switch in mucosal dendritic cells from a tolerogenic to a pro-inflammatory phenotype (Figliuolo da Paz et al., 2019). Nevertheless, whether Dab2-mediated modulation of aforesaid inflammation by regulating endocytosis of the plasma membrane cargo is unclear.

On the contrary, Dab2 has been shown to potentially regulate LDL receptor (LDLR) endocytosis, and consequently, LDL uptake and cholesterol metabolism as the PTB/PID domain of Dab2 can bind to the NPXY (Asn-Pro-X-Tyr) motif expressed on LDLR. Lipid uptake is mediated by the LDLR through clathrin-dependent endocytosis and the adaptor proteins Arh and Dab2 can specifically interact with the NPXF motif of LDLR and recruit clathrin/AP-2 to facilitate internalization (Tao et al., 2016b). The latter studies suggest that the deletion of both Dab2 and Arh in liver endothelial cells dramatically elevates serum LDL and cholesterol levels, which is different from a single knockout of either Dab2 or Arh. The authors conclude that Arh and Dab2 work together to regulate hepatic cholesterol synthesis through LDLR endocytosis (Tao et al., 2016b).

It is notable that despite the multiple physiological roles of endocytic adaptor proteins in governing cell signaling, adhesion, nutrient uptake, and synaptic transmission, malfunction of these proteins cause a suite of endocytic defects that perturb cholesterol homeostasis and inaugurate cardiovascular disease, and produce developmental defects, cancer and neurological disorders (**Figure 4**). There are numerous molecular mechanisms that remain to be uncovered to determine how these adaptor proteins function. In particular, more work is required to understand how epsins and Dab2 act in a cell context-dependent manner as well as elucidate their interacting partners, post-translational modifications, and their role in the development and progression of diseases.

TARGETING EPSINS AND Dab2 TO TREAT ATHEROSCLEROSIS

Statins remain the most commonly used drugs to treat or prevent atherosclerosis by lowering cholesterol levels in the circulation (Endo et al., 1976; Goldstein and Brown, 2015); although, anti-hypertensive drugs, such as anti-platelet medications, beta blockers, angiotensin-converting enzyme (ACE) inhibitors, and calcium channel blockers are also used to reduce the symptoms of this disease. Unfortunately, due to their potential side effects in multiple organ systems combined with an increased risk for developing diabetes and cancer (Ramkumar et al., 2016), the safety of wide-spread use of statins remains questionable. Consequently, the identification of new therapeutic targets is warranted.

Promising alternatives to reduce atherosclerosis include targeted therapies for the renin-angiotensin system (RAS) and administration of CD47 blocking antibodies to target macrophages (Lu et al., 2008; Kojima et al., 2016). Targeted

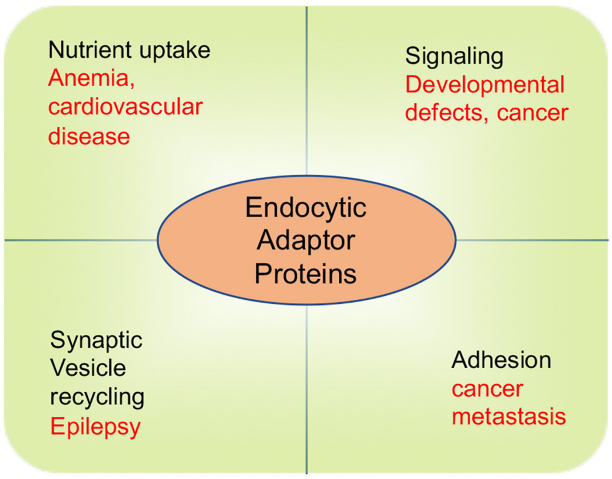

FIGURE 4 | The role of endocytic adaptor proteins in physiological and pathophysiological processes. Physiological processes are depicted by words in black color. Pathological consequences of endocytic defects are depicted by words in red color.

therapy of PCSK9 in the liver to manage cholesterol levels is another recent alternative (Rader and Daugherty, 2008; Goldstein and Brown, 2015) and Amgen has recently been marketing an antibody to this protein. In addition, anti-inflammatory therapies are being developed to combat atherosclerosis (Rader and Daugherty, 2008; Tabas and Glass, 2013; Li et al., 2019, 2020). In particular, the CANTOS trial clearly suggests that reducing inflammation in patients with prior cardiovascular events using anti-Interleukin-1β antibodies (i.e., Canakinumab) significantly diminishes the risk of recurrent myocardial infarction (Ridker et al., 2017). At the same time, selectively targeting the activated aortic endothelium has proven more difficult despite its obvious potential for treating atherosclerosis.

In our studies, we have shown that endothelial and macrophage epsins are possible therapeutic targets for the treatment of atherosclerosis (Brophy et al., 2019; Dong et al., 2020). Based on the molecular mechanism that we have uncovered, it may be possible to treat this disease by: (1) targeting atheroma-specific epsins using lipid nanoparticle-based delivery of siRNAs to mitigate inflammatory signaling, (2) blocking epsin binding of IP3R1 or LRP1 using UIM-containing peptides in both the endothelium and macrophages, and (3) using an adeno-associated virus gene therapy approach to downregulate epsin expression in lesions.

While several studies show that Dab2 plays an important role in cellular trafficking of LDLR, the relationship between Dab2 and the development of atherosclerosis remains somewhat obscure. A recent study shows that a Dab2 gene variant is associated with increased coronary artery disease risk (Wang et al., 2020). In another study, quercetin attenuated the progression of atherosclerosis by regulating dendritic cell maturation by upregulating Dab2 expression (Lin et al., 2017). Giving the important role of epsins and Dab2 in endocytosis and the regulation of LDLR and LRP trafficking, fully uncovering the regulatory roles of these proteins in different cells and tissues may result in the development of new anti-atherosclerotic therapeutics.

PERSPECTIVE

Because of the complexity of atherosclerosis, there have been few effective drugs developed to treat this disease despite decades-long relentless efforts (Weber and Noels, 2011; Libby, 2012; Ridker et al., 2017). As epsins are ubiquitin-binding proteins that play important roles in the vascular system as well as the initiation and progression of atherosclerosis, these endocytic adaptors could represent an important therapeutic target for this disease. Using genetically modified mice, we have demonstrated that the loss of epsins in the aortic endothelium or macrophages inhibits atherosclerosis (Brophy et al., 2019; Dong et al., 2020). Mechanistically, epsins bind IP3R1 in the endothelium and LRP-1 in macrophages via their UIM domain to potentiate atherosclerosis. Targeting epsins in atherosclerotic plaques using liposome nanoparticles containing epsins siRNAs, UIM-containing peptides as competitive inhibitors, or by using a gene therapy approach, may open new avenues to treat atherosclerosis. At the same time, a detailed knowledge of Dab2-receptor interactions in atherosclerosis may identify additional, therapeutically relevant avenues of investigation. In addition, as other endocytic adaptor proteins, such as Numb and Arh, have been implicated in regulating the uptake of cholesterol or cholesterol synthesis (Tao et al., 2016a; Azarnia Tehran et al., 2019). Modulating levels of these endocytic adaptor proteins in cell-restrictive manner would offer equally inspiring opportunity to intervene diseased conditions including dyslipidemia. Thus, developing novel class of drugs that potentially target these endocytic adaptors should offer great promise to circumvent the challenge for the management of dyslipidemia and to reduce cardiovascular diseases.

AUTHOR CONTRIBUTIONS

KC, YD, BW, DC, S-LC, JS, and HC wrote the manuscript. KC and HC created the figures. All authors contributed to the article and approved the submitted version.

FUNDING

This work was supported in part by the NIH Grants R01HL093242, R01HL130845, R01HL133216, R01HL137229, R01HL141858, R01HL146134, and R01HL141853 to HC, as well as an Established Investigator Award and a Transformational Project Award from American Heart Association to HC.

REFERENCES

Adamson, S. E., Griffiths, R., Moravec, R., Senthivinayagam, S., Montgomery, G., Chen, W., et al. (2016). Disabled homolog 2 controls macrophage phenotypic polarization and adipose tissue inflammation. *J. Clin. Invest.* 126, 1311–1322. doi: 10.1172/JCI79590

Adamson, S. E., Polanowska-Grabowska, R., Marqueen, K., Griffiths, R., Angdisen, J., Breevoort, S. R., et al. (2018). Deficiency of Dab2 (Disabled Homolog 2) in myeloid cells exacerbates inflammation in liver and atherosclerotic plaques in LDLR (low-density lipoprotein receptor)-null mice-brief report. *Arterioscler Thromb. Vasc. Biol.* 38, 1020–1029. doi: 10.1161/ATVBAHA.117.310467

Azarnia Tehran, D., Lopez-Hernandez, T., and Maritzen, T. (2019). Endocytic adaptor proteins in health and disease: lessons from model organisms and human mutations. *Cells* 8:1345. doi: 10.3390/cells8111345

Bhattacharjee, S., Lee, Y., Zhu, B., Wu, H., Chen, Y., and Chen, H. (2020). Epsins in vascular development, function and disease. *Cell Mol. Life Sci.* doi: 10.1007/s00018-020-03642-4 [Epub ahead of print],

Bobryshev, Y. V., Ivanova, E. A., Chistiakov, D. A., Nikiforov, N. G., and Orekhov, A. N. (2016). Macrophages and their role in atherosclerosis: pathophysiology and transcriptome analysis. *Biomed. Res. Int.* 2016:9582430. doi: 10.1155/2016/9582430

Bode, F., Baumann, K., and Kinne, R. (1975). Biochemical aspects of pinocytosis in kidney. *Contrib. Nephrol.* 1, 21–27. doi: 10.1159/000398225

Bories, G. F. P., and Leitinger, N. (2017). Macrophage metabolism in atherosclerosis. *FEBS Lett.* 591, 3042–3060. doi: 10.1002/1873-3468.12786

Bork, P., and Margolis, B. (1995). A phosphotyrosine interaction domain. *Cell* 80, 693–694. doi: 10.1016/0092-8674(95)90347-x

Brophy, M. L., Dong, Y., Tao, H., Yancey, P. G., Song, K., Zhang, K., et al. (2019). Myeloid-specific deletion of epsins 1 and 2 reduces atherosclerosis by preventing LRP-1 downregulation. *Circ. Res.* 124, e6–e19. doi: 10.1161/CIRCRESAHA.118.313028

Cardano, M., Zasso, J., Ruggiero, L., Di Giacomo, G., Marcatili, M., Cremona, O., et al. (2019). Epsins regulate mouse embryonic stem cell exit from pluripotency and neural commitment by controlling notch activation. *Stem Cells Int.* 2019:4084351. doi: 10.1155/2019/4084351

Chang, B., Tessneer, K. L., McManus, J., Liu, X., Hahn, S., Pasula, S., et al. (2015). Epsin is required for Dishevelled stability and Wnt signalling activation in colon cancer development. *Nat. Commun.* 6:6380. doi: 10.1038/ncomms7380

Charo, I. F., and Taubman, M. B. (2004). Chemokines in the pathogenesis of vascular disease. *Circ. Res.* 95, 858–866. doi: 10.1161/01.RES.0000146672.10582.17

Chen, H., and De Camilli, P. (2005). The association of epsin with ubiquitinated cargo along the endocytic pathway is negatively regulated by its interaction with clathrin. *Proc. Natl. Acad. Sci. U.S.A.* 102, 2766–2771. doi: 10.1073/pnas.0409719102

Chen, H., Fre, S., Slepnev, V. I., Capua, M. R., Takei, K., Butler, M. H., et al. (1998). Epsin is an EH-domain-binding protein implicated in clathrin-mediated endocytosis. *Nature* 394, 793–797. doi: 10.1038/29555

Chen, H., Ko, G., Zatti, A., Di Giacomo, G., Liu, L., Raiteri, E., et al. (2009). Embryonic arrest at midgestation and disruption of Notch signaling produced by the absence of both epsin 1 and epsin 2 in mice. *Proc. Natl. Acad. Sci. U.S.A.* 106, 13838–13843. doi: 10.1073/pnas.0907008106

Chen, H., Slepnev, V. I., Di Fiore, P. P., and De Camilli, P. (1999). The interaction of epsin and Eps15 with the clathrin adaptor AP-2 is inhibited by mitotic phosphorylation and enhanced by stimulation-dependent dephosphorylation in nerve terminals. *J. Biol. Chem.* 274, 3257–3260. doi: 10.1074/jbc.274.6.3257

Chistiakov, D. A., Bobryshev, Y. V., and Orekhov, A. N. (2016). Macrophage-mediated cholesterol handling in atherosclerosis. *J. Cell Mol. Med.* 20, 17–28. doi: 10.1111/jcmm.12689

De Camilli, P., Chen, H., Hyman, J., Panepucci, E., Bateman, A., and Brunger, A. T. (2002). The ENTH domain. *FEBS Lett.* 513, 11–18. doi: 10.1016/s0014-5793(01)03306-3

Dong, J., Saunders, D., Silasi-Mansat, R., Yu, L., Zhu, H., Lupu, F., et al. (2018). Therapeutic efficacy of a synthetic epsin mimetic peptide in glioma tumor model: uncovering multiple mechanisms beyond the VEGF-associated tumor angiogenesis. *J. Neurooncol.* 138, 17–27. doi: 10.1007/s11060-018-2766-z

Dong, Y., Lee, Y., Cui, K., He, M., Wang, B., Bhattacharjee, S., et al. (2020). Epsin-mediated degradation of IP3R1 fuels atherosclerosis. *Nat. Commun.* 11:3984. doi: 10.1038/s41467-020-17848-4

Dong, Y., Wu, H., Dong, J., Song, K., Rahman, H. A., Towner, R., et al. (2017). Mimetic peptide of ubiquitin-interacting motif of epsin as a cancer therapeutic-perspective in brain tumor therapy through regulating VEGFR2 signaling. *Vessel Plus* 1, 3–11. doi: 10.20517/2574-1209.2016.01

Dong, Y., Wu, H., Rahman, H. N., Liu, Y., Pasula, S., Tessneer, K. L., et al. (2015). Motif mimetic of epsin perturbs tumor growth and metastasis. *J. Clin. Invest.* 125, 4349–4364. doi: 10.1172/JCI80349

Drahos, K. E., Welsh, J. D., Finkielstein, C. V., and Capelluto, D. G. (2009). Sulfatides partition disabled-2 in response to platelet activation. *PLoS One* 4:e8007. doi: 10.1371/journal.pone.0008007

Eberhard, D. A., Cooper, C. L., Low, M. G., and Holz, R. W. (1990). Evidence that the inositol phospholipids are necessary for exocytosis. Loss of inositol phospholipids and inhibition of secretion in permeabilized cells caused by a bacterial phospholipase C and removal of ATP. *Biochem. J.* 268, 15–25. doi: 10.1042/bj2680015

Eden, E. R., Sun, X. M., Patel, D. D., and Soutar, A. K. (2007). Adaptor protein disabled-2 modulates low density lipoprotein receptor synthesis in fibroblasts from patients with autosomal recessive hypercholesterolaemia. *Hum. Mol. Genet.* 16, 2751–2759. doi: 10.1093/hmg/ddm232

Endo, A., Kuroda, M., and Tanzawa, K. (1976). Competitive inhibition of 3-hydroxy-3-methylglutaryl coenzyme A reductase by ML-236A and ML-236B fungal metabolites, having hypocholesterolemic activity. *FEBS Lett.* 72, 323–326. doi: 10.1016/0014-5793(76)80996-9

Falk, E. (2006). Pathogenesis of atherosclerosis. *J. Am. Coll. Cardiol.* 47, C7–C12. doi: 10.1016/j.jacc.2005.09.068

Fang, P., Zhang, D., Cheng, Z., Yan, C., Jiang, X., Kruger, W. D., et al. (2014). Hyperhomocysteinemia potentiates hyperglycemia-induced inflammatory monocyte differentiation and atherosclerosis. *Diabetes* 63, 4275–4290. doi: 10.2337/db14-0809

Fargion, S., Porzio, M., and Fracanzani, A. L. (2014). Nonalcoholic fatty liver disease and vascular disease: state-of-the-art. *World J. Gastroenterol.* 20, 13306–13324. doi: 10.3748/wjg.v20.i37.13306

Fazili, Z., Sun, W., Mittelstaedt, S., Cohen, C., and Xu, X. X. (1999). Disabled-2 inactivation is an early step in ovarian tumorigenicity. *Oncogene* 18, 3104–3113. doi: 10.1038/sj.onc.1202649

Figliuolo da Paz, V., Jamwal, D. R., Gurney, M., Midura-Kiela, M., Harrison, C. A., Cox, C., et al. (2019). Rapid downregulation of DAB2 by toll-like receptor activation contributes to a pro-inflammatory switch in activated dendritic cells. *Front. Immunol.* 10:304. doi: 10.3389/fimmu.2019.00304

Ford, M. G., Mills, I. G., Peter, B. J., Vallis, Y., Praefcke, G. J., Evans, P. R., et al. (2002). Curvature of clathrin-coated pits driven by epsin. *Nature* 419, 361–366. doi: 10.1038/nature01020

Galkina, E., and Ley, K. (2009). Immune and inflammatory mechanisms of atherosclerosis (*). *Annu. Rev. Immunol.* 27, 165–197. doi: 10.1146/annurev.immunol.021908.132620

Gertler, F. B., Bennett, R. L., Clark, M. J., and Hoffmann, F. M. (1989). Drosophila abl tyrosine kinase in embryonic CNS axons: a role in axonogenesis is revealed through dosage-sensitive interactions with disabled. *Cell* 58, 103–113. doi: 10.1016/0092-8674(89)90407-8

Goldstein, J. L., and Brown, M. S. (2015). A century of cholesterol and coronaries: from plaques to genes to statins. *Cell* 161, 161–172. doi: 10.1016/j.cell.2015.01.036

Groh, L., Keating, S. T., Joosten, L. A. B., Netea, M. G., and Riksen, N. P. (2018). Monocyte and macrophage immunometabolism in atherosclerosis. *Semin. Immunopathol.* 40, 203–214. doi: 10.1007/s00281-017-0656-7

Hilgendorf, I., Swirski, F. K., and Robbins, C. S. (2015). Monocyte fate in atherosclerosis. *Arterioscler Thromb. Vasc. Biol.* 35, 272–279. doi: 10.1161/ATVBAHA.114.303565

Hocevar, B. A. (2019). Loss of disabled-2 expression in pancreatic cancer progression. *Sci. Rep.* 9:7532. doi: 10.1038/s41598-019-43992-z

Holdt, L. M., and Teupser, D. (2012). Recent studies of the human chromosome 9p21 locus, which is associated with atherosclerosis in human populations. *Arterioscler Thromb. Vasc. Biol* 32, 196–206. doi: 10.1161/ATVBAHA.111.232678

Howell, B. W., Hawkes, R., Soriano, P., and Cooper, J. A. (1997). Neuronal position in the developing brain is regulated by mouse disabled-1. *Nature* 389, 733–737. doi: 10.1038/39607

Howell, B. W., Lanier, L. M., Frank, R., Gertler, F. B., and Cooper, J. A. (1999). The disabled 1 phosphotyrosine-binding domain binds to the internalization signals of transmembrane glycoproteins and to phospholipids. *Mol. Cell Biol.* 19, 5179–5188. doi: 10.1128/mcb.19.7.5179

Inoue, A., Sato, O., Homma, K., and Ikebe, M. (2002). DOC-2/DAB2 is the binding partner of myosin VI. *Biochem. Biophys. Res. Commun.* 292, 300–307. doi: 10.1006/bbrc.2002.6636

Jaggi, U., Yang, M., Matundan, H. H., Hirose, S., Shah, P. K., Sharifi, B. G., et al. (2020). Increased phagocytosis in the presence of enhanced M2-like macrophage responses correlates with increased primary and latent HSV-1 infection. *PLoS Pathog.* 16:e1008971. doi: 10.1371/journal.ppat.1008971

Joffe, A. M., Bakalar, M. H., and Fletcher, D. A. (2020). Macrophage phagocytosis assay with reconstituted target particles. *Nat. Protoc.* 15, 2230–2246. doi: 10.1038/s41596-020-0330-8

Kang, Y. L., Yochem, J., Bell, L., Sorensen, E. B., Chen, L., and Conner, S. D. (2013). Caenorhabditis elegans reveals a FxNPxY-independent low-density lipoprotein receptor internalization mechanism mediated by epsin1. *Mol. Biol. Cell* 24, 308–318. doi: 10.1091/mbc.E12-02-0163

Ko, G., Paradise, S., Chen, H., Graham, M., Vecchi, M., Bianchi, F., et al. (2010). Selective high-level expression of epsin 3 in gastric parietal cells, where it is localized at endocytic sites of apical canaliculi. *Proc. Natl. Acad. Sci. U.S.A.* 107, 21511–21516. doi: 10.1073/pnas.1016390107

Kojima, Y., Volkmer, J. P., McKenna, K., Civelek, M., Lusis, A. J., Miller, C. L., et al. (2016). CD47-blocking antibodies restore phagocytosis and prevent atherosclerosis. *Nature* 536, 86–90. doi: 10.1038/nature18935

Langridge, P. D., and Struhl, G. (2017). Epsin-dependent ligand endocytosis activates notch by force. *Cell* 171, 1383–1396.e12. doi: 10.1016/j.cell.2017.10.048

Li, L., Han, L., Zhang, J., Liu, X., Ma, R., Hou, X., et al. (2016). Epsin2 promotes polarity establishment and meiotic division through activating Cdc42 in mouse oocyte. *Oncotarget* 7, 50927–50936. doi: 10.18632/oncotarget.10815

Li, X., Fang, P., Li, Y., Kuo, Y. M., Andrews, A. J., Nanayakkara, G., et al. (2016). Mitochondrial reactive oxygen species mediate lysophosphatidylcholine-induced endothelial cell activation. *Arterioscler Thromb. Vasc. Biol.* 36, 1090–1100. doi: 10.1161/ATVBAHA.115.306964

Li, X., Fang, P., Sun, Y., Shao, Y., Yang, W. Y., Jiang, X., et al. (2020). Anti-inflammatory cytokines IL-35 and IL-10 block atherogenic lysophosphatidylcholine-induced, mitochondrial ROS-mediated innate immune activation, but spare innate immune memory signature in endothelial cells. *Redox Biol.* 28:101373. doi: 10.1016/j.redox.2019.101373

Li, X., Fang, P., Yang, W. Y., Chan, K., Lavallee, M., Xu, K., et al. (2017). Mitochondrial ROS, uncoupled from ATP synthesis, determine endothelial activation for both physiological recruitment of patrolling cells and pathological recruitment of inflammatory cells. *Can. J. Physiol. Pharmacol.* 95, 247–252. doi: 10.1139/cjpp-2016-0515

Li, X., Fang, P., Yang, W. Y., Wang, H., and Yang, X. (2019). IL-35, as a newly proposed homeostasis-associated molecular pattern, plays three major functions including anti-inflammatory initiator, effector, and blocker in cardiovascular diseases. *Cytokine* 122:154076. doi: 10.1016/j.cyto.2017.06.003

Li, X., Shao, Y., Sha, X., Fang, P., Kuo, Y. M., Andrews, A. J., et al. (2018a). IL-35 (Interleukin-35) suppresses endothelial cell activation by inhibiting mitochondrial reactive oxygen species-mediated site-specific acetylation of H3K14 (Histone 3 Lysine 14). *Arterioscler Thromb. Vasc. Biol.* 38, 599–609. doi: 10.1161/ATVBAHA.117.310626

Li, X., Wang, L., Fang, P., Sun, Y., Jiang, X., Wang, H., et al. (2018b). Lysophospholipids induce innate immune transdifferentiation of endothelial cells, resulting in prolonged endothelial activation. *J. Biol. Chem.* 293, 11033–11045. doi: 10.1074/jbc.RA118.002752

Libby, P. (2012). Inflammation in atherosclerosis. *Arterioscler Thromb. Vasc. Biol.* 32, 2045–2051. doi: 10.1161/ATVBAHA.108.179705

Lin, W., Wang, W., Wang, D., and Ling, W. (2017). Quercetin protects against atherosclerosis by inhibiting dendritic cell activation. *Mol. Nutr. Food Res.* 61:1700031. doi: 10.1002/mnfr.201700031

Liu, K., and Czaja, M. J. (2013). Regulation of lipid stores and metabolism by lipophagy. *Cell Death Differ.* 20, 3–11. doi: 10.1038/cdd.2012.63

Liu, X., Pasula, S., Song, H., Tessneer, K. L., Dong, Y., Hahn, S., et al. (2014). Temporal and spatial regulation of epsin abundance and VEGFR3 signaling are required for lymphatic valve formation and function. *Sci. Signal.* 7:ra97. doi: 10.1126/scisignal.2005413

Lu, H., Rateri, D. L., Feldman, D. L., Charnigo, R. J. Jr., Fukamizu, A., Ishida, J., et al. (2008). Renin inhibition reduces hypercholesterolemia-induced atherosclerosis in mice. *J. Clin. Invest.* 118, 984–993. doi: 10.1172/JCI32970

Lusis, A. J. (2000). Atherosclerosis. *Nature* 407, 233–241. doi: 10.1038/35025203

Mai, J., Virtue, A., Shen, J., Wang, H., and Yang, X. F. (2013). An evolving new paradigm: endothelial cells–conditional innate immune cells. *J. Hematol. Oncol.* 6:61. doi: 10.1186/1756-8722-6-61

Maurer, M. E., and Cooper, J. A. (2005). Endocytosis of megalin by visceral endoderm cells requires the Dab2 adaptor protein. *J. Cell Sci.* 118(Pt 22), 5345–5355. doi: 10.1242/jcs.02650

Moore, K. J., Sheedy, F. J., and Fisher, E. A. (2013). Macrophages in atherosclerosis: a dynamic balance. *Nat. Rev. Immunol.* 13, 709–721. doi: 10.1038/nri3520

Moore, R., Cai, K. Q., Tao, W., Smith, E. R., and Xu, X. X. (2013). Differential requirement for Dab2 in the development of embryonic and extra-embryonic tissues. *BMC Dev. Biol.* 13:39. doi: 10.1186/1471-213X-13-39

Morris, S. M., Arden, S. D., Roberts, R. C., Kendrick-Jones, J., Cooper, J. A., Luzio, J. P., et al. (2002a). Myosin VI binds to and localises with Dab2, potentially linking receptor-mediated endocytosis and the actin cytoskeleton. *Traffic* 3, 331–341. doi: 10.1034/j.1600-0854.2002.30503.x

Morris, S. M., and Cooper, J. A. (2001). Disabled-2 colocalizes with the LDLR in clathrin-coated pits and interacts with AP-2. *Traffic* 2, 111–123. doi: 10.1034/j.1600-0854.2001.020206.x

Morris, S. M., Tallquist, M. D., Rock, C. O., and Cooper, J. A. (2002b). Dual roles for the Dab2 adaptor protein in embryonic development and kidney transport. *EMBO J.* 21, 1555–1564. doi: 10.1093/emboj/21.7.1555

Oldham, C. E., Mohney, R. P., Miller, S. L., Hanes, R. N., and O'Bryan, J. P. (2002). The ubiquitin-interacting motifs target the endocytic adaptor protein epsin for ubiquitination. *Curr. Biol.* 12, 1112–1116. doi: 10.1016/s0960-9822(02)00900-4

Orlov, V. S. (1988). The theory of pinocytosis. Factors determining the dynamics of pinocytosis in capillary endothelium. *Biofizika* 33, 117–120.

Palmal, S., Maity, A. R., Singh, B. K., Basu, S., Jana, N. R., and Jana, N. R. (2014). Inhibition of amyloid fibril growth and dissolution of amyloid fibrils by curcumin-gold nanoparticles. *Chemistry* 20, 6184–6191. doi: 10.1002/chem.201400079

Paoletti, R., Bolego, C., Poli, A., and Cignarella, A. (2006). Metabolic syndrome, inflammation and atherosclerosis. *Vasc. Health Risk Manag.* 2, 145–152. doi: 10.2147/vhrm.2006.2.2.145

Pastrana, J. L., Sha, X., Virtue, A., Mai, J., Cueto, R., Lee, I. A., et al. (2012). Regulatory T cells and Atherosclerosis. *J. Clin. Exp. Cardiolog.* 2012(Suppl. 12), 2. doi: 10.4172/2155-9880.S12-002

Pasula, S., Cai, X., Dong, Y., Messa, M., McManus, J., Chang, B., et al. (2012). Endothelial epsin deficiency decreases tumor growth by enhancing VEGF signaling. *J. Clin. Invest.* 122, 4424–4438. doi: 10.1172/JCI64537

Pearse, B. M., Smith, C. J., and Owen, D. J. (2000). Clathrin coat construction in endocytosis. *Curr. Opin. Struct. Biol.* 10, 220–228. doi: 10.1016/s0959-440x(00)00071-3

Polo, S., Sigismund, S., Faretta, M., Guidi, M., Capua, M. R., Bossi, G., et al. (2002). A single motif responsible for ubiquitin recognition and monoubiquitination in endocytic proteins. *Nature* 416, 451–455. doi: 10.1038/416451a

Rader, D. J., and Daugherty, A. (2008). Translating molecular discoveries into new therapies for atherosclerosis. *Nature* 451, 904–913. doi: 10.1038/nature06796

Rahman, H. A., Wu, H., Dong, Y., Pasula, S., Wen, A., Sun, Y., et al. (2016). Selective targeting of a novel epsin-VEGFR2 interaction promotes VEGF-mediated angiogenesis. *Circ. Res.* 118, 957–969. doi: 10.1161/CIRCRESAHA.115.307679

Ramkumar, S., Raghunath, A., and Raghunath, S. (2016). Statin therapy: review of safety and potential side effects. *Acta Cardiol. Sin.* 32, 631–639. doi: 10.6515/acs20160611a

Reine, J., Rylance, J., Ferreira, D. M., Pennington, S. H., Welters, I. D., Parker, R., et al. (2020). The whole blood phagocytosis assay: a clinically relevant test of neutrophil function and dysfunction in community-acquired pneumonia. *BMC Res. Notes* 13:203. doi: 10.1186/s13104-020-05034-0

Ridker, P. M., Everett, B. M., Thuren, T., MacFadyen, J. G., Chang, W. H., Ballantyne, C., et al. (2017). Antiinflammatory therapy with canakinumab for atherosclerotic disease. *N. Engl. J. Med.* 377, 1119–1131. doi: 10.1056/NEJMoa1707914

Rosenbauer, F., Kallies, A., Scheller, M., Knobeloch, K. P., Rock, C. O., Schwieger, M., et al. (2002). Disabled-2 is transcriptionally regulated by ICSBP and augments macrophage spreading and adhesion. *EMBO J.* 21, 211–220. doi: 10.1093/emboj/21.3.211

Rosenthal, J. A., Chen, H., Slepnev, V. I., Pellegrini, L., Salcini, A. E., Di Fiore, P. P., et al. (1999). The epsins define a family of proteins that interact with components of the clathrin coat and contain a new protein module. *J. Biol. Chem.* 274, 33959–33965. doi: 10.1074/jbc.274.48.33959

Sakamoto, C., Kawamoto, C., Takeuchi, K., Miyamoto, I., and Shuntoh, H. (2004). Fission yeast epsin, Ent1p is required for endocytosis and involved in actin organization. *Kobe J. Med. Sci.* 50, 47–57.

Salcini, A. E., Chen, H., Iannolo, G., De Camilli, P., and Di Fiore, P. P. (1999). Epidermal growth factor pathway substrate 15, Eps15. *Int. J. Biochem. Cell Biol.* 31, 805–809. doi: 10.1016/s1357-2725(99)00042-4

Schutte-Nutgen, K., Edeling, M., Mendl, G., Krahn, M. P., Edemir, B., Weide, T., et al. (2019). Getting a Notch closer to renal dysfunction: activated Notch suppresses expression of the adaptor protein Disabled-2 in tubular epithelial cells. *FASEB J.* 33, 821–832. doi: 10.1096/fj.201800392RR

Shao, Y., Saredy, J., Yang, W. Y., Sun, Y., Lu, Y., Saaoud, F., et al. (2020). Vascular endothelial cells and innate immunity. *Arterioscler Thromb. Vasc. Biol* 40, e138–e152. doi: 10.1161/ATVBAHA.120.314330

Shapiro, M. D., and Fazio, S. (2017). Apolipoprotein B-containing lipoproteins and atherosclerotic cardiovascular disease. *F1000Res.* 6:134. doi: 10.12688/f1000research.9845.1

Sheng, Z., He, J., Tuppen, J. A., Sun, W., Fazili, Z., Smith, E. R., et al. (2000). Structure, sequence, and promoter analysis of human disabled-2 gene (DAB2). *Genomics* 70, 381–386. doi: 10.1006/geno.2000.6383

Sheng, Z., Smith, E. R., He, J., Tuppen, J. A., Martin, W. D., Dong, F. B., et al. (2001). Chromosomal location of murine disabled-2 gene and structural comparison with its human ortholog. *Gene* 268, 31–39. doi: 10.1016/s0378-1119(01)00401-2

Smirnov, A., Solga, M. D., Lannigan, J., and Criss, A. K. (2020). Using imaging flow cytometry to quantify neutrophil phagocytosis. *Methods Mol. Biol.* 2087, 127–140. doi: 10.1007/978-1-0716-0154-9_10

Song, K., Cai, X., Dong, Y., Wu, H., Wei, Y., Shankavaram, U., et al. (2020). Epsins 1 and 2 promote NEMO linear ubiquitination via LUBAC to drive breast cancer development. *J. Clin. Invest.* doi: 10.1172/JCI129374 [Epub ahead of print],

Song, K., Wu, H., Rahman, H. N., Dong, Y., Wen, A., Brophy, M. L., et al. (2017). Endothelial epsins as regulators and potential therapeutic targets of tumor angiogenesis. *Cell Mol. Life Sci.* 74, 393–398. doi: 10.1007/s00018-016-2347-2

Spradling, K. D., McDaniel, A. E., Lohi, J., and Pilcher, B. K. (2001). Epsin 3 is a novel extracellular matrix-induced transcript specific to wounded epithelia. *J. Biol. Chem.* 276, 29257–29267. doi: 10.1074/jbc.M101663200

Sun, L., Yang, X., Yuan, Z., and Wang, H. (2020). Metabolic reprogramming in immune response and tissue inflammation. *Arterioscler Thromb. Vasc. Biol.* 40, 1990–2001. doi: 10.1161/ATVBAHA.120.314037

Swirski, F. K., and Nahrendorf, M. (2013). Leukocyte behavior in atherosclerosis, myocardial infarction, and heart failure. *Science* 339, 161–166. doi: 10.1126/science.1230719

Szymanska, M., Fosdahl, A. M., Raiborg, C., Dietrich, M., Liestol, K., Stang, E., et al. (2016). Interaction with epsin 1 regulates the constitutive clathrin-dependent internalization of ErbB3. *Biochim. Biophys. Acta* 1863, 1179–1188. doi: 10.1016/j.bbamcr.2016.03.011

Tabas, I., and Glass, C. K. (2013). Anti-inflammatory therapy in chronic disease: challenges and opportunities. *Science* 339, 166–172. doi: 10.1126/science.1230720

Tao, W., Moore, R., Meng, Y., Smith, E. R., and Xu, X. X. (2016a). Endocytic adaptors Arh and Dab2 control homeostasis of circulatory cholesterol. *J. Lipid Res.* 57, 809–817. doi: 10.1194/jlr.M063065

Tao, W., Moore, R., Smith, E. R., and Xu, X. X. (2016b). Endocytosis and physiology: insights from disabled-2 deficient mice. *Front. Cell Dev. Biol.* 4:129. doi: 10.3389/fcell.2016.00129

Tessneer, K. L., Cai, X., Pasula, S., Dong, Y., Liu, X., Chang, B., et al. (2013a). Epsin family of endocytic adaptor proteins as oncogenic regulators of cancer progression. *J. Can. Res. Updates* 2, 144–150. doi: 10.6000/1929-2279.2013.02.03.2

Tessneer, K. L., Pasula, S., Cai, X., Dong, Y., Liu, X., Yu, L., et al. (2013b). Endocytic adaptor protein epsin is elevated in prostate cancer and required for cancer progression. *ISRN Oncol.* 2013:420597. doi: 10.1155/2013/420597

Tessneer, K. L., Pasula, S., Cai, X., Dong, Y., McManus, J., Liu, X., et al. (2014). Genetic reduction of vascular endothelial growth factor receptor 2 rescues aberrant angiogenesis caused by epsin deficiency. *Arterioscler Thromb. Vasc. Biol.* 34, 331–337. doi: 10.1161/ATVBAHA.113.302586

Tian, X., Hansen, D., Schedl, T., and Skeath, J. B. (2004). Epsin potentiates Notch pathway activity in *Drosophila* and *C. elegans*. *Development* 131, 5807–5815. doi: 10.1242/dev.01459

Traub, L. M. (2003). Sorting it out: AP-2 and alternate clathrin adaptors in endocytic cargo selection. *J. Cell Biol.* 163, 203–208. doi: 10.1083/jcb.200309175

Wang, W., and Struhl, G. (2004). Drosophila Epsin mediates a select endocytic pathway that DSL ligands must enter to activate Notch. *Development* 131, 5367–5380. doi: 10.1242/dev.01413

Wang, Y., Wang, Y., Adi, D., He, X., Liu, F., Abudesimu, A., et al. (2020). Dab2 gene variant is associated with increased coronary artery disease risk in Chinese Han population. *Medicine (Baltimore)* 99:e20924. doi: 10.1097/MD.0000000000020924

Weber, C., and Noels, H. (2011). Atherosclerosis: current pathogenesis and therapeutic options. *Nat. Med.* 17, 1410–1422. doi: 10.1038/nm.2538

Wu, H., Rahman, H. N. A., Dong, Y., Liu, X., Lee, Y., Wen, A., et al. (2018). Epsin deficiency promotes lymphangiogenesis through regulation of VEGFR3 degradation in diabetes. *J. Clin. Invest.* 128, 4025–4043. doi: 10.1172/JCI96063

Xi, H., Zhang, Y., Xu, Y., Yang, W. Y., Jiang, X., Sha, X., et al. (2016). Caspase-1 inflammasome activation mediates homocysteine-induced pyrop-apoptosis in endothelial cells. *Circ. Res.* 118, 1525–1539. doi: 10.1161/CIRCRESAHA.116.308501

Xie, X., Cho, B., and Fischer, J. A. (2012). Drosophila Epsin's role in Notch ligand cells requires three Epsin protein functions: the lipid binding function of the ENTH domain, a single Ubiquitin interaction motif, and a subset of the C-terminal protein binding modules. *Dev. Biol.* 363, 399–412. doi: 10.1016/j.ydbio.2012.01.004

Xu, X. X., Yang, W., Jackowski, S., and Rock, C. O. (1995). Cloning of a novel phosphoprotein regulated by colony-stimulating factor 1 shares a domain with the *Drosophila* disabled gene product. *J. Biol. Chem.* 270, 14184–14191. doi: 10.1074/jbc.270.23.14184

Yang, J., Zhang, L., Yu, C., Yang, X. F., and Wang, H. (2014). Monocyte and macrophage differentiation: circulation inflammatory monocyte as biomarker for inflammatory diseases. *Biomark. Res.* 2:1. doi: 10.1186/2050-7771-2-1

Yin, Y., Li, X., Sha, X., Xi, H., Li, Y. F., Shao, Y., et al. (2015). Early hyperlipidemia promotes endothelial activation via a caspase-1-sirtuin 1 pathway. *Arterioscler Thromb. Vasc. Biol.* 35, 804–816. doi: 10.1161/ATVBAHA.115.305282

Yin, Y., Pastrana, J. L., Li, X., Huang, X., Mallilankaraman, K., Choi, E. T., et al. (2013). Inflammasomes: sensors of metabolic stresses for vascular inflammation. *Front. Biosci. (Landmark Ed)* 18:638–649.

Yu, X. H., Fu, Y. C., Zhang, D. W., Yin, K., and Tang, C. K. (2013). Foam cells in atherosclerosis. *Clin. Chim. Acta* 424, 245–252. doi: 10.1016/j.cca.2013.06.006

Zhang, D., Fang, P., Jiang, X., Nelson, J., Moore, J. K., Kruger, W. D., et al. (2012). Severe hyperhomocysteinemia promotes bone marrow-derived and resident inflammatory monocyte differentiation and atherosclerosis in LDLr/CBS-deficient mice. *Circ. Res.* 111, 37–49. doi: 10.1161/CIRCRESAHA.112.269472

Zhong, C., Yang, X., Feng, Y., and Yu, J. (2020). Trained immunity: an underlying driver of inflammatory atherosclerosis. *Front. Immunol.* 11:284. doi: 10.3389/fimmu.2020.00284

Conflict of Interest: The authors declare that the research was conducted in the absence of any commercial or financial relationships that could be construed as a potential conflict of interest.

Copyright © 2020 Cui, Dong, Wang, Cowan, Chan, Shyy and Chen. This is an open-access article distributed under the terms of the Creative Commons Attribution License (CC BY). The use, distribution or reproduction in other forums is permitted, provided the original author(s) and the copyright owner(s) are credited and that the original publication in this journal is cited, in accordance with accepted academic practice. No use, distribution or reproduction is permitted which does not comply with these terms.

frontiers in Cell and Developmental Biology

REVIEW
published: 14 January 2021
doi: 10.3389/fcell.2020.627647

Molecular Mechanisms Controlling Lymphatic Endothelial Junction Integrity

*Pieter R. Norden and Tsutomu Kume**

Department of Medicine, Feinberg School of Medicine, Feinberg Cardiovascular and Renal Research Institute, Northwestern University, Chicago, IL, United States

The lymphatic system is essential for lipid absorption/transport from the digestive system, maintenance of tissue fluid and protein homeostasis, and immune surveillance. Despite recent progress toward understanding the cellular and molecular mechanisms underlying the formation of the lymphatic vascular system, the nature of lymphatic vessel abnormalities and disease in humans is complex and poorly understood. The mature lymphatic vasculature forms a hierarchical network in which lymphatic endothelial cells (LECs) are joined by functionally specialized cell-cell junctions to maintain the integrity of lymphatic vessels. Blind-ended and highly permeable lymphatic capillaries drain interstitial fluid via discontinuous, button-like LEC junctions, whereas collecting lymphatic vessels, surrounded by intact basement membranes and lymphatic smooth muscle cells, have continuous, zipper-like LEC junctions to transport lymph to the blood circulatory system without leakage. In this review, we discuss the recent advances in our understanding of the mechanisms by which lymphatic button- and zipper-like junctions play critical roles in lymphatic permeability and function in a tissue- and organ-specific manner, including lacteals of the small intestine. We also provide current knowledge related to key pathways and factors such as VEGF and RhoA/ROCK signaling that control lymphatic endothelial cell junctional integrity.

Keywords: lymphatic vessel junction, button-like junction, zipper-like junction, VEGF signaling, RhoA/ROCK, Notch, FOXC, Angiopoietin

OPEN ACCESS

Edited by:
Bin Ren,
University of Alabama at Birmingham, United States

Reviewed by:
Sathish Srinivasan,
Oklahoma Medical Research Foundation, United States
Seiji Yamamoto,
University of Toyama, Japan

***Correspondence:**
Tsutomu Kume
t-kume@northwestern.edu

Specialty section:
This article was submitted to Signaling, a section of the journal Frontiers in Cell and Developmental Biology

Received: *09 November 2020*
Accepted: *18 December 2020*
Published: *14 January 2021*

Citation:
Norden PR and Kume T (2021) Molecular Mechanisms Controlling Lymphatic Endothelial Junction Integrity. Front. Cell Dev. Biol. 8:627647. doi: 10.3389/fcell.2020.627647

FORMATION OF THE LYMPHATIC VASCULAR SYSTEM

The development of the lymphatic vascular system in the mouse begins shortly after blood circulation is established (Escobedo and Oliver, 2016; Kazenwadel and Harvey, 2016; Semo et al., 2016). At approximately embryonic day (E) 9.5, a subpopulation of lymphatic endothelial progenitors located in the anterior cardinal vein become positive for Prospero-related homeobox 1 (Prox1) expression, which is the master regulator of the lymphatic vascular phenotype (Wigle and Oliver, 1999; Francois et al., 2008), and competent for differentiation into lymphatic endothelial cells (LECs) (Lee et al., 2009; Yamazaki et al., 2009; Srinivasan et al., 2010; Srinivasan and Oliver, 2011; Aranguren et al., 2013). Once LEC identity is specified (at ∼E10.0), Prox1+ lymphatic endothelial progenitors that express the vascular endothelial growth factor receptor 3 (VEGFR-3) bud off via stimulation by the VEGF-C ligand derived from the mesenchyme and migrate dorsolaterally from the cardinal and intersomitic veins, creating chains of interconnected cells

that subsequently form the primary lymph sacs and superficial lymphatic vessels (Karkkainen et al., 2004; Francois et al., 2012; Yang et al., 2012; Hagerling et al., 2013). Recent evidence also indicates that non-venous derived lymphatic precursors contribute to the lymphatic vasculature in the developing skin, heart, and mesentery (Klotz et al., 2015; Martinez-Corral et al., 2015; Stanczuk et al., 2015). These primary lymphatic structures develop into the lymphatic vascular network through the proliferation, sprouting, and survival of LECs, and this process is regulated by lymphangiogenic signaling such as the VEGF-C/D-VEGFR-3 and Angiopoietin (Angpt)-TEK (Tie2) pathways (Potente and Makinen, 2017). By E14.5, the network extends throughout the mouse embryo (Coso et al., 2014); then, beginning at E15.5-E16.0, the primary lymphatic vasculature undergoes remodeling and maturation to form a hierarchical lymphatic vascular network composed of lymphatic capillaries, precollecting and collecting lymphatic vessels (**Figure 1A**). The morphological changes associated with lymphatic remodeling and maturation also continue after birth.

FORMATION AND REGULATION OF SPECIALIZED LYMPHATIC ENDOTHELIAL CELL JUNCTIONS

Lymphatic capillaries (also called initial lymphatics) are blind-ended and highly permeable, because their basement membrane is discontinuous, and they are not covered by pericytes or lymphatic smooth muscle cells. Furthermore, lymphatic

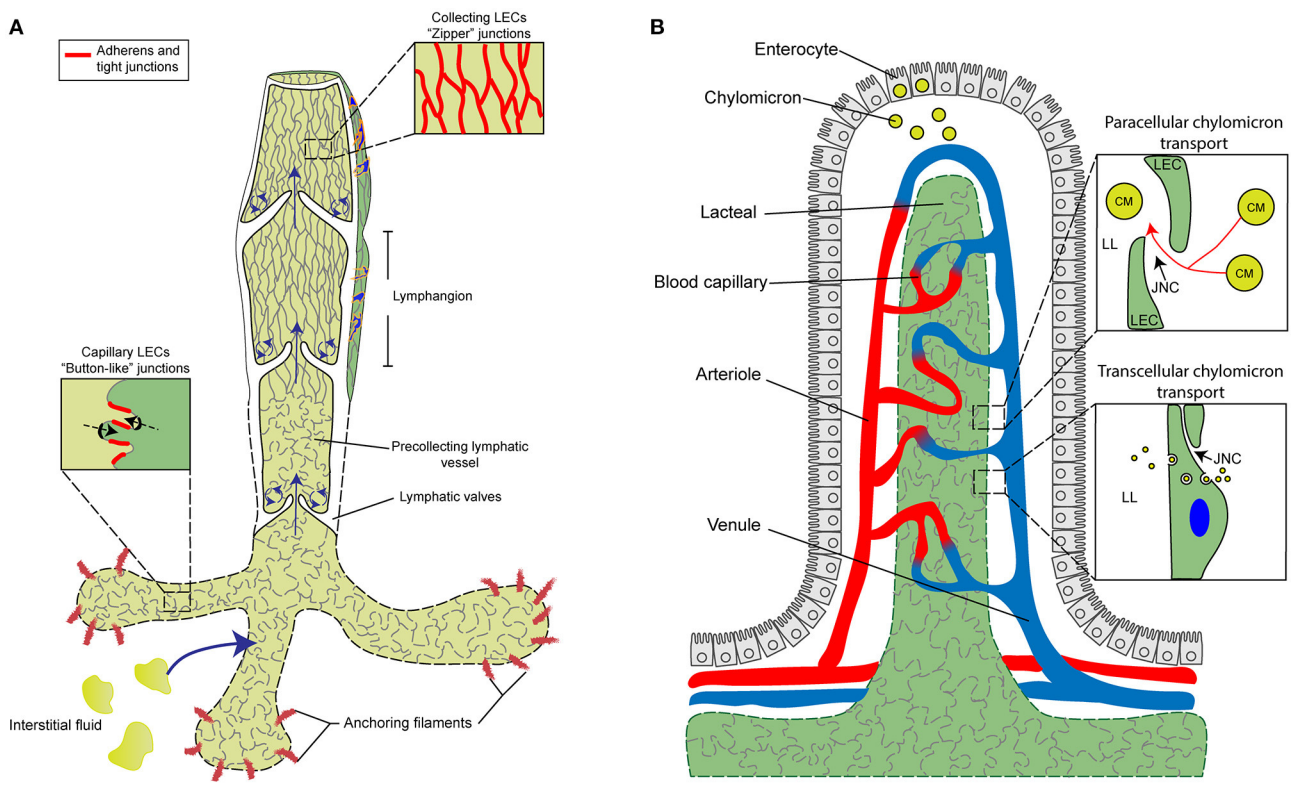

FIGURE 1 | Characterization and function of cell junctions in the general lymphatic vasculature and lymphatic lacteals. **(A)** The general lymphatic vasculature is organized into lymphatic capillaries, pre-collecting, and collecting lymphatic vessels. The lymphatic capillaries have sparse basement membrane and consist of oak-leaf shaped lymphatic endothelial cells (LECs) characterized by the presence of "button-like" cell junctions formed by discontinuous adherens and tight junction protein complexes. Additionally, lymphatic capillaries are tightly connected to the extracellular matrix (ECM) via anchoring filaments. Local hydrostatic pressure then facilitates the opening of overlapping junctions by stretching anchoring filaments, which then promotes the uptake of interstitial fluid and migration of immune cells into the lymphatic vasculature. In contrast to capillaries, collecting vessel LECs function to transport lymph and exhibit continuous "zipper-like" cell junctions and are surrounded by basement membrane and lymphatic smooth muscle cells (blue). Collecting vessels are also arranged into lymphangion regions, separated by intraluminal lymphatic valves, which then help to maintain the unidirectional transport of lymph. The formation of valve LECs is driven by biomechanical transduction of exposure to oscillatory shear stress and valve LECs are attached to specialized ECM and lack lymphatic smooth muscle coverage. **(B)** Specialized lymphatic vessels, known as lacteals, are present in each villus of the small intestine. Lacteals are blind-ended lymphatic vessels consisting of LECs with "button-like" junctions surrounded by a blood vasculature capillary network and differentiated, specialized epithelial cells forming the villus. Lacteals function in the maintenance of intestinal homeostasis and gut immunity as well as digestive fat absorption. Specialized absorptive cells in the villus known as enterocytes are responsible for the uptake of fatty acids and monoglycerides from the intestinal lumen, which are then combined with proteins to form chylomicrons that are secreted and transported to the lacteals. Open regions of "button"-like junctions in the lacteals facilitate paracellular chylomicron transport into the lacteal lumen whereas transcellular chylomicron transport is mediated by pinocytic vesicle uptake and transport across the LEC cytoplasm into the lymphatic lumen. CM, chylomicron; JNC, junction; LEC, lymphatic endothelial cell; LL, lacteal lumen.

capillaries are joined by discontinuous, button-like junctions at the border of oak leaf-shaped endothelial cells as they take up interstitial fluid and serve as entrance points for immune cells that infiltrate from blood vessels (**Figure 1A**). Such specialized button-like junctions are present in many tissues, including the trachea, diaphragm, dermis, and small intestine (Baluk et al., 2007; Dejana et al., 2009a; Yao et al., 2012; Bernier-Latmani and Petrova, 2017; Duong and Vestweber, 2020; Zhang et al., 2020). In contrast, continuous, zipper-like junctions are formed in the endothelium of collecting lymphatic vessels, which are surrounded by intact basement membranes and lymphatic smooth muscle cells and contain intraluminal valves. Collecting vessels then transport lymph to the circulatory system via lymph nodes (Martinez-Corral and Makinen, 2013; Petrova and Koh, 2018).

During mouse embryonic development, continuous zipper-like lymphatic junctions are initially formed in Prox1+ cells budding from the cardinal vein and in the jugular lymph sacs at E12.5 as well as in the tracheal lymphatic plexus at E 16.5 (Yao et al., 2012). The transformation to button-like junctions in the initial lymphatics of the trachea and diaphragm begins at E17.5 before birth and is mostly complete by postnatal day (P) 28 (Yao et al., 2012). In contrast, collecting lymphatic vessels maintain zipper-like junctions. While initial lymphatics of P4 neonatal mice contain intermediate cell-junctions between zippers and buttons, treatment with dexamethasone, an anti-inflammatory corticosteroid, promotes button junction formation (Yao et al., 2012). Sustained inflammation by *Mycoplasma pulmonis* infection in the respiratory tract induces button-to-zipper junctional conversion in the existing initial lymphatics of the trachea (Yao et al., 2012), whereas zipper-like junctions are present in growing tips of lymphatic sprouts in the tracheal mucosa (Baluk et al., 2007). Similar to neonatal lymphatics, the button-to-zipper transformation in inflammation can be reversed by the treatment of dexamethasone (Yao et al., 2012). These findings indicate the plasticity of LEC junction integrity between zippers and buttons both in development and inflammation.

The integrity of LEC junctions is tightly regulated by cell junction molecular complexes. Particular attention has been paid for the role of the adherens junction molecule vascular endothelial (VE)-cadherin in lymphatic junction stability in different tissues/organs such as mesenteric and dermal lymphatics, lacteals, and lymphatic valves (Hagerling et al., 2018; Yang et al., 2019; Duong and Vestweber, 2020; Petrova and Koh, 2020; Zhang et al., 2020). VE-cadherin is present in both button- and zipper-like junctions in the lymphatic endothelium, whereas its localization is particularly restricted in buttons at LEC borders (Baluk et al., 2007; Yao et al., 2012). Endothelial adhesion is stabilized by anchoring the VE-cadherin cytoplasmic tail to the actin cytoskeleton. In the blood endothelium, VEGF-A/VEGFR-2-mediated activation of the small GTPase RhoA/Rho-associated protein kinase (ROCK) signaling leads to cytoskeletal rearrangement of cortical actin into perpendicular stress fibers binding to VE-cadherin, thereby regulating cell junctions and vascular permeability (Dejana et al., 2009b; Dorland and Huveneers, 2017; Szymborska and Gerhardt, 2018). As described below, accumulating evidence suggest that the RhoA/ROCK pathway controls LEC junction integrity (Zhang et al., 2018; Frye et al., 2020; Norden et al., 2020).

ANGIOPOIETIN 2-DEPENDENT FORMATION OF BUTTON-LIKE JUNCTIONS IN LYMPHATIC CAPILLARIES

The Angiopoietin (Angpt)/TEK (Tie2) signaling pathway, which controls blood vessel stability and remodeling, is also required for the formation and maintenance of lymphatic vessels (Eklund et al., 2017; Saharinen et al., 2017; Akwii et al., 2019; Petrova and Koh, 2020). While the function of the Angpt2 ligand in blood vessels is context-dependent, it acts as an agonist for the TEK receptor in LECs during lymphangiogenesis (Gale et al., 2002; Dellinger et al., 2008; Shen et al., 2014; Yuen et al., 2014; Zheng et al., 2014; Souma et al., 2018). Notably, Angpt2 regulates the transformation of zipper-like junctions into button-like junctions during lymphatic vessel development (Zheng et al., 2014) (**Table 1**). The treatment of an Angpt2 blocking antibody does not affect zipper-like patterns in the sprouting front of lymphatic vessels of the mouse embryonic skin, whereas it blocks the transformation into button-like junctions in the plexus behind the sprouts in initial lymphatics, accompanied by a defect in phosphorylation of VE-cadherin that is associated with destabilization of cell-cell junctions. Dexamethasone-mediated induction of button-like junction formation in the sprouting vessel front, as well as the following plexus, is also inhibited by the Angpt2 blocking antibody. However, Angpt2 is only required for junction remodeling but is dispensable for the maintenance of button-like junctions of initial lymphatics. Similarly, the zipper-to-button junction transformation in initial lymphatics is inhibited in the neonatal mesentery and adult skin of *Angpt2* mutant mice (Zheng et al., 2014). Furthermore, both blocking antibody mediated inhibition of Angpt2 and genetic deletion of *Angpt2* lead to the disruption of LEC junctions in mesenteric collecting vessels leading to chyle leakage. This indicates that Angpt2 is also essential for the maintenance of junctional integrity in lymphatic collecting vessels.

KEY SIGNALING PATHWAYS THAT REGULATE LACTEAL JUNCTIONS IN THE SMALL INTESTINE

Lacteals are blunt-ended, tube-like lymphatic capillaries in small intestinal villi which are essential for dietary fat absorption, gut immunity, and intestinal fluid homeostasis. Lacteal endothelial cells contain a mix of button-like and zipper-like junctions (Bernier-Latmani and Petrova, 2017; Petrova and Koh, 2018, 2020; Cifarelli and Eichmann, 2019) (**Figure 1B**). Here, dietary lipids are packaged into chylomicrons in enterocytes of the intestinal epithelium, and chylomicron entry into the lacteal lumen is thought to be mediated by paracellular transport through open button-like junctions (Casley-Smith, 1962; Sabesin and Frase, 1977; Bernier-Latmani et al., 2015; Zhang et al., 2018), although other studies have shown a transcellular transport

TABLE 1 | Factors involved in regulating lymphatic cell junctions.

Factor	Function	References
Angpt2	Essential for the formation of button-like junction in initial lymphatics	Zheng et al., 2014
	Maintains junctional integrity of collecting vessels	
VEGF-C	Secreted from villus macrophages	Suh et al., 2019
	VEGF-C/VEGFR-3 signaling controls button junctions in lacteals	
VEGFR-2	VEGF-A/VEGFR-2 signaling regulates zipper junctions in lacteals	Zhang et al., 2018
DLL4	Essential for lacteal regeneration via maintaining button junctions	Bernier-Latmani et al., 2015
	Downstream of VEGFR-2/3	
Calcrl	Upstream of Notch/DLL4 signaling in lacteal junctional integrity	Davis et al., 2017
	Controls the transcellular and paracellular transport pathways of chylomicrons	Davis et al., 2019
FOXC1/FOXC2	Required for LEC junction integrity in lymphatic valves, collecting vessels, and dermal lymphatics	Norden et al., 2020 Fatima et al., 2016
S1PR1/LPAR1	Crosstalk between LPAR1 and S1PR1 promotes porous LEC junctions of lymph nodes	Hisano et al., 2019
EphrinB2/EphB4	Maintains LEC junctions via RhoA-dependent cytoskeletal organization	Frye et al., 2020
RhoA/ROCK	Essential for LEC junction formation in lacteals, lymphatic valves and collecting vessels	Zhang et al., 2018 Norden et al., 2020
	Involved in EphrinB2/EphB4- and S1P/S1PR1-dependent junctional/cytoskeletal changes	Frye et al., 2020 Geng et al., 2020

mechanism (Dixon et al., 2009; Dixon, 2010; Reed et al., 2013). The formation and function of intestinal lacteals, including LEC junctions, are tightly regulated by several signaling pathways. The initial development of intestinal lymphatic vessels is dependent on activation of the VEGF-C/VEGFR-3/phosphatidylinositol 3-kinase (PI3K) pathway (Kim et al., 2007; Stanczuk et al., 2015). Unlike quiescent lymphatic vessels located in other adult tissues, lacteals are continuously maintained in a regenerative, slowly proliferative state undergoing lymphangiogenesis through the VEGF-C/VEGFR-3 pathway (Bernier-Latmani et al., 2015; Nurmi et al., 2015), which is attributable to the constant regeneration of the intestinal structure, including the intestinal epithelium containing stem cell populations, in order to maintain gut homeostasis (Barker, 2014). Moreover, intestinal villus SMCs and macrophages are reported to produce VEGF-C to regulate lacteal maintenance (Nurmi et al., 2015; Suh et al., 2019).

The continuous regeneration of lacteals is also regulated by Notch signaling. Expression of the Notch ligand Delta-like ligand 4 (DLL4) in lacteals is mediated by activation of VEGFR-2 and VEGFR-3 signaling, and LEC-specific deletion of *Dll4* in mice results in lacteal regression, reduced button-like junction formation, and impaired dietary fat uptake (Bernier-Latmani et al., 2015). Thus, Notch/DLL4 signaling is critical for lacteal maintenance and junctional integrity (**Table 1**). DLL4 expression in lacteals is also controlled by the peptide hormone adrenomedullin (AM) and its receptor, calcitonin receptor–like receptor (gene = *CALCRL*, protein = CLR) (Davis et al., 2017). Consistent with evidence that mutations in *Calcrl* are associated with autosomal recessive non-immune hydrops fetalis with lymphatic dysplasia in humans (Mackie et al., 2018), global deletion of *Calcrl* in mice causes systemic lymphatic insufficiency and lymphangiectasia (Hoopes et al., 2012). LEC-specific *Calcrl* mutant mice exhibit small intestinal lymphangiectasia, characterized by dilated lacteals and protein-losing enteropathy (Davis et al., 2017). Importantly, *Calcrl*-mutant lacteals contain more continuous cell junctions with reduced expression of DLL4 compared to controls (Davis et al., 2017) (**Table 1**). Indomethacin challenge to induce severe enteropathy that recapitulates human Crohn's disease leads to impaired lipid uptake and junctional barriers in the intestine of LEC-specific *Calcrl* mutant mice. Recent evidence also indicates that CLR signaling controls the critical balance between transcellular and paracellular transport pathways of lipids in lacteals (Davis et al., 2019). Collectively, these studies identify molecular interactions involving the VEGF-C/VEGFR-3, Notch/DLL4, and AM/CLR pathways in intestinal lacteal regeneration, integrity, and function (**Table 1**).

Lacteals are surrounded by villus blood capillaries. Recent studies demonstrate that the close localization of the intestinal blood and lymphatic vessels is important to maintain the junctional integrity and dietary fat uptake of lacteals. Within the villi, the bioavailability of VEGF-A is restricted by VEGFR-1 and NRP1, both of which are highly expressed on blood capillaries, but not on lacteals (Zhang et al., 2018). As decoy receptors, they bind VEGF-A and compete for VEGFR-2. Lack of VEGFR-1 and NPR1 in mice increases VEGF-A availability in the villi, which in turn activates VEGFR-2 signaling in lacteals and induces the button-to-zipper junctional transformation, thereby preventing chylomicron uptake into lacteals. Such lacteal junction zippering protects mice from high-fat diet-induced obesity (Zhang et al., 2018) (**Figure 2A**). In contrast, high VEGF-A bioavailability disrupts cell junctions of villus blood capillaries. This discrepancy between lacteals and villus blood capillaries appears to be associated with VEGFR-2-dependent activation of RhoA/ROCK/phosphorylated myosin light chain (pMLC) signaling in the regulation of cytoskeletal organization (Ridley, 2001; Hall, 2012; Knipe et al., 2015). The RhoA/ROCK pathway regulates stress fiber formation and focal adhesion dynamics in

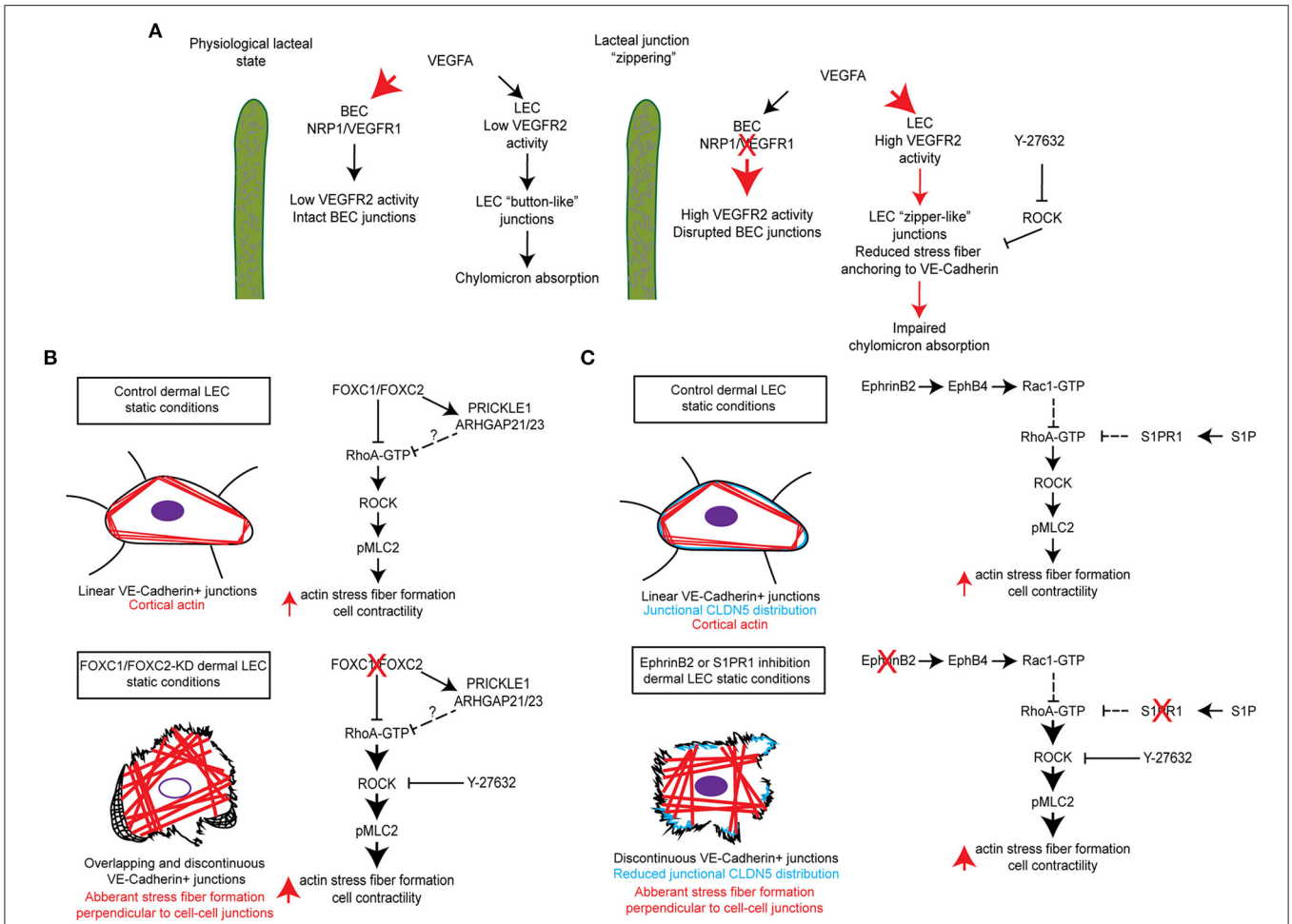

FIGURE 2 | Molecular mechanisms regulating RhoA/ROCK signaling and cytoskeletal activity in maintenance of lymphatic junctional integrity. **(A)** In the lacteals, blood endothelial cell (BEC) expression of the receptors NRP1 and VEGFR-1 regulates the bioavailability of VEGFA resulting in low VEGFR-2 signaling activity in BECs, which maintains intact BEC junctions, and low VEGFR-2 signaling activity in LECs, which maintains "button-like" junctions and facilitates chylomicron absorption. Inducible endothelial-specific deletion of NRP1 and VEGFR-1 results in high VEGFA bioavailability and activation of BEC and LEC VEGFR-2, which results in disrupted BEC junctions and the formation of "zipper-like" junctions in LECs by reducing actin stress fiber anchoring to VE-Cadherin. This in turn impairs chylomicron absorption into lacteals. Moreover, chemical inhibition of ROCK by Y-27632 also reduces stress fiber anchoring to VE-Cadherin and induces the formation of LEC "zipper-like" junctions under physiological conditions (Zhang et al., 2018). **(B)** siRNA-mediated knockdown of FOXC1 and FOXC2 in human dermal lymphatic endothelial cells (HDLECs) induced the formation of overlapping and discontinuous VE-Cadherin+ cell junctions and stimulated aberrant actin stress fiber formation perpendicular to VE-Cadherin+ cell junctions. Treatment of cells with the ROCK inhibitor Y-27632 was able to rescue this impaired phenotype and restore continuous junctions in HDLECs. It is postulated that transcriptional regulation of a molecular signaling complex, consisting of the planar cell polarity signaling component PRICKLE1 and the RhoA GTPase activating proteins (GAPs) Arhgap21 and Arhgap23, by FOXC1 and FOXC2 negatively regulates downstream Rho/ROCK signaling as previously described (Norden et al., 2020). **(C)** siRNA-mediated knockdown of the ligand EphrinB2, subsequently resulting in impaired signaling through its receptor EphB4, was shown to reduce Rac1 GTPase activation in HDLECs. Furthermore, antibody mediated inhibition of EphrinB2 resulted in the formation of discontinuous cell junctions, which was accompanied by reduced junctional CLDN5 distribution and stimulation of aberrant actin stress fiber formation (Frye et al., 2020). In contrast, siRNA-mediated knockdown or chemical inhibition of S1PR1 in HDLECs was shown to enhance RhoA GTPase activation, which also resulted in the formation of discontinuous cell junctions and reduced junctional CLDN5 distribution (Geng et al., 2020). In both instances, pretreatment of HDLECs with Y-27632 was able to rescue the impaired phenotype induced by inhibition of either EphrinB2/EphB4 or S1PR1 signaling.

blood endothelial cell barrier function and permeability (Carbajal et al., 2000; Van Nieuw Amerongen et al., 2000; Wojciak-Stothard et al., 2001; Spindler et al., 2010; Bowers et al., 2016; Cerutti and Ridley, 2017). As endothelial junctions are maintained by a balance of the actin cytoskeleton and myosin-based actin pulling forces anchoring to endothelial junctions, RhoA/ROCK-dependent cytoskeletal dynamics controls endothelial junction integrity (Dorland and Huveneers, 2017). In cultured LECs, VEGFR-2 activation induces junction zippering by reducing actin stress fiber anchoring to perpendicularly formed VE-cadherin, which is attributable to the inhibition of ROCK activity (Zhang et al., 2018). Furthermore, treatment of neonatal mice with the ROCK inhibitor Y27632 enhances lacteal zipper junction formation and reduces chylomicron transport into

mesenteric lymphatic vessels, whereas the ROCK inhibition does not affect junctions of villus blood capillaries (Zhang et al., 2018) (**Table 1**, **Figure 2A**). Considering these differences in the vasculature of the villi, further studies are needed to elucidate the molecular mechanisms underlying opposing effects of VEGFR-2 signaling on blood and lymphatic endothelial cell junctions.

FOXC1 AND FOXC2 TRANSCRIPTION FACTORS AS REGULATORS OF LEC JUNCTIONAL INTEGRITY

FOXC1 and FOXC2 are closely related members of the FOX transcription factor family and have numerous essential roles in cardiovascular development, health, and disease (De Val and Black, 2009; Kume, 2009; Lam et al., 2013). Mutations or changes in the copy number of human *FOXC1* are associated with autosomal-dominant Axenfeld-Rieger syndrome, which is characterized by anterior segment abnormalities in the eye and extraocular defects (Tumer and Bach-Holm, 2009; Seifi and Walter, 2018), while inactivating mutations in human *FOXC2* are responsible for the autosomal dominant syndrome Lymphedema-distichiasis, which is characterized by obstructed lymph drainage in the limbs, venous valve failure, and by the growth of extra eyelashes (distichiasis) that arise from the meibomian glands (Mansour et al., 1993; Fang et al., 2000). FOXC2 expression is upregulated in LECs by oscillatory shear stress (OSS) and is highly enriched in the valve sinuses of lymphatic collecting vessels (Sabine et al., 2012, 2015). FOXC2 is an essential regulator of connexin 37 (Cx37) and calcineurin/NFAT signaling during lymphatic valve initiation (Petrova et al., 2004; Norrmen et al., 2009; Sabine et al., 2012) and is critical for the maintenance of lymphatic valves via regulation of LEC junctional integrity (Sabine et al., 2015). Corresponding with evidence that individuals with *FOXC2* mutations have hyperplastic lymphatic vessels (Mansour et al., 1993; Brice et al., 2002), FOXC2 as well as FOXC1 are essential negative regulators of developmental lymphangiogenesis (Fatima et al., 2016). Of note, dermal LEC junctions stained with VE-cadherin and Lyve1 are disrupted in the dorsal embryonic skin of E14.5 LEC-specific double mutant mice for *Foxc1* and *Foxc2*, suggesting that lack of the two genes impairs the junctional integrity of dermal lymphatic vessels (Fatima et al., 2016).

A recent study further demonstrates a complementary role of FOXC1 in addition to FOXC2 as key mediators of mechanotransduction in the regulation of LEC junctional integrity (Norden et al., 2020). Unlike FOXC2, FOXC1 is not increased in LECs by OSS, but by laminar shear stress (LSS), and FOXC1 is highly enriched in LECs located at the leading free-edge of the intraluminal side of valve leaflets that are exposed to LSS in mesenteric lymphatic valves of the adult mice (Norden et al., 2020). Inducible endothelial cell (EC)-specific *Foxc1* deletion in mice impairs postnatal lymphatic valve maturation, whereas EC-deletion of *Foxc2* induces valve degeneration, which is exacerbated in EC-specific compound *Foxc1* and *Foxc2* mutant mice. Mechanistically, *in vitro* loss of FOXC1 or FOXC2 induces hyper-activation of contractile stress fibers in LECs, which is rescued by the ROCK inhibitor Y27632. Pharmacological inhibition of ROCK by the treatment with Y27632 also improves LEC barrier integrity of mesenteric collecting vessels in both single EC-*Foxc2* and compound EC-*Foxc1; Foxc2* mutant mice, while valve degeneration is partially rescued in only EC-*Foxc2* mutants (Norden et al., 2020). These findings elucidate a key contribution of FOXC1 and FOXC2 in regulating lymphatic valve maintenance and LEC junction integrity via RhoA/ROCK-dependent cytoskeletal organization (**Table 1**, **Figure 2B**).

RECEPTOR CROSSTALK OF LYSOPHOSPHOLIPIDS, SPHINGOSINE 1-PHOSPHATE (S1P) AND LYSOPHOSPHATIDIC ACID (LPA)

S1P and LPA, structurally related lipid mediators, activate G protein–coupled receptors (GPCRs) to regulate various cellular processes, including cytoskeletal dynamics (Moolenaar and Hla, 2012; Proia and Hla, 2015). Despite evidence that the two lysophospholipids have redundant functions, the precise mechanisms of crosstalk between the S1P and LPA signaling pathways remain poorly understood. A genome-wide CRISPR/dCas9–based GPCR signaling screen recently identified the LPAR1 receptor as a key regulator of the S1PR1 receptor-mediated signaling coupling to the antagonistic, β-arrestin-dependent receptor internalization pathway (Hisano et al., 2019). High resolution imaging of cell-cell junctions of sinus-lining LECs of mouse lumbar, popliteal, brachial, and mesenteric lymph nodes reveals both continuous and punctate VE-cadherin+ LEC junctions. In mice treated with the LPAR1 inhibitor AM095 or in *Lpar1* mutant mice, S1PR1 coupling to β-arrestin is suppressed in sinus-lining LECs of lymph nodes, accompanied by a decrease in punctate junctions and an increase in continuous junctions. These findings suggest that LPAR1 signaling attenuates S1P signaling and enhances the junctional porosity of sinus LECs by suppressing the formation of continuous junctions. As LPAR1 signaling controls RhoA/ROCK-mediated cytoskeletal dynamics (Ridley, 2001; Hall, 2012; Knipe et al., 2015), LPA treatment induces stress fiber formation, increased phosphorylation of MLC, and the formation of punctate, intracellular gaps in VE-cadherin-stained cell junctions in human umbilical vein endothelial cells (HUVECs), whereas S1PR1 activation stimulates continuous, zipper-like junctions with cortical F-actin formation. Moreover, it was recently shown that S1PR1 signaling suppresses RhoA GTPase activation in cultured LECs, whereas its blockade results in the formation of discontinuous LEC junctions, which is rescued by ROCK inhibitor Y-27632 (Geng et al., 2020) (**Figure 2C**). In contrast to activation of LPAR1 or S1PR1 individually in HUVECs, combined activation of both LPAR1 and S1PR1 results in a hybrid of continuous cell junctions interspersed with punctate VE-cadherin+ structures at the termini of actin-rich stress fibers. Furthermore, LPAR1 signaling attenuates S1PR1-induced barrier function *in vivo*. In mice treated with the LPAR1 inhibitor AM095, the retention of

lymphocytes in lymph nodes is enhanced, suggesting that LPAR1 signaling is critical for the regulation of lymphatic sinus junctional porosity. Together, these results indicate that the crosstalk of S1PR1 and LPAR1 signaling regulates the junctional architecture, barrier function, and lymphocyte egress in sinus-lining LECs of lymph nodes (Hisano et al., 2019) (**Table 1**). Additionally, S1P signaling regulates the formation of button-like junctions of the diaphragm initial lymphatics (Pham et al., 2010). However, whether there is a similar crosstalk mechanism between S1PR1 and LPAR1 in the initial lymphatics remains to be investigated.

THE EPHRINB2-EPHB4 SIGNALING PATHWAY IN LEC JUNCTION STABILITY

The transmembrane ligand EphrinB2 and its receptor EphB4 are essential for both blood and lymphatic vessel development (Adams et al., 1999; Gerety et al., 1999; Makinen et al., 2005; Zhang et al., 2015; Yoshimatsu et al., 2020). However, the role of this signaling pathway in vessel integrity remains largely unknown. Frye et al. shows that postnatal EC-deletion of *EphrinB2* or *EphB4* in mice results in disruption of cell junctions in different lymphatic vascular beds, including dermal and mesenteric collecting lymphatic vessels as well as the subcapsular sinus of the inguinal lymph nodes, whereas the EphrinB2/EphB4 pathway is dispensable for blood vessel integrity (Frye et al., 2020). *In vitro* studies reveal that inhibition of EphrinB2 by a blocking antibody in LECs causes disruption of cortical actin along with an increase in central actin (radial actin and actin stress fibers) and monolayer permeability. As increased actin stress fibers are associated with enhanced RhoA activity, which is negatively regulated by Rac1 (Wu et al., 2009), inhibition of EphB4 activity by Ephrin B2 knockdown in LECs reduces Rac1 activity, thereby increasing RhoA activity. Furthermore, pretreatment with the ROCK inhibitor Y-27632 inhibits the EphrinB2 blockade-induced junctional and cytoskeletal effects in LECs. Together, basal EphrinB2/EphB4 signaling controls the stability of LEC junctions via RhoA/ROCK-dependent regulation of cytoskeletal contractility (Frye et al., 2020) (**Table 1**, **Figure 2C**).

CONCLUDING REMARKS

Given the plasticity of specialized lymphatic endothelial cell junctions, zipper- and button-like junctions are tightly maintained to keep lymphatic vessel integrity and function for tissue homeostasis. It has become increasingly evident that disrupted LEC junctions are potentially associated with various diseases, including lymphatic leakage present in chylothorax and lymphedema, metabolic syndrome, and impaired immune surveillance (Cifarelli and Eichmann, 2019; Jiang et al., 2019; Xiao et al., 2019; Norden and Kume, 2020; Zhang et al., 2020). The recent seminal studies summarized in this review provide compelling evidence that RhoA/ROCK signaling regulates LEC junction integrity in different vascular beds (Zhang et al., 2018; Hisano et al., 2019; Frye et al., 2020; Norden et al., 2020) (**Table 1**, **Figure 2**). LECs are known to have the ability to undergo endothelial-to-mesenchymal transition (EndMT) by acquiring a mesenchymal cell phenotype, including loss of cell-cell junctions (Ichise et al., 2014; Dejana et al., 2017; Yoshimatsu et al., 2020). Another recent study demonstrates that as a non-Smad pathway, RhoA/ROCK signaling participates in TGF-β-induced EndMT of human dermal LECs *in vitro* (Yoshimatsu et al., 2020). This observation also reinforces the importance of RhoA/ROCK activity in the regulation of LEC junction integrity. As shown in rodent models (Zhang et al., 2018), selective targeting RhoA/ROCK signaling in lacteals of the small intestine is clinically of significance to a novel therapeutic approach for the treatment of obesity and metabolic dysfunction. ROCK inhibitors have been shown to have beneficial effects in experimental animal models of cardiovascular and metabolic disease (Kikuchi et al., 2007; Shi and Wei, 2013; Okin and Medzhitov, 2016), as well as for treatment of cerebral vasospasm, a condition in which the blood vessels in the brain narrow and blood flow is reduced (Shibuya et al., 1992; Zhao et al., 2006; Liu et al., 2012). Yet, additional comprehensive studies are needed to fully elucidate the mechanisms by which the signaling pathways associated with transcriptional regulation control LEC junction integrity. Investigations into the molecular and cellular mechanisms that support the formation, maintenance, and function of lymphatic vessels will have critical implications for the development and optimization of potential therapeutic targets to modulate LEC junctions, permeability and function in disease characterized by dysregulated inflammation, lipid metabolism, and immune responses.

AUTHOR CONTRIBUTIONS

PN contributed to the editing of the manuscript and making the figures. TK contributed to the concepts, writing, editing, and final formatting of the manuscript. All authors contributed to the article and approved the submitted version.

FUNDING

This work was supported by the National Institutes of Health Grants R01HL126920 and R01HL144129 (to TK) and 5T32HL094293 (to PN).

REFERENCES

Adams, R. H., Wilkinson, G. A., Weiss, C., Diella, F., Gale, N. W., Deutsch, U., et al. (1999). Roles of ephrinB ligands and EphB receptors in cardiovascular development: demarcation of arterial/venous domains, vascular morphogenesis, and sprouting angiogenesis. *Genes Dev.* 13, 295–306. doi: 10.1101/gad.13.3.295

Akwii, R. G., Sajib, M. S., Zahra, F. T., and Mikelis, C. M. (2019). Role of Angiopoietin-2 in vascular physiology and pathophysiology. *Cells* 8:471. doi: 10.3390/cells8050471

Aranguren, X. L., Beerens, M., Coppiello, G., Wiese, C., Vandersmissen, I., Lo Nigro, A., et al. (2013). COUP-TFII orchestrates venous and lymphatic endothelial identity by homo- or hetero-dimerisation with PROX1. *J. Cell Sci*. 126, 1164–1175. doi: 10.1242/jcs.116293

Baluk, P., Fuxe, J., Hashizume, H., Romano, T., Lashnits, E., Butz, S., et al. (2007). Functionally specialized junctions between endothelial cells of lymphatic vessels. *J. Exp. Med*. 204, 2349–2362. doi: 10.1084/jem.20062596

Barker, N. (2014). Adult intestinal stem cells: critical drivers of epithelial homeostasis and regeneration. *Nat. Rev. Mol. Cell Biol*. 15, 19–33. doi: 10.1038/nrm3721

Bernier-Latmani, J., Cisarovsky, C., Demir, C. S., Bruand, M., Jaquet, M., Davanture, S., et al. (2015). DLL4 promotes continuous adult intestinal lacteal regeneration and dietary fat transport. *J. Clin. Invest.* 125, 4572–4586. doi: 10.1172/JCI82045

Bernier-Latmani, J., and Petrova, T. V. (2017). Intestinal lymphatic vasculature: structure, mechanisms and functions. *Nat. Rev. Gastroenterol. Hepatol*. 14, 510–526. doi: 10.1038/nrgastro.2017.79

Bowers, S. L., Norden, P. R., and Davis, G. E. (2016). Molecular signaling pathways controlling vascular tube morphogenesis and pericyte-induced tube maturation in 3D extracellular matrices. *Adv. Pharmacol.* 77, 241–280. doi: 10.1016/bs.apha.2016.04.005

Brice, G., Mansour, S., Bell, R., Collin, J. R., Child, A. H., Brady, A. F., et al. (2002). Analysis of the phenotypic abnormalities in lymphoedema-distichiasis syndrome in 74 patients with FOXC2 mutations or linkage to 16q24. *J. Med. Genet*. 39, 478–483. doi: 10.1136/jmg.39.7.478

Carbajal, J. M., Gratrix, M. L., Yu, C. H., and Schaeffer, R. C. Jr. (2000). ROCK mediates thrombin's endothelial barrier dysfunction. *Am. J. Physiol. Cell Physiol*. 279, C195–204. doi: 10.1152/ajpcell.2000.279.1.C195

Casley-Smith, J. R. (1962). The identification of chylomicra and lipoproteins in tissue sections and their passage into jejunal lacteals. *J. Cell Biol*. 15, 259–277. doi: 10.1083/jcb.15.2.259

Cerutti, C., and Ridley, A. J. (2017). Endothelial cell-cell adhesion and signaling. *Exp. Cell Res*. 358, 31–38. doi: 10.1016/j.yexcr.2017.06.003

Cifarelli, V., and Eichmann, A. (2019). The intestinal lymphatic system: functions and metabolic implications. *Cell Mol. Gastroenterol. Hepatol*. 7, 503–513. doi: 10.1016/j.jcmgh.2018.12.002

Coso, S., Bovay, E., and Petrova, T. V. (2014). Pressing the right buttons: signaling in lymphangiogenesis. *Blood* 123, 2614–2624. doi: 10.1182/blood-2013-12-297317

Davis, R. B., Ding, S., Nielsen, N. R., Pawlak, J. B., Blakeney, E. S., and Caron, K. M. (2019). Calcitonin-receptor-like receptor signaling governs intestinal lymphatic innervation and lipid uptake. *ACS Pharmacol. Transl. Sci*. 2, 114–121. doi: 10.1021/acsptsci.8b00061

Davis, R. B., Kechele, D. O., Blakeney, E. S., Pawlak, J. B., and Caron, K. M. (2017). Lymphatic deletion of calcitonin receptor-like receptor exacerbates intestinal inflammation. *JCI Insight* 2:e92465. doi: 10.1172/jci.insight.92465

De Val, S., and Black, B. L. (2009). Transcriptional control of endothelial cell development. *Dev. Cell* 16, 180–195. doi: 10.1016/j.devcel.2009.01.014

Dejana, E., Hirschi, K. K., and Simons, M. (2017). The molecular basis of endothelial cell plasticity. *Nat. Commun*. 8:14361. doi: 10.1038/ncomms 14361

Dejana, E., Orsenigo, F., Molendini, C., Baluk, P., and Mcdonald, D. M. (2009a). Organization and signaling of endothelial cell-to-cell junctions in various regions of the blood and lymphatic vascular trees. *Cell Tissue Res*. 335, 17–25. doi: 10.1007/s00441-008-0694-5

Dejana, E., Tournier-Lasserve, E., and Weinstein, B. M. (2009b). The control of vascular integrity by endothelial cell junctions: molecular basis and pathological implications. *Dev. Cell* 16, 209–221. doi: 10.1016/j.devcel.2009.01.004

Dellinger, M., Hunter, R., Bernas, M., Gale, N., Yancopoulos, G., Erickson, R., et al. (2008). Defective remodeling and maturation of the lymphatic vasculature in Angiopoietin-2 deficient mice. *Dev. Biol.* 319, 309–320. doi: 10.1016/j.ydbio.2008.04.024

Dixon, J. B. (2010). Mechanisms of chylomicron uptake into lacteals. *Ann. N. Y. Acad. Sci.* 1207, E52–57. doi: 10.1111/j.1749-6632.2010.05716.x

Dixon, J. B., Raghunathan, S., and Swartz, M. A. (2009). A tissue-engineered model of the intestinal lacteal for evaluating lipid transport by lymphatics. *Biotechnol. Bioeng*. 103, 1224–1235. doi: 10.1002/bit.22337

Dorland, Y. L., and Huveneers, S. (2017). Cell-cell junctional mechanotransduction in endothelial remodeling. *Cell. Mol. Life Sci*. 74, 279–292. doi: 10.1007/s00018-016-2325-8

Duong, C. N., and Vestweber, D. (2020). Mechanisms ensuring endothelial junction integrity beyond VE-cadherin. *Front. Physiol*. 11:519. doi: 10.3389/fphys.2020.00519

Eklund, L., Kangas, J., and Saharinen, P. (2017). Angiopoietin-Tie signalling in the cardiovascular and lymphatic systems. *Clin. Sci*. 131, 87–103. doi: 10.1042/CS20160129

Escobedo, N., and Oliver, G. (2016). Lymphangiogenesis: origin, specification, and cell fate determination. *Annu. Rev. Cell Dev. Biol*. 32, 677–691. doi: 10.1146/annurev-cellbio-111315-124944

Fang, J., Dagenais, S. L., Erickson, R. P., Arlt, M. F., Glynn, M. W., Gorski, J. L., et al. (2000). Mutations in FOXC2 (MFH-1), a forkhead family transcription factor, are responsible for the hereditary lymphedema-distichiasis syndrome. *Am. J. Hum. Genet*. 67, 1382–1388. doi: 10.1086/316915

Fatima, A., Wang, Y., Uchida, Y., Norden, P., Liu, T., Culver, A., et al. (2016). Foxc1 and Foxc2 deletion causes abnormal lymphangiogenesis and correlates with ERK hyperactivation. *J. Clin. Invest.* 126, 2437–2451. doi: 10.1172/JCI80465

Francois, M., Caprini, A., Hosking, B., Orsenigo, F., Wilhelm, D., Browne, C., et al. (2008). Sox18 induces development of the lymphatic vasculature in mice. *Nature* 456, 643–647. doi: 10.1038/nature07391

Francois, M., Short, K., Secker, G. A., Combes, A., Schwarz, Q., Davidson, T. L., et al. (2012). Segmental territories along the cardinal veins generate lymph sacs via a ballooning mechanism during embryonic lymphangiogenesis in mice. *Dev. Biol*. 364, 89–98. doi: 10.1016/j.ydbio.2011.12.032

Frye, M., Stritt, S., Ortsater, H., Hernandez Vasquez, M., Kaakinen, M., Vicente, A., et al. (2020). EphrinB2-EphB4 signalling provides Rho-mediated homeostatic control of lymphatic endothelial cell junction integrity. *Elife* 9:57732. doi: 10.7554/eLife.57732.sa2

Gale, N. W., Thurston, G., Hackett, S. F., Renard, R., Wang, Q., Mcclain, J., et al. (2002). Angiopoietin-2 is required for postnatal angiogenesis and lymphatic patterning, and only the latter role is rescued by Angiopoietin-1. *Dev. Cell* 3, 411–423. doi: 10.1016/S1534-5807(02)00217-4

Geng, X., Yanagida, K., Akwii, R. G., Choi, D., Chen, L., Ho, Y., et al. (2020). S1PR1 regulates the quiescence of lymphatic vessels by inhibiting laminar shear stress-dependent VEGF-C signaling. *JCI Insight* 5:e137652. doi: 10.1172/jci.insight.137652

Gerety, S. S., Wang, H. U., Chen, Z. F., and Anderson, D. J. (1999). Symmetrical mutant phenotypes of the receptor EphB4 and its specific transmembrane ligand ephrin-B2 in cardiovascular development. *Mol. Cell* 4, 403–414. doi: 10.1016/S1097-2765(00)80342-1

Hagerling, R., Hoppe, E., Dierkes, C., Stehling, M., Makinen, T., Butz, S., et al. (2018). Distinct roles of VE-cadherin for development and maintenance of specific lymph vessel beds. *EMBO J*. 37:e98271. doi: 10.15252/embj.201798271

Hagerling, R., Pollmann, C., Andreas, M., Schmidt, C., Nurmi, H., Adams, R. H., et al. (2013). A novel multistep mechanism for initial lymphangiogenesis in mouse embryos based on ultramicroscopy. *EMBO J*. 32, 629–644. doi: 10.1038/emboj.2012.340

Hall, A. (2012). Rho family GTPases. *Biochem. Soc. Trans*. 40, 1378–1382. doi: 10.1042/BST20120103

Hisano, Y., Kono, M., Cartier, A., Engelbrecht, E., Kano, K., Kawakami, K., et al. (2019). Lysolipid receptor cross-talk regulates lymphatic endothelial junctions in lymph nodes. *J. Exp. Med*. 216, 1582–1598. doi: 10.1084/jem.20181895

Hoopes, S. L., Willcockson, H. H., and Caron, K. M. (2012). Characteristics of multi-organ lymphangiectasia resulting from temporal deletion of calcitonin receptor-like receptor in adult mice. *PLoS ONE* 7:e45261. doi: 10.1371/journal.pone.0045261

Ichise, T., Yoshida, N., and Ichise, H. (2014). FGF2-induced Ras-MAPK signalling maintains lymphatic endothelial cell identity by upregulating endothelial-cell-specific gene expression and suppressing TGFbeta signalling through Smad2. *J. Cell Sci*. 127, 845–857. doi: 10.1242/jcs.137836

Jiang, X., Tian, W., Nicolls, M. R., and Rockson, S. G. (2019). The lymphatic system in obesity, insulin resistance, and cardiovascular diseases. *Front. Physiol*. 10:1402. doi: 10.3389/fphys.2019.01402

Karkkainen, M. J., Haiko, P., Sainio, K., Partanen, J., Taipale, J., Petrova, T. V., et al. (2004). Vascular endothelial growth factor C is required for sprouting

of the first lymphatic vessels from embryonic veins. *Nat. Immunol*. 5, 74–80. doi: 10.1038/ni1013

Kazenwadel, J., and Harvey, N. L. (2016). Morphogenesis of the lymphatic vasculature: a focus on new progenitors and cellular mechanisms important for constructing lymphatic vessels. *Dev. Dyn*. 245, 209–219. doi: 10.1002/dvdy.24313

Kikuchi, Y., Yamada, M., Imakiire, T., Kushiyama, T., Higashi, K., Hyodo, N., et al. (2007). A Rho-kinase inhibitor, fasudil, prevents development of diabetes and nephropathy in insulin-resistant diabetic rats. *J. Endocrinol*. 192, 595–603. doi: 10.1677/JOE-06-0045

Kim, K. E., Sung, H. K., and Koh, G. Y. (2007). Lymphatic development in mouse small intestine. *Dev. Dyn*. 236, 2020–2025. doi: 10.1002/dvdy.21200

Klotz, L., Norman, S., Vieira, J. M., Masters, M., Rohling, M., Dube, K. N., et al. (2015). Cardiac lymphatics are heterogeneous in origin and respond to injury. *Nature* 522, 62–67. doi: 10.1038/nature14483

Knipe, R. S., Tager, A. M., and Liao, J. K. (2015). The Rho kinases: critical mediators of multiple profibrotic processes and rational targets for new therapies for pulmonary fibrosis. *Pharmacol. Rev*. 67, 103–117. doi: 10.1124/pr.114.009381

Kume, T. (2009). "The cooperative roles of Foxc1 and Foxc2 in cardiovascular development," in *Forkhead Transcription Factors: Vital Elements in Biology and Medicine, Vol 665*, ed K. Maiese (New York, NY: Springer), 63–77. doi: 10.1007/978-1-4419-1599-3_5

Lam, E. W., Brosens, J. J., Gomes, A. R., and Koo, C. Y. (2013). Forkhead box proteins: tuning forks for transcriptional harmony. *Nat. Rev. Cancer* 13, 482–495. doi: 10.1038/nrc3539

Lee, S., Kang, J., Yoo, J., Ganesan, S. K., Cook, S. C., Aguilar, B., et al. (2009). Prox1 physically and functionally interacts with COUP-TFII to specify lymphatic endothelial cell fate. *Blood* 113, 1856–1859. doi: 10.1182/blood-2008-03-145789

Liu, G. J., Wang, Z. J., Wang, Y. F., Xu, L. L., Wang, X. L., Liu, Y., et al. (2012). Systematic assessment and meta-analysis of the efficacy and safety of fasudil in the treatment of cerebral vasospasm in patients with subarachnoid hemorrhage. *Eur. J. Clin. Pharmacol*. 68, 131–139. doi: 10.1007/s00228-011-1100-x

Mackie, D. I., Al Mutairi, F., Davis, R. B., Kechele, D. O., Nielsen, N. R., Snyder, J. C., et al. (2018). hCALCRL mutation causes autosomal recessive nonimmune hydrops fetalis with lymphatic dysplasia. *J. Exp. Med*. 215, 2339–2353. doi: 10.1084/jem.20180528

Makinen, T., Adams, R. H., Bailey, J., Lu, Q., Ziemiecki, A., Alitalo, K., et al. (2005). PDZ interaction site in ephrinB2 is required for the remodeling of lymphatic vasculature. *Genes Dev*. 19, 397–410. doi: 10.1101/gad.330105

Mansour, S., Brice, G. W., Jeffery, S., and Mortimer, P. (1993). "Lymphedema-distichiasis syndrome," in *GeneReviews(R)*, eds. R. A. Pagon, M. P. Adam, H. H. Ardinger, T. D. Bird, C. R. Dolan, C. T. Fong, et al. (Seattle, WA: University of Washington), 1–25.

Martinez-Corral, I., and Makinen, T. (2013). Regulation of lymphatic vascular morphogenesis: implications for pathological (tumor)lymphangiogenesis. *Exp. Cell Res*. 319, 1618–1625. doi: 10.1016/j.yexcr.2013.01.016

Martinez-Corral, I., Ulvmar, M. H., Stanczuk, L., Tatin, F., Kizhatil, K., John, S. W., et al. (2015). Nonvenous origin of dermal lymphatic vasculature. *Circ. Res*. 116, 1649–1654. doi: 10.1161/CIRCRESAHA.116.306170

Moolenaar, W. H., and Hla, T. (2012). SnapShot: bioactive lysophospholipids. *Cell* 148, 378–378e372. doi: 10.1016/j.cell.2012.01.013

Norden, P. R., and Kume, T. (2020). The role of lymphatic vascular function in metabolic disorders. *Front. Physiol*. 11:404. doi: 10.3389/fphys.2020.00404

Norden, P. R., Sabine, A., Wang, Y., Demir, C. S., Liu, T., Petrova, T. V., et al. (2020). Shear stimulation of FOXC1 and FOXC2 differentially regulates cytoskeletal activity during lymphatic valve maturation. *Elife* 9:e53814. doi: 10.7554/eLife.53814.sa2

Norrmen, C., Ivanov, K. I., Cheng, J., Zangger, N., Delorenzi, M., Jaquet, M., et al. (2009). FOXC2 controls formation and maturation of lymphatic collecting vessels through cooperation with NFATc1. *J. Cell Biol*. 185, 439–457. doi: 10.1083/jcb.200901104

Nurmi, H., Saharinen, P., Zarkada, G., Zheng, W., Robciuc, M. R., and Alitalo, K. (2015). VEGF-C is required for intestinal lymphatic vessel maintenance and lipid absorption. *EMBO Mol. Med*. 7, 1418–1425. doi: 10.15252/emmm.201505731

Okin, D., and Medzhitov, R. (2016). The effect of sustained inflammation on hepatic mevalonate pathway results in hyperglycemia. *Cell* 165, 343–356. doi: 10.1016/j.cell.2016.02.023

Petrova, T. V., Karpanen, T., Norrmen, C., Mellor, R., Tamakoshi, T., Finegold, D., et al. (2004). Defective valves and abnormal mural cell recruitment underlie lymphatic vascular failure in lymphedema distichiasis. *Nat. Med*. 10, 974–981. doi: 10.1038/nm1094

Petrova, T. V., and Koh, G. Y. (2018). Organ-specific lymphatic vasculature: from development to pathophysiology. *J. Exp. Med*. 215, 35–49. doi: 10.1084/jem.20171868

Petrova, T. V., and Koh, G. Y. (2020). Biological functions of lymphatic vessels. *Science* 369:4063. doi: 10.1126/science.aax4063

Pham, T. H., Baluk, P., Xu, Y., Grigorova, I., Bankovich, A. J., Pappu, R., et al. (2010). Lymphatic endothelial cell sphingosine kinase activity is required for lymphocyte egress and lymphatic patterning. *J. Exp. Med*. 207, 17–27. doi: 10.1084/jem.20091619

Potente, M., and Makinen, T. (2017). Vascular heterogeneity and specialization in development and disease. *Nat. Rev. Mol. Cell Biol*. 18, 477–494. doi: 10.1038/nrm.2017.36

Proia, R. L., and Hla, T. (2015). Emerging biology of sphingosine-1-phosphate: its role in pathogenesis and therapy. *J. Clin. Invest*. 125, 1379–1387. doi: 10.1172/JCI76369

Reed, A. L., Rowson, S. A., and Dixon, J. B. (2013). Demonstration of ATP-dependent, transcellular transport of lipid across the lymphatic endothelium using an *in vitro* model of the lacteal. *Pharm. Res*. 30, 3271–3280. doi: 10.1007/s11095-013-1218-x

Ridley, A. J. (2001). Rho family proteins: coordinating cell responses. *Trends Cell Biol*. 11, 471–477. doi: 10.1016/S0962-8924(01)02153-5

Sabesin, S. M., and Frase, S. (1977). Electron microscopic studies of the assembly, intracellular transport, and secretion of chylomicrons by rat intestine. *J. Lipid Res*. 18, 496–511.

Sabine, A., Agalarov, Y., Maby-El Hajjami, H., Jaquet, M., Hagerling, R., Pollmann, C., et al. (2012). Mechanotransduction, PROX1, and FOXC2 cooperate to control connexin37 and calcineurin during lymphatic-valve formation. *Dev. Cell*. 22, 430–445. doi: 10.1016/j.devcel.2011.12.020

Sabine, A., Bovay, E., Demir, C. S., Kimura, W., Jaquet, M., Agalarov, Y., et al. (2015). FOXC2 and fluid shear stress stabilize postnatal lymphatic vasculature. *J. Clin. Invest*. 125, 3861–3877. doi: 10.1172/JCI80454

Saharinen, P., Eklund, L., and Alitalo, K. (2017). Therapeutic targeting of the angiopoietin-TIE pathway. *Nat. Rev. Drug Discov*. 16, 635–661. doi: 10.1038/nrd.2016.278

Seifi, M., and Walter, M. A. (2018). Axenfeld-rieger syndrome. *Clin. Genet*. 93, 1123–1130. doi: 10.1111/cge.13148

Semo, J., Nicenboim, J., and Yaniv, K. (2016). Development of the lymphatic system: new questions and paradigms. *Development* 143, 924–935. doi: 10.1242/dev.132431

Shen, B., Shang, Z., Wang, B., Zhang, L., Zhou, F., Li, T., et al. (2014). Genetic dissection of tie pathway in mouse lymphatic maturation and valve development. *Arterioscler. Thromb. Vasc. Biol*. 34, 1221–1230. doi: 10.1161/ATVBAHA.113.302923

Shi, J., and Wei, L. (2013). Rho kinases in cardiovascular physiology and pathophysiology: the effect of fasudil. *J. Cardiovasc. Pharmacol*. 62, 341–354. doi: 10.1097/FJC.0b013e3182a3718f

Shibuya, M., Suzuki, Y., Sugita, K., Saito, I., Sasaki, T., Takakura, K., et al. (1992). Effect of AT877 on cerebral vasospasm after aneurysmal subarachnoid hemorrhage. Results of a prospective placebo-controlled double-blind trial. *J. Neurosurg*. 76, 571–577. doi: 10.3171/jns.1992.76.4.0571

Souma, T., Thomson, B. R., Heinen, S., Carota, I. A., Yamaguchi, S., Onay, T., et al. (2018). Context-dependent functions of angiopoietin 2 are determined by the endothelial phosphatase VEPTP. *Proc. Natl. Acad. Sci. U. S. A*. 115, 1298–1303. doi: 10.1073/pnas.1714446115

Spindler, V., Schlegel, N., and Waschke, J. (2010). Role of GTPases in control of microvascular permeability. *Cardiovasc. Res*. 87, 243–253. doi: 10.1093/cvr/cvq086

Srinivasan, R. S., Geng, X., Yang, Y., Wang, Y., Mukatira, S., Studer, M., et al. (2010). The nuclear hormone receptor Coup-TFII is required for the initiation and early maintenance of Prox1 expression in lymphatic endothelial cells. *Genes Dev*. 24, 696–707. doi: 10.1101/gad.1859310

Srinivasan, R. S., and Oliver, G. (2011). Prox1 dosage controls the number of lymphatic endothelial cell progenitors and the formation of the lymphovenous valves. *Genes Dev*. 25, 2187–2197. doi: 10.1101/gad.16974811

Stanczuk, L., Martinez-Corral, I., Ulvmar, M. H., Zhang, Y., Lavina, B., Fruttiger, M., et al. (2015). cKit lineage hemogenic endothelium-derived cells contribute to mesenteric lymphatic vessels. *Cell Rep.* 10, 1708–1721. doi: 10.1016/j.celrep.2015.02.026

Suh, S. H., Choe, K., Hong, S. P., Jeong, S. H., Makinen, T., Kim, K. S., et al. (2019). Gut microbiota regulates lacteal integrity by inducing VEGF-C in intestinal villus macrophages. *EMBO Rep*. 20:e46927. doi: 10.15252/embr.201846927

Szymborska, A., and Gerhardt, H. (2018). Hold me, but not too tight-endothelial cell-cell junctions in angiogenesis. *Cold Spring Harb. Perspect. Biol*. 10:e029223. doi: 10.1101/cshperspect.a029223

Tumer, Z., and Bach-Holm, D. (2009). Axenfeld-Rieger syndrome and spectrum of PITX2 and FOXC1 mutations. *Eur. J. Hum. Genet*. 17, 1527–1539. doi: 10.1038/ejhg.2009.93

Van Nieuw Amerongen, G. P., Van Delft, S., Vermeer, M. A., Collard, J. G., and Van Hinsbergh, V. W. (2000). Activation of RhoA by thrombin in endothelial hyperpermeability: role of Rho kinase and protein tyrosine kinases. *Circ. Res*. 87, 335–340. doi: 10.1161/01.RES.87.4.335

Wigle, J. T., and Oliver, G. (1999). Prox1 function is required for the development of the murine lymphatic system. *Cell* 98, 769–778. doi: 10.1016/S0092-8674(00)81511-1

Wojciak-Stothard, B., Potempa, S., Eichholtz, T., and Ridley, A. J. (2001). Rho and Rac but not Cdc42 regulate endothelial cell permeability. *J. Cell Sci*. 114, 1343–1355.

Wu, Y. I., Frey, D., Lungu, O. I., Jaehrig, A., Schlichting, I., Kuhlman, B., et al. (2009). A genetically encoded photoactivatable Rac controls the motility of living cells. *Nature* 461, 104–108. doi: 10.1038/nature08241

Xiao, C., Stahel, P., Nahmias, A., and Lewis, G. F. (2019). Emerging role of lymphatics in the regulation of intestinal lipid mobilization. *Front. Physiol*. 10:1604. doi: 10.3389/fphys.2019.01604

Yamazaki, T., Yoshimatsu, Y., Morishita, Y., Miyazono, K., and Watabe, T. (2009). COUP-TFII regulates the functions of Prox1 in lymphatic endothelial cells through direct interaction. *Genes Cells* 14, 425–434. doi: 10.1111/j.1365-2443.2008.01279.x

Yang, Y., Cha, B., Motawe, Z. Y., Srinivasan, R. S., and Scallan, J. P. (2019). VE-cadherin is required for lymphatic valve formation and maintenance. *Cell Rep*. 28, 2397–2412e2394. doi: 10.1016/j.celrep.2019.07.072

Yang, Y., Garcia-Verdugo, J. M., Soriano-Navarro, M., Srinivasan, R. S., Scallan, J. P., Singh, M. K., et al. (2012). Lymphatic endothelial progenitors bud from the cardinal vein and intersomitic vessels in mammalian embryos. *Blood* 120, 2340–2348. doi: 10.1182/blood-2012-05-428607

Yao, L. C., Baluk, P., Srinivasan, R. S., Oliver, G., and Mcdonald, D. M. (2012). Plasticity of button-like junctions in the endothelium of airway lymphatics in development and inflammation. *Am. J. Pathol.* 180, 2561–2575. doi: 10.1016/j.ajpath.2012.02.019

Yoshimatsu, Y., Kimuro, S., Pauty, J., Takagaki, K., Nomiyama, S., Inagawa, A., et al. (2020). TGF-beta and TNF-alpha cooperatively induce mesenchymal transition of lymphatic endothelial cells via activation of Activin signals. *PLoS ONE* 15:e0232356. doi: 10.1371/journal.pone.0232356

Yuen, D., Grimaldo, S., Sessa, R., Ecoiffier, T., Truong, T., Huang, E., et al. (2014). Role of angiopoietin-2 in corneal lymphangiogenesis. *Invest. Ophthalmol. Vis. Sci*. 55, 3320–3327. doi: 10.1167/iovs.13-13779

Zhang, F., Zarkada, G., Han, J., Li, J., Dubrac, A., Ola, R., et al. (2018). Lacteal junction zippering protects against diet-induced obesity. *Science* 361, 599–603. doi: 10.1126/science.aap9331

Zhang, F., Zarkada, G., Yi, S., and Eichmann, A. (2020). Lymphatic endothelial cell junctions: molecular regulation in physiology and diseases. *Front. Physiol*. 11:509. doi: 10.3389/fphys.2020.00509

Zhang, G., Brady, J., Liang, W. C., Wu, Y., Henkemeyer, M., and Yan, M. (2015). EphB4 forward signalling regulates lymphatic valve development. *Nat. Commun*. 6:6625. doi: 10.1038/ncomms7625

Zhao, J., Zhou, D., Guo, J., Ren, Z., Zhou, L., Wang, S., et al. (2006). Effect of fasudil hydrochloride, a protein kinase inhibitor, on cerebral vasospasm and delayed cerebral ischemic symptoms after aneurysmal subarachnoid hemorrhage. *Neurol. Med. Chir*. 46, 421–428. doi: 10.2176/nmc.46.421

Zheng, W., Nurmi, H., Appak, S., Sabine, A., Bovay, E., Korhonen, E. A., et al. (2014). Angiopoietin 2 regulates the transformation and integrity of lymphatic endothelial cell junctions. *Genes Dev*. 28, 1592–1603. doi: 10.1101/gad.237677.114

Conflict of Interest: The authors declare that the research was conducted in the absence of any commercial or financial relationships that could be construed as a potential conflict of interest.

Copyright © 2021 Norden and Kume. This is an open-access article distributed under the terms of the Creative Commons Attribution License (CC BY). The use, distribution or reproduction in other forums is permitted, provided the original author(s) and the copyright owner(s) are credited and that the original publication in this journal is cited, in accordance with accepted academic practice. No use, distribution or reproduction is permitted which does not comply with these terms.

frontiers in Cell and Developmental Biology

ORIGINAL RESEARCH
published: 12 February 2021
doi: 10.3389/fcell.2021.616610

TGF-β-Induced Endothelial to Mesenchymal Transition Is Determined by a Balance Between SNAIL and ID Factors

*Jin Ma[1,2], Gerard van der Zon[1,2], Manuel A. F. V. Gonçalves[1], Maarten van Dinther[1,2], Midory Thorikay[1,2], Gonzalo Sanchez-Duffhues[1] and Peter ten Dijke[1,2]**

[1] Department of Cell Chemical Biology, Leiden University Medical Center, Leiden, Netherlands, [2] Oncode Institute, Leiden University Medical Center, Leiden, Netherlands

Endothelial-to-mesenchymal transition (EndMT) plays an important role in embryonic development and disease progression. Yet, how different members of the transforming growth factor-β (TGF-β) family regulate EndMT is not well understood. In the current study, we report that TGF-β2, but not bone morphogenetic protein (BMP)9, triggers EndMT in murine endothelial MS-1 and 2H11 cells. TGF-β2 strongly upregulates the transcription factor SNAIL, and the depletion of *Snail* is sufficient to abrogate TGF-β2-triggered mesenchymal-like cell morphology acquisition and EndMT-related molecular changes. Although SLUG is not regulated by TGF-β2, knocking out *Slug* also partly inhibits TGF-β2-induced EndMT in 2H11 cells. Interestingly, in addition to SNAIL and SLUG, BMP9 stimulates inhibitor of DNA binding (ID) proteins. The suppression of *Id1*, *Id2,* or *Id3* expression facilitated BMP9 in inducing EndMT and, in contrast, ectopic expression of ID1, ID2, or ID3 abrogated TGF-β2-mediated EndMT. Altogether, our results show that SNAIL is critical and indispensable for TGF-β2-mediated EndMT. Although SLUG is also involved in the EndMT process, it plays less of a crucial role in it. In contrast, ID proteins are essential for maintaining endothelial traits and repressing the function of SNAIL and SLUG during the EndMT process. These data suggest that the control over endothelial vs. mesenchymal cell states is determined, at least in part, by a balance between the expression of SNAIL/SLUG and ID proteins.

Keywords: bone morphogenetic protein, endothelial cell, EndMT, inhibitor of DNA binding, transcription factor, transforming growth factor-β2

OPEN ACCESS

Edited by:
Bin Ren,
University of Alabama at Birmingham,
United States

Reviewed by:
Katie Finegan,
The University of Manchester,
United Kingdom
Christian Hiepen,
Freie Universität Berlin, Germany

***Correspondence:**
Peter ten Dijke
P.ten_Dijke@lumc.nl

Specialty section:
This article was submitted to Signaling, a section of the journal Frontiers in Cell and Developmental Biology

Received: *12 October 2020*
Accepted: *20 January 2021*
Published: *12 February 2021*

Citation:
Ma J, van der Zon G, Gonçalves MAFV, van Dinther M, Thorikay M, Sanchez-Duffhues G and ten Dijke P (2021) TGF-β-Induced Endothelial to Mesenchymal Transition Is Determined by a Balance Between SNAIL and ID Factors. Front. Cell Dev. Biol. 9:616610. doi: 10.3389/fcell.2021.616610

INTRODUCTION

In diverse physiological and pathological processes, endothelial cells show remarkable plasticity as they lose endothelial properties and differentiate into mesenchymal cells, a process termed endothelial-to-mesenchymal transition (EndMT) (Dejana and Lampugnani, 2018). EndMT is a gradual and reversible dynamic process, which shares similarities with epithelial-to-mesenchymal transition (EMT) (Saito, 2013). Epithelial cells can acquire different EMT features with mixed epithelial/mesenchymal phenotype. This has recently been described as epithelial cell plasticity (Yang et al., 2020). Unlike EMT, however, our current understanding of the molecular mechanisms

that control EndMT are limited. When cobblestone-shaped endothelial cells (ECs) undergo EndMT, they gradually lose their tight junctions and acquire a mesenchymal-like identity and the appearance of elongated fibroblasts. In order to monitor the transition of ECs toward fibroblast-like cells, a number of proteins can be studied. For example, during EndMT the cells progressively express less cell-cell adhesion- and endothelial-specific proteins, such as vascular endothelial (VE)-cadherin, platelet/EC adhesion molecule-1 (CD31/PECAM-1), tyrosine kinase with immunoglobulin-like, and epidermal growth factor (EGF)-like domains 1 (TIE1), TIE2, and von Willebrand factor (vWF), while mesenchymal factors accumulate, including N-cadherin, α-smooth muscle actin (α-SMA), smooth muscle protein 22α (SM22α), fibronectin, and fibroblast specific protein-1 (FSP-1). EndMT participates in different physiological and pathological processes (Potenta et al., 2008; Yoshimatsu and Watabe, 2011; Hong et al., 2018; Souilhol et al., 2018). Thus, specific modulation of EndMT may provide a therapeutic benefit. For example, targeting of EndMT might be beneficial in treating human disorders, whereas controlled induction of EndMT might be a potential application in tissue engineering and wound healing (Ma et al., 2020). To allow for clinical translation of EndMT modulating approaches, more insights into the underlying molecular and cellular mechanisms of EndMT are needed.

As a complex biological process, EndMT is triggered by, among other factors, numerous cytokines and is modulated by diverse signaling pathways. Extensive studies have shown that TGF-β family proteins, including TGF-βs (Van Meeteren and Ten Dijke, 2012), activins and bone morphogenetic proteins (BMPs) (Zeisberg et al., 2007; Medici et al., 2010; Zhang et al., 2018), all have a pivotal function in controlling EndMT, as well as, EMT (Miyazono, 2009). TGF-β2 was found to be the most potent TGF-β isoform in inducing EndMT, and the most relevant TGF-β isoform involved in regulating EndMT during heart cushion development (Camenisch et al., 2002b; Azhar et al., 2009). However, knowledge regarding the effects and mechanisms by which BMPs control EndMT, remains incomplete. For instance, BMP4 activates EndMT, whereas its close relative BMP7 has been reported to antagonize it (Zeisberg et al., 2007; Medici et al., 2010). Notably, the effect of BMP9 on EndMT remains to be determined despite the fact that BMP9 is one of the major BMP ligands in ECs (Suzuki et al., 2010; Dyer et al., 2014).

TGF-β and BMPs initiate cellular responses by binding to specific cell surface transmembrane type I and type II receptors, including type I (TβRI) and type II (TβRII) receptors for TGF-β; and BMP type I receptors (BMPRIs) and BMP type II receptor (BMPRII) for BMPs (Massagué, 2008). Upon ligand-induced heteromeric complex formation, the activated receptor complex phosphorylates receptor-regulated downstream effectors, termed SMADs. TβRI induces phosphorylation of SMAD2/3 and BMPRI mediates phosphorylation of SMAD1/5/8 (Derynck and Budi, 2019). Activated R-SMADs partner with the common mediator SMAD4 and translocate into the nucleus, where they induce the expression of specific sets of target genes, such as *plasminogen activator inhibitor-1* (*PAI1*) and *Ids* (*Id1, Id2, Id3,* and *Id4*). The former and latter genes are upregulated by exposure to TGF-β and BMPs stimuli, respectively (Pepper et al., 1991; Dennler et al., 1998; Hollnagel et al., 1999; Korchynskyi and Ten Dijke, 2002).

The members of the SNAIL family of transcription factors, which includes SNAIL and SLUG (a.k.a. SNAIL1 and SNAIL2, respectively), contain Cys_2His_2 zinc-finger motifs that bind to E-boxes (5′-CAGGTG-3′) located in certain gene promoters (Nieto, 2002). Upon TGF-β and BMP stimulation, SNAIL proteins are upregulated and bind to the promoters of endothelial-related genes to decrease endothelial protein expression, resulting in ECs with diminished endothelial function and gradually enhanced acquisition of a mesenchymal cell morphology. These EMT-inducing transcription factors may work together and have specific functions in orchestrating the complex EndMT/EMT process (Yang et al., 2020). Of notice, there are somewhat conflicting reports regarding the role of ID proteins in EMT and EndMT, in part likely caused by cellular context-dependent factors. Indeed, although high ID1 expression has been correlated with enhanced EMT in advanced bladder tumor stages (Hu et al., 2013), and promotion of carcinogenesis and metastasis in lung cancer (Castañón et al., 2017), ID1 has also been described to antagonize EMT in mouse NMuMG mammary epithelial cells (Kondo et al., 2004). ID proteins have been shown to dimerize with the transcription factor E2A, which promotes EMT by directly binding to gene regulatory sequences (Massari and Murre, 2000). Thus, how TGF-β and BMPs regulate EndMT and how does the interplay between SNAIL family members and ID proteins influences EndMT, remain poorly understood.

In the present study, we investigated whether the TGF-β family ligands TGF-β2 and BMP9 are capable of inducing EndMT in two murine endothelial cell lines, i.e., pancreatic microvascular endothelial cells (MS-1) and lymphatic endothelial cells (2H11). We show that TGF-β2 upregulates specific EndMT transcription factors and that SNAIL, in particular, is required for EndMT. In contrast, BMP9 fails to induce full-fledged EndMT, although it strongly induces transient expression of EndMT-associated transcription factors. Mechanistically, IDs that accumulate in response to BMP9 stimulation, exhibit opposite effects to those triggered by SNAIL family proteins and antagonize TGF-β2-mediated EndMT. Given the role of TGF-β and BMPs in regulating EndMT in postnatal disease processes, our results provide important insights that may guide future therapeutic interventions based on the modulation of EndMT.

MATERIALS AND METHODS

Materials

Recombinant human TGF-β2 was a kind gift from Joachim Nickel, University of Wurzburg. Human BMP9 (3209-BP/CF) and mouse BMP9 (5566-BP) were obtained from R&D systems. Human BMP6 was a kind gift from Slobodan Vukicevic, University of Zagreb. Human TGF-β1 (HZ-1011) was purchased from HumanZyme. Human TGF-β3 was a kind gift from Andrew Hinck, University of Pittsburgh. Mouse TGF-β2 (7346-B2) was purchased from Bio-Techne. Puromycin (P9620) was obtained from Sigma-Aldrich. The Blasticidin (R21001) and

the ID proteins chemical inhibitor AGX51 (HY-129241), were purchased from Invitrogen to MedChem Express, respectively.

Cell Culture

Murine pancreatic microvascular endothelial cells (MS-1) and murine lymphoid endothelial cells (2H11) were cultured on 0.1% (w/v) gelatin (G1890, Sigma-Aldrich) in Dulbecco's modified Eagles's medium (DMEM, 11965092, Thermo Fisher Scientific) supplemented with 10% fetal bovine serum (FBS, 16000044, Thermo Fisher Scientific) and 100 IU ml^{-1} penicillin/streptomycin. Human embryonic kidney 293T cells were cultured in DMEM supplemented with 10% FBS and 100 IU ml^{-1} penicillin/streptomycin. All cell lines were maintained in a 5% CO_2 humidified air incubator at 37°C and were regularly checked for the absence of mycoplasma infection.

Quantitative Reverse Transcription PCR (RT-qPCR)

Total RNAs were isolated using the NucleoSpin RNA II kit (740955, BIOKE) according to the instructions provided by the manufacturer. After quantifying the RNA concentration by Nanodrop (Isogen, Maarssen, Netherlands), reverse transcription was performed on the same amount of RNA using the RevertAid First Strand cDNA Synthesis Kit (K1621, Thermo Fisher Scientific). After the cDNA synthesis, RT-qPCR was conducted with GoTaq qPCR Master Mix (A6001, Promega) using the CFX Connect Detection System (1855201, Bio-Rad). The expression levels of all target genes were determined using the $\Delta\Delta$Ct method and were normalized for *Gapdh* expression on a per sample basis. All DNA primer sequences that were used in the study are shown in **Supplementary Table S1**.

Western Blot Analysis

Cells were lysed in radioimmunoprecipitation assay (RIPA) lysis buffer containing a protease inhibitor cocktail (11836153001, Roche). After spinning down cellular debris at $1.2 \times 10^4 \times$ g for 5 min, protein concentrations were quantified by using the bicinchoninic acid (BCA) protein assay kit (23235, Thermo Fisher Scientific). Next, the proteins were boiled for 5 min and then loaded and separated through sodium dodecyl sulfate polyacrylamide gel electrophoresis (SDS-PAGE). The resolved proteins were then transferred onto 45 μm polyvinylidene difluoride (PVDF) membranes (IPVH00010, Merck Millipore). After blocking the membranes with 5% non-fat dry milk for 1 h at room temperature in tris-buffered saline with Tween 20 (TBST), the membranes were sequentially incubated with primary and secondary antibodies. The signals were visualized by using the Clarity™ Western ECL Substrate (1705060, Bio-Rad) and the ChemiDoc Imaging System (17001402, Bio-Rad). The primary antibodies used for immunoblotting were diluted 1,000 fold in TBST and were raised against the following proteins: phospho-SMAD1/5 (9516S, Cell Signaling), phospho-SMAD2 (pSMAD2, home-made (Persson et al., 1998), SNAIL (3879, Cell Signaling), SLUG (9585, Cell Signaling), SMAD1 (6944S, Cell Signaling), SMAD2 (3103S, Cell Signaling), ID1 (sc-133104, Santa Cruz), ID2 (sc-489, Santa Cruz), ID3 (sc-490, Santa Cruz), α/β-Tubulin (2148, Cell Signaling), glyceraldehyde 3-phosphate dehydrogenase (GAPDH, MAB374, Merck Millipore), Vinculin (V9131, Sigma-Aldrich). Western blotting for GAPDH, Tubulin or Vinculin were performed to serve as protein loading controls. All experiments were repeated at least three times, and representative results are shown. Use of technical or biological replicates is indicated in the figure legends. Protein amounts were quantified by densitometry using ImageJ (National Institutes of Health, United States).

Lentiviral Vector Production and Stable Transduction of Cell Lines

Lentiviral vectors were produced in HEK293T cells by co-transfecting each of the lentiviral vector transfer constructs together with expression plasmids pCMV-VSVG, pMDLg-RRE (gag/pol), and pRSV-REV using polyethyleneimine (PEI) as previously described (Zhang et al., 2012). The transfection medium was replaced by fresh medium after 24 h and, after 48 h, harvested cell supernatants were centrifuged at 200 × g for 3 min and filtered through 0.45 μm pore-sized filters (4614, Pall Corporation). The clarified supernatants containing the lentiviral vector particles were stored at −80°C until further use. To generate *Snail* and *Slug* knockout cell lines, 2H11 and MS-1 cells were firstly transduced by adding Cas9-expressing lentiviral vector (Cas9BST-1EA, Sigma-Aldrich) supernatant together with 10 μg ml^{-1} of polybrene (107689, Sigma-Aldrich) for 24 h. The transduced cells were selected with 4 μg ml^{-1} blasticidin for 48 h to obtain stable Cas9-expressing cells. Next, the cells were transduced with lentiviral vectors expressing guide RNAs targeting *Snail* or *Slug* and were further selected by adding puromycin (1 μg ml^{-1} for MS-1 and 4 μg ml^{-1} for 2H11). The depletion of SNAIL and SLUG protein efficiencies were determined by western blot analysis.

The annotated map and sequence of the gRNA acceptor lentiviral vector construct AA19_pLKO.1-puro.U6.sgRNA.*Bve*I-Dys.Stuffer are available in **Supplementary Figure S1**. This plasmid was generated by inserting into the *Bcl*I site of pLKO.1-puro.U6.sgRNA.*Bfu*AI.stuffer (Addgene plasmid #50920) a 3431-bp DNA fragment derived from the human dystrophin-coding sequence (Kearns et al., 2014). This stuffer DNA segment contains four additional *Bve*I recognition sites required for efficient *Bve*I plasmid digestion. The digestion of AA19_pLKO.1-puro.U6.sgRNA.*Bve*I-Dys.Stuffer with *Bve*I creates CGGT and GTTT 5′ overhangs permitting directional ligation to the ACCG and AAAC 5′ overhangs, respectively, of annealed oligodeoxyribonucleotides corresponding to a gRNA spacer (Maggio et al., 2016). Spacer sequences of *Snail*- and *Slug*-targeting gRNAs were identified by running the CHOPCHOP algorithm http://chopchop.cbu.uib.no/ (Montague et al., 2014; Labun et al., 2019). The lists of candidate gene knockout gRNAs were shortened by additional screening for potential off-target activity with the aid of Cas-OFFinder http://www.rgenome.net/cas-offinder/ (Bae et al., 2014). The oligonucleotide sequences corresponding to the selected gRNAs are listed in **Supplementary Table S2**. Lentiviral vectors for the expression of mouse *Id1*, *Id2,* and *Id3* were made and used to generate stable

cell lines overexpressing these proteins. In brief, the pLV-*Id1* plasmid was made by digesting pcDNA3-*Id1* with *Nde*I (ER0581, Thermo Fisher Scientific) and *Xho*I (ER0692, Thermo Fisher Scientific) and isolating and subcloning the *Id1* fragment into pLV-IRES-Puro containing a FLAG-tag at the N-terminal cut with same two enzymes. The pLV-*Id2* and pLV-*Id3* constructs were made by cloning the *Id2* and *Id3* fragments isolated from *Bcu*I (ER1251, Thermo Fisher Scientific) and *Xba*I (ER0682, Thermo Fisher Scientific) digested pCDEF3-Id2 or pBluescript KS(-)-*Id3* vectors into the same enzymes cut pLV-IRES-Puro with a FLAG-tag at the N-terminal, respectively. To generate MS-1 and 2H11 stable cell lines overexpressing ID1, ID2, or ID3, the respective cells were exposed for 24 h to clarified supernatants containing lentiviral vectors expressing *Id1*, *Id2,* or *Id3* and polybrene at a final concentration of 10 μg ml^{-1}. At 48 h post-transduction, the cells were subjected to puromycin selection (1 μg ml^{-1} for MS-1 and 4 μg ml^{-1} for 2H11). The ectopic expression of ID1, ID2, and ID3 was checked at both the RNA and protein levels.

Cell Proliferation Assay

One thousand MS-1 and 2H11 cells in 200 μl of regular culture medium were seeded in wells of a 96-well microplate Essen ImageLock^{TM} (4379, Essen Bioscience). Thereafter, the plate was placed in an IncuCyte ZOOM instrument (Essen Bioscience). The cells were monitored in real-time by taking images every 4 h for 2 days in total. The relative cell confluence was analyzed and quantified through the instrument's software.

In vitro Migration Assay

Approximately 2.5 $\times$ 10^4 MS-1 and 2H11 cells in 100 μl of regular culture medium were seeded in wells of a 96-well microplate Essen ImageLock^{TM} and were incubated overnight to allow for cell attachment. Subsequently, a WoundMaker^{TM} device (4563, Essen Bioscience) containing 96 pins was used to scratch homogeneous micron-wide wounds through the cell monolayers. After the removal of debris and detached cells, the monolayers were washed with serum-free medium twice, after which 100 μl of fresh serum-free medium was added to each well. Then the plate was placed in the IncuCyte instrument, and the cells were monitored in real-time by acquiring images every 2 h for 22 h with the wound width being analyzed by the instrument's software.

Small Interfering RNA Transfections

MS-1 cells were transfected with 40 nM of non-targeting (NT; 4390843, Dharmacon), *Id1* (*Id1*; L-040701-01-0005, Dharmacon), *Id2* (*Id2*; L-060495-00-0005, Dharmacon), or *Id3* (*Id3*; L-046495-00-0005, Dharmacon) small interfering RNAs (siRNAs) mixed with siRNA transfection reagent DharmaFECT 1 (T-2001, GE Healthcare Dharmacon). 2H11 cells were transfected with 80 nM of NT or *Id1/2/3* siRNAs using DharmaFECT 3 transfect reagent (T-2003, GE Healthcare Dharmacon). The siRNA and transfection reagent mixtures were incubated in serum-free medium for 20 min at room temperature before being added to the cells. The cells subjected to target gene knockdown were analyzed at 24 h post-transfection. The target gene knockdown frequencies were assessed by mRNA expression analyses using qRT-PCR.

EndMT Assays

MS-1 and 2H11 cells were cultured in wells of 6-well plates in medium containing 10% FBS and were subsequently treated with recombinant human TGF-β2 (1 ng ml^{-1}) or recombinant human BMP9 (5 ng ml^{-1}) for 3 days to investigate their effects on EndMT. Where indicated, lower TGF-β2 concentrations were also used to induce EndMT. For example, MS-1 and 2H11 cells were treated for 3 days with TGF-β2 at 0.1 and 0.2 ng ml^{-1}, respectively, and cell morphology changes were assessed. The cell morphology was quantified by measuring the cell elongation ratios. This was performed by calculating the ratio of cell length to cell width using ImageJ. Cell elongation ratios of fifty cells in each experiment were determined and results from three independent biological replicates are presented.

Immunofluorescence Staining

After stimulating the cells with TGF-β2 or BMP9, the cells were fixed with 4% formalin and were permeabilized with 0.1% triton X-100. Subsequently, the MS-1 cell samples were blocked with 3% bovine serum albumin (BSA, A-6003, Sigma-Aldrich) in phosphate-buffered saline (PBS) for 45 min at room temperature and then incubated with primary antibodies directed against PECAM-1 (1:500, 553370, Becton Dickinson) and SM22α (1:500, ab14106, Abcam); whereas 2H11 samples were incubated with a primary antibody raised against SM22α (1:500, ab14106, Abcam). Primary antibody incubations took place at room temperature for 45 min. After washing three times with PBS, the MS-1 cell samples were exposed to PBS containing secondary antibody donkey anti-rat Alexa 488 (1:1,000, A21208, Invitrogen) and goat anti-rabbit Alexa 594 (1:1000, A11012, Invitrogen); whereas the 2H11 cell samples were incubated with Alexa Fluor 488 Phalloidin (1:1,000, A12379, Thermo Fisher Scientific) and Goat anti-rabbit Alexa 594 at a dilution of 1:1,000. Secondary antibody treatments took place at room temperature in the dark for 45 min. The nuclei were stained with 4′,6-diamidino-2 phenylindole (DAPI, H-1200, Vector Laboratories). Images were taken by confocal microscopy (SP8, Leica Microsystems). The intensity of the fluorescence signals in each confocal image was quantified by ImageJ. All experiments were repeated at least three times, and representative results are shown.

Statistical Analyses

Results were compared by unpaired Student's *t*-test. Differences were considered significant when $p < 0.05$.

RESULTS

TGF-β2 Induces EndMT Whilst BMP9 Does Not

TGF-β family proteins are key regulators of endothelial cell function (Ma et al., 2020) and TGF-β ligands are known as the most important drivers of EndMT (Suzuki et al., 2010;

Ten Dijke et al., 2012). Among the three TGF-β isoforms (i.e., TGF-β1, TGF-β2, and TGF-β3), TGF-β2 has been linked as a pivotal factor in EndMT during atrioventricular (AV) cushion formation (Camenisch et al., 2002a; Sabbineni et al., 2018), being therefore chosen as primary TGF-β isoform in our experimental studies. The TGF-β family member BMP9 has been shown to mediate vascular quiescence and stimulate proliferation of stem cell-derived endothelial cells (MESECs), by activating high-affinity receptors in these cells (Suzuki et al., 2010). In order to gain deeper insights into the mechanisms by which these two cytokines regulate endothelial (dys)function, we characterized the EndMT response in the murine endothelial cell lines MS-1 and 2H11 cells for which previously TGF-β was found to induce a prominent EndMT response (Walter-Yohrling et al., 2004; Mihira et al., 2012). We first investigated the expression of TGF-β receptors by RT-qPCR in these two cell lines. As shown in **Supplementary Figures S2A,B**, both cell lines express ALK5 (encoded by *Tgfbr1*), ALK1 (encoded by *Acvrl1*), TGFβRII (encoded by *Tgfbr2*), BMPRII (encoded by *Bmpr2*), betaglycan (encoded by *Tgfbr3*) (albeit at relatively low levels), and endoglin (encoded by *Eng*) mRNA, suggesting that they are signaling proficient for TGF-β and BMP9.

Next, MS-1 and 2H11 cells were treated with TGF-β2 or BMP9 for 3 days to study whether they have an effect on EndMT. We started by examining the effects of these treatments on MS-1 cell morphology. In the absence of exogenous ligand stimulation, MS-1 cells displayed a cobblestone-like phenotype and tended to remain closely attached to each other. However, upon challenge with TGF-β2 for 3 days, the MS-1 cells showed a spindle-shaped morphology (**Figure 1A**, upper panel). Interestingly, upon treatment with BMP9 for 3 days, no apparent morphological changes were observed (**Figure 1A**, upper panel). To confirm this change in cell shape, the elongation ratios of individual cells were measured and plotted in **Supplementary Figure S3A**. Moreover, to determine whether this lack of effect is specific for BMP9, we challenged the MS-1 cells with BMP6. After addition of BMP6, which, in contrast to BMP9, signals via ALK2 instead of ALK1, also no loss of endothelial morphology was observed in MS-1 cells (**Supplementary Figure S4**). This data suggests that MS-1 cells undergo EndMT in response to TGF-β2, whilst BMP9 does not seem capable of inducing EndMT, at least in a robust fashion.

Next, we sought to confirm these findings by studying the expression of EndMT-related markers. As shown in **Figures 1B,C**, the mRNA expression levels of the mesenchymal cell markers genes *Acta2* (encoding α-SMA) and *Tagln* (encoding SM22α) were significantly increased in the presence of TGF-β2, yet they were only slightly altered by BMP9 exposure. Besides, the expression of the endothelial marker *Kdr* (encoding vascular endothelial growth factor receptor) was attenuated by TGF-β2, while it was promoted by BMP9 (**Figure 1D**). These results indicate a possible role of BMP9 in maintaining endothelial properties. Consistent with these findings, microscopy analysis of EndMT-related protein expression by immunofluorescence staining revealed that the synthesis of the endothelial protein PECAM-1 was strongly down-regulated in response to TGF-β2, yet it was barely affected upon BMP9 treatment (**Figure 1E**). The expression of the mesenchymal protein SM22α was profoundly enhanced by TGF-β2, while no effect was observed on its expression upon BMP9 stimulation. The quantification of the PECAM-1 and SM22α fluorescence intensity in MS-1 is shown in **Supplementary Figures S5A,B**. Thus, we conclude that, in contrast to BMP9, TGF-β2 induces robust EndMT in MS-1 cells.

To further investigate EndMT responses of ECs to TGF-β2 and BMP9, we performed similar experiments in 2H11 cells. In response to TGF-β2 treatments for 3 days, 2H11 cells became elongated and acquired a mesenchymal-like morphology, which was not observed when these cells were exposed, also for 3 days, to BMP9 (**Figure 1A**, lower panel). To confirm this change in cell shape, the elongation ratios of individual cells were measured and plotted in **Supplementary Figure S3B**. Next, the expression of the EndMT marker SM22α and that of the filamentous actin (F-actin) stress fibers were checked by microscopy analysis using immunodetection and fluorophore-conjugated phalloidin staining, respectively. As shown in **Figure 1E** (lower panel), TGF-β2 augmented SM22α and F-actin amounts, while BMP9 did not. The quantification of the F-actin and SM22α fluorescence intensity in 2H11 is shown in **Supplementary Figures S5C,D**. These results demonstrate that, similarly to MS-1 cells, 2H11 cells respond to TGF-β2 by undergoing EndMT, whereas they are incapable of doing so once treated with BMP9.

The Effects of TGF-β2 and BMP9 on SNAIL and SLUG Expression in ECs

EndMT-related transcription factors such as SNAIL and SLUG, contribute to the initiation and maintenance of EndMT processes (Kokudo et al., 2008; Cooley et al., 2014). Hence, we next aimed to study how these factors are regulated by TGF-β2 and how critical are they in inducing EndMT in MS-1 and 2H11 cells. First, *Snail* and *Slug* mRNA expression levels were examined in MS-1 cells treated with TGF-β2 or BMP9 (**Figures 2A–C**). After stimulation with TGF-β2, which promoted SMAD2 phosphorylation without influencing total SMAD2 protein levels, *Snail* mRNA levels were significantly increased in a time-dependent manner in MS-1 cells (**Figure 2A**). Indeed, *Snail* mRNA levels increased 1. 3-, 1. 7-, and 2.3-fold following 3, 6, and 24 h treatments with TGF-β2, respectively (**Figure 2A**). In response to BMP9, its intracellular effectors SMAD1/5 became phosphorylated in MS-1 cells (**Figure 2B**). Interestingly, *Snail* expression was strongly induced by BMP9, yet the maximum expression levels were not maintained with longer BMP9 incubation periods (**Figure 2A**). Indeed, *Snail* expression was increased 2.1- and 2.2-fold after 3 and 6 h treatments with BMP9, respectively, however, after 24 h incubations with BMP9, *Snail* expression was stimulated 1.7-fold in MS-1 cells (**Figure 2A**). We confirmed the TGF-β2- and BMP9-dependent induction patterns of SNAIL expression at the protein level in MS-1 cells (**Figure 2B**). Consistent with the changes in mRNA expression levels, increased SNAIL protein amounts were maintained in MS-1 cells treated with TGF-β2 for 6 and 24 h. In BMP9-treated MS-1 cells, these increased amounts were clearly observed at the 6 h time-point, but far less at 24 h (**Figure 2B**). Conversely, significant increases in SLUG expression levels were observed neither upon TGF-β2 nor BMP9 stimulation (**Figures 2B,C**). Quantification of the SNAIL

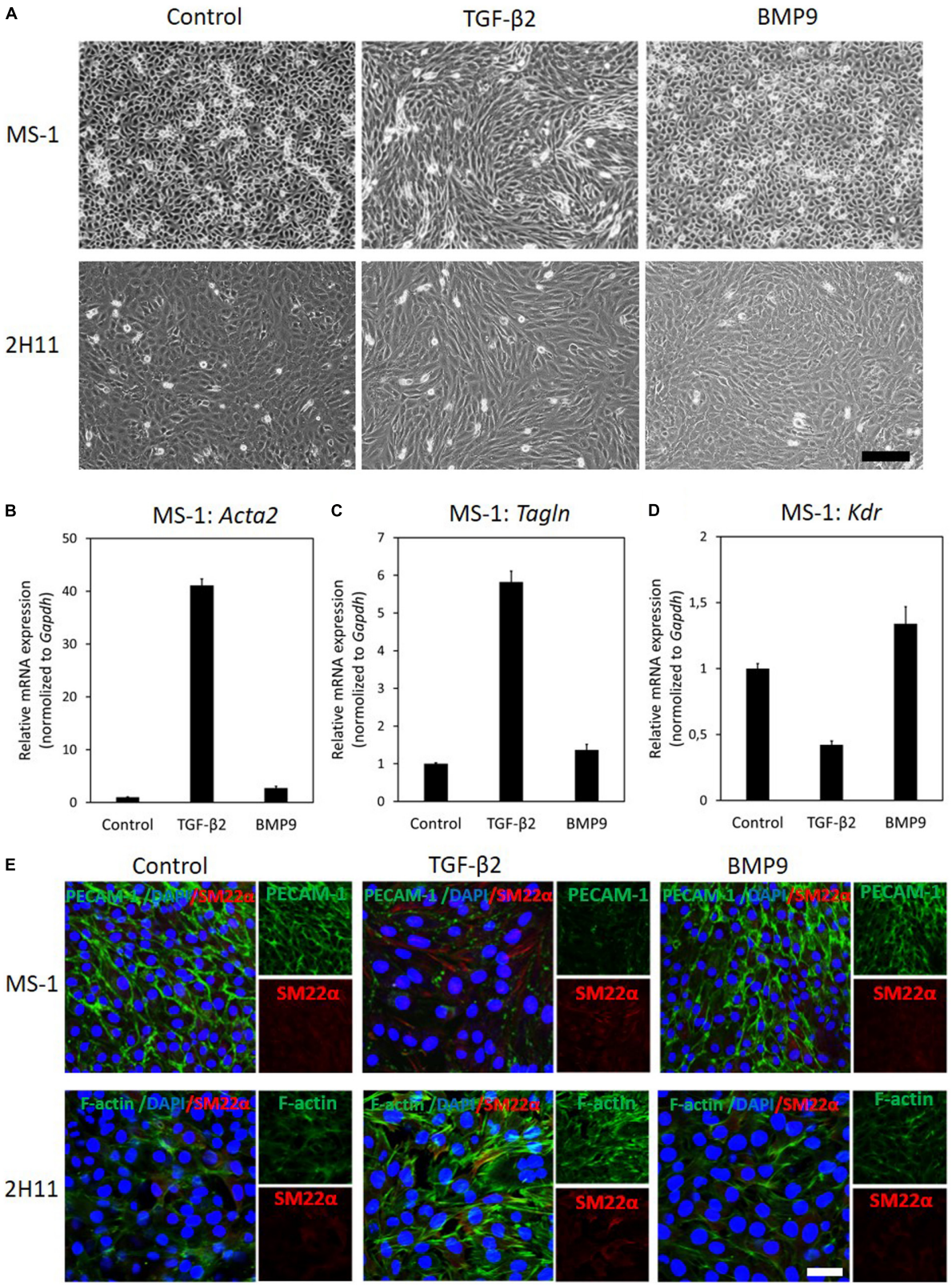

FIGURE 1 | TGF-β2 induces EndMT whilst BMP9 does not. **(A)** Assessing cell morphological changes induced by TGF-β2 and BMP9. Brightfield microscopy images of MS-1 (upper panel) and 2H11 (lower panel) cells showing distinct cell morphologies (i.e., cobblestone or fibroblast-like) after TGF-β2 (1 ng ml^{-1}) and BMP9

(Continued)

FIGURE 1 | Continued
(5 ng ml^{-1}) treatments for 3 days. Scale bar: 200 μm. **(B–D)** RT-qPCR analysis of endothelial and mesenchymal markers in MS-1 cells. MS-1 cells were exposed to medium containing TGF-β2 (1 ng ml^{-1}) or BMP9 (5 ng ml^{-1}) or medium containing ligand buffer (control) for 3 days. The expression of mesenchymal cell marker genes *Acta2* **(B)** and *Tagln* **(C)** and endothelial cell marker gene *Kdr* **(D)** was quantified by RT-qPCR. Expression levels were normalized to those of the housekeeping gene *Gapdh*. Results are expressed as mean ± SD. Representative results from three independent experiments are shown. **(E)** Fluorescence microscopy analysis of endothelial and mesenchymal markers in MS-1 and 2H11 cells. MS-1 and 2H11 cells were incubated in medium containing TGF-β2 (1 ng ml^{-1}) or BMP9 (5 ng ml^{-1}) or medium containing ligand buffer (control) for 3 days. The expression of the endothelial cell marker PECAM-1 (green) and mesenchymal cell marker SM22α (red) in nuclei (blue) stained MS-1 cells (upper panel) and mesenchymal cell markers F-actin (green) and SM22α (red) in nuclei (blue) stained 2H11 cells (lower panel) were assessed by using immunofluorescent staining, respectively. Representative results from at least three independent experiments are shown. Scale bar: 50 μm.

and SLUG western blot results in MS-1 cells by densitometry analysis was performed in three independent experiments (**Supplementary Figures S6A,B**). Further experiments revealed that the induction of SNAIL expression by TGF-β2 and BMP9 occurred in a concentration-dependent manner, while SLUG expression was not influenced (**Supplementary Figures S7A,B**).

We also examined the effects of TGF-β2 and BMP9 on the expression of SNAIL in MS-1 cells exposed to these ligands for 3 days. As shown in **Figure 2D**, *Snail* mRNA expression levels were increased 9.3- and 2.8-fold after TGF-β2 and BMP9 treatments for 3 days, respectively. The SNAIL protein was significantly upregulated upon incubations with TGF-β2 and BMP9 for 3 days (**Figure 2E**). The quantification of SNAIL expression, resulting from three independent experiments, showed 2.1- and 1.6-fold increases in response to TGF-β2 and BMP9, respectively (**Supplementary Figure S8A**). Thus, in contrast to SLUG, SNAIL might be a key mediator of TGF-β2-induced EndMT in MS-1 cells. While BMP9 induces SNAIL, albeit in a transient "bell-shaped" response, this upregulation seems insufficient to mediate a substantial EndMT response in MS-1 cells.

Next, to further investigate the function of SNAIL and SLUG during TGF-β2-induced EndMT, we performed a similar set of experiments in the 2H11 cell line. TGF-β2 significantly enhanced the expression of SNAIL both at the mRNA and protein levels. Maximal 1.7-fold induction of *Snail* mRNA expression was reached by exposing 2H11 cells to TGF-β2 for 6 h (**Figure 2F**). The SNAIL protein amounts also increased after 6 and 24 h treatments with TGF-β2 (**Figure 2G**). BMP9 greatly stimulated *Snail* expression that reached a level 7.2-fold higher than that measured in untreated 2H11 cells at 3 h (**Figure 2F**). However, at the 6 and 24 h timepoints, *Snail* expression decreased to levels 5.6- and 2.8-fold higher, respectively, than those detected in BMP9-untreated 2H11 controls (**Figure 2F**). The synthesis of SNAIL protein was potently induced by BMP9 at 3 h, with its amounts being progressively reduced after exposing 2H11 cells to BMP9 for 6 and 24 h (**Figure 2G**). The quantification of these expression levels is shown in **Supplementary Figure S6C**. Interestingly, the expression of SLUG protein in 2H11 cells was induced 4.4-fold after a 24 h incubation period with BMP9, while it was not influenced by TGF-β2 (**Figure 2G**). The quantification of changes in SLUG protein expression levels is shown in **Supplementary Figure S6D**. In addition, *Slug* mRNA expression was strongly upregulated by BMP9, but not by TGF-β2, after 3, 6, and 24 h stimulation in 2H11 (**Figure 2H**). Upon a 3 days stimulation, SNAIL expression was significantly promoted by TGF-β2 and BMP9 at both the mRNA and protein levels (**Figures 2I,J**). In contrast, after a 3 days stimulation, *Slug* expression was unchanged by BMP9 while it was only slightly inhibited by TGF-β2 (**Figure 2K**). The quantification of SNAIL and SLUG expression based on three independent experiments is shown in **Supplementary Figures S8B,C**. This data suggests that SNAIL family factors, especially SNAIL, have a role in driving the TGF-β2-induced EndMT process in 2H11 cells.

We also investigated the effects of TGF-β2 and BMP9 on *Twist* and *Zeb1* mRNA expression. We found that *Twist* was expressed at very low levels in MS-1 cells (data not shown). In MS-1 cells, *Zeb1* was not regulated by TGF-β2, and was even suppressed by BMP9 (**Supplementary Figure S9A**). In contrast, in 2H11 cells, *Zeb1* was induced by TGF-β2 and was not regulated by BMP9 (**Supplementary Figure S9B**). In this study, we have therefore focused on *Snail* family transcription factors.

As in the previous experiments we used human ligands on mouse cell lines (i.e., MS-1 and 2H11), we next tested whether these two mouse cell lines response similarly to human and mouse TGF-β2 and BMP9. As shown in **Supplementary Figures S10A–D**, ligands from both species induced similar to identical responses with respect to SMAD phosphorylation and SNAIL expression. Moreover, we assessed the responses of ECs to the three different TGF-β isoforms, i.e., TGF-β1, TGF-β2, and TGF-β in MS-1 cells. As shown in **Supplementary Figure S11**, all three TGF-β isoforms induced SMAD2 phosphorylation and SNAIL expression in a similar manner.

Together, the results described above sparked our interest in investigating the reason as to why BMP9 greatly induces the expression of transcription factors SNAIL and SLUG and yet it cannot induce EndMT.

Depletion of *Snail* Attenuates TGF-β2-Induced EndMT

As the expression levels of SNAIL were greatly induced by TGF-β2 in MS-1 cells, we investigated the effect of *Snail* depletion on TGF-β2-driven/mediated EndMT by using CRISPR/Cas9-mediated gene knockouts. We generated two independent guide RNAs (gRNAs) to create insertions and deletions (INDELs) at the endogenous *Snail* gene locus resulting in the disruption of the coding sequence by frameshifting. The sequences of the oligonucleotides used for assembling the gRNA expression constructs are listed in **Supplementary Table S2**. The knockout of *Snail* was verified by checking the absence of SNAIL protein using western blot analysis of MS-1 cells expressing *Snail*-targeting Cas9:gRNA complexes (**Figure 3A**). Interestingly,

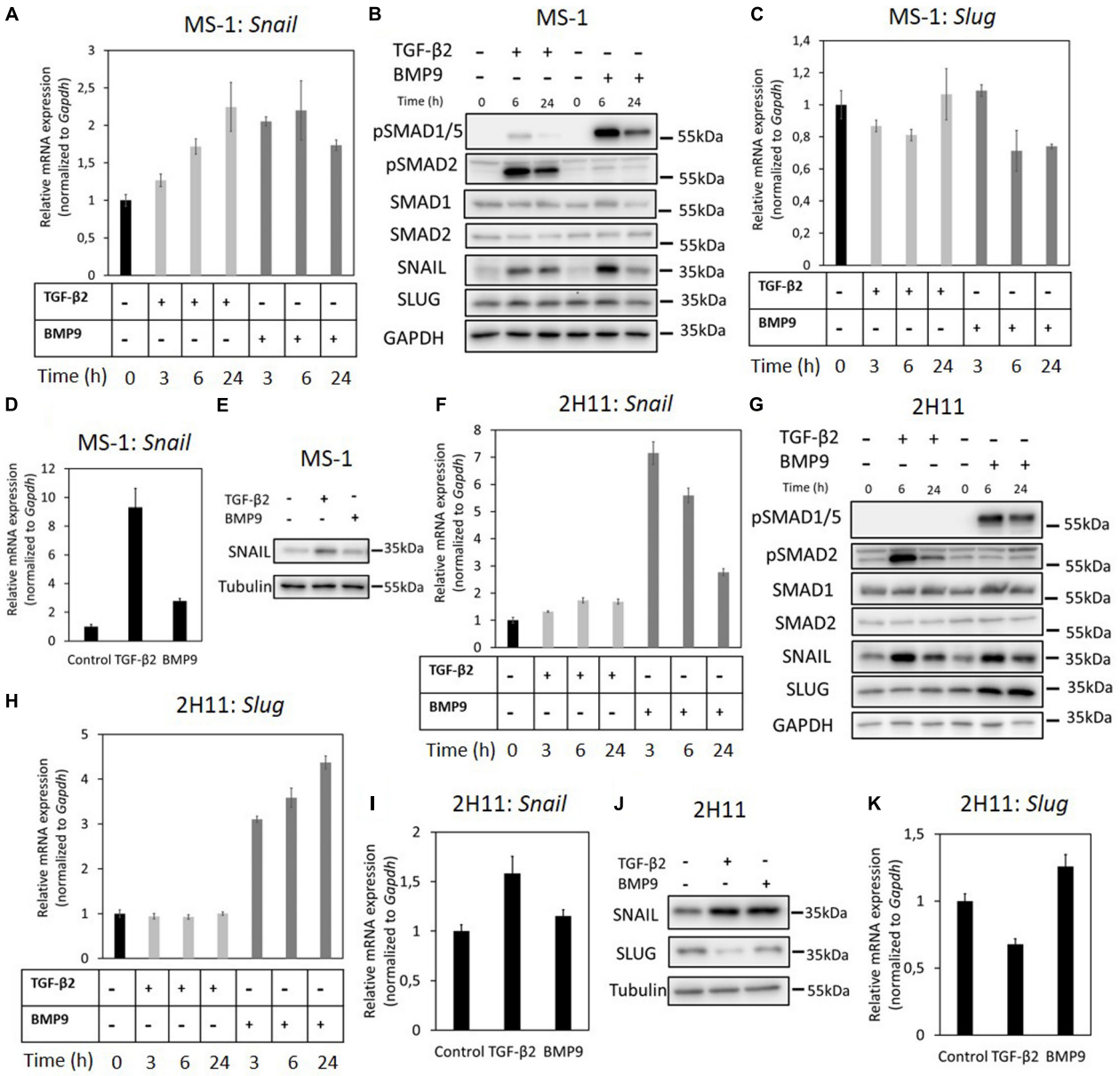

FIGURE 2 | Effects of TGF-β2 and BMP9 on SNAIL and SLUG expression. **(A)** RT-qPCR analysis of the effects of TGF-β2 (1 ng ml^{-1}) and BMP9 (5 ng ml^{-1}) on *Snail* mRNA expression after 3, 6, and 24 h treatments in MS-1 cells. **(B)** Western blot analysis of the effects of TGF-β2 (1 ng ml^{-1}) and BMP9 (5 ng ml^{-1}) on SNAIL and SLUG protein expression after 6 and 24 h treatments in MS-1 cells. **(C)** RT-qPCR analysis of the effects of TGF-β2 (1 ng ml^{-1}) and BMP9 (5 ng ml^{-1}) on *Slug* mRNA expression after 3, 6, and 24 h treatments in MS-1 cells. **(D)** RT-qPCR analysis of the effects of TGF-β2 (1 ng ml^{-1}) and BMP9 (5 ng ml^{-1}) on *Snail* mRNA expression after 3 days treatments in MS-1 cells. **(E)** Western blot analysis of the effects of TGF-β2 (1 ng ml^{-1}) and BMP9 (5 ng ml^{-1}) on SNAIL protein expression after 3 days treatments in MS-1 cells. **(F)** RT-qPCR analysis of the effects of TGF-β2 (1 ng ml^{-1}) and BMP9 (5 ng ml^{-1}) on *Snail* mRNA expression after 3, 6, and 24 h treatments in 2H11 cells. **(G)** Western blot analysis of the effects of TGF-β2 (1 ng ml^{-1}) and BMP9 (5 ng ml^{-1}) on SNAIL and SLUG proteins expression after 6 and 24 h treatments in 2H11 cells. **(H)** RT-qPCR analysis of the effects of TGF-β2 (1 ng ml^{-1}) and BMP9 (5 ng ml^{-1}) on *Slug* mRNA expression after 3, 6, and 24 h treatments in 2H11 cells. **(I)** RT-qPCR analysis of the effects of TGF-β2 (1 ng ml^{-1}) and BMP9 (5 ng ml^{-1}) on *Snail* mRNA expression after 3 days treatments in 2H11 cells. **(J)** Western blot analysis of the effects of TGF-β2 (1 ng ml^{-1}) and BMP9 (5 ng ml^{-1}) on SNAIL and SLUG proteins expression after 3 days treatments in 2H11 cells. **(K)** RT-qPCR analysis of the effects of TGF-β2 (1 ng ml^{-1}) and BMP9 (5 ng ml^{-1}) on *Slug* mRNA expression after 3 days treatments in 2H11 cells. All the mRNA expression levels were normalized to those of the housekeeping gene *Gapdh*. Results are expressed as mean ± SD. Representative results from three independent experiments are shown.

SLUG expression was slightly increased upon permanent loss of SNAIL (**Figure 3A**). By real-time tracking of cell numbers, we found that *Snail* depletion decreased MS-1 cell proliferation and/or viability (**Figure 3B**). Furthermore, *Snail* knockout in MS-1 cells promoted cell migration in a wound healing assay (**Figure 3C**). Under routine MS-1 cell culture conditions, obvious

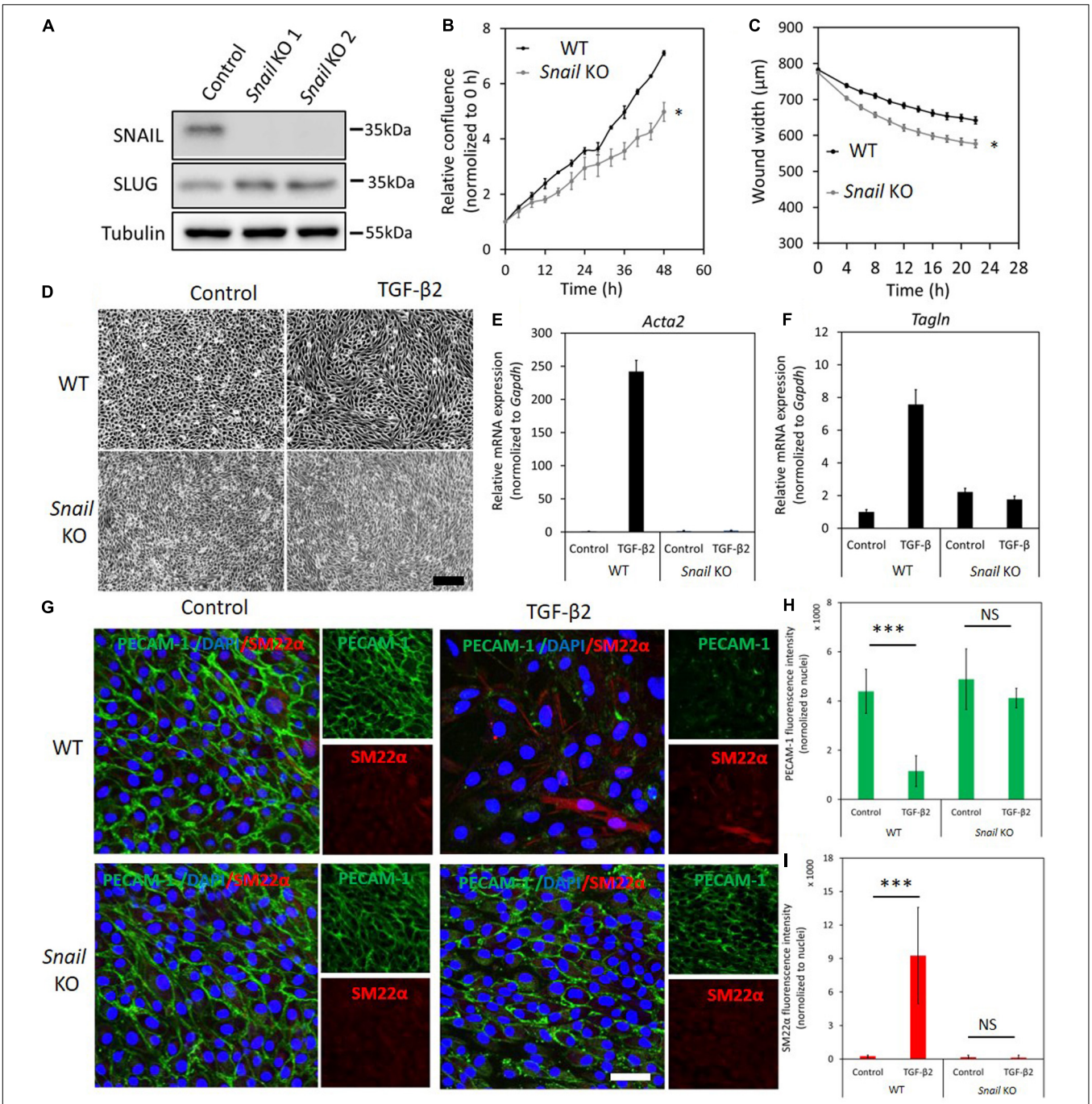

FIGURE 3 | Depletion of *Snail* attenuates TGF-β2-induced EndMT in MS-1 cells. **(A)** Western blot analysis of the *Snail* depletion with two independent guide RNAs using CRISPR/Cas9-based gene editing in MS-1 cells. **(B)** The effect of *Snail* depletion on MS-1 cells proliferation. **(C)** The effect of *Snail* depletion on MS-1 cells migration ability. $^{*}p < 0.05$. **(D)** Assessing cell morphological changes induced by TGF-β2 in parental MS-1 and *Snail* knockout MS-1 cells. Brightfield microscopy images of parental MS-1 (upper panel) and *Snail* knockout MS-1 (lower panel) cells showing distinct cell morphologies (i.e., cobblestone or fibroblast-like) after TGF-β2 (0.1 ng ml^{-1}) treatment for 3 days. Scale bar: 200 μm. **(E,F)** RT-qPCR analysis of mesenchymal cell markers in MS-1 cells. Parental and *Snail* knockout MS-1 cells were exposed to medium containing TGF-β2 (1 ng ml^{-1}) or medium containing ligand buffer (control) for 3 days. The expression of mesenchymal cell marker genes *Acta2* **(E)** and *Tagln* **(F)** was quantified by RT-qPCR. Expression levels were normalized to those of the housekeeping gene *Gapdh*. Results are expressed as mean ± SD. Representative results from three independent experiments are shown. **(G)** Fluorescence microscopy analysis of endothelial and mesenchymal cell markers in MS-1. Parental MS-1 and *Snail* knockout MS-1 cells were incubated in medium containing TGF-β2 (1 ng ml^{-1}) or medium containing ligand buffer (control) for 3 days. The expression of the endothelial cell marker PECAM-1 (green) and mesenchymal cell marker SM22α (red) in nuclei (blue) stained parental MS-1 (upper panel) and *Snail* knockout MS-1 (lower panel) cells were assessed by using immunofluorescent staining, respectively. Scale bar: 50 μm. **(H,I)** Quantified mean fluorescence intensity of PECAM-1 **(H)** and SM22α **(I)**. At least six representative images from three independent experiments were quantified. Results are expressed as mean ± SD. NS, not significant; $^{***}p < 0.001$.

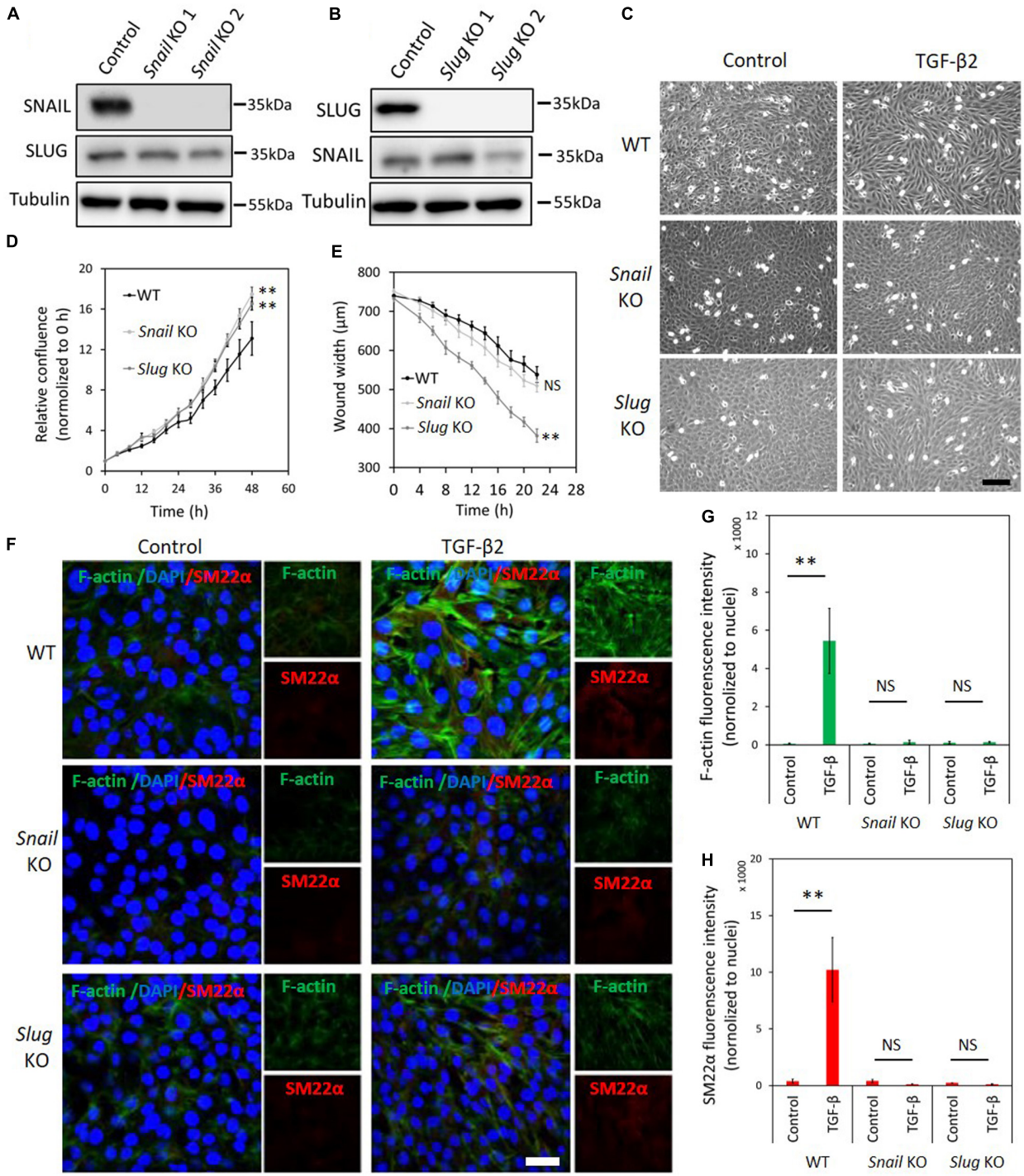

FIGURE 4 | Depletion of *Snail* or *Slug* attenuates TGF-β2-induced EndMT in 2H11 cells. **(A,B)** Western blot analysis of the SNAIL **(A)** and SLUG **(B)** depletion with two independent guide RNAs using CRISPR/Cas9-based gene editing in 2H11 cells. **(C)** Assessing cell morphological changes induced by TGF-β2 in parental 2H11, *Snail* knockout 2H11 and *Slug* knockout 2H11 cells. Brightfield microscopy images of parental 2H11 (upper panel), *Snail* knockout 2H11 (middle panel) and *Slug* knockout 2H11 (lower panel) cells showing distinct cell morphologies (i.e., cobblestone or fibroblast-like) after TGF-β2 (0.2 ng ml^{-1}) treatment for 3 days. Scale bar: 200 μm. **(D)** The effects of *Snail* and *Slug* depletion on 2H11 cells proliferation. **(E)** The effects of *Snail* and *Slug* depletion on 2H11 cells migration ability. $^{**}p < 0.005$. **(F)** Fluorescence microscopy analysis of mesenchymal markers in 2H11 cells. Parental 2H11, *Snail* knockout and *Slug* knockout 2H11 cells were incubated in medium containing TGF-β2 (1 ng ml^{-1}) or medium containing ligand buffer (control) for 3 days. The expression of mesenchymal cell markers F-actin (green) and SM22α (red) in nuclei (blue) stained parental 2H11 (upper panel), *Snail* knockout 2H11 (middle panel) and *Slug* knockout 2H11 (lower panel) cells were assessed by using immunofluorescent staining. Scale bar: 50 μm. **(G,H)** Quantified mean fluorescence intensity of F-actin **(G)** and SM22α **(H)**. At least six representative images from three independent experiments were quantified. Results are expressed as mean ± SD. NS, not significant; $^{**}p < 0.005$.

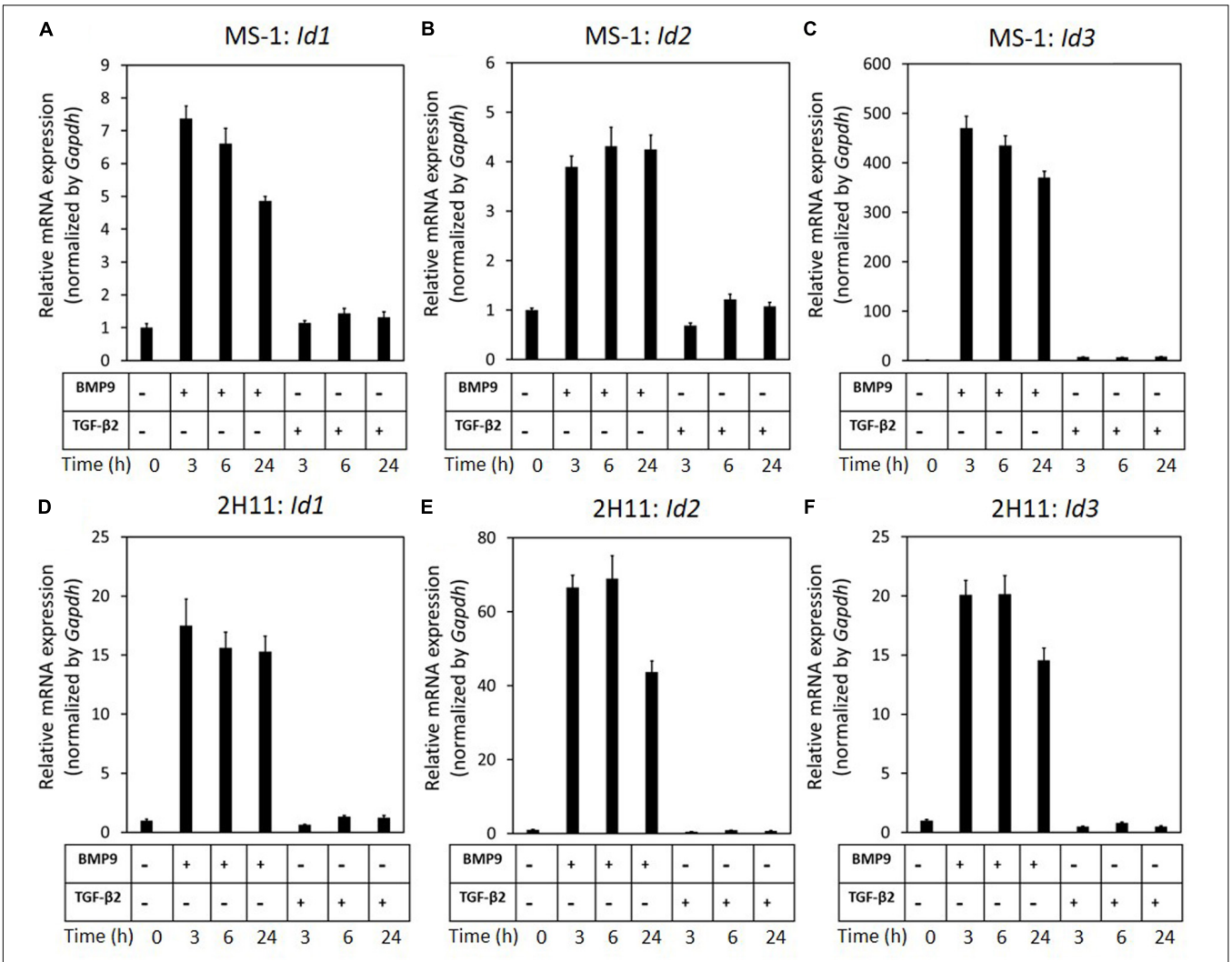

FIGURE 5 | BMP9 induces *Id1*, *Id2,* and *Id3* expression, but not TGF-β2, in both MS-1 and 2H11 cells. **(A–C)** RT-qPCR analysis of the effects of BMP9 (5 ng ml^{-1}) and TGF-β2 (1 ng ml^{-1}) on *Id1* **(A)**, *Id2* **(B)** and *Id3* **(C)** mRNA expression after 3, 6, and 24 h treatments in MS-1 cells. **(D–F)** RT-qPCR analysis of the effects of BMP9 (5 ng ml^{-1}) and TGF-β2 (1 ng ml^{-1}) on *Id1* **(D)**, *Id2* **(E)**, and *Id3* **(F)** mRNA expression after 3, 6, and 24 h treatments in 2H11 cells. Expression levels were normalized to those of the housekeeping gene *Gapdh*. Results are expressed as mean ± SD. Representative results from three independent experiments are shown.

morphological changes were observed neither in parental nor *Snail* knockout MS-1 cells (**Figure 3D**).

Next, we examined the effect of *Snail* depletion on TGF-β2-induced EndMT in MS-1 cells. *Snail* knockout MS-1 cells showed slightly less TGF-β2-induced morphological changes toward a mesenchymal shape when compared to parental MS-1 cells (**Supplementary Figure S12**). To further assess this response, we determined whether a low concentration of TGF-β2 is sufficient to induce EndMT (**Supplementary Figure S13**). Stimulating MS-1 cells with TGF-β2 ligand at 0.1 ng ml^{-1} for 3 days sufficed to trigger cell morphology changes. As expected, morphological changes were readily observed in parental MS-1 cells, whereas in *Snail* knockout MS-1 cells the depletion of *Snail* compromised TGF-β2-mediated EndMT morphological changes (**Figure 3D**), To confirm this change in cell shape, the elongation ratios of individual cells were measured and plotted in **Supplementary Figure S14**. This notion was strengthened by the analysis of mRNA expression levels of *Acta2* and *Tagln*, encoding the mesenchymal marker proteins α-SMA and SM22α, respectively. As shown in **Figures 3E,F**, the TGF-β2-dependent induction of *Acta2* and *Tagln* expression in MS-1 cells was lost upon *Snail* depletion. These results were further verified by fluorescence microscopy analysis upon immunostaining for the endothelial PECAM-1 and mesenchymal SM22α markers (**Figures 3G–I**). After treatment with TGF-β2 for 3 days, cultures of the parental MS-1 cells showed a significant decrease in PECAM-1 accumulation and higher frequencies of SM22α-positive cells than those detected in mock-treated controls (**Figure 3G** upper panel and **Figures 3H,I**). In contrast, in cultures of *Snail* knockout MS-1 cells, neither PECAM-1 protein amounts nor SM22α-positive cell frequencies were altered by TGF-β2 treatments (**Figure 3G** lower panel and

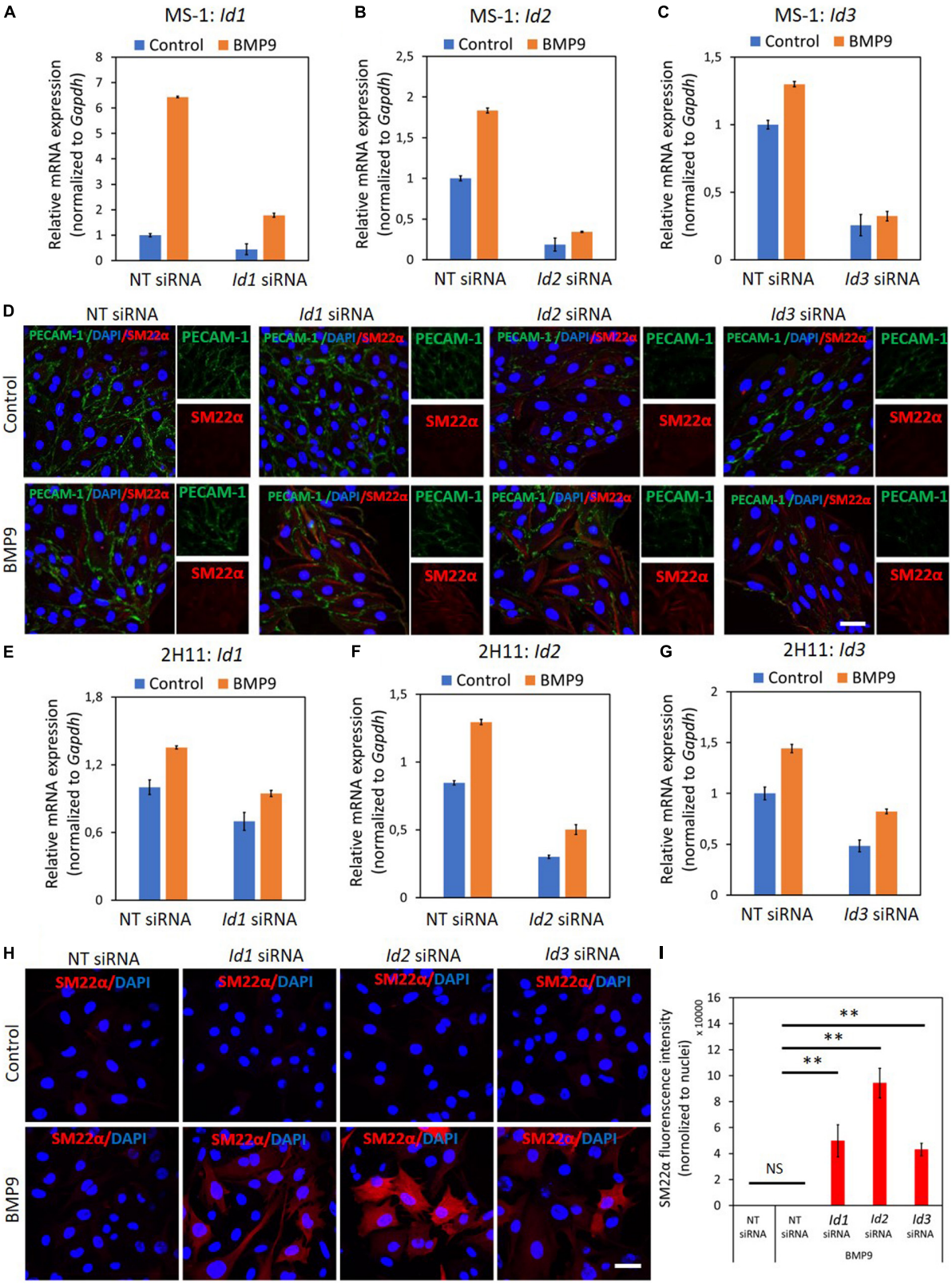

FIGURE 6 | ID proteins are critical in the BMP9-dependent maintenance of endothelial cell phenotypes. **(A–C)** RT-qPCR analysis of the siRNA-mediated silencing of endogenous and BMP9-induced *Id1* **(A)**, *Id2* **(B)** and *Id3* **(C)** mRNA expression in MS-1 cells. Expression levels were normalized to those of the housekeeping gene

(Continued)

FIGURE 6 | Continued
Gapdh. Results are expressed as mean ± SD. Representative results from three independent experiments are shown. **(D)** Fluorescence microscopy analysis of endothelial and mesenchymal markers in MS-1 cells. Non-targeting knockdown, *Id1* knockdown, *Id2* knockdown and *Id3* knockdown MS-1 cells were incubated in medium containing BMP9 (5 ng ml^{-1}) or medium containing ligand buffer (control) for 3 days. The expression of endothelial cell marker PECAM-1 (green) and mesenchymal cell marker SM22α (red) in nuclei (blue) stained MS-1 cells were assessed by using immunofluorescent staining. Scale bar: 50 μm. **(E–G)** RT-qPCR analysis of the siRNA-mediated silencing of endogenous and BMP9-induced *Id1* **(E)**, *Id2* **(F)**, and *Id3* **(G)** mRNA expression in MS-1 cells. The expression levels were normalized to those of the housekeeping gene *Gapdh*. Results are expressed as mean ± SD. Representative results from three independent experiments are shown. **(H)** Fluorescence microscopy analysis of mesenchymal marker in 2H11 cells. Non-targeting knockdown, *Id1* knockdown, *Id2* knockdown and *Id3* knockdown 2H11 cells were incubated in medium containing BMP9 (5 ng ml^{-1}) or medium containing ligand buffer (control) for 3 days. The expression of mesenchymal cell marker SM22α (red) in nuclei (blue) stained 2H11 cells was assessed by using immunofluorescent staining. Scale bar: 50 μm. **(I)** Quantified mean fluorescence intensity of SM22α. At least six representative images from three repeated experiments were quantified. Results are expressed as mean ± SD. NS, not significant; $^{**}p < 0.005$.

Figures 3H,I). These results suggest that SNAIL is essential for TGF-β2-induced EndMT in MS-1 cells.

To unveil the function of SNAIL and SLUG in TGF-β2-mediated EndMT in 2H11 cells, we applied two independent gRNAs to knockout either *Snail* or *Slug* by CRISPR/Cas9-mediated gene editing (**Figures 4A,B**). Under normal cell culture conditions, the morphology of 2H11 cells was not overtly affected upon *Snail* or *Slug* depletion (**Figure 4C**). Unlike in MS-1 cells, in 2H11 cells either *Snail* or *Slug* deficiencies promoted cell proliferation and/or viability (**Figure 4D**). Moreover, when compared with parental 2H11 cells, *Slug* knockout increased 2H11 cell migration, whereas *Snail* knockout did not (**Figure 4E**). Exposure to TGF-β2 failed to confer a mesenchymal morphology to *Snail* knockout 2H11 cells (**Figure 4C**). In contrast, *Slug* knockout cells kept responding to TGF-β2 by undergoing the morphological changes characteristic of EndMT (**Figure 4C**). To confirm this change in cell shape, the elongation ratios of individual cells were measured and plotted in **Supplementary Figure S15**. These findings were consolidated by examining the level of mesenchymal cell protein SM22α and by using Phalloidin to determine the presence and localization of F-actin fibers in 2H11 cells. As shown in **Figures 4F–H**, consistent with the effects on cell morphology, the loss of *Snail* dramatically blocked the TGF-β2-induced accumulation of the mesenchymal protein SM22α as well as F-actin in 2H11 cells. Interestingly, *Slug* knocked-out 2H11 cells also presented a decreased build-up of SM22α and F-actin fibers in response to TGF-β2 (**Figures 4F–H**). Together, our findings demonstrated that SNAIL plays a critical role in TGF-β2-mediated EndMT, while not as crucial as SNAIL, SLUG also participates to some extent in TGF-β2-mediated EndMT.

ID Proteins Are Critical in the BMP9-Dependent Maintenance of Endothelial Cell Phenotypes

Our previous results revealed that while BMP9 strongly induces SNAIL and SLUG expression in ECs, it is unable to trigger EndMT. We hence hypothesized that BMP9, in contrast to TGF-β2, selectively induces genes that negatively regulate the EndMT process and, in these investigations, focused on BMP signaling *Id* target genes. As expected, we found that BMP9 stimulation readily induced *Id1/2/3* expression in MS-1 cells (**Figures 5A–C**). This observation is in striking contrast with the limited increase of *Id2* expression in MS-1 cells exposed for 3 h to TGF-β2, and with the unaffected *Id1* and *Id2* gene expression levels in these cells even after 6 and 24 h treatments with TGF-β2 (**Figures 5A–C**). In contrast to its marginal effect on *Id1* and *Id2* expression, albeit to low levels, TGF-β2 did augment *Id3* expression in MS-1 cells after 3, 6, and 24 h incubations. These findings on the differential effects of TGF-β2 and BMP9 on the expression of ID proteins in MS-1 cells were generically observed in 2H11 cells as well (**Figures 5D–F**). The upregulation of *Id1/2/3* by BMP9, and not by TGF-β2, led us to investigate the role of Id proteins as possible negative regulators of the EndMT process.

To this end, we transiently knocked-down ID proteins expression by transfecting siRNAs targeting *Id1*, *Id2*, or *Id3*. As shown in **Figures 6A–C**, both steady-state and BMP9-induced *Id1*, *Id2,* and *Id3* mRNA levels were decreased after separately transfecting siRNA targeting *Id1*, *Id2,* or *Id3* into MS-1 cells. To investigate whether suppressing the expression of a specific *Id* gene influences the expression of the other two *Id* genes, we checked the levels of each of the three Id proteins in MS-1 and 2H11 cells subjected to knockdown of individual *Id* gene transcripts. As shown in **Supplementary Figure S16A**, *Id2* and *Id3* expression levels were not overtly influenced by knocking down *Id1* expression in MS-1 cells. Likewise, neither *Id1* and *Id3* nor *Id1* and *Id2* expression levels were substantially affected by knocking down *Id2* or *Id3*, respectively, in MS-1 cells (**Supplementary Figure S16A**). However, in 2H11 cells, inhibiting the expression of one of the *Id* genes slightly downregulate the other two tested *Id* members (**Supplementary Figure S16B**). We further treated the *Id1*, *Id2,* and *Id3* knocked down MS-1 cells with BMP9 for 3 days and stained these cells for markers associated with EndMT (i.e., PECAM-1 and SM22α). As shown in **Figure 6D**, whereas BMP9 did not trigger clear marker changes in MS-1 cells transfected with the non-targeting (NT) siRNA control, this ligand did increase the expression of the mesenchymal cell marker SM22α in MS-1 cells knocked down for *Id1*, *Id2,* or *Id3* (**Figure 6D**). The quantification of the SM22α fluorescence intensity is shown in **Supplementary Figure S17A**. Significantly, BMP9 had a lesser obvious effect on altering the expression of the endothelial cell marker PECAM-1 in MS-1 cells knocked down for *Id1*, *Id2* or *Id3* when compared to the changes that it triggered in SM22α expression (**Figure 6D**). The quantification of PECAM-1 fluorescence intensity is shown in **Supplementary Figure S17B**. Importantly, knocking down of *Id* genes in 2H11 cells (**Figures 6E–G**) was sufficient for triggering BMP9-induced EndMT, as observed by increased SM22α

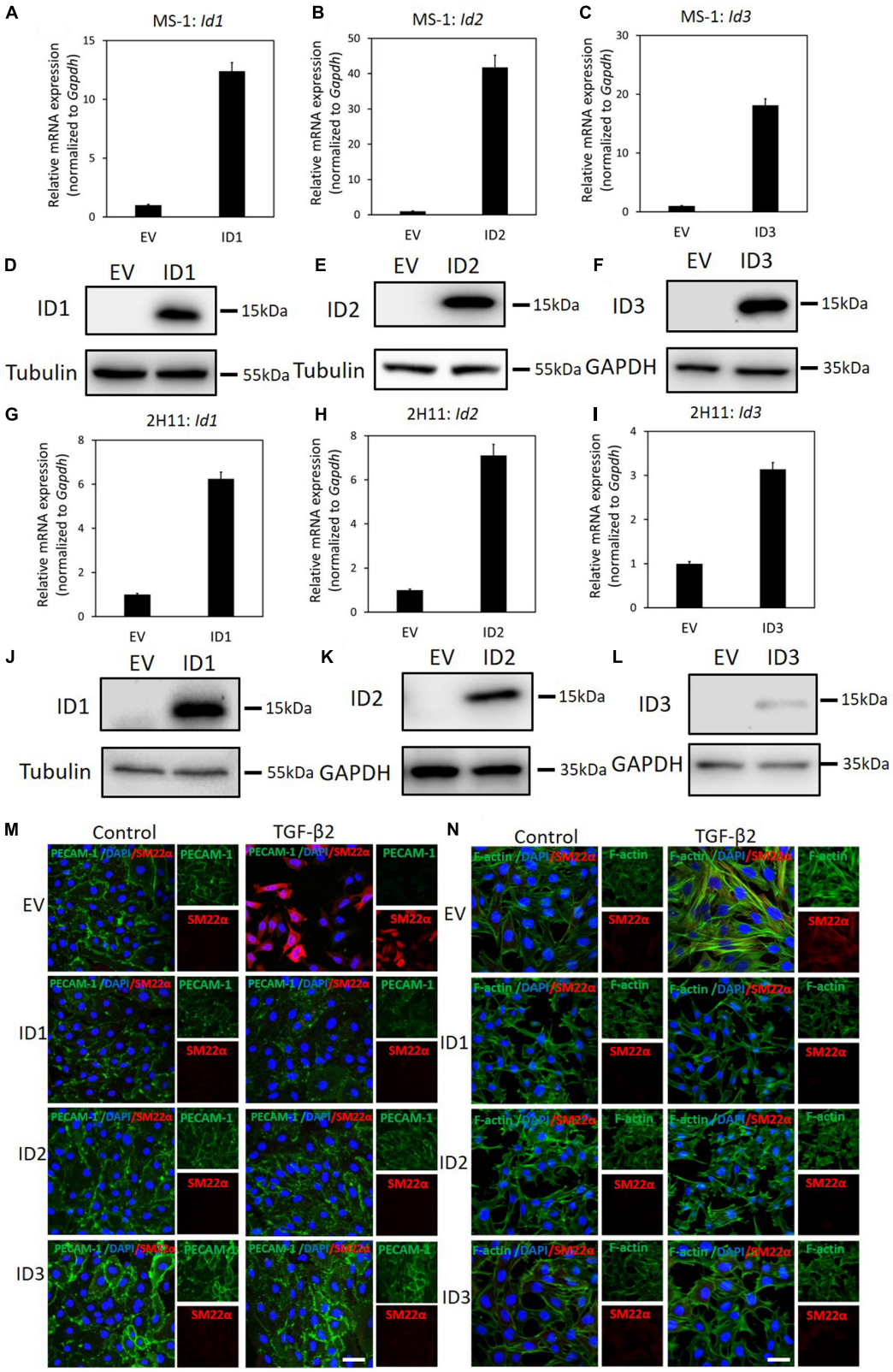

FIGURE 7 | ID proteins antagonize TGF-β2-induced EndMT. **(A–C)** RT-qPCR analysis of lentivirus-mediated ectopic expression of *Id1* **(A)**, *Id2* **(B)**, and *Id3* **(C)** mRNA in MS-1 cells. Expression levels were normalized to those of the housekeeping gene *Gapdh*. Results are expressed as mean ± SD. **(D–F)** Western blot analysis of

(Continued)

FIGURE 7 | Continued
lentivirus-mediated ectopic expression of ID1**(D)**, ID2 **(E)**, and ID3 **(F)** proteins in MS-1 cells. **(G–I)** RT-qPCR analysis of lentivirus-mediated ectopic expression of *Id1***(G)**, *Id2* **(H)**, and *Id3* **(I)** mRNA in 2H11 cells. Expression levels were normalized to those of the housekeeping gene *Gapdh*. Results are expressed as mean ± SD. **(J–L)** Western blot analysis of lentivirus-mediated ectopic expression of ID1**(J)**, ID2 **(K)**, and ID3 **(L)** proteins in 2H11 cells. **(M)** Fluorescence microscopy analysis of endothelial and mesenchymal markers in MS-1 cells. Empty vector (EV) expressing MS-1, ID1-overexpressing, ID2-overexpressing and ID3-overexpressing MS-1 cells were incubated in medium containing TGF-β2 (1 ng ml^{-1}) or medium containing ligand buffer (control) for 3 days. The expression of endothelial cell marker PECAM-1 (green) and mesenchymal cell marker SM22α (red) in nuclei (blue) stained MS-1 cells were assessed by using immunofluorescent staining. Scale bar: 50 μm. **(N)** Fluorescence microscopy analysis of mesenchymal markers in 2H11 cells. Empty vector (EV) expressing 2H11, ID1-overexpressing, ID2-overexpressing and ID3-overexpressing 2H11 cells were incubated in medium containing TGF-β2 (1 ng ml^{-1}) or medium containing ligand buffer (control) for 3 days. The expression of mesenchymal cell markers F-actin (green) SM22α (red) in nuclei (blue) stained 2H11 cells were assessed by using immunofluorescent staining. Representative results from three independent experiments are shown. Scale bar: 50 μm.

expression, whereas BMP9 did not upregulate SM22α expression in control cells transfected with NT siRNA (**Figures 6H,I**). Thus, *Id* depletion facilitates BMP9 in inducing, at least partially, an EndMT response.

To further validate this conclusion, we used the Id chemical inhibitor AGX51, which is known to inhibit the ID1-E47 interaction, leading to ubiquitin-mediated degradation of IDs (Wojnarowicz et al., 2019, 2020). We firstly titrated AGX51 (0–80 μM) in MS-1 and 2H11 cells for 24 h to determine an effective concentration. Significantly, consistent suppression of ID1, ID2, and ID3 levels started to be observed when the cells were treated with ≥ 20 μM of AGX51 (**Supplementary Figures S18A,B**). However, at these AGX51 concentrations, cells showed obvious signs of toxicity (data not shown). In any case, incubation of MS-1 cells with AGX51 led to a marked decrease in endothelial PECAM-1 marker expression and a concomitant enhancement in mesenchymal SM22α marker expression (**Supplementary Figure S18C**). Similarly, in the presence of AGX51, 2H11 cells showed a mesenchymal-like phenotype as the amounts of SM22α and F-actin fibers were both strongly increased (**Supplementary Figure S18D**). These results indicate that inhibition of ID proteins by AGX51 triggers the acquisition of EndMT hallmarks by MS-1 and 2H11 cells.

ID Proteins Antagonize TGF-β2-Induced EndMT

We have demonstrated that genetic and pharmacological inhibition of ID proteins favors BMP9-induced EndMT. Next, we wondered whether upregulation of ID proteins may prevent TGF-β-induced EndMT. To test this, ID1/2/3 were stably expressed in MS-1 and 2H11 cells using lentiviral vectors, as shown by RT-qPCR and western blot analysis (**Figures 7A–L**). As shown in **Figure 7M**, upon ectopic expression of ID1, ID2, or ID3, TGF-β2 failed to increase the expression of SM22α, while the expression of PECAM-1 was partially stabilized. The quantification of the fluorescence intensity of SM22α and PECAM-1 is shown in **Supplementary Figures S19A,B**. This result suggests that constitutive expression of ID1, ID2, or ID3 antagonizes TGF-β2-mediated EndMT in MS-1 cells. Similarly, overexpression of ID1, ID2, or ID3 favored the retention of the endothelial phenotype in 2H11 cells exposed to TGF-β2 (**Figure 7N**). In **Supplementary Figures S19C,D** the quantification of the fluorescence intensities corresponding to the F-actin and SM22α markers in 2H11 is shown. Therefore, we conclude that ID proteins predispose endothelial cells to maintain an endothelial phenotype by interfering with EndMT stimuli.

BMP9 Does Not Antagonize TGF-β2-Induced EndMT

Our results indicate that the Ids induced by BMP9 contribute to maintaining an endothelial cell phenotype, while TGF-β2 actives SNAIL to drive endothelial cells toward a fibroblast-like appearance. To investigate the interplay between BMP9 and TGF-β2 in the context of EndMT, we analyzed changes in the expression of endothelial and mesenchymal markers upon concomitant or sequential stimulation of MS-1cells with TGF-β2 and BMP9 (**Figures 8A–C**). As shown in **Figure 8A**, after 4 days of TGF-β2 stimulation, the expression of PECAM-1 decreased while SM22α increased, as expected. Interestingly, when the cells were treated with a TGF-β2 and BMP9 combination for 4 days, TGF-β2-induced EndMT was not affected, suggesting that the upregulation of SM22α and the down-regulation of PECAM-1 were not influenced by BMP9 (**Figure 8A**). Moreover, EndMT still occurred in MS-1 cells upon a treatment of TGF-β2 for 2 days followed by a 2 day BMP9 stimulation or vice versa (**Figure 8A**). The quantification of fluorescence intensities derived from PECAM-1- and SM22α-directed confocal microscopy analyses of three independent experiments is shown in **Figures 8B,C**. Thus, 2 days of TGF-β2 treatment is sufficient to induce EndMT with neither the concomitant nor sequential presence of BMP9 affecting this process. To obtain further insights on the non-antagonizing effect of BMP9 on TGF-β2-induced EndMT, we studied SNAIL and ID1 expression changes after exposing MS-1 cells to TGF-β2 and BMP9 either individually or simultaneously (**Figure 8D**). BMP9 enhanced TGF-β2 activation of the TGF-β signaling pathway, as BMP9 upregulated TGF-β2-induced SMAD2 phosphorylation, when compared to cells exposed exclusively to TGF-β2. Moreover, SNAIL expression was strongly raised in the presence of both BMP9 and TGF-β2 when compared to its expression in cells treated with BMP9 and TGF-β2 individually. Interestingly, the induction of ID1 in combined treatments was similar to that induced by BMP9 only. Quantification of SNAIL, pSMAD2 and ID1 amounts by densitometry analysis of western blots are shown in **Supplementary Figures S20A–C**. The augmented expression of SNAIL, and retained ID1 expression, might explain why BMP9 fails to inhibit TGF-β2 induced EndMT.

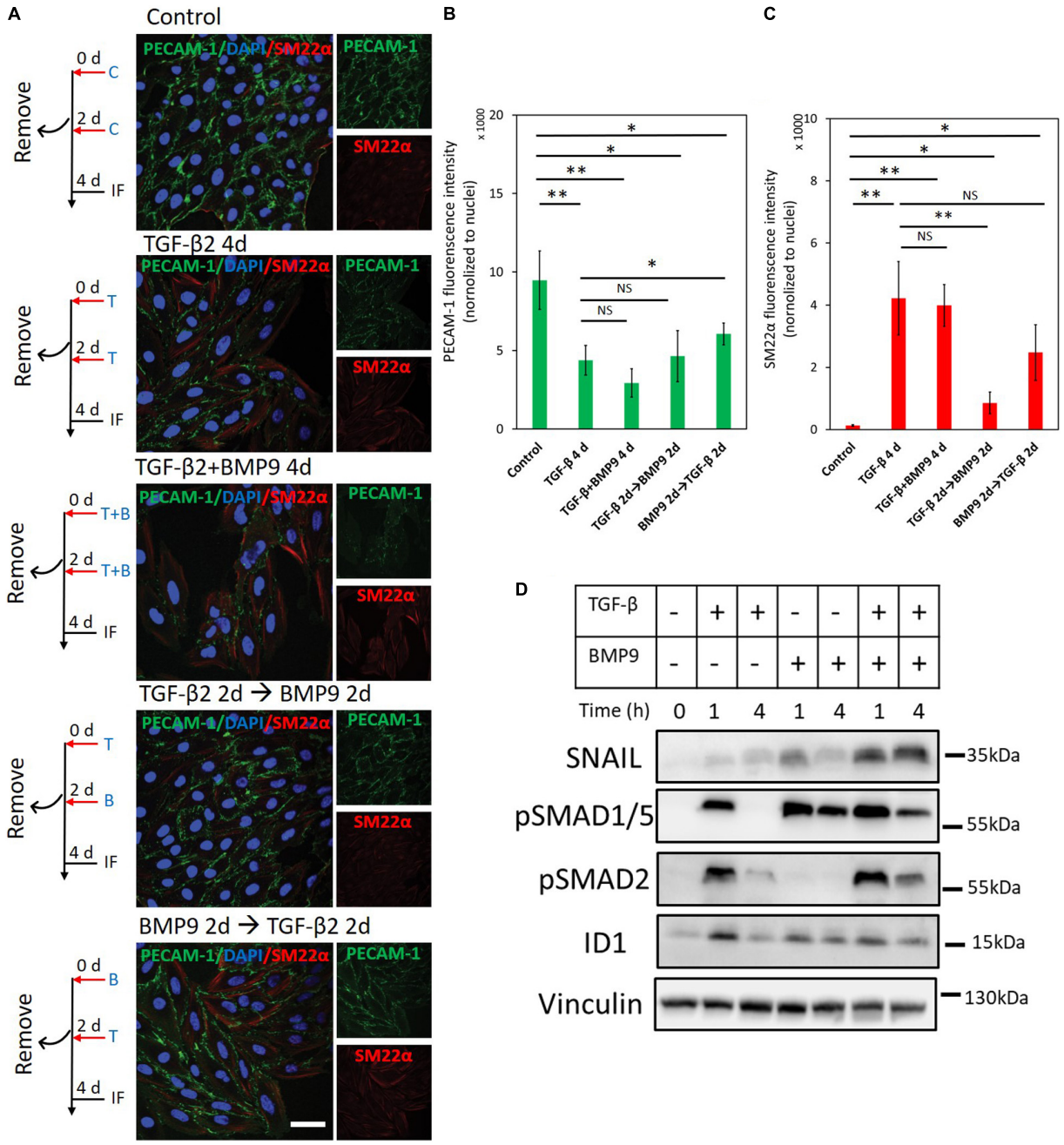

FIGURE 8 | BMP9 does not antagonize TGF-β2-induced EndMT. **(A)** Fluorescence microscopy analysis of endothelial and mesenchymal markers in MS-1 cells. MS-1 cells were incubated in medium containing ligand buffer (control, C) or TGF-β2 (1 ng ml^{-1}, T) and BMP9 (5 ng ml^{-1}, B) for 4 days, or firstly incubated with TGF-β2 (1 ng ml^{-1}) for 2 days and then change to BMP9 (5 ng ml^{-1}) for 2 days, or firstly incubated with BMP9 (5 ng ml^{-1}) for 2 days and then change to TGF-β2 (1 ng ml^{-1}) for 2 days. The expression of the endothelial cell marker PECAM-1 (green) and the mesenchymal cell marker SM22α (red) in nuclei (blue) stained MS-1 cells were assessed by using immunofluorescent staining. Scale bar: 50 μm. **(B,C)** Quantified mean fluorescence intensity of PECAM-1 **(B)** and SM22α **(C)**. At least four representative images from three independent experiments were quantified. Results are expressed as mean ± SD. NS, not significant; *$p < 0.05$, **$p < 0.005$. **(D)** Western blot analysis of the effects of TGF-β2 (1 ng ml^{-1}) or/and BMP9 (5 ng ml^{-1}) on pSmad1/5, pSMAD2, SNAIL, and ID1 proteins expression after 1 and 4 h treatments in MS-1 cells.

DISCUSSION

Emerging evidence points to a pivotal role of EndMT in both embryonic development and clinical disorders (Ma et al., 2020). Moreover, targeting specific EndMT pathways is also gaining considerable interest for its exploitation in tissue engineering (Hong et al., 2018; Ma et al., 2020). Previous studies have highlighted the role of TGF-β family proteins as the main drivers

and regulators of multistep and dynamic EndMT processes. However, in order to target and manipulate EndMT for biomedical applications, a further/deeper understanding of the underlying mechanisms is warranted. In this study, we report that TGF-β2 triggers EndMT in two murine endothelial cell lines, i.e., MS-1 and 2H11. By using CRISPR/Cas9-based gene editing, we generated cell lines knocked-out for either *Snail* or *Slug* that served to demonstrate that SNAIL is required for TGF-β2-induced EndMT. When compared to SNAIL, SLUG had a less effect in the induction of EndMT by TGF-β2 in 2H11 cells. Additionally, we found that while BMP9 strongly induced a burst of SNAIL and SLUG expression, it was nonetheless unable to elicit a substantial EndMT response. Mechanistically, we observed that BMP9-induced ID proteins antagonize EndMT, as inhibition of *Id1*, *Id2,* or *Id3* mRNA expression in ECs enabled BMP9 to trigger EndMT. Moreover, ectopic expression of these ID proteins individually attenuated TGF-β-mediated EndMT. Thus, whereas SNAIL is a key mediator, ID proteins function as gatekeepers of the EndMT process (**Figure 9**). We further showed that TGF-β2 is a strong inducer of EndMT in MS-1 and 2H11 cells, which is in line with previous reports (Yoshimatsu and Watabe, 2011; Ten Dijke et al., 2012). In contrast to TGF-β2, and similarly to BMP6, BMP9, either failed to induce or prevented EndMT (**Figure 1** and **Supplementary Figure S2**). Related to these findings, it is noteworthy mentioning that Medici and co-workers showed that, like TGF-β2, BMP4 can trigger EndMT in a BMP type I receptor/ALK2-dependent manner in both human umbilical vein endothelial cells (HUVECs) and human cutaneous microvascular endothelial cells (HCMECs) (Medici et al., 2010). BMP7 has been reported to act as an EndMT suppressor and being able to abrogate TGF-β1-induced EndMT in human coronary endothelial cells and cardiac fibrosis (Zeisberg et al., 2007). BMP9 and BMP10 have been shown to mediate the closure of the ductus arteriosus at birth via inducing EndMT (Levet et al., 2015). Since endothelial cells exhibit broad degrees of specialization in different organs (Dejana et al., 2017; Pinto et al., 2018), our results suggest that BMPs regulate EndMT in a cell- and/or tissue-specific manner.

The SNAIL family of transcription factors members have been considered to be key modulators of EndMT processes (Kokudo et al., 2008; Medici et al., 2011; Ma et al., 2020). We found that SNAIL expression was strongly stimulated by TGF-β2 (**Figure 2**). The genetic depletion of *Snail* in 2H11 and MS-1 cells inhibited EndMT, indicating that SNAIL is essential for TGF-β2-induced EndMT in these cells (**Figures 3**, **4**). Unlike our results, Mihira and colleagues reported that *Snail* inhibition failed to abrogate TGF-β2-induced α-SMA expression and EndMT in MS-1 cells (Mihira et al., 2012). In contrast to the transient siRNA-induced knockdown of *Snail* expression performed by Mihira et al., we permanently ablated *Snail* by CRISPR/Cas9-induced knockout. Together, these data suggest that low levels of SNAIL may be sufficient to mediate EndMT in MS-1 cells. Moreover, we demonstrated that the CRISPR/Cas9-induced depletion of *Slug* could partially inhibit TGF-β2-induced EndMT in 2H11 cells (**Figure 4**). Our laboratory has previously shown the importance of SLUG in regulating the expression of the endothelial cell marker PECAM-1 and in calcific differentiation of ECs (Sánchez-Duffhues et al., 2015). In the case of the transcription factors *Twist* and *Zeb1*, that are regulated by TGF-β2 and/or BMP9, we were unable to obtain consistent results in MS-1 and 2H11 cells, which might indicate that the function of these two transcription factors in EndMT is not as key as that of SNAIL in most ECs.

When investigating the effect of SNAIL and SLUG through cell proliferation and migration assays, we found that the depletion of SNAIL inhibited the proliferation of MS-1 cells and promoted the proliferation of 2H11 cells (**Figures 3B**, **4D**). This is in line with previous publications in which opposite effects were also reported regarding the role of SNAIL in regulating cell numbers (Yang et al., 2017; Liu et al., 2019). In cell migration assays, we found that SNAIL promoted and failed to promote significant cell motility in MS-1 and 2H11 cells, respectively (**Figures 3C**, **4E**). A number of earlier reports demonstrated that SNAIL enhances the migration of MDA-MB-231 cells (Wu et al., 2009; Ito et al., 2016). Hence, the differential effects of SNAIL and SLUG on cell proliferation and migration might result from different cell origins or expression patterns of other proteins that are alternatively controlled by SNAIL or SLUG deficiency. Further research is warranted to dissect these possibilities.

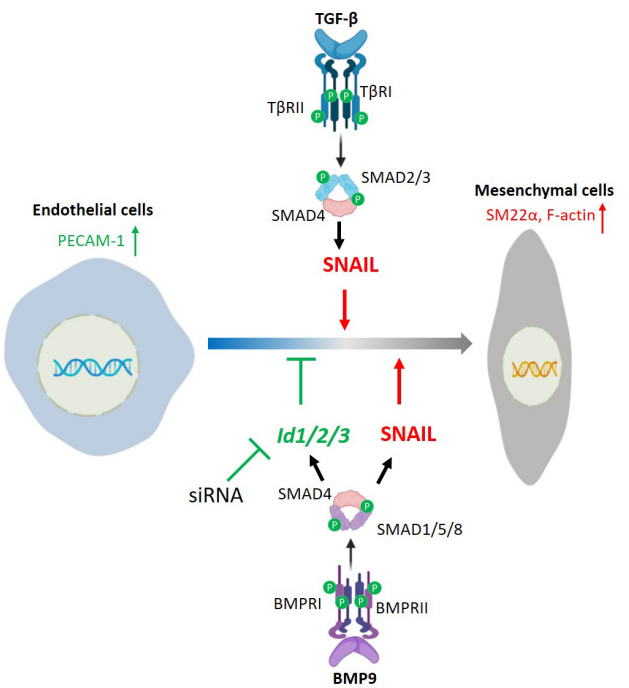

FIGURE 9 | Schematic of a working model by which TGF-β and BMP9 regulate EndMT. TGF-β/SMAD signaling induces EndMT by promoting SNAIL expression. BMP9/SMAD signaling promotes SNAIL and ID1/2/3 expression, and stimulates EndMT only when BMP9-induced expression of *Id1/2/3* is silenced.

In contrast to the SNAIL family of transcription factors, ID proteins were identified as EndMT suppressors. Our data demonstrates that the depletion of either *Id1*, *Id2,* or *Id3* was sufficient for letting BMP9 to induce the expression of the mesenchymal cell marker SM22α in both endothelial cell lines (i.e., MS-1 and 2H11) (**Figure 6**). As corollary, this data indicates that BMP9 promotes the acquisition of EndMT features by MS-1 and 2H11 cells when the expression of ID proteins is dampened. Furthermore, ectopic expression of ID1, ID2 or ID3 prevented the build-up of mesenchymal cell markers in ECs upon TGF-β2 treatment (**Figure 7**), indicating a critical negative regulatory role of IDs on initiating and/or driving the EndMT process. These results may explain the fact that BMP9 strongly increased SNAIL (and even SLUG) expression yet, it was unable to induce EndMT. Indeed, BMP9 induced robust activation of *Id* gene expression, whose products likely went on to oppose SNAIL- and SLUG-mediated EndMT. Interestingly, in cells incubated with TGF-β2 and BMP9, the latter ligand was unable to inhibit TGF-β2-induced EndMT (**Figure 8**). This observation may be caused by the augmented TGF-β2-dependent induction of SNAIL expression despite a retained induction of ID expression in response to BMP9.

To the best of our knowledge, there are no previous studies on the effect of IDs on the EndMT process, whilst the role of IDs in EMT remains controversial (Kondo et al., 2004; Hu et al., 2013; Stankic et al., 2013; Castañón et al., 2017). For instance, after dimerizing with E2A, IDs act as negative regulators of EMT by preventing E2A-mediated suppression of epithelial-specific protein expression (Kondo et al., 2004; Stankic et al., 2013). Other studies, however, demonstrated that ID members, in particular ID1, favored the EMT process in tumor cells (Hu et al., 2013; Castañón et al., 2017).

In summary, our work provides new insights into the role of SNAIL and SLUG in EndMT pathways controlled by TGF-β family members. Furthermore, we identified ID proteins ID1, ID2, and ID3 as critical EndMT suppressors. These findings may be further explored to, by taking into account the balance between SNAIL and ID family members, pharmacologically modulate EndMT for scientific or therapeutic purposes. Regarding the latter aspect, our results may contribute to develop novel approaches permitting a precise control over EndMT for the treatment of fibrotic diseases or for devising tissue engineering applications.

DATA AVAILABILITY STATEMENT

The raw data supporting the conclusions of this article will be made available by the authors, without undue reservation, to any qualified researcher.

AUTHOR CONTRIBUTIONS

JM, GZ, and MT performed the experiments. MG designed the gRNA acceptor construct AA19_pLKO.1-puro.U6.sgRNA.*Bve*I-Dys and the gRNA oligos for CRISPR/Cas9-mediated gene knockouts. JM and PD analyzed the data. JM wrote the manuscript. GS-D, MG, and PD edited and critically revised the manuscript. PD conceived and supervised the project. All authors revised the content and approved the final manuscript.

FUNDING

Work in our laboratory on the role of TGF-β in EndMT was supported by CGC.NL and the Netherlands Cardio Vascular Research Initiative: the Dutch Heart Foundation, the Dutch Federation of University Medical Centers, the Netherlands Organization for Health Research and Development, and the Royal Netherlands Academy of Sciences Grant awarded to the Phaedra-Impact (http://www.phaedraresearch.nl) and the Reconnect consortia. JM was supported by the Chinese Scholarship Council. GS-D was sponsored by FOP Italia and AFM-Telethon (#22379) and a grant from La Marató-TV3.

ACKNOWLEDGMENTS

We thank A. Hinck, S. Vukicevic, and J. Nickel for gifts of recombinant ligands.

SUPPLEMENTARY MATERIAL

The Supplementary Material for this article can be found online at: https://www.frontiersin.org/articles/10.3389/fcell.2021.616610/full#supplementary-material

Supplementary Table 1 | Primers used for qRT-PCR.

Supplementary Table 2 | Gene targets and gRNA oligonucleotides for CRISPR/Cas9-mediated knockout studies.

REFERENCES

Azhar, M., Runyan, R. B., Gard, C., Sanford, L. P., Miller, M. L., Andringa, A., et al. (2009). Ligand−specific function of transforming growth factor beta in epithelial−mesenchymal transition in heart development. *Dev. Dyn.* 238, 431–442. doi: 10.1002/dvdy.21854

Bae, S., Park, J., and Kim, J.-S. (2014). Cas-OFFinder: a fast and versatile algorithm that searches for potential off-target sites of Cas9 RNA-guided endonucleases. *Bioinformatics* 30, 1473–1475. doi: 10.1093/bioinformatics/btu048

Camenisch, T. D., Molin, D. G., Person, A., Runyan, R. B., Gittenberger-De Groot, A. C., Mcdonald, J. A., et al. (2002a). Temporal and distinct TGFb ligand requirements during mouse and avian endocardial cushion morphogenesis. *Dev. Biol. Orlando* 248, 170–181.

Camenisch, T. D., Molin, D. G., Person, A., Runyan, R. B., Gittenberger-De Groot, A. C., Mcdonald, J. A., et al. (2002b). Temporal and distinct TGFb ligand requirements during mouse and avian endocardial cushion morphogenesis. *De. Biol.* 248, 170–181. doi: 10.1006/dbio.2002.0731

Castañón, E., Soltermann, A., López, I., Román, M., Ecay, M., Collantes, M., et al. (2017). The inhibitor of differentiation-1 (Id1) enables lung cancer

liver colonization through activation of an EMT program in tumor cells and establishment of the pre-metastatic niche. *Cancer Lett.* 402, 43–51. doi: 10.1016/j.canlet.2017.05.012

Cooley, B. C., Nevado, J., Mellad, J., Yang, D., Hilaire, C. S., Negro, A., et al. (2014). TGF-β signaling mediates endothelial-to-mesenchymal transition (EndMT) during vein graft remodeling. *Sci. Transl. Med.* 6, ra234–ra227.

Dejana, E., Hirschi, K. K., and Simons, M. (2017). The molecular basis of endothelial cell plasticity. *Nat. Commun.* 8, 1–11. doi: 10.1007/978-1-59259-253-1_1

Dejana, E., and Lampugnani, M. G. (2018). Endothelial cell transitions. *Science* 362, 746–747. doi: 10.1126/science.aas9432

Dennler, S., Itoh, S., Vivien, D., Ten Dijke, P., Huet, S., and Gauthier, J. M. (1998). Direct binding of Smad3 and Smad4 to critical TGFβ−inducible elements in the promoter of human plasminogen activator inhibitor−type 1 gene. *EMBO J.* 17, 3091–3100. doi: 10.1093/emboj/17.11.3091

Derynck, R., and Budi, E. H. (2019). Specificity, versatility, and control of TGF-β family signaling. *Sci. Signal.* 12:eaav5183. doi: 10.1126/scisignal.aav5183

Dyer, L. A., Pi, X., and Patterson, C. (2014). The role of BMPs in endothelial cell function and dysfunction. *Trends Endocrinol. Metab.* 25, 472–480. doi: 10.1016/j.tem.2014.05.003

Hollnagel, A., Oehlmann, V., Heymer, J., Rüther, U., and Nordheim, A. (1999). Id genes are direct targets of bone morphogenetic protein induction in embryonic stem cells. *J. Biol. Chem.* 274, 19838–19845. doi: 10.1074/jbc.274.28.19838

Hong, L., Du, X., Li, W., Mao, Y., Sun, L., and Li, X. (2018). EndMT: a promising and controversial field. *Eur. J. Cell Biol.* 97, 493–500. doi: 10.1016/j.ejcb.2018.07.005

Hu, H., Wang, Y. L., Wang, G. W., Wong, Y. C., Wang, X. F., Wang, Y., et al. (2013). *A novel role of Id-1 in regulation of epithelial-to-mesenchymal transition in bladder cancer*. Amsterdam: Elsevier, 1242–1253.

Ito, K., Park, S. H., Nayak, A., Byerly, J. H., and Irie, H. Y. (2016). PTK6 inhibition suppresses metastases of triple-negative breast cancer via SNAIL-dependent E-cadherin regulation. *Cancer Res.* 76, 4406–4417. doi: 10.1158/0008-5472.can-15-3445

Kearns, N. A., Genga, R. M., Enuameh, M. S., Garber, M., Wolfe, S. A., and Maehr, R. (2014). Cas9 effector-mediated regulation of transcription and differentiation in human pluripotent stem cells. *Dev.* 141, 219–223. doi: 10.1242/dev.103341

Kokudo, T., Suzuki, Y., Yoshimatsu, Y., Yamazaki, T., Watabe, T., and Miyazono, K. (2008). Snail is required for TGFβ-induced endothelial-mesenchymal transition of embryonic stem cell-derived endothelial cells. *J. Cell Sci.* 121, 3317–3324. doi: 10.1242/jcs.028282

Kondo, M., Cubillo, E., Tobiume, K., Shirakihara, T., Fukuda, N., Suzuki, H., et al. (2004). A role for Id in the regulation of TGF-β-induced epithelial–mesenchymal transdifferentiation. *Cell Death Differ.* 11, 1092–1101. doi: 10.1038/sj.cdd.4401467

Korchynskyi, O., and Ten Dijke, P. (2002). Identification and functional characterization of distinct critically important bone morphogenetic protein-specific response elements in the Id1 promoter. *J. Biol. Chem.* 277, 4883–4891. doi: 10.1074/jbc.m111023200

Labun, K., Montague, T. G., Krause, M., Torres Cleuren, Y. N., Tjeldnes, H., and Valen, E. (2019). CHOPCHOP v3: expanding the CRISPR web toolbox beyond genome editing. *Nucleic Acids Res.* 47, W171–W174.

Levet, S., Ouarné, M., Ciais, D., Coutton, C., Subileau, M., Mallet, C., et al. (2015). BMP9 and BMP10 are necessary for proper closure of the ductus arteriosus. *Proc. Natl. Acad. Sci.* 112, E3207–E3215.

Liu, M., Hancock, S. E., Sultani, G., Wilkins, B. P., Ding, E., Osborne, B., et al. (2019). Snail-overexpression induces epithelial-mesenchymal transition and metabolic reprogramming in human pancreatic ductal adenocarcinoma and non-tumorigenic ductal cells. *J. Clin. Med.* 8:822. doi: 10.3390/jcm8060822

Ma, J., Sanchez-Duffhues, G., Goumans, M.-J., and Ten Dijke, P. (2020). TGF-β-induced endothelial to mesenchymal transition in disease and tissue engineering. *Front. Cell Dev. Biol.* 8:260. doi: 10.3389/fcell.2020.00260

Maggio, I., Stefanucci, L., Janssen, J. M., Liu, J., Chen, X., Mouly, V., et al. (2016). Selection-free gene repair after adenoviral vector transduction of designer nucleases: rescue of dystrophin synthesis in DMD muscle cell populations. *Nucleic Acids Res.* 44, 1449–1470. doi: 10.1093/nar/gkv1540

Massagué, J. (2008). TGFβ in cancer. *Cell* 134, 215–230.

Massari, M. E., and Murre, C. (2000). Helix-loop-helix proteins: regulators of transcription in eucaryotic organisms. *Mol. Cell Biol.* 20, 429–440. doi: 10.1128/mcb.20.2.429-440.2000

Medici, D., Potenta, S., and Kalluri, R. (2011). Transforming growth factor-β2 promotes Snail-mediated endothelial–mesenchymal transition through convergence of Smad-dependent and Smad-independent signalling. *Biochem. J.* 437, 515–520. doi: 10.1042/bj20101500

Medici, D., Shore, E. M., Lounev, V. Y., Kaplan, F. S., Kalluri, R., and Olsen, B. R. (2010). Conversion of vascular endothelial cells into multipotent stem-like cells. *Nat. Med.* 16:1400. doi: 10.1038/nm.2252

Mihira, H., Suzuki, H. I., Akatsu, Y., Yoshimatsu, Y., Igarashi, T., Miyazono, K., et al. (2012). TGF-β-induced mesenchymal transition of MS-1 endothelial cells requires Smad-dependent cooperative activation of Rho signals and MRTF-A. *J. Biochem.* 151, 145–156. doi: 10.1093/jb/mvr121

Miyazono, K. (2009). Transforming growth factor-β signaling in epithelial-mesenchymal transition and progression of cancer. *Proc. Jpn Acad. Ser B* 85, 314–323. doi: 10.2183/pjab.85.314

Montague, T. G., Cruz, J. M., Gagnon, J. A., Church, G. M., and Valen, E. (2014). CHOPCHOP: a CRISPR/Cas9 and TALEN web tool for genome editing. *Nucleic Acids Res.* 42, W401–W407.

Nieto, M. A. (2002). The snail superfamily of zinc-finger transcription factors. *Nat. Rev. Mol. Cell Biol.* 3, 155–166. doi: 10.1038/nrm757

Pepper, M. S., Montesano, R., Orci, L., and Vassalli, J.-D. (1991). Plasminogen activator inhibitor-1 is induced in microvascular endothelial cells by a chondrocyte-derived transforming growth factor-beta. *Biochem. Biophys. Res. Commun.* 176, 633–638. doi: 10.1016/s0006-291x(05)80231-1

Persson, U., Izumi, H., Souchelnytskyi, S., Itoh, S., Grimsby, S., Engström, U., et al. (1998). The L45 loop in type I receptors for TGF−β family members is a critical determinant in specifying Smad isoform activation. *FEBS Lett.* 434, 83–87. doi: 10.1016/s0014-5793(98)00954-5

Pinto, M. T., Melo, F. U. F., Malta, T. M., Rodrigues, E. S., Placa, J. R., Silva, W. A. Jr., et al. (2018). Endothelial cells from different anatomical origin have distinct responses during SNAIL/TGF-β2-mediated endothelial-mesenchymal transition. *Am. J. Transl.* 10:4065.

Potenta, S., Zeisberg, E., and Kalluri, R. (2008). The role of endothelial-to-mesenchymal transition in cancer progression. *Br. J. Cancer* 99, 1375–1379. doi: 10.1038/sj.bjc.6604662

Sabbineni, H., Verma, A., and Somanath, P. R. (2018). Isoform−specific effects of transforming growth factor β on endothelial−to−mesenchymal transition. *J. Cell. Physiol.* 233, 8418–8428. doi: 10.1002/jcp.26801

Saito, A. (2013). EMT and EndMT: regulated in similar ways? *J. Biochem.* 153, 493–495. doi: 10.1093/jb/mvt032

Sánchez-Duffhues, G., De Vinuesa, A. G., Lindeman, J. H., Mulder-Stapel, A., Deruiter, M. C., Van Munsteren, C., et al. (2015). SLUG is expressed in endothelial cells lacking primary cilia to promote cellular calcification. *Arterioscler. Thromb. Vasc. Biol.* 35, 616–627. doi: 10.1161/atvbaha.115.305268

Souilhol, C., Harmsen, M. C., Evans, P. C., and Krenning, G. (2018). Endothelial–mesenchymal transition in atherosclerosis. *Cardiovasc. Res.* 114, 565–577. doi: 10.1093/cvr/cvx253

Stankic, M., Pavlovic, S., Chin, Y., Brogi, E., Padua, D., Norton, L., et al. (2013). TGF-β-Id1 signaling opposes Twist1 and promotes metastatic colonization via a mesenchymal-to-epithelial transition. *Cell Rep.* 5, 1228–1242. doi: 10.1016/j.celrep.2013.11.014

Suzuki, Y., Ohga, N., Morishita, Y., Hida, K., Miyazono, K., and Watabe, T. (2010). BMP-9 induces proliferation of multiple types of endothelial cells in vitro and in vivo. *J. Cell Sci.* 123, 1684–1692. doi: 10.1242/jcs.061556

Ten Dijke, P., Egorova, A. D., Goumans, M.-J. T., Poelmann, R. E., and Hierck, B. P. (2012). TGF-β signaling in endothelial-to-mesenchymal transition: the role of shear stress and primary cilia. *Sci. Signal* 5, t2–t2.

Van Meeteren, L. A., and Ten Dijke, P. (2012). Regulation of endothelial cell plasticity by TGF-β. *Cell Tissue Res.* 347, 177–186. doi: 10.1007/s00441-011-1222-6

Walter-Yohrling, J., Morgenbesser, S., Rouleau, C., Bagley, R., Callahan, M., Weber, W., et al. (2004). Murine endothelial cell lines as models of tumor endothelial cells. *Clin. Cancer Res.* 10, 2179–2189. doi: 10.1158/1078-0432.ccr-03-1013

Wojnarowicz, P. M., E Silva, R. L., Ohnaka, M., Lee, S. B., Chin, Y., Kulukian, A., et al. (2019). A small-molecule pan-Id antagonist inhibits pathologic ocular neovascularization. *Cell Rep.* 29, 62.–75.

Wojnarowicz, P. M., Escalono, M. G., Huang, Y.-H., Desai, B., Chin, Y., Shah, R., et al. (2020). Anti-tumor effects of an Id antagonist with no acquired resistance. *bioRxiv* doi: 10.1101/2020.01.06.894840

Wu, Y., Deng, J., Rychahou, P. G., Qiu, S., Evers, B. M., and Zhou, B. P. (2009). Stabilization of snail by NF-κB is required for inflammation-induced cell migration and invasion. *Cancer Cell* 15, 416–428. doi: 10.1016/j.ccr.2009.03.016

Yang, J., Antin, P., Berx, G., Blanpain, C., Brabletz, T., Bronner, M., et al. (2020). Guidelines and definitions for research on epithelial–mesenchymal transition. *Nat. Rev. Mole. Cell Biol.* 21, 341–352.

Yang, X., Han, M., Han, H., Wang, B., Li, S., Zhang, Z., et al. (2017). Silencing Snail suppresses tumor cell proliferation and invasion by reversing epithelial-to-mesenchymal transition and arresting G2/M phase in non-small cell lung cancer. *Int. J. Oncol.* 50, 1251–1260. doi: 10.3892/ijo.2017.3888

Yoshimatsu, Y., and Watabe, T. (2011). Roles of TGF-β signals in endothelial-mesenchymal transition during cardiac fibrosis. *Int. J. Inflam.* 2011:724080.

Zeisberg, E. M., Tarnavski, O., Zeisberg, M., Dorfman, A. L., Mcmullen, J. R., Gustafsson, E., et al. (2007). Endothelial-to-mesenchymal transition contributes to cardiac fibrosis. *Nat. Med.* 13, 952–961.

Zhang, H., Liu, Y., Yan, L., Du, W., Zhang, X., Zhang, M., et al. (2018). Bone morphogenetic protein−7 inhibits endothelial−mesenchymal transition in pulmonary artery endothelial cell under hypoxia. *J. Cell Physiol.* 233, 4077–4090. doi: 10.1002/jcp.26195

Zhang, L., Zhou, F., Drabsch, Y., Gao, R., Snaar-Jagalska, B. E., Mickanin, C., et al. (2012). USP4 is regulated by AKT phosphorylation and directly deubiquitylates TGF-β type I receptor. *Nat. Cell Biol.* 14, 717–726. doi: 10.1038/ncb2522

Conflict of Interest: The authors declare that the research was conducted in the absence of any commercial or financial relationships that could be construed as a potential conflict of interest.

Copyright © 2021 Ma, van der Zon, Gonçalves, van Dinther, Thorikay, Sanchez-Duffhues and ten Dijke. This is an open-access article distributed under the terms of the Creative Commons Attribution License (CC BY). The use, distribution or reproduction in other forums is permitted, provided the original author(s) and the copyright owner(s) are credited and that the original publication in this journal is cited, in accordance with accepted academic practice. No use, distribution or reproduction is permitted which does not comply with these terms.

frontiers in Cell and Developmental Biology

MINI REVIEW
published: 16 February 2021
doi: 10.3389/fcell.2021.642352

Notch Signaling in Vascular Endothelial Cells, Angiogenesis, and Tumor Progression: An Update and Prospective

Abdellah Akil[1†], Ana K. Gutiérrez-García[1†], Rachael Guenter[1†], J. Bart Rose[1,2], Adam W. Beck[1], Herbert Chen[1,2] and Bin Ren[1,2]*

[1] Department of Surgery, School of Medicine, University of Alabama at Birmingham, Birmingham, AL, United States, [2] O'Neal Comprehensive Cancer Center, School of Medicine, University of Alabama at Birmingham, Birmingham, AL, United States

The Notch signaling pathway plays an essential role in a wide variety of biological processes including cell fate determination of vascular endothelial cells and the regulation of arterial differentiation and angiogenesis. The Notch pathway is also an essential regulator of tumor growth and survival by functioning as either an oncogene or a tumor suppressor in a context-dependent manner. Crosstalk between the Notch and other signaling pathways is also pivotal in tumor progression by promoting cancer cell growth, migration, invasion, metastasis, tumor angiogenesis, and the expansion of cancer stem cells (CSCs). In this review, we provide an overview and update of Notch signaling in endothelial cell fate determination and functioning, angiogenesis, and tumor progression, particularly in the development of CSCs and therapeutic resistance. We further summarize recent studies on how endothelial signaling crosstalk with the Notch pathway contributes to tumor angiogenesis and the development of CSCs, thereby providing insights into vascular biology within the tumor microenvironment and tumor progression.

Keywords: angiogenesis, arteriolar niche, cancer stem cell, Notch signaling, tumor microenvironment

OPEN ACCESS

Edited by:
Arie Horowitz,
Université de Rouen, France

Reviewed by:
Paola Rizzo,
University of Ferrara, Italy
Mohit Kumar Jolly,
Indian Institute of Science (IISc), India

***Correspondence:**
Bin Ren
bren@uabmc.edu;
ren.science@gmail.com

† These authors have contributed equally to this work

Specialty section:
This article was submitted to Signaling, a section of the journal Frontiers in Cell and Developmental Biology

Received: *15 December 2020*
Accepted: *19 January 2021*
Published: *16 February 2021*

Citation:
Akil A, Gutiérrez-García AK, Guenter R, Rose JB, Beck AW, Chen H and Ren B (2021) Notch Signaling in Vascular Endothelial Cells, Angiogenesis, and Tumor Progression: An Update and Prospective. Front. Cell Dev. Biol. 9:642352. doi: 10.3389/fcell.2021.642352

OVERVIEW OF THE NOTCH SIGNALING PATHWAY

The Notch signaling pathway is highly conserved across all vertebrate species and orchestrates a diverse range of functions including cell growth, differentiation, and patterning. In mammals, this pathway features four transmembrane receptors (Notch 1–4) that interact with five canonical transmembrane ligands (Jagged 1, 2; Delta-like ligand 1, 3, and 4) (Aquila et al., 2019). Canonical Notch signaling has been more widely characterized than non-canonical Notch signaling. Activation of the canonical Notch pathway begins when a Notch receptor extracellularly interacts with a Notch ligand, which subsequently initiates proteolytic cleavage of the receptor. This cleavage precedes two sequential proteolytic events that require the enzymes including the disintegrin metalloproteinase domain-containing protein 10 (ADAM10) and the γ-secretase. The series of cleavage events following the initial Notch receptor–ligand interaction result in the release of the Notch receptor intracellular domain (NICD) from the cell membrane. The NICD then translocates to the nucleus where it acts as a transcriptional coactivator in cooperation with recombination of signal-binding protein for the immunoglobulin kappa J region (RBPJ).

The NICD–RBPJ interaction initiates transcription of Notch target genes to regulate cell fate determination, migration, differentiation, and proliferation under both normal and malignant conditions (**Figure 1**). Consequently, Notch signaling can control the expression of a group of target genes that ultimately impact critical cellular functions (D'Souza et al., 2010; Kangsamaksin et al., 2014).

In contrast, non-canonical Notch signaling can be initiated by a non-canonical ligand and may not require cleavage of the Notch receptors. In some forms of non-canonical signaling, there is no involvement of RBPJ, which may reflect interactions with other signaling pathways upstream of the NICD–RBPJ complex (Andersson et al., 2011). Given the diverse roles of Notch signaling in different contexts, it is not surprising that defects in Notch ligands or perturbations in the overall Notch pathway have been associated with genetic disorders and cancers.

NOTCH SIGNALING IN ENDOTHELIAL CELLS AND ANGIOGENESIS

Angiogenesis in general refers to the formation of new blood vessels from preexisting vasculature, a process that is vital for normal tissue growth, development, and wound healing (Ren et al., 2019; Liu et al., 2020). Blood vessels make up complex vascular networks composed of arteries (arteriogenesis and *de novo* arteriogenesis), capillaries (vasculogenesis), and veins (venogenesis). These networks supply oxygen and nutrients to all tissues and remove wastes in the body in support of tissue growth and organ function under physiological and pathological conditions (Sitohy et al., 2011; Nagy and Dvorak, 2012; Ren et al., 2019). The process of generating new blood vessels occurs through several different mechanisms. One mechanism is the sprouting angiogenesis. This process is initiated by the release of growth factors from cells and requires the coordination of a series of cellular processes. One key process is the selection of a migrating tip cell at the end of the sprout, a tightly coordinated balance between newly forming endothelial cells (ECs), and the maintenance of existing vascular tubes (Otrock et al., 2007; Blanco and Gerhardt, 2013).

Studies suggest that Notch signaling plays an essential role in angiogenesis through interactions with the Notch ligands, in addition to crosstalk with other pathways such as vascular endothelial growth factor (VEGF) signaling. Delta-like ligand 4 (DLL4) has been shown to be a critical Notch ligand for stimulating angiogenesis (Benedito et al., 2009;

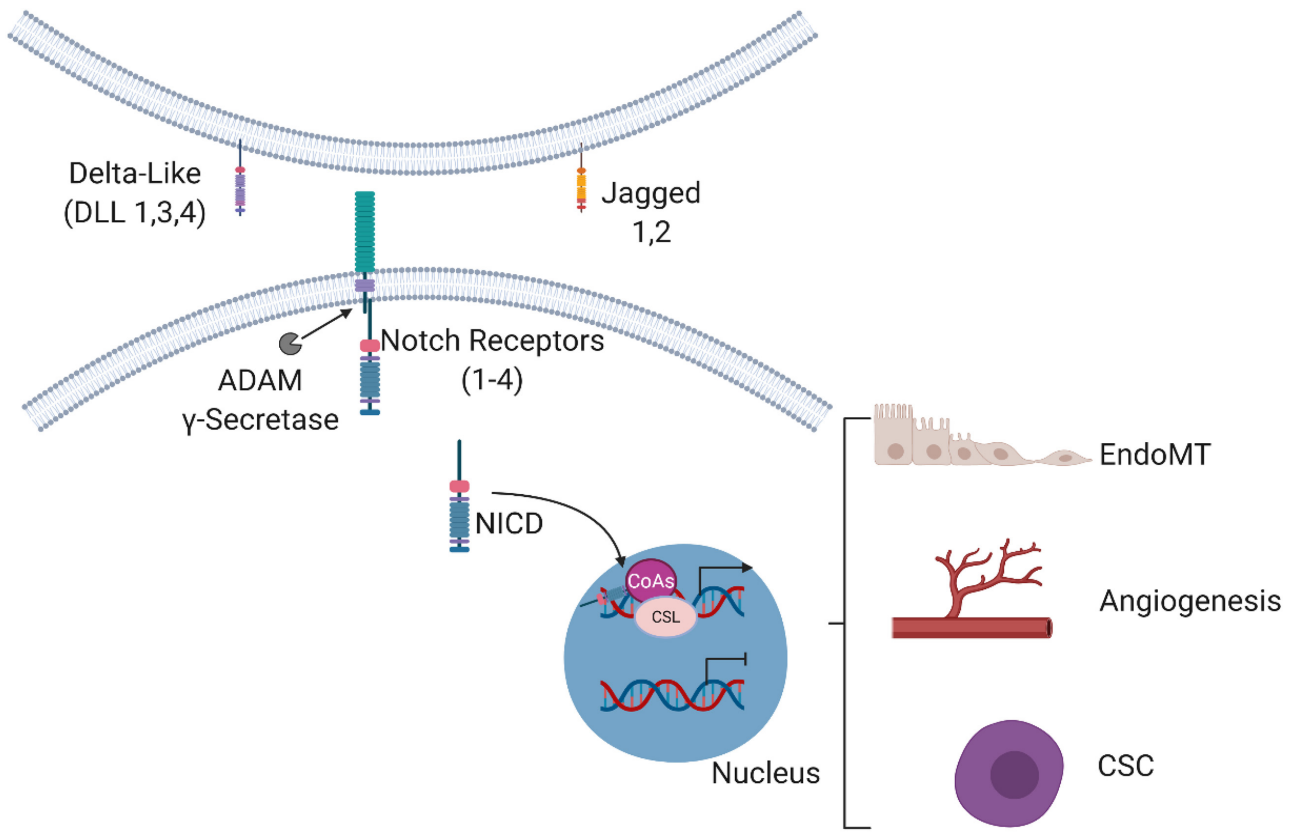

FIGURE 1 | Overview of the Notch signaling pathway. Binding of the Notch ligands (Delta-like 1, Delta-like 3, Delta-like 4, Jagged 1 and Jagged 2) to the transmembrane Notch receptors (Notch 1–4) results in proteolytic cleavage events by ADAM and γ-secretase to mediate the release of the Notch intracellular domain (NICD). The NICD then enters the nucleus and interacts with cofactors to regulate the expression of target genes involved in EndoMT, angiogenesis, and CSC biology.

Blanco and Gerhardt, 2013; Oon et al., 2017; Naito et al., 2020). However, another Notch ligand, Jagged1 (Jag1), can compete with DLL4 to negatively regulate angiogenesis (Taslimi and Das, 2018). This concept was recently illustrated in an *in vitro* study showing that Jag1 is a potent pro-angiogenic regulator capable of antagonizing DLL4–mediated Notch signaling in angiogenesis (Benedito et al., 2009).

Moreover, Notch signaling may directly and/or indirectly regulate angiogenesis through crosstalk with VEGF receptors (VEFGRs) (Garcia and Kandel, 2012; Luo et al., 2019). For instance, in a murine retinal model, DLL4 may act downstream of VEGF as a negative regulator of VEGF-mediated angiogenesis (Suchting et al., 2007). Notch signaling can therefore influence both the induction and the cessation of angiogenesis through different mechanisms. This apparent involvement of Notch signaling emphasizes its potential role as a target for controlling angiogenesis.

The ability of Notch signaling to dictate angiogenetic processes becomes important in the context of aberrant angiogenesis. Pathological angiogenesis plays an important role in abnormal vessel growth and contributes to the pathogenesis of such human diseases as diabetic retinopathy, ischemic cardiovascular diseases, inflammatory processes (rheumatoid arthritis), and cancer (Carmeliet, 2005). In cancer, angiogenesis is critical for disease progression. Abnormal angiogenesis in the tumor microenvironment (TME) can promote tumor growth and progression (Carmeliet, 2005). Therefore, targeting different aspects of the Notch signaling pathway may be a feasible approach to inhibiting pathogenic angiogenesis. For example, therapeutically inhibiting DLL4 in murine ischemic retinas has shown potential to promote the growth of normal blood vessels to partially reverse ischemic conditions (Lobov and Mikhailova, 2018). In addition, blocking the DLL4/Notch1 interaction in cancer is being explored in clinical trials because DLL4 inhibition has been shown to cause non-productive vessel formation within the TME, thereby inhibiting tumor growth (Kuhnert et al., 2011). Designing targeted treatments against Notch signaling may thus demonstrate therapeutic potential by regulating angiogenesis in different disease contexts.

Notch signaling is also implicated in arteriogenesis and *de novo* arteriogenesis, the growth of functional collateral arteries from preexisting arterio-arteriolar anastomoses and *de novo* arterial development, in which smooth muscle cells (SMCs) cover ECs (Heil et al., 2006). The preferential expression of DLL4 on arterial ECs highlights the importance of Notch signaling in arteriogenesis (Shutter et al., 2000; Liu et al., 2003). In fact, DLL4/Notch1 signaling may function downstream of VEGF during arteriogenesis and likely supports the survival and differentiation of arterial ECs (Lawson et al., 2001). However, the complete function of Notch signaling during arteriogenesis has yet to be delineated.

It is plausible that the Notch pathway interacts with other factors, such as CD36, to produce differential responses via regulation of VEGFR2 signaling. CD36 is a well-known anti-angiogenic receptor that is mainly expressed in microvascular ECs (MVECs) and arteriolar ECs in the vascular system. CD36 downregulation has been linked to the upregulation of pro-angiogenic and arterial genes (Ren et al., 2016). Several studies have demonstrated the association of CD36 expression with both angiogenesis and *de novo* arteriogenesis in adult organisms under oncogenic and pathological conditions (Ren et al., 2011, 2016; Dong et al., 2017). However, the relationship between CD36 and Notch signaling remains largely unknown. Jabs et al. (2018) demonstrated that in CD36 transcription is upregulated by molecules known to function downstream of Notch in vascular ECs. In addition, Notch signaling may play a significant role during arteriogenesis by interacting with such other factors as VEGF, FoxO1, and potentially CD36 (Ren et al., 2010, 2011, 2016; Ren, 2018). This potential interaction could be a *de novo* process, particularly under pathological conditions and occur within the TME (Ren et al., 2019).

Notch Signaling in Endothelial Differentiation and Fate Determination

Regulation of cell fate decisions is a hallmark characteristic of Notch signaling. In the vasculature, a primary effect of Notch signaling is the promotion of stalk/tip cell specification (Mack and Iruela-Arispe, 2018). During angiogenesis, Notch signaling coordinates tip versus stalk phenotypes within a growing sprout. Expression of DLL4 at the end of the sprout (tip cell) activates Notch1 in the stalk cell (Blanco and Gerhardt, 2013).

Crosstalk between VEGF and Notch signaling is fundamental to sprout formation, vascular EC maintenance, and the establishment of EC heterogeneity (Blanco and Gerhardt, 2013). When Notch is inactivated at the onset of angiogenesis, there is a significant expansion of tip cells at the expense of stalk cells (Mack and Iruela-Arispe, 2018). Moreover, Notch inactivation can result in the loss of vascular hierarchy as tip cells are unable to organize tubes or form stable junctional complexes (Mack and Iruela-Arispe, 2018). Thus, Notch signaling is required for vascular stabilization and differentiation of the emerging vascular tree through the suppression of EC proliferation and stabilization of cell–cell junctions.

Notch signaling also plays a role to prevent excessive sprouting. Upon DLL4-mediated Notch activation, the induction of tip cells is repressed by a process called "lateral inhibition." During lateral inhibition, VEGF signaling promotes the upregulation of DLL4 in tip cells, which in turn trans-activates Notch in the neighboring cells. Interestingly, a recent mathematical model of Notch-Jagged signaling revealed intriguing aspects about the existence of a third EC state. In addition to the two EC states (Tip or Stalk), Boareto et al. (2015) reported a novel hybrid state that exhibits intermediary tip and stalk cell characteristics, which may result from the asymmetric effects of the Notch intracellular domain. This allows neighboring cells to attain either opposite or similar fates, depending on which ligand is dominant (Delta-mediated signaling drives neighboring cells to have an opposite fate versus Jagged-mediated signaling drives the cell to maintain a similar fate). Additionally, Venkatraman et al. (2016) further confirmed the presence of a hybrid state apart from the traditional tip and stalk states. They showed that EC patterning dynamics does not solely depend upon the presence of Jag and this hybrid

state can be found in both normal and pathological conditions. More evidence was provided by Koon et al. (2018), who, in addition to providing a computational model, also demonstrated the presence of the hybrid state by immunofluorescent stains for the known tip cell markers Delta and CD34. Importantly, the canonical tip cells, stalk cells and hybrid cells can be distinguished based upon the fluorescent signal intensity and the position of cells.

Notch signaling is also required for the proper formation of vascular branches. Recent studies have demonstrated that Notch regulates endothelial branching in response to other pathways, including BMP and SMAD1/5/8 signaling (Mack and Iruela-Arispe, 2018). SMAD6, an inhibitory protein that filters input signals from SMAD1/5/8, is regulated intrinsically by Notch levels (Mouillesseaux et al., 2016). The distribution of vascular sprouts depends upon the "Notch status" of a given cell within the sprout. Furthermore, the decision to form a new sprout or to widen the original vessel relies upon differential expression patterns of Notch-DLL4, BMP, and VEGF between cells (Mack and Iruela-Arispe, 2018) (**Figure 2**).

Lawson et al. (2001) showed in zebrafish embryos that the loss of Notch signaling leads to molecular defects in arterial venous differentiation. This finding might constitute an important link between blood flow and maintenance of Notch1 expression in adult arteries. We recently showed that a lipid signaling mediator lysophosphatidic acid (LPA) may promote angiogenesis and induce the arteriolar differentiation of vascular ECs via protein kinase PKD-1, a process in which the expression of DLL4 may play an important role (Ren et al., 2011, 2016; Best et al., 2018; Jiang et al., 2020). Acting via transcription factor FoxO1, PKD-1 could dictate arterial fate by the regulation of MVEC transdifferentiation (Ren et al., 2016; Ren, 2018). This may be associated with its regulation of CD36 transcription and fatty acid metabolism (Ren et al., 2016; Dong et al., 2017). Furthermore, Notch signaling may interact with the MAPK/Erk1/2 pathway, downstream of PKD-1 signaling, to promote arterial differentiation through inducing expression of ephrin B2, Hey2, and DLL4 during arteriogenesis under either developmental or ischemic conditions (Ren et al., 2010, 2016).

A recent study that combined computational modeling with *in vivo* experiments demonstrated that a VEGF-mediated positive signaling feedback can shape the timing, magnitude, and robustness of determining tip cell identity for angiogenic branching, which is terminated by DLL4-Notch signaling. Mechanistically, the induction of expression of tm4sf18 (an atypical tetraspanin) dictates the speed and robustness of EC selection for angiogenesis by stimulating VEGF signaling (Page et al., 2019). Intriguingly, this study demonstrates that Tm4sf18-mediated positive feedback appears to be specific to VEGF-induced arterial EC sprouting, implicating its functional role in *de novo* arteriogenesis.

On the other hand, Guarani et al. (2011) showed that NAD-dependent deacetylase sirtuin-1 (SIRT1) acts as an intrinsic negative modulator of Notch signaling in ECs. They also found that acetylation of the NICD on conserved lysine residues controls the amplitude and duration of Notch responses by

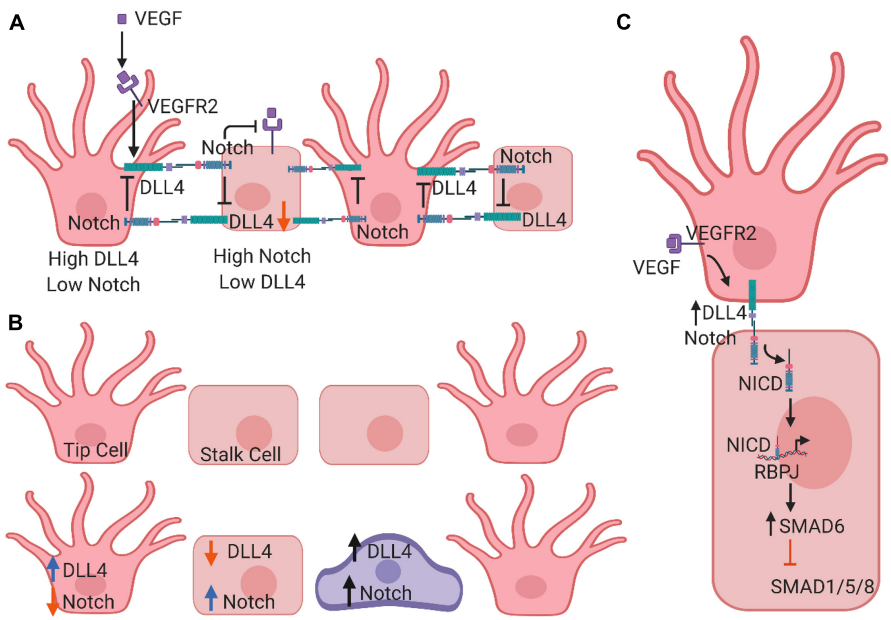

FIGURE 2 | Schematic models of Notch signaling in vascular endothelial cell (EC) differentiation. **(A)** In endothelial tip cells, VEGF signaling induces DLL4 expression, which activates Notch1 signaling. In endothelial stalk cells, activation of Notch signaling via DLL4 suppresses differentiation toward a tip cell phenotype. **(B)** Graphic representation of lateral inhibition to show a classical salt and pepper pattern where tip cells are separated exactly by one stalk cell. DLL4 of one cell binds to the Notch receptor of the adjacent cell, and Notch inhibits DLL4 expression and the VEGFR2 signaling within the same cell. **(C)** Mathematic model of Notch signaling in asymmetric patterning. Cells do not necessarily adopt a canonical salt and pepper pattern. Instead, two tip cells might be separated by a few stalk cells, which could be determined by Jag. It is also possible that an intermediary tip cell may express similar DLL4 and Notch expression. Both theories involve a third EC state.

altering NICD protein turnover. SIRT1 associates with NICD and functions as a NICD deacetylase, which opposes acetylation-induced NICD stabilization. Consequently, ECs lacking SIRT1 activity are sensitized to Notch signaling, resulting in impaired growth, sprout elongation, and enhanced Notch target gene expression in response to DLL4 stimulation, thereby adopting a non-sprouting, stalk-cell-like phenotype. *In vivo*, inactivation of SIRT1 in zebrafish and mice reduces vascular branching due to enhanced Notch signaling (Guarani et al., 2011).

Notch Signaling in Proliferation and Apoptosis of Both Endothelial and Cancer Cells

The formation of a new blood vessel requires not only the selection of an endothelial tip cell, but also EC proliferation to enable sprout growth in length and diameter (Phng and Gerhardt, 2009). Notch signaling is required for the stabilization and differentiation of the emerging vascular trees, and it does so by suppressing EC proliferation and stabilization of cell–cell junctions. Several studies have shown that Notch signaling inhibits proliferation in ECs (Noseda et al., 2004; Liu G. et al., 2006; Harrington et al., 2008; Trindade et al., 2008). Notch signaling can inhibit the sprouting of ECs during the growth of blood vessels through the direct interaction between Notch receptors and DLL4 (Lobov and Mikhailova, 2018), further suggesting that DLL4 plays a fundamental role in vascular development and angiogenesis.

The Notch pathway also plays a significant role in apoptosis of both ECs and cancer cells. Notch appears to regulate apoptosis through extensive networks involving cell cycle, growth, and survival pathways. The Notch receptors seemingly play opposite roles in the endothelium. For instance, Notch1 and Notch4 prevent apoptosis induced by lipopolysaccharides (LPS) by increasing the levels of Bcl2 (Rizzo et al., 2013), TNF-α, and turbulent blood flow (Walshe et al., 2011). The activation of Notch signaling in human umbilical vein ECs (HUVECs) by estrogens promotes EC survival in response to TNF-α via signaling crosstalk between E2 and the Notch pathway (Fortini et al., 2017). This protective role may be attributable to Notch1-mediated Akt phosphorylation (Fortini et al., 2017) and estradiol-mediated protection via the estrogen receptor-β. On the other hand, Notch2 sensitizes ECs to apoptosis by inhibiting the expression of survivin, a key anti-apoptotic regulator (Quillard et al., 2009). Furthermore, during vascular remodeling, the activation of Notch signaling can cause EC apoptosis and thereby disrupt the balance of EC proliferation and regeneration (Dejana et al., 2017). Specifically, an increase of Notch3 can downregulate the expression of the anti-apoptotic gene *Bcl-1* in ECs, leading to apoptosis (Kartalaei et al., 2015; Dejana et al., 2017). The effects of Notch signaling on apoptosis has also been discussed by Aquila et al. (2019) in a recent review.

In the context of cancer, Notch signaling has been associated with multiple mechanisms of apoptosis. For example, the activation of Notch1 in colon cancer inhibits apoptosis by repressing p27 expression (Hristova et al., 2013; Meisel et al., 2020). Other studies have reported that the inhibition of Notch signaling by miRNAs leads to an increase in cancer cell apoptosis. For example, Du et al. (2017) showed that miR-145 induces glioma cell apoptosis by inhibiting Notch signaling through the binding of Bcl2/adenovirus E1b interacting protein 3 (BNIP3) to its 3′-UTR in glioma cells. Additionally, Li et al. (2018) demonstrated that overexpression of miR-22 promotes apoptosis in ovarian cancer cells by suppressing Notch signaling. Therefore, the Notch pathway could represent a promising therapeutic target in certain types of cancer since suppression of Notch signaling results in the loss of the malignant phenotype in both *in vitro* and *in vivo* models. However, the toxicity of Notch inhibitors to normal cells should be considered. To minimize the side effects, cancer-specific targeting should be an optimal strategy.

Notch Signaling in Endothelial to Mesenchymal Transition

Endothelial-to-mesenchymal transition (EndoMT) is a process where ECs lose their endothelial-specific phenotype and progressively acquire mesenchymal properties such as formation of spindle-shaped elongated cell morphology, loss of cell–cell junctions and polarity, and increased cellular motility, loss of endothelial markers (such as CD31 or vascular endothelial (VE) cadherin), and the acquirement of mesenchymal features [such as expression of N-cadherin, fibroblast-specific protein 1 (FSP1), or α-smooth muscle actin (αSMA)] (Zeisberg et al., 2007a; Azhar et al., 2009).

As major components of the vascular networks in the TME, ECs demonstrate plasticity and the potential to transdifferentiate into mesenchymal cells via EndoMT. EndoMT has been shown to participate in critical embryonic developmental processes and the pathogenesis in a variety of genetic and acquired human diseases including cancer-associated fibrosis (Zeisberg et al., 2007a), cardiac fibrosis (Zeisberg et al., 2007b), and atherosclerosis (Chen P.Y. et al., 2015). A recent review highlighted important roles of EndoMT within the TME during tumor progression and the acquisition of therapeutic resistance (Clere et al., 2020). Cells that underwent EndoMT increased expression of the Snail family proteins, which plays a critical role in disrupting cell–cell junctions (Potenta et al., 2008). Furthermore, Notch can either directly induce or suppress gene expression. As an example, Notch signaling can upregulate Snail and Slug to ultimately initiate EndoMT in developmental and pathological conditions (Niessen et al., 2008; Welch-Reardon et al., 2015) (**Figure 3**).

In addition to the complete epithelial-to-mesenchymal transition (EMT)/EndoMT, the concept of partial EMT/EndoMT has emerged recently, which was described by Welch-Reardon et al. (2015). Examples of a partial EndoMT process include angiogenic sprouting, the crosstalk between Notch and VEGF pathways in hypoxic tumors to form unstable and leaky vessels (Holderfield and Hughes, 2008), and a process involving tubulogenesis (cells temporarily lose apical-basal polarity and gain migratory capacity, but never fully acquire all mesenchymal phenotypes) (Welch-Reardon et al., 2015). However, the molecular signaling and mechanisms by which epithelial or endothelial cells undergo either complete or partial

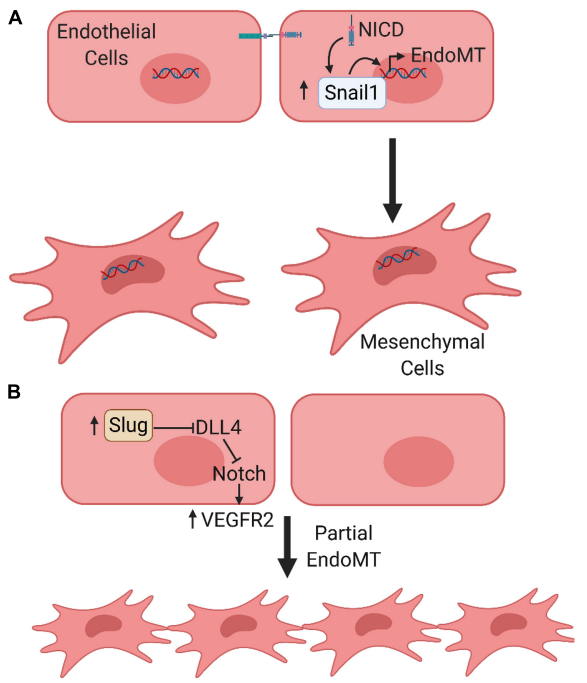

FIGURE 3 | Notch signaling regulates endothelial to mesenchymal transition. **(A)** Notch signaling induces an endothelial to mesenchymal transition (EndoMT). As an example, active NICD regulates the expression of Snail1, a key EndoMT transcription factor to promote EndoMT. **(B)** Partial EndoMT, where cells temporarily lose apical-basal polarity and gain migratory capacity, while retaining intercellular junctions and undergoing collective rather than individualized cell migration.

EMT/EndoMT are largely unknown. Welch-Reardon et al. (2015) proposed that Notch signaling, being a contact-dependent pathway, may play an important role in the case of sprouting angiogenesis (Welch-Reardon et al., 2015). Their recent study demonstrated that endothelial Slug activity may be involved in driving the transition of ECs toward a partial EndoMT state. This activity promotes sprouting angiogenesis by modulation of Notch signaling via transcriptional repression of DLL4 and upregulation of VEGFR2 (Hultgren et al., 2020). It should also be noted that anti-angiogenic signaling could be involved in the regulation of arterial sprouting and angiogenesis under complex physiological conditions *in vivo*, particularly under pathological conditions such as tumor angiogenesis (Ren et al., 2006, 2009, 2016; Kazerounian et al., 2011). The association between this process, EndoMT and the Notch pathway warrants further exploration.

Notch activation in conjunction with sprouting angiogenesis could be a crucial determinant of either partial or full EndoMT. However, other signaling pathways such as Wnt and TGF-β signaling pathway are also capable of promoting partial EndoMT. Mechanistic studies have demonstrated a role for both TGF-β and bone morphogenic protein (BMP) in conjunction with Notch signaling to regulate EndoMT in embryonic heart formation (Thiery and Sleeman, 2006). In addition, the role of Notch signaling in EndoMT is prominent during heart valve development, arterial venous differentiation, and the remodeling of the primitive vascular plexus (Lin et al., 2012). Intriguingly, inhibition of Notch signaling abrogates TGF-β-stimulated EndoMT in HUVECs (Chen X. et al., 2015).

While the interaction between Notch and EndoMT is pivotal during tumor progression via a complex modulation of both the tumor and the surrounding stroma (Nie et al., 2014). Ghiabi et al. (2015) showed that xenograft cells from two different breast cancer cell lines, MDA-MB-231 and MCF-7, promoted the acquisition of a contact-dependent mesenchymal phenotype in ECs that contributed to the generation of a pro-tumoral niche. The authors concluded that Notch signaling likely induces a tumor-fostered mesenchymal phenotype in ECs, while the endothelial characteristics of ECs remain unchanged (the cells maintain EC traits). This suggests that Notch signaling might promote partial EndoMT. In the context of CSCs, Marín-Ramos et al. (2019) demonstrated that Notch signaling is necessary for TGF-β-stimulated EndoMT in glioblastoma.

These studies strongly support a role for Notch signaling in the development of multiple biological processes and diseases through regulation of EndoMT. Significantly, it is worth investigating whether and how Notch signaling contributes to the development of metastatic niche in tumor progression and therapeutic resistance through promoting EndoMT and/or partial EndoMT, either of which might play a critical role in the regulation of TME plasticity and CSC heterogeneity.

NOTCH SIGNALING IN TUMOR PROGRESSION

Overview

Dysregulated Notch signaling has been documented in a variety of human cancers including melanoma (Ntziachristos et al., 2014), lymphoma (Aster et al., 2017), glioma (Teodorczyk and Schmidt, 2014), breast cancer (Guo et al., 2011), ovarian cancer (Ntziachristos et al., 2014), head and neck cancer (Ntziachristos et al., 2014), colorectal cancer (Ntziachristos et al., 2014), pancreatic adenocarcinoma (Ntziachristos et al., 2014), hepatocellular carcinoma (Ntziachristos et al., 2014), glioblastoma (Ntziachristos et al., 2014), thyroid cancer (Guenter et al., 2021), and neuroendocrine cancer (Ren et al., 2019). Given the involvement of Notch signaling in many different cancers, this pathway has become a key target for developing therapeutics to treat broad spectrum of patients. However, the role of Notch signaling in tumorigenesis often depends upon the type of cancer. Depending upon the context, Notch activation can be either oncogenic or tumor suppressive. The opposing roles of Notch signaling may be attributed to the innate function of Notch in a cell type-dependent manner, and to crosstalk between Notch signaling and other cellular pathways.

Oncogenic Notch signaling activation is often linked to an increase in cellular proliferation, inhibition of apoptosis, suppression of cellular differentiation, and the induction of CSC features (Aster et al., 2017; Brzozowa-Zasada et al., 2017). In T-cell acute lymphoblastic leukemia (ALL), a mutation that causes constitutive activation of Notch1 drives tumorigenesis by

regulating Notch-dependent transcription factors that promote cell growth, proliferation, and self-renewal (Weng et al., 2004; Sanchez-Martin and Ferrando, 2017). In ovarian cancer, aberrant activation of Notch signaling contributes to chemoresistance, while overexpression of the Notch3 receptor correlates with advanced stage disease, metastasis, and poor overall survival (Jung et al., 2010; Brzozowa-Zasada et al., 2017).

The tumor suppressive role of Notch has been described in other malignancies including bladder squamous cell carcinoma (bladder SCC), medullary thyroid cancer (MTC), and skin cancer (Weng and Aster, 2004; Dotto, 2008; Rampias et al., 2014; Jaskula-Sztul et al., 2015; Tamagnone et al., 2018). In bladder SCC, mutations that ablate Notch activity lead to an earlier onset of disease and more aggressive tumor progression (Nowell and Radtke, 2017). In MTC, overexpression of Notch1 and Notch3 may limit tumor cell growth and proliferation *in vitro* and *in vivo* in a dose-dependent manner (Jaskula-Sztul et al., 2011, 2015). Similarly, mice that conditionally lack Notch1 in keratinocytes demonstrate increased keratinocyte proliferation and delayed terminal differentiation, thereby leading to increased susceptibility of skin cancer formation (Rangarajan et al., 2001; Weng and Aster, 2004).

The crosstalk between Notch and other cell signaling pathways may explain some of the contrasting tumorigenic consequences that are observed in different types of cancer. Notch signaling is known to interact with multiple other oncogenic signaling pathways such as epidermal growth factor receptor (EGFR), platelet-derived growth factor (PDGF), NF-κB, Akt, Hedgehog, mTOR, Ras, Wnt, estrogen receptor (ER), and androgen receptor (AR) signaling (Guo et al., 2011; Baker et al., 2014; Jeon et al., 2014; Qiu et al., 2014; Meurette and Mehlen, 2018; Hibdon et al., 2019; Katoh and Katoh, 2020).

The interaction of Notch1 with NFκB promotes tumor progression in colorectal adenocarcinoma through inhibition of apoptosis via the upregulation of the Bcl-xL (Gopalakrishnan et al., 2014). The communication between Notch and EGFR signaling may lead to more aggressive disease due to acquired resistance to EGFR-targeted chemotherapeutics through enhanced EMT characteristics (Xie et al., 2013), a behavior often associated with cancer aggressiveness. Notch signaling likely contributes to EMT through Notch1-mediated down-regulation of E-cadherin (epithelial marker) and up-regulation of Vimentin and Snail (mesenchymal markers) (Yuan et al., 2014; Kar et al., 2019).

Conversely, Notch1 functions as a tumor suppressor to transform high-grade adenomas into low-grade ones in murine models of colon cancer by epigenetically suppressing Wnt pathway target genes (Kim et al., 2012). In addition, pharmacologic activation of both Notch1 and Raf-1 signaling in MTC cells reduces aberrant secretion of hormones and tumor cell proliferation, suggesting a tumor suppressive role for Notch1 signaling in this context.

To better understand the role of Notch signaling in tumor development, it is important to consider the innate function of Notch in the cell or tissue type being studied. Just as the impact of Notch signaling varies among cancer types, it also varies among normal tissue types. For example, Notch signaling plays different roles during the normal development of different cell types in the pancreas. The Notch pathway plays a pivotal role in deciding the fate of progenitor cells as either exocrine cells (acinar/ductal cells) or endocrine cells (Islets of Langerhans) by lateral inhibition (Hald et al., 2003; Ahnfelt-Rønne et al., 2007; Kim et al., 2010; de Back et al., 2013; Pézeron et al., 2014; Li et al., 2016).

In summary, Notch signaling has a significant functional role in a broad spectrum of human cancers. The oncogenic involvement of Notch signaling across different cancer types has emphasized its centralized role in the regulation of tumor formation, progression, and therapeutic resistance. The distinct role of Notch signaling in tumor progression emphasizes the need for further studies to better understand this pathway in a cellular- and tumor type-dependent manner. A deeper understanding of Notch signaling in various biological settings and pathological conditions may reveal key opportunities for effective therapies that target Notch in tumors. We will discuss the role of Notch signaling in tumor angiogenesis, cancer stem cells (CSCs), therapeutic resistance, and signaling crosstalk between CSCs and vascular ECs as well as the clinical potential of targeting the Notch signaling pathway in more detail.

Notch Signaling in Tumor Angiogenesis

Tumor angiogenesis is characterized by excessive endothelial sprouting from preexisting blood vessels, which leads to overgrowth of randomly organized tumor vessels including venous and arteriolar vessels and capillaries (Sitohy et al., 2011; Nagy and Dvorak, 2012; De Palma et al., 2017; Ren et al., 2019; Yunus et al., 2019). The growth of new vascular networks or blood vessels within the TME is pivotal during tumor growth and progression, as newly formed and proliferating cancer cells require a supply of oxygen and nutrients to survive and remove waste products (Carmeliet, 2005; Jain and Carmeliet, 2012). They may also serve as a favorable niche for CSCs and as a channel system for both metastatic CSCs and the infiltration of immune cells.

Stimulation of neoangiogenesis in the TME depends upon the induction of such pro-angiogenic factors as VEGF and basic fibroblast growth factor (bFGF) (Yancopoulos et al., 2000; Lieu et al., 2011; Lugano et al., 2020). The crosstalk between pro-angiogenic and anti-angiogenic factors may determine angiogenic status throughout tumor progression (Ren, 2016), in which angiogenic receptors play a critical role in mediating angiogenic signaling. In fact, there is a *Yin and Yang* balance between pro-angiogenic and anti-angiogenic signaling to control overall angiogenic responses. During this dynamic angiogenic process, angiogenic receptors may serve as a pivotal axis to regulate the angiogenic functions of corresponding ligands. As an example, VEGFR2 is critical for upregulating VEGF signaling, while CD36 signaling may function as a critical negative regulator of angiogenesis (Ren, 2016).

Several studies have highlighted the critical role of Notch signaling in the overall regulation of tumor angiogenesis (Siekmann and Lawson, 2007; Suchting et al., 2007). The Notch ligands DLL4 and Jag1 are the best characterized Notch pathway factors that have roles in tumor angiogenesis. DLL4 is highly expressed in tumor ECs and its expression can be regulated by

VEGF, bFGF, and by low oxygen conditions (hypoxia) through hypoxia-inducible factor 1α (HIF1α) (Dufraine et al., 2008). The importance of DLL4 in tumor angiogenic processes is highlighted by the fact that silencing its expression leads to an inhibition of proliferation and migration of ECs (Patel et al., 2005; Rehman and Wang, 2006).

Intriguingly, tumor vasculature becomes disorganized and overgrown upon pharmacologic inhibition of DLL4, ultimately reducing overall tumor growth due to dysfunctional tumor angiogenesis (Dufraine et al., 2008). Given the ability of DLL4 to regulate tumor angiogenesis, strategies that target Notch/DLL4 signaling may show therapeutic potential against cancers. Unlike DLL4, Jag1 is overexpressed in cancer cells. It is suspected that Jag1 serves as a communication factor between cancer cells and tumor-associated ECs (TECs) to activate Notch signaling and induce angiogenesis by increasing cell proliferation and stabilizing vessels (Dufraine et al., 2008).

Notch signaling also regulates tumor angiogenesis and metastasis in a context-dependent manner. Notch signaling can upregulate Jag1 to antagonize the DLL4-dependent 'stalk' phenotype, thereby promoting EC sprouting and proliferation (Bridges et al., 2011; Simons et al., 2016). Activation of Notch signaling in ECs may either promote or inhibit metastasis in the lung (Wieland et al., 2017) and liver (Wohlfeil et al., 2019), respectively. Sustained endothelial Notch1 signaling facilitates metastasis by generating a senescent, pro-inflammatory endothelium in human carcinomas and melanoma (Wieland et al., 2017). Intriguingly, Notch activation in liver ECs protects hepatic metastasis by regulating endothelial-tumor cell adhesion independent of angiocrine signaling in malignant melanoma and colorectal carcinoma (Wohlfeil et al., 2019). These studies indicate the complex roles of the Notch pathway in tumor progression. Further investigation into the mechanisms by which Notch signaling regulates both cancer cells and TECs within the TME is warranted for the discovery of novel and effective strategies to control tumor progression.

Notch Signaling in Cancer Stem Cells (CSCs)

Accumulating evidence in CSC research suggests that the principles of anti-cancer treatments should be revised with consideration for the intrinsic heterogeneity of cancer cells. CSCs are a subpopulation of cells within a tumor that are able to promote neoplastic initiation, growth, survival, and metastasis (Al-Hajj et al., 2003; Li et al., 2007; Zhang et al., 2008). CSCs are hierarchically organized cancer cell populations within tumors and can also be defined by their ability to self-renew, exclusively retain tumorigenic potential, and generate heterogeneous lineages of cancer cells. Additionally, CSCs are resistant to a variety of conventional chemotherapies and radiotherapies, which leads to the failures of most conventional cancer therapies (Kim et al., 2009).

Notch signaling has emerged as a key pathway in CSCs. This signaling pathway may be involved in the regulation of survival, plasticity, and self-renewal of CSCs. Blockade of the Notch pathway using γ-secretase inhibitors can decrease CSC numbers, increase apoptosis, and limit tumorsphere formation efficiency, a measure of cancer stemness (Abel et al., 2014). However, the precise mechanisms by which Notch signaling promotes and maintains CSCs are still being investigated.

The expression of both Notch receptors and ligands have been correlated with CSC-like phenotypes in a variety of cancers, with a number of studies in breast cancers (Bray, 2006; Xiao et al., 2017; Yang et al., 2020). Breast cancer cell lines contain functional CSCs with distinct molecular signatures and metastatic capacities (Charafe-Jauffret et al., 2009). Aberrant Notch signaling also plays an important role in the invasive properties of breast CSCs (Dontu et al., 2004; Sansone et al., 2007; Guo et al., 2011). Higher Notch1 expression is associated with a transition from ductal carcinoma *in situ* to invasive cancer and may worsen overall and recurrence-free survival (Yuan et al., 2015). In particular, the activation of Notch3 through an IL-6 driven feed forward loop is able to promote self-renewal of breast CSCs (Sansone et al., 2016). In addition, the activation of Notch signaling may enhance the CSC-like properties of breast cancer cells likely via interaction with and the activation of LPA/PKD-1 signaling axis (Bray, 2006; Jiang et al., 2020).

Furthermore, the interaction of Notch1 with the erythropoietin receptor (EpoR), a protein expressed on the surface of breast CSCs, can lead to the maintenance of stemness through continuous self-renewal (Phillips et al., 2007). Notch1 also promotes the stem cell phenotype via activation of c-Jun signaling in a triple negative breast cancer (TNBC) (Xie et al., 2017). It has been speculated that the mechanism by which Notch promotes stemness is through activation of NF−κB as a means of resisting apoptosis (Baker et al., 2018; Najafi et al., 2019). A recent study demonstrates that the serine-threonine kinase receptor associated protein (STRAP) is oncogenic and regulates stemness behavior and drug response in colorectal cancer via mediating the epigenetic activation of Notch signaling (Jin et al., 2017).

Finally, it should be noted that heterogeneous CSC subsets in primary tumors have varied EMT phenotypes, in which Notch signaling may play a critical role. A recent study demonstrated that Notch-Jag1 signaling triggered by inflammatory cytokines can lead to varying EMT phenotypes within the TME (Bocci et al., 2019). The authors of this study also showed that breast CSCs with a mesenchymal-like ($CD44^+/CD24^-$) phenotype reside at the invasive edge of the tumor, whereas a population of hybrid epithelial-mesenchymal (E/M) CSCs are localized within the tumor interior. Thus, a primary tumor may contain spatially distributed cells with varying extents of EMT. This spatial distribution of CSCs and EMT heterogeneity may be attributed to a TGF-β diffusion gradient and cell–cell communication through Notch-Jag1 signaling induced by inflammatory cytokines such as IL-6. Furthermore, knockdown of Jag1 in the hybrid E/M SUM149 TNBC cell line suggests a role for Notch-Jag1 signaling in the maintenance of the CSC phenotype (Bocci et al., 2019). Despite the limitation of modeling itself and associated experimental evidence, this study provides insight into a concept regarding the spatiotemporal patterning of CSC subsets in the TME in response to Notch signaling, which may occur in a variety of other cancer types.

Notch Signaling in Cancer Therapeutic Resistance

The Notch signaling pathway may be a key factor in the context of anti-cancer drug resistance (Wang et al., 2010; Zou et al., 2013). Specifically, the activation of Jag1/Notch1 signaling has been associated with chemoresistance in many human tumors, including ovarian cancer (Liu et al., 2014), and the activation of the Notch1 signaling induces resistance to cisplatin (Liu et al., 2013; Wang et al., 2014; Zeng et al., 2020). Studies that investigate Notch in the context of drug resistance emphasize that Notch signaling can regulate the maintenance and self-renewal of CSCs and induce the EMT phenotype, both features associated with drug resistance and metastasis (Liu et al., 2013; Wang et al., 2014; Zeng et al., 2020).

Different chemotherapeutic agents can upregulate the expression of CSC-related markers and stimulate the expansion of CSCs (Phi et al., 2018; Yang et al., 2020). A recent study reported a significant increase in the percentage of $CD44^+/CD24^-$/low breast CSCs in biopsies specimens following chemotherapy (Abraham et al., 2005), suggesting that modulating Notch in breast cancers may be a promising strategy to reduce drug resistance by eliminating the CSC subpopulation (Shah et al., 2018; Najafi et al., 2019). In glioblastoma, $CD133^+$ CSCs are resistant to several chemotherapeutic agents (Liu Z.J. et al., 2006).

Additionally, CSCs are more resistant to radiation than non-CSCs (Rycaj and Tang, 2014; Arnold et al., 2020). Radiation can increase the percentage of $CD133^+$ CSCs *in vitro* and *in vivo* (Liu Z.J. et al., 2006; Kawamoto et al., 2012). This phenomenon was also seen in breast cancers, where tumors were found to be enriched for the $CD44^+/CD24^-$ CSC subpopulation following exposure to radiation (Gao et al., 2016). In these CSC-enriched subpopulations, Notch signaling was preferentially activated in response to radiation exposure, suggesting its possible role for this pathway in radiation resistance of breast CSCs (Gao et al., 2016). This is supported by multiple studies showing that CSCs activity is regulated by Notch signaling (Kanwar et al., 2010; Gao et al., 2016; Yang et al., 2020).

Blocking Notch signaling in tumors could reduce drug resistance and CSC properties, potentially leading to increased effectiveness of chemotherapeutics. This concept is beginning to be explored pre-clinically and has shown promising early results. In xenograft models of pancreatic cancer, the combination of a small molecule Notch inhibitor with gemcitabine reduced tumor proliferation and angiogenesis, leading to an overall reduction in tumor growth and metastasis (Yabuuchi et al., 2013; Zou et al., 2013).

In summary, Notch signaling appears to play a role in cancer drug resistance, potentially by regulating the CSC subpopulation. Therefore, targeting Notch signaling may demonstrate therapeutic potential for cancers by overcoming drug resistance. This may be accomplished by eliminating CSCs and/or EMT-type cells that are typically believed to be the "root cause" of tumor recurrence and metastasis. To develop more effective therapies, it is essential to have a better understanding of the molecular mechanisms by which Notch signaling mediates the CSC phenotype in certain cancers to promote drug resistance. Additional studies are also necessary to understand the potential clinical impact of using Notch inhibition strategy to target CSCs in either a single or combination treatment regimen.

Notch Signaling Crosstalk Between Cancer Stem Cells and Vascular Endothelial Cells

The crosstalk between tumor cells and their microenvironment is crucial for cancer cell self-renewal, tumor growth, and metastasis (Butler et al., 2010; Hanahan and Weinberg, 2011). Notch pathway activation by signals within the TME may be an additional mechanism by which Notch controls the activity of CSCs (Ingangi et al., 2019). In colorectal cancer, Notch signaling may not be essential for bulk tumorigenesis, but signaling crosstalk between Notch1 and FGF/WNT pathway could be responsible for orchestrating the TME for CSC maintenance (Germann et al., 2014; Mourao et al., 2019). This concept is supported by the fact that Notch signaling mediates cell–cell communication (Lai, 2004; Stylianou et al., 2006).

A major component of the TME is the vascular niche, which is composed of a vascular basement, pericytes (capillaries), and smooth muscle cells (arteriolar and venous vessels) surrounding ECs (Ping et al., 2016; Ingangi et al., 2019). A seminal study along with our recent work have demonstrated that some aggressive cancer cells may prefer high perfusion that provides nutrients and oxygen rather than hypoxia conditions as CSCs and aggressive cancer cells tend to localize themselves near blood vessels and arterioles within the TME (Kumar et al., 2019; Jiang et al., 2020).

Vascular ECs are an essential component of blood-vessel walls, which are the main driver of new blood vessel formation including initiation of vessel sprouting and vessel maturation. Notch signaling in vascular ECs may promote the stem cell phenotype including self-renewal of CSCs and tumor progression (Zhu et al., 2011; Lu et al., 2013; Cao et al., 2014, 2017; Ghiabi et al., 2014). It has been suggested that ECs regulate the homeostasis of CSCs directly via cellular contact or indirectly by releasing a distant specific growth factor called stem cell-active trophogens (Plaks et al., 2015; Ingangi et al., 2019; Jiang et al., 2020). For example, ECs in TNBC can enhance self-renewal, survival, and pro-metastatic properties of the breast CSCs through direct cell–cell contact mediated by Notch signaling *in vitro* (Ghiabi et al., 2014).

In glioblastoma, Notch signaling can induce CSC features through bFGF and regulate the EC-mediated acquisition of CSC properties (Fessler et al., 2015; Bradshaw et al., 2016; Bazzoni and Bentivegna, 2019; Jiang et al., 2020). Inhibition of Notch signaling can suppress the self-renewal of glioblastoma CSCs by reducing the number of ECs (Bradshaw et al., 2016). In fact, co-culture of ECs with glioblastoma CSCs increases the self-renewal capability and maintains an undifferentiated status of the CSCs through direct cell–cell contact and indirect paracrine signaling involving DLL4/Notch (Nandhu et al., 2014; Rostama et al., 2014).

Beyond the self-renewal potential and the capacity to generate heterogeneous cancer cell populations, CSCs can

transdifferentiate into ECs and develop vascular mimicry (Jain and Carmeliet, 2012; Huang et al., 2015). CSCs in glioblastoma, breast cancer, and ovarian cancer are able to differentiate into ECs (Jain and Carmeliet, 2012; Fan et al., 2013; Qian and Rankin, 2019). They also participate in vascular mimicry under hypoxic conditions (Fan et al., 2013; Qian and Rankin, 2019). Hypoxia is believed to play an important role in the CSC-mediated production of angiogenic factors and the maintenance of "stemness" within the CSC subpopulation (Qian and Rankin, 2019). The interaction between Notch signaling and HIF1α under hypoxic conditions (Qiang et al., 2012; De Francesco et al., 2018) suggests a potential role of Notch pathway in the development of vascular mimicry within the TME. Intriguingly, Notch signaling may also promote the development of the arteriolar niche within the TME that can maintain CSC features during tumor progression (Jiang et al., 2020).

In conclusion, the Notch pathway may determine the fate of both ECs and CSCs and mediate crosstalk between these two cell types. However, several studies indicate that the differentiation of CSCs is not a one-way route, but instead might be a reversible process that can be directed by signals from the TME (Huang et al., 2015). Furthermore, a recent study suggested that CSCs can differentiate to not only ECs but also tumor cells themselves, indicating the potential to generate endothelial phenotypes and directly participate in tumor angiogenesis and cancer cell plasticity (Dudley, 2012; Hida et al., 2018). Further studies are necessary to fully understand how the Notch pathway in the TME participates in the crosstalk between CSCs and ECs and when and how CSCs differentiate into ECs and/or tumor cells.

Clinical Potential of Inhibiting Notch Signaling

Given the critical roles of Notch signaling in endothelial cell biology, angiogenesis, and the expansion of CSCs in a variety of tumors, targeting the Notch pathway holds great therapeutic potential. Unfortunately, there are no approved drugs that target this pathway for cancer treatment in the clinic. A recent review has discussed the therapeutic implications of cardiovascular disease and cardiotoxicity caused by anti-cancer drugs (Aquila et al., 2019). Our recent review also provides an update on the use of gamma secretase inhibitors (GSIs) to inhibit Notch signaling for cancer treatment (McCaw et al., 2020). However, much remains to be ascertained before optimal approaches targeting Notch signaling can be developed to treat patients with cardiovascular diseases and cancers.

One approach to inhibit the Notch pathway is through suppression of the proteolytic step that leads to the generation of the active Notch intracellular domain (NICD). Gamma-secretase is the orchestrating enzyme of the crucial proteolytic activity that releases the NICD and is a key player in the canonical Notch signaling pathway. GSIs prevent cleavage of the NICD by blocking the proteolytic function of presenilin enzymes, thereby preventing Notch pathway activation (Cook et al., 2018). Therefore, GSIs can inactivate Notch signaling in cancer cells and lead to impaired cancer cell growth and tumor progression. GSIs may also suppress angiogenesis in solid tumors by interfering in the crosstalk between the tumor and the vasculature (McCaw et al., 2020). Several different forms of GSIs have been tested for antitumor effects (Shih and Wang, 2007; McCaw et al., 2020). Phase I clinical trials using Notch inhibitors (MK0752, PF-03084014, RO4929097) either alone or in combination with other agents (Cook et al., 2018; McCaw et al., 2020) have been conducted in advanced breast cancers, lung cancer, melanoma. These studies strongly suggest a potential clinical application for GSIs in cancer therapeutics. However, the side effects associated with GSIs pose a major clinical challenge, since γ-secretase does not exclusively target Notch signaling in cancer cells alone. In addition to GSIs, a bi-specific antibody (ABL001) that targets both VEGF and DLL4 is currently being evaluated in a phase I clinical trial. This trial aims to assess the safety and tolerability of the bi-specific antibody in patients who did not respond to current chemotherapy or targeted therapy (Yeom et al., 2021).

Furthermore, inhibition of Notch signaling has shown efficacy in reducing CSC features, thereby limiting tumor progression *in vivo*. In murine models of colorectal cancer, blocking Notch signaling with an anti-DLL4 antibody reduced the frequency of CSCs, delayed recurrence of tumors, and decreased metastasis (Hoey et al., 2009; Najafi et al., 2019). Inhibition of Notch signaling by GSIs abolished the formation of secondary mammospheres from a variety of human breast cancer cell lines and patient samples (Grudzien et al., 2010), leading to the observation that Notch inhibition could overcome treatment resistance (McCaw et al., 2020). In an animal breast cancer model, GSIs alone do not reduce tumor volume. Comparatively, trastuzumab (HER2-targeted therapy) alone does indeed drastically decrease tumor volume but does not prevent recurrence. However, combining GSIs with trastuzumab stops the recurrence of HER2-positive tumors in mice (Pandya et al., 2011). The results of this study indicate that Notch inhibition through GSIs targets CSCs, while trastuzumab targets the tumor bulk. In combination, these two targeted mechanisms can eliminate the tumor and prevent recurrence. This approach may be attributed to the evidence that Notch signaling is essential for the maintenance of CSCs and the development of the arteriolar niche to promote the self-renewal of CSCs (Shutter et al., 2000; Lawson et al., 2001; Liu et al., 2003; Trindade et al., 2008; Jiang et al., 2020). Since Notch signaling is crucial in many biological processes, targeting alternative pathways that are critical for Notch signaling-mediated pathology could be tested as potential strategies for cancer treatment.

SUMMARY AND PERSPECTIVES

In many human cancers, the activation of Notch signaling can crosstalk with numerous oncogenic signaling pathways, such as Wnt and Hedgehog signaling, cytokines, and oncogenic kinases. This crosstalk plays an important role in tumor angiogenesis and growth, invasion, metastasis, and therapeutic resistance. As a major signaling pathway in tumor progression, Notch has been extensively studied in the context of angiogenesis and CSC biology. In vascular ECs, this pathway is essential for the determination of cellular fate, proliferation, apoptosis and

EndoMT. Importantly, Notch signaling plays an essential role in arteriolar differentiation and the determination of angiogenic phenotype as well as in tumor initiation, EMT-driven metastatic growth, and the self-renewal of CSCs (Ranganathan et al., 2011). Furthermore, this signaling may contribute to CSC-mediated chemoresistance in many different types of cancer (Zhang et al., 2008; Meng et al., 2009; Ulasov et al., 2011; McAuliffe et al., 2012) and radiation resistance (Gao et al., 2016). In summary, Notch pathway activation is associated with more aggressive cancer via the regulation of angiogenesis and CSC features in a variety of tumors (**Figure 4**).

However, it should be noted that Notch signaling is characterized by its context-dependent consequences, exerting either tumor-suppressive or oncogenic effects. Using a reverse genetic CRISPR screen to functionally assess about 500 long tail gene mutations that occur in human head and neck squamous cell carcinoma (HNSCC), Loganathan et al. (2020) recently identified 15 tumor-suppressor genes with activities that converged on the Notch signaling pathway. This suggests that Notch inactivation drives HNSCC growth given that Notch itself is mutated at a high frequency in this type of cancer. In addition, Bill et al. (2020) demonstrated that EGF-like domain 7 (EGFL7), a secreted protein that plays an important role in acute myeloid leukemia (AML), contributes to Notch silencing in AML by antagonizing canonical Notch ligand binding. However, whether oncogenic or tumor suppressive, targeting Notch signaling holds promising therapeutic potential for cancer treatment.

Due to its driving role in many types of cancer, significant attention has been paid in recent years toward the development of clinically valuable antagonists of Notch signaling. However, there are still many gaps to uncover in this field due to the heterogeneity and complexity of the molecular biology in human cancers including neuroendocrine tumors and breast cancers as well as in cardiovascular diseases. In terms of cancer treatment, a popular new strategy is the development of target-selective "smart" drugs based upon the foundation of characterized molecular mechanisms. The crosstalk between Notch signaling and many other oncogenic signaling pathways in carcinogenesis presents multiple opportunities for the design of new drugs aimed at blocking these interactions. However, this would require new studies to better understand the precise mechanisms by which Notch signaling pathway and molecular signaling critical to the Notch pathway promotes or inhibits tumor progression. In addition, developing innovative tools to more accurately predict their prognosis, and designing and testing personalized treatment strategies would be helpful to facilitate the optimal Notch targeting in cancer patients.

Research in the past decade has focused upon eliminating tumor recurrence by targeting CSCs. Targeting Notch may be an optimal therapeutic strategy to disrupt the arteriolar niche and eradicate CSCs. However, targeting the Notch pathway may elicit cardiovascular toxicities because of its critical role in the maintenance of cardiovascular homeostasis by EC DLL4-Notch signaling (Potente et al., 2011; Goel and Mercurio, 2013). Through molecular profiling and screening, potential co-targeting options could be found to use Notch inhibition as a strategy to benefit patients (Mollen et al., 2018). Additional research will be required to determine the cellular and molecular mechanisms, as well as the precise role of Notch in different cancer types. This will enable deep investigations into the use of Notch-targeting agents and their combination with current therapeutic regimens to achieve optimal treatment efficacy.

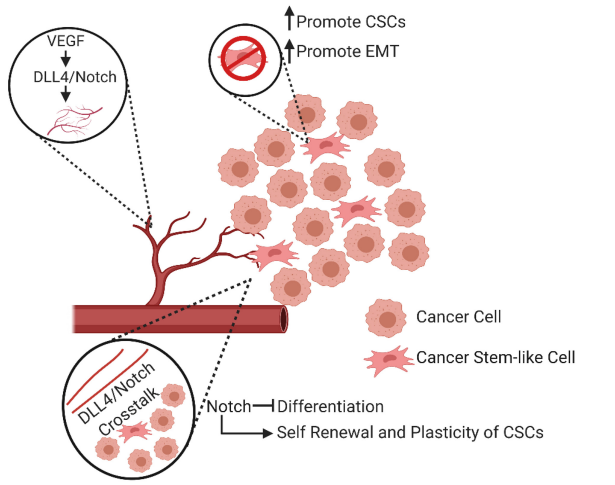

FIGURE 4 | Diverse involvement of Notch signaling in angiogenesis and CSCs. The interaction between VEGF and DLL4/Notch signaling regulates angiogenesis. In addition, active Notch signaling can promote the development of the CSC phenotype, the renewal and plasticity of CSCs, and promote an epithelial to mesenchymal transition (EMT).

AUTHOR CONTRIBUTIONS

AA, AG-G, and RG wrote the manuscript. AG-G made the figures. JR, AB, and HC reviewed the manuscript. BR conceptualized and wrote the manuscript. All authors approved the submitted version.

FUNDING

This work was partially supported by the National Institute of Health Grant R01HL136423 (to BR) and by the Bioengineering Surgery Collaborative Award, University of Alabama at Birmingham (to BR and AB).

ACKNOWLEDGMENTS

BR's work has been supported by the National Institute of Health (HL136423; BR), the American Cancer Society (86-004-26; Institution Fund to BR, the Medical College of Wisconsin), the American Heart Association (13SDG14800019; BR), the Ann's Hope Foundation (FP00011709; BR), and Bioengineering Surgery Collaborative Award, University of Alabama at Birmingham (BR and AP). We apologize to those colleagues whose work could not be cited directly owing to space constraints.

REFERENCES

Abel, E. V., Kim, E. J., Wu, J., Hynes, M., Bednar, F., Proctor, E., et al. (2014). The notch pathway is important in maintaining the cancer stem cell population in pancreatic cancer. *PLoS One* 9:e91983. doi: 10.1371/journal.pone.0091983

Abraham, B. K., Fritz, P., McClellan, M., Hauptvogel, P., Athelogou, M., and Brauch, H. (2005). Prevalence of CD44+/CD24-/low cells in breast cancer may not be associated with clinical outcome but may favor distant metastasis. *Clin. Cancer Res.* 11, 1154–1159.

Ahnfelt-Rønne, J., Hald, J., Bødker, A., Yassin, H., Serup, P., and Hecksher-Sørensen, J. (2007). Preservation of proliferating pancreatic progenitor cells by Delta-Notch signaling in the embryonic chicken pancreas. *BMC Devel. Biol.* 7:63. doi: 10.1186/1471-213X-7-63

Al-Hajj, M., Wicha, M. S., Benito-Hernandez, A., Morrison, S. J., and Clarke, M. F. (2003). Prospective identification of tumorigenic breast cancer cells. *Proc. Natl. Acad. Sci.* 100, 3983–3988.

Andersson, E. R., Sandberg, R., and Lendahl, U. (2011). Notch signaling: simplicity in design, versatility in function. *Development* 138, 3593–3612. doi: 10.1242/dev.063610

Aquila, G., Kostina, A., Vieceli Dalla Sega, F., Shlyakhto, E., Kostareva, A., Marracino, L., et al. (2019). The Notch pathway: a novel therapeutic target for cardiovascular diseases? *Exp. Opin. Therap. Targets* 23, 695–710. doi: 10.1080/14728222.2019.1641198

Arnold, C. R., Mangesius, J., Skvortsova, I.-I., and Ganswindt, U. (2020). The Role of Cancer Stem Cells in Radiation Resistance. *Front. Oncol.* 10:164. doi: 10.3389/fonc.2020.00164

Aster, J. C., Pear, W. S., and Blacklow, S. C. (2017). The varied roles of Notch in cancer. *Annu. Rev. Pathol. Mechan. Dis.* 12, 245–275. doi: 10.1146/annurev-pathol-052016-100127

Azhar, M., Runyan, R. B., Gard, C., Sanford, L. P., Miller, M. L., Andringa, A., et al. (2009). Ligand−specific function of transforming growth factor beta in epithelial−mesenchymal transition in heart development. *Devel. Dynam.* 238, 431–442. doi: 10.1002/dvdy.21854

Baker, A., Wyatt, D., Bocchetta, M., Li, J., Filipovic, A., Green, A., et al. (2018). Notch-1-PTEN-ERK1/2 signaling axis promotes HER2+ breast cancer cell proliferation and stem cell survival. *Oncogene* 37, 4489–4504. doi: 10.1038/s41388-018-0251-y

Baker, A., Zlobin, A., and Osipo, C. (2014). Notch-EGFR/HER2 bidirectional crosstalk in breast cancer. *Front. Oncol.* 4:360. doi: 10.3389/fonc.2014.00360

Bazzoni, R., and Bentivegna, A. (2019). Role of notch signaling pathway in glioblastoma pathogenesis. *Cancers* 11:292. doi: 10.3390/cancers11030292

Benedito, R., Roca, C., Sörensen, I., Adams, S., Gossler, A., Fruttiger, M., et al. (2009). The notch ligands Dll4 and Jagged1 have opposing effects on angiogenesis. *Cell* 137, 1124–1135. doi: 10.1016/j.cell.2009.03.025

Best, B., Moran, P., and Ren, B. (2018). VEGF/PKD-1 signaling mediates arteriogenic gene expression and angiogenic responses in reversible human microvascular endothelial cells with extended lifespan. *Mol. Cell. Biochem.* 446, 199–207. doi: 10.1007/s11010-018-3286-z

Bill, M., Pathmanathan, A., Karunasiri, M., Shen, C., Burke, M. H., and Ranganathan, P. (2020). EGFL7 Antagonizes NOTCH Signaling and Represents a Novel Therapeutic Target in Acute Myeloid Leukemia. *Clin. Cancer Res.* 26, 669–678. doi: 10.1158/1078-0432.ccr-19-2479

Blanco, R., and Gerhardt, H. (2013). VEGF and Notch in tip and stalk cell selection. *Cold Spring Harbor. Perspect. Med.* 3:a006569. doi: 10.1101/cshperspect.a006569

Boareto, M., Jolly, M. K., Lu, M., Onuchic, J. N., Clementi, C., and Ben-Jacob, E. (2015). Jagged–Delta asymmetry in Notch signaling can give rise to a Sender/Receiver hybrid phenotype. *Proc. Natl. Acad. Sci.* 112, E402–E409.

Bocci, F., Gearhart-Serna, L., Boareto, M., Ribeiro, M., Ben-Jacob, E., Devi, G. R., et al. (2019). Toward understanding cancer stem cell heterogeneity in the tumor microenvironment. *Proc. Natl. Acad. Sci.* 116, 148–157. doi: 10.1073/pnas.1815345116

Bradshaw, A., Wickremsekera, A., Tan, S. T., Peng, L., Davis, P. F., and Itinteang, T. (2016). Cancer stem cell hierarchy in glioblastoma multiforme. *Front. Surg.* 3:21. doi: 10.3389/fsurg.2016.00021

Bray, S. J. (2006). Notch signalling: a simple pathway becomes complex. *Nat. Rev. Mole. Cell Biol.* 7, 678–689. doi: 10.1038/nrm2009

Bridges, E., Oon, C. E., and Harris, A. (2011). Notch regulation of tumor angiogenesis. *Fut. Oncol.* 7, 569–588. doi: 10.2217/fon.11.20

Brzozowa-Zasada, M., Piecuch, A., Michalski, M., Segiet, O., Kurek, J., Harabin-Słowińska, M., et al. (2017). Notch and its oncogenic activity in human malignancies. *Eur. Surg.* 49, 199–209. doi: 10.1007/s10353-017-0491-z

Butler, J. M., Kobayashi, H., and Rafii, S. (2010). Instructive role of the vascular niche in promoting tumour growth and tissue repair by angiocrine factors. *Nat. Rev. Cancer* 10, 138–146. doi: 10.1038/nrc2791

Cao, Z., Ding, B. S., Guo, P., Lee, S. B., Butler, J. M., Casey, S. C., et al. (2014). Angiocrine factors deployed by tumor vascular niche induce B cell lymphoma invasiveness and chemoresistance. *Cancer Cell* 25, 350–365. doi: 10.1016/j.ccr.2014.02.005

Cao, Z., Scandura, J. M., Inghirami, G. G., Shido, K., Ding, B. S., and Rafii, S. (2017). Molecular Checkpoint Decisions Made by Subverted Vascular Niche Transform Indolent Tumor Cells into Chemoresistant Cancer Stem Cells. *Cancer Cell* 31, 110–126. doi: 10.1016/j.ccell.2016.11.010

Carmeliet, P. (2005). Angiogenesis in life, disease and medicine. *Nature* 438, 932–936. doi: 10.1038/nature04478

Charafe-Jauffret, E., Ginestier, C., Iovino, F., Wicinski, J., Cervera, N., Finetti, P., et al. (2009). Breast cancer cell lines contain functional cancer stem cells with metastatic capacity and a distinct molecular signature. *Cancer Res.* 69, 1302–1313. doi: 10.1158/0008-5472.can-08-2741

Chen, P. Y., Qin, L., Baeyens, N., Li, G., Afolabi, T., Budatha, M., et al. (2015). Endothelial-to-mesenchymal transition drives atherosclerosis progression. *J. Clin. Invest.* 125, 4514–4528. doi: 10.1172/jci82719

Chen, X., Cai, J., Zhou, X., Chen, L., Gong, Y., Gao, Z., et al. (2015). Protective Effect of Spironolactone on Endothelial-to-Mesenchymal Transition in HUVECs via Notch Pathway. *Cell. Physiol. Biochem.* 36, 191–200. doi: 10.1159/000374063

Clere, N., Renault, S., and Corre, I. (2020). Endothelial-to-Mesenchymal Transition in Cancer. *Front. Cell. Dev. Biol.* 8:747. doi: 10.1038/sj.bjc.6604662

Cook, N., Basu, B., Smith, D.-M., Gopinathan, A., Evans, J., Steward, W. P., et al. (2018). A phase I trial of the γ-secretase inhibitor MK-0752 in combination with gemcitabine in patients with pancreatic ductal adenocarcinoma. *Br. J. Cancer* 118, 793–801. doi: 10.1038/bjc.2017.495

de Back, W., Zhou, J. X., and Brusch, L. (2013). On the role of lateral stabilization during early patterning in the pancreas. *J. Roy. Soc. Interf.* 10:20120766. doi: 10.1098/rsif.2012.0766

De Francesco, E. M., Maggiolini, M., and Musti, A. M. (2018). Crosstalk between notch, HIF-1α and GPER in breast cancer EMT. *Int. J. Mol. Sci.* 19:2011. doi: 10.3390/ijms19072011

De Palma, M., Biziato, D., and Petrova, T. V. (2017). Microenvironmental regulation of tumour angiogenesis. *Nat. Rev. Cancer* 17, 457–474. doi: 10.1038/nrc.2017.51

Dejana, E., Hirschi, K. K., and Simons, M. (2017). The molecular basis of endothelial cell plasticity. *Nat. Commun.* 8:13461.

Dong, L., Yuan, Y., Opansky, C., Chen, Y., Aguilera-Barrantes, I., Wu, S., et al. (2017). Diet-induced obesity links to ER positive breast cancer progression via LPA/PKD-1-CD36 signaling-mediated microvascular remodeling. *Oncotarget* 8:22550. doi: 10.18632/oncotarget.15123

Dontu, G., Jackson, K. W., McNicholas, E., Kawamura, M. J., Abdallah, W. M., and Wicha, M. S. (2004). Role of Notch signaling in cell-fate determination of human mammary stem/progenitor cells. *Breast Cancer Res.* 6, 1–11.

Dotto, G. P. (2008). Notch tumor suppressor function. *Oncogene* 27, 5115–5123. doi: 10.1038/onc.2008.225

D'Souza, B., Meloty-Kapella, L., and Weinmaster, G. (2010). Canonical and non-canonical notch ligands. *Curr. Top. Dev. Biol.* 92, 73–129. doi: 10.1016/s0070-2153(10)92003-6

Du, Y., Li, J., Xu, T., Zhou, D.-D., Zhang, L., and Wang, X. (2017). MicroRNA-145 induces apoptosis of glioma cells by targeting BNIP3 and Notch signaling. *Oncotarget* 8:61510. doi: 10.18632/oncotarget.18604

Dudley, A. C. (2012). Tumor endothelial cells. *Cold Spr. Harbor. Perspect. Med.* 2:a006536.

Dufraine, J., Funahashi, Y., and Kitajewski, J. (2008). Notch signaling regulates tumor angiogenesis by diverse mechanisms. *Oncogen* 27, 5132–5137. doi: 10.1038/onc.2008.227

Fan, Y. L., Zheng, M., Tang, Y. L., and Liang, X. H. (2013). A new perspective of vasculogenic mimicry: EMT and cancer stem cells. *Oncol. Lett.* 6, 1174–1180. doi: 10.3892/ol.2013.1555

Fessler, E., Borovski, T., and Medema, J. P. (2015). Endothelial cells induce cancer stem cell features in differentiated glioblastoma cells via bFGF. *Mole. Cancer* 14, 1–12.

Fortini, F., Vieceli Dalla Sega, F., Caliceti, C., Aquila, G., Pannella, M., Pannuti, A., et al. (2017). Estrogen receptor beta-dependent Notch1 activation protects vascular endothelium against tumor necrosis factor alpha (TNFalpha)-induced apoptosis. *J. Biol. Chem.* 292, 18178–18191. doi: 10.1074/jbc.m117.790121

Gao, X., Sishc, B. J., Nelson, C. B., Hahnfeldt, P., Bailey, S. M., and Hlatky, L. (2016). Radiation-induced reprogramming of pre-senescent mammary epithelial cells enriches putative CD44+/CD24-/low stem cell phenotype. *Front. Oncol.* 6:138. doi: 10.3389/fonc.2016.00138

Garcia, A., and Kandel, J. J. (2012). Notch: a key regulator of tumor angiogenesis and metastasis. *Histol. Histopathol.* 27:151.

Germann, M., Xu, H., Malaterre, J., Sampurno, S., Huyghe, M., Cheasley, D., et al. (2014). Tripartite interactions between Wnt signaling, Notch and Myb for stem/progenitor cell functions during intestinal tumorigenesis. *Stem Cell Res.* 13, 355–366. doi: 10.1016/j.scr.2014.08.002

Ghiabi, P., Jiang, J., Pasquier, J., Maleki, M., Abu-Kaoud, N., Halabi, N., et al. (2015). Breast cancer cells promote a notch-dependent mesenchymal phenotype in endothelial cells participating to a pro-tumoral niche. *J. Transl. Med.* 13:27. doi: 10.1186/s12967-015-0386-3

Ghiabi, P., Jiang, J., Pasquier, J., Maleki, M., Abu-Kaoud, N., Rafii, S., et al. (2014). Endothelial cells provide a notch-dependent pro-tumoral niche for enhancing breast cancer survival, stemness and pro-metastatic properties. *PLoS One* 9:e112424. doi: 10.1371/journal.pone.0112424

Goel, H. L., and Mercurio, A. M. (2013). VEGF targets the tumour cell. *Nat. Rev. Cancer* 13, 871–882. doi: 10.1038/nrc3627

Gopalakrishnan, N., Sivasithamparam, N. D., and Devaraj, H. (2014). Synergistic association of Notch and NFκB signaling and role of Notch signaling in modulating epithelial to mesenchymal transition in colorectal adenocarcinoma. *Biochimie* 107, 310–318. doi: 10.1016/j.biochi.2014.09.020

Grudzien, P., Lo, S., Albain, K. S., Robinson, P., Rajan, P., Strack, P. R., et al. (2010). Inhibition of Notch signaling reduces the stem-like population of breast cancer cells and prevents mammosphere formation. *Anticancer Res.* 30, 3853–3867.

Guarani, V., Deflorian, G., Franco, C. A., Krüger, M., Phng, L. K., Bentley, K., et al. (2011). Acetylation-dependent regulation of endothelial Notch signalling by the SIRT1 deacetylase. *Nature* 473, 234–238. doi: 10.1038/nature09917

Guenter, R., Patel, Z., and Chen, H. (2021). Notch signaling in thyroid cancer. *Adv. Exp. Med. Biol.* 1287, 155–168. doi: 10.1007/978-3-030-55031-8_10

Guo, S., Liu, M., and Gonzalez-Perez, R. R. (2011). Role of Notch and its oncogenic signaling crosstalk in breast cancer. *Biochim. Biophys. Acta* 1815, 197–213. doi: 10.1016/j.bbcan.2010.12.002

Hald, J., Hjorth, J. P., German, M. S., Madsen, O. D., Serup, P., and Jensen, J. (2003). Activated Notch1 prevents differentiation of pancreatic acinar cells and attenuate endocrine development. *Devel. Biol.* 260, 426–437. doi: 10.1016/s0012-1606(03)00326-9

Hanahan, D., and Weinberg, R. A. (2011). Hallmarks of cancer: the next generation. *Cell* 144, 646–674. doi: 10.1016/j.cell.2011.02.013

Harrington, L. S., Sainson, R. C., Williams, C. K., Taylor, J. M., Shi, W., Li, J.-L., et al. (2008). Regulation of multiple angiogenic pathways by Dll4 and Notch in human umbilical vein endothelial cells. *Microvascul. Res.* 75, 144–154. doi: 10.1016/j.mvr.2007.06.006

Heil, M., Eitenmüller, I., Schmitz—Rixen, T., and Schaper, W. (2006). Arteriogenesis versus angiogenesis: similarities and differences. *J. Cell. Mole. Med.* 10, 45–55. doi: 10.1111/j.1582-4934.2006.tb00290.x

Hibdon, E. S., Razumilava, N., Keeley, T. M., Wong, G., Solanki, S., Shah, Y. M., et al. (2019). Notch and mTOR Signaling Pathways Promote Human Gastric Cancer Cell Proliferation. *Neoplasia* 21, 702–712. doi: 10.1016/j.neo.2019.05.002

Hida, K., Maishi, N., Annan, D. A., and Hida, Y. (2018). Contribution of tumor endothelial cells in cancer progression. *Int. J. Mole. Sci.* 19:1272. doi: 10.3390/ijms19051272

Hoey, T., Yen, W. C., Axelrod, F., Basi, J., Donigian, L., Dylla, S., et al. (2009). DLL4 Blockade Inhibits Tumor Growth and Reduces Tumor-Initiating Cell Frequency. *Cell. Stem Cell* 5, 168–177. doi: 10.1016/j.stem.2009.05.019

Holderfield, M. T., and Hughes, C. C. (2008). Crosstalk between vascular endothelial growth factor, notch, and transforming growth factor-β in vascular morphogenesis. *Circul. Res.* 102, 637–652. doi: 10.1161/circresaha.107.167171

Hristova, N. R., Tagscherer, K. E., Fassl, A., Kopitz, J., and Roth, W. (2013). Notch1-dependent regulation of p27 determines cell fate in colorectal cancer. *Int. J. Oncol.* 43, 1967–1975. doi: 10.3892/ijo.2013.2140

Huang, Z., Wu, T., Liu, A. Y., and Ouyang, G. (2015). Differentiation and transdifferentiation potentials of cancer stem cells. *Oncotarget* 6:39550. doi: 10.18632/oncotarget.6098

Hultgren, N. W., Fang, J. S., Ziegler, M. E., Ramirez, R. N., Phan, D. T. T., Hatch, M. M. S., et al. (2020). Slug regulates the Dll4-Notch-VEGFR2 axis to control endothelial cell activation and angiogenesis. *Nat. Commun.* 11:5400.

Ingangi, V., Minopoli, M., Ragone, C., Motti, M. L., and Carriero, M. V. (2019). Role of microenvironment on the fate of disseminating cancer stem cells. *Front. Oncol.* 9:82. doi: 10.3389/fonc.2019.00082

Jabs, M., Rose, A. J., Lehmann, L. H., Taylor, J., Moll, I., and Sijmonsma, T. P. (2018). Inhibition of endothelial notch signaling impairs fatty acid transport and leads to metabolic and vascular remodeling of the adult heart. *Circulation* 137, 2592–2608. doi: 10.1161/CIRCULATIONAHA.117.029733

Jain, R. K., and Carmeliet, P. (2012). SnapShot: tumor angiogenesis. *Cell* 149, 1408–1408.

Jaskula-Sztul, R., Eide, J., Tesfazghi, S., Dammalapati, A., Harrison, A. D., Yu, X. M., et al. (2015). Tumor-suppressor role of notch3 in medullary thyroid carcinoma revealed by genetic and pharmacological induction. *Mole. Cancer Therap.* 14, 499–512. doi: 10.1158/1535-7163.MCT-14-0073

Jaskula-Sztul, R., Pisarnturakit, P., Landowski, M., Chen, H., and Kunnimalaiyaan, M. (2011). Expression of the active Notch1 decreases MTC tumor growth in vivo. *J. Surg. Res.* 171, 23–27. doi: 10.1016/j.jss.2011.03.035

Jeon, H. M., Kim, S. H., Jin, X., Park, J. B., Kim, S. H., Joshi, K., et al. (2014). Crosstalk between glioma-initiating cells and endothelial cells drives tumor progression. *Cancer Res.* 74, 4482–4492. doi: 10.1158/0008-5472

Jiang, Y. G., Hao, Y. C., Guenter, J. J., Lathia, R., Beck, J., Hattaway, A., et al. (2020). LPA/PKD-1 signaling promotes development of arteriolar niche that supports self-renewal of breast cancer stem cells and stemness. *bioRxiv*.

Jin, L., Vu, T., Yuan, G., and Datta, P. K. (2017). STRAP Promotes Stemness of Human Colorectal Cancer via Epigenetic Regulation of the NOTCH Pathway. *Cancer Res.* 77, 5464–5478. doi: 10.1158/0008-5472.can-17-0286

Jung, S. G., Kwon, Y. D., Song, J. A., Back, M. J., Lee, S. Y., Lee, C., et al. (2010). Prognostic significance of Notch 3 gene expression in ovarian serous carcinoma. *Cancer Sci.* 101, 1977–1983. doi: 10.1111/j.1349-7006.2010.01641.x

Kangsamaksin, T., Tattersall, Ian W., and Kitajewski, J. (2014). Notch functions in developmental and tumour angiogenesis by diverse mechanisms1. *Biochem. Soc. Transac.* 42, 1563–1568. doi: 10.1042/BST20140233

Kanwar, S. S., Yu, Y., Nautiyal, J., Patel, B. B., and Majumdar, A. P. (2010). The Wnt/β-catenin pathway regulates growth and maintenance of colonospheres. *Mole. Cancer* 9, 1–13.

Kar, R., Jha, N. K., Jha, S. K., Sharma, A., Dholpuria, S., Asthana, N., et al. (2019). A "NOTCH" deeper into the epithelial-to-mesenchymal transition (EMT) program in breast cancer. *Genes* 10:96.

Kartalaei, P. S., Yamada-Inagawa, T., Vink, C. S., de Pater, E., van der Linden, R., and Marks-Bluth, J. (2015). Whole-transcriptome analysis of endothelial to hematopoietic stem cell transition reveals a requirement for Gpr56 in HSC generation. *J. Exp. Med.* 12, 93–106. doi: 10.1084/jem.20140767

Katoh, M., and Katoh, M. (2020). Precision medicine for human cancers with Notch signaling dysregulation. *Int. J. of Mole. Med.* 45, 279–297.

Kawamoto, A., Tanaka, K., Saigusa, S., Toiyama, Y., Morimoto, Y., Fujikawa, H., et al. (2012). Clinical significance of radiation-induced CD133 expression in residual rectal cancer cells after chemoradiotherapy. *Exp. Therap. Med.* 3, 403–409. doi: 10.3892/etm.2011.438

Kazerounian, S., Duquette, M., Reyes, M. A., Lawler, J. T., Song, K., Perruzzi, C., et al. (2011). Priming of the vascular endothelial growth factor signaling pathway by thrombospondin-1. *CD36* 117, 4658–4666. doi: 10.1182/blood-2010-09-305284

Kim, H.-A., Koo, B.-K., Cho, J.-H., Kim, Y.-Y., Seong, J., Chang, H. J., et al. (2012). Notch1 counteracts WNT/β-catenin signaling through chromatin modification in colorectal cancer. *J. Clin. Investig.* 122, 3248–3259. doi: 10.1172/jci61216

Kim, W., Shin, Y.-K., Kim, B.-J., and Egan, J. M. (2010). Notch signaling in pancreatic endocrine cell and diabetes. *Biochem. Biophys. Res. Commun.* 392, 247–251. doi: 10.1016/j.bbrc.2009.12.115

Kim, Y., Joo, K. M., Jin, J., and Nam, D.-H. (2009). Cancer stem cells and their mechanism of chemo-radiation resistance. *Int. J. Stem Cells* 2:109. doi: 10.15283/ijsc.2009.2.2.109

Koon, Y. L., Zhang, S., Rahmat, M. B., Koh, C. G., and Chiam, K.-H. (2018). Enhanced Delta-Notch lateral inhibition model incorporating intracellular notch heterogeneity and tension-dependent rate of Delta-Notch binding that reproduces sprouting angiogenesis patterns. *Scient. Rep.* 8, 1–15.

Kuhnert, F., Kirshner, J. R., and Thurston, G. (2011). Dll4-Notch signaling as a therapeutic target in tumor angiogenesis. *Vascular Cell* 3:20. doi: 10.1186/2045-824x-3-20

Kumar, S., Sharife, H., Kreisel, T., Mogilevsky, M., Bar-Lev, L., Grunewald, M., et al. (2019). Intra-Tumoral Metabolic Zonation and Resultant Phenotypic Diversification Are Dictated by Blood Vessel Proximity. *Cell. Metab.* 30:e6.

Lai, E. C. (2004). Notch signaling: control of cell communication and cell fate. *Development* 131, 965–973. doi: 10.1242/dev.01074

Lawson, N. D., Scheer, N., Pham, V. N., Kim, C.-H., Chitnis, A. B., Campos-Ortega, J. A., et al. (2001). Notch signaling is required for arterial-venous differentiation during embryonic vascular development. *Development* 128, 3675–3683.

Li, C., Heidt, D. G., Dalerba, P., Burant, C. F., Zhang, L., Adsay, V., et al. (2007). Identification of pancreatic cancer stem cells. *Cancer Res.* 67, 1030–1037.

Li, X.-Y., Zhai, W.-J., and Teng, C.-B. (2016). Notch signaling in pancreatic development. *Int. J. Mole. Sci.* 17:48. doi: 10.3390/ijms17010048

Li, Y., Gu, Y., Tang, N., Liu, Y., and Zhao, Z. (2018). miR-22-notch signaling pathway is involved in the regulation of the apoptosis and autophagy in human ovarian cancer cells. *Biol. Pharmaceut. Bull.* 41, 1237–1242. doi: 10.1248/bpb.b18-00084

Lieu, C., Heymach, J., Overman, M., Tran, H., and Kopetz, S. (2011). Beyond VEGF: inhibition of the fibroblast growth factor pathway and antiangiogenesis. *Clin. Cancer Res.* 17, 6130–6139. doi: 10.1158/1078-0432.ccr-11-0659

Lin, F., Wang, N., and Zhang, T. C. (2012). The role of endothelial–mesenchymal transition in development and pathological process. *IUBMB Life* 64, 717–723. doi: 10.1002/iub.1059

Liu, G., Yuan, X., Zeng, Z., Tunici, P., Ng, H. I, Abdulkadir, R., et al. (2006). Analysis of gene expression and chemoresistance of CD133+ cancer stem cells in glioblastoma. *Mole. Cancer* 5:67.

Liu, H., Mei, F. C., Yang, W., Wang, H., Wong, E., Cai, J., et al. (2020). Epac1 inhibition ameliorates pathological angiogenesis through coordinated activation of Notch and suppression of VEGF signaling. *Sci. Adv.* 6:eaay3566. doi: 10.1126/sciadv.aay3566

Liu, M. X., Siu, M. K., Liu, S. S., Yam, J. W., Ngan, H. Y., and Chan, D. W. (2014). Epigenetic silencing of microRNA-199b-5p is associated with acquired chemoresistance via activation of JAG1-Notch1 signaling in ovarian cancer. *Oncotarget* 5:944. doi: 10.18632/oncotarget.1458

Liu, Y. P., Yang, C. J., Huang, M. S., Yeh, C. T., Wu, A. T. H., Lee, Y. C., et al. (2013). Cisplatin selects for multidrug-resistant CD133+ cells in lung adenocarcinoma by activating notch signaling. *Cancer Res.* 73, 406–416. doi: 10.1158/0008-5472.can-12-1733

Liu, Z. J., Xiao, M., Balint, K., Soma, A., Pinnix, C. C., and Capobianco, A. J. (2006). Inhibition of endothelial cell proliferation by Notch1 signaling is mediated by repressing MAPK and PI3K/Akt pathways and requires MAML1. *FASEB J.* 20, 1009–1011. doi: 10.1096/fj.05-4880fje

Liu, Z.-J., Shirakawa, T., Li, Y., Soma, A., Oka, M., Dotto, G. P., et al. (2003). Regulation of Notch1 and Dll4 by vascular endothelial growth factor in arterial endothelial cells: implications for modulating arteriogenesis and angiogenesis. *Mole. Cell. Biol.* 23, 14–25. doi: 10.1128/mcb.23.1.14-25.2003

Lobov, I., and Mikhailova, N. (2018). The role of Dll4/Notch signaling in normal and pathological ocular angiogenesis: Dll4 controls blood vessel sprouting and vessel remodeling in normal and pathological conditions. *J. Ophthalmol.* 2018:11.

Loganathan, S. K., Schleicher, K., Malik, A., Quevedo, R., Langille, E., Teng, K., et al. (2020). Rare driver mutations in head and neck squamous cell carcinomas converge on NOTCH signaling. *Science* 367, 1264–1269. doi: 10.1126/science.aax0902

Lu, J., Ye, X., Fan, F., Xia, L., Bhattacharya, R., Bellister, S., et al. (2013). Endothelial cells promote the colorectal cancer stem cell phenotype through a soluble form of Jagged-1. *Cancer Cell* 23, 171–185. doi: 10.1016/j.ccr.2012.12.021

Lugano, R., Ramachandran, M., and Dimberg, A. (2020). Tumor angiogenesis: Causes, consequences, challenges and opportunities. *Cell. Mole. Life Sci.* 77, 1745–1770. doi: 10.1007/s00018-019-03351-7

Luo, Z., Shang, X., Zhang, H., Wang, G., Massey, P. A., Barton, S. R., et al. (2019). Notch signaling in osteogenesis, osteoclastogenesis, and angiogenesis. *Am. J. Pathol.* 189, 1495–1500. doi: 10.1016/j.ajpath.2019.05.005

Mack, J. J., and Iruela-Arispe, M. L. (2018). NOTCH regulation of the endothelial cell phenotype. *Curr. Opin. Hematol.* 25:212. doi: 10.1097/moh.0000000000000425

Marín-Ramos, N. I., Jhaveri, N., Thein, T. Z., Fayngor, R. A., Chen, T. C., and Hofman, F. M. (2019). NEO212, a conjugate of temozolomide and perillyl alcohol, blocks the endothelial-to-mesenchymal transition in tumor-associated brain endothelial cells in glioblastoma. *Cancer Lett.* 442, 170–180. doi: 10.1016/j.canlet.2018.10.034

McAuliffe, S. M., Morgan, S. L., Wyant, G. A., Tran, L. T., Muto, K. W., and Chen, Y. S. (2012). Targeting Notch, a key pathway for ovarian cancer stem cells, sensitizes tumors to platinum therapy. *Proc. Natl. Acad. Sci. U. S. A.* 109, E2939–E2948.

McCaw, T. R., Inga, E., Chen, H., Jaskula-Sztul, R., Dudeja, V., Bibb, J. A., et al. (2020). Gamma secretase inhibitors in cancer: a current perspective on clinical performance. *Oncologist* 7:2020.

Meisel, C. T., Porcheri, C., and Mitsiadis, T. A. (2020). Cancer Stem Cells, Quo Vadis? The Notch Signaling Pathway in Tumor Initiation and Progression. *Cells* 9:1879. doi: 10.3390/cells9081879

Meng, R. D., Shelton, C. C., Li, Y. M., Qin, L. X., Notterman, D., Paty, P. B., et al. (2009). gamma-Secretase inhibitors abrogate oxaliplatin-induced activation of the Notch-1 signaling pathway in colon cancer cells resulting in enhanced chemosensitivity. *Cancer Res.* 69, 573–582. doi: 10.1158/0008-5472.can-08-2088

Meurette, O., and Mehlen, P. (2018). Notch Signaling in the Tumor Microenvironment. *Cancer Cell.* 34, 536–548. doi: 10.1016/j.ccell.2018.07.009

Mollen, E. W. J., Ient, J., Tjan-Heijnen, V. C. G., Boersma, L. J., Miele, L., Smidt, M. L., et al. (2018). Moving Breast Cancer Therapy up a Notch. *Front. Oncol.* 8:518. doi: 10.3389/fonc.2018.00518

Mouillesseaux, K. P., Wiley, D. S., Saunders, L. M., Wylie, L. A., Kushner, E. J., Chong, D. C., et al. (2016). Notch regulates BMP responsiveness and lateral branching in vessel networks via SMAD6. *Nat. Commun.* 7, 1–12.

Mourao, L., Jacquemin, G., Huyghe, M., Nawrocki, W. J., Menssouri, N., Servant, N., et al. (2019). Lineage tracing of Notch1-expressing cells in intestinal tumours reveals a distinct population of cancer stem cells. *Sci. Rep.* 9:888.

Nagy, J. A., and Dvorak, H. F. (2012). Heterogeneity of the tumor vasculature: the need for new tumor blood vessel type-specific targets. *Clin. Exp. Metast.* 29, 657–662. doi: 10.1007/s10585-012-9500-6

Naito, H., Iba, T., and Takakura, N. (2020). Mechanisms of new blood-vessel formation and proliferative heterogeneity of endothelial cells. *Int. Immunol.* 32, 295–305. doi: 10.1093/intimm/dxaa008

Najafi, M., Farhood, B., and Mortezaee, K. (2019). Cancer stem cells (CSCs) in cancer progression and therapy. *J. Cell. Physiol.* 234, 8381–8395. doi: 10.1002/jcp.27740

Nandhu, M. S., Hu, B., Cole, S. E., Erdreich-Epstein, A., Rodriguez-Gil, D. J., and Viapiano, M. S. (2014). Novel paracrine modulation of Notch–DLL4 signaling by fibulin-3 promotes angiogenesis in high-grade gliomas. *Cancer Res.* 74, 5435–5448. doi: 10.1158/0008-5472.can-14-0685

Nie, L., Lyros, O., Medda, R., Jovanovic, N., Schmidt, J. L., Otterson, M. F., et al. (2014). Endothelial-mesenchymal transition in normal human esophageal endothelial cells cocultured with esophageal adenocarcinoma cells: role of IL-1β and TGF-β2. *Am. J. Physiol. Cell. Physiol.* 307, C859–C877.

Niessen, K., Fu, Y., Chang, L., Hoodless, P. A., McFadden, D., and Karsan, A. (2008). Slug is a direct Notch target required for initiation of cardiac cushion cellularization. *J. Cell Biol.* 182, 315–325. doi: 10.1083/jcb.200710067

Noseda, M., Chang, L., McLean, G., Grim, J. E., Clurman, B. E., Smith, L. L., et al. (2004). Notch activation induces endothelial cell cycle arrest and participates in contact inhibition: role of p21Cip1 repression. *Mole. Cell. Biol.* 24, 8813–8822. doi: 10.1128/mcb.24.20.8813-8822.2004

Nowell, C. S., and Radtke, F. (2017). Notch as a tumour suppressor. *Nat. Rev. Cancer* 17, 145–159. doi: 10.1038/nrc.2016.145

Ntziachristos, P., Lim, J. S., Sage, J., and Aifantis, I. (2014). From fly wings to targeted cancer therapies: A centennial for notch signaling. *Cancer Cell.* 25, 318–334. doi: 10.1016/j.ccr.2014.02.018

Oon, C. E., Bridges, E., Sheldon, H., Sainson, R. C. A., Jubb, A., Turley, H., et al. (2017). Role of Delta-like 4 in Jagged1-induced tumour angiogenesis and tumour growth. *Oncotarget* 8, 40115–40131. doi: 10.18632/oncotarget.16969

Otrock, Z. K., Mahfouz, R. A. R., Makarem, J. A., and Shamseddine, A. I. (2007). Understanding the biology of angiogenesis: Review of the most important molecular mechanisms. *Blood Cells Mol. Dis.* 39, 212–220. doi: 10.1016/j.bcmd.2007.04.001

Page, D. J., Thuret, R., Venkatraman, L., Takahashi, T., Bentley, K., and Herbert, S. P. (2019). Positive Feedback Defines the Timing, Magnitude, and Robustness of Angiogenesis. *Cell. Rep.* 27, 3139–3151e5.

Pandya, K., Meeke, K., Clementz, A. G., Rogowski, A., Roberts, J., Miele, L., et al. (2011). Targeting both Notch and ErbB-2 signalling pathways is required for prevention of ErbB-2-positive breast tumour recurrence. *Br. J. Cancer* 105, 796–806. doi: 10.1038/bjc.2011.321

Patel, N. S., Li, J. L., Generali, D., Poulsom, R., Cranston, D. W., and Harris, A. L. (2005). Up-regulation of delta-like 4 ligand in human tumor vasculature and the role of basal expression in endothelial cell function. *Cancer Res.* 65, 8690–8697. doi: 10.1158/0008-5472.CAN-05-1208

Pézeron, G., Millen, K., Boukhatmi, H., and Bray, S. (2014). Notch directly regulates the cell morphogenesis genes Reck, talin and trio in adult muscle progenitors. *J. Cell Sci.* 127, 4634–4644. doi: 10.1242/jcs.151787

Phi, L. T. H. I, Sari, N., Yang, Y.-G., Lee, S.-H., Jun, N., Kim, K. S., et al. (2018). Cancer stem cells (CSCs) in drug resistance and their therapeutic implications in cancer treatment. *Stem Cells Int.* 2018:5416923.

Phillips, T. M., Kim, K., Vlashi, E., McBride, W. H., and Pajonk, F. (2007). Effects of recombinant erythropoietin on breast cancer-initiating cells. *Neoplasia* 9, 1122–1129. doi: 10.1593/neo.07694

Phng, L.-K., and Gerhardt, H. (2009). Angiogenesis: a team effort coordinated by notch. *Devel. Cell* 16, 196–208. doi: 10.1016/j.devcel.2009.01.015

Ping, Y.-F., Zhang, X., and Bian, X.-W. (2016). Cancer stem cells and their vascular niche: Do they benefit from each other? *Cancer Lett.* 380, 561–567. doi: 10.1016/j.canlet.2015.05.010

Plaks, V., Kong, N., and Werb, Z. (2015). The cancer stem cell niche: How essential is the niche in regulating stemness of tumor cells? *Cell Stem Cell.* 16, 225–238. doi: 10.1016/j.stem.2015.02.015

Potenta, S., Zeisberg, E., and Kalluri, R. (2008). The role of endothelial-to-mesenchymal transition in cancer progression. *Br. J. Cancer* 99, 1375–1379. doi: 10.1038/sj.bjc.6604662

Potente, M., Gerhardt, H., and Carmeliet, P. (2011). Basic and therapeutic aspects of angiogenesis. *Cell* 146, 873–887. doi: 10.1016/j.cell.2011.08.039

Qian, J., and Rankin, E. B. (2019). *Hypoxia-induced phenotypes that mediate tumor heterogeneity, in Hypoxia and Cancer Metastasis*. Netherland: Springer, 43–55.

Qiang, L., Wu, T., Zhang, H., Lu, N., Hu, R., Wang, Y., et al. (2012). HIF-1 α is critical for hypoxia-mediated maintenance of glioblastoma stem cells by activating Notch signaling pathway. *Cell Death Diff.* 19, 284–294. doi: 10.1038/cdd.2011.95

Qiu, M., Bao, W., Wang, J., Yang, T., He, X., Liao, Y., et al. (2014). FOXA1 promotes tumor cell proliferation through AR involving the Notch pathway in endometrial cancer. *BMC Cancer* 14, 1–17. doi: 10.1186/1471-2407-14-78

Quillard, T., Devalliere, J., Chatelais, M., Coulon, F., Séveno, C., Romagnoli, M., et al. (2009). Notch2 signaling sensitizes endothelial cells to apoptosis by negatively regulating the key protective molecule survivin. *PLoS One* 4:e8244. doi: 10.1371/journal.pone.0008244

Rampias, T., Vgenopoulou, P., Avgeris, M., Polyzos, A., Stravodimos, K., Valavanis, C., et al. (2014). A new tumor suppressor role for the Notch pathway in bladder cancer. *Nat. Med.* 20, 1199–1205. doi: 10.1038/nm.3678

Ranganathan, P., Weaver, K. L., and Capobianco, A. J. (2011). Notch signalling in solid tumours: a little bit of everything but not all the time. *Nat. Rev. Cancer* 11, 338–351. doi: 10.1038/nrc3035

Rangarajan, A., Talora, C., Okuyama, R., Nicolas, M., Mammucari, C., Oh, H., et al. (2001). Notch signaling is a direct determinant of keratinocyte growth arrest and entry into differentiation. *EMBO J.* 20, 3427–3436. doi: 10.1093/emboj/20.13.3427

Rehman, A. O., and Wang, C.-Y. (2006). Notch signaling in the regulation of tumor angiogenesis. *Trends Cell Biol.* 16, 293–300. doi: 10.1016/j.tcb.2006.04.003

Ren, B. (2016). Protein kinase D1 signaling in angiogenic gene expression and VEGF-mediated angiogenesis. *Front. Cell Devel. Biol.* 4:37. doi: 10.3389/fcell.2016.00037

Ren, B. (2018). FoxO1 transcriptional activities in VEGF expression and beyond: a key regulator in functional angiogenesis? *J. Pathol.* 245, 255–257. doi: 10.1002/path.5088

Ren, B., Best, B., Ramakrishnan, D. P., Walcott, B. P., Storz, P., and Silverstein, R. L. (2016). LPA/PKD-1-FoxO1 signaling axis mediates endothelial cell CD36 transcriptional repression and proangiogenic and proarteriogenic reprogramming. *Arterioscl. Thromb. Vascul. Biol.* 36, 1197–1208. doi: 10.1161/atvbaha.116.307421

Ren, B., Deng, Y., Mukhopadhyay, A., Lanahan, A. A., Zhuang, Z. W., Moodie, K. L., et al. (2010). ERK1/2-Akt1 crosstalk regulates arteriogenesis in mice and zebrafish. *J. Clin. Investig.* 120, 1217–1228. doi: 10.1172/jci39837

Ren, B., Hale, J., Srikanthan, S., and Silverstein, R. L. (2011). Lysophosphatidic acid suppresses endothelial cell CD36 expression and promotes angiogenesis via a PKD-1–dependent signaling pathway. *Blood J. Am. Soc. Hematol.* 117, 6036–6045. doi: 10.1182/blood-2010-12-326017

Ren, B., Rose, J. B., Liu, Y., Jaskular-Sztul, R., Contreras, C., Beck, A., et al. (2019). Heterogeneity of vascular endothelial cells, de novo arteriogenesis and therapeutic implications in pancreatic neuroendocrine tumors. *J. Clin. Med.* 8:1980. doi: 10.3390/jcm8111980

Ren, B., Song, K., Parangi, S., Jin, T., Ye, M., Humphreys, R., et al. (2009). A double hit to kill tumor and endothelial cells by TRAIL and antiangiogenic 3TSR. *Cancer Res.* 69, 3856–3865. doi: 10.1158/0008-5472.can-08-2940

Ren, B., Yee, K. O., Lawler, J., and Khosravi-Far, R. (2006). Regulation of tumor angiogenesis by thrombospondin-1. *Biochim. Biophys. Acta* 1765, 178–188.

Rizzo, P., Miele, L., and Ferrari, R. (2013). The Notch pathway: a crossroad between the life and death of the endothelium. *Eur. Heart J.* 34, 2504–2509. doi: 10.1093/eurheartj/ehs141

Rostama, B., Peterson, S. M., Vary, C. P. H., and Liaw, L. (2014). Notch signal integration in the vasculature during remodeling. *Vascul. Pharmacol.* 63, 97–104. doi: 10.1016/j.vph.2014.10.003

Rycaj, K., and Tang, D. G. (2014). Cancer stem cells and radioresistance. *Int. J. Radiat. Biol.* 90, 615–621.

Sanchez-Martin, M., and Ferrando, A. (2017). The NOTCH1-MYC highway toward T-cell acute lymphoblastic leukemia. *Blood* 129, 1124–1133. doi: 10.1182/blood-2016-09-692582

Sansone, P., Ceccarelli, C., Berishaj, M., Chang, Q., Rajasekhar, V. K., Perna, F., et al. (2016). Self-renewal of CD133 hi cells by IL6/Notch3 signalling regulates endocrine resistance in metastatic breast cancer. *Nat. Commun.* 7, 1–10. doi: 10.1155/2016/2498764

Sansone, P., Storci, G., Giovannini, C., Pandolfi, S., Pianetti, S., Taffurelli, M., et al. (2007). p66Shc/Notch−3 interplay controls self−renewal and hypoxia survival in human stem/progenitor cells of the mammary gland expanded in vitro as mammospheres. *Stem Cells* 25, 807–815. doi: 10.1634/stemcells.2006-0442

Shah, D., Wyatt, D., Baker, A. T., Simms, P., Peiffer, D. S., Fernandez, M., et al. (2018). Inhibition of HER2 increases JAGGED1-dependent breast cancer stem cells: Role for membrane JAGGED1. *Clin. Cancer Res.* 24, 4566–4578. doi: 10.1158/1078-0432.ccr-17-1952

Shih, I.-M., and Wang, T.-L. (2007). Notch signaling, γ-secretase inhibitors, and cancer therapy. *Cancer Res.* 67, 1879–1882. doi: 10.1158/0008-5472.can-06-3958

Shutter, J. R., Scully, S., Fan, W., Richards, W. G., Kitajewski, J., Deblandre, G. A., et al. (2000). Dll4, a novel Notch ligand expressed in arterial endothelium. *Genes Devel.* 14, 1313–1318.

Siekmann, A. F., and Lawson, N. D. (2007). Notch signalling and the regulation of angiogenesis. *Cell Adhes. Migr.* 1, 104–106. doi: 10.4161/cam.1.2.4488

Simons, M., Gordon, E., and Claesson-Welsh, L. (2016). Mechanisms and regulation of endothelial VEGF receptor signalling. *Nat. Rev. Mol. Cell Biol.* 17, 611–625. doi: 10.1038/nrm.2016.87

Sitohy, B., Nagy, J. A., Jaminet, S. C., and Dvorak, H. F. (2011). Tumor-surrogate blood vessel subtypes exhibit differential susceptibility to anti-VEGF therapy. *Cancer Res.* 71, 7021–7028. doi: 10.1158/0008-5472.can-11-1693

Stylianou, S., Clarke, R. B., and Brennan, K. (2006). Aberrant activation of notch signaling in human breast cancer. *Cancer Res.* 66, 1517–1525. doi: 10.1158/0008-5472.can-05-3054

Suchting, S., Freitas, C., le Noble, F., Benedito, R., Bréant, C., Duarte, A., et al. (2007). The Notch ligand Delta-like 4 negatively regulates endothelial tip cell formation and vessel branching. *Proc. Natl. Acad. Sci.* 104, 3225–3230. doi: 10.1073/pnas.0611177104

Tamagnone, L., Zacchigna, S., and Rehman, M. (2018). Taming the Notch transcriptional regulator for cancer therapy. *Molecules* 23:431. doi: 10.3390/molecules23020431

Taslimi, S., and Das, S. (2018). *Angiogenesis and Angiogenesis Inhibitors in Brain Tumors, in Handbook of Brain Tumor Chemotherapy, Molecular Therapeutics, and Immunotherapy*. New York: Elsevier, 361–371.

Teodorczyk, M., and Schmidt, M. H. H. (2014). Notching on cancer's door: Notch signaling in brain tumors. *Front. Oncol.* 4:341. doi: 10.3389/fonc.2014.00341

Thiery, J. P., and Sleeman, J. P. (2006). Complex networks orchestrate epithelial–mesenchymal transitions. *Nat. Rev. Mole. Cell Biol.* 7, 131–142. doi: 10.1038/nrm1835

Trindade, A., Ram Kumar, S., Scehnet, J. S., Lopes-da-Costa, L., Becker, J., Jiang, W., et al. (2008). Overexpression of delta-like 4 induces arterialization and attenuates vessel formation in developing mouse embryos. *Blood J. Am. Soc. Hematol.* 112, 1720–1729. doi: 10.1182/blood-2007-09-112748

Ulasov, I. V., Nandi, S., Dey, M., Sonabend, A. M., and Lesniak, M. S. (2011). Inhibition of Sonic hedgehog and Notch pathways enhances sensitivity of CD133(+) glioma stem cells to temozolomide therapy. *Mol. Med.* 17, 103–112. doi: 10.2119/molmed.2010.00062

Venkatraman, L., Regan, E. R., and Bentley, K. (2016). Time to decide? Dynamical analysis predicts partial tip/stalk patterning states arise during angiogenesis. *PLoS One* 11:e0166489. doi: 10.1371/journal.pone.0166489

Walshe, T. E., Connell, P., Cryan, L., Ferguson, G., Gardiner, T., Morrow, D., et al. (2011). Microvascular retinal endothelial and pericyte cell apoptosis in vitro: role of Hedgehog and Notch signaling. *Investig. Ophthalmol. Visual Sci.* 52, 4472–4483. doi: 10.1167/iovs.10-7061

Wang, L., Jin, F., Qin, A., Hao, Y., Dong, Y., Ge, S., et al. (2014). Targeting Notch1 signaling pathway positively affects the sensitivity of osteosarcoma to cisplatin by regulating the expression and/or activity of Caspase family. *Mole. Cancer* 13:139. doi: 10.1186/1476-4598-13-139

Wang, Z., Li, Y., Ahmad, A., Azmi, A. S., Banerjee, S., Kong, D., et al. (2010). Targeting Notch signaling pathway to overcome drug resistance for cancer therapy. *Biochim. Biophys. Acta* 1806, 258–267. doi: 10.1016/j.bbcan.2010.06.001

Welch-Reardon, K. M., Wu, N., and Hughes, C. C. (2015). A role for partial endothelial–mesenchymal transitions in angiogenesis? *Arterioscl. Thromb. Vascul. Biol.* 35, 303–308. doi: 10.1161/atvbaha.114.303220

Weng, A. P., and Aster, J. C. (2004). Multiple niches for Notch in cancer: Context is everything. *Curr. Opin. Genet. Dev.* 14, 48–54. doi: 10.1016/j.gde.2003.11.004

Weng, A. P., Ferrando, A. A., Lee, W., Morris, J. P., Silverman, L. B., Sanchez-Irizarry, C., et al. (2004). Activating mutations of NOTCH1 in human T cell acute lymphoblastic leukemia. *Science* 306, 269–271. doi: 10.1126/science.1102160

Wieland, E., Rodriguez-Vita, J., Liebler, S. S., Mogler, C., Moll, I., and Herberich, S. E. (2017). Endothelial Notch1 Activity Facilitates Metastasis. *Cancer Cell* 31, 355–367. doi: 10.1016/j.ccell.2017.01.007

Wohlfeil, S. A., Hafele, V., Dietsch, B., Schledzewski, K., Winkler, M., and Zierow, J. (2019). Hepatic Endothelial Notch Activation Protects against Liver Metastasis by Regulating Endothelial-Tumor Cell Adhesion Independent of Angiocrine Signaling. *Cancer Res.* 79, 598–610. doi: 10.1158/0008-5472.can-18-1752

Xiao, W., Gao, Z., Duan, Y., Yuan, W., and Ke, Y. (2017). Notch signaling plays a crucial role in cancer stem-like cells maintaining stemness and mediating chemotaxis in renal cell carcinoma. *J. Exp. Clin. Cancer Res.* 36:41.

Xie, M., He, C.-S., Wei, S.-H., and Zhang, L. (2013). Notch-1 contributes to epidermal growth factor receptor tyrosine kinase inhibitor acquired resistance in non-small cell lung cancer in vitro and in vivo. *Eur. J. Cancer* 49, 3559–3572. doi: 10.1016/j.ejca.2013.07.007

Xie, X., Kaoud, T. S., Edupuganti, R., Zhang, T., Kogawa, T., Zhao, Y., et al. (2017). c-Jun N-terminal kinase promotes stem cell phenotype in triple-negative breast cancer through upregulation of Notch1 via activation of c-Jun. *Oncogene* 36, 2599–2608. doi: 10.1038/onc.2016.417

Yabuuchi, S., Pai, S. G., Campbell, N. R., De Wilde, R. F., De Oliveira, E., Korangath, P., et al. (2013). Notch signaling pathway targeted therapy suppresses tumor progression and metastatic spread in pancreatic cancer. *Cancer Lett.* 335, 41–51. doi: 10.1016/j.canlet.2013.01.054

Yancopoulos, G. D., Davis, S., Gale, N. W., Rudge, J. S., Wiegand, S. J., and Holash, J. (2000). Vascular-specific growth factors and blood vessel formation. *Nature* 407, 242–248. doi: 10.1038/35025215

Yang, L., Shi, P., Zhao, G., Xu, J., Peng, W., Zhang, J., et al. (2020). Targeting cancer stem cell pathways for cancer therapy. *Sign. Transduct. Target. Ther.* 5, 1–35. doi: 10.1155/2019/8549020

Yeom, D.-H., Lee, Y.-S., Ryu, I., Lee, S., Sung, B., Lee, H.-B., et al. (2021). ABL001, a Bispecific Antibody Targeting VEGF and DLL4, with Chemotherapy, Synergistically Inhibits Tumor Progression in Xenograft Models. *Int. J. Mole. Sci.* 22:241. doi: 10.3390/ijms22010241

Yuan, X., Wu, H., Han, N., Xu, H., Chu, Q., Yu, S., et al. (2014). Notch signaling and EMT in non-small cell lung cancer: Biological significance and therapeutic application. *J. Hematol. Oncol.* 7, 87.

Yuan, X., Zhang, M., Wu, H., Xu, H., Han, N., Chu, Q., et al. (2015). Expression of Notch1 Correlates with Breast Cancer Progression and Prognosis. *PLoS One* 10:e0131689. doi: 10.1371/journal.pone.0131689

Yunus, M., Jansson, P. J., Kovacevic, Z., Kalinowski, D. S., and Richardson, D. R. (2019). Tumor-induced neoangiogenesis and receptor tyrosine kinases - Mechanisms and strategies for acquired resistance. *Biochim. Biophys. Acta Gen. Subj* 1863, 1217–1225. doi: 10.1016/j.bbagen.2019.04.017

Zeisberg, E. M., Potenta, S., Xie, L., Zeisberg, M., and Kalluri, R. (2007a). Discovery of endothelial to mesenchymal transition as a source for carcinoma-associated fibroblasts. *Cancer Res.* 67, 10123–10128. doi: 10.1158/0008-5472.can-07-3127

Zeisberg, E. M., Tarnavski, O., Zeisberg, M., Dorfman, A. L., McMullen, J. R., Gustafsson, E., et al. (2007b). Endothelial-to-mesenchymal transition contributes to cardiac fibrosis. *Nat. Med.* 13, 952–961.

Zeng, D., Liang, Y. K., Xiao, Y. S., Wei, X. L., Lin, H. Y., Wu, Y., et al. (2020). Inhibition of Notch1 reverses EMT and chemoresistance to cisplatin via direct downregulation of MCAM in triple-negative breast cancer cells. *Int. J. Cancer* 147, 490–504. doi: 10.1002/ijc.32911

Zhang, S., Balch, C., Chan, M. W., Lai, H. C., Matei, D., Schilder, J. M., et al. (2008). Identification and characterization of ovarian cancer-initiating cells from primary human tumors. *Cancer Res.* 68, 4311–4320. doi: 10.1158/0008-5472.can-08-0364

Zhu, T. S., Costello, M. A., Talsma, C. E., Flack, C. G., Crowley, J. G., Hamm, L. L., et al. (2011). Endothelial cells create a stem cell niche in glioblastoma by providing NOTCH ligands that nurture self-renewal of cancer stem-like cells. *Cancer Res.* 71, 6061–6072. doi: 10.1158/0008-5472.can-10-4269

Zou, J., Li, P., Lu, F., Liu, N., Dai, J., Ye, J., et al. (2013). Notch1 is required for hypoxia-induced proliferation, invasion and chemoresistance of T-cell acute lymphoblastic leukemia cells. *J. Hematol. Oncol.* 6:3. doi: 10.1186/1756-8722-6-3

Conflict of Interest: The authors declare that the research was conducted in the absence of any commercial or financial relationships that could be construed as a potential conflict of interest.

Copyright © 2021 Akil, Gutiérrez-García, Guenter, Rose, Beck, Chen and Ren. This is an open-access article distributed under the terms of the Creative Commons Attribution License (CC BY). The use, distribution or reproduction in other forums is permitted, provided the original author(s) and the copyright owner(s) are credited and that the original publication in this journal is cited, in accordance with accepted academic practice. No use, distribution or reproduction is permitted which does not comply with these terms.

frontiers in Cell and Developmental Biology

ORIGINAL RESEARCH
published: 18 February 2021
doi: 10.3389/fcell.2021.643810

Chronic Inhibition of mROS Protects Against Coronary Endothelial Dysfunction in Mice With Diabetes

*Hang Xing[1], Zhiqi Zhang[1], Guangbin Shi[1], Yixin He[1], Yi Song[1], Yuhong Liu[1], Elizabeth O. Harrington[2], Frank W. Sellke[1] and Jun Feng[1]**

[1] Cardiothoracic Surgery Research Laboratory, Cardiovascular Research Center, Department of Surgery, Rhode Island Hospital, Alpert Medical School of Brown University, Providence, RI, United States, [2] Vascular Research Laboratory, Providence VA Medical Center, Department of Medicine, Alpert Medical School of Brown University, Providence, RI, United States

Diabetes is associated with coronary endothelial dysfunction. Persistent oxidative stress during diabetes contributes to coronary endothelial dysfunction. The mitochondria are main sources of reactive oxygen species (ROS) in diabetes, and mitochondria-targeted antioxidant mito-Tempo can prevent mitochondrial reactive oxygen species (mROS) generation in a variety of disorders. Inhibition/inactivation of small-conductance Ca^{2+}-activated K^+ (SK) channels contribute to diabetic downregulation of coronary endothelial function/relaxation. However, few investigated the role of mROS on endothelial dysfunction/vasodilation and endothelial SK channel downregulation in diabetes. The aim of present study was to investigate the chronic administration of mito-Tempo, on coronary vasodilation, and endothelial SK channel activity of mice with or without diabetes. Mito-Tempo (1 mg/kg/day) was applied to the mice with or without diabetes (n = 10/group) for 4 weeks. *In vitro* relaxation response of pre-contracted arteries was examined in the presence or absence of the vasodilatory agents. SK channel currents of the isolated mouse heart endothelial cells were measured using whole-cell patch clamp methods. At baseline, coronary endothelium-dependent relaxation responses to ADP and the selective SK channel activator NS309 and endothelial SK channel currents were decreased in diabetic mice compared with that in non-diabetic (ND) mice ($p < 0.05$). After a 4-week treatment with mito-Tempo, coronary endothelium-dependent relaxation response to ADP or NS309 and endothelial SK channel currents in the diabetic mice was significantly improved when compared with that in untreated diabetic mice ($p < 0.05$). Interestingly, coronary relaxation responses to ADP and NS309 and endothelial SK channel currents were not significantly changed in ND mice after mito-Tempo treatment, as compared to that of untreated control group. Chronic inhibition of endothelial mROS appears to improve coronary endothelial function/dilation and SK channel activity in diabetes, and mROS inhibitors may be a novel strategy to treat vascular complications in diabetes.

Keywords: coronary endothelial function, mitochondrial reactive oxygen species, diabetes, potassium channels, coronary microcirculation

OPEN ACCESS

Edited by:
Bin Ren,
University of Alabama at Birmingham, United States

Reviewed by:
Longhou Fang,
Houston Methodist Research Institute, United States
Tong Lu,
Mayo Clinic, United States

***Correspondence:**
Jun Feng
jfeng@lifespan.org

Specialty section:
This article was submitted to Signaling, a section of the journal Frontiers in Cell and Developmental Biology

Received: *18 December 2020*
Accepted: *29 January 2021*
Published: *18 February 2021*

Citation:
Xing H, Zhang Z, Shi G, He Y, Song Y, Liu Y, Harrington EO, Sellke FW and Feng J (2021) Chronic Inhibition of mROS Protects Against Coronary Endothelial Dysfunction in Mice With Diabetes. Front. Cell Dev. Biol. 9:643810. doi: 10.3389/fcell.2021.643810

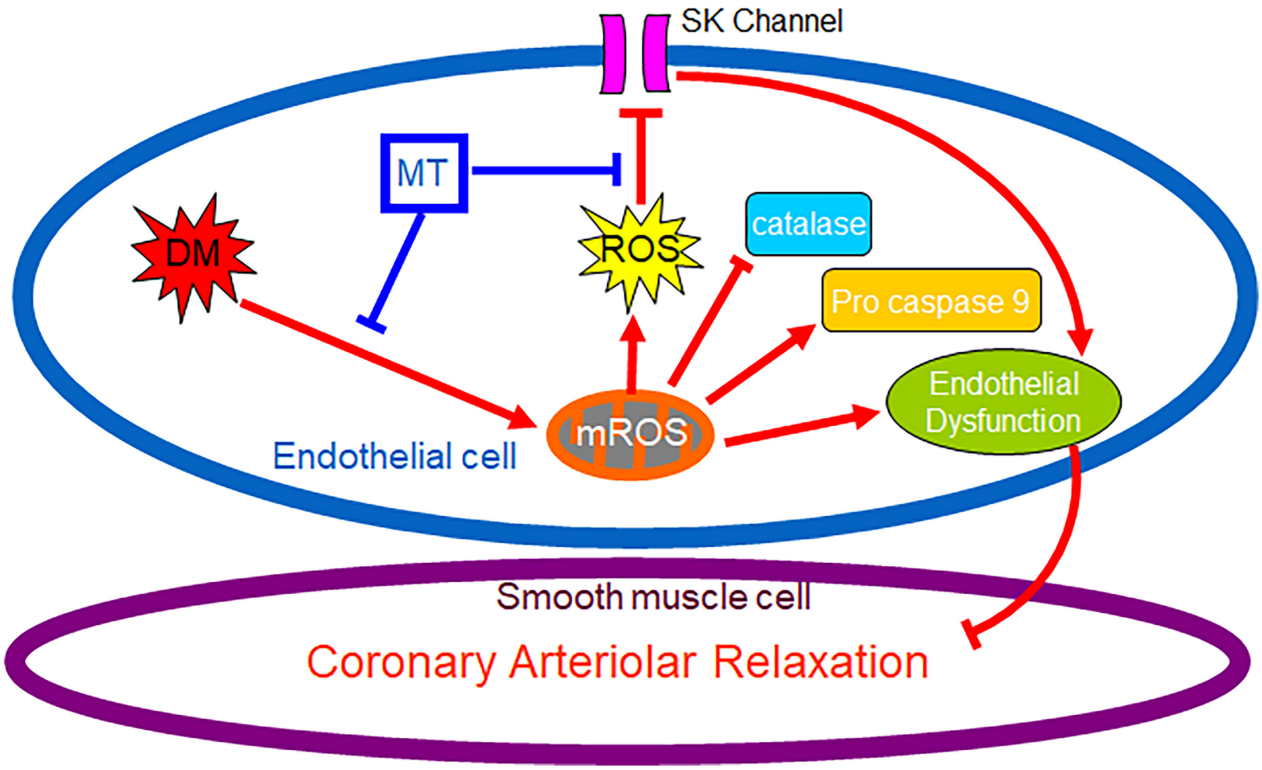

GRAPHICAL ABSTRACT | Chronic hyperglycemia during diabetes causes persistent overproduction of mitochondrial ROS (mROS), resulting in inhibition of endothelial SK channel activity, impairment of coronary endothelium-dependent relaxation and dysregulation of antioxidant/pro-cell death enzyme. Chronic inhibition of mROS with mito-Tempo prevents endothelial mROS production resulting in increasing endothelial SK currents, enhancing antioxidant enzyme production, and improving coronary endothelium-dependent relaxation.

INTRODUCTION

Macro- and micro-vascular diseases are the principal contributors to the increased morbidity and mortality associated with diabetes (DM) with the mortality rate of diabetic patients 3–4 times that of the general population (Haffner et al., 1998; Wilson et al., 2005). Diabetes is associated with coronary endothelial dysfunction (Emani et al., 2009; Ismail-Beigi et al., 2010; Feng et al., 2011, 2012a,b); a major risk factor of cardiovascular complications of DM. Given that DM affects 20% of the United States population and is increasing dramatically in prevalence, this remains a considerable clinical problem. Thus, investigation into mitochondrial reactive oxygen species (mROS) impact of diabetic regulation of endothelial function/protection in the coronary circulation with translational research model is a crucial step linking bench to bedside. Endothelial dysfunction from DM is associated with altered metabolism and inactivation of small conductance calcium-activated-potassium (SK) channels in the animal and human coronary vasculature (Makino et al., 2000; Ding et al., 2005; Burnham et al., 2006; Leo et al., 2011; Feng et al., 2012b, 2017; Liu et al., 2015, 2018, 2020). However, the precise mechanisms responsible for diabetic inactivation of SK and coronary endothelial dysfunction are still undefined.

Persistent oxidative stress during DM contributes to coronary endothelial dysfunction by reducing endothelial nitric oxide (eNOS) syntheses, increasing eNOS uncoupling (Si et al., 2006). The mitochondria are main sources of reactive oxygen species (ROS) in DM (Kizhakekuttu et al., 2012; Cho et al., 2013), and mitochondria-targeted antioxidants can prevent mROS generation in a variety of disorders (O'Malley et al., 2006; Graham et al., 2009; Galkin et al., 2014; Szczesny et al., 2014; Sada et al., 2016). However, few have evaluated the effects of chronic mROS inhibition on coronary endothelial function and SK channel activity *in vivo* in the setting of diabetes. Mito-Tempo, a mitochondria-targeted antioxidant, has been shown to reduce cellular levels of ROS, which shows promise in protecting cells against oxidative stress and cell damage (Park et al., 2016; Chen et al., 2017). However, its efficacy in preventing coronary endothelial and SK channel dysfunction in the setting of DM has not been investigated. Thus, we hypothesized that DM induces persistent overproduction of coronary endothelial mROS, resulting in impairment of coronary endothelium-dependent relaxation and dysfunction of endothelial SK channel. We further hypothesized that chronic inhibition of mROS during diabetes would suppress endothelial mROS overproduction resulting in improving coronary endothelium-dependent relaxation and enhancing endothelial SK channel function. Using genetically modified, obesity/type-2-DM mice, we investigated the effects of chronic treatment with mito-Tempo on coronary endothelium-dependent relaxation

and endothelial SK channel function, as well as endothelial mROS production.

MATERIALS AND METHODS

Animals

C57BL/6J mice (male, 12 weeks old) served as control of non-diabetic (ND) group (n = 20). Genetically modified mice exhibiting type-2 DM and obesity (BKS.Cg - *Dock7*^{m} +/+ *Lepr*^{db}/J male, 12 weeks old, n = 20), were used in this study (Jackson Laboratory, Bar Harbor, Maine). All experiments were approved by the Institutional Animal Care and Use Committee of the Rhode Island Hospital.

Mito-Tempo Treatment and Mouse Heart Harvesting

The mice were divided into following 4 groups (n = 10/group): (1) the untreated control ND mice received saline i.p. injection; (2) mito-Tempo treated ND mice received 1 mg/kg/day mito-Tempo i.p., injection; (3) the untreated DM mice saline i.p., injection; and (4) mito-Tempo treated DM mice received 1 mg/kg/day mito-Tempo i.p., injection. After 4 weeks of treatment, the mice were anesthetized using inhalant isoflurane and thoracotomy was performed and the heart was removed. The heart tissue was placed in cold Krebs buffer in preparation for *in vitro* microvascular study or preserved in cell culture medium for endothelial cell isolation or stored in liquid nitrogen for molecular analysis.

Vascular Reactivity

After the mouse hearts (n = 6/group) were removed from the 4 experimental groups, they were immediately placed into cold (4°C) Krebs buffer [(in millimoles per liter): NaCl 119.0, NaHCO3 25.0, KCl 4.6, KH2PO4 1.2, $MgSO_4$ 1.2, $CaCl_2$ 1.8, and glucose 11.0]. The mouse small coronary (LAD) arteries (70–120 μm internal diameters) (Zhang et al., 2020) were dissected using a 10–60X dissecting microscope (Olympus Optical, Tokyo, Japan). Vessel studies were performed *in vitro* in a pressurized (40-mmHg) no-flow state using video-microscopy as previously described (Zhang et al., 2020). After 60-min period of equilibration, the vessel was pre-constricted with the thromboxane A2 analog U46619 (4×10^{-7}–1×10^{-6} M) or endothelin-1 (10^{-7} M) and then receive the vasodilatory agents, sodium nitroprusside (SNP, 1×10^{-9}–1×10^{-4} M), or adenosine 5′dephosphate (ADP, 1×10^{-9}–1×10^{-4} M) or the selective SK channel activator NS309 (1×10^{-9}–1×10^{-4} M), respectively (Feng et al., 2008; Liu et al., 2008, 2015, 2018; Zhang et al., 2020).

Endothelial Cell Isolation and Culture

Mouse heart endothelial cells (MHECs) were isolated from the harvested heart of DM- and ND-mice (n=4/group), and cultured as previously described (Liu et al., 2015). MHECs (passage 0) were grown in the DMEM with 20% FCS + Pen/Strep + 100 μg/mL Heparin (Sigma) + 100 μg/mL ECGS (Biomedical Technologies, Stoughton, MA) + 1× non-essential amino acids + 2 mM L-glutamine + 1× sodium pyruvate + 25 mM HEPES in a humidified incubator with 5%CO_2 at 37°C according to the manufacturer's protocols and our previous study. Results were obtained, in triplicate, using three independent batches of isolation per group (Zhang et al., 2020).

SK Channel Recording in MHECs

The cultured MHECs (passage 0) from mice with or without DM were washed twice with Ca^{2+-}free DMEM, incubated with 0.05% trypsin and 0.02% EDTA for 1–2 min. An Axopatch-200B amplifier and pClamp 10.6 (Molecular Devices, Foster City, United States) were used to record and analyze K^+ currents of MHECs in the whole-cell configuration in the voltage-clamp mode. The bath solution contained (in mM): 140 NaCl, 5 KCl, 1 $CaCl_2$, 2 $MgCl_2$, 10 HEPES, 30 glucose (pH 7.4). The patch pipette resistance was 1–3 MΩ and filled with the pipette solution contained (mM): 110 K-Aspartate, 20 KCl, 1 $MgCl_2$, 8.5 $CaCl_2$, 10 HEPES, 8 NaCl, 0.01 Niflumic acid and 10 BAPTA (pH 7.2, with calculated free Ca^{2+} 400 nM). The cells were examined every 5 s at the holding potential of −50 mV by 150 ms test pulses between −100 and +100 mV in 20 mV increments. Sampling rate was 10 kHz with low-pass filter set at 2 KHz. The effect of selective SK channel activator NS309 (10^{-6} M) on the whole cell K^+ currents was examined. The specificity of NS309 was confirmed by simultaneous application of the selective SK (SK2/SK3) blocker apamin (10^{-7} M) and SK4 (IK) blocker TRAM34 (10^{-5} M) (Zhang et al., 2020).

Measurement of mROS in the MHECs

Mouse heart endothelial cells were loaded with 5 μmol/L MitoSox Red and 100 nmol/L MitoTracker Green FM (Invitrogen) for 10 min at 37°C. Images were taken on a Zeiss LSM710 confocal microscope (Carl Zeiss GmbH, Germany) using an argon laser excitation (514 nm) with emission collection through a 560 nm long pass filter. The mean values of the whole cell fluorescence of MitoSOX^{TM} Red were obtained with ImageJ software (Liu et al., 2020).

Immunoblot

The methods for whole cell protein purification, Western blotting and imaging quantification have been described previously. Membranes were incubated overnight at 4°C with primary antibodies against catalase and procaspase 9 (Cell Signaling, Danvers, MA, United States). After washing with TBST, membranes were incubated with the appropriate secondary antibody conjugated to horseradish peroxidase. All membranes were also incubated with GAPDH (glyceraldehyde-3-phosphate) or alpha-tubulin (Cell Signaling Tech. Danvers, MA, United States) as loading controls (Feng et al., 2017; Liu et al., 2020; Zhang et al., 2020).

Statistical Analysis

Data are presented as the standard deviation (SD) or mean and standard error of the mean (SEM). Vascular responses are expressed as percent relaxation of the pre-constricted diameter. Data of vascular reactivity and channel current activity

were analyzed using two-way repeated-measures ANOVA with a *post hoc* Bonferroni test. Other data were analyzed by either one-way ANOVA or Student's *t*-test (GraphPad Software, Inc, San Diego, CA, United States). *P*-values < 0.05 were considered significant.

RESULTS

Mice Characteristics

The effects of DM and 4-week treatment with mito-Tempo on mouse body weight and blood glucose levels are summarized in **Figure 1**. At baseline, the body weight (**Figure 1A**) and blood glucose (**Figure 1B**) of genetically modified DM mice were higher than that of ND mice ($p < 0.0001$). Four-week treatment with mito-Tempo did not change the body weight and blood glucose levels, as compared to their non-treated controls ($P > 0.05$), respectively.

The Effects of DM and Mito-Tempo Treatment on Small Coronary Arterial Relaxation

The endothelium-independent vasodilator SNP, the endothelium-dependent vasodilator ADP, and the endothelium-dependent/SK channel activator NS309 induced dose-dependent relaxation response in the mouse small coronary arteries (**Figure 2**). There were no significant differences in the responses to the endothelium-independent vasodilator SNP between ND and DM mice or mito-Tempo treated groups vs. control untreated groups (**Figure 2**). However, in the control untreated (saline) groups, DM significantly reduced the relaxation response to ADP and NS309 compared to that of ND group ($p < 0.05$). Four-week treatment with mito-Tempo significantly improved relaxation response to ADP and NS309 in the DM vessels, as compared with that in untreated DM vessels ($p < 0.05$). Interestingly, 4-week treatment with mito-Tempo failed to affect

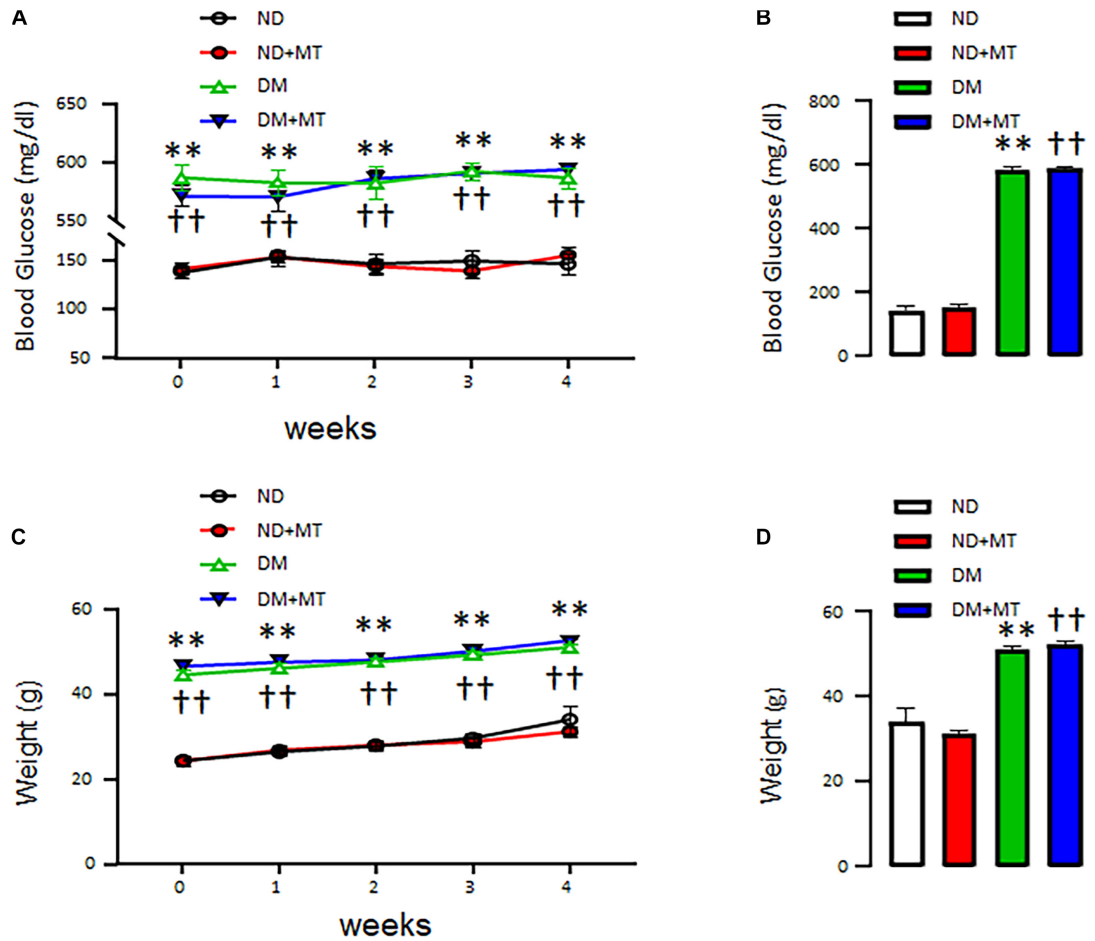

FIGURE 1 | The effects of chronic treatment with mito-Tempo (MT) on body weight and blood glucose level in diabetic (DM) and non-diabetic (ND) mice. Mice (8 weeks of age) were intraperitoneal injection mito-Tempo (1 mg/kg) for 4 weeks; DM + MT = diabetic mice treated with mito-Tempo for 4 weeks, ND + MT = non-diabetic mice treated with mito-Tempo for 4 weeks; **(A)** Blood glucose level of DM mice was significantly higher than ND mice ($p < 0.01$), chronic MT treatment had no effect on body weight in both mice ($p > 0.05$), **(B)** Bar graph showing blood glucose of DM and ND mice after 4 week treatment with MT, **(C)** Body weight of DM mice was significantly higher than ND mice ($p < 0.01$), chronic treatment with MT had no effect on body weight in both mice ($p > 0.05$), and **(D)** Bar graph showing body weight of DM and ND mice after 4 weeks chronic treatment of MT; $^{**}p < 0.01$ vs ND mice; $^{\dagger\dagger}p < 0.01$ vs. ND + MT.

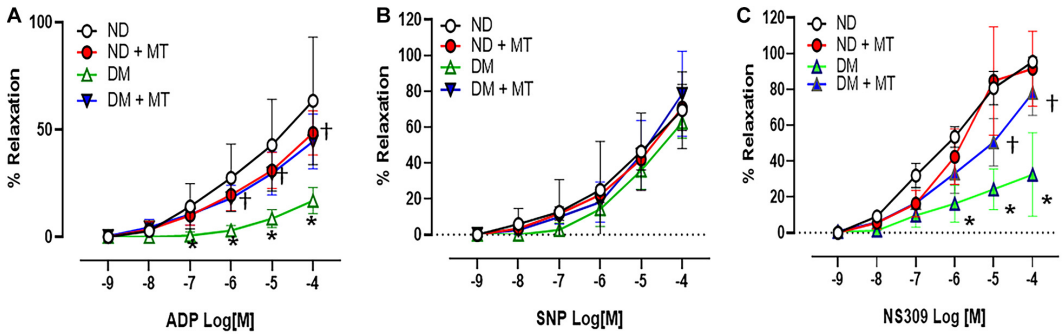

FIGURE 2 | Effects of chronic treatment with mito-Tempo (MT) on mouse small coronary arterial relaxation in responses to vasodilators. **(A)** Mouse small coronary arterial relaxation responses to endothelium-dependent vasodilators ADP in diabetic (DM) and non-diabetic (DM) mice after 4-week treatment with mito-Tempo (1 mg/kg/day), DM + MT = diabetic mice treated with mito-Tempo for 4 weeks, ND + MT = non-diabetic mice treated with mito-Tempo for 4 weeks; **(B)** Mouse small coronary arterial relaxation responses to endothelium-independent vasodilators SNP in ND and DM mice after chronic treatment with mito-Tempo, n = 5–6/group. **(C)** Mouse small coronary arterial relaxation responses to the selective SK channel activator NS309 in ND and DM mice and after chronic treatment with MT, n = 6–8/group, *$p < 0.05$ ND vs.DM, †$p < 0.05$ DM + mito-Tempo vs. DM.

the relaxation response to ADP and NS309 of small coronary arteries in ND mice, as compared to the untreated ND mice ($p > 0.05$).

The Effects of DM and Mito-Tempo Treatment on Endothelial SK-Currents of MHECs

The basal endothelial K^+ currents were significantly diminished in the MHECs with DM compared to ND (**Figure 3**, $p < 0.05$). Application of the SK channel activator NS 309 enhanced endothelial SK current in both of ND and DM cells, however, the response to NS309 was significantly diminished in the DM mice compared to that of ND (**Figure 3**). Four-week treatment with mito-Tempo significantly enhanced endothelial K^+ currents in the DM cells compared to untreated DM cells (**Figure 3**, $p < 0.05$). Subsequent application of SK blockers, apamin (10^{-7} M) and TRAM34 (10^{-6} M), prevented NS309-indued effects on K^+ currents in both ND and DM groups (**Figure 3**). In contrast, 4-week treatment with mito-Tempo failed to affect endothelial K^+ currents in the ND mice ($p > 0.05$).

The Effects of DM and Mito-Tempo Treatment on mROS in MHECs

The untreated MHECs of DM mice had significantly higher levels of mROS than their ND counterparts (**Figure 4**, $p < 0.05$). In the DM groups, 4-week treatment with mito-TEMPO significantly reduced mROS ($p < 0.05$) compared to untreated DM. In contrast, in the ND groups, 4-week treatment with mito-TEMPO did not affect mROS levels compared to untreated ND ($p < 0.05$).

The Effects of DM and Mito-Tempo Treatment on Catalase and Pro-caspase 9 Expression

DM significantly decreased protein expression of catalase but enhanced pro-caspase 9 in the LV myocardium compared to that of ND (**Figure 5**, $p < 0.05$), respectively. Treatment of the diabetic mice with mito-Tempo significantly increased protein expression of catalase but decreased pro-caspase 9 in the DM heart compared to that of untreated diabetic mice ($p < 0.05$), respectively. In contrast, chronic treatment with mito-Tempo failed to affect catalase and pro-caspase 9 expression in the ND mice.

DISCUSSION

We and others have previously reported that DM is associated with coronary endothelial dysfunction in animals and humans (Feng et al., 2012a; Liu et al., 2015, 2018, 2020; Zhang et al., 2020). The current study confirmed these previous findings by demonstrating that DM reduced mouse coronary endothelium-dependent relaxation/function. ROS generated during diabetic hyperglycemia are implicated in the development of diabetic vascular complications (Baynes, 1991; Li and Shah, 2004). Elevated levels of oxygen-derived free radicals are the initial source of endothelial dysfunction in DM. ROS not only reduce nitric oxide (NO) bioavailability via uncoupled eNOS, but also facilitate the production and/or action of endothelium-dependent constricting factors (EDCFs) (Srinivasan et al., 2013). Thus, the endothelial balance tips toward vasoconstrictor responses over the course of diabetes (Shi and Vanhoutte, 2009). Mitochondrial dysfunction plays a key role in endothelial dysfunction in DM. Emerging evidence shows that mitochondria are the dominant mechanisms of ROS production in the diabetic heart/vessels (Shenouda et al., 2011; Kizhakekuttu et al., 2012; Liu et al., 2020). The current study further indicates that DM significantly increases endothelial mROS in the MHECs. Four-week application of mito-Tempo in the mice with DM prevented mROS overproduction in MHECs and improved coronary endothelial function. Consistent with previous studies in animals and humans (Ding et al., 2005; Burnham et al., 2006; Leo et al., 2011; Liu et al., 2015, 2020; Zhang et al., 2020), in the current study we confirmed that DM decreased coronary relaxation response to the SK activators and endothelial SK current activity, suggesting that diabetic inhibition of SK channels may contribute to coronary endothelial dysfunction.

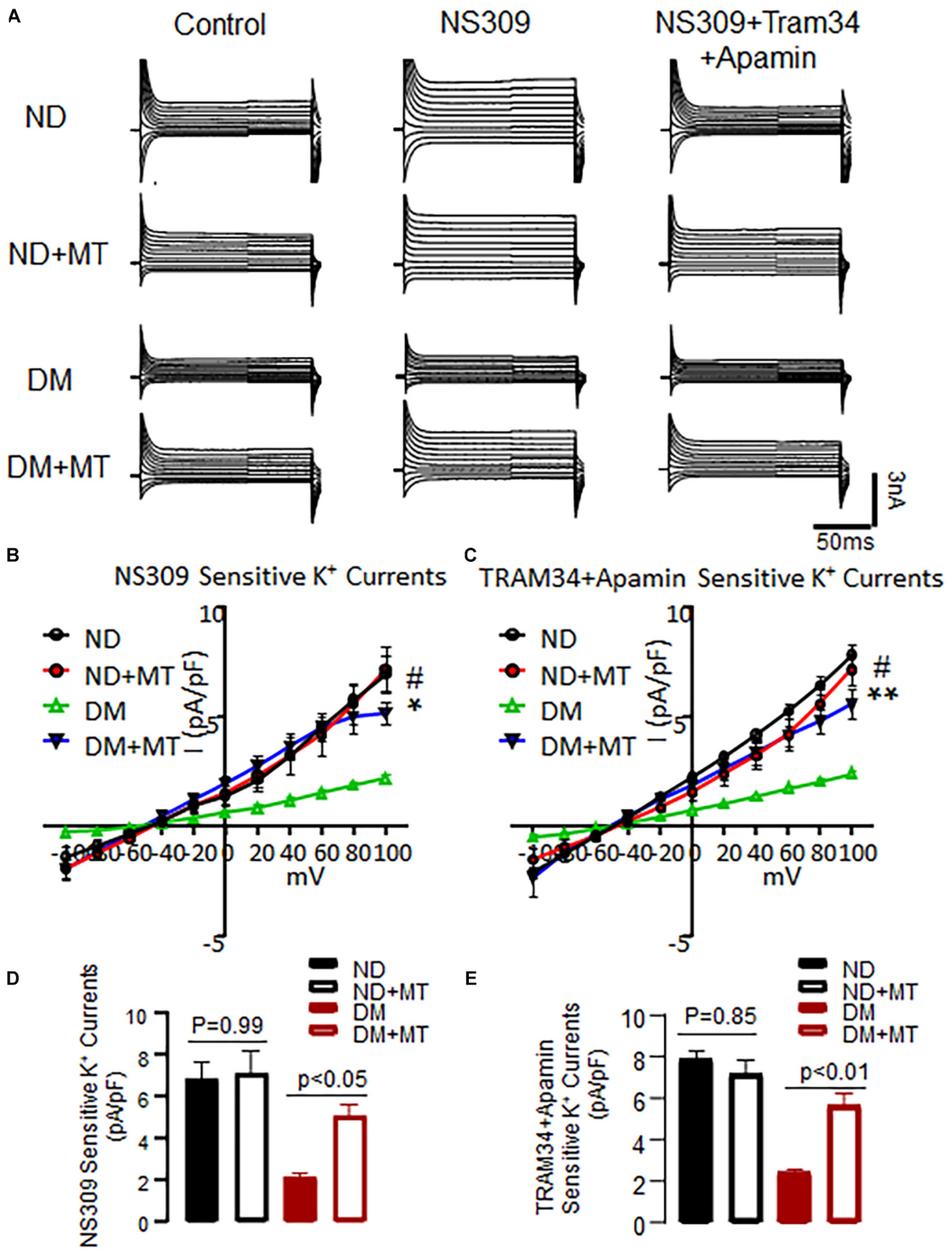

FIGURE 3 | Chronic treatment with mito-Tempo (MT) significantly increased SK channels current in mouse heart endothelial cells (MHECs) of diabetics (DM) and non-diabetics (ND). **(A)** Representative traces of the whole cell currents of MHECs treated with or without MT. **(B)** Four-week treatment with MT increased SK channels current in responses to NS309 in MHECs of DM, $n = 6$/group, $^{*}p < 0.05$ DM + MT vs. DM, $\#p < 0.01$ ND vs. DM, DM + MT = diabetic mice treated with mito-Tempo for 4 weeks, ND + MT = non-diabetic mice treated with mito-Tempo for 4 weeks; **(C)** NS309-sensitive K^{+} currents were blocked by simultaneous co-application of the selective SK2/SK3 blocker Apamin and SK4 blocker TRAM34. $n = 6$/group, $^{**}p < 0.01$ DM + MT vs. DM, $\#p < 0.01$ ND vs. DM. **(D,E)** Cumulative bar graph of NS309-activated currents and TRAM34 + Apamin blocked currents at +100 mV showing that was significantly increased in DM + MT MHECs compared with DM MHECs. $n = 5$/group.

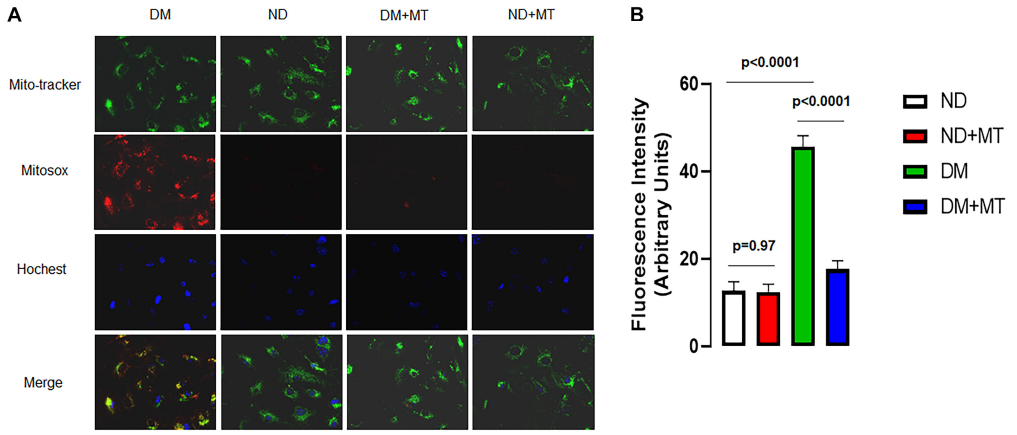

FIGURE 4 | The effects of 4-week treatment with mito-Tempo (1 mg/kg/day) on the production of mitochondrial ROS (mROS) in the mouse heart endothelial cells (MHECs) from diabetic (DM) and non-diabetic (ND) mice, **(A)** MHECs were loaded with mitochondrial marker mitotracker (green) and mROS marker (red), and Hochest 33342 (blue); **(B)** bar graph showing the analysis of fluorescence intensity (mROS signals) in the experimental groups. *n* = 4/group.
DM + mito-Tempo = diabetic mice treated with mito-Tempo for 4 weeks, ND + mito-Tempo = non-diabetic mice treated with mito-Tempo for 4 weeks.

There are several novel findings in the current study. First, chronic treatment with mito-Tempo in mice *in vivo* caused significant reduction in coronary endothelial mROS, and improved coronary endothelial function as demonstrated by enhanced coronary relaxation response to endothelium-dependent vasodilator ADP. Second, chronic treatment with mito-Tempo *in vivo* significantly increased the relaxation response of diabetic coronary vasculature by the selective SK activator NS309. Third, chronic treatment with mito-Tempo improved SK current activity of MHECs in the diabetic mice. Finally, chronically treating the healthy mice with mito-Tempo did not affect coronary endothelial function and SK channel activity, suggesting that mROS play little role during normal condition. This finding was confirmed by the results that there were few endothelial mROS tested in the normal MHECs in mice without diabetes. Under physiological condition, endothelial cells largely depend on cytosolic glycolysis for generation of ATP and for its energy supply, which does occur in the mitochondria.

Endothelial cells release endothelium-derived relaxing factors (EDRF), such as NO, prostacyclin (PGI_2), endothelium-dependent hyperpolarizing factors (EDHF) (Vanhoutte and Shimokawa, 1989; Feletou and Vanhoutte, 2009). SK channels are largely responsible for coronary arteriolar relaxation mediated by EDHF (Vanhoutte and Shimokawa, 1989; Feletou and Vanhoutte, 2009). Previous studies have demonstrated that ADP induced coronary vasodilation is endothelium- and NO-dependent (Vanhoutte and Shimokawa, 1989; Myers et al., 1992; Faraci et al., 2004). Inhibition of mROS with mito-Tempo in the diabetic mice improved coronary relaxation in response ADP, suggesting that mito-Tempo may potentiate endothelial eNOS coupling. In addition, we and others have observed that the selective SK activator NS309 induced coronary dilation partially via NO signaling pathway (Sheng et al., 2009; Dalsgaard et al., 2010; Zhang et al., 2020), suggesting that there is potential cross-talk between NO and EDHF in the endothelium. It can be assumed that mito-Tempo treatment may augment the cross talk between NO and EDHF in the endothelium leading to NS309-enhancemenet of coronary dilatation and SK channel activation in the diabetic mice.

Compelling evidences suggest that diabetes and hyperglycemia inhibits large-conductance Ca^{2+}-activated K^+ channel (BK) and voltage-gated K^+ channel (Kv) function on vascular smooth muscle cells (Liu et al., 2001; Lu et al., 2006). This effect is mediated by direct oxidation of key cysteine residues in the bowl region of this channel (Tang et al., 2004; Lu et al., 2006), inhibition of Akt signaling, facilitation of the FOXO-3a/FBXO-dependent BK-β1 degradation (Lu et al., 2006, 2012), and other oxidation of vascular K^+ channels, such as peroxynitrite (Liu et al., 2002; Cheng et al., 2011). However, mechanisms responsible for diabetic downregulation of endothelial SK channels are still largely unknown. A recent study also indicates that diabetic oxidation and nitration of endothelial SK channels may be one of the potential mechanisms (Cheng et al., 2018). Interesting, we recently observed that diabetic dysregulation of pyridine nucleotide NADH may also contribute to the inactivation of coronary endothelial SK channels (Liu et al., 2020). Furthermore, the enhancement of antioxidant enzyme expression in the diabetic heart may account for endothelial protective effects of chronic mROS inhibition.

However, some studies suggested that ROS or H_2O_2 may be some of EDHFs contributing to the maintenance of vascular relaxation in settings of metabolic syndrome. Acute administration of H_2O_2 (high dose) can cause vasodilation, whereas catalase can block H_2O_2 induced vasodilation (Matoba et al., 2002; Hatoum et al., 2005). This discrepancy between the previous studies and the current findings may be due to the animal models used in the studies; that is acute metabolic syndrome versus chronic diabetes. Thus, the data suggest that persistent overproduction of ROS is detrimental for coronary endothelial function during chronic hyperglycemia or chronic diabetes.

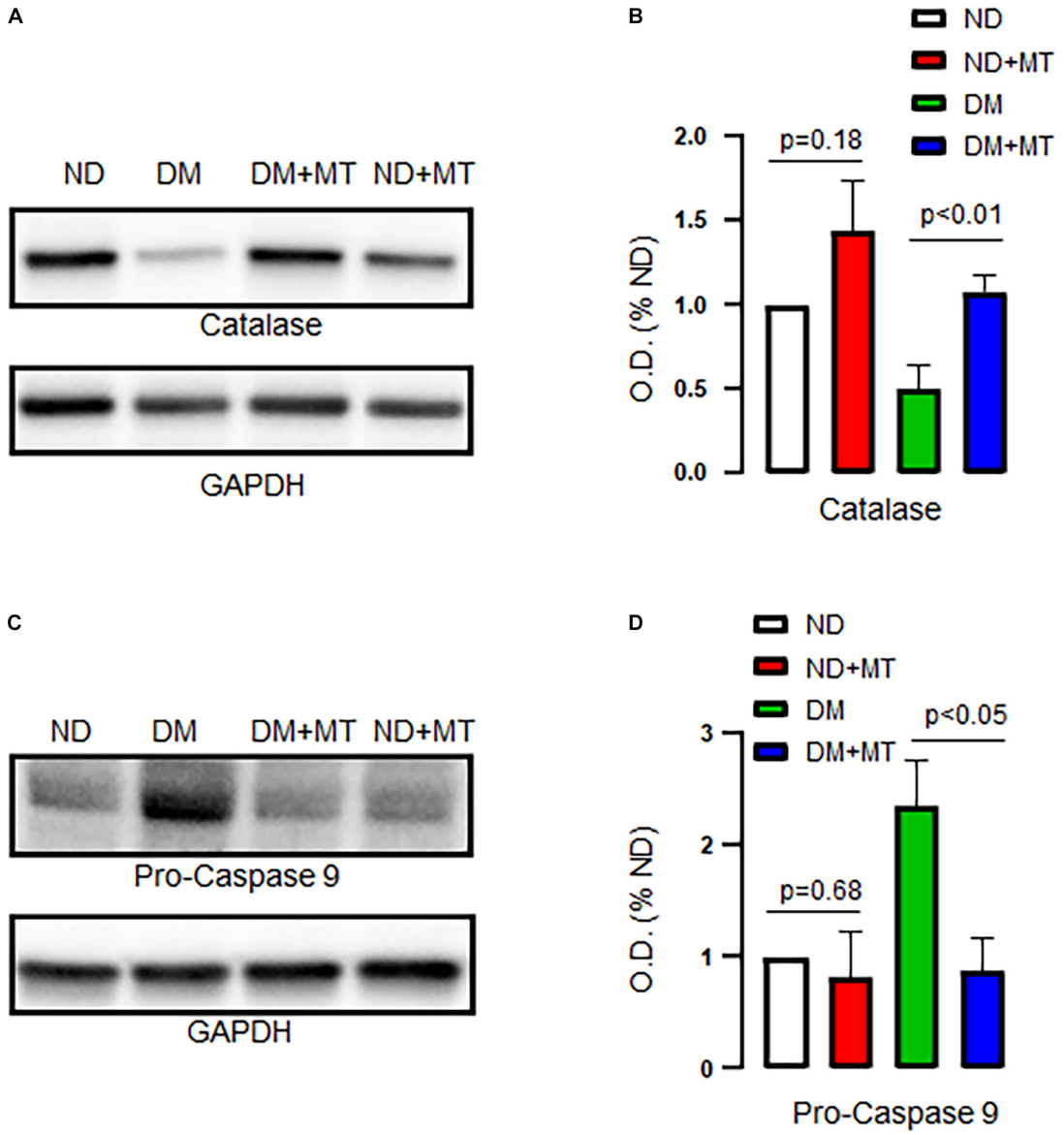

FIGURE 5 | Effects of chronic treatment with mito-Tempo (MT) on catalase and pro-caspase 9 in ND and DM heart tissue samples. **(A)** Representative immunoblots for catalase. **(B)** Densitometric analysis of signal intensity in the catalase protein expression of heart tissue samples in DM and ND mice treated with or without mito-Tempo; DM + MT = diabetic mice treated with mito-Tempo for 4 weeks, ND + MT = non-diabetic mice treated with mito-Tempo for 4 weeks; *n* = 6/group; **(C)** Representative immunoblots of ECs for pro-caspase 9. **(D)** Densitometric analysis of signal intensity in the pro-caspase 9 protein expression of heart tissue samples in DM and ND mice after chronic treatment with mito-Tempo. *n* = 6/group.

There are still some limitations in the current study. For example, we did not measure SK protein expression in the mouse heart after mito-Tempo treatment. It has been established that SK2, SK3, and SK4 are predominantly expressed in the mouse heart (Tuteja et al., 2005). SK2 and SK3 mainly present in the cardiomyocytes, whereas SK3 and SK4 (IK) in the endothelial cells. We have recently observed that there were no significant differences in protein expression of SK3 and SK4 between ND and DM MHECs (Zhang et al., 2020) or between patients with ND and patients with DM in the atrial myocardium/coronary endothelial cells, (Liu et al., 2015, 2018, 2020) suggesting that DM may affect endothelial SK gating or trafficking instead of the total protein levels. However, we did not conclusively distinguish the effects of diabetes and mito-Tempo on SK expression in the mouse heart endothelial and cardiomyocytes in the current study.

This is the first study to observe that the activation of endothelial SK channels may contribute to mROS inhibition-induced protection of coronary endothelial function/relaxation. Our study strongly suggests that persistent over-production mROS causes coronary endothelial dysfunction and chronic inhibition of mROS may provide therapeutic effects on diabetic complications.

DATA AVAILABILITY STATEMENT

The raw data supporting the conclusions of this article will be made available by the authors, without undue reservation.

ETHICS STATEMENT

The animal study was reviewed and approved by the Institutional Animal Care and Use Committee of the Rhode Island Hospital.

AUTHOR CONTRIBUTIONS

HX carried out ion channel recoding experiments, all the data analysis, and draft the primary manuscript. ZZ, YS, and YL performed animal handling, *in vitro* vessel reactivity experiments and related data analysis. GS, YH, and EH performed cell culture, mROS, and protein analysis. JF, EH, and FS obtained funding, critical revision and supervised the project. All authors were involved in writing and editing the manuscript.

FUNDING

This work was supported by grants from the National Institutes of Health R01HL127072-01A1 and 1R01HL136347-01, NIGMS/NIH grant (pilot project) 1P20GM103652 to JF and core services 1P20GM103652 to EH. This work was supported in part by 3R01HL136347-04S1 to JF, R01-HL46716 to FS, and RO1HL128831 to FS.

ACKNOWLEDGMENTS

The authors thank Julie Braza of the COBRE-Core Facility at Ocean State Research Institute, Providence VA Medical Center for the assistance in endothelial cell isolation/culture.

SUPPLEMENTARY MATERIAL

The Supplementary Material for this article can be found online at: https://www.frontiersin.org/articles/10.3389/fcell.2021.643810/full#supplementary-material

REFERENCES

Baynes, J. W. (1991). Role of oxidative stress in development of complications in diabetes. *Diabetes* 40, 405–412. doi: 10.2337/diabetes.40.4.405

Burnham, M. P., Johnson, I. T., and Weston, A. H. (2006). Impaired small-conductance Ca2+-activated K+ channel-dependent EDHF responses in Type II diabetic ZDF rats. *Br. J. Pharmacol.* 148, 434–441. doi: 10.1038/sj.bjp.0706748

Chen, M. L., Zhu, X. H., Ran, L., Lang, H. D., Yi, L., and Mi, M. T. (2017). Trimethylamine-N-Oxide induces vascular inflammation by activating the NLRP3 inflammasome through the SIRT3-SOD2-mtROS signaling pathway. *J. Am. Heart Assoc.* 6:e006347. doi: 10.1161/JAHA.117.006347

Cheng, Z., Jiang, X., Kruger, W. D., Pratico, D., Gupta, S., Mallilankaraman, K., et al. (2011). Hyperhomocysteinemia impairs endothelium-derived hyperpolarizing factor-mediated vasorelaxation in transgenic cystathionine beta synthase-deficient mice. *Blood* 118, 1998–2006. doi: 10.1182/blood-2011-01-333310

Cheng, Z., Shen, X., Jiang, X., Shan, H., Cimini, M., Fang, P., et al. (2018). Hyperhomocysteinemia potentiates diabetes-impaired EDHF-induced vascular relaxation: role of insufficient hydrogen sulfide. *Redox Biol.* 16, 215–225. doi: 10.1016/j.redox.2018.02.006

Cho, Y. E., Basu, A., Dai, A., Heldak, M., and Makino, A. (2013). Coronary endothelial dysfunction and mitochondrial reactive oxygen species in type 2 diabetic mice. *Am. J. Physiol. Cell Physiol.* 305, C1033–C1040. doi: 10.1152/ajpcell.00234.2013

Dalsgaard, T., Kroigaard, C., Misfeldt, M., Bek, T., and Simonsen, U. (2010). Openers of small conductance calcium-activated potassium channels selectively enhance NO-mediated bradykinin vasodilatation in porcine retinal arterioles. *Br. J. Pharmacol.* 160, 1496–1508. doi: 10.1111/j.1476-5381.2010.00803.x

Ding, H., Hashem, M., Wiehler, W. B., Lau, W., Martin, J., Reid, J., et al. (2005). Endothelial dysfunction in the streptozotocin-induced diabetic apoE-deficient mouse. *Br. J. Pharmacol.* 146, 1110–1118. doi: 10.1038/sj.bjp.0706417

Emani, S., Ramlawi, B., Sodha, N. R., Li, J., Bianchi, C., and Sellke, F. W. (2009). Increased vascular permeability after cardiopulmonary bypass in patients with diabetes is associated with increased expression of vascular endothelial growth factor and hepatocyte growth factor. *J. Thorac. Cardiovasc. Surg.* 138, 185–191. doi: 10.1016/j.jtcvs.2008.12.024

Faraci, F. M., Lynch, C., and Lamping, K. G. (2004). Responses of cerebral arterioles to ADP: eNOS-dependent and eNOS-independent mechanisms. *Am. J. Physiol. Heart Circ. Physiol.* 287, H2871–H2876. doi: 10.1152/ajpheart.00392.2004

Feletou, M., and Vanhoutte, P. M. (2009). EDHF: an update. *Clin. Sci.* 117, 139–155. doi: 10.1042/CS20090096

Feng, J., Anderson, K., Singh, A. K., Ehsan, A., Mitchell, H., Liu, Y., et al. (2017). Diabetes upregulation of cyclooxygenase 2 contributes to altered coronary reactivity after cardiac surgery. *Ann. Thorac. Surg.* 104, 568–576. doi: 10.1016/j.athoracsur.2016.11.025

Feng, J., Chu, L. M., Dobrilovic, N., Liu, Y., Singh, A. K., and Sellke, F. W. (2012a). Decreased coronary microvascular reactivity after cardioplegic arrest in patients with uncontrolled diabetes mellitus. *Surgery* 152, 262–269. doi: 10.1016/j.surg.2012.04.009

Feng, J., Liu, Y., Chu, L. M., Singh, A. K., Dobrilovic, N., Fingleton, J. G., et al. (2012b). Changes in microvascular reactivity after cardiopulmonary bypass in patients with poorly controlled versus controlled diabetes. *Circulation* 126(11 Suppl. 1), S73–S80. doi: 10.1161/CIRCULATIONAHA.111.084590

Feng, J., Liu, Y., Clements, R. T., Sodha, N. R., Khabbaz, K. R., Senthilnathan, V., et al. (2008). Calcium-activated potassium channels contribute to human coronary microvascular dysfunction after cardioplegic arrest. *Circulation* 118(14 Suppl.), S46–S51. doi: 10.1161/CIRCULATIONAHA.107.755827

Feng, J., Liu, Y., Khabbaz, K. R., Hagberg, R., Robich, M. P., Clements, R. T., et al. (2011). Decreased contractile response to endothelin-1 of peripheral microvasculature from diabetic patients. *Surgery* 149, 247–252. doi: 10.1016/j.surg.2010.07.003

Galkin, I. I., Pletjushkina, O. Y., Zinovkin, R. A., Zakharova, V. V., Birjukov, I. S., Chernyak, B. V., et al. (2014). Mitochondria-targeted antioxidants prevent TNFalpha-induced endothelial cell damage. *Biochemistry* 79, 124–130. doi: 10.1134/S0006297914020059

Graham, D., Huynh, N. N., Hamilton, C. A., Beattie, E., Smith, R. A., Cocheme, H. M., et al. (2009). Mitochondria-targeted antioxidant MitoQ10 improves endothelial function and attenuates cardiac hypertrophy. *Hypertension* 54, 322–328. doi: 10.1161/HYPERTENSIONAHA.109.130351

Haffner, S. M., Lehto, S., Ronnemaa, T., Pyorala, K., and Laakso, M. (1998). Mortality from coronary heart disease in subjects with type 2 diabetes and in nondiabetic subjects with and without prior myocardial infarction. *N. Engl. J. Med.* 339, 229–234. doi: 10.1056/NEJM199807233390404

Hatoum, O. A., Binion, D. G., Miura, H., Telford, G., Otterson, M. F., and Gutterman, D. D. (2005). Role of hydrogen peroxide in ACh-induced dilation of human submucosal intestinal microvessels. *Am. J. Physiol. Heart Circ. Physiol.* 288, H48–H54. doi: 10.1152/ajpheart.00663.2004

Ismail-Beigi, F., Craven, T., Banerji, M. A., Basile, J., Calles, J., Cohen, R. M., et al. (2010). Effect of intensive treatment of hyperglycaemia on microvascular

outcomes in type 2 diabetes: an analysis of the ACCORD randomised trial. *Lancet* 376, 419–430. doi: 10.1016/S0140-6736(10)60576-4

Kizhakekuttu, T. J., Wang, J., Dharmashankar, K., Ying, R., Gutterman, D. D., Vita, J. A., et al. (2012). Adverse alterations in mitochondrial function contribute to type 2 diabetes mellitus-related endothelial dysfunction in humans. *Arterioscler. Thromb. Vasc. Biol.* 32, 2531–2539. doi: 10.1161/ATVBAHA.112.256024

Leo, C. H., Hart, J. L., and Woodman, O. L. (2011). Impairment of both nitric oxide-mediated and EDHF-type relaxation in small mesenteric arteries from rats with streptozotocin-induced diabetes. *Br. J. Pharmacol.* 162, 365–377. doi: 10.1111/j.1476-5381.2010.01023.x

Li, J. M., and Shah, A. M. (2004). Endothelial cell superoxide generation: regulation and relevance for cardiovascular pathophysiology. *Am. J. Physiol. Regul. Integr. Comp. Physiol.* 287, R1014–R1030. doi: 10.1152/ajpregu.00124.2004

Liu, Y., Cole, V., Lawandy, I., Ehsan, A., Sellke, F. W., and Feng, J. (2018). Decreased coronary arteriolar response to KCa channel opener after cardioplegic arrest in diabetic patients. *Mol. Cell. Biochem.* 445, 187–194. doi: 10.1007/s11010-017-3264-x

Liu, Y., Kabakov, A. Y., Xie, A., Shi, G., Singh, A. K., Sodha, N. R., et al. (2020). Metabolic regulation of endothelial SK channels and human coronary microvascular function. *Int. J. Cardiol.* 312, 1–9. doi: 10.1016/j.ijcard.2020.03.028

Liu, Y., Sellke, E. W., Feng, J., Clements, R. T., Sodha, N. R., Khabbaz, K. R., et al. (2008). Calcium-activated potassium channels contribute to human skeletal muscle microvascular endothelial dysfunction related to cardiopulmonary bypass. *Surgery* 144, 239–244. doi: 10.1016/j.surg.2008.03.032

Liu, Y., Terata, K., Chai, Q., Li, H., Kleinman, L. H., and Gutterman, D. D. (2002). Peroxynitrite inhibits Ca2+-activated K+ channel activity in smooth muscle of human coronary arterioles. *Circ. Res.* 91, 1070–1076. doi: 10.1161/01.res.0000046003.14031.98

Liu, Y., Terata, K., Rusch, N. J., and Gutterman, D. D. (2001). High glucose impairs voltage-gated K(+) channel current in rat small coronary arteries. *Circ. Res.* 89, 146–152. doi: 10.1161/hh1401.093294

Liu, Y., Xie, A., Singh, A. K., Ehsan, A., Choudhary, G., Dudley, S., et al. (2015). Inactivation of endothelial small/intermediate conductance of calcium-activated potassium channels contributes to coronary arteriolar dysfunction in diabetic patients. *J. Am. Heart Assoc.* 4:e002062. doi: 10.1161/JAHA.115.002062

Lu, T., Chai, Q., Yu, L., d'Uscio, L. V., Katusic, Z. S., He, T., et al. (2012). Reactive oxygen species signaling facilitates FOXO-3a/FBXO-dependent vascular BK channel beta1 subunit degradation in diabetic mice. *Diabetes* 61, 1860–1868. doi: 10.2337/db11-1658

Lu, T., He, T., Katusic, Z. S., and Lee, H. C. (2006). Molecular mechanisms mediating inhibition of human large conductance Ca2+-activated K+ channels by high glucose. *Circ. Res.* 99, 607–616. doi: 10.1161/01.RES.0000243147.41792.93

Makino, A., Ohuchi, K., and Kamata, K. (2000). Mechanisms underlying the attenuation of endothelium-dependent vasodilatation in the mesenteric arterial bed of the streptozotocin-induced diabetic rat. *Br. J. Pharmacol.* 130, 549–556. doi: 10.1038/sj.bjp.0703354

Matoba, T., Shimokawa, H., Kubota, H., Morikawa, K., Fujiki, T., Kunihiro, I., et al. (2002). Hydrogen peroxide is an endothelium-derived hyperpolarizing factor in human mesenteric arteries. *Biochem. Biophys. Res. Commun.* 290, 909–913. doi: 10.1006/bbrc.2001.6278

Myers, P. R., Guerra, R. Jr., and Harrison, D. G. (1992). Release of multiple endothelium-derived relaxing factors from porcine coronary arteries. *J. Cardiovasc. Pharmacol.* 20, 392–400. doi: 10.1097/00005344-199209000-00008

O'Malley, Y., Fink, B. D., Ross, N. C., Prisinzano, T. E., and Sivitz, W. I. (2006). Reactive oxygen and targeted antioxidant administration in endothelial cell mitochondria. *J. Biol. Chem.* 281, 39766–39775. doi: 10.1074/jbc.M608268200

Park, J. B., Nagar, H., Choi, S., Jung, S. B., Kim, H. W., Kang, S. K., et al. (2016). IDH2 deficiency impairs mitochondrial function in endothelial cells and endothelium-dependent vasomotor function. *Free Radic. Biol. Med.* 94, 36–46. doi: 10.1016/j.freeradbiomed.2016.02.017

Sada, K., Nishikawa, T., Kukidome, D., Yoshinaga, T., Kajihara, N., Sonoda, K., et al. (2016). Hyperglycemia induces cellular hypoxia through production of mitochondrial ROS followed by suppression of Aquaporin-1. *PLoS One* 11:e0158619. doi: 10.1371/journal.pone.0158619

Sheng, J. Z., Ella, S., Davis, M. J., Hill, M. A., and Braun, A. P. (2009). Openers of SKCa and IKCa channels enhance agonist-evoked endothelial nitric oxide synthesis and arteriolar vasodilation. *FASEB J.* 23, 1138–1145. doi: 10.1096/fj.08-120451

Shenouda, S. M., Widlansky, M. E., Chen, K., Xu, G., Holbrook, M., Tabit, C. E., et al. (2011). Altered mitochondrial dynamics contributes to endothelial dysfunction in diabetes mellitus. *Circulation* 124, 444–453. doi: 10.1161/CIRCULATIONAHA.110.014506

Shi, Y., and Vanhoutte, P. M. (2009). Reactive oxygen-derived free radicals are key to the endothelial dysfunction of diabetes. *J. Diabetes* 1, 151–162. doi: 10.1111/j.1753-0407.2009.00030.x

Si, H., Heyken, W. T., Wolfle, S. E., Tysiac, M., Schubert, R., Grgic, I., et al. (2006). Impaired endothelium-derived hyperpolarizing factor-mediated dilations and increased blood pressure in mice deficient of the intermediate-conductance Ca2+-activated K+ channel. *Circ. Res.* 99, 537–544. doi: 10.1161/01.RES.0000238377.08219.0c

Srinivasan, S., Spear, J., Chandran, K., Joseph, J., Kalyanaraman, B., and Avadhani, N. G. (2013). Oxidative stress induced mitochondrial protein kinase A mediates cytochrome c oxidase dysfunction. *PLoS One* 8:e77129. doi: 10.1371/journal.pone.0077129

Szczesny, B., Modis, K., Yanagi, K., Coletta, C., Le Trionnaire, S., Perry, A., et al. (2014). AP39, a novel mitochondria-targeted hydrogen sulfide donor, stimulates cellular bioenergetics, exerts cytoprotective effects and protects against the loss of mitochondrial DNA integrity in oxidatively stressed endothelial cells in vitro. *Nitric Oxide* 41, 120–130. doi: 10.1016/j.niox.2014.04.008

Tang, X. D., Garcia, M. L., Heinemann, S. H., and Hoshi, T. (2004). Reactive oxygen species impair Slo1 BK channel function by altering cysteine-mediated calcium sensing. *Nat. Struct. Mol. Biol.* 11, 171–178. doi: 10.1038/nsmb725

Tuteja, D., Xu, D., Timofeyev, V., Lu, L., Sharma, D., Zhang, Z., et al. (2005). Differential expression of small-conductance Ca^{2+}-activated K^{+} channels SK1, SK2, and SK3 in mouse atrial and ventricular myocytes. *Am. J. Physiol. Heart Circ. Physiol.* 289, H2714–H2723. doi: 10.1152/ajpheart.00534.2005

Vanhoutte, P. M., and Shimokawa, H. (1989). Endothelium-derived relaxing factor and coronary vasospasm. *Circulation* 80, 1–9. doi: 10.1161/01.cir.80.1.1

Wilson, P. W., D'Agostino, R. B., Parise, H., Sullivan, L., and Meigs, J. B. (2005). Metabolic syndrome as a precursor of cardiovascular disease and type 2 diabetes mellitus. *Circulation* 112, 3066–3072. doi: 10.1161/CIRCULATIONAHA.105.539528

Zhang, Z., Shi, G., Liu, Y., Xing, H., Kabakov, A. Y., Zhao, A. S., et al. (2020). Coronary endothelial dysfunction prevented by small-conductance calcium-activated potassium channel activator in mice and patients with diabetes. *J. Thorac. Cardiovasc. Surg.* 160, e263–e280. doi: 10.1016/j.jtcvs.2020.01.078

Conflict of Interest: The authors declare that the research was conducted in the absence of any commercial or financial relationships that could be construed as a potential conflict of interest.

Copyright © 2021 Xing, Zhang, Shi, He, Song, Liu, Harrington, Sellke and Feng. This is an open-access article distributed under the terms of the Creative Commons Attribution License (CC BY). The use, distribution or reproduction in other forums is permitted, provided the original author(s) and the copyright owner(s) are credited and that the original publication in this journal is cited, in accordance with accepted academic practice. No use, distribution or reproduction is permitted which does not comply with these terms.

frontiers in Cell and Developmental Biology

ORIGINAL RESEARCH
published: 22 February 2021
doi: 10.3389/fcell.2021.634242

Mitogen-Inducible Gene 6 Inhibits Angiogenesis by Binding to SHC1 and Suppressing Its Phosphorylation

Lixian Liu, Liying Xing, Rongyuan Chen, Jianing Zhang, Yuye Huang, Lijuan Huang, Bingbing Xie, Xiangrong Ren, Shasha Wang, Haiqing Kuang, Xianchai Lin, Anil Kumar, Jong Kyong Kim, Chunsik Lee and Xuri Li**

State Key Laboratory of Ophthalmology, Zhongshan Ophthalmic Center, Sun Yat-sen University, Guangzhou, China

The mitogen-inducible gene 6 (MIG6) is an adaptor protein widely expressed in vascular endothelial cells. However, it remains unknown thus far whether it plays a role in angiogenesis. Here, using comprehensive *in vitro* and *in vivo* model systems, we unveil a potent anti-angiogenic effect of MIG6 in retinal development and neovascularization and the underlying molecular and cellular mechanisms. Loss of function assays using genetic deletion of *Mig6* or siRNA knockdown increased angiogenesis *in vivo* and *in vitro*, while MIG6 overexpression suppressed pathological angiogenesis. Moreover, we identified the cellular target of MIG6 by revealing its direct inhibitory effect on vascular endothelial cells (ECs). Mechanistically, we found that the anti-angiogenic effect of MIG6 is fulfilled by binding to SHC1 and inhibiting its phosphorylation. Indeed, SHC1 knockdown markedly diminished the effect of MIG6 on ECs. Thus, our findings show that MIG6 is a potent endogenous inhibitor of angiogenesis that may have therapeutic value in anti-angiogenic therapy.

Keywords: MIG6, angiogenesis, SHC1, endothelial cell, ocular neovascularization

OPEN ACCESS

Edited by:
Bin Ren,
University of Alabama at Birmingham,
United States

Reviewed by:
Jack Lawler,
Beth Israel Deaconess Medical Center and Harvard Medical School,
United States
Qiulun Lu,
Nanjing Medical University, China
Biao Yan,
Fudan University, China

****Correspondence:***
Xuri Li
lixr6@mail.sysu.edu.cn
Chunsik Lee
chunsik@mail.sysu.edu.cn

Specialty section:
This article was submitted to Signaling, a section of the journal Frontiers in Cell and Developmental Biology

Received: *27 November 2020*
Accepted: *05 February 2021*
Published: *22 February 2021*

Citation:
Liu L, Xing L, Chen R, Zhang J, Huang Y, Huang L, Xie B, Ren X, Wang S, Kuang H, Lin X, Kumar A, Kim JK, Lee C and Li X (2021) Mitogen-Inducible Gene 6 Inhibits Angiogenesis by Binding to SHC1 and Suppressing Its Phosphorylation. Front. Cell Dev. Biol. 9:634242. doi: 10.3389/fcell.2021.634242

INTRODUCTION

The blood vessel network is vital for both normal physiology and numerous diseases. Blood vessels not only transport oxygen and nutrient to tissues and cells required for their functions and maintenance, they also have unique functions by serving as a regulator of vascular tone, organ development, immunity, and blood-organ communication (Karaman et al., 2018; Li and Carmeliet, 2018). However, uncontrolled growth of new blood vessel can result in life-threatening pathologies, such as cancer and many other neovascular diseases (Apte et al., 2019; Li et al., 2019). Angiogenesis therefore needs to be tightly controlled to avoid overproduction of blood vessels. Currently, the majority of the studies have focused on angiogenic factors. Much knowledge in this aspect has been gained and anti-angiogenic therapies targeting angiogenic factors, such as VEGF, have been used to treat patients with neovascular diseases (Apte et al., 2019). However, despite the great success, drug resistance can develop over time, suggesting the involvement of multiple factors and pathways, such as genetic instability of tumor cells that up-regulates pro-angiogenic factors to overcome the inhibitor (Ribatti, 2016; Haibe et al., 2020). Given the presence of diverse and abundant angiogenic factors, endogenous anti-angiogenic factors would be constantly required to keep the angiogenic factors in check but less is known in this aspect. Indeed, decreased or the lack of the expression of anti-angiogenic factors may often be the reason of pathological neovascularization (Murugeswari et al., 2008; Zhang et al., 2020). Studying such endogenous anti-angiogenic molecules is therefore of critical importance.

MIG6 is a ubiquitously expressed cytoplasmic adaptor protein that modulates many cell surface receptors (Zhang and Vande Woude, 2007; Sasaki et al., 2018). MIG6 is involved in diverse biological events, including suppressing the epidermal growth factor receptor (EGFR) pathway (Ferby et al., 2006; Zhang and Vande Woude, 2007; Park et al., 2015). However, MIG6 has many EGFR-independent functions. For example, MIG6 induces cell cycle arrest in an EGFR-independent manner (Sasaki et al., 2018). MIG6 is widely expressed in various types of cells and tissues (Jin et al., 2007; Zhang and Vande Woude, 2007; Anastasi et al., 2016), including the vascular system (Jin et al., 2009; Lee et al., 2014). The expression of MIG6 is rapidly induced by various growth factors and cellular stresses under pathological conditions (Zhang and Vande Woude, 2007). However, it remains thus far unknown whether it plays a role in angiogenesis.

Here, we utilized both knockout mice and cultured endothelial cells and examined the effect of MIG6 on angiogenesis. We found that MIG6 is a potent endogenous inhibitor of angiogenesis. Genetic deletion of *Mig6* increased retinal angiogenesis in mice, and its overexpression inhibited hypoxia-induced retinal neovascularization. Overexpression of MIG6 reduced aortic and choroidal microvessel growth, and suppressed endothelial cell proliferation, migration and sprouting. Mechanistically, we show that the anti-angiogenic effect of MIG6 is exerted by inhibiting SHC1 signaling. Our thus findings reveal a new function for MIG6 as an endogenous inhibitor of angiogenesis, which may have implications in anti-angiogenic therapy.

MATERIALS AND METHODS

Mice

All animal experiments were approved by the Animal Use and Care Committee of Zhongshan Ophthalmic Center, Sun Yat-sen University (2015-098). The *Mig6* knockout mice were kindly provided by Dr. George Vande Woude at Van Andel Institute (Grand Rapids, MI, USA). *Mig6* knockout mice used for experiments were bred on C57Bl/6J background for more than six generations and littermates were used for experiments.

Cell Culture and Reagents

The primary human retinal endothelial cells (HREC) were purchased from Angio-Proteomie (Boston, MA, USA) and cultured in endothelial cell medium (ScienCell Research, Carlsbad, CA, USA) containing endothelial cell growth supplement (ECGS), 5% FCS, and penicillin/streptomycin. HREC within 8 passages were used for experiments.

Retinopathy of Prematurity (ROP) Mouse Model

C57Bl6J mice at post-natal day 7 (P7) were exposed to 75% oxygen for 5 days, after which the mice were intravitreally injected with 1 μl of adenovirus expressing GFP (Ad-GFP, CV10001, 1.0×10^{13} pfu/ml, Vigene Biosciences, Rockville, MD, USA) or adenovirus expressing human MIG6 (Ad-MIG6, VH894726, 1.0×10^{13} pfu/ml, Vigene Biosciences, Rockville, MD, USA), and then returned to normoxia for additional 5 days. Mouse eyes were collected at P17 and the retinal neovascularization areas were analyzed using whole mount retinae stained with IB4-Alexa 488 (I21411, Invitrogen, Waltham, MA, USA). Neovascularization areas were outlined and quantified as the percentage of the total area of the retina using ImageJ (NIH, Bethesda, MD, USA).

Isolation and Culture of Murine Primary Vascular Endothelial Cells

Murine primary endothelial cells were isolated from lungs of 6-week old mice. Lungs were harvested and digested with collagenase type I (17100017, ThermoFisher Scientific, Waltham, MA, USA). The digested tissues were pelleted and resuspended in PBS with 0.1% BSA and incubated with rat anti-mouse CD31 conjugated Dynabeads at room temperature for 15 min. The bead-bound cells were recovered using a magnetic separator and resuspended in complete culture medium (DMEM containing 20% FBS, supplemented with 100 μg/ml heparin, 100 μg/ml ECGS, non-essential amino acids, L-glutamine and antibiotics). Primary ECs within 3 passages were used for experiments.

siRNA Knockdown and Adenovirus Infection of Endothelial Cells

For siRNA knockdown, ECs were transfected with human MIG6 siRNA (5′-CUACACUUUCUGAUUUCAA-3′) (Liu et al., 2012), human SHC1 siRNA (5′ CUACUUGGUUCGGUACAUGGG-3′) (Lundgren et al., 2006), or non-targeting scrambled negative control (Ribobio, Guangzhou, China) using ESCORT III (L3037, Sigma). For adenoviral infection, ECs were infected with Ad-MIG6 or Ad-GFP at an MOI of 10 for 48 h.

Antibodies

Antibodies used in Western blots were as the following: anti-β-actin (A5316, Sigma), anti-tubulin (T6734, Sigma), anti-MIG6 (WH0054206M1, Sigma), anti-pTyr239/240 SHC1 (2434, Cell Signaling), anti-SHC1 (610878, BD Bioscience), anti-phospho-p44/42 MAPK (9101, Cell Signaling), anti-p44/42 MAPK (9102, Cell Signaling), anti-GST (2625, Cell Signaling), and anti-HA tag (A01244, GenScript). Immunoreactivity was detected using horseradish-peroxidase (HRP)-conjugated secondary antibody (RAG0072 for anti-rabbit, GAM0072 for anti-mouse, 1:5,000 dilution, Multi Sciences, Hangzhou, China).

Construction of SHC1 Deletion Mutants

The cDNA encoding human SHC1 in pcDNA 3.1 (+) vector was obtained from GenScript (Piscataway, NJ, USA) and subcloned into a pLV-3xHA vector (Inovogen, Chongqing, China). The deletion mutants of SHC1 ΔPTB (deletion of amino acids 30–210 corresponding to protein tyrosine binding domain), ΔPro-rich (deletion of amino acids 300–366 corresponding to proline-rich domain), and ΔSH2 (deletion of amino acids 377–469 corresponding to SH2 domain) were generated using a Quickchange site-directed mutagenesis kit (Agilent Technologies) according to the manufacturer's instructions. The sequences of the oligonucleotides used to generate Shc1 mutants are as follows:

(1) ΔPTB
CCGGACTCAGATCTCGAATT (forward)
TACCCGGTAGAATTATCTAGGGATC (reverse)
(2) ΔPro-rich
ATCCAGAAGTCCGCAAACAGTCGGTGTCCATGG CTGAG (forward)
CTGTTTGCGGACTTCTGGA (reverse)
(3) ΔSH2
CTGAGCAGCTCCGAGGGGAGGAGCGGAAACTGTC TAGAGG (forward)
CTCCCCTCGGAGCTG (reverse)

The deletion mutants were verified by sequencing and expressed in 293T cells by transfection using Fugene 6 (Promega, Madison, WI, USA). Two days after transfection, pull-down assays were performed to examine the binding of MIG6.

Purification of GST Fusion Protein and Pull-Down Assays

The glutathione S-transferase (GST) fusion MIG6 protein was generated by expressing human full-length MIG6 cDNA subcloned into a pGEX-4T-1 (GE Healthcare Life Sciences) in *E. coli*. For GST-Mig6 pull-down assay, 2 μg of GST-MIG6 fusion protein was added to 30 μl of glutathione magnetic beads (L00327, GenScript) and incubated at 4°C for 2 h. The protein-bound beads were then washed three times with RIPA buffer (R0010, Solarbio, Beijing, China) and incubated with the cell lysates of 293T cells transfected with SHC1 plasmids at 4°C for overnight. The beads were then washed with RIPA buffer and subjected to Western blot analysis.

Co-immunoprecipitation of MIG6 and SHC1

HRECs were homogenized in RIPA lysis buffer with a protease and phosphatase inhibitor tablet (88668, Thermo Fisher Scientific) following EGF (50 ng/ml, PeproTech) stimulation for 30 min. The cell lysates were incubated with an anti-MIG6 antibody (sc-46167, Santa Cruz Biotechnology) for overnight at 4°C and precipitated using immobilized protein A/G plus-agarose (sc-2003, Santa Cruz Biotechnology). Immunoprecipitated protein complexes were subjected to Western blot analysis.

Cell Proliferation and Viability Assay

Cell proliferation was determined using a Click-iT EdU Imaging Kit with Alexa Fluor 594 (C10086, Invitrogen) according to the manufacturer's instruction. Images were obtained and analyzed by ImageJ. For cell viability, 5×10^3 cells of MIG6-knockdown or MIG6-overexpressing HRECs were seeded in 96-well plates. The cells were incubated for 24 h and viable cells were assessed using an MTT (3-(4,5-dimethylthiazol-2-yl)-2,5-diphenyltetrazolium bromide, CT02, Sigma) method.

Tube Formation Assay

96-well plates were coated with 50 μl/well of growth factor reduced Matrigel (356230, BD Biosciences). The plates were incubated at 37°C for 30 min to allow Matrigel to polymerize. The HRECs were suspended in serum-free endothelial medium after treatment with siMIG6 or siMIG6 + siSHC1 and subsequently plated at 10,000 cells/100 μl/well on top of Matrigel in triplicates. After 6 h, the formation of tube-like structures was taken and analyzed using ImageJ.

EC Spheroid Sprouting Assay

3.2×10^5 of HRECs (800 cells/spheroid) were trypsinized and suspended in EC medium (ScienCell Research) containing 20% methylcellulose (Methocel, M0512, Sigma). 100 μl/well of HRECs were in a round-bottom 96-well plate and incubated overnight for spheroid formation. EC spheroids were resuspended in collagen I solution (800 μl of collagen, 200 μl of 10x M199 media, 240 μl of 0.25N of NaOH, 200 μl 0.2M of HEPES, 360 μl of H_2O) and added 50 μl collagen solution in a 96-well plate and incubate at 37°C for 20 min. EC spheroids were centrifuged at 300 × g and resuspended in media after collecting from a 96-well plate. 80% Methocel (80% Methocel + 20% FBS) with collagen I solution were mixed and resuspended EC spheroids and transfer to a 96-well plate. After incubation at 37°C for 15 min, serum-free media was added on top of the gel. After 24 h, the images were obtained and the sprouts and their total length were analyzed using an ImageJ.

Aortic Ring Assay

Aorta from *Mig6* knockout mice and wild-type littermates were excised and the surrounding tissues were removed. After aortic rings were cut into pieces (1 mm in length) and were placed on the top of growth factor-reduced Matrigel (354230, Corning) in 24-well plates and incubated for 7 days. Images of individual explants were obtained using a phase-contrast microscope, and converted to binary mode using a low-pass filter and threshold transformation using ImageJ. The areas of sprouting microvessels were quantified using ImageJ.

Choroid Sprouting Assay

Mouse eyes were enucleated from wild-type and *Mig6* knockout mice. After the cornea and the lens were removed, the choroid-scleral complex was separated from the retina and cut into ∼1 × 1 mm pieces. The choroid-scleral complex was placed in growth factor-reduced Matrigel (354230, Corning) for a week. The areas of sprouting microvessels were quantified using ImageJ.

Immunofluorescence Staining and Analysis of Mouse Retinal Vasculature

The mouse retinal vascularized area of wild-type and *Mig6* knockout mice at P5 was stained using Alexa fluor 488-conjugated IB4 (I21411, Invitrogen) and anti-Erg (ab92513, Abcam) antibody. DAPI (D3571, Thermo Fisher Scientific) was used for nuclear staining. Images were acquired and the vascularized retinal areas quantified using ImageJ.

Transwell Cell Migration Assay

HRECs (7.5×10^4) in serum-free media were seeded to the upper chamber of the transwell system with 8 μm pore size (3422, Corning) for 24 h after 2 days infection with Ad-Control or Ad-MIG6. Each 50 ng/ml of either EGF (PeproTech) or VEGFA

(100-20, PeproTech) was added in the bottom chamber. After 24 h, the bottom chamber was stained with DAPI (Thermo Fisher Scientific) and images were taken to analyze. The number of migrated cells per area was quantified using ImageJ.

Statistical Analysis

Comparisons between two groups were analyzed using an unpaired or paired Student's *t*-test (two-tailed) using GraphPad Prism (GraphPad Software, La Jolla, CA, USA). Data are

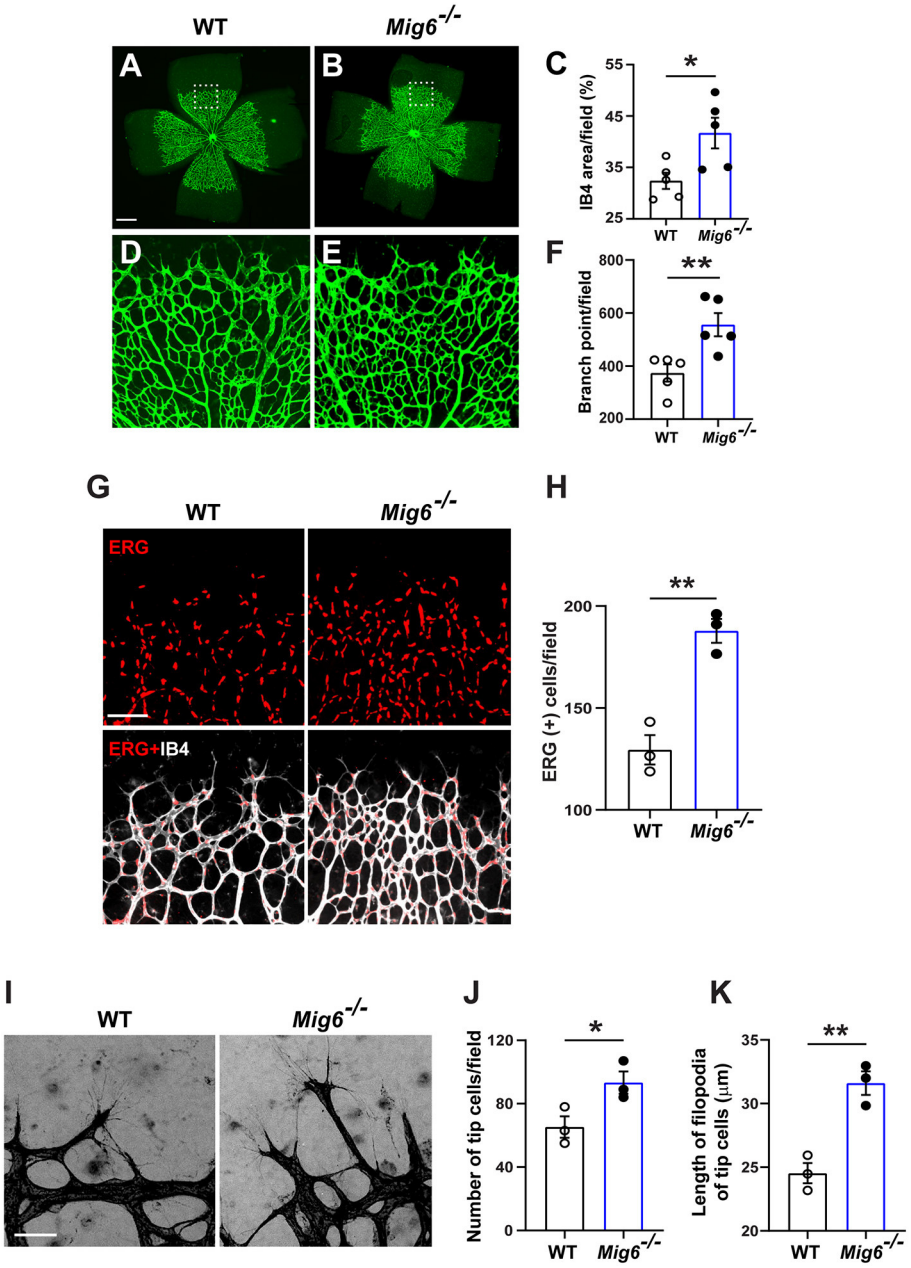

FIGURE 1 | Increased retinal angiogenesis in *Mig6* deficient mice. **(A,B)** Representative images of whole mount retinae of wild-type (WT) and *Mig6*$^{-/-}$ mice at P5 stained for IB4 (green). **(C)** Quantification of retinal blood vessel densities stained with IB4 in WT and *Mig6*$^{-/-}$ mice ($n = 5$ fields per retina). **(D,E)** Higher magnification of dotted regions in whole mount retinae of WT **(D)** and *Mig6*$^{-/-}$ **(E)** mice. **(F)** IB4 staining (green) in **(D)** and **(E)** showing more vascular branch points in the retinae of *Mig6*$^{-/-}$ mice at P5 ($n = 5$ fields per retina). **(G)** Whole mount retinae co-stained for ERG (red) and IB4 (white) to label endothelial cells in WT and *Mig6*$^{-/-}$ mice at P5. **(H)** Quantification of ERG^{+} ECs in the front of retinal vascular plexus ($n = 3$ fields per retina) in WT and *Mig6*$^{-/-}$ mice at P5. **(I)** Images of retinal blood vessel tip cells and their filopodia extensions at the angiogenic front of WT and *Mig6*$^{-/-}$ retinae at P5. **(J)** Quantification of the number of retinal blood vessel tip cells per field ($n = 3$ fields per retina) in WT and *Mig6*$^{-/-}$ mice at P5. **(K)** Measurement of the length of filopodia of tip cells per field ($n = 3$ fields per retina). Scale bars: 50 μm for **(A)** and **(I)**; 100 μm for **(G)**. Data represent mean ± SEM. * $p < 0.05$, ** $p < 0.01$ (two-tailed paired Student's *t*-test).

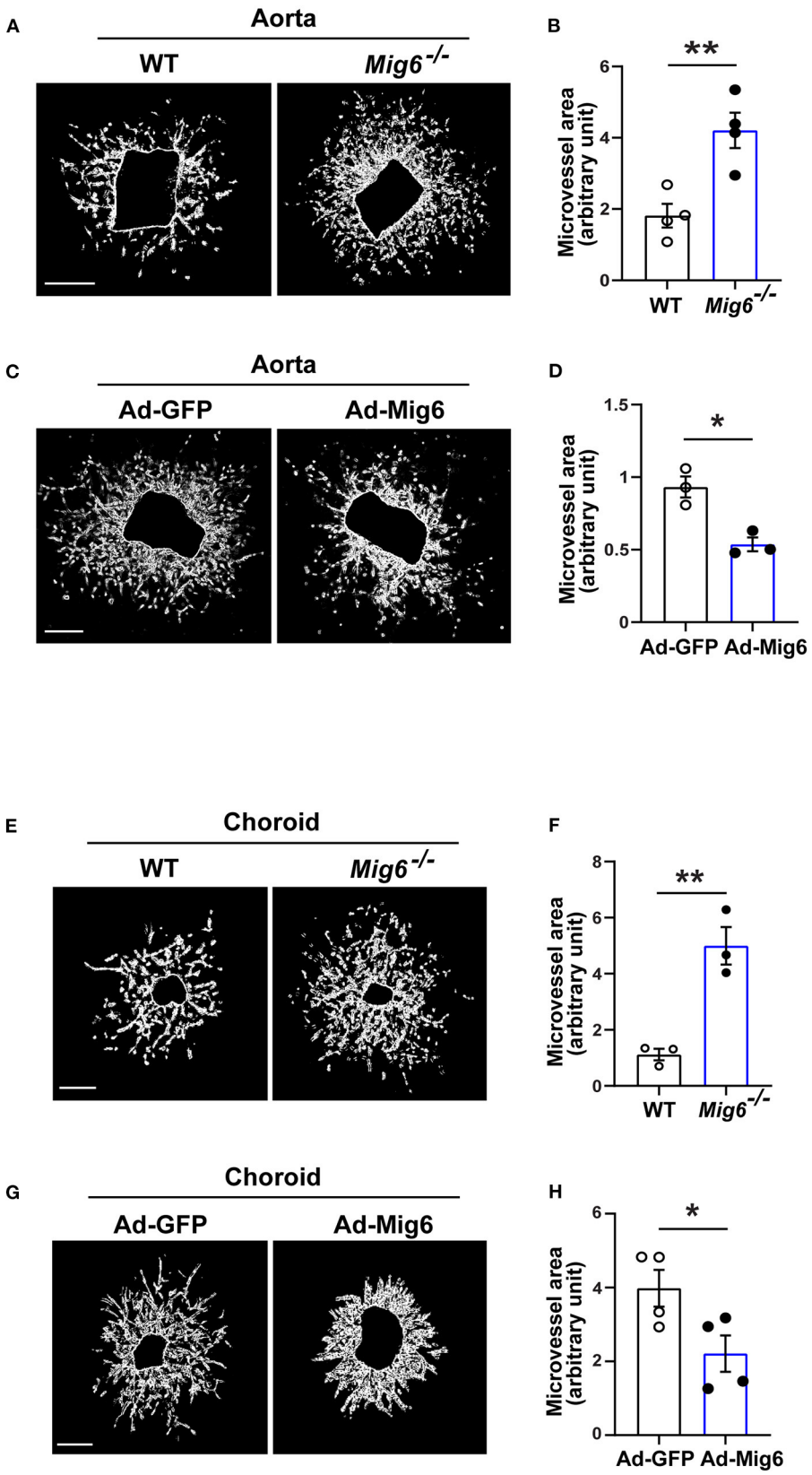

FIGURE 2 | MIG6 suppresses microvessel outgrowth. **(A)** Mouse aortic rings from WT or *Mig6*$^{-/-}$ aorta incubated for 7 days. **(B)** Quantification of vascular sprouting area per aortic ring in **(A)**. $n = 4$ aortic rings per group. **(C)** Mouse aortic rings infected with Ad-GFP or Ad-MIG6 and incubated for 7 days. **(D)** Quantification of

(Continued)

FIGURE 2 | vascular sprouting area per aortic ring in **(C)**. $n = 3$ aortic rings per group. **(E)** Mouse choroidal tissues of WT or *Mig6*$^{-/-}$ mice incubated for 7 days. **(F)** Quantification of vascular sprouting area per choroid tissue in **(E)**. $n = 3$ choroids per group. **(G)** Mouse choroidal tissues infected with Ad-GFP or Ad-MIG6 and incubated for 7 days. **(H)** Quantification of vascular sprouting area per choroid tissue in **(G)**. $n = 3$ choroids per group. Scale bars: 500 μm for **(A)**; 250 μm for **(C,E,G)**. The data are shown as the mean ± SEM from at least three independent experiments. * $p < 0.05$, ** $p < 0.01$ (two-tailed paired Student's *t*-test).

presented as mean ± SEM. $p < 0.05$ was considered statistically significant.

RESULTS

MIG6 Is Expressed in Various Types of Vascular Endothelial Cells (ECs) From Different Human Organs

To obtain insight into the expression of MIG6 in vascular endothelial cells, we searched the public database Human Protein Atlas (www.proteinatlas.org), in which the expression levels of MIG6 are derived from published single cell RNA sequencing studies. We found that MIG6 is expressed in ECs from various tissues/organs, including skin, liver, prostate, lung, heart muscle, eye, placenta, and testis (**Supplementary Table 1**), indicating a potential effect of MIG6 on ECs.

Genetic Deletion of *Mig6* Increases Retinal Angiogenesis

MIG6 has also been shown to be expressed in mouse vascular system (Zhang and Vande Woude, 2007; Jin et al., 2009). However, it remains unknown thus far whether it plays a role in angiogenesis. To address this, we evaluated vascular formation in the retinae of *Mig6* knockout mice. Isolectin B4 (IB4) staining showed that *Mig6* knockout mice displayed higher retinal blood vessel density and branch points at postnatal day 5 (P5) (**Figures 1A–F**), while no difference was found in total retinal areas (**Supplementary Figure 1A**). Immunofluorescence staining of ERG, an endothelial cell (EC) nuclear marker, revealed a higher number of ECs in the retinae of *Mig6* knockout mice (**Figures 1G,H**). Notably, more tip cells and longer filopodia extensions of tip cells, known to be critical for angiogenesis (Gerhardt et al., 2003; Ochsenbein et al., 2016), were found in the retinae of *Mig6* knockout mice (**Figures 1I–K**). Together, these findings show that loss of *Mig6* increased retinal angiogenesis.

MIG6 Inhibits Aortic and Choroidal Microvessel Growth

We next investigated whether MIG6 affected angiogenesis in other tissues. An aortic ring assay showed that gene deletion of *Mig6* significantly increased microvessel growth (**Figures 2A,B**), while MIG6 overexpression by adenovirus markedly inhibited microvessel sprouting (**Figures 2C,D**). Choroidal neovascularization is a devastating pathology that can cause blindness (Shao et al., 2013). We therefore tested whether MIG6 affected choroidal angiogenesis using a choroidal sprouting assay. We found that *Mig6* deficient choroids gave rise to more microvessels than those of wild type (WT) choroids (**Figures 2E,F**), whereas MIG6 overexpression significantly inhibited choroidal microvessel sprouting (**Figures 2G,H**). Thus, apart from the retina, MIG6 also inhibits angiogenesis in other tissues, such as in the aorta and choroids.

MIG6 Inhibits Endothelial Cell Proliferation, Migration, and Tube Formation

Although MIG6 is expressed in various types of endothelial cells (**Supplementary Table 1**) (Jin et al., 2009; Lee et al., 2014), it remains thus far unknown whether it regulates EC functions. We therefore investigated into this using both gain- and loss-of-function assays. An EdU incorporation assay revealed that Mig6 overexpression (**Figure 3A**) markedly inhibited the proliferation of human retinal endothelial cells (HREC) (**Figures 3B,C**), while MIG6 knockdown (**Figure 3D**) increased HREC proliferation (**Figures 3E,F**). This finding was further supported by an MTT assay showing that MIG6 knockdown increased and MIG6 overexpression decreased HREC proliferation, respectively (**Supplementary Figures 1B,C**). Moreover, an HREC migration assay showed that overexpression of MIG6 inhibited HREC migration (**Supplementary Figures 2A–C**), and MIG6 knockdown enhanced HREC tube formation (**Figures 3G,H**). Furthermore, an HREC spheroid assay revealed that MIG6 knockdown markedly increased the number and length of EC sprouts in HREC (**Figures 3I–K**). Thus, multiple assays showed that MIG6 overexpression inhibits HREC proliferation, migration, and tube formation.

MIG6 Inhibits Ischemia-Induced Retinal Neovascularization

Led by our observation on the anti-angiogenic effect of MIG6, we further tested whether MIG6 could inhibit pathological neovascularization using a mouse model of retinopathy of prematurity (ROP) (Connor et al., 2009) (**Figure 4A**). Adenoviruses encoding MIG6 were intravitreally injected at P12 to overexpress MIG6, with Ad-GFP as a control (**Supplementary Figure 3**). After 5 days, the retinae were collected to analyze neovascularization. The retinae treated with Ad-MIG6 displayed less neovascularization and fewer neovascular tufts compared with the Ad-GFP retinae (**Figures 4B,C**), demonstrating that MIG6 overexpression inhibits retinal neovascularization.

MIG6 Binds to SHC1

SHC1 has a central role in the signaling of many tyrosine kinases (Zheng et al., 2013; Ahn et al., 2017) and binds to the pY[I/E/Y/L][X][I/L/M] motif (X representing any of the 20 amino acids), which is found in MIG6 (YYLL: 394Tyr-397Leu) (Wills and Jones, 2012; Suen et al., 2013). We therefore tested whether it binds to MIG6. A co-immunoprecipitation assay revealed that SHC1 formed complex with MIG6 in HREC, which was augmented by EGF treatment (**Figures 5A,B**).

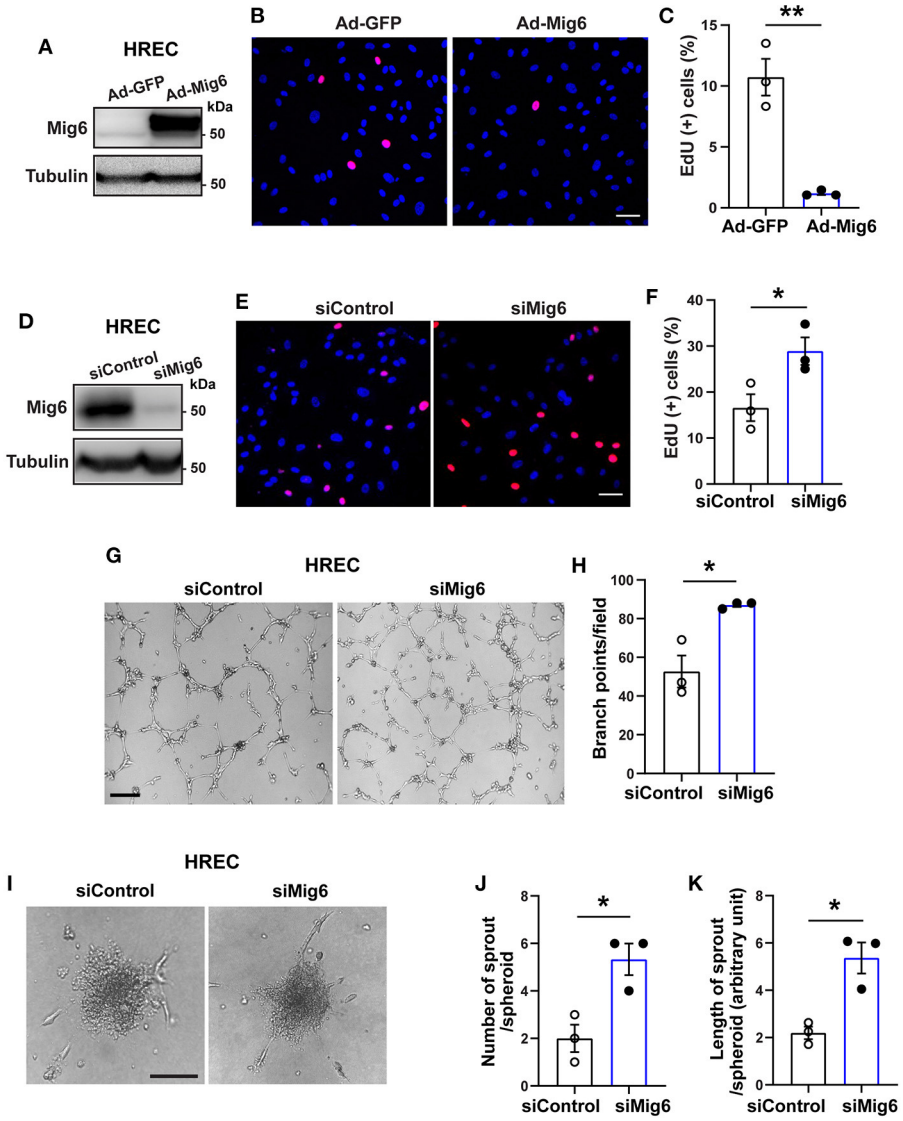

FIGURE 3 | MIG6 inhibits endothelial cell proliferation, migration, tube formation, and sprouting. **(A)** Western blot for MIG6 overexpression in HRECs treated with Ad-MIG6. **(B)** Representative images for EdU incorporation in MIG6-overexpressing HRECs. **(C)** Bar graphs represent the mean ± SEM of % EdU+ cells per field in **(B)**. **(D)** Western blot for MIG6 expression in MIG6 knockdown HRECs. **(E)** Images showing EdU incorporation in MIG6 knockdown HRECs. **(F)** Bar graphs represent the mean ± SEM of % EdU+ cells per field in **(E)**. **(G)** Tube formation in HRECs upon control (siControl) or MIG6 siRNA (siMIG6)-mediated knockdown. **(H)** Quantification of the number of the branch points per field in **(G)**. **(I)** Representative images of EC spheroids using siMIG6 HREC for 48 h. **(J)** Quantification of the number of sprouts per EC spheroid in **(I)**. **(K)** Quantification of the total sprout length per EC spheroid in **(I)**. Scale bars: 50 μm for **(B,E)**; 100 μm for **(G)**; 500 μm for **(I)**. The data are shown as mean ± SEM from three independent experiments. * $p < 0.05$, ** $p < 0.01$ (two-tailed paired Student's *t*-test).

To determine the domain of the SHC1 bound by MIG6, GST-conjugated MIG6 fusion protein (GST-MIG6) and the truncated mutants of SHC1 protein were produced (**Figure 5C**, **Supplementary Figures 4A,B**). The GST-MIG6 protein bound to the full-length and deletion mutant of SHC1 lacking the proline-rich domain (deletion of amino acids 300–366) but not to the mutants lacking PTB (deletion of amino acids 30–210) or SH2 domain (deletion of amino acids 377–469) (**Figure 5D**), suggesting that the PTB and SH2 domains of SHC1 are critical for MIG6 binding.

MIG6 Inhibits SHC1 Phosphorylation

It is known that phosphorylation of SHC1 is critical in promoting cell proliferation, migration, and survival (Zheng et al., 2013; Ahn et al., 2017; Wright et al., 2019). We therefore examined whether MIG6 affected SHC1 phosphorylation. We found that gene deletion of *Mig6* increased SHC1 phosphorylation at both the basal level and after EGF stimulation in primary mouse lung ECs (**Figures 6A,B**). Moreover, MIG6 overexpression decreased SHC1 phosphorylation in HRECs (**Figures 6C,D**), while opposite effects were observed after MIG6

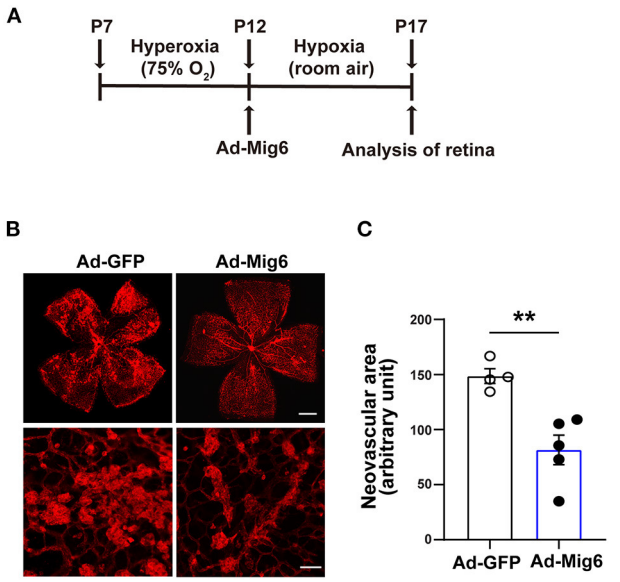

FIGURE 4 | MIG6 inhibits pathological angiogenesis. **(A)** Timeline of the retinopathy of prematurity model. P7 neonatal mice were exposed to hyperoxia for 5 days. Intravitreal injection of adenovirus expressing GFP or MIG6 was executed at P12. Mice were then returned to room air until P17. **(B)** Images of whole mount retinae at P17 stained with IB4-Alexa 594 (top). High magnification images of neovascular tufts in the retinae infected with Ad-GFP or Ad-MIG6 (bottom). **(C)** Quantification of neovascular areas in retinal whole mounts in **(B)**. $n = 4$ fields per Ad-GFP treated retina, $n = 5$ fields per Ad-Mig6 treated retina. Scale bars: 300 μm for the top panel of **(B)**; 50 μm for the bottom panel of **(B)**. The data are shown as mean ± SEM. ** $p < 0.01$ (two-tailed paired Student's *t*-test).

knockdown (**Supplementary Figures 5A–D**). These data thus demonstrate that MIG6 has a critical suppressive effect on SHC1 phosphorylation.

We next verified whether SHC1 played a role in modulating MIG6 function. We found that SHC1 knockdown by siRNA markedly reduced MIG6 knockdown-induced tube formation in HRECs (**Figures 6E,F**), demonstrating that SHC1 is required for the inhibitory effect of MIG6 on angiogenesis. Moreover, at a molecular level, we found that SHC1 knockdown also abolished siMIG6-induced ERK1/2 activation in the presence of EGF in HREC (**Figures 6G,H**). Taken together, our data show that MIG6 has a potent anti-angiogenic effect by binding to SHC1 and inhibiting its phosphorylation (**Figure 7**).

DISCUSSION

Uncontrolled growth of blood vessels can result in many devastating neovascular diseases. Therefore, a tight regulation of angiogenesis is essential to prevent overgrowth of blood vessels and consequential exacerbation or development of neovascular diseases. Given the presence diverse and abundant angiogenic factors, naturally occurring endogenous anti-angiogenic factors would be critical to counteract excessive pro-angiogenic activities to maintain vascular homeostasis. Yet, currently, less is known about such endogenous anti-angiogenic factors as opposed to the pro-angiogenic factors. In this study, we identified MIG6 as a potent endogenous inhibitor of angiogenesis by investigating the functions of MIG6 in multiple experimental systems. Furthermore, we reveal the molecular mechanism underlying the anti-angiogenic functions of MIG6, which implicates the inhibition of SHC1 signaling driven by MIG6 binding-mediated inhibition of SHC1 phosphorylation.

MIG6 is widely expressed in vascular cells (**Supplementary Table 1**) (Jin et al., 2009; Lee et al., 2014). Yet, little is known whether MIG6 functions in them. Here, we found *Mig6* knockout mice displayed increased blood vessel density and number of branch points in the retinae, demonstrating an anti-angiogenic effect of MIG6 in retinal vascularization. Indeed, *in vitro*, MIG6 inhibits EC proliferation, viability and sprouting. It remains unclear thus far whether MIG6 regulates pathological neovascularization. We found in this work that overexpression of MIG6 suppressed retinal neovascularization in a mouse model of retinopathy of prematurity, providing evidence for a role of MIG6 in pathological neovascularization. It has been shown that *Mig6* deficiency led to endometrial hyperplasia (Jin et al., 2007) and neointimal hyperplasia (Lee et al., 2014), thus raising the possibility that MIG6 deficiency-induced angiogenesis might contribute to these pathological conditions. Further studies are needed to verify this.

Our findings of the anti-angiogenic effects of MIG6 present different observations from another gene knockout study, which reported the opposite roles of MIG6 in angiogenesis by showing that neovascularization is reduced compared with wild-type lungs, and pro-angiogenic factors, including VEGF-A, are downregulated at P3 in *Mig6* knockout lungs (Jin et al., 2009). At least one of the reasons for this discrepancy might be due to differential expression of MIG6 in different tissues during development (Jin et al., 2009). Additionally, in our current work, the *Mig6* knockout mice used were bred on C57Bl/6J background for more than six generations. In the Jin et al. (2009) study, however, it was not clearly indicated whether C57Bl6 strain was used. In addition, the Mig6 knockout mice used in the Jin *et al.* study were produced by crossing $Mig6^{fl/fl}$ with Rosa26-Cre-ERT2, which was a different targeting strategy compared with that of our knockout mice, which is global knockout without any *Cre* recombination.

However, in line with our findings, vascular smooth muscle cells (SMCs) in SMC-specific *Mig6* conditional knockout mice displayed an increased cell migration and proliferation (Lee et al., 2014). Due to this SMC phenotype, it cannot rule out the possibility that some of the effect of MIG6 deletion on angiogenesis could be secondary to SMC defect, if any. It indeed has been reported that the EC-SMC interplay affects collective EC movements driving capillary elongation in the aortic ring assay (Arima et al., 2011). On the other hand, our HREC proliferation, tube formation and spheroid assays showed a direct effect of MIG6 on them. Also, ERG (an EC marker) staining showed more ERG+ cells in *Mig6* KO mice, indicating that MIG6 has a direct effect on ECs. Moreover, MIG6 activities vary since it interacts with a wide range of receptor tyrosine kinases (RTK), such as c-Met, FGFR2, and PDGFR (Pante et al., 2005; Zhang

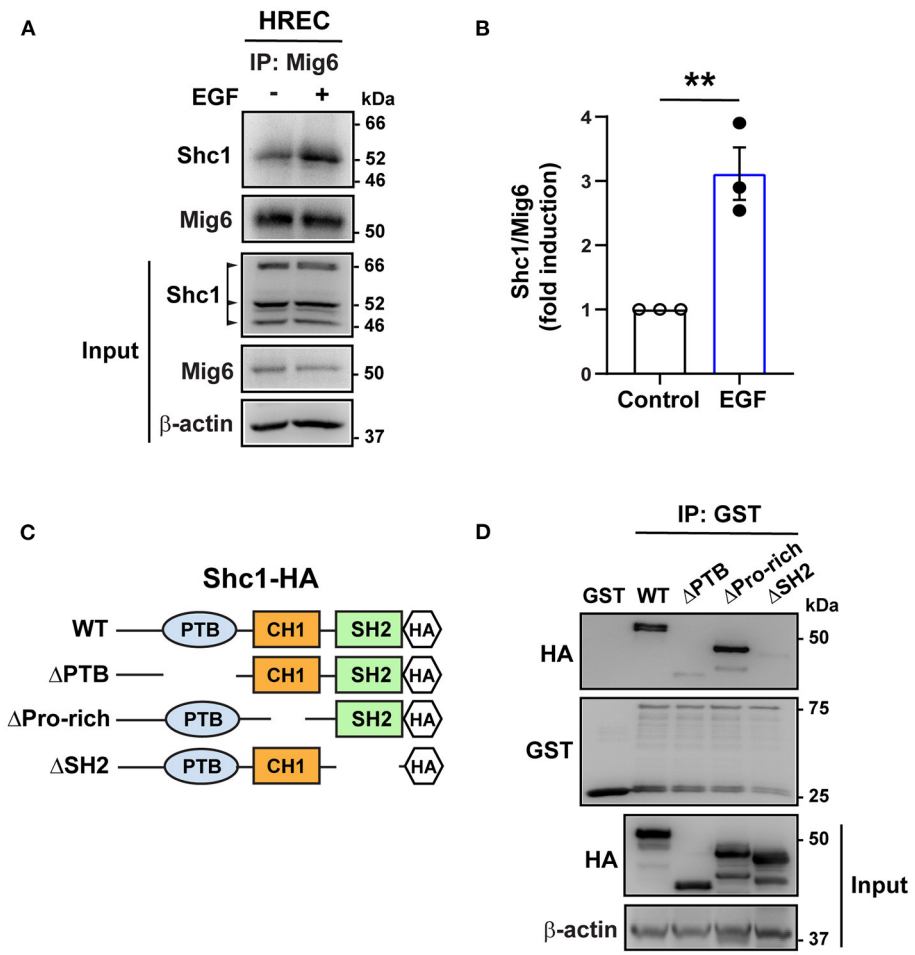

FIGURE 5 | MIG6 binds to SHC1 through PTB and SH2 domains. **(A)** Immunoprecipitation (IP) followed by Western blot showing binding of MIG6 with SHC1 in HRECs, which was further augmented by EGF (50 ng/ml) treatment. **(B)** MIG6 binding to SHC1 was analyzed by densitometry and normalized by total MIG6. Fold induction relative to the control is shown as the mean ± SEM from three independent experiments. ** $p < 0.01$ (two-tailed paired Student's *t*-test). **(C)** Schematic representation of SHC1 deletion mutants. The full-length (WT) and the truncated deletion mutants of SHC1 were tagged with HA in their C-terminus. The truncated mutants of SHC1 lack the PTB domain (ΔPTB: deletion of amino acids 30–210), proline-rich domain (ΔPro-rich: deletion of amino acids 300–366) in CH1 (collagen homology 1) region, and the SH2 domain (ΔSH2: deletion of amino acids 377–469). **(D)** Association of MIG6 with the truncated mutants of SHC1 was determined by GST pull-down assay, showing that MIG6 binding is mediated by the PTB and SH2 domains in SHC1.

and Vande Woude, 2007; Borad et al., 2014; Migliore et al., 2018). Furthermore, a recent study showed that Akt is a novel binding partner of MIG6 to modulate its activation in several types of cancer cells expressing a low level of EGFR (Cairns et al., 2018). As such, by interacting with different signaling molecules depending on their expression status, MIG6 may appear to be multi-functional in different cell types or tissues.

The signaling pathway of MIG6 is poorly understood thus far. In this study, we found that MIG6 forms complex with SHC1, an intracellular adaptor protein that is highly expressed in the vascular system (Lai and Pawson, 2000; Sweet et al., 2012). Moreover, we show that the PTB and SH2 domains in SHC1 are critical regions for MIG6 binding, which leads to the inhibition of the SHC1 downstream signaling. Gene deletion of *Mig6* increased SHC1 phosphorylation in ECs, demonstrating the inhibitory effect of MIG6 on SHC1 phosphorylation. Importantly, SHC1 knockdown largely abolished MIG6 depletion-induced EC tube formation and the increased ERK1/2 activation by EGF in ECs, suggesting that the anti-angiogenic function of MIG6 is mediated by its suppressive effect on SHC1. Indeed, SHC1 has been shown to be pro-angiogenic by promoting EC proliferation, survival and blood vessel maturation (Saucier et al., 2004; Sweet et al., 2012). Noteworthy, SHC1 has a critical role in inducing VEGF expression (Saucier et al., 2004) and enhancing the activities of several angiogenic pathways, including VEGFR2 (Lai and Pawson, 2000; Sweet et al., 2012), raising the question whether MIG6 affects the angiogenic activities of the VEGFA-VEGFR2 pathway. Future studies are needed to address this.

In summary, we demonstrate that MIG6 deficiency increases angiogenesis both *in vivo* and *in vitro*. We also show that MIG6

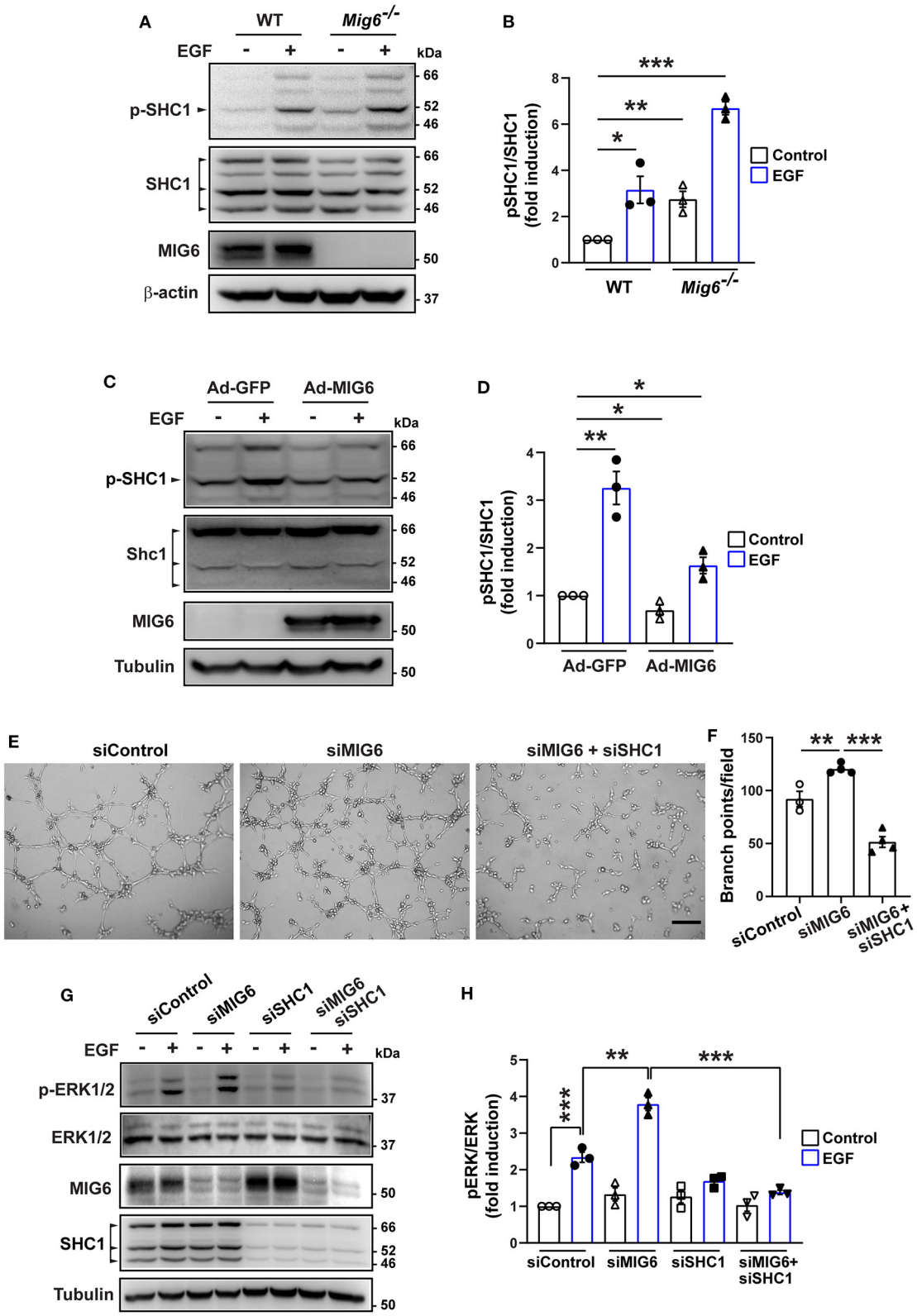

FIGURE 6 | MIG6 has a potent anti-angiogenic effect by inhibiting SHC1 phosphorylation and the subsequent ERK1/2 activation. **(A)** Western blots showing that gene deletion of *Mig6* increases SHC1 phosphorylation in mouse primary lung ECs at the baseline level and in the presence of EGF. **(B)** Tyrosine phosphorylation of

(Continued)

FIGURE 6 | SHC1 (pTyr239/240 SHC1) was analyzed by densitometry and normalized by total SHC1. Fold induction relative to the control is shown as the mean ± SEM from three independent experiments. **(C)** Western blots showing that overexpression of MIG6 decreases SHC1 phosphorylation in HRECs at the baseline level and in the presence of EGF. **(D)** Tyrosine phosphorylation of SHC1 (pTyr239/240 SHC1) was analyzed by densitometry and normalized by total SHC1. Fold induction relative to the control is shown as the mean ± SEM from three independent experiments. **(E)** Images of tube formation assay showing that SHC1 knockdown abolished siMIG6-induced tube formation of HRECs. **(F)** Quantification of the branch points per field in **(E)**. The graph is shown as the mean ± SEM from three independent experiments. **(G)** Western blots showing that SHC1 knockdown abolished siMIG6-induced ERK1/2 phosphorylation in HRECs. **(H)** Phosphorylation of ERK1/2 was analyzed by densitometry and normalized by total ERK1/2. Three isoforms of SHC1 are indicated by the arrowhead **(A,C)**. Fold induction relative to the control is shown as the mean ± SEM from three independent experiments. * $p < 0.05$, ** $p < 0.01$, *** $p < 0.001$ (two-tailed paired Student's *t*-test).

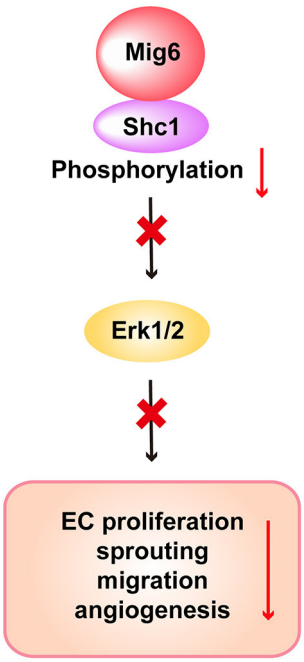

FIGURE 7 | Scheme of the proposed function of MIG6 and the underlying mechanism in endothelial cells. Shown is the proposed working model displaying that MIG6 restrains SHC1 signaling pathway by binding to it and inhibiting its phosphorylation, leading to reduced ERK1/2 activation and EC proliferation and migration, thus resulting in the inhibition of angiogenesis.

antagonizes SHC1 signaling to inhibit angiogenesis. Our results demonstrate that the signaling axis of MIG6 and SHC1 plays a critical role in keeping angiogenesis balanced. Our work provides new insights into the pathogenesis of neovascular diseases, and may have therapeutic implications in anti-angiogenic therapy.

DATA AVAILABILITY STATEMENT

The original contributions presented in the study are included in the article/**Supplementary Material**, further inquiries can be directed to the corresponding authors.

ETHICS STATEMENT

The animal study was reviewed and approved by Animal Use and Care Committee of Zhongshan Ophthalmic Center, Sun Yat-sen University.

AUTHOR CONTRIBUTIONS

LL and LX designed and performed experiments, analyzed data, and wrote a part of the manuscript. RC, YH, JZ, LH, BX, XR, SW, HK, and XLin performed experiments and analyzed data. AK and JK provided critical experimental tools and suggestions. CL and XLi designed and supervised experiments, analyzed data, and wrote the manuscript. All authors contributed to the article and approved the submitted version.

FUNDING

This study is supported by the State Key Laboratory of Ophthalmology (SKLO), Zhongshan Ophthalmic Center (ZOC) at the Sun Yat-sen University, the National Natural Science Foundation of China (81670855), and a Key Program of Guangzhou Scientific Research Plan (201804020010).

SUPPLEMENTARY MATERIAL

The Supplementary Material for this article can be found online at: https://www.frontiersin.org/articles/10.3389/fcell.2021.634242/full#supplementary-material

REFERENCES

Ahn, R., Sabourin, V., Bolt, A. M., Hébert, S., Totten, S., De Jay, N., et al. (2017). The Shc1 adaptor simultaneously balances Stat1 and Stat3 activity to promote breast cancer immune suppression. *Nat. Commun.* 8:14638. doi: 10.1038/ncomms14638

Anastasi, S., Lamberti, D., Alemà, S., and Segatto, O. (2016). Regulation of the ErbB network by the MIG6 feedback loop in physiology, tumor suppression and responses to oncogene-targeted therapeutics. *Semin. Cell Dev. Biol.* 50, 115–124. doi: 10.1016/j.semcdb.2015.10.001

Apte, R. S., Chen, D. S., and Ferrara, N. (2019). VEGF in signaling and disease: beyond discovery and development. *Cell* 176, 1248–1264. doi: 10.1016/j.cell.2019.01.021

Arima, S., Nishiyama, K., Ko, T., Arima, Y., Hakozaki, Y., Sugihara, K., et al. (2011). Angiogenic morphogenesis driven by dynamic and heterogeneous collective endothelial cell movement. *Development* 138, 4763–4776. doi: 10.1242/dev.068023

Borad, M. J., Champion, M. D., Egan, J. B., Liang, W. S., Fonseca, R., Bryce, A. H., et al. (2014). Integrated genomic characterization reveals novel, therapeutically relevant drug targets in FGFR and EGFR pathways

in sporadic intrahepatic cholangiocarcinoma. *PLoS Genet.* 10:e1004135. doi: 10.1371/journal.pgen.1004135

Cairns, J., Fridley, B. L., Jenkins, G. D., Zhuang, Y., Yu, J., and Wang, L. (2018). Differential roles of ERRFI1 in EGFR and AKT pathway regulation affect cancer proliferation. *EMBO Rep.* 19:e44767. doi: 10.15252/embr.201744767

Connor, K. M., Krah, N. M., Dennison, R. J., Aderman, C. M., Chen, J., Guerin, K. I., et al. (2009). Quantification of oxygen-induced retinopathy in the mouse: a model of vessel loss, vessel regrowth and pathological angiogenesis. *Nat. Protoc.* 4, 1565–1573. doi: 10.1038/nprot.2009.187

Ferby, I., Reschke, M., Kudlacek, O., Knyazev, P., Pantè, G., Amann, K., et al. (2006). Mig6 is a negative regulator of EGF receptor-mediated skin morphogenesis and tumor formation. *Nat. Med.* 12, 568–573. doi: 10.1038/nm1401

Gerhardt, H., Golding, M., Fruttiger, M., Ruhrberg, C., Lundkvist, A., Abramsson, A., et al. (2003). VEGF guides angiogenic sprouting utilizing endothelial tip cell filopodia. *J. Cell Biol.* 161, 1163–1177. doi: 10.1083/jcb.200302047

Haibe, Y., Kreidieh, M., El Hajj, H., Khalifeh, I., Mukherji, D., Temraz, S., et al. (2020). Resistance mechanisms to anti-angiogenic therapies in cancer. *Front. Oncol.* 10:221. doi: 10.3389/fonc.2020.00221

Jin, N., Cho, S. N., Raso, M. G., Wistuba, I., Smith, Y., Yang, Y., et al. (2009). Mig-6 is required for appropriate lung development and to ensure normal adult lung homeostasis. *Development* 136, 3347–3356. doi: 10.1242/dev.032979

Jin, N., Gilbert, J. L., Broaddus, R. R., Demayo, F. J., and Jeong, J. W. (2007). Generation of a Mig-6 conditional null allele. *Genesis* 45, 716–721. doi: 10.1002/dvg.20348

Karaman, S., Leppänen, V. M., and Alitalo, K. (2018). Vascular endothelial growth factor signaling in development and disease. *Development* 145:dev151019. doi: 10.1242/dev.151019

Lai, K. M., and Pawson, T. (2000). The ShcA phosphotyrosine docking protein sensitizes cardiovascular signaling in the mouse embryo. *Genes. Dev.* 14, 1132–1145. doi: 10.1101/gad.14.9.1132

Lee, J. H., Choung, S., Kim, J. M., Lee, J. U., Kim, K. S., Kim, H. J., et al. (2014). Mig-6 gene knockout induces neointimal hyperplasia in the vascular smooth muscle cell. *Dis. Markers* 2014:549054. doi: 10.1155/2014/549054

Li, X., and Carmeliet, P. (2018). Targeting angiogenic metabolism in disease. *Science* 359, 1335–1336. doi: 10.1126/science.aar5557

Li, X., Sun, X., and Carmeliet, P. (2019). Hallmarks of endothelial cell metabolism in health and disease. *Cell Metab.* 30, 414–433. doi: 10.1016/j.cmet.2019.08.011

Liu, N., Matsumoto, M., Kitagawa, K., Kotake, Y., Suzuki, S., Shirasawa, S., et al. (2012). Chk1 phosphorylates the tumour suppressor Mig-6, regulating the activation of EGF signalling. *EMBO J.* 31, 2365–2377. doi: 10.1038/emboj.2012.88

Lundgren, T. K., Scott, R. P., Smith, M., Pawson, T., and Ernfors, P. (2006). Engineering the recruitment of phosphotyrosine binding domain-containing adaptor proteins reveals distinct roles for RET receptor-mediated cell survival. *J. Biol. Chem.* 281, 29886–29896. doi: 10.1074/jbc.M600473200

Migliore, C., Morando, E., Ghiso, E., Anastasi, S., Leoni, V. P., Apicella, M., et al. (2018). miR-205 mediates adaptive resistance to MET inhibition via ERRFI1 targeting and raised EGFR signaling. *EMBO Mol. Med.* 10:e8746. doi: 10.15252/emmm.201708746

Murugeswari, P., Shukla, D., Rajendran, A., Kim, R., Namperumalsamy, P., and Muthukkaruppan, V. (2008). Proinflammatory cytokines and angiogenic and anti-angiogenic factors in vitreous of patients with proliferative diabetic retinopathy and eales' disease. *Retina* 28, 817–824. doi: 10.1097/IAE.0b013e31816576d5

Ochsenbein, A. M., Karaman, S., Proulx, S. T., Berchtold, M., Jurisic, G., Stoeckli, E. T., et al. (2016). Endothelial cell-derived semaphorin 3A inhibits filopodia formation by blood vascular tip cells. *Development* 143, 589–594. doi: 10.1242/dev.127670

Pante, G., Thompson, J., Lamballe, F., Iwata, T., Ferby, I., Barr, F. A., et al. (2005). Mitogen-inducible gene 6 is an endogenous inhibitor of HGF/Met-induced cell migration and neurite growth. *J. Cell Biol.* 171, 337–348. doi: 10.1083/jcb.200502013

Park, E., Kim, N., Ficarro, S. B., Zhang, Y., Lee, B. I., Cho, A., et al. (2015). Structure and mechanism of activity-based inhibition of the EGF receptor by Mig6. *Nat. Struct. Mol. Biol.* 22, 703–711. doi: 10.1038/nsmb.3074

Ribatti, D. (2016). Tumor refractoriness to anti-VEGF therapy. *Oncotarget* 7, 46668–46677. doi: 10.18632/oncotarget.8694

Sasaki, M., Terabayashi, T., Weiss, S. M., and Ferby, I. (2018). The tumor suppressor MIG6 controls mitotic progression and the G2/M DNA damage checkpoint by stabilizing the WEE1 kinase. *Cell Rep.* 24, 1278–1289. doi: 10.1016/j.celrep.2018.06.064

Saucier, C., Khoury, H., Lai, K. M., Peschard, P., Dankort, D., Naujokas, M. A., et al. (2004). The Shc adaptor protein is critical for VEGF induction by Met/HGF and ErbB2 receptors and for early onset of tumor angiogenesis. *Proc. Natl. Acad. Sci. U. S. A.* 101, 2345–2350. doi: 10.1073/pnas.0308065101

Shao, Z., Friedlander, M., Hurst, C. G., Cui, Z., Pei, D. T., Evans, L. P., et al. (2013). Choroid sprouting assay: an ex vivo model of microvascular angiogenesis. *PLoS ONE* 8:e69552. doi: 10.1371/journal.pone.0069552

Suen, K. M., Lin, C. C., George, R., Melo, F. A., Biggs, E. R., Ahmed, Z., et al. (2013). Interaction with Shc prevents aberrant Erk activation in the absence of extracellular stimuli. *Nat. Struct. Mol. Biol.* 20, 620–627. doi: 10.1038/nsmb.2557

Sweet, D. T., Chen, Z., Wiley, D. M., Bautch, V. L., and Tzima, E. (2012). The adaptor protein Shc integrates growth factor and ECM signaling during postnatal angiogenesis. *Blood* 119, 1946–1955. doi: 10.1182/blood-2011-10-384560

Wills, M. K., and Jones, N. (2012). Teaching an old dogma new tricks: twenty years of Shc adaptor signalling. *Biochem. J.* 447, 1–16. doi: 10.1042/BJ20120769

Wright, K. D., Miller, B. S., El-Meanawy, S., Tsaih, S. W., Banerjee, A., Geurts, A. M., et al. (2019). The p52 isoform of SHC1 is a key driver of breast cancer initiation. *Breast Cancer Res.* 21:74. doi: 10.1186/s13058-019-1155-7

Zhang, K., Li, M., Yin, L., Fu, G., and Liu, Z. (2020). Role of thrombospondin-1 and thrombospondin-2 in cardiovascular diseases (Review). *Int. J. Mol. Med.* 45, 1275–1293. doi: 10.3892/ijmm.2020.4507

Zhang, Y. W., and Vande Woude, G. F. (2007). Mig-6, signal transduction, stress response and cancer. *Cell Cycle* 6, 507–513. doi: 10.4161/cc.6.5.3928

Zheng, Y., Zhang, C., Croucher, D. R., Soliman, M. A., St.-Denis, N., Pasculescu, A., et al. (2013). Temporal regulation of EGF signalling networks by the scaffold protein Shc1. *Nature* 499, 166–171. doi: 10.1038/nature 12308

Conflict of Interest: The authors declare that the research was conducted in the absence of any commercial or financial relationships that could be construed as a potential conflict of interest.

Copyright © 2021 Liu, Xing, Chen, Zhang, Huang, Huang, Xie, Ren, Wang, Kuang, Lin, Kumar, Kim, Lee and Li. This is an open-access article distributed under the terms of the Creative Commons Attribution License (CC BY). The use, distribution or reproduction in other forums is permitted, provided the original author(s) and the copyright owner(s) are credited and that the original publication in this journal is cited, in accordance with accepted academic practice. No use, distribution or reproduction is permitted which does not comply with these terms.

frontiers in Cell and Developmental Biology

HYPOTHESIS AND THEORY
published: 23 March 2021
doi: 10.3389/fcell.2021.660609

Reconciling VEGF With VPF: The Importance of Increased Vascular Permeability for Stroma Formation in Tumors, Healing Wounds, and Chronic Inflammation

*Harold F. Dvorak**

Department of Pathology, Beth Israel Deaconess Medical Center, Harvard Medical School, Boston, MA, United States

OPEN ACCESS

Edited by:
Ramani Ramchandran, Medical College of Wisconsin, United States

Reviewed by:
Domenico Ribatti, University of Bari Aldo Moro, Italy
Bingmei M. Fu, The City College of New York (CUNY), United States
Kaustubh Datta, University of Nebraska Medical Center, United States

***Correspondence:**
Harold F. Dvorak
hdvorak@comcast.net

Specialty section:
This article was submitted to Signaling, a section of the journal Frontiers in Cell and Developmental Biology

Received: *29 January 2021*
Accepted: *04 March 2021*
Published: *23 March 2021*

Citation:
Dvorak HF (2021) Reconciling VEGF With VPF: The Importance of Increased Vascular Permeability for Stroma Formation in Tumors, Healing Wounds, and Chronic Inflammation. Front. Cell Dev. Biol. 9:660609. doi: 10.3389/fcell.2021.660609

It is widely believed that vascular endothelial growth factor (VEGF) induces angiogenesis by its direct mitogenic and motogenic actions on vascular endothelial cells. However, these activities are only detected when endothelial cells are cultured at very low (0.1%) serum concentrations and would not be expected to take place at the much higher serum levels found in angiogenic sites *in vivo*. This conundrum can be resolved by recalling VEGF's original function, that of an extremely potent vascular permeability factor (VPF). *In vivo* VPF/VEGF increases microvascular permeability such that whole plasma leaks into the tissues where it undergoes clotting by tissue factor that is expressed on tumor and host connective tissue cells to deposit fibrin and generate serum. By providing tissue support and by reprogramming the gene expression patterns of cells locally, fibrin and serum can together account for the formation of vascular connective tissue stroma. In sum, by increasing vascular permeability, VPF/VEGF triggers the "wound healing response," setting in motion a fundamental pathophysiological process that induces the mature stroma that is found not only in healing wounds but also in solid tumors and chronic inflammatory diseases. Once initiated by increased vascular permeability, this response may be difficult to impede, perhaps contributing to the limited success of anti-VEGF therapies in treating cancer.

Keywords: VPF/VEGF, vascular permeability, tumors, wound healing, chronic inflammation, delayed hypersensitivity, angiogenesis, stroma

INTRODUCTION

Normal tissues are comprised of two compartments: *parenchyma* and *stroma*. For example, the *parenchyma* of normal skin is the epidermis, a multi-layered squamous epithelium; skin's *stroma* is the dermis, a "connective tissue" comprised of blood vessels, lymphatics, fibroblasts and their products (primarily collagen but also including glycosaminoglycans and proteoglycans), small amounts of interstitial fluid (a plasma protein-*poor* transudate of blood plasma), and small numbers of inflammatory cells (mostly macrophages and lymphocytes). The dermal stroma supports the

epidermal parenchyma in three ways: it provides *nutrition* (oxygen, sugars, amino acids, etc.) and *waste disposal* (carbon dioxide, metabolic products) via the blood vasculature and lymphatics, and provides a collagenous matrix for physical *support*.

Like normal tissues, tumors are comprised of a parenchyma (the tumor cells) and a stroma that is of host origin. *All* tumors require stroma for survival and growth. As in normal tissues, stroma is necessary for tumor cell nutrition, waste product disposal, and support. However, not all tumors need to generate new stroma. Liquid tumors such as leukemias have inbuilt host stroma; the blood in which they circulate serves as stroma, affording abundant oxygen and nutrients as well as an efficient means for clearing waste products via the lungs, kidneys and bile system. Therefore, leukemic cells require no additional stroma beyond the blood plasma in which they circulate.

At least initially, when very small, *solid* tumors can make use of the stroma provided by the normal tissues in which they arise; indeed, some primary tumors (e.g., some glioblastomas) continue to "live off the land," growing in cuffs around pre-existing host blood vessels (Holash et al., 1999). Tumor metastases to lungs and liver may also make use of pre-existing host blood vessels to supply their needs (Bridgeman et al., 2017). However, most solid primary tumors and their metastases require new stroma (Dvorak, 2015b, 2019). This newly generated stroma includes the same components found in the dermis and other normal tissues, though the overall composition and arrangement may differ. The *amount* of new stroma generated varies widely among different solid tumors. In many desmoplastic carcinomas, stroma comprises the bulk of the tumor mass. However, the amount of stroma is not correlated with tumor malignancy and some highly malignant tumors have relatively small amounts of stroma. Nonetheless, all tumors have and require stroma.

A critical question then arises: how do solid tumors generate the new stroma that they need for survival and growth? Often this question has been reduced to one of new blood vessel formation, i.e., how do tumors induce "angiogenesis"? However, angiogenic blood vessels, though necessary and important, are but one component of tumor stroma, and often only a minor component as measured by mass.

BEFORE PROCEEDING, A NECESSARY PRIMER ON VASCULAR PERMEABILITY

An understanding of vascular permeability is foundational to a comprehension of the pathogenesis of stroma formation as occurs in tumors, healing wounds and chronic inflammatory diseases. The endothelium lining microvessels provides the primary barrier to the passage of plasma across the vasculature. In normal tissues, such as the dermis, capillaries exhibit a *basal* level of permeability such that plasma water and small solutes (generally $\leq$40 kD) pass readily through the interface between neighboring endothelial cells (Feng et al., 2000; Nagy et al., 2008, 2012; Dvorak, 2015a,b). However, this inter-endothelial cell pathway does not permit the easy passage of larger molecules such as plasma proteins ($\geq$60 kD). Nonetheless, plasma proteins do cross the normal capillary endothelium in small amounts, but primarily, it is thought, by a different pathway, i.e., by way of vesicles (caveolae). Caveolae are 70 nm vesicles that open to and then bud off from the luminal capillary endothelial surface, traverse the endothelial cytoplasm, and discharge their plasma cargo into the tissues after fusing with the abluminal plasma membrane (Majno and Palade, 1961 #152; Majno et al., 1961 #153; Palade, 1988 #271). Vascular permeabilizing agents such as histamine greatly increase the efflux of large molecules; at least in humans and guinea pigs, they act primarily on *venular* (rather than *capillary*) endothelium to open two potential pathways, about whose relative importance there remains controversy (Feng et al., 1996, 1997, 1999, 2000; Majno and Joris, 2004; Nagy et al., 2008, 2012; Dvorak, 2015a,b): (1) A *transcellular* pathway involving the vesiculo-vacuolar organelle (VVO), an organelle comprised of hundreds of interconnected vesicles and vacuoles that spans venular cytoplasm from lumen to albumen. The stomata connecting these vesicles and vacuoles with each other and with the luminal and abluminal plasma membranes are normally closed but open in response to vascular permeabilizing agents to form transcellular channels through which whole plasma can flow. (2) An *intercellular* pathway generated by the pulling apart of adjacent endothelial cells to create gaps which allow the passage of whole plasma. The permeabilizing stimulus and resulting increased vascular permeability may be transient (as in the case of a mosquito bite) or chronic (as in tumors, healing wounds, and chronic inflammation), but in all cases results in an outpouring of a plasma protein-*rich* fluid that is both qualitatively and quantitatively different from the plasma protein-*poor* fluid bathing normal tissues. Further, when the stimulus is chronic, the capillaries and venules undergo profound structural changes, differentiating into ultrathin, intrinsically hyperpermeable *mother vessels*, as well as other abnormal vessel types (Dvorak et al., 1996; Pettersson et al., 2000; Nagy et al., 2006, 2007, 2010).

DELAYED HYPERSENSITIVITY AS A PARADIGM FOR PATHOLOGICAL STROMA FORMATION

Initial insights into the mechanisms of tumor stroma generation came from a surprising source, a form of cellular immunity known as *delayed hypersensitivity* (DH) (Colvin et al., 1973; Dvorak et al., 1974; Colvin and Dvorak, 1975). DH epitomizes the response of the body to allergens (e.g., poison ivy), foreign proteins (e.g., the tuberculin reaction), infectious agents (e.g., bacteria, viruses), and allografts. DH therefore has a prominent role in many important diseases, including tuberculosis, various other infections, contact allergy, rheumatoid arthritis, psoriasis and organ transplantation. DH is antibody-*independent*, mediated by T lymphocytes and macrophages, and can be passively transferred with lymphocytes but not with antibodies. Of course, many immunogens induce both cellular and humoral immune responses.

In the early 1970s, we reinvestigated DH skin reactions to tuberculin and other immunogens (Colvin et al., 1973;

Dvorak et al., 1974; Colvin and Dvorak, 1975). We discovered two surprising new features of these reactions: (1) Hyperpermeability of the dermal vasculature to plasma proteins and other circulating macromolecules, and (2) Abundant dermal deposits of cross-linked fibrin. These two findings were linked causally. The hyperpermeability of the dermal microvasculature led to the extravasation of a plasma protein-*rich* exudate that included fibrinogen and other clotting factors, in contrast to the plasma-*poor* transudate of normal tissues. Further, clotting took place extra vascularly, converting extravasated plasma to *serum* and extravasated fibrinogen to cross-linked *fibrin*. Deposited fibrin took the form of a water trapping gel[1] that was responsible for the induration characteristic of these reactions (Dvorak et al., 1979a,b #71).

These new findings were both unexpected and puzzling. First, increased vascular permeability had not previously been associated with cellular immunity; instead, microvascular hyperpermeability was thought to be a property of certain antibody-mediated reactions in which mast cells and basophils degranulate to release histamine, a well-known vascular permeabilizing factor. However, antihistamines did not inhibit DH reactions. Second, what was the significance, if any, of the clotting of plasma that generated serum and deposited fibrin?

STROMA GENERATION IN SOLID TUMORS FOLLOWS THE PATTERN OF DH

Our new findings in DH reactions prompted us to determine whether similar events took place when tumors were used as antigens. For these studies we transplanted Line 1 and Line 10 bile duct carcinomas subcutaneously into guinea pigs, i.e., the same animal species preferred for studies of DH[2]. Over the course of a week or two, both tumors became organized such that clumps of tumor cells became dispersed within a newly generated vascularized collagenous stroma (Dvorak et al., 1979a). Line 1 tumors had a more abundant stroma than that of Line 10 tumors, but the organizational pattern was the same and was reproducible upon multiple transplants. Both tumors provoked a lymphocyte response, similar to that found in DH reactions elicited by tuberculin and other immunogens. Further, the vasculature supplying both tumors was hyperpermeable to circulating high molecular weight dextrans and plasma proteins and deposits of cross-linked fibrin were found intermixed within the collagenous stroma (Dvorak et al., 1979a,b).

The combination of lymphocyte infiltrate, leaky blood vessels and fibrin deposits implied that these tumors had elicited a DH-type immune response. However, evaluation of these tumors at very early times after transplant demonstrated that increased vascular permeability and clotting occurred independent of immunity. Within 48 h after transplant, long before the possibility of an immune response, tumors were already arranged in a pattern similar to that found at later times except that clumps of malignant cells were separated from each other not by vascularized collagenous stroma but by fluid-filled spaces that included strands of fibrillar material. Immunohistochemistry identified these fibrils as fibrin or fibrin-related proteins and electron microscopy demonstrated the characteristic banding pattern of cross-linked fibrin. Further, when subjected to a solvent that extracted soluble elements (such as fibrinogen, non-cross-linked fibrin, fibrin degradation products) much of this fibrillar material remained behind, confirming its identity as cross-linked fibrin (Dvorak et al., 1984; Dvorak, 2015b, 2019).

In sum, within hours of transplant, tumors became organized into a pattern in which tumor cell clumps were separated from each other by a provisional stroma comprised of fibrin gel that over time was replaced by vascularized connective tissue. Thus, although these tumors did indeed induce a cellular immune response, the immune response could not account for the vascular hyperpermeability and fibrin deposition demonstrated at early times after transplant. Similar fibrin deposits were found in the stroma of many different cancers growing *in situ* in patients (Dvorak et al., 1981a; Harris et al., 1982), establishing the generality of these findings and negating the possibility that the trauma of tumor transplantation or some other artifact was responsible for fibrin deposition.

CANCER AND THE CLOTTING SYSTEM

An association between cancer and blood clotting was not a new concept in the 1970s. Vascular thrombosis is a fairly common cause of cancer death, and abnormal hemostasis has long been associated with cancer [reviewed in Carr et al. (1985), Dvorak and Rickles (2005)]. Armand Trousseau long ago recognized migratory thrombophlebitis (Trousseau's sign) as a predictor of underlying malignancy, the thought being that tumors shed procoagulant activities into the blood where they induce intravascular clotting. Some leukemias also express procoagulant activities that can induce disseminated intravascular coagulation. Several tumor cell-associated procoagulant activities have been identified. Most important among these is tissue factor, a cell membrane associated lipoprotein that activates the extrinsic clotting pathway and is widely expressed by tumor cells, including Line 1 and Line 10 carcinomas and many other animal and human tumor cells (Van De Water et al., 1985). In addition, these and many other tumors shed microparticles (exosomes) that also express tissue factor, allowing clotting to be initiated at a distance away from the tumor cells themselves (Dvorak et al., 1981b).

What was new from our work was the finding that clotting took place *extra vascularly*, such that fibrin was deposited and

[1]Gels are semi-solid structures in which small amounts of polymers of various types (in this case cross-linked fibrin) trap large amounts of fluid (here plasma), thus restricting fluid flow. Common examples include gelatin ("Jello"), and, of course, blood clots that form within blood vessels *in vivo* or in blood or plasma that is allowed to clot in a test tube.

[2]Guinea pigs provide a better animal model of human cellular immunity (and probably of cancer) than mice. However, guinea pigs suffer from a number of disadvantages that have limited their usefulness: they are more expensive to purchase and maintain, more difficult to inbreed (only two inbred strains are currently available), have few available transplantable tumor strains, and their genetics have been much less well studied.

serum generated *outside* rather *within* the blood vasculature. As in DH reactions, extravascular clotting was readily explained by the hyperpermeability of the tumor vasculature that allowed extravasated fibrinogen and other clotting proteins to come into contact with tumor cell- and exosome-associated tissue factor.

FIBRIN DEPOSITION IS A GENERALIZED RESPONSE TO VASCULAR HYPERPERMEABILITY

It was possible that there was something special about the DH and tumor microenvironments that allowed clotting of extravasated plasma. Therefore, to test the linkage between increased vascular permeability and clotting, we injected histamine and other vascular permeabilizing agents into normal guinea pig skin or other tissues and harvested the injection sites 20 min later (Dvorak et al., 1985). Such injections caused only brief pulses of increased vascular permeability that nonetheless resulted in deposits of cross-linked fibrin. Thus, even brief pulses of increased vascular permeability in otherwise normal tissues are sufficient to induce extravascular clotting and fibrin deposition. Clotting in these normal tissues was associated with fibroblasts and other host connective tissue cells that express tissue factor. That normal dermal cells express tissue factor is not surprising from an evolutionary point of view. Connective tissue cells are not normally exposed to the clotting proteins present in blood; however, when so exposed following tissue injury, the tissue factor they express is available to provide a protective function, activating clotting, depositing fibrin, and so limiting the extent of bleeding.

VASCULAR PERMEABILITY FACTOR (VPF), THE MEDIATOR OF TUMOR-ASSOCIATED VASCULAR HYPERPERMEABILITY

Because the cause of clotting in solid tumors was attributable to the tissue factor expressed by tumor and host connective tissue cells, the important unresolved question was the cause of the vascular hyperpermeability that led to extravasation of fibrinogen and other plasma proteins. To address this question, we cultured tumor cells in serum-free medium and tested supernatants for the presence of a possible secreted vascular permeability-inducing "factor" (Dvorak et al., 1979b; Senger et al., 1983). We found that a wide variety of tumors secreted such an activity. Using the Miles assay[3] to assess column fractions, we purified this vascular permeability factor (VPF) to homogeneity. VPF turned out to be an N-glycosylated dimeric protein that rapidly induced permeability to plasma proteins and other circulating macromolecules with a molar potency some 50,000 times that of histamine (Senger et al., 1986; Yeo et al., 1991). It did not degranulate mast cells to release vascular permeabilizing factors such as histamine, nor was its activity inhibited by anti-histamines; instead, it acted directly on vascular endothelium. An antibody raised to the N-terminal sequence of VPF blocked its vascular permeabilizing activity and inhibited accumulation of ascites fluid in tumors growing in the peritoneal cavity (Senger et al., 1983). Many animal and human cancer cells were found to express this same protein (Senger et al., 1986).

Vascular permeability factor was thus the missing factor responsible for the vascular hyperpermeability characteristic of solid tumors. VPF rendered the microvasculature leaky to plasma and plasma proteins, resulting in extravascular clotting and fibrin deposition as tumor- and host cell-associated tissue factor triggered the extrinsic clotting system (**Figure 1**). Fibrin accumulation in tumors was limited by fibrinolysis that was mediated by another tumor cell-secreted product, plasminogen activator [reviewed in Dvorak (2015b, 2019)]. Plasminogen, like other plasma proteins, extravasates from leaky blood vessels, and is cleaved by plasminogen activator to generate the potent fibrinolytic protease plasmin. Thus, fibrin accumulation in tumors, as well as in other sites of increased vascular permeability, reflects a balance struck between clotting with fibrin deposition on the one hand and fibrinolysis on the other. The net amount of fibrin present initially seems to predict the amount of mature stroma that subsequently replaces it, perhaps thereby explaining differences in the amounts of mature stroma found among different solid tumors.

PARALLELS BETWEEN TUMOR STROMA GENERATION AND WOUND HEALING

Speculations concerning a relationship between tumor stroma generation and wound healing go back at least as far as Virchow but were supported by little hard data. Nonetheless, two reports stand out. The first of these demonstrated that when the Rous sarcoma virus was injected intravenously into chickens, tumors formed preferentially at sites of incidental minor injury, i.e., at local sites where wound healing was taking place (Dolberg et al., 1985). A second important report by Majno demonstrated that in rat skin wounds there were two waves of increased vascular permeability [summarized in Majno and Joris (2004)]. The first wave was attributable to the injury itself which caused bleeding; this was generally staunched within a few minutes by platelet activation and clotting. However, a second wave of vascular hyperpermeability developed sometime later. This second phase of vascular hyperpermeability led to extravasation of whole plasma but not blood cells. It peaked at around 15 h after injury and persisted for a day or more. The mechanisms responsible for this second, unexpected round of vascular hyperpermeability were not known.

[3] Ashley Miles developed an assay for evaluating the permeability inducing properties of small molecules such as histamine (Feldberg and Miles, 1953). We used this assay to assess the VPF produced by tumor cells (Dvorak et al., 1979b; Senger et al., 1983). Putative permeability inducing agents were injected intradermally into the depilated flank skin of guinea pigs. Evans blue dye was then injected intravenously. This low molecular weight dye binds to plasma proteins and so tracks their distribution, generating prominent blue spots in skin sites injected with factors that induce vascular permeability to macromolecules. Permeability can be quantitated by measuring the amount of accumulated dye (Sitohy et al., 2017).

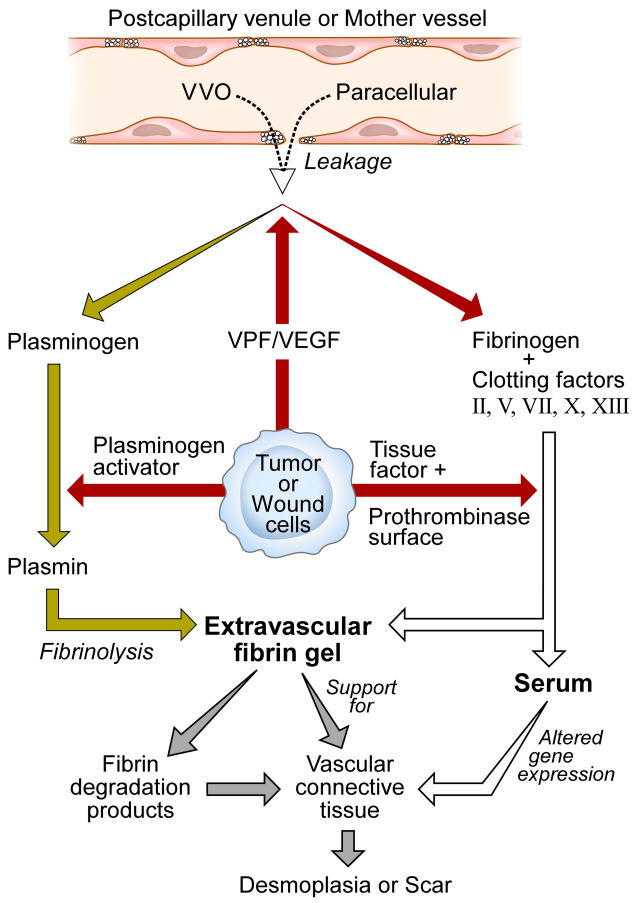

FIGURE 1 | Schematic diagram of stroma formation in tumors and wounds. Vascular permeability factor/vascular endothelial growth factor (VPF/VEGF) initiates the wound healing response by increasing vascular permeability. As a result, whole plasma including plasma proteins extravasate by way of *transcellular* (VVO) and/or *paracellular* pathways. Tumor, connective tissue, and wound cells express tissue factor to trigger the extrinsic clotting system, generating serum, and depositing fibrin. Fibrin provides support for tumor cells and the ingrowth of new blood vessels and fibroblasts that synthesize collagen and other structural proteins. Fibrin degradation products are proangiogenic. Serum reprograms the gene expression patterns of tumor and host connective tissue cells. Over time, vascular connective tissue is replaced by dense fibrous connective tissue stroma termed scar in wounds and desmoplasia in tumors. Modified from Dvorak (2019, Figure 3) and Dvorak (2015b, Figure 1) with permissions.

We confirmed Majno's findings and demonstrated that VPF was responsible for this second wave of vascular hyperpermeability (Brown et al., 1992). Several hours after wounding, VPF expression was highly upregulated in regenerating epidermal cells immediately adjacent to wound sites, as well as in macrophages scattered in the dermis (Brown et al., 1992). Upregulation of VPF expression was attributable to the local hypoxia characteristic of wound sites that stimulates VPF expression through the HIF-1 pathway (Semenza, 2014). As a consequence of this heightened vascular permeability, fibrinogen and other plasma proteins leaked and clotting took place, converting extravasated plasma to serum and fibrinogen to cross-linked fibrin, just as occurred in tumors and in response to vascular permeabilizing agents in normal tissues. Further, as wound healing progressed, new blood vessels formed, relieving local hypoxia and thereby turning down VPF expression. A similar increase in VPF expression was found at other sites of wounding, e.g., myocardial infarcts in the heart (Li et al., 1996) and following local brain injury (Stiver et al., 2004). We concluded that tumors are "wounds that do not heal," or, perhaps put better, tumors are wounds that continually exhibit elements of healing but do not heal the host (Dvorak, 1986, 2015b, 2019); instead, the healing process actually facilitates tumor survival and growth.

We subsequently demonstrated that VPF was also the previously unknown agent responsible for inducing the vascular hyperpermeability found in DH reactions (Brown et al., 1995) and in chronic inflammatory diseases such as psoriasis (Detmar et al., 1994) and rheumatoid arthritis (Fava et al., 1994). The same sequence of events followed in all of these examples: VPF induced vascular hyperpermeability which led to plasma extravasation, extravascular clotting, conversion of plasma to serum and extravasated fibrinogen to cross-linked fibrin. Fibrin was then degraded to varying extents by plasmin as extravasated plasma plasminogen was activated to plasmin by locally secreted plasminogen activator (**Figure 1**).

GENERATION OF MATURE TUMOR STROMA

Together the findings just summarized demonstrate the mechanisms by which increased vascular permeability leads to fibrin deposition in solid tumors, healing wounds, DH reactions, chronic inflammatory diseases, and in normal tissues in which vascular permeability to plasma and plasma proteins has been increased by VPF, histamine or other vascular permeabilizing agents. However, they do not explain the means by which tumor fibrin deposits are replaced over time by mature, vascularized connective tissue stroma. Therefore, there was considerable excitement when it was found that VPF was a weak though highly selective growth and pro-migratory factor for cultured vascular endothelium and that it was also able to induce angiogenesis *in vivo* (Connolly et al., 1989; Keck et al., 1989; Leung et al., 1989). VPF was immediately recognized as Judah Folkman's long sought after "tumor angiogenesis factor" (Folkman, 1971) and was rechristened vascular endothelial growth factor (VEGF) (Leung et al., 1989). It was surmised that VPF/VEGF induced mature tumor stroma by causing endothelial cell division and migration.

However, there are two problems with this analysis. First, as noted above, angiogenic blood vessels comprise only one element of tumor stroma. In addition to new angiogenic blood vessels, solid tumors, and healing wounds feature greatly enlarged feeder arteries, draining veins, and several other abnormal vessel types (Pettersson et al., 2000; Fu et al., 2007; Nagy et al., 2007, 2010). How do these other vessel types form? Also not accounted for is the generation of important structural components such as collagen, proteoglycans, and glycosaminoglycans, as well as the

fibroblasts and other cell types responsible for their synthesis; together these structural elements often comprise the bulk of the tumor mass.

The second and equally significant problem with this analysis is that of the highly restrictive conditions under which VPF/VEGF can act as an endothelial cell growth and motility factor. While VPF/VEGF is selectively mitogenic and motogenic for endothelial cells *in vitro*, such activity is detected only when endothelial cells are cultured in very low (typically 0.1%) serum. However, as shown above, the tumor microenvironment *in vivo* includes high serum concentrations that can approach those found when whole plasma is clotted. Tumor-induced ascites fluid may be taken as a proxy for the interstitial fluid in which solid tumors are bathed. Tumor ascites fluid typically has a high protein content, e.g., >25 g/dL (Tarn and Lapworth, 2010). While much of this protein content results from the death of tumor and other suspended cells, plasma-derived albumin content typically exceeds 2 g/dL, i.e., a plasma albumin content corresponding to 40% of that of whole plasma. Further, ascites fluid commonly becomes bloody and under these conditions plasma protein levels can approach those of whole blood. In such high serum concentrations, VPF/VEGF would not be expected to have mitogenic or motogenic activity on endothelial cells.

Together these two problems pose a conundrum. VPF/VEGF is able to induce the formation of mature, vascularized connective tissue stroma *in vivo* but apparently has no mitogenic or motogenic activity on endothelial cells under the conditions found in tumor stroma and of course in healing wounds. How is this conundrum to be resolved? It is possible that as yet unexplained circumstances *in vivo* allow VPF/VEGF to induce endothelial cell division and migration despite high local serum concentrations. However, there is a much simpler and I think more satisfactory explanation that depends on VPF/VEGF's original activity as a highly potent vascular permeabilizing factor. By inducing vascular permeability *in vivo*, VPF/VEGF generates both *serum* and *fibrin* and together these can explain the formation of mature vascularized connective tissue stroma.

First, *serum* exerts powerful effects on cell gene expression. Chang et al. (2004) found that when fibroblasts were cultured in 10% serum, dramatic changes took place in the expression (up- or down-regulation) of a core group of some 677 genes, as compared when these cells were grown in low (0.1%) serum, i.e., under the conditions in which VPF/VEGF is effective as an endothelial cell mitogen and motogen[4]. Further, these same changes in gene expression are evident in important autochthonous human cancers (e.g., breast, prostate) where they correlate with the degree of tumor malignancy. The consequences of these multiple changes in gene expression are likely complex and difficult to assess, but the genes involved encode transcription factors, cell surface receptors, G protein signaling proteins, etc. and thus modulate many important cell pathways.

Second and equally important, *fibrin* has significant biological activities and is an important link in the chain of events leading to mature stroma generation. These activities were demonstrated convincingly by a simple experiment in which purified fibrin, prepared *in vitro*, was implanted in the skin of normal guinea pigs (Dvorak et al., 1987). The fibrin so deposited was gradually replaced by vascularized collagenous stroma, just as occurred in tumors and in healing wounds. The mechanisms by which these changes take place are not well understood, but fibrin has a number of properties that likely contribute [reviewed in Dvorak (2019)]. Fibrin provides structure as a provisional stroma. It binds many different integrins and so provides a promiscuous matrix for attachment, support and migration of fibroblasts, tumor and endothelial cells. In addition, fibrin can induce growth factor expression and it binds to and thereby sequesters growth factors, preventing their degradation by tissue proteases. Finally, several of fibrin's breakdown products have angiogenic activity.

In sum, once VPF/VEGF increases vascular permeability, clotting is activated in the extravascular space to generate serum and fibrin which together initiate a chain of events that leads to the formation of mature vascularized connective tissue stroma (**Figure 1**). The details of this process are likely to be complex and remain to be fully ascertained[5]. However, after VPF/VEGF has induced increased vascular permeability, there would seem to be no further need for it to act as an endothelial cell growth or motility factor.

A NEW HYPOTHESIS

The data summarized here have led to a new hypothesis that can better explain the mechanisms by which VPF/VEGF acts *in vivo* to induce stroma formation; it also offers a possible explanation for the limited effectiveness of anti-VEGF cancer therapies. The hypothesis states that VPF/VEGF induces stroma primarily by way of its potent "VPF" function. Increased vascular permeability introduces a plasma protein-rich exudate into tissues that sets in motion a fundamental pathophysiological process, the "wound healing response," which, once triggered, proceeds on "autopilot" (**Figure 1**). Tissue factor, expressed by many tumor cells and also by host connective tissue cells, initiates clotting of extravasated plasma to generate serum and to deposit fibrin; serum dramatically alters the gene expression pattern of tissue cells and, together with fibrin, promotes and supports the ingrowth of fibroblasts and new blood vessels. Because tumors and healing wounds are bathed in protein-rich serum, VEGF's mitogenic and motogenic actions on endothelial cells are likely to be severely limited. Over time fibrin is replaced by vascular connective tissue stroma, and finally by largely avascular connective tissue termed *scar* in wounds and *desmoplasia* in tumors. Simply introducing purified fibrin prepared *in vitro* into tissues can replicate this response (Dvorak et al., 1987 #75). Tumors thus can be regarded as parasites that by secreting VPF/VEGF trick the host into thinking that a wound is present, thereby inducing the host to trigger the wound healing response.

[4]It would be desirable to repeat these experiments with endothelial cells, but that is difficult because endothelial cells do not do well when cultured for long in low serum concentrations.

[5]For example, other leaked plasma proteins such as fibronectin, vitronectin, etc. have known biological activities that are likely to contribute but their roles in stroma formation have not as yet been investigated.

In this manner, tumors induce the stroma they require for survival and growth. By continuing to secrete VPF/VEGF indefinitely, tumors behave as wounds that are always healing but never heal. The healing process benefits the tumor at the expense of the host. Chronic inflammatory diseases make use of the same wound healing process, again by secreting VPF/VEGF. Anti-VEGF approaches to cancer have met with limited success, perhaps because once plasma has leaked into tissues, a powerful process has been set in motion that is difficult to impede.

DATA AVAILABILITY STATEMENT

The original contributions presented in the study are included in the article/supplementary material, further inquiries can be directed to the corresponding author.

ETHICS STATEMENT

The animal study was reviewed and approved by Beth Israel Deaconess Animal Care Committee.

AUTHOR CONTRIBUTIONS

HFD was entirely responsible for the work reported here.

FUNDING

This work was supported by NIH grants PO1 CA92644 and RO1CA142262, by SDG, and by a contract from the National Foundation for Cancer Research.

REFERENCES

Bridgeman, V. L., Vermeulen, P. B., Foo, S., Bilecz, A., Daley, F., Kostaras, E., et al. (2017). Vessel co-option is common in human lung metastases and mediates resistance to anti-angiogenic therapy in preclinical lung metastasis models. *J. Pathol.* 241, 362–374. doi: 10.1002/path.4845

Brown, L. F., Olbricht, S. M., Berse, B., Jackman, R. W., Matsueda, G., Tognazzi, K. A., et al. (1995). Overexpression of vascular permeability factor (VPF/VEGF) and its endothelial cell receptors in delayed hypersensitivity skin reactions. *J. Immunol.* 154, 2801–2807.

Brown, L. F., Yeo, K. T., Berse, B., Yeo, T. K., Senger, D. R., Dvorak, H. F., et al. (1992). Expression of vascular permeability factor (vascular endothelial growth factor) by epidermal keratinocytes during wound healing. *J. Exp. Med.* 176, 1375–1379. doi: 10.1084/jem.176.5.1375

Carr, J. M., Dvorak, A. M., and Dvorak, H. F. (1985). Circulating membrane vesicles in leukemic blood. *Cancer Res.* 45(Pt 2), 5944–5951.

Chang, H. Y., Sneddon, J. B., Alizadeh, A. A., Sood, R., West, R. B., Montgomery, K., et al. (2004). Gene expression signature of fibroblast serum response predicts human cancer progression: similarities between tumors and wounds. *PLoS Biol.* 2:E7. doi: 10.1371/journal.pbio.0020007

Colvin, R. B., and Dvorak, H. F. (1975). Role of the clotting system in cell-mediated hypersensitivity. II. Kinetics of fibrinogen/fibrin accumulation and vascular permeability changes in tuberculin and cutaneous basophil hypersensitivity reactions. *J. Immunol.* 114(Pt 2), 377–387.

Colvin, R. B., Johnson, R. A., Mihm, M. C. Jr., and Dvorak, H. F. (1973). Role of the clotting system in cell-mediated hypersensitivity. I. Fibrin deposition in delayed skin reactions in man. *J. Exp. Med.* 138, 686–698. doi: 10.1084/jem.138.3.686

Connolly, D. T., Heuvelman, D. M., Nelson, R., Olander, J. V., Eppley, B. L., Delfino, J. J., et al. (1989). Tumor vascular permeability factor stimulates endothelial cell growth and angiogenesis. *J. Clin. Invest.* 84, 1470–1478. doi: 10.1172/JCI114322

Detmar, M., Brown, L. F., Claffey, K. P., Yeo, K. T., Kocher, O., Jackman, R. W., et al. (1994). Overexpression of vascular permeability factor/vascular endothelial growth factor and its receptors in psoriasis. *J. Exp. Med.* 180, 1141–1146. doi: 10.1084/jem.180.3.1141

Dolberg, D. S., Hollingsworth, R., Hertle, M., and Bissell, M. J. (1985). Wounding and its role in RSV-mediated tumor formation. *Science* 230, 676–678. doi: 10.1126/science.2996144

Dvorak, A. M., Kohn, S., Morgan, E. S., Fox, P., Nagy, J. A., and Dvorak, H. F. (1996). The vesiculo-vacuolar organelle (VVO): a distinct endothelial cell structure that provides a transcellular pathway for macromolecular extravasation. *J. Leukoc Biol.* 59, 100–115. doi: 10.1002/jlb.59.1.100

Dvorak, H. F. (1986). Tumors: wounds that do not heal. Similarities between tumor stroma generation and wound healing. *N. Engl. J. Med.* 315, 1650–1659. doi: 10.1056/NEJM198612253152606

Dvorak, H. F. (2015a). Tumor stroma, tumor blood vessels, and antiangiogenesis therapy. *Cancer J.* 21, 237–243. doi: 10.1097/PPO.0000000000000124

Dvorak, H. F. (2015b). Tumors: wounds that do not heal-redux. *Cancer Immunol. Res.* 3, 1–11. doi: 10.1158/2326-6066.CIR-14-0209

Dvorak, H. F. (2019). Tumors: wounds that do not heal-a historical perspective with a focus on the fundamental roles of increased vascular permeability and clotting. *Semin. Thromb. Hemost.* 45, 576–592. doi: 10.1055/s-0039-1687908

Dvorak, H. F., Dickersin, G. R., Dvorak, A. M., Manseau, E. J., and Pyne, K. (1981a). Human breast carcinoma: fibrin deposits and desmoplasia. Inflammatory cell type and distribution. Microvasculature and infarction. *J. Natl. Cancer Inst.* 67, 335–345.

Dvorak, H. F., Quay, S. C., Orenstein, N. S., Dvorak, A. M., Hahn, P., Bitzer, A. M., et al. (1981b). Tumor shedding and coagulation. *Science* 212, 923–924. doi: 10.1126/science.7195067

Dvorak, H. F., Dvorak, A. M., Manseau, E. J., Wiberg, L., and Churchill, W. H. (1979a). Fibrin gel investment associated with line 1 and line 10 solid tumor growth, angiogenesis, and fibroplasia in guinea pigs. Role of cellular immunity, myofibroblasts, microvascular damage, and infarction in line 1 tumor regression. *J Natl. Cancer Inst.* 62, 1459–1472.

Dvorak, H. F., Orenstein, N. S., Carvalho, A. C., Churchill, W. H., Dvorak, A. M., Galli, S. J., et al. (1979b). Induction of a fibrin-gel investment: an early event in line 10 hepatocarcinoma growth mediated by tumor-secreted products. *J. Immunol.* 122, 166–174.

Dvorak, H. F., Harvey, V. S., Estrella, P., Brown, L. F., McDonagh, J., and Dvorak, A. M. (1987). Fibrin containing gels induce angiogenesis. Implications for tumor stroma generation and wound healing. *Lab. Invest.* 57, 673–686.

Dvorak, H. F., Harvey, V. S., and McDonagh, J. (1984). Quantitation of fibrinogen influx and fibrin deposition and turnover in line 1 and line 10 guinea pig carcinomas. *Cancer Res.* 44, 3348–3354.

Dvorak, H. F., Mihm, M. C. Jr., Dvorak, A. M., Johnson, R. A., Manseau, E. J., Morgan, E., et al. (1974). Morphology of delayed type hypersensitivity reactions in man. I. Quantitative description of the inflammatory response. *Lab. Invest.* 31, 111–130.

Dvorak, H. F., and Rickles, F. R. (2005). "Hemostasis and thrombosis in cancer," in *Hemostasis and Thrombosis. Basic Principles and Clinical Practice*, 5th Edn, eds R. W. Colman, J. Hirsh, V. J. Marder, A. W. Clowes, and J. N. George (Philadelphia: Lippincott Williams & Wilkins).

Dvorak, H. F., Senger, D. R., Dvorak, A. M., Harvey, V. S., and McDonagh, J. (1985). Regulation of extravascular coagulation by microvascular permeability. *Science* 227, 1059–1061. doi: 10.1126/science.3975602

Fava, R. A., Olsen, N. J., Spencer-Green, G., Yeo, K. T., Yeo, T. K., Berse, B., et al. (1994). Vascular permeability factor/endothelial growth factor (VPF/VEGF): accumulation and expression in human synovial fluids and rheumatoid synovial tissue. *J. Exp. Med.* 180, 341–346. doi: 10.1084/jem.180.1.341

Feldberg, W., and Miles, A. A. (1953). Regional variations of increased permeability of skin capillaries induced by a histamine liberator and their relation to the histamine content of the skin. *J. Physiol.* 120, 205–213. doi: 10.1113/jphysiol.1953.sp004885

Feng, D., Nagy, J. A., Dvorak, A. M., and Dvorak, H. F. (2000). Different pathways of macromolecule extravasation from hyperpermeable tumor vessels. *Microvasc. Res.* 59, 24–37. doi: 10.1006/mvre.1999.2207

Feng, D., Nagy, J. A., Hipp, J., Dvorak, H. F., and Dvorak, A. M. (1996). Vesiculo-vacuolar organelles and the regulation of venule permeability to macromolecules by vascular permeability factor, histamine, and serotonin. *J. Exp. Med.* 183, 1981–1986. doi: 10.1084/jem.183.5.1981

Feng, D., Nagy, J. A., Hipp, J., Pyne, K., Dvorak, H. F., and Dvorak, A. M. (1997). Reinterpretation of endothelial cell gaps induced by vasoactive mediators in guinea-pig, mouse and rat: many are transcellular pores. *J. Physiol.* 504(Pt 3), 747–761. doi: 10.1111/j.1469-7793.1997.747bd.x

Feng, D., Nagy, J. A., Pyne, K., Hammel, I., Dvorak, H. F., and Dvorak, A. M. (1999). Pathways of macromolecular extravasation across microvascular endothelium in response to VPF/VEGF and other vasoactive mediators. *Microcirculation* 6, 23–44. doi: 10.1080/713773925

Folkman, J. (1971). Tumor angiogenesis: therapeutic implications. *N. Engl. J. Med.* 285, 1182–1186. doi: 10.1056/NEJM197111182852108

Fu, Y., Nagy, J., Dvorak, A., and Dvorak, H. F. (2007). "Tumor blood vessels: structure and function," in *Cancer Drug Discovery and Function. Antiangiogenic Agents in Cancer Therapy*, eds B. Teicher and L. Ellis (Totowa, NJ: Humana Press).

Harris, N. L., Dvorak, A. M., Smith, J., and Dvorak, H. F. (1982). Fibrin deposits in Hodgkin's disease. *Am. J. Pathol.* 108, 119–129.

Holash, J., Maisonpierre, P. C., Compton, D., Boland, P., Alexander, C. R., Zagzag, D., et al. (1999). Vessel cooption, regression, and growth in tumors mediated by angiopoietins and VEGF. *Science* 284, 1994–1998. doi: 10.1126/science.284.5422.1994

Keck, P. J., Hauser, S. D., Krivi, G., Sanzo, K., Warren, T., Feder, J., et al. (1989). Vascular permeability factor, an endothelial cell mitogen related to PDGF. *Science* 246, 1309–1312. doi: 10.1126/science.2479987

Leung, D. W., Cachianes, G., Kuang, W. J., Goeddel, D. V., and Ferrara, N. (1989). Vascular endothelial growth factor is a secreted angiogenic mitogen. *Science* 246, 1306–1309. doi: 10.1126/science.2479986

Li, J., Brown, L. F., Hibberd, M. G., Grossman, J. D., Morgan, J. P., and Simons, M. (1996). VEGF, flk-1, and flt-1 expression in a rat myocardial infarction model of angiogenesis. *Am. J. Physiol.* 270(Pt 2), H1803–H1811.

Majno, G., and Joris, I. (2004). *Cells, Tissues, and Diseases. Principles of General Pathology*. New York, NY: Oxford University Press.

Majno, G., and Palade, G. E. (1961). Studies on inflammation. 1. The effect of histamine and serotonin on vascular permeability: an electron microscopic study. *J. Biophys. Biochem. Cytol.* 11, 571–605.

Majno, G., Palade, G. E., and Schoefl, G. I. (1961). Studies on inflammation. II. The site of action of histamine and serotonin along the vascular tree: a topographic study. *J. Biophys. Biochem. Cytol.* 11, 607–626.

Nagy, J. A., Benjamin, L., Zeng, H., Dvorak, A. M., and Dvorak, H. F. (2008). Vascular permeability, vascular hyperpermeability and angiogenesis. *Angiogenesis* 11, 109–119. doi: 10.1007/s10456-008-9099-z

Nagy, J. A., Chang, S. H., Shih, S. C., Dvorak, A. M., and Dvorak, H. F. (2010). Heterogeneity of the tumor vasculature. *Semin. Thromb. Hemost.* 36, 321–331. doi: 10.1055/s-0030-1253454

Nagy, J. A., Dvorak, A. M., and Dvorak, H. F. (2012). Vascular hyperpermeability, angiogenesis, and stroma generation. *Cold Spring Harb. Perspect. Med.* 2:a006544. doi: 10.1101/cshperspect.a006544

Nagy, J. A., Dvorak, H. F., and Dvorak, A. M. (2007). VEGF-A and the induction of pathological angiogenesis. *Annu. Rev. Pathol. Mech. Dis.* 2, 251–275. doi: 10.1146/annurev.pathol.2.010506.134925

Nagy, J. A., Feng, D., Vasile, E., Wong, W. H., Shih, S. C., Dvorak, A. M., et al. (2006). Permeability properties of tumor surrogate blood vessels induced by VEGF-A. *Lab. Invest.* 86, 767–780. doi: 10.1038/labinvest.3700436

Palade, G. (1988). "The microivascular endothelium revisited," in *Endothelial Cell Biology in Health and Disease*, eds N. Simionescu and M. Simionescu (New York, NY: Plenum Press).

Pettersson, A., Nagy, J. A., Brown, L. F., Sundberg, C., Morgan, E., Jungles, S., et al. (2000). Heterogeneity of the angiogenic response induced in different normal adult tissues by vascular permeability factor/vascular endothelial growth factor. *Lab. Invest.* 80, 99–115. doi: 10.1038/labinvest.3780013

Semenza, G. L. (2014). Oxygen sensing, hypoxia-inducible factors, and disease pathophysiology. *Annu. Rev. Pathol.* 9, 47–71. doi: 10.1146/annurev-pathol-012513-104720

Senger, D. R., Galli, S. J., Dvorak, A. M., Perruzzi, C. A., Harvey, V. S., and Dvorak, H. F. (1983). Tumor cells secrete a vascular permeability factor that promotes accumulation of ascites fluid. *Science* 219, 983–985. doi: 10.1126/science.6823562

Senger, D. R., Perruzzi, C. A., Feder, J., and Dvorak, H. F. (1986). A highly conserved vascular permeability factor secreted by a variety of human and rodent tumor cell lines. *Cancer Res.* 46, 5629–5632.

Sitohy, B., Chang, S., Sciuto, T. E., Masse, E., Shen, M., Kang, P. M., et al. (2017). Early actions of anti-vascular endothelial growth factor/vascular endothelial growth factor receptor drugs on angiogenic blood vessels. *Am. J. Pathol.* 187, 2337–2347. doi: 10.1016/j.ajpath.2017.06.010

Stiver, S. I., Tan, X., Brown, L. F., Hedley-Whyte, E. T., and Dvorak, H. F. (2004). VEGF-A angiogenesis induces a stable neovasculature in adult murine brain. *J. Neuropathol. Exp. Neurol.* 63, 841–855. doi: 10.1093/jnen/63.8.841

Tarn, A. C., and Lapworth, R. (2010). Biochemical analysis of ascitic (peritoneal) fluid: what should we measure? *Ann. Clin. Biochem.* 47(Pt 5), 397–407. doi: 10.1258/acb.2010.010048

Van De Water, L., Tracy, P. B., Aronson, D., Mann, K. G., and Dvorak, H. F. (1985). Tumor cell generation of thrombin via functional prothrombinase assembly. *Cancer Res.* 45(Pt 1), 5521–5525.

Yeo, T. K., Senger, D. R., Dvorak, H. F., Freter, L., and Yeo, K. T. (1991). Glycosylation is essential for efficient secretion but not for permeability-enhancing activity of vascular permeability factor (vascular endothelial growth factor). *Biochem. Biophys. Res. Commun.* 179, 1568–1575. doi: 10.1016/0006-291x(91)91752-x

Conflict of Interest: The author declares that the research was conducted in the absence of any commercial or financial relationships that could be construed as a potential conflict of interest.

Copyright © 2021 Dvorak. This is an open-access article distributed under the terms of the Creative Commons Attribution License (CC BY). The use, distribution or reproduction in other forums is permitted, provided the original author(s) and the copyright owner(s) are credited and that the original publication in this journal is cited, in accordance with accepted academic practice. No use, distribution or reproduction is permitted which does not comply with these terms.

frontiers in Cell and Developmental Biology

MINI REVIEW
published: 29 March 2021
doi: 10.3389/fcell.2021.664696

Endothelial Cell Behavior Is Determined by Receptor Clustering Induced by Thrombospondin-1

Verônica Morandi[1], Jim Petrik[2] and Jack Lawler[3]**

[1] Rio de Janeiro State University (UERJ), Rio de Janeiro, Brazil, [2] University of Guelph, Guelph, ON, Canada, [3] Beth Israel Deaconess Medical Center, Harvard Medical School, Boston, MA, United States

The thrombospondins (TSPs) are a family of multimeric extracellular matrix proteins that dynamically regulate cellular behavior and response to stimuli. In so doing, the TSPs directly and indirectly affect biological processes such as embryonic development, wound healing, immune response, angiogenesis, and cancer progression. Many of the direct effects of Thrombospondin 1 (TSP-1) result from the engagement of a wide range of cell surface receptors including syndecans, low density lipoprotein receptor-related protein 1 (LRP1), CD36, integrins, and CD47. Different or even opposing outcomes of TSP-1 actions in certain pathologic contexts may occur, depending on the structural/functional domain involved. To expedite response to external stimuli, these receptors, along with vascular endothelial growth factor receptor 2 (VEGFR2) and Src family kinases, are present in specific membrane microdomains, such as lipid rafts or tetraspanin-enriched microdomains. The molecular organization of these membrane microdomains and their constituents is modulated by TSP-1. In this review, we will describe how the presence of TSP-1 at the plasma membrane affects endothelial cell signal transduction and angiogenesis.

Keywords: angiogenesis, CD36, syndecan, thrombospondin, CD47, integrin, endothelial cell

OPEN ACCESS

Edited by:
Bin Ren,
University of Alabama at Birmingham, United States

Reviewed by:
David D. Roberts,
National Institutes of Health (NIH), United States
Jun Feng,
Alpert Medical School, Brown University, United States

****Correspondence:***
Jack Lawler
jlawler@bidmc.harvard.edu
Jim Petrik
jpetrik@uoguelph.ca

Specialty section:
This article was submitted to Signaling, a section of the journal Frontiers in Cell and Developmental Biology

Received: *05 February 2021*
Accepted: *10 March 2021*
Published: *29 March 2021*

Citation:
Morandi V, Petrik J and Lawler J (2021) Endothelial Cell Behavior Is Determined by Receptor Clustering Induced by Thrombospondin-1. Front. Cell Dev. Biol. 9:664696. doi: 10.3389/fcell.2021.664696

INTRODUCTION

Like most biological processes, formation of the vasculature is temporally and spatially regulated by a balance of the signals that are elicited by stimulators and inhibitors. The temporal changes in the levels of these factors in the microenvironment determines endothelial cell behavior. In normal adult tissue, the endothelium is in a quiescent state, but it can respond rapidly to form new capillaries through a process termed angiogenesis. To facilitate a rapid response, the constituents of the pro- and anti-angiogenic pathways are co-localized to specific regions of the plasma membrane, such as lipid rafts and tetraspanin-enriched microdomains (Garcia-Parajo et al., 2014). The recruitment of specific proteins and lipids to these clusters is a critical determinant of their function. This spatial compartmentalization of the pathway components facilitates the efficient regulation of signal transduction that is essential for correct physiological response.

Thrombospondin 1 (TSP-1) is a founding member of the matricellular family of proteins (Adams and Lawler, 2011). These proteins are expressed primarily at the cell surface where they participate in the dynamic changes that cells undergo in response to extracellular stimuli. TSP-1 is involved in cell-to-cell junctions in synapses and immune cell interactions (Soto-Pantoja et al., 2015; Risher et al., 2018). As an example of the simplest form of cell-to-cell interaction, TSP-1 forms a molecular bridge between integrins on apoptotic neutrophils and CD36 on macrophages (Ren and Savill, 1995). TSP-1 is also highly expressed in supramolecular attack particles that are

made by cytotoxic T lymphocytes (Balint et al., 2020). A molecular layer of TSP-1 on the attack particles presumably functions to engage the target cell (Balint et al., 2020). TSP-1 also participates in the lateral association of membrane proteins within a single cell, such as endothelial cells where it affects the association of proteins involved in angiogenesis pathways. Taken together, the data indicate that TSP-1 brings membrane proteins together, either on the same cell or adjacent cells, to regulate cellular behavior.

Thrombospondin 1 is a large multimeric extracellular matrix protein that is expressed at sites of normal tissue development, remodeling, and repair (Adams and Lawler, 2011). In cutaneous wounds, TSP-1 is deposited by platelets to accelerate wound closure (Agah et al., 2002). Its coordinated expression with vascular endothelial growth factor (VEGF) is important for normal ovarian follicular development (Michaely et al., 2004). As a physiological activator of latent TGFβ, TSP-1 is also involved in fibrotic and immune response (Murphy-Ullrich and Suto, 2018). Additionally, TSP-1 expression is altered during pathological conditions such as myocardial infarction and cancer (Frangogiannis et al., 2005; Stenina-Adognravi et al., 2018).

Thrombospondin 1 antagonizes angiogenesis through multiple mechanisms, several of which suppress the bioavailability of VEGF. TSP-1 inhibits MMP9 activity and suppresses the release of VEGF from the extracellular matrix (Rodriguez-Manzaneque et al., 2001). TSP-1 also binds VEGF and supports its clearance through an lipoprotein receptor-related protein (LRP)-dependent mechanism (Greenaway et al., 2007). A significant portion of the direct anti-angiogenic activity of TSP-1 maps to the three, thrombospondin type 1 repeats, designated 3TSR (Russell et al., 2015). These repeats, which were first identified in TSP-1, contain binding sites for TGFβ and CD36 (Tan et al., 2002). As described below, the binding of TSP-1 to CD36 activates apoptosis pathways in endothelial cells.

The ability of TSP-1 to strongly bind heparin has long been identified and used as a strategic tool for purifying the protein from human platelets (Lawler et al., 1978; Sipes et al., 2018). Physiologically, this affinity for heparin may reflect the capacity of TSP-1 to bind to heparan sulfate (HS) and to heparan sulfate proteoglycans (HSPG; Sun et al., 1989). Binding to HS/HSPG has direct consequences for the role played by TSP-1 in endothelial cell adhesion, proliferation, motility, differentiation, and in the modulation of activity of angiogenic growth factors (Vischer et al., 1988; Vogel et al., 1993; Nunes et al., 2008).

The globular pentraxin-like heparin-binding N-terminal domain (HBD) of TSP-1 bears the main high-affinity sites for binding to heparin/HS (Clezardin et al., 1997). A prototypical BBXB consensus heparin/HS-binding motif (where B represents basic amino acids) in the HBD is represented by the amino acid sequence MKKTRG (residues 79-84), while the sequences ARKGSGRR (residues 22–29) and TRDLASIARLRIAKGVNDNF (residues 170–189) lack this BBXB configuration. However, both are enriched in positively charged residues, essential for the electrostatic interactions playing a major role in the binding of heparin/HS to proteins (Munoz and Linhardt, 2004). Heparin-binding sites have also been identified in the three type-I repeats or properdin-like domains (Guo et al., 1992; Yu et al., 2000) but, while studies have confirmed the essential requirement for the HBD in the interaction of TSP-1 with heparin/HS chains, it remains unclear whether these secondary heparin binding sites are indeed functional in the intact molecule (Yu et al., 2000). So far, TSP-1 interactions with perlecan (Vischer et al., 1997; Feitsma et al., 2000), decorin (Winnemoller et al., 1992; Merle et al., 1997), and some members of the syndecan (SDC) family of HSPG (see below) have already been described.

In this review, we will focus on the well-characterized interactions of TSP-1 with SDCs, lipoprotein receptor-related protein 1 (LRP1), CD36, integrins, and CD47 in the context of endothelial cell phenotype and angiogenesis (**Figure 1**). We will discuss how the downstream signals elicited by engagement of these receptors are integrated to determine endothelial cell behavior.

SYNDECANS AS RECEPTORS FOR TSP-1

Mammalian SDCs comprise four cell surface members bearing type-I (single-pass) core proteins, with highly conserved short cytoplasmic domains, a transmembrane domain and a varying length extracellular domain, covalently substituted with HS chains (chondroitin or dermatan-sulfate chains may also be present occasionally, to a lesser extent) (Couchman, 2003). SDCs act as receptors or coreceptors for extracellular matrix, growth factors, chemokines, interleukins, and morphogens (Chung et al., 2016) and can engage laterally with other classes of receptors, such as integrins and tyrosine kinase receptors for growth factors (FGFR1, EGFR, among others) (Couchman, 2003), thus contributing to the triggering and modulation of pivotal signaling including PKCα, Akt, and Wnt pathways (Gondelaud and Ricard-Blum, 2019). Indeed, there is growing evidence that SDCs are key parts of processes that involve tissue remodeling, such as development, cancer, inflammation, and tissue repair (Chung et al., 2016). TSP-1 bound to a HSPG recognized by a monoclonal antibody later shown to react specifically with the SDC1 isoform, in mammary epithelial cells (Sun et al., 1989). Both molecules were also found colocalized during lung development (Corless et al., 1992).

Although all four isoforms of SDC have been to some extent implicated in the modulation of endothelial angiogenic differentiation (De Rossi and Whiteford, 2014), a major role for syndecan-4 (SDC-4) seems to prevail over other SDC isoforms, in the context of angiogenesis associated with inflammatory and mechanical stimuli, as well as with injuries occurring in the cardiovascular system (Matsui et al., 2011; Vuong et al., 2015; Russo et al., 2020). SDC-4-null mice exhibit delayed dermal wound repair and defective angiogenesis (Echtermeyer et al., 2001).

Among SDCs, SDC-4 isoform has a unique role in the formation of fibronectin (FN)-induced focal adhesions, in cooperation with β1-integrin receptors (Woods and Couchman, 1994). As other matricellular proteins found in the ECM, TSP-1 destabilizes focal adhesions (Murphy-Ullrich and Sage, 2014),

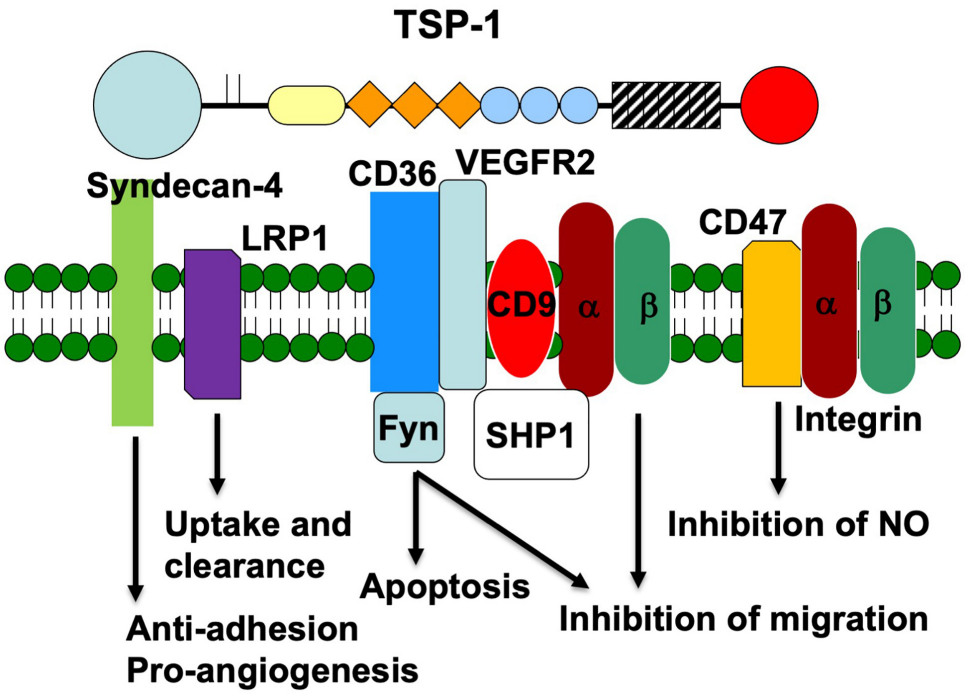

FIGURE 1 | Schematic representation of the endothelial cell receptors that interact with the various domains of TSP-1. The receptors are placed under the domain with which they interact. The signaling proteins that associate with each receptor and the signal that is transduced are also indicated.

and this activity was specifically located in the HBD domain of TSP-1, in endothelial models (Murphy-Ullrich et al., 1993; Vogel et al., 1993). Interestingly, pro-angiogenic activities of TSP-1 have also been attributed to HBD (Chandrasekaran et al., 2000; Taraboletti et al., 2000; Ferrari do Outeiro-Bernstein et al., 2002).

A 18 kDa HBD comprising the amino acid sequence 1–174—but not intact TSP-1—was able to stimulate tubulogenesis (Ferrari do Outeiro-Bernstein et al., 2002) when physically incorporated into fibrin plugs, a 3D support largely considered as a "provisional matrix" comparable to inflammatory edema and tumor microenvironments (Dvorak, 2015). The two sequences known for both containing affinity for GAGs (TSP-HepI, aa 17–35 and TSP-HepII, aa 78–94) and destabilizing focal adhesions (Murphy-Ullrich et al., 1993) retained the major pro-angiogenic activity of HBD (Nunes et al., 2008). Competitive binding assays indicated that the two TSP-1 motifs could exert their effects by interfering with the recognition of the high-affinity C-terminal heparin-binding domain of FN (FN HepII) by cell surface SDC-4. However, it is important to note that this interference in the action of FN did not affect the maintenance of cell viability, since pathways activated by SDC-4 in its regular role in focal adhesions, e.g., its ability to promote the sequential activation of protein-kinase C-α (PKC-α, a hallmark of SDC-4 activation) and phosphoinositide 3-kinase (PI3K), which in turn activates Akt/protein-kinase B (PKB; Oh et al., 1997; Ilan et al., 1998), were also activated by the HBD domain and its angiogenic peptides TSP-HepI and TSP-HepII (Nunes et al., 2008). These data suggest that, in tissue remodeling microenvironments, the N-terminal HBD possibly generated by proteases may provide the appropriate level of adhesion relaxation of endothelial cells engaged in tubulogenesis, while preserving cell viability.

Additional evidence for the biological relevance of pro-angiogenic activities of the HBD domain of TSP-1 came from studies performed with endothelial colony-forming cells (ECFC), or endothelial progenitor cells, isolated from human cord blood (Dias et al., 2012). Besides stimulating endothelial tubulogenesis of ECFC, as previously observed with adult primary endothelial cells (HUVECs; Nunes et al., 2008), TSP-HepI peptide strongly potentiated FGF-2 angiogenic activity *in vivo*, in the Matrigel plug model.

Adhesion to established endothelial layers is one of the key steps of endothelial progenitor recruitment to ischemic/inflammatory sites. It was shown that the overnight pre-conditioning of ECFC with soluble TSP-HepI (but not with intact TSP-1) significantly increased the adhesion of progenitors to HUVEC monolayers under shear flow (Dias et al., 2012). Interestingly, pre-conditioning with TSP-HepI also resulted in augmented levels of α6 integrin chain on ECFC surfaces. The presence of a neutralizing anti-SDC-4 antibody during the pre-conditioning of ECFC with TSP-HepI inhibited their adhesion to HUVEC monolayers by 84%. While the exact mechanisms for these effects remain to be explored, these data suggested a role of HBD domain in "priming" SDC-4/α6β1 cooperation.

The study of the crystal structure of the HBD (amino acids 1–240) and its complex with a synthetic pentameric heparin (Tan et al., 2008) has shown that, although the positively charged residues of TSP-HepI and TSP-HepII are well separated on the primary sequence of HBD, they congregate to form a patch in

the tertiary structure of the domain. Thus, these heparin-binding motifs used for SDC-4 recognition might be accessible in native N-terminal fragments rapidly cleaved *in vitro* and in variable sizes by several proteases relevant to the vascular compartment (Bonnefoy and Legrand, 2000; Morandi, 2009).

LRP1 AS A RECEPTOR FOR TSP-1

The low density LRP1 is a large cell surface receptor that mediates the endocytosis of a number of different ligands including apolipoprotein E-enriched lipoproteins, protease inhibitor complexes, and matrix proteins including TSP-1 (Lillis et al., 2005). LRP1 is a member of the low-density lipoprotein (LDL) receptor family, which contains seven members that are closely related including the LDL receptor, very low density lipoprotein (VLDL) receptor, apoE receptor2, multiple epidermal growth factor-like domains 7 (MEGF7), glycoprotein 330 (gp330/megalin/LRP2), LRP1, and LRP1B. Similar to the other family members, LRP1 contains several modular structures including cysteine-rich complement-type repeats, EGF repeats, β-propeller domains, a transmembrane domain, and a cytoplasmic domain (Herz et al., 1990). LRP-1 is expressed by many tissues including liver, lung, and brain and in multiple cell types including hepatocytes, fibroblasts, smooth muscle cells, neurons, and macrophages (Moestrup et al., 1992).

Similar to the other family members, LRP1 is an endocytic receptor that at least partly functions to regulate the concentration of extracellular ligand by transporting these ligands through clathrin-coated pits into intracellular vesicles. LRP1 internalizes more than 40 ligands from the pericellular and extracellular environment, including proteinases, ECM proteins, growth factors, and cell surface receptors (Strickland et al., 2002).

Lipoprotein receptor-related protein 1 recognizes a vast number of different ligands and thus mechanisms must be present to inhibit premature association with ligands in the endoplasmic reticulum and allow for proper targeting to the plasma membrane. To facilitate this, the chaperone receptor associated protein (RAP) binds LRP1 with high affinity at multiple sites and antagonizes ligand binding while it is in the endoplasmic reticulum (Herz et al., 1991; Williams et al., 1992).

Lipoprotein receptor-related protein 1 binds TSP-1 at the N-terminal heparin-binding domain, resulting in internalization and degradation in lysosomes (Chen et al., 1996). Through this internalization, TSP-1 can act as a bridging molecule between LRP1 and extracellular ligands and facilitate their clearance. TSP1/LRP-1 binding has been reported to be an important mechanism of clearing matrix metalloproteinases (MMPs) from the extracellular space (Bein and Simons, 2000; Yang et al., 2001). TSP-1 can also associate with cell surface proteoglycans and undergo endocytosis and degradation in an LRP-1-dependent fashion (Godyna et al., 1995; Mikhailenko et al., 1995). LRP-1 and TSP-1 can also act as co-receptors and in the presence of calreticulin can initiate a signaling cascade that results in focal adhesion disassembly (Orr et al., 2003). In the ovary, TSP-1 has been shown to participate in the clearance of VEGF via LRP1, reducing VEGF bioavailability and inhibiting ovarian follicular angiogenesis (Greenaway et al., 2007). TSP-1 also reduces the bioavailability of fibroblast growth factor 2 and hepatocyte growth factor/scatter factor (HGF/SF; Margosio et al., 2003).

CD36 AS A RECEPTOR FOR TSP-1

CD36 is a transmembrane glycoprotein that is a member of the class B scavenger receptor family. It functions as a long chain fatty acid translocase and a receptor for TSP-1, TSP-2, and collagen (Silverstein and Febbraio, 2009). Through these interactions, CD36 participates in a wide range of physiological processes, including fatty acid metabolism, atherosclerosis, and angiogenesis. CD36 mediates the inhibition of endothelial cell migration and proliferation by TSP-1. Significant quantities of CD36 are found in platelets, macrophages, adipocytes and endothelial cells (Silverstein and Febbraio, 2009). In general, CD36 is expressed on small, but not large, vessel endothelial cells (Luscinskas and Lawler, 1994). Whereas the expression of integrins on tumor vessels was found to vary with the stage of tumor progression in the Rip-Tag model of pancreatic cancer, CD36 is expressed at all stages (Xie et al., 2011). CD36 is a well characterized receptor for TSP-1 in endothelial cells (Jimenez et al., 2000). Engagement of CD36 by TSP-1 activates Fyn, JNK, and p38MAPK to induce apoptosis through activation of caspase-8- and -9-dependent pathways (Jimenez et al., 2000).

The membrane localization of CD36 and its mobility in the plasma membrane has been well studied. CD36 has been reported to be enriched in lipid rafts and tetraspanin-enriched microdomains (Miao et al., 2001; Thorne et al., 2006). The tetraspanins are a family of proteins that contain four transmembrane domains (Hemler, 2014; van Deventer et al., 2020). They undergo homo- and heterotypic association to form distinct regions in the plasma membrane that are enriched in integrins and other membrane proteins. The N- and C-terminals of CD36 contain short intracellular sequences that do not contain consensus sequences for the docking of signal transduction proteins. Thus, CD36 is thought to initiate signal transduction indirectly through complex formation with lipids, integrins and itself. In platelets, the association of CD36 with the Src family kinase Lyn is reportedly mediated by lipids (Thorne et al., 2006). However, the specific Src family kinase that is immunoprecipitated with CD36 depends upon the presence of TSP-1 (Sun et al., 2009). In endothelial cells from wild-type mice, CD36 associates with Fyn and the quantity of Fyn that co-immunoprecipitates with CD36 increases when 3TSR is added. In TSP-1-null endothelial cells, Src replaces Fyn.

In 2006, Daviet et al. (1997) reported that CD36 exists as monomers and dimers in the plasma membrane. Whereas the addition of TSP-1 increases the formation of CD36 dimers in the membrane, TSP-1 did not induce dimerization of a soluble form of CD36. A more recent study reported that over-expression of CD36 in an immortalized endothelial cell line resulted in 40% of the CD36 molecules localizing to nanoclusters that contained as many as 75 CD36 molecules (Githaka et al., 2016). These nanoclusters are enriched in Fyn and F-actin. The size of the clusters and the phosphorylation of Fyn increases after addition of TSP-1 or an anti-CD36 IgM molecule (Githaka et al., 2016). The formation of

nanoclusters is likely facilitated by the fact the CD36 mobility in the plasma membrane is restricted by the cytoskeleton (Jaqaman et al., 2011).

The clustering of CD36 promotes signal transduction through recruitment of other membrane proteins, such as integrins, and signaling molecules, such as Fyn and Syk (**Figure 2**; Kazerounian et al., 2011). Complex formation of CD36 with the tetraspanins CD9, CD81, and CD151 in platelets and endothelial cells has been reported (Miao et al., 2001; Kazerounian et al., 2011). In addition, association with αv, α5, β1, and β2 integrins has been detected (Kazerounian et al., 2011). Since TSP-1 can engage integrins in the absence of CD36 (see below), it may form multivalent complexes with these proteins. In monocytes, the interaction of Syk with CD36 is reportedly mediated by integrins and FcRγ (Heit et al., 2013).

In the context of angiogenesis, the association of CD36 with VEGF receptor 2 (VEGFR2) is a particularly intriguing one because it places receptors involved in pro- and anti-angiogenic signaling in close proximity and raises the possibility that these complexes function as molecular angiogenic switches (Primo et al., 2005). Interestingly, this interaction is markedly reduced in the absence of TSP-1 (Primo et al., 2005; Zhang et al., 2009). VEGFR2 is a key receptor for the stimulation of endothelial cell proliferation and migration by VEGF during physiological and pathological angiogenesis (Simons et al., 2016). The close juxtaposition of a pro-angiogenic signaling receptor with CD36 offers a second pathway through which TSP-1 can antagonize angiogenesis. This pathway involves the recruitment of the phosphatase SHP1 to the CD36/VEGFR2 complex (Chu et al., 2013). SHP1 dephosphorylates VEGFR2 and suppresses the recruitment of pro-angiogenic, downstream signaling proteins. Addition of TSP-1 increases the quantity of SHP1 associated with VEGFR2 in endothelial and ovarian cancer cells (Russell et al., 2015). The inhibition of VEGFR2 phosphorylation by TSP-1 is disrupted when CD36 is mutated so as to lose its ability to interact with β1 integrins (Primo et al., 2005).

Taken together, the data indicate that CD36 forms complexes with multiple other membrane proteins to affect endothelial behavior. Extracellular TSP-1 affects endothelial cell response to stimuli by modulating the composition of these complexes. The complexes that form may be heterogeneous in their composition and size.

INTEGRIN BINDING TO TSP-1

The integrins are a family of heterodimeric membrane proteins that function as receptors for extracellular matrix molecules, including collagens, FN, vitronectin, and laminins (Hynes, 2002; Luo et al., 2007). The term integrin was coined to reflect the integral role of these protein complexes as mediators of communication between the extracellular matrix and the cytoskeleton (Tamkun et al., 1986). In addition, a subset of integrins can activate TGFβ (Munger et al., 1999; Mu et al., 2002). An early comparison of platelet GPIIb/GPIIIa and endothelial cell αVβ3 was one of the first indications that integrins are an extensive family of proteins, with various members expressed on virtually all cell types (Charo et al., 1986). Integrins are differentially expressed on large vessel and microvascular endothelial cells, and by various growth factors and cytokines (Luscinskas and Lawler, 1994). As indicated above, integrins are included in tetraspanin-enriched microdomains where they can associate with CD36 and VEGFR-2 in a TSP-1-dependent manner. The αv, α5, β1, and β2 integrins have been reported to be present in these complexes (Hemler, 2014; van Deventer et al., 2020).

A direct RGD-dependent interaction of TSP-1 with αvβ3 has been reported (Lawler et al., 1988; Chen et al., 2000). The RGD sequence of TSP-1 lies within the type 3 repeats, which are a contiguous set of calcium-binding sites. Removal of calcium results in a significant change in the conformation of the TSP-1 molecule and increases exposure of the RGD sequence (Sun et al., 1992). The structure of the type 3 repeats is stabilized by calcium and intrachain disulfide bonds (Tan et al., 2002). Sun et al. (1992) reported that partial reduction of the disulfide bonds in TSP-1 increases the exposure of the RGD sequence. A follow-up study by Hotchkiss et al. (1998) found a disulfide bond isomerase at the plasma membrane of endothelial cells that increased the accessibility of the RGD sequence of TSP-1. Microvascular endothelial cell attachment to and chemotaxis toward TSP-1 are inhibited by antibodies to β3 (Lawler et al., 1988; Taraboletti et al., 1990). TSP-1 may serve as a substrate for endothelial αvβ3 in wounds where high quantities of TSP-1 are deposited by activated platelets.

TSP-1 inhibits the migration of human umbilical vein endothelial cells, which lack CD36, through an integrin β1-dependent mechanism (Short et al., 2005). This pathway for inhibition of migration appears to involve PI3K. Interestingly, an antibody to β1 integrin also inhibits VEGF-induced migration of microvascular endothelial cells that do express CD36 in the presence of an anti-CD36 antibody (Short et al., 2005). These data underscore the close interaction between CD36 and integrins that may arise from their physical proximity in the plasma membrane.

As described above, the NH_2 domain of TSP-1 promotes angiogenesis through SDC-4 (Ferrari do Outeiro-Bernstein et al., 2002; Dias et al., 2012). This domain has also been reported to enhance angiogenesis through the α9β1 integrin on microvascular endothelial cells through pathways that involve Erk1/2 and paxillin (Staniszewska et al., 2007). The α3β1 and α4β1 integrins have also been reported to bind to the NH_2 domain of TSP-1 (Chandrasekaran et al., 2000; Calzada et al., 2004). The binding of α4β1 to TSP-1 was observed with venous but not microvascular endothelial cells (Calzada et al., 2004). The interaction of α3β1 and α4β1 integrins with TSP-1 reportedly promotes angiogenesis.

CD47 AS A RECEPTOR FOR TSP-1

CD47 is a 50 kDa transmembrane receptor, also known as integrin-associated protein (IAP), that was initially identified as a protein lost from red blood cells in patients with Rh-null hemolytic anemia (Miller et al., 1987). CD47 consists of an extracellular N-terminal IgV domain, five transmembrane

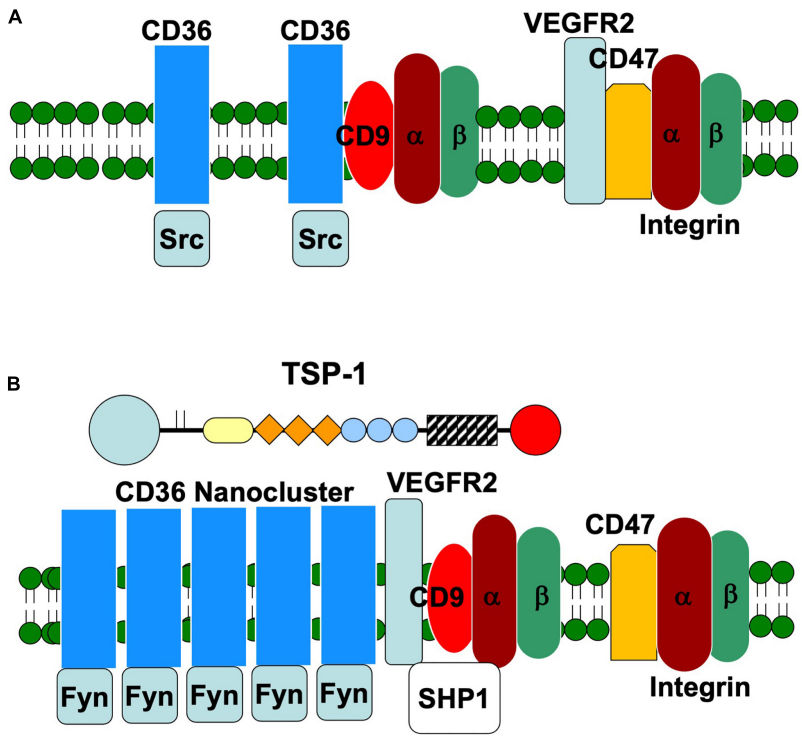

FIGURE 2 | Schematic representation of the organization of endothelial membrane proteins in the absence **(A)** and presence **(B)** of TSP-1. In the absence of TSP-1, Src co-immunoprecipitates with CD36. Fyn is preferentially associated with CD36 in the presence of TSP-1 and the formation of CD36 nanoclusters amplifies Fyn-mediated signal transduction. The presence of TSP-1 also promotes the dissociation of VEGFR2 from CD47 and the association of VEGFR2 with CD36. Integrins and SHP1 also complex with VEGFR2.

domains, and a short C-terminal intracellular tail (Mawby et al., 1994). Four alternatively spliced isoforms of CD47 exist, differing in the length of their cytoplasmic tails (Reinhold et al., 1995). CD47 has two main roles: as a ligand for the signal-regulatory protein alpha (SIRPα) and as a receptor for TSP-1. The CD47-SIRPα axis delivers inhibitory signals for phagocytosis and conveys a "don't eat me" signal that has important functions in hematopoiesis and innate immune surveillance (Tsai et al., 2010; McCracken et al., 2015; Horrigan and Reproducibility Project: Cancer Biology, 2017). Initial studies reported that CD47 is bound by TSP-1 at two peptide motifs on the carboxy-terminal domain (Gao et al., 2017). While partial conservation of some of these residues is found in TSP-2 and -4, CD47 only binds to TSP-1 with high affinity (Isenberg et al., 2009). Some molecules of CD47 contain proteoglycan side chains that are important for high-affinity TSP-1 binding and signaling (Kaur et al., 2011). The interaction with the proteoglycan moieties may be specific to TSP-1.

Thrombospondin 1 binding to CD47 has an inhibitory influence on VEGF signaling. CD47 constitutively associates with VEGFR2 on endothelial (Kaur et al., 2010) and tumor (Russell et al., 2015) cells. Binding of CD47 by TSP-1 inhibits the association between CD47 and VEGFR-2 and disrupts VEGFR2 phosphorylation (Kaur et al., 2010). Ligation by TSP-1 prevents VEGFR2 autophosphorylation, which decreases activation of endothelial nitric oxide synthase (eNOS) associated with Akt phosphorylation. This is consistent with the increased Akt phosphorylation seen in retinal vasculature (Sun et al., 2009) and in ovarian peri-follicular vasculature (Greenaway et al., 2007) of TSP-1 null mice. Similar to the receptor clustering seen with CD36, recent evidence suggests that clustering of CD47 is also required for the high-affinity binding of TSP-1 (Wang et al., 2020). These results suggest that in addition to the amount of CD47 available, the distribution pattern of the receptor is important in regulating TSP-1 signaling.

Activation of CD47 by TSP-1 ultimately inhibits Ca^{2+}/calmodulin-mediated activation of eNOS (Bauer et al., 2010), activation of soluble guanylate cyclase (sGC) by nitric oxide (NO; Isenberg et al., 2006), and downstream activation of cGMP-dependent protein kinase (Isenberg et al., 2008b). At physiologic concentrations of TSP-1 (100–200 pM), CD47 is thought to be the dominant receptor for the ligand in inhibiting activation of soluble guanylate cyclase or cGMP-dependent protein kinase (Isenberg et al., 2006, 2008b). Using a systems biology approach, it was determined that enhancing binding of TSP-1 to CD47 decreases the amount of unbound TSP-1 and protects TSP-1 from cleavage, enhancing the anti-angiogenic effect of the ligand (Rohrs et al., 2016).

By disrupting TSP-1/CD47 signaling, angiogenesis can be enhanced, which can have therapeutic benefit. Both TSP-1 and CD47 null mice have decreased necrosis and improved healing in the cutaneous flap model and in full-thickness skin grafts.

Skin grafts implanted on wild-type mice fail due to a lack of angiogenesis and tissue perfusion, while those grafted onto TSP-1 or CD47 null mice survive (Isenberg et al., 2008a). Similarly, pancreatic islet grafts have improved survival in TSP-1 null mice, due to increased angiogenesis (Olerud et al., 2008). Using function blocking antibodies to TSP-1 or CD47 has also been shown to reestablish perfusion in ischemic tissues in rodents and pigs (Isenberg et al., 2007, 2008a). In cancer, CD47 null mice had elevated VEGF and VEGFR2 expression and there was increased angiogenesis and accelerated tumor progression in a syngeneic murine model of prostate cancer (Gao et al., 2017).

In addition to its role in angiogenesis, TSP-1/CD47 binding is also involved in regulating tumor immunity. Ligation of CD47 on immune cells inactivates antitumor adaptive immunosurveillance and directly inhibits TCR-mediated T cell activation (Li et al., 2001, 2002). Through CD47, TSP-1 also reduces VEGF-induced immunosuppression in tumors (Kaur et al., 2014), and enhances antitumor immunity by stimulating CD8+cytotoxic T cells (Soto-Pantoja et al., 2014). TSP-1 signaling via CD47 also regulate NK and DC functions that impact adaptive immunity (Weng et al., 2014).

CONCLUSION AND FUTURE DIRECTIONS

In this review, we have highlighted the interaction of TSP-1 with endothelial membrane proteins (**Figure 1**). Through these many interactions, TSP-1 is able to direct the formation of supramolecular complexes that vary in composition over time to modulate the endothelial cell's response to environmental stimuli (Kazerounian and Lawler, 2018). The data indicate that endothelial cell behavior is determined at the level of the plasma membrane and thus early in the signal generation. The remodeling of membrane protein complexes that form in response to TSP-1 serves to integrate signals from pro- and anti-angiogenic stimuli. In the presence of TSP-1, VEGFR2 dissociates from CD47 and complexes with CD36, which results in enhanced association with integrins and SHP1, leading to dephosphorylation of VEGFR2 and suppression of VEGF signal transduction. TSP-1 also initiates an anti-angiogenic signal through CD36 that leads to decreased endothelial cell migration and apoptosis. This pathway is amplified by the ability of TSP-1 to drive the formation of CD36 nanoclusters, which in turn cluster Fyn. It is important to determine how the concentrations of TSP-1 and VEGF affect the above processes. Does the quantity of the various supramolecular complexes have a linear effect on the net signal, or are there thresholds that must be exceeded in order to initiate response in a stepwise fashion? Can the negative signal elicited by TSP-1 be reversed at some stages and not at others? In addition, our understanding of the role of integrins and their ligands in the way in which endothelial cells respond to TSP-1 is far from complete.

Since tumor growth experiments in TSP-1-null mice indicate that the absence of the intact molecule leads to increased angiogenesis, the pro-angiogenic activity of the NH_2 domain may be masked or outweighed by the anti-angiogenic activity of the TSRs and the C-terminal domain (Lawler et al., 2001; Xie et al., 2011). In addition, the type 3 repeats have been reported to inhibit angiogenesis by binding to fibroblast growth factor 2 (FGF2; Colombo et al., 2010). Proteolytic cleavage of TSP-1 may produce pro- and anti-angiogenic domains with distinct biological properties. Indeed, the first study to show that TSP-1 is anti-angiogenic detected a proteolytic fragment of TSP-1 in the condition media of p53 deficient fibroblasts from Li-Fraumeni patients (Dameron et al., 1994). This fragment was produced by a proteolytic cleavage between the HBD and the TSRs. We need to better understand the physiological conditions that lead to the release of the HBD from the intact molecule and the disposition of the two or more fragments that are produced. Do the two fragments have different biodistribution and/or stability? Like the intact molecule, the HBD has multiple ligands, including proteoglycans, LPR1, calreticulin and integrins.

AUTHOR CONTRIBUTIONS

All authors listed have made a substantial, direct and intellectual contribution to the work, and approved it for publication.

FUNDING

This work was supported by operating grants to JP from the Canadian Institutes for Health Research, Cancer Research Society, and Ovarian Cancer Canada. The project was also supported by a CAO Pilot Grant from the Beth Israel Deaconess Medical Center. VM received supports from the Brazilian federal agencies CAPES and CNPq, and from FAPERJ (a public funding organism of the Rio de Janeiro State).

ACKNOWLEDGMENTS

We thank Sami Lawler for editing the text.

REFERENCES

Adams, J. C., and Lawler, J. (2011). The thrombospondins. *Cold Spring Harb. Perspect. Biol.* 3:a009712.

Agah, A., Kyriakides, T. R., Lawler, J., and Bornstein, P. (2002). The lack of thrombospondin-1 (TSP1) dictates the course of wound healing in double-TSP1/TSP2-null mice. *Am. J. Pathol.* 161, 831–839. doi: 10.1016/s0002-9440(10)64243-5

Balint, S., Muller, S., Fischer, R., Kessler, B. M., Harkiolaki, M., Valitutti, S., et al. (2020). Supramolecular attack particles are autonomous killing entities released from cytotoxic T cells. *Science.* 368, 897–901. doi: 10.1126/science.aay9207

Bauer, E. M., Qin, Y., Miller, T. W., Bandle, R. W., Csanyi, G., Pagano, P. J., et al. (2010). Thrombospondin-1 supports blood pressure by limiting eNOS activation and endothelial-dependent vasorelaxation. *Cardiovasc. Res.* 88, 471–481. doi: 10.1093/cvr/cvq218

Bein, K., and Simons, M. (2000). Thrombospondin type 1 repeats interact with matrix metalloproteinase 2. Regulation of metalloproteinase activity. *J. Biol. Chem.* 275, 32167–32173. doi: 10.1074/jbc.m003834200

Bonnefoy, A., and Legrand, C. (2000). Proteolysis of subendothelial adhesive glycoproteins (fibronectin, thrombospondin, and von Willebrand factor) by plasmin, leukocyte cathepsin G, and elastase. *Thromb. Res.* 98, 323–332. doi: 10.1016/s0049-3848(99)00242-x

Calzada, M. J., Zhou, L., Sipes, J. M., Zhang, J., Krutzsch, H. C., Iruela-Arispe, M. L., et al. (2004). Alpha4beta1 integrin mediates selective endothelial cell responses to thrombospondins 1 and 2 in vitro and modulates angiogenesis in vivo. *Circ. Res.* 94, 462–470. doi: 10.1161/01.res.0000115555.05668.93

Chandrasekaran, L., He, C. Z., Al-Barazi, H., Krutzsch, H. C., Iruela-Arispe, M. L., and Roberts, D. D. (2000). Cell contact-dependent activation of alpha3beta1 integrin modulates endothelial cell responses to thrombospondin-1. *Mol. Biol. Cell.* 11, 2885–2900. doi: 10.1091/mbc.11.9.2885

Charo, I. F., Fitzgerald, L. A., Steiner, B., Rall, S. C. Jr., Bekeart, L. S., and Phillips, D. R. (1986). Platelet glycoproteins IIb and IIIa: evidence for a family of immunologically and structurally related glycoproteins in mammalian cells. *Proc. Natl. Acad. Sci. U.S.A.* 83, 8351–8355. doi: 10.1073/pnas.83.21.8351

Chen, H., Herndon, M. E., and Lawler, J. (2000). The cell biology of thrombospondin-1. *Matrix Biol.* 19, 597–614. doi: 10.1016/s0945-053x(00)00107-4

Chen, H., Sottile, J., Strickland, D. K., and Mosher, D. F. (1996). Binding and degradation of thrombospondin-1 mediated through heparan sulphate proteoglycans and low-density-lipoprotein receptor-related protein: localization of the functional activity to the trimeric N-terminal heparin-binding region of thrombospondin-1. *Biochem. J.* 318(Pt 3), 959–963. doi: 10.1042/bj3180959

Chu, L. Y., Ramakrishnan, D. P., and Silverstein, R. L. (2013). Thrombospondin-1 modulates VEGF signaling via CD36 by recruiting SHP-1 to VEGFR2 complex in microvascular endothelial cells. *Blood.* 122, 1822–1832. doi: 10.1182/blood-2013-01-482315

Chung, H., Multhaupt, H. A., Oh, E. S., and Couchman, J. R. (2016). Minireview: syndecans and their crucial roles during tissue regeneration. *FEBS Lett.* 590, 2408–2417. doi: 10.1002/1873-3468.12280

Clezardin, P., Lawler, J., Amiral, J., Quentin, G., and Delmas, P. (1997). Identification of cell adhesive active sites in the N-terminal domain of thrombospondin-1. *Biochem. J.* 321(Pt 3), 819–827. doi: 10.1042/bj3210819

Colombo, G., Margosio, B., Ragona, L., Neves, M., Bonifacio, S., Annis, D. S., et al. (2010). Non-peptidic thrombospondin-1 mimics as fibroblast growth factor-2 inhibitors: an integrated strategy for the development of new antiangiogenic compounds. *J. Biol. Chem.* 285, 8733–8742. doi: 10.1074/jbc.m109.085605

Corless, C. L., Mendoza, A., Collins, T., and Lawler, J. (1992). Colocalization of thrombospondin and syndecan during murine development. *Dev. Dyn.* 193, 346–358. doi: 10.1002/aja.1001930408

Couchman, J. R. (2003). Syndecans: proteoglycan regulators of cell-surface microdomains? *Nat. Rev. Mol. Cell Biol.* 4, 926–937. doi: 10.1038/nrm1257

Dameron, K. M., Volpert, O. V., Tainsky, M. A., and Bouck, N. (1994). Control of angiogenesis in fibroblasts by p53 regulation of thrombospondin-1. *Science.* 265, 1582–1584. doi: 10.1126/science.7521539

Daviet, L., Malvoisin, E., Wild, T. F., and McGregor, J. L. (1997). Thrombospondin induces dimerization of membrane-bound, but not soluble CD36. *Thromb. Haemost.* 78, 897–901. doi: 10.1055/s-0038-1657649

De Rossi, G., and Whiteford, J. R. (2014). Syndecans in angiogenesis and endothelial cell biology. *Biochem. Soc. Trans.* 42, 1643–1646. doi: 10.1042/bst20140232

Dias, J. V., Benslimane-Ahmim, Z., Egot, M., Lokajczyk, A., Grelac, F., Galy-Fauroux, I., et al. (2012). A motif within the N-terminal domain of TSP-1 specifically promotes the proangiogenic activity of endothelial colony-forming cells. *Biochem. Pharmacol.* 84, 1014–1023. doi: 10.1016/j.bcp.2012.07.006

Dvorak, H. F. (2015). Tumors: wounds that do not heal-redux. *Cancer Immunol. Res.* 3, 1–11. doi: 10.1158/2326-6066.cir-14-0209

Echtermeyer, F., Streit, M., Wilcox-Adelman, S., Saoncella, S., Denhez, F., Detmar, M., et al. (2001). Delayed wound repair and impaired angiogenesis in mice lacking syndecan-4. *J. Clin. Invest.* 107, R9–R14. doi: 10.1007/978-3-642-27814-3_85-2

Feitsma, K., Hausser, H., Robenek, H., Kresse, H., and Vischer, P. (2000). Interaction of thrombospondin-1 and heparan sulfate from endothelial cells. Structural requirements of heparan sulfate. *J. Biol. Chem.* 275, 9396–9402. doi: 10.1074/jbc.275.13.9396

Ferrari do Outeiro-Bernstein, M. A., Nunes, S. S., Andrade, A. C., Alves, T. R., Legrand, C., and Morandi, V. (2002). A recombinant NH(2)-terminal heparin-binding domain of the adhesive glycoprotein, thrombospondin-1, promotes endothelial tube formation and cell survival: a possible role for syndecan-4 proteoglycan. *Matrix Biol.* 21, 311–324. doi: 10.1016/s0945-053x(02)00010-0

Frangogiannis, N. G., Ren, G., Dewald, O., Zymek, P., Haudek, S., Koerting, A., et al. (2005). Critical role of endogenous thrombospondin-1 in preventing expansion of healing myocardial infarcts. *Circulation.* 111, 2935–2942. doi: 10.1161/circulationaha.104.510354

Gao, L., Chen, K., Gao, Q., Wang, X., Sun, J., and Yang, Y. G. (2017). CD47 deficiency in tumor stroma promotes tumor progression by enhancing angiogenesis. *Oncotarget* 8, 22406–22413. doi: 10.18632/oncotarget.9899

Garcia-Parajo, M. F., Cambi, A., Torreno-Pina, J. A., Thompson, N., and Jacobson, K. (2014). Nanoclustering as a dominant feature of plasma membrane organization. *J. Cell Sci.* 127(Pt 23), 4995–5005. doi: 10.1242/jcs.146340

Githaka, J. M., Vega, A. R., Baird, M. A., Davidson, M. W., Jaqaman, K., and Touret, N. (2016). Ligand-induced growth and compaction of CD36 nanoclusters enriched in Fyn induces Fyn signaling. *J. Cell Sci.* 129, 4175–4189. doi: 10.1242/jcs.188946

Godyna, S., Liau, G., Popa, I., Stefansson, S., and Argraves, W. S. (1995). Identification of the low density lipoprotein receptor-related protein (LRP) as an endocytic receptor for thrombospondin-1. *J. Cell Biol.* 129, 1403–1410. doi: 10.1083/jcb.129.5.1403

Gondelaud, F., and Ricard-Blum, S. (2019). Structures and interactions of syndecans. *FEBS J.* 286, 2994–3007. doi: 10.1111/febs.14828

Greenaway, J., Lawler, J., Moorehead, R., Bornstein, P., Lamarre, J., and Petrik, J. (2007). Thrombospondin-1 inhibits VEGF levels in the ovary directly by binding and internalization via the low density lipoprotein receptor-related protein-1 (LRP-1). *J. Cell Physiol.* 210, 807–818. doi: 10.1002/jcp.20904

Guo, N. H., Krutzsch, H. C., Negre, E., Vogel, T., Blake, D. A., and Roberts, D. D. (1992). Heparin- and sulfatide-binding peptides from the type I repeats of human thrombospondin promote melanoma cell adhesion. *Proc. Natl. Acad. Sci. U.S.A.* 89, 3040–3044. doi: 10.1073/pnas.89.7.3040

Heit, B., Kim, H., Cosio, G., Castano, D., Collins, R., Lowell, C. A., et al. (2013). Multimolecular signaling complexes enable Syk-mediated signaling of CD36 internalization. *Dev. Cell.* 24, 372–383. doi: 10.1016/j.devcel.2013.01.007

Hemler, M. E. (2014). Tetraspanin proteins promote multiple cancer stages. *Nat. Rev. Cancer* 14, 49–60. doi: 10.1038/nrc3640

Herz, J., Goldstein, J. L., Strickland, D. K., Ho, Y. K., and Brown, M. S. (1991). 39-kDa protein modulates binding of ligands to low density lipoprotein receptor-related protein/alpha 2-macroglobulin receptor. *J. Biol. Chem.* 266, 21232–21238. doi: 10.1016/s0021-9258(18)54845-6

Herz, J., Kowal, R. C., Goldstein, J. L., and Brown, M. S. (1990). Proteolytic processing of the 600 kd low density lipoprotein receptor-related protein (LRP) occurs in a trans-Golgi compartment. *EMBO J.* 9, 1769–1776. doi: 10.1002/j.1460-2075.1990.tb08301.x

Horrigan, S. K., and Reproducibility Project: Cancer Biology (2017). Replication study: the CD47-signal regulatory protein alpha (SIRPa) interaction is a therapeutic target for human solid tumors. *Elife* 6:e18173.

Hotchkiss, K. A., Matthias, L. J., and Hogg, P. J. (1998). Exposure of the cryptic Arg-Gly-Asp sequence in thrombospondin-1 by protein disulfide isomerase. *Biochim. Biophys. Acta.* 1388, 478–488. doi: 10.1016/s0167-4838(98)00211-8

Hynes, R. O. (2002). Integrins: bidirectional, allosteric signaling machines. *Cell.* 110, 673–687.

Ilan, N., Mahooti, S., and Madri, J. A. (1998). Distinct signal transduction pathways are utilized during the tube formation and survival phases of in vitro angiogenesis. *J. Cell Sci.* 111(Pt 24), 3621–3631.

Isenberg, J. S., Annis, D. S., Pendrak, M. L., Ptaszynska, M., Frazier, W. A., Mosher, D. F., et al. (2009). Differential interactions of thrombospondin-1, -2, and -4 with CD47 and effects on cGMP signaling and ischemic injury responses. *J. Biol. Chem.* 284, 1116–1125. doi: 10.1074/jbc.m804860200

Isenberg, J. S., Ridnour, L. A., Dimitry, J., Frazier, W. A., Wink, D. A., and Roberts, D. D. (2006). CD47 is necessary for inhibition of nitric oxide-stimulated vascular cell responses by thrombospondin-1. *J. Biol. Chem.* 281, 26069–26080. doi: 10.1074/jbc.m605040200

Isenberg, J. S., Romeo, M. J., Abu-Asab, M., Tsokos, M., Oldenborg, A., Pappan, L., et al. (2007). Increasing survival of ischemic tissue by targeting CD47. *Circ. Res.* 100, 712–720. doi: 10.1161/01.res.0000259579.35787.4e

Isenberg, J. S., Romeo, M. J., Maxhimer, J. B., Smedley, J., Frazier, W. A., and Roberts, D. D. (2008a). Gene silencing of CD47 and antibody ligation of thrombospondin-1 enhance ischemic tissue survival in a porcine model: implications for human disease. *Ann. Surg.* 247, 860–868. doi: 10.1097/sla.0b013e31816c4006

Isenberg, J. S., Romeo, M. J., Yu, C., Yu, C. K., Nghiem, K., Monsale, J., et al. (2008b). Thrombospondin-1 stimulates platelet aggregation by blocking the antithrombotic activity of nitric oxide/cGMP signaling. *Blood.* 111, 613–623. doi: 10.1182/blood-2007-06-098392

Jaqaman, K., Kuwata, H., Touret, N., Collins, R., Trimble, W. S., Danuser, G., et al. (2011). Cytoskeletal control of CD36 diffusion promotes its receptor and signaling function. *Cell.* 146, 593–606. doi: 10.1016/j.cell.2011.06.049

Jimenez, B., Volpert, O. V., Crawford, S. E., Febbraio, M., Silverstein, R. L., and Bouck, N. (2000). Signals leading to apoptosis-dependent inhibition of neovascularization by thrombospondin-1. *Nat. Med.* 6, 41–48. doi: 10.1038/71517

Kaur, S., Chang, T., Singh, S. P., Lim, L., Mannan, P., Garfield, S. H., et al. (2014). CD47 signaling regulates the immunosuppressive activity of VEGF in T cells. *J. Immunol.* 193, 3914–3924. doi: 10.4049/jimmunol.1303116

Kaur, S., Kuznetsova, S. A., Pendrak, M. L., Sipes, J. M., Romeo, M. J., Li, Z., et al. (2011). Heparan sulfate modification of the transmembrane receptor CD47 is necessary for inhibition of T cell receptor signaling by thrombospondin-1. *J. Biol. Chem.* 286, 14991–15002. doi: 10.1074/jbc.m110.179663

Kaur, S., Martin-Manso, G., Pendrak, M. L., Garfield, S. H., Isenberg, J. S., and Roberts, D. D. (2010). Thrombospondin-1 inhibits VEGF receptor-2 signaling by disrupting its association with CD47. *J. Biol. Chem.* 285, 38923–38932. doi: 10.1074/jbc.m110.172304

Kazerounian, S., and Lawler, J. (2018). Integration of pro- and anti-angiogenic signals by endothelial cells. *J. Cell Commun. Signal.* 12, 171–179. doi: 10.1007/s12079-017-0433-3

Kazerounian, S., Duquette, M., Reyes, M. A., Lawler, J. T., Song, K., Perruzzi, C., et al. (2011). Priming of the vascular endothelial growth factor signaling pathway by thrombospondin-1, CD36, and spleen tyrosine kinase. *Blood.* 117, 4658–4666. doi: 10.1182/blood-2010-09-305284

Lawler, J. W., Slayter, H. S., and Coligan, J. E. (1978). Isolation and characterization of a high molecular weight glycoprotein from human blood platelets. *J. Biol. Chem.* 253, 8609–8616. doi: 10.1016/s0021-9258(17)34336-3

Lawler, J., Miao, W. M., Duquette, M., Bouck, N., Bronson, R. T., and Hynes, R. O. (2001). Thrombospondin-1 gene expression affects survival and tumor spectrum of p53-deficient mice. *Am. J. Pathol.* 159, 1949–1956. doi: 10.1016/s0002-9440(10)63042-8

Lawler, J., Weinstein, R., and Hynes, R. O. (1988). Cell attachment to thrombospondin: the role of ARG-GLY-ASP, calcium, and integrin receptors. *J. Cell Biol.* 107(6 Pt 1), 2351–2361. doi: 10.1083/jcb.107.6.2351

Li, S. S., Ivanoff, A., Bergstrom, S. E., Sandstrom, A., Christensson, B., van Nerven, J., et al. (2002). T lymphocyte expression of thrombospondin-1 and adhesion to extracellular matrix components. *Eur. J. Immunol.* 32, 1069–1079. doi: 10.1002/1521-4141(200204)32:4<1069::aid-immu1069>3.0.co;2-e

Li, Z., He, L., Wilson, K., and Roberts, D. (2001). Thrombospondin-1 inhibits TCR-mediated T lymphocyte early activation. *J Immunol.* 166, 2427–2436. doi: 10.4049/jimmunol.166.4.2427

Lillis, A. P., Mikhailenko, I., and Strickland, D. K. (2005). Beyond endocytosis: LRP function in cell migration, proliferation and vascular permeability. *J. Thromb. Haemost.* 3, 1884–1893. doi: 10.1111/j.1538-7836.2005.01371.x

Luo, B. H., Carman, C. V., and Springer, T. A. (2007). Structural basis of integrin regulation and signaling. *Annu. Rev. Immunol.* 25, 619–647. doi: 10.1146/annurev.immunol.25.022106.141618

Luscinskas, F. W., and Lawler, J. (1994). Integrins as dynamic regulators of vascular function. *FASEB J.* 8, 929–938. doi: 10.1096/fasebj.8.12.7522194

Margosio, B., Marchetti, D., Vergani, V., Giavazzi, R., Rusnati, M., Presta, M., et al. (2003). Thrombospondin 1 as a scavenger for matrix-associated fibroblast growth factor 2. *Blood.* 102, 4399–4406. doi: 10.1182/blood-2003-03-0893

Matsui, Y., Ikesue, M., Danzaki, K., Morimoto, J., Sato, M., Tanaka, S., et al. (2011). Syndecan-4 prevents cardiac rupture and dysfunction after myocardial infarction. *Circ. Res.* 108, 1328–1339. doi: 10.1161/circresaha.110.235689

Mawby, W. J., Holmes, C. H., Anstee, D. J., Spring, F. A., and Tanner, M. J. (1994). Isolation and characterization of CD47 glycoprotein: a multispanning membrane protein which is the same as integrin-associated protein (IAP) and the ovarian tumour marker OA3. *Biochem. J.* 304(Pt 2), 525–530. doi: 10.1042/bj3040525

McCracken, M. N., Cha, A. C., and Weissman, I. L. (2015). Molecular pathways: activating T cells after cancer cell phagocytosis from blockade of CD47 "Don't Eat Me" signals. *Clin. Cancer Res.* 21, 3597–3601. doi: 10.1158/1078-0432.ccr-14-2520

Merle, B., Malaval, L., Lawler, J., Delmas, P., and Clezardin, P. (1997). Decorin inhibits cell attachment to thrombospondin-1 by binding to a KKTR-dependent cell adhesive site present within the N-terminal domain of thrombospondin-1. *J. Cell Biochem.* 67, 75–83. doi: 10.1002/(sici)1097-4644(19971001)67:1<75::aid-jcb8>3.0.co;2-t

Miao, W. M., Vasile, E., Lane, W. S., and Lawler, J. (2001). CD36 associates with CD9 and integrins on human blood platelets. *Blood* 97, 1689–1696. doi: 10.1182/blood.v97.6.1689

Michaely, P., Li, W. P., Anderson, R. G., Cohen, J. C., and Hobbs, H. H. (2004). The modular adaptor protein ARH is required for low density lipoprotein (LDL) binding and internalization but not for LDL receptor clustering in coated pits. *J. Biol. Chem.* 279, 34023–34031. doi: 10.1074/jbc.m405242200

Mikhailenko, I., Kounnas, M. Z., and Strickland, D. K. (1995). Low density lipoprotein receptor-related protein/alpha 2-macroglobulin receptor mediates the cellular internalization and degradation of thrombospondin. A process facilitated by cell-surface proteoglycans. *J. Biol. Chem.* 270, 9543–9549. doi: 10.1074/jbc.270.16.9543

Miller, Y. E., Daniels, G. L., Jones, C., and Palmer, D. K. (1987). Identification of a cell-surface antigen produced by a gene on human chromosome 3 (cen-q22) and not expressed by Rhnull cells. *Am. J. Hum. Genet.* 41, 1061–1070.

Moestrup, S. K., Gliemann, J., and Pallesen, G. (1992). Distribution of the alpha 2-macroglobulin receptor/low density lipoprotein receptor-related protein in human tissues. *Cell. Tissue Res.* 269, 375–382. doi: 10.1007/bf00353892

Morandi, V. (2009). The N-terminal domain of thrombospondin-1: a key for the dual effect of TSP-1 in angiogenesis and cancer progression? *ScientificWorldJournal.* 9, 133–136. doi: 10.1100/tsw.2009.11

Mu, D., Cambier, S., Fjellbirkeland, L., Baron, J. L., Munger, J. S., Kawakatsu, H., et al. (2002). The integrin alpha(v)beta8 mediates epithelial homeostasis through MT1-MMP-dependent activation of TGF-beta1. *J. Cell Biol.* 157, 493–507. doi: 10.1083/jcb.200109100

Munger, J. S., Huang, X., Kawakatsu, H., Griffiths, M. J., Dalton, S. L., Wu, J., et al. (1999). The integrin alpha v beta 6 binds and activates latent TGF beta 1: a mechanism for regulating pulmonary inflammation and fibrosis. *Cell* 96, 319–328. doi: 10.1016/s0092-8674(00)80545-0

Munoz, E. M., and Linhardt, R. J. (2004). Heparin-binding domains in vascular biology. *Arterioscler. Thromb. Vasc. Biol.* 24, 1549–1557. doi: 10.1161/01.atv.0000137189.22999.3f

Murphy-Ullrich, J. E., and Sage, E. H. (2014). Revisiting the matricellular concept. *Matrix Biol.* 37, 1–14. doi: 10.1016/j.matbio.2014.07.005

Murphy-Ullrich, J. E., and Suto, M. J. (2018). Thrombospondin-1 regulation of latent TGF-beta activation: a therapeutic target for fibrotic disease. *Matrix Biol.* 68-69, 28–43. doi: 10.1016/j.matbio.2017.12.009

Murphy-Ullrich, J. E., Gurusiddappa, S., Frazier, W. A., and Hook, M. (1993). Heparin-binding peptides from thrombospondins 1 and 2 contain focal adhesion-labilizing activity. *J. Biol. Chem.* 268, 26784–26789. doi: 10.1016/s0021-9258(19)74381-6

Nunes, S. S., Outeiro-Bernstein, M. A., Juliano, L., Vardiero, F., Nader, H. B., Woods, A., et al. (2008). Syndecan-4 contributes to endothelial tubulogenesis through interactions with two motifs inside the pro-angiogenic N-terminal domain of thrombospondin-1. *J. Cell Physiol.* 214, 828–837. doi: 10.1002/jcp.21281

Oh, E. S., Woods, A., and Couchman, J. R. (1997). Syndecan-4 proteoglycan regulates the distribution and activity of protein kinase C. *J. Biol. Chem.* 272, 8133–8136. doi: 10.1074/jbc.272.13.8133

Olerud, J., Johansson, M., Lawler, J., Welsh, N., and Carlsson, P. O. (2008). Improved vascular engraftment and graft function after inhibition of the angiostatic factor thrombospondin-1 in mouse pancreatic islets. *Diabetes.* 57, 1870–1877. doi: 10.2337/db07-0724

Orr, A. W., Pedraza, C. E., Pallero, M. A., Elzie, C. A., Goicoechea, S., Strickland, D. K., et al. (2003). Low density lipoprotein receptor-related protein is a calreticulin coreceptor that signals focal adhesion disassembly. *J. Cell Biol.* 161, 1179–1189. doi: 10.1083/jcb.200302069

Primo, L., Ferrandi, C., Roca, C., Marchio, S., di Blasio, L., Alessio, M., et al. (2005). Identification of CD36 molecular features required for its in vitro angiostatic activity. *FASEB J.* 19, 1713–1715. doi: 10.1096/fj.05-3697fje

Reinhold, M. I., Lindberg, F. P., Plas, D., Reynolds, S., Peters, M. G., and Brown, E. J. (1995). In vivo expression of alternatively spliced forms of integrin-associated protein (CD47). *J. Cell Sci.* 108(Pt 11), 3419–3425.

Ren, Y., and Savill, J. (1995). Proinflammatory cytokines potentiate thrombospondin-mediated phagocytosis of neutrophils undergoing apoptosis. *J. Immunol.* 154, 2366–2374.

Risher, W. C., Kim, N., Koh, S., Choi, J. E., Mitev, P., Spence, E. F., et al. (2018). Thrombospondin receptor alpha2delta-1 promotes synaptogenesis and spinogenesis via postsynaptic Rac1. *J. Cell Biol.* 217, 3747–3765. doi: 10.1083/jcb.201802057

Rodriguez-Manzaneque, J. C., Lane, T. F., Ortega, M. A., Hynes, R. O., Lawler, J., and Iruela-Arispe, M. L. (2001). Thrombospondin-1 suppresses spontaneous tumor growth and inhibits activation of matrix metalloproteinase-9 and mobilization of vascular endothelial growth factor. *Proc. Natl. Acad. Sci. U.S.A.* 98, 12485–12490. doi: 10.1073/pnas.171460498

Rohrs, J. A., Sulistio, C. D., and Finley, S. D. (2016). Predictive model of thrombospondin-1 and vascular endothelial growth factor in breast tumor tissue. *NPJ Syst. Biol. Appl.* 2:16030.

Russell, S., Duquette, M., Liu, J., Drapkin, R., Lawler, J., and Petrik, J. (2015). Combined therapy with thrombospondin-1 type I repeats (3TSR) and chemotherapy induces regression and significantly improves survival in a preclinical model of advanced stage epithelial ovarian cancer. *FASEB J.* 29, 576–588. doi: 10.1096/fj.14-261636

Russo, T. A., Banuth, A. M. M., Nader, H. B., and Dreyfuss, J. L. (2020). Altered shear stress on endothelial cells leads to remodeling of extracellular matrix and induction of angiogenesis. *PLoS One.* 15:e0241040. doi: 10.1371/journal.pone.0241040

Short, S. M., Derrien, A., Narsimhan, R. P., Lawler, J., Ingber, D. E., and Zetter, B. R. (2005). Inhibition of endothelial cell migration by thrombospondin-1 type-1 repeats is mediated by beta1 integrins. *J. Cell Biol.* 168, 643–653. doi: 10.1083/jcb.200407060

Silverstein, R. L., and Febbraio, M. (2009). CD36, a scavenger receptor involved in immunity, metabolism, angiogenesis, and behavior. *Sci. Signal.* 2:re3. doi: 10.1126/scisignal.272re3

Simons, M., Gordon, E., and Claesson-Welsh, L. (2016). Mechanisms and regulation of endothelial VEGF receptor signalling. *Nat. Rev. Mol. Cell Biol.* 17, 611–625. doi: 10.1038/nrm.2016.87

Sipes, J. M., Murphy-Ullrich, J. E., and Roberts, D. D. (2018). Thrombospondins: purification of human platelet thrombospondin-1. *Methods Cell Biol.* 143, 347–369. doi: 10.1016/bs.mcb.2017.08.021

Soto-Pantoja, D. R., Kaur, S., and Roberts, D. D. (2015). CD47 signaling pathways controlling cellular differentiation and responses to stress. *Crit. Rev. Biochem. Mol. Biol.* 50, 212–230. doi: 10.3109/10409238.2015.1014024

Soto-Pantoja, D. R., Terabe, M., Ghosh, A., Ridnour, L. A., DeGraff, W. G., Wink, D. A., et al. (2014). CD47 in the tumor microenvironment limits cooperation between antitumor T-cell immunity and radiotherapy. *Cancer Res.* 74, 6771–6783. doi: 10.1158/0008-5472.can-14-0037-t

Staniszewska, I., Zaveri, S., Del Valle, L., Oliva, I., Rothman, V. L., Croul, S. E., et al. (2007). Interaction of alpha9beta1 integrin with thrombospondin-1 promotes angiogenesis. *Circ. Res.* 100, 1308–1316. doi: 10.1161/01.res.0000266662.98355.66

Stenina-Adognravi, O., Muppala, S., and Gajeton, J. (2018). Thrombospondins and remodeling of the tumor microenvironment. *Vessel Plus* 2, 30. doi: 10.20517/2574-1209.2018.40

Strickland, D. K., Gonias, S. L., and Argraves, W. S. (2002). Diverse roles for the LDL receptor family. *Trends Endocrinol. Metab.* 13, 66–74. doi: 10.1016/s1043-2760(01)00526-4

Sun, J., Hopkins, B. D., Tsujikawa, K., Perruzzi, C., Adini, I., Swerlick, R., et al. (2009). Thrombospondin-1 modulates VEGF-A-mediated Akt signaling and capillary survival in the developing retina. *Am. J. Physiol. Heart Circ. Physiol.* 296, H1344–H1351.

Sun, X., Mosher, D. F., and Rapraeger, A. (1989). Heparan sulfate-mediated binding of epithelial cell surface proteoglycan to thrombospondin. *J. Biol. Chem.* 264, 2885–2889. doi: 10.1016/s0021-9258(19)81695-2

Sun, X., Skorstengaard, K., and Mosher, D. F. (1992). Disulfides modulate RGD-inhibitable cell adhesive activity of thrombospondin. *J. Cell Biol.* 118, 693–701. doi: 10.1083/jcb.118.3.693

Tamkun, J. W., DeSimone, D. W., Fonda, D., Patel, R. S., Buck, C., Horwitz, A. F., et al. (1986). Structure of integrin, a glycoprotein involved in the transmembrane linkage between fibronectin and actin. *Cell.* 46, 271–282. doi: 10.1016/0092-8674(86)90744-0

Tan, K., Duquette, M., Liu, J. H., Dong, Y., Zhang, R., Joachimiak, A., et al. (2002). Crystal structure of the TSP-1 type 1 repeats: a novel layered fold and its biological implication. *J. Cell Biol.* 159, 373–382.

Tan, K., Duquette, M., Liu, J. H., Shanmugasundaram, K., Joachimiak, A., Gallagher, J. T., et al. (2008). Heparin-induced cis- and trans-dimerization modes of the thrombospondin-1 N-terminal domain. *J. Biol. Chem.* 283, 3932–3941. doi: 10.1074/jbc.m705203200

Taraboletti, G., Morbidelli, L., Donnini, S., Parenti, A., Granger, H. J., Giavazzi, R., et al. (2000). The heparin binding 25 kDa fragment of thrombospondin-1 promotes angiogenesis and modulates gelatinase and TIMP-2 production in endothelial cells. *FASEB J.* 14, 1674–1676. doi: 10.1096/fj.99-0931fje

Taraboletti, G., Roberts, D., Liotta, L. A., and Giavazzi, R. (1990). Platelet thrombospondin modulates endothelial cell adhesion, motility, and growth: a potential angiogenesis regulatory factor. *J. Cell Biol.* 111, 765–772. doi: 10.1083/jcb.111.2.765

Thorne, R. F., Law, E. G., Elith, C. A., Ralston, K. J., Bates, R. C., and Burns, G. F. (2006). The association between CD36 and Lyn protein tyrosine kinase is mediated by lipid. *Biochem. Biophys. Res. Commun.* 351, 51–56. doi: 10.1016/j.bbrc.2006.09.156

Tsai, R. K., Rodriguez, P. L., and Discher, D. E. (2010). Self inhibition of phagocytosis: the affinity of 'marker of self' CD47 for SIRPalpha dictates potency of inhibition but only at low expression levels. *Blood Cells Mol. Dis.* 45, 67–74. doi: 10.1016/j.bcmd.2010.02.016

van Deventer, S., Arp, A. B., and van Spriel, A. B. (2020). Dynamic plasma membrane organization: a complex symphony. *Trends Cell Biol.* 31, 119–129. doi: 10.1016/j.tcb.2020.11.004

Vischer, P., Feitsma, K., Schon, P., and Volker, W. (1997). Perlecan is responsible for thrombospondin 1 binding on the cell surface of cultured porcine endothelial cells. *Eur. J. Cell Biol.* 73, 332–343.

Vischer, P., Volker, W., Schmidt, A., and Sinclair, N. (1988). Association of thrombospondin of endothelial cells with other matrix proteins and cell attachment sites and migration tracks. *Eur. J. Cell Biol.* 47, 36–46.

Vogel, T., Guo, N. H., Krutzsch, H. C., Blake, D. A., Hartman, J., Mendelovitz, S., et al. (1993). Modulation of endothelial cell proliferation, adhesion, and motility by recombinant heparin-binding domain and synthetic peptides from the type I repeats of thrombospondin. *J. Cell Biochem.* 53, 74–84. doi: 10.1002/jcb.240530109

Vuong, T. T., Reine, T. M., Sudworth, A., Jenssen, T. G., and Kolset, S. O. (2015). Syndecan-4 is a major syndecan in primary human endothelial cells in vitro, modulated by inflammatory stimuli and involved in wound healing. *J. Histochem. Cytochem.* 63, 280–292. doi: 10.1369/0022155415568995

Wang, F., Liu, Y. H., Zhang, T., Gao, J., Xu, Y., Xie, G. Y., et al. (2020). Aging-associated changes in CD47 arrangement and interaction with thrombospondin-1 on red blood cells visualized by super-resolution imaging. *Aging Cell.* 19:e13224.

Weng, T. Y., Huang, S. S., Yen, M. C., Lin, C. C., Chen, Y. L., Lin, C. M., et al. (2014). A novel cancer therapeutic using thrombospondin 1 in dendritic cells. *Mol. Ther.* 22, 292–302. doi: 10.1038/mt.2013.236

Williams, S. E., Ashcom, J. D., Argraves, W. S., and Strickland, D. K. (1992). A novel mechanism for controlling the activity of alpha 2-macroglobulin receptor/low density lipoprotein receptor-related protein. Multiple regulatory sites for 39-kDa receptor-associated protein. *J. Biol. Chem.* 267, 9035–9040. doi: 10.1016/s0021-9258(19)50384-2

Winnemoller, M., Schon, P., Vischer, P., and Kresse, H. (1992). Interactions between thrombospondin and the small proteoglycan decorin: interference with cell attachment. *Eur. J. Cell Biol.* 59, 47–55.

Woods, A., and Couchman, J. R. (1994). Syndecan 4 heparan sulfate proteoglycan is a selectively enriched and widespread focal adhesion component. *Mol. Biol. Cell* 5, 183–192. doi: 10.1091/mbc.5.2.183

Xie, L., Duncan, M. B., Pahler, J., Sugimoto, H., Martino, M., Lively, J., et al. (2011). Counterbalancing angiogenic regulatory factors control the rate of cancer progression and survival in a stage-specific manner. *Proc. Natl. Acad. Sci. U.S.A.*. 108, 9939–9944. doi: 10.1073/pnas.1105041108

Yang, Z., Strickland, D. K., and Bornstein, P. (2001). Extracellular matrix metalloproteinase 2 levels are regulated by the low density lipoprotein-related scavenger receptor and thrombospondin 2. *J. Biol. Chem.* 276, 8403–8408. doi: 10.1074/jbc.m008925200

Yu, H., Tyrrell, D., Cashel, J., Guo, N. H., Vogel, T., Sipes, J. M., et al. (2000). Specificities of heparin-binding sites from the amino-terminus and type 1 repeats of thrombospondin-1. *Arch. Biochem. Biophys.* 374, 13–23. doi: 10.1006/abbi.1999.1597

Zhang, X., Kazerounian, S., Duquette, M., Perruzzi, C., Nagy, J. A., Dvorak, H. F., et al. (2009). Thrombospondin-1 modulates vascular endothelial growth factor activity at the receptor level. *FASEB J.* 23, 3368–3376. doi: 10.1096/fj.09-131649

Conflict of Interest: The authors declare that the research was conducted in the absence of any commercial or financial relationships that could be construed as a potential conflict of interest.

Copyright © 2021 Morandi, Petrik and Lawler. This is an open-access article distributed under the terms of the Creative Commons Attribution License (CC BY). The use, distribution or reproduction in other forums is permitted, provided the original author(s) and the copyright owner(s) are credited and that the original publication in this journal is cited, in accordance with accepted academic practice. No use, distribution or reproduction is permitted which does not comply with these terms.

frontiers in Cell and Developmental Biology

REVIEW
published: 29 April 2021
doi: 10.3389/fcell.2021.672447

The Role of Histone Protein Acetylation in Regulating Endothelial Function

Zhi Fang[1,2], Xiang Wang[1], Xiaoran Sun[1], Wenquan Hu[1] and Qing R. Miao[1]**

[1] Department of Foundations of Medicine, New York University Long Island School of Medicine, Mineola, NY, United States,
[2] Department of Neurology, Tongji Medical College, Union Hospital, Huazhong University of Science and Technology, Wuhan, China

Endothelial cell (EC), consisting of the innermost cellular layer of all types of vessels, is not only a barrier composer but also performing multiple functions in physiological processes. It actively controls the vascular tone and the extravasation of water, solutes, and macromolecules; modulates circulating immune cells as well as platelet and leukocyte recruitment/adhesion and activation. In addition, EC also tightly keeps coagulation/fibrinolysis balance and plays a major role in angiogenesis. Therefore, endothelial dysfunction contributes to the pathogenesis of many diseases. Growing pieces of evidence suggest that histone protein acetylation, an epigenetic mark, is altered in ECs under different conditions, and the acetylation status change at different lysine sites on histone protein plays a key role in endothelial dysfunction and involved in hyperglycemia, hypertension, inflammatory disease, cancer and so on. In this review, we highlight the importance of histone acetylation in regulating endothelial functions and discuss the roles of histone acetylation across the transcriptional unit of protein-coding genes in ECs under different disease-related pathophysiological processes. Since histone acetylation changes are conserved and reversible, the knowledge of histone acetylation in endothelial function regulation could provide insights to develop epigenetic interventions in preventing or treating endothelial dysfunction-related diseases.

Keywords: epigenetic regulation, histone acetylation, acetyltransferase, deacetylase, endothelial dysfunction

OPEN ACCESS

Edited by:
Xiaofeng Yang,
Temple University, United States

Reviewed by:
Bin Ren,
University of Alabama at Birmingham, United States
Jun Yu,
Temple University, United States

***Correspondence:**
Wenquan Hu
wenquan.hu@nyulangone.org
Qing R. Miao
qing.miao@nyulangone.org

Specialty section:
This article was submitted to Signaling, a section of the journal Frontiers in Cell and Developmental Biology

Received: *25 February 2021*
Accepted: *06 April 2021*
Published: *29 April 2021*

Citation:
Fang Z, Wang X, Sun X, Hu W and Miao QR (2021) The Role of Histone Protein Acetylation in Regulating Endothelial Function. Front. Cell Dev. Biol. 9:672447. doi: 10.3389/fcell.2021.672447

INTRODUCTION

Endothelial cells (ECs), mostly in the inner layer of blood vessels are co-existing with ever-changing environmental conditions, such as fluid shear stress, fluctuations of blood pressure, glucose and cytokines, nutrition availability, as well as pollutant molecules (Potente and Makinen, 2017; Sturtzel, 2017). Sensitive response to rapid changes in both internal and external cues is essential for ECs to maintain cellular homeostasis. Histone post-translational modifications (PTMs) represent crucial epigenetic mechanisms governing the ability of ECs in response to intracellular and extracellular stimuli.

To date, more than 100 different histone modifications have been detected by mass spectrometry or specific antibodies (Choudhary et al., 2014). In all eukaryotes ranging from yeast to humans, DNA is compacted more than 10,000-fold into the nucleus as chromatin. The basic structural subunit of chromatin is the nucleosome, which is comprised of 147 bp of DNA wrapped around

a histone octamer core. Each nucleosome core is consisted of two copies of each of the histones: H2A, H2B, H3, and H4 (Tessarz and Kouzarides, 2014). Initially, histones were regarded as merely structural components which act as a repressive barrier to the nuclear processes requiring access to DNA. However, research over the past two decades has illustrated that histone proteins are critical for the organization and function of chromatin. Dynamic histone PTMs, largely occur at the amino-terminal tail of histones, can fundamentally regulate chromatin structure and gene transcription by spatially and temporally coordinating the shifting between condensed/transcriptionally silenced states and accessible/transcriptionally active states (Shahbazian and Grunstein, 2007). Among the diverse histone PTMs, histone acetylation has been recognized as a fundamental process that strongly affects gene expression regulation (Allfrey et al., 1964).

Growing pieces of evidence suggest that histone protein acetylation is altered in ECs under different conditions. The changes of acetylation status at different lysine sites on histone protein strongly affect EC gene expression and thus lead to endothelial dysfunction, which is involved in the pathogenesis of many cardiovascular disease processes. In this review, we will generally introduce histone acetylation and the related writers and erasers and highlight the importance of histone acetylation in regulating endothelial functions and discuss the roles of histone acetylation across the transcriptional unit of protein-coding genes in ECs under different disease-related pathophysiological processes, including vascular tone, inflammation, oxidative stress, angiogenesis, barrier function, thrombosis, and coagulation.

HISTONE ACETYLATION

A common form of histone PTMs and, indeed, one of the first discovered is acetylation (**Figure 1**). Histone acetylation has been linked to active transcription (Phillips, 1963). Mechanically, negatively charged acetyl groups covalently added to specific lysine residues in histone can diminish the electrostatic affinity between histone proteins and DNA, thus disrupts the interaction of these histones with the DNA, leading to chromatin relaxation that enables the activation of gene transcription. Moreover, this modification can serve as docking sites for proteins involved in gene activation, such as transcriptional activators and chromatin remodeling complexes (Marmorstein and Zhou, 2014).

Histone acetylation is a highly reversible process operated in a highly regulated manner. A lysine residue becomes acetylated by the action of the histone acetyltransferases (HATs, also referred to as "writers"), which transfer acetyl group from acetyl-coenzyme A (acetyl-CoA) onto the ε-amino group of target lysine residues. To date, 37 mammalian proteins have been suggested to possess endogenous HAT activity, which can be further classified into at least five different subfamilies based on their structural homologies: the CBP/p300, GCN5/PCAF, MYST, the nuclear receptor coactivator family, and basal transcription families (**Figures 2A,B**; Javaid and Choi, 2017; Sheikh and Akhtar, 2019). However, due to the lack of validated evidence of HAT activities, the latter two subfamilies will not be further discussed in this review. The reverse reaction is catalyzed by histone deacetylases (HDACs, also referred to as "erasers"). In mammals, there are 18 HDAC enzymes that can be grouped into two distinct categories with different catalytic mechanisms: Zn^{2+}-dependent HDACs and NAD^{+}-dependent sirtuin (Sir2 orthologs) deacetylases (**Figures 2C,D**). On the basis of their domain structures and sequence similarities, they can be further divided into five groups: Class I comprises HDAC1, HDAC2, HDAC3, and HDAC8; the Class IIa includes HDAC4, HDAC5, HDAC7, and HDAC9; class IIb includes HDAC6 and HDAC10; Class III comprise SIRT1, SIRT2, SIRT3, SIRT4, SIRT5, SIRT6, and SIRT7; and the Class IV protein HDAC11 (Seto and Yoshida, 2014; Zhao et al., 2018). Just as histone acetylation is accomplished by "writers" and "erasers," their actions to govern DNA transcription are mediated by "readers." According to domain structure, various "readers" can be roughly classified into three categories, including BRD, double PHD finger (DPF), and YEATS domains (Gillette and Hill, 2015; Gong et al., 2016). Emerging evidence has also highlighted the importance of acetylation readers, and some have been implicated in physiological and pathological processes of ECs.

Histone Acetyltransferases- Writers

GCN5/PCAF Family

General control non-derepressible 5 (GCN5, also called KAT2A) was one of the first proteins found to possess HAT activity (Mutlu and Puigserver, 2020). It was also the first histone acetyltransferase confirmed to link histone acetylation to transcriptional activation (Verdin and Ott, 2015). Following its discovery, some other HATs, including PCAF, which contain similar domain structures, have also been identified and consist of the GCN5/PCAF subfamily of HAT proteins. This family of HAT proteins contains PCAF-specific N-terminal domains, a HAT domain of around 160 residues, and a conserved bromodomain within the C-terminal, responsible for recognizing and binding acetyl-lysine recruiting transcriptional machinery to regulate gene expression (Downey, 2020).

GCN5 and PCAF both function as part of unique multi-subunit complexes, where they act as the catalytic HAT domain. For example, GCN5/PCAF is found in the complexes of Spt-Ada-GCN5 acetyltransferase (SAGA) and Ada Two A Containing (ATAC) (**Figures 3A,B**; Helmlinger and Tora, 2017). While the HAT module within the SAGA complex preferentially acetylates histone H3K9 and H3K14 lysine residues *in vivo*, GCN5 within the ATAC complex mainly acetylates H4K5, H4K12, and H4K16 (Spedale et al., 2012). Although the exact function of the ATAC complex remains elusive, it has been well demonstrated that following transcriptional activation, GCN5–SAGA mediates H3 acetylation throughout the gene body recruitment of the ATP-dependent chromatin remodeler SWI/SNF to target genes, which initiates a cascade of chromatin remodeling events that promotes gene transcription (Helmlinger et al., 2020).

CBP/p300 Family

CREB-binding protein [CREB (cyclic-AMP response element-binding protein) binding protein, CBP] and its close paralog EP300 (E1A binding protein p300) consist of another major group of HATs, which are now collectively referred

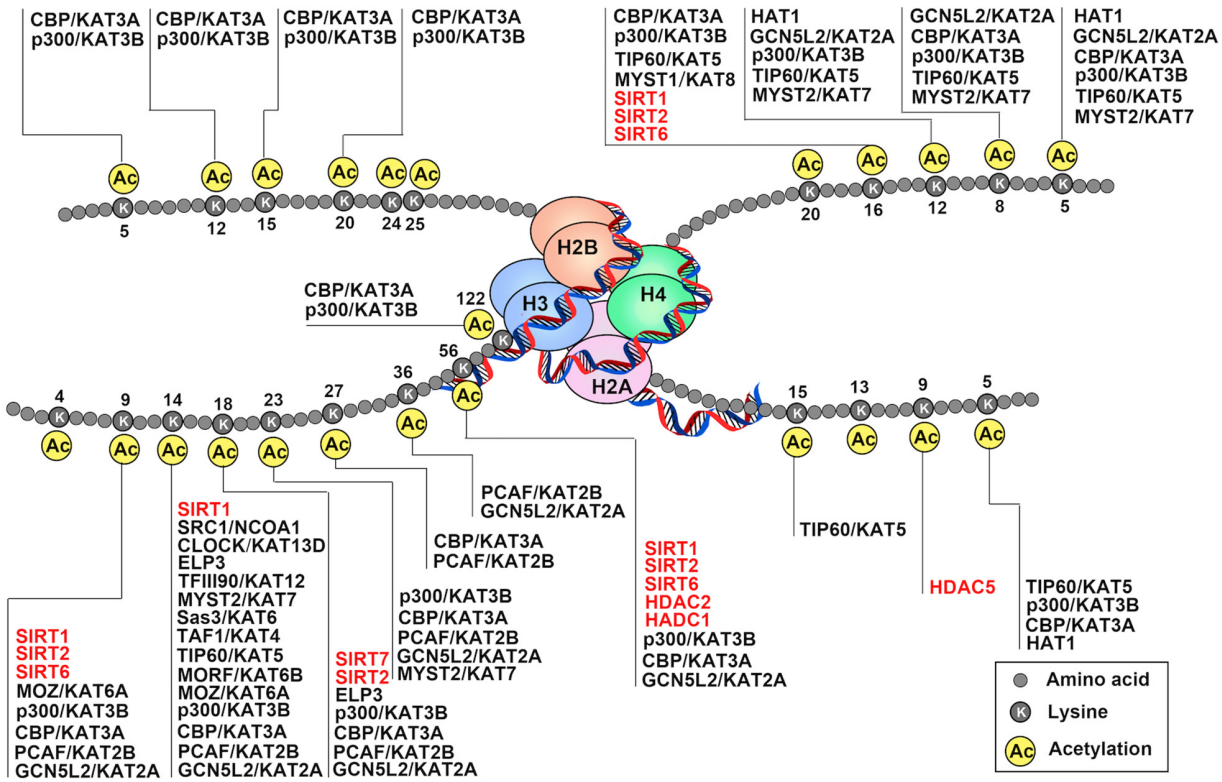

FIGURE 1 | Schematic drawing of histone acetylation. DNA is wound around nucleosomes, which are composed of eight histone molecules with two copies of histones H2A, H2B, H3, and H4. Each histone molecule has a long tail rich in lysine residues (K), which are acetylation modification sites. Gene activation and repression are regulated by acetylation of core histone, and histone acetylation is mediated by coactivators (histone acetyltransferase: HATs) and corepressors (histone deacetylases: HDACs). The addition of acetyl-groups to the tails of histone core proteins leads to a relaxing state of chromatin and includes active transcription. In turn, removel of acetyl-groups from the tails of histone core proteins leads to the adoption of a condensed state of chromatin and transcriptional repression.

to as CBP/p300 because of extensive structural homology and functional redundancy (Breen and Mapp, 2018). Both proteins are pivotal transcriptional coactivators integrating and coordinating transcriptional activation (Lipinski et al., 2019).

The members of this family are large proteins (with about 2,400 amino acids) that do not have defined molecular complexes but harbor multiple functional domains, including a considerably larger HAT domain of about 500 residues, a bromodomain to capture acetyl-lysine, and some other functional domains including the nuclear receptor-interacting box, cysteine/histidine-rich module, phospho-CREB interacting module, and glutamine-rich domain that can regulate enzyme activity and mediate diverse protein-protein interactions (**Figure 2B**; Bordoli et al., 2001; He et al., 2021). CBP/p300 facilitates the gene transcription not only through acetylation of histones and transcription factors but also acts as "hubs" that link chromatin-modifying proteins and basal transcriptional machinery (Rando and Chang, 2009). More importantly, recent advances reveal that CBP/p300 can be recruited by enhancers and mediate the acetylation of H3K18 and H3K27, which stimulates the establishment of an active enhancer state and facilitates transcriptional activation (Heintzman et al., 2007; Hnisz et al., 2013; Arner et al., 2015). For example, p300 was found to locate to the tissue-specific enhancers and drive the expression of adjacent genes in the forebrain or limb tissues during mouse embryonic development at a specific time point (Visel et al., 2009). Given that dynamic regulation of enhancers at specific sets of genes involving cellular differentiation, CBP/p300 can orchestrate the transcription of a series of developmentally essential genes in a temporal-specific and cell type-specific manner.

MYST Family

The MYST family of HAT proteins was first reported in 1996 (Reifsnyder et al., 1996), originally named for its founding members in yeast and mammals. The family currently comprises five human HATs: MOZ (MYST3/KAT6a), MORF (MYST4/KAT6b), HBO1 (MYST2/KAT7), MOF (MYST1/KAT8), and TIP60 (HTATIP/KAT5). They are defined together by the presence of a highly conserved 370 residue MYST domain, which consists of an acetyl-CoA-binding motif homologous to the canonical acetyl-CoA binding domain of GCN5/PCAF family and a C2HC zinc finger domain (Thomas and Voss, 2007). Besides the MYST domain, many members contain additional structural features, such as cysteine-rich, zinc-binding domain within the HAT regions and N-terminal

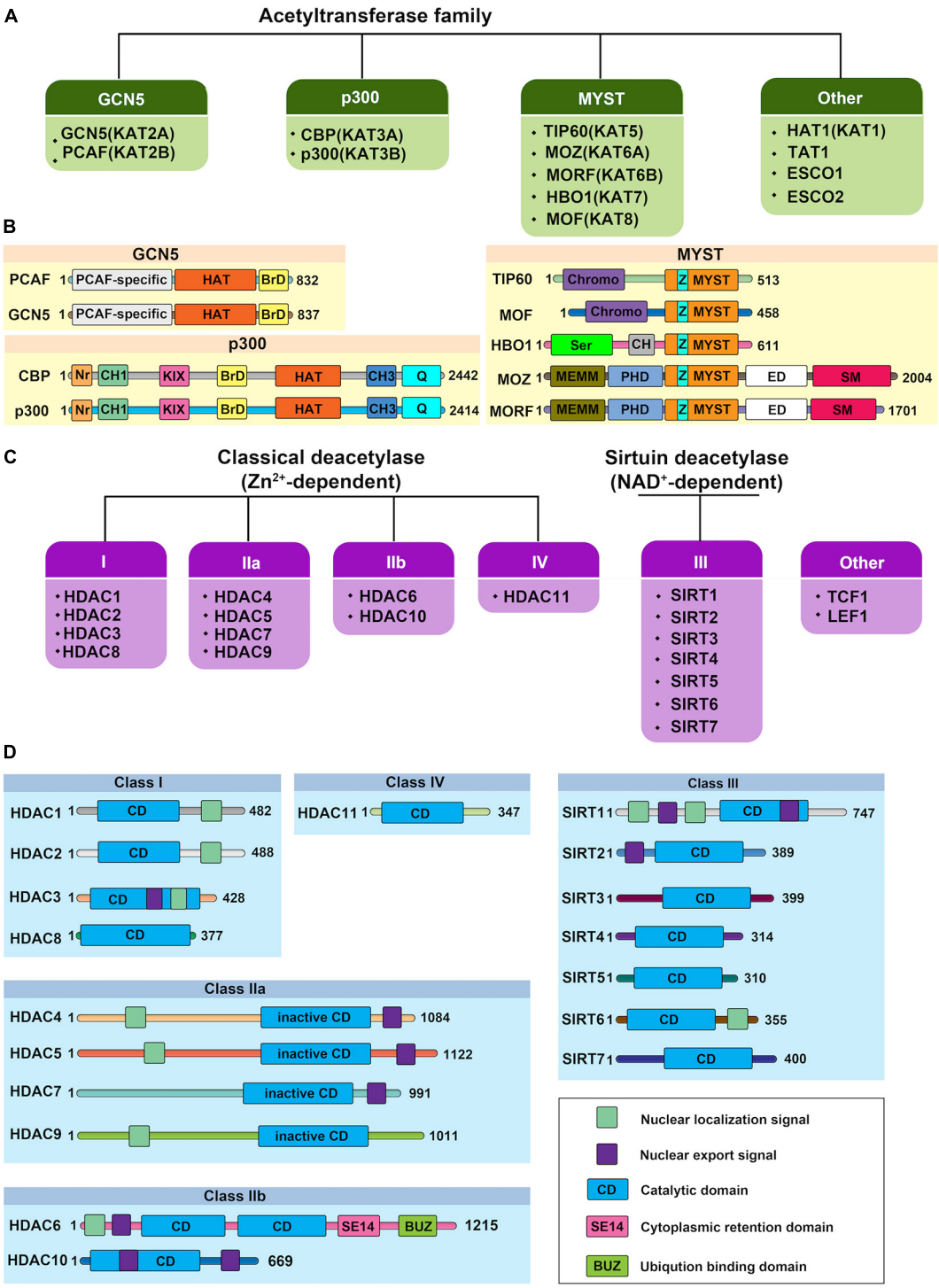

FIGURE 2 | Protein structure of human histone acetylases and deacetylases. **(A)** The canonical histone acetyltransferases (HATs) are classified into three prominent families: GCN5, p300, and MYST. The other HATs are relatives dissimilar to each other. **(B)** Protein structure of human histone acetyltransferases. BrD, bromodomain; Nr, nuclear receptor-interacting box; CH, cysteine/histidine-rich module; KIX, phospho-CREB interacting module; Q, glutamine-rich domain; HAT, the lysine acetyltransferase catalytic domain; Chromo, chromodomain; Ser, serine-rich domain; NEMM, N-terminal part of MOZ or MORF; PHD, PHD zinc finger; ED, glutamate/aspartate-rich region; SM, serine/methionine-rich domain; MYST, MYST histone acetyltransferase domain; Z: C2HC zinc finger domain within the MYST domain. Numbers indicate the length of each protein. **(C)** Histone deacetylases (HDACs) are divided into two categories: the classical Zn^{2+}-dependent HDACs and NAD^{+}-dependent sirtuin deacetylases. Based on their phylogenetic conservation and sequence similarities, the HDACs are further classified into five major families: Class I, Class IIa, Class IIb, Class III, and Class IV. **(D)** Protein structure of human histone deacetylases. Protein domains of HDAC isoenzymes are presented above. Most HDACs possess a nuclear localization and/or export signal. Numbers indicate the length of each protein.

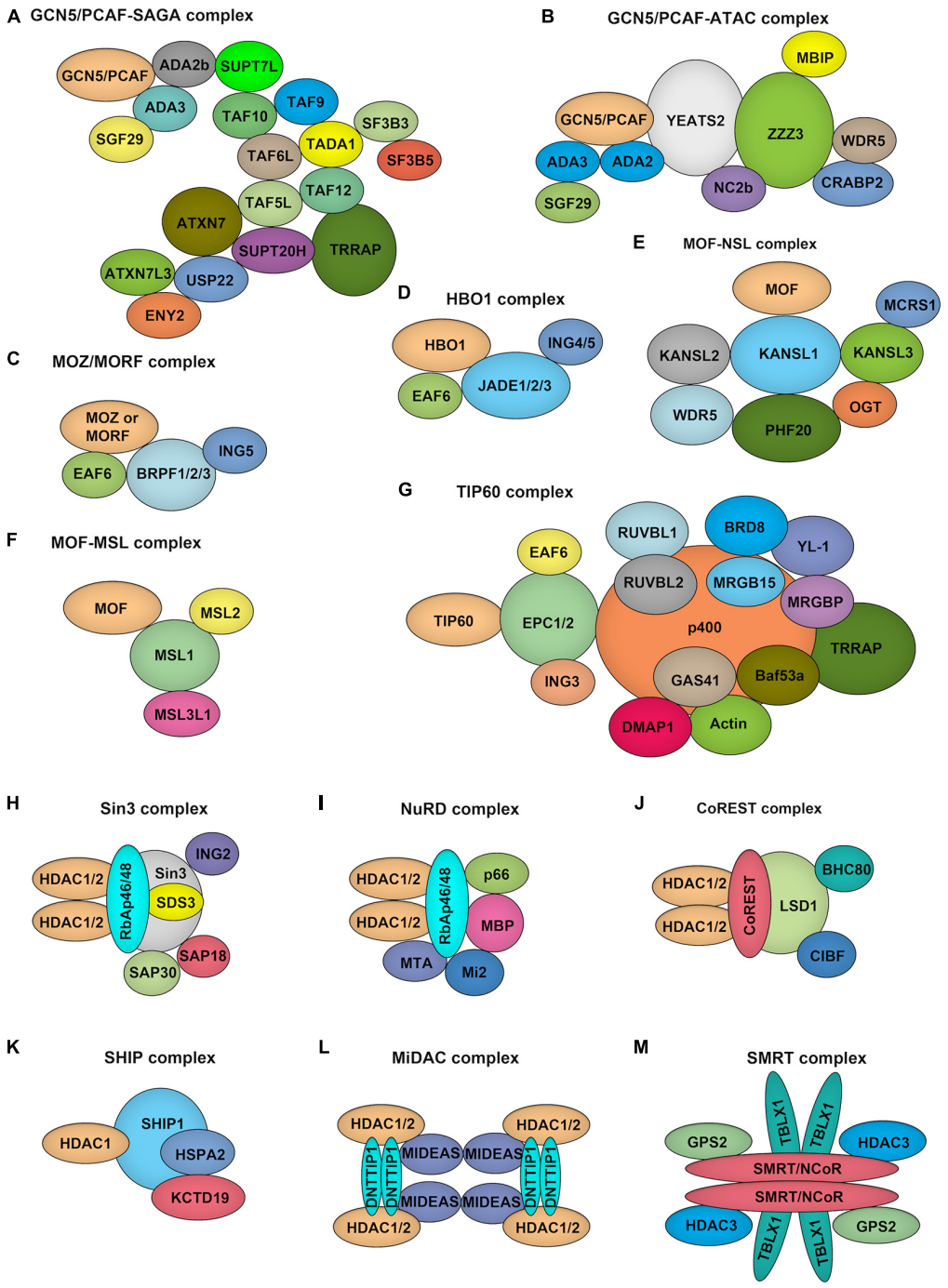

FIGURE 3 | Composition of HATs and HDACs containing multiprotein complexes. **(A–G)**. Depiction of the major histone acetyltransferase complexes: GCN5/PCAF-SAGA **(A)** and GCN5/PCAF-ATAC **(B)**, MOZ/MORF-ING5 **(C)**, HBO1-JADE **(D)**, MOF-NSL **(E)**, MOF-MSL **(F)**, TIP60 **(G)**, which contains two HATs. **(H–M)**, Overview of class I HDAC containing complexes. Sin3 complex **(H)**: The Sin3 complex is comprised of HDAC1 and HDAC2, delivering enzymatic activity and the structural components Sin3, RbAp46, RbAp48, SAP18, SAP30, and SDS3. NuRD complex **(I)**: RbAp46, RbAp48, HDAC1, and HDAC2 are also found in the NuRD complex, together with the NuRD specific factors MTA, Mi-2, p66, and MBD. CoREST complex **(J)**: The CoREST complex consists of CoREST, CIBF, BHC80, HDAC1, HDAC2 and is targeted to DNA via the REST protein. SHIP complex **(K)**: The SHIP complex was identified recently as a testis specific complex containing SHIP1, HDAC1, HSPA2, and KCTD19. MiDAC complex **(L)**: The mitotic deacetylase complex (MiDAC) is a recently identified histone deacetylase (HDAC) complex using proteomics in cells that are blocked in mitosis by nocodazole. MiDAC contains HDAC1/2, a protein called DNTTIP1 (deoxynucleotidyltransferase terminal-interacting protein 1), and the MIDEAS (mitotic deacetylase-associated SANT domain protein) co-repressor protein. SMRT/NCoR complex **(M)**: The core of the complex consists of SMRT/NCoR bound to TBL1 (transducin beta-like protein 1), GPS2 (G protein pathway suppressor 2), and HDAC3 proteins.

chromodomains (**Figure 2B**; Wiesel-Motiuk and Assaraf, 2020). Based on additional notable domain regions, this family of HATs can be further classified into three subgroups: (1) MOZ and MORF, (2) MOF and TIP60, as well as (3) HBO1 alone. For example, MOZ and MORF contain two PHD-type zinc finger domains, while MOF and TIP60 are characterized by a conserved chromodomain (Santos-Rosa and Caldas, 2005).

The MYST family proteins usually form complexes with other transcriptional cofactors to coordinate transcriptional activation and transcriptional silencing. MOZ and MORF were co-purified from HeLa cells in the ING5 complex, which is consisted of MOZ/MORF, EAF, ING5, and BRPF1/2/3 (**Figure 3C**; Pillus, 2008). This complex can localize to the promoter regions of target genes to acetylate H3K9 and H3K23, leading to transcriptional activation. MOF occurs in two complexes identified as the MSL (male-specific lethal) complex and the NSL (non-specific lethal) complex (**Figures 3E,F**; Feller et al., 2012). Either MOF–MSL complex or MOF-NSL complex can trigger H4K16 acetylation at the promoter region to promote transcription, and, most intriguingly, the MOF-NSL complex can be recruited to H3K4 dimethylation positive promoters where it acetylates H4K16. In contrast, the MOF-MSL complex strongly binds to H4K20 monomethylation positive promoters in active gene bodies. TIP60 exists in a multi-subunit protein complex called NuA4 (**Figure 3G**; Xu et al., 2016), which shows an affinity for multiple histone acetylation sites, including H3K14, H3K27 H3K18, and H3K27. HBO1 functions in the context of a multi-protein complex called HBO1-JADE (**Figure 3D**), which contains ING4/5, MEAF6, and JADE1/2/3 for H3K14 acetylation throughout the gene body as well as promoters (Saksouk et al., 2009). This complex also shows an affinity for H3K4 dimethylation and trimethylation positive regions.

Histone Deacetylases—Erasers

Zn^{2+}-Dependent HDACs

Among the zinc-dependent HDACs, Class I, II, and IV HDACs share a conserved HDAC domain (**Figure 2D**). However, they have quite different characteristics. Class I HDACs majorly localize to the nucleus of mammalian cells with robust deacetylase activity. These family proteins usually function as the catalytic core within multi-subunit transcriptional repressor complexes. HDAC1/2 exist in the complexes of NuRD (nucleosome remodeling and deacetylase), SHIP (a testis-specific protein possessing putative DNA binding and chromatin remodeling properties), SIN3 (switch-independent 3), CoREST (corepressor of REST), and MiDAC (mitotic deacetylase) while HDAC3 primarily acts in NCOR1/SMRT repressor protein complex (**Figures 3H–M**; Kelly and Cowley, 2013; Millard et al., 2017). These complexes play essential roles for Class I HDACs to recruit them to specific target gene regions and activate their enzymatic activity. Due to the absence of a catalytic residue in the HDAC domain, class IIa HDACs, including HDAC4, HDAC5, HDAC7, and HDAC9, possess weak deacetylase activity. However, they still can serve as transcriptional repressors by forming complexes with NCOR1/SMRT (Kelly and Cowley, 2013). Also, the function of class IIa HDACs toward histone proteins is under the control of the shuttling between the cytoplasm and nucleus. Distinguished from other zinc-dependent HDACs, the class IIb family member HDAC6 is a unique member of the HDAC family that not only deacetylates histone but also targets cytoskeleton structure, including α-tubulin and cortactin (Li T. et al., 2018). For the other class IIb HDACs, HDAC10, although it can form a repressor complex with SMRT, has relatively low lysine deacetylase activity but is a robust polyamine deacetylase (Fischer et al., 2002; Hai et al., 2017). As the exclusive class IV HDAC, HDAC11 is the newest member of the HDAC family and shares the catalytic domain both of class I and II HDACs. However, it has been reported that the defatty-acylase activity of HDAC11 is over 10,000 times more than its deacetylase activity (Liu et al., 2020).

NAD^{+}-Dependent Sirtuin Deacetylases

Sirtuin deacetylases, which have a conserved nicotinamide adenine dinucleotide (NAD)-binding and catalytic domain, are NAD^{+}-dependent lysine deacetylases or ADP-ribosyltransferases. They were first identified in the yeast, referred to as the class III histone deacetylases (Carafa et al., 2016; Kida and Goligorsky, 2016). To date, seven different SIRT proteins have been identified in mammals. However, growing evidence suggests several members, including SIRT4, SIRT5 have weak deacetylase activity. Instead, extensive studies have clearly shown that SIRT proteins can catalyze the removal of diverse acyl groups from target proteins such as malonyl, succinyl, propionyl, and long-chain fatty acyl (Bosch-Presegue and Vaquero, 2015).

Besides the common deacetylase domain, SIRTs contain quite different N- and C-terminal structural features, which may explain their specified subcellular localization and functions: SIRT1, SIRT2, and SIRT6 can shuttle from nucleus to the cytoplasm; SIRT3, SIRT4, and SIRT5 are majorly mitochondrial proteins; SIRT7 localizes to nuclear and nucleolar compartment (**Figure 2B**; D'Onofrio et al., 2018; Singh et al., 2018).

ROLE OF ENDOTHELIAL HISTONE ACETYLATION IN MULTIPLE PHYSIOLOGICAL PROCESSES

Vascular Tone

Nitric oxide (NO) is a vessel dilator regulating vascular tone (Balligand and Cannon, 1997; Alderton et al., 2001). The production of NO is regulated by the activation of nitric oxide synthase (NOS). Endothelial NOS (eNOS, also called NOS3) is constitutively expressed in vascular ECs (Wilcox et al., 1997) and plays a key role in vascular wall homeostasis and regulation of vascular tone (Balligand and Cannon, 1997; Wilcox et al., 1997; Alderton et al., 2001). Fish et al. (2005) reported that the expression of eNOS is controlled by an EC-specific histone code. Different from non-ECs, the endothelial nucleosomes that encompassed the eNOS core promoter and proximal downstream coding regions are highly enriched in acetylated histones H3K9, H4K12, and di- and tri-methylated H3K4, which are selectively associated with functionally competent RNA polymerase II complexes in ECs (Fish et al., 2005).

Proper expression of eNOS, which is required for maintaining the normal endothelial function, is regulated by histone acetylation under multiple stimuli (**Table 1**). Laminar shear stress (SS) has an acute stimulation of eNOS mRNA transcription (Dimmeler et al., 1999; Fleming and Busse, 1999; Boo et al., 2002). Chen et al. (2008) reported that shear stress increases p300 histone acetyltransferase activity by 2.5-fold and stimulates acetylation of histones H3 and H4 at the promoter region of the eNOS shear stress response element (SSRE) and extended 3′ toward the eNOS coding region, resulting in the opening of chromatin at the SSRE and rapid transcriptional increase of eNOS. Different from shear stress, Fish et al. (2010) demonstrated that hypoxia causes a rapid decrease in the transcription of the eNOS gene. Hypoxia rapidly evicts histone 2A (H2A.Z) from eNOS proximal promoter, and after longer durations of hypoxia exposure, acetylation of histone H3K9, H3K14, H4K5, H4K8, H4K12, and methylation of histone H3K4 decrease on eNOS proximal promoter (Fish et al., 2010). However, there is a controversy on hypoxia-induced histone acetylation mediating eNOS expression. In a rat model of hypoxia-induced persistent pulmonary hypertension of the newborn (PPHN), eNOS expression in pulmonary vascular ECs exhibits an increase with significantly higher levels of acetylated histone H3 and H4 at the proximal promoter of the eNOS gene (Xu et al., 2010). Postberg et al. (2015) also reported the increased acetylation of histone H3K9 and H2A.Z and eNOS expression after hypoxia. Chao et al. (2018) further reported that early hypoxia exposure (neonatal exposure to hyperoxia) leads to histone modification patterns as H2A.Z and H3K9 hyperacetylation and a substantial increase of the baseline expression of eNOS and STAT3. This histone modification pattern persists and becomes a signature that alters the response of ECs exposed to hypoxia later (Chao et al., 2018). In contrast, eNOS expression is decreased in another PPHN model induced by prenatal ductus arteriosus constriction in lamb. The decreased expression of eNOS is associated with DNA CpG methylation in the gene promoter region accompanied by decreased Sp1 occupancy, H4K12 acetylation, and increased H3K9 trimethylation around Sp1 binding sites (Ke et al., 2018). In human umbilical artery ECs (HUAECs), inhibition of HDAC activity using HDAC inhibitor Trichostatin A (TSA) leads to rapidly increased histone acetylation at the eNOS promoter and increases eNOS mRNA levels (Yang et al., 2012; Postberg et al., 2015). Histone H3K9 acetylation at the eNOS gene transcription start site is directly correlated with eNOS mRNA levels (Postberg et al., 2015). However, HDAC inhibition with TSA decreases eNOS mRNA while paradoxically increasing its promoter activity, suggesting a more complicated mechanism involving HDAC and histone acetylation mediated eNOS mRNA expression (Rossig et al., 2002). The suppression effect of HDAC inhibitor TSA on eNOS expression was further confirmed by Bogaard et al. (2011). Similarly, HDAC inhibitor vorinostat was reported to reduce eNOS expression more than 50% in a mouse model of diabetic nephropathy (Advani et al., 2011), and class I-specific HDAC inhibitor Valproic Acid (VPA) was demonstrated to decrease eNOS expression in HUVECs as well (Murugavel et al., 2018).

TABLE 1 | Histone acetylation involved in the expression of vascular tone mediators.

Stimuli	Histone acetylation	HAT or HDAC involved	Targeting	References
Laminar shear stress	H3ac, H4ac	p300	eNOS (SSRE region)	Chen et al., 2008
Hypoxia	H2A.Zac, H3K9, H3K14, H4K5, H4K8, H4K12		eNOS	Fish et al., 2010
	H3ac, H4ac		eNOS	Xu et al., 2010
	H3K9ac, H2A.Zac		eNOS (STAT3 binding)	Postberg et al., 2015; Chao et al., 2018
Persistent pulmonary hypertension of newborn	H4K12ac		eNOS (Sp1 binding)	Ke et al., 2018
27nt small RNA	H3K9ac, H3K12ac, H3K23ac, H4K8ac, H4K12ac	HDAC3	eNOS	Zhang et al., 2008
DJ-1/park7	H3ac	HDAC1	eNOS	Won et al., 2014
Athero protective pulsatile shear stress	H3K27ac		ITPR3 (KLF4 binding)	He et al., 2019
Pathogenic factors of hypertension	H3K9ac	SIRT6	Nkx3.2	Guo et al., 2019
Pathogenic factors of heart failure	H3K56ac	SIRT3, p300	eNOS, arginase II	Su et al., 2020
Maternal nutrient restriction	H3K9ac, H3K18ac, H4ac		ET-1 (HIF-1a binding)	Xu et al., 2013
Shear stress	H3K14ac	CBP	c-fos, c-jun	Illi et al., 2003

The 27nt small RNA, generated from 27nt repeat polymorphism in eNOS intron 4, inhibits eNOS expression. In human aortic ECs (HAECs), the 27 nt small RNA duplex induces hyperacetylation in H3K8, H3K12, H3K23, and H4K9, H4K12 at the 27 nt repeat element and DNA methylation in a region approximately 750nt upstream of the intron 4 repeats of eNOS gene, which is interacted with Non-O (Non-POU Domain Containing Octamer Binding portion) and HDAC3 proteins. The latter deacetylated H3 and H4 at the eNOS core promoter, thereby reduces the expression of eNOS. Treatment with HDAC3 small interfering RNA (siRNA) significantly mitigates the 27 nt small RNA-suppressed expression of eNOS (Zhang et al., 2008). DJ-1/park7, a multifunctional protein, is reported to be implicated in the regulation of vascular contractility and blood pressure by the impairment of NO production through epigenetic inhibition of eNOS expression. HDAC1 recruitment in the eNOS promoter regions is significantly increased in ECs isolated from DJ-1/park7$^{-/-}$ mice compared with control mice. Moreover, the acetylation of H3 histones in the eNOS promoter regions is decreased in DJ-1/park7$^{-/-}$ mice. These

DJ-1/park7-dependent epigenetic characteristics in mouse ECs are also appreciated in HUVECs (Won et al., 2014).

Besides by directly binding of acetylated histone proteins on the eNOS promoter region, eNOS expression is also regulated by indirectly histone acetylation-dependent regulation. Atheroprotective pulsatile shear stress induces KLF4-dependent binding of acetylated H3K27 at the ITPR3 promotor region and increases chromatin accessibility, RNA polymerase II recruitment, and ITPR3 transcription. The ITPR3 induction further elevates the expression of eNOS and NO bioavailability (He et al., 2019).

Histone deacetylase SIRT6 in ECs has pleiotropic protective actions, which include promoting endothelium-dependent vasodilatation and vascular NO bioavailability. It induces the expression of GATA-binding protein 5 (GATA5), a novel regulator of blood pressure, through inhibiting NK3 homeobox 2 (Nkx3.2) transcription by deacetylating histone H3K9, thereby regulating GATA5-mediated signaling pathways to prevent endothelial injury (Guo et al., 2019). Histone deacetylase SIRT3 deletion in ECs causes cardiac remodeling and diastolic dysfunction (He et al., 2017), associated closely with vascular tone. Knockout of SIRT3 results in significant increases in p300 expression and histone H3K56 acetylation. P300 inhibitor C646 significantly reduced levels of p300 and H3K56 acetylation and increased eNOS expression (Su et al., 2020). As a product of eNOS, NO also modulates essential endothelial functions and gene expression through histone deacetylation. Mechanistically, NO induces class II HDAC4, and HDAC5 nuclear shuttling via activation of the protein phosphatase 2A (PP2A) (Illi et al., 2008).

Endothelin-1 (ET1), another critical vasoconstrictor secreted by EC, plays a crucial role in vascular tone. ET1-mediated vascular tone increases with age and contributes to the pathogenesis of hypertension (Stauffer et al., 2008). The maternal nutrient restriction increases the acetylation of histone H3K9, H3K18, and H4 and hypoxia-inducible factor-1α (HIF-1α) binding levels at the gene promoter of ET1 in pulmonary vascular ECs (PVEC) of intrauterine growth retardation (IUGR) newborn rats and continues up to 6 weeks after birth. These epigenetic changes result in endothelial dysfunction, and IUGR rats are highly sensitive to hypoxia later in life, causing more significant pulmonary arterial hypertension (PAH) (Xu et al., 2013).

Except for eNOS, shear stress (SS) modulates the expression of several other genes in ECs and regulates vascular tone (Illi et al., 2003; Iring et al., 2019). In HUVECs, SS activates ribosomal S6 kinase-2 and mitogen- and stress-activated kinase-1 protein kinases and promotes the formation of CREB/CBP transcriptional complexes thus increases the histone acetyltransferase activity and acetylates histone H3K14 within the c-fos and c-jun promoters. Consequently, shear stress increases the expression of transcription factors c-fos and c-jun and initiates the transcription of c-fos and c-jun-targeted genes in ECs (Illi et al., 2003).

Inflammation

As an important player in the inflammation process, EC participates in multiple cytokine production and secretion and responds to cytokines stimuli through the mechanism of involving histone acetylation, as summarized in **Table 2**.

Histone acetylation mediates cytokine expression and secretion in various infectious diseases. After dengue virus infection, the infected monocytes, ECs, and epithelial cells increase the secretion of interleukin 8 (IL-8) and results in an increased serum level of IL-8 significantly. The induction of IL-8 is associated with the hyperacetylation of histone H3 and H4 at the IL-8 promoter in addition to the transcription activated by NF-kB (Bosch et al., 2002). Intracellular *Listeria monocytogenes* infection induces time-dependent acetylation of histone H4K8 and H3K14 at the IL-8 promoter in HUVEC, as well as recruitment of the histone acetylase CBP (Schmeck et al., 2005). Inhibition of RhoA, Rac1, and Cdc42 in HUVEC reduces *Listeria*-promoted recruitment of NF-kB/p65 and RNA polymerase II to the IL-8 promoter, as well as acetylation of histone H4 and H3K14 at the IL-8 gene promoter (Schmeck et al., 2006). Inflammatory activation of the endothelium by *Chlamydophila pneumonia* infection is involved in the development of chronic vascular lesions. *Chlamydophila pneumonia*-induced expression of inflammatory genes (IL-6, IL-8, G-CSF, GM-CSF, MIP-1β, and IFN-γ) in ECs is regulated by Rho-GTPase–related acetylation of histone H3 and H4 (Schmeck et al., 2008). Integrin engagement, contributing to antigenotoxic effects of lung endothelium, increases the acetylation of core histone H3 at the promoters of intercellular adhesion molecule-1 (ICAM-1) and vascular cell adhesion molecule-1 (VCAM-1), similar to the effect of HDAC inhibitor TSA (Rose et al., 2005). However, the effect of HDAC inhibitors on VCAM-1 in ECs is opposite under TNF-α stimulation. Inoue et al. (2006) and Hebbel et al. (2010) reported that HDAC inhibitors TSA and suberoylanilide hydroxamic acid (SAHA) greatly reduced TNF-α-stimulated VCAM-1 expression in ECs. As another case of histone acetylation-mediated cytokine expression in HUVECs, BTB, and CNC homology 1 (Bach1), a basic leucine zipper transcription factor, recruits HDAC1 to the IL-8 promoter and decreases histone H3 and H4 acetylation at the transcription factor 4 (TCF4)-binding site of IL-8 promoter (Jiang et al., 2015). Though histone hyperacetylation is involved in promoting inflammatory cytokine production and secretion, HDAC inhibitors, generally increasing histone acetylation, have a suppressive effect on inflammatory cytokine production induced by lipopolysaccharide (LPS) or TNF-α. A reduction in IL-6 and IL-8 gene expression by HDAC inhibitors, such as butyrate, propionate, and TSA, is observed in HUVECs (Li M. et al., 2018). HDAC inhibitor butyrate also suppresses gene expression and LPS-induced secretion of pro-inflammatory genes CCL2, IL-6, and IL-1β, via enhancing histone H3K9/14 and H2A.Z acetylation and the associated upregulation of oxidative stress-protective genes IRS1, Catalase, SOD2, FOXO3A, and PGC-1α expression in human microvascular ECs (HMEC-1) (Chriett et al., 2019).

Inflammatory response changes during blood vessel maturation and this change has been demonstrated to go through histone H3 acetylation mediated E-selectin expression in response to TNF-α stimulus during blood vessel maturation (Hamada et al., 2014). In many chronic diseases, histone

TABLE 2 | Inflammation signals mediated by histone acetylation in ECs.

Stimuli	Histone acetylation	HAT or HDAC involved	Targeting	References
Dengue virus infection	H3ac, H4ac		IL-8	Bosch et al., 2002
Listeria monocytogenes infection	H4K8ac, H3K14ac	CBP	IL-8	Schmeck et al., 2005
	H4ac, H3K14ac		IL-8 (NF-κB/p65 binding)	Schmeck et al., 2006
Chlamydophila pneumoniae infection	H3ac, H4ac		Cytokines (p65/RelA binding)	Schmeck et al., 2008
Bach1	H3ac, H4ac	HDAC1	IL-8	Jiang et al., 2015
Integrin engagement	H3ac		ICAM-1, VCAM-1	Rose et al., 2005
TNF-α stimulus during blood vessel maturation	H3ac		E-selectin	Hamada et al., 2014
LDL	H3K9ac, H3K14ac		p66shc	Kim et al., 2012
oxLDL	H3K14ac, H4ac	CBP, p300, HDAC1, HDAC2	IL-8, MCP-1	Dje N'Guessan et al., 2009
Hyperglycemia or RAGE	H3K9ac		Cox2 (NF-κB binding)	Perrone et al., 2009
Lysophosphatidylcholine	H3K14ac		ICAM-1 (AP-1 binding)	Li X. et al., 2018; Lu et al., 2019
Angiotensin II	H3ac		CSF1	Shao et al., 2019
Tumor angiogenic growth factors	H3ac		ICAM-1	Hellebrekers et al., 2006
Estrogen	H3ac, H4ac	CBP	MHC II	Adamski et al., 2004
IL-1β	H3K27ac		Genomic sites occupied by NOTCH1-RBPJ	Poulsen et al., 2018
TNF-α	H3ac		Netrin-1	Passacquale et al., 2015
TNF-α or IL-1β	H3K27ac, H4ac	HDAC2	RNASE1	Bedenbender et al., 2019
Polychlorinated biphenyls	H3ac	p300, HADC1, HDAC2	IL-6, CRP, ICAM-1, VCAM-1, IL-1α, IL-1β	Liu et al., 2016
Epigallocatechin-3-gallate	H3K9ac, H3K14ac	HDAC5, HDAC7, p300, CBP	Chromatin relaxation	Ciesielski et al., 2020

acetylation plays a critical role in endothelial dysfunction associated with inflammation. Hypercholesterolemia induces p66shc-mediated proinflammatory endothelial dysfunction and atheromatous plaque formation by inducing ICAM-1 and reducing thrombomodulin (TM). Mechanistically, low-density lipoprotein (LDL) promotes hypomethylation of two CpG dinucleotides and acetylation of histone H3K9 and H3K14 in the p66shc promoter, thus increasing endothelial p66shc expression (Kim et al., 2012). Similar to LDL, oxidized low-density lipoprotein (oxLDL) also has a proinflammation feature. It induces lectin-like oxidized LDL receptor-1 (LOX-1) and extracellular regulated kinases (ERK1/2)-dependent acetylation of histone H3K14 and H4 binding onto the promoters of IL-8 and monocyte-chemoattractant protein-1 (MCP-1). Consequently, oxLDL increases the expression and secretion of IL-8 and MCP-1 in ECs (Dje N'Guessan et al., 2009). Clinically used statins, which block 3-hydroxy-3-methylglutaryl coenzyme A (HMG Co-A), has a beneficial effect on atherosclerosis depending at least in part on the inhibition of the release of proinflammatory cytokines (Liao and Laufs, 2005). The use of statins alters the histone modification by reducing the recruitment of CBP/p300, NF-kB, and RNA polymerase II but increasing the binding of HDAC1 and HDAC2 at the promoters of IL-8 and MCP-1 genes (Dje N'Guessan et al., 2009). Thioredoxin-interacting protein (TXNIP) plays a causative role in diabetic vascular complications by increasing proinflammatory factor cyclooxygenase (COX)-2 expression in ECs. It induces COX-2 expression by abolishing H3K9 tri-methylation and increasing H3K9 acetylation at the proximal COX-2 promoter bearing the NF-kB-binding site (Perrone et al., 2009). However, HDAC inhibitor TSA decreases LPS-induced COX-2 expression in HUVECs, which is caused by the non-acetylation effect of TSA and may be due to JNK and p38MAPK dephosphorylation induced by TSA activated MKP-1 (Hsu et al., 2011). Lysophosphatidylcholine (LPC) induces mitochondrial reactive oxygen species-dependent site-specific H3K14 acetylation, therefore increases the binding of proinflammatory transcription factor AP-1 in the promoter of ICAM-1 and induces ICAM-1 transcription in HAECs. However, IL-35, an anti-inflammatory cytokine, suppresses LPC-induced monocyte adhesion via ICAM-1 mediated regulation (Li X. et al., 2018). The further RNA-seq and ChIP-seq analysis results demonstrated that LPC induces H3K14 acetylation in the genomic DNA that encodes LPC-induced immunity pathway genes including ICAM-1 (Lu et al., 2019).

Angiotensin II (Ang II), a causative factor for hypertension, has been documented to stimulate endothelium-derived colony-stimulating factor (CSF1), which is a key molecule controlling the production, differentiation, and function of macrophage) transcription (da Cunha et al., 2005). Shao et al. (2019) demonstrated that Ang II upregulates both acetylated H3 and tri-methylated H3K4 and downregulates dimethyl H3K9 surrounding the proximal CSF1 promoter via BRG1 interaction with histone methyltransferase SET1A and histone demethylase JMJD1A. In the tumor, another chronic disease,

it has been demonstrated that tumor cells could go immune escape through histone acetylation mediated endothelial dysfunction. As a mediator of leukocyte-EC adhesion, ICAM-1 expression in tumor ECs is epigenetically silenced by promoter histone modifications (histone H3 deacetylation and histone H3K4 demethylation) while restored by HDAC inhibitor TSA (Hellebrekers et al., 2006).

Except for the production of cytokines, the responses of ECs to cytokine or inflammatory stimuli also are associated with histone acetylation. Estrogen has immunomodulatory effects and reduces the class II MHC expression, which has been demonstrated to go through attenuating the acetylation of histone H3 and H4 and the association of CBP within the class II MHC promoter (Adamski et al., 2004). Histone H3K27 acetylation is required for proinflammatory cytokine IL-1β-induced rapid recruitment of NF-κB subunit RELA to genomic sites occupied by NOTCH1-RBPJ (Poulsen et al., 2018). Netrin-1, a neuroimmune guidance cue (Boyer and Gupton, 2018), has chemorepellent action of the endothelium against monocyte chemotaxis. TNF-α-induced NF-κB activation upregulates the nuclear isoform of netrin-1 while simultaneously reducing secreted netrin-1 through histone H3 hyperacetylation. Besides, aspirin, a COX inhibitor that is widely used as an antiplatelet agent but exerts anti-inflammatory properties as well (Desborough and Keeling, 2017), also regulates the TNF-α-induced secretion of netrin-1 via epigenetic modification. Mechanistically, aspirin reduces HDAC/HAT ratio and induces higher expression of acetylated histone H3 (Passacquale et al., 2015). Upon long-term inflammation, high amounts of proinflammatory cytokines affect endothelial function by downregulating RNase1, a circulating extracellular endonuclease regulating vascular homeostasis of extracellular RNA and acting as a vessel- and tissue-protective enzyme (Fischer et al., 2007; Cabrera-Fuentes et al., 2015). In HUVECs, TNF-α, or IL-1β stimulation reduces the expression of RNase1 by inducing hypoacetylation of histone H3K27 and histone H4 via accumulation of HDAC2 to the RNASE1 promoter, while class I HDAC specific inhibitor MS275 abolishes the changes (Bedenbender et al., 2019). Lipoxin A4 (LXA4), a primary stop signal of inflammation, exerts potent bioactions by activating a specific G protein-coupled receptor ALX/FPR2. Activation of p300 restores chromatin accessibility and significantly increases ALX/FPR2 mRNA and protein levels in pulmonary artery ECs (PAECs). Changes in the histone acetylation status enhance ALX/FPR2 signaling in response to LXA4 (Simiele et al., 2016).

Environmental pollutants, such as polychlorinated biphenyls (PCBs), are also reported to induce endothelial inflammation via histone acetylation. PCB 126 exposure increases the expression of vascular inflammatory mediators, including IL-6, C-reactive protein (CRP), ICAM-1, VCAM-1, and IL-1α/β in EA.hy926 human ECs (Liu et al., 2016). Anti-inflammatory polyphenol epigallocatechin-3-gallate (EGCG), the main green tea polyphenol, is demonstrated to abolish nuclear translocation of p65, decrease chromatin binding of p65, and p300, and increase chromatin binding of HDAC1/2, therefore deacetylate histone H3 and deactivate the proinflammatory genes (Liu et al., 2016). Besides, EGCG also increases the chromatin marks of H3K9 and H3K14 acetylation as well as H3K4 and H3K9 trimethylation, presenting a broad epigenetic potential in affecting the expression and activity of epigenome modulators including HDAC5 and 7, p300, CBP, Lysine Demethylase 1A (LSD1) or KMT2A (Ciesielski et al., 2020).

Oxidative Stress

Oxidative stress is a complicated factor affecting EC functions. ECs produce both reactive oxygen species (ROS) and anti-oxidative molecules. The proper balance is required to maintain normal endothelial function. Multiple stimuli affect the balance, and excessive ROS causes endothelial dysfunction. Among these processes, histone acetylation plays an important role, as summarized in **Table 3**. Inactivation of the p66Shc adaptor protein confers EC resistance to oxidative stress. However, high-glucose induces overexpression of p66Shc. It has been reported that p66Shc-deficient mice are protected against age-related and hyperglycemia-induced endothelial dysfunction. SIRT1 inhibits high glucose-induced upregulation of p66Shc via decreasing the acetylation of histone H3 binding onto the p66Shc promoter (Zhou et al., 2011). The p66Shc gene overexpression induced by high-glucose is epigenetically regulated by promoter CpG hypomethylation (Paneni et al., 2012) and histone H3K9 acetylation along with enhanced transcriptional factor p53 binding (Mishra et al., 2019). Besides mediating the endothelial response to oxidative stress, p66Shc is also emerging as a key molecule responsible for ROS generation and vascular damage. Methyltransferase SUV39H1, demethylase JMJD2C, and acetyltransferase SRC-1 are found to be associated with reduced di- and tri-methylation as well as acetylation of H3K9 on the p66Shc promoter in visceral fat arteries (VFA), which results in the elevated expression of p66Shc and ROS-related endothelial dysfunction in VFA (Costantino et al., 2019).

Hydrogen peroxide (H_2O_2), ROS inducer, upregulates p53 and acetylation of H3K14 and H4K16 due to the decreased activity of SIRT1. Paeonol, a phenolic compound isolated mainly from Moutan cortex, the root bark of the Chinese Peony tree, significantly increases the deacetylase activity of SIRT1 in HUVECs. Pretreatment with paeonol substantially decreases the H_2O_2–upregulated levels of acetylated H3K14 and H4K16 (Jamal et al., 2014). NADPH oxidase (NOX) promotes ROS production in ECs. In response to hypoxia-reoxygenation (HR), chromatin remodeling protein BRG1 is recruited to the NOX promoter region and induces acetylation of histones H3 and H4 and methylation of histone H3K9 surrounding the NOX promoter (Li Z. et al., 2018). In human EA.hy926 ECs, siRNA-mediated knockdown of HDAC3 leads to a significant downregulation of NOX family member Nox4 expression. Also, HDAC inhibitor Scriptaid leads to the enhanced acetylation of histone H4 and H3K27, and decreases Nox4 transcription by preventing the binding of transcription factor c-Jun and RNA polymerase IIa to the Nox4 promoter due to hyperacetylation-mediated steric inhibition (Siuda et al., 2012).

Extracellular superoxide dismutase (EC-SOD, SOD3) is the major antioxidant enzyme present in the vascular wall. The expression of antioxidant genes in PAECs is regulated by epigenetic mechanisms (Zelko et al., 2011). HDAC inhibitor

TABLE 3 | Histone acetylation involved in endothelial mediated oxidative stress.

Stimuli	Histone acetylation	HAT or HDAC involved	Targeting	References
Hyper glycemia	H3K9ac	SIRT1, SRC-1	p66shc (p53 binding)	Zhou et al., 2011; Paneni et al., 2012; Costantino et al., 2019; Mishra et al., 2019
H2O2	H3K14ac, H4K16ac	SIRT1	p53	Jamal et al., 2014
HDACi scriptaid	H4ac, H3K27ac	HDAC3	Nox4 (c-jun binding)	Siuda et al., 2012
HDAC inhibitors	H3K27ac		SOD3	Zelko and Folz, 2015
Exendin-4	H3ac	HDAC activity	SOD3	Yasuda et al., 2016
CAPE	H3ac	HDAC1	SOD3 (MEF2A binding)	Ohashi et al., 2017
Hyper glycemia	H3K9ac, H3K27ac	HDAC2	SOD2	Hou et al., 2018
Oxidative stress	H4K16ac	SIRT1	Antioxidant genes (FoxO3a and PGC-1 binding)	Olmos et al., 2013

Scriptaid-mediated augmentation of SOD3 expression is associated with increased histone H3K27 acetylation and H3K4 trimethylation at the promoter of the SOD3 gene (Zelko and Folz, 2015). Exendin-4, a glucagon-like peptide-1 receptor agonist, significantly induces the expression of SOD3 in human retinal microvascular ECs (HRECs) by decreasing HDAC activity and enhancing the status of histone H3 acetylation at the SOD3 proximal promoter and (Yasuda et al., 2016). Moreover, Caffeic acid phenethyl ester (CAPE) increases the transcription of SOD3 through HDAC1-regulated histone acetylation in HRECs (Ohashi et al., 2017). Except for SOD3, SOD2 (Superoxide Dismutase 2, also called MnSOD) is also regulated by histone acetylation. Diabetes-induced HDAC2 upregulation diminishes the acetylation of histone H3K9 and H3K27, therefore, reduces SOD2 expression. The reduced SOD2 expression promotes oxidative stress and contributes to diabetes-related endothelial dysfunction (Hou et al., 2018). SIRT1 activates the expression of antioxidant genes in ECs by deacetylating and increasing the transcription factors FOXO3a and PGC-1α, however reducing H4K16 acetylation and increasing elongating Pol II recruitment occurring at these genes (Olmos et al., 2013).

Angiogenesis

Angiogenesis is a process of new blood vessel formation, which is the well-characterized function of ECs. As summarized in **Table 4**, histone acetylation is found to be crucial in regulating angiogenesis.

In response to angiogenic signals, histone cell cycle regulation defective homolog A (HIRA) is induced in ECs and mediates the incorporation of CBP acetylated H3K56 at the chromatin domain of VEGFR1, which then induces transcription of several angiogenic genes in ECs (Dutta et al., 2010). Upon VEGF stimulation, angiogenic genes VEGFR1, VEGFR2, and angiopoietin 2 (ANGPT2) in HUVECs are induced via increased promotor binding of transcription factor E2F1, which is correlated with the recruitment of p300 and PCAF and acetylation of histones and E2F1 (Pillai et al., 2010). Zhang et al. (2013) also reported that the greatest change of H3K27 acetylation (H3K27ac) is associated tightly with p300 in VEGF-stimulated HUVECs. Dynamic H3K27ac deposition and associated changes in chromatin conformation require p300 activity instead of altered nucleosome occupancy or changes in DNase I hypersensitivity (Zhang et al., 2013). Moreover, human metallothionein 1G (hMT1G) is upregulated upon VEGF stimulation in HAECs. VEGF stimulation leads to dissociation of HDAC1 from the promoter, acetylation of histones, and increased binding of transcription factor E2F1. The upregulation of hMT1G contributes to the proangiogenic functions of VEGF (Joshi et al., 2005). Seryl-tRNA synthetase (SerRS) plays an essential role in regulating vascular development by acetylated histone-mediated regulation of VEGFA expression. In particular, SerRS blocks the binding of c-Myc, the major transcription factor promoting VEGFA, to VEGFA promoter and recruits SIRT2 to erase c-Myc-promoted acetylation of H4K16 so as to intervene c-Myc-dependent VEGFA expression (Shi et al., 2014).

Vascular endothelial cadherin (VE-cadherin) is the primary determinant of EC junction integrity during vascular development and angiogenesis. During angiogenesis and neovascularization processes, VEGF induces the binding of myocardin-related transcription factor-A (MRTF-A) to the Serum Response Factor (SRF)-binding site within the VE-cadherin promoter. MRTF-A and p300 synergistically augment VE-cadherin expression by enhancing acetylation of H3K9, H3K14, and H4 at the SRF-binding site within the VE-cadherin promoter (Shu et al., 2015). Osteoporosis-associated downregulation of zinc-finger transcription factor ZEB1 in ECs reduces CBP/p300 mediated acetylation of H3K4, H3K14, and H3K18 within the promoters of Dll4 and Notch1, thereby epigenetically suppressing Notch signaling, a critical pathway that controls bone angiogenesis and osteogenesis (Fu et al., 2020).

NF-kB signal is induced by antiangiogenic molecules and has a dual effect on downstream transcription through histone acetylation regulation. On the one hand, NF-kB acts as an activator of proapoptotic Fas ligand via recruiting p300 and acetylated histones H3 and H4 at its promotor. On the other hand, NF-kB acts as a repressor of antiapoptotic cFLIP [cellular FLICE (FADD-like IL-1β-converting enzyme)-inhibitory protein] via reducing the HDAC1 and p300 coordinated histone acetylation and recruitment of transcription factor NFAT critically required for cFLIP transcription (Aurora et al., 2010). Administration of low, safe doses of exogenous carbon monoxide (CO) was demonstrated to enhance EC migration and angiogenesis in the acetylated H3K9, H3K18,

TABLE 4 | Histone acetylation associated with angiogenesis.

Stimuli	Histone acetylation	HAT or HDAC involved	Targeting	References
Angiogenic signals	H3K56ac	CBP	VEGFR1	Dutta et al., 2010
VEGF stimulation	H3ac	PCAF	VEGFR1, VEGFR2, ANGPT2 (E2F1 binding)	Pillai et al., 2010
VEGF stimulation	H3K27ac	p300	Angiogenic genes	Zhang et al., 2013
SerRS	H4K16ac	SIRT2	VEGFA (c-myc binding)	Shi et al., 2014
VEGF stimulation	H3K9ac, H3K14 ac, H4ac	p300	VE-cadherin (SRF binding)	Shu et al., 2015
Osteoporosis (ZEB1 loss)	H3K4ac, H3K14ac, H3K18ac	p300, CBP	Dll4, NOTCH1	Fu et al., 2020
NF-kB signal	H3ac, H4ac	p300, HDAC1	cFLIP, NFAT	Aurora et al., 2010
CO	H3K9ac, H3K18ac, H3K23ac	HDAC3 (implied)	Angiogenic genes	Li et al., 2014
KAT7 KO	H3K14ac, H4ac	KAT7	VEGFR2	Yan et al., 2018
VEGF stimulation and HDAC inhibitors	H3K9ac	HDAC1 (implied)	Angiogenic genes	Jin et al., 2011
HDAC7 KO	H3ac	HDAC7	AKAP12	Turtoi et al., 2012

and H3K23 dependent manner, nuclear receptor Rev-erbα, a haem-containing transcription factor, responds to CO stimulation, recruits the HDAC/nuclear Receptor Corepressor (N-CoR) complex, and thus suppresses the transcription of genes responsible for EC migration and angiogenesis (Li et al., 2014).

Histone acetyltransferase and deacetylase are potentially involved in regulating angiogenesis through the alteration of histone acetylation. KAT7 participates in regulating VEGFR-2 transcription by promoting the acetylation of H3K14 and H4 and RNA polymerase II binding. Depletion of KAT7 reduces VEGFR2 expression and disrupts angiogenic potential in HUVECs (Yan et al., 2018). HDAC inhibitor VPA results in hyperacetylated H3K9 and greatly enhances the VEGF-promoted spheroid sprouting of HUVECs (Jin et al., 2011). HDAC inhibitor LBH589 induces the acetylation of histone H3 and non-histone protein α-tubulin and induces G2-M cell cycle arrest, inhibits the VEGF-induced expression of ANGPT2, survivin, HIF-1α, and CXCR4 possibly due to histone acetylation modulated upregulation of tumor suppressor genes, such as p53 and VHL (Von Hippel–Lindau) (Qian et al., 2006). Novel HDAC inhibitor N-hydroxy-7-(2-naphthylthio) heptanomide (HNHA) showed a similar effect on histone H3 and non-histone protein α-tubulin to LBH589 (Kim et al., 2009). HDAC inhibitor TSA significantly reduces sVEGFR1 basal expression, suggesting that histone acetylation is involved in activating sVEGFR1 (Choi et al., 2018). The depletion of HDAC7 in HUVEC results in the overexpression of A-kinase anchor protein 12 (AKAP12), which is a tumor/angiogenesis suppressor gene responsible for the inhibition of migration and tube formation. Mechanistically, H3 histone proteins associated with AKAP12 promoter are highly acetylated following the removal of HDAC7, leading to an increase in its mRNA and protein levels (Turtoi et al., 2012). Intriguingly, regulation of gene locus-specific histone acetylation status by the interaction between a lipid signaling mediator LPA and HDAC7 may downregulate the transcription of angiogenic regulator CD36 via protein kinase D pathway, thereby promoting angiogenesis (Ren et al., 2011, 2016).

Barrier Function

The endothelial barrier in all organ beds allows the free exchange of water but is restrictive to varying degrees to the transport of solutes (Malik et al., 1989). Functional changes in EC, to a large extent, influence the barrier function. As listed in **Table 5**, many studies have demonstrated the histone acetylation changes affect the barrier function.

High glucose impairs the endothelial barrier through multiple histone acetylation mediated signals. Zhong and Kowluru reported that diabetes activates retinal Matrix metalloproteinases (MMP)-9 via LSD1 mediated decrease of histone H3K9 di-methylation. The decreased H3K9 methylation frees up that lysine 9 for acetylation and facilitates the recruitment of p65 to MMP-9 promoter, thus resulting in MMP-9 activation in retinal ECs (Zhong and Kowluru, 2013). Li et al. (2017) demonstrated high glucose suppresses claudins-5 and -11 gene expression in human cardiac microvascular ECs, possibly due to inhibition of acetylated H3K9 in claudin-5 and claudin-11

TABLE 5 | EC barrier function mediated by histone acetylation.

Stimuli	Histone acetylation	HAT or HDAC involved	Targeting	References
Hyperglycemia	H3K9ac		MMP-9 (p65 binding)	Zhong and Kowluru, 2013
	H3K9ac		Claudin-5, Claudin-11	Li et al., 2017
	H3K9ac, H3K14ac	p300, SIRT1	ET-1, TGF-β1	Mortuza et al., 2015
LPS	H3K9ac and H3K18ac		VE-cadherin	Thangavel et al., 2014
Scald injury	H3K9ac		VEGF, MPO	Tang et al., 2018
HDAC inhibitors	H3K9ac, H3K14ac		MDR1 (AHR binding)	You et al., 2019

gene promoters. Mortuza et al. (2015) revealed that high glucose induces p300 expression, and reduces SIRT1 levels, thus increases the acetylation of H3K9 and H3K14, which is attributed to the upregulation of ET1 and TGFβ1. These changes contribute to high glucose-induced endothelial hyperpermeability (Mortuza et al., 2015). In pulmonary ECs, combinatorial treatment with DNA methyltransferase (DNMT) inhibitor Aza and HDAC inhibitor TSA mitigate the LPS increased endothelial permeability due to the enhanced acetylation of H3K9 and H3K18 on the VE-cadherin promoter (Thangavel et al., 2014). HDAC inhibitor VPA treatment significantly alleviates the microvascular permeability and water content of the lung, lowers VEGF and MPO levels, and promotes the acetylation of H3K9 following scald injury (Tang et al., 2018). In brain ECs, multidrug resistance protein 1 (MDR1, ABCB1, P-glycoprotein) is a critical efflux transporter that extrudes chemicals from the blood–brain barrier and limits neuronal exposure to xenobiotics. HDAC inhibitor SAHA upregulates the expression and activity of the MDR1 transporter in immortalized human brain capillary EC hCMEC/D3 by increasing H3K9/K14 acetylation and facilitating aryl hydrocarbon receptor (AHR) binding at the MDR1 promoter (You et al., 2019).

TABLE 6 | Histone acetylation associated with thrombosis and coagulation.

Stimuli	Histone acetylation	HAT or HDAC involved	Targeting	References
HDAC inhibitors	H4ac		t-PA	Arts et al., 1995; Dunoyer-Geindre and Kruithof, 2011
HDAC inhibitors	H3K9ac, H3K18ac, H3K23ac, H3K27ac, H4K8ac, H4K16ac	HDAC3, HDAC5, HDAC7	t-PA	Larsson et al., 2012
Atherosclerosis	H4K16ac	SIRT1	PAI-1	Wan et al., 2014
Irradiation	H4ac	HDAC1, PCAF	vWF	Peng et al., 2007
Hypoxia	H4ac		vWF	Mojiri et al., 2019
Senescence	H3K9ac		TF	Kurz et al., 2014

Thrombosis and Coagulation

Several studies revealed the involvement of histone acetylation modification in EC mediated coagulation and thrombosis (**Table 6**). Tissue-type plasminogen activator (t-PA) plays a key role in the onset of the fibrinolytic process by converting the zymogen plasminogen into the active enzyme plasmin. Stimulated release of t-PA is pivotal for an intravascular fibrinolytic response and protects the circulation from occluding thrombosis. Arts et al. (1995) reported for the first time that t-PA expression could be regulated by histone acetylation. HDAC inhibitors butyrate, TSA, MS275, and VPA were demonstrated to induce a dose-dependent increase of t-PA expression in ECs, which involves histone H3 and H4 acetylation (Arts et al., 1995; Dunoyer-Geindre and Kruithof, 2011; Larsson et al., 2012). VPA induced t-PA expression is associated with increased acetylation of H3K9, H3K18, H3K23, H3K27, H4K8, and H4K16 at the t-PA promoter (Larsson et al., 2012) and dependent on the proximal GC boxes in the t-PA promoter and may involve interactions with transcription factors Sp2, Sp4, and KLF5 (Ulfhammer et al., 2016). The effect of VPA on t-PA expression was then confirmed *in vivo* (Svennerholm et al., 2014; Larsson et al., 2016). Plasminogen activator inhibitor-1 (PAI-1), the most important serine protease inhibitor of t-PA (Van De Craen et al., 2012), has shown beneficial effects on age-related vascular diseases. PAI-1 is induced in senescent HUVECs and aortas of eld mice. SIRT1 is able to reverse the change by binding to the PAI-1 promoter, resulting in a decreased acetylation of H4K16 at the PAI-1 promoter region (Wan et al., 2014). Clinical study has demonstrated that HDAC inhibitor VPA reduces in exhaustion during repeated and prolonged cumulative stimulated t-PA release and decreases basal PAI-1 levels (Svennerholm et al., 2015), which suggested potentially positive effects of HDAC inhibitors on the expression of t-PA and PAI-1. Von Willebrand factor (vWF), playing an essential role in regulating the balance between blood clotting and bleeding, also is regulated by histone acetylation. Peng et al. (2007) reported that irradiation induces thrombus formation via vWF elevation. The irradiation-caused changes in the association of NF-Y with HDAC1 and PCAF lead to the increased acetylated histone H4 and PCAF recruitment to the vWF promoter, which results in subsequently increased vWF transcription in HUVECs (Peng et al., 2007). Mojiri et al. (2019) reported that, in response to hypoxia, Nuclear Factor IB (NFIB) repressor disassociates from the vWF promoter due to the increased acetylation of the promoter-associated histone H4, and thus increases vWF expression. Tissue factor (TF), another protein involved in coagulation, is demonstrated to lose inducibility during senescence, which occurs following chromatin remodeling at the TF promoter resulting from hypoacetylation of histone H3K9 (Kurz et al., 2014). However, HDAC inhibitors TSA and SAHA were reported to greatly attenuate TF expression induced by TNF-α despite of its effect of promoting histone acetylation (Wang et al., 2007; Hebbel et al., 2010).

Others

Except for vascular tone, inflammation, oxidative stress, angiogenesis, barrier function, and thrombosis and coagulation, histone acetylation is also involved in other EC-associated pathological processes, including endothelial mesenchymal transition (EndMT), senescence, and metabolism. Fu et al. (2009) reported that Notch and TGFβ synergistically upregulate a subset of genes by recruiting Smad3 to both Smad and DNA-binding protein CSL binding sites and cooperatively inducing histone H4 acetylation. Zhang et al. (2016) demonstrated that aging-related transcriptional regulator p49/STRAP alters histone acetylation status and impacts mitochondrial dynamics, thereby reducing mitochondrial function and

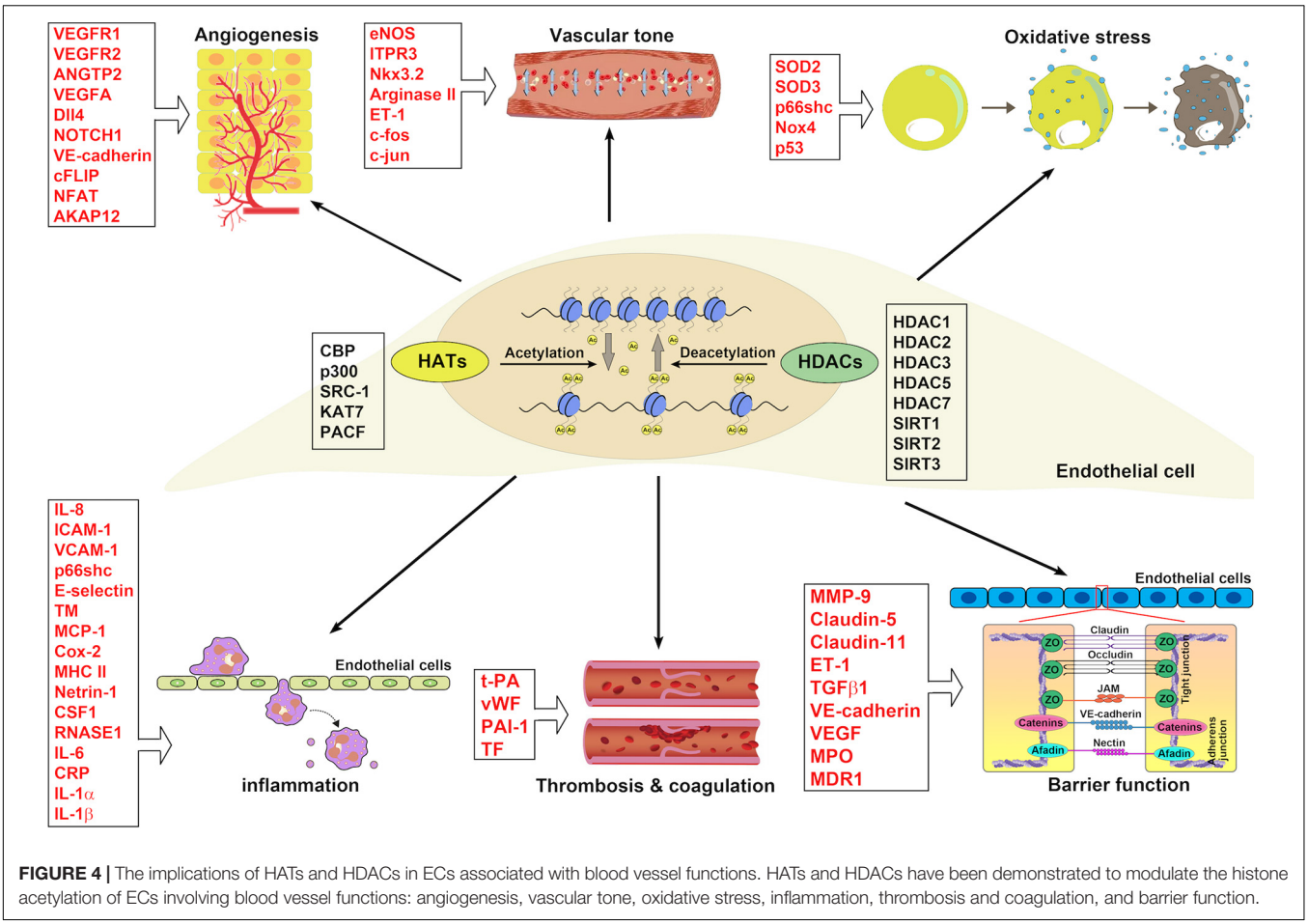

FIGURE 4 | The implications of HATs and HDACs in ECs associated with blood vessel functions. HATs and HDACs have been demonstrated to modulate the histone acetylation of ECs involving blood vessel functions: angiogenesis, vascular tone, oxidative stress, inflammation, thrombosis and coagulation, and barrier function.

cardiac performance during mammalian senescence. Zhong et al. found the so-called metabolic memory phenomenon in diabetic retinopathy. This phenomenon is mediated by HDAC activation due to the increased expression of HDAC1, 2, 8 genes and compromised HAT activity, as evidenced by the decreased histone H3 acetylation in the retina and its capillary cells (Zhong and Kowluru, 2010). Pirola et al. (2011) uncovered hyperglycemia-mediated induction of genes and pathways associated with endothelial dysfunction occur through modulation of acetylated H3K9/K14, which is inversely correlated with methyl-CpG content (Pirola et al., 2011). Chen et al. (2010) reported that p300 critically regulates glucose-induced gene expression in ECs via binding to gene promoters and augmenting histone acetylation. In HUVECs, high glucose treatment increases p300 production accompanied by increased binding of p300 to ET-1 and fibronectin promoters and increased transcription of vasoactive factors and extracellular matrix (ECM) proteins (Chen et al., 2010). Tanegashima et al. (2017) demonstrated that fasting-induced production of the ketone body β-hydroxybutyrate (β-OHB) enhances expression of the glucose transporter gene Slc2a1 (Glut1) via HDAC2 mediated H3K9 acetylation at the critical cis-regulatory region of the Slc2a1 gene in brain microvascular ECs.

CONCLUSION AND FUTURE PERSPECTIVE

Histone acetylation has been found to be involved in the pathogenesis of EC dysfunction in the last two decades. The acetylation of histone at different lysine residues alters under various stimuli and affects gene expression in ECs (**Figure 4**), therefore mediating endothelial functions. In regards to acetylated histone-mediated gene expression, HATs and HDACs are indispensable. The fact that histone acetylation can be reversed makes it an ideal target for drug treatment. With the development of HDAC inhibitors, which could inhibit HDACs, therefore, promoting histone acetylation, modulation of histone acetylation becomes achievable. In the oncology field, HDAC inhibitors have already been tested in clinical trials for treating solid and hematological malignancies (O'Connor et al., 2015; Sekeres et al., 2017; Tambo et al., 2017; Gray et al., 2019; Rodriguez et al., 2020).

The application of HDAC inhibitors in EC dysfunction-related disease is promising but still in its infantile stage. Many challenges are awaiting to be conquered. The side effects of HDAC inhibitors on the acetylation of non-histone proteins and other non-acetylation effects may limit their application. For example, the non-selective HDAC inhibitor vorinostat,

inhibiting the activities of class I and class II HDAC enzymes, potentially increases the lysine acetylation status of more than 1,700 non-histone proteins (Choudhary et al., 2009). HDAC inhibitor LBH589 and HNHA have an acetylation effect on non-histone protein α-tubulin (Qian et al., 2006; Kim et al., 2009). HDAC inhibitor TSA could acetylate non-histone protein p53 (Zeng et al., 2003) and has ubiquitination effect on histone acetyltransferase p300 (Hakami et al., 2016). HDAC inhibitor VPA could induce ERK1/2 phosphorylation independent of the HDAC inhibition effect (Michaelis et al., 2006). In ECs, except for the histone deacetylation effect, HDACs were also reported to deacetylate non-histone proteins. HDAC1 was demonstrated to deacetylate p53 and transactivate the p21 under laminar flow (Zeng et al., 2003). SIRT1 activates the expression of antioxidant genes in ECs by deacetylating and increasing the activity of the transcription factors FOXO3a and PGC-1α (Olmos et al., 2013). Furthermore, many HDACs form corepressor complexes to silence gene activity, which again amplifies the potential non-specific effects that HDAC inhibitors can have within the cell (Krishna et al., 2015). Therefore, there is a critical need for further investigation to elucidate the roles of HDACs and HATs in regulating the acetylation of non-histone proteins in ECs.

Not all the HATs and HDACs, which are potentially involved in endothelial dysfunction-related histone acetylation, have been elucidated. The systemic study using individual HATs and HDACs endothelial-specific knockout mice should be essential for filling up our current knowledge gaps. Same HAT or HDAC may regulate different genes that have beneficial or detrimental EC functions in various physiological and pathological settings. HDAC1 has an anti-inflammatory effect via histone acetylation mediated IL-8 expression (Jiang et al., 2015) and pro-oxidative stress through SOD3 as well (Ohashi et al., 2017). Though HDAC2 could decrease pro-inflammatory gene expression (Liu et al., 2016), it also inhibits anti-oxidative stress gene SOD3 expression (Hou et al., 2018). It could be another challenge in how to target HDAC mediated histone acetylation for modulating endothelial functions precisely. In addition, histone acetylation and methylation always work together. The complexity of histone posttranslational modification in ECs needs our endeavor to be revealed in the future.

AUTHOR CONTRIBUTIONS

QM provided the outline of the manuscript. ZF, XW, and XS searched the literature for the article and wrote the manuscript. WH coordinated and revised the content and prepared the figures. ZF prepared the tables. QM supervised the work and completed the final editing. All authors discussed its content and edited the submitted manuscript.

FUNDING

This work was supported in part by start-up funds from NYU Langone Hospital-Long Island, NIH R01HL141733 to QM.

REFERENCES

Adamski, J., Ma, Z., Nozell, S., and Benveniste, E. N. (2004). 17beta-Estradiol inhibits class II major histocompatibility complex (MHC) expression: influence on histone modifications and cbp recruitment to the class II MHC promoter. *Mol. Endocrinol.* 18, 1963–1974. doi: 10.1210/me.2004-0098

Advani, A., Huang, Q., Thai, K., Advani, S. L., White, K. E., Kelly, D. J., et al. (2011). Long-term administration of the histone deacetylase inhibitor vorinostat attenuates renal injury in experimental diabetes through an endothelial nitric oxide synthase-dependent mechanism. *Am. J. Pathol.* 178, 2205–2214. doi: 10.1016/j.ajpath.2011.01.044

Alderton, W. K., Cooper, C. E., and Knowles, R. G. (2001). Nitric oxide synthases: structure, function and inhibition. *Biochem. J.* 357(Pt 3), 593–615. doi: 10.1042/0264-6021:3570593

Allfrey, V. G., Faulkner, R., and Mirsky, A. E. (1964). Acetylation and methylation of histones and their possible role in the regulation of Rna synthesis. *Proc. Natl. Acad. Sci. U.S.A.* 51, 786–794. doi: 10.1073/pnas.51.5.786

Arner, E., Daub, C. O., Vitting-Seerup, K., Andersson, R., Lilje, B., Drablos, F., et al. (2015). Transcribed enhancers lead waves of coordinated transcription in transitioning mammalian cells. *Science* 347, 1010–1014. doi: 10.1126/science.1259418

Arts, J., Lansink, M., Grimbergen, J., Toet, K. H., and Kooistra, T. (1995). Stimulation of tissue-type plasminogen activator gene expression by sodium butyrate and trichostatin A in human endothelial cells involves histone acetylation. *Biochem. J.* 310(Pt 1), 171–176. doi: 10.1042/bj3100171

Aurora, A. B., Biyashev, D., Mirochnik, Y., Zaichuk, T. A., Sanchez-Martinez, C., Renault, M. A., et al. (2010). NF-kappaB balances vascular regression and angiogenesis via chromatin remodeling and NFAT displacement. *Blood* 116, 475–484. doi: 10.1182/blood-2009-07-232132

Balligand, J. L., and Cannon, P. J. (1997). Nitric oxide synthases and cardiac muscle. Autocrine and paracrine influences. *Arterioscler. Thromb. Vasc. Biol.* 17, 1846–1858. doi: 10.1161/01.atv.17.10.1846

Bedenbender, K., Scheller, N., Fischer, S., Leiting, S., Preissner, K. T., Schmeck, B. T., et al. (2019). Inflammation-mediated deacetylation of the ribonuclease 1 promoter via histone deacetylase 2 in endothelial cells. *FASEB J.* 33, 9017–9029. doi: 10.1096/fj.201900451R

Bogaard, H. J., Mizuno, S., Hussaini, A. A., Toldo, S., Abbate, A., Kraskauskas, D., et al. (2011). Suppression of histone deacetylases worsens right ventricular dysfunction after pulmonary artery banding in rats. *Am. J. Respir. Crit. Care Med.* 183, 1402–1410. doi: 10.1164/rccm.201007-1106OC

Boo, Y. C., Hwang, J., Sykes, M., Michell, B. J., Kemp, B. E., Lum, H., et al. (2002). Shear stress stimulates phosphorylation of eNOS at Ser(635) by a protein kinase A-dependent mechanism. *Am. J. Physiol. Heart Circ. Physiol.* 283, H1819–H1828. doi: 10.1152/ajpheart.00214.2002

Bordoli, L., Husser, S., Luthi, U., Netsch, M., Osmani, H., and Eckner, R. (2001). Functional analysis of the p300 acetyltransferase domain: the PHD finger of p300 but not of CBP is dispensable for enzymatic activity. *Nucleic Acids Res.* 29, 4462–4471. doi: 10.1093/nar/29.21.4462

Bosch, I., Xhaja, K., Estevez, L., Raines, G., Melichar, H., Warke, R. V., et al. (2002). Increased production of interleukin-8 in primary human monocytes and in human epithelial and endothelial cell lines after dengue virus challenge. *J. Virol.* 76, 5588–5597. doi: 10.1128/jvi.76.11.5588-5597.2002

Bosch-Presegue, L., and Vaquero, A. (2015). Sirtuin-dependent epigenetic regulation in the maintenance of genome integrity. *FEBS J.* 282, 1745–1767. doi: 10.1111/febs.13053

Boyer, N. P., and Gupton, S. L. (2018). Revisiting Netrin-1: one who guides (Axons). *Front. Cell Neurosci.* 12:221. doi: 10.3389/fncel.2018.00221

Breen, M. E., and Mapp, A. K. (2018). Modulating the masters: chemical tools to dissect CBP and p300 function. *Curr. Opin. Chem. Biol.* 45, 195–203. doi: 10.1016/j.cbpa.2018.06.005

Cabrera-Fuentes, H. A., Niemann, B., Grieshaber, P., Wollbrueck, M., Gehron, J., Preissner, K. T., et al. (2015). RNase1 as a potential mediator of remote ischaemic preconditioning for cardioprotectiondagger. *Eur. J. Cardiothorac. Surg.* 48, 732–737. doi: 10.1093/ejcts/ezu519

Carafa, V., Rotili, D., Forgione, M., Cuomo, F., Serretiello, E., Hailu, G. S., et al. (2016). Sirtuin functions and modulation: from chemistry to the clinic. *Clin. Epigenetics* 8:61. doi: 10.1186/s13148-016-0224-3

Chao, C. M., van den Bruck, R., Lork, S., Merkle, J., Krampen, L., Weil, P. P., et al. (2018). Neonatal exposure to hyperoxia leads to persistent disturbances in pulmonary histone signatures associated with NOS3 and STAT3 in a mouse model. *Clin. Epigenetics* 10:37. doi: 10.1186/s13148-018-0469-0

Chen, S., Feng, B., George, B., Chakrabarti, R., Chen, M., and Chakrabarti, S. (2010). Transcriptional coactivator p300 regulates glucose-induced gene expression in endothelial cells. *Am. J. Physiol. Endocrinol. Metab.* 298, E127–E137. doi: 10.1152/ajpendo.00432.2009

Chen, W., Bacanamwo, M., and Harrison, D. G. (2008). Activation of p300 histone acetyltransferase activity is an early endothelial response to laminar shear stress and is essential for stimulation of endothelial nitric-oxide synthase mRNA transcription. *J. Biol. Chem.* 283, 16293–16298. doi: 10.1074/jbc.M801803200

Choi, S., Uehara, H., Wu, Y., Das, S., Zhang, X., Archer, B., et al. (2018). RNA activating-double stranded RNA targeting flt-1 promoter inhibits endothelial cell proliferation through soluble FLT-1 upregulation. *PLoS One* 13:e0193590. doi: 10.1371/journal.pone.0193590

Choudhary, C., Kumar, C., Gnad, F., Nielsen, M. L., Rehman, M., Walther, T. C., et al. (2009). Lysine acetylation targets protein complexes and co-regulates major cellular functions. *Science* 325, 834–840. doi: 10.1126/science.1175371

Choudhary, C., Weinert, B. T., Nishida, Y., Verdin, E., and Mann, M. (2014). The growing landscape of lysine acetylation links metabolism and cell signalling. *Nat. Rev. Mol. Cell Biol.* 15, 536–550. doi: 10.1038/nrm3841

Chriett, S., Dabek, A., Wojtala, M., Vidal, H., Balcerczyk, A., and Pirola, L. (2019). Prominent action of butyrate over beta-hydroxybutyrate as histone deacetylase inhibitor, transcriptional modulator and anti-inflammatory molecule. *Sci. Rep.* 9:742. doi: 10.1038/s41598-018-36941-9

Ciesielski, O., Biesiekierska, M., and Balcerczyk, A. (2020). Epigallocatechin-3-gallate (EGCG) alters histone acetylation and methylation and impacts chromatin architecture profile in human endothelial cells. *Molecules* 25:2326. doi: 10.3390/molecules25102326

Costantino, S., Paneni, F., Virdis, A., Hussain, S., Mohammed, S. A., Capretti, G., et al. (2019). Interplay among H3K9-editing enzymes SUV39H1, JMJD2C and SRC-1 drives p66Shc transcription and vascular oxidative stress in obesity. *Eur. Heart J.* 40, 383–391. doi: 10.1093/eurheartj/ehx615

da Cunha, V., Tham, D. M., Martin-McNulty, B., Deng, G., Ho, J. J., Wilson, D. W., et al. (2005). Enalapril attenuates angiotensin II-induced atherosclerosis and vascular inflammation. *Atherosclerosis* 178, 9–17. doi: 10.1016/j.atherosclerosis.2004.08.023

Desborough, M. J. R., and Keeling, D. M. (2017). The aspirin story - from willow to wonder drug. *Br. J. Haematol.* 177, 674–683. doi: 10.1111/bjh.14520

Dimmeler, S., Fleming, I., Fisslthaler, B., Hermann, C., Busse, R., and Zeiher, A. M. (1999). Activation of nitric oxide synthase in endothelial cells by Akt-dependent phosphorylation. *Nature* 399, 601–605. doi: 10.1038/21224

Dje N'Guessan, P., Riediger, F., Vardarova, K., Scharf, S., Eitel, J., et al. (2009). Statins control oxidized LDL-mediated histone modifications and gene expression in cultured human endothelial cells. *Arterioscler. Thromb. Vasc. Biol.* 29, 380–386. doi: 10.1161/ATVBAHA.108.178319

D'Onofrio, N., Servillo, L., and Balestrieri, M. L. (2018). SIRT1 and SIRT6 signaling pathways in cardiovascular disease protection. *Antioxid Redox Signal.* 28, 711–732. doi: 10.1089/ars.2017.7178

Downey, M. (2020). Non-histone protein acetylation by the evolutionarily conserved GCN5 and PCAF acetyltransferases. *Biochim. Biophys. Acta Gene Regul. Mech.* 1864:194608. doi: 10.1016/j.bbagrm.2020.194608

Dunoyer-Geindre, S., and Kruithof, E. K. (2011). Epigenetic control of tissue-type plasminogen activator synthesis in human endothelial cells. *Cardiovasc. Res.* 90, 457–463. doi: 10.1093/cvr/cvr028

Dutta, D., Ray, S., Home, P., Saha, B., Wang, S., Sheibani, N., et al. (2010). Regulation of angiogenesis by histone chaperone HIRA-mediated incorporation of lysine 56-acetylated histone H3.3 at chromatin domains of endothelial genes. *J. Biol. Chem.* 285, 41567–41577. doi: 10.1074/jbc.M110.190025

Feller, C., Prestel, M., Hartmann, H., Straub, T., Soding, J., and Becker, P. B. (2012). The MOF-containing NSL complex associates globally with housekeeping genes, but activates only a defined subset. *Nucleic Acids Res.* 40, 1509–1522. doi: 10.1093/nar/gkr869

Fischer, D. D., Cai, R., Bhatia, U., Asselbergs, F. A., Song, C., Terry, R., et al. (2002). Isolation and characterization of a novel class II histone deacetylase. HDAC10. *J. Biol. Chem.* 277, 6656–6666. doi: 10.1074/jbc.M108055200

Fischer, S., Gerriets, T., Wessels, C., Walberer, M., Kostin, S., Stolz, E., et al. (2007). Extracellular RNA mediates endothelial-cell permeability via vascular endothelial growth factor. *Blood* 110, 2457–2465. doi: 10.1182/blood-2006-08-040691

Fish, J. E., Matouk, C. C., Rachlis, A., Lin, S., Tai, S. C., D'Abreo, C., et al. (2005). The expression of endothelial nitric-oxide synthase is controlled by a cell-specific histone code. *J. Biol. Chem.* 280, 24824–24838. doi: 10.1074/jbc.M502115200

Fish, J. E., Yan, M. S., Matouk, C. C., St Bernard, R., Ho, J. J., Gavryushova, A., et al. (2010). Hypoxic repression of endothelial nitric-oxide synthase transcription is coupled with eviction of promoter histones. *J. Biol. Chem.* 285, 810–826. doi: 10.1074/jbc.M109.067868

Fleming, I., and Busse, R. (1999). Signal transduction of eNOS activation. *Cardiovasc. Res.* 43, 532–541. doi: 10.1016/s0008-6363(99)00094-2

Fu, R., Lv, W. C., Xu, Y., Gong, M. Y., Chen, X. J., Jiang, N., et al. (2020). Endothelial ZEB1 promotes angiogenesis-dependent bone formation and reverses osteoporosis. *Nat. Commun.* 11:460. doi: 10.1038/s41467-019-14076-3

Fu, Y., Chang, A., Chang, L., Niessen, K., Eapen, S., Setiadi, A., et al. (2009). Differential regulation of transforming growth factor beta signaling pathways by Notch in human endothelial cells. *J. Biol. Chem.* 284, 19452–19462. doi: 10.1074/jbc.M109.011833

Gillette, T. G., and Hill, J. A. (2015). Readers, writers, and erasers: chromatin as the whiteboard of heart disease. *Circ. Res.* 116, 1245–1253. doi: 10.1161/CIRCRESAHA.116.303630

Gong, F., Chiu, L. Y., and Miller, K. M. (2016). Acetylation reader proteins: linking acetylation signaling to genome maintenance and cancer. *PLoS Genet.* 12:e1006272. doi: 10.1371/journal.pgen.1006272

Gray, J. E., Saltos, A., Tanvetyanon, T., Haura, E. B., Creelan, B., Antonia, S. J., et al. (2019). Phase I/ib study of pembrolizumab plus vorinostat in advanced/metastatic non-small cell lung cancer. *Clin. Cancer Res.* 25, 6623–6632. doi: 10.1158/1078-0432.CCR-19-1305

Guo, J., Wang, Z., Wu, J., Liu, M., Li, M., Sun, Y., et al. (2019). Endothelial SIRT6 Is vital to prevent hypertension and associated cardiorenal injury through targeting Nkx3.2-GATA5 signaling. *Circ. Res.* 124, 1448–1461. doi: 10.1161/CIRCRESAHA.118.314032

Hai, Y., Shinsky, S. A., Porter, N. J., and Christianson, D. W. (2017). Histone deacetylase 10 structure and molecular function as a polyamine deacetylase. *Nat. Commun.* 8:15368. doi: 10.1038/ncomms15368

Hakami, N. Y., Dusting, G. J., and Peshavariya, H. M. (2016). Trichostatin A, a histone deacetylase inhibitor suppresses NADPH Oxidase 4-Derived redox signalling and angiogenesis. *J. Cell Mol. Med.* 20, 1932–1944. doi: 10.1111/jcmm.12885

Hamada, K., Osaka, M., and Yoshida, M. (2014). Cell density impacts epigenetic regulation of cytokine-induced E-selectin gene expression in vascular endothelium. *PLoS One* 9:e90502. doi: 10.1371/journal.pone.0090502

He, M., Huang, T. S., Li, S., Hong, H. C., Chen, Z., Martin, M., et al. (2019). Atheroprotective Flow Upregulates ITPR3 (Inositol 1,4,5-Trisphosphate Receptor 3) in vascular endothelium via KLF4 (Kruppel-Like Factor 4)-Mediated histone modifications. *Arterioscler. Thromb. Vasc. Biol.* 39, 902–914. doi: 10.1161/ATVBAHA.118.312301

He, X., Zeng, H., Chen, S. T., Roman, R. J., Aschner, J. L., Didion, S., et al. (2017). Endothelial specific SIRT3 deletion impairs glycolysis and angiogenesis and causes diastolic dysfunction. *J. Mol. Cell Cardiol.* 112, 104–113. doi: 10.1016/j.yjmcc.2017.09.007

He, Z. X., Wei, B. F., Zhang, X., Gong, Y. P., Ma, L. Y., and Zhao, W. (2021). Current development of CBP/p300 inhibitors in the last decade. *Eur. J. Med. Chem.* 209:112861. doi: 10.1016/j.ejmech.2020.112861

Hebbel, R. P., Vercellotti, G. M., Pace, B. S., Solovey, A. N., Kollander, R., Abanonu, C. F., et al. (2010). The HDAC inhibitors trichostatin A and suberoylanilide hydroxamic acid exhibit multiple modalities of benefit for the vascular pathobiology of sickle transgenic mice. *Blood* 115, 2483–2490. doi: 10.1182/blood-2009-02-204990

Heintzman, N. D., Stuart, R. K., Hon, G., Fu, Y., Ching, C. W., Hawkins, R. D., et al. (2007). Distinct and predictive chromatin signatures of transcriptional promoters and enhancers in the human genome. *Nat. Genet.* 39, 311–318. doi: 10.1038/ng1966

Hellebrekers, D. M., Castermans, K., Vire, E., Dings, R. P., Hoebers, N. T., Mayo, K. H., et al. (2006). Epigenetic regulation of tumor endothelial cell anergy: silencing of intercellular adhesion molecule-1 by histone modifications. *Cancer Res.* 66, 10770–10777. doi: 10.1158/0008-5472.CAN-06-1609

Helmlinger, D., Papai, G., Devys, D., and Tora, L. (2020). What do the structures of GCN5-containing complexes teach us about their function? *Biochim. Biophys. Acta Gene Regul. Mech.* 1864:194614. doi: 10.1016/j.bbagrm.2020.194614

Helmlinger, D., and Tora, L. (2017). Sharing the SAGA. *Trends Biochem. Sci.* 42, 850–861. doi: 10.1016/j.tibs.2017.09.001

Hnisz, D., Abraham, B. J., Lee, T. I., Lau, A., Saint-Andre, V., Sigova, A. A., et al. (2013). Super-enhancers in the control of cell identity and disease. *Cell* 155, 934–947. doi: 10.1016/j.cell.2013.09.053

Hou, Q., Hu, K., Liu, X., Quan, J., and Liu, Z. (2018). HADC regulates the diabetic vascular endothelial dysfunction by targetting MnSOD. *Biosci. Rep.* 38:BSR20181042. doi: 10.1042/BSR20181042

Hsu, Y. F., Sheu, J. R., Lin, C. H., Chen, W. C., Hsiao, G., Ou, G., et al. (2011). MAPK phosphatase-1 contributes to trichostatin A inhibition of cyclooxygenase-2 expression in human umbilical vascular endothelial cells exposed to lipopolysaccharide. *Biochim. Biophys. Acta* 1810, 1160–1169. doi: 10.1016/j.bbagen.2011.08.015

Illi, B., Dello Russo, C., Colussi, C., Rosati, J., Pallaoro, M., Spallotta, F., et al. (2008). Nitric oxide modulates chromatin folding in human endothelial cells via protein phosphatase 2A activation and class II histone deacetylases nuclear shuttling. *Circ. Res.* 102, 51–58. doi: 10.1161/CIRCRESAHA.107.157305

Illi, B., Nanni, S., Scopece, A., Farsetti, A., Biglioli, P., Capogrossi, M. C., et al. (2003). Shear stress-mediated chromatin remodeling provides molecular basis for flow-dependent regulation of gene expression. *Circ. Res.* 93, 155–161. doi: 10.1161/01.RES.0000080933.82105.29

Inoue, K., Kobayashi, M., Yano, K., Miura, M., Izumi, A., Mataki, C., et al. (2006). Histone deacetylase inhibitor reduces monocyte adhesion to endothelium through the suppression of vascular cell adhesion molecule-1 expression. *Arterioscler. Thromb. Vasc. Biol.* 26, 2652–2659. doi: 10.1161/01.ATV.0000247247.89787.e7

Iring, A., Jin, Y. J., Albarran-Juarez, J., Siragusa, M., Wang, S., Dancs, P. T., et al. (2019). Shear stress-induced endothelial adrenomedullin signaling regulates vascular tone and blood pressure. *J. Clin. Invest.* 129, 2775–2791. doi: 10.1172/JCI123825

Jamal, J., Mustafa, M. R., and Wong, P. F. (2014). Paeonol protects against premature senescence in endothelial cells by modulating Sirtuin 1 pathway. *J. Ethnopharmacol.* 154, 428–436. doi: 10.1016/j.jep.2014.04.025

Javaid, N., and Choi, S. (2017). Acetylation- and methylation-related epigenetic proteins in the context of their targets. *Genes* 8:196. doi: 10.3390/genes8080196

Jiang, L., Yin, M., Wei, X., Liu, J., Wang, X., Niu, C., et al. (2015). Bach1 represses wnt/beta-catenin signaling and angiogenesis. *Circ. Res.* 117, 364–375. doi: 10.1161/CIRCRESAHA.115.306829

Jin, G., Bausch, D., Knightly, T., Liu, Z., Li, Y., Liu, B., et al. (2011). Histone deacetylase inhibitors enhance endothelial cell sprouting angiogenesis in vitro. *Surgery* 150, 429–435. doi: 10.1016/j.surg.2011.07.001

Joshi, B., Ordonez-Ercan, D., Dasgupta, P., and Chellappan, S. (2005). Induction of human metallothionein 1G promoter by VEGF and heavy metals: differential involvement of E2F and metal transcription factors. *Oncogene* 24, 2204–2217. doi: 10.1038/sj.onc.1208206

Ke, X., Johnson, H., Jing, X., Michalkiewicz, T., Huang, Y. W., Lane, R. H., et al. (2018). Persistent pulmonary hypertension alters the epigenetic characteristics of endothelial nitric oxide synthase gene in pulmonary artery endothelial cells in a fetal lamb model. *Physiol. Genomics* 50, 828–836. doi: 10.1152/physiolgenomics.00047.2018

Kelly, R. D., and Cowley, S. M. (2013). The physiological roles of histone deacetylase (HDAC) 1 and 2: complex co-stars with multiple leading parts. *Biochem. Soc. Trans.* 41, 741–749. doi: 10.1042/BST20130010

Kida, Y., and Goligorsky, M. S. (2016). Sirtuins, cell senescence, and vascular aging. *Can. J. Cardiol.* 32, 634–641. doi: 10.1016/j.cjca.2015.11.022

Kim, J. H., Kim, J. H., Oh, M., Yu, Y. S., Kim, K. W., and Kwon, H. J. (2009). N-hydroxy-7-(2-naphthylthio) heptanomide inhibits retinal and choroidal angiogenesis. *Mol. Pharm.* 6, 513–519. doi: 10.1021/mp800178b

Kim, Y. R., Kim, C. S., Naqvi, A., Kumar, A., Kumar, S., Hoffman, T. A., et al. (2012). Epigenetic upregulation of p66shc mediates low-density lipoprotein cholesterol-induced endothelial cell dysfunction. *Am. J. Physiol. Heart Circ. Physiol.* 303, H189–H196. doi: 10.1152/ajpheart.01218.2011

Krishna, S. M., Trollope, A. F., and Golledge, J. (2015). The relevance of epigenetics to occlusive cerebral and peripheral arterial disease. *Clin. Sci.* 128, 537–558. doi: 10.1042/CS20140491

Kurz, D. J., Payeli, S., Greutert, H., Briand Schumacher, S., Luscher, T. F., and Tanner, F. C. (2014). Epigenetic regulation of tissue factor inducibility in endothelial cell senescence. *Mech. Ageing Dev.* 140, 1–9. doi: 10.1016/j.mad.2014.07.002

Larsson, P., Alwis, I., Niego, B., Sashindranath, M., Fogelstrand, P., Wu, M. C., et al. (2016). Valproic acid selectively increases vascular endothelial tissue-type plasminogen activator production and reduces thrombus formation in the mouse. *J. Thromb. Haemost.* 14, 2496–2508. doi: 10.1111/jth.13527

Larsson, P., Ulfhammer, E., Magnusson, M., Bergh, N., Lunke, S., El-Osta, A., et al. (2012). Role of histone acetylation in the stimulatory effect of valproic acid on vascular endothelial tissue-type plasminogen activator expression. *PLoS One* 7:e31573. doi: 10.1371/journal.pone.0031573

Li, B., Li, Y., Liu, K., Wang, X., Qi, J., Wang, B., et al. (2017). High glucose decreases claudins-5 and -11 in cardiac microvascular endothelial cells: antagonistic effects of tongxinluo. *Endocr. Res.* 42, 15–21. doi: 10.3109/07435800.2016.1163723

Li, M., Gallo, D., Csizmadia, E., Otterbein, L. E., and Wegiel, B. (2014). Carbon monoxide induces chromatin remodelling to facilitate endothelial cell migration. *Thromb. Haemost.* 111, 951–959. doi: 10.1160/TH13-09-0748

Li, M., van Esch, B., Henricks, P. A. J., Folkerts, G., and Garssen, J. (2018). The anti-inflammatory effects of short chain fatty acids on lipopolysaccharide- or tumor necrosis factor alpha-stimulated endothelial cells via activation of GPR41/43 and inhibition of HDACs. *Front. Pharmacol.* 9:533. doi: 10.3389/fphar.2018.00533

Li, T., Zhang, C., Hassan, S., Liu, X., Song, F., Chen, K., et al. (2018). Histone deacetylase 6 in cancer. *J. Hematol. Oncol.* 11:111. doi: 10.1186/s13045-018-0654-9

Li, X., Shao, Y., Sha, X., Fang, P., Kuo, Y. M., Andrews, A. J., et al. (2018). IL-35 (Interleukin-35) suppresses endothelial cell activation by inhibiting mitochondrial reactive oxygen species-mediated site-specific acetylation of H3K14 (Histone 3 Lysine 14). *Arterioscler. Thromb. Vasc. Biol.* 38, 599–609. doi: 10.1161/ATVBAHA.117.310626

Li, Z., Zhang, X., Liu, S., Zeng, S., Yu, L., Yang, G., et al. (2018). BRG1 regulates NOX gene transcription in endothelial cells and contributes to cardiac ischemia-reperfusion injury. *Biochim. Biophys. Acta Mol. Basis Dis.* 1864, 3477–3486. doi: 10.1016/j.bbadis.2018.08.002

Liao, J. K., and Laufs, U. (2005). Pleiotropic effects of statins. *Annu. Rev. Pharmacol. Toxicol.* 45, 89–118. doi: 10.1146/annurev.pharmtox.45.120403.095748

Lipinski, M., Del Blanco, B., and Barco, A. (2019). CBP/p300 in brain development and plasticity: disentangling the KAT's cradle. *Curr. Opin. Neurobiol.* 59, 1–8. doi: 10.1016/j.conb.2019.01.023

Liu, D., Perkins, J. T., and Hennig, B. (2016). EGCG prevents PCB-126-induced endothelial cell inflammation via epigenetic modifications of NF-kappaB target genes in human endothelial cells. *J. Nutr. Biochem.* 28, 164–170. doi: 10.1016/j.jnutbio.2015.10.003

Liu, S. S., Wu, F., Jin, Y. M., Chang, W. Q., and Xu, T. M. (2020). HDAC11: a rising star in epigenetics. *Biomed. Pharmacother.* 131:110607. doi: 10.1016/j.biopha.2020.110607

Lu, Y., Sun, Y., Drummer, C. T., Nanayakkara, G. K., Shao, Y., Saaoud, F., et al. (2019). Increased acetylation of H3K14 in the genomic regions that encode trained immunity enzymes in lysophosphatidylcholine-activated human aortic endothelial cells - Novel qualification markers for chronic disease risk factors and conditional DAMPs. *Redox Biol.* 24:101221. doi: 10.1016/j.redox.2019.101221

Malik, A. B., Lynch, J. J., and Cooper, J. A. (1989). Endothelial barrier function. *J. Invest. Dermatol.* 93(2 Suppl.), 62S–67S. doi: 10.1111/1523-1747.ep12581072

Marmorstein, R., and Zhou, M. M. (2014). Writers and readers of histone acetylation: structure, mechanism, and inhibition. *Cold Spring Harb. Perspect. Biol.* 6:a018762. doi: 10.1101/cshperspect.a018762

Michaelis, M., Suhan, T., Michaelis, U. R., Beek, K., Rothweiler, F., Tausch, L., et al. (2006). Valproic acid induces extracellular signal-regulated kinase 1/2 activation and inhibits apoptosis in endothelial cells. *Cell Death Differ.* 13, 446–453. doi: 10.1038/sj.cdd.4401759

Millard, C. J., Watson, P. J., Fairall, L., and Schwabe, J. W. R. (2017). Targeting class i histone deacetylases in a "Complex" environment. *Trends Pharmacol. Sci.* 38, 363–377. doi: 10.1016/j.tips.2016.12.006

Mishra, M., Duraisamy, A. J., Bhattacharjee, S., and Kowluru, R. A. (2019). Adaptor protein p66Shc: a link between cytosolic and mitochondrial dysfunction in the development of diabetic retinopathy. *Antioxid Redox Signal* 30, 1621–1634. doi: 10.1089/ars.2018.7542

Mojiri, A., Alavi, P., Lorenzana Carrillo, M. A., Nakhaei-Nejad, M., Sergi, C. M., Thebaud, B., et al. (2019). Endothelial cells of different organs exhibit heterogeneity in von Willebrand factor expression in response to hypoxia. *Atherosclerosis* 282, 1–10. doi: 10.1016/j.atherosclerosis.2019.01.002

Mortuza, R., Feng, B., and Chakrabarti, S. (2015). SIRT1 reduction causes renal and retinal injury in diabetes through endothelin 1 and transforming growth factor beta1. *J. Cell Mol. Med.* 19, 1857–1867. doi: 10.1111/jcmm.12557

Murugavel, S., Bugyei-Twum, A., Matkar, P. N., Al-Mubarak, H., Chen, H. H., Adam, M., et al. (2018). Valproic acid induces endothelial-to-mesenchymal transition-like phenotypic switching. *Front. Pharmacol.* 9:737. doi: 10.3389/fphar.2018.00737

Mutlu, B., and Puigserver, P. (2020). GCN5 acetyltransferase in cellular energetic and metabolic processes. *Biochim. Biophys. Acta Gene Regul. Mech.* 1864:194626. doi: 10.1016/j.bbagrm.2020.194626

O'Connor, O. A., Horwitz, S., Masszi, T., Van Hoof, A., Brown, P., Doorduijn, J., et al. (2015). Belinostat in patients with relapsed or refractory Peripheral T-Cell lymphoma: results of the pivotal phase II BELIEF (CLN-19) study. *J. Clin. Oncol.* 33, 2492–2499. doi: 10.1200/JCO.2014.59.2782

Ohashi, A., Yasuda, H., Kamiya, T., Hara, H., and Adachi, T. (2017). CAPE increases the expression of SOD3 through epigenetics in human retinal endothelial cells. *J. Clin. Biochem. Nutr.* 61, 6–13. doi: 10.3164/jcbn.16-109

Olmos, Y., Sanchez-Gomez, F. J., Wild, B., Garcia-Quintans, N., Cabezudo, S., Lamas, S., et al. (2013). SirT1 regulation of antioxidant genes is dependent on the formation of a FoxO3a/PGC-1alpha complex. *Antioxid Redox Signal* 19, 1507–1521. doi: 10.1089/ars.2012.4713

Paneni, F., Mocharla, P., Akhmedov, A., Costantino, S., Osto, E., Volpe, M., et al. (2012). Gene silencing of the mitochondrial adaptor p66(Shc) suppresses vascular hyperglycemic memory in diabetes. *Circ. Res.* 111, 278–289. doi: 10.1161/CIRCRESAHA.112.266593

Passacquale, G., Phinikaridou, A., Warboys, C., Cooper, M., Lavin, B., Alfieri, A., et al. (2015). Aspirin-induced histone acetylation in endothelial cells enhances synthesis of the secreted isoform of netrin-1 thus inhibiting monocyte vascular infiltration. *Br. J. Pharmacol.* 172, 3548–3564. doi: 10.1111/bph.13144

Peng, Y., Stewart, D., Li, W., Hawkins, M., Kulak, S., Ballermann, B., et al. (2007). Irradiation modulates association of NF-Y with histone-modifying cofactors PCAF and HDAC. *Oncogene* 26, 7576–7583. doi: 10.1038/sj.onc.1210565

Perrone, L., Devi, T. S., Hosoya, K., Terasaki, T., and Singh, L. P. (2009). Thioredoxin interacting protein (TXNIP) induces inflammation through chromatin modification in retinal capillary endothelial cells under diabetic conditions. *J. Cell Physiol.* 221, 262–272. doi: 10.1002/jcp.21852

Phillips, D. M. (1963). The presence of acetyl groups of histones. *Biochem. J.* 87, 258–263. doi: 10.1042/bj0870258

Pillai, S., Kovacs, M., and Chellappan, S. (2010). Regulation of vascular endothelial growth factor receptors by Rb and E2F1: role of acetylation. *Cancer Res.* 70, 4931–4940. doi: 10.1158/0008-5472.CAN-10-0501

Pillus, L. (2008). MYSTs mark chromatin for chromosomal functions. *Curr. Opin. Cell Biol.* 20, 326–333. doi: 10.1016/j.ceb.2008.04.009

Pirola, L., Balcerczyk, A., Tothill, R. W., Haviv, I., Kaspi, A., Lunke, S., et al. (2011). Genome-wide analysis distinguishes hyperglycemia regulated epigenetic signatures of primary vascular cells. *Genome Res.* 21, 1601–1615. doi: 10.1101/gr.116095.110

Postberg, J., Kanders, M., Forcob, S., Willems, R., Orth, V., Hensel, K. O., et al. (2015). CpG signalling, H2A.Z/H3 acetylation and microRNA-mediated deferred self-attenuation orchestrate foetal NOS3 expression. *Clin. Epigenetics* 7:9. doi: 10.1186/s13148-014-0042-4

Potente, M., and Makinen, T. (2017). Vascular heterogeneity and specialization in development and disease. *Nat. Rev. Mol. Cell Biol.* 18, 477–494. doi: 10.1038/nrm.2017.36

Poulsen, L. C., Edelmann, R. J., Kruger, S., Dieguez-Hurtado, R., Shah, A., Stav-Noraas, T. E., et al. (2018). Inhibition of endothelial NOTCH1 signaling attenuates inflammation by reducing cytokine-mediated histone acetylation at inflammatory enhancers. *Arterioscler. Thromb. Vasc. Biol.* 38, 854–869. doi: 10.1161/ATVBAHA.117.310388

Qian, D. Z., Kato, Y., Shabbeer, S., Wei, Y., Verheul, H. M., Salumbides, B., et al. (2006). Targeting tumor angiogenesis with histone deacetylase inhibitors: the hydroxamic acid derivative LBH589. *Clin. Cancer Res.* 12, 634–642. doi: 10.1158/1078-0432.CCR-05-1132

Rando, O. J., and Chang, H. Y. (2009). Genome-wide views of chromatin structure. *Annu. Rev. Biochem.* 78, 245–271. doi: 10.1146/annurev.biochem.78.071107.134639

Reifsnyder, C., Lowell, J., Clarke, A., and Pillus, L. (1996). Yeast SAS silencing genes and human genes associated with AML and HIV-1 Tat interactions are homologous with acetyltransferases. *Nat. Genet.* 14, 42–49. doi: 10.1038/ng0996-42

Ren, B., Best, B., Ramakrishnan, D. P., Walcott, B. P., Storz, P., and Silverstein, R. L. (2016). LPA/PKD-1-FoxO1 signaling axis mediates endothelial cell CD36 transcriptional repression and proangiogenic and proarteriogenic reprogramming. *Arterioscler. Thromb. Vasc. Biol.* 36, 1197–1208. doi: 10.1161/ATVBAHA.116.307421

Ren, B., Hale, J., Srikanthan, S., and Silverstein, R. L. (2011). Lysophosphatidic acid suppresses endothelial cell CD36 expression and promotes angiogenesis via a PKD-1-dependent signaling pathway. *Blood* 117, 6036–6045. doi: 10.1182/blood-2010-12-326017

Rodriguez, C. P., Wu, Q. V., Voutsinas, J., Fromm, J. R., Jiang, X., Pillarisetty, V. G., et al. (2020). A Phase II trial of pembrolizumab and vorinostat in recurrent metastatic head and neck squamous cell carcinomas and salivary gland cancer. *Clin. Cancer Res.* 26, 837–845. doi: 10.1158/1078-0432.CCR-19-2214

Rose, J. L., Huang, H., Wray, S. F., and Hoyt, D. G. (2005). Integrin engagement increases histone H3 acetylation and reduces histone H1 association with DNA in murine lung endothelial cells. *Mol. Pharmacol.* 68, 439–446. doi: 10.1124/mol.104.010876

Rossig, L., Li, H., Fisslthaler, B., Urbich, C., Fleming, I., Forstermann, U., et al. (2002). Inhibitors of histone deacetylation downregulate the expression of endothelial nitric oxide synthase and compromise endothelial cell function in vasorelaxation and angiogenesis. *Circ. Res.* 91, 837–844. doi: 10.1161/01.res.0000037983.07158.b1

Saksouk, N., Avvakumov, N., Champagne, K. S., Hung, T., Doyon, Y., Cayrou, C., et al. (2009). HBO1 HAT complexes target chromatin throughout gene coding regions via multiple PHD finger interactions with histone H3 tail. *Mol. Cell* 33, 257–265. doi: 10.1016/j.molcel.2009.01.007

Santos-Rosa, H., and Caldas, C. (2005). Chromatin modifier enzymes, the histone code and cancer. *Eur. J. Cancer* 41, 2381–2402. doi: 10.1016/j.ejca.2005.08.010

Schmeck, B., Beermann, W., N'Guessan, P. D., Hocke, A. C., Opitz, B., Eitel, J., et al. (2008). Simvastatin reduces *Chlamydophila* pneumoniae-mediated histone modifications and gene expression in cultured human endothelial cells. *Circ. Res.* 102, 888–895. doi: 10.1161/CIRCRESAHA.107.161307

Schmeck, B., Beermann, W., van Laak, V., Opitz, B., Hocke, A. C., Meixenberger, K., et al. (2006). Listeria monocytogenes induced Rac1-dependent signal transduction in endothelial cells. *Biochem. Pharmacol.* 72, 1367–1374. doi: 10.1016/j.bcp.2006.06.033

Schmeck, B., Beermann, W., van Laak, V., Zahlten, J., Opitz, B., Witzenrath, M., et al. (2005). Intracellular bacteria differentially regulated endothelial cytokine release by MAPK-dependent histone modification. *J. Immunol.* 175, 2843–2850. doi: 10.4049/jimmunol.175.5.2843

Sekeres, M. A., Othus, M., List, A. F., Odenike, O., Stone, R. M., Gore, S. D., et al. (2017). Randomized phase II study of azacitidine alone or in combination with lenalidomide or with vorinostat in higher-risk myelodysplastic syndromes and chronic myelomonocytic leukemia: north american intergroup study SWOG S1117. *J. Clin. Oncol.* 35, 2745–2753. doi: 10.1200/JCO.2015.66.2510

Seto, E., and Yoshida, M. (2014). Erasers of histone acetylation: the histone deacetylase enzymes. *Cold Spring Harb. Perspect. Biol.* 6:a018713. doi: 10.1101/cshperspect.a018713

Shahbazian, M. D., and Grunstein, M. (2007). Functions of site-specific histone acetylation and deacetylation. *Annu. Rev. Biochem.* 76, 75–100. doi: 10.1146/annurev.biochem.76.052705.162114

Shao, J., Weng, X., Zhuo, L., Yu, L., Li, Z., Shen, K., et al. (2019). Angiotensin II induced CSF1 transcription is mediated by a crosstalk between different epigenetic factors in vascular endothelial cells. *Biochim. Biophys. Acta Gene Regul. Mech.* 1862, 1–11. doi: 10.1016/j.bbagrm.2018.10.001

Sheikh, B. N., and Akhtar, A. (2019). The many lives of KATs - detectors, integrators and modulators of the cellular environment. *Nat. Rev. Genet.* 20, 7–23. doi: 10.1038/s41576-018-0072-4

Shi, Y., Xu, X., Zhang, Q., Fu, G., Mo, Z., Wang, G. S., et al. (2014). tRNA synthetase counteracts c-Myc to develop functional vasculature. *eLife* 3:e02349. doi: 10.7554/eLife.02349

Shu, X. Z., Zhang, L. N., Zhang, R., Zhang, C. J., He, H. P., Zhou, H., et al. (2015). Histone acetyltransferase p300 promotes MRTF-A-mediates transactivation of VE-cadherin gene in human umbilical vein endothelial cells. *Gene* 563, 17–23. doi: 10.1016/j.gene.2015.02.076

Simiele, F., Recchiuti, A., Patruno, S., Plebani, R., Pierdomenico, A. M., Codagnone, M., et al. (2016). Epigenetic regulation of the formyl peptide receptor 2 gene. *Biochim. Biophys. Acta* 1859, 1252–1258. doi: 10.1016/j.bbagrm.2016.07.007

Singh, C. K., Chhabra, G., Ndiaye, M. A., Garcia-Peterson, L. M., Mack, N. J., and Ahmad, N. (2018). The role of sirtuins in antioxidant and redox signaling. *Antioxid Redox Signal* 28, 643–661. doi: 10.1089/ars.2017.7290

Siuda, D., Zechner, U., El Hajj, N., Prawitt, D., Langer, D., Xia, N., et al. (2012). Transcriptional regulation of Nox4 by histone deacetylases in human endothelial cells. *Basic Res. Cardiol.* 107:283. doi: 10.1007/s00395-012-0283-3

Spedale, G., Timmers, H. T., and Pijnappel, W. W. (2012). ATAC-king the complexity of SAGA during evolution. *Genes Dev.* 26, 527–541. doi: 10.1101/gad.184705.111

Stauffer, B. L., Westby, C. M., and DeSouza, C. A. (2008). Endothelin-1, aging and hypertension. *Curr. Opin. Cardiol.* 23, 350–355. doi: 10.1097/HCO.0b013e328302f3c6

Sturtzel, C. (2017). Endothelial cells. *Adv. Exp. Med. Biol.* 1003, 71–91. doi: 10.1007/978-3-319-57613-8_4

Su, H., Zeng, H., He, X., Zhu, S. H., and Chen, J. X. (2020). Histone acetyltransferase p300 inhibitor improves coronary flow reserve in SIRT3 (Sirtuin 3) knockout mice. *J. Am. Heart Assoc.* 9:e017176. doi: 10.1161/JAHA.120.017176

Svennerholm, K., Bergh, N., Larsson, P., Jern, S., Johansson, G., Biber, B., et al. (2014). Histone deacetylase inhibitor treatment increases coronary t-PA release in a porcine ischemia model. *PLoS One* 9:e97260. doi: 10.1371/journal.pone.0097260

Svennerholm, K., Haney, M., Biber, B., Ulfhammer, E., Saluveer, O., Larsson, P., et al. (2015). Histone deacetylase inhibition enhances tissue plasminogen activator release capacity in atherosclerotic man. *PLoS One* 10:e0121196. doi: 10.1371/journal.pone.0121196

Tambo, Y., Hosomi, Y., Sakai, H., Nogami, N., Atagi, S., Sasaki, Y., et al. (2017). Phase I/II study of docetaxel combined with resminostat, an oral hydroxamic acid HDAC inhibitor, for advanced non-small cell lung cancer in patients previously treated with platinum-based chemotherapy. *Invest. New Drugs* 35, 217–226. doi: 10.1007/s10637-017-0435-2

Tanegashima, K., Sato-Miyata, Y., Funakoshi, M., Nishito, Y., Aigaki, T., and Hara, T. (2017). Epigenetic regulation of the glucose transporter gene Slc2a1 by beta-hydroxybutyrate underlies preferential glucose supply to the brain of fasted mice. *Genes Cells* 22, 71–83. doi: 10.1111/gtc.12456

Tang, F. B., Dai, Y. L., Zhou, G. Y., Zhang, W. H., Wang, H. B., Li, Y. G., et al. (2018). Valproic acid treatment inhibits vasopermeability and improves survival in rats with lethal scald injury. *J. Burn Care Res.* 39, 209–217. doi: 10.1097/BCR.0000000000000568

Tessarz, P., and Kouzarides, T. (2014). Histone core modifications regulating nucleosome structure and dynamics. *Nat. Rev. Mol. Cell Biol.* 15, 703–708. doi: 10.1038/nrm3890

Thangavel, J., Malik, A. B., Elias, H. K., Rajasingh, S., Simpson, A. D., Sundivakkam, P. K., et al. (2014). Combinatorial therapy with acetylation and methylation modifiers attenuates lung vascular hyperpermeability in endotoxemia-induced mouse inflammatory lung injury. *Am. J. Pathol.* 184, 2237–2249. doi: 10.1016/j.ajpath.2014.05.008

Thomas, T., and Voss, A. K. (2007). The diverse biological roles of MYST histone acetyltransferase family proteins. *Cell Cycle* 6, 696–704. doi: 10.4161/cc.6.6.4013

Turtoi, A., Mottet, D., Matheus, N., Dumont, B., Peixoto, P., Hennequiere, V., et al. (2012). The angiogenesis suppressor gene AKAP12 is under the epigenetic control of HDAC7 in endothelial cells. *Angiogenesis* 15, 543–554. doi: 10.1007/s10456-012-9279-8

Ulfhammer, E., Larsson, P., Magnusson, M., Karlsson, L., Bergh, N., and Jern, S. (2016). Dependence of proximal GC boxes and binding transcription factors in the regulation of basal and valproic acid-induced expression of t-PA. *Int. J. Vasc. Med.* 2016:7928681. doi: 10.1155/2016/7928681

Van De Craen, B., Declerck, P. J., and Gils, A. (2012). The biochemistry, physiology and pathological roles of PAI-1 and the requirements for PAI-1 inhibition in vivo. *Thromb. Res.* 130, 576–585. doi: 10.1016/j.thromres.2012.06.023

Verdin, E., and Ott, M. (2015). 50 years of protein acetylation: from gene regulation to epigenetics, metabolism and beyond. *Nat. Rev. Mol. Cell Biol.* 16, 258–264. doi: 10.1038/nrm3931

Visel, A., Blow, M. J., Li, Z., Zhang, T., Akiyama, J. A., Holt, A., et al. (2009). ChIP-seq accurately predicts tissue-specific activity of enhancers. *Nature* 457, 854–858. doi: 10.1038/nature07730

Wan, Y. Z., Gao, P., Zhou, S., Zhang, Z. Q., Hao, D. L., Lian, L. S., et al. (2014). SIRT1-mediated epigenetic downregulation of plasminogen activator inhibitor-1 prevents vascular endothelial replicative senescence. *Aging Cell* 13, 890–899. doi: 10.1111/acel.12247

Wang, J., Mahmud, S. A., Bitterman, P. B., Huo, Y., and Slungaard, A. (2007). Histone deacetylase inhibitors suppress TF-kappaB-dependent agonist-driven tissue factor expression in endothelial cells and monocytes. *J. Biol. Chem.* 282, 28408–28418. doi: 10.1074/jbc.M703586200

Wiesel-Motiuk, N., and Assaraf, Y. G. (2020). The key roles of the lysine acetyltransferases KAT6A and KAT6B in physiology and pathology. *Drug Resist. Updat.* 53:100729. doi: 10.1016/j.drup.2020.100729

Wilcox, J. N., Subramanian, R. R., Sundell, C. L., Tracey, W. R., Pollock, J. S., Harrison, D. G., et al. (1997). Expression of multiple isoforms of nitric oxide synthase in normal and atherosclerotic vessels. *Arterioscler. Thromb. Vasc. Biol.* 17, 2479–2488. doi: 10.1161/01.atv.17.11.2479

Won, K. J., Jung, S. H., Jung, S. H., Lee, K. P., Lee, H. M., Lee, D. Y., et al. (2014). DJ-1/park7 modulates vasorelaxation and blood pressure via epigenetic modification of endothelial nitric oxide synthase. *Cardiovasc. Res.* 101, 473–481. doi: 10.1093/cvr/cvt274

Xu, P., Li, C., Chen, Z., Jiang, S., Fan, S., Wang, J., et al. (2016). The NuA4 core complex acetylates nucleosomal histone H4 through a double recognition mechanism. *Mol. Cell* 63, 965–975. doi: 10.1016/j.molcel.2016.07.024

Xu, X. F., Lv, Y., Gu, W. Z., Tang, L. L., Wei, J. K., Zhang, L. Y., et al. (2013). Epigenetics of hypoxic pulmonary arterial hypertension following intrauterine growth retardation rat: epigenetics in PAH following IUGR. *Respir. Res.* 14:20. doi: 10.1186/1465-9921-14-20

Xu, X. F., Ma, X. L., Shen, Z., Wu, X. L., Cheng, F., and Du, L. Z. (2010). Epigenetic regulation of the endothelial nitric oxide synthase gene in persistent pulmonary hypertension of the newborn rat. *J. Hypertens* 28, 2227–2235. doi: 10.1097/HJH.0b013e32833e08f1

Yan, M. S., Turgeon, P. J., Man, H. J., Dubinsky, M. K., Ho, J. J. D., El-Rass, S., et al. (2018). Histone acetyltransferase 7 (KAT7)-dependent intragenic histone acetylation regulates endothelial cell gene regulation. *J. Biol. Chem.* 293, 4381–4402. doi: 10.1074/jbc.RA117.001383

Yang, D., Xie, P., and Liu, Z. (2012). Ischemia/reperfusion-induced MKP-3 impairs endothelial NO formation via inactivation of ERK1/2 pathway. *PLoS One* 7:e42076. doi: 10.1371/journal.pone.0042076

Yasuda, H., Ohashi, A., Nishida, S., Kamiya, T., Suwa, T., Hara, H., et al. (2016). Exendin-4 induces extracellular-superoxide dismutase through histone H3 acetylation in human retinal endothelial cells. *J. Clin. Biochem. Nutr.* 59, 174–181. doi: 10.3164/jcbn.16-26

You, D., Wen, X., Gorczyca, L., Morris, A., Richardson, J. R., and Aleksunes, L. M. (2019). Increased MDR1 transporter expression in human brain endothelial cells through enhanced histone acetylation and activation of aryl hydrocarbon receptor signaling. *Mol. Neurobiol.* 56, 6986–7002. doi: 10.1007/s12035-019-1565-7

Zelko, I. N., and Folz, R. J. (2015). Regulation of oxidative stress in pulmonary artery endothelium. modulation of extracellular superoxide dismutase and NOX4 expression using histone deacetylase Class I inhibitors. *Am. J. Respir. Cell Mol. Biol.* 53, 513–524. doi: 10.1165/rcmb.2014-0260OC

Zelko, I. N., Stepp, M. W., Vorst, A. L., and Folz, R. J. (2011). Histone acetylation regulates the cell-specific and interferon-gamma-inducible expression of extracellular superoxide dismutase in human pulmonary arteries. *Am. J. Respir. Cell Mol. Biol.* 45, 953–961. doi: 10.1165/rcmb.2011-0012OC

Zeng, L., Zhang, Y., Chien, S., Liu, X., and Shyy, J. Y. (2003). The role of p53 deacetylation in p21Waf1 regulation by laminar flow. *J. Biol. Chem.* 278, 24594–24599. doi: 10.1074/jbc.M301955200

Zhang, B., Day, D. S., Ho, J. W., Song, L., Cao, J., Christodoulou, D., et al. (2013). A dynamic H3K27ac signature identifies VEGFA-stimulated endothelial enhancers and requires EP300 activity. *Genome Res.* 23, 917–927. doi: 10.1101/gr.149674.112

Zhang, M. X., Zhang, C., Shen, Y. H., Wang, J., Li, X. N., Chen, L., et al. (2008). Effect of 27nt small RNA on endothelial nitric-oxide synthase expression. *Mol. Biol. Cell* 19, 3997–4005. doi: 10.1091/mbc.E07-11-1186

Zhang, X., Williams, E. D., Azhar, G., Rogers, S. C., and Wei, J. Y. (2016). Does p49/STRAP, a SRF-binding protein (SRFBP1), modulate cardiac mitochondrial function in aging? *Exp. Gerontol* 82, 150–159. doi: 10.1016/j.exger.2016.06.008

Zhao, S., Zhang, X., and Li, H. (2018). Beyond histone acetylation-writing and erasing histone acylations. *Curr. Opin. Struct. Biol.* 53, 169–177. doi: 10.1016/j.sbi.2018.10.001

Zhong, Q., and Kowluru, R. A. (2010). Role of histone acetylation in the development of diabetic retinopathy and the metabolic memory phenomenon. *J. Cell Biochem.* 110, 1306–1313. doi: 10.1002/jcb.22644

Zhong, Q., and Kowluru, R. A. (2013). Regulation of matrix metalloproteinase-9 by epigenetic modifications and the development of diabetic retinopathy. *Diabetes* 62, 2559–2568. doi: 10.2337/db12-1141

Zhou, S., Chen, H. Z., Wan, Y. Z., Zhang, Q. J., Wei, Y. S., Huang, S., et al. (2011). Repression of P66Shc expression by SIRT1 contributes to the prevention of hyperglycemia-induced endothelial dysfunction. *Circ. Res.* 109, 639–648. doi: 10.1161/CIRCRESAHA.111.243592

Conflict of Interest: The authors declare that the research was conducted in the absence of any commercial or financial relationships that could be construed as a potential conflict of interest.

Copyright © 2021 Fang, Wang, Sun, Hu and Miao. This is an open-access article distributed under the terms of the Creative Commons Attribution License (CC BY). The use, distribution or reproduction in other forums is permitted, provided the original author(s) and the copyright owner(s) are credited and that the original publication in this journal is cited, in accordance with accepted academic practice. No use, distribution or reproduction is permitted which does not comply with these terms.

frontiers in Cell and Developmental Biology

ORIGINAL RESEARCH
published: 04 May 2021
doi: 10.3389/fcell.2021.657662

FOXC2 Autoregulates Its Expression in the Pulmonary Endothelium After Endotoxin Stimulation in a Histone Acetylation-Dependent Manner

*Sheng Xia[1†], Wei Yu[1†], Heather Menden[1], Scott T. Younger[2] and Venkatesh Sampath[1]**

[1] Department of Pediatrics, Children's Mercy Kansas City, MO, United States, [2] Center for Pediatric Genomic Medicine, Children's Mercy Kansas City, MO, United States

OPEN ACCESS

Edited by:
Xiaofeng Yang,
Temple University, United States

Reviewed by:
Ruijing Zhang,
Second Hospital of Shanxi Medical University, China
Owais Bhat,
Virginia Commonwealth University, United States

***Correspondence:**
Venkatesh Sampath
vsampath@cmh.edu

[†] These authors have contributed equally to this work and share first authorship

Specialty section:
This article was submitted to Signaling, a section of the journal Frontiers in Cell and Developmental Biology

Received: 23 January 2021
Accepted: 12 April 2021
Published: 04 May 2021

Citation:
Xia S, Yu W, Menden H, Younger ST and Sampath V (2021) FOXC2 Autoregulates Its Expression in the Pulmonary Endothelium After Endotoxin Stimulation in a Histone Acetylation-Dependent Manner. Front. Cell Dev. Biol. 9:657662. doi: 10.3389/fcell.2021.657662

The innate immune response of pulmonary endothelial cells (EC) to lipopolysaccharide (LPS) induces Forkhead box protein C2 (FOXC2) activation through Toll Like Receptor 4 (TLR4). The mechanisms by which FOXC2 expression is regulated in lung EC under LPS stimulation remain unclear. We postulated that FOXC2 regulates its own expression in sepsis, and its transcriptional autoregulation directs lymphatic EC cell-fate decision. Bioinformatic analysis identified potential FOXC2 binding sites in the *FOXC2* promoter. In human lung EC, we verified using chromatin immunoprecipitation (ChIP) and luciferase assays that FOXC2 bound to its own promoter and stimulated its expression after LPS stimulation. Chemical inhibition of histone acetylation by garcinol repressed LPS-induced histone acetylation in the *FOXC2* promoter region, and disrupted LPS-mediated FOXC2 binding and transcriptional activation. CRISPR/dCas9/gRNA directed against FOXC2-binding-element (FBE) suppressed LPS-stimulated FOXC2 binding and autoregulation by blocking FBEs in the *FOXC2* promoter, and repressed expression of lymphatic EC markers. In a neonatal mouse model of sterile sepsis, LPS-induced FOXC2 binding to FBE and FOXC2 expression in lung EC was attenuated with garcinol treatment. These data reveal a new mechanism of LPS-induced histone acetylation-dependent *FOXC2* autoregulation.

Keywords: FOXC2, autoregulation, endothelium, sepsis, lung

INTRODUCTION

FOXC2 is a member of the forkhead box (FOX) transcription factor family (Seo et al., 2006). It plays a critical role in vascular development. FOXC2 is a key transcription regulator involved in VEGF regulated vascular formation and remodeling in physiological and pathological conditions. VEGFA activates FOXC2 through kinase insert domain receptor (KDR) pathway in arterial endothelium, and then FOXC2 binds to delta like canonical Notch ligand 4 (DLL4) promoter and upregulates DLL4 expression, which in turn activates Notch signaling (Hayashi and Kume, 2008). Subsequently hes related family bHLH transcription factor with YRPW motif 1 (HEY1) and HEY2, downstream of DLL4/Notch signaling, collaborating with SRY-box transcription factor 7 (Sox7)/Sox18, lead to arterial specification through EphrinB2 activation (Hayashi and Kume, 2008). Unrelated to the role of FOXC2 in developmental signaling, we showed that systemic lipopolysaccharide (LPS)

upregulates *Dll4* expression through TLR4-ERK-FOXC2 axis to program endothelial cell (EC) specification and induce inflammatory angiogenesis in the neonatal mouse lung (Xia et al., 2018).

Loss of one copy of *FOXC2* in humans causes hereditary lymphedema distichiasis (LD) syndrome and primary valve failure in veins of lower extremities (Finegold et al., 2001). *Foxc2* haploinsufficient mice serve as a model for human LD syndrome (Fang et al., 2000), while *Foxc2* homozygous conventional knockout mice die embryologically after day E13.5 up to shortly after birth because of branchial arch and skeletal anomalies (Kume, 2009). In lymphatic endothelial cells, VEGFC/VEGFR3 activates FOXC2 to regulate lymphatic development, growth, function and survival (Petrova et al., 2004). FOXC2 also plays an important role in the later stages of lymphatic development by regulating the morphogenesis of lymphatic valves, stabilize postnatal lymphatic vasculature, and interactions of the lymphatic endothelium with vascular mural cells (Sabine et al., 2015). In pathological states, FOXC2 overexpression is involved in cancer progression through several mechanisms, including epithelial mesenchymal transition (EMT) (Mani et al., 2007; Cui et al., 2015; Paranjape et al., 2016). FOXC2-AS1 overexpression promotes proliferation and migration of vascular smooth muscle cells and tumor cells (Yang et al., 2019; Zhang et al., 2019). Regulation of FOXC2 expression in native and diseased states is not fully understood. The miR-548c-5p clusters regulates FOXC2 transcription (Christofides et al., 2019) and LncRNA FOXC2-AS1 stabilizes *FOXC2* mRNA by forming double stranded RNA to promote FOXC2 expression (Zhang et al., 2017). Histone deacetylase 5 (HDAC5) negatively regulates FOXC2 expression during mouse embryonic development (Lagha et al., 2010). The methylation and histone acetylation of chromatin structure plays essential roles in regulation of EC function (Ohtani and Dimmeler, 2011; Zhou et al., 2011; Li et al., 2020). HDAC5 represses angiogenic genes in EC, and VEGFA induces HDAC5 nuclear export, which allows histone acetyltransferases (HATs) to acetylate transcriptional factors and histones to activate gene expression (Urbich et al., 2009; Zhang et al., 2013; Fish et al., 2017). As a key transcriptional regulator in VEGF signaling pathways (Hayashi and Kume, 2009), FOXC2 binding affinity to Fox-binding element (FBE) may be regulated by chromatin acetylation in EC.

Bronchopulmonary dysplasia (BPD) is a chronic lung disease that develops in premature babies exposed to hyperoxia and sepsis. The aberrant vasculature and alveolar structure were observed in the lungs in which BPD developed (Thébaud and Abman, 2007; Baker and Abman, 2015). Srinivasan et al. (2017) found that over-represented SNPs in proximity to *FOXC2* in premature infants with all sepsis, which indicates *FOXC2* expression level decides susceptibility to infection in neonatal lungs. Our previous study shows that *FOXC2* expression is stimulated by LPS in the mouse lung endothelium and in isolated human pulmonary microvascular endothelial cells (HPMEC) (Xia et al., 2018), but how LPS stimulates *FOXC2* expression remains unknown. Considering the varied roles played by FOXC2 in embryonic development and pathological states, it is imperative to examine the mechanisms underlying *FOXC2* expression. In this study, we hypothesized that FOXC2 expression is self-regulated by FOXC2 transcriptional activation and its binding affinity to FBE is regulated by histone acetylation during sepsis.

MATERIALS AND METHODS

Cell Culture and Reagents

Immortalized HPMEC (HPMEC-Im) was generated as described before (Nitkin et al., 2020). Briefly, primary human lung EC purchased from a commercial source (ScienCell) underwent lentiviral transformation to generate an immortal cell line, and immunostaining for PECAM1, ERG and oxLDL uptake were used to confirm EC specificity. Primary HPMEC and HPMEC-Im were grown in endothelial cell medium (ECM) supplemented with fetal bovine serum (FBS), antibiotics, and endothelial cell growth serum (ECGS) as recommended by the manufacturer (ScienCell) in a humidified incubator containing 5% CO_2 at 37°C. HPMEC-Im were transfected overnight with the indicated plasmids or empty plasmids (mock) with Lipofectamine 3000 (Thermo-Fisher) as per the manufacturer's protocol. Ultrapure LPS was purchased commercially from Invivogen. Garcinol was purchased from Santa Cruse. For experiments with inhibitors, primary HPMEC and HPMEC-Im were pre-treated with 25 μM Garcinol for 45 min prior to the addition of LPS (0.5 μg/ml).

Animal Model

Care of mice before and during the experimental procedures was conducted in accordance with the policies at the University of Missouri- Kansas City Lab Animal Resource Center (Protocol 1510) and the National Institutes of Health guidelines for the care and use of laboratory animals. All protocols had prior approval from the University of Missouri- Kansas City Institutional Animal Care and Use Committee. Wildtype C57BL/6 strain was obtained commercially from Charles River (Burlington, MA). LPS injections (2 mg/kg) to the mice were given intraperitoneally (i.p), and sterile saline used for controls (Sigma, St. Louis, MO) with or without 25 μmol/kg Garcinol pretreatment. Mice were then euthanized using a 100 μl i.p injection pentobarbital, exsanguinated with the cessation of a heartbeat, and the lungs were harvested and utilized as described below.

Plasmids and Lentiviral Vector

The FOXC2 CA, generated by cloning the FOXC2 DBD in-frame with the VP16 transcriptional activation domain (Gerin et al., 2009), was a gift from Dr. Ormond MacDougald. pIRES-Puro-EGFP-FOXC2 CA was generated as described before (Xia et al., 2018). Human *FOXC2* gene was amplified with 5′-tgagctagccca ccatgcaggcgcgctactccgtgtccga-3′ and 5′-agtctcgagtcagtatttcgtgc agtcgtaggagtaggg-3′ from HPMEC genomic DNA and cloned into pIRES-Puro-EGFP (Addgene) to generate pIRES-Puro-EGFP-FOXC2 WT. Oligos 5′-caccgtccgggattcctagaggga-3′ and 5′-aaactccctctaggaatcccggac-3′; 5′-caccgcgagggaaactcagtttgt-3′ and 5′-aaacacaaactgagtttccctcgc-3′; 5′-caccgattggctcaaagttccggg-3′ and 5′-aaaccccggaactttgagccaatc-3′ were annealed to generate double-strand gRNA templates next to FBEs about −1.7, −0.9,

and −0.45 kb in *FOXC2* promoter and then cloned into phU6-gRNA plasmid, respectively, to generate phU6-gRNA targeting FBEs in FOXC2 promoter for FBE dCas9/gRNA assay. 0.45 and 2 kb upstream DNA of *FOXC2* promoter regions were amplified with 5′-actgctagccgctttcagcaagaagacttttgaaacttttcc-3′ and 5′-tgagagcgagagagcgcgagaga-3′; 5′-tattggaaataagtggcacgcc-3′ and 5′-tgagagcgagagagcgcgagaga-3′ from HPMEC genomic DNA and cloned into pGL4.10 to generate pGL4.10-FOXC2-Pomoter respectively for luciferase assay.

Lentiviral vector containing the dCas9 (Gilbert et al., 2013; Richardson et al., 2018) and packing vectors, psPAX2 and pMD2.G, were purchased from Addgene. These plasmids were transfected into HEK293T (Takara) using calcium phosphate transfection to produce lentivirus containing dCas9. After 2 days of transfection, supernatant containing lentiviral particles were harvest and used to transduce HPMEC-Im cells in the presence of polybrene (Santa Cruz) at 8 μ g/ml.

Luciferase Assay

pGL4.10 -FOXC2-Promoter, pGL4.75 Renilla and pIRES-Puro-EGFP-FOXC2 WT (or CA) plasmids were co-transfected into HPMEC-Im cultured in 96-well plate. Next day, luciferase assay was applied with Dual-Glo® Luciferase Assay System (Promega) according to the manufacturer's instructions.

Chromatin Immunoprecipitation (ChIP)

HPMEC-Im were treated with LPS for 0.5 h, with or without garcinol pretreatment, and then ChIP was applied according to the manufacturer's instructions (Thermo Fisher Scientific). Rabbit anti FOXC2 antibody (Abcam, Cambridge, MA) was used to pull down FOXC2 binding DNA and rabbit anti acetylated H3K27antibody (Abcam, Cambridge, MA) was used to pull down H3K27ac binding DNA. qPCR was performed to quantify pulled-down DNA with *FOXC2* promoter primers: −1.7 kb, 5′-cccgtgtttagccttgttaaag-3′ and 5′-ctaggaatcccggacagtttg-3′; −0.9 kb, 5′-cctcgataggttatccttgacg-3′ and 5′-tggattggaatggcaggg-3′; −0.5 kb, 5′-tgattggctcaaagttccgg-3′ and 5′-aagaggccaagtccctttag-3′.

Mice were treated with LPS for 3 h, with or without garcinol pretreatment, and then lung EC were isolated. ChIP was applied according to the manufacturer's instructions (Thermo Fisher Scientific, Rockford, IL). Anti-FOXC2 antibody (Abcam, Cambridge, MA) was used to pull down FOXC2 binding DNA. qPCR was performed to quantify pulled-down DNA with mouse *Foxc2* promoter primers: 5′-cgactggagatgttgaaggaa-3′ and 5′-attttatgccaaccttgacgc-3′

CRISPR/dCas9/gRNA

HPMEC-Im was transduced by lentivirus containing dCas9 and then screened with 200 mg/L hygromycin to generate dCas9 stable cell line HPMEC-Im/dCas9. Mixed FBE gRNAs were transfected into dCas9 stable HPMEC.

Isolation of Murine Endothelial Cells

For endothelial cell isolation, all lobes of the lung from 2 neonatal C57BL/6 pups (4–7 days old) were pooled per condition. The isolation of mouse lung endothelial cells was done as described previously (Menden et al., 2019).

Quantification of mRNA Expression Using Quantitative RT-PCR (qRT-PCR)

Total RNA was extracted from HPMEC and mouse lung EC using the PureLink RNA Mini Kit (Life Technologies) following the manufacturer's instruction and cDNA was synthesized from 1 μg of RNA using an iScript cDNA synthesis kit (Bio-Rad, Hercules, CA) according to the manufacturer's instruction. qRT-PCR was run on a Bio-Rad IQ5 with SYBR green master mix (Bio-Rad). The primers for mouse and human target genes, and mouse *Actb* and human 18S were purchased commercially from Sigma. mouse *Actb* and human 18S were used as the housekeeping gene. The relative gene expression was calculated using the Pfaffl method.

Immunoprecipitation for Phosphorylation Studies

HPMEC-Im grown to the 90% confluence in 60-mm dishes had various treatments, and lysates were used for immunoprecipitation studies. It was done as described previously (Xia et al., 2018).

Immunoblotting for Quantifying Changes in Protein Expression

HPMEC-Im and mouse lung tissue were homogenized in RIPA lysis buffer containing commercially available protease and phosphatase inhibitors (Sigma) with after LPS treatment, with the clarified lysates used for immunoblotting. Immunoblotting was done following standard protocol. The primary antibodies used were: goat anti-FOXC2 [Santa Cruz Biotechnology (SCBT), Santa Cruz, CA], mouse anti- CRISPR-Cas9 (Abcam, Cambridge, MA), mouse anti-phospho-Serine [(p)Ser], mouse anti-phospho-Threonine [(p)Thr] and mouse anti-ACTB (Sigma). Densitometry was performed using ImageJ Software (NIH, Bethesda, MD) and changes were normalized to ACTB.

Immunofluorescent (IF) Staining

IF was done as in our previous study (Menden et al., 2019). The lungs of the mouse pups were fixed in formalin and frozen, and sections were cut onto slides. The slides were stained with rabbit anti FOXC2 antibody (23066-1-AP, Thermo Fisher Scientific, Rockford, IL) and rat anti PECAM antibody (550274, BD Biosciences, San Jose, CA). $n = 3$–4 per group.

Statistical Analysis

Data are presented as mean ± SD or median with interquartile range. $P < 0.05$ was considered significant. For cell culture experiments, data are from a minimum of three independent experiments with adequate technical replicates used for quantification. All animal data were obtained in littermate controls. For animal experiments, a minimum of 3 animals were used for each experimental group. RNA quantification and PCR results had 2–3 technical replicates. For all data, we initially

examined whether distribution of data was Gaussian using the D'Agostino-Pearson omnibus normality test. If data were normally distributed, then ANOVA with a *post hoc* Tukey test was used for analysis. If data did not meet Gaussian assumptions, a Mann-Whitney *U*-test was used for analysis. For most analysis, fold-changes were calculated related to expression/changes in untreated controls. Statistical analysis was done using Graphpad Prism 7.0 (San Diego, CA).

Study Approvals

Lab experiments were reviewed and approved under the University of Missouri-Kansas City IBC, protocol number 18–28. Animal experiments were reviewed and approved under the University of Missouri-Kansas City IACUC, protocol number 1510-02.

RESULTS

FOXC2 Expression Is Upregulated by LPS and FOXC2-CA in HMPEC-Im

To study whether LPS stimulates *FOXC2* expression in HPMEC-Im, we compared *FOXC2* mRNA and protein expression with or without LPS stimulation. qRT-PCR showed *FOXC2* mRNA expression increased 6 h after LPS treatment (**Figure 1A**), and immunoblotting demonstrated protein expression increased

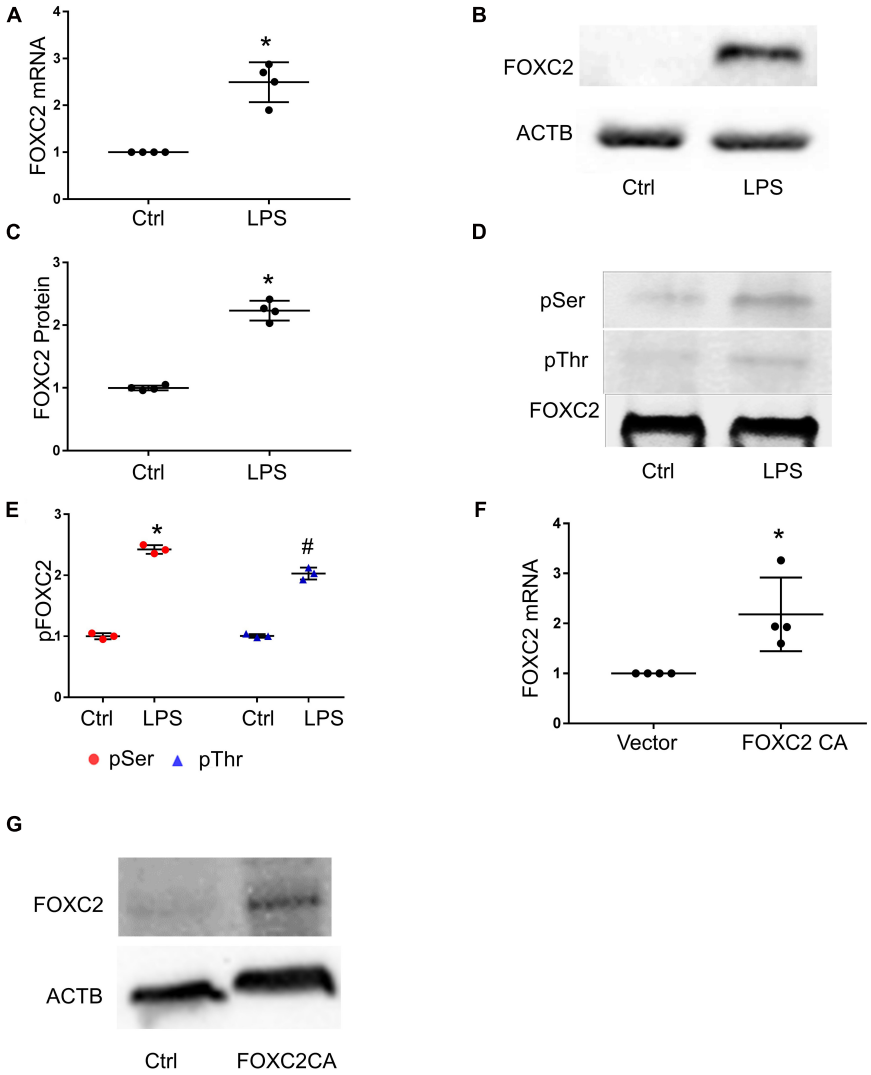

FIGURE 1 | FOXC2 expression is upregulated by LPS and FOXC2 CA in HMPEC-Im. **(A)** *FOXC2* mRNA was assessed by qRT-PCR 4 h after 0.5 μg/ml LPS treatment. $n = 4$ per group; $^{*}p < 0.01$, LPS vs. Ctrl. **(B)** FOXC2 protein was quantified by immunoblotting after overnight 0.5 μg/ml LPS treatment, with densitometry shown graphically **(C)**. $n = 4$ per group; $^{*}p < 0.05$, LPS vs. Ctrl. **(D)** FOXC2 protein was immunoprecipitated from cell lysates at 30 min after LPS, and serine and threonine phosphorylation was assessed by immunoblotting, with densitometry shown graphically **(E)**. $n = 3$ per group, $^{*}p < 0.0001$, LPS pSer vs. Ctrl pSer; $^{\#}p < 0.005$, LPS pThr vs. Ctrl pThr. **(F)** Cells were collected 2 days after transfection of *FOXC2C CA* plasmid and empty control plasmid respectively, and *FOXC2* mRNA was quantified. $n = 4$ per group; $^{*}p < 0.05$, FOXC2 CA vs. vector. **(G)** Immunoblotting showed FOXC2CA stimulated FOXC2 expression.

18 h after LPS treatment (**Figures 1B,C**). Serine and threonine phosphorylation of FOXC2, required for its transcriptional activation (Ivanov et al., 2013), was induced by LPS in HPMEC-Im at 30 min (**Figures 1D,E**). To determine whether FOXC2 can stimulate its own expression, FOXC2-CA, a peptide containing the nuclear binding domain of FOXC2, was transfected and overexpressed in HPMEC-Im. We noted that *FOXC2* mRNA expression increased (**Figure 1F**) using qRT-PCR with primers that specifically detect endogenous *FOXC2* mRNA. FOXC2 protein expression was also increased after FOXC2-CA transfection (**Figure 1G**). These data reveal that LPS activates FOXC2 protein by serine and threonine phosphorylation and stimulates FOXC2 expression potentially through a positive feedback loop.

Luciferase Assay Demonstrates That FOXC2 Promoter Is Activated by FOXC2 WT and FOXC2 CA

As we found that FOXC2 CA can stimulate *FOXC2* expression in HPMEC-Im, we studied whether FOXC2 directly regulates self-expression in HPMEC-Im. Analyzing the *FOXC2* promoter sequences in several species on PROMO server, we found potential FBEs in the *FOXC2* promoter regions of zebra fish, chicken, mouse and human (**Figure 2A**). So, we posited that FOXC2 binds to and regulates its own promoter. 17 potential FBEs predicted by JASPAR, whose relative scores are more than 0.8, distribute from −2000 to −456 bp upstream of human *FOXC2* gene (**Table 1**). We next cloned the 2 kb human *FOXC2* upstream DNA sequence into a luciferase reporter plasmid. Luciferase assays revealed that the promoter activity increased 9- and 4-fold with FOXC2 WT and CA overexpression, respectively (**Figures 2B,C**). We then truncated the 2 kb *FOXC2* upstream DNA to 0.45 kb containing no FBE, placed it in front of luciferase reporter and performed luciferase assays. We found that 0.45 kb activity was much lower than 2 kb activity when FOXC2 WT was over expressed (**Figure 2D**). These data indicate that FOXC2 may activate its own transcriptional activity through FBEs.

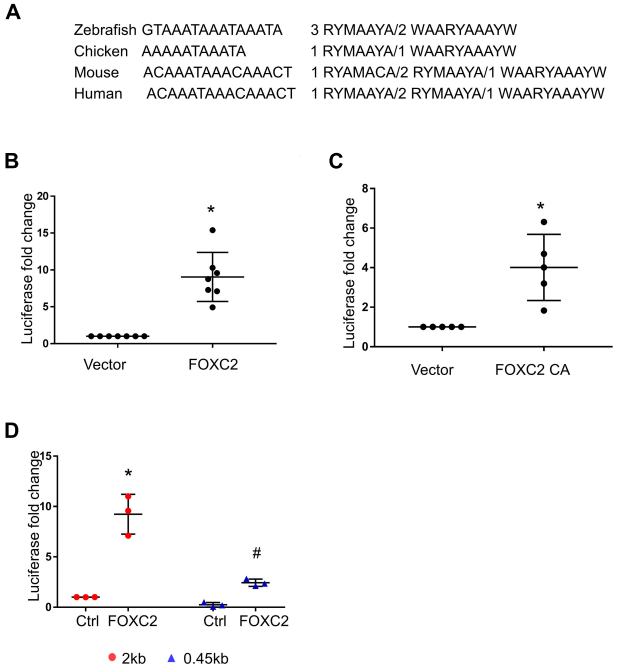

FIGURE 2 | Luciferase assay demonstrates that FOXC2 promoter is activated by FOXC2 WT and FOXC2 CA in HPMEC-Im. **(A)** Overlapped FBEs in Zebrafish, Chicken, mouse and human in 2 kb FOXC2 upstream region. **(B,C)** 2 kb DNA upstream sequence of human *FOXC2* transcriptional start site (TSS) was cloned into pGL4.10 (luc2) and co-transfected with expression plasmids containing *FOXC2 CA* and *FOXC2 WT,* respectively. **(B)** FOXC2 WT overexpression stimulated luciferase reporter activity. $n = 7$ per group; $^{*}p < 0.001$. **(C)** FOXC2 CA increased luciferase activity. $n = 5$ per group, $^{*}p < 0.005$. **(D)** 0.45 kb upstream sequence of *FOXC2 TSS* was cloned into pGL4.10 (luc2) and co-transfected with *FOXC2 WT* plasmid. FOXC2-induced luciferase activity of 0.45 kb promoter was 3.8-fold less than that of the 2 kb promoter. $n = 3$ per group; $^{*}p < 0.05$, FOXC2-stimulated 2 kb vs. 2 kb; $^{\#}p < 0.01$, FOXC2-stimulated 2 kb vs. FOXC2-stimulated 0.45 kb.

LPS Enhances FOXC2 Expression by Stimulating Histone Acetylation and FOXC2 Binding Affinity

Luciferase assay demonstrated that over-expressed FOXC2 activates its own promoter, so we next determined to identify the mechanisms by which LPS induces *FOXC2* expression. Histone lysine acetylation and deacetylation is essential chromatin modification for genes epigenetic regulation (Grunstein, 1997; Jenuwein and Allis, 2001). The expression of several genes in the VEGF pathway is regulated by HDACs (Fraineau et al., 2015) and *FOXC2* expression is regulated by HDAC5 in mouse embryos (Lagha et al., 2010), so we posited that LPS induces FOXC2 expression by stimulating histone acetylation within the FOXC2 promoter region. To test this hypothesis, three pairs of primers were designed to cover two FBE enriched locations at −1.7 and −0.9 kb, and the FBE from –445 to −456 bp (**Supplementary Figure 1**). At first, we checked histone acetylation in response to LPS. Immunoblotting showed that H3K27 was widely acetylated 30 min after LPS treatment (**Figures 3A,B**), consistent with previous reports (Lauterbach et al., 2019). To investigate histone acetylation in FOXC2 promoter region, we performed ChIP assay with anti-H3K27ac antibody and confirmed that three locations in *FOXC2* promoter were acetylated in response to 30-min LPS treatment (**Figure 3C**). P300/CBP is a major histone acetyl-transferase that is stimulated by LPS (Hassa et al., 2003; Liu et al., 2018), so we used garcinol, an inhibitor specifically targeting p300/CBP(IC50 approximately 7 μM) and P300/CBP-associated factor complex(IC50 approximately 5 μM) (Balasubramanyam et al., 2004), repressed LPS-induced acetylation of FOXC2 promoter sites queried (**Figure 3C**). To study whether histone acetylation in FBE influences FOXC2 binding, we applied ChIP with anti-FOXC2 antibody and revealed that FOXC2 binding to those three locations was increased with LPS treatment, but it was significantly suppressed with garcinol pretreatment (**Figure 3D**).

To study whether histone acetylation and FOXC2 binding affinity in FOXC2 promoter region regulates FOXC2 expression in HPMEC-Im, we did qRT-PCR and immunoblotting. We demonstrated that FOXC2 LPS-stimulated FOXC2

mRNA and protein expression levels were suppressed with garcinol pretreatment (**Figures 3E–G**). We also confirmed that LPS stimulated *FOXC2* expression is suppressed with garcinol pretreatment in primary HPMEC (**Figure 3H**). These studies identify that histone acetylation in FOXC2 promoter region is important to LPS-stimulated FOXC2 binding and *FOXC2* expression.

CRISPR/dCas9/FBE gRNA Blocks FOXC2 Binding and Represses Autoregulation

To confirm that FOXC2 binding to its promoter upregulates its expression in pathological conditions, we utilized CRISPR/dCas9, a nuclease dead Cas9 retaining the ability to bind to target DNA based on the gRNA targeting sequence, to investigate whether blocking FBE can prevent FOXC2 binding and inducing transcriptional activity. At first, we generated dCas9 stable HPMEC-Im cell line with lentivirus and confirmed the cells expressed dCas9 with immunoblotting (**Figure 4A**). Three gRNAs mixture targeting FBE enriched regions in *FOXC2* promoter, was transfected into dCas9stable expressed HPMEC-Im. LPS-induced *FOXC2* mRNA and protein expression was reduced dramatically after 4-h and overnight LPS treatments, respectively in FBE gRNAs transfected cells by comparing to scramble gRNA transfected cells (**Figures 4B–D**). To verify whether reduced *FOXC2* mRNA expression was caused by FBE blocking, we applied ChIP and found that LPS-induced FOXC2 binding to FBEs was totally inhibited by FBE gRNA/dCas9 (**Figure 4E**). These data verify that FBEs in FOXC2 promoter plays an important role of regulating *FOXC2* expression in response to LPS, FBE blocking by gRNA/dCas9 prevents FOXC2 binding and autoregulation.

TABLE 1 | 17 potential FEBs predicted by JASPAR, whose relative scores are more than 0.8, distribute from −456 to −2000 bp upstream of human *FOXC2* mRNA (NM_005251.2).

Sequence	Score	Relative score	Strand
CAAATAAACAAA	12.813	0.933425979	+
GGAATAAATAAT	7.92393	0.856966601	+
TAAATAAGTATA	7.78859	0.854849912	+
TCCACAAATAAA	6.97316	0.84209754	+
AAAATAAATTTT	6.88391	0.840701689	+
TAATCAAATAAT	6.83889	0.839997682	–
TAAATAATCAGT	6.60866	0.836397124	+
AAAGTAAAAACT	6.14274	0.82911063	+
TCAGTCCACAAA	6.13537	0.828995446	+
AAAAAAATCAAT	5.84931	0.824521662	–
CAACAAAACAAA	5.73341	0.822709108	+
TGTCTCAACATC	5.58709	0.820420851	+
AAAACAAAAAAA	5.45669	0.818381568	+
TGATTAAATAAG	5.44639	0.818220387	+
CAAATAATTAAT	5.15087	0.813598808	–
AATACAAATGTT	4.68596	0.806328132	+
CACCTCAATAAT	4.30528	0.800374752	–

FBE Blocking in *FOXC2* Promoter Suppresses Expression of Lymphatic EC Markers

FOXC2 regulates lymphatic development and programs lymphatic EC specification (Petrova et al., 2004; Sabine et al., 2015). To investigate whether repression of *FOXC2* expression through blocking FBEs alters EC characters in HPMEC-Im, we tested lymphatic EC markers 2 days after gRNAs transfection and revealed that lymphatic EC markers (Podgrabinska et al., 2002; Wilting et al., 2002; Shinoda et al., 2016), such as *PROX1*, *LYVE1,* and *THY1,* were reduced with repression of FOXC2 expression (**Figure 4F**). These data suggest that FOXC2 autoregulation may play a role in lymphatic EC specification.

FOXC2 Autoregulation in Mouse Lung EC

To confirm our *in vitro* finding *in vivo*, we evaluated LPS-induced histone acetylation, FOXC2 binding and expression in the developing mouse lung. Day of life 7 mouse pups were treated with intraperitoneal LPS, with or without garcinol pretreatment. At first, we treated with mice with different dosage of garcinol and found that 25 μmol/kg garcinol efficiently blocked LPS-induced H3K27 acetylation (**Figure 5A**). We next examined the effect of garcinol on LPS-induced FOXC2 expression in P7 mouse lung EC. Immunoblotting lung EC lysates (PECAM pull down) showed that LPS-induced FOXC2 expression was repressed by 25 μmol/kg garcinol (**Figures 5B,C**). Additionally, immunofluorescence studies indicated that FOXC2 lung EC expression (PECAM – red; FOXC2-green) induced by LPS at 24 h was inhibited with garcinol (**Figure 5E**). There is only one FBE-enriched location in mice (**Figure 2A**), and ChIP with anti-FOXC2 antibody revealed that LPS enhanced FOXC2 binding to this location, and this binding was repressed by garcinol pretreatment in P7 mouse lung EC (**Figure 5D**). These data revealed that LPS stimulated FOXC2 expression through the same mechanism in HPMEC *in vitro* and mouse lung EC *in vivo*.

DISCUSSION

FOXC2 is a major transcriptional regulator of lymphatic development and EC phenotype specification (Petrova et al., 2004; Sabine et al., 2015; Xia et al., 2018). FOXC2 phosphorylation regulates FOXC2-mediated transcription in lymphatic EC and pulmonary EC (Ivanov et al., 2013; Xia et al., 2018). Previous studies reveal that Foxc2 expression is regulated by miR-548c-5p clusters, LncRNA FOXC2-AS1 and HDAC5 (Lagha et al., 2010; Zhang et al., 2017; Christofides et al., 2019). While our previous study showed that LPS strongly induces FOXC2 in lung and retinal EC *in vivo* and *in vitro* the mechanisms were not determined (Xia et al., 2018). In this study we demonstrate that FOXC2 autoregulates its own expression, under native and inflammatory states. Using gain of function and loss of function approaches we identify that FBEs in the FOXC2 promoter are the key of self-regulation. We demonstrate FOXC2 binding affinity to its promoter is enhanced by histone acetylation in response to LPS, and repression of

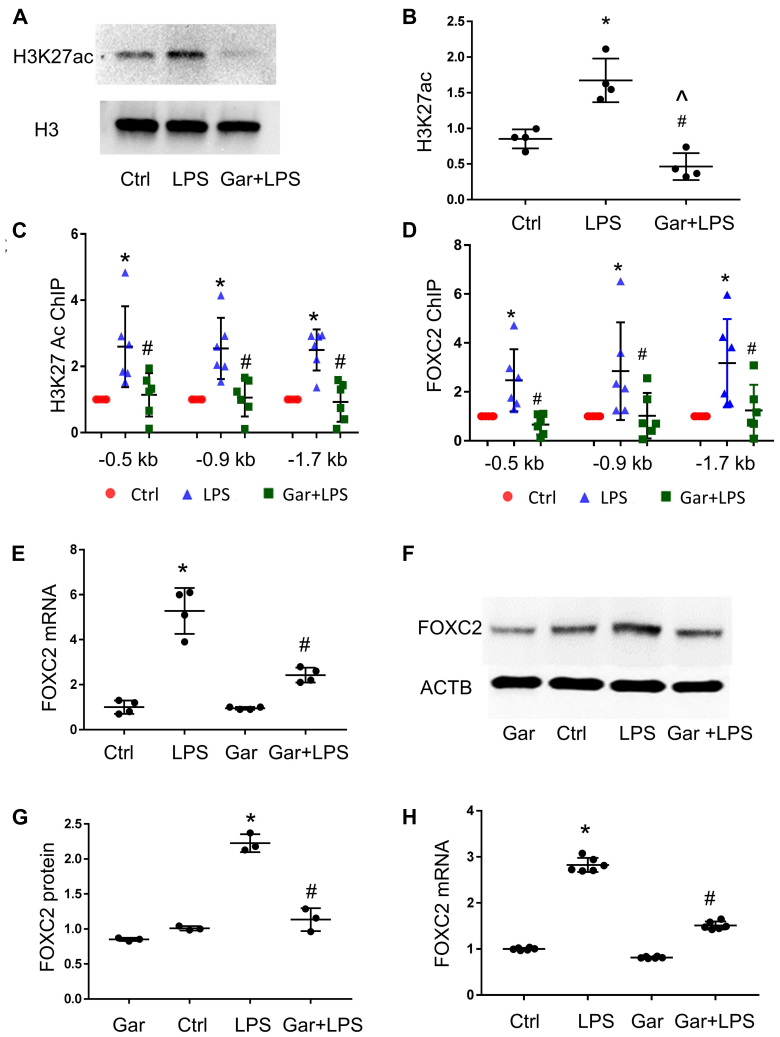

FIGURE 3 | LPS enhances FOXC2 expression by stimulating histone acetylation and FOXC2 binding affinity in HPMEC. **(A)** Acetylated H3K27 (H3K27ac) protein was quantified by immunoblotting from HPMEC-Im cell lysates 30 min after LPS with or without Garcinol (Gar) pretreatment, with densitometry shown graphically **(B)**. $n = 4$ per group; $^{*}p < 0.05$, LPS vs. Ctrl; $^{\#}p < 0.05$, LPS + Gar vs. LPS, $\hat{}p < 0.05$, LPS + Gar vs. Ctrl. **(C)** ChIP with anti-acetylated H3K27 antibody was performed at 30 min after LPS treated HPMEC-Im, with or without garcinol pretreatment. $n = 6$ per group; $^{*}P < 0.01$, LPS vs. ctrl; $^{\#}p < 0.05$, LPS + Gar vs. LPS. **(D)** ChIP with anti-FOXC2 antibody was performed 30 min after LPS treated HPMEC-Im, with or without garcinol pretreatment. $n = 6$ per group; $^{*}P < 0.05$, LPS vs. ctrl; $^{\#}p < 0.05$, LPS + Gar vs. LPS. **(E)** *FOXC2* mRNA was quantified by qRT-PCR 4 h after LPS treated HMPEC-Im, with or without garcinol pretreatment. $n = 4$ per group; $^{*}P < 0.01$, LPS vs. ctrl; $^{\#}P < 0.05$, LPS + Gar vs. LPS. **(F)** FOXC2 protein was quantified by immunoblotting after 16 h LPS treated HPMEC-Im, with or without garcinol pretreatment, with densitometry shown graphically **(G)**. $n = 3$ per group; $^{*}p < 0.005$, LPS vs. ctrl; $^{\#}p < 0.001$, LPS + Gar vs. LPS. **(H)** *FOXC2* mRNA was quantified by qRT-PCR 4 h after LPS treated primary HPMEC, with or without garcinol pretreatment. $n = 6$ per group; $^{*}P < 0.0001$, LPS vs. ctrl; $^{\#}P < 0.0001$, LPS + Gar vs. LPS.

histone acetylation inhibits its autoregulatory expression in human and mouse lung EC. Interestingly, blocking FBEs using a CRISPR/dCas9/gRNA strategy strongly represses FOXC2 autoregulation, and suppresses the expression of markers typically associated with lymphatic EC specification. Our data uncover a novel mechanism of *FOXC2* self-regulation in EC, potentially significant to FOXC2's developmental and pathological role.

Prior work demonstrated that FOXC2 expression is regulated by LPS in primary HPMEC (Xia et al., 2018). Primary HPMEC are fragile, and so we generated HPMEC-Im because it facilitates stable gene-modification such as dCas9 through several passages unlike primary EC. We overexpressed FOXC2 CA and confirmed that FOXC2 stimulated its mRNA and protein expression in HMPEC-Im. Subsequent studies where a 2 kb DNA upstream promoter region of FOXC2 gene was used to regulate luciferase expression revealed that both FOXC2 WT and CA upregulated its promoter's transcription activity. However, FOXC2 overexpression and luciferase assay can't distinguish whether FOXC2 regulates its transcription expression directly or indirectly. We analyzed *FOXC2* promoter regions in zebrafish, chicken, mouse and human, and found putative FBE in all of them. So, we hypothesized that FOXC2 could bind to its promoter and regulate its transcription expression.

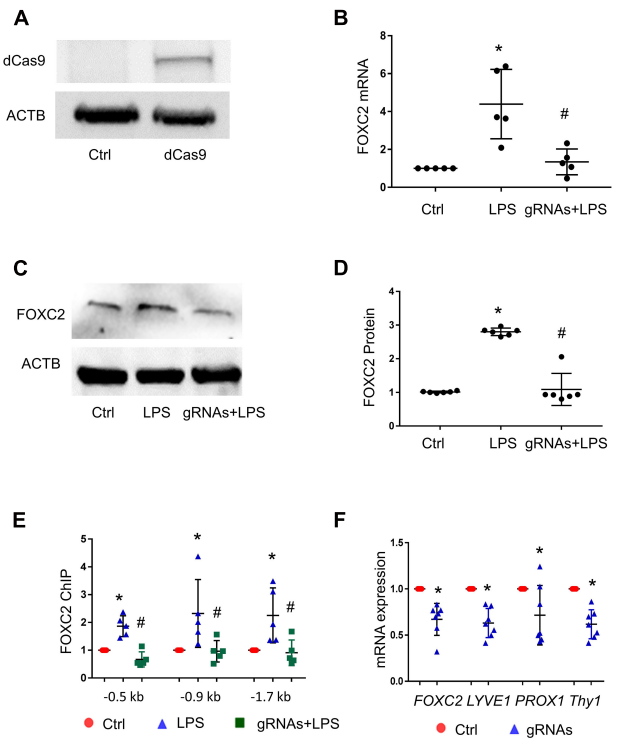

FIGURE 4 | CRISPR/dCas9/FBE gRNA blocks LPS-stimulated FOXC2 binding, represses autoregulation in HPMEC-lm, and alters EC character. **(A)** dCas9 protein expression in stable cell line of HPMEC-lm/dCas9 was shown by immunoblotting, but no expression in control HPMEC-lm. **(B)** *FOXC2* RNA expression was quantified by qTR-PCR 2 days after gRNA mix were transfected into HPMEC-lm/dCas9, with or without 4-h LPS treatment. $n = 5$ per group, $^{*}p < 0.05$, LPS vs. Ctrl; $^{\#}p < 0.05$, gRNAs + LPS vs. LPS. **(C)** FOXC2 protein was quantified by immunoblotting from cell lysate 6 h after LPS treatment with or without gRNAs transfection, with densitometry shown graphically **(D)**. $n = 6$, $^{*}p < 0.01$, LPS vs. ctrl; $^{\#}P < 0.001$, gRNAs + LPS vs. LPS. **(E)** ChIP with anti-FOXC2 antibody was performed 30 min after LPS treatment of gRNAs transfected HPMEC-lm/dCas9. $n = 5$ per group, $^{*}p < 0.05$, LPS vs. ctrl; $^{\#}p < 0.05$ gRNAs + LPS vs. LPS. **(F)** FOXC2, LYVE-1, PROX-1 and Thy1 RNA expression was quantified 2 days after gRNAs were transfected into HPMEC-lm/dCas9. $n = 7$ per group, $^{*}p < 0.05$.

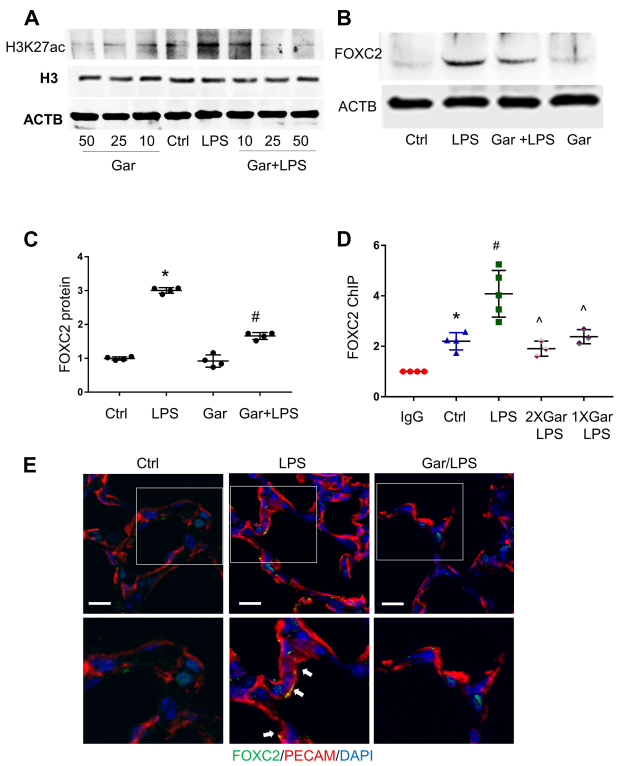

FIGURE 5 | LPS-induced FOXC2 autoregulation is histone acetylation dependent in mouse lung. **(A)** Mouse lungs were collected after 3 h LPS treatment, with or without different dosages of garcinol pretreatment (2 h). Protein expression of histone H3 and acetylated histone H3 was shown by immunoblotting. **(B)** Mouse lung EC were isolated after 3 h LPS treatment at P5, with or without 2 h garcinol pretreatment. FOXC2 protein in mouse lung EC was quantified by immunoblotting, with densitometry shown graphically **(C)**. $n = 4$ per group, $^{*}p < 0.0001$, LPS vs. Ctrl; $^{\#}p < 0.0001$, Gar + LPS vs. LPS. **(D)** Mouse lung EC were isolated after 3 h LPS with or without garcinol co-treatment) at P7. ChIP with anti-FOXC2 antibody was performed with mouse lung EC. $n \geq 3$ per group; $^{*}p < 0.05$, ctrl vs. IgG; $^{\#}p < 0.05$, LPS vs. ctrl; $^{\wedge}p < 0.05$, LPS + Gar vs. LPS. **(E)** Mouse lungs were cryopreserved at P7 after 24 h LPS treatment, with or without garcinol pre-treatment. FOXC2 (green) and PECAM (red) IF staining was applied. Lower panels present the magnified images in the boxes of the up panels. White arrows point to the EC (red) which express FOXC2 (green). $n = 3$–4 per group; scale bars: 10 μm.

JASPAR (jaspar.genereg.net) predicted 17 potential FBEs (**Table 1**), whose relative scores are more than 0.8 and which distribute from −2000 to −456 bp upstream of human *FOXC2* gene (**Supplementary Figure 1**). Three overlapped FBE hotspots were found: 6 putative FBEs localize between −1752 to −1782, 2 putative sites are between −1572 to −1588, and 3 putative sites are between −915 to −940. We also searched FBE in 2 kb DNA fragment manually. According to FOXC binding motif as "RYAMACA" (R = G/A, Y = T/C, M = A/C) (Chen et al., 2019), there is only one potential FBE, CAAATAAACAAA, which represents the highest JASPAR relative score and localizes between −1752 to −1782. However, according to FBE as "RYMAAYA" and "WAARYAAAYW" (Kaufmann and Knöchel, 1996; Carlsson and Mahlapuu, 2002; Samatar et al., 2002; Hayashi and Kume, 2008), three putative FBEs locate between −1752 to −1782 as JASPAR predicted, and two lie at −942 and −632 separately, which are not predicted by JASPAR. With collective consideration, we deigned two pairs of primers for ChIP and two gRNAs for dCas9 repressor, which target two putative FBE hotspots, −1752 to −1782 and −915 to −940 separately, and one pair of primers target the first FBE, which locates at −456. Luciferase assay demonstrated that 0.45 kb *FOXC2* upstream DNA significantly lost self-regulation function, indicating those FBEs are necessary for FOXC2 autoregulation. Retained FOXC2-induced activity of 0.45 kb may be cause by FOXC2 indirect binding or regulation. To uncover that, more studies will be conducted.

Most genes in VEGF signaling pathway are regulated by HDACs and HATs (Urbich et al., 2009; Zhang et al., 2013; Fish et al., 2017), which change chromatin accessibility and regulate gene transcription (Voss and Thomas, 2018). LPS is known to

induce histone modification (Hamon and Cossart, 2008). Loss of HDAC5 function stimulates *Foxc2* expression in mouse embryos (Lagha et al., 2010). So, we posited that *FOXC2* autoregulated self-expression might be dependent on histone acetylation after stimulation by LPS. We demonstrate by ChIP that FOXC2 binds to its promoter and its binding affinity is enhanced by LPS treatment. Our data also reveal that garcinol, a HAT inhibitor, that is specific to p300 and PCAF (Balasubramanyam et al., 2004; Kim et al., 2020; Wang et al., 2020; Kopytko et al., 2021), represses LPS-stimulated histone acetylation at *FOXC2* promoter, FOXC2 binding affinity and FOXC2 expression in HPMEC-Im. Our data shows that LPS-stimulated FOXC2 expression in primary HPMEC is also repressed by garcinol consistent with our data in immortalized HPMEC. Our data, while consistent with other studies showing that LPS promotes histone acetylation uncover FOXC2 as a target for histone acetylation dependent FOXC2 expression. Although our studies clearly demonstrate the role of histone acetylation in FOXC2 expression both *in vivo* and *in vitro*, a minor limitation is that we did not identify the precise histone acetylase that mediates FOXC2 promoter acetylation.

To validate FOXC2 binds its promoter, we used a loss of function approach by blocking two putative FBE hotspots (−1752 to −1782 and −915 to −940) and one FBE at −456 in the upstream of FOXC2 gene utilizing CRISPR/dCas9/gRNAs technologies. We identify that dCas9/gRNAs specifically target those FBEs and repress LPS-stimulated *FOXC2* expression with ChIP, qRT-PCR and immunoblotting, respectively. After we revealed the mechanism of *FOXC2* autoregulation in human lung EC *in vitro*, we pursued studies to confirm FOXC2 autoregulation *in vivo*. With the same strategy we predicted FBEs in mouse *Foxc2* upstream DNA, we only found one FBE hotspot (**Figure 2A**) within 2 kb mouse *Foxc2* upstream DNA. With ChIP, we demonstrated that FOXC2 bound to the FBEs hotspot in mouse lung EC after intraperitoneal LPS injections, and garcinol pretreatment repressed FOXC2 binding and LPS-induced FOXC2 expression *in vivo*. These data uncover that LPS-induced FOXC2-mediated autoregulation is HAT dependent in mouse lung EC. FOXC1 and FOXC2 are closely related FOX family members and collaboratively work together to regulates VEGF downstream genes in arterial EC (Seo et al., 2006). Both ChIP and dCas9/gRNA can't differentiate FOXC2 binding to its promoter directly or indirectly, and EMSA can't define it too when two FOXC member proteins, which share the same FBE, are added. So, in this study, we only applied ChIP and gRNA/dCas9 to prove that FOXC2 binds to its promoter and regulates its expression.

To study how *FOXC2* autoregulation influences EC cell fate, we transfected mixed FBE-targeted gRNAs into dCas9 stable expressed HPMEC-Im and analyzed expression of lymphatic markers. After blocking FOXC2 autoregulation, EC had decreased expression of lymphatic EC specification markers, which suggests that *FOXC2* autoregulation may play an important role in EC programing and differentiation during lung development. CRISPR/dCas9 strategy is broadly used to study DNA-protein interaction and gene expression regulation, but dCas9 footprint covers 78.1 bp ± 37.9 bp (Josephs et al., 2015). So, the other transcription factor binding element may be blocked when dCas9/gRNAs target to FBEs. To overcome this disadvantage, mutations of FBEs in *FOXC2* promoter will be studied in the future.

Collectively, using human lung EC, as well as a sterile sepsis model in neonatal mice, we demonstrate that FOXC2 regulates its own expression through a histone acetylation-dependent positive feedback loop during TLR4 stimulation in developing lung EC. Our data demonstrates a direct link between lung EC innate immune signaling and FOXC2 self-regulation as suggested by our previous study (Xia et al., 2018). Further, we show that suppression of FBE on the FOXC2 promoter using CRISPR/dCas9/gRNA strategy suppresses the native expression of lymphatic EC specification markers such as *Lyve1* and Thy1. The implications of FOXC2 transcriptional activation and autoregulation during LPS stimulation to lung EC inflammatory signaling and fate specification in chronic models of inflammation is an area of future investigation. Further, whether exaggerated FOXC2 autoregulation underlies FOXC2's role in cancer remains to be determined.

DATA AVAILABILITY STATEMENT

The original contributions presented in the study are included in the article/**Supplementary Material**, further inquiries can be directed to the corresponding author/s.

ETHICS STATEMENT

The animal study was reviewed and approved by Care of mice before and during the experimental procedures was conducted in accordance with the policies at the University of Missouri-Kansas City Lab Animal Resource Center (Protocol 1510) and the National Institutes of Health guidelines for the care and use of laboratory animals. All protocols had prior approval from the University of Missouri- Kansas City Institutional Animal Care and Use Committee.

AUTHOR CONTRIBUTIONS

VS and SX: conception and design. SX, WY, and HM: data collection. VS, SX, WY, HM, and SY: analysis and interpretation, drafting and editing the manuscript. All authors contributed to the article and approved the submitted version.

FUNDING

HM, SX, and VS were supported by 1R01 HL128374-05; NIH/NHLBI (VS) and WY, HM, SX, and VS were supported by CMRI Start-up (VS).

SUPPLEMENTARY MATERIAL

The Supplementary Material for this article can be found online at: https://www.frontiersin.org/articles/10.3389/fcell.2021.657662/full#supplementary-material

REFERENCES

Baker, C. D., and Abman, S. H. (2015). Impaired Pulmonary Vascular Development in Bronchopulmonary Dysplasia. *Neonatology* 107, 344–351. doi: 10.1159/000381129

Balasubramanyam, K., Altaf, M., Varier, R. A., Swaminathan, V., Ravindran, A., Sadhale, P. P., et al. (2004). Polyisoprenylated benzophenone, garcinol, a natural histone acetyltransferase inhibitor, represses chromatin transcription and alters global gene expression. *J. Biol. Chem.* 279, 33716–33726. doi: 10.1074/jbc.M402839200

Carlsson, P., and Mahlapuu, M. (2002). Forkhead transcription factors: key players in development and metabolism. *Dev. Biol.* 250, 1–23. doi: 10.1006/dbio.2002.0780

Chen, X., Wei, H., Li, J., Liang, X., Dai, S., Jiang, L., et al. (2019). Structural basis for DNA recognition by FOXC2. *Nucleic Acids Res.* 47, 3752–3764. doi: 10.1093/nar/gkz077

Christofides, A., Papagregoriou, G., Dweep, H., Makrides, N., Gretz, N., Felekkis, K., et al. (2019). Evidence for miR-548c-5p regulation of FOXC2 transcription through a distal genomic target site in human podocytes. *Cell. Mol. Life Sci.* 2019:03294. doi: 10.1007/s00018-019-03294-z

Cui, Y.-M., Jiao, H.-L., Ye, Y.-P., Chen, C.-M., Wang, J.-X., Tang, N., et al. (2015). FOXC2 promotes colorectal cancer metastasis by directly targeting MET. *Oncogene* 34, 4379–4390. doi: 10.1038/onc.2014.368

Fang, J., Dagenais, S. L., Erickson, R. P., Arlt, M. F., Glynn, M. W., Gorski, J. L., et al. (2000). Mutations in FOXC2 (MFH-1), a forkhead family transcription factor, are responsible for the hereditary lymphedema-distichiasis syndrome. *Am. J. Hum. Genet.* 67, 1382–1388. doi: 10.1086/316915

Finegold, D. N., Kimak, M. A., Lawrence, E. C., Levinson, K. L., Cherniske, E. M., Pober, B. R., et al. (2001). Truncating mutations in FOXC2 cause multiple lymphedema syndromes. *Hum. Mol. Genet.* 10, 1185–1189. doi: 10.1093/hmg/10.11.1185

Fish, J. E., Gutierrez, M. C., Dang, L. T., Khyzha, N., Chen, Z., Veitch, S., et al. (2017). Dynamic regulation of VEGF-inducible genes by an ERK/ERG/p300 transcriptional network. *Dev.* 144, 2428–2444. doi: 10.1242/dev.146050

Fraineau, S., Palii, C. G., Allan, D. S., and Brand, M. (2015). Epigenetic regulation of endothelial-cell-mediated vascular repair. *FEBS J.* 282, 1605–1629. doi: 10.1111/febs.13183

Gerin, I., Bommer, G. T., Lidell, M. E., Cederberg, A., Enerback, S., and McDougald, O. A. (2009). On the role of FOX transcription factors in adipocyte differentiation and insulin-stimulated glucose uptake. *J. Biol. Chem.* 284, 10755–10763. doi: 10.1074/jbc.M809115200

Gilbert, L. A., Larson, M. H., Morsut, L., Liu, Z., Brar, G. A., Torres, S. E., et al. (2013). XCRISPR-mediated modular RNA-guided regulation of transcription in eukaryotes. *Cell* 154:442. doi: 10.1016/j.cell.2013.06.044

Grunstein, M. (1997). Histone acetylation in chromatin structure and transcription. *Nature* 389, 349–352. doi: 10.1038/38664

Hamon, M. A., and Cossart, P. (2008). Histone Modifications and Chromatin Remodeling during Bacterial Infections. *Cell Host Microbe* 4, 100–109. doi: 10.1016/j.chom.2008.07.009

Hassa, P. O., Buerki, C., Lombardi, C., Imhof, R., and Hottiger, M. O. (2003). Transcriptional Coactivation of Nuclear Factor-κB-dependent Gene Expression by p300 Is Regulated by Poly(ADP)-ribose Polymerase-1. *J. Biol. Chem.* 278, 45145–45153. doi: 10.1074/jbc.M307957200

Hayashi, H., and Kume, T. (2008). Foxc transcription factors directly regulate DII4 and hey2 expression by interacting with the VEGF-notch signaling pathways in endothelial cells. *PLoS One* 3, 1–9. doi: 10.1371/journal.pone.0002401

Hayashi, H., and Kume, T. (2009). Foxc2 transcription factor as a regulator of angiogenesis via induction of integrin β3 expression. *Cell Adhes. Migr.* 3, 24–26. doi: 10.4161/cam.3.1.7252

Ivanov, K. I., Agalarov, Y., Valmu, L., Samuilova, O., Liebl, J., Houhou, N., et al. (2013). Phosphorylation Regulates FOXC2-Mediated Transcription in Lymphatic Endothelial Cells. *Mol. Cell. Biol.* 33, 3749–3761. doi: 10.1128/mcb.01387-12

Jenuwein, T., and Allis, C. D. (2001). Translating the histone code. *Science* 293, 1074–1080. doi: 10.1126/science.1063127

Josephs, E. A., Kocak, D. D., Fitzgibbon, C. J., McMenemy, J., Gersbach, C. A., and Marszalek, P. E. (2015). Structure and specificity of the RNA-guided endonuclease Cas9 during DNA interrogation, target binding and cleavage. *Nucleic Acids Res.* 43, 8924–8941. doi: 10.1093/nar/gkv892

Kaufmann, E., and Knöchel, W. (1996). Five years on the wings of fork head. *Mech. Dev.* 57, 3–20. doi: 10.1016/0925-4773(96)00539-4

Kim, J. Y., Jo, J., Leem, J., and Park, K. K. (2020). Inhibition of P300 by garcinol protects against cisplatin-induced acute kidney injury through suppression of oxidative stress, inflammation, and tubular cell death in mice. *Antioxidants* 9, 1–16. doi: 10.3390/antiox9121271

Kopytko, P., Piotrowska, K., Janisiak, J., and Tarnowski, M. (2021). Garcinol—a natural histone acetyltransferase inhibitor and new anti-cancer epigenetic drug. *Int. J. Mol. Sci.* 22, 1–11. doi: 10.3390/ijms22062828

Kume, T. (2009). Novel insights into the differential functions of Notch ligands in vascular formation. *J. Angiogenes. Res.* 1:8. doi: 10.1186/2040-2384-1-8

Lagha, M., Sato, T., Regnault, B., Cumano, A., Zuniga, A., Licht, J., et al. (2010). Transcriptome analyses based on genetic screens for Pax3 myogenic targets in the mouse embryo. *BMC Genomics* 11:696. doi: 10.1186/1471-2164-11-696

Lauterbach, M. A., Hanke, J. E., Serefidou, M., Mangan, M. S. J., Kolbe, C. C., Hess, T., et al. (2019). Toll-like Receptor Signaling Rewires Macrophage Metabolism and Promotes Histone Acetylation via ATP-Citrate Lyase. *Immunity* 51, 997.e–1011.e. doi: 10.1016/j.immuni.2019.11.009

Li, P., Ge, J., and Li, H. (2020). Lysine acetyltransferases and lysine deacetylases as targets for cardiovascular disease. *Nat. Rev. Cardiol.* 17, 96–115. doi: 10.1038/s41569-019-0235-9

Liu, Q., Yang, H., Xu, S., and Sun, X. (2018). Downregulation of p300 alleviates LPS-induced inflammatory injuries through regulation of RhoA/ROCK/NF-κB pathways in A549 cells. *Biomed. Pharmacother.* 97, 369–374. doi: 10.1016/j.biopha.2017.10.104

Mani, S. A., Yang, J., Brooks, M., Schwaninger, G., Zhou, A., Miura, N., et al. (2007). Mesenchyme Forkhead 1 (FOXC2) plays a key rofile:///C:/Users/benxi/Downloads/25381815.nbib file:///C:/Users/benxi/Downloads/26804168.nbib le in metastasis and is associated with aggressive basal-like breast cancers. *Proc. Natl. Acad. Sci. U. S. A.* 104, 10069–10074. doi: 10.1073/pnas.0703900104

Menden, H., Xia, S., Mabry, S. M., Noel-MacDonnell, J., Rajasingh, J., Ye, S. Q., et al. (2019). Histone deacetylase 6 regulates endothelial MyD88-dependent canonical TLR signaling, lung inflammation, and alveolar remodeling in the developing lung. *Am. J. Physiol. Cell. Mol. Physiol.* 317, L332–L346. doi: 10.1152/ajplung.00247.2018

Nitkin, C. R., Xia, S., Menden, H., Yu, W., Xiong, M., Heruth, D. P., et al. (2020). FOSL1 is a novel mediator of endotoxin/lipopolysaccharide-induced pulmonary angiogenic signaling. *Sci. Rep.* 10, 1–14. doi: 10.1038/s41598-020-69735-z

Ohtani, K., and Dimmeler, S. (2011). Epigenetic regulation of cardiovascular differentiation. *Cardiovasc. Res.* 90, 404–412. doi: 10.1093/cvr/cvr019

Paranjape, A. N., Soundararajan, R., Werden, S. J., Joseph, R., Taube, J. H., Liu, H., et al. (2016). Inhibition of FOXC2 restores epithelial phenotype and drug sensitivity in prostate cancer cells with stem-cell properties. *Oncogene* 35, 5963–5976. doi: 10.1038/onc.2015.498

Petrova, T. V., Karpanen, T., Norrmén, C., Mellor, R., Tamakoshi, T., Finegold, D., et al. (2004). Defective valves and abnormal mural cell recruitment underlie lymphatic vascular failure in lymphedema distichiasis. *Nat. Med.* 10, 974–981. doi: 10.1038/nm1094

Podgrabinska, S., Braun, P., Velasco, P., Kloos, B., Pepper, M. S., Skobe, M., et al. (2002). Molecular characterization of lymphatic endothelial cells. *Proc. Natl. Acad. Sci. U. S. A.* 99, 16069–16074. doi: 10.1073/pnas.242401399

Richardson, C. D., Kazane, K. R., Feng, S. J., Zelin, E., Bray, N. L., Schäfer, A. J., et al. (2018). CRISPR–Cas9 genome editing in human cells occurs via the Fanconi anemia pathway. *Nat. Genet.* 50, 1132–1139. doi: 10.1038/s41588-018-0174-0

Sabine, A., Bovay, E., Demir, C. S., Kimura, W., Jaquet, M., Agalarov, Y., et al. (2015). FOXC2 and fluid shear stress stabilize postnatal lymphatic vasculature. *J. Clin. Invest.* 125, 3861–3877. doi: 10.1172/JCI80454

Samatar, A. A., Wang, L., Mirza, A., Koseoglu, S., Liu, S., and Kumar, C. C. (2002). Transforming growth factor-β2 is a transcriptional target for Akt/protein kinase B via forkhead transcription factor. *J. Biol. Chem.* 277, 28118–28126. doi: 10.1074/jbc.M203686200

Seo, S., Fujita, H., Nakano, A., Kang, M., Duarte, A., and Kume, T. (2006). The forkhead transcription factors, Foxc1 and Foxc2, are required for arterial

specification and lymphatic sprouting during vascular development. *Dev. Biol.* 294, 458–470. doi: 10.1016/j.ydbio.2006.03.035

Shinoda, K., Hirahara, K., Iinuma, T., Ichikawa, T., Suzuki, A. S., Sugaya, K., et al. (2016). Thy1+ IL-7+ lymphatic endothelial cells in iBALT provide a survival niche for memory T-helper cells in allergic airway inflammation. *Proc. Natl. Acad. Sci. U. S. A.* 113, E2842–E2851. doi: 10.1073/pnas.1512600113

Srinivasan, L., Page, G., Kirpalani, H., Murray, J. C., Das, A., Higgins, R. D., et al. (2017). Genome-wide association study of sepsis in extremely premature infants. *Arch. Dis. Child. - Fetal Neonatal Ed.* 102, F439L–F445. doi: 10.1136/archdischild-2016-311545

Thébaud, B., and Abman, S. H. (2007). Bronchopulmonary dysplasia: Where have all the vessels gone? Roles of angiogenic growth factors in chronic lung disease. *Am. J. Respir. Crit. Care Med.* 175, 978–985. doi: 10.1164/rccm.200611-1660PP

Urbich, C., Rössig, L., Kaluza, D., Potente, M., Boeckel, J. N., Knau, A., et al. (2009). HDAC5 is a repressor of angiogenesis and determines the angiogenic gene expression pattern of endothelial cells. *Blood* 113, 5669–5679. doi: 10.1182/blood-2009-01-196485

Voss, A. K., and Thomas, T. (2018). Histone Lysine and Genomic Targets of Histone Acetyltransferases in Mammals. *Bioessays* 40:e1800078. doi: 10.1002/bies.201800078

Wang, J., Wu, M., Zheng, D., Zhang, H., Lv, Y., Zhang, L., et al. (2020). Garcinol inhibits esophageal cancer metastasis by suppressing the p300 and TGF-β1 signaling pathways. *Acta Pharmacol. Sin.* 41, 82–92. doi: 10.1038/s41401-019-0271-3

Wilting, J., Papoutsi, M., Christ, B., Nicolaides, K. H., von Kaisenberg, C. S., Borges, J., et al. (2002). The transcription factor Prox1 is a marker for lymphatic endothelial cells in normal and diseased human tissues. *FASEB J.* 16, 1271–1273. doi: 10.1096/fj.01-1010fje

Xia, S., Menden, H. L., Korfhagen, T. R., Kume, T., and Sampath, V. (2018). Endothelial immune activation programmes cell-fate decisions and angiogenesis by inducing angiogenesis regulator DLL4 through TLR4-ERK-FOXC2 signalling. *J. Physiol.* 596, 1397–1417. doi: 10.1113/JP275453

Yang, H., Chen, T., Xu, S., Zhang, S., and Zhang, M. (2019). Long noncoding RNA FOXC2-AS1 predicts poor survival in breast cancer patients and promotes cell proliferation. *Oncol. Res.* 27, 219–226. doi: 10.3727/096504018X15213126075068

Zhang, B., Day, D. S., Ho, J. W., Song, L., Cao, J., Christodoulou, D., et al. (2013). A dynamic H3K27ac signature identifies VEGFA-stimulated endothelial enhancers and requires EP300 activity. *Genome Res.* 23, 917–927. doi: 10.1101/gr.149674.112

Zhang, C.-L., Zhu, K.-P., and Ma, X.-L. (2017). Antisense lncRNA FOXC2-AS1 promotes doxorubicin resistance in osteosarcoma by increasing the expression of FOXC2. *Cancer Lett.* 396, 66–75. doi: 10.1016/j.canlet.2017.03.018

Zhang, C., Li, H., and Guo, X. (2019). FOXC2-AS1 regulates phenotypic transition, proliferation and migration of human great saphenous vein smooth muscle cells. *Biol. Res.* 52, 1–10. doi: 10.1186/s40659-019-0266-z

Zhou, B., Margariti, A., Zeng, L., and Xu, Q. (2011). Role of histone deacetylases in vascular cell homeostasis and arteriosclerosis. *Cardiovasc. Res.* 90, 413–420. doi: 10.1093/cvr/cvr003

Conflict of Interest: The authors declare that the research was conducted in the absence of any commercial or financial relationships that could be construed as a potential conflict of interest.

Copyright © 2021 Xia, Yu, Menden, Younger and Sampath. This is an open-access article distributed under the terms of the Creative Commons Attribution License (CC BY). The use, distribution or reproduction in other forums is permitted, provided the original author(s) and the copyright owner(s) are credited and that the original publication in this journal is cited, in accordance with accepted academic practice. No use, distribution or reproduction is permitted which does not comply with these terms.

frontiers in Cell and Developmental Biology

ORIGINAL RESEARCH
published: 14 May 2021
doi: 10.3389/fcell.2021.672625

Loss of Primary Cilia Protein IFT20 Dysregulates Lymphatic Vessel Patterning in Development and Inflammation

*Delayna Paulson[1,2], Rebecca Harms[1,2], Cody Ward[1,2], Mackenzie Latterell[1,2], Gregory J. Pazour[3] and Darci M. Fink[1,2]**

[1] Department of Chemistry and Biochemistry, South Dakota State University, Brookings, SD, United States, [2] BioSNTR, South Dakota State University, Brookings, SD, United States, [3] Program in Molecular Medicine, University of Massachusetts Medical School, Worcester, MA, United States

Microenvironmental signals produced during development or inflammation stimulate lymphatic endothelial cells to undergo lymphangiogenesis, in which they sprout, proliferate, and migrate to expand the vascular network. Many cell types detect changes in extracellular conditions via primary cilia, microtubule-based cellular protrusions that house specialized membrane receptors and signaling complexes. Primary cilia are critical for receipt of extracellular cues from both ligand-receptor pathways and physical forces such as fluid shear stress. Here, we report the presence of primary cilia on immortalized mouse and primary adult human dermal lymphatic endothelial cells *in vitro* and on both luminal and abluminal domains of mouse corneal, skin, and mesenteric lymphatic vessels *in vivo*. The purpose of this study was to determine the effects of disrupting primary cilia on lymphatic vessel patterning during development and inflammation. Intraflagellar transport protein 20 (IFT20) is part of the transport machinery required for ciliary assembly and function. To disrupt primary ciliary signaling, we generated global and lymphatic endothelium-specific IFT20 knockout mouse models and used immunofluorescence microscopy to quantify changes in lymphatic vessel patterning at E16.5 and in adult suture-mediated corneal lymphangiogenesis. Loss of IFT20 during development resulted in edema, increased and more variable lymphatic vessel caliber and branching, as well as red blood cell-filled lymphatics. We used a corneal suture model to determine ciliation status of lymphatic vessels during acute, recurrent, and tumor-associated inflammatory reactions and wound healing. Primary cilia were present on corneal lymphatics during all of the mechanistically distinct lymphatic patterning events of the model and assembled on lymphatic endothelial cells residing at the limbus, stalk, and vessel tip. Lymphatic-specific deletion of IFT20 cell-autonomously exacerbated acute corneal lymphangiogenesis resulting in increased lymphatic vessel density and branching. These data are the first functional studies of primary cilia on lymphatic endothelial cells and reveal a new dimension in regulation of lymphatic vascular biology.

Keywords: primary cilia, lymphatic, lymphangiogenesis, lymphatic development, corneal inflammation, IFT20, vascular patterning

OPEN ACCESS

Edited by:
Ramani Ramchandran, Medical College of Wisconsin, United States

Reviewed by:
Tsutomu Kume, Northwestern University, United States
Iain Drummond, Mount Desert Island Biological Laboratory, United States

***Correspondence:**
Darci M. Fink
darci.fink@sdstate.edu

Specialty section:
This article was submitted to Signaling, a section of the journal Frontiers in Cell and Developmental Biology

Received: *26 February 2021*
Accepted: *15 April 2021*
Published: *14 May 2021*

Citation:
Paulson D, Harms R, Ward C, Latterell M, Pazour GJ and Fink DM (2021) Loss of Primary Cilia Protein IFT20 Dysregulates Lymphatic Vessel Patterning in Development and Inflammation. Front. Cell Dev. Biol. 9:672625. doi: 10.3389/fcell.2021.672625

INTRODUCTION

Regulation of lymphatic vessel patterning is critical for the establishment of lymphatic vascular networks during development and pathological tissue remodeling events such as inflammation and wound healing. Lymphatic expansion is driven by a set of cellular mechanisms that activate and mobilize individual endothelial cells residing in a pre-existing vessel to sprout, proliferate, undergo directional chemotaxis, and remodel intercellular junctions to form new vessels. Properly patterned lymphatic vessels govern tissue fluid homeostasis and transport soluble antigens and immune cells to draining lymph nodes. During development, lymphatic patterning begins at approximately E9.5 when COUPTFII and SOX18 upregulate expression of PROX1 in venous endothelial cells of the cardinal vein to establish the first lymphatic endothelial cells (LECs; Wigle and Oliver, 1999; Petrova et al., 2002; François et al., 2008; Johnson et al., 2008; Srinivasan et al., 2010; Hägerling et al., 2013). These cells form lymph sacs, which expand to form lymphatic vessels separated from the blood circulation by lymphovenous valves (Cha et al., 2016; Geng et al., 2016). Further proliferation, branching, and maturation establishes a network of lymphatic vasculature throughout the embryo consisting of blind-ended capillaries that coalesce into lymphatic collecting vessels invested with smooth muscle cells and containing intraluminal valves (Lutter et al., 2012; Scallan et al., 2016). Inflammation activates existing lymphatic capillaries to undergo lymphangiogenesis, thus increasing capacity to transport edematous fluid and support egress of antigen presenting cells and lymphocytes out of inflamed tissue (Baluk et al., 2005; Maruyama et al., 2005; Pflicke and Sixt, 2009; Tal et al., 2011).

Lymphatic vessel patterning and function are dysregulated and contribute to disease pathology in many conditions, including chronic inflammation, lymphedema, and malignancy (Skobe et al., 2001; Schwager and Detmar, 2019; Oliver et al., 2020). The canonical mechanism governing both developmental and inflammation-associated lymphangiogenesis is VEGF-C stimulating VEGFR-2/3 on LECs, along with co-receptor NRP-2 (Karkkainen et al., 2004; Haiko et al., 2008; Kataru et al., 2009; Xu et al., 2010; Kelley et al., 2013). Other factors induce lymphangiogenesis in specific contexts including angiopoietins (Gale et al., 2002; Morisada et al., 2005; Tammela et al., 2005; Dellinger et al., 2008), TNF-α(Ji et al., 2014), FGF-2 (Cao et al., 2012), IGF1/2 (Björndahl et al., 2005), EGF (Marino et al., 2013), HGF (Cao et al., 2006), PDGF-BB (Cao et al., 2004), and NGF (Fink et al., 2014). Despite the identification of these lymphangiogenic factors, the mechanisms governing lymphatic vessel patterning are not fully understood. This is particularly evident in studies of viral infection (Loo et al., 2017), lymphatic vessel regression (Baluk et al., 2005; Cursiefen et al., 2006; Kelley et al., 2011), and chronic inflammation (Kelley et al., 2013) in which lymphatic vessel remodeling events are highly variable and do not follow current paradigms. This evidence suggests that additional unknown elements regulate lymphatic vessel patterning.

Primary cilia are non-motile sensory organelles that govern proliferation, migration, cell polarity, and fluid shear stress sensing in other cell types, including blood endothelial cells. Primary cilia house receptor-ligand signaling pathways such as Hedgehog (Huangfu et al., 2003; Huangfu and Anderson, 2005; Clement et al., 2009), Wnt (Jonassen et al., 2008; McDermott et al., 2010), Notch (Ezratty et al., 2011; Grisanti et al., 2016; Chen et al., 2017), PDGFRα (Schneider et al., 2005; Noda et al., 2016; Schmid et al., 2018), and TGF-β (Clement et al., 2013), as well as mechanosensation machinery (Praetorius and Spring, 2001), such as polycystins PKD1/2 (Pazour et al., 2002; Nauli et al., 2008). Disruption of primary cilia signaling dysregulates formation of lumenized structures such as kidney tubules (Pazour et al., 2000; Jonassen et al., 2008) and breast ducts (McDermott et al., 2010), and causes cardiovascular disease (Pala et al., 2018). Studies across *in vivo* systems including zebrafish and mice have established that disruption of pathways known to function via primary cilia in other cell types dysregulates lymphangiogenesis (James et al., 2013; Murtomaki et al., 2013; Coxam et al., 2014; Fatima et al., 2014; Outeda et al., 2014; Huang et al., 2015; Betterman et al., 2020). A single previous report (Bailey et al., 2009) identified acetylated α-tubulin+ structures on LYVE-1+ cells in thin sections of pancreatic ductal adenocarcinoma, suggesting that primary cilia may modulate tumor-stroma interactions in the tumor microenvironment. When and how LECs express primary cilia across tissues, developmental stages, inflammation states, and vessel domains is not known. The purpose of this study was to determine if and when primary cilia are present on mammalian LECs and how they regulate lymphatic vessel patterning.

We used immunofluorescence microscopy to demonstrate that LECs possess primary cilia both *in vitro* and *in vivo* across diverse microenvironmental conditions. Based on primary cilia function in other cell types, we hypothesized that primary cilia on LECs regulate cellular behaviors important for lymphangiogenesis. To evaluate how loss of primary cilia impacts lymphatic vessel patterning, we knocked out intraflagellar transport protein 20 (IFT20), a protein critical for primary cilia assembly and ciliary cargo transport, and assessed lymphangiogenesis during mouse development and corneal inflammation. This paper presents the primary cilium as a novel LEC organelle with regulatory functions during lymphatic vessel patterning and discusses the implications of primary cilia signaling for fundamental lymphatic endothelial biology.

MATERIALS AND METHODS

Lymphatic Endothelial Cell Culture and Immunofluorescence

Immortalized mouse mesenteric lymphatic endothelial cells (SVLECs) were a kind gift from J. Steven Alexander (Ando et al., 2005) (Louisiana State University Health Shreveport) and were routinely cultured with Dulbecco's Modified Eagle's Medium (Corning, 10-017-CV) supplemented with 10% fetal bovine

Abbreviations: FOV, field of view; LEC, lymphatic endothelial cell; MIP, maximum intensity projection; RBC, red blood cell; RT, room temperature.

serum (Thermo Fisher Scientific) and penicillin/streptomycin (Thermo Fisher Scientific) at 37°C and 5% CO_2. Primary human dermal lymphatic endothelial cells (HDLECs) obtained from PromoCell (c-12217) were routinely cultured with Endothelial Cell Growth Medium MV 2 (PromoCell, c-22022) supplemented with the corresponding SupplementMix (PromoCell, c-39226) at 37°C and 5% CO_2. Under serum starvation protocols, SVLECs and HDLECs were cultured with 0 and 0.1% serum at 37°C and 5% CO_2 for 24 and 48 h, respectively. For immunofluorescence staining protocols, SVLECs were seeded on sterile poly-L-lysine coated coverslips (Corning), and HDLECs were seeded on sterile uncoated coverslips (Thermo Fisher Scientific). Both SVLECs and HDLECs were fixed in chilled methanol for 20 min. Cells were then blocked and permeabilized in a solution containing 0.15% Triton-X 100 and 1% bovine serum albumen (BSA) in 1× PBS. Primary antibodies were incubated for one hour at room temperature (RT) in the blocking solution followed by PBS washes. Secondary antibodies were incubated for 45 min at RT in the blocking solution followed by PBS washes. Coverslips were mounted in Fluoromount-G with DAPI (Thermo Fisher Scientific, 00-4959-52) and imaged by epifluorescence microscopy.

Mice

All experimental procedures were approved by the Institutional Animal Care and Use Committees of South Dakota State University or the University of Massachusetts Medical School. C57BL/6J (Stock# 000664), Prox1CreERT2 (*Prox1*$^{TM3(cre/ERT2)Gco}$/J, Stock# 022075), and Lyve1Cre (B6;129P2-*Lyve1*$^{TM1.1(EGFP/cre)Cys}$/J, Stock# 012601) mice were purchased from Jackson Laboratories. Lyve1CreERT2 (Connor et al., 2016) mice were a kind gift from Dr. Richard M. Tempero (Boys Town National Research Hospital, Omaha, NE, United States). Development of *Ift20*$^{fl/fl}$ mice was described previously (Jonassen et al., 2008). Development of global and LEC-specific IFT20 knockout (KO) mice is described below. Development of Lyve1CreERT2;tdTomato mice with LEC-specific expression of tdTomato reporter protein was described previously (Connor et al., 2016). Adult mice were euthanized by ketamine/xylazine overdose or CO_2 inhalation and cervical dislocation. Embryos were collected following euthanasia of pregnant dams. Mice were genotyped by standard PCR methods.

Development of Global and LEC-Specific IFT20 KO Mice

Ift20$^{fl/fl}$ females were bred to *Ift20*$^{null/+}$;CAGG-CreER^{TM} (Hayashi and McMahon, 2001) males. E0.5 was designated as noon on the day of plug identification. CAGG-CreER^{TM} recombinase activity was induced in pregnant dams at E7.5 by oral gavage of tamoxifen suspended in vegetable oil (100 μL, 10 mg/mL). Embryos were harvested at E16.5 and fixed in 10% formalin overnight at 4°C. Following fixation, embryos were rinsed with PBS and stored in 70% ethanol.

Lymphatic endothelial cell-specific IFT20 KO strains were generated by crossing *Ift20*$^{fl/fl}$ mice with Cre-positive mice (Prox1CreERT2, Lyve1CreERT2, or Lyve1Cre). Cre-positive progeny of this cross bearing a single floxed *Ift20* allele were then crossed with *Ift20*$^{fl/fl}$ mice to generate the desired experimental *Ift20*$^{fl/fl}$;Cre-positive genotype. Littermates of mixed genotypes were included in control groups, including mice that were Cre-positive or Cre-negative and heterozygous or wild type for floxed *Ift20*. For CreERT2 lines, 4-hydroxytamoxifen (Sigma-Aldrich, H7904-25MG) was suspended in sunflower seed oil and injected intraperitoneally on three consecutive days (200 μL, 5 mg/mL).

Corneal Inflammation Assays

The corneal model of suture-mediated inflammation, wound recovery, and recurrent inflammation was previously described (Kelley et al., 2011, 2013; Fink et al., 2014). Briefly, we placed four 10-0 prolene monofilament sutures into the healthy mouse cornea and left them in place for 7 days to induce inflammation. Sutures were removed on day 7 and corneas healed for 14 days. To induce recurrent inflammation, we placed four sutures into corneas after wound healing (day 21) and left them in place for 7 days. Homeostasis control corneas were harvested from unmanipulated mice. Surgery was performed under general (ketamine 100 mg/kg, xylazine 10 mg/kg) and topical (proparacaine hydrochloride, USP, 0.5%) anesthesia. Pain was controlled with slow-release buprenorphine (0.1 mg/kg, Zoopharm), and subcutaneous saline was administered to prevent dehydration. Gentamicin ophthalmic ointment (USP, 0.3%) was applied post-operatively.

Corneal Tumor Model

B16-F10 mouse melanoma cells were obtained from ATCC (CRL-6475) and routinely cultured with Dulbecco's Modified Eagle's Medium (Corning, 10-017-CV) supplemented with 10% fetal bovine serum (Thermo Fisher Scientific) and penicillin/streptomycin (Thermo Fisher Scientific) at 37°C and 5% CO_2. To model a tumor microenvironment, B16-F10 cells were injected into healthy Lyve1CreERT2;tdTomato mouse corneas on the same day as suturing with four 10-0 prolene monofilament sutures. Injections were performed under general and topical anesthesia and pain was controlled as described above. Lymphatic vessel growth was observed by intravital imaging using a Zeiss SteREO Discovery.V8 fluorescence stereomicroscope on day 7 (data not shown). Corneas were harvested on day 8.

Whole-Mount Tissue Immunofluorescence

The following mouse tissues were immunostained and imaged as whole-mounts: adult ear, adult cornea, adult mesentery, E16.5 skin, and E16.5 mesentery. Adult mouse ears were dissected to separate ventral and dorsal halves, then fixed in 4% PFA at RT for 2 h. Adult mouse eyes were enucleated and fixed in 1% PFA for 1 h at RT. The cornea was then dissected out and fixed in 1% PFA for an additional hour at RT. Adult mouse mesentery samples were dissected onto a supportive plastic mesh and fixed in 4% PFA at RT for 1 h. E16.5 IFT20 KO embryos were fixed overnight in 10% formalin. Skin and mesentery were dissected from IFT20 KO embryos for whole-mount staining. Following

fixation, whole-mount tissue samples were rehydrated in 1X PBS for one hour at RT and blocked and permeabilized for one hour at RT in PBS++, a solution containing 5.2% BSA, 0.3% Triton X-100, and 0.2% sodium azide in 1X PBS at pH 7.4. Primary and secondary antibodies were applied in PBS++ overnight at RT. Following primary and secondary antibody incubations, three 1 h washes were completed in PBS+, a solution containing 0.2% BSA, 0.3% Triton X-100, and 0.2% sodium azide in 1X PBS at pH 7.4. Samples were mounted in Fluoromount-G without DAPI (Thermo Fisher Scientific, 00-4958-02).

Antibodies

Primary antibodies used in cell and tissue immunofluorescence include: rabbit anti-mouse LYVE-1 1:200 (abcam, ab33682), goat anti-human PROX-1 1:200 (R&D Systems, AF2727), mouse anti-mouse ARL13B 1:200 and 1:4,000 (Neuromab, 75-287), rabbit anti-mouse IFT20 1:1,000 (Proteintech, 13615-1-AP), goat anti-mouse NRP-2 1:200 (R&D Systems, AF567), goat anti-human podocalyxin 1:100 (R&D Systems, AF1658), goat anti-mouse integrin α-9 1:100 (R&D Systems, AF3827), rat anti-mouse LYVE-1 1:50 (Santa Cruz, sc-65647), and rat anti-mouse pHH3 1:100 (Sigma Aldrich, H9908). Directly conjugated primary antibodies used in whole-mount tissue immunofluorescence include: mouse anti-mouse 611B1-AF647 1:500 (Santa Cruz, sc-23950 AF647) and mouse anti-mouse smooth muscle actin-Cy3 1:300 (Sigma-Aldrich, C6198). Secondary antibodies used in cell and tissue immunofluorescence at concentrations of 1:10,000 and 1:500, respectively, include: goat anti-mouse 488, donkey anti-rabbit 488, goat anti-mouse 555, chicken anti-goat 647 (Invitrogen), donkey anti-rabbit 555 (abcam), donkey anti-rat 594 (Thermo Fisher Scientific), chicken anti-goat 488 (Thermo Fisher Scientific), goat anti-rat 550 (Thermo Fisher Scientific), and goat anti-rat 647 (Thermo Fisher Scientific). Primary antibodies used for Western blot analysis include: rabbit anti-mouse/human PROX-1 1:1,000 (abcam, ab101851) and mouse anti-mouse β-actin 1:1,000 (Santa Cruz, sc-47778). Secondary antibodies include: donkey anti-mouse IRDye 800CW 1:15,000 (Licor, 926-32212) and donkey anti-rabbit IRDye 680RD 1:15,000 (Licor, 926-68073).

Microscopy

Epifluorescence microscopy was performed using a DMI 4000 B microscope (Leica) with a KUBler CODIX EL6000 light source (Leica) and a Zyla 4.2 sCMOS camera (ANDOR). Two photon microscopy was performed using a FLUOVIEW FVMPE-RS Multi Photon Laser Scanning Microscope (Olympus) and InSight and MaiTai tunable lasers (SpectraPhysics). Laser scanning confocal microscopy was performed using a FLUOVIEW FV1200 scanning confocal microscope (Olympus) interfaced with an IX81 microscope (Olympus) using 488, 559, and 635 laser lines. A spinning disk confocal microscope with fully automated iMIC platform (Till Photonics), four lasers (445, 515, 561, and 645nm), and a CMOS camera was used to image whole-mount corneas. A Zeiss Stemi 305 compact stereo dissecting microscope with a 1080P HP digital video camera was used to image intact embryos and perform surgery and dissections. A Zeiss SteREO Discovery.V8 fluorescence stereomicroscope and a Zeiss Axio Zoom.V16 fluorescence stereo zoom microscope with Apotome2 structured illumination module and Axiocam 503 monochrome cameras were used to image tissues and perform surgery. Z-slice thickness from confocal and two photon microscopy is indicated in figure legends.

Image Analysis

Primary cilia *in vitro* were counted manually using the cell counter plugin in Fiji (NIH ImageJ) (**Figure 1E**). Lymphatic vessel densities were quantified by manually outlining lymphatic vessel area on maximum intensity projections (MIPs) using the freehand selections plugin in Fiji (**Figure 2G**), manual object identification in CellProfiler (**Figure 3E**), or by overlaying a grid onto a MIP and counting grid squares in Fiji (**Figures 4B,I,M** and **Supplementary Figure 6C**). Lymphatic vessel diameters, junctions, and branches were measured and counted manually using the segmented lines plugin and cell counter plugin, respectively, in Fiji (**Figures 2H–J**, 4J,N and **Supplementary Figure 6D**). Lymphatic vessel area filled with red blood cells was determined by dividing lymphatic vessel area containing red blood cells by total lymphatic vessel area per field of view from MIPs. Both of these areas were determined by manual object identification in CellProfiler (**Figure 3E**). Blood vessel junctions and branches per junction were counted using the cell counter plugin in Fiji while scrolling through a z-stack (**Figure 3C**). Primary cilia on LECs *in vivo* were identified by trimming confocal z-stacks to remove z-slices above and below lymphatic vasculature. Primary cilia on trimmed MIPs were then counted by automated primary object identification in CellProfiler. The primary cilia count was then masked with manually identified lymphatic vessel area in CellProfiler to identify primary cilia on LECs (**Figure 2B**). Total primary cilia on full stack MIPs were quantified by automated primary object identification in CellProfiler and related to the tissue volume imaged (**Figure 2B**), where one volume unit was set to 300 μm^3. For primary cilia per lymphatic vessel area unit, the lymphatic vessel area was multiplied by two to account for the top and bottom surfaces of the vessel. The data is presented as primary cilia per lymphatic vessel area unit, where one area unit was defined as 75 μm^2 (**Figure 2B**). Primary cilia on LECs *in vivo* were also identified manually using the cell counter plugin in Fiji by identifying primary cilia projecting from lymphatic endothelial cells while scrolling through confocal z-stacks (**Figure 4B**). The lymphatic vessel area was multiplied by two and one unit set equal to 75 μm^2 as above. Percent ciliated LECs was determined by counting PROX-1+ nuclei in confocal z-stacks and identifying primary cilia projecting from each individual LEC, also expressing tdTomato (**Supplementary Figure 5B**). Percent proliferating LECs in E16.5 skin was determined using the cell counter plugin in Fiji to identify PROX-1+ and PROX-1/pHH3 double positive LECs in confocal z-stacks (**Supplementary Figure 4C**). Percent proliferating LECs in adult cornea was quantified using automated primary object identification in CellProfiler. PROX-1+ LECs were masked with pHH3+ nuclei to determine the number of proliferating LECs (**Supplementary Figures 4D,E**). Image brightness and contrast were adjusted in some cases to improve signal/noise for visualization in thick tissue samples.

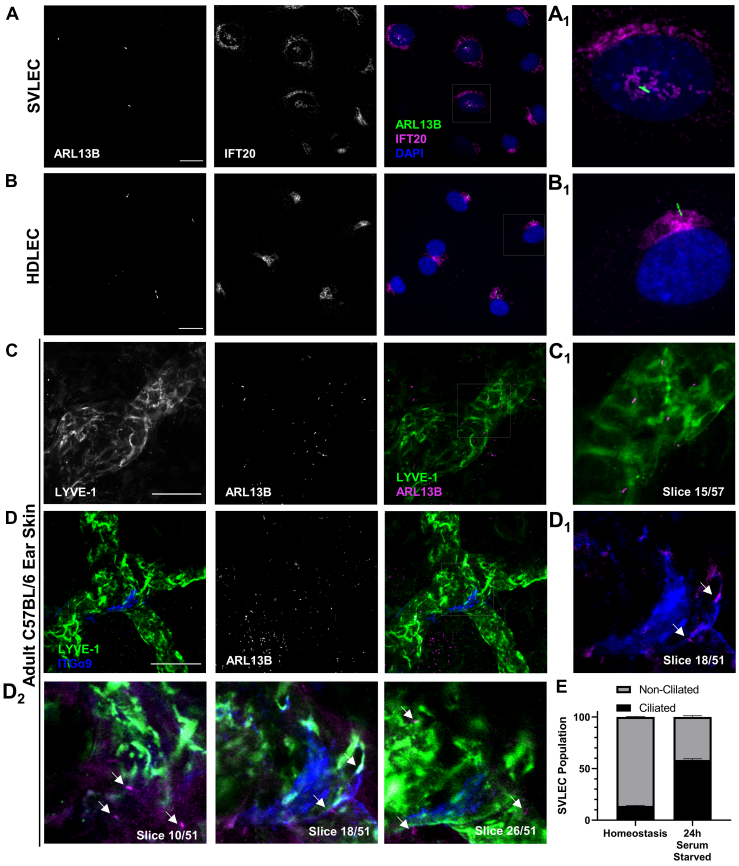

FIGURE 1 | PC assemble on LECs both *in vitro* and *in vivo*. **(A,B)** Epifluorescence microscopy of serum starved SVLECs **(A)** and HDLECs **(B)** immunostained with antibodies against ARL13B and IFT20, and nuclei labeled with DAPI reveals primary cilia on immortalized mouse and primary human LECs *in vitro*. **(A_1,B_1)** Single cell from panels **(A,B)**. **(C,D)** Maximum intensity projections (MIPs) from laser scanning confocal z-stacks of adult C57BL/6J whole mount ear skin immunostained with antibodies against LYVE-1, ARL13B, and ITGα9 reveal primary cilia on both luminal and abluminal surfaces of lymphatic vessels *in vivo*. **(C_1)** A single 1 μm z-slice shows abluminal primary cilia on a LYVE-1 positive lymphatic vessel. **(D_{1-2})** Intraluminal primary cilia are observed near lymphatic valves identified by ITGα9. Arrows indicate both luminal and abluminal primary cilia. **(E)** Quantification of **(A)** represented as an average of three biological replicates. Each biological replicate included at least three fields of view from each of at least two technical replicates. **(C,D)** Images are representative from three animals. **(A,B)** Scale bar = 20 μm. **(C,D)** Scale bar = 50 μm.

Western Blotting

Immortalized mouse mesenteric lymphatic endothelial cells from confluent 9.6 cm^2 wells (six-well plates) were lysed using RIPA buffer (Thermo Fisher Scientific, 89900) plus 1X Halt protease and phosphatase inhibitors with EDTA (Thermo Fisher Scientific) and cleared by centrifugation. Cell lysates were subjected to Western blot analysis using the XCell II^{TM} Blot Module system (Invitrogen, EI9051). PVDF membranes were probed with primary antibodies against PROX-1 and β-actin as a loading control followed by Licor IRDye secondary antibodies. Membranes were imaged using a LI-COR Odyssey CLx imager with near-infrared Western blot detection and analyzed using ImageStudioLite software.

Statistics

Data were analyzed using GraphPad Prism 8 and 9 software (GraphPad Software, Inc.) using Student's or Welch's T-Test or One-Way ANOVA with Dunnett's Multiple Comparisons Post-Test. *p* values and replicates are indicated in figure legends. Error bars show mean and standard deviation.

RESULTS

Primary Cilia Assemble on Lymphatic Endothelial Cells *in vitro* and *in vivo*

Our first goal was to definitively identify the presence or absence of primary cilia on LECs in culture and in mouse tissue. Using immunofluorescence microscopy, we identified ARL13B+ primary cilia on LECs *in vitro* on both SVLECs (**Figure 1A**) and primary adult HDLECs (**Figure 1B**). We confirmed that SVLECs express the master regulator LEC transcription factor PROX-1 by Western blot and form tubes in an *in vitro* tubulogenesis assay (**Supplementary Figure 1**). Immunofluorescence staining confirmed expression of IFT20

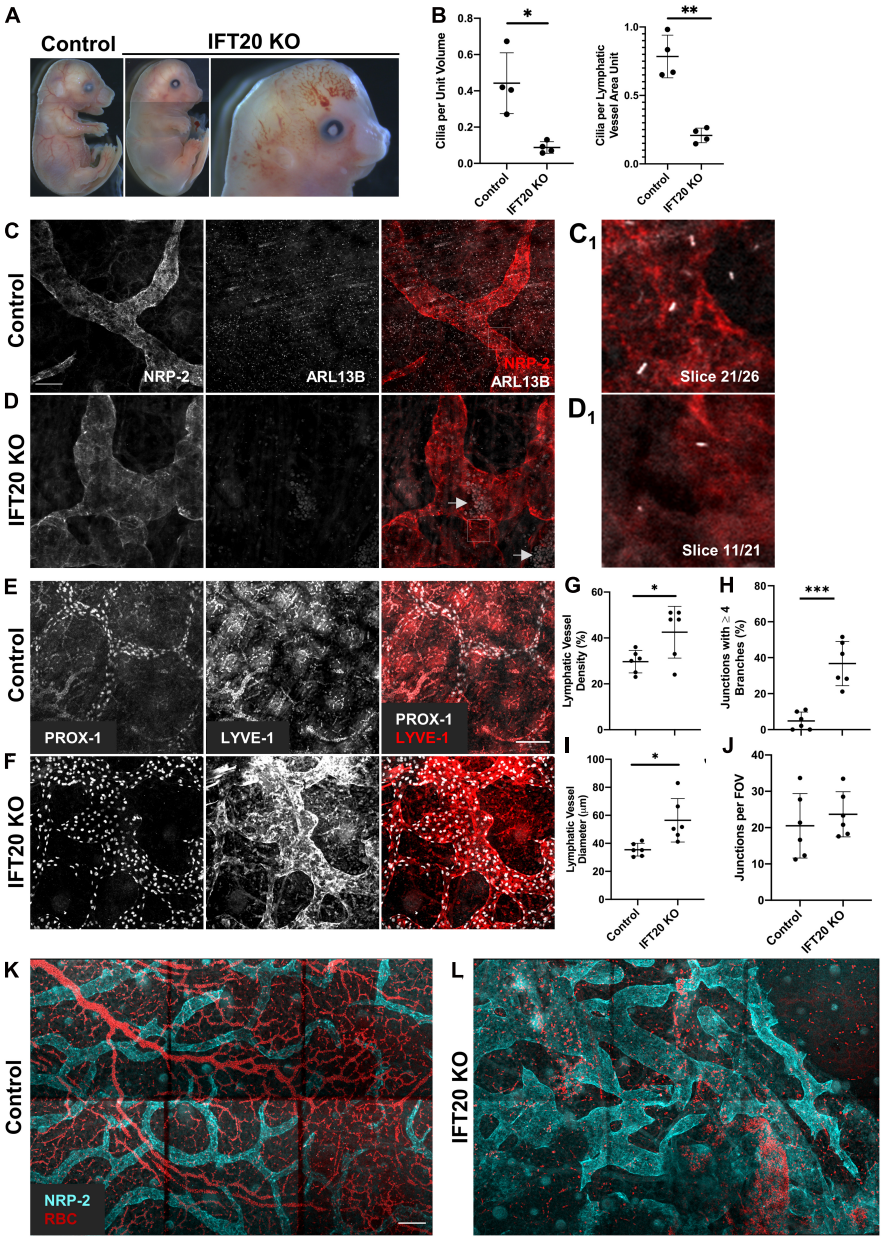

FIGURE 2 | Global IFT20 KO mice show severe lymphatic vessel patterning defects at E16.5. **(A)** Administration of tamoxifen to pregnant dams at E7.5 causes polydactyly, craniofacial abnormalities, hydrops, and abnormal vasculature with gross hemorrhaging in IFT20 KO embryos at E16.5 vs. control. Images of entire embryo were generated by aligning separate images of head, abdomen, and rump. **(B)** Quantification of panels **(C,D)** where "unit volume" represents 300 μm^3 of tissue, approximating the volume of a single cell, and "LV area unit" represents 75 μm^2 of lymphatic vessel. Each data point represents a per embryo average of at least 2 fields of view and is from 4 control and 4 KO animals across 3 litters. **(C,D)** MIPs from laser scanning confocal z-stacks of whole mount skin immunostained with antibodies against neuropilin-2 (NRP-2) and ARL13B. Arrows in panel **(D)** indicate autofluorescent red blood cells in lymphatic vessel lumens. **(C_1,D_1)** Single 1 μm z-slices showing primary cilia on the abluminal surface of NRP-2 positive lymphatic vessels. **(E,F)** MIPs from multiphoton z-stacks of full thickness skin samples immunostained with antibodies against LYVE-1 and PROX-1 show malformed lymphatic vasculature of significantly greater vessel density, diameter, and branching in the IFT20 KO **(F)** vs. control **(E)**. **(G–J)** Quantification of panels **(E,F)** where each data point represents a per embryo average of at least 3 fields of view and is from 6 KO and 6 control embryos across 4 litters. **(K,L)** MIPs from tiled multiphoton z-stacks of full thickness skin samples immunostained with antibodies for NRP-2 further demonstrate lymphatic patterning defects in the mutant **(L)** vs. control **(K)**. Autofluorescent red blood cells are shown in red and suggest hemorrhaging in the IFT20 KO (**L**). Scale bars = 50 μm. ***$p < 0.0001$; **$p < 0.005$; *$p < 0.05$.

in SVLECs and HDLECs and marked the position of the Golgi apparatus. Approximately 60% of SVLECs displayed primary cilia under serum starvation, while approximately 18% were ciliated in complete media (**Figure 1E**). This is consistent with findings in other cell types in which serum starvation causes cell cycle arrest, thus enabling primary cilium

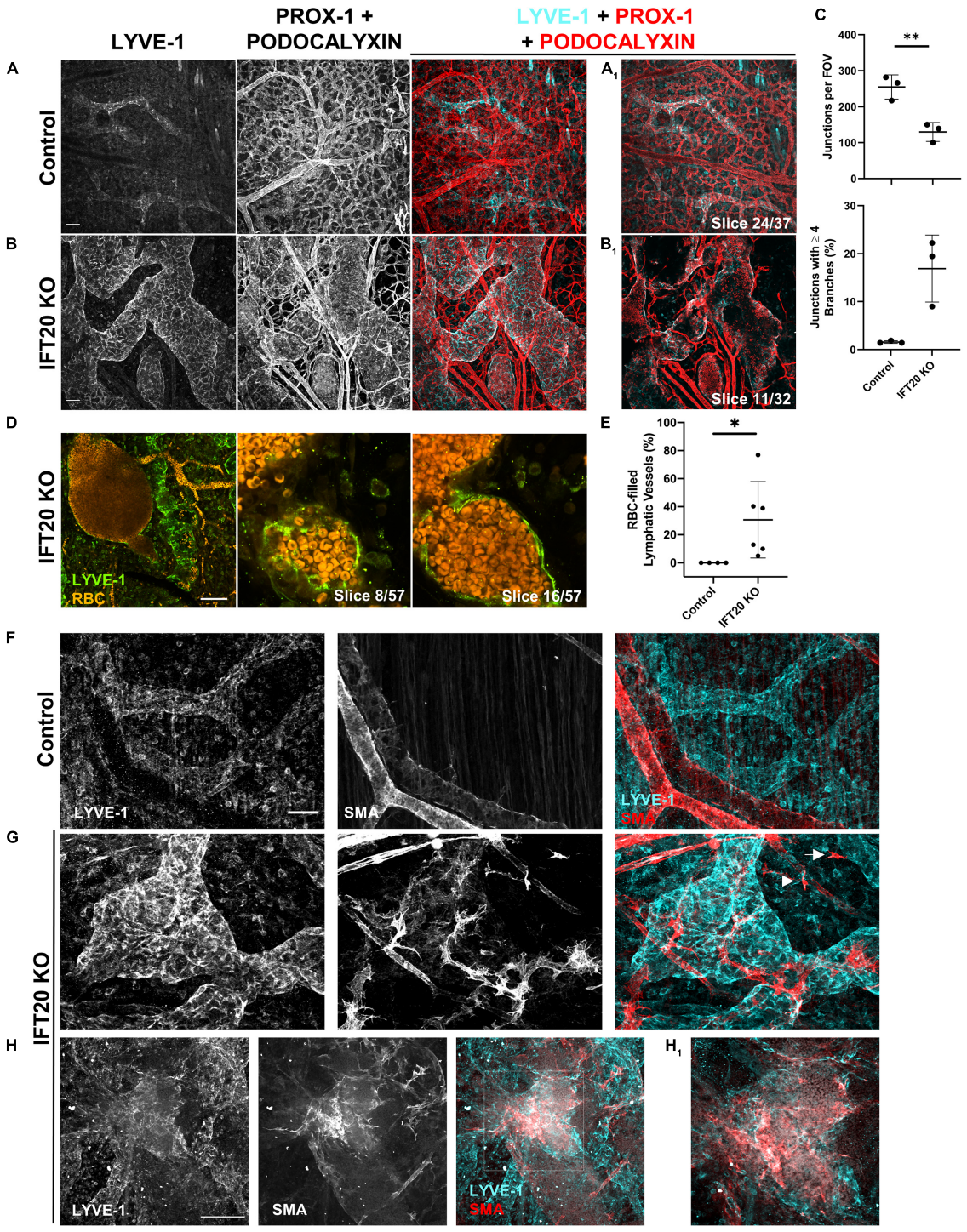

FIGURE 3 | Lymphatic vessels in E16.5 IFT20 KO skin have intraluminal red blood cells and aberrant SMA+ cell coverage. **(A,B)** MIPs from laser scanning confocal z-stacks from whole mount control **(A)** and IFT20 KO **(B)** skin immunostained with antibodies against LYVE-1, PROX-1, and podocalyxin, a sialoglycoprotein expressed in both blood and lymphatic endothelium. **(A_1,B_1)** Single 1 μm z-slices. **(C)** Quantification of blood vessel junctions from panels **(A,B)** where each data point represents a per embryo average of at least 2 fields of view and is from 3 KO and 3 control embryos. **(D)** MIP and single 1 μm z-slices from two photon z-stacks of whole-mount skin immunostained for LYVE-1. Autofluorescent RBCs are shown in orange. **(E)** Quantification of RBC-filled lymphatics from whole-mount skin immunostained for NRP-2 (as in **Figures 2C,D**), where each data point represents a per embryo average of at least 4 fields of view and is from 4 control and 6 KO animals across 5 litters. **(F–H)** MIPs from laser scanning confocal z-stacks of whole-mount skin immunostained with antibodies against LYVE-1 and smooth muscle actin (SMA) showing aberrant SMA+ recruitment to lymphatic vessels and single SMA+ cells (*arrows*) in the interstitium in the IFT20 KO **(G,H)**. **(H_1)** Single 1 μm z-slice. Scale bars = 50 μm. $^{**}p < 0.005$; $^{*}p < 0.05$.

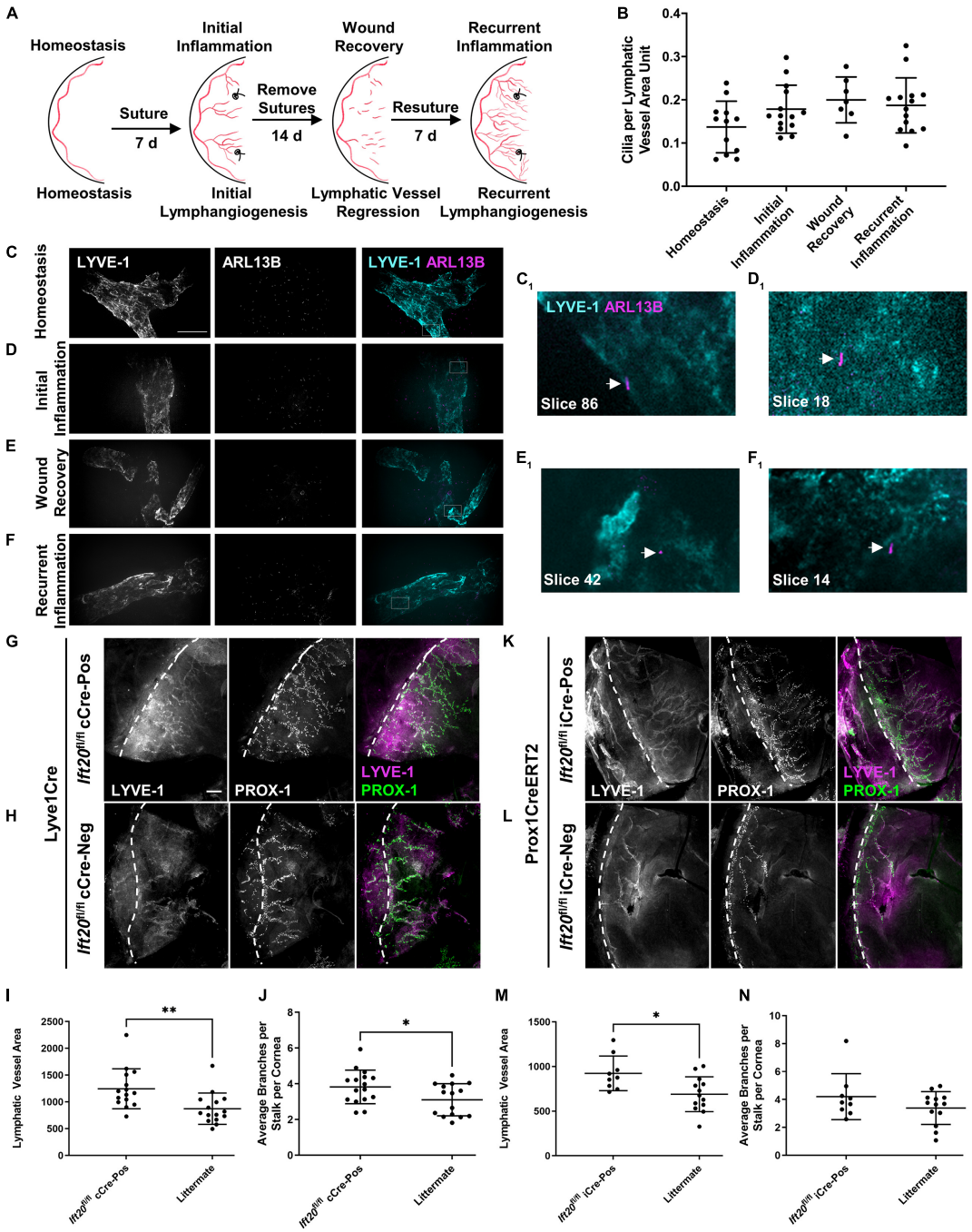

FIGURE 4 | PC assemble on corneal LECs and are differentially expressed depending on inflammatory status, and IFT20 KO exacerbates corneal lymphangiogenesis. **(A)** Sequential suturing, suture removal, and resuturing in the adult mouse cornea provides an animal model to study acute and recurrent inflammation-induced lymphangiogenesis and lymphatic vessel regression during wound recovery. **(B)** Quantifications of panels **(C–F)** where each data point represents a per animal average, where "LV area unit" represents 75 μm^2 of lymphatic vessel. Corneas under the following inflammatory microenvironments were immunostained with antibodies against ARL13B, acetylated α-tubulin (not shown), and LYVE-1: **(C)** homeostasis, **(D)** initial inflammation, **(E)** wound recovery, and **(F)** recurrent inflammation. **(C–F)** MIPs from spinning disk confocal z-stacks of whole mount corneas demonstrate the presence of primary cilia on corneal LECs during all phases of the model with a trend to increase following activation of lymphatic vessels by inflammation. (**C_1–F_1**) Arrows indicate abluminal primary cilia on LECs in a single 0.15 μm z-slice. For each condition, 2–5 fields of view were analyzed from each of at least seven mice across four experiments. Scale bar = 50 μm. **(G–N)** Initial corneal lymphangiogenesis was stimulated by placing sutures in each quadrant of the cornea of Lyve1Cre;*Ift20*$^{fl/fl}$ **(G–J)** or Prox1CreERT2;*Ift20*$^{fl/fl}$ **(K–N)** mice and littermate controls for 7 days. Littermates of all intermediate genotypes including Cre-negative and *Ift20*$^{fl/+}$ were included. Corneas were harvested and immunostained with antibodies against LYVE-1 and PROX-1 and imaged by epifluorescence microscopy. **(I,J,M,N)** Quantifications of **(G,H,K,L)** where each data point represents a per animal average from fields of view encompassing the entire cornea. Scale bar = 200 μm. cCre = constitutive Cre. iCre = inducible Cre. Dashed lines indicate limbus. $^{**}p < 0.005$; $^{*}p < 0.05$.

assembly. Immunofluorescence staining of adult C57BL/6 ear skin revealed primary cilia present on LYVE-1+ lymphatic vessels in homeostasis (**Figures 1C,D**). Analysis of single 1 μm z-slices from laser scanning confocal z-stacks showed the presence of primary cilia on both the abluminal (**Figures 1C1,D2**, slices 10, 26) and luminal (**Figures 1D1,D2**, slice 18) domains of lymphatic vessels. The intraluminal space was identified by the presence of integrin-α9+ lymphatic valves (Bazigou et al., 2009; **Figure 1D**). Our analysis did not directly interrogate or identify primary cilia on mature valve LECs, rather valves were used to identify intraluminal z-planes. A 3D surface rendering of LYVE-1 and ARL13B signals confirmed the presence of cilia projecting both out toward the interstitium and into the lymphatic vessel lumen (**Supplementary Figure 2**). Analysis of E16.5 mouse mesenteric lymphatic vessels also showed both luminal and abluminal primary cilia, demonstrating conservation of ciliation during development of mesenteric lymphatic vessels, which form through aggregation of LEC progenitors and lymphvasculogenesis rather than sprouting from embryonic veins (Stanczuk et al., 2015; **Supplementary Figure 3**). Our *in vitro* experiments demonstrate that primary cilia on LECs adopt the expected perinuclear cellular localization and can be induced by serum starvation. These are conserved features of primary cilia *in vitro* across many cell types and indicate that regulation of ciliary dynamics is likely similar in LECs. Our *in vivo* data show that primary cilia are present on luminal and abluminal domains of LECs organized into functional vessels in mammalian tissue, suggesting that they may perform domain-specific functions.

IFT20 KO Causes Lymphatic Vessel Patterning Defects During Mammalian Development

Given that we had now identified primary cilia on mouse and human LECs *in vitro* and on mouse lymphatic vessels *in vivo*, we next wanted to know if primary cilia are important for lymphatic vessel patterning during mouse development. To disrupt primary cilia *in vivo*, we developed a tamoxifen-inducible global IFT20 KO mouse model (*Ift20*$^{fl/fl}$;CAGG-CreER^{TM}). IFT20 is required for primary cilia assembly and traffic of cargo, including signaling receptors, from the Golgi to the cilium and up its length via anterograde intraflagellar transport as part of the IFT-B complex (Follit et al., 2006, 2008; Schmid et al., 2018). We induced deletion of IFT20 at E7.5, just before LECs begin sprouting from the cardinal vein, and harvested embryos at E16.5, when dorsal lymphatic vessels have come together at the midline and mesenteric lymphatics are beginning to form valves. Though extraciliary functions of IFT20 have been identified (Finetti et al., 2009, 2020), IFT20 KO embryos phenocopied common developmental defects of other ciliopathy models, including hydrops/edema, polydactyly, and craniofacial abnormalities (**Figure 2A**). A subset of KO embryos also displayed gross hemorrhage and vascular ballooning (**Figure 2A**, right panel). As expected, primary cilia incidence was reduced both in the skin overall and on LECs specifically (**Figure 2B**). Embryonic edema has been attributed to cardiac defects in some mouse models. Other models, such as Prox1CreERT2;*Cdh5*$^{fl/fl}$ and *Pkd1*$^{-/-}$, demonstrate normal heart development and attribute edema directly to lymphatic malfunction (Outeda et al., 2014; Hägerling et al., 2018). In addition to edema, our IFT20 KO model recapitulated common lymphatic developmental defects, such as dilated and variable lumen size, disrupted branching, and intraluminal red blood cells (Srinivasan and Oliver, 2011). Two photon microscopy of whole-mount embryonic skin immunostained for LYVE-1, PROX-1, and NRP-2 revealed malformed lymphatic vasculature with increased lymphatic vessel density and branching vs. littermate controls (**Figures 2C–L**). Lymphatic vessel diameter was increased in both overall caliber and range, with areas of either significant dilation or constriction evident in KO samples. Number of vessels meeting at junctions was increased in KOs, with nearly 40% of junctions composed of four or more branches. Number of junctions per field of view did not change. LEC proliferation, as measured by colocalization of phosphorylated histone H3 and PROX-1, trended to increase in KO vs. control but was not statistically significant (**Supplementary Figures 4A–C**). This result correlates with the increased lymphatic vessel density and junction complexity, but indicates that dramatically increased proliferation is not a feature of the IFT20 KO lymphatic vasculature at this time point during development. Red blood cells were also visualized inside lymphatic vessel lumens (**Figure 2D**, arrows). Formation of lymphatic vessel valves is not complete until approximately E18 (Koltowska et al., 2013), thus we were unable to evaluate valve formation in these E16.5 skin samples. Our data demonstrate that IFT20 KO reduces the prevalence of primary cilia overall and on LECs, induces common ciliopathy phenotypes, and dysregulates lymphatic vessel patterning.

Lymphatic Vessels Are Filled With Red Blood Cells and Recruit Smooth Muscle Actin+ Cells in IFT20 KO Embryos

Our analysis of E16.5 IFT20 KO dorsal skin identified LYVE-1/PROX-1+ lymphatic vessels with autofluorescent intraluminal red blood cells (RBCs; **Figure 2D**, arrows) as well as extravascular RBCs. The presence of RBCs in lymphatic vessels is a feature of many developmental lymphangiogenesis mutants and has been attributed to failure to adequately separate blood and lymphatic vasculatures due to lymphovenous valve insufficiency, to improper blood-lymphatic vessel anastomoses, or to clearing of extravascular RBCs from the interstitium following blood vessel hemorrhage. To visualize blood and lymphatic vasculature together, we immunostained skin for LYVE-1, PROX-1, and podocalyxin. Podocalyxin is a sialoglycoprotein that is expressed by both blood and lymphatic endothelial cells. This staining strategy resulted in lymphatic vessels labeled with all three markers and blood vessels labeled with podocalyxin only (**Figures 3A,B**). Blood vessel branching was dysregulated in IFT20 KOs (**Figure 3C**). Blood vessel junctions per field of view were decreased approximately by half in KO vs. control, while number of junctions composed of four or more branches was increased to more than 15%. As expected RBCs were restricted

to blood vessel lumens in control embryo samples. In contrast, RBCs were present both free in the interstitium and within the lumen of lymphatic vessels in IFT20 KO skin. RBCs tightly packed the lumen of some sections of lymphatic vessels, while in areas of more uniform lumen caliber RBCs were more sparsely distributed, suggesting flow (**Figure 3D**). Overall, on average 30% of lymphatic vessels by area were filled with RBCs across six IFT20 KO embryos, ranging up to more than 70% (**Figure 3E**).

Aberrant recruitment of smooth muscle cells to lymphatic vessels is a feature of other models of vascular malformation. Blood vessels are invested with vascular smooth muscle cells to increase structural integrity and reduce hemorrhage. Lymphatic vessels are exposed to much lower intraluminal pressure than blood vessels. In mice, lymphatic collecting vessels are not supported by lymphatic smooth muscle cells until P14, and lymphatic capillaries lack mural cell coverage entirely. To determine if smooth muscle cell localization is disrupted by loss of primary cilia, we immunostained for smooth muscle actin (SMA) and LYVE-1. As expected, SMA+ cells in control skin smoothly covered LYVE-1-negative blood vessels (**Figure 3F**). In IFT20 KO skin, SMA+ cells with numerous filopodia were aberrantly recruited to lymphatic vessels (**Figure 3G**), covering large patches in some cases (**Figure 3H**). Single SMA+ cells not associated with vessels were also present in KO skin (**Figure 3G**, arrows).

In summary, CAGG-CreER^{TM}-mediated loss of IFT20 disrupts not only lymphatic but also blood vessel patterning and integrity. Blood vessel branching overall was reduced, while complexity at individual junctions was increased. Free RBCs and RBCs in the lymphatic vessel lumen suggest compromised blood vessel integrity, which may be explained in part by mislocalization of SMA+ cells individually in the interstitium and to lymphatic vessels.

Primary Cilia Assemble on Corneal Lymphatic Vessels During Acute, Recurrent, and Tumor-Associated Inflammation and Wound Healing, and IFT20 KO Exacerbates Corneal Lymphangiogenesis in a LEC-Autonomous Manner During Acute Inflammation

To determine if primary cilia on LECs regulate lymphatic patterning in settings beyond development, we quantified primary cilia on corneal lymphatic vessels during distinct pathological conditions. We used a well-characterized corneal model of inflammation, wound healing, and recurrent inflammation to induce three diverse corneal lymphatic patterning events: initial lymphangiogenesis, lymphatic vessel regression, and recurrent lymphangiogenesis (Kelley et al., 2011, 2013; **Figure 4A**). In this model, placement of sutures in the cornea induces inflammation and activates LECs restricted to the limbus vasculature during homeostasis to sprout, proliferate, and migrate to expand the lymphatic vasculature into the corneal parenchyma. This initial lymphangiogenesis is dependent on VEGF-C. Removing sutures promotes resolution of inflammation, during which lymphatic vessels regress by unknown mechanisms. Resuturing causes recurrent lymphangiogenesis, also termed lymphatic vessel memory (Kelley et al., 2013), in which regressed lymphatic vessel fragments reorganize independent of VEGF-C to form a complex, robust lymphatic network. Primary cilia were present on corneal lymphatic vessels during all phases of this dynamic tissue injury model (**Figures 4B–F**). Stimulation of LECs to undergo lymphangiogenesis trended to increase cilia incidence in all subsequent phases of the model vs. homeostasis, though this was not statistically significant. Expression of primary cilia across diverse inflammation states suggests that primary cilia-dependent signaling may influence lymphatic patterning by complementing known mechanisms of lymphangiogenesis regulation or by supporting novel mechanisms.

We next wanted to determine if primary cilia on LECs could cell-autonomously regulate lymphatic vessel patterning. We used lymphatic-specific constitutive and tamoxifen-inducible Cres to disrupt IFT20 in adult mouse LECs and studied corneal lymphangiogenesis during initial inflammation using the model described above (**Figure 4A**). IFT20 KO driven by constitutive Lyve1Cre or tamoxifen-inducible Prox1CreERT2 increased new lymphatic vessel growth toward corneal sutures. (**Figures 4G–L**). At harvest on day 7, lymphatic vessel density was increased in *Ift20*$^{fl/fl}$;Cre-positive mice vs. littermate controls in both models (**Figures 4I,M**). Branching was also significantly increased in the constitutive Cre model (**Figures 4J,N**). In some animals, a large number of very short branches sprouting from stalks was observed (**Figure 4G**). This together with our finding of highly ciliated tip cells (**Supplementary Figure 5**) indicates that cilia may be especially important for regulation of tip cell identity and function. LEC proliferation was not significantly increased at this time point during initial inflammation in either model (**Supplementary Figures 4D–I**). We also performed these experiments in Lyve1CreERT2;*Ift20*$^{fl/fl}$ mice, but increased lymphangiogenesis in that model did not reach statistical significance (**Supplementary Figure 6**). These results demonstrate LEC-autonomous regulation of inflammation-associated corneal lymphangiogenesis by primary cilia.

We then turned to a mouse melanoma model to study tumor-associated corneal lymphangiogenesis. To monitor lymphatic vessel growth toward tumors, we performed these experiments in Lyve1CreERT2;tdTomato mice in which LECs express tdTomato fluorescent reporter protein. We sutured mouse corneas, injected B16-F10 cells into a corneal micropocket, and allowed tumor-associated lymphangiogenesis to proceed for 8 days (**Supplementary Figure 5A**). We immunostained corneas for acetylated α-tubulin and PROX-1. Primary cilia and a subset of corneal nerves expressed acetylated α-tubulin. We quantified the incidence of primary cilia on populations of lymphatic endothelial cells expected to perform different functions based on their localization within the vascular network: limbus cells, stalk/branch cells, and tip cells. LECs residing in limbus lymphatic vessels are mostly quiescent during later stages of corneal lymphatic vessel remodeling but, as the source of nascent lymphatic vessels, can be stimulated to sprout and

proliferate. LECs residing in a stalk connected to the limbus or in a branch emanating from a stalk proliferate along the long axis of the vessel to increase its length. Tip cells are typically non-proliferative and provide directionality to vascular expansion through signal gradient detection, filopodia extension, and chemotaxis (Connor et al., 2016; Geng et al., 2020). We identified primary cilia on limbus, stalk/branch, and tip LECs in this model (**Supplementary Figures 5B–E**). Approximately 40% of limbus and stalk/branch LECs and nearly 80% of tip cells were ciliated. In addition to likely functions in chemosensing, LEC primary cilia in the tumor microenvironment may be responsible for sensing changes in tissue stiffness or regulate properties of lymphatic vessels relevant to tumor metastasis such as intercellular junctions.

These data show that primary cilia are present on corneal lymphatic vessels under a wide variety of microenvironmental conditions. LECs residing in distinct functional domains of lymphatic vessels (limbus, stalk/branch, tip) assemble primary cilia. Tip cells especially may employ primary cilia-dependent signaling pathways during lymphangiogenesis. Taken together these data suggest that ciliary signaling may be important for both maintenance of lymphatic vessels during homeostasis and during diverse lymphatic vessel remodeling events that characterize inflammation, wound healing, recurrent inflammation, and the tumor microenvironment.

DISCUSSION

Despite swift progress in the field of lymphatic vessel biology since the identification of lymphatic-specific markers around the turn of the century, the mechanisms regulating lymphatic vessel patterning in some physiological settings remain unclear. In this work we demonstrate that LECs possess primary cilia both *in vitro* and *in vivo* and that disruption of *Ift20*, a critical component of the intraflagellar transport machinery and a required element for ciliary assembly, results in profound lymphatic vessel patterning defects during both mammalian development and inflammation. While the developmental and inflammation-associated lymphangiogenesis phenotypes we observed in our models were not identical, they were complimentary in that lymphatic vessel density and complexity of branching were increased in both conditions and within the spectrum of phenotypes reported in other studies of dysregulation of embryonic or corneal lymphangiogenesis. This suggests that signaling through primary cilia governs cellular LEC activities important for lymphangiogenesis, such as proliferation, chemotaxis, lumen formation, shear flow sensing, and intercellular junction organization.

Primary Cilia on Lymphatic Endothelial Cells

The diversity of microenvironments and vessel domains in which primary cilia are present on LECs implicates them broadly in lymphatic vascular biology. While primary cilia assemble on LECs *in vitro* as well as *in vivo* in development and in inflammatory and tumor microenvironments, the functioning primary cilia-dependent signaling and sensory mechanisms may be unique in each condition. We demonstrate that primary cilia are present on both the abluminal and luminal surfaces of adult and embryonic lymphatic vessels, including near lymphatic valves, though we did not directly visualize primary cilia on valve LECs. In other lumenized structures such as kidney tubules and blood vessels, primary cilia predominantly project into the lumen, serving as flow sensors (Nauli et al., 2008; AbouAlaiwi et al., 2009; Goetz et al., 2014), including regulation of vascular regression in retina (Vion et al., 2018). Intraluminal cilia in blood vessels have recently been implicated in regulation of vascular integrity independent of flow (Eisa-Beygi et al., 2018). Thus, primary cilia within the lymphatic vessel lumen may complement known mechanisms of shear stress sensing or perform flow-independent functions and may regulate lymphatic vessel regression. Abluminal cilia may be involved in direct interactions with extracellular matrix or other cells in the interstitium, such as immune cells and fibroblasts, and may also play a more prominent role in receptor-ligand mediated signaling or in sensing other microenvironmental attributes such as matrix stiffness (Frye et al., 2018). We also show that primary cilia are present on regions of corneal lymphatic vessels with distinct functional roles during lymphangiogenesis. Primary cilia are present on LECs residing in the quiescent limbus, proliferating stalk/branch, and chemosensing tip of nascent lymphatic vessels. Primary cilia localized to discrete vessel domains may themselves be specialized to regulate specific aspects of a coordinated lymphangiogenesis response, such as proliferation vs. gradient sensing. LEC-specific IFT20 KO exacerbated inflammation-associated lymphangiogenesis, strongly influencing overall lymphatic vessel density as well as branching in some specimens. While key aspects of developmental and initial inflammation-associated lymphangiogenesis are clearly regulated by canonical VEGF-C/VEGFR-2/3 mechanisms, our data provide evidence for additional complexity that may complement, augment, oppose, or modify this pathway through primary cilia-dependent mechanisms. We also demonstrate the presence of primary cilia on LECs during lymphatic vessel regression, recurrent lymphangiogenesis, and tumor-associated lymphangiogenesis, three mechanistically distinct, poorly understood lymphatic remodeling events with significant implications for wound healing, chronic inflammation, and metastasis. Thus, elucidation of primary cilia-dependent signaling mechanisms on LECs under these conditions may provide new targets for therapeutic modulation of disease. Taken together, LEC primary cilia are likely an important feature of the lymphatic vascular signaling machinery with diverse functions depending on the microenvironment, activation state, and vascular domain of the LEC on which they reside.

Primary Cilia in Lymphatic Vessel Development

Our IFT20 KO model demonstrates defective lymphatic vessel patterning during development. Similar developmental lymphatic abnormalities occurred when pathways known to function via primary cilia in other cell types were disrupted

globally or in LECs. For example, PKD1/2 KO mice displayed edema, dilated lymphatics, and altered lymphatic branching. This was attributed to failed LEC polarity and disorganization of actin stress fibers and VE-cadherin junctions (Coxam et al., 2014; Outeda et al., 2014; Huang et al., 2015). Similarly, loss of TGFBR1/2 reduced LEC filopodia formation, disrupted branching, and caused lymphatic hyperplasia and edema (James et al., 2013). *Fat4* was recently identified as a LEC target gene of transcription factor GATA2, which regulates many aspects of lymphatic specification and maturation. FAT4 is an atypical cadherin that localizes to primary cilia and regulates planar cell polarity (Saburi et al., 2008). FAT4 KO during developmental lymphangiogenesis caused edema and defects in vessel caliber and branching due to disrupted LEC polarity (Betterman et al., 2020). Furthermore, LEC-specific KO of NOTCH1 caused edema and lymphatic hyperplasia, including increased proliferation, sprouting, and junction reorganization (Murtomaki et al., 2013; Fatima et al., 2014). These studies together with our data suggest that the primary cilium may function as a hub for these signaling mechanisms in LECs as in other cell types.

Human primary lymphedema may also be linked to dysregulation of primary cilia function. HKLLS1 (Hennekam lymphangiectasia-lymphedema syndrome 1, OMIM #235510) can be caused by mutation of *FAT4*, and in addition to lymphedema may also present with camptodactyly or syndactyly (Alders et al., 2014), digit aberrations common in ciliopathies (Baker and Beales, 2009; Norris and Grimes, 2012). Similarly, mutation of *KIF11*, a microtubule-based motor protein, results in MLCRD (microcephaly with or without chorioretinopathy, lymphedema, or mental retardation, OMIM #152950) syndrome (Ostergaard et al., 2012). KIF11 has recently been shown to regulate primary cilia assembly dynamics (Zalenski et al., 2020) and been implicated in human retinal ciliopathy (Birtel et al., 2017). Future work is needed to determine how LEC primary cilia may influence the pathogenesis of human disease.

Vascular Integrity and Flow Sensing

Two striking features of E16.5 IFT20 KO skin are blood-filled lymphatic vessels and aberrant localization of SMA+ cells singly within the interstitium and on lymphatic vessels. Lymphovenous valves form at the interface of blood and lymphatic vasculatures during expansion of the first lymphatic capillaries following upregulation of PROX-1 in venous endothelial cells. Blood-lymph separation is then reinforced by interactions between podoplanin on LECs and CLEC receptors on platelets (Bertozzi et al., 2010; Hess et al., 2013). Lymphovenous valve insufficiency is a feature of several lymphedema mouse models with disruptions in genes including *Prox1, Foxc2, Cx37, Gata2, Pdpn,* or *Clec2* (Uhrin et al., 2010; Hess et al., 2013; Geng et al., 2016; Bianchi et al., 2018). The extent of blood-filled lymphatics in our model suggests that lymphovenous valve insufficiency may be a consequence of loss of primary cilia. In blood endothelium, primary cilia are important for maintaining blood vessel integrity in an endothelial cell-autonomous manner (AbouAlaiwi et al., 2009; Kallakuri et al., 2015; Eisa-Beygi et al., 2018; Liu et al., 2018). Our data also support this model, as our analysis revealed widespread extravascular RBCs in IFT20 KO skin. Blood vessel integrity may also have been compromised due to recruitment of SMA+ cells to dilated lymphatic vessels in embryonic skin. Aberrant localization of SMA+ cells on lymphatic vessels has been linked to defects in lymph flow and flow sensing in developmental lymphangiogenesis mutants including *Foxc2*$^{-/-}$, *Ang2*$^{-/-}$, and *Clec2*$^{-/-}$(Petrova et al., 2004; Dellinger et al., 2008; Sweet et al., 2015), though we cannot assign a LEC-autonomous recruitment mechanism in our model because of our use of the global Cre deleter. It is possible that changes in sensing external forces, such as vessel dilation leading to endothelial stretch (Stratman et al., 2020) or reduced fluid shear stress sensing could induce chemoattractant expression to recruit SMCs. For example, *Foxc2*$^{-/-}$ mouse embryos showed dilated lymphatic vessels with associated SMA+ cells. FOXC2 is a multifunctional flow-dependent transcription factor (Sabine et al., 2015; Norden et al., 2020) and negative regulator of collagen IV production and PDGF-B secretion, which recruits SMCs. Thus, loss of FOXC2 upregulated PDGF-B and collagen IV and recruited mural cells to mutant dermal lymphatic vessels (Petrova et al., 2004). Future studies should determine the role of LEC primary cilia in complementing known mechanisms of fluid shear stress sensing and mechanotrasduction (Sabine et al., 2012;2015; Gordon et al., 2020), such as primary cilium-localized mechanosensative ion channels that have been implicated in lymphatic function including PIEZO1 and TRPV4 (Lee et al., 2015; Behringer et al., 2017; Choi et al., 2019; Miyazaki et al., 2019; Solari et al., 2020), modulation of FOXC2 expression or phosphorylation (Ivanov et al., 2013; Dieterich et al., 2017), and mural cell recruitment or lack thereof.

CONCLUSION

This study presents the LEC primary cilium as a novel regulator of lymphatic vessel patterning. Studying primary cilia-dependent signaling is a new approach to identify mechanisms of lymphatic vessel patterning and function not fully explained by current paradigms. Ongoing work in our laboratory seeks to elucidate the molecular mechanisms by which primary cilia-dependent signaling controls LEC activities, such as sprouting and migration, that are required for lymphatic vessel remodeling events. Studying primary cilia function on LECs is a new enterprise for the field of lymphatic vessel biology. Understanding how primary cilia sense and transmit extracellular soluble and mechanical signals to modify LEC signaling networks has the potential to elucidate fundamental aspects of LEC biology and may identify new targetable mechanisms of lymphatic vessel regulation.

DATA AVAILABILITY STATEMENT

The raw data supporting the conclusions of this article will be made available by the authors, without undue reservation.

ETHICS STATEMENT

The animal study was reviewed and approved by Institutional Animal Care and Use Committees of South Dakota State University or the University of Massachusetts Medical School.

AUTHOR CONTRIBUTIONS

DF and GP designed the study and wrote the manuscript. DF, RH, and GP generated mice. All authors designed and performed experiments and reviewed the manuscript.

FUNDING

This work was supported by the National Institutes of Health GM140458 to DF and GM060992 to GP, by the South Dakota Board of Regents through NSF/EPSCoR 1355423 (BioSNTR) and FY20 Collaborative Research Award "IMAGEN: Biomaterials in South Dakota" (Dr. Steve Smith, PI, South Dakota School of Mines and Technology), and by the Department of Chemistry and Biochemistry at South Dakota State University.

ACKNOWLEDGMENTS

We thank Aleesha Anderson, Heather Collazo, Courtney Ekle, Khalil Ford, Nicholas Goeman, Taylor Hietpas, Ryan Krump, Collin Livingston, Ahana Majumder, Chase Petersen, and Miah Schallenkamp for their contributions to experiments. We acknowledge use of the SDSU Functional Genomics Core Facility, which was supported in part by NSF/EPSCoR grant no. 0091948 and by the State of South Dakota. We thank Richard M. Tempero of Boys Town National Research Hospital, Omaha, NE for the Lyve1CreERT2 strain and J. Steven Alexander of Louisiana State University Health Shreveport for the SVLEC cell line. We also thank Sathish Srinivasan at the Oklahoma Medical Research Foundation for his help and advice.

SUPPLEMENTARY MATERIAL

The Supplementary Material for this article can be found online at: https://www.frontiersin.org/articles/10.3389/fcell.2021.672625/full#supplementary-material

REFERENCES

AbouAlaiwi, W. A., Takahashi, M., Mell, B. R., Jones, T. J., Ratnam, S., Kolb, R. J., et al. (2009). Ciliary Polycystin-2 Is a Mechanosensitive Calcium Channel Involved in Nitric Oxide Signaling Cascades. *Circ. Res.* 104, 860–869. doi: 10.1161/circresaha.108.192765

Alders, M., Al-Gazali, L., Cordeiro, I., Dallapiccola, B., Garavelli, L., Tuysuz, B., et al. (2014). Hennekam syndrome can be caused by FAT4 mutations and be allelic to Van Maldergem syndrome. *Hum. Genet.* 133, 1161–1167. doi: 10.1007/s00439-014-1456-y

Ando, T., Jordan, P., Joh, T., Wang, Y., Jennings, M. H., Houghton, J., et al. (2005). Isolation and Characterization of A Novel Mouse Lymphatic Endothelial Cell Line: SV-LEC. *Lymphat. Res. Biol.* 3, 105–115. doi: 10.1089/lrb.2005.3.105

Bailey, J. M., Mohr, A. M., and Hollingsworth, M. A. (2009). Sonic hedgehog paracrine signaling regulates metastasis and lymphangiogenesis in pancreatic cancer. *Oncogene* 28, 3513–3525. doi: 10.1038/onc.2009.220

Baker, K., and Beales, P. L. (2009). Making sense of cilia in disease: The human ciliopathies. *Am. J. Medical Genet. Part C Semin. Med. Genet.* 151C, 281–295. doi: 10.1002/ajmg.c.30231

Baluk, P., Tammela, T., Ator, E., Lyubynska, N., Achen, M. G., Hicklin, D. J., et al. (2005). Pathogenesis of persistent lymphatic vessel hyperplasia in chronic airway inflammation. *J. Clin. Invest.* 115, 247–257. doi: 10.1172/jci22037

Bazigou, E., Xie, S., Chen, C., Weston, A., Miura, N., Sorokin, L., et al. (2009). Integrin-alpha9 is required for fibronectin matrix assembly during lymphatic valve morphogenesis. *Dev. Cell* 17, 175–186. doi: 10.1016/j.devcel.2009.06.017

Behringer, E. J., Scallan, J. P., Jafarnejad, M., Castorena-Gonzalez, J. A., Zawieja, S. D., Moore, J. E., et al. (2017). Calcium and electrical dynamics in lymphatic endothelium. *J. Physiol.* 595, 7347–7368. doi: 10.1113/jp274842

Bertozzi, C. C., Schmaier, A. A., Mericko, P., Hess, P. R., Zou, Z., Chen, M., et al. (2010). Platelets regulate lymphatic vascular development through CLEC-2–SLP-76 signaling. *Blood* 116, 661–670. doi: 10.1182/blood-2010-02-270876

Betterman, K. L., Sutton, D. L., Secker, G. A., Kazenwadel, J., Oszmiana, A., Lim, L., et al. (2020). Atypical cadherin Fat4 orchestrates lymphatic endothelial cell polarity in response to flow. *J. Clin. Invest.* 130, 3315–3328. doi: 10.1172/jci99027

Bianchi, R., Russo, E., Bachmann, S. B., Proulx, S. T., Sesartic, M., Smaadahl, N., et al. (2018). Postnatal Deletion of Podoplanin in Lymphatic Endothelium Results in Blood Filling of the Lymphatic System and Impairs Dendritic Cell Migration to Lymph Nodes. *Arterioscler. Thromb. Vasc. Biol.* 37, 108–117. doi: 10.1161/atvbaha.116.308020

Birtel, J., Gliem, M., Mangold, E., Tebbe, L., Spier, I., Müller, P. L., et al. (2017). Novel Insights Into the Phenotypical Spectrum of KIF11-Associated Retinopathy, Including a New Form of Retinal CiliopathyNovel Insights in KIF11-Related Retinopathy. *Invest. Ophth. Vis. Sci.* 58, 3950–3959. doi: 10.1167/iovs.17-21679

Björndahl, M., Cao, R., Nissen, L. J., Clasper, S., Johnson, L. A., Xue, Y., et al. (2005). Insulin-like growth factors 1 and 2 induce lymphangiogenesis in vivo. *Proc. Natl. Acad. Sci. U S A.* 102, 15593–15598. doi: 10.1073/pnas.0507865102

Cao, R., Björndahl, M. A., Gallego, M. I., Chen, S., Religa, P., Hansen, A. J., et al. (2006). Hepatocyte growth factor is a lymphangiogenic factor with an indirect mechanism of action. *Blood* 107, 3531–3536. doi: 10.1182/blood-2005-06-2538

Cao, R., Björndahl, M. A., Religa, P., Clasper, S., Garvin, S., Galter, D., et al. (2004). PDGF-BB induces intratumoral lymphangiogenesis and promotes lymphatic metastasis. *Cancer Cell* 6, 333–345. doi: 10.1016/j.ccr.2004.08.034

Cao, R., Ji, H., Feng, N., Zhang, Y., Yang, X., Andersson, P., et al. (2012). Collaborative interplay between FGF-2 and VEGF-C promotes lymphangiogenesis and metastasis. *Proc. Natl. Acad. Sci. U S A.* 109, 15894–15899. doi: 10.1073/pnas.1208324109

Cha, B., Geng, X., Mahamud, R., Fu, J., Mukherjee, A., Kim, Y., et al. (2016). Mechanotransduction activates canonical Wnt/β-catenin signaling to promote lymphatic vascular patterning and the development of lymphatic and lymphovenous valves. *Genes Dev.* 30, 1454–1469. doi: 10.1101/gad.282400.116

Chen, X., Gays, D., Milia, C., and Santoro, M. M. (2017). Cilia Control Vascular Mural Cell Recruitment in Vertebrates. *Cell Rep.* 18, 1033–1047. doi: 10.1016/j.celrep.2016.12.044

Choi, D., Park, E., Jung, E., Cha, B., Lee, S., Yu, J., et al. (2019). Piezo1 incorporates mechanical force signals to genetic program that governs lymphatic valve development and maintenance. *JCI Insight* 4:125068. doi: 10.1172/jci.insight.125068

Clement, C. A., Ajbro, K. D., Koefoed, K., Vestergaard, M. L., Veland, I. R., Henriques, et al. (2013). TGF-β Signaling Is Associated with Endocytosis at the Pocket Region of the Primary Cilium. *Cell Rep.* 3, 1806–1814. doi: 10.1016/j.celrep.2013.05.020

Clement, C. A., Kristensen, S. G., Møllgård, K., Pazour, G. J., Yoder, B. K., Larsen, L. A., et al. (2009). The primary cilium coordinates early cardiogenesis and hedgehog signaling in cardiomyocyte differentiation. *J. Cell Sci.* 122, 3070–3082. doi: 10.1242/jcs.049676

Connor, A. L., Kelley, P. M., and Tempero, R. M. (2016). Lymphatic endothelial lineage assemblage during corneal lymphangiogenesis. *Lab. Invest.* 96, 270–282. doi: 10.1038/labinvest.2015.147

Coxam, B., Sabine, A., Bower, N. I., Smith, K. A., Pichol-Thievend, C., Skoczylas, R., et al. (2014). Pkd1 Regulates Lymphatic Vascular Morphogenesis during Development. *Cell Rep.* 7, 623–633. doi: 10.1016/j.celrep.2014.03.063

Cursiefen, C., Maruyama, K., Jackson, D. G., Streilein, J. W., and Kruse, F. E. (2006). Time Course of Angiogenesis and Lymphangiogenesis After Brief Corneal Inflammation. *Cornea* 25, 443–447. doi: 10.1097/01.ico.0000183485.85636.ff

Dellinger, M., Hunter, R., Bernas, M., Gale, N., Yancopoulos, G., Erickson, R., et al. (2008). Defective remodeling and maturation of the lymphatic vasculature in Angiopoietin-2 deficient mice. *Dev. Biol.* 319, 309–320. doi: 10.1016/j.ydbio.2008.04.024

Dieterich, L. C., Ducoli, L., Shin, J. W., and Detmar, M. (2017). Distinct transcriptional responses of lymphatic endothelial cells to VEGFR-3 and VEGFR-2 stimulation. *Sci. Data* 4:170106. doi: 10.1038/sdata.2017.106

Eisa-Beygi, S., Benslimane, F. M., El-Rass, S., Prabhudesai, S., Abdelrasoul, M. K. A., Simpson, P. M., et al. (2018). Characterization of Endothelial Cilia Distribution During Cerebral-Vascular Development in Zebrafish (Danio rerio). *Arterioscler. Thromb. Vasc. Biol.* 38, 2806–2818. doi: 10.1161/atvbaha.118.311231

Ezratty, E. J., Stokes, N., Chai, S., Shah, A. S., Williams, S. E., and Fuchs, E. (2011). A role for the primary cilium in Notch signaling and epidermal differentiation during skin development. *Cell* 145, 1129–1141. doi: 10.1016/j.cell.2011.05.030

Fatima, A., Culver, A., Culver, F., Liu, T., Dietz, W. H., Thomson, B. R., et al. (2014). Murine Notch1 is required for lymphatic vascular morphogenesis during development: Role of Notch1 In Lymphatic Vessel Development. *Dev. Dynam.* 243, 957–964. doi: 10.1002/dvdy.24129

Finetti, F., Cassioli, C., Cianfanelli, V., Onnis, A., Paccagnini, E., Kabanova, A., et al. (2020). The intraflagellar transport protein IFT20 controls lysosome biogenesis by regulating the post-Golgi transport of acid hydrolases. *Cell Death Differ.* 27, 310–328. doi: 10.1038/s41418-019-0357-y

Finetti, F., Paccani, S. R., Riparbelli, M. G., Giacomello, E., Perinetti, G., Pazour, G. J., et al. (2009). Intraflagellar transport is required for polarized recycling of the TCR/CD3 complex to the immune synapse. *Nat. Cell Biol.* 11:ncb1977. doi: 10.1038/ncb1977

Fink, D. M., Connor, A. L., Kelley, P. M., Steele, M. M., Hollingsworth, M. A., and Tempero, R. M. (2014). Nerve Growth Factor Regulates Neurolymphatic Remodeling during Corneal Inflammation and Resolution. *PLoS One* 9:e112737. doi: 10.1371/journal.pone.0112737

Follit, J. A., Agustin, J. T. S., Xu, F., Jonassen, J. A., Samtani, R., Lo, C. W., et al. (2008). The Golgin GMAP210/TRIP11 anchors IFT20 to the Golgi complex. *PLoS Genet.* 4:e1000315. doi: 10.1371/journal.pgen.1000315

Follit, J. A., Tuft, R. A., Fogarty, K. E., and Pazour, G. J. (2006). The Intraflagellar Transport Protein IFT20 Is Associated with the Golgi Complex and Is Required for Cilia Assembly. *Mol. Biol. Cell* 17, 3781–3792. doi: 10.1091/mbc.e06-02-0133

François, M., Caprini, A., Hosking, B., Orsenigo, F., Wilhelm, D., Browne, C., et al. (2008). Sox18 induces development of the lymphatic vasculature in mice. *Nature* 456, 643–647. doi: 10.1038/nature07391

Frye, M., Taddei, A., Dierkes, C., Martinez-Corral, I., Fielden, M., Ortsäter, H., et al. (2018). Matrix stiffness controls lymphatic vessel formation through regulation of a GATA2-dependent transcriptional program. *Nat. Commun.* 9:1511. doi: 10.1038/s41467-018-03959-6

Gale, N. W., Thurston, G., Hackett, S. F., Renard, R., Wang, Q., McClain, J., et al. (2002). Angiopoietin-2 Is Required for Postnatal Angiogenesis and Lymphatic Patterning, and Only the Latter Role Is Rescued by Angiopoietin-1. *Dev. Cell* 3, 411–423. doi: 10.1016/s1534-5807(02)00217-4

Geng, X., Cha, B., Mahamud, R., Lim, K.-C., Silasi-Mansat, R., Uddin, M. K. M., et al. (2016). Multiple mouse models of primary lymphedema exhibit distinct defects in lymphovenous valve development. *Dev. Biol.* 409, 218–233. doi: 10.1016/j.ydbio.2015.10.022

Geng, X., Yanagida, K., Akwii, R. G., Choi, D., Chen, L., Ho, Y., et al. (2020). S1PR1 regulates the quiescence of lymphatic vessels by inhibiting laminar shear stress-dependent VEGF-C signaling. *JCI Insight* 5:137652. doi: 10.1172/jci.insight.137652

Goetz, J. G., Steed, E., Ferreira, R. R., Roth, S., Ramspacher, C., Boselli, F., et al. (2014). Endothelial Cilia Mediate Low Flow Sensing during Zebrafish Vascular Development. *Cell Rep.* 6, 799–808. doi: 10.1016/j.celrep.2014.01.032

Gordon, E., Schimmel, L., and Frye, M. (2020). The Importance of Mechanical Forces for in vitro Endothelial Cell Biology. *Front. Physiol.* 11:684. doi: 10.3389/fphys.2020.00684

Grisanti, L., Revenkova, E., Gordon, R. E., and Iomini, C. (2016). Primary cilia maintain corneal epithelial homeostasis by regulation of the Notch signaling pathway. *Development* 143, 2160–2171. doi: 10.1242/dev.132704

Hägerling, R., Hoppe, E., Dierkes, C., Stehling, M., Makinen, T., Butz, S., et al. (2018). Distinct roles of VE−cadherin for development and maintenance of specific lymph vessel beds. *EMBO J.* 37:201798271. doi: 10.15252/embj.201798271

Hägerling, R., Pollmann, C., Andreas, M., Schmidt, C., Nurmi, H., Adams, R. H., et al. (2013). A novel multistep mechanism for initial lymphangiogenesis in mouse embryos based on ultramicroscopy. *EMBO J.* 32, 629–644. doi: 10.1038/emboj.2012.340

Haiko, P., Makinen, T., Keskitalo, S., Taipale, J., Karkkainen, M. J., Baldwin, M. E., et al. (2008). Deletion of Vascular Endothelial Growth Factor C (VEGF-C) and VEGF-D Is Not Equivalent to VEGF Receptor 3 Deletion in Mouse Embryos. *Mol. Cell Biol.* 28, 4843–4850. doi: 10.1128/mcb.02214-07

Hayashi, S., and McMahon, A. P. (2001). Efficient Recombination in Diverse Tissues by a Tamoxifen-Inducible Form of Cre: A Tool for Temporally Regulated Gene Activation/Inactivation in the Mouse. *Dev. Biol.* 244, 305–318. doi: 10.1006/dbio.2002.0597

Hess, P. R., Rawnsley, D. R., Jakus, Z., Yang, Y., Sweet, D. T., Fu, J., et al. (2013). Platelets mediate lymphovenous hemostasis to maintain blood-lymphatic separation throughout life. *J. Clin. Invest.* 124, 273–284. doi: 10.1172/jci70422

Huang, J. L., Woolf, A. S., Kolatsi-Joannou, M., Baluk, P., Sandford, R. N., Peters, D. J. M., et al. (2015). Vascular Endothelial Growth Factor C for Polycystic Kidney Diseases. *J. Am. Soc. Nephrol.* 27, 69–77. doi: 10.1681/asn.2014090856

Huangfu, D., and Anderson, K. V. (2005). Cilia and Hedgehog responsiveness in the mouse. *Proc. Natl. Acad. Sci. U S A.* 102, 11325–11330. doi: 10.1073/pnas.0505328102

Huangfu, D., Liu, A., Rakeman, A. S., Murcia, N. S., Niswander, L., and Anderson, K. V. (2003). Hedgehog signalling in the mouse requires intraflagellar transport proteins. *Nature* 426, 83–87. doi: 10.1038/nature02061

Ivanov, K. I., Agalarov, Y., Valmu, L., Samuilova, O., Liebl, J., Houhou, N., et al. (2013). Phosphorylation Regulates FOXC2-Mediated Transcription in Lymphatic Endothelial Cells. *Mol. Cell Biol.* 33, 3749–3761. doi: 10.1128/mcb.01387-12

James, J. M., Nalbandian, A., and Mukouyama, Y. (2013). TGFβ signaling is required for sprouting lymphangiogenesis during lymphatic network development in the skin. *Development* 140, 3903–3914. doi: 10.1242/dev.095026

Ji, H., Cao, R., Yang, Y., Zhang, Y., Iwamoto, H., Lim, S., et al. (2014). TNFR1 mediates TNF-α-induced tumour lymphangiogenesis and metastasis by modulating VEGF-C-VEGFR3 signalling. *Nat. Commun.* 5:4944. doi: 10.1038/ncomms5944

Johnson, N. C., Dillard, M. E., Baluk, P., McDonald, D. M., Harvey, N. L., Frase, S. L., et al. (2008). Lymphatic endothelial cell identity is reversible and its maintenance requires Prox1 activity. *Gene Dev.* 22, 3282–3291. doi: 10.1101/gad.1727208

Jonassen, J. A., Agustin, J. S., Follit, J. A., and Pazour, G. J. (2008). Deletion of IFT20 in the mouse kidney causes misorientation of the mitotic spindle and cystic kidney disease. *J. Cell Biol.* 183, 377–384. doi: 10.1083/jcb.200808137

Kallakuri, S., Yu, J. A., Li, J., Li, Y., Weinstein, B. M., Nicoli, S., et al. (2015). Endothelial Cilia Are Essential for Developmental Vascular Integrity in Zebrafish. *J. Am. Soc. Nephrol.* 26, 864–875. doi: 10.1681/asn.2013121314

Karkkainen, M. J., Haiko, P., Sainio, K., Partanen, J., Taipale, J., Petrova, T. V., et al. (2004). Vascular endothelial growth factor C is required for sprouting of the first lymphatic vessels from embryonic veins. *Nat. Immunol.* 5, 74–80. doi: 10.1038/ni1013

Kataru, R. P., Jung, K., Jang, C., Yang, H., Schwendener, R. A., Baik, J. E., et al. (2009). Critical role of CD11b+ macrophages and VEGF in inflammatory lymphangiogenesis, antigen clearance, and inflammation resolution. *Blood* 113, 5650–5659. doi: 10.1182/blood-2008-09-176776

Kelley, P. M., Connor, A. L., and Tempero, R. M. (2013). Lymphatic Vessel Memory Stimulated by Recurrent Inflammation. *Am. J. Pathol.* 182, 2418–2428. doi: 10.1016/j.ajpath.2013.02.025

Kelley, P. M., Steele, M. M., and Tempero, R. M. (2011). Regressed lymphatic vessels develop during corneal repair. *Lab. Invest.* 91, 1643–1651. doi: 10.1038/labinvest.2011.121

Koltowska, K., Betterman, K. L., Harvey, N. L., and Hogan, B. M. (2013). Getting out and about: the emergence and morphogenesis of the vertebrate lymphatic vasculature. *Development* 140, 1857–1870. doi: 10.1242/dev.089565

Lee, K. L., Guevarra, M. D., Nguyen, A. M., Chua, M. C., Wang, Y., and Jacobs, C. R. (2015). The primary cilium functions as a mechanical and calcium signaling nexus. *Cilia* 4:7. doi: 10.1186/s13630-015-0016-y

Liu, M., Zhao, J., Zhou, Q., Peng, Y., Zhou, Y., and Jiang, Y. (2018). Primary Cilia Deficiency Induces Intracranial Aneurysm. *Shock* 49, 604–611. doi: 10.1097/shk.0000000000000961

Loo, C. P., Nelson, N. A., Lane, R. S., Booth, J. L., Hardin, S. C. L., Thomas, A., et al. (2017). Lymphatic Vessels Balance Viral Dissemination and Immune Activation following Cutaneous Viral Infection. *Cell Rep.* 20, 3176–3187. doi: 10.1016/j.celrep.2017.09.006

Lutter, S., Xie, S., Tatin, F., and Makinen, T. (2012). Smooth muscle–endothelial cell communication activates Reelin signaling and regulates lymphatic vessel formation. *J. Cell Biol.* 197, 837–849. doi: 10.1083/jcb.201110132

Marino, D., Angehrn, Y., Klein, S., Riccardi, S., Baenziger-Tobler, N., Otto, V. I., et al. (2013). Activation of the epidermal growth factor receptor promotes lymphangiogenesis in the skin. *J. Dermatol. Sci.* 71, 184–194. doi: 10.1016/j.jdermsci.2013.04.024

Maruyama, K., Ii, M., Cursiefen, C., Jackson, D. G., Keino, H., Tomita, M., et al. (2005). Inflammation-induced lymphangiogenesis in the cornea arises from CD11b-positive macrophages. *J. Clin. Invest.* 115, 2363–2372. doi: 10.1172/jci23874

McDermott, K. M., Liu, B. Y., Tlsty, T. D., and Pazour, G. J. (2010). Primary cilia regulate branching morphogenesis during mammary gland development. *Curr. Biol. CB* 20, 731–737. doi: 10.1016/j.cub.2010.02.048

Miyazaki, A., Sugimoto, A., Yoshizaki, K., Kawarabayashi, K., Iwata, K., Kurogoushi, R., et al. (2019). Coordination of WNT signaling and ciliogenesis during odontogenesis by piezo type mechanosensitive ion channel component 1. *Sci. Rep.* 9:14762. doi: 10.1038/s41598-019-51381-9

Morisada, T., Oike, Y., Yamada, Y., Urano, T., Akao, M., Kubota, Y., et al. (2005). Angiopoietin-1 promotes LYVE-1-positive lymphatic vessel formation. *Blood* 105, 4649–4656. doi: 10.1182/blood-2004-08-3382

Murtomaki, A., Uh, M. K., Choi, Y. K., Kitajewski, C., Borisenko, V., Kitajewski, J., et al. (2013). Notch1 functions as a negative regulator of lymphatic endothelial cell differentiation in the venous endothelium. *Development* 140, 2365–2376. doi: 10.1242/dev.083865

Nauli, S. M., Kawanabe, Y., Kaminski, J. J., Pearce, W. J., Ingber, D. E., and Zhou, J. (2008). Endothelial cilia are fluid shear sensors that regulate calcium signaling and nitric oxide production through polycystin-1. *Circulation* 117, 1161–1171. doi: 10.1161/circulationaha.107.710111

Noda, K., Kitami, M., Kitami, K., Kaku, M., and Komatsu, Y. (2016). Canonical and noncanonical intraflagellar transport regulates craniofacial skeletal development. *Proc. Natl. Acad. Sci. U S A.* 113, E2589–E2597. doi: 10.1073/pnas.1519458113

Norden, P. R., Sabine, A., Wang, Y., Demir, C. S., Liu, T., Petrova, T. V., et al. (2020). Shear stimulation of FOXC1 and FOXC2 differentially regulates cytoskeletal activity during lymphatic valve maturation. *Elife* 9:e53814. doi: 10.7554/elife.53814

Norris, D. P., and Grimes, D. T. (2012). Mouse models of ciliopathies: the state of the art. *Dis. Model. Mech.* 5, 299–312. doi: 10.1242/dmm.009340

Oliver, G., Kipnis, J., Randolph, G. J., and Harvey, N. L. (2020). The Lymphatic Vasculature in the 21st Century: Novel Functional Roles in Homeostasis and Disease. *Cell* 182, 270–296. doi: 10.1016/j.cell.2020.06.039

Ostergaard, P., Simpson, M. A., Mendola, A., Vasudevan, P., Connell, F. C., van Impel, A., et al. (2012). Mutations in KIF11 Cause Autosomal-Dominant Microcephaly Variably Associated with Congenital Lymphedema and Chorioretinopathy. *Am. J. Hum. Genet.* 90, 356–362. doi: 10.1016/j.ajhg.2011.12.018

Outeda, P., Huso, D. L., Fisher, S. A., Halushka, M. K., Kim, H., Qian, F., et al. (2014). Polycystin Signaling Is Required for Directed Endothelial Cell Migration and Lymphatic Development. *Cell Rep.* 7, 634–644. doi: 10.1016/j.celrep.2014.03.064

Pala, R., Jamal, M., Alshammari, Q., and Nauli, S. M. (2018). The Roles of Primary Cilia in Cardiovascular Diseases. *Cells* 7:233. doi: 10.3390/cells7120233

Pazour, G. J., Agustin, J. T. S., Follit, J. A., Rosenbaum, J. L., and Witman, G. B. (2002). Polycystin-2 localizes to kidney cilia and the ciliary level is elevated in orpk mice with polycystic kidney disease. *Curr. Biol.* 12, R378–R380. doi: 10.1016/s0960-9822(02)00877-1

Pazour, G. J., Dickert, B. L., Vucica, Y., Seeley, E. S., Rosenbaum, J. L., Witman, G. B., et al. (2000). Chlamydomonas IFT88 and Its Mouse Homologue, Polycystic Kidney Disease Gene Tg737, Are Required for Assembly of Cilia and Flagella. *J. Cell Biol.* 151, 709–718. doi: 10.1083/jcb.151.3.709

Petrova, T. V., Karpanen, T., Norrmén, C., Mellor, R., Tamakoshi, T., Finegold, D., et al. (2004). Defective valves and abnormal mural cell recruitment underlie lymphatic vascular failure in lymphedema distichiasis. *Nat. Med.* 10, 974–981. doi: 10.1038/nm1094

Petrova, T. V., Mäkinen, T., Mäkelä, T. P., Saarela, J., Virtanen, I., Ferrell, R. E., et al. (2002). Lymphatic endothelial reprogramming of vascular endothelial cells by the Prox-1 homeobox transcription factor. *EMBO J.* 21, 4593–4599. doi: 10.1093/emboj/cdf470

Pflicke, H., and Sixt, M. (2009). Preformed portals facilitate dendritic cell entry into afferent lymphatic vessels. *J. Exp. Medicine* 206, 2925–2935. doi: 10.1084/jem.20091739

Praetorius, H. A., and Spring, K. R. (2001). Bending the MDCK Cell Primary Cilium Increases Intracellular Calcium. *J. Membr. Biol.* 184, 71–79. doi: 10.1007/s00232-001-0075-4

Sabine, A., Agalarov, Y., Maby-El Hajjami, H., Jaquet, M., Hägerling, R., Pollmann, C., et al. (2012). Mechanotransduction, PROX1, and FOXC2 Cooperate to Control Connexin37 and Calcineurin during Lymphatic-Valve Formation. *Dev. Cell* 22, 430–445. doi: 10.1016/j.devcel.2011.12.020

Sabine, A., Bovay, E., Demir, C. S., Kimura, W., Jaquet, M., Agalarov, Y., et al. (2015). FOXC2 and fluid shear stress stabilize postnatal lymphatic vasculature. *J. Clin. Invest.* 125, 3861–3877. doi: 10.1172/jci80454

Saburi, S., Hester, I., Fischer, E., Pontoglio, M., Eremina, V., Gessler, M., et al. (2008). Loss of Fat4 disrupts PCP signaling and oriented cell division and leads to cystic kidney disease. *Nat. Genet.* 40, 1010–1015. doi: 10.1038/ng.179

Scallan, J. P., Zawieja, S. D., Castorena-Gonzalez, J. A., and Davis, M. J. (2016). Lymphatic pumping: mechanics, mechanisms and malfunction. *J. Physiol.* 594, 5749–5768. doi: 10.1113/jp272088

Schmid, F. M., Schou, K. B., Vilhelm, M. J., Holm, M. S., Breslin, L., Farinelli, P., et al. (2018). IFT20 modulates ciliary PDGFRα signaling by regulating the stability of Cbl E3 ubiquitin ligasesIFT20 controls Cbl-mediated inhibition of PDGFRα. *J. Cell Biol.* 217, 151–161. doi: 10.1083/jcb.201611050

Schneider, L., Clement, C. A., Teilmann, S. C., Pazour, G. J., Hoffmann, E. K., Satir, P., et al. (2005). PDGFRαα Signaling Is Regulated through the Primary Cilium in Fibroblasts. *Curr. Biol.* 15, 1861–1866. doi: 10.1016/j.cub.2005.09.012

Schwager, S., and Detmar, M. (2019). Inflammation and Lymphatic Function. *Front. Immunol.* 10:308. doi: 10.3389/fimmu.2019.00308

Skobe, M., Hawighorst, T., Jackson, D. G., Prevo, R., Janes, L., Velasco, P., et al. (2001). Induction of tumor lymphangiogenesis by VEGF-C promotes breast cancer metastasis. *Nat. Med.* 7, 192–198. doi: 10.1038/84643

Solari, E., Marcozzi, C., Bistoletti, M., Baj, A., Giaroni, C., Negrini, D., et al. (2020). TRPV4 channels' dominant role in the temperature modulation of intrinsic contractility and lymph flow of rat diaphragmatic lymphatics. *Am. J. Physiol. Heart C* 319, H507–H518. doi: 10.1152/ajpheart.00175.2020

Srinivasan, R. S., and Oliver, G. (2011). Prox1 dosage controls the number of lymphatic endothelial cell progenitors and the formation of the lymphovenous valves. *Gene Dev.* 25, 2187–2197. doi: 10.1101/gad.16974811

Srinivasan, R. S., Geng, X., Yang, Y., Wang, Y., Mukatira, S., Studer, M., et al. (2010). The nuclear hormone receptor Coup-TFII is required for the initiation and early maintenance of Prox1 expression in lymphatic endothelial cells. *Genes Dev.* 24, 696–707. doi: 10.1101/gad.1859310

Stanczuk, L., Martinez-Corral, I., Ulvmar, M. H., Zhang, Y., Laviña, B., Fruttiger, M., et al. (2015). cKit Lineage Hemogenic Endothelium-Derived Cells Contribute to Mesenteric Lymphatic Vessels. *Cell Rep.* 10, 1708–1721. doi: 10.1016/j.celrep.2015.02.026

Stratman, A. N., Burns, M. C., Farrelly, O. M., Davis, A. E., Li, W., Pham, V. N., et al. (2020). Chemokine mediated signalling within arteries promotes vascular

smooth muscle cell recruitment. *Commun. Biol.* 3:734. doi: 10.1038/s42003-020-01462-7

Sweet, D. T., Jiménez, J. M., Chang, J., Hess, P. R., Mericko-Ishizuka, P., Fu, J., et al. (2015). Lymph flow regulates collecting lymphatic vessel maturation in vivo. *J. Clin. Invest.* 125, 2995–3007. doi: 10.1172/jci79386

Tal, O., Lim, H. Y., Gurevich, I., Milo, I., Shipony, Z., Ng, L. G., et al. (2011). DC mobilization from the skin requires docking to immobilized CCL21 on lymphatic endothelium and intralymphatic crawling. *J. Exp. Medicine* 208, 2141–2153. doi: 10.1084/jem.20102392

Tammela, T., Saaristo, A., Lohela, M., Morisada, T., Tornberg, J., Norrmeìn, C., et al. (2005). Angiopoietin-1 promotes lymphatic sprouting and hyperplasia. *Blood* 105, 4642–4648. doi: 10.1182/blood-2004-08-3327

Uhrin, P., Zaujec, J., Breuss, J. M., Olcaydu, D., Chrenek, P., Stockinger, H., et al. (2010). Novel function for blood platelets and podoplanin in developmental separation of blood and lymphatic circulation. *Blood* 115, 3997–4005. doi: 10.1182/blood-2009-04-216069

Vion, A.-C., Alt, S., Klaus-Bergmann, A., Szymborska, A., Zheng, T., Perovic, T., et al. (2018). Primary cilia sensitize endothelial cells to BMP and prevent excessive vascular regressionPrimary cilium and vascular regression. *J. Cell Biol.* 217, 1651–1665. doi: 10.1083/jcb.201706151

Wigle, J. T., and Oliver, G. (1999). Prox1 Function Is Required for the Development of the Murine Lymphatic System. *Cell* 98, 769–778. doi: 10.1016/s0092-8674(00)81511-1

Xu, Y., Yuan, L., Mak, J., Pardanaud, L., Caunt, M., Kasman, I., et al. (2010). Neuropilin-2 mediates VEGF-C–induced lymphatic sprouting together with VEGFR3Nrp-2 mediates lymphatic sprouting. *J. Cell Biol.* 188, 115–130. doi: 10.1083/jcb.200903137

Zalenski, A. A., Majumder, S., De, K., and Venere, M. (2020). An interphase pool of KIF11 localizes at the basal bodies of primary cilia and a reduction in KIF11 expression alters cilia dynamics. *Sci. Rep.* 10:13946. doi: 10.1038/s41598-020-70787-4

Conflict of Interest: The authors declare that the research was conducted in the absence of any commercial or financial relationships that could be construed as a potential conflict of interest.

Copyright © 2021 Paulson, Harms, Ward, Latterell, Pazour and Fink. This is an open-access article distributed under the terms of the Creative Commons Attribution License (CC BY). The use, distribution or reproduction in other forums is permitted, provided the original author(s) and the copyright owner(s) are credited and that the original publication in this journal is cited, in accordance with accepted academic practice. No use, distribution or reproduction is permitted which does not comply with these terms.

frontiers in Cell and Developmental Biology

ORIGINAL RESEARCH
published: 19 May 2021
doi: 10.3389/fcell.2021.689469

Single-Cell Transcriptomics Reveals Endothelial Plasticity During Diabetic Atherogenesis

Guizhen Zhao[1], Haocheng Lu[1], Yuhao Liu[1,2], Yang Zhao[1], Tianqing Zhu[1], Minerva T. Garcia-Barrio[1], Y. Eugene Chen[1] and Jifeng Zhang[1]**

[1] Frankel Cardiovascular Center, Department of Internal Medicine, University of Michigan Medical Center, Ann Arbor, MI, United States, [2] Department of Internal Medicine, The Second Xiangya Hospital, Central South University, Changsha, China

Atherosclerosis is the leading cause of cardiovascular diseases, which is also the primary cause of mortality among diabetic patients. Endothelial cell (EC) dysfunction is a critical early step in the development of atherosclerosis and aggravated in the presence of concurrent diabetes. Although the heterogeneity of the organ-specific ECs has been systematically analyzed at the single-cell level in healthy conditions, their transcriptomic changes in diabetic atherosclerosis remain largely unexplored. Here, we carried out a single-cell RNA sequencing (scRNA-seq) study using EC-enriched single cells from mouse heart and aorta after 12 weeks feeding of a standard chow or a diabetogenic high-fat diet with cholesterol. We identified eight EC clusters, three of which expressed mesenchymal markers, indicative of an endothelial-to-mesenchymal transition (EndMT). Analyses of the marker genes, pathways, and biological functions revealed that ECs are highly heterogeneous and plastic both in normal and atherosclerotic conditions. The metabolic transcriptomic analysis further confirmed that EndMT-derived fibroblast-like cells are prominent in atherosclerosis, with diminished fatty acid oxidation and enhanced biological functions, including regulation of extracellular-matrix organization and apoptosis. In summary, our data characterized the phenotypic and metabolic heterogeneity of ECs in diabetes-associated atherogenesis at the single-cell level and paves the way for a deeper understanding of endothelial cell biology and EC-related cardiovascular diseases.

Keywords: single-cell RNA-sequencing, endothelial cell, transcriptomic heterogeneity, diabetes, atherosclerosis

OPEN ACCESS

Edited by:
Xiaofeng Yang,
Temple University, United States

Reviewed by:
Ying Shao,
Temple University, United States
Owais Bhat,
Virginia Commonwealth University, United States

****Correspondence:***
Jifeng Zhang
jifengz@umich.edu
Y. Eugene Chen
echenum@umich.edu

Specialty section:
This article was submitted to Signaling, a section of the journal Frontiers in Cell and Developmental Biology

Received: *31 March 2021*
Accepted: *20 April 2021*
Published: *19 May 2021*

Citation:
Zhao G, Lu H, Liu Y, Zhao Y, Zhu T, Garcia-Barrio MT, Chen YE and Zhang J (2021) Single-Cell Transcriptomics Reveals Endothelial Plasticity During Diabetic Atherogenesis. Front. Cell Dev. Biol. 9:689469. doi: 10.3389/fcell.2021.689469

INTRODUCTION

Atherosclerosis is the primary pathological basis of myocardial infarction, ischemic stroke, and peripheral vascular diseases, which represent a leading cause of death worldwide (Lusis, 2000; Herrington et al., 2016). Atherosclerosis accounts for virtually 80% of all deaths among diabetic patients (Aronson and Rayfield, 2002). Prolonged exposure to hyperglycemia is recognized as a major factor in the pathogenesis of atherosclerosis associated with diabetes. Hyperglycemia induces a large number of alterations in the vascular tissue at the cellular level that potentially accelerate the atherosclerotic process (Aronson and Rayfield, 2002; Calkin and Allen, 2006; Funk et al., 2012). Growing evidence indicates that endothelial cell (EC) dysfunction is a critical early event in the diabetes-associated development of atherosclerosis (Hansson, 2005).

Endothelial cells exist in the whole body and play an essential role in tissue homeostasis by assisting vessel formation and function, and building a barrier between blood and tissue cells

(Cines et al., 1998). ECs exhibit considerable structural and functional heterogeneity depending on the tissue in which they reside, which have been demonstrated by recent single-cell RNA sequencing (scRNA-seq) studies (Feng et al., 2019; Kalluri et al., 2019; Kalucka et al., 2020; Paik et al., 2020). In cardiac development, specifically, certain ECs within the endocardium undergo a process named endothelial-mesenchymal transition (EndMT) to give rise to mesenchymal cells, which play a crucial role in endocardial cushion formation (Camenisch et al., 2002; Dejana et al., 2017). In addition, EndMT makes a major contribution to the suboptimal repair of damaged heart tissue after ischemic injury, which has also been shown through scRNA-seq (Tombor et al., 2021). Throughout life, ECs residing in the vessel wall are exposed to various mechanical stresses (Chiu and Chien, 2011; Mahmoud et al., 2017; Demos et al., 2020), inflammatory stimuli (Hajra et al., 2000; Fan et al., 2012), and metabolic alteration (Patella et al., 2015; Kuo et al., 2017; Theodorou and Boon, 2018). The extended exposure gradually leads to endothelial activation and EndMT. Recently, multiple studies extended our understanding of EndMT and demonstrated that it promotes atherosclerosis progression (Souilhol et al., 2018). Using an endothelial-lineage tracing system, EndMT-derived fibroblast-like cells were identified in mouse atherosclerotic plaques (Evrard et al., 2016). In addition to ECs undergoing EndMT to fibroblast-like cells, there may be unidentified subpopulations of ECs within the atherosclerotic lesions that remain to be explored.

The recent advent of scRNA-seq has enabled the transcriptomic analysis of a large number of cells at the single-cell resolution (Liu et al., 2019; Kalucka et al., 2020; Rohlenova et al., 2020), which provides insights into the transcriptional signature in individual cells. Here we performed scRNA-seq using endothelial-enriched single cells obtained from the mouse heart and aorta following feeding of a 12-week diabetogenic diet with cholesterol (DDC) or standard chow (Chow) diet to determine the differential gene transcription during atherosclerosis progression. Integrated analysis of scRNA-seq data revealed that ECs are heterogenous in the cardiovascular system under normal and atherosclerotic conditions. Diet-induced diabetic atherosclerosis dramatically altered EC transcriptomic profiles, including reprograming into mesenchymal cells. In addition, we identified diminished fatty acid oxidation (FAO) in the ECs undergoing mesenchymal transition in atherosclerosis, which underscore metabolic targets that control the development of atherosclerosis.

RESULTS

Single-Cell RNA Sequencing Revealed Eight Endothelial Cell Clusters in the Cardiovascular System

The EC heterogeneity across healthy tissues has been characterized using scRNA-seq technology (Feng et al., 2019; Kalluri et al., 2019; Kalucka et al., 2020; Paik et al., 2020). However, the EC plasticity in pathological conditions remains unexplored. To determine EC heterogeneity in diabetic atherosclerosis, we performed scRNA-seq analysis on the ECs collected from *Ldlr* null ($Ldlr^{-/-}$) mice fed a diabetogenic high-fat diet with cholesterol (DDC) (Subramanian et al., 2008) or a standard Chow for 12 weeks (**Figure 1A**). The mice fed a DDC showed increased body weight, impaired glucose tolerance and insulin sensitivity compared to chow-fed mice (**Supplementary Figures 1A–C**). Additionally, a significant increase in plasma total cholesterol (TC) and triglycerides (TG) were noticed in the DDC-fed mice relative to the chow-fed mice (**Supplementary Figure 1D**). Next, the ECs from the heart and aorta were enzymatically isolated and purified from three mice from each group using a collagenase protocol (Hu et al., 2018). Single cells from the two groups were subsequently bar-coded and sequenced using the 10X Genomics Chromium platform (**Figure 1A**). The median reads per cell were 243,312 for Chow group and 276,821 for DDC group, and transcripts detected per cell were 1551 and 1297, respectively (**Supplementary Table 1**).

scRNA-seq data analysis was performed using Seurat version 4.0. As a quality control, we eliminated the cells that expressed gene counts >3000 or <200, and those expressing >10% mitochondrial unique molecular identifier (UMI) counts to remove doublets and damaged cells during the sample preparation. Subsequently, data integration, and unsupervised graph-based clustering were performed to group the cells according to their gene-expression profile and uniform manifold approximation and projection (UMAP) plot was used for visualization (**Figure 1B**). In total, 12 cell clusters were singled out in the integrated datasets (**Figure 1C**). To define the identity of each cell cluster, we performed differential expression analysis [by average log2(fold change)] between each cluster and all other clusters (**Supplementary Table 2**) and assigned a specific cell type to each cluster based on the established lineage-specific marker genes (**Figures 1D,E**). Next, we selected 8 EC clusters based on the expression of *Cdh5*, *Pecam1*, *Tek,* or *Vwf* (**Figures 1D,E**), and excluded contaminating macrophages (cluster 8) which featured expression of *Cd68*, *Adgre1*, and *Lgals3*; fibroblasts (cluster 5) which showed high expression of the collagens/collagen-binding proteins, *Dcn, Col1a1*, and *Col3a1*; and vascular smooth muscle cells (SMC, cluster 12) which highly expressed the SMC canonical markers, *Myh11*, *Acta2*, and *Tagln* (**Figure 1E**). Of note, the gene expression profile of cluster 11, without the expression of the canonical EC markers, could not support the lineage assignment as ECs, thus these cells were also excluded from further analysis.

Endothelial Cell Subpopulations Show Transcriptomic and Functional Heterogeneity

Eight EC subpopulations were identified (**Figure 2A**) with positive expression of EC marker genes *Cdh5* and *Pecam1* (**Figure 2B**). Next, we sought to determine the proportion of each subpopulation, and perform differential gene expression and gene set enrichment analysis (**Figures 2C**, **3** and **Supplementary Table 3**). Notably, EC_1, EC_2, EC_3, and EC_4 are the major clusters, accounting for 85.8% of the total ECs, while the other four EC clusters (EC_5, EC_6, EC_7, and EC_8) only account

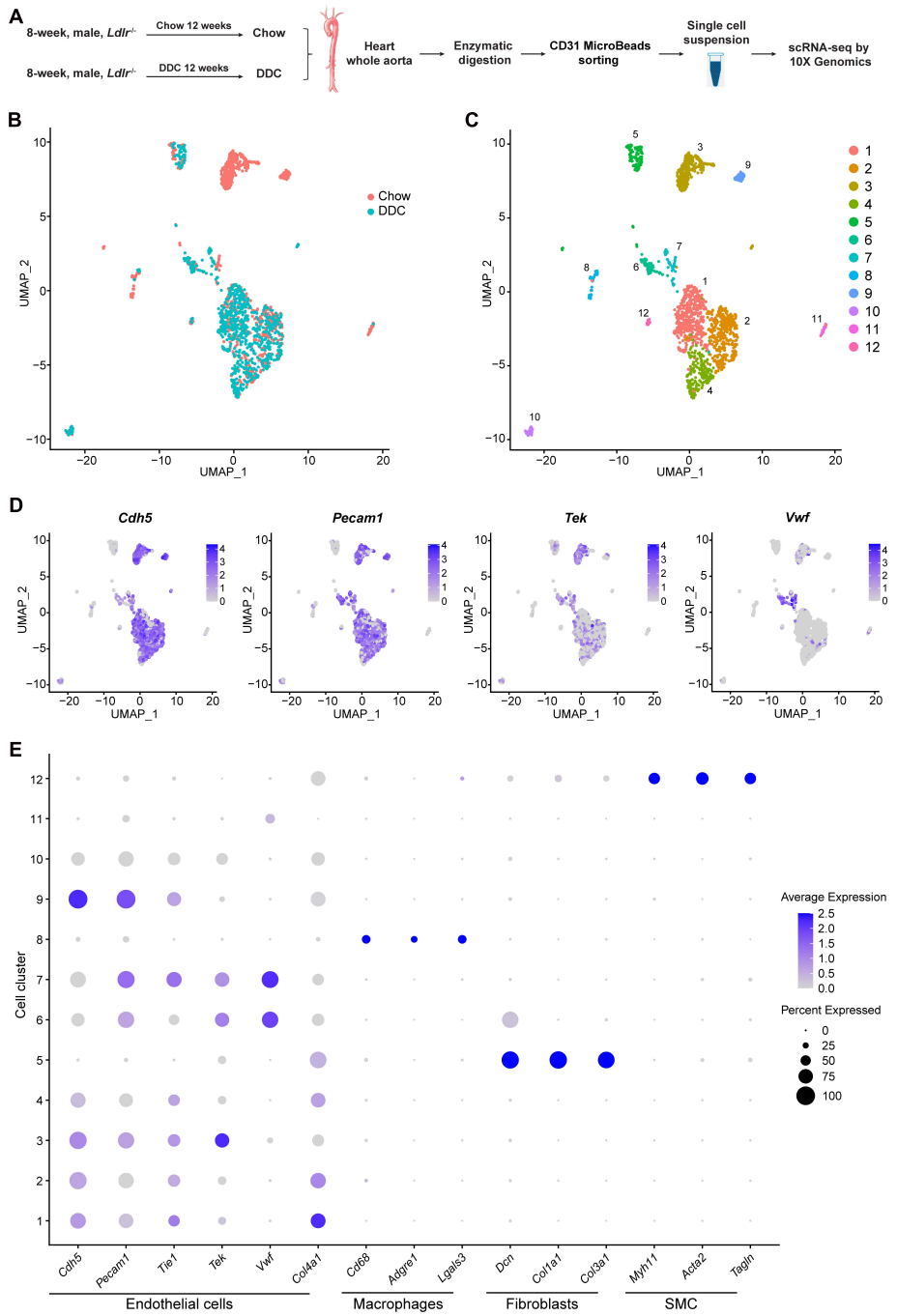

FIGURE 1 | Identification of cell clusters present in the mouse heart and aorta by single-cell RNA sequencing (scRNA-seq). **(A)**, Schematic diagram indicating the procedure for scRNA-seq. Chow, *Ldlr*$^{-/-}$ mice fed a standard chow for 12 weeks. DDC, *Ldlr*$^{-/-}$ mice fed a diabetogenic diet with 0.15% cholesterol for 12 weeks. The cells isolated from each group were pooled from three mice. **(B)**, Uniform Manifold Approximation and Projection (UMAP) plot of aggregate cells from Chow and DDC group. Colors denote different groups. After quality control, 1014 and 770 cells from Chow and DDC were captured for clustering analysis. **(C)**, UMAP plot of aggregated cells from the three groups with colors denoting different cell clusters. **(D)**, Expression of endothelial cell (EC) marker genes (*Cdh5*, *Pecam1*, *Tek,* and *Vwf*) was visualized by Feature plots. **(E)**, Dot plot of selected marker genes for each cluster and lineage. Dot size indicates the percentage of cells expressing each gene, and dot color represents the average expression level. SMC, smooth muscle cells.

for 14.2% (**Figure 2C**). We identified the top 5 marker genes [sorted by average log2(fold change)] for each cluster relative to all other EC clusters, and these genes were plotted using a heatmap (**Supplementary Table 4** and **Figure 2D**). The two largest subpopulations, EC_1 and EC_2, accounted for 32 and 26.3% of all ECs, respectively, and showed high expression

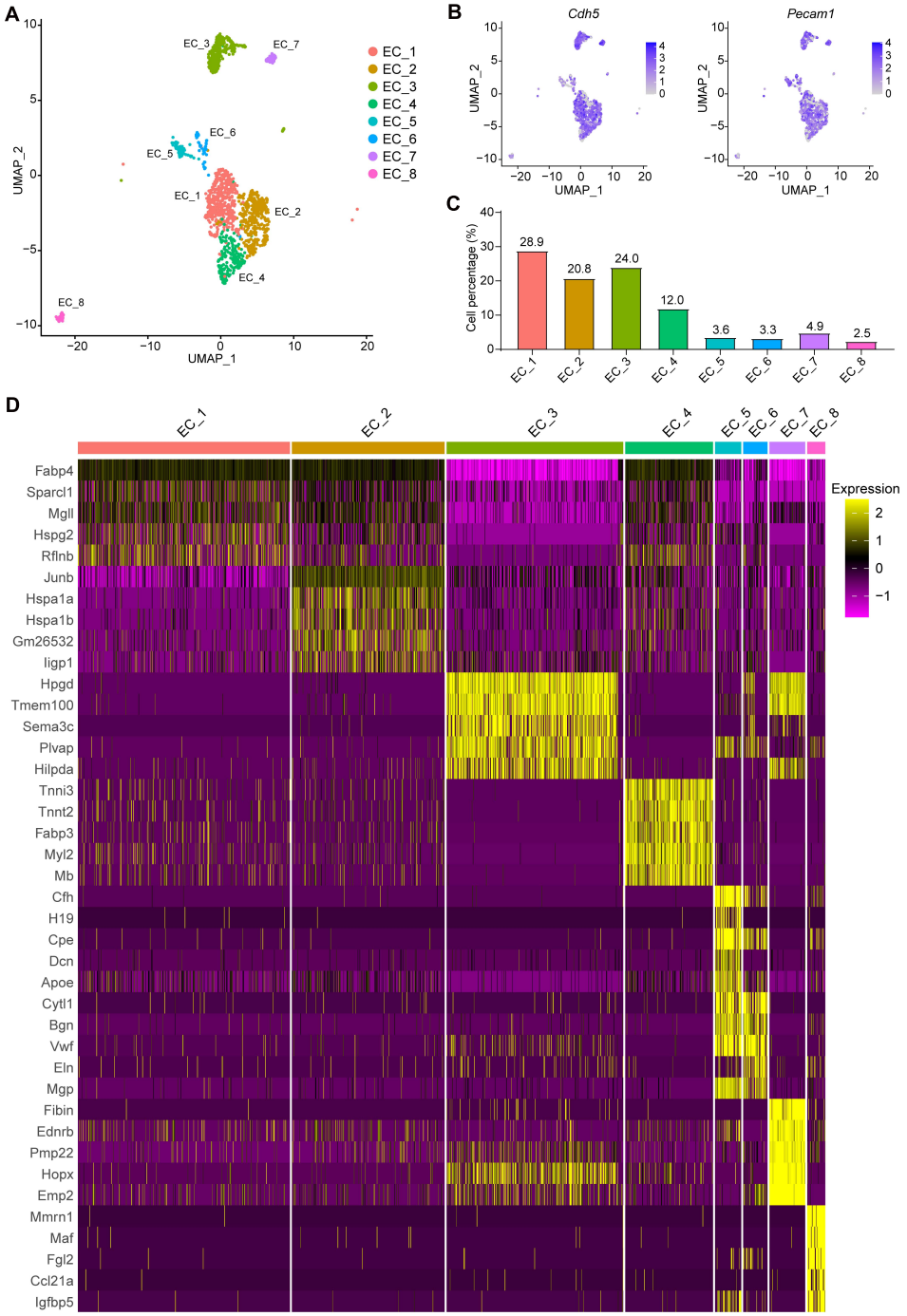

FIGURE 2 | Categorization of endothelial cell subpopulations. **(A)**, UMAP plot of the aggregate ECs with positive expression of *Cdh5*, *Pecam1*, *Tek,* or *Vwf*. Eight EC clusters were identified in the aggregate arterial ECs. **(B)**, Feature plot of EC marker genes *Cdh5* and *Pecam1* in the EC clusters. **(C)**, Percentage of cells in each EC cluster. **(D)**, The top5 markers for each cluster were selected based on the average Log2(fold change). The FindAllmarkers function in Seurat v4.0 was performed using non-parametric Wilcoxon rank sum test with parameters min.pct = 0.25, thresh.use = 0.25, only.positive = TRUE and return.thresh = 0.01, to find all markers for each cluster.

of genes involved in fatty acid metabolism (*Fabp4*, *Cd36,* and *MgII*) (Elmasri et al., 2009; Son et al., 2018; Theodorou and Boon, 2018) and angiogenesis markers (*Flt1* and *Kdr*) (Kanno et al., 2000; Zachary and Gliki, 2001) (**Supplementary Table 3**). Accordingly, the GO terms of vascular development, cell growth, and response to growth factors were enriched in these two EC clusters (**Supplementary Figures 2A,B**). Additionally, we found that EC_2 expressed the highest levels of the two best-known

mechanosensitive genes, *Klf2*(Doddaballapur et al., 2015) and *Klf4* (Sangwung et al., 2017), and showed enrichment for the GO term regulation of cellular response to stress (**Supplementary Table 3** and **Supplementary Figure 2B**), indicating EC_2 displaying an atheroprotective endothelial phenotype. Based on the markers specific to EC_3 (**Supplementary Table 3**), blood vessel morphogenesis, cell junction organization, and adherence junction organization showed selective enrichment in this cluster (**Supplementary Figure 2C**), suggesting its contribution to maintaining the endothelial barrier function. Interestingly, EC_4 demonstrated a high expression of *Fabp3*, *Myl2,* and *Myl3*, which have been reported to be selectively expressed in heart tissue (Andersen et al., 2012; Tsukahara et al., 2014; Sheikh et al., 2015) (**Figure 2D**). In line with recent scRNA-seq studies of cardiac ECs (Feng et al., 2019; Tombor et al., 2021), the GO terms, including electron transport chain, aerobic respiration, proton transmembrane transporter activity and mitochondrial electron transport, and the KEGG pathways including, cardiac muscle contraction, mitochondrial fatty acid beta-oxidation, glycolysis, and pyruvate metabolism, were enriched in EC_4 cluster (**Supplementary Figure 2C**), suggesting that EC_4 belongs to the cardiac lineage and exhibits distinct functional and metabolic signatures from those in the vascular ECs.

We then investigated the expression profiles enriched for EC_5, EC_6, EC_7, and EC_8. Interestingly, we found that EC_5 and EC_6 highly expressed both endothelial marker genes (*Pecam1*, *Cdh5,* and *Vwf*) and mesenchymal marker genes (Piera-Velazquez and Jimenez, 2019; Ma et al., 2020) (*Dcn*, *Mgp*, *Eln,* and *Fn1*) (**Figures 2B,D** and **Supplementary Table 3**), resembling the signature of endothelial-mesenchymal transition (EndMT). Moreover, the GO terms of vascular development, extracellular matrix organization (extracelluar matrix structural constituent for EC_5 and collagen-containing extracellular matrix for EC_6) and response to growth factor stimulus were enriched in these two EC clusters, further supporting that EC_5 and EC_6 acquire a mesenchymal state (**Supplementary Figure 3A,B**). Similarly, EC_8 also showed EndMT features, characterized by the expression of EC marker gene *Pecam1* and mesenchymal marker genes, including *Vim*, *Fn1,* and *Tgfbr2* (Frid et al., 2002; Derada Troletti et al., 2019; Piera-Velazquez and Jimenez, 2019) (**Figure 2B** and **Supplementary Table 3**) and are enriched for the GO term of vascular development, tissue remodeling and mesenchyme development (**Supplementary Figure 3D**). Additionally, EC_8 highly expressed *Fgl2* (encoded fibrinogen like protein 2), *Ccl21a,* and *Il7,* which are involved in cell adhesion and EC activation (Liu et al., 2003; Yuan et al., 2015). Unlike EC_5, EC_6, and EC_8, the EC_7 cluster selectively expresses genes associated with actin cytoskeleton organization, blood vessel morphogenesis, cell junction organization, and endothelium development, suggesting that this EC cluster may be involved in maintaining endothelial function (**Supplementary Figure 3C**).

To further identify the cellular functions of each EC cluster, we performed GO and KEGG enrichment analysis of the gene sets of these clusters (**Figure 3**). We found that all EC clusters shared the GO terms associated with the developmental process, cellular component organization or biogenesis, and metabolic process

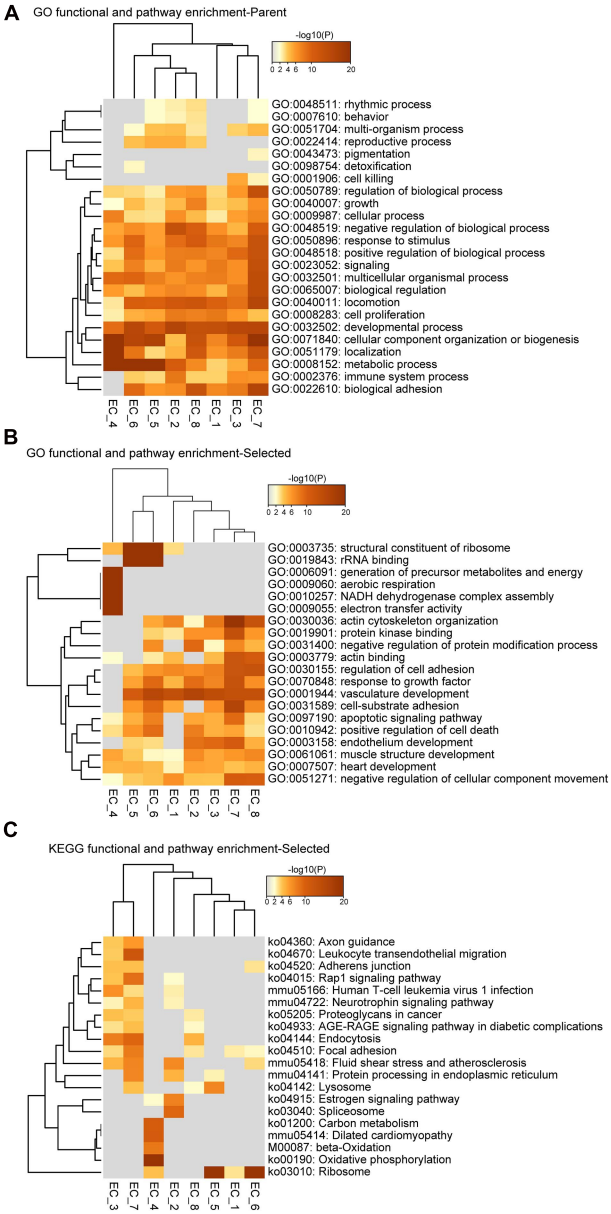

FIGURE 3 | Functional and pathway enrichment analysis of endothelial cell subpopulations. **(A–C)**, Heatmap showing the Gene Ontology (GO) and KEGG-terms enrichment of all the cluster-specific genes for the 8 EC clusters.

(**Figure 3A**). The vascular development pathway demonstrated selective enrichment in all EC clusters except EC_4 (**Figure 3B**), further supporting its endocardial lineage assignment which is distinct from the other seven EC clusters. Additionally, as shown in **Figures 3B,C**, we found that EC_4 showed enrichment of NADH dehydrogenase activity, electron transfer activity, beta-oxidation, carbon metabolism, and oxidative phosphorylation, which is in line with previous reports that endocardial ECs have high metabolic demands to execute their biological functions in the high-energy-requiring heart (Eelen et al., 2015; Xiong et al., 2018; Shimizu et al., 2020).

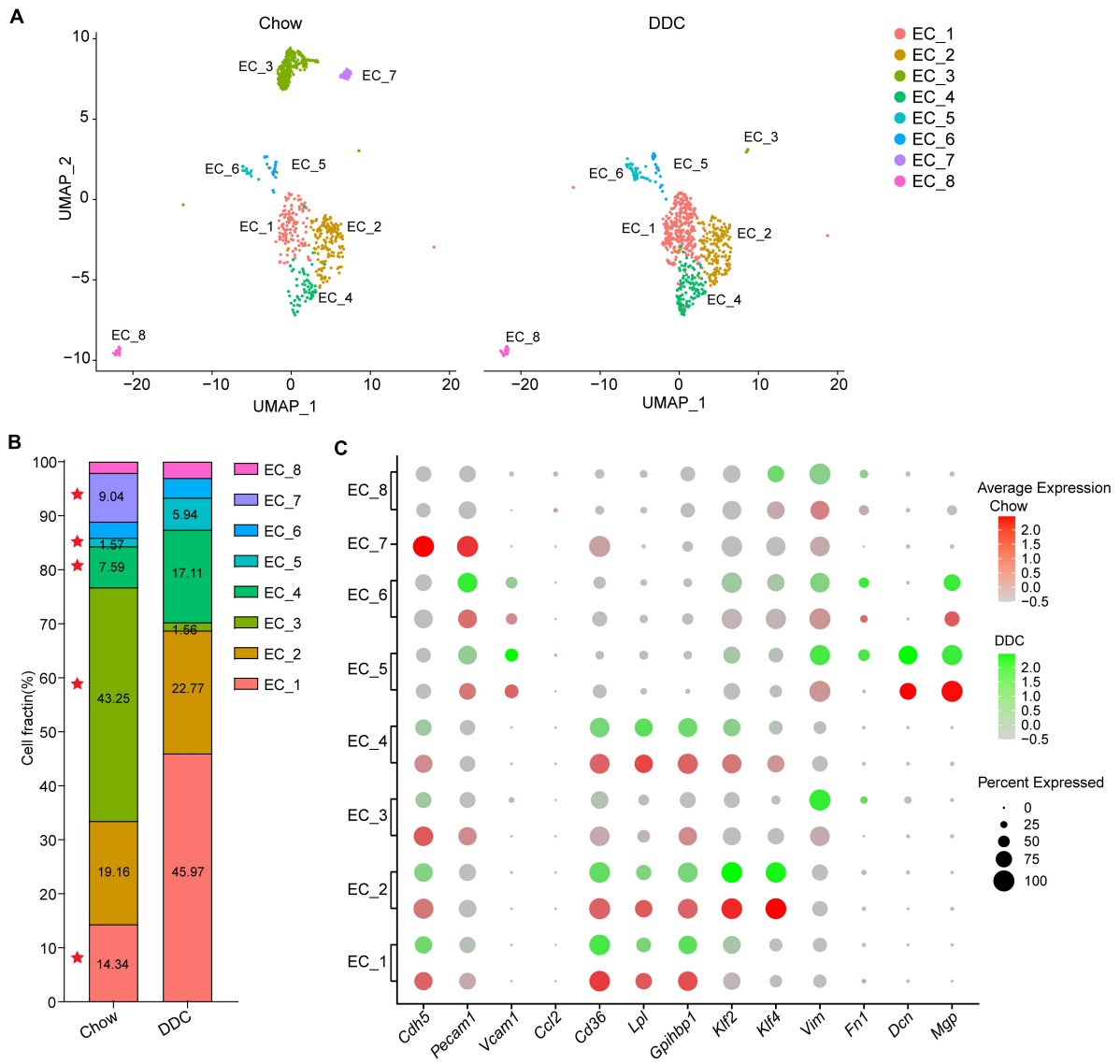

FIGURE 4 | Diet-induced changes in endothelial cell subpopulations. **(A)**, UMAP plot of EC clusters from Chow ($n = 830$) and DDC ($n = 707$) groups (n is the number of cells qualified for analysis in each group). Colors denote different EC clusters. **(B)**, Cell cluster percentages across two experimental groups (Chow and DDC). **(C)**, Dot plot showing the expression of EC marker genes and genes associated with inflammation, lipid metabolism, stress response and endothelial-mesenchymal transition (EndMT) in all EC clusters across the two experimental conditions.

Identification of Endothelial Cell Plasticity in Diabetic Atherosclerosis

To determine the cellular response of the EC subpopulations during atherosclerosis at the single-cell level, we analyzed the scRNA-seq profiles from Chow and DDC groups (**Figure 4A**). Compared with the Chow group, DDC feeding resulted in expansions of EC_1, EC_4, and EC_5 subpopulations and significantly decreased EC_3 and EC_7 subpopulations (**Figure 4B**). There is no discernable difference between the two groups in EC_6 and EC_8 subpopulations. Compared with other EC clusters, EC_1 showed a high expression of lipid-handling genes, including *Cd36*, *Lpl,* and *Gpihbp1*, suggesting a functional specialization in lipid uptake and metabolism (**Figure 4C** and **Supplementary Figure 4A**). Accordingly, the PPAR signaling pathway was also enriched in the EC_1 cluster (**Supplementary Figure 2A**), in line with the master role of PPAR signaling in regulating lipid-handling genes and circulating fatty acids (Kanda et al., 2009; Mehrotra et al., 2014). Similarly, EC_4 highly expressed *Cd36* (Son et al., 2018), *Lpl* (Wang et al., 2007), and *Gpihbp1* (Chiu Amy et al., 2016) (**Figure 4C** and **Supplementary Figure 4A**), since cardiac tissues are highly oxidative and catabolize fatty acids as a source of energy under normal conditions (Schoonderwoerd and Stam, 1992; Son et al., 2018). Interestingly, DDC induced expansions of these two clusters, but did not affect the expression of lipid-handling

genes (**Figures 4B,C** and **Supplementary Figure 4A**). Desipe not transforming to foam cells or accumulating cholesterol as macrophages or SMCs in the atherosclerotic plaques, ECs express transporters for cholesterol and have the biochemical pathways for cholesterol homeostasis (Hassan et al., 2006). Mutiple proteins, such as ATP-binding cassette transporter A1 (ABCA1), ABC G subfamily (ABCG1), and SR-B1 (encoded by *Scarb1*) are involved in endothelial cholesterol homeostasis (Hassan et al., 2006; Stamatikos et al., 2019). Of note, *Abca1*, *Abcg1,* and *Scarb1* showed heterogeneous expression by EC clusters (**Figure 4C** and **Supplementary Figure 4A**). *Abca1* was expressed in EC_5 and EC_8, while *Abcg1* and *Scarb1* expressed in EC_7, consistent with previous reports that ABCA1 only weakly expressed in human vascular ECs (Hassan et al., 2006). These data suggest the functional heterogeneity of cholesterol metabolism in individual EC clusters. Pathological conditions, including hyperlipidemia, hyperglycemia, disturbed flow, and vascular inflammation, lead to endothelial activation and EndMT (Piera-Velazquez and Jimenez, 2019). Consistently, we found that EC_5 showed high expression of the pro-inflammatory gene *Vcam1*, and mesenchymal marker genes *Vim*, *Fn1*, *Dcn,* and *Mgp*, and these genes were increased in the DDC group compared to the Chow group (**Figure 4C** and **Supplementary Figure 4B**), suggesting that mesenchymal activation contributes to the expansion of this cluster of ECs. Of note, different from the expression profiles of *Fn1*, *Dcn,* and *Mgp*, *Vim* was broadly expressed in all EC clusters albeit highly expressed in EC_5, EC_6, and EC_8, particularly in DDC condition, suggesting EndMT is a process in which loss of EC markers and gain of multiple mesenchymal markers. Compared to the other subpopulations, EC_3 and EC_7 showed high expression of the canonical EC markers, but low expression of pro-inflammatory genes, lipid-handling genes, and mesenchymal marker genes (e.g., *Fn1*, *Dcn,* and *Mgp*) (**Figure 4C** and **Supplementary Figure 4B**). In addition, the proportion of these two clusters were dramatically decreased after DDC feeding. Notably, the EC_7 cluster accounts for 9.04% in the Chow group, and they disappeared upon DDC feeding (**Figure 4B**). These data indicate that the reduction of EC_3 and EC_7 may be caused by EC apoptosis or EndMT, both occurring during atherogenesis.

Identification of Endothelial to Mesenchymal Transition During Atherosclerosis

Our analysis of the transcriptomic and functional profiles for each EC subpopulation suggests that ECs undergo phenotypic changes and metabolic programming during the development of atherosclerosis. The cluster dendrogram in **Figure 5A** suggests that EC_1, EC_2, and EC_4 are more similar to each other. The similarity between EC_3 and EC_7, and the similarity between EC_5 and EC_6 are also shown in **Figure 5A**. We next sought to explore if ECs underwent a trans-differentiation trajectory during atherogenesis and if EC trans-differentiation was associated with metabolic-related transcriptomic changes. Thus, we used Slingshot to perform trajectory inference analysis of the ECs from the two experimental groups. EC_8, EC_5, EC_6, EC_1, and EC_2 clusters were distributed in the global path along the development axis, predicting the potential hierarchy between mesenchymal clusters and mature EC clusters (**Figure 5B**). This prediction provides further evidence that EndMT contributes to atherosclerosis, as previously established by lineage tracing (Evrard et al., 2016). To further characterize the ECs undergoing EndMT, we compared the transcriptome of ECs that express mesenchymal markers, to ECs lacking those marker genes. As expected, the EndMT cells (EndMT$^+$), including EC_5, EC_6, and EC_8, highly expressed mesenchymal and extracellular matrix genes, such as *Tgfbr2*, *Fn1*, *Eln*, *Vim*, *Dcn,* and *Mgp* (**Figures 5C,D** and **Supplementary Figure 4B**). In contrast, EC clusters, including EC_1, EC_2, EC_3, EC_4, and EC_7, that did not undergo EndMT (EndMT$^-$) showed high expression of genes involved in glycolysis (*Aldoa*, *Gapdh*, *Gpi1,* and *Pfkfb3*), fatty acid metabolism (*Cd36* and *Fabp4*), vasculoprotection (*Klf2* and *Klf4*) and angiogenic response (*Id1* and *Ets1*) (**Figures 5C,D** and **Supplementary Figure 4A**). Next, the specific genes found in EndMT$^+$ cells when compared with EndMT$^-$ cells (**Supplementary Table 5**) were subjected to GO analysis. As shown in **Figure 5E**, EndMT$^+$ cells exhibited induction of many well-known biological processes associated with proatherogenic pathways, including extracellular matrix organization, apoptosis, and adhesion molecule binding (**Figure 5E**). These results suggest that the ECs in a mesenchymal state show a pro-atherogenic phenotype.

Since EC metabolic reprogramming is known to play a critical role in endothelial plasticity and EndMT (Rohlenova et al., 2020), we performed a detailed analysis of the gene expression signatures related to glycolysis, fatty acid and glutamine metabolism, as well as TCA cycle (**Figure 5F**). In normal ECs, glycolysis is the main energy supplier, accounting for > 85% of the total ATP production (Krützfeldt et al., 1990; De Bock et al., 2013), which safeguards ECs against oxidative stress in oxygen-replete. Interestingly, EndMT$^+$ cells showed reduced expression of glycolytic enzyme genes, including *Gpi1* and *Gapdh*, while increased expression of *Pkm*, *Pgk1*, *Pgam1,* and *Pfkl*, compared to EndMT$^-$ cells, suggesting a glycolytic reprogramming during EndMT. Although ECs rely primarily on glycolysis as their ATP source, some studies demonstrated that fatty acid oxidation (FAO) is required to maintain EC fate and restrain EndMT (Schoors et al., 2015; Xiong et al., 2018). Consistently, EndMT$^+$ cells displayed reduced expression of genes associated with fatty acid metabolism, including *Fabp4*, *Cd36*, *Gpihbp1,* and *Mgll*, further supporting that FAO inhibition potentiates EndMT (Xiong et al., 2018).

Endothelial to Mesenchymal Transition Is Increased in Atherosclerosis

The contribution of EndMT to atherosclerosis progression has been documented using endothelial lineage tracking in a mouse atherosclerosis model (Evrard et al., 2016). Consistently, our data showed that DDC markedly increased the proportion of EndMT$^+$ cells relative to the Chow group (DDC, 12.59% vs. Chow, 6.63%) (**Figures 6A,B**). EndMT is characterized by the loss of EC features and acquisition of mesenchymal

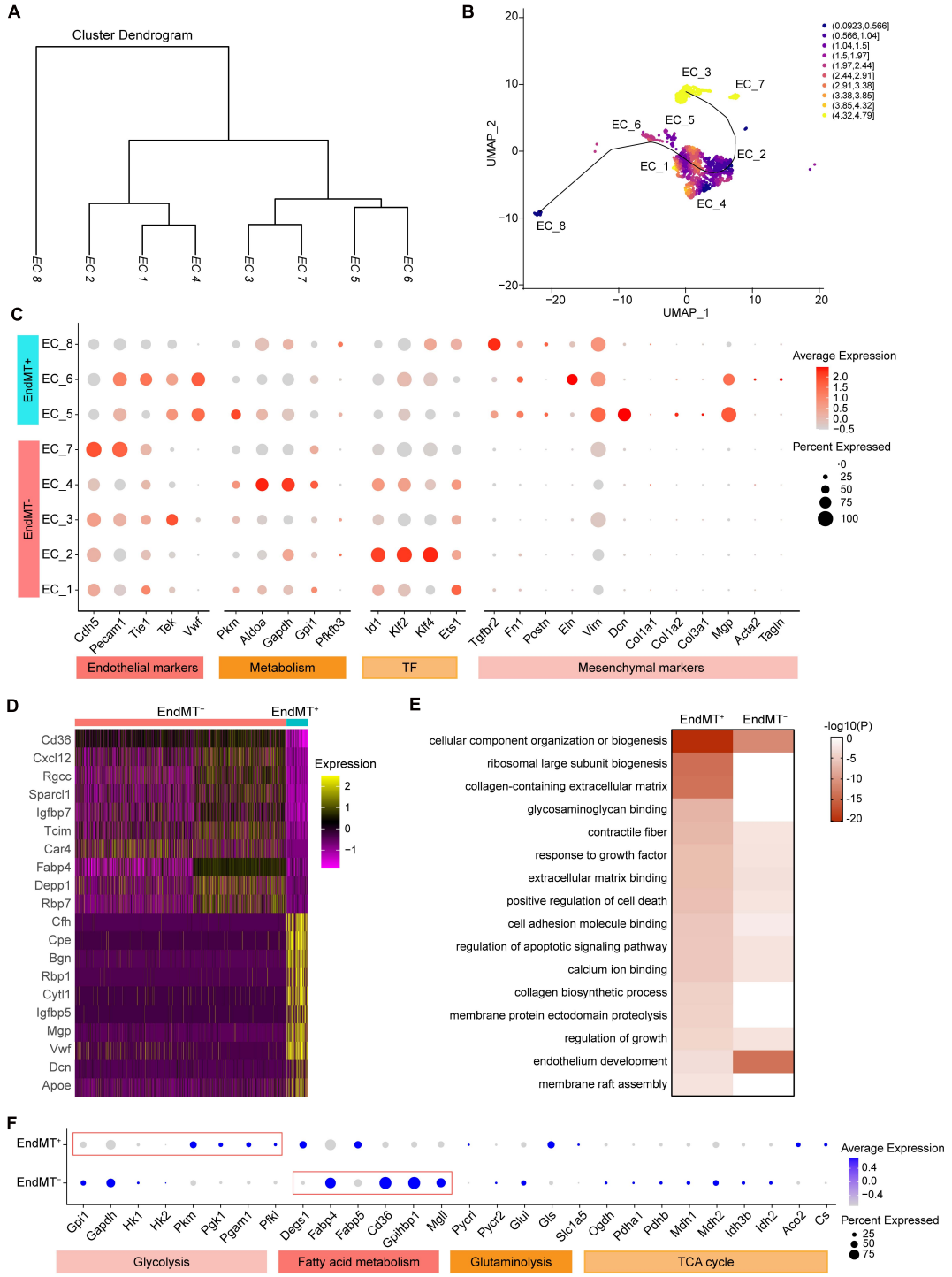

FIGURE 5 | Identification of endothelial cell subpopulations undergoing mesenchymal transition. **(A)**, Dendrogram summarizing the similarity of the EC clusters in the aggregate arterial ECs according to average RNA expression. **(B)**, Two-dimensional representation of EC clusters using UMAP, with trajectory inferred by the interpretation of Slingshot and tradeSeq analysis. Color indicates imbalance score. Regions with a high score indicate that the local cell distribution is unbalanced compared to the overall distribution. **(C)**, Dot plot showing the marker genes associated with EC identity, metabolism, transcription factor, and mesenchymal identity in EndMT^{-} (EC marker positive and mesenchymal marker negative) and EndMT^{+} (EC marker positive and mesenchymal marker positive). Size depicts the percentage of cell expressing each gene, and color indicates the expression level. **(D)**, Heatmap showing the top10 genes selected from all markers of EndMT^{-} and EndMT^{+} cells based on the average Log2(fold change). **(E)**, Heatmap showing the representative GO-terms enrichment of the specific genes in EndMT^{+} cells in comparison to EndMT^{-} cells. The color indicates the -$\log_{10}$(P) value. **(F)**, Dot plot showing the expression of genes associated with glycolysis, fatty acid metabolism, glutaminolysis, and tricarboxylic acid (TCA) cycle comparing EndMT^{-} and EndMT^{+} cells.

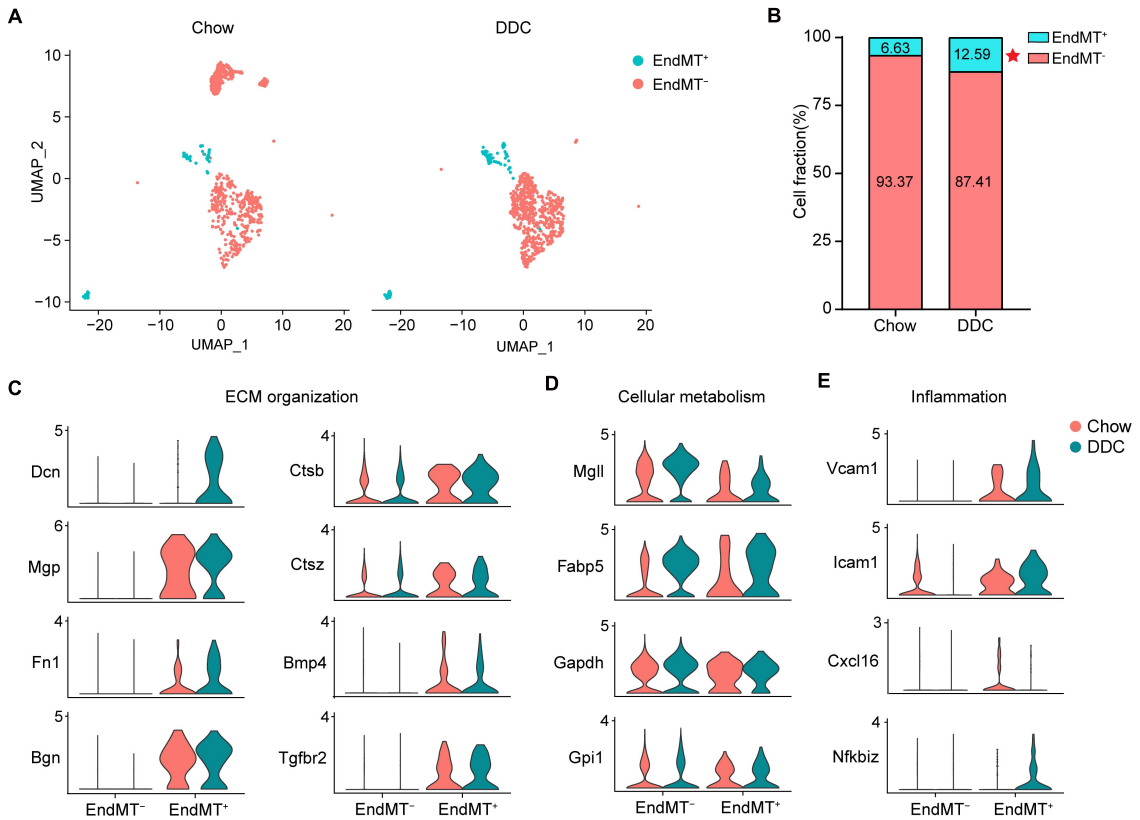

FIGURE 6 | Activated endothelial cells show distinct transcriptional features. **(A)**, UMAP plot of EndMT$^-$ and EndMT$^+$ cells across the two experimental groups. **(B)**, The percentage of EndMT$^-$ and EndMT$^+$ cells across the two experimental groups. *$P < 0.05$ using Chi-square test. **(C–E)**, Violin plot showing the genes associated with ECM organization **(C)**, cellular metabolism **(D)**, and inflammation **(E)** in EndMT$^-$ and EndMT$^+$ cells across the two experimental groups.

characteristics, including enhanced extracellular matrix (ECM) organization (Dahal et al., 2017), metabolic program (Xiong et al., 2018), and enhanced inflammation (Chen et al., 2015). Next, we further analyzed the alteration of the genes associated with those EndMT characteristics between the two experimental groups. As shown in **Figure 6C**, the ECM genes, such as *Dcn*, *Mgp*, *Fn1,* and *Bgn* were markedly increased in EndMT$^+$ cell, and DDC feeding further enhanced the expression of *Dcn* and *Fn1*, in line with a prior study identifying that ECs transform toward a mature fibroblast-like phenotype during atherosclerosis progression (Souilhol et al., 2018). Additionally, EndMT$^+$ cells showed increased expression of *Ctsb*, *Ctsz*, *Bmp4,* and *Tgfbr2*, all involved in ECM organization, and the ECM degradation enzymes *Ctsb* and *Ctsz* were further increased upon DDC feeding (**Figure 6C**), suggesting that DDC diet may induce plaque instability. To further address the metabolic program during EndMT between Chow and DDC groups, we analyzed the marker genes of fatty acid metabolism (*Mgll* and *Fabp5*) and glycolysis (*Gapdh* and *Gpi1*). We found that DDC feeding increased the cells expressing *Mgll* and *Fabp5*, in both the EndMT$^-$ and EndMT$^+$ cells, despite no alterations of the expression levels (**Figure 6D**). Moreover, the pro-inflammatory genes (*Vcam1*, *Icam1,* and *Cxcl16*) and the NF-κB pathway gene (*Nfkbiz*) were highly expressed in the EndMT$^+$ cells, and DDC feeding further increased the expression of *Vcam1*, *Icam1,* and *Nfkbiz*, suggesting DDC enhances inflammatory response during EndMT (**Figure 6E**). These data suggest that EndMT occurs in atherosclerosis and that DDC feeding enhances the EndMT process.

DISCUSSION

Endothelial cell heterogeneity is a hallmark of blood vessel biology, with subpopulations identified across different tissues and within a particular vascular bed to meet the distinct physiological needs (Feng et al., 2019; Kalucka et al., 2020; Paik et al., 2020). The scRNA-seq technology has enabled the unbiased and systematic analysis of the transcriptomes of various cell populations at the single-cell resolution at once. Herein, we performed a detailed analysis, via scRNA-seq, of the cardiac and aortic EC gene expression signatures during atherosclerosis. We identified 8 EC populations in the normal tissues and characterized the heterogeneity of the transcriptome and biological process signatures of each population. Furthermore, through the integrated analysis of the ECs across normal and atherosclerotic conditions, we identified three EC clusters undergoing EndMT to a fibroblast-like phenotype, which were

expanded in atherosclerosis and exhibited a metabolic switch compared with the other EC subpopulations.

It was reported that EndMT-derived fibroblast-like cells contribute to the atherosclerotic plaques, using the endothelial-lineage tracing mouse model (Evrard et al., 2016). In our study, 12.59% of ECs acquire a fibroblast phenotype in atherosclerotic conditions, which is much lower than the extent of EndMT-derived fibroblast-like cells (22.8%) in the lineage tracing study. Nevertheless, among the entire EC-derived fibroblasts, 11.1% of cells co-expressed endothelial and fibroblast markers, which is closer to the proportion in our study (12.59%). The unbiased nature of the present study further strengthens those previous findings. However, as a limitation, our study was performed using the CD31-enriched ECs, therefore, the ECs that translate toward a more mature fibroblast phenotype and lose the endothelial markers cannot be captured in the present study. Furthermore, both our study and the endothelial-lineage tracing study similarly demonstrated that ECs which undergo EndMT rarely give rise to vascular smooth muscle cells (VSMCs) in plaques. However, some studies showed that VSMCs or immune cells arise from EndMT in angiogenesis (Rohlenova et al., 2020) or in carotid artery exposed to disturbed flow (Andueza et al., 2020). Unexpectedly, we also identified the presence of EndMT-derived fibroblast-like cells in the Chow group (6.63% $EndMT^+$ of total ECs). Similarly, a recent scRNA-seq study revealed the presence of angiogenic and proliferating ECs in healthy tissues (Kalucka et al., 2020). Although limited EC proliferative potential has been described in the suboptimal repair of damaged heart tissue after ischemic injury, whether these activated/proliferative ECs in the healthy tissues represent an ongoing EC repair/regeneration process remains to be further determined. Collectively, these data strengthen the evidences of phenotypic heterogeneity of ECs residing in different tissues and response to environmental conditions.

An additional level of EC heterogeneity was observed when analyzing GO biological processes for distinct EC populations. The EndMT-derived fibroblast-like cells show signatures of genes associated with extracellular matrix organization, cell apoptosis and cytokine production, which are representative key functions for fibroblasts in atherosclerosis (Brokopp et al., 2011; Evrard et al., 2016). Moreover, our findings defined that fibroblasts are the primary mesenchymal cell type derived from EndMT in atherosclerosis, which is consistent with previous reports (Evrard et al., 2016; Wesseling et al., 2018). Although the functional importance of EndMT in atherosclerotic plaque formation has been well-established (Chen et al., 2015; Evrard et al., 2016; Souilhol et al., 2018; Piera-Velazquez and Jimenez, 2019), the transcriptomic and functional heterogeneity of mesenchymal cells in atherosclerosis has yet to be elucidated. Here we identified three clusters of $EndMT^+$ cells and characterized their distinct gene profiles and functional characteristics, which extend our understanding of the mesenchymal heterogeneity in atherosclerotic plaques. A recent report (Tombor et al., 2021) suggests that the EndMT in the myocardial infarction area is a reversible process, and that inhibition of TGF-β signaling could reduce the expansion of these cells. Moreover, inhibition of EndMT driving transcription factors such as *Snail* and *Slug*, has been shown to prevent EC migration and *in vitro* angiogenesis (Welch-Reardon et al., 2014; Hultgren et al., 2020). However, more studies and deeper analysis will be needed to investigate the implications of these observations in the EndMT process in atherosclerosis.

As another phenotypic readout of our scRNA-seq analysis, we also characterized the metabolic transcriptome signatures that differ between EndMT positive and negative ECs. In agreement with the observation that metabolic adaptations of ECs contribute to endothelial plasticity and EndMT in response to various physiological and pathological stimuli (Eelen et al., 2015; Theodorou and Boon, 2018; Rohlenova et al., 2020; Tombor et al., 2021), the immature ECs, which express mesenchymal markers, have a more robust glycolytic gene signature than the mature ECs. In turn, mature ECs highly express genes associated with fatty acid signaling and the TCA cycle despite still generating >85% of their ATP glycolytically. During the process of atherosclerosis, pro-inflammatory cytokines enhance glycolysis in ECs, and in turn enhanced glycolysis can drive pro-inflammatory programs, thereby constituting a vicious cycle resulting in sustained pro-inflammatory signaling in ECs (Theodorou and Boon, 2018). Here, we identified increased expression of glycolytic enzymes during EndMT. In agreement with a previous study (Xiong et al., 2018), our scRNA-seq data also revealed that EndMT in ECs is accompanied with an inhibition of FAO, suggesting that endothelial FAO may be a critical regulator of the EndMT process. Metabolic adaptations were also identified in cardiac ECs after myocardial infarction (Tombor et al., 2021) and ECs in choroidal neovascularization (Rohlenova et al., 2020). These findings further illustrate the extensive phenotypic plasticity and potential of ECs to adapt their metabolic signatures, presumably to fine-tune their function in different vascular compartments and in response to physiological and pathological conditions.

As the pump of the circulatory system, the heart has multiple types of ECs, including endocardial ECs, coronary vascular ECs, and aorta-specific ECs. Recent scRNA-seq studies have identified the transcriptome signatures of these ECs (Feng et al., 2019). Through gene expression analysis, *Cytl1* and *Npr3* were reported to be expressed in endocardial ECs, while *Fabp4* and *Cd36* were identified as the markers of coronary vascular ECs, and *Edh3* and *Fam167b* as the top 2 genes specifically expressed in aorta-specific ECs. Although our study was not designed to explore the transcriptomic differences in the organ-specific ECs, we were able to identify a cluster of cardiac ECs, EC_4, which distinguish themselves from those in other organs by specifically expressing genes involved in electron transport, cardiac muscle contraction, pyruvate and lipid metabolism. However, the cell lineage of the cardiac EC cluster singled out in our study was not able to be identified based on the markers featured in the three types of cardiac ECs reported in that prior study.

In summary, we report an unbiased single-cell transcriptomic approach to delineate the heterogeneity of cardiovascular ECs from normal and diabetic atherosclerotic conditions in mice. The identification of three ECs that very strongly recapitulate endothelial-derived fibroblasts, clearly confirms the existence of cells expressing mesenchymal markers at the single-cell level,

and therefore supports the many studies reporting EndMT in atherosclerosis and other cardiovascular diseases. We also characterized the metabolic heterogeneity of ECs, which may serve as a valuable source for researchers in the field. The insights provided by our data can lead to a better understanding of endothelial biology and pathobiology and further facilitate the development of therapeutics for atherosclerosis.

MATERIALS AND METHODS

Animals and Diet

The B6.129S7-*Ldlr*^{tm1Her}/J (*Ldlr*$^{-/-}$, stock No. 002207) mice were purchased from The Jackson Laboratory (Bar Harbor, ME). Eight-week-old male *Ldlr*$^{-/-}$ mice were fed either a standard rodent chow (Chow, LabDiet 5L0D, 13% fat) or a diabetogenic diet with 0.15% cholesterol (Subramanian et al., 2008) (DDC; Envigo, TD.180368, a diet formulated with 59.1% kcal from fat and 24% sucrose with 0.15% cholesterol added) for 12 weeks. The diabetogenic diet provides 35.7% calories from fat and 37.8% from carbohydrates. Animals were housed in cages with microisolator filter tops, maintained on a 12-h light/dark cycle in a temperature-controlled room, and given free access to food and water. All animal care and experimental procedures were approved by the Institutional Animal Care & Use Committee (IACUC) from the University of Michigan and complied with the National Institutes of Health (NIH) Guidelines for the care and use of laboratory animals.

Oral Glucose Tolerance (OGTT) and Insulin Tolerance Test (ITT)

For OGTT, mice on standard chow or DDC were fasted overnight. Next, glucose was administered (2g/kg, gavage) and blood glucose levels were measured at the indicated time points thereafter. For ITT, mice were administered human insulin (Humulin R, 1 U/kg, i.p.) following 6 h of fasting. Blood glucose levels were measured at indicated time points after insulin administration.

Endothelial Cell Preparation

At the end of the experiments, mice were anesthetized by using carbon dioxide (CO_2) in accordance with the NIH Guidelines for the euthanasia of animals and then perfused with 10 ml of PBS through left ventricular puncture. Preparation of the single-cell suspension of the arterial endothelial cells was performed as previously described (Hu et al., 2018). In brief, the heart and whole aorta from three mice for each group were harvested and dissected into small pieces. Samples were incubated in digestion solution [DMEM (ThermoFisher Scientific, 21063-045), 2mg/ml collagenase I (Worthington Biochemical Corporation, LS004196), 60 U/ml DNase I (Roche Diagnostics, 1010459001)] at 37°C for 30–45 min with shaking. At the end of incubation, DMEM containing 10% FBS was added to the samples to stop the digestion and filtered through a 40 μm strainer. The cell suspension was centrifuged at 400 g for 8 min at 4°C, and the pellet was re-suspended in a DPBS-based wash buffer (WB, containing 1% FBS and 2 mM EDTA). Next, the cell suspension was enriched for ECs using CD31 MicroBeads (Miltenyi Biotec, 130097418) according to the manufacturer's instructions. The CD31-enriched single-cell suspension was washed with WB and stained with Viable dye eFluor 450 (Thermo Fisher Scientific, 50-112-8817). Doublets were gated out prior to FACS sorting, and the viable cells were sorted into a collecting tube with DMEM containing 20% FBS.

Single-Cell RNA Sequencing (scRNA-seq)

Standard 10× Chromium Single Cell 3' Solution v3.1 (10X Genomics Gemcode Technology) protocols were followed for scRNA-seq. Briefly, single cells with specific 10X Barcode Gel Beads and unique molecular identifiers were partitioned into the Gel Bead-in-Emulsion (GEM) in the GemCode instrument, where cell lysis and bar-coded reverse transcription of RNA ensued, followed by amplification, shearing, and 5' adaptor and sample index attachment. Libraries were sequenced on the sequencing platform Illumina NovaSeq 6000. The sequencing depths among the samples were: 243,312 mean reads per cell for the Chow group; 276,821 mean reads per cell for the DDC group. The fraction reads in cells for each sample were >85%. The median number of genes detected per cell (also named as median genes per cell) for Chow and DDC were 1551 and 1297, respectively.

Processing of scRNA-seq Data

The raw scRNA-seq data was processed using the 10X Genomics Cell Ranger software (v5.0.1). The CellRanger mkfastq command was used to generate Fastq files. Subsequently, sequencing data were mapped to the pre-build mouse reference genome (mm10, version 1.2.0). The mapping rate of the reads mapped to the genome for the three samples was more than 93%. The CellRanger count command was run on the individual Fastq datasets to produce expression data. The Cellranger aggr program was run to generate the aggregate dataset.

scRNA-seq Data Analysis

After aggregation of the three samples, R package Seurat v4.0 was used for cell filtration, normalization, principal component analysis, variable genes finding, clustering analysis, and UMAP dimensional reduction. The datasets were trimmed by removing the cells expressing fewer than 200 genes and the genes expressed in fewer than five cells. Cells with an expression of >3000 genes were filtered out for exclusion of possible cell aggregates. Cells containing >10% mitochondrial genes were presumed to be of poor quality and were also filtered out. Data were then log-normalized for the subsequent analyses. Principal component analysis (PCA) was used for dimension reduction, followed by clustering analysis in principal component analysis space using a graph-based clustering approach. UMAP was then used for the two-dimensional visualization of the identified clusters. The Seurat functions DotPlot, Vlnplot, FeaturePlot, and Heatmap

were used to visualize the gene expression with dot plot, violin plot, feature plot, and heatmap, respectively. Markers for a specific cluster against all remaining cells were identified by using the Seurat function FindAllMarkers.

Statistical Analysis

The data corresponding to mouse body weight, plasma glucose, total cholesterol, and triglyceride were presented as mean ± standard error of the mean. Statistical analysis was performed using GraphPad Prism 8.0 Software (GraphPad Software, San Diego, CA, United States). All data were tested for normality and similar variance. Then, unpaired *t*-test was used to compare the body weight, plasma total cholesterol, and triglyceride. Two-way ANOVA followed by Bonferroni test was used to compare the plasma glucose concentration between Chow and DDC groups at the indicated time.

DATA AVAILABILITY STATEMENT

The datasets presented in this study can be found in online repositories. The names of the repository/repositories and accession number(s) can be found below: https://www.ncbi.nlm.nih.gov/geo/, GSE169332.

ETHICS STATEMENT

The animal study was reviewed and approved by the Institutional Animal Care & Use Committee (IACUC) from the University of Michigan.

AUTHOR CONTRIBUTIONS

GZ, HL, YL, and YZ performed the experiments. GZ performed data analysis. GZ and JZ wrote the article. TZ and MG-B provided technical support and contributed to the discussion of the article. MG-B did critical editing. YEC, JZ, and GZ designed research and discussed the results. All authors contributed to the article and approved the submitted version.

FUNDING

This work was partially supported by the National Institutes of Health grants (HL138139 to JZ and HL137214, HL109946, and HL134569 to YEC) and American Heart Association Grant (20P0ST35110064 to GZ).

ACKNOWLEDGMENTS

We thank Judith S. Opp and other staff members in the Advanced Genomics Core at the University of Michigan for their support for single-cell RNA sequencing.

SUPPLEMENTARY MATERIAL

The Supplementary Material for this article can be found online at: https://www.frontiersin.org/articles/10.3389/fcell.2021.689469/full#supplementary-material

REFERENCES

Andersen, P. S., Hedley, P. L., Page, S. P., Syrris, P., Moolman-Smook, J. C., McKenna, W. J., et al. (2012). A novel Myosin essential light chain mutation causes hypertrophic cardiomyopathy with late onset and low expressivity. *Biochem. Res. Int.* 2012:685108. doi: 10.1155/2012/685108

Andueza, A., Kumar, S., Kim, J., Kang, D. W., Mumme, H. L., Perez, J. I., et al. (2020). Endothelial reprogramming by disturbed flow revealed by single-cell RNA and chromatin accessibility study. *Cell Rep.* 33:108491. doi: 10.1016/j.celrep.2020.108491

Aronson, D., and Rayfield, E. J. (2002). How hyperglycemia promotes atherosclerosis: molecular mechanisms. *Cardiovasc. Diabetol.* 1:1.

Brokopp, C. E., Schoenauer, R., Richards, P., Bauer, S., Lohmann, C., Emmert, M. Y., et al. (2011). Fibroblast activation protein is induced by inflammation and degrades type I collagen in thin-cap fibroatheromata. *Eur. Heart J.* 32, 2713–2722. doi: 10.1093/eurheartj/ehq519

Calkin, A. C., and Allen, T. J. (2006). Diabetes mellitus-associated atherosclerosis. *Am. J. Cardiovasc. Drugs* 6, 15–40. doi: 10.2165/00129784-200606010-00003

Camenisch, T. D., Schroeder, J. A., Bradley, J., Klewer, S. E., and McDonald, J. A. (2002). Heart-valve mesenchyme formation is dependent on hyaluronan-augmented activation of ErbB2-ErbB3 receptors. *Nat. Med.* 8, 850–855. doi: 10.1038/nm742

Chen, P.-Y., Qin, L., Baeyens, N., Li, G., Afolabi, T., Budatha, M., et al. (2015). Endothelial-to-mesenchymal transition drives atherosclerosis progression. *J. Clin. Invest.* 125, 4514–4528. doi: 10.1172/JCI82719

Chiu Amy, P.-L., Wan, A., Lal, N., Zhang, D., Wang, F., Vlodavsky, I., et al. (2016). Cardiomyocyte VEGF regulates endothelial cell GPIHBP1 to relocate lipoprotein lipase to the coronary lumen during diabetes mellitus. *Arterioscler. Thromb. Vasc. Biol.* 36, 145–155. doi: 10.1161/ATVBAHA.115.306774

Chiu, J.-J., and Chien, S. (2011). Effects of disturbed flow on vascular endothelium: pathophysiological basis and clinical perspectives. *Physiol. Rev.* 91, 327–387. doi: 10.1152/physrev.00047.2009

Cines, D. B., Pollak, E. S., Buck, C. A., Loscalzo, J., Zimmerman, G. A., McEver, R. P., et al. (1998). Endothelial cells in physiology and in the pathophysiology of vascular disorders. *Blood* 91, 3527–3561.

Dahal, S., Huang, P., Murray, B. T., and Mahler, G. J. (2017). Endothelial to mesenchymal transformation is induced by altered extracellular matrix in aortic valve endothelial cells. *J. Biomed. Mater. Res. A* 105, 2729–2741. doi: 10.1002/jbm.a.36133

De Bock, K., Georgiadou, M., Schoors, S., Kuchnio, A., Wong, B. W., Cantelmo, A. R., et al. (2013). Role of PFKFB3-driven glycolysis in vessel sprouting. *Cell* 154, 651–663. doi: 10.1016/j.cell.2013.06.037

Dejana, E., Hirschi, K. K., and Simons, M. (2017). The molecular basis of endothelial cell plasticity. *Nat. Commun.* 8:14361. doi: 10.1038/ncomms14361

Demos, C., Williams, D., and Jo, H. (2020). Disturbed flow induces atherosclerosis by Annexin A2-mediated integrin activation. *Circ. Res.* 127, 1091–1093. doi: 10.1161/circresaha.120.317909

Derada Troletti, C., Fontijn, R. D., Gowing, E., Charabati, M., van Het Hof, B., Didouh, I., et al. (2019). Inflammation-induced endothelial to mesenchymal transition promotes brain endothelial cell dysfunction and occurs during multiple sclerosis pathophysiology. *Cell Death Dis.* 10:45. doi: 10.1038/s41419-018-1294-2

Doddaballapur, A., Michalik, K. M., Manavski, Y., Lucas, T., Houtkooper, R. H., You, X., et al. (2015). Laminar shear stress inhibits endothelial cell metabolism via KLF2-mediated repression of PFKFB3. *Arterioscler. Thromb. Vasc. Biol.* 35, 137–145. doi: 10.1161/atvbaha.114.304277

Eelen, G., de Zeeuw, P., Simons, M., and Carmeliet, P. (2015). Endothelial cell metabolism in normal and diseased vasculature. *Circ. Res.* 116, 1231–1244. doi: 10.1161/CIRCRESAHA.116.302855

Elmasri, H., Karaaslan, C., Teper, Y., Ghelfi, E., Weng, M., Ince, T. A., et al. (2009). Fatty acid binding protein 4 is a target of VEGF and a regulator of cell proliferation in endothelial cells. *Faseb J.* 23, 3865–3873. doi: 10.1096/fj.09-134882

Evrard, S. M., Lecce, L., Michelis, K. C., Nomura-Kitabayashi, A., Pandey, G., Purushothaman, K. R., et al. (2016). Endothelial to mesenchymal transition is common in atherosclerotic lesions and is associated with plaque instability. *Nat. Commun.* 7:11853. doi: 10.1038/ncomms11853

Fan, Y., Guo, Y., Zhang, J., Subramaniam, M., Song, C.-Z., Urrutia, R., et al. (2012). Krüppel-like factor-11, a transcription factor involved in diabetes mellitus, suppresses endothelial cell activation via the nuclear factor-κB signaling pathway. *Arterioscler. Thromb. Vasc. Biol.* 32, 2981–2988. doi: 10.1161/ATVBAHA.112.300349

Feng, W., Chen, L., Nguyen, P. K., Wu, S. M., and Li, G. (2019). Single cell analysis of endothelial cells identified organ-specific molecular signatures and heart-specific cell populations and molecular features. *Front. Cardiovasc. Med.* 6:165. doi: 10.3389/fcvm.2019.00165

Frid, M. G., Kale, V. A., and Stenmark, K. R. (2002). Mature vascular endothelium can give rise to smooth muscle cells via endothelial-mesenchymal transdifferentiation: *in vitro* analysis. *Circ. Res.* 90, 1189–1196. doi: 10.1161/01.res.0000021432.70309.28

Funk, S. D., Yurdagul, A. Jr., and Orr, A. W. (2012). Hyperglycemia and endothelial dysfunction in atherosclerosis: lessons from type 1 diabetes. *Int. J. Vasc. Med.* 2012, 569654–569654. doi: 10.1155/2012/569654

Hajra, L., Evans, A. I., Chen, M., Hyduk, S. J., Collins, T., and Cybulsky, M. I. (2000). The NF-κB signal transduction pathway in aortic endothelial cells is primed for activation in regions predisposed to atherosclerotic lesion formation. *Proc. Natl. Acad. Sci. U.S.A.* 97:9052. doi: 10.1073/pnas.97.16.9052

Hansson, G. K. (2005). Inflammation, atherosclerosis, and coronary artery disease. *New Engl. J. Med.* 352, 1685–1695. doi: 10.1056/NEJMra043430

Hassan, H. H., Denis, M., Krimbou, L., Marcil, M., and Genest, J. (2006). Cellular cholesterol homeostasis in vascular endothelial cells. *Can. J. Cardiol.* 22 Suppl B(Suppl B), 35b–40b. doi: 10.1016/s0828-282x(06)70985-0

Herrington, W., Lacey, B., Sherliker, P., Armitage, J., and Lewington, S. (2016). Epidemiology of atherosclerosis and the potential to reduce the global burden of atherothrombotic disease. *Circ. Res.* 118, 535–546. doi: 10.1161/circresaha.115.307611

Hu, W., Lu, H., Zhang, J., Fan, Y., Chang, Z., Liang, W., et al. (2018). Krüppel-like factor 14, a coronary artery disease associated transcription factor, inhibits endothelial inflammation via NF-κB signaling pathway. *Atherosclerosis* 278, 39–48. doi: 10.1016/j.atherosclerosis.2018.09.018

Hultgren, N. W., Fang, J. S., Ziegler, M. E., Ramirez, R. N., Phan, D. T. T., Hatch, M. M. S., et al. (2020). Slug regulates the Dll4-Notch-VEGFR2 axis to control endothelial cell activation and angiogenesis. *Nat. Commun.* 11:5400. doi: 10.1038/s41467-020-18633-z

Kalluri, A. S., Vellarikkal, S. K., Edelman, E. R., Nguyen, L., Subramanian, A., Ellinor, P. T., et al. (2019). Single-cell analysis of the normal mouse aorta reveals functionally distinct endothelial cell populations. *Circulation* 140, 147–163. doi: 10.1161/CIRCULATIONAHA.118.038362

Kalucka, J., de Rooij, L., Goveia, J., Rohlenova, K., Dumas, S. J., Meta, E., et al. (2020). Single-cell transcriptome atlas of murine endothelial cells. *Cell* 180, 764–779.e720. doi: 10.1016/j.cell.2020.01.015

Kanda, T., Brown, J. D., Orasanu, G., Vogel, S., Gonzalez, F. J., Sartoretto, J., et al. (2009). PPARgamma in the endothelium regulates metabolic responses to high-fat diet in mice. *J. Clin. Invest.* 119, 110–124. doi: 10.1172/jci36233

Kanno, S., Oda, N., Abe, M., Terai, Y., Ito, M., Shitara, K., et al. (2000). Roles of two VEGF receptors, Flt-1 and KDR, in the signal transduction of VEGF effects in human vascular endothelial cells. *Oncogene* 19, 2138–2146. doi: 10.1038/sj.onc.1203533

Krützfeldt, A., Spahr, R., Fau Mertens, S., Mertens, S., Fau Siegmund, B., Siegmund, B., et al. (1990). Metabolism of exogenous substrates by coronary endothelial cells in culture. *J. Mol. Cell Cardiol.* 22, 1393–1404. doi: 10.1016/0022-2828(90)90984-a

Kuo, A., Lee, M. Y., and Sessa, W. C. (2017). Lipid droplet biogenesis and function in the endothelium. *Circ. Res.* 120, 1289–1297. doi: 10.1161/circresaha.116.310498

Liu, M., Leibowitz, J. L., Clark, D. A., Mendicino, M., Ning, Q., Ding, J. W., et al. (2003). Gene transcription of fgl2 in endothelial cells is controlled by Ets-1 and Oct-1 and requires the presence of both Sp1 and Sp3. *Eur. J. Biochem.* 270, 2274–2286. doi: 10.1046/j.1432-1033.2003.03595.x

Liu, X., Chen, W., Li, W., Li, Y., Priest, J. R., Zhou, B., et al. (2019). Single-Cell RNA-Seq of the developing cardiac outflow tract reveals convergent development of the vascular smooth muscle cells. *Cell Rep.* 28, 1346–1361e1344. doi: 10.1016/j.celrep.2019.06.092

Lusis, A. J. (2000). Atherosclerosis. *Nature* 407, 233–241. doi: 10.1038/35025203

Ma, J., Sanchez-Duffhues, G., Goumans, M.-J., and ten Dijke, P. (2020). TGF-β-induced endothelial to mesenchymal transition in disease and tissue engineering. *Front. Cell Dev. Biol.* 8:260. doi: 10.3389/fcell.2020.00260

Mahmoud, M. M., Serbanovic-Canic, J., Feng, S., Souilhol, C., Xing, R., Hsiao, S., et al. (2017). Shear stress induces endothelial-to-mesenchymal transition via the transcription factor Snail. *Sci. Rep.* 7:3375. doi: 10.1038/s41598-017-03532-z

Mehrotra, D., Wu, J., Papangeli, I., and Chun, H. J. (2014). Endothelium as a gatekeeper of fatty acid transport. *Trends Endocrinol. Metab.* 25, 99–106. doi: 10.1016/j.tem.2013.11.001

Paik, D. T., Tian, L., Williams, I. M., Rhee, S., Zhang, H., Liu, C., et al. (2020). Single-Cell RNA sequencing unveils unique transcriptomic signatures of organ-specific endothelial cells. *Circulation* 142, 1848–1862. doi: 10.1161/CIRCULATIONAHA.119.041433

Patella, F., Schug, Z. T., Persi, E., Neilson, L. J., Erami, Z., Avanzato, D., et al. (2015). Proteomics-based metabolic modeling reveals that fatty acid oxidation (FAO) controls endothelial cell (EC) permeability. *Mol. Cell Proteomics* 14, 621–634. doi: 10.1074/mcp.M114.045575

Piera-Velazquez, S., and Jimenez, S. A. (2019). Endothelial to mesenchymal transition: role in physiology and in the pathogenesis of human diseases. *Physiol. Rev.* 99, 1281–1324. doi: 10.1152/physrev.00021.2018

Rohlenova, K., Goveia, J., Garcia-Caballero, M., Subramanian, A., Kalucka, J., Treps, L., et al. (2020). Single-Cell RNA sequencing maps endothelial metabolic plasticity in pathological angiogenesis. *Cell Metab.* 31, 862–877.e814. doi: 10.1016/j.cmet.2020.03.009

Sangwung, P., Zhou, G., Nayak, L., Chan, E. R., Kumar, S., Kang, D. W., et al. (2017). KLF2 and KLF4 control endothelial identity and vascular integrity. *JCI Insight* 2:e91700. doi: 10.1172/jci.insight.91700

Schoonderwoerd, K., and Stam, H. (1992). Lipid metabolism of myocardial endothelial cells. *Mol. Cell. Biochem.* 116, 171–179. doi: 10.1007/BF01270585

Schoors, S., Bruning, U., Missiaen, R., Queiroz, K. C., Borgers, G., Elia, I., et al. (2015). Fatty acid carbon is essential for dNTP synthesis in endothelial cells. *Nature* 520, 192–197. doi: 10.1038/nature14362

Sheikh, F., Lyon, R. C., and Chen, J. (2015). Functions of myosin light chain-2 (MYL2) in cardiac muscle and disease. *Gene* 569, 14–20. doi: 10.1016/j.gene.2015.06.027

Shimizu, T., Maruyama, K., Kawamura, T., Urade, Y., and Wada, Y. (2020). PERK participates in cardiac valve development via fatty acid oxidation and endocardial-mesenchymal transformation. *Sci. Rep.* 10:20094. doi: 10.1038/s41598-020-77199-4

Son, N.-H., Basu, D., Samovski, D., Pietka, T. A., Peche, V. S., Willecke, F., et al. (2018). Endothelial cell CD36 optimizes tissue fatty acid uptake. *J. Clin. Invest.* 128, 4329–4342. doi: 10.1172/JCI99315

Souilhol, C., Harmsen, M. C., Evans, P. C., and Krenning, G. (2018). Endothelial-mesenchymal transition in atherosclerosis. *Cardiovasc. Res.* 114, 565–577. doi: 10.1093/cvr/cvx253

Stamatikos, A., Dronadula, N., Ng, P., Palmer, D., Knight, E., Wacker, B. K., et al. (2019). ABCA1 overexpression in endothelial cells *In Vitro* Enhances ApoAI-mediated cholesterol efflux and decreases inflammation. *Hum. Gene. Ther.* 30, 236–248. doi: 10.1089/hum.2018.120

Subramanian, S., Han, C. Y., Chiba, T., McMillen, T. S., Wang, S. A., Haw, A. III, et al. (2008). Dietary cholesterol worsens adipose tissue macrophage accumulation and atherosclerosis in obese LDL receptor-deficient mice. *Arterioscler. Thromb. Vasc. Biol.* 28, 685–691. doi: 10.1161/ATVBAHA.107.157685

Theodorou, K., and Boon, R. A. (2018). Endothelial cell metabolism in atherosclerosis. *Front. Cell Dev. Biol.* 6:82. doi: 10.3389/fcell.2018.00082

Tombor, L. S., John, D., Glaser, S. F., Luxan, G., Forte, E., Furtado, M., et al. (2021). Single cell sequencing reveals endothelial plasticity with transient mesenchymal activation after myocardial infarction. *Nat. Commun.* 12:681. doi: 10.1038/s41467-021-20905-1

Tsukahara, R., Haniu, H., Matsuda, Y., and Tsukahara, T. (2014). Heart-type fatty-acid-binding protein (FABP3) is a lysophosphatidic acid-binding protein in human coronary artery endothelial cells. *FEBS Open Bio* 4, 947–951. doi: 10.1016/j.fob.2014.10.014

Wang, J., Xian, X., Huang, W., Chen, L., Wu, L., Zhu, Y., et al. (2007). Expression of LPL in endothelial-intact artery results in lipid deposition and vascular cell adhesion molecule-1 upregulation in both LPL and ApoE-deficient mice. *Arterioscler. Thromb. Vasc. Biol.* 27, 197–203. doi: 10.1161/01.ATV.0000249683.80414.d9

Welch-Reardon, K. M., Ehsan, S. M., Wang, K., Wu, N., Newman, A. C., Romero-Lopez, M., et al. (2014). Angiogenic sprouting is regulated by endothelial cell expression of Slug. *J. Cell Sci.* 127(Pt 9), 2017–2028. doi: 10.1242/jcs.143420

Wesseling, M., Sakkers, T. R., de Jager, S. C. A., Pasterkamp, G., and Goumans, M. J. (2018). The morphological and molecular mechanisms of epithelial/endothelial-to-mesenchymal transition and its involvement in atherosclerosis. *Vascul. Pharmacol.* 106, 1–8. doi: 10.1016/j.vph.2018.02.006

Xiong, J., Kawagishi, H., Yan, Y., Liu, J., Wells, Q. S., Edmunds, L. R., et al. (2018). A metabolic basis for endothelial-to-mesenchymal transition. *Mol. Cell* 69, 689–698.e7. doi: 10.1016/j.molcel.2018.01.010

Yuan, S., Zhang, S., Zhuang, Y., Zhang, H., Bai, J., and Hou, Q. (2015). Interleukin-17 Stimulates STAT3-mediated endothelial cell activation for neutrophil recruitment. *Cell. Physiol. Biochem.* 36, 2340–2356. doi: 10.1159/000430197

Zachary, I., and Gliki, G. (2001). Signaling transduction mechanisms mediating biological actions of the vascular endothelial growth factor family. *Cardiovasc. Res.* 49, 568–581. doi: 10.1016/s0008-6363(00)00268-6

Conflict of Interest: The authors declare that the research was conducted in the absence of any commercial or financial relationships that could be construed as a potential conflict of interest.

Copyright © 2021 Zhao, Lu, Liu, Zhao, Zhu, Garcia-Barrio, Chen and Zhang. This is an open-access article distributed under the terms of the Creative Commons Attribution License (CC BY). The use, distribution or reproduction in other forums is permitted, provided the original author(s) and the copyright owner(s) are credited and that the original publication in this journal is cited, in accordance with accepted academic practice. No use, distribution or reproduction is permitted which does not comply with these terms.

frontiers in Cell and Developmental Biology

REVIEW
published: 26 May 2021
doi: 10.3389/fcell.2021.688388

Sinner or Saint?: Nck Adaptor Proteins in Vascular Biology

*Mabruka Alfaidi[1], Matthew L. Scott[1] and Anthony Wayne Orr[1,2,3]**

[1] Department of Pathology and Translational Pathobiology, Louisiana State University Health – Shreveport, Shreveport, LA, United States, [2] Department of Cell Biology and Anatomy, LSU Health – Shreveport, Shreveport, LA, United States, [3] Department of Molecular & Cellular Physiology, LSU Health – Shreveport, Shreveport, LA, United States

The Nck family of modular adaptor proteins, including Nck1 and Nck2, link phosphotyrosine signaling to changes in cytoskeletal dynamics and gene expression that critically modulate cellular phenotype. The Nck SH2 domain interacts with phosphotyrosine at dynamic signaling hubs, such as activated growth factor receptors and sites of cell adhesion. The Nck SH3 domains interact with signaling effectors containing proline-rich regions that mediate their activation by upstream kinases. In vascular biology, Nck1 and Nck2 play redundant roles in vascular development and postnatal angiogenesis. However, recent studies suggest that Nck1 and Nck2 differentially regulate cell phenotype in the adult vasculature. Domain-specific interactions likely mediate these isoform-selective effects, and these isolated domains may serve as therapeutic targets to limit specific protein-protein interactions. In this review, we highlight the function of the Nck adaptor proteins, the known differences in domain-selective interactions, and discuss the role of individual Nck isoforms in vascular remodeling and function.

Keywords: actin cytoskeleton, receptor tyrosine kinase, SH2/SH3 domains, developmental biology, vascular biology, Nck1/Nck2, adaptor proteins, binding parners

OPEN ACCESS

Edited by:
Xiaofeng Yang,
Temple University, United States

Reviewed by:
Jingyan Han,
Boston University, United States
Jianxin Sun,
Thomas Jefferson University, United States

***Correspondence:**
Anthony Wayne Orr
aorr@lsuhsc.edu

Specialty section:
This article was submitted to Signaling, a section of the journal Frontiers in Cell and Developmental Biology

Received: *30 March 2021*
Accepted: *28 April 2021*
Published: *26 May 2021*

Citation:
Alfaidi M, Scott ML and Orr AW (2021) Sinner or Saint?: Nck Adaptor Proteins in Vascular Biology. Front. Cell Dev. Biol. 9:688388. doi: 10.3389/fcell.2021.688388

ADAPTOR PROTEINS IN SIGNAL TRANSDUCTION RESEARCH

Mammalian cells express more than 500 kinases and more than 200 phosphatases that regulate nearly every aspect of cellular function. Regulated spatial organization enhances the specificity of these kinase and phosphatase reactions to generate specific cellular outputs. To accomplish this organization, the cell utilizes a host of modular adaptor proteins to mediate specific protein-protein interactions through various interacting domains (Birge et al., 1996). While lacking enzymatic activity, these modular adaptor proteins utilize various interacting domains to regulate a variety of cellular processes, and their deletion often results in embryonic lethality (Bladt et al., 2003). This review focuses on the non-catalytic region of tyrosine kinase (Nck) family of adaptor proteins that couples tyrosine phosphorylation to changes in cell morphology, gene expression, and function in a variety of vascular diseases. In it, we discuss the classic role of Nck adaptor proteins in cytoskeletal remodeling and vascular morphogenesis and new roles for Nck isoforms in the regulation of gene expression and vascular cell phenotype.

Nck FAMILY OF SIGNALING ADAPTORS

The Nck family of Src homology 2 (SH2) and SH3 domain-containing adaptor proteins, including Nck1 (Nckα) and Nck2 (Nckβ, Grb4) were first identified in 1990 (Lehmann et al., 1990) and were subsequently isolated from multiple organs, including the brain, heart, lung, liver, and kidney (Li et al., 1992; Park and Rhee, 1992). The Nck1 gene localizes to chromosome 3q21 in a region mutated in various cancers (Chen et al., 1998), and genome-wide association studies (GWAS) link Nck1 single nucleotide polymorphisms (SNPs) with obesity, dyslipidemia, circulating leukocyte counts, platelet counts, and coronary artery disease (Locke et al., 2015; van der Harst and Verweij, 2018; Chen M. H. et al., 2020). The Nck2 gene localizes to chromosome 2 band q12 (2q12) in a region linked to neurological development (Chen et al., 1998; Griggs et al., 2009; Hladilkova et al., 2015), and GWAS analysis link Nck2 SNPs to drug addiction, Alzheimer's Disease, and platelet levels (Liu et al., 2013; Chen M. H. et al., 2020; Schwartzentruber et al., 2021). While Nck1 shows similar expression across adult tissues, Nck2 shows higher expression in the spleen and skeletal muscle and lower expression in the liver (Chen et al., 1998; Bladt et al., 2003; Latreille et al., 2011). In addition, several studies have shown altered Nck1/2 expression in disease states. Multiple cancer models show enhanced Nck1 expression, driven at least in part by the expression of the Nck1-antisense (AS) LncRNA, which competes for miR-137 binding to Nck1 mRNA (Deshpande et al., 2019; Chang et al., 2020; Liu et al., 2020). Similarly, metastatic melanoma cell lines shower higher Nck2 expression compared to non-metastatic melanoma (de Wit et al., 2005; Labelle-Cote et al., 2011). In addition, cardiometabolic disease is also associated with elevated Nck1 expression, as Nck1 expression is enhanced in endothelial cells overlying human atherosclerotic plaques compared to healthy vessels and in adipocytes in white adipose tissue from obese or aging mice (Haider et al., 2018; Alfaidi et al., 2020a). However, Nck2 shows reduced expression in white adipose tissue from obese humans (Dusseault et al., 2016), suggesting Nck1 and Nck2 may play differential roles in cardiometabolic disease. While differential expression may be due to altered transcription, Nck1 and Nck2 also show differential regulation by post-translational degradation. In podocytes, c-Cbl mediates the ubiquitination of Nck1, but not Nck2, on Lys178 resulting in selective Nck1 degradation (Buvall et al., 2013).

Despite being expressed by different genes, Nck1 and Nck2 in humans share 68% amino acid identity and 79% similarity (**Figure 1A**) and possess both conserved and distinct downstream signaling partners (Chen et al., 1998; Lettau et al., 2009; **Figure 1B**). The C-terminal SH2 domain in Nck binds to specific phosphotyrosine residues (pTyr) at dynamic signaling hubs, such as activated growth factor receptors and sites of cell adhesion (Becker et al., 2000). Through its three tandem SH3 domains, Nck interacts with proteins containing proline-rich regions to form a local signaling scaffold to recruit proteins involved in cytoskeletal remodeling and regulation of gene expression (Pawson, 1995; McCarty, 1998; Lettau et al., 2009; Chaki and Rivera, 2013).

Nck 1/2 DOMAINS AND INTERACTING PROTEINS

The modular architecture of adaptor proteins allows for numerous individual and potentially simultaneous protein-protein interactions (McCarty, 1998). Over the past decade, more than 60 Nck interaction partners have been identified, mostly involved in actin cytoskeleton organization (Bokoch et al., 1996; Galisteo et al., 1996; Lu et al., 1997; Bokoch, 2003). While many Nck1/2 binding partners interact with both isoforms, some interactions preferentially occur with select Nck isoforms and may therefore confer isoform-selective functions (Lettau et al., 2009, 2010; Jacquet et al., 2018). In this section, we discuss the structure, function, specificity, and regulation of the SH2 and SH3 domains that make up the Nck family adaptor proteins.

SH2 Domains

Phosphotyrosine promotes signaling complex formation by recruiting signaling proteins with phosphotyrosine-binding (PTB) domains, such as SH2 domains and PTB domains. SH2 domains consist of ∼100 amino acids forming a central anti-parallel β-sheet and two flanking α-helices that bind short phosphotyrosine motifs in interacting proteins (**Figure 1C**; Waksman et al., 1992; Liu B. A. et al., 2006). A positively charged pocket with a conserved Arg residue on one side of the central β-sheet contributes to high-affinity phosphotyrosine binding, whereas an extended binding surface on the other side contains more variable residues that contribute to domain-selective interactions with sequences C-terminal to phosphotyrosine (Waksman et al., 1992). The human and mouse genome encodes for 120 SH2 domains across 110 different proteins that regulate protein interaction (adaptors, scaffolds), phosphorylation, small GTPase activation, cytoskeletal and chromatin remodeling, signal regulation, and protein ubiquitination (Liu B. A. et al., 2006).

The Nck1 and Nck2 SH2 domains show both similarities and differences in their binding properties. The Nck1 and Nck2 SH2 domains bind to a similar pY-D/E-x-V/P consensus sequence in target proteins (**Figure 1A**), although alterations in the C-terminal amino acids may affect binding specificity and affinity (Frese et al., 2006). Phosphorylation of Platelet Endothelial Cell Adhesion Molecule-1 (PECAM-1) on Tyr663 (pYTEV) supports binding to both the Nck1 and Nck2 SH2 domain (Machida et al., 2007; Alfaidi et al., 2020b), whereas phosphorylation on the similar Tyr686 (pYSEV) site did not support binding of either Nck1 or Nck2 (Machida et al., 2007). Moreover, both Nck1 SH2 and Nck2 SH2 bind to platelet derived growth factor (PDGF) and epidermal growth factor (EGF) receptors, but the Nck2 SH2 domain binds with a higher affinity than the Nck1 SH2 domain (Chen et al., 1998). This differential affinity may be due to Nck1 SH2 domains and Nck2 SH2 domains binding at different sites, as the PDGF receptor phosphotyrosine residue pY751 specifically interacts with Nck1 (Nishimura et al., 1993), whereas pY1009 specifically interacts with Nck2 (Chen et al., 2000). Similarly, phosphorylated ephrinB1 associates specifically with the Nck2 SH2 domain but not with the Nck1 SH2 domain (Stein et al., 1998; Pesti et al., 2012). Additional information on Nck1/2 SH2

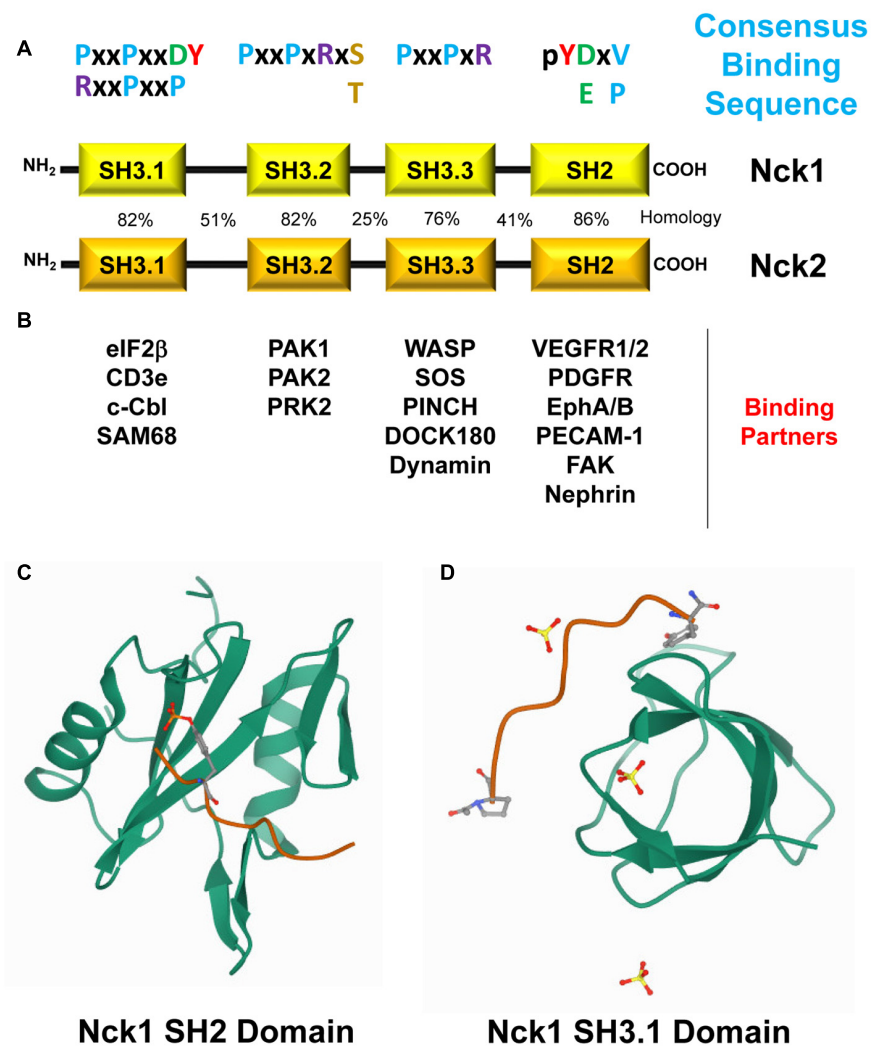

FIGURE 1 | (A) Modular Structure of Nck1 and Nck2 and their binding partners. Nck1 and Nck2 consist of one C-terminal Src-homology domain 2 (SH2) and three N-terminal SH3 domains. The sequence homology in humans (%) of each domain, their consensus binding sequence, and their known binding partners are shown. **(B)** Selected Nck binding partners and the domains of Nck that mediate these interactions are shown. **(C)** The Nck1 SH2 domain (PBD ID: 2CI9, RCSB Protein Data Bank, https://www.rcsb.org/) complexed with a phosphotyrosine peptide (Frese et al., 2006). **(D)** The Nck1 SH3.1 domain (PBD ID: 5QU2, RCSB Protein Data Bank, https://www.rcsb.org/) complexed with a PPPVPNPDY peptide (Richter et al., unpublished).

identified binding partners and their interacting sequences are provided in **Table 1**.

SH3 Domains

Proline-rich regions in proteins bind to a variety of domains, such as SH3 domains, WW domains, and EVH domains. SH3 domains represent one of the largest families of modular domains, with humans expressing over 300 SH3 domains in over 200 proteins (Mayer and Gupta, 1998; Teyra et al., 2017). Composed of ∼60 amino acids, SH3 domains consist of five or six β-sheets arranged in two tightly packed anti-parallel β sheets forming a β-barrel (**Figure 1D**; Musacchio et al., 1992). The hydrophobic binding pocket of SH3 domains is enriched in aromatic and carboxylic amino acids with a conserved WPY triad critical for binding to proline-rich peptides (Musacchio et al., 1992; Chakrabarti and Janin, 2002). Mutation of the conserved Trp (W) residues in the WPY triad often results in significantly reduced binding efficiency (Lim and Richards, 1994; Lee et al., 1995). The hydrophobic binding pocket interacts with PxxP motifs in target proteins, while an adjacent RT loop and n-Src loop interacts with positively charged Arg/Lys residues on either side of the PxxP motif (Teyra et al., 2017). Proline-rich sequences can be divided into Class I motifs (RxxPxxP) and Class II motifs (PxxPxR) depending upon the relative position of the charged amino acids. However, several SH3 domains can bind peptides outside of this basic structure, such as R/K-rich peptides, thereby conferring greater specificity to the SH3 domain interactions (Teyra et al., 2017). While the SH3 does not show the same requirement for phosphorylation as observed for SH2 domains, phosphorylation of Ser and Thr residues adjacent to the conserved Arg/Lys

residues (PxxPxRS/T) often results in reduced binding affinity (Howe and Juliano, 2000; Yurdagul Chen et al., 2013).

Several proteins interact with one or more of the Nck SH3 domains (**Table 2**; Pawson, 1995; Bokoch et al., 1996; Galisteo et al., 1996; Wang et al., 2000; Lettau et al., 2010). However, most interactions have not been tested for Nck1/2 selectivity (Lettau et al., 2010). Nck has three N-terminal SH3 domains, often referred to as SH3.1, SH3.2, and SH3.3. The Nck1 and Nck2 SH3.1 domain shows specificity for both class I and class II proline-rich sequences, with enhanced affinity to the class II sequence containing the PxxPxxDY motif (Aitio et al., 2008; Saksela and Permi, 2012). Phosphorylation of this Tyr residue abolishes ligand-binding affinity (Kesti et al., 2007; Takeuchi et al., 2008). The SH3.2 and SH3.3 domains exhibit high affinity for PxxPxR motif, with the second SH2 domain preferring a PxxPxRxS/T motif such as that found in the classic Nck-binding partner p21 activated kinase (PAK; Liu J. et al., 2006). The group I PAKs (PAK1/2/3) function as downstream effectors of the small GTPases Cdc42 and Rac-1. PAK normally exists as a transinhibited dimer, with an autoinhibitory domain of one PAK molecule binding and inhibiting the kinase domain of a second PAK. PAK activation involves its recruitment to phosphotyrosine-based signaling hubs in the plasma membrane through interaction with modular adaptor proteins, such as Nck and Grb2 (Li et al., 1992, 2001). PAK, through its conserved proline-rich region, binds to Nck SH3.2 and to a lesser extent to Nck SH3.3 (Bokoch et al., 1996; Galisteo et al., 1996; Lu et al., 1997; Bokoch, 2003). Upon membrane targeting, PAK can interact with active, GTP-bound Rac and cdc42 to relieve autoinhibition and promote PAK kinase activity. Active PAK contributes to cytoskeleton remodeling, actomyosin contractility, and activation of signaling pathways that regulate gene transcription (Manser et al., 1997; Bokoch, 2003).

Due to its inducible nature, Nck1/2 is generally recruited to signaling hubs through interaction between its SH2 domain and phosphotyrosine. However, this isn't always the case. Nck's SH3.1 domain can interact with PxxDY motifs on target proteins, such as the T cell receptor (TCR), to initiate signaling complex formation (Gil et al., 2002; Lettau et al., 2010). Nck binds to TCR initially through its SH3.1 domain and this binding recruits Src kinase through the other Nck SH3 domains to phosphorylate TCR and facilitate a secondary SH2-mediated Nck binding to tyrosine phosphorylated TCR (Gil et al., 2002; Lettau et al., 2010).

TABLE 1 | Some of the known Nck1/2 SH2 binding partners.

Binding partner	Binding site	Nck isoform	pTyr sequence	Reference
PDGFRB	PY751	Nck1	VDpYVPMLDMK	Nishimura et al., 1993
EPHB1	PY594	Nck1	KIpYIDPFTYE	Becker et al., 2000
PDGFR	PY1009	Nck2	VLpYTAVQPNE	Chen et al., 2000
FAK	pY397	Nck2	DDpYAEIIDEE	Goicoechea et al., 2002
VEGFR2	pY1214	Nck1/2?	FHpYDNTAGIS	Lamalice et al., 2006
Flt-1 (VEGFR1)	pY1333	Nck1/2?	VLpYSTPPI	Ito et al., 1998
Flt-1 (VEGFR1)	pY1213	Nck1/2?	VRpYVNAFKFM	Igarashi et al., 1998
Nephrin	pY1193	Nck1/2?	PLpYDEVQMGP	Verma et al., 2006
Cortactin	pY421	Nck1/2?	pYEDAASFKAE	Oser et al., 2009
PECAM-1	pY663	Nck1/2	VQpYTEVQVSS	Machida et al., 2007; Alfaidi et al., 2020b
BCR-Abl	pY177	Nck2, not tested for Nck1	PFpYVNVEFHH	Coutinho et al., 2000

PY, phosphotyrosine; PDGFR, platelet derived growth factor receptor; VEGFR, vascular endothelial growth factor receptor; PECAM-1, platelet endothelial adhesion molecule 1; BCR, B-cell receptor; FGFR, fibroblast growth factor receptor; FAK, focal adhesion kinase.

TABLE 2 | Some of the known Nck1/2 SH3 binding partners.

Binding partner	SH3 domain involved	Nck isoform	Proline rich sequence	Reference
PAK	SH3.2; less SH3.3	Nck1	KPPAPPMRNTSTM	Bokoch et al., 1996; Galisteo et al., 1996; Bokoch, 2003
WASP	SH3.1, SH3.2, SH3.3	Nck1	GRSGPXPPXP	Rivero-Lezcano et al., 1995
CYFIP2	SH3.1	Nck2	Uncharacterized	Lettau et al., 2010
FasL	SH3.2, less SH3.3	Nck2	PPLPLPPLKKR	Lettau et al., 2006
eIF beta	SH3.1, SH3.3	Nck1/2?	Uncharacterized	Kebache et al., 2002
Cortactin	SH3?	Nck1/2?	KPPVPPKP	Kruchten et al., 2008
CD3ε	SH3.1	Nck1/2?	NKERPPPVPNPDY	Sun et al., 2011
R-Ras	SH3.2; less SH3.3	Nck1/2?	PPSPPSAPRKK	Wang et al., 2000
SAM68	SH3.1	Nck1/2	Uncharacterized	Lawe et al., 1997
NIK	SH3	Nck2, not tested for Nck1	SODPCPPSRS/PRVPVRTTSR	Su et al., 1997

PAK, P21-activated kinase; WASP, Wiskott-Aldrich syndrome protein; CYFIP2, cytoplasmic FMR1-interacting protein 2; FasL, Fas ligand; TCR, T cell receptor; FAK, focal adhesion kinase; SAM68, SRC associated in mitosis of 68 kDa; NIK, Nck inducing kinase; SAPK, stress activated protein kinase; eIF, eukaryotic initiation factor.

Phosphorylation and Intramolecular Interactions

While Nck1/2 undergoes inducible interaction with phosphotyrosine motifs and phosphorylation-inhibitable interactions with proline-rich motifs, another mode of Nck regulation may involve regulation of intramolecular interactions. Intramolecular interactions constrain the activity of several known kinases (e.g., Src, Janus, ZAP70), but less is known about intramolecular interactions regulating adaptor protein function (Kurochkina and Guha, 2013). Takeuchi and colleagues demonstrated a self-inhibitory intramolecular interaction between the Nck SH3.2 domain and a K/RxK/RRxxS sequence in the linker region between the SH3.1 and SH3.2 domain (Takeuchi et al., 2010). This interaction masks the Nck SH3.2 domain and may serve as a mechanism to limit Nck protein complex formation in the absence of stimulus (**Figure 2A**). Since this work used purified Nck protein, the relevance of the autoinhibited conformation to Nck function within the cell remains to be determined. Interestingly, the linker region between the Nck SH3.1 and SH3.2 domains is a site of extensive phosphorylation. While Nck1/2 undergoes phosphorylation in a variety of conditions (Li et al., 1992; Park and Rhee, 1992; Schmitz et al., 1997; Dionne et al., 2018), the function of these phosphorylation events remain virtually unknown. However, the inclusion of the Ser residue in this intramolecular inhibitory sequence (Ser85) may allow for phosphorylation-dependent relief of autoinhibition (**Figures 2B,C**). Multiple groups have shown Nck phosphorylation on Ser85 is associated with cell stimulation (Dephoure et al., 2008; Mayya et al., 2009; Konakahara et al., 2012; Dionne et al., 2018). Shear stress, H_2O_2, and hypoxia/reoxygenation injury all induce PAK2-Nck1/2 interactions, consistent with this interaction being inhibited under unstimulated conditions (Yurdagul Chen et al., 2013; Chen et al., 2015). In addition, phosphorylation of the conserved WPY triad in the Nck SH3 domains inhibits SH3 interactions as a negative feedback mechanism (**Figure 2D**) (Dionne et al., 2018). Proteomic analysis of liver ischemia-reperfusion injury identified Nck1 as a prominent tyrosine-phosphorylated protein (Emadali et al., 2007), suggesting that Nck tyrosine phosphorylation may be relevant to human disease. In addition to SH3 inhibition, Nck tyrosine phosphorylation sites may also induce intramolecular interactions with the Nck SH2 domain to inhibit SH2 domain function or may serve as a binding site for other SH2 and PTB domain containing proteins to enlarge the signaling complex.

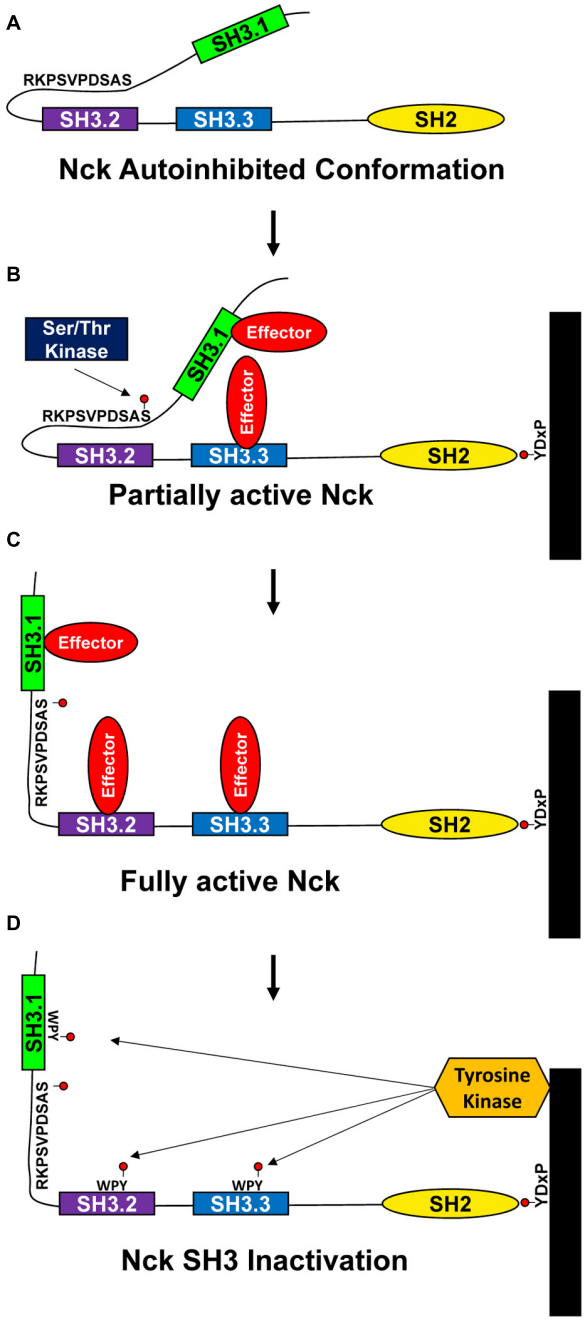

FIGURE 2 | Proposed model for Nck1/2 regulation. **(A)** Intramolecular interactions between the Nck1/2 SH3.2 domain and a peptide in the linker between the SH3.1 and SH3.2 domains may limit SH3.2 interactions with other targets. **(B,C)** Phosphorylation of Ser85 in response to cell stimulation may reduce this intramolecular interaction to activate Nck1/2, allowing recruitment of effector proteins. **(D)** Tyrosine phosphorylation within the WPY motifs in the SH3 domains may limit SH3 domain interactions to inactivate Nck1/2.

MAJOR FUNCTIONS OF Nck 1/2

The Nck SH2/SH3 domains couple sites of tyrosine phosphorylation to the activation of downstream signaling partners that regulate cytoskeletal remodeling, gene transcription, protein translation, and cell survival (Li et al., 1992; Pawson and Scott, 1997; McCarty, 1998; Pawson and Nash, 2003; Pesti et al., 2012; Oeste and Alarcon, 2015; Porter and Day, 2016). However, depending on the extracellular stimulus and cell type, Nck1 and Nck2 may be capable of selectively regulating different responses within the cell (McCarty, 1998). In this section, we discuss the known role for Nck1/2 signaling in the regulation of cell function, and we identify potential roles for isoform-specific functions of Nck1 and Nck2 in this regard.

Cytoskeletal Remodeling and Cell Migration

Several previous reviews describe the important role for Nck1/2 in the regulation of cytoskeletal remodeling and cell migration (Li et al., 2001; Chaki and Rivera, 2013). Both Nck1 and Nck2 bind to hubs of tyrosine phosphorylation, such as pro-migratory activated growth factor receptors, chemorepulsive guidance molecule receptors, and sites of cell-matrix adhesions (Li et al., 1992; Meisenhelder and Hunter, 1992). After targeting these sites, Nck1/2 recruits and regulates several proteins involved in actin remodeling and cell migration (Li et al., 1992; Meisenhelder and Hunter, 1992). Nck1/2 recruitment to tyrosine phosphorylated receptor tyrosine kinases in the leading edge of migrating cells recruits the WASP/WAVE proteins to enhance Arp2/3 complex activation and actin branching (**Figure 3A**; Li et al., 2001; Chaki and Rivera, 2013). PAK recruitment and activation promotes turnover of actin filaments and integrin adhesions to enhance actin dynamics at the leading edge (Zhao et al., 2000; Stoletov et al., 2001). As such, Nck deficient cells fail to induce cytoskeletal remodeling and membrane ruffles in response to growth factor stimulation (Rivera et al., 2006). In addition, Nck1/2 recruitment to the leading edge regulates polarized cell migration by mediating activation of the polarity complex (cdc42, atypical PKC), suggesting roles in both actin dynamics and directed cell migration (Chaki et al., 2013). As cells migrate, formation of cell matrix adhesions stabilizes protrusions, perpetuate actin remodeling signaling, and mediate the actomyosin propulsive force (Huttenlocher and Horwitz, 2011). However, large adhesion sites limit cell migration by hindering release of cell-matrix adhesions during tail retraction (Huttenlocher and Horwitz, 2011). Nck1/2 binds to focal adhesion kinase (FAK) to facilitate recruitment to cell matrix adhesions. Focal adhesion targeting enhances cell migration through PAK recruitment, recruitment of the PAK-associated RacGEF, β-Pix, and focal adhesion turnover (Zhao et al., 2000; Stoletov et al., 2001). While Nck1 and Nck2 are often ascribed redundant roles in cell migration, this is not always the case. Silencing of Nck2, but not Nck1, blunts nerve growth factor-induced neurite outgrowth, associated with diminished paxillin levels (Guan et al., 2007). In contrast, axon retraction in response to EphA3 activation requires Nck1 binding (Hu et al., 2009). Furthermore, although both Nck1 and Nck2 expression can drive podosome formation, Nck2 deletion showed a stronger reduction than Nck1 deletion in reducing podosome-associated matrix invasion (Chaki et al., 2019).

Transcription Factor Activation

Nck recruitment to phosphotyrosine signaling hubs promotes the activation of several signaling pathways that regulate gene expression. Tyrosine kinases classically activate the mitogen-activated protein kinase (MAPK) pathways resulting in activation of the c-fos/c-jun transcription factor, activated protein-1 (AP-1). Activation of c-fos by the ERK/MAPK pathway classically involves the SH2/SH3 adaptor protein Grb2, which recruits the RasGEF Son of Sevenless (SOS) to drive Ras-dependent ERK signaling (Buday and Downward, 1993; Egan et al., 1993; Gale et al., 1993). While early studies with Nck1/2 show SOS binding and Nck-dependent c-fos activation (Hu et al., 1995; Okada and Pessin, 1996; Gupta and Mayer, 1998), Nck1/2 does not contribute to ERK activation in response to several growth factors (Tanaka et al., 1995; Roche et al., 1996; Rockow et al., 1996). However, Nck1/2 regulates the c-jun N-terminal kinase (JNK) pathway by multiple mechanisms. Nck1/2 recruits Nck-Interacting Kinase (NIK; mitogen activated protein 4 kinase 4, MAP4K4) driving NIK-dependent JNK activation (**Figure 3B**; Su et al., 1997; Becker et al., 2000; Machida et al., 2004). In addition, Nck1/2 can also promote JNK through activation of Traf2- and Nck-interacting kinase (TNIK) or PAK (Schmitz et al., 2001; Poitras et al., 2003; Hahn et al., 2009; Shitashige et al., 2010). In contrast to the MAPK cascades, Nck1 shows a preferential activation of the proinflammatory transcription factors nuclear factor κ-light-chain-enhancer of activated B cells (NF-κB) and nuclear factor of activated T cells (NFAT; **Figure 3B**). Nck1, but not Nck2, mediates endothelial NF-κB activation in response to shear stress (Alfaidi et al., 2020a), and Nck1 recruitment to the T cell receptor drives PAK1-dependent NFAT activation (Yablonski et al., 1998; Ngoenkam et al., 2014). Finally, Nck1/2 binds phosphorylated nephrin in podocytes and sequesters/inactivates Lats1, thereby enhancing activation of the mechanically regulated transcription factor Yap, a key regulator of cell growth and proliferation (Keyvani Chahi et al., 2016).

Protein Translation and Endoplasmic Reticulum Stress

In addition to regulating mRNA transcription, Nck adaptor proteins also regulate mRNA translation. Insulin stimulation promotes Nck1 recruitment into the enhanced ribosomal fraction through interactions between the Nck1 SH3.1/SH3.3 domains and eukaryotic initiation factor eIF2β (Kebache et al., 2002). Additionally, Nck1 upregulation enhances protein translation, suggesting that this targeting to the enhanced ribosomal fraction may promote translation (Kebache et al., 2002).

Nck signaling also regulates multiple aspects of the unfolded protein response (UPR) during endoplasmic reticulum (ER) stress. When misfolded proteins accumulate in the ER, UPR activation transiently slows translation and enhances expression of ER chaperones to facilitate cell recovery. The UPR consists of three distinct ER resident transmembrane stress sensors: protein kinase R-like ER kinase (PERK), inositol-requiring enzyme 1 alpha (IRE1a), and activating transcription factor 6 (ATF6) (Welihinda et al., 1999; Harding et al., 2000; Zhang et al., 2002). PERK phosphorylation stimulates eIF2α phosphorylation and inhibition of eIF2α-dependent mRNA translation (Cao and Kaufman, 2012). However, select genes, such as ATF4, show enhanced expression following eIF2α phosphorylation, allowing ATF4 to drive the expression of the antioxidant response, ER chaperones, and the apoptosis-associated protein CHOP. PERK phosphorylation on Y561 (pY^{561}DxVxxD/E) recruits Nck1 to limit PERK activation and eIF2α phosphorylation (**Figure 3C**; Yamani et al., 2014). In addition, Nck recruits the phosphatase PP1c into this complex to dephosphorylate eIF2α (Latreille and Larose, 2006). IRE1α activation promotes

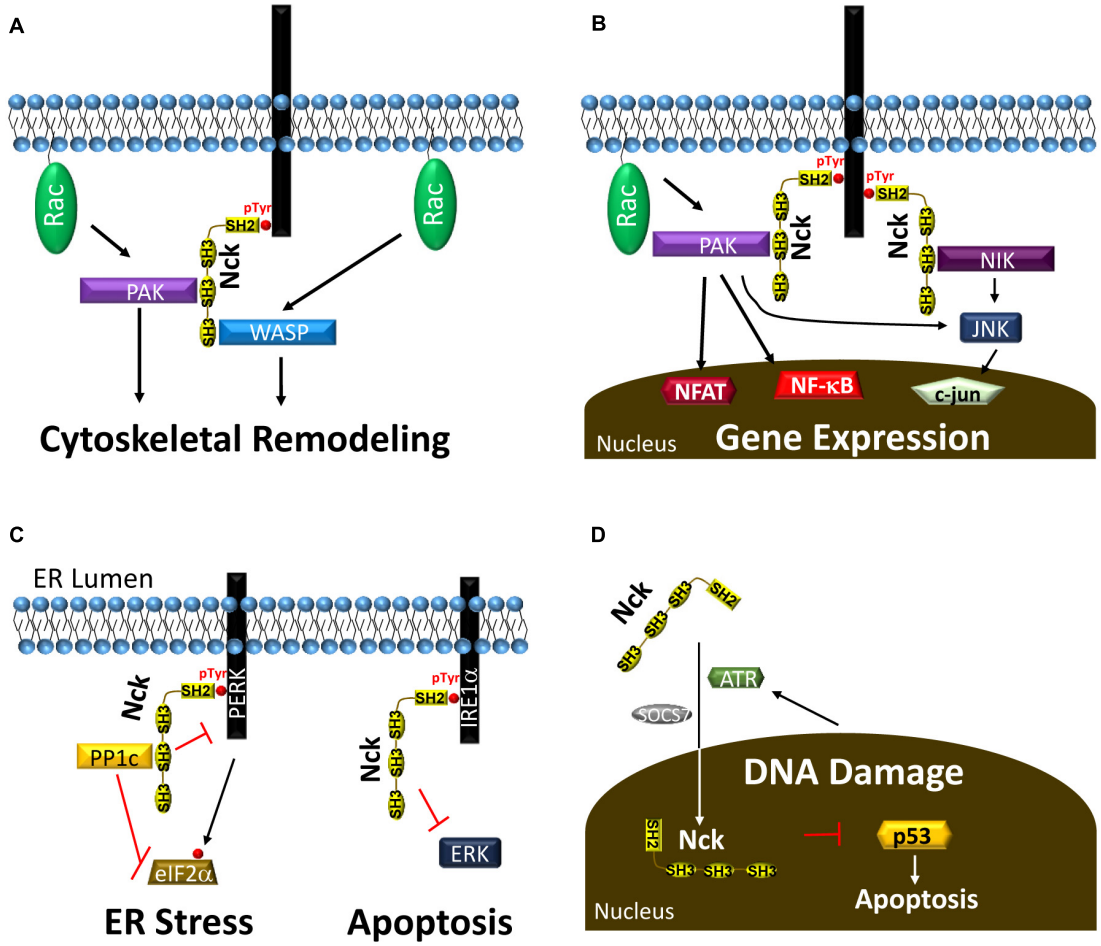

FIGURE 3 | (A) Nck recruitment to tyrosine phosphorylated proteins recruits PAK and WASP to enhance their activation by the small GTPase RAC, leading to cytoskeletal remodeling and cell migration. **(B)** Nck recruitment to phosphotyrosine enhances activation of several proteins, such as PAK and NIK, that activate transcription factors to affect gene expression. **(C)** Nck1 recruitment to the ER membrane through interactions with PERK and IRE1α reduces ER stress and ER stress-associated apoptosis. **(D)** ATR and SOCS7 drive Nck translocation into the nucleus following DNA damage to reduce p53-dependent apoptosis.

the stabilizing splicing of the Xbp1 transcription factor, thereby allowing it to translocate to the nucleus and drive expression of ER chaperones and ER biogenesis genes (Cao and Kaufman, 2012). IRE1α phosphorylation promotes activation of JNK and NF-κB to drive proinflammatory gene expression (Cao and Kaufman, 2012). Nck interacts with proline-rich regions in IRE1α under normal conditions and represses ERK activation (**Figure 3C**). Activation of IRE1α in response to ER stress causes Nck1 release and ERK activation to promote cell survival (Nguyen et al., 2004). Therefore, Nck1 interactions with IRE1α and PERK serve to limit UPR signaling, and loss of Nck1 enhances cell survival following ER stress (Yamani et al., 2014, 2015).

Cell Proliferation and Cell Survival

Nck1 and Nck2 show elevated expression in multiple cancers associated with enhanced proliferation and reduced apoptosis (Li et al., 1992; Labelle-Cote et al., 2011; Zhang et al., 2017). A five-fold overexpression of Nck drives the formation of an oncogenic foci (Li et al., 1992). In T cells, inhibiting the interaction between the Nck1 SH3.1 domain and the TCR with a small molecule inhibitor (AX-024) significantly reduces T cell proliferation both *in vitro* and *in vivo* (Borroto et al., 2014; Richter et al., 2020). While few studies have addressed the mechanisms by which Nck regulates cell proliferation, JNK inhibition reduces cell cycle progression in a variety of cell types (Himes et al., 2006; Wagner and Nebreda, 2009).

Nck expression regulates apoptosis through multiple mechanisms. Nck accumulates in the nucleus following DNA damage through an ATR- and suppressor of cytokine signaling 7 (SOCS7)-dependent mechanism, and Nck-depleted cells show enhanced apoptosis in response to DNA damage (**Figure 3D**; Errington and Macara, 2013). Depletion of either Nck1 or Nck2 enhances DNA damage-associated p53 activation and early apoptosis; however, Nck2 depletion had a significantly stronger effect (Errington and Macara, 2013). In contrast, Nck signaling can also promote apoptosis. Nck-dependent JNK activation promotes B cell apoptosis following B cell receptor activation

(Mizuno et al., 2002), and Nck signaling is required for ER stress-induced CHOP expression and apoptosis (Li et al., 2013).

Nck 1/2 IN VASCULAR BIOLOGY

Vascular Development

Nck1 and Nck2 are functionally redundant during development, as neither loss of Nck1 nor Nck2 expression in mice show any phenotypic changes (Bladt et al., 2003). However, deleting both Nck1 and Nck2 *in utero* results in embryonic lethality with defective chorion-allantoic fusion and axial rotation (Bladt et al., 2003). The Drosophila Nck homolog, Dock, regulates actin dynamics to facilitate neuronal growth cone guidance (Clemens et al., 1996; Rao and Zipursky, 1998; Li et al., 2001) and synapse formation (Desai et al., 1999). Similarly, neuronal-specific deletion of both Nck1 and Nck2 in mice results in deficient organization of the neuronal circuits critical for walking (Fawcett et al., 2007), such that neuronal Nck1/2 deficient mice display a hopping gate. Nck1/2 signaling within the developing spinal cord is required for outgrowth and growth cone architecture (Fawcett et al., 2007; Lane et al., 2015), and Nck has been identified as an essential downstream signaling component for EphB2-regulated axon guidance/growth cone collapse in rat cortical neurons (Srivastava et al., 2013). Regarding the vascular system, endothelial-specific deletion of both Nck1 and Nck2 during development results in embryonic lethality between E10 and E11 due to impaired angiogenesis, with reduced vessel branching and pericyte coverage (Clouthier et al., 2015). Endothelial cells from Nck1/2 knockout mice show significantly reduced migratory capacity, delayed cell spreading, and poor turnover of cell-matrix adhesions (Clouthier et al., 2015), consistent with a defect in angiogenesis. Interestingly, the endothelial-specific Nck1/2 deficient mice show defects in myocardial trabeculation and endocardial cushion formation (Clouthier et al., 2015). Endothelial-to-mesenchymal transition (EndMT), a phenotypic conversion involving reduced expression of endothelial marker genes (e.g., VE-cadherin) and enhanced expression of mesenchymal markers (e.g., smooth muscle actin, fibroblast-specific protein 1, fibronectin) (Chen P. Y. et al., 2020), drives endocardial cushion formation (Camenisch et al., 2002). Endothelial Nck1/2 deletion enhanced endothelial marker expression and reduced EndMT marker expression, suggesting that endothelial Nck1/2 signaling may affect endocardial cushion formation through EndMT regulation (Clouthier et al., 2015). In addition to fibronectin expression, fibronectin fibrillogenesis during EndMT requires contractility-dependent formation of elongated α5β1-rich fibrillar adhesions (Georgiadou and Ivaska, 2017). Consistent with Nck1/2-dependent fibronectin deposition in EndMT, endothelial Nck1/2 deletion reduces both adhesion length and α5β1-fibronectin adhesion force (Chaki et al., 2013).

Postnatal Angiogenesis

In postnatal tissue, angiogenesis contributes to both physiological and pathological effects. In wound healing and tissue ischemia, angiogenesis enhances blood flow to promote tissue healing and homeostasis. However, in diabetic retinopathy, age-related macular degeneration, arthritis, and cancer, angiogenesis contributes to disease pathogenesis (Herbert and Stainier, 2011; Potente et al., 2011). In sprouting angiogenesis, quiescent endothelial cells respond to angiogenic factors by loosening cell-cell junctions and enhancing the production of matrix-degrading enzymes to allow for invasion of the adjacent tissue (Herbert and Stainier, 2011; Potente et al., 2011). Classic angiogenic factors, such as vascular endothelial growth factor (VEGF) and platelet-derived growth factor-B (PDGF-B), induce vascular cell migration and proliferation to promote new blood vessel formation (Lindblom et al., 2003; Koch and Claesson-Welsh, 2012).

Endothelial Nck1 and Nck2 in Angiogenesis

Tissue ischemia and inflammation drive local VEGF production, enhancing endothelial migration and sprout formation through the endothelial VEGF receptor 2 (VEGFR2). Although several studies have shown Nck recruitment to VEGFR2 (Stoletov et al., 2004; Wang et al., 2007), the specific isoforms involved remain unknown. A membrane-permeable peptide corresponding to a Nck-binding sequence in PAK1 (KPPAPPMRNTSTM, PAK-Nck peptide) significantly reduces endothelial migration *in vitro* and angiogenesis *in vivo* (Kiosses et al., 2002). Mice deficient in both Nck1 and Nck2 show deficient front-rear endothelial polarity in sprouting vessels, associated with severe angiogenic defects in the postnatal retina (Dubrac et al., 2016). While endothelial-specific Nck2 deletion partially reduces branchpoints and vascular density, Nck1 deletion has no effect on angiogenesis during retinal postnatal angiogenesis (Dubrac et al., 2016). Similarly, Nck1/2 deletion, and to a lesser extent endothelial-specific Nck2 deletion, reduces pathological angiogenesis in the oxygen-induced retinopathy model, whereas Nck1 deletion has no or minimal effect (Dubrac et al., 2016). Endothelial cells lacking both Nck1 and Nck2 show reduced migration and PAK2 activation in response to VEGF and the guidance molecule Slit2 (Stoletov et al., 2001, 2004; Chaki and Rivera, 2013; Dubrac et al., 2016), associated with reduced PAK activation and diminished focal adhesion dynamics. Similarly, endothelial cells deficient for Nck1/2 show reduced endothelial lumen formation in 3D culture (Chaki et al., 2015), associated with the reduced activation of the polarity pathway (cdc42, atypical PKC). In addition to polarity and actin dynamics, endothelial invasion into surrounding tissue often requires matrix degradation through the formation of podosomes, actin-based protrusions rich in proteolytic enzymes. Increasing Nck1/2 expression in endothelial cells drives podosome formation, whereas Nck1/2 depletion reduces pososomes (Chaki et al., 2019). Deletion of Nck2, and to a lesser extent Nck1, reduces endothelial cell invasion of a matrigel matrix, whereas rescuing Nck2 expression enhances matrigel invasion and gelatin degradation (Chaki et al., 2019). Interestingly, focal adhesion kinase phosphorylation on Y397 recruits Nck2 through an SH2-dependent mechanism, suggesting that Nck2 may play a preferential role in mediating

cytoskeletal remodeling signaling from the focal adhesion (Goicoechea et al., 2002).

Pericyte Nck1 and Nck2 in Angiogenesis

Following the sprouting process, tube formation results in the initiation of blood flow and in vessel stabilization through pericyte recruitment (Herbert and Stainier, 2011; Potente et al., 2011). Endothelial cell-derived PDGF-B enhances pericyte recruitment via the pericyte PDGF receptor-β (PDGFRβ), whereas endothelial-specific deletion of PDGF-B results in diminished angiogenesis associated with reduced pericyte coverage and impaired vessel stability (Lindblom et al., 2003; Dubrac et al., 2018). Although PDGFRβ-dependent Nck1/2 recruitment has not been explored in pericytes, fibroblast PDGFRβ activation recruits both Nck1 and Nck2, with Nck1 binding to pTyr751 and Nck2 binding to pTyr1009 (Nishimura et al., 1993; Guan et al., 2009). Compared to Nck1 deletion alone, pericyte-specific Nck1/2 knockout mice show reduced angiogenesis associated with reduced vessel sprouts, reduced branchpoints, and diminished pericyte coverage (Dubrac et al., 2018). However, the effect of pericyte Nck1 or Nck2 deletion alone remains unknown. Nck1/2 knockdown in pericytes reduces PDGF-B-induced wound healing, associated with diminished PAK activation (Dubrac et al., 2018). In fibroblasts, deletion of either Nck1 or Nck2 reduces PDGF-B-induced migration (Ruusala et al., 2008), whereas overexpression of Nck1 or Nck2 SH2 domain or the SH3.2 domain (dominant-negative inhibitors of domain interactions) similarly blunts cell motility (Guan et al., 2009). The requirement for the SH2 domain (PDGFRβ-binding) and the SH3.2 domain (PAK-binding) is consistent with the PAK-dependent mechanism for reduced migration in Nck1/2 deficient pericytes (Dubrac et al., 2018).

Vascular Permeability

The vascular endothelium provides a selective barrier limiting the efflux of fluid and plasma proteins into the surrounding tissue. Excessive fluid accumulation drives organ dysfunction in a variety of pathologies, and the leak of plasma proteins into atherosclerosis-prone arterial regions precedes plaque formation (LaMack et al., 2005; Orr et al., 2005) and may contribute to plaque-associated inflammation (Orr et al., 2005; Popov and Simionescu, 2006; Finney et al., 2017). Endothelial barrier integrity is mediated by endothelial adherens junctions (VE-cadherin, PECAM-1) and the tight junctions (claudin-5, occludin, JAMs). While endothelial transcytosis mediates active transcellular permeability (e.g, LDL), turnover of cell-cell adhesions and elevated cytoskeletal tension facilitate passive leak of fluids and plasma proteins through the induction of paracellular pores (Mundi et al., 2018). Phosphorylation of VE-cadherin in adherens junctions loosens its association with catenins and promotes adherens junction disassembly (Gavard, 2014). Additionally, myosin-mediated contractility significantly promotes vascular permeability (Sun et al., 2011). Therefore, the formation of paracellular pores likely requires both phosphorylation-dependent loosening of cell-cell junctions and contractility-dependent tension on cell-cell junctions.

PAK-Nck Interaction in Vascular Permeability

Multiple lines of evidence suggest that Nck1/2 signaling critically regulates vascular permeability. Several permeability-inducing factors (VEGF, basic fibroblast growth factor, histamine, thrombin, and disturbed flow) promote PAK recruitment to endothelial cell-cell junctions (**Figure 4**; Stockton et al., 2004; Orr et al., 2007). Treatment with the PAK-Nck blocking peptide reduces PAK recruitment to cell-cell junctions, blunts myosin light chain phosphorylation, and limits paracellular pore formation in response to these factors (Stockton et al., 2004; Orr et al., 2007). In addition to PAK-dependent contractility, PAK-mediated VE-cadherin phosphorylation enhances both β-arrestin-mediated VE-cadherin endocytosis and endothelial permeability (Gavard and Gutkind, 2006). Furthermore, treating mice with the PAK-Nck peptide reduces vascular permeability in atherosclerosis, ischemia-reperfusion injury, and acute lung injury (Stockton et al., 2004; Orr et al., 2007; Reutershan et al., 2007; Chen et al., 2015). However, conflicting reports cloud the role of PAK in the permeability response. PAK activation promotes vascular integrity in several models (Garcia et al., 2001; Birukova et al., 2007), and deleting the major endothelial PAK isoform, PAK2, results in increased vascular permeability (Radu et al., 2015). Many of the studies implicating PAK as barrier protective suggest the lower expressed PAK1 isoform mediates these effects. However, these studies do not examine the relative roles of PAK1 and PAK2 in these processes, the specificity of the reagents for PAK1 is questionable, and the PAK1 knockout shows no permeability defects (Garcia et al., 2001; Birukova et al., 2007; Radu et al., 2015). One potential explanation for these discrepancies might involve the mechanism of PAK-recruitment to cell-cell junctions. Most studies showing PAK signaling enhances barrier function utilize signals that activate the cAMP/Protein Kinase A (PKA) pathway. PKA phosphorylates PAK2 within the Nck-binding sequence (KPPAPPVRMSST) and inhibits the PAK-Nck interaction, similar to the PAK-Nck blocking peptide (Howe and Juliano, 2000; Funk et al., 2010; Yurdagul Chen et al., 2013). However, PAK has additional proline-rich sequences that can bind Grb2 and β-Pix, and the interaction between PAK and β-Pix mediates the barrier-protective properties of PAK (Birukova et al., 2007). Therefore, PKA-mediated PAK2 phosphorylation may alter its function from barrier destabilizing to barrier protective, dependent upon changing which protein recruits PAK to the cell-cell junction.

Nck1 and Nck2 in Vascular Permeability

While these studies suggest a potential role for Nck in permeability, work from our laboratory has examined the mechanisms of Nck recruitment to the cell-cell junction and Nck isoform-specific signaling. Both shear stress and oxidant stress promote PECAM-1 tyrosine phosphorylation and the co-immunoprecipitation of Nck1/2 with PECAM-1 (**Figure 4**; Chen et al., 2015; Alfaidi et al., 2020b). PECAM-1 can be tyrosine phosphorylated at Y663 and Y686, and PECAM-1 lacking these sites fails to recruit Nck (Chen et al., 2015). While both pTyr sites (Y^{663}TEV, Y^{686}SEV) are similar to the Nck SH2-binding consensus sequence (Y-D/E-x-V/P) (Frese et al., 2006), isolated Nck1 SH2 and Nck2 SH2 domains

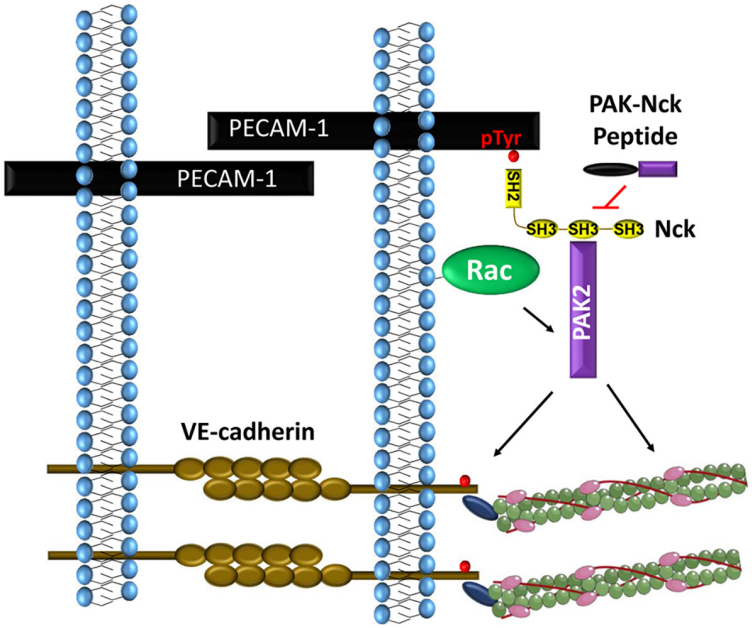

FIGURE 4 | PECAM-1 phosphorylation recruits Nck1 and Nck2 to endothelial cell-cell junctions. Nck1-dependent PAK activation promotes VE-cadherin phosphorylation and local myosin-dependent contractility to induce paracellular pore formation.

show preferential interaction with the phospho-Tyr663 sequence (Machida et al., 2007). In response to shear stress, PECAM-1 phosphorylation recruits both Nck1 and Nck2. However, only deletion of Nck1 reduces shear stress-induced PAK2 activation and endothelial permeability, whereas Nck2 deletion paradoxically enhances both PAK activation and endothelial permeability (Alfaidi et al., 2020b). Domain-swap experiments combining the Nck1 SH2 domain with the Nck2 SH3 domains (and vice versa) suggest that the Nck1 and Nck2 SH2 domains play redundant roles in shear-induced endothelial permeability, whereas the Nck1 SH3 domains critically mediate this effect (Alfaidi et al., 2020b). This is consistent with the current model of PECAM-1 interaction with both Nck1 and Nck2, but only Nck1 mediating subsequent PAK activation. Since both Nck1 and Nck2 can promote PAK membrane translocation and activation (Bokoch, 2003), the reason for the preferential activation of PAK by Nck1 in this context is currently unknown. However, consistent with cell culture models, endothelial-specific Nck1 deletion reduces vascular permeability at sites of disturbed flow, whereas endothelial-specific Nck2 deletion does not (Alfaidi et al., 2020b). Since endothelial-specific Nck1 deletion does not result in a lethal phenotype similar to PAK2 deletion (Radu et al., 2015; Alfaidi et al., 2020b), Nck1 deletion may not limit all endothelial PAK2 signaling but rather the specific PAK2 signaling at the cell-cell junctions that promotes permeability.

Proinflammatory Gene Expression

Endothelial activation, the conversion from a quiescent phenotype to a leaky, proinflammatory phenotype, contributes to a variety of cardiovascular diseases (Pober and Sessa, 2007). Proinflammatory cytokines (TNFα, IL-1β) and oxidized phospholipids promote endothelial activation, primarily through activation of the transcription factor NF-κB (Collins and Cybulsky, 2001). In atherosclerosis, disturbed blood flow patterns at vessel branchpoints, curvatures, and bifurcations induce cytoskeletal stiffening, elevated oxidant stress, and low levels of chronic NF-κB activation that primes these areas for further activation by atherogenic stimuli (Hajra et al., 2000; Hahn and Schwartz, 2009; Fang and Davies, 2012). Inhibiting NF-κB activation in endothelial cells protects mice from atherosclerotic plaque formation (Gareus et al., 2008), underscoring the importance of endothelial activation to atherosclerotic plaque formation. In contrast to disturbed flow, uniform laminar flow reduces endothelial activation and limits endothelial proinflammatory gene expression in response to circulating proatherogenic stimuli.

Laminar and disturbed flow induce distinct endothelial morphologies, which may contribute to their differential activation state. In response to laminar flow, transient activation of cytoskeletal remodeling pathways (e.g., integrin activation, focal adhesion kinase, Rac, PAK) promote both cytoskeletal remodeling in the direction of flow and activation of proinflammatory transcription factors, like NF-κB and YAP/TAZ, to induce proinflammatory gene expression (Hahn and Schwartz, 2009; Yurdagul and Orr, 2016). However, as cells align, these pathways are muted, and endothelial cells adopt a quiescent phenotype (Hahn and Schwartz, 2009; Yurdagul and Orr, 2016). In disturbed flow, sustained NF-κB activation occurs due to the inability of the cells to align, resulting in chronic activation of cytoskeletal remodeling signals (Hahn and Schwartz, 2009; Yurdagul and Orr, 2016).

PAK-Nck Interactions in Endothelial Proinflammatory Gene Expression

Early evidence for Nck's role in proinflammatory endothelial activation derived from experiments utilizing the PAK-Nck peptide to inhibit PAK activation. Treating endothelial cells with the PAK-Nck peptide inhibited disturbed-flow-induced NF-κB activation, JNK activation, and proinflammatory gene expression (**Figure 5**; Orr et al., 2008; Hahn et al., 2009; Funk et al., 2010), and treating atherosclerosis-prone ApoE knockout mice with the PAK-Nck peptide prevented NF-κB activation, JNK activation, and proinflammatory gene expression at sites of disturbed flow *in vivo*. Mutation of the PKA-dependent phosphorylation site (Ser20) that inhibits the PAK-Nck interaction enhanced disturbed flow-induced NF-κB activation, suggesting that Nck-binding critically mediates this effect (Funk et al., 2010; Yurdagul Chen et al., 2013). Like disturbed flow, treatment with the PAK-Nck peptide significantly blunts the proinflammatory response to oxidative stress (**Figure 5**; Orr et al., 2008), and treating mice with the PAK-Nck peptide blunts inflammation in the cremaster ischemia-reperfusion injury model and the LPS-induced lung injury model (Reutershan et al., 2007; Chen et al., 2015). However, the selectivity of this peptide for Nck is questionable, as this peptide could target several other SH3 domain-containing proteins (Teyra et al., 2017). In addition, this peptide may target other non-endothelial cell types, as treating neutrophils with the PAK-Nck peptide significantly affects their cytoskeletal remodeling and cell migration (Reutershan et al., 2007).

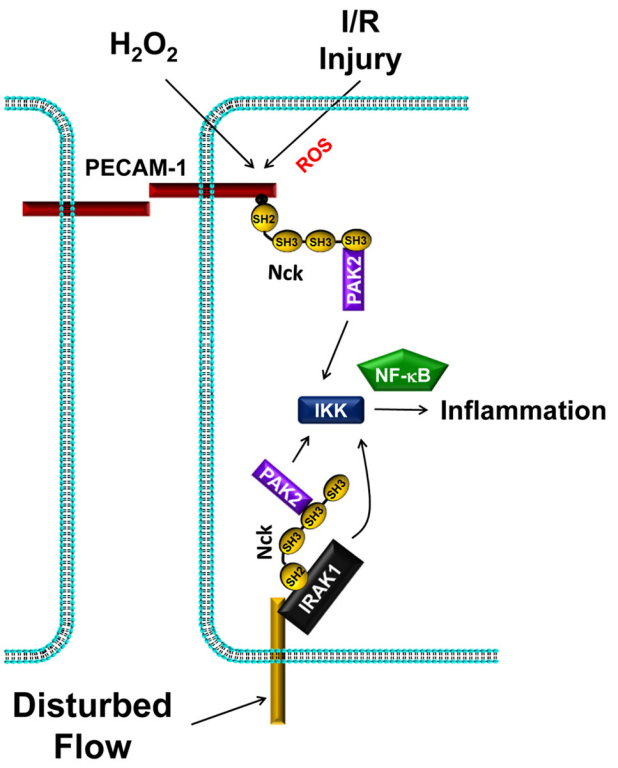

FIGURE 5 | Nck1/2 recruitment to tyrosine phosphorylated proteins promote IKK-dependent NF-κB activation and proinflammatory gene expression. Oxidative stress (H2O2, ischemia/reperfusion injury) promotes Nck1/2 recruitment through PECAM-1 phosphorylation. In disturbed flow, Nck1 recruitment to IRAK-1 promotes NF-κB activation through a pathway that may or may not involve PAK2.

Nck1 and Nck2 in Endothelial Proinflammatory Gene Expression

Work from our group sought to determine the direct role of Nck1/2 in vascular inflammation. Endothelial cells treated with siRNA targeting both Nck1 and Nck2 show reduced activation of NF-κB and the upstream IκB kinase (IKK) complex in response to exogenous (H_2O_2) and endogenous (hypoxia/reoxygenation) oxidative stress (**Figure 5**; Chen et al., 2015). Likewise, endothelial Nck1/2 depletion inhibits H_2O_2 and hypoxia/reoxygenation-induced expression of the proinflammatory adhesion molecules intercellular adhesion molecule-1 (ICAM-1) and vascular cell adhesion molecule-1 (VCAM-1; Chen et al., 2015). Similarly, Nck1/2 depletion prevents disturbed flow-induced NF-κB activation and ICAM-1/VCAM-1 expression (Alfaidi et al., 2020a). However, Nck1 and Nck2 play different roles in this regard. Nck1-depleted endothelial cells showed significantly less NF-κB activation and ICAM-1/VCAM-1 expression in response to disturbed flow, whereas Nck2 depleted endothelial cells do not (Alfaidi et al., 2020a). Furthermore, endothelial cells isolated from Nck1/2 double knockout mice fail to induce NF-κB activation and ICAM-1/VCAM-1 expression in response to disturbed flow, and re-expression of Nck1, but not Nck2, in these cells restores these proinflammatory responses (Alfaidi et al., 2020a). Moreover, atherosclerosis-prone ApoE knockout mice with a global Nck1 deletion show significantly reduced atherosclerotic plaque formation associated with diminished proinflammatory gene expression and leukocyte-positive plaque area (Alfaidi et al., 2020a). In contrast, endothelial-specific Nck2 knockout does not affect plaque formation or plaque-associated inflammation. While the effect of Nck1 deletion could be due to effects on leukocyte recruitment, bone marrow chimeras suggest that vessel wall Nck1 drives its proatherogenic effects (Alfaidi et al., 2020a).

Domain-swap experiments and point mutations in the Nck1 SH2 and SH3 domains suggest that specific Nck1 domains mediate this proinflammatory effect. Experiments with the Nck1/Nck2 chimeras suggest that the Nck1 SH2 domain critically mediates these proinflammatory signals, whereas the Nck2 SH3 domains can mediate the proinflammatory response when coupled with the Nck1 SH2 domain (Alfaidi et al., 2020a). Point mutations in the Nck1 SH2 targeting the critical Arg residue in the SH2 binding pocket (R308M) verify that disturbed flow-induced proinflammatory signaling requires the Nck1 SH2 domain (Alfaidi et al., 2020a). While the Nck1 and Nck2 SH3 domains appear to be redundant, inactivating point mutations in the Nck1 SH3 domains targeting the critical WPY triad (SH3.1 W38K, SH3.2 W143K, SH3.3 W229K) suggest that the Nck1 SH3.1 domain critically mediates flow-induced NF-κB activation and ICAM-1/VCAM-1 expression (Alfaidi et al., 2020a). This data is in conflict with the body of literature using the PAK-Nck peptide that should target the Nck SH3.2 domain to block interactions with PAK2. However, the SH3.1 domain provides a

potential useful therapeutic target, as it is a non-canonical class I/II SH3 domain with an atypical PxLPxxDY binding sequence (Teyra et al., 2017).

While current data support a role for PAK in mediating endothelial activation, other Nck1-binding partners may also contribute to the inflammatory response. A study by Jacquet *et al.,* utilizing spatial proteomics to identify Nck1- and Nck2-selective binding partners, demonstrates a selective interaction between Nck1 and the interleukin-1 (IL-1) receptor (IL-1R) signaling partner IL-1R activated kinase-1 (IRAK-1) (Jacquet et al., 2018). IL-1 interaction with IL-1R initiates a signaling complex with MyD88 and IRAK-4 that recruits IRAK-1 to the plasma membrane, resulting in IRAK-1 phosphorylation on Thr209 (Abbate et al., 2020; Su et al., 2020). Active IRAK-1 binds TRAF6, and the resulting signaling complex becomes ubiquitinated with non-proteolytic K63-ubiquitin chains that recruit and facilitate IKK complex activation (Abbate et al., 2020; Su et al., 2020). Disturbed flow enhances endothelial Nck1-IRAK-1 interactions and Nck1-dependent IRAK-1 activation (**Figure 5**; Alfaidi et al., 2020a). While wildtype mice show enhanced endothelial IRAK-1 activation at sites of disturbed flow and in atherosclerotic plaques, Nck1 knockout mice show reduced IRAK-1 activation (Alfaidi et al., 2020a). Furthermore, IRAK-1 depletion significantly blunts disturbed flow-induced NF-κB activation and proinflammatory gene expression (Alfaidi et al., 2020a).

Smooth Muscle Cell Function

Whereas several studies address the role of Nck1/2 signaling in endothelial cells and pericytes, only a few studies examine Nck1/2 signaling in vascular smooth muscle cells. Atherosclerosis-prone global Nck1 knockout mice show reduced smooth muscle cell incorporation into the plaque (Alfaidi et al., 2020a), which is typically driven by smooth muscle phenotypic modulation, migration, and proliferation. However, the role of Nck1/2 signaling in smooth muscle phenotype and smooth muscle migration has not been addressed. In fibroblasts, Nck1/2 deletion significantly reduces migration toward the classic smooth muscle cell mitogen PDGF-B, consistent with a potential role for Nck1/2 in mediating smooth muscle migration (Chen et al., 2000; Ruusala et al., 2008; Guan et al., 2009). In addition, multiple studies have shown a role for Nck1/2 in angiotensin-induced smooth muscle proliferation, as Nck1/2 depletion reduces angiotensin-induced smooth muscle proliferation associated with reduced activation of PAK and JNK (Voisin et al., 1999; Schmitz et al., 2001). Similarly, Nck1/2 depletion in fibroblasts blunts PDGF-B-induced proliferation (Roche et al., 1996). While these findings are suggestive, understanding how Nck1 and Nck2 signaling affects smooth muscle function will require additional studies.

CURRENT CLINICAL THERAPIES TARGETING Nck ADAPTOR PROTEINS

The small molecule inhibitor AX-024 blocks the interaction between the Nck1 SH3.1 domain and the TCR and significantly reduces T cell proliferation both *in vitro* and *in vivo* (Borroto et al., 2014; Richter et al., 2020), suggesting that it may serve as a viable treatment for autoimmune diseases, such as psoriasis, autoimmune dermatitis, and multiple sclerosis (Borroto et al., 2016). This compound can be given orally, subcutaneously or intravenously and was well tolerated in mice even with higher doses. Phase Ia/Ib clinical trials have been completed in healthy human volunteers (Borroto et al., 2016; Flemming, 2017), but no efficacy data is currently available. In a mouse model of imiquimod-induced psoriasis, oral treatment with AX-024 significantly reduced skin thickening and inflammation. In ovalbumin-antigen-induced asthma model, AX-024 prevented airway sensitization and inflammation, and in an experimental model of autoimmune encephalopathy (a model of multiple sclerosis), treatment with AX-024 was more effective than the currently available treatment (Borroto et al., 2016; Flemming, 2017).

CONCLUSION AND FUTURE DIRECTIONS

The Nck family of SH2/SH3 adaptors proteins link activation of phosphotyrosine signaling hubs (activated growth factor receptors, sites of cell adhesion) to cytoskeletal dynamics and changes in gene expression driving cell proliferation, survival, and phenotypic changes. Nck1/2 signaling contributes to endothelial and pericyte cell migration to regulate vascular development and vascular remodeling in postnatal angiogenesis. In addition, Nck1/2 signaling contributes to the regulation of vascular phenotypic changes, such as endothelial activation and EndMT, through effects on gene transcription and protein translation. While several of these functions are redundant between Nck1 and Nck2, isoform selective effects have been described in multiple model systems, with Nck1 primarily implicated in vascular cell phenotype and Nck2 primarily implicated in vascular cytoskeletal remodeling and cell migration.

Future Directions in Nck Research

Due to the similarity in domain structure and function, Nck1 and Nck2 have classically been viewed as redundant signaling mediators during organismal development. However, recent research highlights the isoform-selective roles of these proteins in various diseases, and new mouse models will be required to allow for selective inhibition of Nck1 and Nck2 in various cell types to fully characterize their context-specific functions. New advances in single cell RNA-Seq also promises to better enable our understanding of how Nck1 and Nck2 expression correlates with cell phenotype. In addition to expression, most binding partners show poor isoform selectivity, suggesting that new techniques may be required to characterize the Nck1-selective and Nck2-selective interacting partners under various conditions. Furthermore, the role of Nck1 and Nck2 post-translational modifications in the regulation of Nck1/2 function remain virtually unknown despite being known to occur for several decades. Future work will need to characterize how

these modifications (primarily phosphorylation) affect Nck1/2 interactions and how they change during disease conditions.

Adaptor proteins provide a uniquely tunable therapeutic target. Redundancy within the receptor tyrosine kinases may limit the efficacy of therapeutics targeting individual enzymes. Therapeutics targeting kinase activity often result in significant negative side effects due to potent inhibition of target protein function and off-target effects on other kinases. In contrast, domain-selective inhibitors of the modular adaptor proteins block only a subset of their downstream effectors to limit specific signaling effects. For example, peptide inhibitors of the Nck1/2 SH3.2 domain reduce angiogenesis and show significant reductions in inflammation and permeability across multiple *in vivo* models. While this combination of effects may be useful for chronic inflammatory conditions like arthritis, the reduction in angiogenesis would likely limit their efficacy in atherosclerotic cardiovascular disease due to a worsened ability to respond to tissue ischemia. Since deficiency in either Nck1 or Nck2 does not disrupt angiogenesis, inhibitors targeting either Nck1 or Nck2 could affect isoform-specific effects without limiting angiogenesis or wound healing. Furthermore, inhibitors that target isoform-specific domains, such as the AX-024 small molecule inhibitor of the Nck1 SH3.1 domain, could further target specific downstream signaling effectors with limited off target effects. As current research focuses on high-throughput analysis of gene expression to identify potential therapeutic targets, analysis of protein-protein interactions and domain-selective protein functions will be necessary to utilize this information to treat human disease.

AUTHOR CONTRIBUTIONS

MA and AO wrote, edited, and generated the figures. MS wrote and edited the manuscript. All authors contributed to the article and approved the submission.

FUNDING

This work was supported by an American Heart Association Postdoctoral Fellowship [AHA grant number 20POST35120288] to MA and [AHA grant number 20POST35220022] to MS and by National Institutes of Health grants [HL098435, HL133497, HL141155, and GM121307] to AO.

REFERENCES

Abbate, A., Toldo, S., Marchetti, C., Kron, J., Van Tassell, B. W., and Dinarello, C. A. (2020). Interleukin-1 and the inflammasome as therapeutic targets in cardiovascular disease. *Circ. Res.* 126, 1260–1280. doi: 10.1161/circresaha.120.315937

Aitio, O., Hellman, M., Kesti, T., Kleino, I., Samuilova, O., Paakkonen, K., et al. (2008). Structural basis of PxxDY motif recognition in SH3 binding. *J. Mol. Biol.* 382, 167–178. doi: 10.1016/j.jmb.2008.07.008

Alfaidi, M., Acosta, C. H., Wang, D., Traylor, J. G., and Orr, A. W. (2020a). Selective role of Nck1 in atherogenic inflammation and plaque formation. *J. Clin. Invest.* 130, 4331–4347.

Alfaidi, M., Bhattarai, U., and Orr, A. W. (2020b). Nck1, But Not Nck2, mediates disturbed flow-induced p21-activated kinase activation and endothelial permeability. *J. Am. Heart. Assoc.* 9:e016099.

Becker, E., Huynh-Do, U., Holland, S., Pawson, T., Daniel, T. O., and Skolnik, E. Y. (2000). Nck-interacting Ste20 kinase couples Eph receptors to c-Jun N-terminal kinase and integrin activation. *Mol. Cell Biol.* 20, 1537–1545. doi: 10.1128/mcb.20.5.1537-1545.2000

Birge, R. B., Knudsen, B. S., Besser, D., and Hanafusa, H. (1996). SH2 and SH3-containing adaptor proteins: redundant or independent mediators of intracellular signal transduction. *Genes Cells* 1, 595–613. doi: 10.1046/j.1365-2443.1996.00258.x

Birukova, A. A., Malyukova, I., Mikaelyan, A., Fu, P., and Birukov, K. G. (2007). Tiam1 and betaPIX mediate Rac-dependent endothelial barrier protective response to oxidized phospholipids. *J. Cell Physiol.* 211, 608–617. doi: 10.1002/jcp.20966

Bladt, F., Aippersbach, E., Gelkop, S., Strasser, G. A., Nash, P., Tafuri, A., et al. (2003). The murine Nck SH2/SH3 adaptors are important for the development of mesoderm-derived embryonic structures and for regulating the cellular actin network. *Mol. Cell Biol.* 23, 4586–4597. doi: 10.1128/mcb.23.13.4586-4597.2003

Bokoch, G. M. (2003). Biology of the p21-activated kinases. *Annu. Rev. Biochem.* 72, 743–781. doi: 10.1146/annurev.biochem.72.121801.161742

Bokoch, G. M., Wang, Y., Bohl, B. P., Sells, M. A., Quilliam, L. A., and Knaus, U. G. (1996). Interaction of the Nck adapter protein with p21-activated kinase (PAK1). *J. Biol. Chem.* 271, 25746–25749. doi: 10.1074/jbc.271.42.25746

Borroto, A., Arellano, I., Blanco, R., Fuentes, M., Orfao, A., Dopfer, E. P., et al. (2014). Relevance of Nck-CD3 epsilon interaction for T cell activation in vivo. *J. Immunol.* 192, 2042–2053. doi: 10.4049/jimmunol.1203414

Borroto, A., Reyes-Garau, D., Jimenez, M. A., Carrasco, E., Moreno, B., Martinez-Pasamar, S., et al. (2016). First-in-class inhibitor of the T cell receptor for the treatment of autoimmune diseases. *Sci. Transl. Med.* 8:370 ra184.

Buday, L., and Downward, J. (1993). Epidermal growth factor regulates p21ras through the formation of a complex of receptor, Grb2 adapter protein, and Sos nucleotide exchange factor. *Cell* 73, 611–620. doi: 10.1016/0092-8674(93)90146-h

Buvall, L., Rashmi, P., Lopez-Rivera, E., Andreeva, S., Weins, A., Wallentin, H., et al. (2013). Proteasomal degradation of Nck1 but not Nck2 regulates RhoA activation and actin dynamics. *Nat. Commun.* 4:2863.

Camenisch, T. D., Molin, D. G., Person, A., Runyan, R. B., Gittenberger-De Groot, A. C., Mcdonald, J. A., et al. (2002). Temporal and distinct TGFbeta ligand requirements during mouse and avian endocardial cushion morphogenesis. *Dev. Biol.* 248, 170–181. doi: 10.1006/dbio.2002.0731

Cao, S. S., and Kaufman, R. J. (2012). Unfolded protein response. *Curr. Biol.* 22, R622–R626.

Chaki, S. P., Barhoumi, R., Berginski, M. E., Sreenivasappa, H., Trache, A., Gomez, S. M., et al. (2013). Nck enables directional cell migration through the coordination of polarized membrane protrusion with adhesion dynamics. *J. Cell Sci.* 126, 1637–1649. doi: 10.1242/jcs.119610

Chaki, S. P., Barhoumi, R., and Rivera, G. M. (2015). Actin remodeling by Nck regulates endothelial lumen formation. *Mol. Biol. Cell* 26, 3047–3060. doi: 10.1091/mbc.e15-06-0338

Chaki, S. P., Barhoumi, R., and Rivera, G. M. (2019). Nck adapter proteins promote podosome biogenesis facilitating extracellular matrix degradation and cancer invasion. *Cancer Med.* 8, 7385–7398. doi: 10.1002/cam4.2640

Chaki, S. P., and Rivera, G. M. (2013). Integration of signaling and cytoskeletal remodeling by Nck in directional cell migration. *Bioarchitecture* 3, 57–63. doi: 10.4161/bioa.25744

Chakrabarti, P., and Janin, J. (2002). Dissecting protein-protein recognition sites. *Proteins* 47, 334–343. doi: 10.1002/prot.10085

Chang, H., Li, B., Zhang, X., and Meng, X. (2020). NCK1-AS1 promotes NCK1 expression to facilitate tumorigenesis and chemo-resistance in ovarian cancer. *Biochem. Biophys. Res. Commun.* 522, 292–299. doi: 10.1016/j.bbrc.2019.11.014

Chen, J., Leskov, I. L., Yurdagul, A. Jr., Thiel, B., Kevil, C. G., Stokes, K. Y., et al. (2015). Recruitment of the adaptor protein Nck to PECAM-1 couples oxidative stress to canonical NF-kappaB signaling and inflammation. *Sci. Signal.* 8:ra20. doi: 10.1126/scisignal.2005648

Chen, M., She, H., Davis, E. M., Spicer, C. M., Kim, L., Ren, R., et al. (1998). Identification of Nck family genes, chromosomal localization, expression, and signaling specificity. *J. Biol. Chem.* 273, 25171–25178. doi: 10.1074/jbc.273.39.25171

Chen, M., She, H., Kim, A., Woodley, D. T., and Li, W. (2000). Nckbeta adapter regulates actin polymerization in NIH 3T3 fibroblasts in response to platelet-derived growth factor bb. *Mol. Cell Biol.* 20, 7867–7880. doi: 10.1128/.20.21.7867-7880.2000

Chen, M. H., Raffield, L. M., Mousas, A., Sakaue, S., Huffman, J. E., Moscati, A., et al. (2020). Trans-ethnic and ancestry-specific blood-cell genetics in 746,667 individuals from 5 global populations. *Cell* 182, 1198–1213.e1114.

Chen, P. Y., Schwartz, M. A., and Simons, M. (2020). Endothelial-to-Mesenchymal transition, vascular inflammation, and atherosclerosis. *Front. Cardiovasc Med.* 7:53. doi: 10.3389/fcvm.2020.00053

Clemens, J. C., Ursuliak, Z., Clemens, K. K., Price, J. V., and Dixon, J. E. (1996). A Drosophila protein-tyrosine phosphatase associates with an adapter protein required for axonal guidance. *J. Biol. Chem.* 271, 17002–17005. doi: 10.1074/jbc.271.29.17002

Clouthier, D. L., Harris, C. N., Harris, R. A., Martin, C. E., Puri, M. C., and Jones, N. (2015). Requisite role for Nck adaptors in cardiovascular development, endothelial-to-mesenchymal transition, and directed cell migration. *Mol. Cell Biol.* 35, 1573–1587. doi: 10.1128/mcb.00072-15

Collins, T., and Cybulsky, M. I. (2001). NF-kappaB: pivotal mediator or innocent bystander in atherogenesis? *J. Clin. Invest.* 107, 255–264. doi: 10.1172/jci10373

Coutinho, S., Jahn, T., Lewitzky, M., Feller, S., Hutzler, P., Peschel, C., et al. (2000). Characterization of Ggrb4, an adapter protein interacting with Bcr-Abl. *Blood* 96, 618–624. doi: 10.1182/blood.v96.2.618.014k06_618_624

de Wit, N. J., Rijntjes, J., Diepstra, J. H., Van Kuppevelt, T. H., Weidle, U. H., Ruiter, D. J., et al. (2005). Analysis of differential gene expression in human melanocytic tumour lesions by custom made oligonucleotide arrays. *Br. J. Cancer* 92, 2249–2261. doi: 10.1038/sj.bjc.6602612

Dephoure, N., Zhou, C., Villen, J., Beausoleil, S. A., Bakalarski, C. E., Elledge, S. J., et al. (2008). A quantitative atlas of mitotic phosphorylation. *Proc. Natl. Acad. Sci. U.S.A.* 105, 10762–10767. doi: 10.1073/pnas.0805139105

Desai, C. J., Garrity, P. A., Keshishian, H., Zipursky, S. L., and Zinn, K. (1999). The Drosophila SH2-SH3 adapter protein Dock is expressed in embryonic axons and facilitates synapse formation by the RP3 motoneuron. *Development* 126, 1527–1535. doi: 10.1242/dev.126.7.1527

Deshpande, R. P., Panigrahi, M., Chandra Sekhar, Y. B. V. K., and Babu, P. P. (2019). Expression and clinicopathological significance of Nck1 in human astrocytoma progression. *Int. J. Neurosci.* 129, 171–178.

Dionne, U., Chartier, F. J. M., Lopez De Los Santos, Y., Lavoie, N., Bernard, D. N., Banerjee, S. L., et al. (2018). Direct phosphorylation of SRC homology 3 domains by tyrosine kinase receptors disassembles ligand-induced signaling networks. *Mol. Cell* 70, 995–1007.e1011.

Dubrac, A., Genet, G., Ola, R., Zhang, F., Pibouin-Fragner, L., Han, J., et al. (2016). Targeting NCK-mediated endothelial cell front-rear polarity inhibits neovascularization. *Circulation* 133, 409–421. doi: 10.1161/circulationaha.115.017537

Dubrac, A., Kunzel, S. E., Kunzel, S. H., Li, J., Chandran, R. R., Martin, K., et al. (2018). NCK-dependent pericyte migration promotes pathological neovascularization in ischemic retinopathy. *Nat. Commun.* 9:3463.

Dusseault, J., Li, B., Haider, N., Goyette, M. A., Cote, J. F., and Larose, L. (2016). Nck2 deficiency in mice results in increased adiposity associated with adipocyte hypertrophy and enhanced adipogenesis. *Diabetes* 65, 2652–2666. doi: 10.2337/db15-1559

Egan, S. E., Giddings, B. W., Brooks, M. W., Buday, L., Sizeland, A. M., and Weinberg, R. A. (1993). Association of Sos Ras exchange protein with Grb2 is implicated in tyrosine kinase signal transduction and transformation. *Nature* 363, 45–51. doi: 10.1038/363045a0

Emadali, A., Metrakos, P. P., Kalantari, F., Boutros, T., Boismenu, D., and Chevet, E. (2007). Proteomic analysis of tyrosine phosphorylation during human liver transplantation. *Proteome Sci.* 5:1.

Errington, T. M., and Macara, I. G. (2013). Depletion of the adaptor protein NCK increases UV-induced p53 phosphorylation and promotes apoptosis. *PLoS One* 8:e76204. doi10.1371/journal.pone.0076204

Fang, Y., and Davies, P. F. (2012). Site-specific microRNA-92a regulation of Kruppel-like factors 4 and 2 in atherosusceptible endothelium. *Arterioscler Thromb. Vasc. Biol.* 32, 979–987. doi: 10.1161/atvbaha.111.244053

Fawcett, J. P., Georgiou, J., Ruston, J., Bladt, F., Sherman, A., Warner, N., et al. (2007). Nck adaptor proteins control the organization of neuronal circuits important for walking. *Proc. Natl. Acad. Sci. U.S.A.* 104, 20973–20978. doi: 10.1073/pnas.0710316105

Finney, A. C., Stokes, K. Y., Pattillo, C. B., and Orr, A. W. (2017). Integrin signaling in atherosclerosis. *Cell Mol. Life Sci.* 74, 2263–2282. doi: 10.1007/s00018-017-2490-4

Flemming, A. (2017). Autoimmune diseases: Inhibitor of adaptor protein shows self-antigen selectivity. *Nat. Rev. Immunol.* 17, 80–81.

Frese, S., Schubert, W. D., Findeis, A. C., Marquardt, T., Roske, Y. S., Stradal, T. E., et al. (2006). The phosphotyrosine peptide binding specificity of Nck1 and Nck2 Src homology 2 domains. *J. Biol. Chem.* 281, 18236–18245. doi: 10.1074/jbc.m512917200

Funk, S. D., Yurdagul, A. Jr., Green, J. M., Jhaveri, K. A., Schwartz, M. A., and Orr, A. W. (2010). Matrix-specific protein kinase A signaling regulates p21-activated kinase activation by flow in endothelial cells. *Circ. Res.* 106, 1394–1403. doi: 10.1161/circresaha.109.210286

Gale, N. W., Kaplan, S., Lowenstein, E. J., Schlessinger, J., and Bar-Sagi, D. (1993). Grb2 mediates the EGF-dependent activation of guanine nucleotide exchange on Ras. *Nature* 363, 88–92. doi: 10.1038/363088a0

Galisteo, M. L., Chernoff, J., Su, Y. C., Skolnik, E. Y., and Schlessinger, J. (1996). The adaptor protein Nck links receptor tyrosine kinases with the serine-threonine kinase Pak1. *J. Biol. Chem.* 271, 20997–21000. doi: 10.1074/jbc.271.35.20997

Garcia, J. G., Liu, F., Verin, A. D., Birukova, A., Dechert, M. A., Gerthoffer, W. T., et al. (2001). Sphingosine 1-phosphate promotes endothelial cell barrier integrity by Edg-dependent cytoskeletal rearrangement. *J. Clin. Invest.* 108, 689–701. doi: 10.1172/jci12450

Gareus, R., Kotsaki, E., Xanthoulea, S., Van Der Made, I., Gijbels, M. J., Kardakaris, R., et al. (2008). Endothelial cell-specific NF-kappaB inhibition protects mice from atherosclerosis. *Cell Metab.* 8, 372–383. doi: 10.1016/j.cmet.2008.08.016

Gavard, J. (2014). Endothelial permeability and VE-cadherin: a wacky comradeship. *Cell Adh. Migr.* 8, 158–164. doi: 10.4161/cam.29026

Gavard, J., and Gutkind, J. S. (2006). VEGF controls endothelial-cell permeability by promoting the beta-arrestin-dependent endocytosis of VE-cadherin. *Nat. Cell Biol.* 8, 1223–1234. doi: 10.1038/ncb1486

Georgiadou, M., and Ivaska, J. (2017). Tensins: bridging AMP-activated protein kinase with integrin activation. *Trends Cell Biol.* 27, 703–711. doi: 10.1016/j.tcb.2017.06.004

Gil, D., Schamel, W. W., Montoya, M., Sanchez-Madrid, F., and Alarcon, B. (2002). Recruitment of Nck by CD3 epsilon reveals a ligand-induced conformational change essential for T cell receptor signaling and synapse formation. *Cell* 109, 901–912. doi: 10.1016/s0092-8674(02)00799-7

Goicoechea, S. M., Tu, Y., Hua, Y., Chen, K., Shen, T. L., Guan, J. L., et al. (2002). Nck-2 interacts with focal adhesion kinase and modulates cell motility. *Int. J. Biochem. Cell Biol.* 34, 791–805. doi: 10.1016/s1357-2725(02)00002-x

Griggs, B. L., Ladd, S., Decker, A., Dupont, B. R., Asamoah, A., and Srivastava, A. K. (2009). Identification of ectodysplasin-A receptor gene deletion at 2q12.2 and a potential autosomal MR locus. *Eur. J. Hum. Genet.* 17, 30–36. doi: 10.1038/ejhg.2008.183

Guan, S., Chen, M., Woodley, D., and Li, W. (2007). Nckbeta adapter controls neuritogenesis by maintaining the cellular paxillin level. *Mol. Cell Biol.* 27, 6001–6011. doi: 10.1128/mcb.01807-06

Guan, S., Fan, J., Han, A., Chen, M., Woodley, D. T., and Li, W. (2009). Non-compensating roles between Nckalpha and Nckbeta in PDGF-BB signaling to promote human dermal fibroblast migration. *J. Invest. Dermatol.* 129, 1909–1920. doi: 10.1038/jid.2008.457

Gupta, R. W., and Mayer, B. J. (1998). Dominant-negative mutants of the SH2/SH3 adapters Nck and Grb2 inhibit MAP kinase activation and mesoderm-specific gene induction by eFGF in Xenopus. *Oncogene* 17, 2155–2165. doi: 10.1038/sj.onc.1202158

Hahn, C., Orr, A. W., Sanders, J. M., Jhaveri, K. A., and Schwartz, M. A. (2009). The subendothelial extracellular matrix modulates JNK activation by flow. *Circ. Res.* 104, 995–1003. doi: 10.1161/circresaha.108.186486

Hahn, C., and Schwartz, M. A. (2009). Mechanotransduction in vascular physiology and atherogenesis. *Nat. Rev. Mol. Cell Biol.* 10, 53–62. doi: 10.1038/nrm2596

Haider, N., Dusseault, J., and Larose, L. (2018). Nck1 deficiency impairs adipogenesis by activation of PDGFRalpha in preadipocytes. *iScience* 6, 22–37. doi: 10.1016/j.isci.2018.07.010

Hajra, L., Evans, A. I., Chen, M., Hyduk, S. J., Collins, T., and Cybulsky, M. I. (2000). The NF-kappa B signal transduction pathway in aortic endothelial cells is primed for activation in regions predisposed to atherosclerotic lesion formation. *Proc. Natl. Acad. Sci. U.S.A.* 97, 9052–9057. doi: 10.1073/pnas.97.16.9052

Harding, H. P., Zhang, Y., Bertolotti, A., Zeng, H., and Ron, D. (2000). Perk is essential for translational regulation and cell survival during the unfolded protein response. *Mol. Cell* 5, 897–904. doi: 10.1016/s1097-2765(00)80330-5

Herbert, S. P., and Stainier, D. Y. (2011). Molecular control of endothelial cell behaviour during blood vessel morphogenesis. *Nat. Rev. Mol. Cell Biol.* 12, 551–564. doi: 10.1038/nrm3176

Himes, S. R., Sester, D. P., Ravasi, T., Cronau, S. L., Sasmono, T., and Hume, D. A. (2006). The JNK are important for development and survival of macrophages. *J. Immunol.* 176, 2219–2228. doi: 10.4049/jimmunol.176.4.2219

Hladilkova, E., Baroy, T., Fannemel, M., Vallova, V., Misceo, D., Bryn, V., et al. (2015). A recurrent deletion on chromosome 2q13 is associated with developmental delay and mild facial dysmorphisms. *Mol. Cytogenet.* 8:57.

Howe, A. K., and Juliano, R. L. (2000). Regulation of anchorage-dependent signal transduction by protein kinase A and p21-activated kinase. *Nat. Cell Biol.* 2, 593–600. doi: 10.1038/35023536

Hu, Q., Milfay, D., and Williams, L. T. (1995). Binding of NCK to SOS and activation of ras-dependent gene expression. *Mol. Cell Biol.* 15, 1169–1174. doi: 10.1128/mcb.15.3.1169

Hu, T., Shi, G., Larose, L., Rivera, G. M., Mayer, B. J., and Zhou, R. (2009). Regulation of process retraction and cell migration by EphA3 is mediated by the adaptor protein Nck1. *Biochemistry* 48, 6369–6378. doi: 10.1021/bi900831k

Huttenlocher, A., and Horwitz, A. R. (2011). Integrins in cell migration. *Cold Spring Harb. Perspect. Biol.* 3:a005074.

Igarashi, K., Isohara, T., Kato, T., Shigeta, K., Yamano, T., and Uno, I. (1998). Tyrosine 1213 of Flt-1 is a major binding site of Nck and SHP-2. *Biochem. Biophys. Res. Commun.* 246, 95–99. doi: 10.1006/bbrc.1998.8578

Ito, N., Wernstedt, C., Engstrom, U., and Claesson-Welsh, L. (1998). Identification of vascular endothelial growth factor receptor-1 tyrosine phosphorylation sites and binding of SH2 domain-containing molecules. *J. Biol. Chem.* 273, 23410–23418. doi: 10.1074/jbc.273.36.23410

Jacquet, K., Banerjee, S. L., Chartier, F. J. M., Elowe, S., and Bisson, N. (2018). Proteomic analysis of NCK1/2 adaptors uncovers paralog-specific interactions that reveal a new role for NCK2 in cell abscission during cytokinesis. *Mol. Cell Proteom.* 17, 1979–1990. doi: 10.1074/mcp.ra118.000689

Kebache, S., Zuo, D., Chevet, E., and Larose, L. (2002). Modulation of protein translation by Nck-1. *Proc. Natl. Acad. Sci. U.S.A.* 99, 5406–5411. doi: 10.1073/pnas.082483399

Kesti, T., Ruppelt, A., Wang, J. H., Liss, M., Wagner, R., Tasken, K., et al. (2007). Reciprocal regulation of SH3 and SH2 domain binding via tyrosine phosphorylation of a common site in CD3epsilon. *J. Immunol.* 179, 878–885. doi: 10.4049/jimmunol.179.2.878

Keyvani Chahi, A., Martin, C. E., and Jones, N. (2016). Nephrin suppresses hippo signaling through the adaptor proteins Nck and WTIP. *J. Biol. Chem.* 291, 12799–12808. doi: 10.1074/jbc.m116.724245

Kiosses, W. B., Hood, J., Yang, S., Gerritsen, M. E., Cheresh, D. A., Alderson, N., et al. (2002). A dominant-negative p65 PAK peptide inhibits angiogenesis. *Circ. Res.* 90, 697–702. doi: 10.1161/01.res.0000014227.76102.5d

Koch, S., and Claesson-Welsh, L. (2012). Signal transduction by vascular endothelial growth factor receptors. *Cold Spring Harb. Perspect. Med.* 2:a006502. doi: 10.1101/cshperspect.a006502

Konakahara, S., Suzuki, Y., Kawakami, T., Saitou, M., Kajikawa, M., Masuho, Y., et al. (2012). A neuronal transmembrane protein LRFN4 complexes with 14-3-3s and NCK1 to induce morphological change in monocytic cells via Rac1-mediated actin cytoskeleton reorganization. *FEBS Lett.* 586, 2251–2259. doi: 10.1016/j.febslet.2012.05.053

Kruchten, A. E., Krueger, E. W., Wang, Y., and Mcniven, M. A. (2008). Distinct phospho-forms of cortactin differentially regulate actin polymerization and focal adhesions. *Am. J. Physiol. Cell Physiol.* 295, C1113–C1122.

Kurochkina, N., and Guha, U. (2013). SH3 domains: modules of protein-protein interactions. *Biophys. Rev.* 5, 29–39. doi: 10.1007/s12551-012-0081-z

Labelle-Cote, M., Dusseault, J., Ismail, S., Picard-Cloutier, A., Siegel, P. M., and Larose, L. (2011). Nck2 promotes human melanoma cell proliferation, migration and invasion in vitro and primary melanoma-derived tumor growth in vivo. *BMC Cancer* 11:443. doi: 10.1186/1471-2407-11-443

LaMack, J. A., Himburg, H. A., Li, X. M., and Friedman, M. H. (2005). Interaction of wall shear stress magnitude and gradient in the prediction of arterial macromolecular permeability. *Ann. Biomed. Eng.* 33, 457–464. doi: 10.1007/s10439-005-2500-9

Lamalice, L., Houle, F., and Huot, J. (2006). Phosphorylation of Tyr1214 within VEGFR-2 triggers the recruitment of Nck and activation of Fyn leading to SAPK2/p38 activation and endothelial cell migration in response to VEGF. *J. Biol. Chem.* 281, 34009–34020. doi: 10.1074/jbc.m603928200

Lane, C., Qi, J., and Fawcett, J. P. (2015). NCK is critical for the development of deleted in colorectal cancer (DCC) sensitive spinal circuits. *J. Neurochem.* 134, 1008–1014. doi: 10.1111/jnc.13137

Latreille, M., Laberge, M. K., Bourret, G., Yamani, L., and Larose, L. (2011). Deletion of Nck1 attenuates hepatic ER stress signaling and improves glucose tolerance and insulin signaling in liver of obese mice. *Am. J. Physiol. Endocrinol. Metab.* 300, E423–E434.

Latreille, M., and Larose, L. (2006). Nck in a complex containing the catalytic subunit of protein phosphatase 1 regulates eukaryotic initiation factor 2alpha signaling and cell survival to endoplasmic reticulum stress. *J. Biol. Chem.* 281, 26633–26644. doi: 10.1074/jbc.m513556200

Lawe, D. C., Hahn, C., and Wong, A. J. (1997). The Nck SH2/SH3 adaptor protein is present in the nucleus and associates with the nuclear protein SAM68. *Oncogene* 14, 223–231. doi: 10.1038/sj.onc.1200821

Lee, C. H., Leung, B., Lemmon, M. A., Zheng, J., Cowburn, D., Kuriyan, J., et al. (1995). A single amino acid in the SH3 domain of Hck determines its high affinity and specificity in binding to HIV-1 Nef protein. *EMBO J.* 14, 5006–5015. doi: 10.1002/j.1460-2075.1995.tb00183.x

Lehmann, J. M., Riethmuller, G., and Johnson, J. P. (1990). Nck, a melanoma cDNA encoding a cytoplasmic protein consisting of the src homology units SH2 and SH3. *Nucleic Acids Res.* 18:1048. doi: 10.1093/nar/18.4.1048

Lettau, M., Pieper, J., Gerneth, A., Lengl-Janssen, B., Voss, M., Linkermann, A., et al. (2010). The adapter protein Nck: role of individual SH3 and SH2 binding modules for protein interactions in T lymphocytes. *Protein Sci.* 19, 658–669. doi: 10.1002/pro.334

Lettau, M., Pieper, J., and Janssen, O. (2009). Nck adapter proteins: functional versatility in T cells. *Cell Commun. Signal.* 7:1. doi: 10.1155/2012/178525

Lettau, M., Qian, J., Linkermann, A., Latreille, M., Larose, L., Kabelitz, D., et al. (2006). The adaptor protein Nck interacts with Fas ligand: guiding the death factor to the cytotoxic immunological synapse. *Proc. Natl. Acad. Sci. U.S.A.* 103, 5911–5916. doi: 10.1073/pnas.0508562103

Li, B., Pi, Z., Liu, L., Zhang, B., Huang, X., Hu, P., et al. (2013). FGF-2 prevents cancer cells from ER stress-mediated apoptosis via enhancing proteasome-mediated Nck degradation. *Biochem. J.* 452, 139–145. doi: 10.1042/bj20121671

Li, W., Fan, J., and Woodley, D. T. (2001). Nck/Dock: an adapter between cell surface receptors and the actin cytoskeleton. *Oncogene* 20, 6403–6417. doi: 10.1038/sj.onc.1204782

Li, W., Hu, P., Skolnik, E. Y., Ullrich, A., and Schlessinger, J. (1992). The SH2 and SH3 domain-containing Nck protein is oncogenic and a common target for phosphorylation by different surface receptors. *Mol. Cell Biol.* 12, 5824–5833. doi: 10.1128/mcb.12.12.5824

Lim, W. A., and Richards, F. M. (1994). Critical residues in an SH3 domain from Sem-5 suggest a mechanism for proline-rich peptide recognition. *Nat. Struct. Biol.* 1, 221–225. doi: 10.1038/nsb0494-221

Lindblom, P., Gerhardt, H., Liebner, S., Abramsson, A., Enge, M., Hellstrom, M., et al. (2003). Endothelial PDGF-B retention is required for proper investment of pericytes in the microvessel wall. *Genes Dev.* 17, 1835–1840. doi: 10.1101/gad.266803

Liu, B. A., Jablonowski, K., Raina, M., Arce, M., Pawson, T., and Nash, P. D. (2006). The human and mouse complement of SH2 domain proteins-establishing the boundaries of phosphotyrosine signaling. *Mol. Cell* 22, 851–868. doi: 10.1016/j.molcel.2006.06.001

Liu, J., Li, M., Ran, X., Fan, J. S., and Song, J. (2006). Structural insight into the binding diversity between the human Nck2 SH3 domains and proline-rich proteins. *Biochemistry* 45, 7171–7184. doi: 10.1021/bi060091y

Liu, X., Zhang, J., Duan, Z., Feng, X., Yu, Y., He, M., et al. (2020). Nck1 promotes the progression of ovarian carcinoma by enhancing the PI3K/AKT/p70S6K signaling. *Hum. Cell* 33, 768–779. doi: 10.1007/s13577-020-00344-8

Liu, Z., Guo, X., Jiang, Y., and Zhang, H. (2013). NCK2 is significantly associated with opiates addiction in African-origin men. *Sci. World J.* 2013:748979.

Locke, A. E., Kahali, B., Berndt, S. I., Justice, A. E., Pers, T. H., Day, F. R., et al. (2015). Genetic studies of body mass index yield new insights for obesity biology. *Nature* 518, 197–206.

Lu, W., Katz, S., Gupta, R., and Mayer, B. J. (1997). Activation of Pak by membrane localization mediated by an SH3 domain from the adaptor protein Nck. *Curr. Biol.* 7, 85–94. doi: 10.1016/s0960-9822(06)00052-2

Machida, K., Thompson, C. M., Dierck, K., Jablonowski, K., Karkkainen, S., Liu, B., et al. (2007). High-throughput phosphotyrosine profiling using SH2 domains. *Mol. Cell* 26, 899–915. doi: 10.1016/j.molcel.2007.05.031

Machida, N., Umikawa, M., Takei, K., Sakima, N., Myagmar, B. E., Taira, K., et al. (2004). Mitogen-activated protein kinase kinase kinase kinase 4 as a putative effector of Rap2 to activate the c-Jun N-terminal kinase. *J. Biol. Chem.* 279, 15711–15714. doi: 10.1074/jbc.c300542200

Manser, E., Huang, H. Y., Loo, T. H., Chen, X. Q., Dong, J. M., Leung, T., et al. (1997). Expression of constitutively active alpha-PAK reveals effects of the kinase on actin and focal complexes. *Mol. Cell Biol.* 17, 1129–1143. doi: 10.1128/mcb.17.3.1129

Mayer, B. J., and Gupta, R. (1998). Functions of SH2 and SH3 domains. *Curr. Top. Microbiol. Immunol.* 228, 1–22. doi: 10.1007/978-3-642-27841-9_5278-2

Mayya, V., Lundgren, D. H., Hwang, S. I., Rezaul, K., Wu, L., Eng, J. K., et al. (2009). Quantitative phosphoproteomic analysis of T cell receptor signaling reveals system-wide modulation of protein-protein interactions. *Sci. Signal.* 2:ra46. doi: 10.1126/scisignal.2000007

McCarty, J. H. (1998). The Nck SH2/SH3 adaptor protein: a regulator of multiple intracellular signal transduction events. *Bioessays* 20, 913–921. doi: 10.1002/(sici)1521-1878(199811)20:11<913::aid-bies6>3.0.co;2-t

Meisenhelder, J., and Hunter, T. (1992). The SH2/SH3 domain-containing protein Nck is recognized by certain anti-phospholipase C-gamma 1 monoclonal antibodies, and its phosphorylation on tyrosine is stimulated by platelet-derived growth factor and epidermal growth factor treatment. *Mol. Cell Biol.* 12, 5843–5856. doi: 10.1128/mcb.12.12.5843

Mizuno, K., Tagawa, Y., Mitomo, K., Watanabe, N., Katagiri, T., Ogimoto, M., et al. (2002). Src homology region 2 domain-containing phosphatase 1 positively regulates B cell receptor-induced apoptosis by modulating association of B cell linker protein with Nck and activation of c-Jun NH2-terminal kinase. *J. Immunol.* 169, 778–786. doi: 10.4049/jimmunol.169.2.778

Mundi, S., Massaro, M., Scoditti, E., Carluccio, M. A., Van Hinsbergh, V. M., Iruela-Arispe, M. L., et al. (2018). Endothelial permeability, LDL deposition, and cardiovascular risk factors-a review. *Cardiovasc. Res.* 114, 35–52. doi: 10.1093/cvr/cvx226

Musacchio, A., Noble, M., Pauptit, R., Wierenga, R., and Saraste, M. (1992). Crystal structure of a Src-homology 3 (SH3) domain. *Nature* 359, 851–855.

Ngoenkam, J., Paensuwan, P., Preechanukul, K., Khamsri, B., Yiemwattana, I., Beck-Garcia, E., et al. (2014). Non-overlapping functions of Nck1 and Nck2 adaptor proteins in T cell activation. *Cell Commun. Signal.* 12:21. doi: 10.1186/1478-811x-12-21

Nguyen, D. T., Kebache, S., Fazel, A., Wong, H. N., Jenna, S., Emadali, A., et al. (2004). Nck-dependent activation of extracellular signal-regulated kinase-1 and regulation of cell survival during endoplasmic reticulum stress. *Mol. Biol. Cell* 15, 4248–4260. doi: 10.1091/mbc.e03-11-0851

Nishimura, R., Li, W., Kashishian, A., Mondino, A., Zhou, M., Cooper, J., et al. (1993). Two signaling molecules share a phosphotyrosine-containing binding site in the platelet-derived growth factor receptor. *Mol. Cell Biol.* 13, 6889–6896. doi: 10.1128/mcb.13.11.6889

Oeste, C. L., and Alarcon, B. (2015). Editorial: Nck has a knack for T cell differentiation. *J. Leukoc. Biol.* 98, 297–298. doi: 10.1189/jlb.2ce0415-181r

Okada, S., and Pessin, J. E. (1996). Interactions between Src homology (SH) 2/SH3 adapter proteins and the guanylnucleotide exchange factor SOS are differentially regulated by insulin and epidermal growth factor. *J. Biol. Chem.* 271, 25533–25538. doi: 10.1074/jbc.271.41.25533

Orr, A. W., Hahn, C., Blackman, B. R., and Schwartz, M. A. (2008). p21-activated kinase signaling regulates oxidant-dependent NF-kappa B activation by flow. *Circ. Res.* 103, 671–679. doi: 10.1161/circresaha.108.182097

Orr, A. W., Sanders, J. M., Bevard, M., Coleman, E., Sarembock, I. J., and Schwartz, M. A. (2005). The subendothelial extracellular matrix modulates NF-kappa B activation by flow: a potential role in atherosclerosis. *J. Cell Biol.* 169, 191–202. doi: 10.1083/jcb.200410073

Orr, A. W., Stockton, R., Simmers, M. B., Sanders, J. M., Sarembock, I. J., Blackman, B. R., et al. (2007). Matrix-specific p21-activated kinase activation regulates vascular permeability in atherogenesis. *J. Cell Biol.* 176, 719–727. doi: 10.1083/jcb.200609008

Oser, M., Yamaguchi, H., Mader, C. C., Bravo-Cordero, J. J., Arias, M., Chen, X., et al. (2009). Cortactin regulates cofilin and N-WASp activities to control the stages of invadopodium assembly and maturation. *J. Cell Biol.* 186, 571–587. doi: 10.1083/jcb.200812176

Park, D., and Rhee, S. G. (1992). Phosphorylation of Nck in response to a variety of receptors, phorbol myristate acetate, and cyclic AMP. *Mol. Cell Biol.* 12, 5816–5823. doi: 10.1128/mcb.12.12.5816

Pawson, T. (1995). Protein modules and signalling networks. *Nature* 373, 573–580. doi: 10.1038/373573a0

Pawson, T., and Nash, P. (2003). Assembly of cell regulatory systems through protein interaction domains. *Science* 300, 445–452. doi: 10.1126/science.1083653

Pawson, T., and Scott, J. D. (1997). Signaling through scaffold, anchoring, and adaptor proteins. *Science* 278, 2075–2080. doi: 10.1126/science.278.5346.2075

Pesti, S., Balazs, A., Udupa, R., Szabo, B., Fekete, A., Bogel, G., et al. (2012). Complex formation of EphB1/Nck/Caskin1 leads to tyrosine phosphorylation and structural changes of the Caskin1 SH3 domain. *Cell Commun. Signal.* 10:36. doi: 10.1186/1478-811x-10-36

Pober, J. S., and Sessa, W. C. (2007). Evolving functions of endothelial cells in inflammation. *Nat. Rev. Immunol.* 7, 803–815. doi: 10.1038/nri2171

Poitras, L., Jean, S., Islam, N., and Moss, T. (2003). PAK interacts with NCK and MLK2 to regulate the activation of jun N-terminal kinase. *FEBS Lett.* 543, 129–135. doi: 10.1016/s0014-5793(03)00424-1

Popov, D., and Simionescu, M. (2006). Cellular mechanisms and signalling pathways activated by high glucose and AGE-albumin in the aortic endothelium. *Archiv. Physiol. Biochem.* 112, 265–273. doi: 10.1080/13813450601094573

Porter, K., and Day, B. (2016). From filaments to function: the role of the plant actin cytoskeleton in pathogen perception, signaling and immunity. *J. Integr. Plant Biol.* 58, 299–311. doi: 10.1111/jipb.12445

Potente, M., Gerhardt, H., and Carmeliet, P. (2011). Basic and therapeutic aspects of angiogenesis. *Cell* 146, 873–887. doi: 10.1016/j.cell.2011.08.039

Radu, M., Lyle, K., Hoeflich, K. P., Villamar-Cruz, O., Koeppen, H., and Chernoff, J. (2015). p21-activated Kinase 2 regulates endothelial development and function through the Bmk1/Erk5 pathway. *Mol. Cell. Biol.* 35, 3990–4005. doi: 10.1128/mcb.00630-15

Rao, Y., and Zipursky, S. L. (1998). Domain requirements for the Dock adapter protein in growth- cone signaling. *Proc. Natl. Acad. Sci. U.S.A.* 95, 2077–2082. doi: 10.1073/pnas.95.5.2077

Reutershan, J., Stockton, R., Zarbock, A., Sullivan, G. W., Chang, D., Scott, D., et al. (2007). Blocking p21-activated kinase reduces lipopolysaccharide-induced acute lung injury by preventing polymorphonuclear leukocyte infiltration. *Am. J. Respir. Crit. Care Med.* 175, 1027–1035. doi: 10.1164/rccm.200612-1822oc

Richter, K., Rufer, A. C., Muller, M., Burger, D., Casagrande, F., Grossenbacher, T., et al. (2020). Small molecule AX-024 reduces T cell proliferation independently of CD3/Nck1 interaction, which is governed by a domain swap in the Nck1-SH3.1 domain. *J. Biol. Chem.* 295, 7849–7864. doi: 10.1074/jbc.ra120.012788

Rivera, G. M., Antoku, S., Gelkop, S., Shin, N. Y., Hanks, S. K., Pawson, T., et al. (2006). Requirement of Nck adaptors for actin dynamics and cell migration stimulated by platelet-derived growth factor B. *Proc. Natl. Acad. Sci. U.S.A.* 103, 9536–9541. doi: 10.1073/pnas.0603786103

Rivero-Lezcano, O. M., Marcilla, A., Sameshima, J. H., and Robbins, K. C. (1995). Wiskott-Aldrich syndrome protein physically associates with Nck through Src homology 3 domains. *Mol. Cell Biol.* 15, 5725–5731. doi: 10.1128/mcb.15.10.5725

Roche, S., Mcglade, J., Jones, M., Gish, G. D., Pawson, T., and Courtneidge, S. A. (1996). Requirement of phospholipase C gamma, the tyrosine phosphatase Syp and the adaptor proteins Shc and Nck for PDGF-induced DNA synthesis: evidence for the existence of Ras-dependent and Ras-independent pathways. *EMBO J.* 15, 4940–4948. doi: 10.1002/j.1460-2075.1996.tb00874.x

Rockow, S., Tang, J., Xiong, W., and Li, W. (1996). Nck inhibits NGF and basic FGF induced PC12 cell differentiation via mitogen-activated protein kinase-independent pathway. *Oncogene* 12, 2351–2359.

Ruusala, A., Pawson, T., Heldin, C. H., and Aspenstrom, P. (2008). Nck adapters are involved in the formation of dorsal ruffles, cell migration, and Rho signaling downstream of the platelet-derived growth factor beta receptor. *J. Biol. Chem.* 283, 30034–30044. doi: 10.1074/jbc.m800913200

Saksela, K., and Permi, P. (2012). SH3 domain ligand binding: what's the consensus and where's the specificity? *FEBS Lett.* 586, 2609–2614. doi: 10.1016/j.febslet.2012.04.042

Schmitz, U., Ishida, M., and Berk, B. C. (1997). Angiotensin II stimulates tyrosine phosphorylation of phospholipase C-gamma-associated proteins. Characterization of a c-Src-dependent 97-kD protein in vascular smooth muscle cells. *Circ. Res.* 81, 550–557. doi: 10.1161/01.res.81.4.550

Schmitz, U., Thommes, K., Beier, I., Wagner, W., Sachinidis, A., Dusing, R., et al. (2001). Angiotensin II-induced stimulation of p21-activated kinase and c-Jun NH2-terminal kinase is mediated by Rac1 and Nck. *J. Biol. Chem.* 276, 22003–22010. doi: 10.1074/jbc.m102450200

Schwartzentruber, J., Cooper, S., Liu, J. Z., Barrio-Hernandez, I., Bello, E., Kumasaka, N., et al. (2021). Genome-wide meta-analysis, fine-mapping and integrative prioritization implicate new Alzheimer's disease risk genes. *Nat. Genet.* 53, 392–402. doi: 10.1038/s41588-020-00776-w

Shitashige, M., Satow, R., Jigami, T., Aoki, K., Honda, K., Shibata, T., et al. (2010). Traf2- and Nck-interacting kinase is essential for Wnt signaling and colorectal cancer growth. *Cancer Res.* 70, 5024–5033. doi: 10.1158/0008-5472.can-10-0306

Srivastava, N., Robichaux, M. A., Chenaux, G., Henkemeyer, M., and Cowan, C. W. (2013). EphB2 receptor forward signaling controls cortical growth cone collapse via Nck and Pak. *Mol. Cell Neurosci.* 52, 106–116. doi: 10.1016/j.mcn.2012.11.003

Stein, E., Huynh-Do, U., Lane, A. A., Cerretti, D. P., and Daniel, T. O. (1998). Nck recruitment to Eph receptor, EphB1/ELK, couples ligand activation to c-Jun kinase. *J. Biol. Chem.* 273, 1303–1308. doi: 10.1074/jbc.273.3.1303

Stockton, R. A., Schaefer, E., and Schwartz, M. A. (2004). p21-activated kinase regulates endothelial permeability through modulation of contractility. *J. Biol. Chem.* 279, 46621–46630. doi: 10.1074/jbc.m408877200

Stoletov, K. V., Gong, C., and Terman, B. I. (2004). Nck and Crk mediate distinct VEGF-induced signaling pathways that serve overlapping functions in focal adhesion turnover and integrin activation. *Exp. Cell Res.* 295, 258–268. doi: 10.1016/j.yexcr.2004.01.008

Stoletov, K. V., Ratcliffe, K. E., Spring, S. C., and Terman, B. I. (2001). NCK and PAK participate in the signaling pathway by which vascular endothelial growth factor stimulates the assembly of focal adhesions. *J. Biol. Chem.* 276, 22748–22755. doi: 10.1074/jbc.m009720200

Su, L. C., Xu, W. D., and Huang, A. F. (2020). IRAK family in inflammatory autoimmune diseases. *Autoimmun. Rev.* 19:102461. doi: 10.1016/j.autrev.2020.102461

Su, Y. C., Han, J., Xu, S., Cobb, M., and Skolnik, E. Y. (1997). NIK is a new Ste20-related kinase that binds NCK and MEKK1 and activates the SAPK/JNK cascade via a conserved regulatory domain. *EMBO J.* 16, 1279–1290. doi: 10.1093/emboj/16.6.1279

Sun, C., Wu, M. H., and Yuan, S. Y. (2011). Nonmuscle myosin light-chain kinase deficiency attenuates atherosclerosis in apolipoprotein E-deficient mice via reduced endothelial barrier dysfunction and monocyte migration. *Circulation* 124, 48–57. doi: 10.1161/circulationaha.110.988915

Takeuchi, K., Sun, Z. Y., Park, S., and Wagner, G. (2010). Autoinhibitory interaction in the multidomain adaptor protein Nck: possible roles in improving specificity and functional diversity. *Biochemistry* 49, 5634–5641. doi: 10.1021/bi100322m

Takeuchi, K., Yang, H., Ng, E., Park, S. Y., Sun, Z. Y., Reinherz, E. L., et al. (2008). Structural and functional evidence that Nck interaction with CD3epsilon regulates T-cell receptor activity. *J. Mol. Biol.* 380, 704–716. doi: 10.1016/j.jmb.2008.05.037

Tanaka, M., Gupta, R., and Mayer, B. J. (1995). Differential inhibition of signaling pathways by dominant-negative SH2/SH3 adapter proteins. *Mol. Cell Biol.* 15, 6829–6837. doi: 10.1128/mcb.15.12.6829

Teyra, J., Huang, H., Jain, S., Guan, X., Dong, A., Liu, Y., et al. (2017). Comprehensive analysis of the human SH3 domain family reveals a wide variety of non-canonical specificities. *Structure* 25, 1598–1610.e1593.

van der Harst, P., and Verweij, N. (2018). Identification of 64 Novel genetic loci provides an expanded view on the genetic architecture of coronary artery disease. *Circ. Res.* 122, 433–443. doi: 10.1161/circresaha.117.312086

Verma, R., Kovari, I., Soofi, A., Nihalani, D., Patrie, K., and Holzman, L. B. (2006). Nephrin ectodomain engagement results in Src kinase activation, nephrin phosphorylation, Nck recruitment, and actin polymerization. *J. Clin. Invest.* 116, 1346–1359. doi: 10.1172/jci27414

Voisin, L., Larose, L., and Meloche, S. (1999). Angiotensin II stimulates serine phosphorylation of the adaptor protein Nck: physical association with the serine/threonine kinases Pak1 and casein kinase I. *Biochem. J.* 341(Pt 1), 217–223. doi: 10.1042/bj3410217

Wagner, E. F., and Nebreda, A. R. (2009). Signal integration by JNK and p38 MAPK pathways in cancer development. *Nat. Rev. Cancer* 9, 537–549. doi: 10.1038/nrc2694

Waksman, G., Kominos, D., Robertson, S. C., Pant, N., Baltimore, D., Birge, R. B., et al. (1992). Crystal structure of the phosphotyrosine recognition domain SH2 of v-src complexed with tyrosine-phosphorylated peptides. *Nature* 358, 646–653. doi: 10.1038/358646a0

Wang, B., Zou, J. X., Ek-Rylander, B., and Ruoslahti, E. (2000). R-Ras contains a proline-rich site that binds to SH3 domains and is required for integrin activation by R-Ras. *J. Biol. Chem.* 275, 5222–5227. doi: 10.1074/jbc.275.7.5222

Wang, Y., Chang, J., Chen, K. D., Li, S., Li, J. Y., Wu, C., et al. (2007). Selective adapter recruitment and differential signaling networks by VEGF vs. shear stress. *Proc. Natl. Acad. Sci. U.S.A.* 104, 8875–8879. doi: 10.1073/pnas.0703088104

Welihinda, A. A., Tirasophon, W., and Kaufman, R. J. (1999). The cellular response to protein misfolding in the endoplasmic reticulum. *Gene Expr.* 7, 293–300.

Yablonski, D., Kane, L. P., Qian, D., and Weiss, A. (1998). A Nck-Pak1 signaling module is required for T-cell receptor-mediated activation of NFAT, but not of JNK. *EMBO J.* 17, 5647–5657. doi: 10.1093/emboj/17.19.5647

Yamani, L., Latreille, M., and Larose, L. (2014). Interaction of Nck1 and PERK phosphorylated at Y(5)(6)(1) negatively modulates PERK activity and PERK regulation of pancreatic beta-cell proinsulin content. *Mol. Biol. Cell* 25, 702–711. doi: 10.1091/mbc.e13-09-0511

Yamani, L., Li, B., and Larose, L. (2015). Nck1 deficiency improves pancreatic beta cell survival to diabetes-relevant stresses by modulating PERK activation and signaling. *Cell Signal.* 27, 2555–2567. doi: 10.1016/j.cellsig.2015.09.016

Yurdagul, A. Jr., Chen, J., Funk, S. D., Albert, P., Kevil, C. G., and Orr, A. W. (2013). Altered nitric oxide production mediates matrix-specific PAK2 and NF-kappaB activation by flow. *Mol. Biol. Cell* 24, 398–408. doi: 10.1091/mbc.e12-07-0513

Yurdagul, A. Jr., and Orr, A. W. (2016). Blood brothers: hemodynamics and cell-matrix interactions in endothelial function. *Antioxid Redox Signal.* 25, 415–434. doi: 10.1089/ars.2015.6525

Zhang, F., Lu, Y. X., Chen, Q., Zou, H. M., Zhang, J. M., Hu, Y. H., et al. (2017). Identification of NCK1 as a novel downstream effector of STAT3 in colorectal

cancer metastasis and angiogenesis. *Cell Signal.* 36, 67–78. doi: 10.1016/j.cellsig.2017.04.020

Zhang, P., Mcgrath, B., Li, S., Frank, A., Zambito, F., Reinert, J., et al. (2002). The PERK eukaryotic initiation factor 2 alpha kinase is required for the development of the skeletal system, postnatal growth, and the function and viability of the pancreas. *Mol. Cell Biol.* 22, 3864–3874. doi: 10.1128/mcb.22.11.3864-3874.2002

Zhao, Z. S., Manser, E., Loo, T. H., and Lim, L. (2000). Coupling of PAK-interacting exchange factor PIX to GIT1 promotes focal complex disassembly. *Mol. Cell Biol.* 20, 6354–6363. doi: 10.1128/.20.17.6354-6363.2000

Conflict of Interest: The authors declare that the research was conducted in the absence of any commercial or financial relationships that could be construed as a potential conflict of interest.

Copyright © 2021 Alfaidi, Scott and Orr. This is an open-access article distributed under the terms of the Creative Commons Attribution License (CC BY). The use, distribution or reproduction in other forums is permitted, provided the original author(s) and the copyright owner(s) are credited and that the original publication in this journal is cited, in accordance with accepted academic practice. No use, distribution or reproduction is permitted which does not comply with these terms.

frontiers in Cell and Developmental Biology

REVIEW
published: 08 June 2021
doi: 10.3389/fcell.2021.691585

AMPK and Pulmonary Hypertension: Crossroads Between Vasoconstriction and Vascular Remodeling

*Qiang Zhao, Ping Song and Ming-Hui Zou**

Center for Molecular and Translational Medicine, Georgia State University, Atlanta, GA, United States

Pulmonary hypertension (PH) is a debilitating and life-threatening disease characterized by increased blood pressure within the pulmonary arteries. Adenosine monophosphate-activated protein kinase (AMPK) is a heterotrimeric serine-threonine kinase that contributes to the regulation of metabolic and redox signaling pathways. It has key roles in the regulation of cell survival and proliferation. The role of AMPK in PH is controversial because both inhibition and activation of AMPK are preventive against PH development. Some clinical studies found that metformin, the first-line antidiabetic drug and the canonical AMPK activator, has therapeutic efficacy during treatment of early-stage PH. Other study findings suggest the use of metformin is preferentially beneficial for treatment of PH associated with heart failure with preserved ejection fraction (PH-HFpEF). In this review, we discuss the "AMPK paradox" and highlight the differential effects of AMPK on pulmonary vasoconstriction and pulmonary vascular remodeling. We also review the effects of AMPK activators and inhibitors on rescue of preexisting PH in animals and include a discussion of gender differences in the response to metformin in PH.

Keywords: AMPK, pulmonary hypertension, pulmonary vascular remodeling, hypoxic pulmonary vasoconstriction, metformin

OPEN ACCESS

Edited by:
Ramani Ramchandran,
Medical College of Wisconsin,
United States

Reviewed by:
Ru-Jeng Teng,
Medical College of Wisconsin,
United States
Reena Singh,
The University of Sydney, Australia

***Correspondence:**
Ming-Hui Zou
mzou@gsu.edu

Specialty section:
This article was submitted to Signaling, a section of the journal Frontiers in Cell and Developmental Biology

Received: *06 April 2021*
Accepted: *18 May 2021*
Published: *08 June 2021*

Citation:
Zhao Q, Song P and Zou M-H (2021) AMPK and Pulmonary Hypertension: Crossroads Between Vasoconstriction and Vascular Remodeling. Front. Cell Dev. Biol. 9:691585. doi: 10.3389/fcell.2021.691585

INTRODUCTION

Pulmonary hypertension (PH) is a disease characterized by high blood pressure that affects the vessels in lungs. These changes result in right ventricular failure and ultimately, premature death (Maron and Leopold, 2015). Adenosine monophosphate-activated protein kinase (AMPK) is a central regulator of energy homeostasis. It is activated under a variety of conditions, including hypoxia, nutrient starvation, and toxin exposure (Towler and Hardie, 2007; Kim et al., 2016; Herzig and Shaw, 2018). AMPK exerts most of its biological effects *via* catalytic α-subunits (α1 and α2) that are ubiquitously expressed in pulmonary vessels (Mihaylova and Shaw, 2011; Hardie, 2013; Kim et al., 2016). AMPK α1 is the predominant subunit in small pulmonary artery-derived pulmonary microvascular endothelial cells (ECs) and vascular smooth muscle cells (VSMCs). AMPK α2 is the predominant subunit in conduit pulmonary artery-derived ECs and VSMCs (Evans et al., 2005; Creighton et al., 2011). The AMPK α1 and AMPK α2 subunits have different effects on survival of pulmonary VSMCs and hypoxic pulmonary vasoconstriction. For example, activation of AMPK α1 stimulates autophagy in pulmonary artery VSMCs, but AMPK α2 activation prevents apoptosis

(Ibe et al., 2013). Under conditions of mild hypoxia, AMPK α1 is activated by liver kinase B1 (LKB1) and is required for hypoxic pulmonary vasoconstriction; the AMPK α2 subunit is required under conditions of severe hypoxia (Moral-Sanz et al., 2018). Because of these characteristics, studies found that use of AMPK-targeting agonists and antagonists results in contradictory effects on PH development. Some studies found that AMPK activators [i.e., metformin (Agard et al., 2009; Dean et al., 2016; Lai et al., 2016; Omura et al., 2016; Zhai et al., 2018; Zhang et al., 2018; Wang et al., 2020), 5-aminoimidazole-4-carboxamide (AICAR) (Huang et al., 2014; Chen et al., 2016; Dean et al., 2016), rosiglitazone/pioglitazone (Hansmann et al., 2007; Satoh et al., 2009; Kim et al., 2010; Legchenko et al., 2018), and apelin (Chandra et al., 2011; Kim, 2014)] are protective against experimental PH. Other studies found that AMPK activation induces hypoxic pulmonary vasoconstriction (Evans, 2006; Robertson et al., 2008; Evans et al., 2009; Moral-Sanz et al., 2018) and that inhibition of AMPK by compound C prevents PH (Ibe et al., 2013). Results from human clinical studies are not currently conclusive on the precise role of AMPK in PH because studies on PH treatment using metformin are currently phase two clinical trials (NCT01884051 and NCT03629340). The AMPK paradox remains relevant.

AMPK: STRUCTURE AND REGULATION

AMPK Structure

Adenosine monophosphate-activated protein kinase is a highly conserved serine/threonine protein kinase complex consisting of a catalytic α-subunit, a scaffolding β-subunit, and a regulatory γ-subunit (**Figure 1**). In eukaryotes, each subunit has multiple distinct isoforms encoded by different genes. The α-subunit has two isoforms, α1 and α2, encoded by genes *Prkaa1* and *Prkaa2*, respectively (Stapleton et al., 1996). It contains a canonical N-terminal Ser/Thr kinase domain (KD), an auto-inhibitory domain (AID), and an adenine nucleotide sensor segment termed an α-linker (Herzig and Shaw, 2018; Yan et al., 2018). AMPK activation requires phosphorylation of critical residues (Thr174 in the AMPK α1 subunit and Thr172 in the AMPK α2 subunit) within the activation loop of the KD in the AMPKα catalytic subunit that is phosphorylated by upstream kinases LKB1 (Hudson et al., 2003), Ca^{2+}/calmodulin-dependent protein kinase β (CaMKKβ) (Woods et al., 2005), or TGF-beta-activated kinase-1 (TAK-1) (Momcilovic et al., 2006). AMPK auto-inhibition requires an AID, which interacts with the KD and causes AMPK to be maintained as an inactive conformation (Chen et al., 2013; Kim et al., 2016). The β-subunit also has two isoforms, β1 and β2, encoded by *Prkab1* and *Prkab2*, respectively (Hudson et al., 2003). The γ-subunit has three isoforms, γ1, γ2, and γ3, encoded by *Prkag1*, *Prkag2*, and *Prkag3*, respectively (Cheung et al., 2000). The γ-subunits contain four tandem cystathionine-β-synthase domains, which enable AMP, ADP, or ATP binding (Xiao et al., 2007). Binding of AMP, and to a lesser extent ADP, to the γ-subunit is an important regulatory feature of the conformational switch that activates the AMPK complex (Hardie et al., 2011; Gowans et al., 2013; Ross et al., 2016a). Each AMPK complex consists of one α-subunit, one β-subunit, and one γ-subunit, and all 12 heterotrimeric combinations are possible (Ross et al., 2016b). Different subunits have distinct organ preferences and expression patterns. For example, the AMPK α1 subunit is mainly expressed in adipose tissue (Ruderman et al., 2003; Rutter et al., 2003; Kelly et al., 2004). The AMPK α2 subunit is predominantly expressed in skeletal muscle and cardiac myocytes (Sakamoto et al., 2005, 2006; Thomson et al., 2007). Isoform-specific roles of AMPK α1/AMPK α2 contribute to the pathogenesis of different diseases (e.g., cardiovascular disease (Ahmad et al., 2005; Sakamoto et al., 2006; Zarrinpashneh et al., 2006; Arad et al., 2007), osteoclastogenesis (Wang et al., 2016), and Alzheimer's disease (Zhao et al., 2020)).

AMPK Signaling Transduction

Adenosine monophosphate-activated protein kinase can be phosphorylated directly by small molecules that mimic cellular decreased ATP-to-ADP or ATP-to-AMP ratios or three upstream AMPK kinases (i.e., LKB1, CaMKKβ and TAK1) (**Figure 1**). Upon changes in ATP/ADP and ATP/AMP ratios that occur during nutrient starvation, AMP binds to the AMPK γ subunit to cause allosteric activation *via* modulation of the phosphorylation state of Thr172 (Xiao et al., 2011; Oakhill et al., 2012; Gowans et al., 2013). LKB1, in a complex with the pseudokinase STRAD and the scaffolding protein MO25, directly phosphorylates AMPK at Thr172 (Lizcano et al., 2004). Study results indicate that LKB1 is the principal route *via* which AMPK is activated in many organs (e.g., skeletal muscle, adipose tissue, and liver) (Shackelford and Shaw, 2009). Whereas, CaMKKβ activates AMPK in response to Ca^{2+} signaling pathways (Hawley et al., 2005; Hong et al., 2005; Hurley et al., 2005). In 2006, TAK1 (i.e., MAPKK kinase-7, MAP3K7) was identified as the third kinase capable of direct AMPK activation (Momcilovic et al., 2006).

Adenosine monophosphate-activated protein kinase can be activated by hypoxia in various tissue and cell types (Mungai et al., 2011; Sallé-Lefort et al., 2016), but long-term hypoxia exposure inhibits AMPK activation (de Theije et al., 2018). Many studies found that activation of AMPK under hypoxia primarily implies LKB1 activity, because AMPK activation is abrogated in LKB1-deleted cells and knockout of CaMKK2, or another upstream kinase, has no effect on AMPK activation in VSMCs under hypoxic conditions (Moral-Sanz et al., 2018). Some studies found that LKB1 seems to only activate the AMPK α2 subunit, because the AMPK α1 subunit remains phosphorylated in LKB1-deficient heart muscle cells (Sakamoto et al., 2006). This result might be explained by differences in abundances and preferences of the AMPK upstream kinase in different cells and organs. Increased production of reactive oxygen species (ROS) in hypoxic conditions contributes to activation of AMPK (Choi et al., 2001; Emerling et al., 2009; Zmijewski et al., 2010; Hinchy et al., 2018). Hypoxia-inducible factor-prolyl-4-hydroxylases (HIF-P4Hs) have a role in the activation of AMPK (Yan et al., 2012; Dengler and Gäbel, 2019).

Once activated, AMPK phosphorylates key proteins in multiple pathways (Marsin et al., 2000; Inoki et al., 2003;

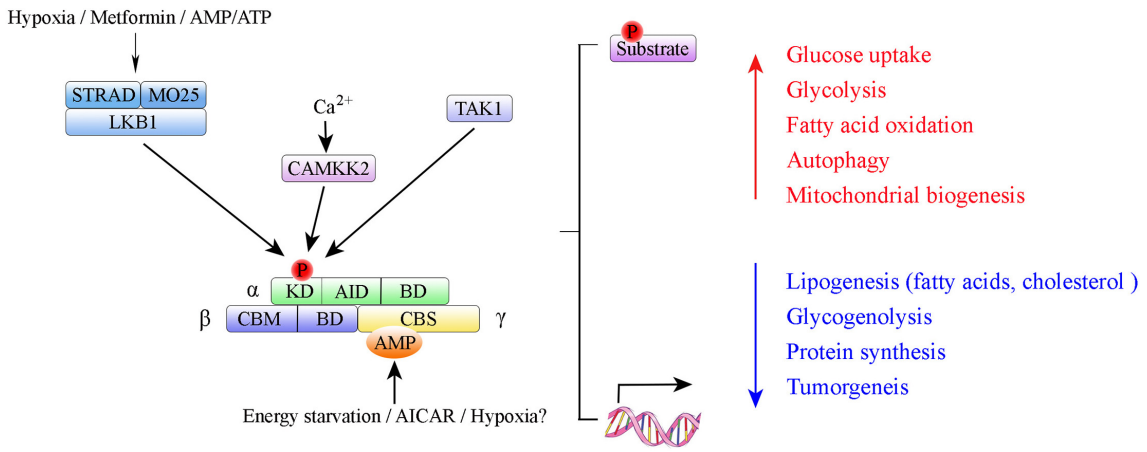

FIGURE 1 | Summary of AMP-activated protein kinase (AMPK) structure and activation. Domain structure of AMPK trimer: α-, β-, and γ-subunits with respective domains. AMPK α subunits: KD, kinase domain containing Thr-172 phosphorylation site; AID, autoinhibitory domain; BD, binding domain. AMPK β subunits: CBM, carbohydrate binding module; BD, binding domain. AMPK γ subunits: CBS, cystathione-β-synthase domain. The upstream kinases LKB1, CAMKK2, and TAK1 are shown above the AMPK complex. LKB1 in complex with STRAD and MO25 activates AMPK; CAMKK2 activated by intracellular calcium.

Gwinn et al., 2008) or directly regulates key enzymes involved in these pathways. These processes occur over time *via* targeting of transcriptional regulators (Koo et al., 2005; Lamia et al., 2009; Bungard et al., 2010; **Figure 1**). The most important aspect of AMPK biology is its role in maintaining the balance between catabolism and anabolism in response to metabolic stress (Towler and Hardie, 2007; Hardie, 2008; Fogarty and Hardie, 2010). Studies have revealed the roles of AMPK in lipid homeostasis [e.g., acetyl-CoA carboxylase (Munday et al., 1988) and HMG-CoA reductase (Carling et al., 1987)], glucose metabolism [e.g., thioredoxin-interacting protein (TXNIP) (Wu et al., 2013) and 6-phosphofructo-2-kinase (Bando et al., 2005)], insulin signaling (Galic et al., 2011; Li Y. et al., 2011; Fullerton et al., 2013; Wu et al., 2015; Emilio et al., 2016; Myers et al., 2017), and food intake and body weight (Kahn et al., 2005; Kola et al., 2005; Kola, 2008). Given those functional attributes in metabolism, AMPK is a major therapeutic target for treatment of metabolic diseases (e.g., type 2 diabetes) and obesity (Viollet et al., 2009; Rojas et al., 2011; Hardie, 2013; Day et al., 2017). A growing body of evidence also points to specific regulation of AMPK and mitochondrial homeostasis, including *via* stimulation of mitochondrial biogenesis (Bergeron et al., 2001; Zong et al., 2002; Garcia-Roves et al., 2008), regulation of mitochondrial dynamics (Ducommun et al., 2015; Toyama et al., 2016), and mitophagy (Wang et al., 2001; Egan et al., 2011).

AMPK and Cardiovascular Disease

Adenosine monophosphate-activated protein kinase has pivotal roles in cardiovascular physiology and in cardiovascular disease states. AMPK α1 is the predominant subunit in VSMCs, ECs, monocytes/macrophages, and adipocytes. AMPK α2 is the predominant subunit in cardiomyocytes (Shirwany and Zou, 2010; Wu and Zou, 2020). The functions of AMPK in cardiovascular disease include contributions to atherosclerosis and to heart failure and hypertension, which have been extensively reviewed elsewhere (Shirwany and Zou, 2010; Wu and Zou, 2020).

PULMONARY HYPERTENSION

Categories

Pulmonary hypertension is a general term used to describe increased blood pressure (mean pulmonary arterial pressure, mPAP, exceeds 25 mmHg at rest) in the lungs (Galiè et al., 2009). At the 5th and 6th World Symposium on PH, it was classified into five groups: pulmonary artery hypertension (PAH, Group 1), PH associated with left heart disease (Group 2), PH associated with lung disease and/or hypoxia (Group 3), PH associated with chronic thromboembolic disease (Group 4), and PH with unclear or multifactorial mechanisms, or both (Group 5) (Galiè and Simonneau, 2013; Simonneau et al., 2019). Each group represents a very broad spectrum of disease etiology, pathobiology, hemodynamic characteristics, and therapeutic approaches (**Table 1**). The detailed features and treatments of pulmonary hypertensive vascular disease in humans have been reviewed elsewhere (Maron and Galiè, 2016; Thenappan et al., 2018). AMPK deficiency has been identified in metabolic syndrome-associated PH (PH-HFpE) (Lai et al., 2016). However, in PAH, AMPK activity and expression can be either inhibited or promoted depending on cell type and branch pulmonary artery diameter (Ibe et al., 2013; Omura et al., 2016; Zhang et al., 2018), which is discussed in section "Clinical Trials of Pulmonary Hypertension Treatment Using Metformin."

Pathology of PH

Although the exact causes of PH remain to be determined, study findings indicate that it results from a combination of sustained pulmonary vasoconstriction and pulmonary vascular remodeling (Stenmark and McMurtry, 2005; Stenmark et al., 2006).

TABLE 1 | Animal models of pulmonary hypertension.

Cause	Histological features	Animal models
Group 1: Pulmonary arterial hypertension (PAH)		
Idiopathic PAH	Pulmonary artery intimal proliferation	Su-Hx rat/mouse
Heritable PAH	Pulmonary artery medical hypertrophy	MCT rat
Drugs/Toxin/Others	Plexiform lesions	Su-Hx-Normoxia
Group 2: Pulmonary hypertension with left heart disease		
Left-sided heart disease	Pulmonary medical hypertrophy Pulmonary vein arterialization Pulmonary interstitial edema	SU5416/Obese ZSF1 rat
Group 3: Pulmonary hypertension associated with lung disease and/or hypoxemia		
High altitudes	Hypoxic pulmonary vasoconstriction	Su-Hx rat/mouse
COPD/Pulmonary fibrosis Obstructive sleep apnea	Muscularization of arterioles	Hypoxia rat/mouse
Group 4: Pulmonary hypertension due to chronic thrombotic and/or embolic disease		
Pulmonary emboli	Thrombi or embolism	Vena cava ligation
Other clotting disorders	Recanalized organized thrombi	
Group 5: Pulmonary hypertension triggered by other health conditions		
Heterogeneous	Heterogeneous	

Pulmonary vasoconstriction is the major contributor to the early phase of the disease; pulmonary vascular structural remodeling becomes progressively more dominant and important over time (Shimoda and Laurie, 2013). Hypoxic pulmonary vasoconstriction is a reflex contraction of vascular smooth muscle in the pulmonary circulation to optimize lung blood flow from low ventilated areas to well-oxygenated areas, and thereby optimize gas exchange and oxygen delivery (Moudgil et al., 2005; Dunham-Snary et al., 2017; Tarry and Powell, 2017). Unlike the systemic circulation, which dilates in the presence of hypoxia, pulmonary arteries constrict in response to alveolar hypoxia (Detar, 1980; Waypa and Schumacker, 2010). Hypoxic pulmonary vasoconstriction is an important homeostatic mechanism used to match regional perfusion and ventilation in the lung (Dunham-Snary et al., 2017; Tarry and Powell, 2017).

Sustained pulmonary vasoconstriction initiates pulmonary vascular structural changes. These changes are characterized by thickening of the intimal and/or medial layers of muscular vessels, which results in concentric pulmonary vascular remodeling (Heath and Edwards, 1958; Tuder, 2017). In human beings, pulmonary vascular remodeling is attributed to lesions that mainly occur in distal pre-capillary arteries, ranging in diameter from 500 to 700 μm. Remodeling involves a change in the maximal lumen diameter (interior and exterior) and accumulation of different vascular cell types in the pulmonary arterial wall (pulmonary artery ECs, VSMCs, and fibroblasts). Pulmonary endothelial dysfunction is the key trigger that drives PH development. It is characterized by either impairment of endothelial-dependent vasodilatation, reduced anticoagulant properties, ROS production, or active EC metabolic changes (Budhiraja et al., 2004; Attinà et al., 2005; Klinger et al., 2013; Ranchoux et al., 2018). Various stimuli (e.g., hypoxia, smoking, disturbed blood flow, and oxidative stress) can lead to endothelial dysfunction (Dummer et al., 2018; Ranchoux et al., 2018). In PH, progressive accumulation of resident VSMCs in pulmonary arteries contributes to expansion of the tunica media. Accumulating evidence also supports involvement of increased VSMC proliferation and inhibition of apoptosis in pulmonary vascular medial layer thickening (Tuder et al., 2007; Lyle et al., 2017; Humbert et al., 2019). Better understanding of the molecular mechanisms underlying pulmonary endothelial dysfunction and VSMC adaptation will greatly enhance our understanding of the pathogenesis of PH, which may help identify new therapeutic strategies. Other promising targets (e.g., fibroblast cell activation and immune system dysregulation) have also been identified as contributing to the pathogenesis of PH (Li M. et al., 2011; Rabinovitch et al., 2014; Plecitá-Hlavatá et al., 2016; Nicolls and Voelkel, 2017).

Animal Models of PH

A variety of pre-clinical PH animal models are available to study this complex disease of diverse etiologies and histopathological features. Each model has its own hemodynamic and microanatomic histological characteristics (**Table 1**). The chronic hypoxia rat/mouse model is the one most widely used to study PH. Exposure of rats/mice to hypoxia causes increased mPAP, pulmonary vasoconstriction, and vascular medial hypertrophy that mimic the pathological features of human PH. However, right ventricular failure is absent (Zhao, 2010; Ryan et al., 2013). Monocrotaline (MCT) is a toxic alkaloid that causes a widespread pneumotoxicity and endothelial injury (Kay et al., 1967; Wilson et al., 1989). A single dose of MCT (60 mg/Kg) is sufficient to induce PH in rats by modulating two key pathological features of human PH, pulmonary vascular remodeling and right ventricular failure (Schoental and Head, 1955; Jasmin et al., 2001; Dumitrascu et al., 2008; Gomez-Arroyo et al., 2012). Sugen 5416 is a vascular endothelial growth factor receptor 2 (VEGFR2) inhibitor. Sugen 5416/hypoxia (Su/Hx) induces severe PH in both rats and mice that is characterized by pulmonary angioobliteration and right ventricular failure (Taraseviciene-Stewart et al., 2001; Sakao and Tatsumi, 2011). These three PH animal models are well-recognized models of Group 1 PH and Group 3 PH (Ryan et al., 2013; Colvin and Yeager, 2014; Sztuka and Jasiñska-Stroschein, 2017). Lai et al. (2016) developed a two-hit model of PH associated with heart failure with preserved ejection fraction (PH-HFpEF). It includes giving a single injection of SU5416 to obese ZSF1 rats. The SU5416/obese ZSF1 rats develop PH that includes a preserved ejection fraction and right and left ventricular hypertrophy. PH-HFpEF develops as a more advanced corollary of PH and diastolic HF, leading to more severe symptoms than those with HFpEF and suffers significant exercise intolerance, frequent hospitalization, and reduced survival (Thenappan et al., 2011; Hoeper et al., 2016).

AMPK AND PULMONARY HYPERTENSION

Role of AMPK in the Predisposition and Development of PH

Researches have revealed the role of AMPK in hypoxic pulmonary vasoconstriction and pulmonary vascular remodeling. Two clinical trials (NCT01884051 and NCT03629340) focusing on PAH treatment with metformin are in progress. However, in various animal models, AMPK has contradictory effects on PH, as both inhibition and activation of AMPK are protective for the development of PH. These seemingly opposing results can be partly explained by the different effects of AMPK signaling in pulmonary vasoconstriction and pulmonary vascular remodeling.

Role of AMPK in Hypoxic Pulmonary Vasoconstriction

Until 1871, it was universally believed that the pulmonary vessels did not respond to a vasomotor system. However, Brown-Séquard (1871) published some results indicating that such a system exists. Subsequently, Bradford and Dean (1894) reported that asphyxia causes PH. von Euler and von Liljestrand (1946) reported that acute hypoxia promotes pulmonary vasoconstriction to increase pulmonary arterial pressure. This study (von Euler and von Liljestrand, 1946) launched the current era of study of hypoxia and pulmonary vasoconstriction.

Hypoxic pulmonary vasoconstriction is an important homeostatic physiological mechanism that optimizes ventilation/perfusion matching, gas exchange, and systemic oxygen delivery. In response to alveolar hypoxia, intrapulmonary arteries constrict to divert blood to better-oxygenated lung segments (Bradford and Dean, 1894; von Euler and von Liljestrand, 1946; McMurtry et al., 1976; Madden et al., 1985; Sylvester et al., 2012; Dunham-Snary et al., 2017). Hypoxic pulmonary vasoconstriction relies on a group of specialized pulmonary VSMCs, which are located in pulmonary arterial segments stripped of the tunica intima and tunica media, but not in similar segments of pulmonary veins or systemic arteries (Bergofsky et al., 1967; Murray et al., 1990a,b; Madden et al., 1992; Weir and Archer, 1995). Hypoxic pulmonary vasoconstriction is triggered by mitochondrial redox signaling that involves voltage-gated potassium channels (Kv) and calcium channels (Weir and Archer, 1995). Hypoxia inhibits Kv channels in pulmonary VSMCs, causing membrane depolarization and opening of voltage-gated calcium channels to initiate Ca^{2+}-mediated pulmonary vasoconstriction (Weir and Archer, 1995; Archer and Michelakis, 2002; Sommer et al., 2008; Dunham-Snary et al., 2017).

Adenosine monophosphate-activated protein kinase has a critical role in hypoxic pulmonary vasoconstriction by linking the oxygen sensor to its effectors (**Figure 2**). Evans et al. (2005, 2006) and Evans (2006) found that physiological hypoxia increases the AMP/ATP ratio in pulmonary VSMCs, followed by increased AMPK activity and phosphorylation of a classical AMPK substrate, acetyl CoA carboxylase (a well-validated marker for AMPK activation). This process is likely to be mediated by binding of AMP to the AMPK γ subunit, which triggers activation of the kinase by, (1) promoting AMPK Thr 172 phosphorylation *via* allosteric regulation (Scott et al., 2002; Kemp, 2004; Oakhill et al., 2010), (2) inhibiting AMPK Thr 172 dephosphorylating (Davies et al., 1995), and (3) facilitating phosphorylation of Thr 172 by the upstream kinase LKB1 (Hawley et al., 2003; Woods et al., 2003; Shaw et al., 2004, 2005). Additional studies found that AMPK activation evokes a slow, sustained, and reversible increase in Ca^{2+} influx *via* cyclic adenosine diphosphate-ribose (cADPR)-dependent mobilization of sarcoplasmic reticulum stores in pulmonary VSMCs and the consequent induction of constriction of pulmonary artery rings (Evans et al., 2005). Consistent with these findings, two different AMPK activators, AICAR and phenformin, evoke intracellular Ca^{2+} influx and reversible constriction of the pulmonary artery rings. The characteristics of this process are strikingly similar to those of hypoxic pulmonary vasoconstriction (Evans et al., 2005). The hypoxia-associated pulmonary vasoconstriction and Ca^{2+} influx is inhibited by the non-selective AMPK antagonist, compound C, upon inhibition of the sarcoplasmic reticulum store-refilling current (Robertson et al., 2008). When hypoxia occurs, AMPK can directly phosphorylate voltage-gated potassium channels (Kv1.5 channels), followed by inhibition of K^+ currents in pulmonary VSMCs. The entry of voltage-dependent Ca^{2+} to initiate the hypoxia-related pulmonary vasoconstriction is thus activated (Moral-Sanz et al., 2016). Downregulation of Kv1.5 expression and activity is also a hallmark of PH (Yuan et al., 1998; Lv et al., 2013). Strong support for this mechanism results from *in vivo* studies performed by Moral-Sanz et al. (2018), who found a key *in vivo* role of AMPK in hypoxic pulmonary vasoconstriction using a combination of AMPK isoform deletion strategies and spectral Doppler ultrasound. Under conditions of mild hypoxia (8% O_2), deletion of AMPK α1, but not AMPK α2, in smooth muscle cells block induction of hypoxia-related pulmonary vasoconstriction. When conditions of severe hypoxia (5% O_2) are present, either AMPK α1 or AMPK α2 deletion attenuates hypoxia-related pulmonary vasoconstriction (Moral-Sanz et al., 2018). The findings that SNPs in the *Prkaa1* gene have been identified in populations that live at high altitudes and who have attenuated hypoxic pulmonary vasoconstriction are consistent with these results (Penaloza and Arias-Stella, 2007; Bigham et al., 2014). In summary, a growing body of evidence supports the hypothesis that AMPK activation is a primary mediator of hypoxic pulmonary vasoconstriction.

Role of AMPK in Pulmonary Vasculature Remodeling

In PH, pulmonary arteries and veins undergo structure changes. This pulmonary vascular remodeling is characterized by proliferation of pulmonary ECs and VSMCs. AMPK has a key role in the pathogenesis of pulmonary vasculature remodeling (**Figure 3**).

AMPK in Endothelial Cells and PH

Both AMPK subunits (AMPK α1 and AMPK α2) are expressed in pulmonary ECs. However, AMPK α1 is mainly expressed in capillary-derived pulmonary microvascular ECs and AMPK α2 is mainly expressed in conduit-derived pulmonary artery ECs

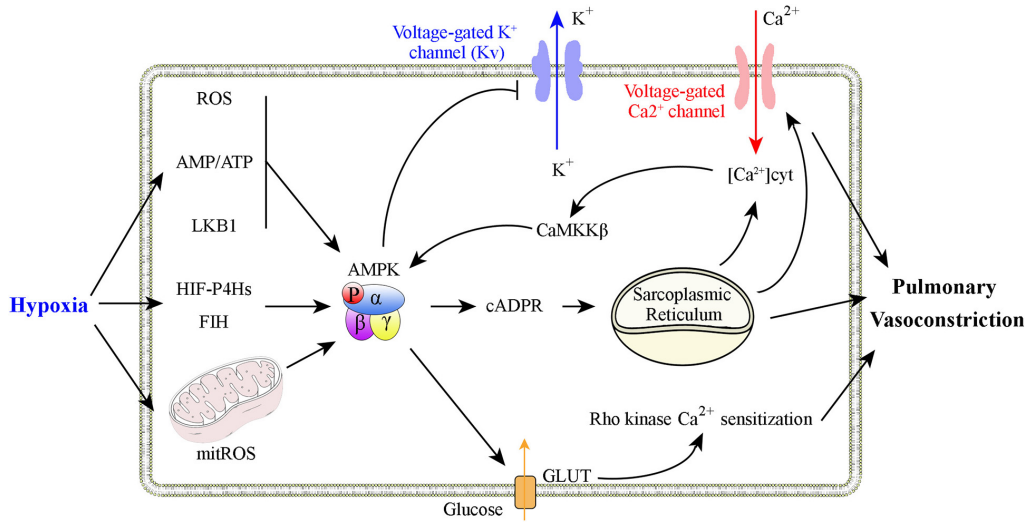

FIGURE 2 | Graphical summary of possible mechanisms that explain how AMPK activation is involved in hypoxic pulmonary vasoconstriction. Physiological hypoxia results in increases in the AMP/ATP ratio, ROS production, and in LKB1 activation to promote AMPK Thr 172 phosphorylation. AMPK activation increases Ca^{2+} levels in pulmonary VSMCs to promote constriction through, (1) inhibition of voltage-dependent K^+ channels, (2) activation of voltage-operated Ca^{2+} channels, and (3) activation of Ca^{2+}-sensing sarcoplasmic reticulum.

(Creighton et al., 2011). Pulmonary endothelial AMPK is down-regulated in pulmonary hypertensive patients and hypoxia-induced PH animals, compared with that from healthy donors or non-PH animals, respectively (Teng et al., 2013; Afolayan et al., 2016; Omura et al., 2016; Rana et al., 2020). EC-specific AMPK knockout mice (EC-AMPK$^{-/-}$) (Omura et al., 2016) and EC-specific AMPK α2 knockout mice (EC-AMPK α2$^{-/-}$) (Zhang et al., 2018) have accelerated development of PH under conditions of hypoxia. Endothelial AMPK exerts protective effects against PH via, (1) paracrine growth mechanism (e.g., PDGF-BB and FGF-2) mediation of the interaction between pulmonary artery ECs and pulmonary VSMCs (Omura et al., 2016), (2) positive regulation of nitric oxide (NO) production *via* endothelial NO synthase (eNOS) phosphorylation (Zhang et al., 2006; Chen et al., 2009; Afolayan et al., 2016), (3) stabilization of angiotensin-converting enzyme 2 (ACE2) to increase angiotensin 1–7 (Ang 1–7) expression and eNOS-derived NO bioavailability (Zhang et al., 2006), (4) Ca^{2+} influx in pulmonary microvascular ECs, which promotes endothelial barrier function (Creighton et al., 2011), (5) notch ligand promotion of angiogenesis (200), and (6) alleviation of EC apoptosis (Ido et al., 2002; Nagata et al., 2009; Enkhjargal et al., 2014).

AMPK in Vascular Smooth Muscle Cells and PH

During PH development, the remodeling process universally involves medial thickening driven by VSMC proliferation/hypertrophy and deposition of extracellular matrix within the tunica media of pulmonary arteries (Lyle et al., 2017). Pulmonary VSMCs express both the AMPK α1 and AMPK α2 subunits of AMPK (Creighton et al., 2011; Ibe et al., 2013). However, AMPK α1 is the predominant subunit in pulmonary VSMCs and contributes up to 80% of total AMPK activity (Evans et al., 2005; Xue et al., 2017). AMPK α1 catalytic activity is much higher in VSMCs from small pulmonary arteries than in those from the main pulmonary arteries (Evans et al., 2005). Unlike AMPK in pulmonary ECs, studies of AMPK in pulmonary VSMCs have found contradictory results. Some studies found that phosphorylated AMPK is increased, while total AMPK levels remain the same, in pulmonary VSMCs from pulmonary hypertensive patients and hypoxia-induced PH mice, compared with those from healthy donors or non-PH mice, respectively (Krymskaya et al., 2011; Ibe et al., 2013). Mechanistically, hypoxia-activated AMPK promotes pulmonary VSMC survival, but AMPK activity pharmacologically inhibited by either compound C or 9-β-d-arabinofuranosyl adenine (Ara-a) abrogates hypoxia-induced pulmonary VSMC proliferation and PH (Ibe et al., 2013; Xue et al., 2017). Ibe et al. (2013) found that although suppression of either AMPK α1 or α2 in pulmonary VSMCs leads to increased cell death, AMPK α1 and AMPK α2 have differential roles. Activation of AMPK α1 stimulates autophagy and promotes pulmonary VSMC survival; activation of AMPK α2 regulates myeloid cell leukemia sequence 1 (MCL-1) to prevent apoptosis (Ibe et al., 2013). In contrast to these results, another series of studies found that phosphorylated AMPK is decreased in pulmonary VSMCs from patients with PH and from mice with hypoxia-induced PH, compared with those from healthy donors or non-PH mice, respectively (Goncharov et al., 2014). AMPK inhibition promotes pulmonary VSMC proliferation and survival, but AMPK pharmacologically activated by metformin or AICAR inhibits hypoxia-induced pulmonary VSMC proliferation and chronic PH (Agard et al., 2009; Goncharov et al., 2014; Wu et al., 2014; Ke et al., 2016; Song et al., 2016; Gui et al., 2017; Liu et al., 2019).

Seemingly contradictory results should be interpreted with caution. In the study that found elevated AMPK phosphorylation in PH and AMPK inhibition-attenuated

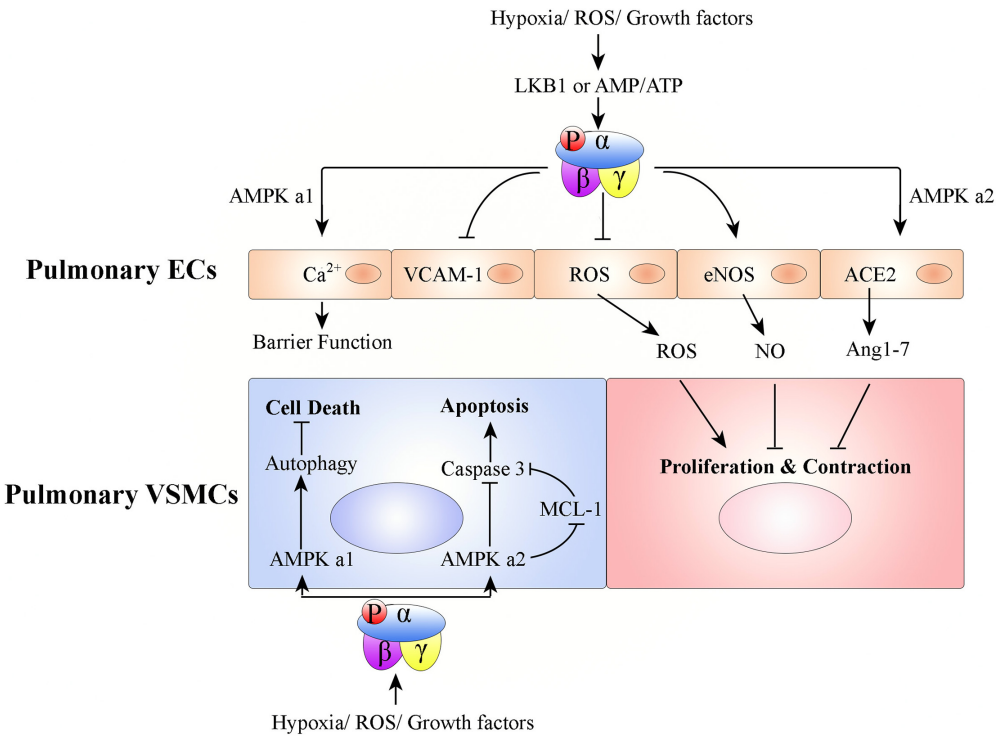

FIGURE 3 | Graphical summary of possible mechanisms associated with how AMPK activation affects pulmonary vascular remodeling. Hypoxia/ROS/growth factors activate AMPK in ECs or VSMCs to promote or inhibit PH development. In pulmonary ECs, AMPK activation protects PH: (1) AMPK α1 activation in pulmonary ECs promotes Ca^{2+} influx to maintain endothelial barrier function, (2) pulmonary endothelial AMPK inhibits VCAM-1 expression to antagonize inflammatory cell infiltration, (3) AMPK activation in pulmonary ECs inhibits ROS production, promotes eNOS-NO bioactivity, and stabilizes ACE2 to increase Ang 1–7 expression. Pulmonary VSMC proliferation and contraction are thus regulated. In pulmonary VSMCs, AMPK α1 activation promotes autophagy-mediated cell survival; AMPK α2 activation inhibits cell apoptosis.

PH (Krymskaya et al., 2011; Ibe et al., 2013), the researchers used pulmonary VSMCs isolated from large-diameter arteries located in a segment of pulmonary arteries just proximal to where lung entry occurs (diameter $\geq$ 0.8 mm). In the study that found AMPK reduction in PH and PH mitigation by AMPK activation (Goncharov et al., 2014), pulmonary VSMCs isolated from small-diameter arteries located in distal pulmonary artery segments (type III, diameter $\leq$ 0.1 mm) were used. Therefore, these discrepancies may be due to different functions of AMPK or different AMPK isoforms, or both, in pulmonary arteries with different diameters. Hypoxic pulmonary vasoconstriction is more vigorous in small pulmonary arteries (Dawson et al., 1977; Grimm et al., 1978; Sylvester et al., 2012), where the AMPK α1 catalytic subunit is predominantly expressed (Evans et al., 2005). The non-selective nature of AMPK activators or inhibitors may be another factor that contributes to these apparent inconsistencies.

AMPK and Pulmonary Hypertension Treatment

AMPK Inhibition Is Preventive for Development of Pulmonary Hypertension

Ibe et al. (2013) found that inhibition of AMPK by compound C prevents development of hypoxia-induced PH. When mice treated with compound C one day before hypoxia exposure (10% oxygen for 3 weeks), compound C prevents hypoxia-induced PH, pulmonary arterial wall thickening, and right ventricular hypertrophy. The activation of AMPK α1 stimulates autophagy, promoting pulmonary VSMCs survival, whereas the activation of AMPK α2 increases the expression of myeloid cell leukemia sequence 1 (MCL-1), inhibiting pulmonary VSMCs apoptosis (Ibe et al., 2013). Consistent with these results, Robertson et al. (2008) and Evans et al. (2009) pre-incubated intrapulmonary arteries (3rd and 4th order branches of the pulmonary arterial tree, 0.2–0.5 mm internal diameter) with compound C (40 mM). Compound C reversed/inhibited hypoxic pulmonary vasoconstriction in a concentration-dependent manner. Functionally, AMPK phosphorylates voltage-gated K^+ channel (Kv2.1) and thereby confers a leftward shift in both the activation and inactivation curves of Kv2.1, which precipitates an increase in the intracellular Ca^{2+} concentration (Evans et al., 2009).

AMPK Activation Is Preventive for Development of Pulmonary Hypertension

A significant body of evidence suggests that AMPK activation is preventive for development of PH. Metformin, the first-line medication for treatment of type 2 diabetes and the canonical

TABLE 2 | Pulmonary hypertension (PH) animal experiments of AMPK.

Therapy	Dose (mg/kg/day)	Route	Time (day)	PH models	Sex	References
AMPK activator with beneficial effects on PH						
Metformin	100–150	p.o.	21–28	MCT rat	M	Zhai et al., 2018; Yoshida et al., 2020
Metformin	100–150	i.p.	21–28	MCT rat	M	Agard et al., 2009; Li et al., 2016
Metformin	100	i.p.	30	MCT rat		Sun et al., 2019
Metformin	100	i.p.	21	Hypoxia rat		Liu et al., 2019
Metformin	100	p.o.	21	Su/Hx rat	F	Dean et al., 2016
Metformin	300	p.o.	31–28	Obese ZSF1 rat	M	Lai et al., 2016
Metformin	300	p.o.	98	SU5416/Obese ZSF1 rat	F	Wang et al., 2020
Metformin	150	i.p.	14	Su/Hx mouse	M	Zhang et al., 2018
Metformin	100	p.o.	21	Hypoxia mouse	M	Omura et al., 2016
AICAR	1?	i.p.	28	Hypoxia rat	M	Huang et al., 2014; Chen et al., 2016
AMPK antagonist with beneficial effects on PH						
Compound C	20	i.p.	21	Hypoxia mouse	M	Ibe et al., 2013
AMPK activators without effects on PH						
Metformin	100	p.o.	14	SuHx mouse	M	Goncharov et al., 2018
Metformin	300	p.o.	42	SuHx rat	M	Goncharov et al., 2018
AICAR	500	p.o.	42	SuHx rat	M	Goncharov et al., 2018

p.o., oral administration (per os); i.p., Intraperitoneal injection.

AMPK activator, demonstrates therapeutic efficacy on PH in animal models. AMPK activation by metformin prevents MCT-induced PH in rats (Agard et al., 2009; Li et al., 2016; Zhai et al., 2018; Sun et al., 2019; Yoshida et al., 2020). In these experimental models, rats were injected with one dose of MCT (60 mg/kg) to induce PH. Metformin (100–150 mg/kg/day, drinking water or intraperitoneal injection, 21–30 days) treatment significantly reduced right ventricular systolic pressure and pulmonary vascular remodeling in rats with MCT-induced PH (Agard et al., 2009; Li et al., 2016; Zhai et al., 2018; Sun et al., 2019; Yoshida et al., 2020). Consistent with these results, metformin has protective effects on hypoxia-induced PH in mice and rats (Huang et al., 2014; Omura et al., 2016; Liu et al., 2019), and a more pronounced PH with angioobliterative lesions in Sugen 5416/hypoxia (SuHx) mice/rats (Dean et al., 2016; Zhang et al., 2018) and SU5416/Obese ZSF1 rats (Lai et al., 2016; Wang et al., 2020). The AMPK activator, AICAR, also prevents PH development in rats with hypoxia-induced PH (Huang et al., 2014; Chen et al., 2016).

In contrast to the results that metformin has protective effects, other researchers reported that their findings did not support the efficacy of metformin in PAH therapy (Goncharov et al., 2018). Goncharov et al. (2018) findings suggested that metformin treatment may be preferentially beneficial for PH with heart failure with preserved ejection fraction (PH-HFpEF, group 2 PH), but that it has limited efficacy for PAH. They induced PAH in a male C57BL/6J mouse model using a 3-week exposure to SuHx. They then gave metformin (100 mg/kg/day, 14 days) in drinking water for 2-weeks post hypoxia exposure. Goncharov et al. found no changes in right ventricular systolic pressure, right ventricular hypertrophy, or pulmonary vascular remodeling in the metformin-treated SuHx mice. They also evaluated the preventive effects of metformin and AICAR in PAH. In these animal models, metformin (300 mg/kg/day, drinking water, 42 days) or AICAR (500 mg/kg/day, intraperitoneal, 42 days) were administrated 1 day before SuHx exposure. They found no changes in right ventricular systolic pressure, right ventricular hypertrophy, or pulmonary vascular remodeling in either the metformin- or AICAR-treated SuHx rats. However, they did not measure phosphorylation levels of AMPK or downstream AMPK pathways. Metformin-induced AMPK activation requires full activation of an upstream kinase (e.g., LKB1), especially at low doses (Choi et al., 2001; Emerling et al., 2009; Zmijewski et al., 2010; Hinchy et al., 2018). Therefore, it is unknown whether the lack of metformin efficacy for PH treatment was associated with AMPK activation.

Different characteristics that likely contribute to apparently contradictory results are presented in **Table 2**. In Dean et al. (2016), AMPK activation by metformin (100 mg/kg/day, oral gavage, 21 days) seems to reverse the PH phenotype induced by SuHx in female rats, in contrast to the findings of Goncharov et al. (2018) that was performed using male rats. Thus, a sex difference might affect the response to metformin treatment of PH. Effects of this difference have been described for other diseases (e.g., obesity, aging, and spontaneous tumorigenesis) (Anisimov et al., 2010; Quan et al., 2016; Park et al., 2017; Bramante et al., 2021).

Clinical Trials of Pulmonary Hypertension Treatment Using Metformin

There has been significant interest in the use of metformin for PH treatment. Liao et al. (2018, 2019) found that a combination therapy using metformin (500 mg, twice daily, 3 months) and bosentan (endothelin receptor antagonist) improves 6-min walk distance and right heart hemodynamics, decreases serum pro-brain natriuretic peptide (pro-BNP) levels, and ameliorates pulmonary vasoconstriction in patients with PH associated with congenital heart defects. Two phase I/II clinical trials of

metformin for PH treatment are in progress (clinicaltrials.gov, NCT01884051 and NCT03629340). Results to date indicate good tolerability and potential clinical efficacy for improvement in right ventricular function in patients with PH who receive metformin therapy (2 g/day, 8 weeks) (Brittain et al., 2020). However, metformin use did not change the 6-min walk distance in those patients (Brittain et al., 2020). Although not yet complete, this clinical study provides new insights into the potential benefits of metformin use on right ventricular failure in patients with PH and indicates the need for more studies of the use of metformin therapeutic intervention in patients with PH and PH-HFpEF.

CONCLUSION AND PERSPECTIVES

In this review, we discussed some seemingly contradictory study results for AMPK and PH development. AMPK has a key role in PH, either during the early process of hypoxic pulmonary vasoconstriction or later during pulmonary vasculature remodeling, or both. However, whether AMPK activation or inhibition is protective against PH remains unclear: (1) AMPK activation triggers hypoxia-induced pulmonary artery constriction. AMPK activator use (e.g., AICAR and Ara-a) prevents hypoxia-induced pulmonary artery constriction and PH. (2) EC-specific deletion of AMPK exaggerates hypoxia-induced PH *in vivo*. This result indicates endothelial AMPK has a protective role during PH development. (3) VSMCs from large pulmonary arteries with AMPK activation have accelerated proliferation and inhibited apoptosis. VSMCs from distal small pulmonary arteries with AMPK inhibition have similar potential. (4) Some animal studies found that the AMPK activators, AICAR and metformin, have beneficial effects on PH treatment. Other study findings suggest that metformin therapy for PH may be limited to use for PH-HFpEF. AMPK activation might have less pronounced pulmonary vascular effects than right ventricular effects, as much evidence has been published suggesting that AMPK activation exerts a protective effect in cardiac dysfunction, ischemic heart, heat failure, and cardiac hypertrophy (Russell et al., 2004; Miller et al., 2008; Ma et al., 2010; Kim et al., 2011; Morrison et al., 2011). (5) Sex differences in the response to metformin used for PH treatment may affect outcomes.

In conclusion, studies found seemingly contradictory results for the relationship between AMPK and PH. In one series of studies, inhibition of AMPK resulted in attenuated hypoxic pulmonary vasoconstriction and pulmonary VSMC proliferation. In another series of studies, activation of AMPK resulted in improved EC function, VSMC apoptosis, and decreased pulmonary vasculature tone. Given that AMPK a1 and AMPK a2 have different expression patterns and different functions in pulmonary arteries of different sizes, the role of AMPK in PH should be studied using a cell-specific and pathological process-specific approach. Studies involving genetically- and specifically-modified AMPK α1 and α2 subunits are needed to clarify their specific roles in PH pathogenesis and treatment.

AUTHOR CONTRIBUTIONS

QZ drafted the manuscript and figures. PS and M-HZ revised the manuscript. All authors contributed to the article and approved the submitted version.

FUNDING

This work was supported in part by National Heart, Lung, and Blood Institute (HL079584, HL080499, HL089920, HL110488, HL128014, HL132500, HL137371, and HL142287), National Cancer Institute (CA213022), and National Institute on Aging (AG047776) (to M-HZ) and HL140954 (PS). QZ is a recipient of Postdoctoral Fellowship Award of American Heart Association (835456).

REFERENCES

Afolayan, A. J., Eis, A., Alexander, M., Michalkiewicz, T., Teng, R.-J., Lakshminrusimha, S., et al. (2016). Decreased endothelial nitric oxide synthase expression and function contribute to impaired mitochondrial biogenesis and oxidative stress in fetal lambs with persistent pulmonary hypertension. *Am. J. Physiol. Lung Cell. Mol. Physiol.* 310, L40–L49.

Agard, C., Rolli-Derkinderen, M., Dumas-de-La-Roque, E., Rio, M., Sagan, C., Savineau, J. P., et al. (2009). Protective role of the antidiabetic drug metformin against chronic experimental pulmonary hypertension. *Br. J. Pharmacol.* 158, 1285–1294. doi: 10.1111/j.1476-5381.2009.00445.x

Ahmad, F., Arad, M., Musi, N., He, H., Wolf, C., Branco, D., et al. (2005). Increased alpha2 subunit-associated AMPK activity and PRKAG2 cardiomyopathy. *Circulation* 112, 3140–3148. doi: 10.1161/circulationaha.105.550806

Anisimov, V. N., Piskunova, T. S., Popovich, I. G., Zabezhinski, M. A., Tyndyk, M. L., Egormin, P. A., et al. (2010). Gender differences in metformin effect on aging, life span and spontaneous tumorigenesis in 129/Sv mice. *Aging (Albany N. Y.)* 2, 945–958. doi: 10.18632/aging.100245

Arad, M., Seidman, C. E., and Seidman, J. G. (2007). AMP-activated protein kinase in the heart. *Circulat. Res.* 100, 474–488.

Archer, S., and Michelakis, E. (2002). The mechanism(s) of hypoxic pulmonary vasoconstriction: potassium channels redox O2 sensors, and controversies. *Physiology* 17, 131–137. doi: 10.1152/nips.01388.2002

Attinà, T., Camidge, R., Newby, D. E., and Webb, D. J. (2005). Endothelin antagonism in pulmonary hypertension, heart failure, and beyond. *Heart* 91, 825–831. doi: 10.1136/hrt.2004.053991

Bando, H., Atsumi, T., Nishio, T., Niwa, H., Mishima, S., Shimizu, C., et al. (2005). Phosphorylation of the 6-phosphofructo-2-kinase/fructose 2,6-bisphosphatase/PFKFB3 family of glycolytic regulators in human cancer. *Clin. Cancer Res.* 11, 5784–5792. doi: 10.1158/1078-0432.ccr-05-0149

Bergeron, R., Ren, J. M., Cadman, K. S., Moore, I. K., Perret, P., Pypaert, M., et al. (2001). Chronic activation of AMP kinase results in NRF-1 activation and mitochondrial biogenesis. *Am. J. Physiol. Endocrinol. Metabol.* 281, E1340–E1346.

Bergofsky, E. H., Holtzman, S., and Study, A. (1967). A study of the mechanisms involved in the pulmonary arterial pressor response to hypoxia. *Circulat. Res.* 20, 506–519. doi: 10.1161/01.res.20.5.506

Bigham, A. W., Julian, C. G., Wilson, M. J., Vargas, E., Browne, V. A., Shriver, M. D., et al. (2014). Maternal PRKAA1 and EDNRA genotypes are associated with birth weight, and PRKAA1 with uterine artery diameter and metabolic

homeostasis at high altitude. *Physiol. Genom.* 46, 687–697. doi: 10.1152/physiolgenomics.00063.2014

Bradford, J. R., and Dean, H. P. (1894). The pulmonary circulation. *J. Physiol.* 16, 34–158.25.

Bramante, C. T., Ingraham, N. E., Murray, T. A., Marmor, S., Hovertsen, S., Gronski, J., et al. (2021). Metformin and risk of mortality in patients hospitalised with COVID-19: a retrospective cohort analysis. *Lancet Health. Longev.* 2, e34–e41.

Brittain, E. L., Niswender, K., Agrawal, V., Chen, X., Fan, R., Pugh, M. E., et al. (2020). Mechanistic phase II clinical trial of metformin in pulmonary arterial hypertension. *J. Am. Heart Associat.* 9:e018349.

Brown-Séquard, C. E. (1871). On the production of hæmorrhage, anæmia, śdema, and emphysema in the lungs by injuries to the base of the brain. *Lancet* 97:6. doi: 10.1016/s0140-6736(02)77750-7

Budhiraja, R., Tuder, R. M., and Hassoun, P. M. (2004). Endothelial dysfunction in pulmonary hypertension. *Circulation* 109, 159–165.

Bungard, D., Fuerth, B. J., Zeng, P.-Y., Faubert, B., Maas, N. L., Viollet, B., et al. (2010). Signaling kinase AMPK activates stress-promoted transcription via histone H2B phosphorylation. *Science* 329, 1201–1205. doi: 10.1126/science.1191241

Carling, D., Zammit, V. A., and Hardie, D. G. (1987). A common bicyclic protein kinase cascade inactivates the regulatory enzymes of fatty acid and cholesterol biosynthesis. *FEBS Lett.* 223, 217–222. doi: 10.1016/0014-5793(87)80292-2

Chandra, S. M., Razavi, H., Kim, J., Agrawal, R., Kundu, R. K., de Jesus Perez, V., et al. (2011). Disruption of the apelin-APJ system worsens hypoxia-induced pulmonary hypertension. *Arterioscler. Thrombos. Vascul. Biol.* 31, 814–820. doi: 10.1161/atvbaha.110.219980

Chen, L., Xin, F.-J., Wang, J., Hu, J., Zhang, Y.-Y., Wan, S., et al. (2013). Conserved regulatory elements in AMPK. *Nature* 498, E8–E10.

Chen, M., Cai, H., Yu, C., Wu, P., Fu, Y., Xu, X., et al. (2016). Salidroside exerts protective effects against chronic hypoxia-induced pulmonary arterial hypertension via AMPKα1-dependent pathways. *Am. J. Transl. Res.* 8, 12–27.

Chen, Z., Peng, I. C., Sun, W., Su, M. I., Hsu, P. H., Fu, Y., et al. (2009). AMP-activated protein kinase functionally phosphorylates endothelial nitric oxide synthase Ser633. *Circulat. Res.* 104, 496–505. doi: 10.1161/circresaha.108.187567

Cheung, P. C., Salt, I. P., Davies, S. P., Hardie, D. G., and Carling, D. (2000). Characterization of AMP-activated protein kinase gamma-subunit isoforms and their role in AMP binding. *Biochem. J.* 346(Pt 3), 659–669. doi: 10.1042/0264-6021:3460659

Choi, S.-L., Kim, S.-J., Lee, K.-T., Kim, J., Mu, J., Birnbaum, M. J., et al. (2001). The regulation of AMP-activated protein kinase by H2O2. *Biochem. Biophys. Res. Commun.* 287, 92–97.

Colvin, K. L., and Yeager, M. E. (2014). Animal models of pulmonary hypertension: matching disease mechanisms to etiology of the human disease. *J. Pulmon. Respirat. Med.* 4:198.

Creighton, J., Jian, M., Sayner, S., Alexeyev, M., and Insel, P. A. (2011). Adenosine monophosphate-activated kinase alpha1 promotes endothelial barrier repair. *FASEB J.* 25, 3356–3365. doi: 10.1096/fj.10-179218

Davies, S. P., Helps, N. R., Cohen, P. T. W., and Hardie, D. G. (1995). 5′-AMP inhibits dephosphorylation, as well as promoting phosphorylation, of the AMP-activated protein kinase. Studies using bacterially expressed human protein phosphatase-2Cα and native bovine protein phosphatase-2Ac. *FEBS Lett.* 377, 421–425. doi: 10.1016/0014-5793(95)01368-7

Dawson, C. A., Grimm, D. J., and Linehan, J. H. (1977). Effects of lung inflation on longitudinal distribution of pulmonary vascular resistance. *J. Appl. Physiol.* 43, 1089–1092. doi: 10.1152/jappl.1977.43.6.1089

Day, E. A., Ford, R. J., and Steinberg, G. R. (2017). AMPK as a therapeutic target for treating metabolic diseases. *Trends Endocrinol. Metabol.* 28, 545–560. doi: 10.1016/j.tem.2017.05.004

de Theije, C. C., Schols, A., Lamers, W. H., Neumann, D., Köhler, S. E., and Langen, R. C. J. (2018). Hypoxia impairs adaptation of skeletal muscle protein turnover- and AMPK signaling during fasting-induced muscle atrophy. *PLoS One* 13:e0203630. doi: 10.1371/journal.pone.0203630

Dean, A., Nilsen, M., Loughlin, L., Salt, I. P., and MacLean, M. R. (2016). Metformin reverses development of pulmonary hypertension via aromatase inhibition. *Hypertension* 68, 446–454. doi: 10.1161/hypertensionaha.116.07353

Dengler, F., and Gäbel, G. (2019). The fast lane of hypoxic adaptation: glucose transport is modulated via a HIF-hydroxylase-AMPK-axis in jejunum epithelium. *Int. J. Mol. Sci.* 20:4993. doi: 10.3390/ijms20204993

Detar, R. (1980). Mechanism of physiological hypoxia-induced depression of vascular smooth muscle contraction. *Am. J. Physiol.* 238, H761–H769.

Ducommun, S., Deak, M., Sumpton, D., Ford, R. J., úñez Galindo, A. N., Kussmann, M., et al. (2015). affinity and mass spectrometry proteomic approach for the discovery of cellular AMPK targets: identification of mitochondrial fission factor as a new AMPK substrate. *Cell. Signal.* 27, 978–988. doi: 10.1016/j.cellsig.2015.02.008

Dumitrascu, R., Koebrich, S., Dony, E., Weissmann, N., Savai, R., Pullamsetti, S. S., et al. (2008). Characterization of a murine model of monocrotaline pyrrole-induced acute lung injury. *BMC Pulmon. Med.* 8:25.

Dummer, A., Rol, N., Szulcek, R., Kurakula, K., Pan, X., Visser, B. I., et al. (2018). Endothelial dysfunction in pulmonary arterial hypertension: loss of cilia length regulation upon cytokine stimulation. *Pulmon. Circulat.* 8:2045894018764629.

Dunham-Snary, K. J., Wu, D., Sykes, E. A., Thakrar, A., Parlow, L. R. G., Mewburn, J. D., et al. (2017). Hypoxic pulmonary vasoconstriction: from molecular mechanisms to medicine. *Chest* 151, 181–192.

Egan, D. F., Shackelford, D. B., Mihaylova, M. M., Gelino, S., Kohnz, R. A., Mair, W., et al. (2011). of ULK1 (hATG1) by AMP-activated protein kinase connects energy sensing to mitophagy. *Science* 331, 456–461. doi: 10.1126/science.1196371

Emerling, B. M., Weinberg, F., Snyder, C., Burgess, Z., Mutlu, G. M., Viollet, B., et al. (2009). Hypoxic activation of AMPK is dependent on mitochondrial ROS but independent of an increase in AMP/ATP ratio. *Free Rad. Biol. Med.* 46, 1386–1391. doi: 10.1016/j.freeradbiomed.2009.02.019

Emilio, P., Mottillo, E. M., Desjardins, J. D., Crane, B. K., Smith, A. E., Green, S. D., et al. (2016). Lack of adipocyte AMPK exacerbates insulin resistance and hepatic steatosis through brown and beige adipose tissue function. *Cell Metab.* 24, 118–129. doi: 10.1016/j.cmet.2016.06.006

Enkhjargal, B., Godo, S., Sawada, A., Suvd, N., Saito, H., Noda, K., et al. (2014). Endothelial AMP-activated protein kinase regulates blood pressure and coronary flow responses through hyperpolarization mechanism in mice. *Arterioscl. Thromb. Vascul. Biol.* 34, 1505–1513. doi: 10.1161/atvbaha.114.303735

Evans, A. M. (2006). AMP-activated protein kinase underpins hypoxic pulmonary vasoconstriction and carotid body excitation by hypoxia in mammals. *Exp. Physiol.* 91, 821–827. doi: 10.1113/expphysiol.2006.033514

Evans, A. M., Hardie, D. G., Peers, C., Wyatt, C. N., Viollet, B., Kumar, P., et al. (2009). Ion channel regulation by AMPK. *Annal. N. Y. Acad. Sci.* 1177, 89–100.

Evans, A. M., Mustard, K. J., Wyatt, C. N., Dipp, M., Kinnear, N. P., and Hardie, D. G. (2006). Does AMP-activated protein kinase couple inhibition of mitochondrial oxidative phosphorylation by hypoxia to pulmonary artery constriction? *Adv. Exp. Med. Biol.* 580, 147–154; discussion 351–9.

Evans, A. M., Mustard, K. J., Wyatt, C. N., Peers, C., Dipp, M., Kumar, P., et al. (2005). Does AMP-activated protein kinase couple inhibition of mitochondrial oxidative phosphorylation by hypoxia to calcium signaling in O_2-sensing cells? *J. Biol. Chem.* 280, 41504–41511. doi: 10.1074/jbc.m510040200

Fogarty, S., and Hardie, D. G. (2010). Development of protein kinase activators: AMPK as a target in metabolic disorders and cancer. *Biochim. Biophys. Acta (BBA) Prot. Proteom.* 1804, 581–591. doi: 10.1016/j.bbapap.2009.09.012

Fullerton, M. D., Galic, S., Marcinko, K., Sikkema, S., Pulinilkunnil, T., Chen, Z.-P., et al. (2013). Single phosphorylation sites in Acc1 and Acc2 regulate lipid homeostasis and the insulin-sensitizing effects of metformin. *Nat. Med.* 19, 1649–1654. doi: 10.1038/nm.3372

Galic, S., Fullerton, M. D., Schertzer, J. D., Sikkema, S., Marcinko, K., Walkley, C. R., et al. (2011). Hematopoietic AMPK β1 reduces mouse adipose tissue macrophage inflammation and insulin resistance in obesity. *J. Clin. Investigat.* 121, 4903–4915. doi: 10.1172/jci58577

Galiè, N., and Simonneau, G. (2013). The fifth world symposium on pulmonary hypertension. *J. Am. Coll. Cardiol.* 62, D1–D3.

Galiè, N., Hoeper, M. M., Humbert, M., Torbicki, A., Vachiery, J. L., Barbera, J. A., et al. (2009). Guidelines for the diagnosis and treatment of pulmonary hypertension. *Eur. Respirat. J.* 34, 1219–1263.

Garcia-Roves, P. M., Osler, M. E., Holmström, M. H., and Zierath, J. R. (2008). Gain-of-function R225Q mutation in AMP-activated protein Kinase γ3 subunit

increases mitochondrial biogenesis in glycolytic skeletal muscle. *J. Biol. Chem.* 283, 35724–35734. doi: 10.1074/jbc.m805078200

Gomez-Arroyo, J. G., Farkas, L., Alhussaini, A. A., Farkas, D., Kraskauskas, D., Voelkel, N. F., et al. (2012). The monocrotaline model of pulmonary hypertension in perspective. *Am. J. Physiol. Lung Cell. Mol. Physiol.* 302, L363–L369.

Goncharov, D. A., Goncharova, E. A., Tofovic, S. P., Hu, J., Baust, J. J., Pena, A. Z., et al. (2018). Metformin therapy for pulmonary hypertension associated with heart failure with preserved ejection fraction versus pulmonary arterial hypertension. *Am. J. Respirat. Crit. Care Med.* 198, 681–684.

Goncharov, D. A., Kudryashova, T. V., Ziai, H., Ihida-Stansbury, K., DeLisser, H., Krymskaya, V. P., et al. (2014). Mammalian target of rapamycin complex 2 (mTORC2) coordinates pulmonary artery smooth muscle cell metabolism, proliferation, and survival in pulmonary arterial hypertension. *Circulation* 129, 864–874. doi: 10.1161/circulationaha.113.004581

Gowans, G. J., Hawley, S. A., Ross, F. A., and Hardie, D. G. (2013). AMP is a true physiological regulator of AMP-activated protein kinase by both allosteric activation and enhancing net phosphorylation. *Cell Metab.* 18, 556–566. doi: 10.1016/j.cmet.2013.08.019

Grimm, D. J., Dawson, C. A., Hakim, T. S., and Linehan, J. H. (1978). Pulmonary vasomotion and the distribution of vascular resistance in a dog lung lobe. *J. Appl. Physiol.* 45, 545–550. doi: 10.1152/jappl.1978.45.4.545

Gui, D., Cui, Z., Zhang, L., Yu, C., Yao, D., Xu, M., et al. (2017). Salidroside attenuates hypoxia-induced pulmonary arterial smooth muscle cell proliferation and apoptosis resistance by upregulating autophagy through the AMPK-mTOR-ULK1 pathway. *BMC Pulmon. Med.* 17:191.

Gwinn, D. M., Shackelford, D. B., Egan, D. F., Mihaylova, M. M., Mery, A., Vasquez, D. S., et al. (2008). AMPK phosphorylation of raptor mediates a metabolic checkpoint. *Mol. Cell* 30, 214–226. doi: 10.1016/j.molcel.2008.03.003

Hansmann, G., Wagner, R. A., Schellong, S., Perez, V. A. d. J., Urashima, T., Wang, L., et al. (2007). Pulmonary arterial hypertension is linked to insulin resistance and reversed by peroxisome proliferator-activated receptor-gamma activation. *Circulation* 115, 1275–1284. doi: 10.1161/circulationaha.106.663120

Hardie, D. G. (2008). AMPK: a key regulator of energy balance in the single cell and the whole organism. *Int. J. Obes.* 32, S7–S12.

Hardie, D. G. (2013). AMPK: a target for drugs and natural products with effects on both diabetes and cancer. *Diabetes* 62, 2164–2172. doi: 10.2337/db13-0368

Hardie, D. G., Carling, D., and Gamblin, S. J. (2011). AMP-activated protein kinase: also regulated by ADP? *Trends Biochem. Sci.* 36, 470–477. doi: 10.1016/j.tibs.2011.06.004

Hawley, S. A., Boudeau, J., Reid, J. L., Mustard, K. J., Udd, L., Mäkelä, T. P., et al. (2003). Complexes between the LKB1 tumor suppressor, STRAD alpha/beta and MO25 alpha/beta are upstream kinases in the AMP-activated protein kinase cascade. *J. Biol.* 2:28.

Hawley, S. A., Pan, D. A., Mustard, K. J., Ross, L., Bain, J., Edelman, A. M., et al. (2005). Calmodulin-dependent protein kinase kinase-β is an alternative upstream kinase for AMP-activated protein kinase. *Cell Metab.* 2, 9–19. doi: 10.1016/j.cmet.2005.05.009

Heath, D., and Edwards, J. E. (1958). The pathology of hypertensive pulmonary vascular disease. *Circulation* 18, 533–547.

Herzig, S., and Shaw, R. J. (2018). AMPK: guardian of metabolism and mitochondrial homeostasis. *Nat. Rev. Mol. Cell Biol.* 19, 121–135. doi: 10.1038/nrm.2017.95

Hinchy, E. C., Gruszczyk, A. V., Willows, R., Navaratnam, N., Hall, A. R., Bates, G., et al. (2018). Mitochondria-derived ROS activate AMP-activated protein kinase (AMPK) indirectly. *J. Biol. Chem.* 293, 17208–17217. doi: 10.1074/jbc.ra118.002579

Hoeper, M. M., Lam, C. S. P., Vachiery, J.-L., Bauersachs, J., Gerges, C., Lang, I. M., et al. (2016). Pulmonary hypertension in heart failure with preserved ejection fraction: a plea for proper phenotyping and further research. *Eur. Heart J.* 38, 2869–2873.

Hong, S.-P., Momcilovic, M., and Carlson, M. (2005). Function of mammalian LKB1 and Ca2+/calmodulin-dependent protein kinase kinase α as Snf1-activating kinases in yeast. *J. Biol. Chem.* 280, 21804–21809. doi: 10.1074/jbc.m501887200

Huang, X., Fan, R., Lu, Y., Yu, C., Xu, X., Zhang, X., et al. (2014). Regulatory effect of AMP-activated protein kinase on pulmonary hypertension induced by chronic hypoxia in rats: in vivo and in vitro studies. *Mol. Biol. Rep.* 41, 4031–4041. doi: 10.1007/s11033-014-3272-9

Hudson, E. R., Pan, D. A., James, J., Lucocq, J. M., Hawley, S. A., Green, K. A., et al. (2003). A novel domain in AMP-activated protein kinase causes glycogen storage bodies similar to those seen in hereditary cardiac arrhythmias. *Curr. Biol.* 13, 861–866. doi: 10.1016/s0960-9822(03)00249-5

Humbert, M., Guignabert, C., Bonnet, S., Dorfmüller, P., Klinger, J. R., Nicolls, M. R., et al. (2019). Pathology and pathobiology of pulmonary hypertension: state of the art and research perspectives. *Eur. Respirat. J.* 53:1801887. doi: 10.1183/13993003.01887-2018

Hurley, R. L., Anderson, K. A., Franzone, J. M., Kemp, B. E., Means, A. R., and Witters, L. A. (2005). The Ca2+/calmodulin-dependent protein kinase kinases are AMP-activated protein kinase kinases. *J. Biol. Chem.* 280, 29060–29066. doi: 10.1074/jbc.m503824200

Ibe, J. C. F., Zhou, Q., Chen, T., Tang, H., Yuan, J. X. J., Raj, J. U., et al. (2013). Adenosine monophosphate-activated protein kinase is required for pulmonary artery smooth muscle cell survival and the development of hypoxic pulmonary hypertension. *Am. J. Respirat. Cell Mol. Biol.* 49, 609–618. doi: 10.1165/rcmb.2012-0446oc

Ido, Y., Carling, D., and Ruderman, N. (2002). Hyperglycemia-induced apoptosis in human umbilical vein endothelial cells: inhibition by the AMP-activated protein kinase activation. *Diabetes* 51, 159–167. doi: 10.2337/diabetes.51.1.159

Inoki, K., Zhu, T., and Guan, K.-L. (2003). TSC2 mediates cellular energy response to control cell growth and survival. *Cell* 115, 577–590. doi: 10.1016/s0092-8674(03)00929-2

Jasmin, J. F., Lucas, M., Cernacek, P., and Dupuis, J. (2001). Effectiveness of a nonselective ET(A/B) and a selective ET(A) antagonist in rats with monocrotaline-induced pulmonary hypertension. *Circulation* 103, 314–318. doi: 10.1161/01.cir.103.2.314

Kahn, B. B., Alquier, T., Carling, D., and Hardie, D. G. (2005). AMP-activated protein kinase: Ancient energy gauge provides clues to modern understanding of metabolism. *Cell Metab.* 1, 15–25. doi: 10.1016/j.cmet.2004.12.003

Kay, J. M., Harris, P., and Heath, D. (1967). Pulmonary hypertension produced in rats by ingestion of *Crotalaria spectabilis* seeds. *Thorax* 22, 176–179. doi: 10.1136/thx.22.2.176

Ke, R., Liu, L., Zhu, Y., Li, S., Xie, X., Li, F., et al. (2016). Knockdown of AMPKα2 promotes pulmonary arterial smooth muscle cells proliferation via mTOR/Skp2/p27(Kip1) signaling pathway. *Int. J. Mol. Sci.* 17:844. doi: 10.3390/ijms17060844

Kelly, M., Keller, C., Avilucea, P. R., Keller, P., Luo, Z., Xiang, X., et al. (2004). AMPK activity is diminished in tissues of IL-6 knockout mice: the effect of exercise. *Biochem. Biophys. Res. Commun.* 320, 449–454. doi: 10.1016/j.bbrc.2004.05.188

Kemp, B. E. (2004). Bateman domains and adenosine derivatives form a binding contract. *J. Clin. Investigat.* 113, 182–184. doi: 10.1172/jci200420846

Kim, A. S., Miller, E. J., Wright, T. M., Li, J., Qi, D., Atsina, K., et al. (2011). A small molecule AMPK activator protects the heart against ischemia–reperfusion injury. *J. Mol. Cell. Cardiol.* 51, 24–32. doi: 10.1016/j.yjmcc.2011.03.003

Kim, E. K., Lee, J. H., Oh, Y. M., Lee, Y. S., and Lee, S. D. (2010). Rosiglitazone attenuates hypoxia-induced pulmonary arterial hypertension in rats. *Respirology (Carlton Vic.)* 15, 659–668. doi: 10.1111/j.1440-1843.2010.01756.x

Kim, J. (2014). Apelin-APJ signaling: a potential therapeutic target for pulmonary arterial hypertension. *Mol. Cell.* 37, 196–201. doi: 10.14348/molcells.2014.2308

Kim, J., Yang, G., Kim, Y., Kim, J., and Ha, J. (2016). AMPK activators: mechanisms of action and physiological activities. *Exp. Mol. Med.* 48:e224. doi: 10.1038/emm.2016.16

Klinger, J. R., Abman, S. H., and Gladwin, M. T. (2013). Nitric oxide deficiency and endothelial dysfunction in pulmonary arterial hypertension. *Am. J. Respirat. Crit. Care Med.* 188, 639–646. doi: 10.1164/rccm.201304-0686pp

Kola, B. (2008). Role of AMP-activated protein kinase in the control of appetite. *J. Neuroendocrinol.* 20, 942–951. doi: 10.1111/j.1365-2826.2008.01745.x

Kola, B., Hubina, E., Tucci, S. A., Kirkham, T. C., Garcia, E. A., Mitchell, S. E., et al. (2005). Cannabinoids and ghrelin have both central and peripheral metabolic and cardiac effects via AMP-activated protein kinase. *J. Biol. Chem.* 280, 25196–25201. doi: 10.1074/jbc.c500175200

Koo, S.-H., Flechner, L., Qi, L., Zhang, X., Screaton, R. A., Jeffries, S., et al. (2005). The CREB coactivator TORC2 is a key regulator of fasting glucose metabolism. *Nature* 437, 1109–1114. doi: 10.1038/nature03967

Krymskaya, V. P., Snow, J., Cesarone, G., Khavin, I., Goncharov, D. A., Lim, P. N., et al. (2011). mTOR is required for pulmonary arterial vascular smooth muscle cell proliferation under chronic hypoxia. *FASEB J.* 25, 1922–1933. doi: 10.1096/fj.10-175018

Lai, Y. C., Tabima, D. M., Dube, J. J., Hughan, K. S., Vanderpool, R. R., Goncharov, D. A., et al. (2016). ESIRT3-AMP-activated protein kinase activation by nitrite and metformin improves hyperglycemia and normalizes pulmonary hypertension associated with heart failure with preserved ejection fraction. *Circulation* 133, 717–731. doi: 10.1161/circulationaha.115.018935

Lamia, K. A., Sachdeva, U. M., DiTacchio, L., Williams, E. C., Alvarez, J. G., Egan, D. F., et al. (2009). AMPK regulates the circadian clock by cryptochrome phosphorylation and degradation. *Science* 326, 437–440. doi: 10.1126/science.1172156

Legchenko, E., Chouvarine, P., Borchert, P., Fernandez-Gonzalez, A., Snay, E., Meier, M., et al. (2018). PPARγ agonist pioglitazone reverses pulmonary hypertension and prevents right heart failure via fatty acid oxidation. *Sci. Transl. Med.* 10:0303.

Li, M., Riddle, S. R., Frid, M. G., El Kasmi, K. C., McKinsey, T. A., Sokol, R. J., et al. (2011). Emergence of fibroblasts with a proinflammatory epigenetically altered phenotype in severe hypoxic pulmonary hypertension. *J. Immunol.* 187, 2711–2722. doi: 10.4049/jimmunol.1100479

Li, S., Han, D., Zhang, Y., Xie, X., Ke, R., Zhu, Y., et al. (2016). Activation of AMPK prevents monocrotaline-induced extracellular matrix remodeling of pulmonary artery. *Med. Sci. Monit. Basic Res.* 22, 27–33. doi: 10.12659/msmbr.897505

Li, Y., Xu, S., Mihaylova, M. M., Zheng, B., Hou, X., Jiang, B., et al. (2011). AMPK Phosphorylates and Inhibits SREBP activity to attenuate hepatic steatosis and atherosclerosis in diet-induced insulin-resistant mice. *Cell Metab.* 13, 376–388. doi: 10.1016/j.cmet.2011.03.009

Liao, S., Li, D., Hui, Z., McLachlan, C. S., and Zhang, Y. (2018). Metformin added to bosentan therapy in patients with pulmonary arterial hypertension associated with congenital heart defects: a pilot study. *ERJ Open Res.* 4, 00060–2018. doi: 10.1183/23120541.00060-2018

Liao, S., Li, D., Hui, Z., McLachlan, C. S., and Zhang, Y. (2019). Chronic dosing with metformin plus bosentan decreases in vitro pulmonary artery contraction from isolated arteries in adults with pulmonary hypertension. *J. Cardiovasc. Thorac. Res.* 11, 189–195. doi: 10.15171/jcvtr.2019.32

Liu, Y., Xu, Y., Zhu, J., Li, H., Zhang, J., Yang, G., et al. (2019). Metformin prevents progression of experimental pulmonary hypertension via inhibition of autophagy and activation of adenosine monophosphate-activated protein kinase. *J. Vascul. Res.* 56, 117–128. doi: 10.1159/000498894

Lizcano, J. M., Göransson, O., Toth, R., Deak, M., Morrice, N. A., Boudeau, J., et al. (2004). LKB1 is a master kinase that activates 13 kinases of the AMPK subfamily, including MARK/PAR-1. *EMBO J.* 23, 833–843. doi: 10.1038/sj.emboj.7600110

Lv, Y., Tang, L.-L., Wei, J.-K., Xu, X.-F., Gu, W., Fu, L.-C., et al. (2013). Decreased Kv1.5 expression in intrauterine growth retardation rats with exaggerated pulmonary hypertension. *Am. J. Physiol. Lung Cell. Mol. Physiol.* 305:L856.

Lyle, M. A., Davis, J. P., and Brozovich, F. V. (2017). Regulation of pulmonary vascular smooth muscle contractility in pulmonary arterial hypertension: implications for therapy. *Front. Physiol.* 8:614–614.

Ma, H., Wang, J., Thomas, D. P., Tong, C., Leng, L., Wang, W., et al. (2010). Impaired macrophage migration inhibitory factor-AMP-activated protein kinase activation and ischemic recovery in the senescent heart. *Circulation* 122, 282–292. doi: 10.1161/circulationaha.110.953208

Madden, J. A., Dawson, C. A., and Harder, D. R. (1985). Hypoxia-induced activation in small isolated pulmonary arteries from the cat. *J. Appl. Physiol.* 59, 113–118. doi: 10.1152/jappl.1985.59.1.113

Madden, J. A., Vadula, M. S., and Kurup, V. P. (1992). Effects of hypoxia and other vasoactive agents on pulmonary and cerebral artery smooth muscle cells. *Am. J. Physiol. Lung Cell. Mol. Physiol.* 263, L384–L393.

Maron, B. A., and Galiè, N. (2016). Diagnosis, treatment, and clinical management of pulmonary arterial hypertension in the contemporary era: a review. *JAMA Cardiol.* 1, 1056–1065. doi: 10.1001/jamacardio.2016.4471

Maron, B. A., and Leopold, J. A. (2015). Emerging concepts in the molecular basis of pulmonary arterial hypertension: part II: neurohormonal signaling contributes to the pulmonary vascular and right ventricular pathophenotype of pulmonary arterial hypertension. *Circulation* 131, 2079–2091. doi: 10.1161/circulationaha.114.006980

Marsin, A. S., Bertrand, L., Rider, M. H., Deprez, J., Beauloye, C., Vincent, M. F., et al. (2000). Phosphorylation and activation of heart PFK-2 by AMPK has a role in the stimulation of glycolysis during ischaemia. *Curr. Biol.* 10, 1247–1255. doi: 10.1016/s0960-9822(00)00742-9

McMurtry, I. F., Davidson, A. B., Reeves, J. T., and Grover, R. F. (1976). Inhibition of hypoxic pulmonary vasoconstriction by calcium antagonists in isolated rat lungs. *Circulat. Res.* 38, 99–104. doi: 10.1161/01.res.38.2.99

Mihaylova, M. M., and Shaw, R. J. (2011). The AMPK signalling pathway coordinates cell growth, autophagy and metabolism. *Nat. Cell Biol.* 13, 1016–1023. doi: 10.1038/ncb2329

Miller, E. J., Li, J., Leng, L., McDonald, C., Atsumi, T., Bucala, R., et al. (2008). Macrophage migration inhibitory factor stimulates AMP-activated protein kinase in the ischaemic heart. *Nature* 451, 578–582. doi: 10.1038/nature06504

Momcilovic, M., Hong, S.-P., and Carlson, M. (2006). Mammalian TAK1 activates Snf1 protein kinase in yeast and phosphorylates AMP-activated protein kinase in vitro. *J. Biol. Chem.* 281, 25336–25343. doi: 10.1074/jbc.m604399200

Moral-Sanz, J., Lewis, S. A., MacMillan, S., Ross, F. A., Thomson, A., Viollet, B., et al. (2018). The LKB1–AMPK-α1 signaling pathway triggers hypoxic pulmonary vasoconstriction downstream of mitochondria. *Sci. Signal.* 11:0296.

Moral-Sanz, J., Mahmoud, A. D., Ross, F. A., Eldstrom, J., Fedida, D., Hardie, D. G., et al. (2016). AMP-activated protein kinase inhibits Kv 1.5 channel currents of pulmonary arterial myocytes in response to hypoxia and inhibition of mitochondrial oxidative phosphorylation. *J. Physiol.* 594, 4901–4915. doi: 10.1113/jp272032

Morrison, A., Yan, X., Tong, C., and Li, J. (2011). Acute rosiglitazone treatment is cardioprotective against ischemia-reperfusion injury by modulating AMPK, Akt, and JNK signaling in nondiabetic mice. *Am. J. Physiol. Heart Circulat. Physiol.* 301, H895–H902.

Moudgil, R., Michelakis, E. D., and Archer, S. L. (2005). Hypoxic pulmonary vasoconstriction. *J. Appl. Physiol.* 98, 390–403.

Munday, M. R., Campbell, D. G., Carling, D., and Hardie, D. G. (1988). Identification by amino acid sequencing of three major regulatory phosphorylation sites on rat acetyl-CoA carboxylase. *Eur. J. Biochem.* 175, 331–338. doi: 10.1111/j.1432-1033.1988.tb14201.x

Mungai, P. T., Waypa, G. B., Jairaman, A., Prakriya, M., Dokic, D., Ball, M. K., et al. (2011). Hypoxia triggers AMPK Activation through reactive oxygen species-mediated activation of calcium release-activated calcium channels. *Mol. Cell. Biol.* 31, 3531–3545. doi: 10.1128/mcb.05124-11

Murray, T. R., Chen, L., Marshall, B. E., and Macarak, E. J. (1990a). Hypoxic contraction of cultured pulmonary vascular smooth muscle cells. *Am. J. Respirat. Cell Mol. Biol.* 3, 457–465. doi: 10.1165/ajrcmb/3.5.457

Murray, T. R., Marshall, B. E., and Macarak, E. J. (1990b). Contraction of vascular smooth muscle in cell culture. *J. Cell. Physiol.* 143, 26–38. doi: 10.1007/978-3-642-66427-4_6

Myers, R. W., Guan, H.-P., Ehrhart, J., Petrov, A., Prahalada, S., Tozzo, E., et al. (2017). pan-AMPK activator MK-8722 improves glucose homeostasis but induces cardiac hypertrophy. *Science* 357, 507–511. doi: 10.1126/science.aah5582

Nagata, D., Kiyosue, A., Takahashi, M., Satonaka, H., Tanaka, K., Sata, M., et al. (2009). A new constitutively active mutant of AMP-activated protein kinase inhibits anoxia-induced apoptosis of vascular endothelial cell. *Hypertens. Res.* 32, 133–139. doi: 10.1038/hr.2008.25

Nicolls, M. R., and Voelkel, N. F. (2017). The roles of immunity in the prevention and evolution of pulmonary arterial hypertension. *Am. J. Respirat. Crit. Care Med.* 195, 1292–1299. doi: 10.1164/rccm.201608-1630pp

Oakhill, J. S., Chen, Z.-P., Scott, J. W., Steel, R., Castelli, L. A., Ling, N., et al. (2010). β-Subunit myristoylation is the gatekeeper for initiating metabolic stress sensing by AMP-activated protein kinase (AMPK). *Proc. Natl. Acad. Sci. U.S.A.* 107, 19237–19241. doi: 10.1073/pnas.1009705107

Oakhill, J. S., Scott, J. W., and Kemp, B. E. (2012). AMPK functions as an adenylate charge-regulated protein kinase. *Trends Endocrinol. Metabol.* 23, 125–132. doi: 10.1016/j.tem.2011.12.006

Omura, J., Satoh, K., Kikuchi, N., Satoh, T., Kurosawa, R., Nogi, M., et al. (2016). Protective roles of endothelial AMP-activated protein kinase against hypoxia-induced pulmonary hypertension in mice. *Circulat. Res.* 119, 197–209. doi: 10.1161/circresaha.115.308178

Park, J. W., Lee, J. H., Park, Y. H., Park, S. J., Cheon, J. H., Kim, W. H., et al. (2017). Sex-dependent difference in the effect of metformin on colorectal cancer-specific mortality of diabetic colorectal cancer patients. *World J. Gastroenterol.* 23, 5196–5205. doi: 10.3748/wjg.v23.i28.5196

Penaloza, D., and Arias-Stella, J. (2007). The heart and pulmonary circulation at high altitudes. *Circulation* 115, 1132–1146. doi: 10.1161/circulationaha.106.624544

Plecitá-Hlavatá, L., Tauber, J., Li, M., Zhang, H., Flockton, A. R., Pullamsetti, S. S., et al. (2016). Constitutive reprogramming of fibroblast mitochondrial metabolism in pulmonary hypertension. *Am. J. Respirat. Cell Mol. Biol.* 55, 47–57. doi: 10.1165/rcmb.2015-0142oc

Quan, H., Zhang, H., Wei, W., and Fang, T. (2016). Gender-related different effects of a combined therapy of Exenatide and Metformin on overweight or obesity patients with type 2 diabetes mellitus. *J. Diab. Complicat.* 30, 686–692. doi: 10.1016/j.jdiacomp.2016.01.013

Rabinovitch, M., Guignabert, C., Humbert, M., and Nicolls, M. R. (2014). Inflammation and immunity in the pathogenesis of pulmonary arterial hypertension. *Circulat. Res.* 115, 165–175. doi: 10.1161/circresaha.113.301141

Rana, U., Callan, E., Entringer, B., Michalkiewicz, T., Joshi, A., Parchur, A. K., et al. (2020). AMP-kinase dysfunction alters notch ligands to impair angiogenesis in neonatal pulmonary hypertension. *Am. J. Respirat. Cell Mol. Biol.* 62, 719–731. doi: 10.1165/rcmb.2019-0275oc

Ranchoux, B., Harvey, L. D., Ayon, R. J., Babicheva, A., Bonnet, S., Chan, S. Y., et al. (2018). Endothelial dysfunction in pulmonary arterial hypertension: an evolving landscape (2017 Grover Conference Series). *Pulmon. Circulat.* 8:2045893217752912.

Robertson, T. P., Mustard, K. J., Lewis, T. H., Clark, J. H., Wyatt, C. N., Blanco, E. A., et al. (2008). AMP-activated protein kinase and hypoxic pulmonary vasoconstriction. *Eur. J. Pharmacol.* 595, 39–43. doi: 10.1016/j.ejphar.2008.07.035

Rojas, J., Arraiz, N., Aguirre, M., Velasco, M., and Bermúdez, V. (2011). AMPK as target for intervention in childhood and adolescent obesity. *Int. J. Obesit.* 2011, 252817–252817.

Ross, F. A., Jensen, T. E., and Hardie, D. G. (2016a). Differential regulation by AMP and ADP of AMPK complexes containing different γ subunit isoforms. *Biochem. J.* 473, 189–199. doi: 10.1042/bj20150910

Ross, F. A., MacKintosh, C., and Hardie, D. G. (2016b). AMP-activated protein kinase: a cellular energy sensor that comes in 12 flavours. *FEBS J.* 283, 2987–3001. doi: 10.1111/febs.13698

Ruderman, N. B., Park, H., Kaushik, V. K., Dean, D., Constant, S., Prentki, M., et al. (2003). AMPK as a metabolic switch in rat muscle, liver and adipose tissue after exercise. *Acta Physiol. Scand.* 178, 435–442. doi: 10.1046/j.1365-201x.2003.01164.x

Russell, R. R. I. I. I., Li, J., Coven, D. L., Pypaert, M., Zechner, C., Palmeri, M., et al. (2004). AMP-activated protein kinase mediates ischemic glucose uptake and prevents postischemic cardiac dysfunction, apoptosis, and injury. *J. Clin. Investigat.* 114, 495–503. doi: 10.1172/jci19297

Rutter, G. A., da Silva Xavier, G., and Leclerc, I. (2003). Roles of 5′-AMP-activated protein kinase (AMPK) in mammalian glucose homoeostasis. *Biochem. J.* 375, 1–16. doi: 10.1042/bj20030048

Ryan, J. J., Marsboom, G., and Archer, S. L. (2013). Rodent models of group 1 pulmonary hypertension. *Handbook Exp. Pharmacol.* 218, 105–149. doi: 10.1007/978-3-662-45805-1_5

Sakamoto, K., McCarthy, A., Smith, D., Green, K. A., Hardie, D. G., Ashworth, A., et al. (2005). Deficiency of LKB1 in skeletal muscle prevents AMPK activation and glucose uptake during contraction. *EMBO J.* 24, 1810–1820. doi: 10.1038/sj.emboj.7600667

Sakamoto, K., Zarrinpashneh, E., Budas, G. R., Pouleur, A. C., Dutta, A., Prescott, A. R., et al. (2006). Deficiency of LKB1 in heart prevents ischemia-mediated activation of AMPKalpha2 but not AMPKalpha1. *Am. J. Physiol. Endocrinol. Metabol.* 290, E780–E788.

Sakao, S., and Tatsumi, K. (2011). The effects of antiangiogenic compound SU5416 in a rat model of pulmonary arterial hypertension. *Respirat. Int. Rev. Thorac. Dis.* 81, 253–261. doi: 10.1159/000322011

Sallé-Lefort, S., Miard, S., Nolin, M.-A., Boivin, L., Paré, M. -È, Debigaré, R., et al. (2016). Hypoxia upregulates Malat1 expression through a CaMKK/AMPK/HIF-1α axis. *Int. J. Oncol.* 49, 1731–1736. doi: 10.3892/ijo.2016.3630

Satoh, K., Fukumoto, Y., Nakano, M., Sugimura, K., Nawata, J., Demachi, J., et al. (2009). Statin ameliorates hypoxia-induced pulmonary hypertension associated with down-regulated stromal cell-derived factor-1. *Cardiovasc. Res.* 81, 226–234. doi: 10.1093/cvr/cvn244

Schoental, R., and Head, M. A. (1955). Pathological changes in rats as a result of treatment with monocrotaline. *Br. J. Cancer* 9, 229–237. doi: 10.1038/bjc.1955.19

Scott, J. W., Norman, D. G., Hawley, S. A., Kontogiannis, L., and Hardie, D. G. (2002). Protein kinase substrate recognition studied using the recombinant catalytic domain of AMP-activated protein kinase and a model substrate. *J. Mol. Biol.* 317, 309–323. doi: 10.1006/jmbi.2001.5316

Shackelford, D. B., and Shaw, R. J. (2009). The LKB1-AMPK pathway: metabolism and growth control in tumour suppression. *Nat. Rev. Cancer* 9, 563–575. doi: 10.1038/nrc2676

Shaw, R. J., Kosmatka, M., Bardeesy, N., Hurley, R. L., Witters, L. A., DePinho, R. A., et al. (2004). The tumor suppressor LKB1 kinase directly activates AMP-activated kinase and regulates apoptosis in response to energy stress. *Proc. Natl. Acad. Sci. U.S.A.* 101, 3329–3335. doi: 10.1073/pnas.0308061100

Shaw, R. J., Lamia, K. A., Vasquez, D., Koo, S. H., Bardeesy, N., Depinho, R. A., et al. (2005). The kinase LKB1 mediates glucose homeostasis in liver and therapeutic effects of metformin. *Science* 310, 1642–1646. doi: 10.1126/science.1120781

Shimoda, L. A., and Laurie, S. S. (2013). Vascular remodeling in pulmonary hypertension. *J. Mol. Med.* 91, 297–309.

Shirwany, N. A., and Zou, M. H. (2010). AMPK in cardiovascular health and disease. *Acta Pharmacol. Sin.* 31, 1075–1084. doi: 10.1038/aps.2010.139

Simonneau, G., Montani, D., Celermajer, D. S., Denton, C. P., Gatzoulis, M. A., Krowka, M., et al. (2019). Haemodynamic definitions and updated clinical classification of pulmonary hypertension. *Eur. Respirat. J.* 53:1801913. doi: 10.1183/13993003.01913-2018

Sommer, N., Dietrich, A., Schermuly, R. T., Ghofrani, H. A., Gudermann, T., Schulz, R., et al. (2008). Regulation of hypoxic pulmonary vasoconstriction: basic mechanisms. *Eur. Respirat. J.* 32, 1639–1651.

Song, Y., Wu, Y., Su, X., Zhu, Y., Liu, L., Pan, Y., et al. (2016). Activation of AMPK inhibits PDGF-induced pulmonary arterial smooth muscle cells proliferation and its potential mechanisms. *Pharmacol. Res.* 107, 117–124. doi: 10.1016/j.phrs.2016.03.010

Stapleton, D., Mitchelhill, K. I., Gao, G., Widmer, J., Michell, B. J., Teh, T., et al. (1996). Mammalian AMP-activated protein kinase subfamily. *J. Biol. Chem.* 271, 611–614.

Stenmark, K. R., and McMurtry, I. F. (2005). Vascular remodeling versus vasoconstriction in chronic hypoxic pulmonary hypertension. *Circul. Res.* 97, 95–98. doi: 10.1161/01.res.00000175934.68087.29

Stenmark, K. R., Fagan, K. A., and Frid, M. G. (2006). Hypoxia-induced pulmonary vascular remodeling. *Circulat. Res.* 99, 675–691.

Sun, Z., Liu, Y., Yu, F., Xu, Y., Yanli, L., and Liu, N. (2019). Long non-coding RNA and mRNA profile analysis of metformin to reverse the pulmonary hypertension vascular remodeling induced by monocrotaline. *Biomed. Pharmacother.* 115:108933. doi: 10.1016/j.biopha.2019.108933

Sylvester, J. T., Shimoda, L. A., Aaronson, P. I., and Ward, J. P. T. (2012). Hypoxic pulmonary vasoconstriction. *Physiol. Rev.* 92, 367–520.

Sztuka, K., and Jasiñska-Stroschein, M. (2017). Animal models of pulmonary arterial hypertension: a systematic review and meta-analysis of data from 6126 animals. *Pharmacol. Res.* 125, 201–214. doi: 10.1016/j.phrs.2017.08.003

Taraseviciene-Stewart, L., Kasahara, Y., Alger, L., Hirth, P., Mc Mahon, G., Waltenberger, J., et al. (2001). Inhibition of the VEGF receptor 2 combined with chronic hypoxia causes cell death-dependent pulmonary endothelial cell proliferation and severe pulmonary hypertension. *FASEB J.* 15, 427–438. doi: 10.1096/fj.00-0343com

Tarry, D., and Powell, M. (2017). Hypoxic pulmonary vasoconstriction. *BJA Educat.* 17, 208–213.

Teng, R.-J., Du, J., Afolayan, A. J., Eis, A., Shi, Y., and Konduri, G. G. (2013). AMP kinase activation improves angiogenesis in pulmonary artery endothelial cells with in utero pulmonary hypertension. *Am. J. Physiol. Lung Cell. Mol. Physiol.* 304, L29–L42.

Thenappan, T., Ormiston, M. L., Ryan, J. J., and Archer, S. L. (2018). Pulmonary arterial hypertension: pathogenesis and clinical management. *BMJ* 360:j5492. doi: 10.1136/bmj.j5492

Thenappan, T., Shah, S. J., Gomberg-Maitland, M., Collander, B., Vallakati, A., Shroff, P., et al. (2011). Clinical characteristics of pulmonary hypertension in patients with heart failure and preserved ejection fraction. *Circulat. Heart Fail.* 4, 257–265.

Thomson, D. M., Porter, B. B., Tall, J. H., Kim, H.-J., Barrow, J. R., and Winder, W. W. (2007). Skeletal muscle and heart LKB1 deficiency causes decreased voluntary running and reduced muscle mitochondrial marker enzyme expression in mice. *Am. J. Physiol. Endocrinol. Metab.* 292, E196–E202.

Towler, M. C., and Hardie, D. G. (2007). AMP-activated protein kinase in metabolic control and insulin signaling. *Circulat. Res.* 100, 328–341. doi: 10.1161/01.res.0000256090.42690.05

Toyama, E. Q., Herzig, S., Courchet, J., Lewis, T. L., Losón, O. C., Hellberg, K., et al. (2016). AMP-activated protein kinase mediates mitochondrial fission in response to energy stress. *Science* 351, 275–281. doi: 10.1126/science.aab4138

Tuder, R. M. (2017). Pulmonary vascular remodeling in pulmonary hypertension. *Cell Tissue Res.* 367, 643–649.

Tuder, R. M., Marecki, J. C., Richter, A., Fijalkowska, I., and Flores, S. (2007). Pathology of pulmonary hypertension. *Clin. Chest Med.* 28, 23–vii.

Viollet, B., Lantier, L., Devin-Leclerc, J., Hebrard, S., Amouyal, C., Mounier, R., et al. (2009). Targeting the AMPK pathway for the treatment of Type 2 diabetes. *Front. Biosci. (Landmark Ed.)* 14:3380–3400. doi: 10.2741/3460

von Euler, U. S., and von Liljestrand, G. (1946). Observations on the pulmonary arterial blood pressure in the cat. *Acta Physiol. Scandinav.* 12, 301–320. doi: 10.1111/j.1748-1716.1946.tb00389.x

Wang, L., Halliday, G., Huot, J. R., Satoh, T., Baust, J. J., Fisher, A., et al. (2020). Treatment with treprostinil and metformin normalizes hyperglycemia and improves cardiac function in pulmonary hypertension associated with heart failure with preserved ejection fraction. *Arterioscl. Thromb. Vascul. Biol.* 40, 1543–1558. doi: 10.1161/atvbaha.119.313883

Wang, Y. -g., Han, X.-g., Yang, Y., Qiao, H., Dai, K. -r., Fan, Q. -m., et al. (2016). Functional differences between AMPK α1 and α2 subunits in osteogenesis, osteoblast-associated induction of osteoclastogenesis, and adipogenesis. *Sci. Rep.* 6:32771.

Wang, Z., Wilson, W. A., Fujino, M. A., and Roach, P. J. (2001). Antagonistic controls of autophagy and glycogen accumulation by Snf1p, the yeast homolog of AMP-activated protein kinase, and the cyclin-dependent kinase Pho85p. *Mol. Cell. Biol.* 21, 5742–5752. doi: 10.1128/mcb.21.17.5742-5752.2001

Waypa, G. B., and Schumacker, P. T. (2010). Hypoxia-induced changes in pulmonary and systemic vascular resistance: where is the O2 sensor. *Respirat. Physiol. Neurobiol.* 174, 201–211. doi: 10.1016/j.resp.2010.08.007

Weir, E. K., and Archer, S. L. (1995). The mechanism of acute hypoxic pulmonary vasoconstriction: the tale of two channels. *FASEB J.* 9, 183–189. doi: 10.1096/fasebj.9.2.7781921

Wilson, D. W., Segall, H. J., Pan, L. C., and Dunston, S. K. (1989). Progressive inflammatory and structural changes in the pulmonary vasculature of monocrotaline-treated rats. *Microvasc. Res.* 38, 57–80. doi: 10.1016/0026-2862(89)90017-4

Woods, A., Dickerson, K., Heath, R., Hong, S. P., Momcilovic, M., Johnstone, S. R., et al. (2005). Ca2+/calmodulin-dependent protein kinase kinase-beta acts upstream of AMP-activated protein kinase in mammalian cells. *Cell Metab.* 2, 21–33. doi: 10.1016/j.cmet.2005.06.005

Woods, A., Johnstone, S. R., Dickerson, K., Leiper, F. C., Fryer, L. G., Neumann, D., et al. (2003). LKB1 is the upstream kinase in the AMP-activated protein kinase cascade. *Curr. Biol.* 13, 2004–2008. doi: 10.1016/j.cub.2003.10.031

Wu, N., Zheng, B., Shaywitz, A., Dagon, Y., Tower, C., Bellinger, G., et al. (2013). AMPK-dependent degradation of TXNIP upon energy stress leads to enhanced glucose uptake via GLUT1. *Mol. Cell* 49, 1167–1175. doi: 10.1016/j.molcel.2013.01.035

Wu, S., and Zou, M. H. (2020). AMPK, mitochondrial function, and cardiovascular disease. *Int. J. Mol. Sci.* 21:4987. doi: 10.3390/ijms21144987

Wu, Y., Liu, L., Zhang, Y., Wang, G., Han, D., Ke, R., et al. (2014). Activation of AMPK inhibits pulmonary arterial smooth muscle cells proliferation. *Exp. Lung Res.* 40, 251–258. doi: 10.3109/01902148.2014.913092

Wu, Y., Song, P., Zhang, W., Liu, J., Dai, X., Liu, Z., et al. (2015). Activation of AMPKα2 in adipocytes is essential for nicotine-induced insulin resistance in vivo. *Nat. Med.* 21, 373–382. doi: 10.1038/nm.3826

Xiao, B., Heath, R., Saiu, P., Leiper, F. C., Leone, P., Jing, C., et al. (2007). Structural basis for AMP binding to mammalian AMP-activated protein kinase. *Nature* 449, 496–500. doi: 10.1038/nature06161

Xiao, B., Sanders, M. J., Underwood, E., Heath, R., Mayer, F. V., Carmena, D., et al. (2011). Structure of mammalian AMPK and its regulation by ADP. *Nature* 472, 230–233. doi: 10.1038/nature09932

Xue, J., Nelin, L. D., and Chen, B. (2017). Hypoxia induces arginase II expression and increases viable human pulmonary artery smooth muscle cell numbers via AMPKα1 signaling. *Am. J. Physiol. Lung Cell. Mol. Physiol.* 312, L568–L578.

Yan, H., Zhang, D. X., Shi, X., Zhang, Q., and Huang, Y. S. (2012). Activation of the prolyl-hydroxylase oxygen-sensing signal cascade leads to AMPK activation in cardiomyocytes. *J. Cell. Mol. Med.* 16, 2049–2059. doi: 10.1111/j.1582-4934.2011.01500.x

Yan, Y., Zhou, X. E., Xu, H. E., and Melcher, K. (2018). Structure and physiological regulation of AMPK. *Int. J. Mol. Sci.* 19:3534. doi: 10.3390/ijms19113534

Yoshida, T., Matsuura, K., Goya, S., Ma, D., Shimada, K., Kitpipatkun, P., et al. (2020). Metformin prevents the development of monocrotaline-induced pulmonary hypertension by decreasing serum levels of big endothelin-1. *Exp. Therap. Med.* 20:149.

Yuan, J. X.-J., Aldinger, A. M., Juhaszova, M., Wang, J., Conte, J. V., Gaine, S. P., et al. (1998). Dysfunctional voltage-gated K+ channels in pulmonary artery smooth muscle cells of patients with primary pulmonary hypertension. *Circulation* 98, 1400–1406. doi: 10.1161/01.cir.98.14.1400

Zarrinpashneh, E., Carjaval, K., Beauloye, C., Ginion, A., Mateo, P., Pouleur, A.-C., et al. (2006). Role of the α2-isoform of AMP-activated protein kinase in the metabolic response of the heart to no-flow ischemia. *Am. J. Physiol. Heart Circulat. Physiol.* 291, H2875–H2883.

Zhai, C., Shi, W., Feng, W., Zhu, Y., Wang, J., Li, S., et al. (2018). Activation of AMPK prevents monocrotaline-induced pulmonary arterial hypertension by suppression of NF-κB-mediated autophagy activation. *Life Sci.* 208, 87–95. doi: 10.1016/j.lfs.2018.07.018

Zhang, J., Dong, J., Martin, M., He, M., Gongol, B., Marin, T. L., et al. (2018). Shyy, AMP-activated protein kinase phosphorylation of angiotensin-converting enzyme 2 in endothelium mitigates pulmonary hypertension. *Am. J. Respirat. Cell Mol. Biol.* 198, 509–520. doi: 10.1164/rccm.201712-2570oc

Zhang, Y., Lee, T. S., Kolb, E. M., Sun, K., Lu, X., Sladek, F. M., et al. (2006). AMP-activated protein kinase is involved in endothelial NO synthase activation in response to shear stress. *Arterioscler. Thromb. Vasc. Biol.* 26, 1281–1287. doi: 10.1161/01.atv.0000221230.08596.98

Zhao, F., Wang, C., and Zhu, X. (2020). Isoform-specific roles of AMPK catalytic α subunits in Alzheimer's disease. *J. Clin. Investigat.* 130, 3403–3405. doi: 10.1172/jci137908

Zhao, L. (2010). Chronic hypoxia-induced pulmonary hypertension in rat: the best animal model for studying pulmonary vasoconstriction and vascular medial hypertrophy. *Drug Discover. Today Dis. Models* 7, 83–88.

Zmijewski, J. W., Banerjee, S., Bae, H., Friggeri, A., Lazarowski, E. R., and Abraham, E. (2010). Exposure to hydrogen peroxide induces oxidation and activation of AMP-activated protein kinase. *J. Biol. Chem.* 285, 33154–33164. doi: 10.1074/jbc.m110.143685

Zong, H., Ren, J. M., Young, L. H., Pypaert, M., Mu, J., Birnbaum, M. J., et al. (2002). AMP kinase is required for mitochondrial biogenesis in skeletal muscle in response to chronic energy deprivation. *Proc. Natl. Acad. Sci. U.S.A.* 99, 15983–15987. doi: 10.1073/pnas.252625599

Conflict of Interest: The authors declare that the research was conducted in the absence of any commercial or financial relationships that could be construed as a potential conflict of interest.

Copyright © 2021 Zhao, Song and Zou. This is an open-access article distributed under the terms of the Creative Commons Attribution License (CC BY). The use, distribution or reproduction in other forums is permitted, provided the original author(s) and the copyright owner(s) are credited and that the original publication in this journal is cited, in accordance with accepted academic practice. No use, distribution or reproduction is permitted which does not comply with these terms.

frontiers in Cell and Developmental Biology

ORIGINAL RESEARCH
published: 10 June 2021
doi: 10.3389/fcell.2021.691801

Endothelial Aryl Hydrocarbon Receptor Nuclear Translocator Mediates the Angiogenic Response to Peripheral Ischemia in Mice With Type 2 Diabetes Mellitus

*Tu Nguyen[1†], Mei Zheng[1†], Maura Knapp[1†], Nikola Sladojevic[1], Qin Zhang[1], Lizhuo Ai[1], Devin Harrison[2], Anna Chen[1], Albert Sitikov[1], Le Shen[3], Frank J. Gonzalez[4], Qiong Zhao[5], Yun Fang[2], James J. K. Liao[1] and Rongxue Wu[1]**

[1] Biological Sciences Division – Cardiology, Department of Medicine, University of Chicago, Chicago, IL, United States, [2] Section of Pulmonary and Critical Care, Department of Medicine, University of Chicago, Chicago, IL, United States, [3] Section of General Surgery, Department of Surgery, University of Chicago, Chicago, IL, United States, [4] Laboratory of Metabolism, Center for Cancer Research, National Cancer Institute, National Institutes of Health, Bethesda, MD, United States, [5] Division of Cardiology, Department of Medicine, Inova Heart and Vascular Institute, Annandale, VA, United States

OPEN ACCESS

Edited by:
Xiaofeng Yang,
Temple University, United States

Reviewed by:
Jingyan Han,
Boston University, United States
Suresh Kumar Verma,
University of Alabama at Birmingham, United States

***Correspondence:**
Rongxue Wu
Rwu3@uchicago.edu

[†] These authors have contributed equally to this work

Specialty section:
This article was submitted to Signaling, a section of the journal Frontiers in Cell and Developmental Biology

Received: 07 April 2021
Accepted: 17 May 2021
Published: 10 June 2021

Citation:
Nguyen T, Zheng M, Knapp M, Sladojevic N, Zhang Q, Ai L, Harrison D, Chen A, Sitikov A, Shen L, Gonzalez FJ, Zhao Q, Fang Y, Liao JJK and Wu R (2021) Endothelial Aryl Hydrocarbon Receptor Nuclear Translocator Mediates the Angiogenic Response to Peripheral Ischemia in Mice With Type 2 Diabetes Mellitus. Front. Cell Dev. Biol. 9:691801. doi: 10.3389/fcell.2021.691801

Hypoxia-inducible factors (HIFs) are the master regulators of angiogenesis, a process that is impaired in patients with diabetes mellitus (DM). The transcription factor aryl hydrocarbon receptor nuclear translocator (ARNT, also known as HIF1β) has been implicated in the development and progression of diabetes. Angiogenesis is driven primarily by endothelial cells (ECs), but both global and EC-specific loss of ARNT-cause are associated with embryonic lethality. Thus, we conducted experiments in a line of mice carrying an inducible, EC-specific ARNT-knockout mutation ($Arnt^{\Delta\ EC,ERT2}$) to determine whether aberrations in ARNT expression might contribute to the vascular deficiencies associated with diabetes. Mice were first fed with a high-fat diet to induce diabetes. $Arnt^{\Delta\ EC,ERT2}$ mice were then adminstrated with oral tamoxifen to disrupt *Arnt* and peripheral angiogenesis was evaluated by using laser-Doppler perfusion imaging to monitor blood flow after hindlimb ischemia. The $Arnt^{\Delta\ EC,ERT2}$ mice had impaired blood flow recovery under both non-diabetic and diabetic conditions, but the degree of impairment was greater in diabetic animals. In addition, siRNA-mediated knockdown of ARNT activity reduced measurements of tube formation, and cell viability in human umbilical vein endothelial cells (HUVECs) cultured under high-glucose conditions. The $Arnt^{\Delta\ EC,ERT2}$ mutation also reduced measures of cell viability, while increasing the production of reactive oxygen species (ROS) in microvascular endothelial cells (MVECs) isolated from mouse skeletal muscle, and the viability of $Arnt^{\Delta\ EC,ERT2}$ MVECs under high-glucose concentrations increased when the cells were treated with an ROS inhibitor. Collectively, these observations suggest that declines in endothelial ARNT expression contribute to the suppressed angiogenic phenotype in diabetic mice, and that the cytoprotective effect of ARNT expression in ECs is at least partially mediated by declines in ROS production.

Keywords: ARNT, endothelial angiogenesis, hindlimb ischemia, diabetic animal, cell death

INTRODUCTION

Diabetes mellitus (DM) is one of the leading causes of death in the United States and is frequently associated with cardiovascular abnormalities (Hadi and Suwaidi, 2007; Severino et al., 2018; Knapp et al., 2019) that can lead to critical limb ischemia and amputation (Falanga, 2005). Vascular deficiencies are caused by both deterioration of the existing vasculature and impairments in angiogenesis (Costa and Soares, 2013). The angiogenic response to injury and other pathological conditions is chiefly regulated by hypoxia-inducible factors (HIFs) such as HIF1α and aryl hydrocarbon receptor nuclear translocator (ARNT, also known as HIF1β). ARNT is a member of the basic helix-loop-helix/Per-ARNT-SIM (bHLH/PAS) nuclear receptor family (Madan et al., 2002) and regulates the expression of genes involved in cell survival, angiogenesis, and glucose metabolism by dimerizing with HIF1α under hypoxic conditions. Thus, *Arnt* deficiencies in mice lead to angiogenic defects and embryonic lethality, while $Arnt^{-/-}$ embryonic stem cells fail to respond to declines in glucose concentration (Maltepe et al., 1997). ARNT also regulates glucose-stimulated insulin secretion in mouse β cells (Pillai et al., 2011) and is severely downregulated (by 98%) in the liver and pancreas of patients with diabetes (Gunton et al., 2005; Pillai et al., 2011), in addition the cardiac-specific loss of ARNT expression in mice leads to a phenotype that mimics diabetic cardiomyopathy (Wu et al., 2014). Hence, ARNT appears to play a key role in diabetes and the pathogenesis of diabetic complications. However, whether changes in ARNT activity may contribute to the vascular deficiencies observed in patients with diabetes remains unclear. Given that endothelial-specific ARNT mutations are generally associated with embryonic lethality (Maltepe et al., 1997), we characterized the angiogenic role of endothelial ARNT expression under diabetic conditions by conducting experiments in mice carrying an inducible, EC-specific ARNT-knockout mutation. The inducible mutation was then induced via oral tamoxifen administration, and the animals were fed with a high-fat diet to induce type 2 DM. Our results indicate that the angiogenic response to peripheral ischemic injury is impaired in diabetic mice and exacerbated by deficiencies in EC ARNT expression. ARNT inactivation is also associated with declines in the angiogenic activity of endothelial cells (ECs) when the cells are cultured under high-glucose conditions.

MATERIALS AND METHODS

Type 2 Diabetes Mellitus Animal Model

Mice with the endothelial-specific knockout of ARNT ($Arnt^{\Delta\ EC,ERT2}$) were generated by crossing $Arnt^{fl/fl}$ mice with VE-cadherin-CreERT2 mice (Okabe et al., 2014). VE-cadherin-CreERT2 mice were generated by The Jackson Laboratory using sperm from the VE-Cadherin-CreERT2 mouse line, which was a gift from Yoshiaki Kubota (Keio University, Tokyo, Japan) to Liao. ARNT deletion was achieved by oral administration of tamoxifen (30 mg/kg body weight) for 2 weeks, which previously shown to be successful in knocking out ARNT (Wu et al., 2014). The type 2 DM model was induced in $Arnt^{\Delta\ EC,ERT2}$ or control mice ($ARNT^{fl/fl}$ with tamoxifen administration) using a high-fat diet that contains 62%Kcal of fat, 21%Kcal of carbohydrate, 18%Kcal of protein and 5.21 Kcal/g (A06071302, purchased from Research Diets) for 8 weeks as published previously by others (Winzell and Ahren, 2004; Wang and Liao, 2012).

All high-fat diet fed mice met the criteria for diabetes. db/db mice were purchased from The Jackson Laboratory and studied at 32 weeks of age. These db/db mice were homozygous for the diabetes spontaneous mutation ($Lepr^{db}$), which enables the manifestation of a series of conditions: morbid obesity, chronic hyperglycemia, pancreatic beta cell atrophy, and eventual hypoinsulinemia. Their insulin and blood sugar levels start to elevate at 10 to 14 days and at 4 to 8 weeks, respectively. db/+ mice served as the control (Guest and Rahmoune, 2019). The type 1 DM model was induced in 8-week-old male C57BL/6J mice using streptozotocin (STZ) 50 mg/kg body weight. Mice were administered STZ daily at 6 pm via IP injection for five consecutive days. All mice were fasted for 6 h before STZ administration. Mice were used for microvascular endothelial cell isolation 2 weeks after STZ injection. All animal experiments were approved by the Institutional Animal Care and Use Committee (IACUC) at the University of Chicago and followed the National Institutes of Health guide on laboratory animals' care and use.

Genotyping

According to the manufacturer's protocol, genetic DNA was isolated from mouse tails using a DNA isolation kit (QIAGEN DNA isolation kit). Genotyping of $Arnt^{fl/fl}$ mice was determined by PCR amplification (forward primer: 5′-CACCTGAGCTAAATTACCAGGCC-3′; reverse primer: 5′-GCATGCTGGCACATGCCTGTCT-3′). Primers were also used for genotyping VE-cadherin-CreERT2 mice (forward primer: 5′-GCG GTC TGG CAG TAA AAA CTA TC-3′; reverse primer: 5′-GTG AAA CAG CAT TGC TGT CAC TT-3′).

Blood Glucose Measurement and Glucose Tolerance Test

Before blood glucose measurement, mice were fasted for 10–12 h. Approximately 50 μl of blood from lateral tail veins was collected per mouse while animals were awake and restrained. For the glucose tolerance test (GTT), mice were fasted for 6 h. Measurements of blood glucose concentration were performed at 0 min (prior to the glucose injection) and at 15, 30, 60, and 120 min after intraperitoneal glucose injection (2 g glucose/kg body weight). GTT was measured using a Freestyle Precision Neo Blood Glucose Monitoring System (Abbott Diabetes Care Ltd., United Kingdom).

Hindlimb Ischemia Model and Hemodynamic Measurement

Unilateral hindlimb ischemia was induced and limb perfusion was assessed as previously described (Li et al., 2007). Shortly after, mice were anesthetized by 2% isoflurane. They then underwent operation with ligation and excision of the femoral artery from

its origin just above the inguinal ligament to its bifurcation at the root of the saphenous and popliteal arteries. Ligation also included inferior epigastric, lateral circumflex, and superficial epigastric artery branches. We used Doppler perfusion imaging before (0 week) and immediately after surgery at 1–4 weeks.

Cell Culture

Human umbilical vein endothelial cells (HUVECs) (ATCC, VA, United States) were cultured in M199 growth medium (Invitrogen, CA, United States) supplemented with 20% fetal calf serum (Gibco) and buffered with 25 mM HEPES, fresh L-glutamine (final concentration, 2 mM), 100 U/ml K- penicillin G, and 100 mcg/ml streptomycin sulfate (Biowhittaker). On the day of use, 100 μg/mL heparin (Sigma) and 50 μg/mL Endothelial Cell Growth Supplement (ECGS, Biomedical Technologies, Inc.) were added to get a final concentration of 0.1 mg/ml of medium. Cells were cultured in T25 vented flasks with a humidified atmosphere of 95% air and 5% CO_2 at 37°C.

Isolation of Murine Skeletal MUSCLE MICROVASCULAR ENDOTHELIAL CELLS (MMVECs)

This method was partly adapted from various studies and protocols focused on isolating ECs from mice (Nakano et al., 2018; Wang et al., 2019), which used mechanical and enzymatic dissociation followed by activated magnetic cell sorting for purification. In brief, the musculus quadriceps femoris was harvested from mice by cutting the tendon from the knee and severing the muscle from the femur to the hip. About 1 g of muscle tissue was finely minced in a solution containing 2 mg/ml collagenase (S5B115583 from Worthington) and PBS with calcium and magnesium (14040-133 from GIBCO) and incubated on a shaker at 37°C for 1 h. After the incubation period, the supernatant was harvested and centrifuged to collect the pellet. Then, the pellet was re-suspended in a solution containing PBS without calcium and magnesium (GIBCO), BSA (Bovine Serum Albumins) (0.1% v/v, Sigma), and platelet endothelial cell adhesion molecule-1 (PECAM1, CD31) (Choi et al., 2015) coated beads (BDB553370, Fisher). After that, the mixture was rotated for 10 min at room temperature and mounted on a magnetic separator. Following 10–12 washes, the cells were re-suspended in growth media containing DMEM with 1 g/L glucose (11885-084 from GIBCO), 20% FBS (v/v from GIBCO), 1% penicillin/streptomycin, 150 μg/mL Endothelial Cell Growth Supplement (ECGS, Biomedical Technologies), and 100 μg/mL heparin (Sigma). The cells were incubated in a 5% CO2 (v/v) and 95% (v/v) air incubator. After the cells reached 90% confluence, we harvested the cells and re-suspended them in PBS without Calcium and Magnesium and BSA (0.1% v/v). Intercellular Adhesion Molecule 2 antibody was used for the second sort.

Isolation and Measurement of ARNT mRNA and Protein

Total RNA was isolated from microvascular endothelial cells (MVECs) derived from mouse organs using Direct-zol RNA Mini-Prep kit (Zymo Research, CA, United States) according to the manufacturer's protocol. cDNA was synthesized from 500 ng of RNA using iScript Reverse Transcription Supermix for RT-qPCR (Bio-Rad Laboratories Inc., CA, United States). Quantitative real-time PCR was performed using iTaq Universal SYBR Green Supermix (Bio-Rad Laboratories Inc., CA, United States) in CFX Connect Real-time System (Bio-Rad Laboratories Inc., CA, United States). qPCR results were normalized to the expression of the endogenous control 18S. Fold changes in the transcripts were determined using the delta cycle threshold (i.e., $\Delta\Delta$Ct) method. The forward and reverse primer sequences used for human ARNT were: 5′-GAA CCA GCC ACA GTG TGA ATG G-3′ and 5′-GAG CCC ATA CAC ATC CTC ATG GAA GAC TGC TG-3′, respectively. All samples were analyzed in triplicates. 18S mRNA levels were used as an internal quantitative control. Endothelial ARNT protein levels from MVECs isolated from DB/DB and control mice were determined by Western blot, as we have published before (Wu et al., 2014). Antibody for ARNT was purchased from Cell Signaling (Cat# 5537). Antibody for Cofilin served as an internal loading control (Abcam, Ca# 42824).

Cell Transfection and Treatment

ARNT knockdown was induced by small interfering RNA (siRNA) directed against ARNT (Ambion, Carlsbad, CA, United States) in HUVECs. HUVECs were transfected with 25 nM of non-targeted or ARNT siRNA mixed with the siRNA transfection reagent Dharma FECT 3 (GE Healthcare Dharmacon). The mixtures were incubated in serum-free medium for 20 min at room temperature before being added to the HUVECs. siRNA transfection was allowed to proceed for 48 h before harvesting whole cells for RNA isolation for real-time PCR. Cells were treated with high glucose followed by 12 h of starvation. Cells in the high glucose (HG) group were cultured in 35 mmol/L D-glucose media (Sigma). Identical concentrations of medium containing 5.5 mmol/L D-glucose plus 29.5 mmol/L mannitol served as the normal glucose (NG) control group. To test whether reactive oxygen species (ROS) inhibitors have a role in the rescue of cell death, MMVECs were pretreated with PBS or mito-TEMPO (Sigma-Aldrich) at 0.5 μM for 30 min before HG was added.

Cell Proliferation and Cell Apoptosis Assay

After transfection with either ARNT-siRNA or control-siRNA, HUVECs (1.1×10^5) were incubated in FBS-free medium for 6 h and then in HG or NG culture medium. HUVECs were harvested from wells using 0.25% trypsin and counted every 24 h for 3 days using the Moxi GO II (Offlo Technologies) according to the manufacturer's protocol. Cell survival in HUVECs and MMVECs was determined by a cell apoptosis assay following 48 h of HG or NG treatment. The cells were washed with PBS and double-stained with FITC-conjugated Annexin V and PI using the Annexin V and PI kit (Offlo Technologies) according to the manufacturer's protocol. Measurements were obtained via Moxi GO II (Offlo Technologies).

In vitro Cell Migration Assessment

Muscle microvascular endothelial cells isolated from mouse skeletal muscle were seeded at a density of 2.0×10^4 cells in Incucyte ImageLock 96 well microplate Essen ImageLock™ overnight with HG or NG media to let cells attach to the well. We then used a WoundMaker™ device (4563, Essen Bioscience) containing 96 pins to scratch homogeneous micron-wide wounds through all the cell monolayers. After washing with PBS, 100 μl of fresh serum-free medium with either NG or HG were added to each well. The plates were then placed into the Incucyte S3 instrument (Essen Bioscience) to scan for relative wound width and confluence every 2 h for 48 h total. Data were analyzed through the instrument's software in accordance with the manufacturer's analysis manual.

Tube Formation Assay

Passage 2–3 HUVECs (followed by ARNT siRNA transfection for 48 h) were cultured at a density of 1.2×10^5 with HG or NG medium in 24 well plates coated with 300 μl of Growth Reduced Matrigel (Corning, NY, United States). After 17 h, the formation of tube-like structures was visualized under a microscope. Images were taken, and the number of meshes, number of extremities, length of branches and segment length were measured and analyzed by the angiogenesis analyzer for Image J, as previously published (Severino et al., 2018).

Measurement of ROS Production

Cultured MMVECs from either ecARNT-/- or control mice were seeded at a density of 2.0×10^4 cells in 96 well plates. Following incubation with NG or HG media for 48 h, the ROS levels were assessed using the Cellular ROS/Superoxide Detection Assay Kit (ab139476 from Abcam), which has been widely and successfully utilized in many different studies (Hu et al., 2019, 2020; Ren et al., 2019; You et al., 2020). The cells were prepared for measurement as instructed by the manufacturer's manual and submitted to the Biotek Synergy two microplate reader set with standard fluorescein (Ex = 488 nm, Em = 520 nm) and rhodamine (Ex = 550 nm, Em = 610 nm).

Statistical Analysis

Results were compared using one-way or two-way analysis of variance (ANOVA) as appropriate followed by the Tukey–Kramer *post hoc* test using GraphPad Prism statistics software (GraphPad Software, Inc.). Data are shown as means ± SEM. P-values < 0.05 were considered to be significantly different.

RESULTS

Endothelial ARNT Expression Is Reduced in Diabetic Mice

We began investigating the role of endothelial ARNT in diabetes by measuring ARNT expression in MVECs isolated from the hearts of diabetic mice. In models of type 1 [streptozotocin [STZ]-induced (Graham et al., 2011)] and type 2 (db/db) diabetes, the abundance of ARNT protein (DB/DB, **Figure 1A**) or mRNA (STZ-induced, **Figure 1B**) was significantly lower in MVECs from diabetic mice than in those from non-diabetic mice. *In vitro*, we were not able to detect a significant reduction in ARNT mRNA in response to HG; however, cell culture with prolonged HG exposure caused a decrease of *Arnt* mRNA in HUVECs (**Supplementary Figure 1**). To explore the role of ecARNT in angiogenesis during diabetes, we conducted a series of studies in mice carrying a tamoxifen-inducible, EC-specific ARNT-knockout ($Arnt^{\Delta\ EC,ERT2}$) mutation. The mutant line was generated by breeding $Arnt^{flox/flox}$ mice in which exon 6 of Arnt is flanked by loxP sequences (Wu et al., 2014), with VE-cadherin-Cre^{ERT2} mice expression of Cre-recombinase is tamoxifen-inducible and regulated by the vascular endothelial (VE) Cadherin promoter (Han et al., 2014; Okabe et al., 2014; **Figure 1C**). After cross-breeding for two generations, PCR analyses of genomic DNA confirmed that the $Arnt^{\Delta\ EC,ERT2}$ genotype was present in ∼1/4 of offspring (**Figure 1D**), and in the absence of tamoxifen treatment, the mice were phenotypically indistinguishable from wild-type mice. Because intraperitoneal injections of tamoxifen have been associated with Cre-driven cardiomyopathy in similar mouse models (Lexow et al., 2013), the $Arnt^{\Delta\ EC,ERT2}$ mice were orally treated with tamoxifen for 2 weeks via our published protocols (Ichikawa et al., 2014; Wu et al., 2014). Cell-type specificity of the *Arnt* disruption in $Arnt^{\Delta\ EC,ERT2}$ mice was confirmed by comparing *ARNT* mRNA abundance in ECs and other cells from $Arnt^{\Delta\ EC,ERT2}$ mice that had not been treated with tamoxifen (**Figure 1E**).

EC-Specific Loss of ARNT Expression Impairs the Angiogenic Response to Peripheral Ischemic Injury in Mice With Type 2 DM

When fed with a high-fat diet, both control and $Arnt^{\Delta\ EC,ERT2}$ mice developed diabetes, as evidenced by increases in body weight (**Figure 2A**) and in blood-glucose levels both under fasting conditions (**Figure 2B**) and in response to intraperitoneal glucose injection (i.e., the GTT, **Figures 2C,D**). Notably, measurements of glucose tolerance did not differ significantly between $Arnt^{\Delta\ EC,ERT2}$ and control mice under either normal or high-fat feeding conditions (**Supplementary Figure 2**), which suggests that ecARNT expression might not influence the development of type 2 diabetes. We next investigated whether ecARNT expression could contribute to ischemia-induced angiogenesis under diabetic conditions. We utilized the murine model of hindlimb ischemia (Niiyama et al., 2009) and evaluated perfusion in the limbs of mice before, immediately after, and 7–28 days after surgically induced hindlimb ischemia (HLI). Blood flow was quantified via laser doppler perfusion imaging, and measurements in the injured limb were normalized to measurements in the uninjured contralateral limb. In non-diabetic animals (i.e., under normal dietary conditions), perfusion of the injured limb was lower in $Arnt^{\Delta\ EC,ERT2}$ mice compared to the control mice on day 7 (1 week), 14 (2 weeks), and 21 (3 weeks) after HLI induction (**Figures 3A,B**). However, measurements in the two groups were similar on day 28 (4 weeks) (**Figures 3A,B**). In diabetic mice (i.e.,

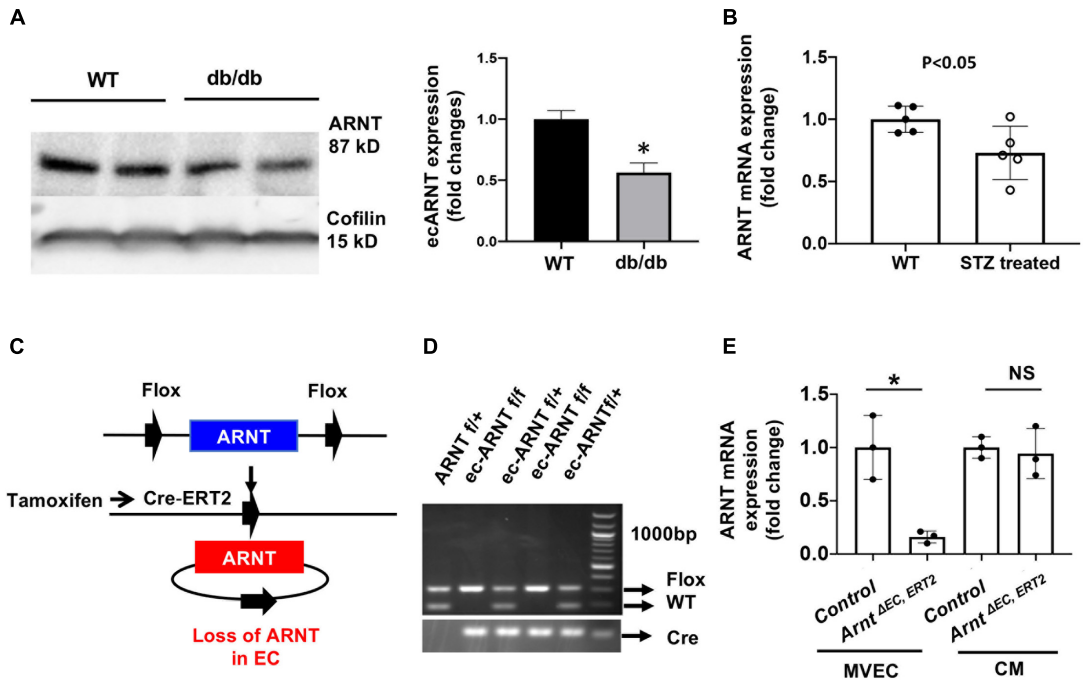

FIGURE 1 | Endothelial ARNT expression in diabetic animals and the generation of inducible endothelial-specific ARNT-deficient adult ($Arnt^{\Delta\ EC,ERT2}$) mice. **(A)** A Representative Western blot and comparison graph of ARNT protein expression levels in mouse microvascular endothelial cells (MVECs) isolated from control (db/+) and diabetic mouse (db/db) organs. **(B)** *ARNT* mRNA expression levels in MVECs isolated from control and STZ-treated diabetic mouse organs. **(C)** Schematic diagram of ecARNT deletion. **(D)** PCR analysis of genomic ARNT DNA. **(E)** *ARNT* mRNA expression levels in MVECs and isolated cardiomyocytes (CM). Data are presented as the mean ± SEM (n = 3–6) mice per group. *P < 0.01 versus WT or control mice.

those fed a high-fat diet), recovery was impaired in both control and ecARNT-KO groups (**Supplementary Figure 3**), which is consistent with the observations previously reported (Hazarika et al., 2007). Also, the difference between measurements in $Arnt^{\Delta\ EC,ERT2}$ and control mice became progressively greater through day 28 (**Supplementary Figure 4** and **Figures 3C,D**). Hence, the loss of ecARNT expression evidently appears to have exacerbated the diabetes-induced impairment of ischemia-induced angiogenesis.

ARNT Inactivation Impairs the Angiogenic Activity of ECs in High-Glucose Conditions

To characterize how deficiencies in endothelial ARNT expression alter the activity of ECs in diabetic animals, HUVECs were transfected with a vector coding for either ARNT-siRNA or a control-siRNA. ARNT knockdown was confirmed by both mRNA and protein expression (**Supplementary Figure 5**). Cells were then cultured under normal or high (35 mM) glucose (NG or HG, respectively) conditions. The NG condition was cultured in medium containing 5.5 mmol/L D-glucose supplemented with 29.5 mM mannitol to ensure osmotic equivalence. When HG-cultured cells were plated onto Matrigel, measurements of tube formation were significantly lower in ARNT-siRNA–transfected HUVECs compared to control-transfected HUVECs, but measurements in the two groups of NG-cultured cells were similar (**Figures 4B–F**). The impaired tube formation was determined by the number of meshes (**Figure 4C**), segment length (**Figure 4D**), number of extremities (**Figure 4E**), and length of branches (**Figure 4F**), which was analyzed by the angiogenesis analyzer for Image J. Of note, to assist our analyses, we used phase contrast of HUVEC network as indicated (**Figure 4A**).

Cell migration and proliferation toward angiogenic stimuli are essential factors for tube formation. Therefore, we performed a cell wound healing assay using an advanced live-cell imaging and analysis system (Incucyte® S3) (**Figure 5A**). The data suggested that *in vivo* wound closure was impaired by high glucose in cells, but not by the loss of ARNT, as migration in MMVECs from $Arnt^{\Delta\ EC,ERT2}$ mice failed to respond to HG (**Figure 5B**). However, cell confluence, used as an indicator of cell proliferation, demonstrated a reduction in MMVECs from ecARNT KO mice when cultured in HG conditions for 2 days (**Figure 5C**). We also measured cell proliferation in HUVECs in the presence of HG or NG conditions for 24 to 72 h. Inconsistent with the previous observation, the results showed that cell proliferation for WT HUVECs was inhibited when treated with high glucose for 72 h, and this inhibition was not due to osmotic pressure (**Figure 5D**). ARNT knockdown-mediated inhibition of cell proliferation was greater than control HUVECs in the presence of HG (**Figure 5E**). Thus, knockdown of ecARNT expression inhibits cell proliferation, which might have contributed to impaired tube formation in HG conditions,

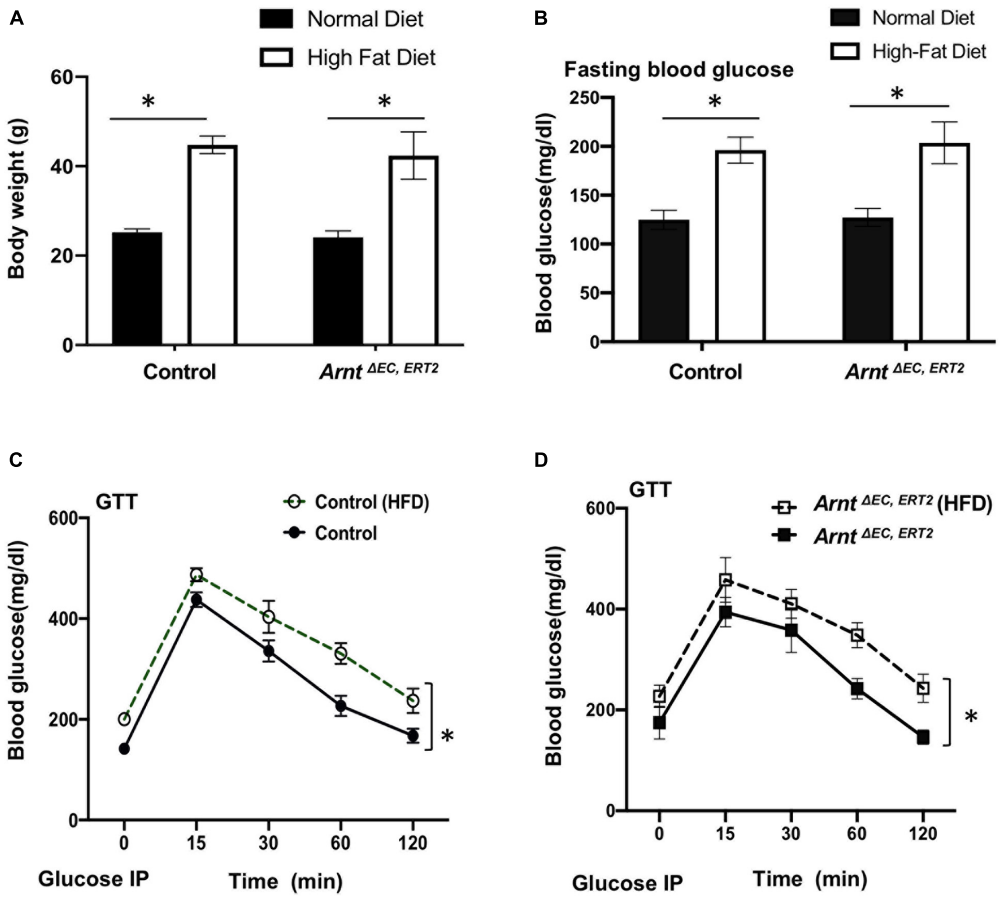

FIGURE 2 | High-fat diet (HFD) induced type-2 diabetic model in both WT control and $Arnt^{\Delta\ EC,ERT2}$ mice. **(A)** Bodyweight in control and $Arnt^{\Delta\ EC,ERT2}$ mice placed on both a standard diet and HFD for 8 weeks as indicated. **(B)** Fasting plasma glucose level in control and $Arnt^{\Delta\ EC,ERT2}$ mice after 8 weeks of standard diet and HFD for as indicated. **(C,D)** Glucose tolerance test (GTT) of control and $Arnt^{\Delta\ EC,ERT2}$ mice after 8 weeks of standard diet and HFD for as indicated. Glucose was administered as a 0.2 g/ml/100 g IP injection. Data are presented as the mean ± SEM (n = 5–8) mice per group. $^{*}P < 0.05$, $^{**}P < 0.01$ versus control mice.

suggesting an essential role for ARNT in angiogenesis in diabetic mellitus. This is in line with our *in vivo* studies.

Aryl hydrocarbon receptor nuclear translocator inactivation was also associated with declines in HUVEC viability when the cells were cultured under HG conditions (**Figure 6A**), and the production of ROS was significantly greater in skeletal-muscle MVECs from $Arnt^{\Delta\ EC,ERT2}$ mice compared to control mice under both NG and HG conditions (**Figure 6B**). Notably, measures of cell viability under HG conditions were also significantly lower for $Arnt^{\Delta\ EC,ERT2}$ MVECs than for control MVECs (**Figure 6C**). In addition, cell viability increased in $Arnt^{\Delta\ EC,ERT2}$ MVECs when the cells were treated with an ROS inhibitor (Mito-TEMPO, 0.5 μM) (**Figure 6C**; Dikalova et al., 2010; Vaka et al., 2018), which suggests that the cytoprotective effect of ARNT in ECs is mediated by declines in ROS production.

DISCUSSION

We are the first to report a reduction in ARNT in mouse MVECs isolated from diabetic animals. We successfully generated mice with an inducible endothelial-specific deletion in *Arnt* (ecARNT KO mice) and showed that these mice have a delayed angiogenic response to peripheral ischemic injury. In addition, loss of ARNT deletion in ECs exacerbated the diabetes-mediated impairment of ischemia-induced angiogenesis. Our *in vitro* studies found that genetic disruption or knockdown of ARNT worsened high glucose-induced endothelial cell dysfunction as measured by the angiogenic response in HUVECs (i.e., cell proliferation and tube formation). Interestingly, ARNT-induced cell death and reduced viability were associated with HG, but not NG cultured cells.

Moreover, we demonstrated that ROS production was significantly elevated in ecARNT KO MMVECs. Under high glucose conditions, increased cell death in ARNT KO MMVECs was rescued using Mito-Tempo (a mitochondrial ROS inhibitor), indicating ARNT protects cells from damages caused by ROS generation during high glucose conditions. Thus, our study demonstrates a direct role for ecARNT in angiogenesis and as an antioxidant in the setting of diabetic complications. Although many factors are likely contributing to impaired angiogenesis in diabetes, our study is the first to report alterations of ARNT

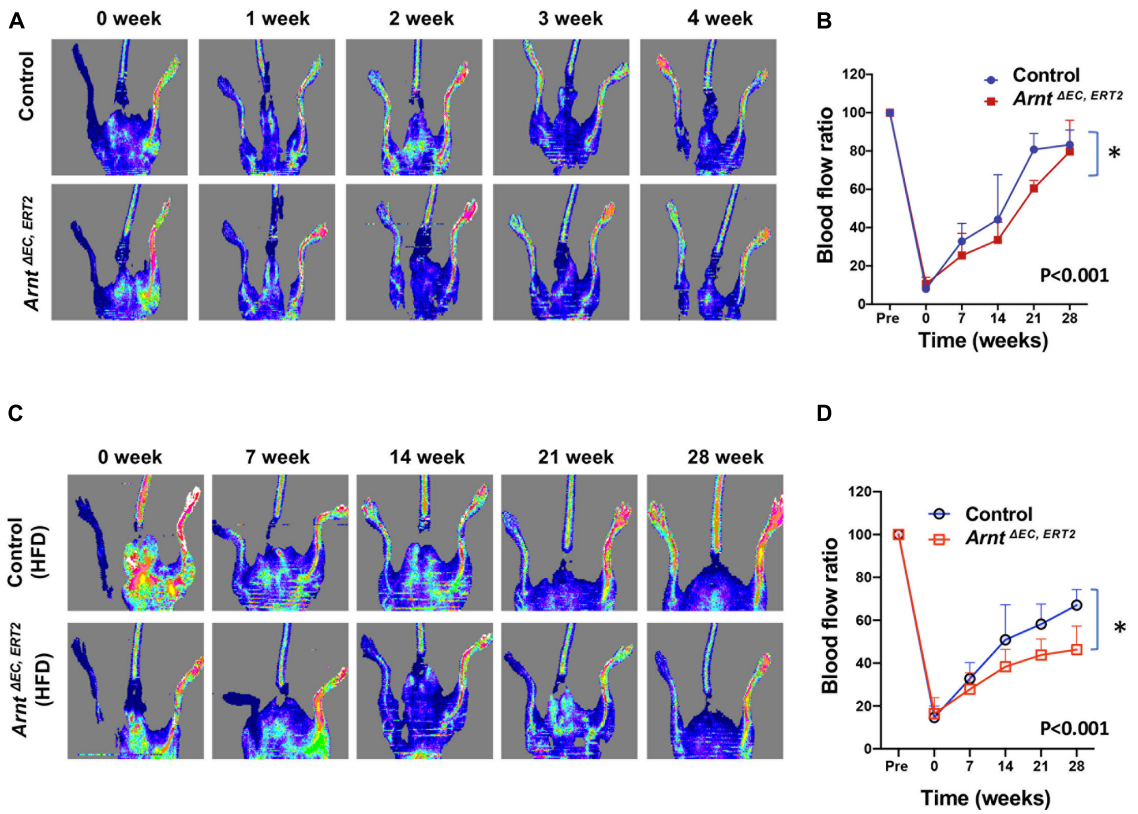

FIGURE 3 | Laser Doppler blood flow analysis for the ischemic hindlimb of *Arnt*$^{\Delta\ EC,ERT2}$ or wild-type control mice with and without high-fat diet (HFD). **(A)** Laser Doppler perfusion imaging of blood flow in the ischemic hindlimb measured in control and *Arnt*$^{\Delta\ EC,ERT2}$ mice fed with a standard diet. Laser Doppler perfusion imaging of blood flow in the ischemic hindlimb was measured immediately (time 0) and 1–4 weeks after surgery. Blood flow is color-coded, with normal perfusion indicated by red and a marked reduction in blood flow indicated by blue. **(B)** Quantitation of blood flow is expressed as the ratio of blood flow in the ischemic (left) hindlimb to that in the normal (right) hindlimb. **(C)** Laser Doppler perfusion imaging of blood flow in the ischemic hindlimb measured in control and *Arnt*$^{\Delta\ EC,ERT2}$ diabetic mice induced with 8 weeks of HFD. **(D)** Quantitation of blood flow as in B. Data are means of values from 8–11 animals per group. $^{*}P < 0.01$ versus corresponding value for wild-type mice.

in the microvascular system as a major contributor to the antioxidant process.

The HIF1//ARNT complex is activated in response to hypoxia. Diabetic tissue damage leads to hypoxia. However, HIF-1 signaling is impaired in diabetes, which may contribute to the development of diabetic complications (Catrina and Zheng, 2021). ARNT has been implicated in the development and progression of diabetes and is severely downregulated in the liver and pancreas of patients with diabetes (Gunton et al., 2005; Pillai et al., 2011). In this study, we observed a reduction in ARNT expression in MVECs isolated from both types 1 and 2 diabetic animal models, which may be caused by high glucose. Additionally, we focused on the role of ARNT in MVECs under hyperglycemic conditions in mice with diabetes. ARNT has been widely studied for its crucial role in angiogenesis. Overexpression of ARNT has previously been shown to rescue growth-restricted fetoplacental angiogenesis (Ji et al., 2019). In addition, ARNT may play a role in tumor angiogenesis via its capacity to bind xenobiotic responsive elements to induce transcription (Hankinson, 1995; Maltepe et al., 2000; Ji et al., 2019). Despite the wide array of studies of ARNT in angiogenesis, the understanding of ARNT's roles in angiogenic abnormalities in DM has been limited so far. In our study, in the absence of ischemia, *Arnt*$^{\Delta\ EC,ERT2}$ mice did not display any vascular abnormalities at baseline, but hindlimb ischemia-induced angiogenic response was slightly delayed in *Arnt*$^{\Delta\ EC,ERT2}$ mice compared to control mice. This impairment was much more pronounced under diabetic conditions. Of note, some diabetic mice with *Arnt*$^{\Delta\ EC,ERT2}$ even developed leg necrosis post hindlimb ischemia.

Given that ARNT is a master regulator of angiogenesis (Su et al., 2015; Ji et al., 2019), its diminished expression in the endothelium in the setting of diabetes may explain why diabetes is the biggest risk factor leading to vascular endothelial dysfunction and delayed tissue repair and regeneration, which eventually manifests as severe vascular complications in diabetic patients (Hadi and Suwaidi, 2007; Severino et al., 2018; Knapp et al., 2019). ARNT reduction in MVECs was observed in both types 1 and 2 diabetic mouse models, suggesting that hyperglycemia, rather than insulin resistance, impairs endothelial ARNT activity. Hence, we used high glucose media to treat HUVECs or primary MMVECs in order to examine angiogenic activity. To be diagnosed with diabetes, one of the criteria

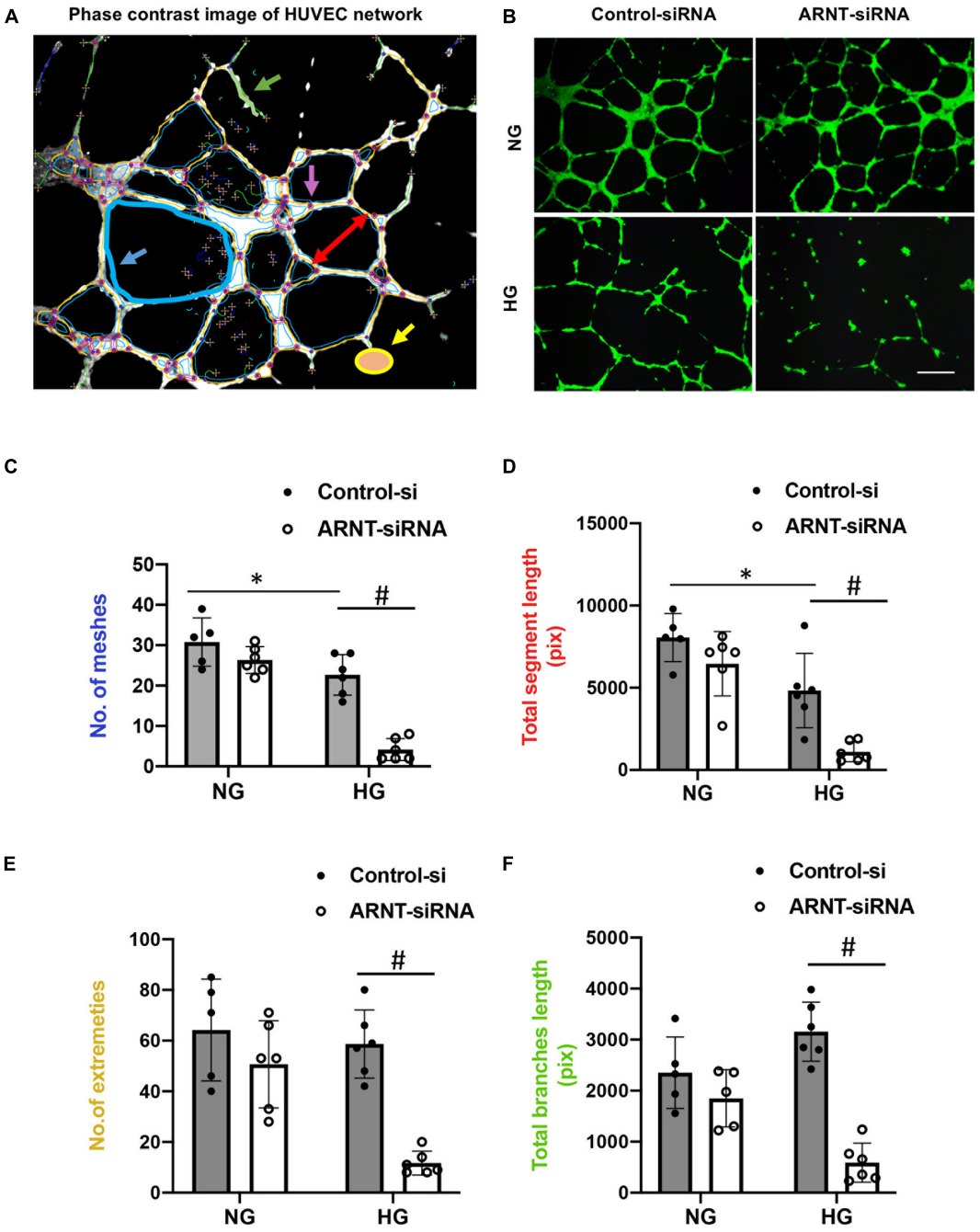

FIGURE 4 | The effects of ARNT knockdown on tube formation in cultured human umbilical vein endothelial cells (HUVECs). Cells were plated on Matrigel pre-coated 24-well plates that were transfected with either ARNT-siRNA or control-siRNA followed by high glucose (HG) and control exposure (NG, identical concentrations of mannitol as an osmotic control group) for an additional 48 h. **(A)** Representative image of HUVEC network, analyzed by the angiogenesis analyzer for Image J. The picture shows meshes (blue), extremities (yellow), branches (green), and segment length (red) as indicated. **(B)** Images of capillary-like tube formation, which mature by 6–16 h. Photomicrograph shows the effect of 35 mM high glucose exposure on tube formation with and without ecARNT knockdown (Scale bar = 200 μm). Summary of analysis is shown. **(C)** Number of meshes. **(D)** Total segment length. **(E)** Number of extremities. **(F)** Total branch length. Data are presented as the mean ± SEM (n = 5–6). $^{*}P < 0.01$ versus Control-si (NG), $^{\#}P < 0.01$ vs. Control-si (HG).

that must be met is a blood glucose level greater than or equal to 30 mM (200 mg/dl). Therefore, we used a culture medium containing 35 mmol glucose as our high-glucose (HG) condition and 5.5 mM (100 vmg/dl) glucose plus 29.5 mmol/L mannitol (as an osmotic control) for our normal glucose (NG) control group. Our data indicated that compared with the control group, ARNT knockdown (KD) using siRNA in HUVECs significantly worsened the HG induced impairment in tube

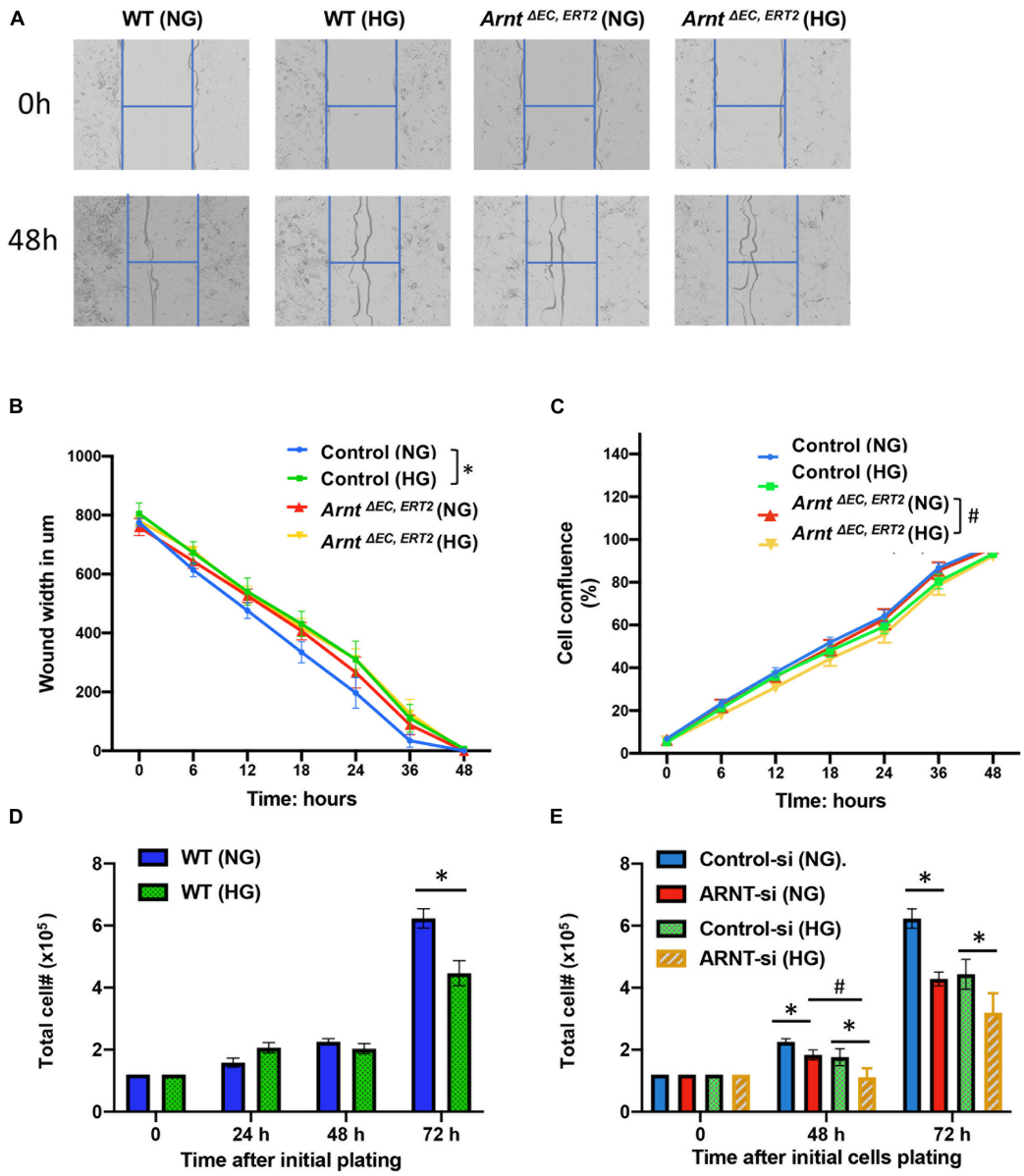

FIGURE 5 | Effect of ecARNT knockdown on high glucose-induced migration dysfunction in MMVEC and proliferation inhibition in HUVECs. **(A)** Representative micrographs of automatically acquired images of real-time live cells using Incucyte® system. Images show that compared to WT HUVECs in osmotic pressure control group (WT and NG), HUVECs with high glucose migrated more slowly $P = 0.0026$, corresponding statistical analysis of HUVEC migration by scratch wound healing assay. All 96-well kinetic trends were viewed at once with Incucyte® PlateGraph and data was exported to calculate different values shown. **(B)** Wound width. $n = 8$, $^{*}p < 0.01$ vs. WT (NG). Please note, migration in HUVECs with ARNT knockdown failed to respond to high glucose exposure **(C)** Cell confluence%, $n = 8$, $^{*}p < 0.001$ vs. WH (NG); $^{\#}P < 0.01$ vs. $Arnt^{\Delta\ EC,ERT2}$ (NG). **(D)** High glucose-mediated reduction in WT HUVEC proliferation over time. **(E)** Effect of ecARNT knockdown on HUVEC proliferation over time following either normal glucose or high glucose exposure. The same number of HUVECs were seeded on Day 0 (1.2×10^5) in 6- well plate. ARNT knockdown was induced with an siRNA transfection. Data are presented as the mean ± SEM ($n = 6$). $^{*}P < 0.01$ versus corresponding control.

formation, which is in line with our *in vivo* observations. Our results are in agreement with previous studies of wounds from diabetic patients, which showed decreased cellular migration, proliferation, and cell survival under HG conditions (Lan et al., 2009). However, ARNT KD did not affect cell migration under HG conditions. HG-mediated inhibition of proliferation in HUVECs was worsened with ARNT KD and HG-induced cell death was only observed in ARNT KD HUVECs, not in control HUVECs. This suggests an important role for ARNT in regulating EC proliferation and cell death under HG conditions, a process that is important in tube formation and angiogenesis.

High glucose in diabetes increases the production of ROS, which can impair cellular functions such as migration and proliferation, and activate apoptosis in β-cells (Volpe et al.,

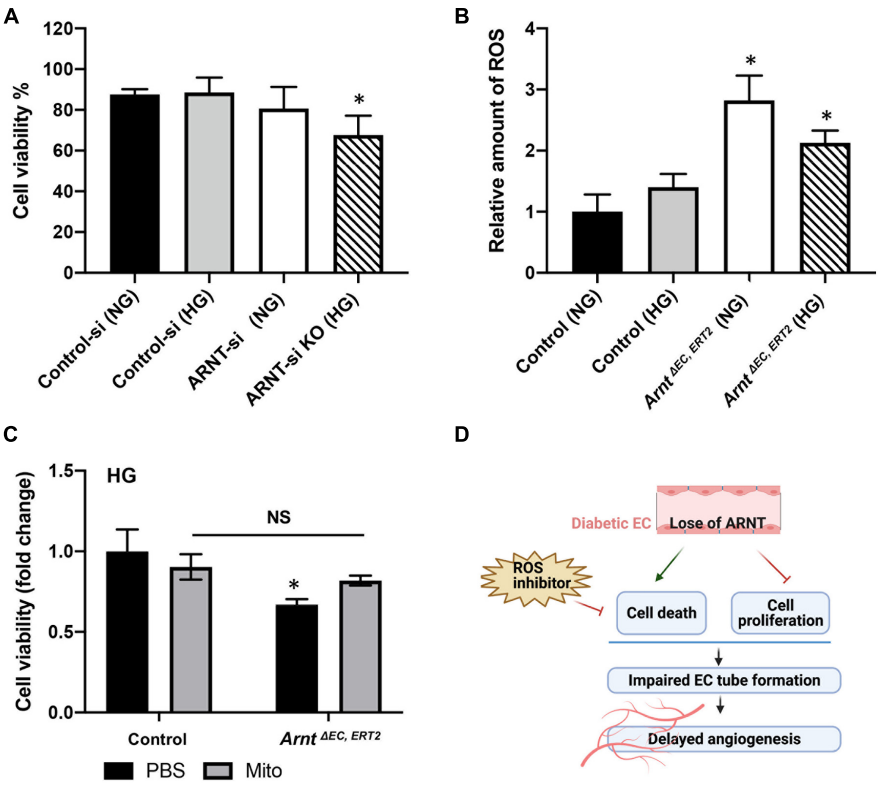

FIGURE 6 | Effects of ARNT expression on cell viability and cellular reactive oxygen species (ROS) production under either high glucose (HG) or normal media (NG) conditions. **(A)** Cell viability in the presence of high glucose or control media with and without ARNT deletion in HUVECs as indicated. ARNT knockdown was induced with an siRNA transfection. The treatment of a control siRNA serves as control. **(B)** ROS levels in MMVECs isolated from *Arnt*$^{\Delta\ EC,ERT2}$ and *Arnt*$^{fl/fl}$ WT mice under high glucose. The ROS levels were assessed using the Cellular ROS/Superoxide Detection Assay Kit from Abcam. **(C)** Effect of inhibition of ROS by Mito-TEMPO on cell viability. Isolated MMVECs from *Arnt*$^{\Delta\ EC,ERT2}$ and *Arnt*$^{fl/fl}$ WT control mice were cultured for 48 h in HG media followed by 24 h of administration of Mito-TEMPO at 0.5 μM. Cell viability was measured as before using the Moxi GO II machine. The data are shown as mean ± SEM (n = 6–8 per group). *P < 0.01. **(D)** Schematic diagram of the role of endothelial ARNT in diabetic angiogenesis.

2018). Our results showed that the ROS levels were notably elevated in ARNT-KO MMVECs as compared to control MMVECs both in NG and HG conditions. We then conducted an experiment that inhibited ROS production using Mito-TEMPO (Dikalova et al., 2010; Vaka et al., 2018) and observed a rescuing effect on cell death in the *Arnt*$^{\Delta\ EC,ERT2}$ HG group. Collectively, these findings suggest an important role for ARNT in acting as an antioxidant responder to protect MVECs under high glucose conditions. This conclusion corroborates a similar finding of the antioxidant role of ARNT previously observed in leukemia (Gu et al., 2013). Although our study demonstrated the critical antioxidant action of ARNT against ROS, it did not reveal the causative relationship between ARNT and the production of ROS. Thus far, knocking down ARNT has been shown to suppress the expression of PDK1 (pyruvate dehydrogenase kinase (1) in certain cancers. This in turn activates PDH (pyruvate dehydrogenase), the TCA cycle enzyme that converts pyruvate to acetyl Co-A to fuel the TCA cycle for oxidative phosphorylation (OXPHOS) (Kim et al., 2006; Huang et al., 2021). The upregulation of OXPHOS in mitochondria ultimately leads to increased ROS production (Li et al., 2013; Reichart et al., 2019; Huang et al., 2021). Unquestionably, these findings are valuable in supporting the causative relationship between ARNT and ROS production but limit ARNT's actions in ROS production to the PDK1-dependent pathway in cancer cells. Nevertheless, the underlying mechanisms in which ARNT could be involved in ROS generation in mitochondria under diabetic conditions is not clear. It is known that PDK4 levels are elevated in diabetes (Wu et al., 1998, 2000; Sugden and Holness, 2002). Therefore, it is in our best interest into investigating whether ecARNT in diabetes would regulate the production of ROS resulting from the upregulation of OXPHOS via a novel PDK4 dependent pathway or through the same pathway regulated by PDK1 above. This future direction is valuable because it will not only further elucidate our understanding of diminished cell proliferation and impaired angiogenesis via a ROS perspective but also allow us to expand our knowledge of the importance of ARNT in regulating genes encoding for glycolytic enzymes to produce energy, which many other studies have proved (Firth et al., 1994, 1995; Semenza et al., 1994, 1996). Despite these promising future directions, this study is the first to establish the connection between ecARNT and impaired angiogenesis in diabetes and demonstrate that ecARNT deficiency in diabetes

mellitus exacerbates angiogenesis impairment via a mechanism that intensifies the negative effects of ROS.

DATA AVAILABILITY STATEMENT

The raw data supporting the conclusions of this article will be made available by the authors, without undue reservation.

ETHICS STATEMENT

The animal study was reviewed and approved by the UCMC Institutional Review Boards at the University of Chicago.

AUTHOR CONTRIBUTIONS

TN and RW conceived of the study design and wrote the manuscript. TN, MZ, MK, and NS performed experiments with assistance from QINZ, LA, DH, AC, AS, and LS. TN, MZ, MK, and NS analyzed the data. FG, YF, QIOZ, and JL reviewed and contributed to the writing of the manuscript. All authors read and approved the final version of the manuscript.

FUNDING

RW is supported by AHA Scientist Development Award (13SDG17270046), NIH (1R01HL140114-01A1), Chicago DRTC (NIH/P30DK020595), and CTSA-ITM Core subsidies funding (throughNIHUL1TR000430). QIOZ is supported by NIH (R01HL083218) and JL is supported by HL136962.

ACKNOWLEDGMENTS

FG provided ARNT Flox/Flox mice. VE-cadherin-CreERT2 mice were provided by JL. Sperm was a gift from Yoshiaki Kubota (Keio University, Tokyo, Japan) to JL. **Figure 6D** was created with BioRender.com.

SUPPLEMENTARY MATERIAL

The Supplementary Material for this article can be found online at: https://www.frontiersin.org/articles/10.3389/fcell.2021.691801/full#supplementary-material

REFERENCES

Catrina, S. B., and Zheng, X. (2021). Hypoxia and hypoxia-inducible factors in diabetes and its complications. *Diabetologia* 64, 709–716. doi: 10.1007/s00125-021-05380-z

Choi, S., Kim, J. A., Kim, K. C., and Suh, S. H. (2015). Isolation and in vitro culture of vascular endothelial cells from mice. *Korean J. Physiol. Pharmacol.* 19, 35–42. doi: 10.4196/kjpp.2015.19.1.35

Costa, P. Z., and Soares, R. (2013). Neovascularization in diabetes and its complications. Unraveling the angiogenic paradox. *Life Sci.* 92, 1037–1045. doi: 10.1016/j.lfs.2013.04.001

Dikalova, A. E., Bikineyeva, A. T., Budzyn, K., Nazarewicz, R. R., McCann, L., Lewis, W., et al. (2010). Therapeutic targeting of mitochondrial superoxide in hypertension. *Circ. Res.* 107, 106–116. doi: 10.1161/circresaha.109.214601

Falanga, V. (2005). Wound healing and its impairment in the diabetic foot. *Lancet* 366, 1736–1743. doi: 10.1016/s0140-6736(05)67700-8

Firth, J. D., Ebert, B. L., Pugh, C. W., and Ratcliffe, P. J. (1994). Oxygen-regulated control elements in the phosphoglycerate kinase 1 and lactate dehydrogenase A genes: similarities with the erythropoietin 3' enhancer. *Proc. Natl. Acad. Sci. U.S.A.* 91, 6496–6500. doi: 10.1073/pnas.91.14.6496

Firth, J. D., Ebert, B. L., and Ratcliffe, P. J. (1995). Hypoxic regulation of lactate dehydrogenase A. Interaction between hypoxia-inducible factor 1 and cAMP response elements. *J. Biol. Chem.* 270, 21021–21027.

Graham, M. L., Janecek, J. L., Kittredge, J. A., Hering, B. J., and Schuurman, H. J. (2011). The streptozotocin-induced diabetic nude mouse model: differences between animals from different sources. *Comp. Med.* 61, 356–360.

Gu, C., Gonzalez, J., Zhang, T., Kamel-Reid, S., and Wells, R. A. (2013). The aryl hydrocarbon receptor nuclear translocator (ARNT) modulates the antioxidant response in AML cells. *Leuk Res.* 37, 1750–1756. doi: 10.1016/j.leukres.2013.10.010

Guest, P. C., and Rahmoune, H. (2019). Characterization of the db/db mouse model of type 2 diabetes. *Methods Mol. Biol.* 1916, 195–201. doi: 10.1007/978-1-4939-8994-2_18

Gunton, J. E., Kulkarni, R. N., Yim, S., Okada, T., Hawthorne, W. J., Tseng, Y. H., et al. (2005). Loss of ARNT/HIF1β mediates altered gene expression and pancreatic-islet dysfunction in human type 2 diabetes. *Cell* 122, 337–349. doi: 10.1016/j.cell.2005.05.027

Hadi, H. A., and Suwaidi, J. A. (2007). Endothelial dysfunction in diabetes mellitus. *Vasc. Health Risk Manag.* 3, 853–876.

Han, Y., Tao, J., Gomer, A., and Ramirez-Bergeron, D. L. (2014). Loss of endothelial-ARNT in adult mice contributes to dampened circulating proangiogenic cells and delayed wound healing. *Vasc. Med.* 19, 429–441. doi: 10.1177/1358863x14559588

Hankinson, O. (1995). The aryl hydrocarbon receptor complex. *Annu. Rev. Pharmacol. Toxicol.* 35, 307–340.

Hazarika, S., Dokun, A. O., Li, Y., Popel, A. S., Kontos, C. D., and Annex, B. H. (2007). Impaired angiogenesis after hindlimb ischemia in type 2 diabetes mellitus: differential regulation of vascular endothelial growth factor receptor 1 and soluble vascular endothelial growth factor receptor 1. *Circ. Res.* 101, 948–956. doi: 10.1161/circresaha.107.160630

Hu, K., Xie, L., Zhang, Y., Hanyu, M., Yang, Z., Nagatsu, K., et al. (2020). Marriage of black phosphorus and Cu(2+) as effective photothermal agents for PET-guided combination cancer therapy. *Nat. Commun.* 11:2778.

Hu, Y. B., Zhang, Y. F., Wang, H., Ren, R. J., Cui, H. L., Huang, W. Y., et al. (2019). miR-425 deficiency promotes necroptosis and dopaminergic neurodegeneration in Parkinson's disease. *Cell Death Dis.* 10:589.

Huang, C. R., Chang, T. W., Lee, C. T., Shen, C. J., Chang, W. C., Chen, B. K., et al. (2021). represses pyruvate dehydrogenase kinase 1 to trigger ROS production and melanoma metastasis. *Oncogenesis* 10:11.

Ichikawa, Y., Ghanefar, M., Bayeva, M., Wu, R., Khechaduri, A., Naga Prasad, S. V., et al. (2014). Cardiotoxicity of doxorubicin is mediated through mitochondrial iron accumulation. *J. Clin. Invest.* 124, 617–630. doi: 10.1172/jci72931

Ji, S., Xin, H., and Su, E. J. (2019). Overexpression of the aryl hydrocarbon receptor nuclear translocator partially rescues fetoplacental angiogenesis in severe fetal growth restriction. *Clin. Sci. (Lond)* 133, 1353–1365. doi: 10.1042/cs20190381

Kim, J. W., Tchernyshyov, I., Semenza, G. L., and Dang, C. V. (2006). HIF-1-mediated expression of pyruvate dehydrogenase kinase: a metabolic switch required for cellular adaptation to hypoxia. *Cell Metab.* 3, 177–185. doi: 10.1016/j.cmet.2006.02.002

Knapp, M., Tu, X., and Wu, R. (2019). Vascular endothelial dysfunction, a major mediator in diabetic cardiomyopathy. *Acta Pharmacol. Sin.* 40, 1–8. doi: 10.1038/s41401-018-0042-6

Lan, C. C., Wu, C. S., Kuo, H. Y., Huang, S. M., and Chen, G. S. (2009). Hyperglycaemic conditions hamper keratinocyte locomotion via sequential inhibition of distinct pathways: new insights on poor wound closure in patients

with diabetes. *Br. J. Dermatol.* 160, 1206–1214. doi: 10.1111/j.1365-2133.2009.09089.x

Lexow, J., Poggioli, T., Sarathchandra, P., Santini, M. P., and Rosenthal, N. (2013). Cardiac fibrosis in mice expressing an inducible myocardial-specific Cre driver. *Dis. Model Mech.* 6, 1470–1476.

Li, X., Fang, P., Mai, J., Choi, E. T., Wang, H., and Yang, X. F. (2013). Targeting mitochondrial reactive oxygen species as novel therapy for inflammatory diseases and cancers. *J. Hematol. Oncol.* 6:19. doi: 10.1186/1756-8722-6-19

Li, Y., Hazarika, S., Xie, D., Pippen, A. M., Kontos, C. D., and Annex, B. H. (2007). In mice with type 2 diabetes, a vascular endothelial growth factor (VEGF)-activating transcription factor modulates VEGF signaling and induces therapeutic angiogenesis after hindlimb ischemia. *Diabetes* 56, 656–665. doi: 10.2337/db06-0999

Madan, A., Varma, S., and Cohen, H. J. (2002). Developmental stage-specific expression of the α and β subunits of the HIF-1 protein in the mouse and human fetus. *Mol. Genet. Metab.* 75, 244–249. doi: 10.1006/mgme.2001.3293

Maltepe, E., Keith, B., Arsham, A. M., Brorson, J. R., and Simon, M. C. (2000). The role of ARNT2 in tumor angiogenesis and the neural response to hypoxia. *Biochem. Biophys. Res. Commun.* 273, 231–238. doi: 10.1006/bbrc.2000.2928

Maltepe, E., Schmidt, J. V., Baunoch, D., Bradfield, C. A., and Simon, M. C. (1997). Abnormal angiogenesis and responses to glucose and oxygen deprivation in mice lacking the protein ARNT. *Nature* 386, 403–407. doi: 10.1038/386403a0

Nakano, H., Nakano, K., and Cook, D. N. (2018). Isolation and purification of epithelial and endothelial cells from mouse lung. *Methods Mol. Biol.* 1799, 59–69. doi: 10.1007/978-1-4939-7896-0_6

Niiyama, H., Huang, N. F., Rollins, M. D., and Cooke, J. P. (2009). Murine model of hindlimb ischemia. *J. Vis. Exp.* 1035.

Okabe, K., Kobayashi, S., Yamada, T., Kurihara, T., Tai-Nagara, I., Miyamoto, T., et al. (2014). Neurons limit angiogenesis by titrating VEGF in retina. *Cell* 159, 584–596. doi: 10.1016/j.cell.2014.09.025

Pillai, R., Huypens, P., Huang, M., Schaefer, S., Sheinin, T., Wettig, S. D., et al. (2011). Aryl hydrocarbon receptor nuclear translocator/hypoxia-inducible factor-1{β} plays a critical role in maintaining glucose-stimulated anaplerosis and insulin release from pancreatic {β}-cells. *J. Biol. Chem.* 286, 1014–1024. doi: 10.1074/jbc.m110.149062

Reichart, G., Mayer, J., Zehm, C., Kirschstein, T., Tokay, T., Lange, F., et al. (2019). Mitochondrial complex IV mutation increases reactive oxygen species production and reduces lifespan in aged mice. *Acta Physiol. (Oxf)* 225:e13214. doi: 10.1111/apha.13214

Ren, G., Zheng, X., Bommarito, M., Metzger, S., Walia, Y., Letson, J., et al. (2019). reduced basal nitric oxide production induces precancerous mammary lesions via ERBB2 and TGFβ. *Sci. Rep.* 9:6688.

Semenza, G. L., Jiang, B. H., Leung, S. W., Passantino, R., Concordet, J. P., Maire, P., et al. (1996). Hypoxia response elements in the aldolase A, enolase 1, and lactate dehydrogenase A gene promoters contain essential binding sites for hypoxia-inducible factor 1. *J. Biol. Chem.* 271, 32529–32537.

Semenza, G. L., Roth, P. H., Fang, H. M., and Wang, G. L. (1994). Transcriptional regulation of genes encoding glycolytic enzymes by hypoxia-inducible factor 1. *J. Biol. Chem.* 269, 23757–23763. doi: 10.1016/s0021-9258(17)31580-6

Severino, P., D'Amato, A., Netti, L., Pucci, M., De Marchis, M., Palmirotta, R., et al. (2018). Diabetes mellitus and ischemic heart disease: the role of Ion Channels. *Int. J. Mol. Sci.* 19:802. doi: 10.3390/ijms19030802

Su, E. J., Xin, H., Yin, P., Dyson, M., Coon, J., Farrow, K. N., et al. (2015). Impaired fetoplacental angiogenesis in growth-restricted fetuses with abnormal umbilical artery doppler velocimetry is mediated by aryl hydrocarbon receptor nuclear translocator (ARNT). *J. Clin. Endocrinol. Metab.* 100, E30–E40.

Sugden, M. C., and Holness, M. J. (2002). Therapeutic potential of the mammalian pyruvate dehydrogenase kinases in the prevention of hyperglycaemia. *Curr. Drug Targets Immune Endocr. Metabol. Disord.* 2, 151–165. doi: 10.2174/1568008023340785

Vaka, V. R., McMaster, K. M., Cunningham, M. W. Jr., Ibrahim, T., Hazlewood, R., Usry, N., et al. (2018). Role of mitochondrial mysfunction and reactive oxygen species in mediating hypertension in the reduced uterine perfusion pressure rat model of preeclampsia. *Hypertension* 72, 703–711. doi: 10.1161/hypertensionaha.118.11290

Volpe, C. M. O., Villar-Delfino, P. H., Dos Anjos, P. M. F., and Nogueira-Machado, J. A. (2018). Cellular death, reactive oxygen species (ROS) and diabetic complications. *Cell Death Dis.* 9:119.

Wang, C. Y., and Liao, J. K. (2012). A mouse model of diet-induced obesity and insulin resistance. *Methods Mol. Biol.* 821, 421–433. doi: 10.1007/978-1-61779-430-8_27

Wang, J., Niu, N., Xu, S., and Jin, Z. G. (2019). A simple protocol for isolating mouse lung endothelial cells. *Sci. Rep.* 9:1458.

Winzell, M. S., and Ahren, B. (2004). The high-fat diet-fed mouse: a model for studying mechanisms and treatment of impaired glucose tolerance and type 2 diabetes. *Diabetes* 53(Suppl. 3), S215–S219.

Wu, P., Blair, P. V., Sato, J., Jaskiewicz, J., Popov, K. M., and Harris, R. A. (2000). Starvation increases the amount of pyruvate dehydrogenase kinase in several mammalian tissues. *Arch. Biochem. Biophys.* 381, 1–7. doi: 10.1006/abbi.2000.1946

Wu, P., Sato, J., Zhao, Y., Jaskiewicz, J., Popov, K. M., and Harris, R. A. (1998). Starvation and diabetes increase the amount of pyruvate dehydrogenase kinase isoenzyme 4 in rat heart. *Biochem. J.* 329(Pt 1), 197–201. doi: 10.1042/bj3290197

Wu, R., Chang, H. C., Khechaduri, A., Chawla, K., Tran, M., Chai, X., et al. (2014). Cardiac-specific ablation of ARNT leads to lipotoxicity and cardiomyopathy. *J. Clin. Invest.* 124, 4795–4806. doi: 10.1172/jci76737

You, L., Chen, J., Liu, W., Xiang, Q., Luo, Z., Wang, W., et al. (2020). Enterovirus 71 induces neural cell apoptosis and autophagy through promoting ACOX1 downregulation and ROS generation. *Virulence* 11, 537–553. doi: 10.1080/21505594.2020.1766790

Conflict of Interest: The authors declare that the research was conducted in the absence of any commercial or financial relationships that could be construed as a potential conflict of interest.

Copyright © 2021 Nguyen, Zheng, Knapp, Sladojevic, Zhang, Ai, Harrison, Chen, Sitikov, Shen, Gonzalez, Zhao, Fang, Liao and Wu. This is an open-access article distributed under the terms of the Creative Commons Attribution License (CC BY). The use, distribution or reproduction in other forums is permitted, provided the original author(s) and the copyright owner(s) are credited and that the original publication in this journal is cited, in accordance with accepted academic practice. No use, distribution or reproduction is permitted which does not comply with these terms.

frontiers in Cell and Developmental Biology

BRIEF RESEARCH REPORT
published: 17 June 2021
doi: 10.3389/fcell.2021.687598

Distinct Signaling Functions of Rap1 Isoforms in NO Release From Endothelium

*Ramoji Kosuru[1], Bandana Singh[1], Sribalaji Lakshmikanthan[1], Yoshinori Nishijima[2], Jeannette Vasquez-Vivar[3], David X. Zhang[2] and Magdalena Chrzanowska[1,4,5]**

[1] Blood Research Institute, Versiti, Milwaukee, WI, United States, [2] Department of Medicine, Medical College of Wisconsin, Milwaukee, WI, United States, [3] Department of Biophysics and Redox Biology Program, Medical College of Wisconsin, Milwaukee, WI, United States, [4] Cardiovascular Center, Medical College of Wisconsin, Milwaukee, WI, United States, [5] Department of Pharmacology and Toxicology, Medical College of Wisconsin, Milwaukee, WI, United States

Small GTPase Rap1 plays a prominent role in endothelial cell (EC) homeostasis by promoting NO release. Endothelial deletion of the two highly homologous Rap1 isoforms, Rap1A and Rap1B, leads to endothelial dysfunction *ex vivo* and hypertension *in vivo*. Mechanistically, we showed that Rap1B promotes NO release in response to shear flow by promoting mechanosensing complex formation involving VEGFR2 and Akt activation. However, the specific contribution of the Rap1A isoform to NO release and the underlying molecular mechanisms through which the two Rap1 isoforms control endothelial function are unknown. Here, we demonstrate that endothelial dysfunction resulting from knockout of both Rap1A and Rap1B isoforms is ameliorated by exogenous L-Arg administration to rescue NO-dependent vasorelaxation and blood pressure. We confirmed that Rap1B is rapidly activated in response to agonists that trigger eNOS activation, and its deletion in ECs attenuates eNOS activation, as detected by decreased Ser1177 phosphorylation. Somewhat surprising was the finding that EC deletion of Rap1A does not lead to impaired agonist-induced vasorelaxation *ex vivo*. Mechanistically, the deletion of Rap1A led to elevated eNOS phosphorylation both at the inhibitory, T495, and the activating Ser1177 residues. These findings indicate that the two Rap1 isoforms act *via* distinct signaling pathways: while Rap1B directly positively regulates eNOS activation, Rap1A prevents negative regulation of eNOS. Notably, the combined deficiency of Rap1A and Rap1B has a severe effect on eNOS activity and NO release with an *in vivo* impact on endothelial function and vascular homeostasis.

Keywords: endothelial (dys)function, vasodilation, nitric oxide signaling, small GTP protein, Rap1A, Rap1B

OPEN ACCESS

Edited by:
Bin Ren,
University of Alabama at Birmingham,
United States

Reviewed by:
Takayuki Matsumoto,
Hoshi University, Japan
Rodrigo Franco,
University of Nebraska-Lincoln,
United States

****Correspondence:***
Magdalena Chrzanowska
mchrzanowska@versiti.org
orcid.org/0000-0003-4182-2126

Specialty section:
This article was submitted to Signaling, a section of the journal Frontiers in Cell and Developmental Biology

Received: *29 March 2021*
Accepted: *21 May 2021*
Published: *17 June 2021*

Citation:
Kosuru R, Singh B, Lakshmikanthan S, Nishijima Y, Vasquez-Vivar J, Zhang DX and Chrzanowska M (2021) Distinct Signaling Functions of Rap1 Isoforms in NO Release From Endothelium. Front. Cell Dev. Biol. 9:687598. doi: 10.3389/fcell.2021.687598

INTRODUCTION

Located at the blood interface, the endothelium controls vessel and organ function by releasing bioactive substances. In response to physical and chemical cues from the environment: laminar shear stress of flowing blood and agonists: bradykinin, acetylcholine, and ATP, endothelial-derived factors modulate vascular smooth muscle tone, maintain non-adhesive lumen surface, and control inflammatory responses in the vascular wall, thereby controlling blood flow. Among EC-derived factors, endothelial nitric oxide synthase NOS (eNOS, NOS3)-produced NO release is fundamental

to vascular homeostasis as disruption of NO production leads to endothelial dysfunction and underlies cardiovascular disease (Widlansky et al., 2003; Vanhoutte et al., 2009). eNOS activity is regulated by Ca^{2+} and Ca^{2+}-regulatory protein, calmodulin, binding of regulatory cofactors, and post-translational modifications, including palmitoylation and phosphorylation (Michel and Feron, 1997). Phosphorylation of Ser1177 and Ser633 sensitizes eNOS to Ca^{2+} and stimulates NO production, whereas Thr495 phosphorylation is inhibitory (Förstermann and Sessa, 2012). We have recently identified small GTPase Rap1 (Ras Association Proximate) (Lakshmikanthan et al., 2015) as a novel factor controlling eNOS-dependent NO release.

Two closely related Rap1 isoforms, Rap1A and Rap1B, are key regulators of vascular homeostasis (Chrzanowska-Wodnicka, 2017). Many studies, in particular in isolated ECs, point to the role of Rap1 in the modulation of cell–matrix and cell–cell adhesion (Boettner and Van Aelst, 2009). The presence of either isoform is required for *de novo* cell–cell junction formation *in vitro* (Lakshmikanthan et al., 2018) and normal vasculogenesis *in vivo* (Chrzanowska-Wodnicka et al., 2015). Interestingly, EC deletion of both Rap1 isoforms after birth and establishment of vascular barriers does not increase vascular permeability in most vascular beds (Lakshmikanthan et al., 2018). Instead, the most profound defect in total Rap1 (Rap1A + Rap1B), EC-specific KO ($Rap1^{i\Delta EC}$) mice is endothelial dysfunction due to a decreased NO bioavailability defect, evidenced by impaired vasorelaxation defect *ex vivo* and hypertension *in vivo* (Lakshmikanthan et al., 2015). Endothelial deletion of Rap1B, the predominant EC Rap1 isoform, leads to a partial vasorelaxation defect (Lakshmikanthan et al., 2014) and impaired NO release in response to shear stress (Lakshmikanthan et al., 2015). Mechanistically, in response to shear flow, Rap1B acts as a mechanosensor promoting the formation of the endothelial junctional mechanosensing complex, VEGFR2 transactivation, and signaling to NO release involving Akt recruitment and Ser1177 phosphorylation of eNOS (Lakshmikanthan et al., 2015). However, the mechanism through which Rap1 controls agonist-induced NO release or the individual contribution of each of the Rap1 isoforms to the control of NO release is unknown.

Herein, taking advantage of novel EC-specific Rap1A ($Rap1A^{i\Delta EC}$) and Rap1 (1A + 1B, $Rap1^{i\Delta EC}$) knockout mice, we investigated the isoforms' contribution to NO release *ex vivo*. Specifically, we examined the involvement of each Rap1 isoform on eNOS phosphorylation at key regulatory sites. Our results confirm the cooperation between the two isoforms in promoting NO release, while they also reveal dramatically distinct functions of the two isoforms in signaling to eNOS and NO release. Physiologically significant, our results bring new information on Rap1 endothelial biology.

MATERIALS AND METHODS

Animals, L-Arginine Treatment, and Blood Pressure Measurement

All mouse procedures were performed according to the Medical College of Wisconsin Institutional Animal Use and Care Committee. Generation of endothelial cell (EC)-specific total Rap1 KO mice [Rap1A + Rap1B knockout, Cadh5(PAC)-$CreERT2^{+/0}$; $Rap1A^{f/f}$ $Rap1B^{f/f}$; $Rap1^{i\Delta EC}$] and EC-specific Rap1A-knockout mice [Cadh5(PAC)-$CreERT2^{+/0}$; $Rap1A^{f/f}$ $Rap1B^{+/+}$; $Rap1A^{i\Delta EC}$] on C57Bl/6J background was previously described (Lakshmikanthan et al., 2015, 2018). Cadh5-Cre-negative mice, or mice injected with carrier oil only, were used as controls. For L-arginine treatment, drinking water was supplemented with L-arginine (6 g/kg/day) (Chen et al., 2003) at weaning until the analyses were completed; control mice received plain water. Systolic blood pressure measurements were performed thrice-weekly in conscious 8- to 12-week-old male and female animals using IITC Life Science Blood Pressure System, as described previously (Kriska et al., 2012; Lakshmikanthan et al., 2015).

Aortic Ring Wire Myography

Endothelium-dependent relaxation of aortic rings in response to acetylcholine was measured as previously described (Mendoza et al., 2010; Lakshmikanthan et al., 2015). Briefly, the thoracic aortae from control and $Rap1^{i\Delta EC}$ mice were dissected and placed in Krebs physiological saline aerated with 21% O_2/5% CO_2. Artery segments were mounted on parallel pins in conventional myographs and maintained at 37°C in Krebs buffer for 60 min. The vessels were then preconstricted with 10 nM phenylephrine or 10 nM thromboxane mimetic U-46619. After constriction, relaxation responses to the increasing concentration of acetylcholine were recorded.

Cell Culture, Transfection, and Treatments

Primary human coronary arteriole endothelial cells (hCAECs) (Lonza #CC-2585) and human pulmonary aorta ECs were cultured with standard methods for no longer than six passages and were used for all *in vitro* experiments. For 30–40% confluent EC, monolayers were transfected with 50 nM Rap1A or Rap1B siGENOME siRNA pool, or with non-targeting siRNA pool (Dharmacon) for 6 h and cultured for an additional 30 h in complete EBM culture medium (Lonza#CC-3156). Prior to biochemical analysis, cells were serum-starved for 4–6 h. To induce eNOS phosphorylation, cells were treated with 500 μM ATP. Ach (10 μM, 60 min)- or bradykinin (1 μM, 60 min)-induced NO release in hPAECs was estimated from the reduction of nitrite to NO and quantified by NO-Analyzer-chemiluminescence using authentic standards as previously described (Cornelius et al., 2009).

Rap1 Activity Assay and Western Blotting

Active, GTP-bound fraction of Rap1 in lysates of ECs subjected to 1 μM bradykinin was measured using RalGDS-GST pull-down method, as previously described (Franke et al., 2000; Lakshmikanthan et al., 2015). Agonist-induced eNOS phosphorylation in ECs was assessed by Western blotting of Tris-glycine 4–12% gradient gel-resolved cell lysates, blotted onto nitrocellulose membranes as previously described (Lakshmikanthan et al., 2015; Singh et al., 2021). The following

antibodies were used for Western Blot analysis: antibodies against phospho-eNOS (Ser-1177) (BD Biosciences #612392), phospho-eNOS (Thr495) (Cell Signaling Technologies #9574), total eNOS (Cell Signaling Technologies #32027), Rap1A/Rap1B (Cell Signaling Technologies #2399), and β-actin (Santa Cruz Biotechnology #sc-47778). Rap1 rabbit monoclonal antibody (clone 26B4, Cell Signaling Technologies #2399) was used for GTP-Rap1 pull-down assay. Horseradish peroxidase-conjugated secondary antibodies followed by chemiluminescence detection using Amersham Imager 600 and analysis software (GE Healthcare) were used for densitometry. Blanked values (following subtraction of the corresponding empty well lane value), normalized within each experiment, were used to calculate fold change in phosphorylation between Rap1-deficient and control conditions.

Statistical Analysis

GraphPad Prism version 5 (GraphPad Software) was used. Statistical significance of group differences was determined using two-tailed unpaired Student's *t*-test with Welch's correction; $^{*}p < 0.05$; $^{**}p < 0.01$; $^{***}p < 0.001$.

RESULTS

Endothelial Dysfunction Resulting From Rap1 Deficiency Is Ameliorated by Exogenous L-Arginine Supplementation

Endothelial Rap1 deficiency of both Rap1 isoforms, Rap1A and Rap1B, significantly impairs endothelial NO production *in vitro* and NO-dependent vasorelaxation, leading to endothelial dysfunction and hypertension *in vivo* (Lakshmikanthan et al., 2015). This effect is concentration-dependent, with partial decrease in single allele, Rap1B-KO mice (Lakshmikanthan et al., 2014). Exogenous administration of NO synthesis precursor, L-arginine as substrate to the ECs increases NO availability and leads to increased vascular relaxation *in vivo* (Palmer et al., 1988; Böger et al., 1998). To test if NO is the main effector of Rap1 in endothelium *in vivo* responsible for endothelial dysfunction in $Rap1^{i\Delta EC}$ mice, we exogenously administered L-arginine to EC-specific Rap1 knockout ($Rap1^{i\Delta EC}$) mice to compensate for decreased eNOS activity and measured endothelium-dependent responses. Depressed NO-dependent vasorelaxation of aortic segments from $Rap1^{i\Delta EC}$ mice (Lakshmikanthan et al., 2015) was restored upon L-arginine treatment to the level similar to control mice (**Figure 1A**). To determine vascular specificity of the L-arginine effect, we blocked NO release with L-nitro-arginine methyl ester (L-NAME) and measured vasorelaxation in the presence of sodium nitroprusside (SNP, EC-independent vasorelaxation). We found that the extent of SNP-induced vasorelaxation of aortic segments was unchanged in $Rap1^{i\Delta EC}$ aortae compared to controls (**Figure 1B**). Likewise, blood pressure, elevated in $Rap1^{i\Delta EC}$ mice (Lakshmikanthan et al., 2015), was lowered to normal levels with L-arginine treatment (**Figure 1C**). These findings demonstrate that compensation for depressed NO production is sufficient to overcome Rap1 deficiency-induced endothelial dysfunction *in vivo* and suggests that NO is the major Rap1 effector in maintaining vessel homeostasis.

Rap1B Acts in a GPCR-Induced Signaling Pathway to eNOS Activation

Decreased vasorelaxation response to ACh of aortic segments from $Rap1B^{i\Delta EC}$ mice suggested that Rap1B is required for agonist-induced NO release. To test this hypothesis directly, we examined the effect of Rap1B deletion on agonist-induced NO release from ECs. In the absence of stimulation, the release of NO was negligible in siControl ECs and not detected in siRap1B ECs (**Figure 2A**). Treatment of ECs with acetylcholine or bradykinin induced significant release of NO (**Figure 2A**). Interestingly, knockdown of Rap1B inhibited bradykinin-induced NO release from ECs (**Figure 2B**). As this finding supported the role of Rap1B in a signaling pathway from GPCR-linked agonist receptors to eNOS activation, we examined the ability of bradykinin to induce Rap1 activation in hCAECs (**Figure 2C**). Consistently with previous results (Lakshmikanthan et al., 2015), we found a considerable level of active Rap1 in quiescent ECs (**Figure 2D**). Nonetheless, bradykinin induced a rapid and significant increase in active Rap1 fraction (**Figure 2D**), consistent with Rap1 acting downstream from GPCR. Next, to determine the involvement of Rap1B in eNOS activation, we examined the effect of siRap1B knockdown on agonist (ATP)-induced eNOS/Ser1177 phosphorylation (**Figure 2E**). Agonist induced rapid and transient eNOS-Ser1177 phosphorylation in siControl ECs (**Figure 2F**). Levels of eNOS-Ser1177 were significantly decreased in siRap1B ECs (**Figure 2F**), consistent with the observed decreased NO release from siRap1B ECs (**Figures 2A,B**). Altogether, these data support a model in which GPCR-induced Rap1B activity promotes agonist-induced eNOS activation (**Figure 4**).

Rap1A Restricts eNOS Inhibition but Is Not Required for Normal Vasorelaxation

Our previous studies of Rap1 isoforms involvement in NO regulation have focused on Rap1B, the predominant Rap1 isoform in ECs (Lakshmikanthan et al., 2014, 2015). In our *ex vivo* studies, we demonstrated a partial vasorelaxation defect in EC-Rap1B KO (Lakshmikanthan et al., 2014) vs. almost complete inhibition of vasorelaxation upon deletion of both Rap1 isoforms (Lakshmikanthan et al., 2015). While this result implicated loss of Rap1A as a contributing factor to decreased NO release, the contribution of Rap1A isoform to NO release has not been directly addressed. To assess the role of Rap1A in NO release, we examined acetylcholine-induced vasorelaxation of aortic rings from $Rap1A^{i\Delta EC}$ mice. Surprisingly, we found that, unlike EC deletion of Rap1B, EC deletion of Rap1A did not lead to impaired vasorelaxation of aortic segments *ex vivo*, compared to controls (**Figure 3A**). EC-independent vasorelaxation to SNP was also unaffected by EC-Rap1A deficiency (**Figure 3B**). To further explore the relationship between Rap1A and NO release regulation, we examined the effect of Rap1A deletion on agonist-induced regulatory eNOS phosphorylation in hCAECs.

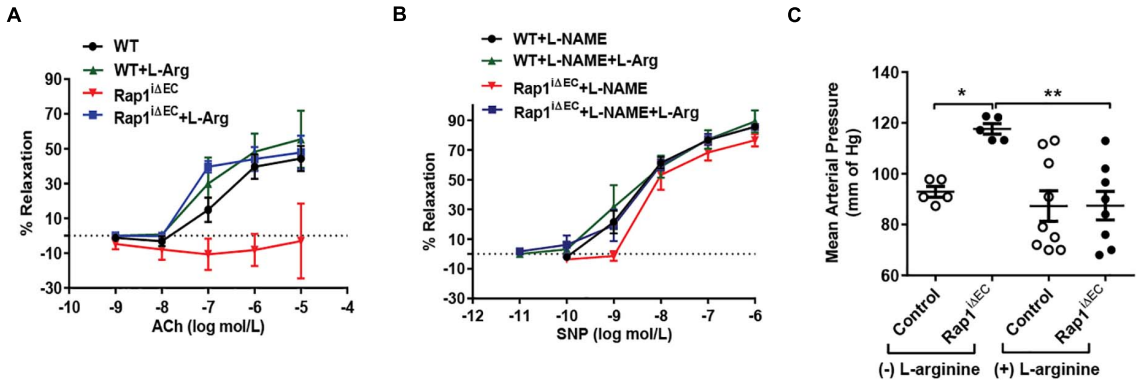

FIGURE 1 | Endothelial dysfunction in Rap1i$^{\Delta EC}$ mice is attenuated by L-arginine (L-Arg) supplementation. **(A,B)** Corrected vasorelaxation. Concentration dependent vasorelaxation of U466169-preconstricted aortae from control (WT) and Rap1$^{i\Delta EC}$ mice treated with or without L-arginine in response to ACh **(A)**, sodium nitroprusside (SNP) **(B)**. SNP response was measured in presence of L-NAME, an NO blocker. Values are means ± SEM (n = 6). **(C)** L-arginine treatment normalizes blood pressure in Rap1$^{i\Delta EC}$ mice. Systolic blood pressure was measured in control (WT) and Rap1$^{i\Delta EC}$ mice with or without L-arginine supplementation in drinking water. Values are means + SEM (n = 5–9).* indicates $p < 0.05$ vs. control without L-arginine; ** indicates $p < 0.01$ vs. Rap1$^{i\Delta EC}$ without L-arginine. One-way ANOVA Tukey's multiple comparison test was applied to compare statistical significance.

We found a significant increase in eNOS-Ser1177 activating phosphorylation in siRap1A hCAECs, compared to siControls (**Figures 3C,D**). Interestingly, Rap1A deletion also increased inhibitory phosphorylation of eNOS-pThr495 (**Figures 3E,F**). In contrast, deletion of Rap1B did not significantly alter eNOS-pThr495 (**Figures 3G,H**). These findings demonstrate that Rap1A and Rap1B direct distinct pathways converging at eNOS activation; while Rap1B promotes the stimulatory eNOS-Ser1177 phosphorylation, Rap1A restricts the inhibitory eNOS-Thr495 phosphorylation (**Figure 4**).

DISCUSSION

The seminal findings of the study are as follows: both Rap1 isoforms contribute to NO release and thus are significant regulators of endothelial homeostasis. Moreover, the two Rap1 isoforms act *via* distinct pathways. Rap1B directly contributes to eNOS activation and NO release, acting in a signaling pathway promoting eNOS activating phosphorylation. In contrast, Rap1A restricts regulatory eNOS phosphorylation events and, in particular, restricts negative eNOS regulation. Significantly, disrupted Rap1A signaling does not functionally affect endothelial function in the presence of Rap1B—NO-dependent vasorelaxation is normal in Rap1A$^{i\Delta EC}$ mice (**Figure 3A**). The importance of Rap1A's modulatory function only becomes evident in the absence of Rap1B (Rap1$^{i\Delta EC}$ mice), where it further impairs vasorelaxation (Lakshmikanthan et al., 2014, 2015) compared to EC-Rap1B-deficient mice (Lakshmikanthan et al., 2014). These findings suggest distinct signaling functions, converging on NO release, by the two—highly homologous—Rap1 proteins.

eNOS Is a Target of Both Rap1 Isoforms

The compound effect of endothelial loss of both Rap1A and Rap1B isoforms is severe endothelial dysfunction and hypertension (Lakshmikanthan et al., 2015). Here, we demonstrate that this phenotype is ameliorated by restoring NO bioavailability (**Figure 1**). Our study demonstrates that the synergistic function of Rap1A and Rap1B occurs *via* distinct signaling pathways, converging at eNOS phosphorylation, and suggests that the two isoforms have distinct effectors. In particular, signaling leading to eNOS phosphorylation is differentially regulated by the two Rap1 isoforms. In response to GPCR agonist stimulation, similarly to EC activation by shear stress (Lakshmikanthan et al., 2015), Rap1B is rapidly activated and promotes phosphorylation on Ser1177, and its deficiency leads to decreased eNOS phosphorylation at Ser1177 and blocks NO release from ECs. In contrast, deletion of Rap1A has a dissimilar effect on eNOS phosphorylation: it increases not only activating Ser1177 phosphorylation but also inhibitory Thr495 phosphorylation.

Dual phosphorylation of Ser1177 and Thr495 determines the activity of eNOS in agonist-stimulated ECs (Fleming et al., 2001; Förstermann and Sessa, 2012). Most GPCR agonists, such as histamine, ATP, thrombin, and bradykinin, regulate phosphorylation of eNOS at Ser1177 and Thr495 *via* different protein kinases; Ser1177 phosphorylation is mediated by protein kinase C (PKC) (Gonçalves Da Silva et al., 2009) and AMP-activated protein kinase (AMPK) (Thors et al., 2004). Thr495 phosphorylation, in turn, is catalyzed by calmodulin-dependent kinase II (CaMKII) (Fleming et al., 2001; Murthy et al., 2017), and dephosphorylation is catalyzed by PP1 in a calcium-dependent manner (Fleming et al., 2001). In addition, dysregulation of the Thr495 phosphorylation site may contribute to increased superoxide, rather than NO, generation by activated eNOS (Lin et al., 2003). Increased phosphorylation of Thr495 in siRap1A ECs suggests that CaMKII activity increases in the absence of Rap1A and that Rap1A acts to suppress CaMKII. Conversely, decreased Ser1177 phosphorylation in response to agonist stimulation in siRap1B ECs implicates Rap1B in positive regulation of PKC or AMPK (**Figure 4**).

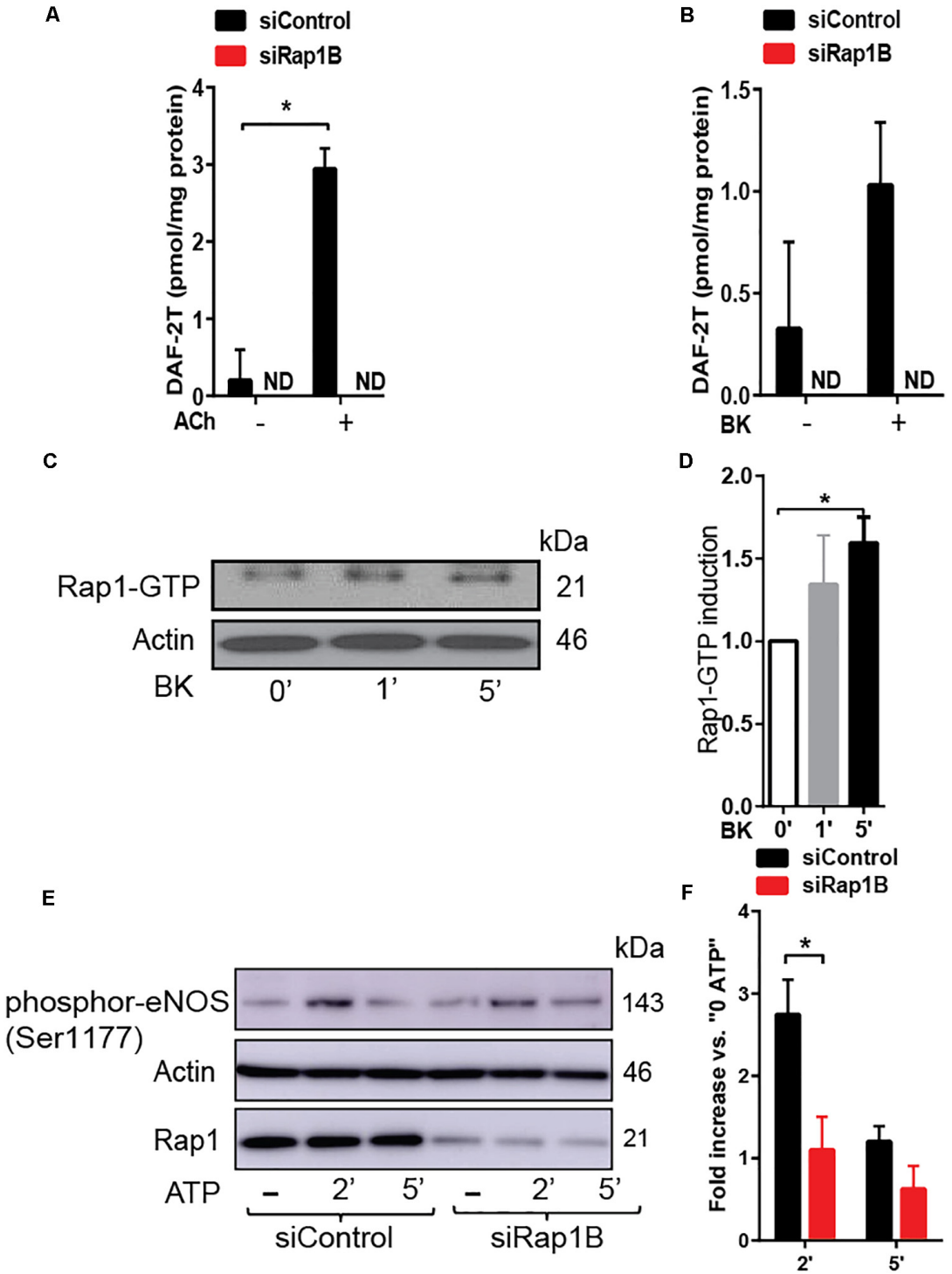

FIGURE 2 | (A,B) RaplB deletion inhibits agonist-induced NO release. NO release measured in HPAECs preincubated with 2 ml DAF-DA (5 μM) + L-arginine 10 μM with or without ACh **(A)** and bradykinin (BK) **(B)** for 30 min at 37°C. Mean values of concentrations calculated using authentic standards are shown (n = 3). ND: not dected. * indicates $p < 0.05$ vs. siControl unstimulated. One-way ANOVA Tukey's multiple comparison test was applied to compare statistical significance. **(C,D)** Rap1 is activated by GPCR agonist that induced nitric oxide (NO). Bradykinin (BK)-induced, GTP-bound Rap1 using Rap1-GTP pulldown assay. Representative immunoblot **(C)** and quantification **(D)** of Rap1 bound to GST-RalGDS beads following 1 and 5 min treatment with BK. Values are means ± SEM (n = 3). * indicates $p < 0.05$ vs. 0' BK. Unpaired t-test was applied to compare statistical significance. **(E,F)** Rap1B deletion attenuates agonist-induced Ser-1177 eNOS phosphorylation. Representative immunoblot **(E)** and quantification **(F)** of fold increase of phosphor-eNOS (Ser1177) vs.0 ATP in siControl and siRap1B HCAECs (n = 4). * indicates $p < 0.05$ vs. siControl 2' ATP. One-way ANOVA Tukey's multiple comparison test was applied to compare statistical significance.

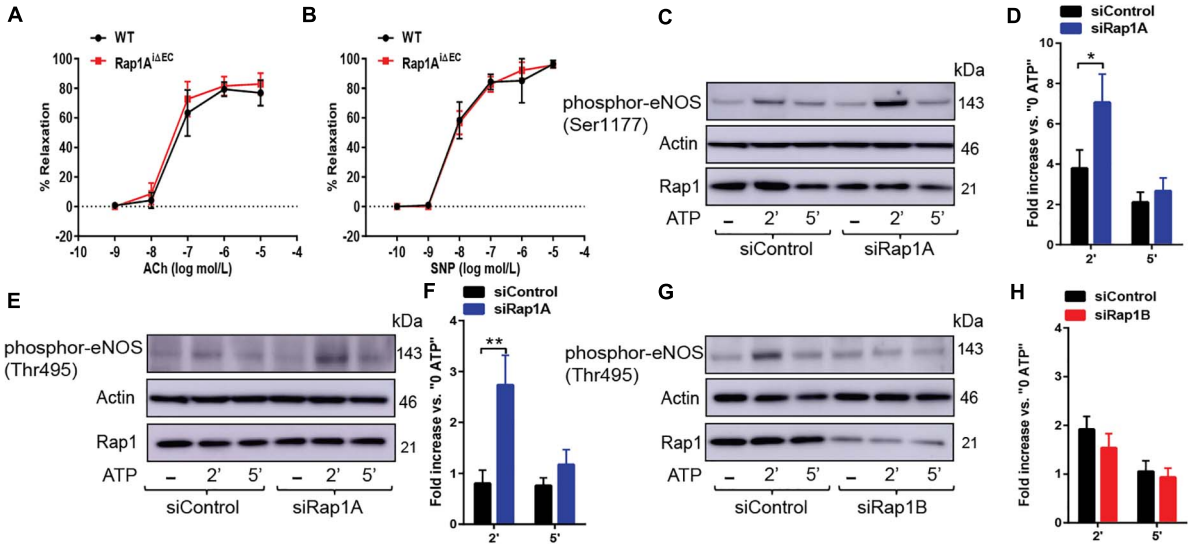

FIGURE 3 | (A,B) Vasorelaxation is not impaired upon EC-deletion of Rap1A isoform alone. Concentration dependent vasorelaxation of phenylephrine-preconstricted aortae from control (WT) and Rap1A$^{i\Delta EC}$ mice treated with ACh **(A)**, and SNP **(B)**. Values are means ± SEM (n = 6). **(C,D)** eNOS Ser1177 phosphorylation is increased in siRap1A ECs. Representative Immunoblot **(C)** and quantification **(D)** of fold increase of Ser1177 vs.0 ATP in siControl and siRap1A HCAECs (n = 6). * indicates $p < 0.05$ vs. siControl 2' ATP. One-way ANOVA Tukey's multiple comparison test was applied to compare statistical significance. **(E,F)** siRap1A knockdown leads to elevated phosphor-eNOS (Thr-495). Representative Immunoblot **(E)** and quantification **(F)** of fold increase of phosphor-eNOS (Thr495) vs.0 ATP in siControl and siRap1A HCAECs (n = 5). **(G,H)** siRap1B leads to decreased eNOS Thr-495 phosphorylation. Representative Immunoblot **(G)** and quantification **(H)** of fold increase of phosphor-eNOS T(hr495) vs.0 ATP in siControl and siRap1B HCAECs (n = 5). ** indicates $p < 0.01$.vs. siControl 2' ATP. One-way ANOVA Tukey's multiple comparison test was applied to compare statistical significance.

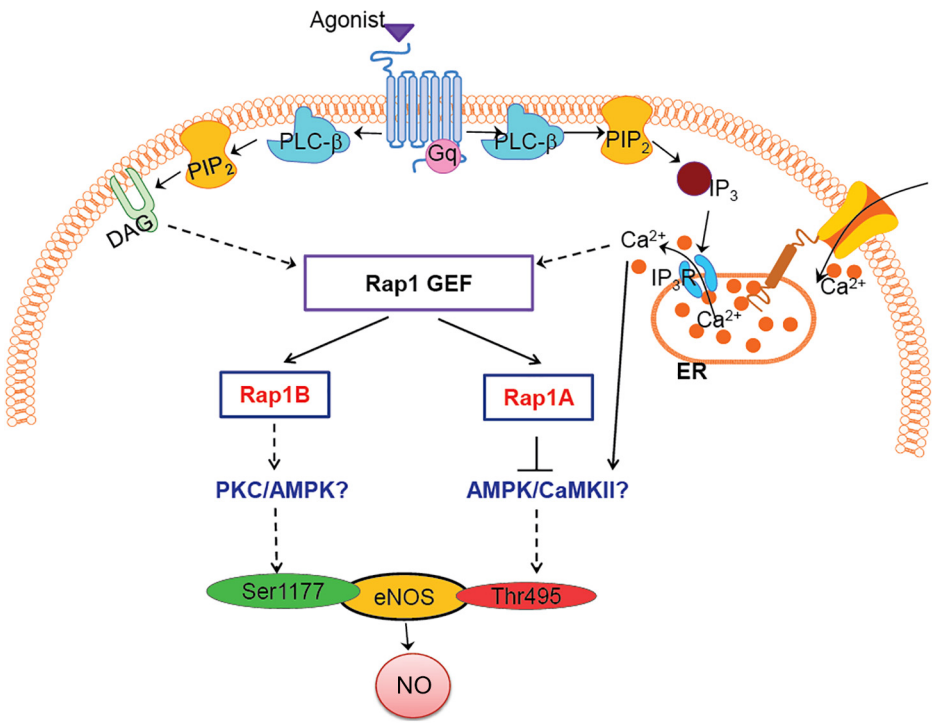

FIGURE 4 | Model: how Rap1A, Rap1B contribute to NO release, role in agonist-induced eNOS activation. Two Rap1 isoforms regulate eNOS activity via distinct signaling pathways; Rap1B promotes eNOS, activating Ser1177 phosphorylation, while Rap1A suppresses Thr495 eNOS phosphorylation, preventing eNOS inhibition. Candidate kinases regulated by Rap1 isoforms, PKC/AMPK/CaMKII, are indicated in blue font.

Physiological Functions of Rap1 Isoforms

Our study addressed, for the first time, the role of Rap1A, the less predominant Rap1 isoform, in contribution to NO release and endothelial function. Previous studies have implicated Rap1A in the regulation of endothelial barrier and vascular integrity (Birukova et al., 2015; Lakshmikanthan et al., 2018) and FGF-dependent angiogenesis (Yan et al., 2008). However, the involvement of Rap1A in regulation of endothelial function has not been addressed—until now. Mechanistically, our study implicates Rap1A in restraining EC response to agonists that stimulate eNOS. However, the impact of Rap1A deficiency on the endothelial phenotype is largely influenced by the presence of Rap1B, as combined deficiency of both isoforms has a more extreme deleterious effect on NO release (Lakshmikanthan et al., 2015) than Rap1B deficiency alone (Lakshmikanthan et al., 2014).

Hypertension in Rap1$^{i\Delta\ EC}$ mice (**Figure 1C**; Lakshmikanthan et al., 2015) is a strong indication of the physiological significance of endothelial Rap1 to the regulation of vascular reactivity. Although most of the mechanistic studies linking eNOS were performed in large vessels, it is likely that similar mechanisms operate in small resistance vessels. Vascular resistance within tissues and organs is largely controlled by small arterioles (40–150 μm) (Durand and Gutterman, 2013). In these vessels, ACh, BK, and shear stress are major regulators of vasodilation. Thus, it is possible that in addition to activated eNOS, prostaglandins and other vasoactive substances referred to as endothelial-derived hyperpolarizing factors (EDHFs), such as hydrogen peroxide (H_2O_2) and epoxyeicosatrienoic acids (EETs), play a role. Whether Rap1 controls the release of other vasoactive factors will be addressed in future studies. Nonetheless, decreased NO production, also resulting from genetic interference with eNOS, results in hypertension (Huang et al., 1995; Shesely et al., 1996) and our studies underscore the importance of both Rap1 isoforms in NO production.

Mechanisms Linking Rap1 Isoforms With NO Release

Our molecular studies point to altered kinase activities resulting in differential eNOS phosphorylation in the absence of Rap1 isoforms, but the exact mechanism remains to be elucidated. In particular, Rap1 proteins may have indirect effect on kinases modulating eNOS activity. Alternative and potentially complementary mechanisms can be envisioned. Rap1A may control NO bioavailability by inhibiting reactive oxygen species (ROS) generation. We have previously shown that in choroid epithelial cells, Rap1A can inhibit NOX-dependent activation (Wang et al., 2014), and a similar mechanism in ECs may exist. Additional studies are needed to fully explain the signaling pathways controlled by Rap1A and Rap1B and their interplay, which is necessary for normal endothelial function.

In sum, our study underscores the importance of both Rap1 isoforms in the production of NO by ECs. Rap1 isoform function is not redundant, and the two isoforms act *via* distinct pathways, converging on NO bioavailability.

DATA AVAILABILITY STATEMENT

The raw data supporting the conclusions of this article will be made available by the authors, without undue reservation.

ETHICS STATEMENT

The animal study was reviewed and approved by the Medical College of Wisconsin Institutional Animal Use and Care Committee.

AUTHOR CONTRIBUTIONS

RK designed and performed eNOS phosphorylation analysis, analyzed data, and edited the manuscript. BS designed and performed L-arginine supplementation experiments and blood pressure measurements, analyzed data, and reviewed the manuscript. SL designed and performed Rap1 activity assay and eNOS phosphorylation analysis and critically reviewed the manuscript. YN designed and performed vasodilation experiments and analyzed vasodilation data. JV-V designed and performed NO measurements, analyzed data, and critically revised the manuscript. DZ designed vasodilation experiments, analyzed data, and critically reviewed the manuscript. MC designed the study, analyzed data, and wrote the manuscript. All authors contributed to the article and approved the submitted version.

FUNDING

This work was funded by NIH Grant R01HL111582 (MC). JV-V was supported by NIH Grants NS081936 and NS114972. DZ was supported by NIH Grant R01HL096647. RK was supported by the Director's Fellowship Award at the Blood Research Institute of Versiti, Wisconsin.

ACKNOWLEDGMENTS

We thank Drs. W. Campbell and T. Kriska for assistance with blood pressure measurements.

REFERENCES

Birukova, A. A., Meng, F., Tian, Y., Meliton, A., Sarich, N., Quilliam, L. A., et al. (2015). Prostacyclin post-treatment improves LPS-induced acute lung injury and endothelial barrier recovery via Rap1. *Biochim. Biophys. Acta* 1852, 778–791. doi: 10.1016/j.bbadis.2014.12.016

Boettner, B., and Van Aelst, L. (2009). Control of cell adhesion dynamics by Rap1 signaling. *Curr. Opin. Cell Biol.* 21, 684–693. doi: 10.1016/j.ceb.2009.06.004

Böger, R. H., Bode-Böger, S. M., Phivthong-Ngam, L., Brandes, R. P., Schwedhelm, E., Mügge, A., et al. (1998). Dietary L-arginine and α-tocopherol reduce vascular oxidative stress and preserve endothelial function in hypercholesterolemic rabbits via different mechanisms. *Atherosclerosis* 141, 31–43. doi: 10.1016/s0021-9150(98)00145-2

Chen, J., Kuhlencordt, P., Urano, F., Ichinose, H., Astern, J., and Huang, P. L. (2003). Effects of chronic treatment with L-arginine on atherosclerosis in ApoE knockout and ApoE/inducible NO synthase double-knockout mice. *Arterioscler. Thromb. Vasc. Biol.* 23, 97–103. doi: 10.1161/01.atv.0000040223.74255.5a

Chrzanowska-Wodnicka, M. (2017). Rap1 in endothelial biology. *Curr. Opin. Hematol.* 24, 248–255. doi: 10.1097/moh.0000000000000332

Chrzanowska-Wodnicka, M., White, G. C., Quilliam, L. A., and Whitehead, K. J. (2015). Small GTPase Rap1 is essential for mouse development and formation of functional vasculature. *PLoS One* 10:e0145689. doi: 10.1371/journal.pone.0145689

Cornelius, J., Tran, T., Turner, N., Piazza, A., Mills, L., Slack, R., et al. (2009). Isotope tracing enhancement of chemiluminescence assays for nitric oxide research. *Biol. Chem.* 390, 181–189. doi: 10.1515/bc.2009.017

Durand, M. J., and Gutterman, D. D. (2013). Diversity in mechanisms of endothelium-dependent vasodilation in health and disease. *Microcirculation* 20, 239–247. doi: 10.1111/micc.12040

Fleming, I., Fisslthaler, B., Dimmeler, S., Kemp, B. E., and Busse, R. (2001). Phosphorylation of Thr(495) regulates Ca(2+)/calmodulin-dependent endothelial nitric oxide synthase activity. *Circ. Res.* 88, E68–E75.

Förstermann, U., and Sessa, W. C. (2012). Nitric oxide synthases: regulation and function. *Eur. Heart J.* 33, 829d–837d.

Franke, B., Van Triest, M., De Bruijn, K. M. T., Van Willigen, G., Nieuwenhuis, H. K., Negrier, C., et al. (2000). Sequential regulation of the small GTPase Rap1 in human platelets. *Mol. Cell. Biol.* 20, 779–785. doi: 10.1128/mcb.20.3.779-785.2000

Gonçalves Da Silva, C., Specht, A., Wegiel, B., Ferran, C., and Kaczmarek, E. (2009). Mechanism of purinergic activation of endothelial nitric oxide synthase in endothelial cells. *Circulation* 119, 871–879. doi: 10.1161/circulationaha.108.764571

Huang, P. L., Huang, Z., Mashimo, H., Bloch, K. D., Moskowitz, M. A., Bevan, J. A., et al. (1995). Hypertension in mice lacking the gene for endothelial nitric oxide synthase. *Nature* 377, 239–242.

Kriska, T., Cepura, C., Magier, D., Siangjong, L., Gauthier, K. M., and Campbell, W. B. (2012). Mice lacking macrophage 12/15-lipoxygenase are resistant to experimental hypertension. *Am. J. Physiol.* 302, H2428–H2438.

Lakshmikanthan, S., Sobczak, M., Li Calzi, S., Shaw, L., Grant, M. B., and Chrzanowska-Wodnicka, M. (2018). Rap1B promotes VEGF-induced endothelial permeability and is required for dynamic regulation of the endothelial barrier. *J. Cell Sci.* 131:jcs207605.

Lakshmikanthan, S., Zheng, X., Nishijima, Y., Sobczak, M., Szabo, A., Vasquez-Vivar, J., et al. (2015). Rap1 promotes endothelial mechanosensing complex formation. NO release and normal endothelial function. *EMBO Rep.* 16, 628–637. doi: 10.15252/embr.201439846

Lakshmikanthan, S., Zieba, B. J., Ge, Z. D., Momotani, K., Zheng, X., Lund, H., et al. (2014). Rap1b in smooth muscle and endothelium is required for maintenance of vascular tone and normal blood pressure. *Arterioscler. Thromb. Vasc. Biol.* 34, 1486–1494. doi: 10.1161/atvbaha.114.303678

Lin, M. I., Fulton, D., Babbitt, R., Fleming, I., Busse, R., Pritchard, K. A. Jr., et al. (2003). Phosphorylation of threonine 497 in endothelial nitric-oxide synthase coordinates the coupling of L-arginine metabolism to efficient nitric oxide production. *J. Biol. Chem.* 278, 44719–44726. doi: 10.1074/jbc.m302836200

Mendoza, S. A., Fang, J., Gutterman, D. D., Wilcox, D. A., Bubolz, A. H., Li, R., et al. (2010). TRPV4-mediated endothelial Ca2+ influx and vasodilation in response to shear stress. *Am. J. Physiol. Heart Circ. Physiol.* 298, H466–H476.

Michel, T., and Feron, O. (1997). Nitric oxide synthases: which, where, how, and why? *J. Clin. Invest.* 100, 2146–2152. doi: 10.1172/jci119750

Murthy, S., Koval, O. M., Ramiro Diaz, J. M., Kumar, S., Nuno, D., Scott, J. A., et al. (2017). Endothelial CaMKII as a regulator of eNOS activity and NO-mediated vasoreactivity. *PLoS One* 12:e0186311. doi: 10.1371/journal.pone.0186311

Palmer, R. M. J., Ashton, D. S., and Moncada, S. (1988). Vascular endothelial cells synthesize nitric oxide from L-arginine. *Nature* 333, 664–666. doi: 10.1038/333664a0

Shesely, E. G., Maeda, N., Kim, H. S., Desai, K. M., Krege, J. H., Laubach, V. E., et al. (1996). Elevated blood pressures in mice lacking endothelial nitric oxide synthase. *Proc. Natl. Acad. Sci. U. S. A.* 93, 13176–13181. doi: 10.1073/pnas.93.23.13176

Singh, B., Kosuru, R., Lakshmikanthan, S., Sorci-Thomas, M. G., Zhang, D. X., Sparapani, R., et al. (2021). Endothelial Rap1 (Ras-Association Proximate 1) restricts inflammatory signaling to protect from the progression of atherosclerosis. *Arterioscler. Thromb. Vasc. Biol.* 41, 638–650. doi: 10.1161/atvbaha.120.315401

Thors, B., Halldórsson, H., and Thorgeirsson, G. (2004). Thrombin and histamine stimulate endothelial nitric-oxide synthase phosphorylation at Ser1177 via an AMPK mediated pathway independent of PI3K-Akt. *FEBS Lett.* 573, 175–180. doi: 10.1016/j.febslet.2004.07.078

Vanhoutte, P. M., Shimokawa, H., Tang, E. H. C., and Feletou, M. (2009). Endothelial dysfunction and vascular disease. *Acta Physiol.* 196, 193–222.

Wang, H., Jiang, Y., Shi, D., Quilliam, L. A., Chrzanowska-Wodnicka, M., Wittchen, E. S., et al. (2014). Activation of Rap1 inhibits NADPH oxidase-dependent ROS generation in retinal pigment epithelium and reduces choroidal neovascularization. *FASEB J.* 28, 265–274. doi: 10.1096/fj.13-240028

Widlansky, M. E., Gokce, N., Keaney, J. F. Jr., and Vita, J. A. (2003). The clinical implications of endothelial dysfunction. *J. Am. Coll. Cardiol.* 42, 1149–1160.

Yan, J. L., Li, F., Ingram, D. A., and Quilliam, L. A. (2008). Rap1a is a key regulator of fibroblast growth factor 2-induced angiogenesis and together with Rap1b controls human endothelial cell functions. *Mol. Cell. Biol.* 28, 5803–5810. doi: 10.1128/mcb.00393-08

Conflict of Interest: The authors declare that the research was conducted in the absence of any commercial or financial relationships that could be construed as a potential conflict of interest.

Copyright © 2021 Kosuru, Singh, Lakshmikanthan, Nishijima, Vasquez-Vivar, Zhang and Chrzanowska. This is an open-access article distributed under the terms of the Creative Commons Attribution License (CC BY). The use, distribution or reproduction in other forums is permitted, provided the original author(s) and the copyright owner(s) are credited and that the original publication in this journal is cited, in accordance with accepted academic practice. No use, distribution or reproduction is permitted which does not comply with these terms.

frontiers in Cell and Developmental Biology

CORRECTION
published: 06 August 2021
doi: 10.3389/fcell.2021.741935

Corrigendum: Distinct Signaling Functions of Rap1 Isoforms in NO Release From Endothelium

*Ramoji Kosuru[1], Bandana Singh[1], Sribalaji Lakshmikanthan[1], Yoshinori Nishijima[2], Jeannette Vasquez-Vivar[3], David X. Zhang[2] and Magdalena Chrzanowska[1,4,5]**

[1] Blood Research Institute, Versiti, Milwaukee, WI, United States, [2] Department of Medicine, Medical College of Wisconsin, Milwaukee, WI, United States, [3] Department of Biophysics and Redox Biology Program, Medical College of Wisconsin, Milwaukee, WI, United States, [4] Cardiovascular Center, Medical College of Wisconsin, Milwaukee, WI, United States, [5] Department of Pharmacology and Toxicology, Medical College of Wisconsin, Milwaukee, WI, United States

Keywords: endothelial (dys)function, vasodilation, nitric oxide signaling, small GTP protein, Rap1A, Rap1B

OPEN ACCESS

Approved by:
Frontiers Editorial Office, Frontiers Media SA, Switzerland

***Correspondence:**
Magdalena Chrzanowska
mchrzanowska@versiti.org
orcid.org/0000-0003-4182-2126

Specialty section:
This article was submitted to Signaling, a section of the journal Frontiers in Cell and Developmental Biology

Received: *15 July 2021*
Accepted: *22 July 2021*
Published: *06 August 2021*

Citation:
Kosuru R, Singh B, Lakshmikanthan S, Nishijima Y, Vasquez-Vivar J, Zhang DX and Chrzanowska M (2021) Corrigendum: Distinct Signaling Functions of Rap1 Isoforms in NO Release From Endothelium. Front. Cell Dev. Biol. 9:741935. doi: 10.3389/fcell.2021.741935

A Corrigendum on

Distinct Signaling Functions of Rap1 Isoforms in NO Release From Endothelium
by Kosuru, R., Singh, B., Lakshmikanthan, S., Nishijima, Y., Vasquez-Vivar, J., Zhang, D. X., et al. (2021). Front. Cell Dev. Biol. 9:687598. doi: 10.3389/fcell.2021.687598

In the original article, we neglected to include the funder Director's Fellowship Award at the Blood Research Institute of Versiti, Wisconsin to Ramoji Kosuru.

The authors apologize for this error and state that this does not change the scientific conclusions of the article in any way. The original article has been updated.

Publisher's Note: All claims expressed in this article are solely those of the authors and do not necessarily represent those of their affiliated organizations, or those of the publisher, the editors and the reviewers. Any product that may be evaluated in this article, or claim that may be made by its manufacturer, is not guaranteed or endorsed by the publisher.

Copyright © 2021 Kosuru, Singh, Lakshmikanthan, Nishijima, Vasquez-Vivar, Zhang and Chrzanowska. This is an open-access article distributed under the terms of the Creative Commons Attribution License (CC BY). The use, distribution or reproduction in other forums is permitted, provided the original author(s) and the copyright owner(s) are credited and that the original publication in this journal is cited, in accordance with accepted academic practice. No use, distribution or reproduction is permitted which does not comply with these terms.

frontiers in Cell and Developmental Biology

MINI REVIEW
published: 21 June 2021
doi: 10.3389/fcell.2021.673396

The Role of BMP Signaling in Endothelial Heterogeneity

*Orjin Han, Boryeong Pak and Suk-Won Jin**

Cell Logistics Research Center, School of Life Sciences, Gwangju Institute of Science and Technology (GIST), Gwangju, South Korea

Bone morphogenetic proteins (BMPs), which compose the largest group of the transforming growth factor-β (TGF-ß) superfamily, have been implied to play a crucial role in diverse physiological processes. The most intriguing feature of BMP signaling is that it elicits heterogeneous responses from cells with equivalent identity, thus permitting highly context-dependent signaling outcomes. In endothelial cells (ECs), which are increasingly perceived as a highly heterogeneous population of cells with respect to their morphology, function, as well as molecular characteristics, BMP signaling has shown to elicit diverse and often opposite effects, illustrating the innate complexity of signaling responses. In this review, we provide a concise yet comprehensive overview of how outcomes of BMP signaling are modulated in a context-dependent manner with an emphasis on the underlying molecular mechanisms and summarize how these regulations of the BMP signaling promote endothelial heterogeneity.

Keywords: heterogeneity, endothelium, BMP signaling, post-translational modification, computational modeling

OPEN ACCESS

Edited by:
Bin Ren,
University of Alabama at Birmingham,
United States

Reviewed by:
Marie-José Goumans,
Leiden University Medical Center,
Netherlands
Chunsik Lee,
Sun Yat-sen University, China

***Correspondence:**
Suk-Won Jin
sukwonjin@gist.ac.kr

Specialty section:
This article was submitted to Signaling, a section of the journal Frontiers in Cell and Developmental Biology

Received: *27 February 2021*
Accepted: *21 May 2021*
Published: *21 June 2021*

Citation:
Han O, Pak B and Jin S-W (2021) The Role of BMP Signaling in Endothelial Heterogeneity. Front. Cell Dev. Biol. 9:673396. doi: 10.3389/fcell.2021.673396

INTRODUCTION

Endothelial cells (ECs) exhibit great heterogeneity (Aird, 2003), in their developmental origin (Bautch and Caron, 2015; Pak et al., 2020), morphology (Sailem and Al Haj Zen, 2020), as well as gene expression (Chi et al., 2003). With technical advances, the concept of endothelial heterogeneity has been re-evaluated and extended at the single-cell level (Nolan et al., 2013; Kalucka et al., 2020), which re-ignited the interest in signaling pathways essential for modulating endothelial heterogeneity in living organisms. In order to contribute to endothelial heterogeneity, signaling pathways should satisfy certain criteria. For instance, signaling pathways that enrich endothelial heterogeneity should not provide essential functions for endothelial survival but rather function as "auxiliary" cues. In addition, such signaling should elicit its effects in a context-dependent manner. Therefore, signaling pathways, which provide non-essential roles and have been shown to elicit angiogenic responses from a selected subtype of ECs without affecting the viability of ECs, are likely to be instrumental in creating endothelial heterogeneity. Conversely, signaling pathways such as vascular endothelial growth factor-A (VEGF-A) signaling, which are indispensable for the survival of ECs and elicit robust responses from all subtypes of ECs (Byrne et al., 2005), are less likely to contribute to endothelial heterogeneity.

As one of the archetypal receptor-ligand-mediated signaling pathways, bone morphogenetic protein (BMP) signaling has gained increasing importance in the development and homeostasis of the vascular system. Its ability to selectively activate ECs in a context-dependent manner without influencing the survival of ECs (Cunha et al., 2017; Goumans et al., 2018) satisfies the aforementioned criteria of a signaling pathway of which function is important for establishing and promoting endothelial heterogeneity. Belonging to the transforming growth factor-β (TGF-β) family, BMP signaling forms the largest subgroup with more than a dozen ligands and four BMP-specific type I (Miyazono et al., 2010). The canonical signaling pathway is initiated by a dimeric ligand binding to its heterotetrameric receptor complex, consisting of two type I and two type II receptors, leading to the phosphorylation of the receptors (**Figure 1A**). The activated receptors, in turn, phosphorylate downstream target SMAD1/5/8, which translocates into the nucleus in association with SMAD4 to modify transcriptomic profiles. In addition, it has been shown that BMP signaling could activate mitogen-activated protein kinase (MAPK) pathway in a context-dependent manner (Massague, 2003).

To better understand how BMP signaling modulates endothelial heterogeneity, it is essential to understand how BMP signaling functions within ECs. However, a simplified schematic diagram fails to capture the complex molecular landscape of BMP signaling, since distinct expression patterns of individual BMP signaling components result in diverse context-dependent outcomes (Seeherman et al., 2019). In addition, certain combinations of ligands and receptors differently regulate signaling, generating diverse cellular responses (Antebi et al., 2017). Moreover, numerous factors modulate the amplitude and duration of BMP signaling to further increase the complexity of BMP signaling. In this review, we provide a general overview of how BMP signaling functions in ECs and contributes to endothelial heterogeneity. We summarize how distinct responses toward BMP stimulation within subtypes of ECs contribute to endothelial heterogeneity.

ENDOTHELIAL HETEROGENEITY AND BMP SIGNALING

Bone morphogenetic protein signaling appears to function as a critical factor that enhances endothelial heterogeneity. During embryogenesis, it has been shown that BMP signaling promotes the specification of venous ECs (Neal et al., 2019), therefore, sets apart arterial and venous fates, and modulates the initial setup of endothelial heterogeneity. Lack of *Alk3* within naïve ECs led to the failure of venous specific marker expression in presumptive venous ECs (Neal et al., 2019). In sprouting angiogenesis, BMP signaling has been shown to modulate dynamics between tip and stalk cell fates during sprouting angiogenesis (Moya et al., 2012), thereby enriching the endothelial heterogeneity.

Based on the subtypes, cellular responses toward BMP stimulation appear to be distinct among ECs which could further reinforce the endothelial heterogeneity. For instance, BMP signaling elicits distinct outcomes in blood ECs (BECs) and lymphatic ECs (LECs), the two major subtypes of ECs (Wiley and Jin, 2011; Coso et al., 2014). Therefore, it appears as if the responses toward BMP ligands in LECs are opposite to those in BECs. Given that the majority of LECs emerge via transdifferentiation of BECs, primarily venous in nature (Oliver and Srinivasan, 2010), it appears that the propensity to respond to a specific BMP ligand alters as a part of the transdifferentiation program. While it is apparent that BECs and LECs distinctively respond to BMP stimulation, it is largely unknown which factors are responsible for creating subtype-specific responses toward BMP stimulation. Considering this built-in redundancy of BMP signaling at the level of ligands, receptors, as well as effectors, it is tempting to speculate that these two subtypes of ECs may utilize pre-dominant receptors and effectors, which could facilitate subtype-specific responses. Recent analyses on the expression of BMP signaling components corroborate this idea (Yoshimatsu et al., 2013; Takeda et al., 2019).

Even within BECs, it has been shown that the responsiveness toward BMP signaling also varies between arterial and venous ECs. For instance, we and others have shown that pro-angiogenic BMP signaling could selectively induce angiogenic responses in venous ECs without affecting arterial ECs (Wiley et al., 2011; Kashiwada et al., 2015). Together, these studies highlight the innate differences of arterial and venous ECs in BMP responsiveness, which appears to modulate sprouting angiogenesis, potentially in conjunction with Notch and VEGF-A signaling. For instance, Notch signaling has been shown to interact with BMP signaling to orchestrate the intricate process of sprouting angiogenesis (Moya et al., 2012). Moreover, Notch renders the responsiveness of ECs toward pro-angiogenic BMP stimuli, BMP2 and BMP6, by regulating the expression of SMAD6, which ultimately contributes to the phosphorylation of SMAD1/5 and a tip cell phenotype (Mouillesseaux et al., 2016). Recent findings also implicated synergistic effects of BMP signaling and VEGF signaling on tip cell-associated markers VEGFR2 and DLL4 (Pulkkinen et al., 2020). Furthermore, Notch signaling also appears to influence BMP signaling at the effector level since the expression of Herp2 in ECs is co-modulated by Notch and BMP6 signaling (Itoh et al., 2004). Taken together, these studies reiterate the significance of BMP signaling and its mutual interaction with other signaling pathways in regulating endothelial behavior during angiogenesis.

FACTORS THAT MODIFY CELLULAR OUTCOMES OF BMP SIGNALING

Bone morphogenetic protein signaling seems to be highly context-dependent, eliciting opposite outcomes in similar cell types (Abe et al., 2000; Shu et al., 2011). It appears that multiple layers of modulation collectively shape the signaling landscape of BMP ligands: Ligand–receptor interaction in diverse combinations which can be further modulated by agonists and antagonists, mechanical forces which are sensed by the cell and transmitted into biochemical cues, and post-transcriptional and post-translational regulations which provide fine-tuning for the signaling pathway, collectively formulate outcomes of BMP

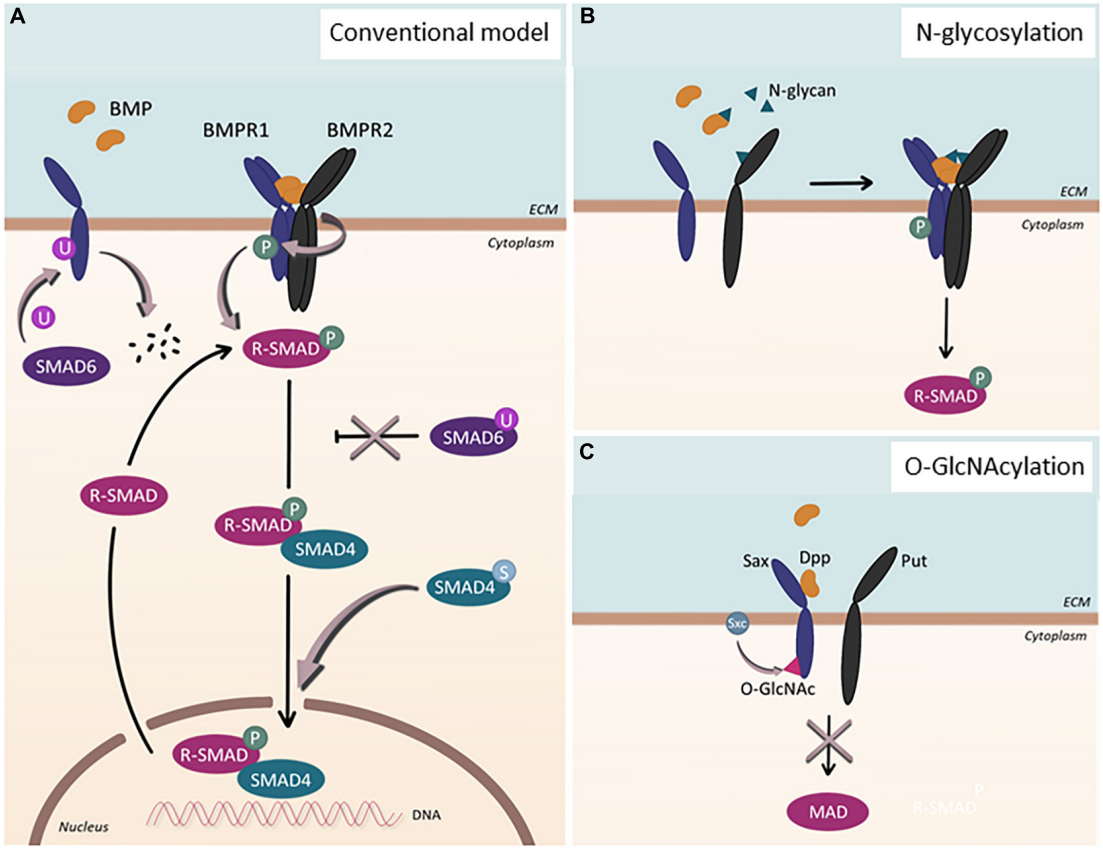

FIGURE 1 | Post-translational modification of BMP signaling components. **(A)** Conventional model of BMP signaling pathway. Upon BMP ligand binding, BMP type 1 receptor (BMPR1) is phosphorylated. Subsequently, R-SMADs, SMAD1/5/8, become phosphorylated and, together with SMAD4, localize into the nucleus to regulate gene transcription. This process can be inhibited by SMAD6. Additional post-translational modifications affect the signaling pathway in various ways: SMAD6 can regulate BMPR1 by facilitating its ubiquitination and subsequent degradation. Upon ubiquitination of SMAD6, SMAD6 loses its ability to inhibit the BMP signaling cascade, which ultimately leads to upregulation of the signaling pathway. When SMAD4 undergoes sumoylation, nuclear accumulation of the protein is enhanced. **(B)** N-glycosylation. N-glycans can bind to BMP ligands as well as to BMP type 2 receptors (BMPR2), enabling proper folding and binding of the proteins. **(C)** O-GlcNAcylation. In *Drosophila*, Sxc facilitates O-GlcNAcylation of Sax, the ortholog for human ALK2, resulting in the attenuation of the signaling pathway.

signaling with a remarkable degree of flexibility and versatility. Only now, we begin to understand the influence of these factors in BMP signaling.

Promiscuity of Ligand–Receptor Interaction

As in other signaling cascades, BMP signaling features a multitude of ligands and receptors, which associate and communicate with each other in diverse ways. However, the multiplicity of these components is not employed equally; most of them exhibit redundant functions. Previous works have shown that a multitude of BMP ligands binds to the same receptor (Mueller and Nickel, 2012) with different affinities (Seeherman et al., 2019). However, there are practical limitations in determining the ligand–receptor promiscuity in living organisms. To circumvent these hurdles, Antebi et al. (2017) resorted to mathematical modeling. By elegantly demonstrating the ligand–receptor promiscuity and the complex reciprocities between its signaling components, they suggested that the redundancy of BMP signaling components might manifest specific signaling-processing capabilities. While this needs to be validated *in vivo*, computational analyses revealed that cells distinguish distinct signaling environments, such as the concentration of ligands and differences in ligand–receptor complexes, to respond to BMP stimulation. Interestingly, inside the signaling-receiving cells, the canonical downstream target SMAD1/5/8 is activated regardless of the signaling-conferring ligand–receptor complex, suggesting the possibility that signaling-receiving cells are only capable of perceiving the sum of BMP ligand stimulation (David and Massague, 2018). This scenario, which is feasible in theory, certainly contradicts the prevailing idea that each BMP ligand retains its unique role *in vivo* (Wang et al., 2014). Therefore, further analyses are warranted to fully understand how the promiscuity of ligand–receptor interaction affects the context-dependent and heterogeneous signaling outcomes of BMP signaling.

Environmental Factors

It has been shown that mechanical forces affect the outcomes of BMP signaling in a number of cell types (Sedlmeier and Sleeman, 2017). For instance, abrogation of α5β1 integrin in vertebrate embryos substantially decreases the response of chondrocytes toward BMP stimulation (Garciadiego-Cazares et al., 2004, 2015). ECs provide another example of responsiveness toward BMP stimulation which is modulated by environmental factors. Previously, shear stress, the mechanical force created by laminar flow, has been implicated in regulating BMP signaling in ECs (Min and Schwartz, 2019; Hiepen et al., 2020). Upon exposure to shear stress, SMAD1/5/8 becomes phosphorylated in both BECs and LECs, dependent on the type and magnitude of shear stress. While turbulent shear stress induced by low oscillatory flow promotes EC proliferation and leads to SMAD1/5/8 phosphorylation (Zhou et al., 2012), laminar shear stress contributes to the quiescence of ECs through the BMP9-ALK1/ENG-SMAD1/5/8 axis (Baeyens et al., 2016), potentially going through the primary cilia (Vion et al., 2018). Interestingly, SMAD1 was most strongly affected by laminar shear stress, whereas SMAD5 and SMAD8 were less responsive (Baeyens et al., 2016). Moreover, the depletion of SMAD4 in human coronary artery ECs impaired the alignment of ECs to blood flow and led to an increased diameter of coronary arteries in developing mice (Poduri et al., 2017). Therefore, it appears that the types of flow, potentially modulating the activity of distinct SMADs, influence outcomes of BMP signaling in ECs. In addition to mechanical forces, recent studies reported hypoxia as one of the potential modulators for BMP signaling. Under hypoxic conditions, differential expression of BMP ligands could be observed in comparison to normoxic conditions (Pulkkinen et al., 2021). Moreover, BMP signaling could also attenuate hypoxic responses in ECs through the ALK1/SMAD/ATOH8 axis, ultimately impeding the development of pulmonary arterial hypertension (PAH) (Morikawa et al., 2019).

Transcriptional and Post-transcriptional Regulation

The responses toward BMP stimulation are further regulated by modifying BMP signaling components. For instance, the transcriptional efficacy of BMP signaling target genes can be modulated by epigenetic factors and other transcriptional co-factors. SMAD1 interacts with p300/CREB-binding protein (CBP) *in vitro* and *in vivo*, which enhances upon phosphorylation of SMAD1 (Nakashima et al., 1999; Pearson et al., 1999). In addition, SMAD1 can form a ternary complex with Notch intracellular domain in the presence of p300/CBP and P/CAF to augment transcriptional activation of Notch target genes (Takizawa et al., 2003). Moreover, chromatin immunoprecipitation analysis in ECs and pulmonary arterial smooth muscle cells revealed that SMAD1/5 preferentially binds to the GC-rich SMAD binding element outside the promoter of known genes, which appears to be mediated by epigenetic factors (Morikawa et al., 2011). Furthermore, responses toward BMP signaling are modulated by post-transcriptional regulation. For instance, numerous miRNAs are involved in BMP signaling-regulated processes (Hata and Kang, 2015). Recent studies provided persuasive evidence of the role of miRNAs in modulating BMP signaling (Dunworth et al., 2014). Therefore, it is apparent that transcriptional as well as post-transcriptional regulation of BMP signaling components could alter the landscape of BMP signaling.

Post-translational Regulation

Post-translational modifications (PTMs) have been shown to contribute to the extensive versatility and complexity of signaling pathways in eukaryotic cells. Perturbations of PTMs have been linked to various diseases, illustrating the significance of PTMs in maintaining cellular homeostasis (Li et al., 2010; Karve and Cheema, 2011). While PTMs in the TGF-β signaling pathway (Xu et al., 2012) have been studied intensively, far less is known about them in BMP signaling. The best-studied PTM in the BMP signaling is phosphorylation, the reversible attachment of a phosphoryl group to its receptors and downstream targets (**Figure 1A**). Upon ligand binding, successive phosphorylation ensues (Nickel and Mueller, 2019); the constitutively active BMPR2 phosphorylates the GS-domain of BMPR1s (Wrana et al., 1994), which, in turn, phosphorylate the SSXS motif of SMAD1/5/8 (Chen et al., 1997; Kretzschmar et al., 1997; Suzuki et al., 1997).

In addition to phosphorylation, ubiquitination and sumoylation, both of which are reversible PTM, have been shown to modulate the context of BMP signaling (Hershko and Ciechanover, 1998) (**Figure 1A**). The primary target of ubiquitination within BMP signaling appears to be SMAD1/5 (Zhu et al., 1999), though other components of BMP signaling, including SMAD6 and ACVR1/ALK2, could also undergo ubiquitination (Zhang et al., 2013; Herhaus et al., 2014; Seo et al., 2019). In addition, several studies have shown that SMAD4 could be sumoylated, which promotes SMAD4 accumulation into the nucleus and prolongs BMP signaling (Lin et al., 2003). Considering the complex interplay between ubiquitination and sumoylation (Liebelt and Vertegaal, 2016), balance between these PTMs may provide additional regulatory input for BMP signaling, which, however, requires further investigation.

Beyond these well-studied PTMs, other less established protein modifications have been acknowledged to be of great significance in modulating BMP signaling outcomes, including methylation, acetylation, O-GlcNAcylation, and acylation (**Figures 1B,C**). For instance, O-GlcNAcylation, which is the addition of a single *O*-linked *N*-acetyl-glucosamine (*O*-GlcNAc) moiety to target proteins, has been shown to fine-tune *Drosophila* BMP type I receptor Saxophone (Sax), an ortholog for human ALK2 (Moulton et al., 2020). In addition, it has been reported that a number of BMP ligands and BMPR2 undergo N-linked glycosylation, the addition of glycan to the target proteins (Garrigue-Antar et al., 2002; Hang et al., 2014; Negreiros et al., 2018). Interestingly, the N-glycosylation consensus of BMPR2 was positioned at a site that is mutated in heritable PAH patients (Pfarr et al., 2011; Lowery et al., 2014), alluding to the importance of this PTM for modulating the activity of BMP signaling. Increasing evidence also suggests

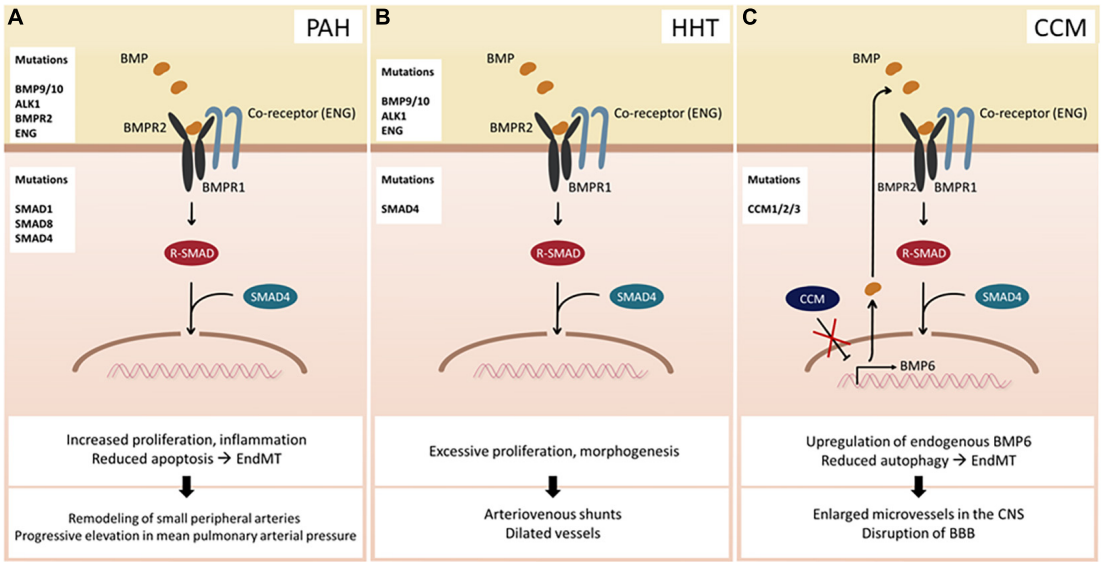

FIGURE 2 | Consequences of BMP signaling dysfunction. **(A)** Pulmonary arterial hypertension (PAH) can occur due to mutations in BMP ligands, receptors, co-receptors, and SMAD proteins. **(B)** Hereditary hemorrhagic telangiectasia (HHT) arises upon mutation of BMP9/10, ALK1, ENG, or SMAD4. **(C)** Cerebral cavernous malformation (CCM) develops when one of the CCM proteins is mutated. Hence, transcriptional activity of BMP6 increases leading to an enhanced BMP signaling. *Abbreviations*: CNS, central nervous system; BBB, blood–brain barrier.

the regulation of BMP signaling by methylation by which the inhibitory effect of Smad6 could be ensured (Xu et al., 2013; Wu et al., 2021).

THE ROLE OF BMP SIGNALING IN ENDOTHELIAL DYSFUNCTION

Numerous studies have suggested that dysregulation of BMP signaling in ECs could lead to various diseases. For instance, mutations in BMPR2 predispose to the onset of PAH (**Figure 2A**), a rare chronic disease characterized by an increase in mean pulmonary arterial pressure, which eventually leads to failure of the right ventricle (Dunmore et al., 2021). Recent studies using next-generation sequencing (NGS) technology have identified more than 800 mutations, including 486 distinct, non-recurrent variants, many of which affect BMP signaling in ECs (Southgate et al., 2020). Moreover, other BMP-related genes have also been implicated with PAH (Graf et al., 2018). Another well-established disease associated with dysfunctional BMP signaling in ECs is hereditary hemorrhagic telangiectasia (HHT) (**Figure 2B**) and cerebral cavernous malformation (CCM) (**Figure 2C**), both of which are autosomal dominant disorders. The clinical hallmarks of HHT are dilated vessels and arteriovenous shunts, which are prone to rupture. To date, mutations in a number of BMP signaling components, including Endoglin, ALK1, SMAD4, and more recently, BMP9 (McAllister et al., 1994; Johnson et al., 1996), have been identified in a smaller group of patients. However, the underlying molecular basis of HHT has not been fully elucidated. CCM is another hereditary condition that leads to enlarged microvessels in the central nervous system, which are susceptible to hemorrhage due to loss-of-function mutations in one of the three autosomal genes collectively known as the *CCM*s (Labauge et al., 2007). Deletion of any of the three genes results in increased synthesis of endogenous BMP6, which, in part, is promoted by KLF4 (Cuttano et al., 2016). Moreover, endothelial-specific deletion of *Ccm1* and *Ccm3* in mice induces endothelial to mesenchymal transition (EndMT), which contributes to the development of vascular lesions (Maddaluno et al., 2013; Malinverno et al., 2019), hinting that dysregulation of BMP signaling plays a key role in the progression of the CCMs. It is worth noting that only a subset of ECs appears to be affected by the pathological conditions caused by dysregulation of BMP signaling. For instance, arteriovenous shunts formed in HHT patients are initiated by a subset of venous ECs, which undergo excessive proliferation and morphogenesis (Brinjikji et al., 2015). In addition, while PAH promotes EndMT, only a subset of ECs in PAH patients transforms into vascular smooth muscle cells (Ranchoux et al., 2015). Therefore, it is fathomable that the effects of dysregulated BMP signaling on ECs are also highly heterogeneous, reminiscent of normal physiological responses toward BMP signaling.

PERSPECTIVES

As we obtain comprehensive knowledge on the role of BMP signaling in endothelial heterogeneity, we are confronted with a plethora of enigmas. Increasing evidence indicates that the complexity of BMP signaling dynamics provides essential regulation on endothelial plasticity. Emerging reports have identified novel fine-tuning regulatory mechanisms for BMP

signaling. While their functions remain largely unknown in the endothelium, given the ubiquitous expression of these regulators, it is plausible that BMP signaling in ECs is similarly modulated. Since the role of BMP signaling in endothelial heterogeneity is still in its infancy, it will be of great importance to elucidate distinct regulatory mechanisms and more importantly its impact on the endothelial phenotype, which ultimately will lead to distinct physiological responses in the body. The plethora of regulatory possibilities provide an additional dimension for regulating distinct BMP signaling components and therefore further enrich the impact of the BMP signaling on endothelial heterogeneity. Not yet identified environmental factors, as well as various PTMs, might give us answers to yet unsolved enigmas and offer novel strategies to overcome limitations faced so far. Therefore, further investigations will provide insights into how such a conceptually simple signaling cascade can give rise to exquisite plasticity and versatility. Moreover, the availability of novel techniques, such as NGS, single-cell analysis, and bioinformatics, will refine our understanding of endothelial dysfunctions and concomitant diseases and ultimately contribute to the development of new therapeutic interventions for various diseases by fully harnessing the heterogeneity and context-dependent properties of BMP signaling.

AUTHOR CONTRIBUTIONS

All authors wrote and edited the manuscript.

FUNDING

This work was supported by grants from the National Research Foundation of Korea (NRF-2016R1A5A1007318 and NRF-2019R1A2C2088125) to S-WJ.

ACKNOWLEDGMENTS

We thank the member of Jin laboratory for helpful discussion and critical reading of the manuscript.

REFERENCES

Abe, E., Yamamoto, M., Taguchi, Y., Lecka-Czernik, B., O'Brien, C. A., Economides, A. N., et al. (2000). Essential requirement of BMPs-2/4 for both osteoblast and osteoclast formation in murine bone marrow cultures from adult mice: antagonism by noggin. *J. Bone Miner. Res.* 15, 663–673. doi: 10.1359/jbmr.2000.15.4.663

Aird, W. C. (2003). Endothelial cell heterogeneity. *Crit. Care Med.* 31, S221–S230. doi: 10.1097/01.CCM.0000057847.32590.C1

Antebi, Y. E., Linton, J. M., Klumpe, H., Bintu, B., Gong, M., Su, C., et al. (2017). Combinatorial signal perception in the BMP pathway. *Cell* 170, 1184–1196. doi: 10.1016/j.cell.2017.08.015

Baeyens, N., Larrivee, B., Ola, R., Hayward-Piatkowskyi, B., Dubrac, A., Huang, B., et al. (2016). Defective fluid shear stress mechanotransduction mediates hereditary hemorrhagic telangiectasia. *J. Cell Biol.* 214, 807–816. doi: 10.1083/jcb.201603106

Bautch, V. L., and Caron, K. M. (2015). Blood and lymphatic vessel formation. *Cold Spring Harb. Perspect. Biol.* 7:a008268. doi: 10.1101/cshperspect.a008268

Brinjikji, W., Iyer, V. N., Sorenson, T., and Lanzino, G. (2015). Cerebrovascular manifestations of hereditary hemorrhagic telangiectasia. *Stroke* 46, 3329–3337. doi: 10.1161/STROKEAHA.115.010984

Byrne, A. M., Bouchier-Hayes, D. J., and Harmey, J. H. (2005). Angiogenic and cell survival functions of vascular endothelial growth factor (VEGF). *J. Cell. Mol. Med.* 9, 777–794. doi: 10.1111/j.1582-4934.2005.tb00379.x

Chen, Y., Bhushan, A., and Vale, W. (1997). Smad8 mediates the signaling of the ALK-2 [corrected] receptor serine kinase. *Proc. Natl. Acad. Sci. U.S.A.* 94, 12938–12943. doi: 10.1073/pnas.94.24.12938

Chi, J. T., Chang, H. Y., Haraldsen, G., Jahnsen, F. L., Troyanskaya, O. G., Chang, D. S., et al. (2003). Endothelial cell diversity revealed by global expression profiling. *Proc. Natl. Acad. Sci. U.S.A.* 100, 10623–10628. doi: 10.1073/pnas.1434429100

Coso, S., Bovay, E., and Petrova, T. V. (2014). Pressing the right buttons: signaling in lymphangiogenesis. *Blood* 123, 2614–2624. doi: 10.1182/blood-2013-12-297317

Cunha, S. I., Magnusson, P. U., Dejana, E., and Lampugnani, M. G. (2017). Deregulated TGF-beta/BMP signaling in vascular malformations. *Circ. Res.* 121, 981–999. doi: 10.1161/CIRCRESAHA.117.309930

Cuttano, R., Rudini, N., Bravi, L., Corada, M., Giampietro, C., Papa, E., et al. (2016). KLF4 is a key determinant in the development and progression of cerebral cavernous malformations. *EMBO Mol. Med.* 8, 6–24. doi: 10.15252/emmm.201505433

David, C. J., and Massague, J. (2018). Contextual determinants of TGFbeta action in development, immunity and cancer. *Nat. Rev. Mol. Cell. Biol.* 19, 419–435. doi: 10.1038/s41580-018-0007-0

Dunmore, B. J., Jones, R. J., Toshner, M. R., Upton, P. D., and Morrell, N. W. (2021). Approaches to treat pulmonary arterial hypertension by targeting bmpr2 - from cell membrane to nucleus. *Cardiovasc. Res.* cvaa350. doi: 10.1093/cvr/cvaa350 [Epub ahead of print].

Dunworth, W. P., Cardona-Costa, J., Bozkulak, E. C., Kim, J. D., Meadows, S., Fischer, J. C., et al. (2014). Bone morphogenetic protein 2 signaling negatively modulates lymphatic development in vertebrate embryos. *Circ. Res.* 114, 56–66. doi: 10.1161/CIRCRESAHA.114.302452

Garciadiego-Cazares, D., Aguirre-Sanchez, H. I., Abarca-Buis, R. F., Kouri, J. B., Velasquillo, C., and Ibarra, C. (2015). Regulation of alpha5 and alphaV integrin expression by GDF-5 and BMP-7 in chondrocyte differentiation and osteoarthritis. *PLoS One* 10:e0127166. doi: 10.1371/journal.pone.0127166

Garciadiego-Cazares, D., Rosales, C., Katoh, M., and Chimal-Monroy, J. (2004). Coordination of chondrocyte differentiation and joint formation by alpha5beta1 integrin in the developing appendicular skeleton. *Development* 131, 4735–4742. doi: 10.1242/dev.01345

Garrigue-Antar, L., Hartigan, N., and Kadler, K. E. (2002). Post-translational modification of bone morphogenetic protein-1 is required for secretion and stability of the protein. *J. Biol. Chem.* 277, 43327–43334. doi: 10.1074/jbc.M207342200

Goumans, M. J., Zwijsen, A., Ten Dijke, P., and Bailly, S. (2018). Bone morphogenetic proteins in vascular homeostasis and disease. *Cold Spring Harb. Perspect. Biol.* 10:a031989. doi: 10.1101/cshperspect.a031989

Graf, S., Haimel, M., Bleda, M., Hadinnapola, C., Southgate, L., Li, W., et al. (2018). Identification of rare sequence variation underlying heritable pulmonary arterial hypertension. *Nat. Commun.* 9:1416. doi: 10.1038/s41467-018-03672-4

Hang, Q., Zhou, Y., Hou, S., Zhang, D., Yang, X., Chen, J., et al. (2014). Asparagine-linked glycosylation of bone morphogenetic protein-2 is required for secretion and osteoblast differentiation. *Glycobiology* 24, 292–304. doi: 10.1093/glycob/cwt110

Hata, A., and Kang, H. (2015). Functions of the bone morphogenetic protein signaling pathway through microRNAs (review). *Int. J. Mol. Med.* 35, 563–568. doi: 10.3892/ijmm.2015.2060

Herhaus, L., Al-Salihi, M. A., Dingwell, K. S., Cummins, T. D., Wasmus, L., Vogt, J., et al. (2014). USP15 targets ALK3/BMPR1A for deubiquitylation to enhance bone morphogenetic protein signalling. *Open Biol.* 4:140065. doi: 10.1098/rsob.140065

Hershko, A., and Ciechanover, A. (1998). The ubiquitin system. *Annu. Rev. Biochem.* 67, 425–479. doi: 10.1146/annurev.biochem.67.1.425

Hiepen, C., Mendez, P. L., and Knaus, P. (2020). It takes two to tango: endothelial TGFbeta/BMP signaling crosstalk with mechanobiology. *Cells* 9:1965. doi: 10.3390/cells9091965

Itoh, F., Itoh, S., Goumans, M. J., Valdimarsdottir, G., Iso, T., Dotto, G. P., et al. (2004). Synergy and antagonism between Notch and BMP receptor signaling pathways in endothelial cells. *EMBO J.* 23, 541–551. doi: 10.1038/sj.emboj.7600065

Johnson, D. W., Berg, J. N., Baldwin, M. A., Gallione, C. J., Marondel, I., Yoon, S. J., et al. (1996). Mutations in the activin receptor-like kinase 1 gene in hereditary haemorrhagic telangiectasia type 2. *Nat. Genet.* 13, 189–195. doi: 10.1038/ng0696-189

Kalucka, J., de Rooij, L., Goveia, J., Rohlenova, K., Dumas, S. J., Meta, E., et al. (2020). Single-cell transcriptome atlas of murine endothelial cells. *Cell* 180:e720. doi: 10.1016/j.cell.2020.01.015

Karve, T. M., and Cheema, A. K. (2011). Small changes huge impact: the role of protein posttranslational modifications in cellular homeostasis and disease. *J. Amino Acids* 2011:207691. doi: 10.4061/2011/207691

Kashiwada, T., Fukuhara, S., Terai, K., Tanaka, T., Wakayama, Y., Ando, K., et al. (2015). Beta-Catenin-dependent transcription is central to Bmp-mediated formation of venous vessels. *Development* 142, 497–509. doi: 10.1242/dev.115576

Kretzschmar, M., Liu, F., Hata, A., Doody, J., and Massague, J. (1997). The TGF-beta family mediator Smad1 is phosphorylated directly and activated functionally by the BMP receptor kinase. *Genes Dev.* 11, 984–995. doi: 10.1101/gad.11.8.984

Labauge, P., Denier, C., Bergametti, F., and Tournier-Lasserve, E. (2007). Genetics of cavernous angiomas. *Lancet Neurol.* 6, 237–244. doi: 10.1016/S1474-4422(07)70053-4

Li, S., Iakoucheva, L. M., Mooney, S. D., and Radivojac, P. (2010). Loss of post-translational modification sites in disease. *Pac. Symp. Biocomput.* 15, 337–347. doi: 10.1142/9789814295291_0036

Liebelt, F., and Vertegaal, A. C. (2016). Ubiquitin-dependent and independent roles of SUMO in proteostasis. *Am. J. Physiol. Cell. Physiol.* 311, C284–C296. doi: 10.1152/ajpcell.00091.2016

Lin, X., Liang, M., Liang, Y. Y., Brunicardi, F. C., and Feng, X. H. (2003). SUMO-1/Ubc9 promotes nuclear accumulation and metabolic stability of tumor suppressor Smad4. *J. Biol. Chem.* 278, 31043–31048. doi: 10.1074/jbc.C300112200

Lowery, J. W., Amich, J. M., Andonian, A., and Rosen, V. (2014). N-linked glycosylation of the bone morphogenetic protein receptor type 2 (BMPR2) enhances ligand binding. *Cell Mol. Life Sci.* 71, 3165–3172. doi: 10.1007/s00018-013-1541-8

Maddaluno, L., Rudini, N., Cuttano, R., Bravi, L., Giampietro, C., Corada, M., et al. (2013). EndMT contributes to the onset and progression of cerebral cavernous malformations. *Nature* 498, 492–496. doi: 10.1038/nature12207

Malinverno, M., Maderna, C., Abu Taha, A., Corada, M., Orsenigo, F., Valentino, M., et al. (2019). Endothelial cell clonal expansion in the development of cerebral cavernous malformations. *Nat. Commun.* 10:2761. doi: 10.1038/s41467-019-10707-x

Massague, J. (2003). Integration of Smad and MAPK pathways: a link and a linker revisited. *Genes Dev.* 17, 2993–2997. doi: 10.1101/gad.1167003

McAllister, K. A., Grogg, K. M., Johnson, D. W., Gallione, C. J., Baldwin, M. A., Jackson, C. E., et al. (1994). Endoglin, a TGF-beta binding protein of endothelial cells, is the gene for hereditary haemorrhagic telangiectasia type 1. *Nat. Genet.* 8, 345–351. doi: 10.1038/ng1294-345

Min, E., and Schwartz, M. A. (2019). Translocating transcription factors in fluid shear stress-mediated vascular remodeling and disease. *Exp. Cell Res.* 376, 92–97. doi: 10.1016/j.yexcr.2019.01.005

Miyazono, K., Kamiya, Y., and Morikawa, M. (2010). Bone morphogenetic protein receptors and signal transduction. *J. Biochem.* 147, 35–51. doi: 10.1093/jb/mvp148

Morikawa, M., Koinuma, D., Tsutsumi, S., Vasilaki, E., Kanki, Y., Heldin, C. H., et al. (2011). ChIP-seq reveals cell type-specific binding patterns of BMP-specific Smads and a novel binding motif. *Nucleic Acids Res.* 39, 8712–8727. doi: 10.1093/nar/gkr572

Morikawa, M., Mitani, Y., Holmborn, K., Kato, T., Koinuma, D., Maruyama, J., et al. (2019). The ALK-1/SMAD/ATOH8 axis attenuates hypoxic responses and protects against the development of pulmonary arterial hypertension. *Sci. Signal.* 12:eaay4430. doi: 10.1126/scisignal.aay4430

Mouillesseaux, K. P., Wiley, D. S., Saunders, L. M., Wylie, L. A., Kushner, E. J., Chong, D. C., et al. (2016). Notch regulates BMP responsiveness and lateral branching in vessel networks via SMAD6. *Nat. Commun.* 7:13247. doi: 10.1038/ncomms13247

Moulton, M. J., Humphreys, G. B., Kim, A., and Letsou, A. (2020). O-GlcNAcylation dampens Dpp/BMP signaling to ensure proper drosophila embryonic development. *Dev. Cell* 53:e333. doi: 10.1016/j.devcel.2020.04.001

Moya, I. M., Umans, L., Maas, E., Pereira, P. N., Beets, K., Francis, A., et al. (2012). Stalk cell phenotype depends on integration of Notch and Smad1/5 signaling cascades. *Dev. Cell* 22, 501–514. doi: 10.1016/j.devcel.2012.01.007

Mueller, T. D., and Nickel, J. (2012). Promiscuity and specificity in BMP receptor activation. *FEBS Lett.* 586, 1846–1859. doi: 10.1016/j.febslet.2012.02.043

Nakashima, K., Wiese, S., Yanagisawa, M., Arakawa, H., Kimura, N., Hisatsune, T., et al. (1999). Developmental requirement of gp130 signaling in neuronal survival and astrocyte differentiation. *J. Neurosci.* 19, 5429–5434. doi: 10.1523/jneurosci.19-13-05429.1999

Neal, A., Nornes, S., Payne, S., Wallace, M. D., Fritzsche, M., Louphrasitthiphol, P., et al. (2019). Venous identity requires BMP signalling through ALK3. *Nat. Commun.* 10:453. doi: 10.1038/s41467-019-08315-w

Negreiros, E., Herszterg, S., Kang, K. H., Camara, A., Dias, W. B., Carneiro, K., et al. (2018). N-linked glycosylation restricts the function of Short gastrulation to bind and shuttle BMPs. *Development* 145:dev167338. doi: 10.1242/dev.167338

Nickel, J., and Mueller, T. D. (2019). Specification of BMP signaling. *Cells* 8:1579. doi: 10.3390/cells8121579

Nolan, D. J., Ginsberg, M., Israely, E., Palikuqi, B., Poulos, M. G., James, D., et al. (2013). Molecular signatures of tissue-specific microvascular endothelial cell heterogeneity in organ maintenance and regeneration. *Dev. Cell* 26, 204–219. doi: 10.1016/j.devcel.2013.06.017

Oliver, G., and Srinivasan, R. S. (2010). Endothelial cell plasticity: how to become and remain a lymphatic endothelial cell. *Development* 137, 363–372. doi: 10.1242/dev.035360

Pak, B., Schmitt, C. E., Choi, W., Kim, J. D., Han, O., Alsio, J., et al. (2020). Analyses of avascular mutants reveal unique transcriptomic signature of non-conventional endothelial cells. *Front. Cell Dev. Biol.* 8:589717. doi: 10.3389/fcell.2020.589717

Pearson, K. L., Hunter, T., and Janknecht, R. (1999). Activation of Smad1-mediated transcription by p300/CBP. *Biochim. Biophys. Acta* 1489, 354–364. doi: 10.1016/s0167-4781(99)00166-9

Pfarr, N., Szamalek-Hoegel, J., Fischer, C., Hinderhofer, K., Nagel, C., Ehlken, N., et al. (2011). Hemodynamic and clinical onset in patients with hereditary pulmonary arterial hypertension and BMPR2 mutations. *Respir. Res.* 12:99. doi: 10.1186/1465-9921-12-99

Poduri, A., Chang, A. H., Raftrey, B., Rhee, S., Van, M., and Red-Horse, K. (2017). Endothelial cells respond to the direction of mechanical stimuli through SMAD signaling to regulate coronary artery size. *Development* 144, 3241–3252. doi: 10.1242/dev.150904

Pulkkinen, H. H., Kiema, M., Lappalainen, J. P., Toropainen, A., Beter, M., Tirronen, A., et al. (2020). BMP6/TAZ-Hippo signaling modulates angiogenesis and endothelial cell response to VEGF. *Angiogenesis* 24, 129–144. doi: 10.1007/s10456-020-09748-4

Pulkkinen, H. H., Kiema, M., Lappalainen, J. P., Toropainen, A., Beter, M., Tirronen, A., et al. (2021). BMP6/TAZ-Hippo signaling modulates angiogenesis and endothelial cell response to VEGF. *Angiogenesis* 24, 129–144.

Ranchoux, B., Antigny, F., Rucker-Martin, C., Hautefort, A., Pechoux, C., Bogaard, H. J., et al. (2015). Endothelial-to-mesenchymal transition in pulmonary hypertension. *Circulation* 131, 1006–1018. doi: 10.1161/CIRCULATIONAHA.114.008750

Sailem, H. Z., and Al Haj Zen, A. (2020). Morphological landscape of endothelial cell networks reveals a functional role of glutamate receptors in angiogenesis. *Sci. Rep.* 10:13829. doi: 10.1038/s41598-020-70440-0

Sedlmeier, G., and Sleeman, J. P. (2017). Extracellular regulation of BMP signaling: welcome to the matrix. *Biochem. Soc. Trans.* 45, 173–181. doi: 10.1042/BST20160263

Seeherman, H. J., Berasi, S. P., Brown, C. T., Martinez, R. X., Juo, Z. S., Jelinsky, S., et al. (2019). A BMP/activin A chimera is superior to native BMPs and induces bone repair in nonhuman primates when delivered in a composite matrix. *Sci. Transl. Med.* 11:eaar4953. doi: 10.1126/scitranslmed.aar4953

Seo, D., Jung, S. M., Park, J. S., Lee, J., Ha, J., Kim, M., et al. (2019). The deubiquitinating enzyme PSMD14 facilitates tumor growth and chemoresistance through stabilizing the ALK2 receptor in the initiation of BMP6 signaling pathway. *EBioMedicine* 49, 55–71. doi: 10.1016/j.ebiom.2019.10.039

Shu, B., Zhang, M., Xie, R., Wang, M., Jin, H., Hou, W., et al. (2011). BMP2, but not BMP4, is crucial for chondrocyte proliferation and maturation during endochondral bone development. *J. Cell. Sci.* 124, 3428–3440. doi: 10.1242/jcs.083659

Southgate, L., Machado, R. D., Graf, S., and Morrell, N. W. (2020). Molecular genetic framework underlying pulmonary arterial hypertension. *Nat. Rev. Cardiol.* 17, 85–95. doi: 10.1038/s41569-019-0242-x

Suzuki, A., Chang, C., Yingling, J. M., Wang, X. F., and Hemmati-Brivanlou, A. (1997). Smad5 induces ventral fates in Xenopus embryo. *Dev. Biol.* 184, 402–405. doi: 10.1006/dbio.1997.8548

Takeda, A., Hollmen, M., Dermadi, D., Pan, J., Brulois, K. F., Kaukonen, R., et al. (2019). Single-cell survey of human lymphatics unveils marked endothelial cell heterogeneity and mechanisms of homing for neutrophils. *Immunity* 51, 561–572. doi: 10.1016/j.immuni.2019.06.027

Takizawa, T., Ochiai, W., Nakashima, K., and Taga, T. (2003). Enhanced gene activation by Notch and BMP signaling cross-talk. *Nucleic Acids Res.* 31, 5723–5731. doi: 10.1093/nar/gkg778

Vion, A. C., Alt, S., Klaus-Bergmann, A., Szymborska, A., Zheng, T., Perovic, T., et al. (2018). Primary cilia sensitize endothelial cells to BMP and prevent excessive vascular regression. *J. Cell. Biol.* 217, 1651–1665. doi: 10.1083/jcb.201706151

Wang, R. N., Green, J., Wang, Z., Deng, Y., Qiao, M., Peabody, M., et al. (2014). Bone morphogenetic protein (BMP) signaling in development and human diseases. *Genes Dis.* 1, 87–105. doi: 10.1016/j.gendis.2014.07.005

Wiley, D. M., and Jin, S. W. (2011). Bone Morphogenetic Protein functions as a context-dependent angiogenic cue in vertebrates. *Semin. Cell Dev. Biol.* 22, 1012–1018. doi: 10.1016/j.semcdb.2011.10.005

Wiley, D. M., Kim, J. D., Hao, J., Hong, C. C., Bautch, V. L., and Jin, S. W. (2011). Distinct signalling pathways regulate sprouting angiogenesis from the dorsal aorta and the axial vein. *Nat. Cell Biol.* 13, 686–692. doi: 10.1038/ncb2232

Wrana, J. L., Attisano, L., Wieser, R., Ventura, F., and Massague, J. (1994). Mechanism of activation of the TGF-beta receptor. *Nature* 370, 341–347. doi: 10.1038/370341a0

Wu, J., Chen, X., Sehgal, P., Zhang, T., Jackson-Weaver, O., Gou, Y., et al. (2021). Arginine methylation of R81 in Smad6 confines BMP-induced Smad1 signaling. *J. Biol. Chem.* 296:100496. doi: 10.1016/j.jbc.2021.100496

Xu, J., Wang, A. H., Oses-Prieto, J., Makhijani, K., Katsuno, Y., Pei, M., et al. (2013). Arginine methylation initiates BMP-induced smad signaling. *Mol. Cell* 51, 5–19. doi: 10.1016/j.molcel.2013.05.004

Xu, P., Liu, J., and Derynck, R. (2012). Post-translational regulation of TGF-beta receptor and Smad signaling. *FEBS Lett.* 586, 1871–1884. doi: 10.1016/j.febslet.2012.05.010

Yoshimatsu, Y., Lee, Y. G., Akatsu, Y., Taguchi, L., Suzuki, H. I., Cunha, S. I., et al. (2013). Bone morphogenetic protein-9 inhibits lymphatic vessel formation via activin receptor-like kinase 1 during development and cancer progression. *Proc. Natl. Acad. Sci. U.S.A.* 110, 18940–18945. doi:10.1073/pnas.1310479110

Zhang, X., Zhang, J., Bauer, A., Zhang, L., Selinger, D. W., Lu, C. X., et al. (2013). Fine-tuning BMP7 signalling in adipogenesis by UBE2O/E2-230K-mediated monoubiquitination of SMAD6. *EMBO J.* 32, 996–1007. doi: 10.1038/emboj.2013.38

Zhou, J., Lee, P. L., Tsai, C. S., Lee, C. I., Yang, T. L., Chuang, H. S., et al. (2012). Force-specific activation of Smad1/5 regulates vascular endothelial cell cycle progression in response to disturbed flow. *Proc. Natl. Acad. Sci. U.S.A.* 109, 7770–7775. doi: 10.1073/pnas.1205476109

Zhu, H., Kavsak, P., Abdollah, S., Wrana, J. L., and Thomsen, G. H. (1999). A SMAD ubiquitin ligase targets the BMP pathway and affects embryonic pattern formation. *Nature* 400, 687–693. doi: 10.1038/23293

Conflict of Interest: The authors declare that the research was conducted in the absence of any commercial or financial relationships that could be construed as a potential conflict of interest.

Copyright © 2021 Han, Pak and Jin. This is an open-access article distributed under the terms of the Creative Commons Attribution License (CC BY). The use, distribution or reproduction in other forums is permitted, provided the original author(s) and the copyright owner(s) are credited and that the original publication in this journal is cited, in accordance with accepted academic practice. No use, distribution or reproduction is permitted which does not comply with these terms.

frontiers in Cell and Developmental Biology

REVIEW
published: 25 June 2021
doi: 10.3389/fcell.2021.691335

Developmental Perspectives on Arterial Fate Specification

*Dongying Chen[1], Martin A. Schwartz[1,2,3] and Michael Simons[1,2]**

[1] Yale Cardiovascular Research Center, Departments of Internal Medicine, Yale University School of Medicine, New Haven, CT, United States, [2] Department of Cell Biology, Yale University School of Medicine, New Haven, CT, United States, [3] Department of Biomedical Engineering, Yale University, New Haven, CT, United States

Blood vessel acquisition of arterial or venous fate is an adaptive phenomenon in response to increasing blood circulation during vascular morphogenesis. The past two decades of effort in this field led to development of a widely accepted paradigm of molecular regulators centering on VEGF and Notch signaling. More recent findings focused on shear stress-induced cell cycle arrest as a prerequisite for arterial specification substantially modify this traditional understanding. This review aims to summarize key molecular mechanisms that work in concert to drive the acquisition of arterial fate in two distinct developmental settings of vascular morphogenesis: *de novo* vasculogenesis of the dorsal aorta and postnatal retinal angiogenesis. We will also discuss the questions and conceptual controversies that potentially point to novel directions of investigation and possible clinical relevance.

Keywords: arterial specification, vasculogenesis, angiogenesis, vascular remodeling, Notch activation, shear stress, VEGF signaling

OPEN ACCESS

Edited by:
Bin Ren,
University of Alabama at Birmingham, United States

Reviewed by:
Yong Fan,
Guangzhou Medical University, China
Chunsik Lee,
Sun Yat-sen University, China
Tsutomu Kume,
Northwestern University, United States

***Correspondence:**
Michael Simons
michael.simons@yale.edu

Specialty section:
This article was submitted to Signaling, a section of the journal Frontiers in Cell and Developmental Biology

Received: *06 April 2021*
Accepted: *18 May 2021*
Published: *25 June 2021*

Citation:
Chen D, Schwartz MA and Simons M (2021) Developmental Perspectives on Arterial Fate Specification. Front. Cell Dev. Biol. 9:691335. doi: 10.3389/fcell.2021.691335

1. INTRODUCTION

Acquisition of distinct arterial and venous identities is a critical step in vascular development. In the past two decades, numerous studies utilizing a variety of models, have placed Notch activation at the center of arterial specification. Studies exploring the role of Notch in arterio-venous (A/V) specification focused on three key areas: (1) how Notch is activated; (2) how Notch induces arterial fate; and (3) coordination of arterial fate acquisition with other developmental processes such as tubulogenesis and angiogenic sprouting. While VEGF-activation of Notch signaling has been considered the key step in arterial specification, recent findings centered on contributions of shear stress-induced Notch activation and cell cycle arrest to this process, raise questions about our traditional understanding of this subject. This review aims to integrate these new developments with the traditional A/V specification paradigm by carefully exploring studies of *de novo* vasculogenesis of the dorsal aorta (DA) during early embryogenesis and vasculature development in the neonatal mouse retina (**Figures 1A,B**). Since arterial specification in these two well-studied settings is subject to distinct regulatory mechanisms in distinct local microenvironments (**Figures 1A,B**), these two complementary models offer opportunities to address general vs specific features of this process. We will also examine key mechanisms responsible for Notch activation and their biological consequences. For a full discussion of signaling pathways involved in arterial and venous specification, readers can also refer to a number of excellent recent reviews (Lin et al., 2007; Roca and Adams, 2007; Aitsebaomo et al., 2008; Swift and Weinstein, 2009; Corada et al., 2014; Fish and Wythe, 2015; Simons and Eichmann, 2015; Mack and Iruela-Arispe, 2018; Red-Horse and Siekmann, 2019).

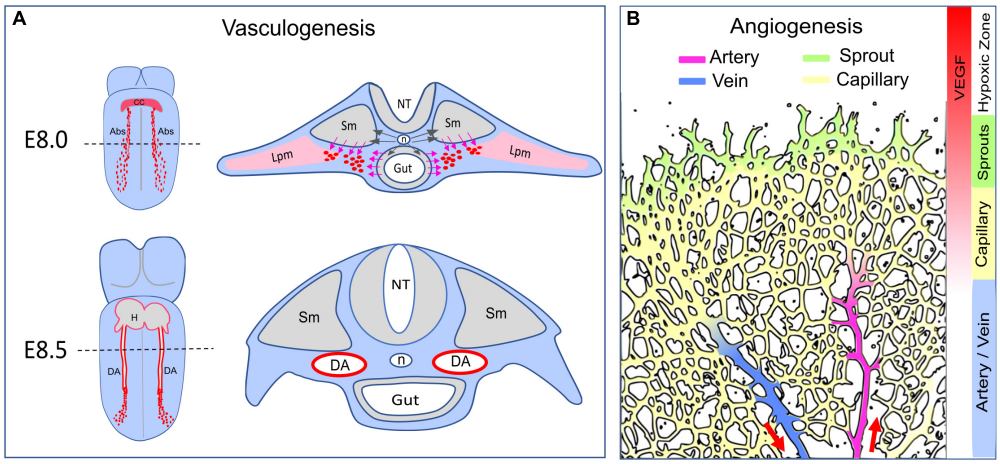

FIGURE 1 | Arterial formation–vasculogenesis versus angiogenesis. **(A)** Formation of the dorsal aorta. Dash lines indicate transverse sections corresponding to the diagrams on the right. At E8.0, Shh (black arrows) released from the notochord (n) triggers VEGF expression in the somite (Sm) and the endoderm (Gut). The angioblasts (Abs, red dots) derived from the lateral plate mesoderm (Lpm) migrate toward the VEGF gradient (pink arrows) and coalesce as an endothelial cord. At E8.5, the dorsal aorta becomes a lumenized vessel connected to the heart (H). The developing vitaline veins and cardinal veins are omitted in this diagram. CC: cardiac crescent. NT: neural tube. **(B)** Arterial formation during postnatal angiogenesis in the retina. Vascular expansion is regulated by antiogenic sprouting at the vascular front, which is induced by a gradient of VEGF released from the neural bed in the avascular (hypoxic) zone. Artery formation is a process of vascular remodeling of the capillary bed. Red arrows indicate the direction of blood flow.

2. ACQUISITION OF ARTERIAL FATE DURING *de novo* VASCULOGENESIS–FORMATION OF THE DORSAL AORTA

During early embryogenesis, vasculature is established in the avascular embryo body. Nascent vessels are formed by emergence of undifferentiated endothelial cells (ECs) from mesodermal progenitors in a stepwise process defined as *de novo* vasculogenesis. Key steps in this process include (a) differentiation of mesodermal cells into angioblasts and ultimately into VEGFR2$^+$/CD31$^+$/VE-Cad$^+$ ECs; (b) assembly of the newly emerged ECs into vascular cords; and (c) cord lumenization leading to establishment of blood flow (Risau and Flamme, 1995; Drake and Fleming, 2000; Crosby et al., 2005; Ferguson et al., 2005; Li et al., 2012; Fish and Wythe, 2015). In mouse embryos, extraembryonic progenitors of the splanchnopleuric mesoderm differentiate into blood islands and subsequently form the primitive vasculature in the yolk sac (Risau and Flamme, 1995; Ferguson et al., 2005; Ross and Boroviak, 2020). In the embryo body proper, the DA is formed by progenitors derived from the lateral plate mesoderm (**Figure 1A**). The DA is the first blood vessel (and the first artery) to form, by E8.25, at the 5 somite (5s) stage (Risau and Flamme, 1995; Drake and Fleming, 2000; Chong et al., 2011; Sato, 2013; Fish and Wythe, 2015; **Figure 1A**). Importantly, angioblasts begin expressing arterial markers Dll4 and Connexin 37 (Cx37) in the endothelial cord of the DA and subsequently gain more arterial markers such as Ephrin B2 and Connexin 40 during the lumenization process (Chong et al., 2011; Wythe et al., 2013; Herman et al., 2018). Slightly later, at approximately E8.5, other groups of mesodermal progenitors contribute to vasculogenesis of the endocardium, the sinus venosus, the vitelline veins and the cardinal veins, thus establishing a primordial circulatory system by the 13s stage (Chong et al., 2011; Fish and Wythe, 2015). At mid-gestation, the pharyngeal arch arteries, which form a rudimentary vascular apparatus that is ultimately remodeled into the aortic arch arteries, are derived from the second heart field mesoderm via vasculogenesis (Li et al., 2012; Wang et al., 2017; Kelly, 2021). Acquisition of arteriovenous identity, the next step during formation of these embryonic vasculatures, is subject to specific molecular controls in distinct and dynamically changing local microenvironments.

2.1 VEGF-MAPK Signaling Regulates the Initial Determination of Arterial Fate

Numerous studies in developing mouse, avians, xenopus and zebrafish embryos have revealed a mechanism involving non-cell autonomous signaling interactions among early embryonic tissues in close proximity, including the notochord, the hypochord (fish and xenopus only), the endoderm and the somites, to tightly control vasculogenesis of the DA (Hogan and Bautch, 2004). Briefly, Shh emanating from the notochord (mouse and zebrafish) and the endoderm (mouse and zebrafish) triggers VEGF expression from the endoderm (mouse and avian), the hypochord (xenopus), and/or the somites (mouse, xenopus, and zebrafish) (Hogan and Bautch, 2004; Sato, 2013; Fish and Wythe, 2015; **Figure 1A**). Once mesodermal precursors acquire the expression of VEGFR2 and differentiate into angioblasts, they migrate away from the lateral plate mesoderm toward the VEGF gradient and coalesce as an endothelial cord of the presumptive DA (Hogan and Bautch, 2004; Sato, 2013; Fish and Wythe, 2015; **Figure 1A**).

Both VEGFR2-null (Shalaby et al., 1995; Sakurai et al., 2005) and VEGFR2-Y1173F (Sakurai et al., 2005) mouse embryos die

at E8.5 with no blood vessel having been formed, including the complete absence of the DA and the extraembryonic yolk sac vasculature, thus demonstrating the indispensable role of VEGF signaling at this time point. The role of Shh in the DA formation and Notch activation is believed to depend on VEGF (Hogan and Bautch, 2004; Castillo and Alvarez, 2011). Unlike VEGFR2-null embryos, the loss of Shh signaling in mouse embryos does not completely compromise DA formation as aggregates of angioblasts and a partially formed lumenized DA are present (Vokes et al., 2004; Coultas et al., 2010). In Shh-deficient embryos, Dll4 expression is reduced, particularly in the cranial portion of the DA, which corresponds to the loss of VEGF expression in the somites of the same segment of the embryo body (Coultas et al., 2010). Indeed, a defective DA formation in Shh-deficient embryos can be rescued by increasing VEGF signaling (Coultas et al., 2010). In zebrafish, Shh deficiency results in a complete loss of VEGF in the somites and Ephrin B2a expression in the DA, which can be rescued by artificial expression of VEGF (Lawson et al., 2002). Collectively, these observations suggest that Shh is required for VEGF expression and that that VEGF expression, in turn, determines Notch signaling and arterial identity of the DA.

The role of VEGF/VEGFR2 in arterial fate determination during DA formation is, however, more complex, as suggested by studies of VEGFR2 downstream signaling. Since phosphorylation of VEGFR2-Y1173 is the primary means of activation of ERK signaling, the lethality of VEGFR2-Y1173F mice has been interpreted to mean that ERK activation by VEGFR2 is indispensable for vasculogenesis. Yet careful analysis of data brings this into question. PLCγ1 is the key effector recruited by VEGFR2-Y1173 to transduce VEGFR2-MAPK signaling (Takahashi et al., 2001). PLCγ1-null mouse embryos exhibit embryonic lethality between E9.5–10.5 (Ji et al., 1997; Liao et al., 2002), 24–48 h after the formation of DA. Not surprisingly, the DA is formed in these PLCγ1-deficient mouse embryos (Ji et al., 1997). In zebrafish embryos with a y10 mutation (a loss-of-function mutation of PLCγ1), the DA forms, as visualized by vascular markers Fli1 and VEGFR2, but arterial markers EphrinB2 and Notch5 are low (Lawson et al., 2003). Ectopic expression of VEGF induces an increase in EphrinB2 expression in the wild type, but fails to do so in y10 fish (Lawson et al., 2003). Consistent with this study, characterization of other PLCγ1-deficient mutations in zebrafish also revealed defective arterial differentiation (Covassin et al., 2009). Given the role of PLCγ1 in transducing VEGFR2-Y1175 signaling to activate PKC-MAPK pathway, these studies support the conclusion that VEGF-MAPK signaling plays a principal role in acquisition of the arterial fate but is not essential for the initial DA formation.

VEGFR2 signaling activates both MAPK and PI3K-AKT pathways. It was proposed that VEGFR2 signals through MAPK to activate the arterial program, while the acquisition of venous fate involves PI3K-AKT activity (Hong et al., 2006; Lin et al., 2007; Fish and Wythe, 2015). Importantly, there is a cross-talk between Akt1 and MAPK cascades, with Akt-induced Ser259 phosphorylation of RAF1 inhibiting ERK activity (Ren et al., 2010). In HUVECs expressing RAF1-S259A, a mutation resistant to phosphorylation by AKT, ERK is constitutively activated, leading to the upregulation of the entire arterial program (Deng et al., 2013). Similarly, a suppression of PI3K-AKT signaling amplifies ERK activation and expression of arterial genes (Hong et al., 2006; Ren et al., 2010; Deng et al., 2013; Wythe et al., 2013). These findings suggest that the balance between PI3K/Akt and PKC/ERK is important for venous vs arterial identities.

There still is some uncertainty whether ERK is required for determination of the arterial fate during *de novo* vasculogenesis. In zebrafish embryos, biphosphorylated ERK (pERK1/2 and Thr202/Tyr204) is detected in the DA and the endothelial progenitors from the lateral plate mesoderm (Hong et al., 2006; Shin et al., 2016). Although experiments using chemical inhibitors suggested a functional role for ERK in arterial specification in zebrafish (Hong et al., 2006; Shin et al., 2016), interpretations of these data are confounded by the dosage and application time windows. ERK inhibition at an early embryonic stage (12 hpf) results in the absence of DA (Hong et al., 2006). In another study, ERK inhibitor at a lower dosage after 16 hpf downregulated Dll4 expression in the DA and the intersomitic angiogenic sprouts but did not affect Ephrin B2 expression (Shin et al., 2016). Besides the potential issue of specificity with chemical inhibition, this observation, however, does not provide a definitive answer to the question whether ERK is required for the initial acquisition of arterial fate. This is because ERK inhibition starts after the formation of DA, a time window when the blood flow can also possibly contribute (see section 2.2 below) and the initiation of ERK inhibition at earlier starting points (before 10 hpf) is not feasible due to severe developmental retardation and necrosis (Shin et al., 2016). A genetic model with a compound deletion of both ERK1/2 isoforms in VEGFR2+ angioblasts prior to the DA formation would be necessary to investigate the function of ERK signaling in regulation of arterial specification during this process.

2.2 Potential Role of Shear Stress in Post-vasculogenic Maintenance of Arterial Identity

The onset of blood flow during mouse embryogenesis begins at E8.25 (6–8s stage), shortly after lumenization of the DA (Ji et al., 2003; McGrath et al., 2003; Chong et al., 2011) as determined by the presence of a small number of red blood cells in the DA. This implies circulation since at E8.25 the yolk sac is the only hematopoietic organ capable of producing primitive erythrocyte (Ji et al., 2003; McGrath et al., 2003). Shear stress has been reported to be critical during embryonic vascular patterning. For example, defective hierarchical remodeling of the yolk sac vasculature is seen in Mcl1a null embryos with deficient contractility of cardiomyocytes (Lucitti et al., 2007). Titin-/- embryos with a weak and spontaneous heartbeat, also show defective lumenization of the DAs and the CVs (May et al., 2004; Gerull, 2015). These effects can be attributed to shear stress rather than oxygen transport because inhibiting blood cell formation, which reduces effective blood viscosity and thus shear stress, had similar effects, and can be rescued by injecting a dextran polymer to restore viscosity (Lucitti et al., 2007).

Does flow contribute to the regulation of arterial identity? It is reported that angioblasts express Dll4 and Cx37 prior to lumen formation in the DA in mouse embryos (Chong et al., 2011; Wythe et al., 2013; Herman et al., 2018). This suggests that arterial fate is predetermined in angioblasts when they aggregate into a solid endothelial cord that is as yet without apico-basal polarization and lumenization (Xu and Cleaver, 2011). After formation of a lumenized DA at E8.0–8.25 (4–8s), aortic ECs start to increase expression of arterial markers including Cx37/40, Dll4, Notch1/4, Hey1, and Nrp1 (Chong et al., 2011; Herman et al., 2018). Though lumenized at this stage, the DA is still a blind vessel as the vitelline vein and the cardinal vein are yet to be formed, meaning that systemic circulation has not been established (Chong et al., 2011; Sato, 2013). The initial acquisition of arterial fate thus occurs prior to the start of blood flow in the embryo proper, excluding shear stress as an important regulator. This conclusion is further supported by the observation that Cx40 and Dll4 are expressed in the endothelial cord of the DA at E8.25 in Rasip1-null embryos, which lack vascular lumens (Chong et al., 2011; Xu and Cleaver, 2011; Xu et al., 2011; Barry et al., 2016).

However, blood flow apparently contributes to the maintenance of arterial identity after embryonic blood circulation is established. Mouse embryos lacking the cardiac sodium-calcium ion exchanger Ncx1 do not have a heartbeat (and thus flow), leading to inhibition of EC Notch activation and expression of Cx40 and EphrinB2 in the DA (Hwa et al., 2017). Similarly, in the aforementioned Rapsi1-null embryos with compromised vascular lumen formation, arterial markers (potentially induced by VEGF) are expressed at E8.25 before flow would normally begin, but Cx40 expression is remarkably decreased at E9.0 when flow would be established in WT embryos (Chong et al., 2011). These observations clearly demonstrate that failure to establish effective blood circulation after 8s results in a decline of arterial identity in the DA, supporting a critical role for shear stress in maintenance of arterial identity.

In summary, VEGF determines the specification of artery fate during DA vasculogenesis, whereas shear stress maintains arterial identity after blood circulation is established. We suggest that VEGF expression from adjacent tissues (e.g., somites) is transient and declines after 8s, after which flow substitutes for VEGF to regulate arterial identity. This pattern resembles events in postnatal retinal angiogenesis, where VEGF initiates sprouting but after blood flow begins and VEGF levels drop, shear stress maintains vascular integrity (Roux et al., 2020).

3. ACQUISITION OF ARTERIAL FATE IN VASCULAR REMODELING DURING ANGIOGENESIS – COORDINATION OF ARTERIAL SPECIFICATION AND SPROUTING

Unlike vasculogenesis, in which a bona fide endothelial lineage is established via mesodermal differentiation, angiogenesis refers to a distinct process of vascular patterning during which new vessels are formed by sprouting from pre-existing vessels (Gariano and Gardner, 2005; Stahl et al., 2010). In the mouse retina, morphogenesis of the retinal vasculature begins on postnatal day 0 (P0) from a tiny vessel at the optic nerve (Gariano and Gardner, 2005; Stahl et al., 2010). Its expansion during the first week after birth is driven by a gradient of hypoxia-induced VEGF released from the neural bed in the peripheral avascular zone (Gerhardt, 2008; **Figure 1B**). When a rudimentary capillary plexus is formed at P2, selected capillary ECs undergo arteriovenous differentiation to become the first arteries and veins (Gariano and Gardner, 2005; Stahl et al., 2010). Starting from P3, the retinal vasculature displays the following stereotypic structures: sprouts at the peripheral angiogenic front, a capillary bed back from the edge, and arteries and veins in an alternating arrangement (Gariano and Gardner, 2005; Stahl et al., 2010; **Figure 1B**). The radial expansion of retinal angiogenesis ceases at P7 when the superficial layer of vessels covers the entire neural bed and the peripheral avascular zone disappears (Gariano and Gardner, 2005; Stahl et al., 2010).

In contrast to the formation of the DA during which arterial fate is determined before the onset of flow, during retinal angiogenesis, arteries and veins emerge from a capillary plexus only in the presence of an effective blood circulation (**Figure 1B**). These results are, therefore, suggestive of the shear stress involvement. In these settings, arteriovenous differentiation transforms a non-hierarchical capillary plexus into a hierarchical vasculature, a process known as vascular remodeling. It is not clear what stimulus triggers the initial selection of ECs in the rudimentary plexus to undergo arteriovenous differentiation and form arteries and veins. Lineage tracing using inducible tip cell-specific Esm1-cre driver disclosed a trajectory of tip-capillary-artery movement (Xu et al., 2014; Pitulescu et al., 2017); by contrast, lineage tracing with artery-specific BMXcre showed that marked ECs remain in the arteries (Ehling et al., 2013). Thus, arterial ECs are derived from capillary ECs but not vice versa. The capillary-to-artery differentiation implies that tip ECs move against blood flow to enter the arteries again pointing toward a role for shear stress in A-V differentiation in this setting.

Similar principles likely apply to two additional instances of vascular development. The first was a follow up study to the work of Lucitti et al. (2007) that demonstrated a requirement for shear stress in remodeling of the primitive extraembryonic yolk sac vasculature in mouse embryos. Subsequent analysis revealed that vascular plexus ECs migrate against blood flow and coalesce to form major vessels as cardiac output (and, hence, shear stress) increases (Udan et al., 2013; Garcia and Larina, 2014). Likewise, in the embryonic pharyngeal arches at mid-gestation, the pharyngeal arch artery connected to the outflow tract of the heart is formed via vascular remodeling that transforms a non-hierarchical primordial vascular plexus into a major artery (Wang et al., 2017; Warkala et al., 2021), a process during which hemodynamic forces possibly play a role.

During angiogenesis, sprouting activity requires VEGF-regulated cell migration and proliferation (Gerhardt et al., 2003; Gerhardt, 2008; Okabe et al., 2014), while artery formation suppresses proliferation and angiogenic sprouting (Hasan et al., 2017). In other words, arterial specification does not occur at the vascular front where proliferation and sprouting

are active. As both tip-stalk conversion and arterial specification are regulated by Notch signaling, the coordination of these two distinct biological processes in an angiogenic vasculature has remained a conundrum.

VEGF-induced Notch signaling regulates acquisition of the tip cell identity and tip-stalk conversion. At the angiogenic front where VEGF level is high, some ECs acquire tip cell identity through a competition mechanism (Ubezio et al., 2016). When an EC is activated by VEGF, it begins to express Dll4, leading to activation of Notch signaling in its neighboring cells. That, in turn, suppresses VEGFR2 expression and, thereby, responsiveness to VEGF, thus preventing these neighboring cells from becoming tip cells. This mechanism is in line with "lateral inhibition" observed in other developmental systems (Williams et al., 2006; Hellstrom et al., 2007b; Gerhardt, 2008; De Smet et al., 2009; Geudens and Gerhardt, 2011). This phenomenon can be recapitulated *in vitro* with an EC monolayer culture in which VEGF stimulation induces a "salt and pepper" pattern of heterogeneous Dll4 expression (Hellstrom et al., 2007a; Ubezio et al., 2016). Postnatal deletion of endothelial VEGFR2 results in the absence of tip cells and capillaries in the retinal vasculature, in which only major vessels are present (Zarkada et al., 2015; Pitulescu et al., 2017). Notch inhibition results in a hypersprouting phenotype that is blocked by VEGFR2-deletion (Zarkada et al., 2015), demonstrating that VEGFR2 signaling is required for angiogenic sprouting and is an essential upstream inducer of Notch signaling. While another study reported an opposite result (Pitulescu et al., 2017), it was likely due to incomplete deletion of VEGFR2. Interestingly, unlike the formation of DA during which VEGF-Notch determines arterial fate, in angiogenesis, sprouting ECs with high level of VEGF-induced Notch activation do not acquire arterial identity. This raises the yet unanswered question of how endothelial sprouts at the angiogenic front with high VEGF-Notch signaling avoid being ectopically arterialized?

4. NOTCH SIGNALING AND ITS BIOLOGICAL CONSEQUENCES – CELL CYCLE ARREST AND ACQUISITION OF ARTERIAL FATE

Notch signaling requires a direct cell-cell contact as both ligands (Dll1,3,4, Jag1, and 2) and receptors (Notch 1,2,3, and 4 in human and mouse, Notch1a, 1b, 2, and 3 in zebrafish) are transmembrane proteins (Kopan and Ilagan, 2009). Among these, Notch1 and 4 are specific to mouse arterial ECs (Reaume et al., 1992; Uyttendaele et al., 1996; Krebs et al., 2000), while Notch1a/b and 3 are expressed in zebrafish arteries (Lawson et al., 2001). Binding of a Notch ligand to its receptor triggers proteolytic cleavage by gamma-secretase and release of the Notch intracellular domain (NICD). Thus liberated, NICD translocates to the nucleus, where it interacts with RBPJ, Mastermind and other transcription regulators to transcriptionally control expression of target genes, including EphrinB2 (Grego-Bessa et al., 2007), Neuropilin1(Nrp1) (Sorensen et al., 2009), Cx37 (Fang et al., 2017), Dll4 (Caolo et al., 2010), Hey (Borggrefe and Oswald, 2009), and Hes (Borggrefe and Oswald, 2009) (**Figure 2**).

Notch activation regulates and is, in turn, regulated by Chicken Ovalbumin Upstream Promoter-transcription factor II (COUP-TFII), an orphan nuclear receptor critical for venous specification (Pereira et al., 1999; Polvani et al., 2019). A loss of endothelial COUP-TFII results in upregulation of Notch and arterial genes *in vivo* and in vitro (You et al., 2005; Chen et al., 2012). COUP-TFII overexpression suppresses Notch signaling and artery formation and promotes venous differentiation (Su et al., 2018).Artificial expression of Notch3 ICD inhibits COUP-TFII expression and prevents vessel differentiation to venous fate in zebrafish cardinal vein (Swift et al., 2014). These data point to the role of Notch activation in regulation of arterial vs. and venous fate specification.

Notch induces cell cycle arrest in multiple biological systems, including hair follicle cells (Deng et al., 2001; Shyu et al., 2009), T and B lymphocytes (Morimura et al., 2000; Joshi et al., 2009), keratinocytes (Rangarajan et al., 2001; Kolly et al., 2005), and cancer (Sriuranpong et al., 2001; Liao et al., 2018). Notch-induced cell cycle arrest in ECs was first implicated in the process of contact inhibition (Chen et al., 2000), during which higher EC density results in upregulation of Notch signaling and cell cycle arrest (Noseda et al., 2004). Artificial expression of Notch ligands Jag1 or Dll4, or the NICD in primary ECs from multiple vascular beds was found to induce cell cycle arrest at G0/G1 and regulate expression of cell cycle regulators (Noseda et al., 2004, 2005; Williams et al., 2006). Notch is also activated by arterial levels of laminar fluid shear stress (FSS), which contributes to the well-known suppression of EC proliferation in this setting (Fang et al., 2017). Further work has shown that cell cycle arrest in late G1 is critical for the arterial phenotype, whereas early G1 arrest is associated with venous specification (Chavkin et al., 2020).

What determines the effect of Notch in cell cycle arrest and arterial fate? A recent study (Fang et al., 2017) surprisingly identified Cx37 as the critical gene induced directly downstream of Notch ICD/RBPJ. Cx37 then induced the CDK inhibitor p27, possibly through a gap junctional transport-independent mechanism. The resultant cell cycle arrest was sufficient to allow arterial specification. This model was supported by a detailed epistatic analysis supporting the FSS-Notch-Cx37-p27 pathway in arterial fate specification.

A non-physiological, extremely high dosage of VEGF (1,000 ng/ml) has been reported to induce cultured EC monolayers to undergo synchronized oscillations in DLL4 expression and Notch activation, instead of the "salt and pepper" pattern seen with physiological VEGF levels (Ubezio et al., 2016). Similarly, intravitreal injection of high dosage of VEGF (300 ng) induced homogenous expression of Dll4 in the entire retinal vasculature at P5 Ubezio et al., 2016. Intriguingly, this treatment inhibited radial expansion and EdU labeling Ubezio et al., 2016, suggesting that synchronized Notch signaling serves as a negative feedback to suppress sprouting and proliferation. Conversely, Notch inhibition using neutralizing Dll4 antibody or Rbpj endothelial knockout

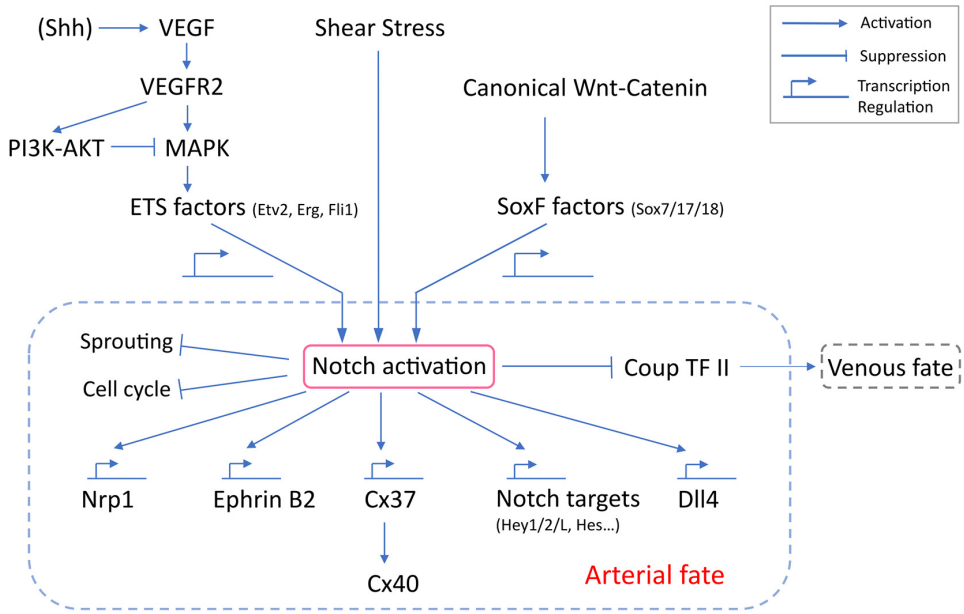

FIGURE 2 | Molecular regulation of Notch activation and arterial specification. VEGF-MAPK activation of Notch depends on ETS factors, which transcriptionally regulate the expression of Notch genes. Canonical Wnt-catenin likely signals through Sox17 to activate Notch. SoxF factors regulates transcription of Notch genes. Despite reports implicating junctional mechanosensary proteins and the interaction with cytoskeleton in response to shear stress, how shear stress activates Notch remains poorly understood. Notch activation is a common downstream outcome and is the central determinant for arterial specification. Notch signaling induces a panel of arterial genes via transcription regulation. Notch also inhibits EC sprouting, induces cell cycle arrest and suppresses venous identity.

reportedly enhanced ERK signaling (presumably induced by VEGF) in the hyperspouting vascular front (Pontes-Quero et al., 2019a; Pontes-Quero et al., 2019b). Surprisingly, high pERK signal correlated with increased expression of the cell cycle inhibitor p21 (Pontes-Quero et al., 2019a,b). Application of Dll4 neutralizing antibody induced proliferation in the capillary bed at 24 h but then strikingly suppressed by 48 h (Pontes-Quero et al., 2019a,b). This observation again suggests a negative feedback mechanism by which high VEGF-ERK signaling elicits a cell cycle arrest via p21, likely independently of Notch signaling.

5. SIGNALING MECHANISMS THAT ACTIVATE NOTCH

Multiple studies have shown that Notch activation is regulated by expression of both its receptor and ligands. Loss of one or both alleles of Dll4 (Duarte et al., 2004; Gale et al., 2004; Krebs et al., 2004), Notch1 knockout (Swiatek et al., 1994), Notch1/4 double knockout (Krebs et al., 2000) or Rbpj knockout (Krebs et al., 2004; Nielsen et al., 2014) in the developing embryo decrease Notch signaling, leading to severe vascular defects. Conversely, increasing either Notch receptor or ligand expression or artificial expression of NICD (Corada et al., 2013) activates Notch signaling. Sequence analysis of putative regulatory regions of Dll4 and Notch4 genes shows binding motifs for ETS family transcription factors (e.g., Fli1 and ERG), RBPJ, β-Catenin, Sox17, and FoxC1/2, suggesting transcriptional regulation of Dll4 and Notch4 by these factors (Corada et al., 2010, 2013; Wythe et al., 2013; Fish et al., 2017). Upstream signaling pathways regulating these transcription factors, including Notch itself, potentially interact to regulate the transcription of Notch genes. In endothelial and non-endothelial systems, Notch signaling can positively regulate the expression of Notch ligands (Dll1, Dll4, and Jag1) and receptors (Notch 1 and 3), thus establishing a positive feed-forward loop (Weng et al., 2006; Qian et al., 2009; Caolo et al., 2010; Chen et al., 2010; Borggrefe and Liefke, 2012).

5.1. VEGF and ETS Family Transcription Factors

At the angiogenic front, VEGF-ERK-induced Dll4 expression and Notch activation are pivotal to regulation of tip-stalk conversion and provide an important negative feedback mechanism regulating VEGFR2 expression to prevent excessive sprouting (Williams et al., 2006). Notch inhibition by a gamma-secretase inhibitor DAPT results in hypersprouting and a hyperdense capillary network with increased ERK activation (Pontes-Quero et al., 2019a). This phenotype is a direct consequence of excessive VEGF-ERK signaling in the absence of Notch-mediated negative feedback. Moreover, macrophage-derived VEGF-C signaling through VEGFR3 has been reported to contribute additively to Notch signaling at the vascular front, as a loss of VEGFR3 leads to hypersprouting similar to Notch inhibition (Tammela et al., 2011).

Studies in HUVECs show that VEGF-ERK signaling can phosphorylate and activate ETS transcription factor ERG, which subsequently binds to DLL4 enhancers and initiates its transcription (Wythe et al., 2013; Fish et al., 2017). In particular, VEGF-activated ERK2 selectively phosphorylates ERG on serine 215 (Ser^{215}), which peaks at 30 min and then declines, a kinetic pattern consistent with VEGF-induced phosphorylation of ERK (peaks at 5–10 min) and Dll4 expression (peaks at 1 h) (Fish et al., 2017). Activated ERG recruits transcriptional co-activator p300 to the Dll4 enhancer to regulate its expression (Fish et al., 2017). Given these observations *in vitro*, it was proposed that during vasculogenesis of the DA, VEGF-MAPK signaling induces Dll4 expression via ETS factor-regulated transcription (Wythe et al., 2013; Fish et al., 2017). However, ERG-deficient mouse embryos did not reveal strong phenotypes in DA formation and arterial specification. Erg exon4-null embryos die at E10.5–11.5 with vascular defects in multiple organs (Vijayaraj et al., 2012). But at E8.5, the DA is formed, despite a modest downregulation of Dll4 (Wythe et al., 2013). Another study reported that global knockout of Erg (Erg-null) is embryonic lethal only at E11.5–12.5, by which point the DA is normally formed (Fish et al., 2017). These observations suggest that vasculogenesis of the DA at E8.5 can be accomplished independent of Erg and that loss of Erg does not completely compromise angiogenic activity needed to support embryonic growth at E9.5–10.5. Postnatal EC deletion of Erg also results in mild reduction of vascular growth and branching in the retina (Fish et al., 2017; Shah et al., 2017). Nevertheless, in zebrafish, combined morpholino inhibition of Erg and Fli1a substantially downregulates Dll4 expression in the DA (Wythe et al., 2013), which suggests that the mild phenotype in Erg-deficient mice is likely due to compensation by other ETS factors.

Erg was found to regulate Notch signaling by balancing expression of Dll4 and Jag1 (Shah et al., 2017), two Notch ligands reported to play opposite roles in angiogenesis (Benedito et al., 2009). Both Dll4 and Jag1 genes have putative binding sites for Erg. Silencing ERG in HUVECs reduced Dll4 but upregulated Jag1 (Shah et al., 2017). The same phenotype is also found in the neonatal retina of mice with endothelial knockout of Erg, though to a lesser extent (Shah et al., 2017).

5.2. Shear Stress

Although studies of DA formation (see section 2.2) and retinal angiogenesis (see section 4) have suggested an important role for shear stress in Notch activation and arterial differentiation, how shear stress activates Notch remains poorly understood. Multiple studies have demonstrated that FSS increases cleavage of Notch 1 and 4, nuclear translocation of their ICDs and expression of target genes (Mack and Iruela-Arispe, 2018). Notch activation by FSS requires expression of its ligands on adjacent cells (Sweet et al., 2013; Polacheck et al., 2017), suggesting that FSS amplifies some aspect of this interaction. Consistent with its junctional localization, a number of studies suggest a connection to the junctional mechanosensory complex, consisting of PECAM-1, VE-cadherin and VEGFRs, that mediates an important subset of FSS responses (Tzima et al., 2005; Givens and Tzima, 2016; Tanaka et al., 2021). Chemical inhibition of VEGFR2 reportedly blocks flow activation of Notch (Masumura et al., 2009). Deletion of SHC, which is important for FSS signaling through the junctional complex also prevents flow activation of Notch (Sweet et al., 2013). The intermediate filament protein vimentin is also required for flow-induced Notch cleavage; this pathway reportedly involves phosphorylation of Vimentin and interaction with Jagged1 (van Engeland et al., 2019). Interestingly, vimentin is also required for signaling through the junctional complex via an interaction with PECAM-1 (Conway et al., 2013). These findings fit well with the close proximity of all these players in cell-cell contacts. Recent data posted on BioRXIV report a requirement for the adhesion GPCR latrophilin-2, another junctional component (Tanaka et al., 2020). Latrophilin-2 is a GPCR studied mainly in neurons (Moreno-Salinas et al., 2019) but also expressed in ECs (Camillo et al., 2020; Tanaka et al., 2020). This studied showed that it is required for flow activation of VEGFRs and downstream events via its GPCR function, and for flow activation of Notch signaling independent of G proteins (Tanaka et al., 2020). Importantly, latrophilin-2 is not required for EC responses to VEGF or Notch ligands in the absence of flow, indicating that it is critical for conferring flow sensitivity to these pathways (Tanaka et al., 2020). Despite these clues, a clear molecular mechanism is currently lacking.

In all of the above studies, Notch signaling contributes to endothelial stabilization, quiescence and arterial specification. In addition to the canonical function of the Notch ICD, junctional stabilization is mediated via a non-canonical mechanism in which the Notch1 transmembrane domain that remains after cleavage interacts with VE-cadherin to enhance barrier function (Polacheck et al., 2017). One limitation with current *in vivo* studies is that there is currently no specific way to inhibit flow activation of Notch signaling as opposed to complete inhibition via deletion of Notch ligands, receptors or other key players. The identification of latrophilin-2 as a component that specifically confers flow sensitivity to this pathway suggests an opportunity for approaches that do not globally inhibit. However, at present, a definitive study to demonstrate the *in vivo* function of flow-induced Notch activation is lacking.

5.3. SoxF Transcription Factors

The SoxF family transcription factors, Sox7, 17, and 18, are implicated in arterial specification. In zebrafish, Sox7 and Sox18 are expressed when lateral DAs fuse to form the single DA, while Sox17 is not detected at this stage (Cermenati et al., 2008). Though in Sox7-null fish embryos, the DA is formed with normal expression of Notch and arterial markers, loss of Sox7 leads to ectopic expression of VEGFR3, which is normally restricted to venous ECs (Hermkens et al., 2015). Also, an A-V shunt forms between the lateral DA and the cardinal vein, so that most of the flow bypasses the systemic blood circulation (Hermkens et al., 2015). The severity and penetrance of this phenotype is increased in Sox7; Sox18 double null fish embryos (Cermenati et al., 2008), suggesting functional redundancy

in these two Sox F factors during early embryonic vascular patterning (Herpers et al., 2008).

In the mouse, Sox17 expression is enriched in developing and mature arteries and arterioles (Matsui et al., 2006; Corada et al., 2013; Zhou et al., 2015), while Sox7 and Sox18 are similarly expressed in arteries, veins and capillaries (Zhou et al., 2015). Similar to Sox7-deficient zebrafish, Sox17-endothelial null mouse embryos develop A-V shunts between the DA and CV (Corada et al., 2013). In the retina, postnatal deletion of Sox7, Sox17, or Sox18 in the endothelium leads to hyper-sprouting with dense capillaries with reduced arterial formation (Corada et al., 2013; Zhou et al., 2015; Kim et al., 2016). The similarity of this phenotype to Notch inhibition suggests possible effects of SoxF factors on Notch activation. Intriguingly, triple deletion of Sox7, Sox17, and Sox18 strikingly enhanced the hypersprouting phenotype with almost no artery formation (Kim et al., 2016), providing evidence of function redundancy among SoxF factors. Moreover, as a direct transcription factor targeting the non-coding regions of Dll4 and Notch4, Sox17 signals upstream of Notch (Corada et al., 2013). This conclusion is supported by the finding that inhibition of Notch *in vitro* and *in vivo* has little impact on Sox17 expression and that artificial expression of Sox17 in primary culture of venous ECs originally lacking Sox17 expression upregulates a panel of Notch and arterial genes (Corada et al., 2013).

It is not clear what upstream physiological stimulus activates the expression of Sox17 during arterial specification. Though VEGF signals upstream of Notch, it does not increase Sox17 expression (Corada et al., 2013). Interestingly, a recent study reported that non-physiological high dose-long duration VEGF treatment (50 ng/ml for 6–36 h) can strikingly upregulated Sox7 and Sox17 protein synthesis via the mTOR pathway without altering mRNA levels (Kim et al., 2016). Further investigations will be needed to understand the precise mechanism to regulate Sox F factors in arterial specification.

5.4. Canonical Wnt-Catenin Signaling

Upon binding of Wnt ligands to Frizzled receptors, β-catenin degradation is inhibited, its levels increase and β-catenin translocates into the nucleus where it functions as a transcriptional regulator (Dejana, 2010). Endothelial deletion of β-catenin is embryonic lethal at E12.5 (Cattelino et al., 2003), but at E9.5 when the DA is fully formed, embryos appear normal in size with no obvious cardiovascular abnormality (Wythe et al., 2013). Another study of β-catenin iECKO, however, reported mild hypersprouting at E9.5, similar to Notch inhibition (Corada et al., 2013). Though the Dll4 promoter region contains β-catenin binding sites, active canonical Wnt signaling was not detected in arterial ECs at E8.5 and E9.5 using Wnt reporter lines (Wythe et al., 2013), which explains the absence of or mild phenotype in this time window. These observations indicate that Wnt-catenin signaling is likely not required for the initial expression of Dll4 during vasculogenesis of the DA at E8.25 and instead functions mainly between E9.5–12.5.

Consistent with direct β-catenin binding to the promoter regions of Dll4 and Notch4 (Corada et al., 2010; Wythe et al., 2013), β-catenin is reported to activate Notch and induce arterial specification. In mouse embryos at E9.5 where β-catenin was genetically stabilized (GOF), sprouting was significantly reduced, with increased Notch signaling and ectopic arterialization (Corada et al., 2010). Additionally, A-V shunt formed between the DA and sinus venosus at E9.5 (Corada et al., 2010), further suggesting defects in A-V identity. Gain or loss of β-catenin signaling up or down regulated Sox17 expression and arterial markers in the postnatal retina and brain, consistent with a model in which Wnt-catenin induces Sox17, which induces Notch (Corada et al., 2013). Other than the endothelium, Wnt-catenin signaling also regulates Sox17 expression in endodermal development (Engert et al., 2013).

6. CONCLUSION

Arterial specification is a critical step in the process of vascular maturation during organogenesis and post-natal angiogenesis. Acquisition and maintenance of arterial identity in different organs in different developmental stages is subject to spatiotemporally distinct molecular mechanisms, with Notch activation being the common downstream determinant of arterial gene expression. Unlike arterial fate specification during organogenesis, arteriogenesis in postnatal setting is much less well understood. Though a wealth of studies has concluded that VEGF-ERK signaling determines arterial fate in angioblasts and in the nascent endothelial lineage during the formation of the DA, it remains uncertain whether the same mechanism applies during postnatal retinal angiogenesis or postnatal arteriogenesis in general. Comparing the DA vasculogenesis model with postnatal retinal angiogenesis is complicated by the concomitant development of angiogenic sprouting and vascular remodeling during the latter, in a microenvironment with a dynamically changing gradient of VEGF. Moreover, the complexity of retinal vasculature is amplified by the presence of shear stress that is also a critical inducer of Notch activation and arterial fate. Despite its obvious critical role, how FSS activates Notch and induces arterial fate specification is poorly understood. Future investigations will be necessary to provide a coordination in such complexity in order to fully understand this process.

AUTHOR CONTRIBUTIONS

DC wrote a complete draft with figures and legends. MS mentored the writing and revised the draft. MAS wrote section "Shear Stress" and edited the rest of the draft. All authors contributed to the article and approved the submitted version.

FUNDING

This study was supported by the grant National Institutes of Health (NIH) P01 HL107205 (MS and MAS).

REFERENCES

Aitsebaomo, J., Portbury, A. L., Schisler, J. C., and Patterson, C. (2008). Brothers and sisters: molecular insights into arterial-venous heterogeneity. *Circ. Res*. 103, 929–939. doi: 10.1161/circresaha.108.184937

Barry, D. M., Koo, Y., Norden, P. R., Wylie, L. A., Xu, K., Wichaidit, C., et al. (2016). Rasip1-mediated rho gtpase signaling regulates blood vessel tubulogenesis via nonmuscle myosin II. *Circ. Res*. 119, 810–826. doi: 10.1161/circresaha.116.309094

Benedito, R., Roca, C., Sorensen, I., Adams, S., Gossler, A., Fruttiger, M., et al. (2009). The notch ligands dll4 and jagged1 have opposing effects on angiogenesis. *Cell* 137, 1124–1135. doi: 10.1016/j.cell.2009.03.025

Borggrefe, T., and Liefke, R. (2012). Fine-tuning of the intracellular canonical notch signaling pathway. *Cell Cycle* 11, 264–276. doi: 10.4161/cc.11.2.18995

Borggrefe, T., and Oswald, F. (2009). The notch signaling pathway: transcriptional regulation at notch target genes. *Cell. Mol. Life Sci*. 66, 1631–1646. doi: 10.1007/s00018-009-8668-7

Camillo, C., Facchinello, N., Gays, D., Villari, G., Gioelli, N., Sandri, C., et al. (2020). Latrophilin 2 controls vascular morphogenesis and function by inhibiting endothelial cell adhesion and yap/taz mechanosignaling. *bioRxiv [preprint]* 2020.2004.2028.065979. doi: 10.1101/2020.04.28.065979

Caolo, V., van den Akker, N. M., Verbruggen, S., Donners, M. M., Swennen, G., Schulten, H., et al. (2010). Feed-forward signaling by membrane-bound ligand receptor circuit: the case of notch delta-like 4 ligand in endothelial cells. *J. Biol. Chem*. 285, 40681–40689. doi: 10.1074/jbc.m110.176065

Castillo, M., and Alvarez, H. (2011). Artery or vein: to be or not to be? *AJNR Am. J. Neuroradiol*. 32, 791–793.

Cattelino, A., Liebner, S., Gallini, R., Zanetti, A., Balconi, G., Corsi, A., et al. (2003). The conditional inactivation of the beta-catenin gene in endothelial cells causes a defective vascular pattern and increased vascular fragility. *J. Cell. Biol*. 162, 1111–1122. doi: 10.1083/jcb.200212157

Cermenati, S., Moleri, S., Cimbro, S., Corti, P., Del Giacco, L., Amodeo, R., et al. (2008). Sox18 and sox7 play redundant roles in vascular development. *Blood* 111, 2657–2666. doi: 10.1182/blood-2007-07-100412

Chavkin, N. W., Genet, G., Poulet, M., Genet, N., Marziano, C., Vasavada, H., et al. (2020). Endothelial cell cycle state determines propensity for arterial-venous fate. *bioRxiv [preprint]* 2020.2008.2012.246512. doi: 10.1101/2020.08.12.246512

Chen, D., Walsh, K., and Wang, J. (2000). Regulation of cdk2 activity in endothelial cells that are inhibited from growth by cell contact. *Arterioscler Thromb. Vasc. Biol*. 20, 629–635. doi: 10.1161/01.atv.20.3.629

Chen, X., Qin, J., Cheng, C. M., Tsai, M. J., and Tsai, S. Y. (2012). Coup-tfII is a major regulator of cell cycle and notch signaling pathways. *Mol. Endocrinol*. 26, 1268–1277. doi: 10.1210/me.2011-1305

Chen, X., Stoeck, A., Lee, S. J., Shih Ie, M., Wang, M. M., and Wang, T. L. (2010). Jagged1 expression regulated by notch3 and wnt/beta-catenin signaling pathways in ovarian cancer. *Oncotarget* 1, 210–218. doi: 10.18632/oncotarget.127

Chong, D. C., Koo, Y., Xu, K., Fu, S., and Cleaver, O. (2011). Stepwise arteriovenous fate acquisition during mammalian vasculogenesis. *Dev. Dyn*. 240, 2153–2165. doi: 10.1002/dvdy.22706

Conway, D. E., Breckenridge, M. T., Hinde, E., Gratton, E., Chen, C. S., and Schwartz, M. A. (2013). Fluid shear stress on endothelial cells modulates mechanical tension across ve-cadherin and pecam-1. *Curr. Biol*. 23, 1024–1030. doi: 10.1016/j.cub.2013.04.049

Corada, M., Morini, M. F., and Dejana, E. (2014). Signaling pathways in the specification of arteries and veins. *Arterioscler Thromb. Vasc. Biol*. 34, 2372–2377. doi: 10.1161/atvbaha.114.303218

Corada, M., Nyqvist, D., Orsenigo, F., Caprini, A., Giampietro, C., Taketo, M. M., et al. (2010). The wnt/beta-catenin pathway modulates vascular remodeling and specification by upregulating dll4/notch signaling. *Dev. Cell*. 18, 938–949. doi: 10.1016/j.devcel.2010.05.006

Corada, M., Orsenigo, F., Morini, M. F., Pitulescu, M. E., Bhat, G., Nyqvist, D., et al. (2013). Sox17 is indispensable for acquisition and maintenance of arterial identity. *Nat. Commun*. 4:2609.

Coultas, L., Nieuwenhuis, E., Anderson, G. A., Cabezas, J., Nagy, A., Henkelman, R. M., et al. (2010). Hedgehog regulates distinct vascular patterning events through vegf-dependent and -independent mechanisms. *Blood* 116, 653–660. doi: 10.1182/blood-2009-12-256644

Covassin, L. D., Siekmann, A. F., Kacergis, M. C., Laver, E., Moore, J. C., Villefranc, J. A., et al. (2009). A genetic screen for vascular mutants in zebrafish reveals dynamic roles for vegf/plcg1 signaling during artery development. *Dev. Biol*. 329, 212–226. doi: 10.1016/j.ydbio.2009.02.031

Crosby, C. V., Fleming, P. A., Argraves, W. S., Corada, M., Zanetta, L., Dejana, E., et al. (2005). Ve-cadherin is not required for the formation of nascent blood vessels but acts to prevent their disassembly. *Blood* 105, 2771–2776. doi: 10.1182/blood-2004-06-2244

De Smet, F., Segura, I., De Bock, K., Hohensinner, P. J., and Carmeliet, P. (2009). Mechanisms of vessel branching: filopodia on endothelial tip cells lead the way. *Arterioscler Thromb. Vasc. Biol*. 29, 639–649. doi: 10.1161/atvbaha.109.185165

Dejana, E. (2010). The role of wnt signaling in physiological and pathological angiogenesis. *Circ. Res*. 107, 943–952. doi: 10.1161/circresaha.110.223750

Deng, W. M., Althauser, C., and Ruohola-Baker, H. (2001). Notch-delta signaling induces a transition from mitotic cell cycle to endocycle in drosophila follicle cells. *Development* 128, 4737–4746. doi: 10.1242/dev.128.23.4737

Deng, Y., Larrivee, B., Zhuang, Z. W., Atri, D., Moraes, F., Prahst, C., et al. (2013). Endothelial raf1/erk activation regulates arterial morphogenesis. *Blood* 121, 3988–3996. . doi: 10.1182/blood-2012-12-474601

Drake, C. J., and Fleming, P. A. (2000). Vasculogenesis in the day 6.5 to 9.5 mouse embryo. *Blood* 95, 1671–1679. doi: 10.1182/blood.v95.5.1671.005k39_1671_1679

Duarte, A., Hirashima, M., Benedito, R., Trindade, A., Diniz, P., Bekman, E., et al. (2004). Dosage-sensitive requirement for mouse dll4 in artery development. *Genes Dev*. 18, 2474–2478. doi: 10.1101/gad.1239004

Ehling, M., Adams, S., Benedito, R., and Adams, R. H. (2013). Notch controls retinal blood vessel maturation and quiescence. *Development* 140, 3051–3061. doi: 10.1242/dev.093351

Engert, S., Burtscher, I., Liao, W. P., Dulev, S., Schotta, G., and Lickert, H. (2013). Wnt/beta-catenin signalling regulates sox17 expression and is essential for organizer and endoderm formation in the mouse. *Development* 140, 3128–3138. doi: 10.1242/dev.088765

Fang, J. S., Coon, B. G., Gillis, N., Chen, Z., Qiu, J., Chittenden, T. W., et al. (2017). Shear-induced notch-cx37-p27 axis arrests endothelial cell cycle to enable arterial specification. *Nat. Commun*. 8:2149.

Ferguson, J. E. 3rd, Kelley, R. W., and Patterson, C. (2005). Mechanisms of endothelial differentiation in embryonic vasculogenesis. *Arterioscler Thromb. Vasc. Biol*. 25, 2246–2254. doi: 10.1161/01.atv.0000183609.55154.44

Fish, J. E., Cantu Gutierrez, M., Dang, L. T., Khyzha, N., Chen, Z., Veitch, S., et al. (2017). Dynamic regulation of vegf-inducible genes by an erk/erg/p300 transcriptional network. *Development* 144, 2428–2444.

Fish, J. E., and Wythe, J. D. (2015). The molecular regulation of arteriovenous specification and maintenance. *Dev. Dyn*. 244, 391–409. doi: 10.1002/dvdy.24252

Gale, N. W., Dominguez, M. G., Noguera, I., Pan, L., Hughes, V., Valenzuela, D. M., et al. (2004). Haploinsufficiency of delta-like 4 ligand results in embryonic lethality due to major defects in arterial and vascular development. *Proc. Natl. Acad. Sci. U.S.A*. 101, 15949–15954. doi: 10.1073/pnas.0407290101

Garcia, M. D., and Larina, I. V. (2014). Vascular development and hemodynamic force in the mouse yolk sac. *Front. Physiol*. 5:308. doi: 10.3389/fphys.2014.00308

Gariano, R. F., and Gardner, T. W. (2005). Retinal angiogenesis in development and disease. *Nature* 438, 960–966. doi: 10.1038/nature04482

Gerhardt, H. (2008). Vegf and endothelial guidance in angiogenic sprouting. *Organogenesis* 4, 241–246. doi: 10.4161/org.4.4.7414

Gerhardt, H., Golding, M., Fruttiger, M., Ruhrberg, C., Lundkvist, A., Abramsson, A., et al. (2003). Vegf guides angiogenic sprouting utilizing endothelial tip cell filopodia. *J. Cell. Biol*. 161, 1163–1177. doi: 10.1083/jcb.200302047

Gerull, B. (2015). The rapidly evolving role of titin in cardiac physiology and cardiomyopathy. *Can. J. Cardiol*. 31, 1351–1359. doi: 10.1016/j.cjca.2015.08.016

Geudens, I., and Gerhardt, H. (2011). Coordinating cell behaviour during blood vessel formation. *Development* 138, 4569–4583. doi: 10.1242/dev.062323

Givens, C., and Tzima, E. (2016). Endothelial mechanosignaling: does one sensor fit all? *Antioxid Redox Signal* 25, 373–388. doi: 10.1089/ars.2015.6493

Grego-Bessa, J., Luna-Zurita, L., del Monte, G., Bolos, V., Melgar, P., Arandilla, A., et al. (2007). Notch signaling is essential for ventricular chamber development. *Dev. Cell*. 12, 415–429. doi: 10.1016/j.devcel.2006.12.011

Hasan, S. S., Tsaryk, R., Lange, M., Wisniewski, L., Moore, J. C., Lawson, N. D., et al. (2017). Endothelial notch signalling limits angiogenesis via control of artery formation. *Nat. Cell. Biol*. 19, 928–940. doi: 10.1038/ncb3574

Hellstrom, M., Phng, L. K., and Gerhardt, H. (2007a). Vegf and notch signaling: the yin and yang of angiogenic sprouting. *Cell. Adh. Migr*. 1, 133–136. doi: 10.4161/cam.1.3.4978

Hellstrom, M., Phng, L. K., Hofmann, J. J., Wallgard, E., Coultas, L., Lindblom, P., et al. (2007b). Dll4 signalling through notch1 regulates formation of tip cells during angiogenesis. *Nature* 445, 776–780. doi: 10.1038/nature05571

Herman, A. M., Rhyner, A. M., Devine, W. P., Marrelli, S. P., Bruneau, B. G., and Wythe, J. D. (2018). A novel reporter allele for monitoring dll4 expression within the embryonic and adult mouse. *Biol. Open*. 7:bio026799.

Hermkens, D. M., van Impel, A., Urasaki, A., Bussmann, J., Duckers, H. J., and Schulte-Merker, S. (2015). Sox7 controls arterial specification in conjunction with hey2 and efnb2 function. *Development* 142, 1695–1704.

Herpers, R., van de Kamp, E., Duckers, H. J., and Schulte-Merker, S. (2008). Redundant roles for sox7 and sox18 in arteriovenous specification in zebrafish. *Circ. Res*. 102, 12–15. doi: 10.1161/circresaha.107.166066

Hogan, K. A., and Bautch, V. L. (2004). Blood vessel patterning at the embryonic midline. *Curr. Top. Dev. Biol*. 62, 55–85. doi: 10.1016/s0070-2153(04)62003-5

Hong, C. C., Peterson, Q. P., Hong, J. Y., and Peterson, R. T. (2006). Artery/vein specification is governed by opposing phosphatidylinositol-3 kinase and map kinase/erk signaling. *Curr. Biol*. 16, 1366–1372. doi: 10.1016/j.cub.2006.05.046

Hwa, J. J., Beckouche, N., Huang, L., Kram, Y., Lindskog, H., and Wang, R. A. (2017). Abnormal arterial-venous fusions and fate specification in mouse embryos lacking blood flow. *Sci. Rep*. 7:11965.

Ji, Q. S., Winnier, G. E., Niswender, K. D., Horstman, D., Wisdom, R., Magnuson, M. A., et al. (1997). Essential role of the tyrosine kinase substrate phospholipase c-gamma1 in mammalian growth and development. *Proc. Natl. Acad. Sci. U.S.A*. 94, 2999–3003. doi: 10.1073/pnas.94.7.2999

Ji, R. P., Phoon, C. K., Aristizabal, O., McGrath, K. E., Palis, J., and Turnbull, D. H. (2003). Onset of cardiac function during early mouse embryogenesis coincides with entry of primitive erythroblasts into the embryo proper. *Circ. Res*. 92, 133–135. doi: 10.1161/01.res.0000056532.18710.c0

Joshi, I., Minter, L. M., Telfer, J., Demarest, R. M., Capobianco, A. J., Aster, J. C., et al. (2009). Notch signaling mediates g1/s cell-cycle progression in t cells via cyclin d3 and its dependent kinases. *Blood* 113, 1689–1698. doi: 10.1182/blood-2008-03-147967

Kelly, R. G. (2021). Integrating matrix signals during arch artery morphogenesis. *Circ Res*. 128, 360–362. doi: 10.1161/circresaha.121.318669

Kim, K., Kim, I. K., Yang, J. M., Lee, E., Koh, B. I., Song, S., et al. (2016). Soxf transcription factors are positive feedback regulators of vegf signaling. *Circ. Res*. 119, 839–852. doi: 10.1161/circresaha.116.308483

Kolly, C., Suter, M. M., and Muller, E. J. (2005). Proliferation, cell cycle exit, and onset of terminal differentiation in cultured keratinocytes: pre-programmed pathways in control of c-myc and notch1 prevail over extracellular calcium signals. *J. Invest. Dermatol*. 124, 1014–1025. doi: 10.1111/j.0022-202x.2005.23655.x

Kopan, R., and Ilagan, M. X. (2009). The canonical notch signaling pathway: unfolding the activation mechanism. *Cell* 137, 216–233. doi: 10.1016/j.cell.2009.03.045

Krebs, L. T., Shutter, J. R., Tanigaki, K., Honjo, T., Stark, K. L., and Gridley, T. (2004). Haploinsufficient lethality and formation of arteriovenous malformations in notch pathway mutants. *Genes Dev*. 18, 2469–2473. doi: 10.1101/gad.1239204

Krebs, L. T., Xue, Y., Norton, C. R., Shutter, J. R., Maguire, M., Sundberg, J. P., et al. (2000). Notch signaling is essential for vascular morphogenesis in mice. *Genes Dev*. 14, 1343–1352.

Lawson, N. D., Mugford, J. W., Diamond, B. A., and Weinstein, B. M. (2003). Phospholipase c gamma-1 is required downstream of vascular endothelial growth factor during arterial development. *Genes Dev*. 17, 1346–1351. doi: 10.1101/gad.1072203

Lawson, N. D., Scheer, N., Pham, V. N., Kim, C. H., Chitnis, A. B., Campos-Ortega, J. A., et al. (2001). Notch signaling is required for arterial-venous differentiation during embryonic vascular development. *Development* 128, 3675–3683. doi: 10.1242/dev.128.19.3675

Lawson, N. D., Vogel, A. M., and Weinstein, B. M. (2002). Sonic hedgehog and vascular endothelial growth factor act upstream of the notch pathway during arterial endothelial differentiation. *Dev. Cell*. 3, 127–136. doi: 10.1016/s1534-5807(02)00198-3

Li, P., Pashmforoush, M., and Sucov, H. M. (2012). Mesodermal retinoic acid signaling regulates endothelial cell coalescence in caudal pharyngeal arch artery vasculogenesis. *Dev. Biol*. 361, 116–124. doi: 10.1016/j.ydbio.2011.10.018

Liao, H. J., Kume, T., McKay, C., Xu, M. J., Ihle, J. N., and Carpenter, G. (2002). Absence of erythrogenesis and vasculogenesis in plcg1-deficient mice. *J. Biol. Chem*. 277, 9335–9341. doi: 10.1074/jbc.m109955200

Liao, W., Li, G., You, Y., Wan, H., Wu, Q., Wang, C., et al. (2018). Antitumor activity of notch1 inhibition in human colorectal carcinoma cells. *Oncol. Rep*. 39, 1063–1071.

Lin, F. J., Tsai, M. J., and Tsai, S. Y. (2007). Artery and vein formation: a tug of war between different forces. *EMBO Rep*. 8, 920–924. doi: 10.1038/sj.embor.7401076

Lucitti, J. L., Jones, E. A., Huang, C., Chen, J., Fraser, S. E., and Dickinson, M. E. (2007). Vascular remodeling of the mouse yolk sac requires hemodynamic force. *Development* 134, 3317–3326. doi: 10.1242/dev.02883

Mack, J. J., and Iruela-Arispe, M. L. (2018). Notch regulation of the endothelial cell phenotype. *Curr. Opin. Hematol*. 25, 212–218. doi: 10.1097/moh.0000000000000425

Masumura, T., Yamamoto, K., Shimizu, N., Obi, S., and Ando, J. (2009). Shear stress increases expression of the arterial endothelial marker ephrinb2 in murine es cells via the vegf-notch signaling pathways. *Arterioscler Thromb. Vasc. Biol*. 29, 2125–2131. doi: 10.1161/atvbaha.109.193185

Matsui, T., Kanai-Azuma, M., Hara, K., Matoba, S., Hiramatsu, R., Kawakami, H., et al. (2006). Redundant roles of sox17 and sox18 in postnatal angiogenesis in mice. *J. Cell. Sci*. 119, 3513–3526. doi: 10.1242/jcs.03081

May, S. R., Stewart, N. J., Chang, W., and Peterson, A. S. (2004). A titin mutation defines roles for circulation in endothelial morphogenesis. *Dev. Biol*. 270, 31–46. doi: 10.1016/j.ydbio.2004.02.006

McGrath, K. E., Koniski, A. D., Malik, J., and Palis, J. (2003). Circulation is established in a stepwise pattern in the mammalian embryo. *Blood* 101, 1669–1676. doi: 10.1182/blood-2002-08-2531

Moreno-Salinas, A. L., Avila-Zozaya, M., Ugalde-Silva, P., Hernandez-Guzman, D. A., Missirlis, F., and Boucard, A. A. (2019). Latrophilins: a neuro-centric view of an evolutionary conserved adhesion g protein-coupled receptor subfamily. *Front. Neurosci*. 13:700. doi: 10.3389/fnins.2019.00700

Morimura, T., Goitsuka, R., Zhang, Y., Saito, I., Reth, M., and Kitamura, D. (2000). Cell cycle arrest and apoptosis induced by notch1 in b cells. *J. Biol. Chem*. 275, 36523–36531. doi: 10.1074/jbc.m006415200

Nielsen, C. M., Cuervo, H., Ding, V. W., Kong, Y., Huang, E. J., and Wang, R. A. (2014). Deletion of rbpj from postnatal endothelium leads to abnormal arteriovenous shunting in mice. *Development* 141, 3782–3792. doi: 10.1242/dev.108951

Noseda, M., Chang, L., McLean, G., Grim, J. E., Clurman, B. E., Smith, L. L., et al. (2004). Notch activation induces endothelial cell cycle arrest and participates in contact inhibition: role of p21cip1 repression. *Mol. Cell. Biol*. 24, 8813–8822. doi: 10.1128/mcb.24.20.8813-8822.2004

Noseda, M., Niessen, K., McLean, G., Chang, L., and Karsan, A. (2005). Notch-dependent cell cycle arrest is associated with downregulation of minichromosome maintenance proteins. *Circ. Res*. 97, 102–104. doi: 10.1161/01.res.0000174380.06673.81

Okabe, K., Kobayashi, S., Yamada, T., Kurihara, T., Tai-Nagara, I., Miyamoto, T., et al. (2014). Neurons limit angiogenesis by titrating vegf in retina. *Cell* 159, 584–596. doi: 10.1016/j.cell.2014.09.025

Pereira, F. A., Qiu, Y., Zhou, G., Tsai, M. J., and Tsai, S. Y. (1999). The orphan nuclear receptor coup-tfII is required for angiogenesis and heart development. *Genes Dev*. 13, 1037–1049. doi: 10.1101/gad.13.8.1037

Pitulescu, M. E., Schmidt, I., Giaimo, B. D., Antoine, T., Berkenfeld, F., Ferrante, F., et al. (2017). Dll4 and notch signalling couples sprouting angiogenesis and artery formation. *Nat. Cell Biol*. 19, 915–927. doi: 10.1038/ncb3555

Polacheck, W. J., Kutys, M. L., Yang, J., Eyckmans, J., Wu, Y., Vasavada, H., et al. (2017). A non-canonical notch complex regulates adherens junctions and vascular barrier function. *Nature* 552, 258–262. doi: 10.1038/nature24998

Polvani, S., Pepe, S., Milani, S., and Galli, A. (2019). Coup-tfII in health and disease. *Cells* 9:101. doi: 10.3390/cells9010101

Pontes-Quero, S., Fernandez-Chacon, M., Luo, W., Lunella, F. F., Casquero-Garcia, V., Garcia-Gonzalez, I., et al. (2019a). High mitogenic stimulation arrests angiogenesis. *Nat. Commun*. 10:2016.

Pontes-Quero, S., Fernandez-Chacon, M., Luo, W., Lunella, F. F., Casquero-Garcia, V., Garcia-Gonzalez, I., et al. (2019b). Publisher correction: high mitogenic stimulation arrests angiogenesis. *Nat. Commun*. 10:2441.

Qian, C. F., Yan, W., Zhang, J. X., Shi, L., Qian, J., Fu, Z., et al. (2009). Notch1 induces enhanced expression of delta-like-1 in the u251mg glioma cell line. *Int. J. Mol. Med*. 24, 445–451.

Rangarajan, A., Talora, C., Okuyama, R., Nicolas, M., Mammucari, C., Oh, H., et al. (2001). Notch signaling is a direct determinant of keratinocyte growth arrest and entry into differentiation. *EMBO J*. 20, 3427–3436. doi: 10.1093/emboj/20.13.3427

Reaume, A. G., Conlon, R. A., Zirngibl, R., Yamaguchi, T. P., and Rossant, J. (1992). Expression analysis of a notch homologue in the mouse embryo. *Dev. Biol*. 154, 377–387. doi: 10.1016/0012-1606(92)90076-s

Red-Horse, K., and Siekmann, A. F. (2019). Veins and arteries build hierarchical branching patterns differently: bottom-up versus top-down. *Bioessays* 41:e1800198.

Ren, B., Deng, Y., Mukhopadhyay, A., Lanahan, A. A., Zhuang, Z. W., Moodie, K. L., et al. (2010). Erk1/2-akt1 crosstalk regulates arteriogenesis in mice and zebrafish. *J. Clin. Invest*. 120, 1217–1228. doi: 10.1172/jci39837

Risau, W., and Flamme, I. (1995). Vasculogenesis. *Annu. Rev. Cell. Dev. Biol*. 11, 73–91.

Roca, C., and Adams, R. H. (2007). Regulation of vascular morphogenesis by notch signaling. *Genes Dev*. 21, 2511–2524. doi: 10.1101/gad.1589207

Ross, C., and Boroviak, T. E. (2020). Origin and function of the yolk sac in primate embryogenesis. *Nat. Commun*. 11:3760.

Roux, E., Bougaran, P., Dufourcq, P., and Couffinhal, T. (2020). Fluid shear stress sensing by the endothelial layer. *Front. Physiol*. 11:861. doi: 10.3389/fphys.2020.00861

Sakurai, Y., Ohgimoto, K., Kataoka, Y., Yoshida, N., and Shibuya, M. (2005). Essential role of flk-1 (vegf receptor 2) tyrosine residue 1173 in vasculogenesis in mice. *Proc. Natl. Acad. Sci. U.S.A*. 102, 1076–1081. doi: 10.1073/pnas.0404984102

Sato, Y. (2013). Dorsal aorta formation: separate origins, lateral-to-medial migration, and remodeling. *Dev. Growth Differ*. 55, 113–129. doi: 10.1111/dgd.12010

Shah, A. V., Birdsey, G. M., Peghaire, C., Pitulescu, M. E., Dufton, N. P., Yang, Y., et al. (2017). The endothelial transcription factor erg mediates angiopoietin-1-dependent control of notch signalling and vascular stability. *Nat. Commun*. 8:16002.

Shalaby, F., Rossant, J., Yamaguchi, T. P., Gertsenstein, M., Wu, X. F., Breitman, M. L., et al. (1995). Failure of blood-island formation and vasculogenesis in flk-1-deficient mice. *Nature* 376, 62–66. doi: 10.1038/376062a0

Shin, M., Beane, T. J., Quillien, A., Male, I., Zhu, L. J., and Lawson, N. D. (2016). Vegfa signals through erk to promote angiogenesis, but not artery differentiation. *Development* 143, 3796–3805.

Shyu, L. F., Sun, J., Chung, H. M., Huang, Y. C., and Deng, W. M. (2009). Notch signaling and developmental cell-cycle arrest in drosophila polar follicle cells. *Mol. Biol. Cell*. 20, 5064–5073. doi: 10.1091/mbc.e09-01-0004

Simons, M., and Eichmann, A. (2015). Molecular controls of arterial morphogenesis. *Circ. Res*. 116, 1712–1724. doi: 10.1161/circresaha.116.302953

Sorensen, I., Adams, R. H., and Gossler, A. (2009). Dll1-mediated notch activation regulates endothelial identity in mouse fetal arteries. *Blood* 113, 5680–5688. doi: 10.1182/blood-2008-08-174508

Sriuranpong, V., Borges, M. W., Ravi, R. K., Arnold, D. R., Nelkin, B. D., Baylin, S. B., et al. (2001). Notch signaling induces cell cycle arrest in small cell lung cancer cells. *Cancer Res*. 61, 3200–3205.

Stahl, A., Connor, K. M., Sapieha, P., Chen, J., Dennison, R. J., Krah, N. M., et al. (2010). The mouse retina as an angiogenesis model. *Invest. Ophthalmol. Vis. Sci*. 51, 2813–2826.

Su, T., Stanley, G., Sinha, R., D'Amato, G., Das, S., Rhee, S., et al. (2018). Single-cell analysis of early progenitor cells that build coronary arteries. *Nature* 559, 356–362. doi: 10.1038/s41586-018-0288-7

Sweet, D. T., Chen, Z., Givens, C. S., Owens, A. P., Rojas, M., and Tzima, E. (2013). Endothelial shc regulates arteriogenesis through dual control of arterial specification and inflammation via the notch and nuclear factor-kappa-light-chain-enhancer of activated b-cell pathways. *Circ. Res*. 113, 32–39.

Swiatek, P. J., Lindsell, C. E., del Amo, F. F., Weinmaster, G., and Gridley, T. (1994). Notch1 is essential for postimplantation development in mice. *Genes Dev*. 8, 707–719.

Swift, M. R., Pham, V. N., Castranova, D., Bell, K., Poole, R. J., and Weinstein, B. M. (2014). Soxf factors and notch regulate nr2f2 gene expression during venous differentiation in zebrafish. *Dev. Biol*. 390, 116–125.

Swift, M. R., and Weinstein, B. M. (2009). Arterial-venous specification during development. *Circ. Res*. 104, 576–588.

Takahashi, T., Yamaguchi, S., Chida, K., and Shibuya, M. (2001). A single autophosphorylation site on kdr/flk-1 is essential for vegf-a-dependent activation of plc-gamma and DNA synthesis in vascular endothelial cells. *EMBO J*. 20, 2768–2778.

Tammela, T., Zarkada, G., Nurmi, H., Jakobsson, L., Heinolainen, K., Tvorogov, D., et al. (2011). Vegfr-3 controls tip to stalk conversion at vessel fusion sites by reinforcing notch signalling. *Nat. Cell. Biol*. 13, 1202–1213.

Tanaka, K., Joshi, D., Timalsina, S., and Schwartz, M. A. (2021). Early events in endothelial flow sensing. *Cytoskeleton (Hoboken) [Online ahead of print]* doi: 10.1002/cm.21652

Tanaka, K., Prendergast, A., Hintzen, J., Kumar, A., Chung, M., Koleske, A., et al. (2020). Latrophilins are essential for endothelial junctional fluid shear stress mechanotransduction. *bioRxiv [preprint]* 2020.2002.2003.932822. doi: 10.1101/2020.02.03.932822

Tzima, E., Irani-Tehrani, M., Kiosses, W. B., Dejana, E., Schultz, D. A., Engelhardt, B., et al. (2005). A mechanosensory complex that mediates the endothelial cell response to fluid shear stress. *Nature* 437, 426–431.

Ubezio, B., Blanco, R. A., Geudens, I., Stanchi, F., Mathivet, T., Jones, M. L., et al. (2016). Synchronization of endothelial dll4-notch dynamics switch blood vessels from branching to expansion. *Elife* 5:e12167.

Udan, R. S., Vadakkan, T. J., and Dickinson, M. E. (2013). Dynamic responses of endothelial cells to changes in blood flow during vascular remodeling of the mouse yolk sac. *Development* 140, 4041–4050.

Uyttendaele, H., Marazzi, G., Wu, G., Yan, Q., Sassoon, D., and Kitajewski, J. (1996). Notch4/int-3, a mammary proto-oncogene, is an endothelial cell-specific mammalian notch gene. *Development* 122, 2251–2259.

van Engeland, N. C. A., Suarez Rodriguez, F., Rivero-Muller, A., Ristori, T., Duran, C. L., Stassen, O., et al. (2019). Vimentin regulates notch signaling strength and arterial remodeling in response to hemodynamic stress. *Sci. Rep*. 9:12415.

Vijayaraj, P., Le Bras, A., Mitchell, N., Kondo, M., Juliao, S., Wasserman, M., et al. (2012). Erg is a crucial regulator of endocardial-mesenchymal transformation during cardiac valve morphogenesis. *Development* 139, 3973–3985.

Vokes, S. A., Yatskievych, T. A., Heimark, R. L., McMahon, J., McMahon, A. P., Antin, P. B., et al. (2004). Hedgehog signaling is essential for endothelial tube formation during vasculogenesis. *Development* 131, 4371–4380.

Wang, X., Chen, D., Chen, K., Jubran, A., Ramirez, A., and Astrof, S. (2017). Endothelium in the pharyngeal arches 3, 4 and 6 is derived from the second heart field. *Dev. Biol*. 421, 108–117.

Warkala, M., Chen, D., Ramirez, A., Jubran, A., Schonning, M., Wang, X., et al. (2021). Cell-extracellular matrix interactions play multiple essential roles in aortic arch development. *Circ. Res*. 128, e27–e44.

Weng, A. P., Millholland, J. M., Yashiro-Ohtani, Y., Arcangeli, M. L., Lau, A., Wai, C., et al. (2006). C-myc is an important direct target of notch1 in t-cell acute lymphoblastic leukemia/lymphoma. *Genes Dev*. 20, 2096–2109.

Williams, C. K., Li, J. L., Murga, M., Harris, A. L., and Tosato, G. (2006). Up-regulation of the notch ligand delta-like 4 inhibits vegf-induced endothelial cell function. *Blood* 107, 931–939.

Wythe, J. D., Dang, L. T., Devine, W. P., Boudreau, E., Artap, S. T., He, D., et al. (2013). Ets factors regulate vegf-dependent arterial specification. *Dev. Cell*. 26, 45–58.

Xu, C., Hasan, S. S., Schmidt, I., Rocha, S. F., Pitulescu, M. E., Bussmann, J., et al. (2014). Arteries are formed by vein-derived endothelial tip cells. *Nat. Commun*. 5:5758.

Xu, K., and Cleaver, O. (2011). Tubulogenesis during blood vessel formation. *Semin. Cell. Dev. Biol*. 22, 993–1004.

Xu, K., Sacharidou, A., Fu, S., Chong, D. C., Skaug, B., Chen, Z. J., et al. (2011). Blood vessel tubulogenesis requires rasip1 regulation of gtpase signaling. *Dev. Cell*. 20, 526–539.

You, L. R., Lin, F. J., Lee, C. T., DeMayo, F. J., Tsai, M. J., and Tsai, S. Y. (2005). Suppression of notch signalling by the coup-tfII transcription factor regulates vein identity. *Nature* 435, 98–104.

Zarkada, G., Heinolainen, K., Makinen, T., Kubota, Y., and Alitalo, K. (2015). Vegfr3 does not sustain retinal angiogenesis without vegfr2. *Proc. Natl. Acad. Sci. U.S.A.* 112, 761–766.

Zhou, Y., Williams, J., Smallwood, P. M., and Nathans, J. (2015). Sox7, sox17, and sox18 cooperatively regulate vascular development in the mouse retina. *PLoS One* 10:e0143650. doi: 10.1371/journal.pone.0143650

Conflict of Interest: The authors declare that the research was conducted in the absence of any commercial or financial relationships that could be construed as a potential conflict of interest.

Copyright © 2021 Chen, Schwartz and Simons. This is an open-access article distributed under the terms of the Creative Commons Attribution License (CC BY). The use, distribution or reproduction in other forums is permitted, provided the original author(s) and the copyright owner(s) are credited and that the original publication in this journal is cited, in accordance with accepted academic practice. No use, distribution or reproduction is permitted which does not comply with these terms.

frontiers in Cell and Developmental Biology

MINI REVIEW
published: 01 July 2021
doi: 10.3389/fcell.2021.697130

Endothelial-Myocardial Angiocrine Signaling in Heart Development

*Hyeonyu Kim[1,2], Mingqiang Wang[1,2] and David T. Paik[1,2]**

[1] Stanford Cardiovascular Institute, Stanford University, Stanford, CA, United States, [2] Department of Medicine, Division of Cardiovascular Medicine, Stanford University School of Medicine, Stanford, CA, United States

Vascular endothelial cells are a multifunctional cell type with organotypic specificity in their function and structure. In this review, we discuss various subpopulations of endothelial cells in the mammalian heart, which spatiotemporally regulate critical cellular and molecular processes of heart development via unique sets of angiocrine signaling pathways. In particular, elucidation of intercellular communication among the functional cell types in the developing heart has recently been accelerated by the use of single-cell sequencing. Specifically, we overview the heterogeneic nature of cardiac endothelial cells and their contribution to heart tube and chamber formation, myocardial trabeculation and compaction, and endocardial cushion and valve formation via angiocrine pathways.

Keywords: endothelial cell, cardiac development, single-cell sequencing, myocardial compaction, cardiomyocyte

OPEN ACCESS

Edited by:
Xiaofeng Yang,
Temple University, United States

Reviewed by:
Kai Jiao,
University of Alabama at Birmingham, United States
Riikka Kivelä,
University of Jyväskylä, Finland

***Correspondence:**
David T. Paik
dtpaik@stanford.edu

Specialty section:
This article was submitted to Signaling, a section of the journal Frontiers in Cell and Developmental Biology

Received: *18 April 2021*
Accepted: *10 June 2021*
Published: *01 July 2021*

Citation:
Kim H, Wang M and Paik DT (2021) Endothelial-Myocardial Angiocrine Signaling in Heart Development. Front. Cell Dev. Biol. 9:697130. doi: 10.3389/fcell.2021.697130

INTRODUCTION

Vascular endothelial cells, which compose the innermost lining of blood vessels, are a multifunctional cell type that dynamically governs tissue function and homeostasis by regulating blood flow, vascular tone, oxygen and nutrient transport, inflammation, and delivery of plasma-borne macromolecules (Aird, 2007; Ricard et al., 2021). Contingent upon the type of tissue or the organ of residence, endothelial cells exhibit a significant level of cellular, molecular, and functional heterogeneity (Augustin and Koh, 2017). Moreover, these organ-specific roles of the endothelial cells are manifested by the unique gene expression signatures that correspond to the organotypic characteristics of the local tissue (Ricard et al., 2021). Recent advances in single-cell sequencing techniques have particularly been advantageous in accelerating our understanding of the organotypic specificity of endothelial cells, as they have been able to eschew the critical limitations of primary endothelial cell culture where removal of endothelial cells from their local microenvironment rapidly promotes endothelial-to-mesenchymal transition (EndoMT) and thereby alters the identity and function of the isolated endothelial cells (Jakab and Augustin, 2020; Paik et al., 2020a). For example, single-cell RNA-sequencing of endothelial cells isolated from 11 major tissues of adult mice led to the profiling of transcriptomic features of quiescent arterial, venous, capillary, and lymphatic endothelial cells (Kalucka et al., 2020), and similarly an organism-wide analysis of *Tabula Muris* dataset unveiled novel markers of organ- and sex-specific endothelial cells in major organs of adult mice (Paik et al., 2020b). Notably, these single-cell transcriptome studies employed predictive analysis of intercellular communication, whereby unique sets of angiocrine (i.e., secreted) factors from endothelial cells were identified in each of the organs investigated.

In this review, we focus on the angiocrine role of heart-specific endothelial cells in cardiac development and the pathological conditions that arise from dysregulation of the

cardiac endothelium. Mammalian heart development encompasses coordinated, spatiotemporal interactions of several cell types in a highly orchestrated manner. Consequently, dysregulation in the intercellular communication or improper generation of any one of the cell types can lead to congenital heart defects and pathological phenotypes (Daniela et al., 2010), which we discuss in this review.

HETEROGENEITY OF CARDIAC ENDOTHELIAL CELLS

In the mammalian heart, endothelial cells are the most abundant cell type next to cardiomyocytes and cardiac fibroblasts, occupying approximately 12 and 8% in cell number in atria and ventricles, respectively (Litviňuková et al., 2020). The precise role of cardiac endothelial cells in cardiac development varies by the specialized function of their subpopulations. Traditionally, pan-endothelial cells in the heart have been identified by the expression of cluster of differentiation 31 (CD31), CD34, CD105 (endoglin), CD144 (vascular endothelial cadherin), CD309 (vascular endothelial growth factor receptor 2), and endothelial nitric oxide synthase (Pratumvinit et al., 2013). Subpopulations of cardiac endothelial cells are classified based on their spatial location in the heart and their gene expression profile (Chen et al., 2014). Endocardial cells for example are specialized endothelial cells unique to the developing heart, which act as a barrier between blood and myocardium in the innermost part of the heart tissue. Endocardial cells are identified by expression of nuclear factor in activated T-cell, cytoplasmic 1 (Nfatc1; de la Pompa et al., 1998; Ranger et al., 1998), natriuretic peptide receptor 3 (Npr3; Hui et al., 2016), and cytokine-like protein 1 (Cytl1; Feng et al., 2019). Coronary endothelial cells expressing apelin (Apln; Tian et al., 2014), fatty acid-binding protein 4 (Fabp4; He et al., 2014), and CD36 (Feng et al., 2019) create and maintain coronary vessels within the myocardium, providing oxygen and nutrients to parenchymal cells and removing waste products. In addition to these two cell types, endothelial cells of the aorta have been shown to express EH domain-containing 3 and family with sequence similarity 167 member B (Fam167b; Feng et al., 2019). Finally, lymphatic endothelial cells that exist in a relatively small number in the heart are marked by the expression of podoplanin (Pdpn; Cimini et al., 2019).

ROLE OF ENDOTHELIAL CELLS IN HEART TUBE AND CHAMBER FORMATION

During cardiac development, cardiac progenitors from the mesodermal primitive streak differentiate into a cardiac crescent, then form a linear heart tube (Clowes et al., 2014). The heart tube has the endocardium as the inner layer and the myocardium as the outer layer, and these two layers are separated by an acellular extracellular matrix (ECM) layer called the cardiac jelly (Eisenberg and Markwald, 1995). Using lineage tracing in mice, endocardium was reported to arise from a precardiac progenitor in the late primitive streak expressing fetal liver kinase 1 (Flk1; Ema et al., 2006; Harris and Black, 2010). Vascular endothelial cells derived from myocardial lineages in the second heart field progenitors were also found to partially contribute to endocardium formation (Verzi et al., 2005; Milgrom-Hoffman et al., 2011). Once the linear heart tube elongates, it undergoes dextral looping and forms chambers through ballooning. During the cardiac chamber ballooning, proliferation of cardiomyocytes is favored in the outer curvature of the heart tube than in the inner curvature, and it has been suggested that this asymmetrical formation of the heart tube is mediated by mechanotransduction via Krüppel-like factor 2 (Klf2). Hence, greater wall shear stress is applied by blood flow on the endocardium in the inner curvature than on the cells in the outer curvature (**Figure 1A**), which further activates Klf2 that functions as a sensor of fluid shear stress through cilia, Polycystins 2, and Trpv4 (Heckel et al., 2015). Expression of Klf2 gene subsequently activates Notch signaling (Li et al., 2020), and it renders a central role in EndoMT in the ventral atrioventricular endocardial cushion (Chang et al., 2011) and the inner curvature (Camenisch et al., 2010). However, more monocilia are present in the outer curvature than the inner curvature (Van der Heiden et al., 2006; Hierck et al., 2008), and hence it has been speculated that Flf2 activation in the inner curvature is mediated by ion channels instead of cilia. However, more detailed mechanisms of the effects of lower shear stress and more cilia in the outer curvature on cardiac chamber ballooning by the enhanced proliferation of cardiomyocytes are to be elucidated.

TRABECULATION AND COMPACTION OF MYOCARDIUM

Trabeculae are bundles of cardiomyocytes protruding from the inner wall of the ventricular chamber. The function of trabeculae is to rapidly increase the number of cardiomyocytes in the ventricular chamber and to facilitate oxygen and nutrient exchange in the myocardium via diffusion with their greater surface area prior to the vascularization by the coronary endothelial cells (Sedmera et al., 2000; Pérez-Pomares and de la Pompa, 2011). Trabeculation, or the formation of trabeculae, is initiated as the endocardial endothelial cells lining the inside of the heart tube penetrate the cardiac jelly in the ventricular outer curvature (Männer and Yelbuz, 2019). In mouse embryos, endocardial cells penetrated the cardiac jelly to reach the myocardium after Notch signaling was activated in the endocardium of the ventricular chamber (Grego-Bessa et al., 2007). As endocardial ridges are generated between the touchdowns between the endocardium and myocardium, a layer of the cardiac jelly becomes ECM bubbles (**Figure 1B**). Subsequently, the trabecular cardiomyocytes enclosed in the ECM bubble start to proliferate, and the trabecular unit grows long toward the ventricular lumen (del Monte-Nieto et al., 2018).

The ECM in the ECM bubble almost disappears as the ECM proteolytic genes ADAM metallopeptidase 1 (Adamts1), matrix metallopeptidase 2 (Mmp2), and hyaluronidase 2 (Hyal2) are activated in the endocardium. During this process, Notch1

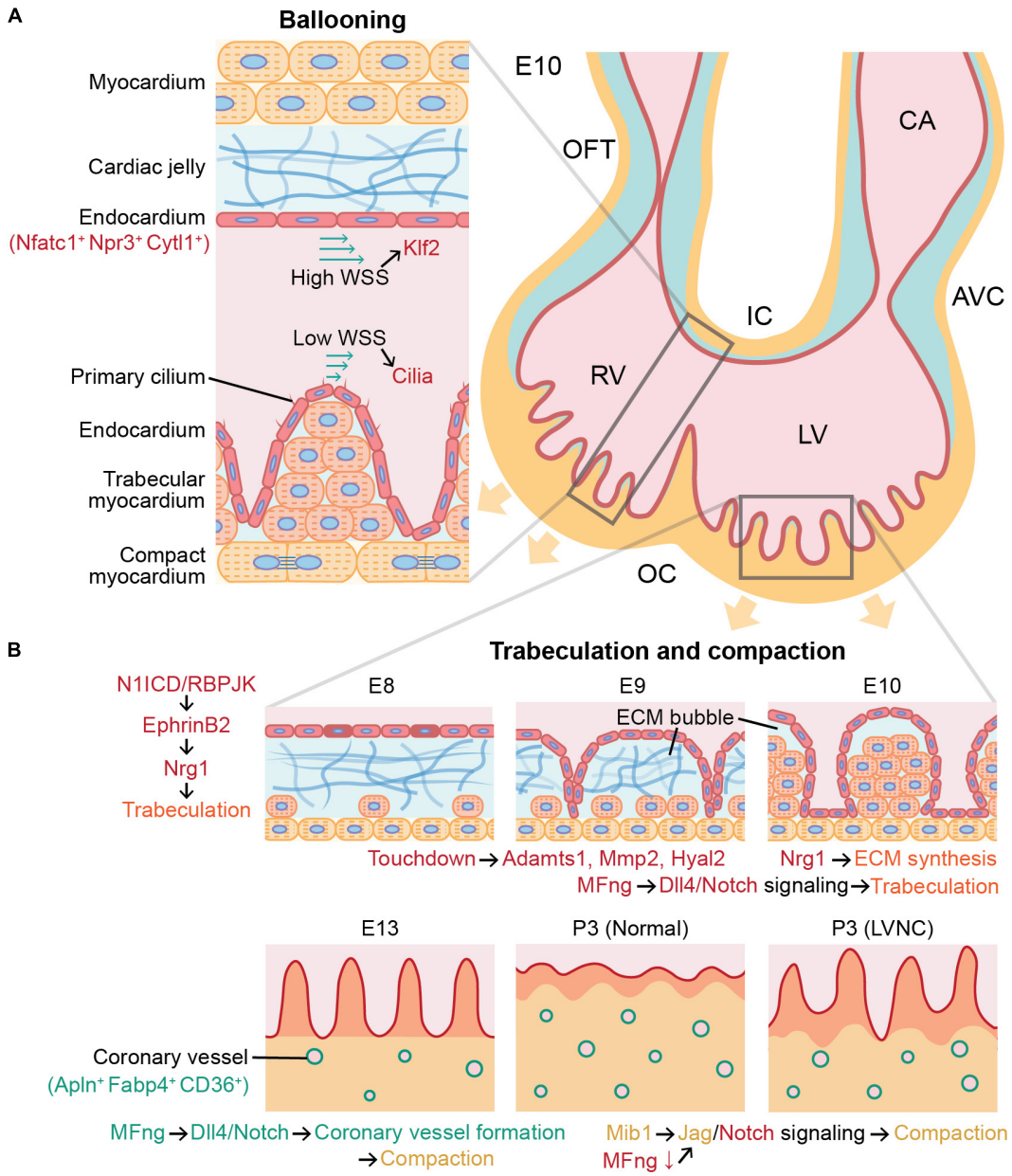

FIGURE 1 | Role of angiocrine signaling in cardiac chamber ballooning, trabeculation, and compaction during cardiac development. Angiocrine signaling of cardiac endothelial cells governs major cellular and molecular processes in mammalian heart development. **(A)** Ballooning is achieved by more active proliferation in the outer curvature (OC) than in the inner curvature (IC), and this asymmetric proliferation between the inner and outer curvatures is associated with Klf2 and cilia signaling in endocardial cells activated by wall shear stress (WSS). **(B)** Initiation of trabeculation and growth of trabeculae (orange) in ECM bubble are regulated by Nrg1 secreted by endocardial cells (red). After trabeculation, compaction requires angiocrine signaling in both coronary endothelial cells (green) and endocardial cells (red). Endothelial dysfunction can cause left ventricular noncompaction (LVNC). Trabecular and compact cardiomyocytes are indicated in orange and yellow, respectively. E10, mouse embryonic day 10; OFT, outflow tract; RV, right ventricle; LV, left ventricle; CA, common atrium; AVC, atrioventricular canal; ECM, extracellular matrix; and P3, postnatal day 3.

intracellular domain (N1ICD)/RBPJK induces the secretion of neuregulin 1 (Nrg1) by activating EphrinB2 in endocardial cells (Grego-Bessa et al., 2007; **Figure 1B**). Nrg1 plays an important role in the growth of trabeculae through paracrine signaling by promoting proliferation of trabecular cardiomyocytes through ErbB2/4 in the myocardium (Liu et al., 2010). This was confirmed by Nrg1, ErbB2, and ErbB4 null mice that did not form trabeculae in ventricular chambers (Yarden and Sliwkowski, 2001). In addition, Nrg1 promotes ECM synthesis and formation of apical ECM bubbles required for rearrangement and growth of trabeculae (del Monte-Nieto et al., 2018), and the trabeculation was poorly developed in the Notch1 mutants

(Grego-Bessa et al., 2007). The ECM secretion by endothelial cells during trabeculation has been confirmed by the single-cell RNA sequencing results of E9.5 and E11.5 mouse heart undergoing trabeculation that showed the high expression of hyaluronan and proteoglycan link protein 1 (Hapln1), a key regulator in developmental ECM interactions in ventricular endothelial cells (DeLaughter et al., 2016).

Moreover, bone morphogenetic protein 10 (Bmp10) is highly expressed in trabecular myocardium and is known to play an important role in trabeculae growth but not in the initiation of trabeculation (Chen et al., 2004). Activation of Bmp10 is also independent of EphrinB2 and Nrg1 expression during trabeculation (Grego-Bessa et al., 2007). Following the trabeculae growth, hypertrabeculation is prevented by endocardial Tie2 expression, which inhibits proliferation of cardiomyocytes (Qu et al., 2019). Single-cell analysis of the ligand-receptor pairs between cardiomyocytes and endocardial cells in E10.5 mouse heart also showed that expression of transforming growth factor beta 1 (Tgfb1), previously characterized to inhibit proliferation of cardiomyocytes, was specifically identified in endocardial cells, and expression of its receptors Tgfbr1 and Tgfbr3 was found in cardiomyocytes (Li et al., 2019). Together, these findings therefore indicate that endocardial cells play a major role in the formation of trabeculae by dynamically regulating promotion and inhibition of cardiomyocyte proliferation and ECM degradation.

At 6–7 weeks of gestation in human and E13.5 in mice, these trabecular structures undergo a compaction process that thickens the ventricular myocardium and smoothens the endocardial surface (Sedmera et al., 2000; MacGrogan et al., 2018). At this time, the myocardium can be divided into trabecular myocardium expressing Nppa in the inner part of the ventricular myocardium and compact myocardium expressing Hey2 in the outer part (Tian et al., 2017). When the myocardium becomes thicker than the diffusion limit due to the rapid proliferation of cardiomyocytes, a hypoxic environment facilitates the formation of coronary vessels in the compact myocardium for the exchange of oxygen and nutrients (Tian et al., 2014; MacGrogan et al., 2018). Using lineage-tracing and clonal analysis tools, it has been revealed that the origin of most coronary endothelial cells is pan-endocardium (Wu et al., 2012; Hui et al., 2018), and about 10% of them are from proepicardium (Katz et al., 2012; Cano et al., 2016). This compaction is continued until postnatal day 28 in mice (Tian et al., 2017), and while some coronary endothelial cells of the postnatal heart are not expanded from embryonic coronary endothelial cells but instead converted from ventricular endocardial cells in the inner part of the myocardium (Tian et al., 2014). Similar to trabeculation, compaction is also largely influenced by endothelial cells through paracrine signaling, and defects in this process can lead to cardiomyopathies such as in the form of left ventricular noncompaction (Wengrofsky et al., 2019).

In autocrine and paracrine signaling during heart development, the Fringe family of glycosyltransferases attaches to the Notch and contributes to ligand selectivity (Panin et al., 1997). In particular, β-1,3-N-Acetylglucosaminyltransferase manic fringe (MFng) modulates the spatiotemporal specificity of Notch-receptor interactions by enhancing Dll4-Notch1 signaling and diminishing Jag-Notch signaling through glycosylation (Panin et al., 1997; Yang et al., 2004; D'Amato et al., 2016b). Expression of MFng is promoted in endocardial during trabeculation, but is required to be down-regulated during compaction to activate myocardial Jag1 and Jag2 signaling to Notch1. In addition to inactivation of MFng, activation of Mib1 gene up-regulates Jag1 in compact cardiomyocytes (D'Amato et al., 2016a). Since Jag1 expression is important for compaction, inactivation of Mib1 causes abnormally thin compact myocardium and large noncompacted trabeculae in mice (Luxán et al., 2013). On the other hand, activation of Dll4 by MFng activation in coronary endothelial cells is required for coronary vessel formation, which is needed for proper myocardial compaction (D'Amato et al., 2016b; Rhee et al., 2018). Therefore, MFng, which promotes Dll4-Notch signaling, must be activated or inactivated depending on the specific type of cardiac endothelial cells for the correct compaction process. In addition, deletion of Jarid2 in both coronary endothelial and endocardial cells increases the methylation at the Notch1 (Mysliwiec et al., 2012) and leads to noncompaction and hypertrabeculation of ventricular myocardium (Mysliwiec et al., 2011).

Compact cardiomyocytes are known to proliferate faster than trabecular cardiomyocytes, which is associated with myocardial growth supported by coronary endothelial cells independent of a blood flow (Giordano et al., 2001; Rhee et al., 2018). These studies show that both endocardial and coronary endothelial cells can impact myocardial compaction via angiocrine pathways by regulating proliferation and cellular maturation of cardiomyocytes. The signaling pathways involved in trabeculation and compaction have been elucidated in *in vivo* models of mice, chicken, and zebrafish, but the detailed mechanisms of spatially restricted cue from the myocardium for the initiation of endocardial cell sprouting and angiocrine signaling between compact cardiomyocytes and coronary endothelial cells are not yet defined.

ENDOCARDIAL CUSHION AND VALVE FORMATION

Following the looping of the heart tube, endocardial cushions are formed by expanding the cardiac jelly between the endocardium and the myocardium (Homan et al., 2019). In the embryonic heart, the endocardial cushions at the atrioventricular canal (AVC) and outflow tract (OFT) develop into atrioventricular (mitral/tricuspid) valves and semilunar (aortic/pulmonic) valves, respectively (Lin et al., 2012). When the valve formation is initiated, valve endothelial cells, a subpopulation of endocardium expressing JB3 (Wunsch et al., 1994) and lining the AVC and OFT, exhibit activated Dll4-Notch signaling (**Figure 2**). In the AVC, endocardial Notch1 signaling activates Wnt4 to induce Bmp2 expression in the adjacent myocardium (Wang et al., 2013). Mouse model studies in loss-of-function or gain-of-function of Notch1 and Bmp2 confirmed that expression of both Bmp2 in the AVC myocardium and N1ICD in the endocardium are required to induce EndoMT (Kisanuki et al.,

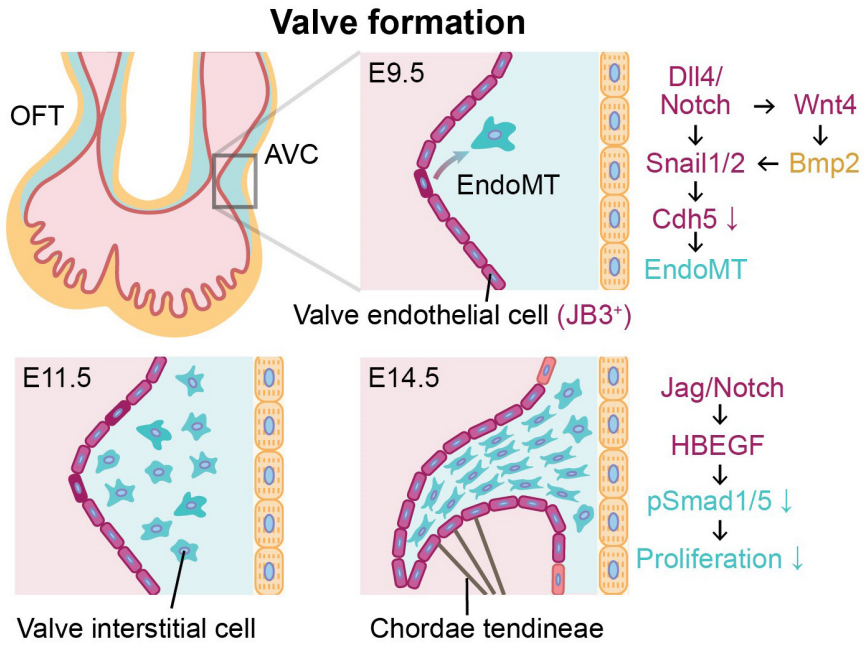

FIGURE 2 | Endothelial-to-mesenchymal transition (EndoMT) of valve endothelial cells expressing JB3 and angiocrine signaling during valve formation between E9.5 and E14.5. Valve formation is initiated by EndoMT of valve endothelial cells (purple) to become valve interstitial cells (blue) in cardiac jelly. During valve formation, the cushion is remodeled and elongated by valve interstitial cells, and the mature valve leaflet is supported by chordae tendineae. Endocardial cells and cardiomyocytes are indicated in red and yellow, respectively. OFT, outflow tract; AVC, atrioventricular canal; E9.5, E11.5, E14.5, mouse embryonic day 9.5, 11.5, 14.5, respectively.

2001; Luna-Zurita et al., 2010; Papoutsi et al., 2018). Notch activation also triggers upregulation of Snail1 and Snail2 expression (Donal et al., 2016) known to inhibit VE-cadherin (Cdh5) whose role is to regulate cell adhesion and cell-to-cell interactions of endocardial cells (Timmerman et al., 2004). Thus, down-regulation of Cdh5 reduces cell-cell contacts between endocardial cells and activates EndoMT. In addition to Notch signaling, Bmp2 has been shown to dramatically up-regulate Snail1 and Snail2 while down-regulating Slug in valve endothelial cells (Niessen et al., 2008). This subsequently leads to decreased expression of Cdh1 and Cdh5, which then promotes EndoMT (Niessen et al., 2008; Kroepil et al., 2012). In addition, expression of Slug in valve endothelial cells induces their migration by repressing VE-cadherin. Therefore, Snail and Slug regulate the initiation of cardiac cushion cellularization by inducing EndoMT (Niessen et al., 2008). Inactivation of Bmp receptor Alk2 in endothelial cells on the other hand results in cardiac cushion EndoMT defects from reduced expression of Snail, but not Slug and Hey2 (Niessen et al., 2008).

Recently, single-cell transcriptomic analysis of valve endothelial cells in the transition state demonstrated that EndoMT was related to PI3K-Akt signaling pathway and AGE-RAGE signaling (Kang et al., 2020). These endocardial-derived valve interstitial cells (VICs) invade the cardiac jelly, proliferate, and remodel the endocardial cushions to form thin elongate valve leaflets (Xiong et al., 2012). With cellular trajectory analysis from single-cell RNA-seq of aortic valve leaflets in calcific aortic valve disease (CAVD) patients, it has been reported that valve endothelial cells may participate in the calcification and thickening of aortic valve disease though more active EndoMT, demonstrated by greater expressions of secreted protein acidic and rich in cysteine and mesenchymal markers (Col1A1 and Cnn1) in transformed valve endothelial cells of CAVD patients than healthy controls (Kang et al., 2020). In the later stages of valve formation, activation of Jag1-Notch1 signaling causes increased Hbegf expression in the endocardium. This inhibits Bmp-phosphorylated Smad1/5 (p-Smad1/5) signaling to restrict proliferation of VICs in cardiac jelly (Donal et al., 2016). Moreover, Jag1 mutants resulted in dysmorphic and thicker valve leaflets due to uncontrolled proliferation of the VICs (Donal et al., 2016). These studies indicate that the investigation of paracrine signaling between the valve endothelial cells and the myocardium should be performed in a spatiotemporally controlled manner to obtain organized and well-functioning heart valves. As the majority of these findings to date have been obtained from animal models, future studies using human induced pluripotent stem cell or 3-dimensional *in vitro* tissue engineering models for embryonic human heart combining with single-cell analysis will be necessary to corroborate and to translate to human cardiac development and disease mechanisms.

CONCLUSION

Angiocrine signaling of cardiac endothelial cells dynamically regulates proliferation and cellular maturation of cardiomyocytes and formation of endocardial cushion during mammalian heart development, playing a critical role in all phases of cardiogenesis.

In this review, we described the angiocrine role of subpopulations of cardiac endothelial cells, including endocardial cells, coronary endothelial cells, and valve endothelial cells during cardiac development reported to date. Nonetheless, the heterogeneic nature of angiocrine signaling within the cardiac arterial, venous, and lymphatic endothelial cells remains poorly understood. Utilizing single-cell omics tools will enable profiling of specialized cell populations and heterogeneity with prediction of intercellular communication, further advancing our understanding of angiocrine function of endothelial cells in cardiac development, homeostasis, and disease. In addition, ongoing clinical trials will reveal whether therapeutics developed based on endocardial-myocardial angiocrine signaling will be effective in combatting human cardiovascular disease, as certain small-molecule candidates associated with nitric oxide-mediated and neuregulin-mediated pathways have been reported to demonstrate a reduction in mortality and improved cardiac output in heart failure patients in early phase clinical trials (Lim et al., 2015). Consequently, thorough elucidation of the role of angiocrine signaling in congenital heart disease will shed light on developing therapeutic strategies using genetic interventions.

AUTHOR CONTRIBUTIONS

HK wrote and revised the manuscript and generated the figures. MW and DP wrote, revised, and approved the submitted version of the manuscript. All authors contributed to the article and approved the submitted version.

FUNDING

We are grateful for funding support from the American Heart Association grant 20POST35210896 (HK) and National Institutes of Health K99 HL150216 and Stanford Cardiovascular Institute Seed Grant (DP).

REFERENCES

Aird, W. C. (2007). Phenotypic heterogeneity of the endothelium. *Circ. Res.* 100, 158–173. doi: 10.1161/01.RES.0000255691.76142.4a

Augustin, H. G., and Koh, G. Y. (2017). Organotypic vasculature: from descriptive heterogeneity to functional pathophysiology. *Science* 357:eaal2379. doi: 10.1126/science.aal2379

Camenisch, T. D., Runyan, R. B., and Markwald, R. R. (2010). "Chapter 6.1–Molecular regulation of cushion morphogenesis," in *Heart Development and Regeneration*, eds N. Rosenthal and R. Harvey (Bostonm MA: Academic Press), 363–387. doi: 10.1016/B978-0-12-381332-9.00018-9

Cano, E., Carmona, R., Ruiz-Villalba, A., Rojas, A., Chau, Y.-Y., Wagner, K. D., et al. (2016). Extracardiac septum transversum/proepicardial endothelial cells pattern embryonic coronary arterio–venous connections. *Proc. Natl. Acad. Sci. U.S.A.* 113, 656–661. doi: 10.1073/pnas.1509834113

Chang, A. C. Y., Fu, Y., Garside, V. C., Niessen, K., Chang, L., Fuller, M., et al. (2011). Notch initiates the endothelial-to-mesenchymal transition in the atrioventricular canal through autocrine activation of soluble guanylyl cyclase. *Dev. Cell* 21, 288–300. doi: 10.1016/j.devcel.2011.06.022

Chen, H., Shi, S., Acosta, L., Li, W., Lu, J., Bao, S., et al. (2004). BMP10 is essential for maintaining cardiac growth during murine cardiogenesis. *Development* 131, 2219–2231. doi: 10.1242/dev.01094

Chen, H. I., Sharma, B., Akerberg, B. N., Numi, H. J., Kivelä, R., Saharinen, P., et al. (2014). The sinus venosus contributes to coronary vasculature through VEGFC-stimulated angiogenesis. *Development* 141, 4500–4512. doi: 10.1242/dev.113639

Cimini, M., Garikipati, V. N. S., de Lucia, C., Cheng, Z., Wang, C., Truongcao, M. M., et al. (2019). Podoplanin neutralization improves cardiac remodeling and function after myocardial infarction. *JCI Insight* 4:e126967. doi: 10.1172/jci.insight.126967

Clowes, C., Boylan, M. G. S., Ridge, L. A., Barnes, E., Wright, J. A., and Hentges, K. E. (2014). The functional diversity of essential genes required for mammalian cardiac development. *Genesis* 52, 713–737. doi: 10.1002/dvg.22794

D'Amato, G., Luxán, G., and de la Pompa, J. L. (2016a). Notch signalling in ventricular chamber development and cardiomyopathy. *FEBS J.* 283, 4223–4237. doi: 10.1111/febs.13773

D'Amato, G., Luxán, G., del Monte-Nieto, G., Martínez-Poveda, B., Torroja, C., Walter, W., et al. (2016b). Sequential Notch activation regulates ventricular chamber development. *Nat. Cell Biol.* 18, 7–20. doi: 10.1038/ncb3280

Daniela, T., Giordano, F. J., and Michael, S. (2010). Cell communications in the heart. *Circulation* 122, 928–937. doi: 10.1161/CIRCULATIONAHA.108.847731

de la Pompa, J. L., Timmerman, L. A., Takimoto, H., Yoshida, H., Elia, A. J., Samper, E., et al. (1998). Role of the NF-ATc transcription factor in morphogenesis of cardiac valves and septum. *Nature* 392, 182–186. doi: 10.1038/32419

del Monte-Nieto, G., Ramialison, M., Adam, A. A. S., Wu, B., Aharonov, A., D'Uva, G., et al. (2018). Control of cardiac jelly dynamics by NOTCH1 and NRG1 defines the building plan for trabeculation. *Nature* 557, 439–445. doi: 10.1038/s41586-018-0110-6

DeLaughter, D. M., Bick, A. G., Wakimoto, H., McKean, D., Gorham, J. M., Kathiriya, I. S., et al. (2016). Single-cell resolution of temporal gene expression during heart development. *Dev. Cell* 39, 480–490. doi: 10.1016/j.devcel.2016.10.001

Donal, M., Gaetano, D., Stanislao, T., Beatriz, M.-P., Guillermo, L., Gonzalo del, M.-N., et al. (2016). Sequential ligand-dependent Notch signaling activation regulates valve primordium formation and morphogenesis. *Circ. Res.* 118, 1480–1497. doi: 10.1161/CIRCRESAHA.115.308077

Eisenberg, L. M., and Markwald, R. R. (1995). Molecular regulation of atrioventricular valvuloseptal morphogenesis. *Circ. Res.* 77, 1–6. doi: 10.1161/01.RES.77.1.1

Ema, M., Takahashi, S., and Rossant, J. (2006). Deletion of the selection cassette, but not cis-acting elements, in targeted Flk1-lacZ allele reveals Flk1 expression in multipotent mesodermal progenitors. *Blood* 107, 111–117. doi: 10.1182/blood-2005-05-1970

Feng, W., Chen, L., Nguyen, P. K., Wu, S. M., and Li, G. (2019). Single cell analysis of endothelial cells identified organ-specific molecular signatures and heart-specific cell populations and molecular features. *Front. Cardiovasc. Med.* 6:165. doi: 10.3389/fcvm.2019.00165

Giordano, F. J., Gerber, H.-P., Williams, S.-P., VanBruggen, N., Bunting, S., Ruiz-Lozano, P., et al. (2001). A cardiac myocyte vascular endothelial growth factor paracrine pathway is required to maintain cardiac function. *Proc. Natl. Acad. Sci. U.S.A.* 98, 5780–5785. doi: 10.1073/pnas.091415198

Grego-Bessa, J., Luna-Zurita, L., del Monte, G., Bolós, V., Melgar, P., Arandilla, A., et al. (2007). Notch signaling is essential for ventricular chamber development. *Dev. Cell* 12, 415–429. doi: 10.1016/j.devcel.2006.12.011

Harris, I. S., and Black, B. L. (2010). Development of the endocardium. *Pediatr. Cardiol.* 31, 391–399. doi: 10.1007/s00246-010-9642-8

He, L., Tian, X., Zhang, H., Wythe, J. D., and Zhou, B. (2014). Fabp4-CreER lineage tracing revealstwo distinctive coronary vascular populations. *J. Cell. Mol. Med.* 18, 2152–2156. doi: 10.1111/jcmm.12415

Heckel, E., Boselli, F., Roth, S., Krudewig, A., Belting, H.-G., Charvin, G., et al. (2015). Oscillatory flow modulates mechanosensitive klf2a expression through trpv4 and trpp2 during heart valve development. *Curr. Biol.* 25, 1354–1361. doi: 10.1016/j.cub.2015.03.038

Hierck, B. P., Van der Heiden, K., Poelma, C., Westerweel, J., and Poelmann, R. E. (2008). Fluid shear stress and inner curvature remodeling of the embryonic heart. Choosing the right lane! *ScientificWorldJournal*. 8:939501. doi: 10.1100/tsw.2008.42

Homan, K. A., Gupta, N., Kroll, K. T., Kolesky, D. B., Skylar-Scott, M., Miyoshi, T., et al. (2019). Flow-enhanced vascularization and maturation of kidney organoids in vitro. *Nat. Methods* 16, 255–262. doi: 10.1038/s41592-019-0325-y

Hui, Z., Lui, K. O., and Bin, Z. (2018). Endocardial cell plasticity in cardiac development, diseases and regeneration. *Circ. Res.* 122, 774–789. doi: 10.1161/CIRCRESAHA.117.312136

Hui, Z., Wenjuan, P., Guang, L., Xiuzhen, H., Lingjuan, H., Xueying, T., et al. (2016). Endocardium minimally contributes to coronary endothelium in the embryonic ventricular free walls. *Circ. Res.* 118, 1880–1893. doi: 10.1161/CIRCRESAHA.116.308749

Jakab, M., and Augustin, H. G. (2020). Understanding angiodiversity: insights from single cell biology. *Development* 147:dev146621. doi: 10.1242/dev.146621

Kalucka, J., de Rooij, L. P. M. H., Goveia, J., Rohlenova, K., Dumas, S. J., Meta, E., et al. (2020). Single-cell transcriptome atlas of murine endothelial cells. *Cell* 180, 764–779.e20. doi: 10.1016/j.cell.2020.01.015

Kang, X., Shangbo, X., Yuming, H., Tingwen, Z., Ming, L., Peng, Z., et al. (2020). Cell-type transcriptome atlas of human aortic valves reveal cell heterogeneity and endothelial to mesenchymal transition involved in calcific aortic valve disease. *Arterioscler. Thromb. Vasc. Biol.* 40, 2910–2921. doi: 10.1161/ATVBAHA.120.314789

Katz, T. C., Singh, M. K., Degenhardt, K., Rivera-Feliciano, J., Johnson, R. L., Epstein, J. A., et al. (2012). Distinct compartments of the proepicardial organ give rise to coronary vascular endothelial cells. *Dev. Cell* 22, 639–650. doi: 10.1016/j.devcel.2012.01.012

Kisanuki, Y. Y., Hammer, R. E., Miyazaki, J., Williams, S. C., Richardson, J. A., and Yanagisawa, M. (2001). Tie2-cre transgenic mice: a new model for endothelial cell-lineage analysis in vivo. *Dev. Biol.* 230, 230–242. doi: 10.1006/dbio.2000.0106

Kroepil, F., Fluegen, G., Totikov, Z., Baldus, S. E., Vay, C., Schauer, M., et al. (2012). Down-regulation of CDH1 is associated with expression of SNAI1 in colorectal adenomas. *PLoS One* 7:e46665. doi: 10.1371/journal.pone.0046665

Li, G., Tian, L., Goodyer, W., Kort, E. J., Buikema, J. W., Xu, A., et al. (2019). Single cell expression analysis reveals anatomical and cell cycle-dependent transcriptional shifts during heart development. *Development* 146:dev173476. doi: 10.1242/dev.173476

Li, X., Lu, Q., Peng, Y., Geng, F., Shao, X., Zhou, H., et al. (2020). Primary cilia mediate Klf2-dependant Notch activation in regenerating heart. *Protein Cell* 11, 433–445. doi: 10.1007/s13238-020-00695-w

Lim, S. L., Lam, C. S. P., Segers, V. F. M., Brutsaert, D. L., and De Keulenaer, G. W. (2015). Cardiac endothelium–myocyte interaction: clinical opportunities for new heart failure therapies regardless of ejection fraction. *Eur. Heart J.* 36, 2050–2060. doi: 10.1093/eurheartj/ehv132

Lin, C.-J., Lin, C.-Y., Chen, C.-H., Zhou, B., and Chang, C.-P. (2012). Partitioning the heart: mechanisms of cardiac septation and valve development. *Development* 139, 3277–3299. doi: 10.1242/dev.063495

Litviňuková, M., Talavera-López, C., Maatz, H., Reichart, D., Worth, C. L., Lindberg, E. L., et al. (2020). Cells of the adult human heart. *Nature* 588, 466–472. doi: 10.1038/s41586-020-2797-4

Liu, J., Bressan, M., Hassel, D., Huisken, J., Staudt, D., Kikuchi, K., et al. (2010). A dual role for ErbB2 signaling in cardiac trabeculation. *Development* 137, 3867–3875. doi: 10.1242/dev.053736

Luna-Zurita, L., Prados, B., Grego-Bessa, J., Luxán, G., del Monte, G., Benguría, A., et al. (2010). Integration of a Notch-dependent mesenchymal gene program and Bmp2-driven cell invasiveness regulates murine cardiac valve formation. *J. Clin. Invest.* 120, 3493–3507. doi: 10.1172/JCI42666

Luxán, G., Casanova, J. C., Martínez-Poveda, B., Prados, B., D'Amato, G., MacGrogan, D., et al. (2013). Mutations in the NOTCH pathway regulator MIB1 cause left ventricular noncompaction cardiomyopathy. *Nat. Med.* 19, 193–201. doi: 10.1038/nm.3046

MacGrogan, D., Münch, J., and de la Pompa, J. L. (2018). Notch and interacting signalling pathways in cardiac development, disease, and regeneration. *Nat. Rev. Cardiol.* 15, 685–704. doi: 10.1038/s41569-018-0100-2

Männer, J., and Yelbuz, T. M. (2019). Functional morphology of the cardiac jelly in the tubular heart of vertebrate embryos. *J. Cardiovasc. Dev. Dis.* 6:12. doi: 10.3390/jcdd6010012

Milgrom-Hoffman, M., Harrelson, Z., Ferrara, N., Zelzer, E., Evans, S. M., and Tzahor, E. (2011). The heart endocardium is derived from vascular endothelial progenitors. *Development* 138, 4777–4787. doi: 10.1242/dev.061192

Mysliwiec, M. R., Bresnick, E. H., and Lee, Y. (2011). Endothelial Jarid2/Jumonji is required for normal cardiac development and proper Notch1 expression. *J. Biol. Chem.* 286, 17193–17204. doi: 10.1074/jbc.M110.205146

Mysliwiec, M. R., Carlson, C. D., Tietjen, J., Hung, H., Ansari, A. Z., and Lee, Y. (2012). Jarid2 (Jumonji, AT rich interactive domain 2) regulates NOTCH1 expression via histone modification in the developing heart. *J. Biol. Chem.* 287, 1235–1241. doi: 10.1074/jbc.M111.315945

Niessen, K., Fu, Y., Chang, L., Hoodless, P. A., McFadden, D., and Karsan, A. (2008). Slug is a direct Notch target required for initiation of cardiac cushion cellularization. *J. Cell Biol.* 182, 315–325. doi: 10.1083/jcb.200710067

Paik, D. T., Cho, S., Tian, L., Chang, H. Y., and Wu, J. C. (2020a). Single-cell RNA sequencing in cardiovascular development, disease and medicine. *Nat. Rev. Cardiol.* 17, 457–473. doi: 10.1038/s41569-020-0359-y

Paik, D. T., Lei, T., Williams, I. M., Siyeon, R., Hao, Z., Chun, L., et al. (2020b). Single-Cell RNA sequencing unveils unique transcriptomic signatures of organ-specific endothelial cells. *Circulation* 142, 1848–1862. doi: 10.1161/CIRCULATIONAHA.119.041433

Panin, V. M., Papayannopoulos, V., Wilson, R., and Irvine, K. D. (1997). Fringe modulates Notch–ligand interactions. *Nature* 387, 908–912. doi: 10.1038/43191

Papoutsi, T., Luna-Zurita, L., Prados, B., Zaffran, S., and de la Pompa, J. L. (2018). Bmp2 and Notch cooperate to pattern the embryonic endocardium. *Development* 145:dev163378. doi: 10.1242/dev.163378

Pérez-Pomares, J. M., and de la Pompa, J. L. (2011). Signaling during epicardium and coronary vessel development. *Circ. Res.* 109, 1429–1442. doi: 10.1161/CIRCRESAHA.111.245589

Pratumvinit, B., Reesukumal, K., Janebodin, K., Ieronimakis, N., and Reyes, M. (2013). Isolation, characterization, and transplantation of cardiac endothelial cells. *Biomed Res. Int.* 2013, 359412. doi: 10.1155/2013/359412

Qu, X., Harmelink, C., and Baldwin, H. S. (2019). Tie2 regulates endocardial sprouting and myocardial trabeculation. *JCI Insight* 5:e96002. doi: 10.1172/jci.insight.96002

Ranger, A. M., Grusby, M. J., Hodge, M. R., Gravallese, E. M., de la Brousse, F. C., Hoey, T., et al. (1998). The transcription factor NF-ATc is essential for cardiac valve formation. *Nature* 392, 186–190. doi: 10.1038/32426

Rhee, S., Chung, J. I., King, D. A., D'amato, G., Paik, D. T., Duan, A., et al. (2018). Endothelial deletion of Ino80 disrupts coronary angiogenesis and causes congenital heart disease. *Nat. Commun.* 9:368. doi: 10.1038/s41467-017-02796-3

Ricard, N., Bailly, S., Guignabert, C., and Simons, M. (2021). The quiescent endothelium: signalling pathways regulating organ-specific endothelial normalcy. *Nat. Rev. Cardiol.* doi: 10.1038/s41569-021-00517-4 [Epub ahead of print].

Sedmera, D., Pexieder, T., Vuillemin, M., Thompson, R. P., and Anderson, R. H. (2000). Developmental patterning of the myocardium. *Anat. Rec.* 258, 319–337. doi: 10.1002/(SICI)1097-0185(20000401)258:4<319::AID-AR1<3.0.CO;2-O

Tian, X., Hu, T., Zhang, H., He, L., Huang, X., Liu, Q., et al. (2014). De novo formation of a distinct coronary vascular population in neonatal heart. *Science* 345, 90–94. doi: 10.1126/science.1251487

Tian, X., Li, Y., He, L., Zhang, H., Huang, X., Liu, Q., et al. (2017). Identification of a hybrid myocardial zone in the mammalian heart after birth. *Nat. Commun.* 8:87. doi: 10.1038/s41467-017-00118-1

Timmerman, L. A., Grego-Bessa, J., Raya, A., Bertrán, E., Pérez-Pomares, J. M., Díez, J., et al. (2004). Notch promotes epithelial-mesenchymal transition during cardiac development and oncogenic transformation. *Genes Dev.* 18, 99–115. doi: 10.1101/gad.276304

Van der Heiden, K., Groenendijk, B. C. W., Hierck, B. P., Hogers, B., Koerten, H. K., Mommaas, A. M., et al. (2006). Monocilia on chicken embryonic endocardium in low shear stress areas. *Dev. Dyn.* 235, 19–28. doi: 10.1002/dvdy.20557

Verzi, M. P., McCulley, D. J., De Val, S., Dodou, E., and Black, B. L. (2005). The right ventricle, outflow tract, and ventricular septum comprise a restricted expression domain within the secondary/anterior heart field. *Dev. Biol.* 287, 134–145. doi: 10.1016/j.ydbio.2005.08.041

Wang, Y., Wu, B., Chamberlain, A. A., Lui, W., Koirala, P., Susztak, K., et al. (2013). Endocardial to myocardial Notch-wnt-bmp axis regulates early heart valve development. *PLoS One* 8:e60244. doi: 10.1371/journal.pone.0060244

Wengrofsky, P., Armenia, C., Oleszak, F., Kupferstein, E., Rednam, C., Mitre, C. A., et al. (2019). Left ventricular trabeculation and noncompaction cardiomyopathy: a review. *EC Clin. Exp. Anat.* 2, 267–283.

Wu, B., Zhang, Z., Lui, W., Chen, X., Wang, Y., Chamberlain, A. A., et al. (2012). Endocardial cells form the coronary arteries by angiogenesis through myocardial-endocardial VEGF signaling. *Cell* 151, 1083–1096. doi: 10.1016/j.cell.2012.10.023

Wunsch, A. M., Little, C. D., and Markwald, R. R. (1994). Cardiac endothelial heterogeneity defines valvular development as demonstrated by the diverse expression of JB3, an antigen of the endocardial cushion tissue. *Dev. Biol.* 165, 585–601. doi: 10.1006/dbio.1994.1278

Xiong, Y., Zhou, B., and Chang, C.-P. (2012). "Analysis of the endocardial-to-mesenchymal transformation of heart valve development by collagen gel culture assay," in *Cardiovascular Development*, eds X. Peng and M. Antonyak (Totowa, NJ: Humana Press), 101–109. doi: 10.1007/978-1-61779-523-7_10

Yang, L.-T., Nichols, J. T., Yao, C., Manilay, J. O., Robey, E. A., and Weinmaster, G. (2004). Fringe glycosyltransferases differentially modulate Notch1 proteolysis induced by Delta1 and Jagged1. *Mol. Biol. Cell* 16, 927–942. doi: 10.1091/mbc.e04-07-0614

Yarden, Y., and Sliwkowski, M. X. (2001). Untangling the ErbB signalling network. *Nat. Rev. Mol. Cell Biol.* 2, 127–137. doi: 10.1038/35052073

Conflict of Interest: The authors declare that the research was conducted in the absence of any commercial or financial relationships that could be construed as a potential conflict of interest.

Copyright © 2021 Kim, Wang and Paik. This is an open-access article distributed under the terms of the Creative Commons Attribution License (CC BY). The use, distribution or reproduction in other forums is permitted, provided the original author(s) and the copyright owner(s) are credited and that the original publication in this journal is cited, in accordance with accepted academic practice. No use, distribution or reproduction is permitted which does not comply with these terms.

frontiers in Cell and Developmental Biology

ORIGINAL RESEARCH
published: 02 August 2021
doi: 10.3389/fcell.2021.672009

Insights Into the Mechanisms of Brain Endothelial Erythrophagocytosis

*Jiahong Sun[1], Prema Vyas[2], Samar Mann[3], Annlia Paganini-Hill[4], Ane C. F. Nunes[5], Wei Ling Lau[5], David H. Cribbs[6], Mark J. Fisher[4] and Rachita K. Sumbria[1,4]**

[1] Department of Biomedical and Pharmaceutical Sciences, School of Pharmacy, Chapman University, Irvine, CA, United States, [2] Henry E. Riggs School of Applied Life Sciences, Keck Graduate Institute, Claremont, CA, United States, [3] Pitzer College, Claremont, CA, United States, [4] Departments of Neurology and Pathology and Laboratory Medicine, University of California, Irvine, Irvine, CA, United States, [5] Division of Nephrology, Department of Medicine, University of California, Irvine, Irvine, CA, United States, [6] Institute for Memory Impairments and Neurological Disorders, University of California, Irvine, Irvine, CA, United States

OPEN ACCESS

Edited by:
Bin Ren,
University of Alabama at Birmingham,
United States

Reviewed by:
Torben Moos,
Aalborg University, Denmark
Anne-Eva Van Der Wijk,
Academic Medical Center,
Netherlands

***Correspondence:**
Rachita K. Sumbria
sumbria@chapman.edu

Specialty section:
This article was submitted to Signaling, a section of the journal Frontiers in Cell and Developmental Biology

Received: 25 February 2021
Accepted: 15 June 2021
Published: 02 August 2021

Citation:
Sun J, Vyas P, Mann S, Paganini-Hill A, Nunes ACF, Lau WL, Cribbs DH, Fisher MJ and Sumbria RK (2021) Insights Into the Mechanisms of Brain Endothelial Erythrophagocytosis. Front. Cell Dev. Biol. 9:672009. doi: 10.3389/fcell.2021.672009

The endothelial cells which form the inner cellular lining of the vasculature can act as non-professional phagocytes to ingest and remove emboli and aged/injured red blood cells (RBCs) from circulation. We previously demonstrated an erythrophagocytic phenotype of the brain endothelium for oxidatively stressed RBCs with subsequent migration of iron-rich RBCs and RBC degradation products across the brain endothelium *in vivo and in vitro*, in the absence of brain endothelium disruption. However, the mechanisms contributing to brain endothelial erythrophagocytosis are not well defined, and herein we elucidate the cellular mechanisms underlying brain endothelial erythrophagocytosis. Murine brain microvascular endothelial cells (bEnd.3 cells) were incubated with tert-butyl hydroperoxide (tBHP, oxidative stressor to induce RBC aging *in vitro*)- or PBS (control)-treated mouse RBCs. tBHP increased the reactive oxygen species (ROS) formation and phosphatidylserine exposure in RBCs, which were associated with robust brain endothelial erythrophagocytosis. TNFα treatment potentiated the brain endothelial erythrophagocytosis of tBHP-RBCs *in vitro*. Brain endothelial erythrophagocytosis was significantly reduced by RBC phosphatidylserine cloaking with annexin-V and with RBC-ROS and phosphatidylserine reduction with vitamin C. Brain endothelial erythrophagocytosis did not alter the bEnd.3 viability, and tBHP-RBCs were localized with early and late endosomes. Brain endothelial erythrophagocytosis increased the bEnd.3 total iron pool, abluminal iron levels without causing brain endothelial monolayer disruption, and ferroportin levels. *In vivo*, intravenous tBHP-RBC injection in aged (17–18 months old) male C57BL/6 mice significantly increased the Prussian blue-positive iron-rich lesion load compared with PBS-RBC-injected mice. In conclusion, RBC phosphatidylserine exposure and ROS are

key mediators of brain endothelial erythrophagocytosis, a process which is associated with increased abluminal iron *in vitro*. tBHP-RBCs result in Prussian blue-positive iron-rich lesions *in vivo*. Brain endothelial erythrophagocytosis may provide a new route for RBC/RBC degradation product entry into the brain to produce iron-rich cerebral microhemorrhage-like lesions.

Keywords: red blood cell, phosphatidylserine, oxidative stress, brain endothelial erythrophagocytosis, iron deposits, cerebral microhemorrhages

INTRODUCTION

Cerebral microhemorrhages (CMHs) are small focal bleeds in the brain that produce the magnetic resonance imaging signatures of cerebral microbleeds (CMBs) (Greenberg et al., 2009). CMBs increase with normal aging and under pathological conditions and are primarily hemorrhagic in origin (e.g., cerebrovascular disruption resulting in red blood cell (RBC) extravasation) (Martinez-Ramirez et al., 2014; Fisher et al., 2018; Lau et al., 2020). However, since CMBs are clinically identified as small magnetic resonance imaging signal voids resulting from the paramagnetic properties of iron in hemosiderin deposits, sources of CMBs that arise due to an increase in hemosiderin iron *via* alternate mechanisms have been suggested (Fisher, 2014; Janaway et al., 2014).

Under physiological conditions, the adhesion of RBCs to the vascular endothelium is negligible. However, an abnormal RBC-vascular endothelial adhesion has been observed in various pathological conditions (Bonomini et al., 2002; Nakagawa et al., 2011; Wautier and Wautier, 2013; Kucukal et al., 2018). Additionally erythrophagocytosis, a well-described feature of macrophages, by which injured/aged erythrocytes are ingested, digested, and cleared from the blood circulation, has been described in peripheral endothelial cells (Fens et al., 2010, 2012; Lee et al., 2011). A similar phagocytic phenotype has also been reported for the brain endothelium, and studies show that the brain endothelium can engulf and extrude emboli to the abluminal (brain) side *via* angiophagy, *in vivo* and *in vitro* (Grutzendler et al., 2014; van der Wijk et al., 2020). Similarly, our recent *in vitro* and *in vivo* work demonstrated an erythrophagocytic phenotype of the brain endothelium with subsequent passage of iron-rich hemoglobin and RBCs across the endothelial monolayer (Chang R. et al., 2018). The passage of iron-rich RBCs (or RBC degradation products) across an intact brain endothelium following erythrophagocytosis may present an alternate source of iron-rich CMH-like lesions (Fisher, 2014; Janaway et al., 2014; Chang R. et al., 2018).

Phosphatidylserine externalization on RBCs is well-recognized as an important signal that initiates their phagocytic removal from the circulation, and this mechanism is widely studied for macrophage-mediated erythrophagocytosis (de Back et al., 2014). Phosphatidylserine exposure on aged/injured RBCs is also a key trigger for erythrophagocytosis of oxidatively stressed or aged RBCs by peripheral endothelial cells (Fens et al., 2008, 2012). Similarly, our previous study reported a marked externalization of RBC phosphatidylserine by tert-butyl hydroperoxide (tBHP), an oxidative stressor used previously to trigger erythrophagocytosis by peripheral endothelial cells (Fens et al., 2012), and we found robust erythrophagocytosis of tBHP-RBCs by murine brain microvascular endothelial cells (Chang R. et al., 2018). Corroborating our findings, a recent study reported increased erythrophagocytosis of aged RBCs by the brain endothelium, which was associated with increased phosphatidylserine externalization and oxidative stress (Catan et al., 2019). These studies together show an association between RBC phosphatidylserine exposure and oxidative stress, and brain endothelial erythrophagocytosis, but a direct role of RBC phosphatidylserine externalization and oxidative stress in this process has not been reported.

The aim of the current study was to provide mechanistic insights into the cellular pathways involved in brain endothelial erythrophagocytosis. Murine RBCs were treated with tBHP to induce oxidative stress and phosphatidylserine externalization to study the role of these mediators in brain endothelial erythrophagocytosis *in vitro* using murine brain microvascular endothelial cells (bEnd.3). We further examined the impact of brain endothelial erythrophagocytosis on the iron-transport machinery of the bEnd.3 cells and the intracellular trafficking of phosphatidylserine exposing tBHP-RBCs by tracing their movement through early endosomes toward late endosomes, the latter being the presumed site of RBC degradation and release of iron-rich degradation products. Finally, we injected tBHP-RBCs into aged mice to provide histological evidence for increased iron-rich Prussian blue-positive lesion development in mice. Overall, our findings provide important mechanistic insights into the cellular pathways involved in, and the alterations to cellular iron homeostasis associated with, brain endothelial erythrophagocytosis.

MATERIALS AND METHODS

Details about the source of the major resources used are in the **Supplementary Material**.

Cell Culture

Murine brain microvascular endothelial cells (bEnd.3 cells; American Type Culture Collection, Manassas, VA, United States) were maintained in Dulbecco's modified Eagle's medium (American Type Culture Collection, Manassas, VA,

Abbreviations: CMBs, cerebral microbleeds; CMHs, cerebral microhemorrhages; H_2DCFDA, 2′,7′-dichlorodihydrofluorescein diacetate; EEA-1, early endosome antigen 1; H&E, hematoxylin and eosin; ICP-MS, inductively coupled plasma mass spectrometry; LAMP-1, lysosome-associated membrane protein 1; PBS, phosphate-buffered saline; RBC, red blood cell; ROS, reactive oxygen species; tBHP, tert-butyl hydroperoxide; TfR, transferrin receptor; ZO-1, zonula occludens - 1.

United States) supplemented with 10% fetal bovine serum and 100 μg/ml penicillin/streptomycin (Sigma-Aldrich, St. Louis, MO, United States) at standard cell culture conditions (5% CO_2, 95% air). Cells between passages 22 and 31 were seeded onto 24- and 6-well plates (Corning, New York, NY, United States), 0.2% gelatin-coated glass coverslips, or Transwells with 0.4-μm-pore polyester membrane inserts of a six-well plate (Corning, New York, NY, United States) at a density of 1×10^5 cells/cm^2, unless otherwise stated.

RBC Preparation and Treatment for *in vitro* Experiments

RBCs in Alsever's solution were derived from 2- to 3-month-old male BALB/c mice (BioIVT, New York, NY, United States). RBCs were resuspended in sterile phosphate-buffered saline (PBS, without Ca^{2+} and Mg^{2+}; Invitrogen, Waltham, MA, United States) as control, or various concentrations (0.3, 1.0, 3.0 mM) of tBHP (Sigma-Aldrich, St. Louis, MO, United States) at 37°C for 30 min. RBCs at a density of 2×10^6/cm^2 were co-incubated with bEnd.3 cells with or without the 7.5-μg annexin-V (BioLegend, San Diego, CA, United States) to cloak phosphatidylserine, the antioxidant vitamin C (15–1,500 μM, Sigma-Aldrich, St. Louis, MO, United States), to reduce ROS, or inflammatory cytokine TNFα (10–100 ng/ml, BioLegend, San Diego, CA, United States). The RBC-to-bEnd.3 ratio was ∼5:1 for these experiments.

ROS Detection

Intracellular ROS were measured by the ROS-reactive fluorescent indicator 2′,7′-dichlorodihydrofluorescein diacetate (H_2DCFDA, Molecular Probes, Carlsbad, CA, United States). Treated RBCs (2×10^6) were incubated with 10 μM H_2DCFDA for 30 min at 37°C. The mean fluorescence intensity of DCF was measured at 485 nm/530 nm (excitation/emission) using a fluorescence plate reader (Molecular Devices, LLC, San Jose, CA, United States).

Phosphatidylserine Exposure Detection and Cloaking, and CD47 Detection

Annexin-V-FITC (BioLegend, San Diego, CA, United States) was used to quantify phosphatidylserine externalization on the RBC surface as per the manufacturer's instructions. Briefly, 1×10^5 RBCs suspended in annexin-V blocking buffer (BD Biosciences, Franklin Lakes, NJ, United States) were incubated with 5 μg of annexin-V-FITC for 15 min in the dark, followed by immediate analysis of the FITC signal using a BD Accuri C6 Plus flow cytometer (BD Biosciences, San Jose, CA, United States). Ten thousand events were recorded for each sample, and RBCs were quantified using logarithmic gain for light scatter and fluorescence channels with gating and background settings defined through the PBS-RBCs. To determine the correct amount of annexin-V required to block phosphatidylserine exposure, phosphatidylserine-exposing RBCs were first incubated with 7.5 μg annexin V (BioLegend, San Diego, CA, United States) and then labeled with annexin-V-FITC (5 μg), followed by FITC detection using flow cytometry. For CD47 detection, 2.5×10^5 RBCs were incubated with the anti-CD47 antibody (1:200 dilution, Santa Cruz Biotechnology, Dallas, TX, United States) in PBS containing 1% bovine serum albumin (Thermo Fisher Scientific, Waltham, MA, United States) for 45 min at room temperature. After washing with PBS, the anti-CD47 antibody was detected using the Alexa Fluor 647-labeled goat anti-rat IgG (H + L) secondary antibody (1:2,000 dilution, Invitrogen, Waltham, MA, United States) for 30 min in the dark, followed by three PBS washes for flow cytometry detection.

Hematoxylin and Eosin (H&E) Staining

H&E staining was performed as described previously (Chang R. et al., 2018). bEnd.3 cells were fixed with 4% paraformaldehyde and then stained with hematoxylin (Sigma-Aldrich, St. Louis, MO, United States) and eosin Y (Sigma-Aldrich, St. Louis, MO, United States) and mounted using Permount (Thermo Fisher Scientific, Waltham, MA, United States). Ten continuous view fields from three random areas per coverslip were imaged at × 40 magnification and manually quantified for total RBC number, RBC-to-bEnd.3 ratio (expressed as %),% of bEnd.3 cells positive for RBC, and % of bEnd.3 cells positive for RBC engulfment, as described previously (Chang R. et al., 2018).

Hemoglobin Measurement

Hemoglobin was measured using 2,7-diaminofluorene (Sigma-Aldrich, St. Louis, MO, United States) as described previously (Chang R. et al., 2018). bEnd.3 cells incubated with RBCs were washed with PBS for total cellular hemoglobin (hemoglobin from attached and engulfed RBCs) or quickly washed with distilled water three times for intracellular hemoglobin (hemoglobin from engulfed RBCs). Cells were lysed with urea lysis buffer (0.2 M Tris–HCl buffer containing 6 M urea, Thermo Fisher Scientific, Waltham, MA, United States) and mixed at a 1:1 ratio with 2,7-diaminofluorene reaction buffer (10 mg 2,7-diaminofluorene in 10 ml urea lysis buffer containing 9% acetic acid and 0.3% hydrogen peroxide). Absorbance was measured at 620 nm using an absorbance plate reader (Molecular Devices, LLC, San Jose, CA, United States). A set of hemoglobin standards (Lee BioSolutions, Maryland Heights, MO, United States) was used to calculate the amount of hemoglobin.

Cell Viability Assay

bEnd.3 cells (7,500 cells/well) seeded in 96-well plates (Corning, New York, NY, United States) were assessed for cell viability using the Cell Counting Kit-8 assay as per the manufacturer's instructions (Dojindo Molecular Technologies, Rockville, MD, United States). Absorbance was measured at 450 nm using an absorbance plate reader (Molecular Devices, LLC, San Jose, CA, United States), and cell viability was adjusted to % of bEnd.3 control group (bEnd.3 cells with no RBC co-incubation).

Immunocytochemistry

After a 48-h incubation with RBCs, bEnd.3 cells were fixed with 2% paraformaldehyde, permeabilized, and blocked with 5% bovine serum albumin (Thermo Fisher Scientific, Waltham, MA, United States) containing 0.1% Triton X-100 (Thermo Fisher Scientific, Waltham, MA, United States). Cells were incubated

with Alexa Fluor 647-labeled anti-early endosome antigen 1 (EEA-1) antibody (1:50 in PBS with 0.75% bovine serum albumin and 0.1% Triton X-100; Santa Cruz Biotechnology, Dallas, TX, United States) or rat anti-lysosome-associated membrane protein 1 (LAMP-1) antibody (the original antibody was diluted 1:2 in 50% glycerol followed by 1:5 dilution in PBS with 0.75% bovine serum albumin and 0.1% Triton X-100; Developmental Studies Hybridoma Bank, Iowa City, IA, United States) overnight at 4°C. The anti-LAMP-1 antibody was detected using the Alexa Fluor 647-labeled goat anti-rat IgG (H + L) secondary antibody (1:200, Santa Cruz Biotechnology, Dallas, TX, United States). Coverslips were mounted with UltraCruz Aqueous Mounting Medium with DAPI (Santa Cruz Biotechnology, Dallas, TX, United States) and imaged at × 63 oil immersion objective with a Leica SP5 confocal microscope (Leica, Wetzlar, Germany). Z-stacks were acquired with a z-step size of 0.5 μm. Each experimental group had at least five coverslips, and 10 images per coverslip were analyzed using ImageJ (NIH, Bethesda, MD, United States). Max projection images were used to count nuclei and nuclei positive for EEA-1/LAMP-1 staining as well as the number of RBCs. The number of EEA-1/LAMP-1-positive RBCs was determined by examining each image in a z-stack to find RBCs localized with EEA-1/LAMP-1 in the same plane. We quantified (1) RBC attachment (expressed as % of number of bEnd.3 cells), (2) RBCs localized to the nucleus (expressed as % of total RBC), (3) EEA-1-/LAMP-1-positive RBCs (expressed as % of total RBCs found in the imaging field of view), and (4) RBCs in the nucleus positive for EEA-1-/LAMP-1 (expressed as a % of RBCs in the nucleus).

Iron Level Measurement

Iron levels in cell samples (total and intracellular iron) and migration of intracellular iron across the bEnd.3 monolayer were measured by Agilent 8900 Triple Quadrupole Inductively Coupled Plasma Mass Spectrometry (ICP-MS; Agilent, Santa Clara, CA, United States). For total cellular and intracellular iron, bEnd.3 cells (9.5×10^5 per well) were seeded in 6-well plates and incubated with 1×10^8 RBCs per well for 48 h. The RBC-to-bEnd.3 ratio was ∼ 25:1 for these experiments. Cells were washed three times with PBS for total cellular iron (iron from attached and engulfed RBCs) or distilled water for intracellular iron (iron from engulfed RBCs). Samples were lysed with 1 ml 4% nitric acid at 80°C for 3 h, after which 250 μl 30% hydrogen peroxide was added and the samples were further digested for 1 h at 90°C.

To measure passage of intracellular iron across the endothelial monolayer, bEnd.3 cells were grown on six-well Transwell inserts (pore size 0.4 μm, Corning New York, NY, United States). The integrity of the bEnd.3 monolayer in Transwell inserts was assessed by measuring the transendothelial electrical resistance using the EVOM2 Epithelial Volt/Ohm Meter and an STX-2 electrode system (World Precision Instruments LLC, Sarasota, FL, United States). After the transendothelial electrical resistance measurements stabilized, 1×10^8 RBCs were added into each insert seeded with the bEnd.3 cells, for 48 h. Apical and basolateral media were collected separately, and 67% nitric acid was added to each sample to result in a final nitric concentration of 4%. Samples were digested for 3 h at 80°C, and 250 μl 30% hydrogen peroxide per 1-ml media sample was added. Samples were further digested at 90°C for 1 h. Standard curves were drawn from calibration blanks with different concentrations (4 nM–4 μM). Iron concentrations from independent samples were calculated based on the calibrated iron standard curve.

Western Blot

bEnd.3 cells were washed with PBS and lysed with radioimmunoprecipitation assay buffer containing cocktail protease inhibitors (Bio-Rad, Hercules, CA, United States) and boiled with Laemmli buffer and 10% 2-mercaptoethanol (Bio-Rad, Hercules, CA, United States). Blots were probed with anti-transferrin receptor (TfR) antibody (1:1,000 dilution; Thermo Fisher Scientific, Waltham, MA, United States) or anti-ferroportin antibody (1:1,000 dilution; Novus Biologicals, Littleton, CO, United States) overnight at 4°C. Membranes were exposed to the appropriate horseradish peroxidase–conjugated secondary antibodies, followed by chemiluminescence detection (Thermo Fisher Scientific, Waltham, MA, United States). Equal protein loading was controlled by re-probing the membrane with anti–β-actin antibody (1:1,000 dilution; Santa Cruz Biotechnology, Dallas, TX, United States). Chemiluminescence was detected using the UVP ChemiDoc-It TS2 Imager (Upland, CA, United States), and Image J (NIH, Bethesda, MD, United States) was used for Western blot signal quantification.

In vivo Prussian Blue-Positive Iron-Rich Lesion Development

All animal procedures were approved by University of California-Irvine's Institutional Animal Care and Use Committee and carried out in compliance with University Laboratory Animal Resources regulations. Blood was collected from 17–18-month-old male C57BL/6 mice (National Institute of Aging, Bethesda, MD, United States) and mixed with 3.2% sodium citrate (0.1/0.9 ml of blood). Blood was centrifuged at 500g for 10 min at 4°C, and RBC pellet was washed with PBS three times. Purified RBCs were resuspended in sterile PBS (without Ca^{2+} and Mg^{2+}; Invitrogen, Waltham, MA, United States) as control, or 3 mM of tBHP (Sigma-Aldrich, St. Louis, MO, United States) at 37°C for 30 min. After centrifuging at 500g for 5 min at 4°C, the RBC pellet was resuspended in sterile PBS. PBS- or tBHP-RBCs (3×10^8 cells per mouse) were then injected intravenously *via* the retro-orbital route under brief isoflurane anesthesia into different 17–18-month-old male C57BL/6 mice ($n = 3$ per group). Seven days after RBC injection, cardiac perfusion was performed, and brains were harvested and fixed with 4% paraformaldehyde. Hemi-brains were cut into 40-μm coronal sections, and every sixth section was used to examine Prussian blue-positive lesions as described previously (Sumbria et al., 2016). Prussian blue-positive lesions were counted at × 20 magnification by a blinded observer, and digital images were used to calculate lesion size (μm^2) and positive area (expressed as a percent of total tissue area analyzed) using the NIH ImageJ software 1.62, as described previously (Sumbria et al., 2016).

Zonula Occludens-1 (ZO-1) Immunostaining

For each mouse ($n = 3$ per group), three coronal sections (600 μm apart and 40 μm thick) prepared as above were used

for ZO-1 immunostaining. Briefly, brain sections were incubated in quenching solution (0.2% Triton X-100 (Thermo Fisher Scientific, Waltham, MA, United States) including 20 mM glycine (Sigma-Aldrich, St. Louis, MO, United States) in PBS) for 1 h, followed by blocking with 0.5% bovine serum albumin (Thermo Fisher Scientific, Waltham, MA, United States) containing 0.3% Triton X-100 (Thermo Fisher Scientific, Waltham, MA, United States) for 1 h. Brain sections were incubated with a rabbit ZO-1 polyclonal antibody (1:100 dilution in blocking buffer, Invitrogen, Waltham, MA, United States) overnight at 4°C. The anti-ZO-1 antibody was detected using Alexa Fluor 647-labeled goat anti-rabbit IgG (H + L) secondary antibody (1:400 dilution in blocking buffer, Invitrogen, Waltham, MA, United States). Brain sections were imaged using a × 60 oil immersion objective with the Nikon Ti-Eclipse microscope (Nikon, Melville, NY, United States), and three cortical images were taken per mouse. Z-stacks were acquired, and max projection images were used to quantify the ZO-1-positive area (expressed as a percent of total tissue area analyzed) using ImageJ (NIH, Bethesda, MD, United States).

Statistical Analysis

The data are shown as means ± SEM. Student's *t*-test or the Mann–Whitney *U* test was used to compare two independent groups, and one-way analysis of variance (ANOVA) with Holm–Sidak *post hoc* test to compare more than two independent groups. To test the effect of two factors, two-way ANOVA with Holm–Sidak *post hoc* test was used. GraphPad Prism 8.0 (GraphPad Software, Inc., La Jolla, CA, United States) was used for statistical analyses, and a $p \leq 0.05$ was considered statistically significant.

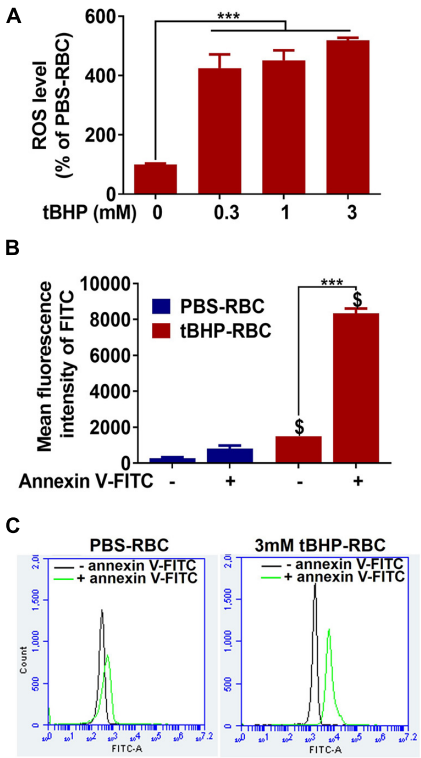

FIGURE 1 | ROS production and phosphatidylserine exposure in PBS- or tBHP-RBCs. ROS level **(A)** and phosphatidylserine exposure **(B,C)** were measured by H_2DCFDA and annexin-V-FITC, respectively, after a 30-min incubation with PBS or tBHP. Data are presented as mean ± SEM of three independent experiments done in duplicate. One-way **(A)** or two-way **(B)** ANOVA with Holm–Sidak *post hoc* test was used. $^{***}p < 0.001$. $^{\$}p < 0.05$ compared with the corresponding PBS-RBC group.

RESULTS

ROS Production and Phosphatidylserine Exposure

As shown in **Figure 1A**, tBHP (0.3–3 mM) induced a 300–400% increase in ROS levels in RBCs compared with PBS-RBCs. tBHP treatment resulted in a >900% increase in annexin-V-FITC-positive RBCs compared with PBS treatment, indicating significant phosphatidylserine exposure in tBHP-RBCs (**Figures 1B,C**).

Temporal Increase in Erythrophagocytosis by bEnd.3 Cells

Our previous study reported a temporal increase in the erythrophagocytosis of tBHP-RBCs (3 mM dose) by the bEnd.3 cells up to 24 h (Chang R. et al., 2018). To further investigate the timeline of erythrophagocytosis of tBHP-RBCs, studies were done following a 24- or 48-h co-incubation of bEnd.3 cells with RBCs. The increased attachment of tBHP-RBCs to the bEnd.3 cells is evident in **Figure 2A**, where the RBCs appear as small red/brown dots on H&E-stained bEnd.3 cells. Compared with the 24-h timepoint, exposure up to 48 h further increased the number of RBCs attached to the bEnd.3 cells (**Figures 2A–C**) and the number of endothelial cells positive for tBHP-RBCs (**Figure 2D**). Although not statistically significant, there was a trend toward an increase in the engulfment of tBHP-RBCs by the bEnd.3 cells at 48 h (**Figure 2E**). No significant erythrophagocytosis with PBS control was observed at 24 or 48 h (**Figures 2A–C**). Based on these results, a 48-h co-incubation of RBCs and bEnd.3 was used for subsequent studies. Interestingly, we saw a dose-dependent increase in brain endothelial erythrophagocytosis of tBHP-RBCs with TNFα (10–100 ng/mL) (**Supplementary Figure 1**).

Role of Phosphatidylserine Exposure in Brain Endothelial Erythrophagocytosis

We used annexin-V to mask the externalized phosphatidylserine on the surface of tBHP-RBCs. As shown in **Figure 3A**, preincubation of tBHP-RBCs with 7.5 μg of annexin-V followed by incubation with annexin-V-FITC reduced the annexin-V-FITC signal equivalent to PBS-control values, indicating complete cloaking of tBHP-induced phosphatidylserine exposure (**Figure 3A**). Phosphatidylserine masking by annexin-V led to a significant decrease in brain endothelial erythrophagocytosis. As shown in **Figure 3**, there was a 78% decrease in the adhesion of tBHP-RBCs, a 69% decrease in the number of RBCs attached per

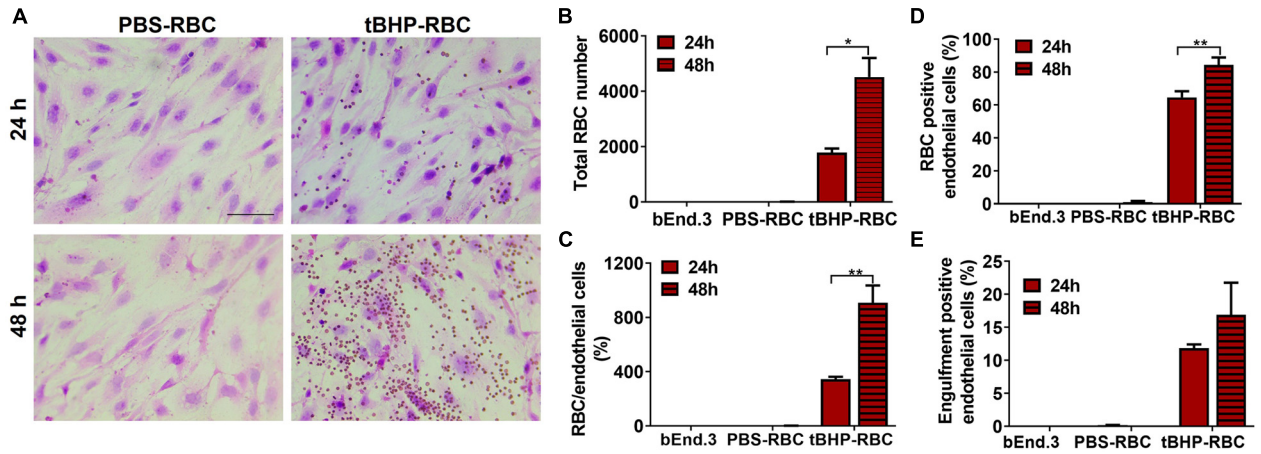

FIGURE 2 | Temporal increase in brain endothelial erythrophagocytosis. Significant time-dependent increase in adhesion **(A–D)** and a trend toward increased engulfment **(E)** of tBHP-RBCs compared with PBS-RBCs using H&E staining and light microscopy. RBCs are seen as small red/brown dots, and bEnd.3 nuclei are stained purple with hematoxylin in A. Data are presented as mean ± SEM of three independent experiments done in duplicates. Two-way ANOVA with Holm–Sidak *post hoc* test was used. $^{*}p < 0.05$, $^{**}p < 0.01$. Scale bar = 50 μm.

bEnd.3 cell, and a 28% decrease in bEnd.3 cells positive for RBCs (**Figures 3B–E**). Further, the bEnd.3 cells positive for engulfed RBCs were reduced by 48% (**Figure 3F**). No significant change in RBC adhesion and/or engulfment was observed in the control PBS-RBC group in the presence of annexin-V (**Figures 3B–F**).

To determine the impact of phosphatidylserine masking on cellular levels of the iron-rich RBC degradation product, hemoglobin, we measured the total and intracellular hemoglobin levels in bEnd.3 cells following a 48-h incubation with RBCs and annexin-V. In the absence of phosphatidylserine cloaking, the total and intracellular hemoglobin levels of bEnd.3 cells incubated with tBHP-RBCs were 6.5 ± 0.4 μg/ml and 2.3 ± 0.1 μg/ml, respectively (**Figure 3G**). These hemoglobin levels were significantly higher than those in the bEnd.3-only group (without RBCs) and PBS-RBC group (**Figure 3G**), further supporting the H&E results (**Figures 3B–F**). In the presence of annexin-V, the total and intracellular hemoglobin levels in bEnd.3 cells incubated with tBHP-RBCs decreased by 77% and 75%, respectively (**Figure 3G**). No significant difference in bEnd.3 cell viability was observed after incubation with PBS- or tBHP-RBCs for 48 h, and in the presence of annexin-V (**Figure 3H**).

Suppression of Brain Endothelial Erythrophagocytosis by Vitamin C

Since tBHP is a robust oxidative inducer and causes phosphatidylserine exposure in RBCs, we investigated if suppression of ROS by antioxidant vitamin C alters phosphatidylserine externalization. A 1-h incubation with vitamin C (1.5–1,500 μM) led to a significant reduction of ROS level in tBHP-RBCs (**Figure 4A**) but had no effect on PBS-RBCs. Notably, vitamin C at a concentration of 1,500 μM led to a full abolishment of ROS accumulation in tBHP-RBCs (**Figure 4A**). Vitamin C (15 and 1,500 μM) also reduced phosphatidylserine exposure of tBHP-RBCs by 38% and 88%, respectively (**Figure 4B**). The above prompted us to investigate the effect of free radical scavenging on brain endothelial erythrophagocytosis. As shown in **Figure 4C**, vitamin C (15 and 1,500 μM) treatment reduced the total cellular hemoglobin level in bEnd.3 cells by 30–47%. Vitamin C (1,500 μM) treatment resulted in a 31% reduction of intracellular hemoglobin level, which shows that vitamin C reduced the engulfment of tBHP-RBCs by the bEnd.3 cells. These results were confirmed by H&E staining (**Figure 4D**).

Intracellular Trafficking of RBCs in Brain Endothelial Cells

We investigated the trafficking of RBCs within the bEnd.3 cells by immunofluorescence to visualize the engulfed RBCs in early and late endosomes. **Figures 5A,B** show tBHP-RBCs (white/yellow) surrounded by an early endosomal marker, EEA-1 (red), and a late endosomal marker, LAMP-1 (red), within the bEnd.3 cells. 3D reconstructions of the z-stack images confirmed the internalization of tBHP-RBCs in the bEnd.3 cells (**Supplementary Figure 2**). Our quantification results show that ∼26% of tBHP-RBCs were co-localized with EEA-1- and LAMP-1-positive vesicles (**Figures 5C,D**). Interestingly, ∼12–15% of tBHP-RBCs were found to co-localize with the nuclear stain DAPI (**Figures 5C,D** and **Supplementary Figure 2**).

Increase in Cellular and Abluminal Iron Following Brain Endothelial Erythrophagocytosis

For brain endothelial erythrophagocytosis to produce iron-rich lesions in the brain, the former must be accompanied with an increase in intracellular iron and subsequent basolateral (abluminal) iron. We therefore measured the accumulation of iron in the bEnd.3 cells and the basolateral iron across the endothelial monolayer by ICP-MS. After a 48-h incubation with tBHP-RBCs, total cellular iron levels (iron from attached

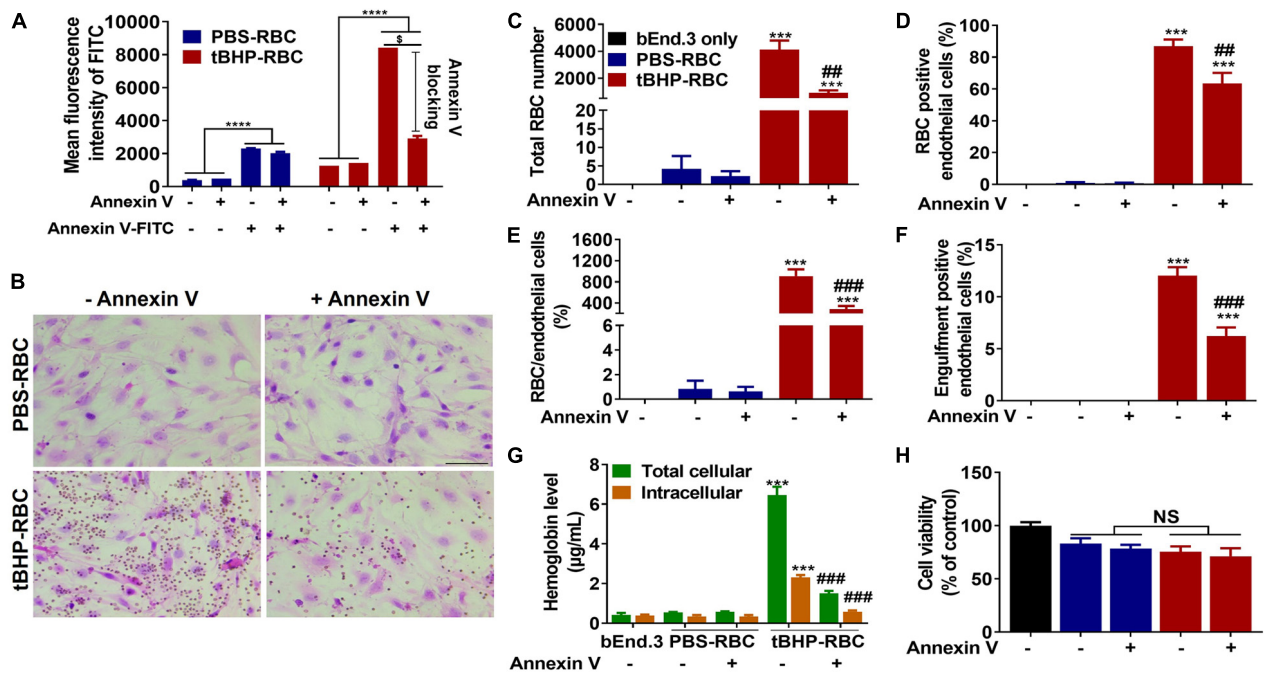

FIGURE 3 | Phosphatidylserine exposure plays an important role in brain endothelial erythrophagocytosis. Phosphatidylserine exposure of tBHP-RBCs was blocked by annexin-V **(A)**. Both RBC adhesion and engulfment were significantly suppressed by annexin-V **(B–F)**. The total cellular and intracellular hemoglobin levels were significantly reduced by annexin-V following a 48-h incubation **(G)**. Erythrophagocytosis did not alter brain endothelial cell viability following the 48-h incubation **(H)**. RBCs are seen as small red/brown dots, and bEnd.3 nuclei are stained purple with hematoxylin in panel **(B)**. Data are presented as mean ± SEM of three independent experiments done in duplicate. One-way **(H)** or two-way **(A,C–G)** ANOVA with Holm–Sidak *post hoc* test was used. $^{***}p < 0.001$, $^{****}p < 0.0001$ compared with the corresponding bEnd.3-only group and PBS-RBC group; $^{\#\#}p < 0.01$, $^{\#\#\#}p < 0.001$ compared with tBHP-RBCs without annexin-V; $^{\$}p < 0.0001$. Scale bar = 50 μm. NS is "not significant".

and engulfed RBCs) of bEnd.3 cells increased by 311% compared with bEnd.3-only and 298% compared with PBS-RBC groups (**Figure 6A**). To further investigate the impact of RBC engulfment on intracellular iron levels, bEnd.3 cells were washed with distilled water to lyse the attached RBCs on the endothelial surface. Intracellular iron levels increased 49% after the incubation of the bEnd.3 cells with tBHP-RBCs compared with PBS-RBCs (**Figure 6B**). An *in vitro* Transwell® system was used to measure iron transmigration across the bEnd.3 monolayer. At 48 h after RBC incubation, basolateral iron levels in the tBHP-RBC group were 205% and 76% higher than those in the bEnd.3-only group and PBS-RBC group, respectively (**Figure 6C**). To rule out the contribution of free iron in the apical medium to the increased basolateral iron levels in **Figure 6C**, we measured free iron levels in the media from PBS- or tBHP-RBCs (in the absence of bEnd.3 cells). No significant differences were observed in the levels of free iron over the course of 48 h between the PBS and tBHP groups (**Supplementary Figure 3A**). No changes in transendothelial electrical resistance (**Supplementary Figures 3B,C**) were observed following PBS- and tBHP-RBC incubation. Further, we investigated the protein levels of the major iron influx transporter, the TfR, and the iron exporter, ferroportin. After a 48-h incubation with tBHP-RBCs, no significant change in TfR protein levels was observed compared with the bEnd.3-only group and PBS-RBC group (**Figure 6D**). A significant 27% increase in ferroportin protein levels was observed in the bEnd.3 cells incubated with tBHP-RBCs compared with the bEnd.3-only and PBS-RBC groups (**Figure 6E**).

In vivo Prussian Blue-Positive CMH-Like Lesion Development

To determine if tBHP-RBCs produce iron-rich CMH-like lesions, aged mice were injected with PBS- or tBHP-RBCs. The mice injected with PBS- or tBHP-RBCs recovered quickly after intravenous RBC injection, appeared normal, and survived the duration of the study (7 days). All aged mice injected with either PBS-RBCs or tBHP-RBCs developed Prussian blue-positive iron-rich lesions. The total Prussian blue-positive area (expressed as a % of brain tissue area analyzed) and size of the individual lesion were, however, greater ($p = 0.05$) in mice injected with tBHP-RBCs than in mice injected with PBS-RBCs (**Figures 7A–C**). No significant difference was observed in the blood–brain barrier tight-junction protein ZO-1-positive area between the mice injected with PBS-RBCs or tBHP-RBCs (**Figure 7D**).

DISCUSSION

Our previous work showed that oxidatively stressed RBCs can undergo robust erythrophagocytosis by the brain endothelium,

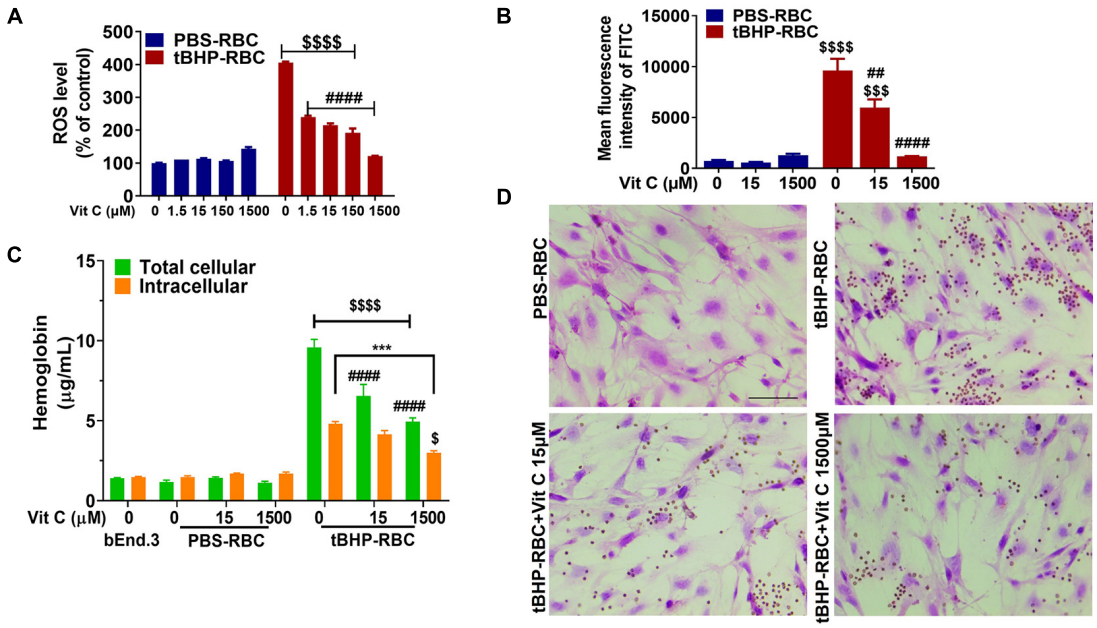

FIGURE 4 | Vitamin C (Vit C) reduced brain endothelial erythrophagocytosis. ROS level **(A)** and phosphatidylserine exposure **(B)** were suppressed by Vit C (15–1,500 μM) after incubation with tBHP-RBCs. The total cellular and intracellular hemoglobin levels of bEnd.3 cells treated with tBHP-RBCs were significantly reduced following a 48-h incubation with Vit C **(C)**. Representative H&E-stained images of bEnd.3 cells following the 48-h incubation with Vit C-treated RBCs **(D)**. RBCs are seen as small red/brown dots, and bEnd.3 nuclei are stained purple with hematoxylin in panel **(D)**. Data are presented as mean ± SEM of three independent experiments done in duplicate. Two-way ANOVA with Holm–Sidak *post hoc* test was used. $^{***}p < 0.001$ as indicated. $^{\#\#}p < 0.01$, $^{\#\#\#\#}p < 0.0001$ compared with the corresponding tBHP-RBC + Vit C 0 μM group. $^{\$}p < 0.05$, $^{\$\$\$}p < 0.001$, $^{\$\$\$\$}p < 0.0001$ tBHP-RBC group compared with the corresponding PBS-RBC and bEnd.3-only groups.

and this process was accompanied by an increase in the migration of an iron-rich RBC degradation product (hemoglobin) and RBCs across the brain endothelium, *in vitro* and *in vivo*, in the absence of vascular disruption (Chang R. et al., 2018). In the present report, we elucidate the cellular mechanisms that contribute to brain endothelial erythrophagocytosis. We show that phosphatidylserine cloaking and oxidative stress reduction significantly attenuate brain endothelial erythrophagocytosis in the *in vitro* murine brain microvascular endothelial cell model. Further, brain endothelial erythrophagocytosis alters endothelial iron homoeostasis and increases abluminal (brain) iron, without loss of the brain endothelial monolayer integrity, *in vitro*. Finally, we provide histological evidence for increased iron-rich Prussian blue-positive lesion load in mice injected with tBHP-RBCs, correlating with the *in vitro* increase in abluminal iron.

RBCs have a life span of 120 days in humans and about 45 days in mice (Gottlieb et al., 2012). ROS accumulation has been suggested to be a key RBC-life-span determinant by causing phosphatidylserine scrambling and externalization. Phosphatidylserine exposure contributes to the recognition of old/damaged RBCs by altering RBC adhesion to professional phagocytes (macrophages), which is followed by erythrophagocytosis and RBC clearance from the circulation (Franco, 2012; Gottlieb et al., 2012). Besides professional phagocytes, other cell types such as smooth muscle cells can phagocytose phosphatidylserine-exposing apoptotic bodies and aged RBCs (Garfield et al., 1975). Endothelial cells, which are in close contact with circulating RBCs, are also reported to have an erythrophagocytic phenotype. Fens et al. (2010) reported that peripheral endothelial cells can phagocytose RBCs subjected to increased oxidative stress and phosphatidylserine exposure. Similarly, a recent study showed that RBC aging and glycation increases phosphatidylserine externalization and oxidative stress in RBCs, which is associated with enhanced RBC phagocytosis by the vascular endothelium (Catan et al., 2019). Overall, the contribution of the endothelium to erythrophagocytosis and clearance of injured RBCs is now increasingly reported, as is the involvement of phosphatidylserine exposure and oxidative stress in endothelial erythrophagocytosis. Our recent work extended these findings to the brain endothelium and showed robust brain endothelial erythrophagocytosis of phosphatidylserine exposing tBHP-RBCs (Chang R. et al., 2018). To establish the definitive contribution of RBC phosphatidylserine exposure to brain endothelial erythrophagocytosis, herein we cloaked phosphatidylserine with annexin-V which has a high binding affinity for phosphatidylserine in a calcium-dependent manner (**Figure 3A**; Lizarbe et al., 2013). Cloaking of RBC phosphatidylserine with annexin-V significantly reduced erythrophagocytosis of tBHP-RBCs by the bEnd.3 cells (**Figures 3B–F**). Annexin-V also significantly reduced total and intracellular hemoglobin, an iron-rich RBC degradation product, in the bEnd.3 cells (**Figure 3G**), confirming the role of RBC surface phosphatidylserine exposure in brain endothelial erythrophagocytosis. Mechanistically, studies

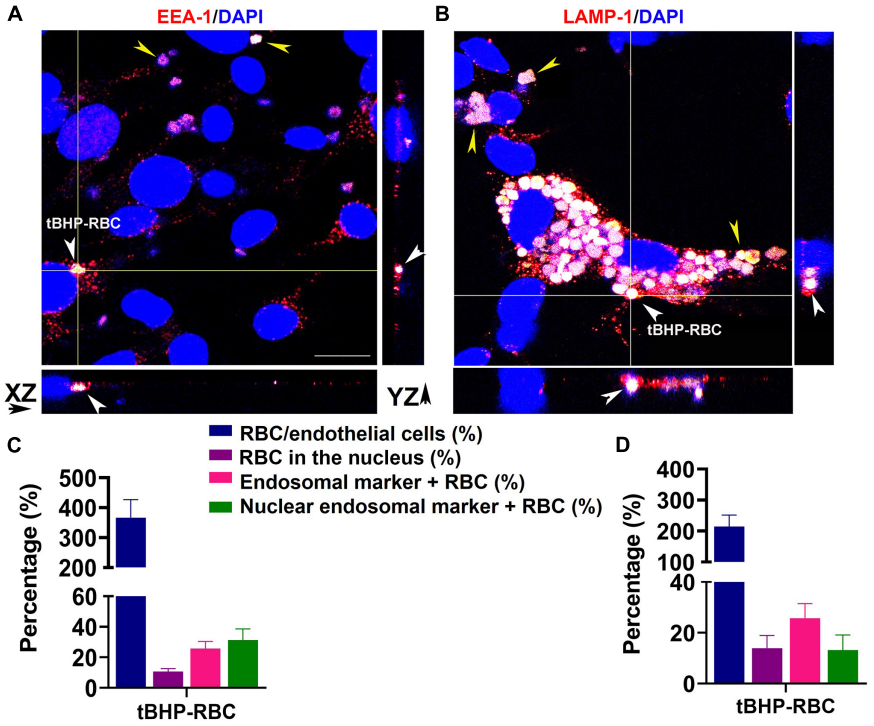

FIGURE 5 | A subset of tBHP-RBCs localized to early and late endosomes. bEnd.3 cells were stained for early endosome antigen 1 (EEA-1; red) **(A)**, lysosome–associated membrane protein 1 (LAMP-1; red) **(B)**, and 4′,6-diamidino-2-phenylindole (DAPI; blue) after a 48-h incubation with PBS- or tBHP-RBCs. RBCs are indicated by yellow arrowheads in panels **(A,B)**. Massive accumulation of tBHP-RBCs within bEnd.3 cells is shown in panel **(B)**. Orthogonal projections from z-stacks of confocal images show tBHP-RBCs co-localized with the endosomal markers in bEnd.3 cells (white arrowheads in **A,B**). Scale bar = 20 μm. Quantification of RBC attachment (expressed as % of number of bEnd.3 cells), RBCs localized to the nucleus (expressed as % of total RBCs; also see **Supplementary Figure 2**), EEA-1- and LAMP-1-positive RBCs (expressed as % of total RBCs), and RBCs in the nucleus positive for EEA-1-/LAMP-1 (expressed as a % of RBCs in the nucleus) (EEA-1: **C** and LAMP-1: **D**). All experiments were repeated at least three times.

show that phosphatidylserine-dependent erythrophagocytosis by endothelial cells is mediated by the α_v integrins or phosphatidylserine-recognizing transmembrane receptors, stabilin-1 and stabilin-2 (Lee et al., 2011; Fens et al., 2012). Besides these, phosphatidylserine-recognizing receptors, including tyrosine kinase receptors, CD300, T-cell immunoglobulin, and mucin domain 1 and 4, are involved in the erythrophagocytosis of phosphatidylserine-exposing RBCs by macrophages, but the involvement of these receptors in endothelial erythrophagocytosis has not been reported and needs further investigation (Klei et al., 2017; Chang C. F. et al., 2018).

Besides RBC phosphatidylserine exposure, tBHP-RBCs showed a dose-dependent increase in intracellular ROS levels in the current study (**Figure 1**). Given that tBHP is a potent oxidative stressor (Fens et al., 2012; Chang R. et al., 2018), we investigated the involvement of oxidative stress in brain endothelial erythrophagocytosis. For this, we incubated tBHP-RBCs with vitamin C, a ROS scavenger. Vitamin C treatment resulted in a 90% reduction of ROS accumulation and phosphatidylserine exposure of tBHP-RBCs (**Figures 4A,B**). Accordingly, we observed a significant reduction in erythrophagocytosis of tBHP-RBCs, indicating that both ROS production and phosphatidylserine exposure play a vital role in the brain endothelial erythrophagocytosis (**Figure 4**). Notably, endothelial cell viability was not altered with brain endothelial erythrophagocytosis up to 48 h, which is consistent with the observations in human peripheral vascular endothelial cells (Catan et al., 2019). It should be noted that despite the almost complete reversal of phosphatidylserine exposure with phosphatidylserine masking with annexin-V (**Figure 3**) and the highest concentration of vitamin C (**Figure 4**), brain endothelial erythrophagocytosis was not completely abolished by these agents. These results suggest the involvement of alternate molecular mechanisms of brain endothelial erythrophagocytosis. In this regard, studies show the involvement of vascular cell adhesion molecule 1 (VCAM-1) and intercellular adhesion molecule 4 (ICAM-4) in erythrocyte adhesion to endothelial cells under pathological conditions (Wautier and Wautier, 2013). The expression of these adhesion molecules is increased by pro-inflammatory cytokines, including TNFα. Although we did not study the role of these adhesion molecules on brain endothelial erythrophagocytosis, treatment of brain endothelial cells and tBHP-RBCs with TNFα significantly enhanced brain endothelial erythrophagocytosis in a dose-dependent manner (**Supplementary Figure 1**), showing the role of inflammation in potentiating brain endothelial erythrophagocytosis, *in vitro*. Besides phosphatidylserine and adhesion molecules, CD47 on the RBC surface is a well-studied "eat me" or "don't eat me"

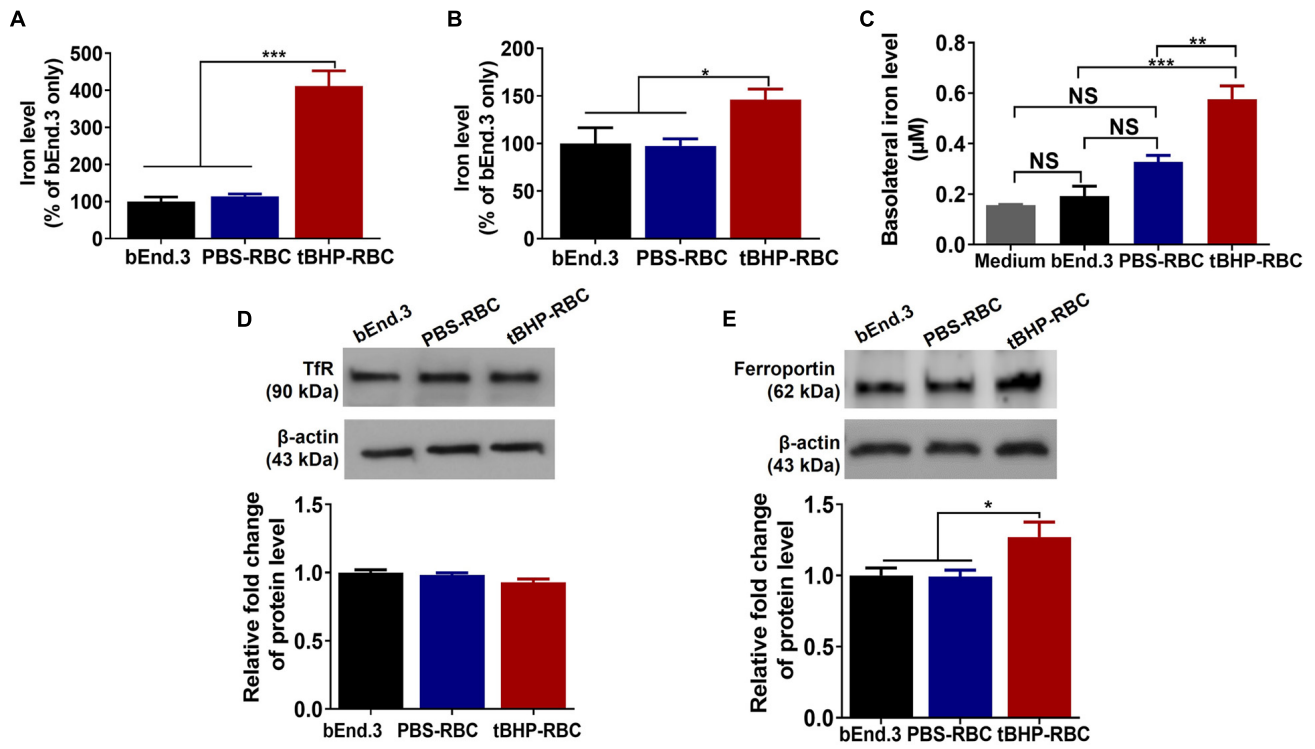

FIGURE 6 | Brain endothelial erythrophagocytosis increased cellular iron load and abluminal iron. Significant increase in total cellular iron (iron from attached and engulfed RBCs) **(A)** and intracellular iron (iron from engulfed RBC) **(B)** in bEnd.3 cells following a 48-h incubation with tBHP-RBCs. Significant increase in basolateral iron levels after the 48-h incubation with tBHP-RBCs **(C)**. No change in the levels of iron importer, transferrin receptor (TfR) **(D)**, but an increase in the levels of iron exporter, ferroportin **(E)**, in bEnd.3 cells after the 48-h incubation with PBS- or tBHP-RBCs. Data are presented as mean ± SEM of three independent experiments done in duplicates. One-way ANOVA with Holm–Sidak *post hoc* test was used. $^{*}p < 0.05$, $^{**}p < 0.01$, $^{***}p < 0.001$. NS is "not significant".

signal and regulates erythrophagocytosis through its interaction with signal-regulatory protein alpha that is expressed on phagocytes including endothelial cells (Burger et al., 2012). We found a significant 27% reduction in CD47 expression in tBHP-RBCs compared with PBS-RBCs (**Supplementary Figure 4**). Future work will be needed to determine the role of the CD47-signal-regulatory protein alpha pathway in brain endothelial erythrophagocytosis.

The intracellular processing of RBCs by macrophages following erythrophagocytosis has been extensively studied and involves engulfment of the damaged/injured RBCs into phagosomes *via* phagocytosis, fusion of the phagosome with the lysosome, lysosomal degradation of the RBC, and release of RBC degradation products into the cytosol (Korolnek and Hamza, 2015). Before fusing with the lysosomes, the phagosomes undergo a regulated sequence of fusion events, which involves fusion with the organelles in the endocytic pathway (Duclos et al., 2000). The endocytic pathway is composed of several distinct compartments based on their functions. For example, early endosomes play a primary role in sorting and recycling, while late endosomal compartments, such as lysosomes, serve as a final destination for proteolytic degradation (Hu et al., 2015). Our results demonstrate that a subset of internalized tBHP-RBCs is co-localized with both early and late endosome markers (**Figure 5**). To examine the fate of the remaining attached RBCs, tBHP- or PBS-RBCs were added to the bEnd.3 monolayer, incubated for 48 h, after which the bEnd.3 media were replaced with fresh media, and the attached RBCs were incubated with the bEnd.3 cells for another 72 h (all the free-floating RBCs were removed with the medium change). The tBHP-RBCs attached to the bEnd.3 cells after 72 h (RBCs appear as black spots in **Supplementary Figure 2D**) were reduced. The total cellular iron levels in the tBHP-RBC-treated bEnd.3 cells were not significantly different from the PBS-RBC-treated bEnd.3 cells, suggesting that the tBHP-RBCs were not present inside the bEnd.3 cells (data not shown). When we measured the iron in the media to determine if the RBCs had internalized and degraded and the resulting iron released to the media, we found a small but significantly higher iron level in the media collected from the bEnd.3 cells incubated with tBHP-RBCs compared with PBS-RBCs (**Supplementary Figure 2E**). These results suggest that with time, the engulfed RBCs are degraded within the lysosome, as implicated by RBCs co-localized with LAMP-1 (**Figure 5**), and the resulting iron released into the media. Contrary to this, a recent study showed that microspheres and emboli are retained in the brain endothelial cells without degradation, triggering their transmigration (van der Wijk et al., 2020). Our previous *in vivo* work showed a similar phenomenon of RBC migration across the brain endothelium (Chang R. et al., 2018), and some of the engulfed RBCs may eventually transmigrate across the brain endothelium. Overall, although

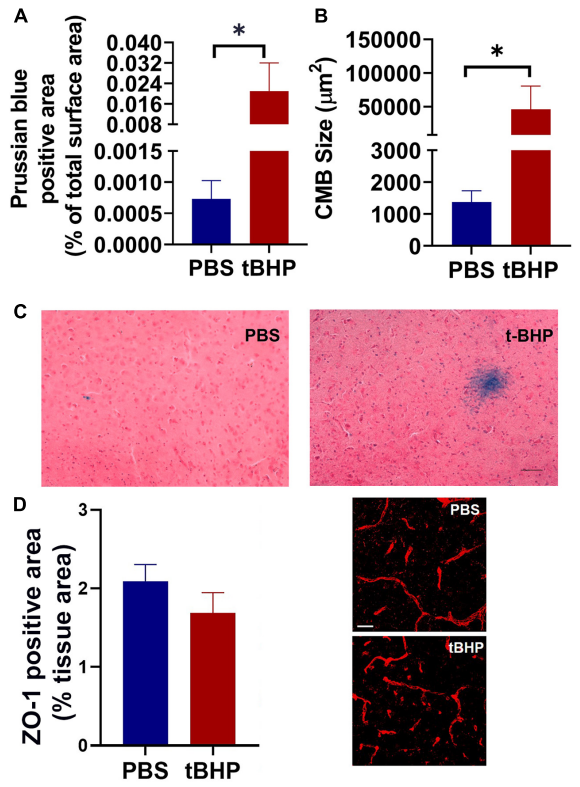

FIGURE 7 | *In vivo* iron-rich Prussian blue-positive cerebral microhemorrhage (CMH)-like lesion development. Aged mice injected with tBHP-RBCs had a higher total Prussian blue-positive lesion area **(A)** and individual lesion size **(B)** compared with the mice injected with PBS-RBCs. Representative Prussian-blue-positive lesions in mice injected with PBS- or tBHP-RBCs **(C)**. No significant difference in the ZO-1-positive area between the mice injected with tBHP-RBCs and PBS-RBCs was observed **(D)**. Data are presented as mean ± SEM of $n = 3$ per group. Scale bar = 200 μm in panel **(C)** and 25 μm in panel **(D)**. $^*p = 0.05$ with a Mann–Whitney U test.

the massive engulfment of tBHP-RBCs by some endothelial cells may overwhelm the abovementioned clearance mechanisms at some point, increase the intracellular iron pool, and trigger endothelial cell apoptosis, we did not observe overt endothelial cell death up to 5 days (48 + 72 h) following RBC incubation (**Supplementary Figure 2D**). However, we, cannot rule out apoptosis, although only a fraction of HUVEC cells showed signs of apoptosis post-erythrophagocytosis following 24 h of incubation (Fens et al., 2012).

We observed RBCs not only in the cytosol but also in the nucleus (**Figure 5** and **Supplementary Figure 2**). Trafficking of cargo to the nucleus has been reported previously and been shown to impact cellular function and regulate gene expression (Olsnes et al., 2003; Chaumet et al., 2015). Further, cellular trafficking is dependent on the size of cargo, such that large cargos (3 μm) are directed to the nucleus for digestion (Keller et al., 2017). It is therefore conceivable that the large size of the RBC sorts them to the nucleus in the current study. This finding of RBC trafficking to the endothelial cell nucleus is novel, and its implication needs to be further investigated.

In the current study, brain endothelial erythrophagocytosis was accompanied with a significant increase in the intracellular iron pool (**Figure 6**), which is consistent with previous work showing an increase in cellular iron load with erythrophagocytosis by professional phagocytes (Knutson et al., 2003). Additionally, and more relevant from the standpoint of iron-rich CMH-like lesion development, we showed an increase in migration of iron across an intact endothelial cell monolayer, providing direct evidence for increased abluminal iron with brain endothelial erythrophagocytosis. These results build on our prior report that brain endothelial erythrophagocytosis was accompanied by passage of hemoglobin across the brain endothelial monolayer with unaltered brain endothelial monolayer integrity (Chang R. et al., 2018). Sources of abluminal iron in the current study could be hemoglobin or cytosolic iron (iron released after lysosomal degradation within the brain endothelial cells) which migrates across the brain endothelial monolayer. These results show that brain endothelial erythrophagocytosis is associated with an increase in abluminal (brain facing) iron load. Once in the brain parenchyma, microglial cells are well equipped to clear RBC and its degradation products, including hemoglobin, *via* scavenger receptors including CD36, CD47, CD163, and CD91 (Pan et al., 2020). Within the microglial cells, hemoglobin can be broken down into free heme followed by free iron that is stored as the insoluble hemosiderin-iron. Similarly, brain iron homeostasis is tightly regulated by the blood–brain barrier transferrin receptors, apotransferrin released by the oligodendrocytes, and iron transporters present on the ependymal surface. Transferrin-bound iron can also be taken up by astrocytes or neurons that express transferrin receptors. Any excess iron released from hemoglobin degradation may be stored as ferritin-iron (Wagner et al., 2003).

Increased cellular iron load after erythrophagocytosis is associated with alterations in iron transport proteins (Knutson et al., 2003). To elucidate the impact of brain endothelial erythrophagocytosis on the brain endothelial iron transporters, we measured levels of TfR, the major iron influx transporter, and ferroportin, the only known iron exporter at the blood–brain barrier (Ganz, 2005; Moos et al., 2007; McCarthy and Kosman, 2015). TfRs are localized to the luminal and abluminal surface of the brain microvasculature (Huwyler and Pardridge, 1998) and facilitate iron uptake into the brain microvascular endothelial cells and export into the brain *via* receptor-mediated transcytosis (Moos et al., 2007). Similarly, studies show that ferroportin is also localized to both the luminal and abluminal surfaces of the brain microvasculature to facilitate iron export from the brain endothelial cells (Wu et al., 2004; McCarthy and Kosman, 2015). In the current study, brain endothelial erythrophagocytosis was not associated with a change in TfR protein levels; however, ferroportin protein levels were significantly increased (**Figure 6**). This is consistent with an increase in ferroportin levels following erythrophagocytosis by macrophages (Knutson et al., 2003) and may be a compensatory response to maintain iron homeostasis and prevent iron overloading within the endothelial cells (Chiou et al., 2019). This also provides a potential explanation for why the brain

endothelial cell viability and brain endothelial integrity are not compromised despite robust erythrophagocytosis and cellular iron increase (**Figure 3** and **Supplementary Figure 3**).

Our previous work provided *in vivo* evidence for migration of tBHP-RBCs across an intact brain endothelium in Tie2-GFP mice, while the PBS-RBCs remained confined to the vasculature (Chang R. et al., 2018). These findings were recently corroborated by a study showing brain endothelial erythrophagocytosis of Plasmodium falciparum-infected RBCs *in vivo* (Adams et al., 2021). In the current study, we show that mice injected with tBHP-RBCs had a greater Prussian blue-positive CMH-like lesion load compared with mice injected with PBS-RBCs (**Figure 7**), supporting the *in vitro* findings of increased abluminal iron with brain endothelial erythrophagocytosis (**Figure 6**). Our previous work using *ex vivo* microscopy demonstrated an intact endothelium at the site of RBC extravasation (Chang R. et al., 2018) as opposed to a ruptured endothelium, which is seen with Prussian blue-positive lesions associated with blood–brain barrier damage (Sumbria et al., 2016). Further, we found no change in the blood–brain barrier tight junction protein ZO-1 seven days after tBHP-RBC injection (**Figure 7**). This is in line with our recent work showing no association between blood–brain barrier changes with CMH development in humans (Wadi et al., 2020). Accordingly, our *in vitro* data and other reports (Catan et al., 2019) show no change in brain endothelial cell viability and permeability with erythrophagocytosis (**Figure 3** and **Supplementary Figure 3**). However, it is important to note that erythrophagocytosis of glycated RBCs is associated with alterations in endothelial function (e.g., reduction in migration and proliferation), and a small increase in apoptotic markers has been reported with endothelial erythrophagocytosis *in vitro* (Fens et al., 2012; Catan et al., 2019). Additionally, engulfment of microspheres by the brain endothelium and subsequent migration into the brain parenchyma is associated with temporary blood–brain barrier opening in a microembolization rat model (van der Wijk et al., 2020). Therefore, the increased RBC or iron load within the brain endothelial cells might trigger temporal endothelial remodeling or dysfunction resulting in blood–brain barrier changes. These changes may further increase the extravasation of RBCs and/or RBC degradation products into the brain, increasing the likelihood of iron-rich lesion development. Future work using intravital imaging will allow us to examine the causal and temporal relationship between brain endothelial erythrophagocytosis and blood–brain barrier permeability at the site of RBC extravasation using tracers followed by Prussian-blue staining to detect iron-rich lesions. These studies will also help elucidate how widespread brain endothelial erythrophagocytosis is, and if brain endothelial erythrophagocytosis-mediated abluminal iron increase is a focal or a diffuse event. Notably, our *in vivo* study showed focal iron deposits associated with tBHP-RBCs.

Overall, based on the results of the current study we propose the following sequence of events whereby brain endothelial erythrophagocytosis may result in iron-rich CMH-like lesion development (**Figure 8**): oxidative stress and

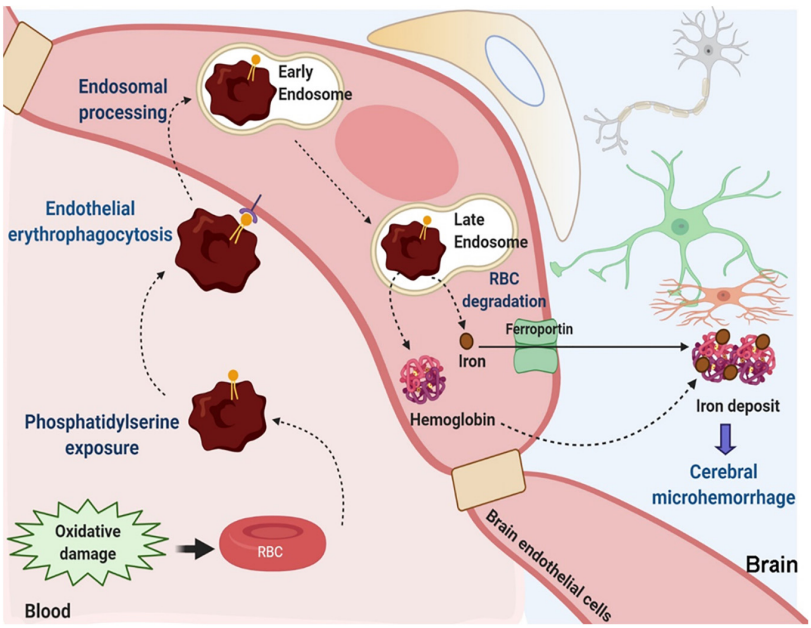

FIGURE 8 | Suggested mechanisms contributing to brain endothelial erythrophagocytosis mediated Prussian blue-positive cerebral lesions. Oxidative stress and phosphatidylserine exposure increase phagocytosis of RBCs by the brain endothelium. Other mechanisms including CD47 reduction may also be involved. Engulfed RBCs undergo endosomal sorting and ultimately undergo degradation within the late endosomes/lysosomes. This increases intracellular pools of iron-rich RBC degradation products, hemoglobin and iron. Free iron may be effluxed from the brain endothelial cells *via* the abluminal iron-exporter ferroportin. Alternatively, hemoglobin may migrate across the brain endothelium. Migration of iron-rich RBC degradation products across the brain endothelial cells can increase the brain abluminal iron, resulting in Prussian blue-positive CMH-like lesion development.

phosphatidylserine exposure increase phagocytosis of RBCs by the brain endothelium. Other mechanisms including CD47 reduction may also contribute to this process. A subset of engulfed RBCs undergoes endosomal sorting and degradation. RBC engulfment and degradation increase intracellular pools of iron-rich RBC degradation products, hemoglobin and iron. Free iron may be effluxed from the brain endothelial cells *via* the iron exporter ferroportin. Additionally, hemoglobin may migrate across the brain endothelium (Chang R. et al., 2018). Both iron and hemoglobin migration across the brain endothelial cells increases brain abluminal iron, which results in Prussian blue-positive CMH-like lesion development.

DATA AVAILABILITY STATEMENT

The original contributions presented in the study are included in the article/**Supplementary Material**, further inquiries can be directed to the corresponding author.

ETHICS STATEMENT

The animal study was reviewed and approved by University of California-Irvine's Institutional Animal Care and Use Committee, and carried out in compliance with University Laboratory Animal Resources regulations.

AUTHOR CONTRIBUTIONS

RKS and MJF conceptualized the study. JS, PV, RKS, and DHC assisted with the experimental design. JS, PV, SM, and RKS performed the experiments and data analysis. AP-H assisted with the data analysis. ACFN and WLL assisted with the *in vivo* study. JS and RKS wrote the first draft of the manuscript. RKS, DHC, and MJF acquired the funding. All authors discussed the results and their implications, and commented on the manuscript. All authors read and approved the final manuscript.

FUNDING

This work was supported by a grants from NINDS R01NS20989 (MJF and DHC) and NIA R01AG062840 (RKS).

ACKNOWLEDGMENTS

The authors thank Jan Michelle Martin, Sriyansh Yarlagadda, Gurnoor Kaur, Rudy Chang, and Matthew Choi for their assistance with confocal imaging quantification, cell culture, and immunostaining; Tiffany Tran and Catherine Huynh for Prussian blue imaging; Han Liu for *in vivo* experiments; and Kyle Ryan McCarty for ICP-MS iron measurement. ICP-MS was performed at the Pomona College Environmental Analysis Laboratories.

SUPPLEMENTARY MATERIAL

The Supplementary Material for this article can be found online at: https://www.frontiersin.org/articles/10.3389/fcell.2021.672009/full#supplementary-material

REFERENCES

Adams, Y., Olsen, R. W., Bengtsson, A., Dalgaard, N., Zdioruk, M., Satpathi, S., et al. (2021). *Plasmodium falciparum* erythrocyte membrane protein 1 variants induce cell swelling and disrupt the blood-brain barrier in cerebral malaria. *J. Exp. Med.* 218:e20201266.

Bonomini, M., Sirolli, V., Gizzi, F., Di Stante, S., Grilli, A., and Felaco, M. (2002). Enhanced adherence of human uremic erythrocytes to vascular endothelium: role of phosphatidylserine exposure. *Kidney Int.* 62, 1358–1363. doi: 10.1111/j.1523-1755.2002.kid560.x

Burger, P., Hilarius-Stokman, P., de Korte, D., van den Berg, T. K., and van Bruggen, R. (2012). CD47 functions as a molecular switch for erythrocyte phagocytosis. *Blood* 119, 5512–5521. doi: 10.1182/blood-2011-10-386805

Catan, A., Turpin, C., Diotel, N., Patche, J., Guerin-Dubourg, A., Debussche, X., et al. (2019). Aging and glycation promote erythrocyte phagocytosis by human endothelial cells: potential impact in atherothrombosis under diabetic conditions. *Atherosclerosis* 291, 87–98. doi: 10.1016/j.atherosclerosis.2019.10.015

Chang, C. F., Goods, B. A., Askenase, M. H., Hammond, M. D., Renfroe, S. C., Steinschneider, A. F., et al. (2018). Erythrocyte efferocytosis modulates macrophages towards recovery after intracerebral hemorrhage. *J. Clin. Invest.* 128, 607–624. doi: 10.1172/jci95612

Chang, R., Castillo, J., Zambon, A. C., Krasieva, T. B., Fisher, M. J., and Sumbria, R. K. (2018). Brain endothelial erythrophagocytosis and hemoglobin transmigration across brain endothelium: implications for pathogenesis of cerebral microbleeds. *Front. Cell. Neurosci.* 12:279. doi: 10.3389/fncel.2018.00279

Chaumet, A., Wright, G. D., Seet, S. H., Tham, K. M., Gounko, N. V., and Bard, F. (2015). Nuclear envelope-associated endosomes deliver surface proteins to the nucleus. *Nat. Commun.* 6:8218.

Chiou, B., Neal, E. H., Bowman, A. B., Lippmann, E. S., Simpson, I. A., and Connor, J. R. (2019). Endothelial cells are critical regulators of iron transport in a model of the human blood-brain barrier. *J. Cereb. Blood Flow. Metab.* 39, 2117–2131. doi: 10.1177/0271678x18783372

de Back, D. Z., Kostova, E. B., van Kraaij, M., van den Berg, T. K., and van Bruggen, R. (2014). Of macrophages and red blood cells; a complex love story. *Front. Physiol.* 5:9. doi: 10.3389/fphys.2014.00009

Duclos, S., Diez, R., Garin, J., Papadopoulou, B., Descoteaux, A., Stenmark, H., et al. (2000). Rab5 regulates the kiss and run fusion between phagosomes and endosomes and the acquisition of phagosome leishmanicidal properties in RAW 264.7 macrophages. *J. Cell Sci.* 113(Pt 19), 3531–3541. doi: 10.1242/jcs.113.19.3531

Fens, M. H., Mastrobattista, E., de Graaff, A. M., Flesch, F. M., Ultee, A., Rasmussen, J. T., et al. (2008). Angiogenic endothelium shows lactadherin-dependent phagocytosis of aged erythrocytes and apoptotic cells. *Blood* 111, 4542–4550. doi: 10.1182/blood-2007-06-094763

Fens, M. H., Storm, G., Pelgrim, R. C., Ultee, A., Byrne, A. T., Gaillard, C. A., et al. (2010). Erythrophagocytosis by angiogenic endothelial cells is enhanced by loss of erythrocyte deformability. *Exp. Hematol.* 38, 282–291. doi: 10.1016/j.exphem.2010.02.001

Fens, M. H., van Wijk, R., Andringa, G., van Rooijen, K. L., Dijstelbloem, H. M., Rasmussen, J. T., et al. (2012). A role for activated endothelial cells in red blood cell clearance: implications for vasopathology. *Haematologica* 97, 500–508. doi: 10.3324/haematol.2011.048694

Fisher, M. (2014). Cerebral microbleeds: where are we now? *Neurology* 83, 1304–1305. doi: 10.1212/wnl.0000000000000871

Fisher, M., Kapur, K., Soo, S., Lyou, Y., Schreiber, S. S., and Kim, M. J. (2018). Disseminated microinfarctions with cerebral microbleeds. *J. Stroke Cerebrovasc. Dis.* 27, e95–e97.

Franco, R. S. (2012). Measurement of red cell lifespan and aging. *Transfus. Med. Hemother.* 39, 302–307. doi: 10.1159/000342232

Ganz, T. (2005). Cellular iron: ferroportin is the only way out. *Cell Metab.* 1, 155–157. doi: 10.1016/j.cmet.2005.02.005

Garfield, R. E., Chacko, S., and Blose, S. (1975). Phagocytosis by muscle cells. *Lab. Invest.* 33, 418–427.

Gottlieb, Y., Topaz, O., Cohen, L. A., Yakov, L. D., Haber, T., Morgenstern, A., et al. (2012). Physiologically aged red blood cells undergo erythrophagocytosis in vivo but not in vitro. *Haematologica* 97, 994–1002. doi: 10.3324/haematol.2011.057620

Greenberg, S. M., Vernooij, M. W., Cordonnier, C., Viswanathan, A., Al-Shahi Salman, R., Warach, S., et al. (2009). Cerebral microbleeds: a guide to detection and interpretation. *Lancet Neurol.* 8, 165–174. doi: 10.1016/s1474-4422(09)70013-4

Grutzendler, J., Murikinati, S., Hiner, B., Ji, L., Lam, C. K., Yoo, T., et al. (2014). Angiophagy prevents early embolus washout but recanalizes microvessels through embolus extravasation. *Sci. Transl. Med.* 6:226ra31. doi: 10.1126/scitranslmed.3006585

Hu, Y. B., Dammer, E. B., Ren, R. J., and Wang, G. (2015). The endosomal-lysosomal system: from acidification and cargo sorting to neurodegeneration. *Transl. Neurodegener.* 4:18.

Huwyler, J., and Pardridge, W. M. (1998). Examination of blood-brain barrier transferrin receptor by confocal fluorescent microscopy of unfixed isolated rat brain capillaries. *J. Neurochem.* 70, 883–886. doi: 10.1046/j.1471-4159.1998.70020883.x

Janaway, B. M., Simpson, J. E., Hoggard, N., Highley, J. R., Forster, G., Drew, D., et al. (2014). Brain haemosiderin in older people: pathological evidence for an ischaemic origin of magnetic resonance imaging (MRI) microbleeds. *Neuropathol. Appl. Neurobiol.* 40, 258–269. doi: 10.1111/nan.12062

Keller, S., Berghoff, K., and Kress, H. (2017). Phagosomal transport depends strongly on phagosome size. *Sci. Rep.* 7:17068.

Klei, T. R., Meinderts, S. M., van den Berg, T. K., and van Bruggen, R. (2017). From the cradle to the grave: the role of macrophages in erythropoiesis and erythrophagocytosis. *Front. Immunol.* 8:73. doi: 10.3389/fimmu.2017.00073

Knutson, M. D., Vafa, M. R., Haile, D. J., and Wessling-Resnick, M. (2003). Iron loading and erythrophagocytosis increase ferroportin 1 (FPN1) expression in J774 macrophages. *Blood* 102, 4191–4197. doi: 10.1182/blood-2003-04-1250

Korolnek, T., and Hamza, I. (2015). Macrophages and iron trafficking at the birth and death of red cells. *Blood* 125, 2893–2897. doi: 10.1182/blood-2014-12-567776

Kucukal, E., Ilich, A., Key, N. S., Little, J. A., and Gurkan, U. A. (2018). Red blood cell adhesion to heme-activated endothelial cells reflects clinical phenotype in sickle cell disease. *Am. J. Hematol.* 93, 1050–1060. doi: 10.1002/ajh.25159

Lau, W. L., Nunes, A. C. F., Vasilevko, V., Floriolli, D., Lertpanit, L., Savoj, J., et al. (2020). Chronic kidney disease increases cerebral microbleeds in mouse and man. *Transl. Stroke Res.* 11, 122–134. doi: 10.1007/s12975-019-00698-8

Lee, S. J., Park, S. Y., Jung, M. Y., Bae, S. M., and Kim, I. S. (2011). Mechanism for phosphatidylserine-dependent erythrophagocytosis in mouse liver. *Blood* 117, 5215–5223. doi: 10.1182/blood-2010-10-313239

Lizarbe, M. A., Barrasa, J. I., Olmo, N., Gavilanes, F., and Turnay, J. (2013). Annexin-phospholipid interactions. Functional implications. *Int. J. Mol. Sci.* 14, 2652–2683. doi: 10.3390/ijms14022652

Martinez-Ramirez, S., Greenberg, S. M., and Viswanathan, A. (2014). Cerebral microbleeds: overview and implications in cognitive impairment. *Alzheimers Res. Ther.* 6:33. doi: 10.1186/alzrt263

McCarthy, R. C., and Kosman, D. J. (2015). Mechanisms and regulation of iron trafficking across the capillary endothelial cells of the blood-brain barrier. *Front. Mol. Neurosci.* 8:31. doi: 10.3389/fnmol.2015.00031

Moos, T., Rosengren Nielsen, T., Skjørringe, T., and Morgan, E. H. (2007). Iron trafficking inside the brain. *J. Neurochem.* 103, 1730–1740. doi: 10.1111/j.1471-4159.2007.04976.x

Nakagawa, K., Kiko, T., Kuriwada, S., Miyazawa, T., Kimura, F., and Miyazawa, T. (2011). Amyloid beta induces adhesion of erythrocytes to endothelial cells and affects endothelial viability and functionality. *Biosci. Biotechnol. Biochem.* 75, 2030–2033. doi: 10.1271/bbb.110318

Olsnes, S., Klingenberg, O., and Wiedlocha, A. (2003). Transport of exogenous growth factors and cytokines to the cytosol and to the nucleus. *Physiol. Rev.* 83, 163–182. doi: 10.1152/physrev.00021.2002

Pan, P., Xu, L., Zhang, H., Liu, Y., Lu, X., Chen, G., et al. (2020). A review of hematoma components clearance mechanism after subarachnoid hemorrhage. *Front. Neurosci.* 14:685. doi: 10.3389/fnins.2020.00685

Sumbria, R. K., Grigoryan, M. M., Vasilevko, V., Krasieva, T. B., Scadeng, M., Dvornikova, A. K., et al. (2016). A murine model of inflammation-induced cerebral microbleeds. *J. Neuroinflammation* 13:218.

van der Wijk, A. E., Georgakopoulou, T., Majolee, J., van Bezu, J. S. M., van der Stoel, M. M., van Het Hof, B. J., et al. (2020). Microembolus clearance through angiophagy is an auxiliary mechanism preserving tissue perfusion in the rat brain. *Acta Neuropathol. Commun.* 8:195.

Wadi, L. C., Grigoryan, M. M., Kim, R. C., Fang, C., Kim, J., Corrada, M. M., et al. (2020). Mechanisms of cerebral microbleeds. *J. Neuropathol. Exp. Neurol.* 42, 1093–1099.

Wagner, K. R., Sharp, F. R., Ardizzone, T. D., Lu, A., and Clark, J. F. (2003). Heme and iron metabolism: role in cerebral hemorrhage. *J. Cereb. Blood Flow Metab.* 23, 629–652. doi: 10.1097/01.wcb.0000073905.87928.6d

Wautier, J. L., and Wautier, M. P. (2013). Molecular basis of erythrocyte adhesion to endothelial cells in diseases. *Clin. Hemorheol. Microcirc.* 53, 11–21. doi: 10.3233/ch-2012-1572

Wu, L. J., Leenders, A. G., Cooperman, S., Meyron-Holtz, E., Smith, S., Land, W., et al. (2004). Expression of the iron transporter ferroportin in synaptic vesicles and the blood-brain barrier. *Brain Res.* 1001, 108–117. doi: 10.1016/j.brainres.2003.10.066

Conflict of Interest: The authors declare that the research was conducted in the absence of any commercial or financial relationships that could be construed as a potential conflict of interest.

Publisher's Note: All claims expressed in this article are solely those of the authors and do not necessarily represent those of their affiliated organizations, or those of the publisher, the editors and the reviewers. Any product that may be evaluated in this article, or claim that may be made by its manufacturer, is not guaranteed or endorsed by the publisher.

Copyright © 2021 Sun, Vyas, Mann, Paganini-Hill, Nunes, Lau, Cribbs, Fisher and Sumbria. This is an open-access article distributed under the terms of the Creative Commons Attribution License (CC BY). The use, distribution or reproduction in other forums is permitted, provided the original author(s) and the copyright owner(s) are credited and that the original publication in this journal is cited, in accordance with accepted academic practice. No use, distribution or reproduction is permitted which does not comply with these terms.

frontiers in Cell and Developmental Biology

REVIEW
published: 27 August 2021
doi: 10.3389/fcell.2021.679995

New Technologies With Increased Precision Improve Understanding of Endothelial Cell Heterogeneity in Cardiovascular Health and Disease

Ashley Dawson[1], Yidan Wang[1], Yanming Li[1], Scott A. LeMaire[1,2] and Ying H. Shen[1,2]**

[1] Division of Cardiothoracic Surgery, Michael E. DeBakey Department of Surgery, Baylor College of Medicine, Houston, TX, United States, [2] Department of Cardiovascular Surgery, Texas Heart Institute, Houston, TX, United States

OPEN ACCESS

Edited by:
Bin Ren,
University of Alabama at Birmingham,
United States

Reviewed by:
Y. Eugene Chen,
University of Michigan, United States
Anton G. Kutikhin,
Research Institute of Complex Problems of Cardiovascular Disease
Russian Academy of Medical Sciences, Russia

***Correspondence:**
Ying H. Shen
hyshen@bcm.edu
Scott A. LeMaire
slemaire@bcm.edu

Specialty section:
This article was submitted to Signaling,
a section of the journal
Frontiers in Cell and Developmental Biology

Received: 12 March 2021
Accepted: 17 June 2021
Published: 27 August 2021

Citation:
Dawson A, Wang Y, Li Y, LeMaire SA and Shen YH (2021) New Technologies With Increased Precision Improve Understanding of Endothelial Cell Heterogeneity in Cardiovascular Health and Disease. Front. Cell Dev. Biol. 9:679995. doi: 10.3389/fcell.2021.679995

Endothelial cells (ECs) are vital for blood vessel integrity and have roles in maintaining normal vascular function, healing after injury, and vascular dysfunction. Extensive phenotypic heterogeneity has been observed among ECs of different types of blood vessels in the normal and diseased vascular wall. Although ECs with different phenotypes can share common functions, each has unique features that may dictate a fine-tuned role in vascular health and disease. Recent studies performed with single-cell technology have generated powerful information that has significantly improved our understanding of EC biology. Here, we summarize a variety of EC types, states, and phenotypes recently identified by using new, increasingly precise techniques in transcriptome analysis.

Keywords: endothelial cell heterogeneity, transcriptomics, endothelial mesenchymal transition, vascular remodeling and arteriogenesis, vascular disease, atherosclerosis, cardiac disease

INTRODUCTION

Endothelial cells (ECs) are vital for maintaining blood vessel integrity in the cardiovascular system. Beyond functioning as a physical barrier, ECs have been shown to play a broader role in vascular physiology and pathology, exhibiting various phenotypes associated with different functions. In addition, ECs have been shown to change phenotype in response to tissue injury, shear stress, physical location, and environmental stimuli. Changes in ECs at the transcriptional level have been compared between healthy and disease states and among different organs. Although phenotypic changes in ECs can promote healing in response to injury, excessive changes are also linked to various types of vascular pathology, including atherosclerosis, fibrosis after heart disease, and other vasculopathies.

Newer techniques such as single-cell analysis have provided even greater precision, improving our understanding of EC heterogeneity and how ECs change in response to stimuli. Data from single-cell RNA sequencing (scRNA-seq) analysis allow for unsupervised clustering of ECs on the basis of each cell's transcriptome. Transcriptomic data collected from ECs in multiple different experiments and among several tissue types and disease states support the existence of a variety of EC phenotypes including quiescent ECs involved in maintaining homeostasis, proliferative

ECs, inflammatory ECs, remodeling ECs, ECs involved in endothelial-mesenchymal transition (EndMT), and ECs involved in angiogenesis (**Figure 1** and **Table 1**).

In this review, we summarize recent technological advancements that have improved our understanding of EC populations, the factors driving phenotypic change, and the ways in which ECs respond to their environment in health and disease.

EC PHENOTYPES

Quiescent ECs and the Promotion of Homeostasis

Cell-Specific Features

Quiescent ECs are common within the healthy vessel wall and promote homeostasis through metabolism, vasodilation, anticoagulation, and anti-inflammation (Ricard et al., 2021). In scRNA-seq studies, clusters associated with normal EC homeostasis have been identified that exhibit increased expression of genes involved in promoting EC stability (*Arhgap18*, *Adm*, and *Hspb1*), as well as lipid metabolism (*Cd36*, *Gpihbp1*, *Lpl*, *Myip*, *Pltp*, and *Scarb1*) (Hippenstiel et al., 2002; Kalluri et al., 2019; Lay et al., 2019). Using scRNA-seq analysis, Lukowski et al. (2019) showed that most ECs in normal mouse descending aorta are in a quiescent G1 phase, which is further supported by the results of cell cycle analysis showing predominantly G1 markers and few proliferative G2M/S phase markers. In a study by Li et al. (2019), the largest cluster of ECs was found to be associated with homeostasis and did not differ in proportion between healthy and diseased cardiac tissues. In another study, which provided a single-cell atlas of mouse ECs, ECs involved in metabolism were identified among different tissue types, indicative of an important and conserved function most likely related to homeostasis and disease resilience (Kalucka et al., 2020; Ricard et al., 2021).

Functions

In healthy tissues, quiescent ECs remain in cell-cycle arrest. However, in the setting of environmental stressors such as disturbed flow or ischemia, ECs may be stimulated to proliferate and promote angiogenesis (Zecchin et al., 2017). Therefore, quiescent ECs may be considered as a baseline from which ECs can undergo phenotypic changes in response to different stimuli.

Regulatory Genes and Pathways

Normal laminar flow has been shown to result in EC quiescence, featuring the downregulation of genes associated with proliferation, inflammation, and apoptosis (Dolan et al., 2012). Protective pathways activated by normal laminar flow include the mitogen-activated protein kinase kinase 5-extracellular signal-regulated kinase 5 (MEK5-ERK5) pathway, which was shown to decrease EndMT and atherogenesis (Moonen et al., 2015). Kruppel-like factor (KLF) 2 and KLF4, downstream effectors of the MEK5-ERK5 pathway, have also been shown to have vasculoprotective effects (Ohnesorge et al., 2010; Moonen et al., 2015). The presence of quiescent ECs and ECs that promote homeostasis in different environments highlights their important functions. ScRNA-seq analysis of ECs has revealed clusters with the activation of gene pathways involved in maintaining homeostasis that are conserved across different tissue types, including the Wnt and mitogen-activated protein kinase (MAPK) pathways (Paik et al., 2020).

Proliferative ECs

Cell-Specific Features

Proliferative ECs have been identified by their increased viability in culture, as well as through transcriptome analyses showing their increased expression of cell-cycle progression genes (Dolan et al., 2012; Vozzi et al., 2018; Khan et al., 2019; Li et al., 2019; Kalucka et al., 2020). ScRNA-seq studies have also identified clusters of proliferative ECs. In mouse tumor cells, specific EC clusters expressed increased levels of proliferation markers including *Cks2*, *Tyms*, *Birc5*, *Cdc20*, *Ccna2*, *Cdca8*, *Mki67*, *Top2a*, and *Rrm2* (Khan et al., 2019; Li et al., 2019). Furthermore, increased expression of these proliferation markers within a distinct subcluster of ECs may be responsible for the overall increased expression of proliferation markers observed in the bulk RNA sequencing of tumor ECs. These findings highlight the impact of more precise sequencing methods in determining the mechanism underlying disease. In a single-cell atlas of ECs among different types of mouse tissues, proliferative ECs were associated with genes such as *Ccdc34*, *Cdkn1a*, *Cks1b*, *Cks2,* and *Tyms*. ScRNA-seq analysis of murine cardiac tissues revealed a cluster of cardiac ECs expressing similar proliferative genes, such as *Mki67*, *Top2a*, *Cks2*, *Birc5*, and *Cdc20*), as well as *Plvap* (Li et al., 2019).

Functions

In a normal state, ECs have low proliferative qualities; however, single-cell analysis of normal tissues has revealed the existence of clusters with gene expression that is consistent with that of proliferative ECs, most likely in areas exposed to disturbed flow or in areas undergoing vasculogenesis. ECs in areas of oscillatory shear stress and disturbed flow have been found to have increased mitotic activity (Chien, 2003). Proliferative ECs are also seen in stalk cells in vasculogenesis (Mack and Iruela-Arispe, 2018). Proliferative ECs are activated in response to vascular injury, hypoxia, and ischemia (Dolan et al., 2012; Vozzi et al., 2018; Li et al., 2019). After MI, an increase in proliferative ECs has been observed in murine hearts (Tombor et al., 2021). EC proliferation may represent a mechanism for maintaining the structural and functional integrity of the endothelium. Further studies may help determine whether these ECs are predominantly a response to vascular stress or a key factor in the promotion of vascular disease.

Regulatory Pathways

Most studies have evaluated proliferative ECs in the setting of disturbed flow. Disturbed flow has been shown to activate yes-associated protein 1 (YAP) and transcriptional coactivator with PDZ-binding motif (TAZ) and ERK1/2 and induce EC proliferation (Bao et al., 2001; Wang et al., 2016; Nakajima and Mochizuki, 2017). Additionally, upon exposure to disturbed

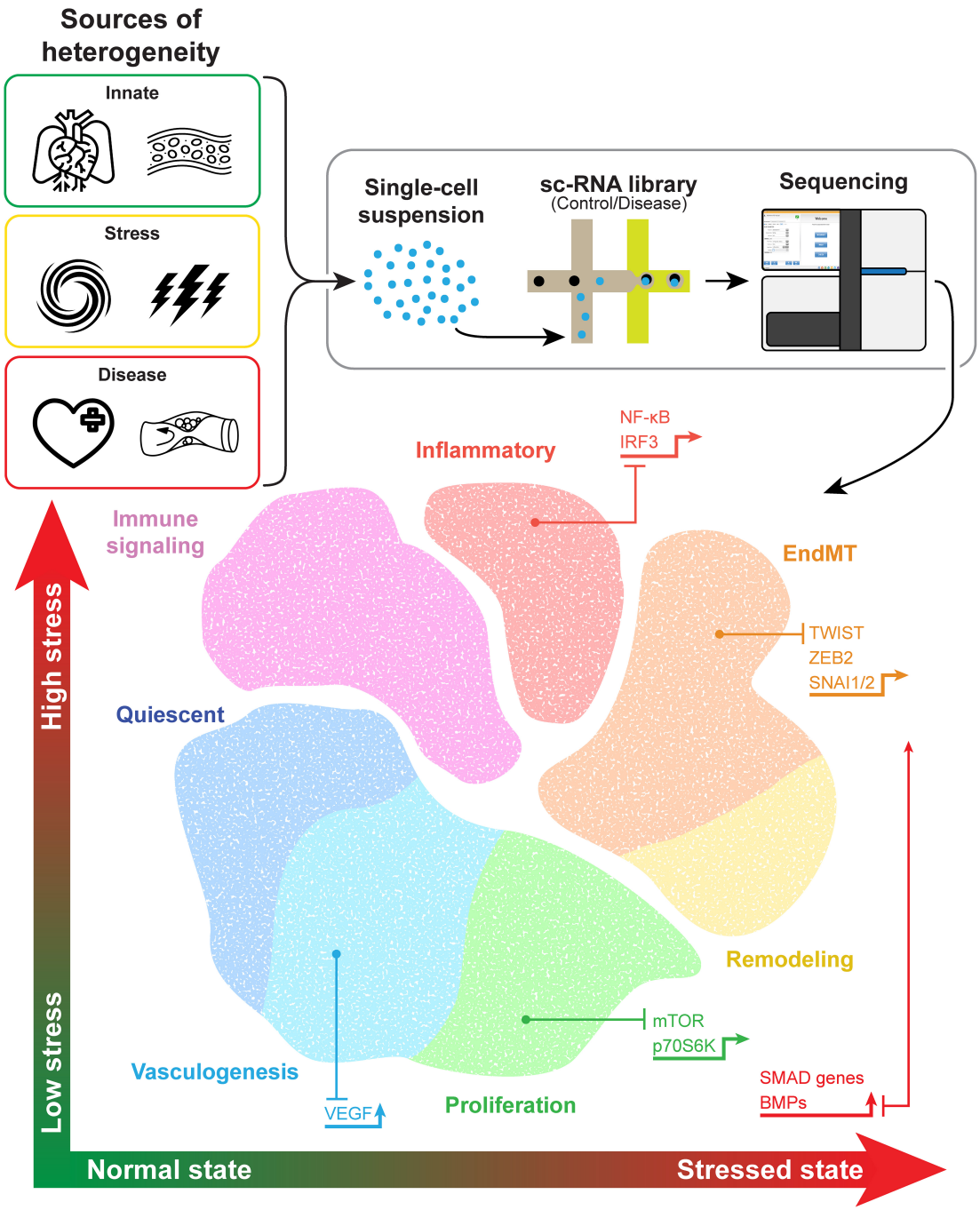

FIGURE 1 | Endothelial cell heterogeneity revealed by cell-specific sequencing. Endothelial cells (ECs) exhibit phenotypic differences that stem from inherent organo-specific, vessel-specific, and site-specific functions. Additionally, ECs can change phenotypes in response to cell stress or vascular disease, with representative pathways and transcription factors promoting different phenotypes, as shown with the associated arrows. The isolation and sequencing of single cells allow for improved precision in determining different endothelial cell phenotypes or cell states. Although distinct phenotypes have been identified, some features overlap, such as proliferative stalk cells in vasculogenesis. Evidence supports a potential phenotypic spectrum of some types of ECs, such as those involved in remodeling and endothelial-mesenchymal transition.

flow, bone morphogenic proteins (BMPs) stimulate SMAD genes, which modulate cyclin-dependent kinases to induce cell cycle progression. Zhou et al. (2012) showed that disturbed flow alone can also activate SMAD1/5, which in turn activates the proliferative factors mTOR and p70S6K. This results in the upregulation of cyclin A, downregulation of p21 and p27 (two inhibitors of cell cycle progression), and increased EC proliferation.

TABLE 1 | Endothelial cell phenotypes identified by transcriptome analysis.

EC phenotype	Stimulus	Transcription factors	Genetic markers in scRNA-seq	EC function	References
Quiescent	Laminar flow	KLF2, KLF4	*Arhgap18, Adm, Apoc, Cd36, Gpihbp1, Hspb1, Lpl, Myip, Pltp, Scarb1*	Maintain homeostasis, lipid metabolism, vasculo-protection	Ohnesorge et al. (2010); Moonen et al. (2015); Schaum et al. (2018); Kalluri et al. (2019)
Proliferative	Disturbed flow, oxidative stress, vascular injury	YAP/TAZ	***Birc5**, Cdca8, Ccna2, Ccdc34, **Cdc20**, Cdkn1a, Cenpa, **Cks2**, Cks1b, Ezh2, Fen1, H2afz, Hmgb2, Hmgn2, Hsp90aa1, Lgals1, Lig1, Lmnb1, Nrm, Pcna, Plvap, **Mki67**, Rrm1, Rrm2, Smc2, Spc24, Stmn1, Tuba1b, **Tyms**, **Top2a***	Vessel repair after injury	Schaum et al. (2018); Khan et al. (2019); Kalucka et al. (2020)
Immune-signaling	Baseline immune surveillance, vascular injury		*Cxcl10, **Ifit1**, **Ifit2**, **Ifit3**, **Ifit3b**, Igtp, Isg15, Stat1, Tgtp2, **Usp18***	Response to T-cells, response to viral proteins	Li et al. (2019); Kalucka et al. (2020)
Inflammatory	Disturbed flow, oxidative stress	IRF3, NF-kB	***Il1b**, Il6, Ccl2, Ccl6, Ccl8, Cd74, **Cxcr4**, **Icam1**, Cd45, **Tnf***	Immune cell recruitment	Vozzi et al. (2018); Tombor et al. (2021)
Remodeling	Disturbed flow		*Adamts genes, Anxa2, **Bgn**, **Col5a**, Emilin, Fnln2, Hmcn1, Mgp, Plat, Plau, Timp3*	ECM degradation and maintenance	Dolan et al. (2012); Kalluri et al. (2019); Li et al. (2019)
Endothelial-mesenchymal transition (EndMT)	Disturbed flow, vascular injury, TGF-β signaling	TWIST, SMAD3, SNAI1/2, ZEB2	***Col1A1**, **Col1A2**, **Col3A1**, Ctgf, Fn1, Postn, Serpine1, Sele*	Vessel repair after injury, fibrosis	Kovacic et al. (2019); Xu et al. (2020); Tombor et al. (2021)
Vasculogenesis	VEGF, hypoxia, ischemia, disturbed flow		Tip cells: ***Angpt2**, **Apln**, Adm, Cldn5, **Cxcr4**, **Dll4**, Ednrb, Efnb2, Esm1, Flt4, Gja4, Hey1, Igfbp3, **Jag**, Kdr, **Kcne3**, Nid2, Nrp1, Nrp2, Notch1, **Plxnd1**, Ramp3, **Robo4*** Stalk cells: *Ackr1, Ehd4, Ki67, Tmem176a/b, Tmem252, Selp, Vwf*	Create new capillaries, vascular healing, promote inflammation	Su et al. (2018); Zhao et al. (2018); Kalluri et al. (2019); Kalucka et al. (2020)

Genes in bold are conserved in the same types of ECs across at least two studies. EC, endothelial cell; ECM, extracellular matrix.

Inflammatory ECs

Cell-Specific Features

Inflammatory, or activated, ECs have been identified by their increased expression of genes involved in inflammatory cell recruitment including *Cxc4*, *Icam1*, *Cd45*, *Tnf*, *Il1b*, and *Ccl8* (Vozzi et al., 2018; Li et al., 2019; Tombor et al., 2021). In a study by Tombor et al. (2021), scRNA-seq analysis early after myocardial infarction (MI) revealed increased populations of inflammatory cardiac ECs (*Tnf*, *Il1b*, *Ccl2*, *Ccl6*, *Ccl8*, and *Cd74*).

Functions

Similar to proliferative ECs, inflammatory and immune-response ECs appear to be stimulated by vascular injury and may be involved in the first steps of vascular repair. However, these ECs promote immune cell recruitment and vascular inflammation, which can cause thrombosis, lipid accumulation, and pathologic remodeling, contributing to the initiation and progression of vascular diseases such as atherosclerosis.

Regulatory Pathways and Transcriptional Factors

Endothelial cells have been shown to be activated to a proinflammatory state by shear stress, oxidative stress, C-reactive protein (CRP), and proinflammatory cytokines (Szmitko et al., 2003). Activation of ECs can lead to a positive feedback cycle and promote further inflammation. Activated ECs release proinflammatory molecules, causing the surrounding cells in the vessel wall to produce cytokines, in turn resulting in increased EC activation. The stimulation of ECs with interleukin (IL)1-β and tumor necrosis factor (TNF)-α induces increased expression of monocyte adhesion molecules, as well as the release of proinflammatory cytokines such as IL-18 and monocyte chemoattractant protein (MCP)-1, which further attract inflammatory cells. Increased levels of CRP seen in states of inflammation inhibit the release of nitric oxide (NO) from ECs and increase the expression of cytokines, monocyte adhesion molecules, MCP-1, and nuclear factor-κB (NF-κB) (Verma et al., 2002; Szmitko et al., 2003).

Nuclear factor-κB is a transcription factor activated by oxidative stress and shear stress and is responsible for the regulation of many proinflammatory genes, including those encoding TNF-α, IL-1, IL-8, and monocyte adhesion molecules in ECs (Xiao et al., 2014). Additionally, activation of pro-inflammatory transcription factor interferon regulatory factor (IRF)-3 by reactive oxygen species (ROS) results in increased expression of ICAM-1 (Mao et al., 2017).

Immune-Signaling ECs

Cell-Specific Features

Other EC phenotypes involved in immune-cell signaling identified by using single-cell analysis include ECs involved in natural killer cell signaling (*Klra3*, *Klra9*, and *Klra10*) and ECs involved in the interferon signaling response (*Ifit1*, *Ifit2*, *Ifit3*, *Ifit3b*, *Usp18*, and *Cxcl10*) (Li et al., 2019). A cluster of ECs involved in the interferon response was also identified in the single-cell atlas of mouse tissues, characterized by the increased expression of *Ifit1*, *Ifit3*, *Ifit3b*, *Igtp*, *Isg15*, *Stat1*, *Tgtp2*, and *Usp18* (Kalucka et al., 2020).

Functions

Immune-signaling ECs appear to be involved in innate immune surveillance, viral responses, and signaling to natural killer cells and T-cells. Like inflammatory ECs, immune-signaling ECs appear to be stimulated by vascular injury, but they are also likely important in baseline cell signaling in healthy tissues. Tissues with increased proportions of immune-surveillance ECs at baseline included those most involved in the immune response, such as liver, spleen, and lung (Kalucka et al., 2020). Interferon signaling through interferon gamma can also result in increased inflammation and decreased extracellular matrix (ECM) production in ECs (Sprague and Khalil, 2009). Li et al. (2019) reported that after MI, a cluster of ECs involved in interferon signaling was increased.

EndMT and Mesenchymal-Like ECs

Cell-Specific Features

Endothelial cells have also been shown to undergo a phenotypic switch toward a mesenchymal phenotype and gain features of other cell types such as fibroblasts or smooth muscle cells (SMCs) (Zeisberg et al., 2007; Ubil et al., 2014; Moonen et al., 2015; Kostina et al., 2016; Kovacic et al., 2019; Xu et al., 2020). By becoming more mesenchymal-like, ECs gain the ability to invade and migrate through the ECM and produce collagen and contractile proteins (Kovacic et al., 2019). In a scRNA-seq study comparing vascular ECs in mice exposed to disturbed flow or stable flow, a small cluster of ECs exposed to chronic disturbed flow had increased expression of a gene associated with disturbed flow (*Thsp1*) and SMC, fibroblast, and immune cell genes (*Acta2*, *Tagln*, *Dcn1*, and *Cd74*), consistent with EndMT (Andueza et al., 2020). In another scRNA-seq analysis of cardiac ECs in mice, a cluster of ECs consistent with EndMT was identified by the increased expression of *Col3a1*, *Fn1*, *Serpine1*, and markers of EC proliferation. An EC cluster tagged by the marker *CDH5* in EC fate–mapped mice also expressed these markers during the initial days after cardiac injury, consistent with EndMT (Tombor et al., 2021). This cluster, which increased 1 week after MI, returned to baseline later in the recovery course, suggestive of a transient EndMT state in response to injury (Tombor et al., 2021). This transient state, in which few EC-traced cells lost their EC markers entirely to become traditional fibroblasts, may explain the differences observed in studies of EndMT levels after vascular injury.

Functions

The effect of EndMT appears to be time dependent, with transient EndMT occurring in the immediate period after injury. Furthermore, chronic disturbed flow is associated with promotion of EndMT in atheroprone regions of the vasculature. This suggests that EndMT may be beneficial for repair after vascular injury but may also perpetuate vascular disease by increasing neointimal hyperplasia and fibrosis in areas of chronic stress (Andueza et al., 2020; Tombor et al., 2021). Additionally, the anti-thrombotic qualities expressed in ECs at baseline are diminished in EndMT, increasing the risk of thrombosis after injury (Hong et al., 2019).

Regulatory Pathways

EndMT has been shown to occur during embryonic development after injury in response to transforming growth factor (TGF)-β, Notch signaling, and inflammatory molecules (Kostina et al., 2016). Canonical TGF-β signaling is considered the driving force of EndMT (van Meeteren and ten Dijke, 2012). *TGFB2* induces EndMT and the increased expression of SMC markers, which reverts to normal levels after *TGFB2* is withdrawn, supportive of a transient phenotype (Tombor et al., 2021). The binding of TGF-β to its receptor activates SMAD genes, promoting the activation of transcription factors associated with EndMT including *TWIST*, *SMAD3*, *ZEB2*, and *SNAI1/2* (Kovacic et al., 2019). Other regulatory pathways involved in EndMT including metabolic, non-coding RNA, and epigenetic regulation pathways are summarized elsewhere in a comprehensive review of EndMT by Kovacic et al. (2019).

Remodeling ECs

Cell-Specific Features

Endothelial cells have been identified that have increased expression of ECM-remodeling genes, such as *ADAMTS* genes, *TIMP3*, and tissue plasminogen activators *PLAT* and *PLAU* (Dolan et al., 2012). In a scRNA-seq study of cardiac ECs, a cluster of ECs was identified with increased expression of ECM-associated genes, such as *Fbln2*, *Anxa2*, *Col5a2*, *Emilin*, *Hmcn1*, *Bgn*, and *Mgp* (Li et al., 2019). Another scRNA-seq analysis revealed a cluster of ECs with the increased expression of ECM genes, such as *Bgn*, *Dcn*, *Fn1*, *Fbln5*, *Lox*, *Mfap5*, *Pcolce2*, and several collagen genes.

Functions

Remodeling ECs are identified by genes associated with the degradation of ECM components (e.g., genes encoding fibrin, fibronectin, laminin, elastin, and collagen). These may be present in healthy tissues at baseline to assist in cell turnover and in response to laminar flow, whereby ECs migrate and realign

to the direction of flow (Brooks et al., 2002; Conway et al., 2010). Remodeling ECs may also be involved in the early steps of angiogenesis, such as ECM breakdown and the rapid assembly/disassembly of focal adhesion molecules to assist with EC migration in vascular sprouts.

Additionally, remodeling ECs may be involved in repair after vascular injury without fully transitioning to an EndMT phenotype. In one study, scRNA analysis of ECs in a murine model of cardiac ischemia revealed a cluster of remodeling ECs that was increased after MI (Li et al., 2019).

Remodeling ECs appear to be involved in both normal vessel homeostasis and in response to cardiovascular injury. Because there is significant overlap in cluster-defining genes between ECs and EndMT cells, additional cell-specific transcriptome studies are needed to help determine whether this is truly a distinct EC phenotype or an early precursor to EndMT cells that respond to cardiovascular injury.

ECs Involved in Angiogenesis

Cell-Specific Features

Phenotypic changes in ECs have been well studied in angiogenesis (Potente et al., 2011; Eelen et al., 2015; Mack and Iruela-Arispe, 2018; Mühleder et al., 2021). During capillary vessel sprouting, ECs can be divided into tip and stalk cells. Tip cells have transcriptome patterns of increased pro-angiogenesis factor expression and NOTCH signaling, whereas stalk cells are more highly proliferative (Mack and Iruela-Arispe, 2018). Single-cell analysis of ECs supports these phenotypes. A study of tumor ECs revealed a cluster with elevated expression of tip cell markers *Kcne3*, *Nid2*, and *Dll4*, as well as a cluster with increased expression of stalk cell markers *Vwf* and *Selp* (Zhao et al., 2018). Intermediate cells that fall between a tip and stalk cell phenotype were also identified. Several markers overlapped with the clusters identified by Li et al. in their single-cell analysis of cardiac tissue, which included one cluster consistent with stalk cells (*Ackr1*, *Ehd4*, *Tmem176a/b*, *Tmem252*, and *Selp*) and one cluster consistent with tip cells/NOTCH signaling (*Dll4*, *Notch1*, *Hey1*, *Jag1*, and *Gja4*) (Li et al., 2019). In another single-cell study of ECs, two EC clusters were identified that were involved in angiogenesis: one expressed genes consistent with tip cells (*Cxcr4*, *Cd34*, *Dll4*, *Flt4*, *Nrp1*, *Nrp2*, and *Plxnd1*), and the other expressed genes consistent with stalk cells (Kalluri et al., 2019).

Functions

In healthy vascular tissue, angiogenesis is important for blood vessel repair and new vessel formation. However, in vascular disease, angiogenesis can occur in response to environmental stimuli such as vessel injury or hypoxia. Pathologic increases in angiogenesis are also seen in tumor vasculature. Angiogenesis and inflammation may be linked, resulting in a positive feedback loop and the progression of vascular disease (Jeong et al., 2021).

Regulatory Pathways

Angiogenesis is stimulated by vascular endothelial growth factor (VEGF). ECs with the highest expression of the receptor gene *VEGFR2* have the greatest pro-angiogenesis response and lead to new vessel formation as tip cells (Eelen et al., 2015). Increased NOTCH signaling from tip cells via *Dll4* results in decreased ERK activity in stalk cells, causing decreased cell-cycle inhibition and increased proliferation (Mühleder et al., 2021). Anti-angiogenesis treatments that block *VEGF* and *Dll4* reduce the proliferation of ECs involved in capillary vessel sprouting, particularly tip cells (Zhao et al., 2018).

INNATE CONTRIBUTIONS TO EC HETEROGENEITY

Environmental stimuli have an important effect on the regulation of EC phenotypes (Aird, 2012). In addition, EC phenotypes differ widely, including organo-specific ECs, location-specific-ECs, and disease-specific ECs. Although these phenotypes may overlap, it is important to understand phenotypic changes within the context of the tissue type and conditions of each experiment. ECs from different types of vessels and tissues have been shown to have unique transcriptomes (Zhao et al., 2018; Kalucka et al., 2020; Paik et al., 2020). Different artery locations expose ECs to different stimuli, such as increased oxygen levels or mechanical stress. Cultured ECs have been shown to have expression patterns that are different than those observed *in vivo*. For example, differences in gene expression between ECs of different arteries *in vivo* are not as evident in cultured ECs (Burridge and Friedman, 2010). Furthermore, differential gene expression between lymphatic ECs and blood vessel ECs is also diminished (Wick et al., 2007). This indicates the importance of environment on EC gene expression. However, cells do retain some distinguishing factors *in vitro*, such as intrinsic transcriptional profiles stemming from vascular bed origin and vessel location, which is supportive of a multifactorial process that leads to cell-specific EC transcriptomes (Wick et al., 2007; Burridge and Friedman, 2010; Kutikhin et al., 2020).

Phenotypic Spectrum of ECs Across Different Vascular Beds

Endothelial cells exhibit unique expression profiles associated with vessel type in four main vessels: arteries, veins, capillaries, and lymphatic vessels. Cell studies conducted *in vitro* have identified EC precursors that express markers of different vessel beds. For example, *Hey2*, *Nos3*, and *Flt1* are expressed as arterial markers; *Klf4* and *Cdh2* as venous markers; and *Lyve1* as a lymphatic EC marker (Kutikhin et al., 2020). In a single-cell analysis of mouse embryonic tissues, arterial and venous populations of ECs were identified that had distinct gene expression profiles. Using single-cell analysis, Kalucka et al. (2020) showed that gene expression across ECs in arteries, capillaries, and veins occurs along a phenotypic spectrum. The highest expression of the traditional EC markers *Vwf* and *Vcam1* was seen at either end of the spectrum, consistent with large vessel arteries or veins. In this study, the EC transcriptomic signatures that were most consistent with large arteries across different tissue types (liver, lung, heart, and kidney) included *Gja4*, *Fbln5*, and *Clu*, whereas those most consistent with large veins included *Apoe*, *Bgn*, and *Plvap*. Some markers such as *Mgp*, which is an inhibitor of tissue calcification, were found

to be specific to both arteries and veins depending upon tissue type. Another analysis, in which endothelial-specific translating ribosome affinity purification (EC-TRAP) and high-throughput RNA sequencing were used, *Ephb4* was identified as a marker for arteries, and *Dll4* as a marker for capillaries (Cleuren et al., 2019).

Of the vessel-specific ECs, heterogeneity among tissue types was highest among capillary ECs, which had the fewest conserved markers across different tissue types, indicating that phenotypic changes in capillary ECs may be responsible for most of the adaptive response to tissue- and environment-specific stimuli. The ability of ECs to change from venous to arterial ECs has also been observed in single-cell studies of EC development (Su et al., 2018).

Lymphatic ECs have been previously identified by the increased expression of *Lyve1* and *Pdpn* and appear distinct from blood vessel ECs (e.g., artery, vein, and capillary ECs) on single-cell analysis (Wick et al., 2007; Kalucka et al., 2020). When multiple datasets from the single-cell analysis of ECs were combined, lymphatic ECs remained clustered together across different tissue types and experiments, indicating a highly conserved and specific transcriptome (Feng et al., 2019). In a scRNA-seq study of lung, heart, liver, and intestinal tissue, a cluster of lymphatic ECs was identified that expressed conserved genes including *Ccl21a*, *Mmrn1*, *Fgl2*, and *Thy1* (Kalucka et al., 2020). In another scRNA-seq study of mouse aorta, a cluster of lymphatic ECs was identified that expressed *Lyve1*, *Prss23*, and *Fxyd6* (Kalluri et al., 2019).

EC Atlases of Multiple Organ Types

As more single-cell studies of ECs are completed, publicly available data can be combined to support more powerful analyses with greater cell counts. A single-cell atlas of murine EC transcriptomes has been formed, and data have been combined for multiple different tissue types. These studies have provided insight into tissue- and vessel-specific transcriptomes, as well as sex-based differences in ECs, supporting the existence of extensive EC heterogeneity (Schaum et al., 2018; Kalucka et al., 2020; Paik et al., 2020). Transcriptional profiles for ECs in different tissues are unique, indicating tissue-specific EC functions, such as roles in membrane transport across the blood-tissue barrier in brain and testes, immunoregulation in spleen and liver, and redox homeostasis in heart tissues (Kalucka et al., 2020; Paik et al., 2020).

When comparing cardiac to vascular ECs, scRNA-seq revealed valvular, coronary artery, and heart wall ECs as clusters separate from vascular ECs (Cui et al., 2019; Feng et al., 2019). *NPR3* was found to be specific to cardiac ECs, whereas vascular ECs were found to have increased expression of ECM genes including *ELN*, *FBLN2,* and *FBLN5* (Cui et al., 2019). *Edh3* and *Fam167b* were identified as aorta-specific EC markers (Feng et al., 2019).

However, some transcriptional profiles are similar among tissues including adipose, heart, aorta, and kidney, indicating that there is at least some degree of overlap and that transcriptional differences seen within one organ system should be considered as potential differences in other systems. Additionally, the overlap of transcriptional phenotypes observed between mouse and human ECs within the same tissue type supports the translation of findings from mouse models to human disease.

Contribution of Sex-Based Differences to EC Heterogeneity

Sexual dimorphism in ECs has been observed and provides insight into sex-based differences that may affect the risk of vascular diseases (Stanhewicz et al., 2018). Compared with men, premenopausal women with hypertriglyceridemia were found to have increased levels of progenitor ECs, along with enhanced production of nitric oxide required for vascular homeostasis, indicating a protective role for these ECs against vascular disease in women (Ren et al., 2020). Additionally, female cultured human umbilical ECs showed higher expression of genes involved in cell proliferation and migration than did male human umbilical ECs. Thus, even *in vitro*, attention should be given to whether cells originate from males or females, and cells from both sexes should ideally be used for *in vitro* studies (Addis et al., 2014). Paik et al. (2020) performed scRNA-seq analysis of mouse ECs from different tissue types and also identified cluster-specific sex-based differences in ECs among mouse tissues, most predominantly in adipose, heart, and kidney tissues. This further emphasizes the importance of studying ECs from both sexes, particularly at a single-cell level, and supports the notion of different transcriptional patterns between sexes as a driving factor in vascular disease.

EFFECTS OF BIOMECHANICAL AND BIOCHEMICAL STRESS ON ECs

The Dose-Dependent Response of ECs to Laminar Shear Stress

Normal laminar flow has been shown to protect against vascular disease, whereby normal laminar flow stimulates EC quiescence and inhibits factors that promote inflammation, such as the Hippo/YAP pathway (Yuan et al., 2020). Dose-dependent gene expression within ECs at different levels of shear stress has been reported and is associated with vascular protection against higher shear stress (Brooks et al., 2002; Ohura et al., 2003; Conway et al., 2010; Dolan et al., 2012; Vozzi et al., 2018). The expression of flow-dependent genes *KLF2* and *KLF4* was not found to increase with increasing laminar flow, but the expression of other genes including inhibitory SMAD genes *SMAD*6 and *SMAD7* and the nitric oxide synthase gene *NOS3* increased with the level of flow (Mandrycky et al., 2020). In a scRNA-seq analysis of cultured ECs, cells exposed to high laminar flow became quiescent and more homogenous in phenotype (Helle et al., 2020). Compared with static conditions, low levels of shear stress were shown to increase EC viability and the expression of EC genes involved in mitosis, indicating a proliferative response (Brooks et al., 2002; Conway et al., 2010). However, as shear stress was increased, EC viability and markers of proliferation decreased, indicating that ECs exhibit a dose-dependent response to shear stress in proliferative pathways (Ohura et al., 2003; Vozzi et al., 2018; Helle et al.,

2020). In the single-cell analysis of ECs exposed to high flow, a spectrum of ECs was identified, with highly proliferative cells on one end and quiescent cells on the other. Many genes in the quiescent cluster were those regulated by Notch pathway activation, such as that seen in laminar shear stress (Mandrycky et al., 2020). Furthermore, under high shear stress conditions, the expression of ECM remodeling genes *MMP2* and *MMP9* was also increased (Sho et al., 2002; Dolan et al., 2012; Mahmoud et al., 2017), and the expression of genes associated with cell-matrix adhesion was decreased (Dolan et al., 2012). This supports previously reported findings that high shear stress induces EC rearrangement, such as ECs becoming elongated and aligning with the direction of flow (Brooks et al., 2002; Conway et al., 2010).

The EC Response to Disturbed Flow

Although changes in EC gene expression have been reported for static-, low-, and high-flow states, disturbed flow is most commonly associated with vascular diseases, such as atherosclerosis (Brown et al., 2016). Shear stress due to disturbed blood flow has been implicated as a driving factor for phenotypic changes in ECs, as evidenced by the unique transcriptional profiles of cells subjected to disturbed flow compared with those subjected to both high and low laminar flow states (Brooks et al., 2002; Conway et al., 2010; Vozzi et al., 2018; Andueza et al., 2020). EC proliferation is triggered by disturbed flow, as shown by the high proportion of ECs in mitosis in areas of disturbed blood flow (Zhou et al., 2012; Lee and Chiu, 2019). Additionally, disturbed flow but not laminar flow has been shown to lead to EndMT, resulting in neointimal hyperplasia and atherogenesis (Moonen et al., 2015). In a study by Andueza et al. (2020), scRNA-seq revealed clusters in ECs exposed to acute disturbed flow that were distinct from clusters in ECs exposed to chronic disturbed flow, indicating a time-dependent relationship between ECs and disturbed flow, with chronic disturbed flow being more closely associated with EndMT. Interestingly, in this analysis, some clusters of ECs were identified as more responsive than others to changes in flow states, suggesting that different EC phenotypes may have varying responses to shear stress and that a specific group of ECs may drive inflammatory and pathologic changes (Andueza et al., 2020). ScRNA-seq analysis showed the upregulation of inflammatory markers in ECs exposed to disturbed flow, particularly chronic disturbed flow (Andueza et al., 2020). Inflammatory adhesion was also highest in flow reversal states that mimic arterial disturbed flow *in vitro* (Conway et al., 2010; Vozzi et al., 2018).

Single-cell analysis of ECs has revealed the presence of quiescent, proliferative, inflammatory, and remodeling EC populations in disease states and under normal conditions. These populations may represent different stages of the endothelial response to laminar and disturbed flow. For example, laminar flow may promote a quiescence phenotype as well as a remodeling phenotype in ECs to allow for realignment with the direction of flow, whereas disturbed flow may promote proliferative, inflammatory, and EndMT phenotypes in ECs. These populations may also represent ECs in different physical locations, with some ECs having greater exposure to changes in flow, or some ECs being predisposed to respond to flow. Future studies with a focus on identifying where each of these unique cell populations are located may reveal cell populations or locations that are at increased risk for a pathologic response to shear stress. Precision spatial genomics provides a method to identify these populations *in situ* (Eng et al., 2019).

EC Changes in Response to Oxidative Stress

Endothelial cells also react to other environmental stressors, such as oxidative stress. Oxidative stress may be associated with risk factors for vascular disease such as smoking, hypertension, and hyperlipidemia. In future cell-specific studies, analyzing the changes in ECs of patients with risk factors for vascular disease may provide more information about how ECs respond to oxidative stress. In previous studies, ROS have been linked to inflammatory gene expression and the promotion of monocyte infiltration into the vascular wall (Kunsch and Medford, 1999). Oxidative stress may upregulate EC expression of the CD40 receptor, a member of the TNF family, and result in CD40-mediated EC activation, which stimulates ROS production, increased leukocyte adhesion, and inflammatory cell recruitment (Nakanishi et al., 2001; Schönbeck and Libby, 2001; Urbich et al., 2002).

EC PHENOTYPES IN CARDIOVASCULAR DISEASE

Endothelial cell clusters unique to vascular disease have been identified. To date, most EC-specific studies have been performed in experimental models of atherosclerosis and heart disease (Li et al., 2019; Andueza et al., 2020; Tombor et al., 2021).

Atherosclerosis

Areas of vessels with disturbed flow are more likely to develop atherosclerosis, such as the carotid bifurcations, aortic arch, and peripheral arterial branch points (Lee and Chiu, 2019). Analysis of EC phenotypes seen in vessels with disturbed flow support the observed increase in proliferative, inflammatory, and EndMT ECs in response to disturbed flow compared with laminar flow (Zhou et al., 2012; Moonen et al., 2015; Andueza et al., 2020). Cell-specific analysis of ECs in human atherosclerotic plaque has shown a transition to inflammatory and EndMT phenotypes (Depuydt et al., 2020).

In an scRNA-seq study (Andueza et al., 2020), EC phenotypes associated with acute disturbed flow were marked by expression of *Ctfg*, *Serpine1*, and *Edn1*. EC phenotypes associated with chronic disturbed flow were marked by *Thsp1*. A cluster of ECs involved in EndMT after exposure to chronic disturbed flow was marked by *Acta2*, *Tagln*, *Dcn1*, and immune cell markers including *CD74*. Transcription factor motifs associated with disturbed flow included *KLF4*, *RELA*, *AP1*, and *STAT1*. Additionally, in a scRNA-seq study (Depuydt et al., 2020) of atherosclerotic plaque, activated ECs were marked by *CD34*,

PECAM1, *TIE1*, *ACKR1*, *PRCP*, and *VCAM1*. EndMT ECs in atherosclerotic plaque were marked by *ACTA2*, *NOTCH3*, and *MYH11*.

Cardiac Disease

Single-cell analysis of murine cardiac ECs after MI revealed an increased proportion of ECs involved in the inflammatory response, proliferation, interferon signaling, vasculogenesis, and remodeling after MI compared with controls. Tombor et al. (2021) reported an increase in EC phenotypes involved in inflammation and proliferation as well as an increase in EndMT in murine cardiac ECs after MI. These EndMT clusters returned to baseline later in the recovery course, suggestive of a transient EndMT state in response to injury (Tombor et al., 2021). However, not all scRNA-seq analyses of ECs in mice after MI show an increase in EndMT during repair after injury (Li et al., 2019), most likely because of variations in the degree of EndMT transition (Kovacic et al., 2019; Tombor et al., 2021). This transient state identified by Tombor et al. (2021), in which very few EC-traced cells lose their EC markers entirely to become traditional fibroblasts, may explain differences between studies of EndMT levels after vascular injuries.

Single-cell analysis of murine hearts after MI revealed the upregulation of *Col3A1*, *Fn1*, and *Serpine1* in EC clusters undergoing transient EndMT and the downregulation of EC marker genes such as *Cdh5* and *Cd36* (Tombor et al., 2021). Overall, the gene ontology terms upregulated in these clusters included ECM organization, collagen synthesis, metabolic activity, angiogenesis, and Wnt signaling. EndMT transition in MI has been associated with Wnt signaling, with ECs that have undergone EndMT marked by increased expression of contractile genes and genes associated with Wnt signaling for 4 days after MI (Aisagbonhi et al., 2011; Tombor et al., 2021).

Neointima Formation and Restenosis

Endothelial cell dysfunction and remodeling are associated with neointima hyperplasia after injury or with restenosis after vascular procedures (Douglas et al., 2013; Moonen et al., 2015). Although neointimal hyperplasia has largely been considered to be due to SMC proliferation, increased attention has been placed on EC involvement. EC recruitment of inflammatory cells as well as EC proliferation and EndMT may contribute to the promotion of neointimal formation (Moonen et al., 2015; Moser et al., 2016).

On histologic analysis, ECs have been found to have an invasive phenotype in neointima formation, with most ECs remaining as ECs rather than undergoing EndMT (Yuan et al., 2017). Performing single-cell analysis of vascular tissues after procedures (e.g., cardiac stents or endovascular procedures) may help identify more precisely the EC-specific changes involved in restenosis and whether there are small populations with pro-inflammatory, proliferative or EndMT phenotypes, as seen in atherosclerotic plaque or after MI.

Calcific Aortic Valve Disease

Endothelial cells have been shown to have an important role in calcific aortic valve disease. As observed in atherosclerosis, ECs exposed to mechanical or shear stress become dysfunctional, with increased lipid deposition and immune cell infiltration (Goody et al., 2020). Calcification of the valve is more commonly found on the fibrosa (outflow) side of the valve, in the area most exposed to disturbed flow. Concordantly, EndMT transition of valvular ECs (VECs) has been identified as a factor in the progression of disease (Ma et al., 2020).

Early changes in human calcific aortic valve ECs consistent with EndMT have been identified by using single-cell analysis (Xu et al., 2020). In this study, one of the clusters of VECs was found to be an early cluster along a trajectory leading to traditional vascular interstitial cells, indicative of EndMT transition in calcific aortic valve disease.

Single-cell analysis of calcific aortic valve disease revealed that two clusters of VECs expressing the marker genes *SELE*, *SERPINE1*, *IL1R1*, and *PI3* were involved in EndMT (Xu et al., 2020). These clusters showed enrichment of the PI3K-Akt and Wnt pathways, which have been found to have a role in EndMT, whereby their upregulation promotes mesenchymal transition (Meadows et al., 2009; Zhong et al., 2018). Additionally, an *in vitro* study of aortic VECs showed that UBE2C (ubiquitin E2 ligase C) responded to disturbed flow by increasing *HIF1α* expression to promote VEC EndMT (Fernandez Esmerats et al., 2019).

Aortic Aneurysms

Much of aortic aneurysm research is focused on SMC mutations and ECM changes. However, because ECs are the first cells to be exposed to environmental stressors and to induce the activation of signaling pathways within the aortic wall, EC phenotype change in aortic aneurysms is an important area of study. Bicuspid aortic valves have been associated with ascending thoracic aortic aneurysms (ATAAs), and the disturbed flow through the valve may stimulate ECs to become proliferative and pro-inflammatory and to undergo EndMT, leading to vascular remodeling and aortic aneurysm formation (van de Pol et al., 2017). ECs are also involved in the angiotensin II signaling pathway, which has been linked to aneurysm development. The endothelial-specific knockout of the angiotensin II *AT1* receptor was shown to protect against thoracic aortic aneurysms (Rateri et al., 2011).

Genes Associated With Aortic Aneurysm Formation in ECs

Few single-cell sequencing studies have focused on EC phenotypes in aortic aneurysm development. In a study of sporadic ATAA by Li et al. (2020), two clusters of ECs were identified. Upon the analysis of differential gene expression, one of the clusters was found to have the majority of differentially expressed genes between sporadic ATAA and control tissues. In this cluster, the transcription factor *ERG* was found to be downregulated in ATAA tissues, along with its downstream genes involved in apoptosis and the response to reactive oxygen species, suggesting that *ERG* may be pathologically downregulated in ATAA.

CONCLUSION

Endothelial cells have dynamic populations with diverse functions. While these functions may overlap, ECs do have distinct transcriptomes, as highlighted by scRNA sequencing. Changes in EC phenotype are influenced by microenvironment, innate organo- and lineage-specific factors, and biomechanical and biochemical stressors.

Alteration of EC gene expression is an early event in vascular disease and plays a critical role in its progression. Identification of potential pathologic phenotypes may help advance precision medicine and guide cell-specific therapies in vascular disease. EC phenotypes identified on scRNA sequencing that are predominantly associated with cell stress include proliferative, inflammatory, and EndMT phenotypes, which may be pathologic if overexpressed. Additionally, knowledge of organo- and lineage-specific transcriptomic signatures may ultimately improve bioengineered tissues, including vascular conduits, and the organo-specific targeting of treatments.

Future studies will be important for expanding upon these phenotypes in different conditions. As more data become available, combining publicly available data obtained under similar conditions will increase the power and precision of analyses.

AUTHOR CONTRIBUTIONS

All authors conceived and designed the review, wrote the manuscript, participated in revising the manuscript, and read and approved the final version of the manuscript.

FUNDING

The research was supported by grants from the American Heart Association (AHA) Vascular Diseases Strategically Focused Research Networks (SFRN) (AHA18SFRN33960114, AHA18SFRN33960163, and AHA18SFRN33960253). SL's work was supported in part by the Jimmy and Roberta Howell Professorship in Cardiovascular Surgery at Baylor College of Medicine.

ACKNOWLEDGMENTS

We thank Nicole Stancel, Ph.D., ELS(D), of the Department of Scientific Publications at the Texas Heart Institute, for her editorial contributions and Scott A. Weldon, MA, CMI, FAMI, for creating the illustration.

REFERENCES

Addis, R., Campesi, I., Fois, M., Capobianco, G., Dessole, S., Fenu, G., et al. (2014). Human umbilical endothelial cells (HUVECs) have a sex: characterisation of the phenotype of male and female cells. *Biol. Sex Diff.* 5:18.

Aird, W. C. (2012). Endothelial cell heterogeneity. *Cold Spring Harb. Perspect. Med.* 2:a006429.

Aisagbonhi, O., Rai, M., Ryzhov, S., Atria, N., Feoktistov, I., and Hatzopoulos, A. K. (2011). Experimental myocardial infarction triggers canonical Wnt signaling and endothelial-to-mesenchymal transition. *Dis. Model Mech.* 4, 469–483. doi: 10.1242/dmm.006510

Andueza, A., Kumar, S., Kim, J., Kang, D. W., Mumme, H. L., Perez, J. I., et al. (2020). Endothelial reprogramming by disturbed flow revealed by single-cell RNA and chromatin accessibility study. *Cell Rep.* 33:108491. doi: 10.1016/j.celrep.2020.108491

Bao, X., Lu, C., and Frangos, J. A. (2001). Mechanism of temporal gradients in shear-induced ERK1/2 activation and proliferation in endothelial cells. *Am. J. Physiol. Heart Circ. Physiol.* 281, H22–H29.

Brooks, A. R., Lelkes, P. I., and Rubanyi, G. M. (2002). Gene expression profiling of human aortic endothelial cells exposed to disturbed flow and steady laminar flow. *Physiol. Genomics* 9, 27–41. doi: 10.1152/physiolgenomics.00075.2001

Brown, A. J., Teng, Z., Evans, P. C., Gillard, J. H., Samady, H., and Bennett, M. R. (2016). Role of biomechanical forces in the natural history of coronary atherosclerosis. *Nat. Rev. Cardiol* 13, 210–220. doi: 10.1038/nrcardio.2015.203

Burridge, K. A., and Friedman, M. H. (2010). Environment and vascular bed origin influence differences in endothelial transcriptional profiles of coronary and iliac arteries. *Am. J. Physiol. Heart Circ. Physiol.* 299, H837–H846.

Chien, S. (2003). Molecular and mechanical bases of focal lipid accumulation in arterial wall. *Prog. Biophys. Mol. Biol.* 83, 131–151. doi: 10.1016/s0079-6107(03)00053-1

Cleuren, A. C. A., van der Ent, M. A., Jiang, H., Hunker, K. L., Yee, A., Siemieniak, D. R., et al. (2019). The in vivo endothelial cell translatome is highly heterogeneous across vascular beds. *Proc. Natl. Acad. Sci. U.S.A.* 116, 23618–23624. doi: 10.1073/pnas.1912409116

Conway, D. E., Williams, M. R., Eskin, S. G., and McIntire, L. V. (2010). Endothelial cell responses to atheroprone flow are driven by two separate flow components: low time-average shear stress and fluid flow reversal. *Am. J. Physiol. Heart Circ. Physiol.* 298, H367–H374.

Cui, Y., Zheng, Y., Liu, X., Yan, L., Fan, X., Yong, J., et al. (2019). Single-cell transcriptome analysis maps the developmental track of the human heart. *Cell Rep.* 26, 1934.e5–1950.e5.

Depuydt, M. A. C., Prange, K. H. M., Slenders, L., Örd, T., Elbersen, D., Boltjes, A., et al. (2020). Microanatomy of the human atherosclerotic plaque by single-cell transcriptomics. *Circ. Res.* 127, 1437–1455.

Dolan, J. M., Sim, F. J., Meng, H., and Kolega, J. (2012). Endothelial cells express a unique transcriptional profile under very high wall shear stress known to induce expansive arterial remodeling. *Am. J. Physiol. Cell Physiol.* 302, C1109–C1118.

Douglas, G., Van Kampen, E., Hale, A. B., McNeill, E., Patel, J., Crabtree, M. J., et al. (2013). Endothelial cell repopulation after stenting determines in-stent neointima formation: effects of bare-metal vs. drug-eluting stents and genetic endothelial cell modification. *Eur. Heart J.* 34, 3378–3388. doi: 10.1093/eurheartj/ehs240

Eelen, G., de Zeeuw, P., Simons, M., and Carmeliet, P. (2015). Endothelial cell metabolism in normal and diseased vasculature. *Circ. Res.* 116, 1231–1244. doi: 10.1161/circresaha.116.302855

Eng, C. L., Lawson, M., Zhu, Q., Dries, R., Koulena, N., Takei, Y., et al. (2019). Transcriptome-scale super-resolved imaging in tissues by RNA seqFISH. *Nature* 568, 235–239. doi: 10.1038/s41586-019-1049-y

Feng, W., Chen, L., Nguyen, P. K., Wu, S. M., and Li, G. (2019). Single cell analysis of endothelial cells identified organ-specific molecular signatures and heart-specific cell populations and molecular features. *Front. Cardiovasc. Med.* 6:165. doi: 10.3389/fcvm.2019.00165

Fernandez Esmerats, J., Villa-Roel, N., Kumar, S., Gu, L., Salim, M. T., Ohh, M., et al. (2019). Disturbed flow increases UBE2C (ubiquitin E2 ligase C) via loss of mir-483-3p, inducing aortic valve calcification by the pVHL (von Hippel-Lindau protein) and HIF-1α (hypoxia-inducible factor-1α) pathway in endothelial cells. *Arterioscler. Thromb. Vasc. Biol.* 39, 467–481. doi: 10.1161/atvbaha.118.312233

Goody, P. R., Hosen, M. R., Christmann, D., Niepmann, S. T., Zietzer, A., Adam, M., et al. (2020). Aortic valve stenosis: from basic mechanisms to novel therapeutic targets. *Arterioscler. Thromb. Vasc. Biol.* 40, 885–900. doi: 10.1161/atvbaha.119.313067

Helle, E., Ampuja, M., Antola, L., and Kivelä, R. (2020). Flow-induced transcriptomic remodeling of endothelial cells derived from human induced pluripotent stem cells. *Front. Physiol.* 11:591450. doi: 10.3389/fphys.2020.591450

Hippenstiel, S., Witzenrath, M., Schmeck, B., Hocke, A., Krisp, M., Krüll, M., et al. (2002). Adrenomedullin reduces endothelial hyperpermeability. *Circ. Res.* 91, 618–625. doi: 10.1161/01.res.0000036603.61868.f9

Hong, L., Du, X., You, T., Sun, L., Li, W., Xiao, L., et al. (2019). Reciprocal enhancement of thrombosis by endothelial-to-mesenchymal transition induced by iliac vein compression. *Life Sci.* 233:116659. doi: 10.1016/j.lfs.2019.116659

Jeong, J.-H., Ojha, U., and Lee, Y. M. (2021). Pathological angiogenesis and inflammation in tissues. *Arch. Pharm. Res.* 44, 1–15. doi: 10.1007/s12272-020-01287-2

Kalluri, A. S., Vellarikkal, S. K., Edelman, E. R., Nguyen, L., Subramanian, A., Ellinor, P. T., et al. (2019). Single-cell analysis of the normal mouse aorta reveals functionally distinct endothelial cell populations. *Circulation* 140, 147–163. doi: 10.1161/circulationaha.118.038362

Kalucka, J., de Rooij, L., Goveia, J., Rohlenova, K., Dumas, S. J., Meta, E., et al. (2020). Single-cell transcriptome atlas of murine endothelial cells. *Cell* 180, 764.e20–779.e20.

Khan, S., Taverna, F., Rohlenova, K., Treps, L., Geldhof, V., de Rooij, L., et al. (2019). EndoDB: a database of endothelial cell transcriptomics data. *Nucleic Acids Res.* 47, D736–D744.

Kostina, A. S., Uspensky, V., Irtyuga, O. B., Ignatieva, E. V., Freylikhman, O., Gavriliuk, N. D., et al. (2016). Notch-dependent EMT is attenuated in patients with aortic aneurysm and bicuspid aortic valve. *Biochim. Biophys. Acta* 1862, 733–740. doi: 10.1016/j.bbadis.2016.02.006

Kovacic, J. C., Dimmeler, S., Harvey, R. P., Finkel, T., Aikawa, E., Krenning, G., et al. (2019). Endothelial to mesenchymal transition in cardiovascular disease: JACC state-of-the-art review. *J. Am. Coll. Cardiol.* 73, 190–209.

Kunsch, C., and Medford, R. M. (1999). Oxidative stress as a regulator of gene expression in the vasculature. *Circ. Res.* 85, 753–766. doi: 10.1161/01.res.85.8.753

Kutikhin, A. G., Tupikin, A. E., Matveeva, V. G., Shishkova, D. K., Antonova, L. V., Kabilov, M. R., et al. (2020). Human peripheral blood-derived endothelial colony-forming cells are highly similar to mature vascular endothelial cells yet demonstrate a transitional transcriptomic signature. *Cells* 9:876. doi: 10.3390/cells9040876

Lay, A. J., Coleman, P. R., Formaz-Preston, A., Ting, K. K., Roediger, B., Weninger, W., et al. (2019). ARHGAP18: a flow-responsive gene that regulates endothelial cell alignment and protects against atherosclerosis. *J. Am. Heart Assoc.* 8:e010057.

Lee, D. Y., and Chiu, J. J. (2019). Atherosclerosis and flow: roles of epigenetic modulation in vascular endothelium. *J. Biomed. Sci.* 26:56.

Li, Y., Ren, P., Dawson, A., Vasquez, H. G., Ageedi, W., Zhang, C., et al. (2020). Single-cell transcriptome analysis reveals dynamic cell populations and differential gene expression patterns in control and aneurysmal human aortic tissue. *Circulation* 142, 1374–1388. doi: 10.1161/circulationaha.120.046528

Li, Z., Solomonidis, E. G., Meloni, M., Taylor, R. S., Duffin, R., Dobie, R., et al. (2019). Single-cell transcriptome analyses reveal novel targets modulating cardiac neovascularization by resident endothelial cells following myocardial infarction. *Eur. Heart J.* 40, 2507–2520. doi: 10.1093/eurheartj/ehz305

Lukowski, S. W., Patel, J., Andersen, S. B., Sim, S. L., Wong, H. Y., Tay, J., et al. (2019). Single-cell transcriptional profiling of aortic endothelium identifies a hierarchy from endovascular progenitors to differentiated cells. *Cell Rep.* 27, 2748.e3–2758.e3.

Ma, X., Zhao, D., Yuan, P., Li, J., Yun, Y., Cui, Y., et al. (2020). Endothelial-to-mesenchymal transition in calcific aortic valve disease. *Acta Cardiol. Sin.* 36, 183–194.

Mack, J. J., and Iruela-Arispe, M. L. (2018). Notch regulation of the endothelial cell phenotype. *Curr. Opin. Hematol.* 25, 212–218. doi: 10.1097/moh.0000000000000425

Mahmoud, M. M., Serbanovic-Canic, J., Feng, S., Souilhol, C., Xing, R., Hsiao, S., et al. (2017). Shear stress induces endothelial-to-mesenchymal transition via the transcription factor snail. *Sci. Rep.* 7:3375.

Mandrycky, C., Hadland, B., and Zheng, Y. (2020). 3D Curvature-instructed endothelial flow response and tissue vascularization. *Sci Adv* 6:eabb3629. doi: 10.1126/sciadv.abb3629

Mao, Y., Luo, W., Zhang, L., Wu, W., Yuan, L., Xu, H., et al. (2017). STING-IRF$_3$ triggers endothelial inflammation in response to free fatty acid-induced mitochondrial damage in diet-induced obesity. *Arterioscler. Thromb. Vasc. Biol.* 37, 920–929. doi: 10.1161/ATVBAHA.117.309017

Meadows, K. N., Iyer, S., Stevens, M. V., Wang, D., Shechter, S., Perruzzi, C., et al. (2009). Akt promotes endocardial-mesenchyme transition. *J. Angiogenes. Res.* 1:2. doi: 10.1186/2040-2384-1-2

Moonen, J. R., Lee, E. S., Schmidt, M., Maleszewska, M., Koerts, J. A., Brouwer, L. A., et al. (2015). Endothelial-to-mesenchymal transition contributes to fibro-proliferative vascular disease and is modulated by fluid shear stress. *Cardiovasc. Res.* 108, 377–386. doi: 10.1093/cvr/cvv175

Moser, J., van Ark, J., van Dijk, M. C., Greiner, D. L., Shultz, L. D., van Goor, H., et al. (2016). Distinct differences on neointima formation in immunodeficient and humanized mice after carotid or femoral arterial injury. *Sci. Rep.* 6:35387.

Mühleder, S., Fernández-Chacón, M., Garcia-Gonzalez, I., and Benedito, R. (2021). Endothelial sprouting, proliferation, or senescence: tipping the balance from physiology to pathology. *Cell. Mol. Life Sci.* 78, 1329–1354. doi: 10.1007/s00018-020-03664-y

Nakajima, H., and Mochizuki, N. (2017). Flow pattern-dependent endothelial cell responses through transcriptional regulation. *Cell Cycle* 16, 1893–1901. doi: 10.1080/15384101.2017.1364324

Nakanishi, K., Yoshimoto, T., Tsutsui, H., and Okamura, H. (2001). Interleukin-18 regulates both Th1 and Th2 responses. *Annu. Rev. Immunol.* 19, 423–474.

Ohnesorge, N., Viemann, D., Schmidt, N., Czymai, T., Spiering, D., Schmolke, M., et al. (2010). Erk5 activation elicits a vasoprotective endothelial phenotype via induction of Kruppel-like factor 4 (KLF4). *J. Biol. Chem.* 285, 26199–26210. doi: 10.1074/jbc.m110.103127

Ohura, N., Yamamoto, K., Ichioka, S., Sokabe, T., Nakatsuka, H., Baba, A., et al. (2003). Global analysis of shear stress-responsive genes in vascular endothelial cells. *J. Atheroscler. Thromb.* 10, 304–313. doi: 10.5551/jat.10.304

Paik, D. T., Tian, L., Williams, I. M., Rhee, S., Zhang, H., Liu, C., et al. (2020). Single-cell RNA sequencing unveils unique transcriptomic signatures of organ-specific endothelial cells. *Circulation* 142, 1848–1862. doi: 10.1161/circulationaha.119.041433

Potente, M., Gerhardt, H., and Carmeliet, P. (2011). Basic and therapeutic aspects of angiogenesis. *Cell* 146, 873–887. doi: 10.1016/j.cell.2011.08.039

Rateri, D. L., Moorleghen, J. J., Balakrishnan, A., Owens, A. P. III, Howatt, D. A., Subramanian, V., et al. (2011). Endothelial cell-specific deficiency of Ang II type 1a receptors attenuates Ang II-induced ascending aortic aneurysms in LDL receptor-/- mice. *Circ. Res.* 108, 574–581. doi: 10.1161/circresaha.110.222844

Ren, Z., Guo, J., Xiao, X., Huang, J., Li, M., Cai, R., et al. (2020). The effect of sex differences on endothelial function and circulating endothelial progenitor cells in hypertriglyceridemia. *Cardiol. Res. Pract.* 2020:2132918.

Ricard, N., Bailly, S., Guignabert, C., and Simons, M. (2021). The quiescent endothelium: signalling pathways regulating organ-specific endothelial normalcy. *Nat. Rev. Cardiol.* doi: 10.1038/s41569-021-00517-4 Online ahead of print

Schaum, N., Karkanias, J., Neff, N. P., May, A. P., Quake, S. R., Wyss-Coray, T., et al. (2018). Single-cell transcriptomics of 20 mouse organs creates a tabula muris. *Nature* 562, 367–372.

Schönbeck, U., and Libby, P. (2001). CD40 signaling and plaque instability. *Circ. Res.* 89, 1092–1103. doi: 10.1161/hh2401.101272

Sho, E., Sho, M., Singh, T. M., Nanjo, H., Komatsu, M., Xu, C., et al. (2002). Arterial enlargement in response to high flow requires early expression of matrix metalloproteinases to degrade extracellular matrix. *Exp. Mol. Pathol.* 73, 142–153. doi: 10.1006/exmp.2002.2457

Sprague, A. H., and Khalil, R. A. (2009). Inflammatory cytokines in vascular dysfunction and vascular disease. *Biochem. Pharmacol.* 78, 539–552. doi: 10.1016/j.bcp.2009.04.029

Stanhewicz, A. E., Wenner, M. M., and Stachenfeld, N. S. (2018). Sex differences in endothelial function important to vascular health and overall cardiovascular disease risk across the lifespan. *Am. J. Physiol. Heart Circ. Physiol.* 315, H1569–H1588.

Su, T., Stanley, G., Sinha, R., D'Amato, G., Das, S., Rhee, S., et al. (2018). Single-cell analysis of early progenitor cells that build coronary arteries. *Nature* 559, 356–362. doi: 10.1038/s41586-018-0288-7

Szmitko, P. E., Wang, C.-H., Weisel, R. D., Almeida, J. R. D., Anderson, T. J., and Verma, S. (2003). New markers of inflammation and endothelial cell activation. *Circulation* 108, 1917–1923. doi: 10.1161/01.cir.0000089190.95415.9f

Tombor, L. S., John, D., Glaser, S. F., Luxán, G., Forte, E., Furtado, M., et al. (2021). Single cell sequencing reveals endothelial plasticity with transient mesenchymal activation after myocardial infarction. *Nat. Commun.* 12:681.

Ubil, E., Duan, J., Pillai, I. C., Rosa-Garrido, M., Wu, Y., Bargiacchi, F., et al. (2014). Mesenchymal-endothelial transition contributes to cardiac neovascularization. *Nature* 514, 585–590. doi: 10.1038/nature13839

Urbich, C., Dernbach, E., Aicher, A., Zeiher, A. M., and Dimmeler, S. (2002). CD40 ligand inhibits endothelial cell migration by increasing production of endothelial reactive oxygen species. *Circulation* 106, 981–986. doi: 10.1161/01.cir.0000027107.54614.1a

van de Pol, V., Kurakula, K., DeRuiter, M. C., and Goumans, M. J. (2017). Thoracic aortic aneurysm development in patients with bicuspid aortic valve: what is the role of endothelial cells? *Front. Physiol.* 8:938. doi: 10.3389/fphys.2017.00938

van Meeteren, L. A., and ten Dijke, P. (2012). Regulation of endothelial cell plasticity by TGF-β. *Cell Tissue Res.* 347, 177–186. doi: 10.1007/s00441-011-1222-6

Verma, S., Wang, C.-H., Li, S.-H., Dumont, A. S., Fedak, P. W. M., Badiwala, M. V., et al. (2002). A self-fulfilling prophecy. *Circulation* 106, 913–919.

Vozzi, F., Campolo, J., Cozzi, L., Politano, G., Di Carlo, S., Rial, M., et al. (2018). Computing of low shear stress-driven endothelial gene network involved in early stages of atherosclerotic process. *BioMed Res. Int.* 2018:5359830.

Wang, L., Luo, J. Y., Li, B., Tian, X. Y., Chen, L. J., Huang, Y., et al. (2016). Integrin-yap/taz-jnk cascade mediates atheroprotective effect of unidirectional shear flow. *Nature* 540, 579–582.

Wick, N., Saharinen, P., Saharinen, J., Gurnhofer, E., Steiner, C. W., Raab, I., et al. (2007). Transcriptomal comparison of human dermal lymphatic endothelial cells ex vivo and in vitro. *Physiol. Genomics* 28, 179–192.

Xiao, L., Liu, Y., and Wang, N. (2014). New paradigms in inflammatory signaling in vascular endothelial cells. *Am. J. Physiol. Heart Circ. Physiol.* 306, H317–H325.

Xu, K., Xie, S., Huang, Y., Zhou, T., Liu, M., Zhu, P., et al. (2020). Cell-type transcriptome atlas of human aortic valves reveal cell heterogeneity and endothelial to mesenchymal transition involved in calcific aortic valve disease. *Arterioscler. Thromb. Vasc. Biol.* 40, 2910–2921.

Yuan, F., Wang, D., Xu, K., Wang, J., Zhang, Z., Yang, L., et al. (2017). Contribution of vascular cells to neointimal formation. *PLoS One* 12:e0168914.

Yuan, P., Hu, Q., He, X., Long, Y., Song, X., Wu, F., et al. (2020). Laminar flow inhibits the Hippo/YAP pathway via autophagy and SIRT1-mediated deacetylation against atherosclerosis. *Cell Death Dis.* 11:141.

Zecchin, A., Kalucka, J., Dubois, C., and Carmeliet, P. (2017). How endothelial cells adapt their metabolism to form vessels in tumors. *Front. Immunol.* 8:1750. doi: 10.3389/fimmu.2017.01750

Zeisberg, E. M., Tarnavski, O., Zeisberg, M., Dorfman, A. L., McMullen, J. R., Gustafsson, E., et al. (2007). Endothelial-to-mesenchymal transition contributes to cardiac fibrosis. *Nat. Med.* 13, 952–961.

Zhao, Q., Eichten, A., Parveen, A., Adler, C., Huang, Y., Wang, W., et al. (2018). Single-cell transcriptome analyses reveal endothelial cell heterogeneity in tumors and changes following antiangiogenic treatment. *Cancer Res.* 78, 2370–2382.

Zhong, A., Mirzaei, Z., and Simmons, C. A. (2018). The roles of matrix stiffness and ß-catenin signaling in endothelial-to-mesenchymal transition of aortic valve endothelial cells. *Cardiovasc. Eng. Technol.* 9, 158–167.

Zhou, J., Lee, P. L., Tsai, C. S., Lee, C. I., Yang, T. L., Chuang, H. S., et al. (2012). Force-specific activation of Smad1/5 regulates vascular endothelial cell cycle progression in response to disturbed flow. *Proc. Natl. Acad. Sci. U. S. A.* 109, 7770–7775.

Conflict of Interest: The authors declare that the research was conducted in the absence of any commercial or financial relationships that could be construed as a potential conflict of interest.

Publisher's Note: All claims expressed in this article are solely those of the authors and do not necessarily represent those of their affiliated organizations, or those of the publisher, the editors and the reviewers. Any product that may be evaluated in this article, or claim that may be made by its manufacturer, is not guaranteed or endorsed by the publisher.

Copyright © 2021 Dawson, Wang, Li, LeMaire and Shen. This is an open-access article distributed under the terms of the Creative Commons Attribution License (CC BY). The use, distribution or reproduction in other forums is permitted, provided the original author(s) and the copyright owner(s) are credited and that the original publication in this journal is cited, in accordance with accepted academic practice. No use, distribution or reproduction is permitted which does not comply with these terms.

frontiers in Cell and Developmental Biology

ORIGINAL RESEARCH
published: 29 September 2021
doi: 10.3389/fcell.2021.693410

Obesity Inhibits Angiogenesis Through TWIST1-SLIT2 Signaling

Tendai Hunyenyiwa[1,2], Kathryn Hendee[1], Kienna Matus[1], Priscilla Kyi[1,2], Tadanori Mammoto[1,3] and Akiko Mammoto[1,2]**

[1] Department of Pediatrics, Medical College of Wisconsin, Milwaukee, WI, United States, [2] Department of Cell Biology, Neurobiology and Anatomy, Medical College of Wisconsin, Milwaukee, WI, United States, [3] Department of Pharmacology and Toxicology, Medical College of Wisconsin, Milwaukee, WI, United States

OPEN ACCESS

Edited by:
Bin Ren,
University of Alabama at Birmingham,
United States

Reviewed by:
Chunsik Lee,
Sun Yat-sen University, China
Reena Singh,
The University of Sydney, Australia
Xiaofeng Yang,
Temple University, United States

***Correspondence:**
Akiko Mammoto
amammoto@mcw.edu
Tadanori Mammoto
tmammoto@mcw.edu

Specialty section:
This article was submitted to Signaling, a section of the journal Frontiers in Cell and Developmental Biology

Received: 10 April 2021
Accepted: 30 August 2021
Published: 29 September 2021

Citation:
Hunyenyiwa T, Hendee K, Matus K, Kyi P, Mammoto T and Mammoto A (2021) Obesity Inhibits Angiogenesis Through TWIST1-SLIT2 Signaling. Front. Cell Dev. Biol. 9:693410. doi: 10.3389/fcell.2021.693410

Angiogenesis is required for functional adipose tissue maintenance, remodeling, and expansion. Physiologically balanced adipogenesis and angiogenesis are inhibited in subcutaneous adipose tissue in obese humans. However, the mechanism by which angiogenesis is inhibited in obese adipose tissue is not fully understood. Transcription factor TWIST1 controls angiogenesis and vascular function. TWIST1 expression is lower in obese human adipose tissues. Here, we have demonstrated that angiogenesis is inhibited in endothelial cells (ECs) isolated from adipose tissues of obese humans through TWIST1-SLIT2 signaling. The levels of TWIST1 and SLIT2 are lower in ECs isolated from obese human adipose tissues compared to those from lean tissues. Knockdown of TWIST1 in lean human adipose ECs decreases, while overexpression of TWIST1 in obese adipose ECs restores SLIT2 expression. DNA synthesis and cell migration are inhibited in obese adipose ECs and the effects are restored by TWIST1 overexpression. Obese adipose ECs also inhibit blood vessel formation in the gel subcutaneously implanted in mice, while these effects are restored when gels are mixed with SLIT2 or supplemented with ECs overexpressing TWIST1. These findings suggest that obesity impairs adipose tissue angiogenesis through TWIST1-SLIT2 signaling.

Keywords: angiogenesis, obesity, adipose tissue, TWIST1, SLIT2

INTRODUCTION

Obesity is regarded as a world epidemic with more than 1 billion people overweight in the world (Huang et al., 2016; GBD 2015 Mortality and Causes of Death Collaborators, 2016) and approximately two-thirds of US adults are overweight or obese (Cao, 2010). Obesity is highly associated with increased morbidity and mortality through its association with cardiovascular disease, type 2 diabetes, hypertension, stroke and certain types of cancer (e.g., colorectal, breast, gastrointestinal, and prostate cancer) (Shibata et al., 2004; Despres, 2006; Despres and Lemieux, 2006; Cao, 2010; O'Sullivan et al., 2018).

Subcutaneous adipose tissue is the largest and safest site to store lipid in the body. In a healthy condition, functional adipogenesis, adipocyte differentiation and hyperplastic expansion maintain

metabolism in the body. However, in an obese condition, hypertrophic adipose tissue is inflamed and the capacity of lipid storage in the subcutaneous adipose tissue is exceeded, which leads to the accumulation of excess amounts of dysfunctional lipids in the ectopic sites (e.g., visceral fat, peri or epicardial fat, liver, skeletal muscles). The deregulated adipose tissue remodeling in an obese condition results in local and systemic insulin resistance and inflammation, consequently increasing the risk of obesity-related diseases (Crewe et al., 2017; Hammarstedt et al., 2018; Chouchani and Kajimura, 2019).

Well-organized functional angiogenesis is necessary for organ development, regeneration and repair from injury (Mammoto and Mammoto, 2019). Under obese conditions, due to its proinflammatory state, endothelial signaling is dysregulated and EC functionality is impaired (Chudek and Wiecek, 2006; Hammarstedt et al., 2018; O'Sullivan et al., 2018). Obese conditions also promote cellular senescence and cell cycle arrest (Yokoyama et al., 2014; Briot et al., 2018; Gustafson et al., 2019; Conley et al., 2020; Smith et al., 2021). While healthy subcutaneous adipose tissue is maintained by physiologically balanced adipogenesis and angiogenesis, inflammatory and anti-angiogenic signals in hypertrophic obese adipose tissues inhibit angiogenesis and disrupt physiological vascular function, which results in local hypoxia, metabolic stress, and tissue dysfunction (Hosogai et al., 2007; Halberg et al., 2009; Pasarica et al., 2009; Cao, 2010; Christiaens and Lijnen, 2010; Xiao et al., 2016; Crewe et al., 2017; Hammarstedt et al., 2018; Chouchani and Kajimura, 2019). These EC dysfunctions, chronic inflammation and impairment of angiogenesis in obese adipose tissues lead to ectopic lipid accumulation and obesity-associated cardiovascular diseases (Friedman, 2000; Shibata et al., 2004; Hosogai et al., 2007; Pasarica et al., 2009; Cao, 2010; Christiaens and Lijnen, 2010; Crewe et al., 2017; Hammarstedt et al., 2018; Chouchani and Kajimura, 2019). Thus, we need to understand the mechanism by which obesity inhibits angiogenesis in adipose tissues.

TWIST1 is a basic helix-loop-helix transcription factor, which regulates vascular development (Li et al., 2014) and function (Mammoto et al., 2013). TWIST1 is involved in obesity- and angiogenesis-associated diseases such as diabetes (Pettersson et al., 2010), chronic obstructive pulmonary disease (COPD) (Nishioka et al., 2015), cancer (Wang et al., 2011), pulmonary fibrosis (Mammoto et al., 2016), and atherosclerosis (Mahmoud et al., 2016, 2017). TWIST1 also controls cellular metabolism; knockdown of TWIST1 in fat cells stimulates oxygen consumption and mitochondrial biogenesis, which results in resistance to obesity (Pan et al., 2009). Inhibition of TWIST1 activity increases the expression of PGC1α that stimulates mitochondrial biogenesis (Finck and Kelly, 2006; Austin and St-Pierre, 2012; Patten and Arany, 2012; Fan and Evans, 2015) and angiogenesis (Arany et al., 2008; Patten and Arany, 2012; Kluge et al., 2013; Rowe et al., 2014) in fat cells (Pan et al., 2009) and aged ECs (Hendee et al., 2021). The SLIT family proteins are extracellular matrix (ECM) proteins and consist of three members (SLIT1-3). SLIT proteins are known as axon guidance molecules and control brain development (Nguyen Ba-Charvet et al., 1999; Wang et al., 1999; Brose and Tessier-Lavigne, 2000). Recently it is reported that SLIT2 promotes thermogenic activity in beige fat tissue and the levels of SLIT2 decrease in the fat tissue of obese mice (Svensson et al., 2016). SLIT2 is expressed in various types of cells including ECs (Urbich et al., 2009; Guijarro-Munoz et al., 2012; Rama et al., 2015; Tavora et al., 2020) and is involved in physiological and pathological angiogenesis (Rama et al., 2015; Liu et al., 2018; Genet et al., 2019; Tavora et al., 2020). However, the role of endothelial TWIST1 and SLIT2 in obese adipose tissue angiogenesis remains unclear.

Here we found that angiogenesis is impaired in adipose tissue ECs isolated from obese humans through TWIST1-SLIT2 signaling. The levels of TWIST1 and SLIT2 are lower in obese adipose ECs and overexpression of TWIST1 or treatment with SLIT2 stimulates EC DNA synthesis and migration *in vitro* and vascular formation in the gel implanted on mice. Modulating TWIST1-SLIT2 signaling in ECs could be a novel therapeutic approach for obesity and obesity-associated diseases.

MATERIALS AND METHODS

Materials

Recombinant human SLIT2 (aa1122–1529) was purchased from R&D Systems (Minneapolis, MN, United States). Anti-β-actin (A5316) monoclonal antibody was from Sigma (St. Louis, MO, United States). Anti-VEGFR2 (2479) antibody was from Cell Signaling (Danvers, MA, United States). Anti-TWIST1 antibody was from Abcam (ab50887, Cambridge, MA, United States) and Santa Cruz Biotechnology (sc-15393, Dallas, TX, United States).

Adipose Endothelial Cell Isolation and Culture

Human subcutaneous adipose tissues [$n = 29$, body mass index (BMI) < 30 or > 30] were obtained as discarded surgical specimens from patients undergoing abdominal surgeries. After surgical removal, samples were placed in ice-cold HEPES buffer and immediately transferred to the laboratory for EC isolation. De-identified patient demographic data were collected using the Generic Clinical Research Database (GCRD) at the Medical College of Wisconsin (MCW). All protocols were approved by the Institutional Review Board of MCW and Froedtert Hospital. The information about sex, age, and BMI of each sample is listed in **Table 1** and sample demographic information is summarized in **Table 2**. Human adipose ECs were isolated as previously described and cultured in 10% FBS/ECM (Mammoto et al., 2018, 2019c, 2020; Hendee et al., 2021). All cell culture experiments were conducted between passages 2–3.

Molecular Biology and Biochemistry Experiments

RNA isolation was performed using an RNeasy mini kit (Qiagen, Valencia, CA, United States). Quantitative reverse transcription (qRT)-PCR was performed using the iScript reverse transcription and iTaq SYBR Green qPCR kit (Bio-Rad, Hercules, CA, United States) then analyzed using the real-time PCR system (Bio-Rad). β2 microglobulin (B2M) was used for overall cDNA content. The primers

TABLE 1 | Sample information.

BMI < 30	Sex	Age	BMI
1	F	47	28
2	M	33	28
3	F	42	26
4	F	47	27
5	F	46	24
6	F	42	27
7	F	51	24
8	F	41	23
9	F	38	29
10	F	30	25
11	F	34	23
12	F	41	24
13	F	33	24
14	F	55	21
15	F	31	19
BMI > 30	**Sex**	**Age**	**BMI**
1	F	50	34
2	F	46	36
3	F	44	37
4	F	32	34
5	F	38	37
6	F	50	44
7	F	36	37
8	F	43	35
9	F	37	31
10	M	40	32
11	F	43	34
12	F	30	45
13	F	43	41
14	F	45	37

TABLE 2 | Sample demographics.

Sample demographics (*n* = 29)	Lean (BMI < 30, *n* = 15)	Obese (BMI > 30, *n* = 14)
Gender, Male/Female	1 (6.6%)/14 (93.4%)	(7.1%)/13 (92.9%)
Age, year (mean ± SEM)	40.73 ± 1.95	41.21 ± 1.61
Body mass index (mean ± SEM)	24.78 ± 0.71	36.81 ± 1.11
Underlying diseases		
Coronary artery disease	0 (0%)	1 (7.1%)
Hypertension	0 (0%)	5 (35.7%)
Hyperlipidemia	0 (0%)	2 (14.2%)
Cancer	1 (6.6%)	3 (21.4%)

used for human B2M and TWIST1 are described before (Mammoto et al., 2018, 2020; Hendee et al., 2021). Primers for human SLIT2 are forward; AGCCGAGGTTCAAAAACGAGA, reverse; GGCAGTGCAAAACACTACAAGA. The protein levels of human SLIT2 were measured using ELISA (MyBioSource, San Diego, CA, United States).

Gene Manipulation

Gene knockdown was conducted by siRNA transfection using siLentFect (Bio-Rad) or lentiviral transduction. Human TWIST1 siRNA was described previously (Mammoto et al., 2020; Hendee et al., 2021). siRNA with an irrelevant sequence (QIAGEN) was used as a control. Lentiviral construct targeting human SLIT2 (SLIT2 shRNA) were CCGGCCTGGAGCTTTCTCACCATATCTCGAGATATGGTG AGAAAGCTCCAGGTTTTTG (MilliporeSigma). Generation of lentiviral vectors was accomplished by a five-plasmid transfection procedure as reported (Mammoto et al., 2009, 2018, 2019b, 2020). Human adipose ECs were incubated with viral stocks in the presence of 5 μg/ml polybrene (Sigma) and 90–100% infection was achieved 3 days later (Mammoto et al., 2009, 2018, 2019b, 2020). Lentivirus with vector alone was used as a control.

Cell Biological Analysis

Human adipose ECs were seeded at a density of 1×10^5 cells/35 mm dish and DNA synthesis was measured using the Click-iT^{TM} EdU Cell Proliferation Kit (Thermofisher, Waltham, MA, United States) (Hendee et al., 2021). The total cells were labeled with Hoechst nuclear dye and cells were imaged using a Nikon A1R confocal laser scanning microscope. Quantification was performed using ImageJ software (NIH). EC migration was analyzed by seeding human adipose ECs (1×10^5 cells/100 μl) in a trans-well chamber (Corning Costar) coated with 0.5% gelatin. 5% FBS was added to the lower chamber to promote migration and cells were incubated for 16 h (Hendee et al., 2021). Cells migrated to the opposite side of the membrane were stained with Wright Giemsa solution (Fisher Scientific) and quantified. The number of surviving cells were counted using trypan blue staining, in which ECs were treated with 0.1% trypan blue (Sigma) in PBS and counted under a light microscope (Salerno et al., 2011; Chen et al., 2015).

Mouse Subcutaneous Gel Implantation

The *in vivo* animal study was carried out in accordance with the recommendations in the Guide for the Care and Use of Laboratory Animals of the National Institutes of Health. The protocol was reviewed and approved by the Animal Care and Use Committee of MCW. NOD SCID gamma (NSG) mice (Jackson Laboratory, stock#, 5557) were used for the study. Human adipose ECs were treated with viral stock expressing GFP for labeling and the transduction efficiency was confirmed before the assay. Fibrin gel was fabricated as previously described, and GFP-labeled human adipose ECs (1×10^6 cells), in which gene expression was manipulated, and human fibroblasts (3×10^5 cells) were mixed in the gel (Mammoto et al., 2018, 2019b, 2020; Hendee et al., 2021). The drops of gels were incubated at 37°C for 30 min and subcutaneously implanted onto the back of the NSG mice (**Supplementary Figure 2A**). The gel was harvested 7 days after implantation, fixed with 4% paraformaldehyde, cryosectioned, and immunohistochemical (IHC) analysis was conducted as described previously (Mammoto et al., 2018, 2019b, 2020; Hendee et al., 2021). The IHC images were taken using a Nikon A1R confocal laser scanning microscope and stacks of optical sections (20-μm thick) were compiled to form three-dimensional images using software associated with a confocal microscope. Morphometric analysis was performed using ImageJ

and AngioTool software. Vascular network formation of GFP-labeled human adipose ECs was evaluated by measuring the area of GFP-labeled blood vessels from five different areas of the gel.

Microarray Data Analysis

Publicly available datasets from eight obese and seven lean adult human subcutaneous adipose samples (NCBI GEO, GSE55200) were utilized, and differential gene expression analysis and volcano plot generation were performed by GEO2R. The total number of genes identified by the array and displayed on the volcano plot was 48,242, with 26,391 being downregulated and 21,851 upregulated. Of these, 859 downregulated and 1,151 upregulated genes possessed adjusted p-values < 0.05 following Benjamini and Hochberg false discovery rate multiple-testing correction of p-values, resulting in a total of 2,010 significantly differentially expressed genes. Thousand three hundred and seventy four of these genes were assigned a GenBank Accession ID. Upon ID conversion to official gene symbol using the Database for Annotation, Visualization, and Integrated Discovery (DAVID) v6.8, 1,302 genes returned with unique conversion IDs. A subset of genes had multiple transcripts appear on the array sharing the same accession ID; these transcripts all changed in the same direction by gene and were encompassed by including the converted gene names only once in the final gene count. Thus, 548 downregulated and 754 upregulated significantly expressed genes underwent Biological Processes Gene Ontology (BP GO) Term analysis through the Functional Annotation Chart tool of the DAVID software. All down and upregulated genes identified in the top 30 BP GO Term categories by p-value were made into a network and color-coded using Ingenuity Pathway Analysis (IPA) software. The network mapped the shortest interactions among TWIST1 and the genes from the Top 30 BP GO Term categories, SLIT2 and the Top 30 BP GO Term genes, and the TWIST1 and SLIT2 groups and the Top 30 BP GO Term genes.

Statistics

All phenotypic analysis was performed by masked observers unaware of the identity of experimental groups. Power analysis was conducted to provide 80% power to detect an effective 20–30% difference between the experimental groups. Error bars (SEM) and p-values were determined from the results of three or more independent experiments. Student's t-test was used for statistical significance for two groups. For more than two groups, one-way ANOVA with a *post hoc* analysis using the Bonferroni test was conducted.

RESULTS

TWIST1 and SLIT2 Expression Is Inhibited in Obese Adipose Endothelial Cells

TWIST1 controls cellular metabolism and is involved in obesity- and angiogenesis-associated diseases (Pettersson et al., 2010; Wang et al., 2011; Nishioka et al., 2015; Mahmoud et al., 2016; Mammoto et al., 2016; Mahmoud et al., 2017). It has been reported that TWIST1 mRNA expression is lower in the adipose tissues from obese humans (Pettersson et al., 2011). Consistently, the levels of TWIST1 were significantly lower in obese human adipose tissues when analyzed using the unbiased publicly available microarray dataset (GSE55200) (**Figure 1A**). To specifically examine the effects of obesity on TWIST1 expression in ECs, we isolated ECs from obese (BMI > 30) vs. lean (BMI < 30) human subcutaneous adipose tissues and measured the mRNA levels of TWIST1. The levels of TWIST1 mRNA in ECs isolated from obese human adipose tissues (BMI > 30) were 71% lower than those in lean human adipose ECs (**Figure 1B**). We confirmed the results using immunoblotting (IB) showing that the TWIST1 protein levels were also 83% lower in ECs isolated from obese human adipose tissues (BMI > 30) compared to those in lean human adipose ECs (**Figure 1C**).

Gene network analysis of microarray dataset (GSE55200) reveals that genes from the top 30 GO Term categories derived from 1,302 significantly differentially expressed genes of lean vs. obese adipose tissues, including angiogenesis, development/differentiation, cell proliferation, adhesion, and inflammatory molecules directly or indirectly interacted with TWIST1 (**Figure 1D**). SLIT2 controls angiogenesis (Rama et al., 2015; Liu et al., 2018; Genet et al., 2019; Tavora et al., 2020) and the levels of Slit2 decrease in the fat tissue of obese mice (Svensson et al., 2016). Consistently, significantly differentially expressed genes of lean vs. obese adipose tissues that interacted with TWIST1 also interacted with SLIT2 (**Figure 1D**). Thus, we next examined the effects of obesity on SLIT2 expression in human adipose ECs. The levels of SLIT2 mRNA in ECs isolated from obese human adipose tissues (BMI > 30) were 66% lower than those in lean human adipose ECs (**Figure 2A**). We also confirmed the results using ELISA; the SLIT2 protein levels in obese human adipose tissue were 60% lower than those in lean adipose tissue (**Figure 2B**).

We next examined whether TWIST1 controls SLIT2 expression in lean and obese adipose ECs. siRNA-based knockdown of TWIST1 in human lean adipose ECs, which downregulated TWIST1 expression (**Figure 2C** and **Supplementary Figure 1A**), decreased the SLIT2 mRNA and protein expression by 64% and 29%, respectively (**Figure 2C**), while TWIST1 overexpression using lentiviral transduction upregulated the SLIT2 expression in obese ECs (**Figure 2D**). These results suggest that downregulation of TWIST1 decreases SLIT2 expression in obese ECs.

TWIST1 and SLIT2 Control DNA Synthesis and Migration in Obese Endothelial Cells *in vitro*

It is reported that capillary density is reduced in obese subcutaneous adipose tissues compared with those in lean animals (Gavin et al., 2005; Halberg et al., 2009; Pasarica et al., 2009; Gealekman et al., 2011; Spencer et al., 2011; Xiao et al., 2016; Crewe et al., 2017; Hammarstedt et al., 2018; Chouchani and Kajimura, 2019). Therefore, we next examined

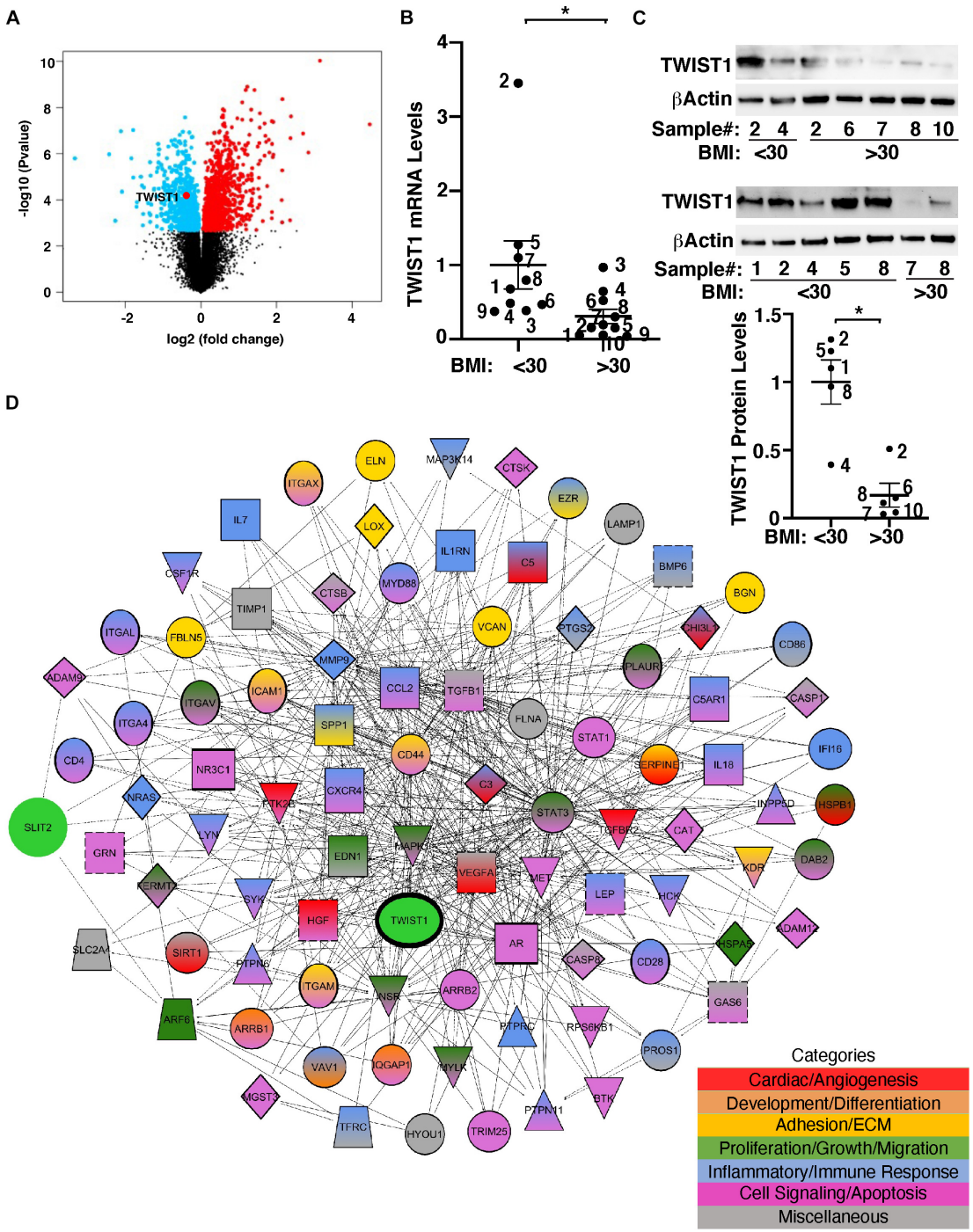

FIGURE 1 | TWIST1 expression in obese human subcutaneous adipose ECs is lower than lean ECs. **(A)** Volcano plot of differentially expressed genes, including TWIST1, in eight obese vs. seven lean adult human subcutaneous adipose samples from the GSE55200 dataset. Blue indicates significantly down-regulated genes and red indicates significantly up-regulated genes with Benjamini and Hochberg adjusted *p*-values < 0.05. **(B)** Graph showing the TWIST1 mRNA levels in ECs isolated from lean (BMI < 30) vs. obese (BMI > 30) human adipose tissues ($n = 9$–10, mean ± SEM, $^*p < 0.05$). The numbers along the dots correspond to the clone numbers in **Table 1**. **(C)** Immunoblots showing the TWIST1 and β-Actin protein levels in ECs isolated from lean (BMI < 30) vs. obese (BMI > 30) human adipose tissues ($n = 5$, mean ± SEM, $^*p < 0.05$). The numbers along the dots correspond to the clone numbers in **Table 1**. **(D)** Network showing connections among TWIST1, SLIT2, and genes from the top 30 BP GO Term categories derived from 1,302 significantly differentially expressed down and upregulated genes with Benjamini and Hochberg adjusted *p*-values < 0.05 from the GSE55200 dataset. Genes are color-coded by GO Term categories. Red, angiogenesis-related genes; Orange, development-related genes; Gold, ECM and cell adhesion-related genes; Dark green, cell proliferation, migration-related genes; Blue, inflammation and/or immune response-related genes; Purple, cell signaling and/or apoptosis-related genes; Gray, miscellaneous category-related genes; Black outlines, genes from the GSE55200 dataset.

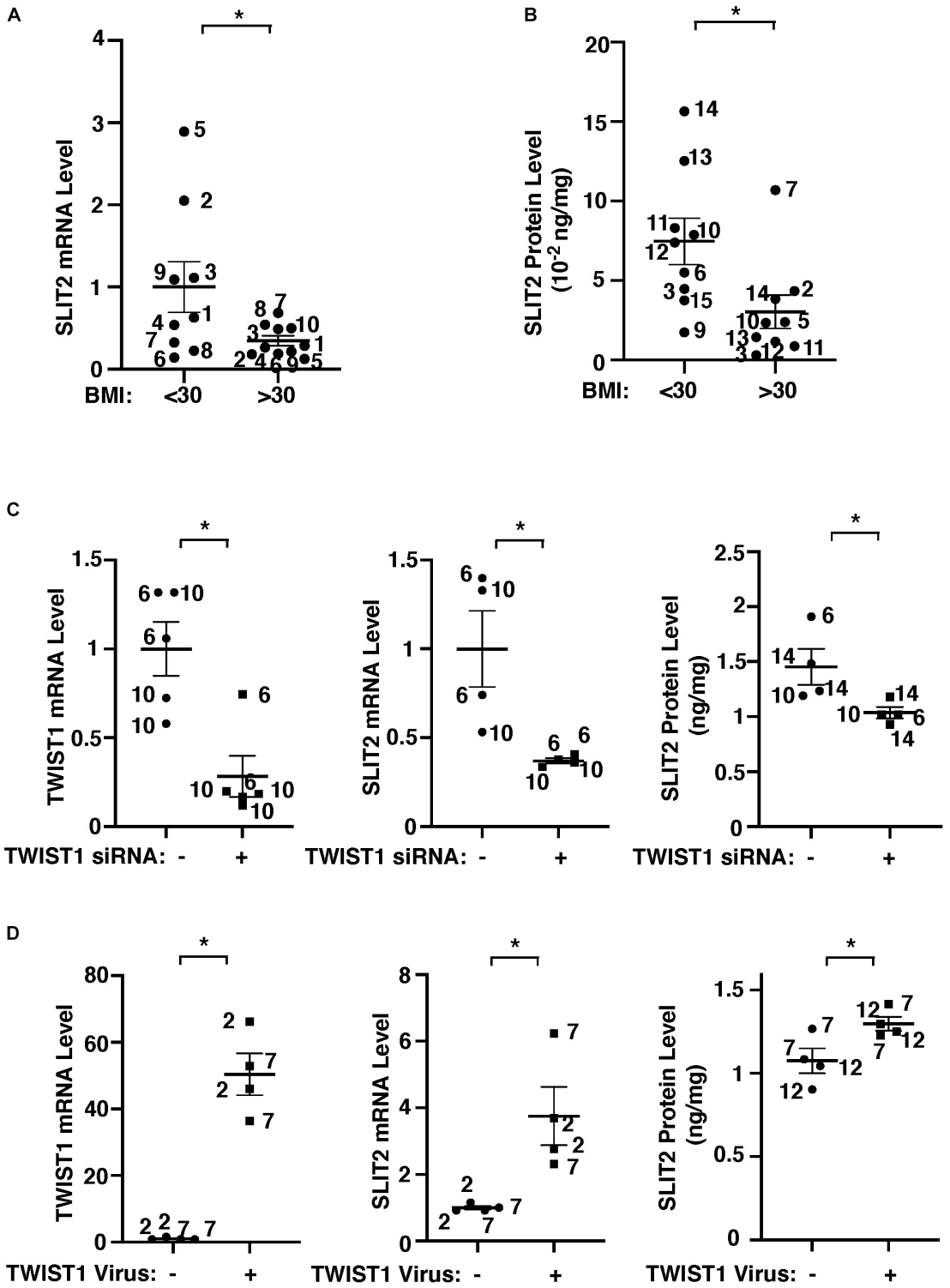

FIGURE 2 | TWIST1 controls SLIT2 expression in lean vs. obese adipose ECs. **(A)** Graph showing SLIT2 mRNA expression in lean vs. obese human adipose ECs (n = 9–10, mean ± SEM, $^*p < 0.05$). **(B)** Graph showing SLIT2 protein expression in lean vs. obese human adipose tissues (n = 9, mean ± SEM, $^*p < 0.05$). **(C)** Graphs showing mRNA expression of TWIST1 and SLIT2 in lean human adipose ECs treated with TWIST1 siRNA or control siRNA with irrelevant sequences (n = 4–5, mean ± SEM, $^*p < 0.05$). Graph showing protein expression of SLIT2 in lean human adipose ECs treated with TWIST1 siRNA or control siRNA with irrelevant sequences (n = 4, mean ± SEM, $^*p < 0.05$). **(D)** Graphs showing mRNA expression of TWIST1 and SLIT2 in obese human adipose ECs treated with lentivirus overexpressing TWIST1 or control virus (n = 4, mean ± SEM, $^*p < 0.05$). Graph showing protein expression of SLIT2 in obese human adipose ECs treated with lentivirus overexpressing TWIST1 or control virus (n = 4, mean ± SEM, $^*p < 0.05$). The numbers along the dots correspond to the clone numbers in **Table 1**.

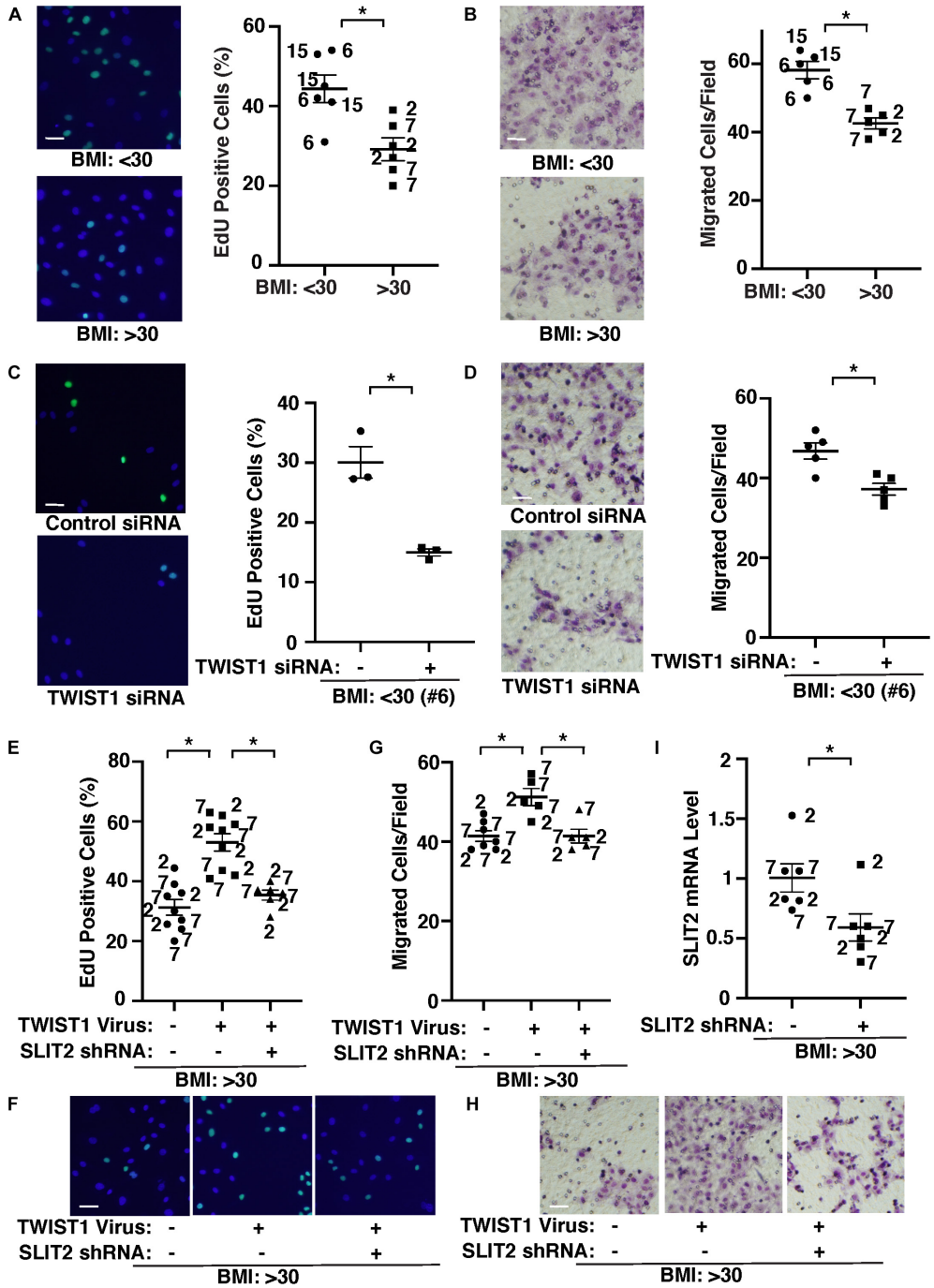

FIGURE 3 | TWIST1-SLIT2 signaling controls DNA synthesis and EC migration in lean vs. obese human adipose ECs. **(A)** Representative images showing EdU positive (green) lean (BMI < 30) vs. obese (BMI > 30) human adipose ECs (*left*). Scale bar, 50 μm. Graph showing DNA synthesis of lean (BMI < 30) vs. obese (BMI > 30) human adipose ECs analyzed using an EdU staining assay (*right*, $n = 6$, mean ± SEM, $^*p < 0.05$). **(B)** Representative images showing lean (BMI < 30) vs. obese (BMI > 30) human adipose ECs migrated to the opposite side of the *trans*-well membrane and stained with Wright Giemsa solution (*left*). Scale bar, 50 μm. Graph showing lean vs. obese human adipose ECs migrating toward 5% FBS (*right*, $n = 5$, mean ± SEM, $^*p < 0.05$). **(C)** Representative images showing EdU positive (green) lean (BMI < 30) human adipose ECs treated with TWIST1 siRNA (*left*). Scale bar, 50 μm. Graph showing EdU-positive lean (BMI < 30) human adipose ECs (clone #6) treated with TWIST1 siRNA (*right*, $n = 3$, mean ± SEM, $^*p < 0.05$). As a control, human adipose ECs were treated with siRNA with irrelevant sequences. **(D)** Representative images showing lean (BMI < 30) human adipose ECs treated with TWIST1 siRNA, migrated to the opposite side of the trans-well membrane and stained with Wright Giemsa solution (*left*). Scale bar, 50 μm. Graph showing lean human adipose ECs (clone #6) treated with TWIST1 siRNA migrating toward 5% FBS (*right*, $n = 5$, mean ± SEM, $^*p < 0.05$). As a control, human adipose ECs were treated with siRNA with irrelevant sequences. **(E)** Graph showing EdU-positive obese (BMI > 30) human adipose ECs treated with lentivirus overexpressing TWIST1 or in combination with SLIT2 shRNA ($n = 6$–9,

(Continued)

FIGURE 3 | (Continued)
mean ± SEM, $*p < 0.05$). As a control, human adipose ECs were treated with control virus (vector alone). **(F)** Representative images showing EdU positive obese (BMI > 30) human adipose ECs treated with lentivirus overexpressing TWIST1 or in combination with SLIT2 shRNA. Scale bar, 50 μm. **(G)** Graph showing obese human adipose ECs treated with lentivirus overexpressing TWIST1 or in combination with SLIT2 shRNA migrating toward 5% FBS (n = 5–7, mean ± SEM, $*p < 0.05$). As a control, human adipose ECs were treated with control virus (vector alone). **(H)** Representative images showing obese (BMI > 30) human adipose ECs treated with lentivirus overexpressing TWIST1 or in combination with SLIT2 shRNA, migrated to the opposite side of the *trans*-well membrane and stained with Wright Giemsa solution. Scale bar, 50 μm. **(I)** Graph showing SLIT2 mRNA levels in obese human adipose ECs treated with lentivirus expressing SLIT2 shRNA (n = 6, mean ± SEM, $*p < 0.05$). As a control, human adipose ECs were treated with control virus (vector alone). The numbers along the dots correspond to the clone numbers in **Table 1**.

the effects of obesity on EC behaviors and whether TWIST1-SLIT2 signaling mediates EC behaviors in obese adipose ECs. DNA synthesis measured by an EdU nuclear incorporation assay decreased by 37% in obese human adipose ECs (**Figure 3A**). EC migration analyzed using a transwell migration assay also decreased by 31% in obese human adipose ECs (**Figure 3B**). When we manipulated the expression of TWIST1 in lean (BMI < 30) vs. obese (BMI > 30) human adipose ECs using siRNA transfection or lentiviral transduction, TWIST1 knockdown, which also suppresses EC survival (**Supplementary Figure 1B**; Salerno et al., 2011; Chen et al., 2015), inhibited DNA synthesis and EC migration in lean human adipose ECs by 54 and 18%, respectively (**Figures 3C,D**), while TWIST1 overexpression stimulated DNA synthesis and EC migration in obese human adipose ECs (**Figures 3E–H**). TWIST1 overexpression-induced stimulation of DNA synthesis and migration in obese human adipose ECs was inhibited when treated with SLIT2 shRNA, which inhibits SLIT2 expression, in combination (**Figure 3I**), suggesting that endothelial TWIST1 mediates inhibition of DNA synthesis and EC migration in obese adipose ECs through SLIT2.

TWIST1 and SLIT2 Control Vascular Network Formation in Obese Endothelial Cells *in vivo*

We also examined the effects of obesity on vascular formation using the mouse gel implantation system, in which fibrin gels supplemented with GFP-labeled lean (BMI < 30) vs. obese (BMI > 30) human adipose ECs were subcutaneously implanted on the back of the immunocompromised NSG mice for 7 days (**Supplementary Figure 2A**; Mammoto et al., 2019c; Hendee et al., 2021). Consistent with *in vitro* study (**Figure 3**), vessel formation derived from GFP-labeled supplemented ECs in the cryosectioned gel was attenuated when gel mixed with GFP-labeled obese human adipose ECs was implanted for 7 days; GFP-labeled vascular area and average vessel length were 46 and 55% lower than that in the gel mixed with lean human adipose ECs (**Figure 4A**). Knockdown of SLIT2 in supplemented lean human adipose ECs suppressed vascular formation in the implanted gel (**Figure 4B**). The supplemented GFP-labeled VEGFR2$^+$ lean human ECs were integrated with host-derived VEGFR2$^+$ ECs in the gel, however these effects were attenuated in the gel supplemented with obese ECs or lean ECs treated with SLIT2 shRNA (**Supplementary Figure 2B**). Supplementation of recombinant SLIT2 protein or overexpression of TWIST1 in supplemented ECs in the gel restored obese EC-derived blood vessel formation and integration with host-derived ECs in the gel, while knockdown of SLIT2 suppressed restoration of vascular formation and integration with host ECs induced by TWIST1 in obese ECs in the implanted gel (**Figure 4C** and **Supplementary Figure 2C**). These results indicate that TWIST1 restores obesity-induced disruption of vascular formation through SLIT2.

DISCUSSION

Impaired angiogenesis and vascular dysfunction in obese adipose tissues contribute to obesity-related diseases. In this report, we have used ECs isolated from lean vs. obese human subcutaneous adipose tissues and demonstrated that vascular formation is inhibited in obese ECs through TWIST1-SLIT2 signaling. The levels of TWIST1 and SLIT2 are lower in obese human adipose ECs compared to those in lean adipose ECs. EC DNA synthesis and migration *in vitro* and blood vessel formation in the gel subcutaneously implanted on the back of mice are suppressed in obese ECs, while TWIST1 overexpression or treatment with SLIT2 protein restores the effects. These results suggest that obesity impairs angiogenesis in subcutaneous adipose ECs through TWIST1-SLIT2 signaling. Modulation of this pathway may be an effective strategy for obesity-related diseases.

While hyperplastic expansion of the adipose tissues maintains healthy metabolism and protects against obesity-related diseases, adipocyte hypertrophy, which is frequently associated with development of obesity (Verboven et al., 2018), leads to adipose tissue dysfunction, inflammation and ectopic lipid accumulation, resulting in the metabolic diseases (Crewe et al., 2017; Hammarstedt et al., 2018; Chouchani and Kajimura, 2019). Impaired angiogenesis is one of the characteristics of hypertrophic adipose tissues. We have found that TWIST1 expression is lower in obese human adipose ECs (**Figure 1**) and overexpression of TWIST1 restores angiogenic activity and blood vessel formation through SLIT2 in obese ECs (**Figures 3**, **4**). Angiogenesis is controlled by multiple angiogenic factors, which is necessary for well-organized physiological blood vessel formation (Carmeliet and Jain, 2011; Chung and Ferrara, 2011; Herbert and Stainier, 2011). TWIST1 interacts with a number of signaling molecules. For example, TWIST1 mediates age-dependent decline in angiogenesis through VEGFR2 expression (Hendee et al., 2021). Increased levels of TWIST1 contribute to pulmonary fibrosis and lung injury through Tie2 signaling (Mammoto et al., 2013, 2016). TWIST1 also mediates hypoxia-induced

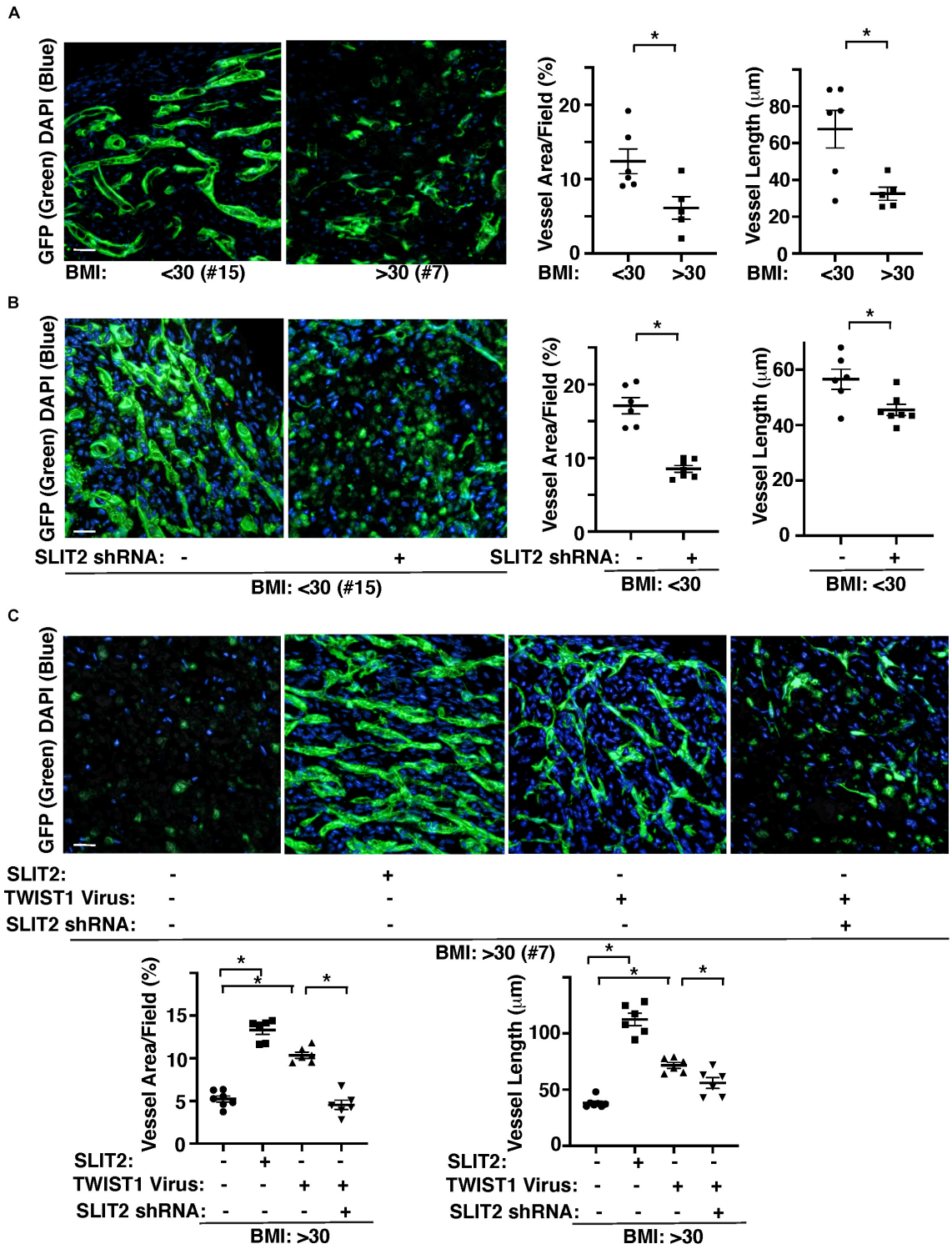

FIGURE 4 | TWIST1-SLIT2 signaling mediates obesity-dependent inhibition of vascular formation in the gel subcutaneously implanted on mice. **(A)** 3D reconstructed immunofluorescence (IF) images showing GFP-labeled vascular formation and DAPI in the fibrin gel supplemented with GFP-labeled lean (BMI < 30, clone #15) vs. obese (BMI > 30, clone #7) human adipose ECs and subcutaneously implanted on NSG mice for 7 days. Scale bar, 50 μm. Graphs showing vascular area and average vessel length in the gel (n = 5–6, mean ± SEM, $^*p < 0.05$). **(B)** 3D reconstructed IF micrographs showing GFP-labeled vascular formation and DAPI in the fibrin gel supplemented with GFP-labeled lean human adipose ECs (clone #15) treated with lentivirus encoding SLIT2 shRNA and subcutaneously implanted on NSG mice for 7 days. As a control, lean human adipose ECs were treated with control virus. Scale bar, 50 μm. Graphs showing vascular area and average vessel length in

(Continued)

FIGURE 4 | (Continued)
the gel (n = 6–7, mean ± SEM, $^*p < 0.05$). **(C)** 3D reconstructed IF micrographs showing GFP-labeled vascular formation and DAPI in the fibrin gel supplemented with GFP-labeled obese human adipose ECs (clone #7) treated with SLIT2 protein, lentivirus overexpressing TWIST1 or in combination with SLIT2 shRNA and subcutaneously implanted on NSG mice for 7 days. As a control, obese human adipose ECs were treated with control virus (vector alone), control shRNA, or control vehicle. Scale bar, 50 μm. Graphs showing vascular area and average vessel length in the gel (n = 6–7, mean ± SEM, $^*p < 0.05$).

pulmonary hypertension by endothelial-to-mesenchymal transition (EndMT) as well as by changing PDGFB expression in ECs (Mammoto et al., 2018, 2020). TWIST1 controls multiple other angiogenic pathways [e.g., VEGF-VEGFR2 (Li et al., 2014), HIF1α (Yang and Wu, 2008), Wnt (Guo et al., 2007), Notch (Chen et al., 2014; Wirrig and Yutzey, 2014), PI3K-AKT (Cheng et al., 2008; Xue et al., 2012), and TGF-β (Mammoto et al., 2018)]. In fact, gene ontology and gene network analysis reveal that TWIST1 interacts with a number of genes that are significantly altered in obese human subcutaneous adipose tissues (**Figure 1D**). These genes directly or indirectly interact with SLIT signaling molecules as well as other genes to modulate cell signaling, proliferation, ECM structures and control angiogenesis. Thus, TWIST1-SLIT2 signaling would be one of the important targets to control angiogenesis in obese ECs. In addition to angiogenic signaling, TWIST1 also binds to PGC1α, which controls mitochondrial biogenesis and metabolism, and inhibits its co-transcriptional activity in fat cells (Pan et al., 2009). We also reported that TWIST1-PGC1α signaling in ECs contributes to age-dependent disruption of angiogenesis (Hendee et al., 2021). TWIST1 may regulate metabolic and mitochondrial signaling and indirectly control angiogenesis. TWIST1 is also involved in DNA methylation that is associated with obesity (Dahl and Guldberg, 2007; Albuquerque et al., 2015; McCullough et al., 2016). Thus, multiple TWIST1 signaling pathways are involved in angiogenesis in obese conditions.

It is reported that TWIST1 is expressed in different types of adipose tissues (brown, subcutaneous, and visceral) (Pan et al., 2009; Pettersson et al., 2010; Dobrian, 2012; Svensson et al., 2016). SLIT2 is also expressed in all kinds of adipose tissues and the expression is suppressed in subcutaneous adipose tissue from high-fat diet-treated obese mice (Svensson et al., 2016). In addition to TWIST1, the levels of TWIST2 are also lower in obese human subcutaneous adipose tissues in another dataset (GSE15524, not shown). The distribution pattern of TWIST1 and TWIST2 seems to be different; the levels of TWIST1 are higher in subcutaneous adipose tissues compared to visceral adipose tissues, which is strongly correlated with BMI and insulin resistance, while Twist2 is more ubiquitously expressed in the body (Pan et al., 2009; Pettersson et al., 2010). Although it remains unknown how the distribution pattern is regulated, TWIST1 may play important roles in development and remodeling of adipose tissues in an obese condition. While our results demonstrate that overexpression of TWIST1 in obese human adipose ECs restores vascular formation (**Figures 3**, **4**), which may restore adipose tissue homeostasis, it is reported that transgenic mice overexpressing Twist1 in the adipose tissue are susceptible to obesity (Pan et al., 2009). This may be because of the differences in the role of TWIST1 depending on cell types and animal species. TWIST1 is expressed in other cell types such as fibroblasts and epithelial cells (Pozharskaya et al., 2009; Yeo et al., 2018) as well, which also alters the effects of TWIST1 in adipose tissues. Further investigation using endothelial-specific Twist1 knockout/overexpressing mice will elucidate the mechanism.

Crosstalk between angiogenesis and adipogenesis is required for the physiological expansion of the adipose tissue, while these processes are disrupted in obese conditions. Hypertrophic obesity is associated with biological pathways related to hypoxia and inflammation (Gustafson et al., 2009; Crewe et al., 2017; Hammarstedt et al., 2018; Chouchani and Kajimura, 2019), which promotes insulin resistance and lipolysis (Tilg and Moschen, 2006; Guilherme et al., 2008; Galic et al., 2010) and inhibits angiogenesis by secreting proinflammatory molecules (e.g., TNFα, NFkB, JNK) and adipokines (Guilherme et al., 2008; Vazquez-Vela et al., 2008; Crewe et al., 2017; Hammarstedt et al., 2018; Chouchani and Kajimura, 2019). Inhibition of angiogenesis due to inflammatory response may feedback to further develop hypoxia in hypertrophic adipose tissues. It is reported that TWIST1 promotes inflammatory pathways, which leads to various pathological conditions such as atherosclerosis, nephropathy, and pulmonary fibrosis (Tan et al., 2017; Hradilkova et al., 2019; Mahmoud et al., 2019; Ren et al., 2020). Binding of SLIT2 with ROBO receptors also triggers proinflammatory signaling (Zhao et al., 2014; Wang et al., 2020). Thus, TWIST1-SLIT2 signaling may control subcutaneous adipose tissue angiogenesis through inflammatory signaling as well.

Adipogenesis in subcutaneous adipose tissues is also regulated by production of ECM proteins and their mechanics (Hammarstedt et al., 2018; Chouchani and Kajimura, 2019; Guzman-Ruiz et al., 2020). Increased deposition of ECM proteins such as collagens (e.g., collagen I, III, IV, VI), fibronectin, and elastin in adipose tissues is associated with infiltration of proinflammatory immune cells, which leads to adipose tissue disorganization and dysfunction in obese conditions (Chouchani and Kajimura, 2019). It is reported that increased adipose tissue fibrosis in the subcutaneous adipose tissues contributes to insulin resistance and metabolic disorder (Sun et al., 2013). ECM stiffness also controls angiogenesis (Mammoto et al., 2009). Since Twist1 is a mechanosensitive gene and senses ECM stiffness (Fattet et al., 2020) and contributes to mechanosensitive pathology [e.g., pulmonary fibrosis (Mammoto et al., 2016), pulmonary hypertension (Mammoto et al., 2018, 2020), cancer (Fattet et al., 2020), atherosclerosis (Mahmoud et al., 2016, 2017)], Twist1 may sense changes in the ECM microenvironment in the obese adipose tissues and control angiogenesis and adipogenesis.

Obesity-mediated inflammation and lipotoxicity through ectopic lipid deposition contribute to vascular remodeling in

ectopic organs (e.g., liver, muscle, pancreas, heart) as well as in tumor tissues, promoting insulin resistance (Kim et al., 2007; Savage, 2009; Virtue and Vidal-Puig, 2010), cardiovascular diseases and tumor progression (Dong et al., 2017). Regarding angiogenesis in obese subcutaneous adipose tissues, consistent with our results, it is demonstrated that angiogenesis is impaired and endothelial function is disrupted in obese subcutaneous adipose tissues, which results in ectopic lipid accumulation and obesity-associated diseases (Hosogai et al., 2007; Halberg et al., 2009; Pasarica et al., 2009; Cao, 2010; Christiaens and Lijnen, 2010; Corvera and Gealekman, 2014; Shimizu et al., 2014; Fuster et al., 2016; Xiao et al., 2016; Crewe et al., 2017; Hammarstedt et al., 2018; Chouchani and Kajimura, 2019). Under obese conditions, due to its proinflammatory state, endothelial signaling and their functionality are impaired (Hosogai et al., 2007; Halberg et al., 2009; Pasarica et al., 2009; Cao, 2010; Christiaens and Lijnen, 2010; Corvera and Gealekman, 2014; Shimizu et al., 2014; Fuster et al., 2016; Xiao et al., 2016; Crewe et al., 2017; Hammarstedt et al., 2018; Chouchani and Kajimura, 2019). Multiple groups have reported that stimulation of angiogenesis in adipose tissue of obese rodents by increasing angiogenic gene expression (e.g., VEGFA, VEGFB, FLT1, FOXO, Angiopoietin2) not only improves local adipose tissue function, but also counteracts systemic metabolic disorders (Sun et al., 2012; Sung et al., 2013; Robciuc et al., 2016; An et al., 2017; Rudnicki et al., 2018; Seki et al., 2018). Thus, the response of ECs to obesity and associated inflammatory and angiogenic signaling may be different among organs and obesity/disease stages due to heterogeneity of ECs and differences in the microenvironment (Mammoto et al., 2009; Mammoto and Mammoto, 2019; Ren et al., 2019). Further time course analysis and investigation of inflammatory gene expression and immune cell infiltration in subcutaneous adipose tissue may elucidate the mechanism.

In this report, we isolated ECs from human subcutaneous adipose tissues of lean vs. obese individuals, which includes a variety of other conditions. Since aging affects angiogenesis (Mammoto et al., 2019a; Hendee et al., 2021), we only used ECs from tissues of young patients (<55 years old). Recent lineage tracing mouse study revealed that subcutaneous adipose tissue expansion pattern is sex dependent; while subcutaneous adipose tissue expansion is through hypertrophy in male mice, increase in adipose tissue is through the combination of hypertrophy and hyperplasia in female mice (Jeffery et al., 2016; Chouchani and Kajimura, 2019). Thus, the pattern and signaling mechanism of adipogenesis and angiogenesis in adipose tissue may be different due to sex, the onset of obesity, and cardiovascular conditions. However, due to tissue availability, most of the human samples in this study are from females. Investigation using a different cohort and a larger sample size will further elucidate the mechanism.

In summary, we have found that vascular formation is inhibited in ECs isolated from obese human subcutaneous adipose tissues through TWIST1-SLIT2 signaling. Modulation of endothelial TWIST1-SLIT2 signaling may be an effective strategy for treating obesity and associated metabolic complications.

DATA AVAILABILITY STATEMENT

Publicly available datasets were analyzed in this study. This data can be found here: NCBI GEO, GSE55200.

ETHICS STATEMENT

The studies involving human participants were reviewed and approved by Institutional Review Board of MCW and Froedtert Hospital. The patients/participants provided their written informed consent to participate in this study. The animal study was reviewed and approved by Animal Care and Use Committee of MCW.

AUTHOR CONTRIBUTIONS

TM and AM conceived and designed the experiments. TH, KH, KM, PK, TM, and AM performed the experiments. TH, KH, TM, and AM analyzed the data, contributed reagents, materials, and analysis tools, and wrote the manuscript. All the authors contributed to the article and approved the submitted version.

FUNDING

This work was supported by funds from NIH R21AG054830 (to AM and TM), R01HL139638 (to AM and TM), R21AG062893 (to AM and TM), R01HL142578 (to AM and TM), and American Heart Association (AHA) 18TPA34170129 (to AM).

SUPPLEMENTARY MATERIAL

The Supplementary Material for this article can be found online at: https://www.frontiersin.org/articles/10.3389/fcell.2021.693410/full#supplementary-material

Supplementary Figure 1 | TWIST1 controls EC survival in human adipose ECs. **(A)** Representative images showing TWIST1 expression and DAPI in lean (BMI < 30) human adipose ECs treated with TWIST1 siRNA (*left*). As a control, human adipose ECs were treated with siRNA with irrelevant sequences. Scale bar, 10 μm. Graph showing integrated density of TWIST1 (*right*, $n = 5$, mean ± SEM, $^*p < 0.05$). **(B)** Representative images showing trypan blue staining of lean (BMI < 30) human adipose ECs treated with TWIST1 siRNA. Scale bar, 25 μm. Graph showing trypan blue excluding lean human adipose ECs treated with TWIST1 siRNA ($n = 5$, mean ± SEM, $^*p < 0.05$). As a control, human adipose ECs were treated with siRNA with irrelevant sequences.

Supplementary Figure 2 | TWIST1-SLIT2 signaling mediates obesity-dependent inhibition of vascular formation in the gel subcutaneously implanted on mice. **(A)** Fibrin gel subcutaneously implanted on the back of a mouse. Scale bar, 1 mm. Arrow indicates the implanted gel. **(B)** 3D reconstructed IF images showing GFP-labeled and VEGFR2-stained vascular formation and DAPI in the fibrin gel supplemented with GFP-labeled lean (BMI < 30, clone #15) vs. obese (BMI > 30, clone #7) human adipose ECs and subcutaneously implanted on NSG mice for 7 days (*top*). 3D reconstructed IF images showing GFP-labeled and VEGFR2-stained vascular formation and DAPI in the fibrin gel supplemented with GFP-labeled lean (BMI < 30, clone #15) human adipose ECs treated with SLIT2 shRNA and subcutaneously implanted on NSG mice for 7 days (*bottom*). Scale bar, 50 μm. **(C)** 3D reconstructed IF micrographs showing GFP-labeled and

VEGFR2-stained vascular formation and DAPI in the fibrin gel supplemented with GFP-labeled obese human adipose ECs (clone #7) treated with SLIT2 protein, lentivirus overexpressing TWIST1 or in combination with SLIT2 shRNA and subcutaneously implanted on NSG mice for 7 days. As a control, obese human adipose ECs were treated with control virus (vector alone), control shRNA, or control vehicle. Scale bar, 50 μm.

REFERENCES

Albuquerque, D., Stice, E., Rodriguez-Lopez, R., Manco, L., and Nobrega, C. (2015). Current review of genetics of human obesity: from molecular mechanisms to an evolutionary perspective. *Mol. Genet. Genomics* 290, 1191–1221. doi: 10.1007/s00438-015-1015-9

An, Y. A., Sun, K., Joffin, N., Zhang, F., Deng, Y., Donze, O., et al. (2017). Angiopoietin-2 in white adipose tissue improves metabolic homeostasis through enhanced angiogenesis. *Elife* 6:e24071.

Arany, Z., Foo, S. Y., Ma, Y., Ruas, J. L., Bommi-Reddy, A., Girnun, G., et al. (2008). HIF-independent regulation of VEGF and angiogenesis by the transcriptional coactivator PGC-1alpha. *Nature* 451, 1008–1012. doi: 10.1038/nature06613

Austin, S., and St-Pierre, J. (2012). PGC1alpha and mitochondrial metabolism–emerging concepts and relevance in ageing and neurodegenerative disorders. *J. Cell Sci.* 125(Pt 21), 4963–4971. doi: 10.1242/jcs.113662

Briot, A., Decaunes, P., Volat, F., Belles, C., Coupaye, M., Ledoux, S., et al. (2018). Senescence alters PPARgamma (peroxisome proliferator-activated receptor gamma)-dependent fatty acid handling in human adipose tissue microvascular endothelial cells and favors inflammation. *Arterioscler. Thromb. Vasc. Biol.* 38, 1134–1146. doi: 10.1161/atvbaha.118.310797

Brose, K., and Tessier-Lavigne, M. (2000). Slit proteins: key regulators of axon guidance, axonal branching, and cell migration. *Curr. Opin. Neurobiol.* 10, 95–102. doi: 10.1016/s0959-4388(99)00066-5

Cao, Y. (2010). Adipose tissue angiogenesis as a therapeutic target for obesity and metabolic diseases. *Nat. Rev. Drug Discov.* 9, 107–115. doi: 10.1038/nrd3055

Carmeliet, P., and Jain, R. K. (2011). Molecular mechanisms and clinical applications of angiogenesis. *Nature* 473, 298–307. doi: 10.1038/nature10144

Chen, C. C., You, J. Y., Gau, J. P., Huang, C. E., Chen, Y. Y., Tsai, Y. H., et al. (2015). Favorable clinical outcome and unique characteristics in association with Twist1 overexpression in de novo acute myeloid leukemia. *Blood Cancer J.* 5:e339. doi: 10.1038/bcj.2015.67

Chen, H. F., Huang, C. H., Liu, C. J., Hung, J. J., Hsu, C. C., Teng, S. C., et al. (2014). Twist1 induces endothelial differentiation of tumour cells through the Jagged1-KLF4 axis. *Nat. Commun.* 5:4697.

Cheng, G. Z., Zhang, W., and Wang, L. H. (2008). Regulation of cancer cell survival, migration, and invasion by Twist: AKT2 comes to interplay. *Cancer Res.* 68, 957–960. doi: 10.1158/0008-5472.can-07-5067

Chouchani, E. T., and Kajimura, S. (2019). Metabolic adaptation and maladaptation in adipose tissue. *Nat. Metab.* 1, 189–200. doi: 10.1038/s42255-018-0021-8

Christiaens, V., and Lijnen, H. R. (2010). Angiogenesis and development of adipose tissue. *Mol. Cell. Endocrinol.* 318, 2–9.

Chudek, J., and Wiecek, A. (2006). Adipose tissue, inflammation and endothelial dysfunction. *Pharmacol. Rep.* 58 Suppl, 81–88.

Chung, A. S., and Ferrara, N. (2011). Developmental and pathological angiogenesis. *Annu. Rev. Cell Dev. Biol.* 27, 563–584. doi: 10.1146/annurev-cellbio-092910-154002

Conley, S. M., Hickson, L. J., Kellogg, T. A., McKenzie, T., Heimbach, J. K., Taner, T., et al. (2020). Human obesity induces dysfunction and early senescence in adipose tissue-derived mesenchymal stromal/stem cells. *Front. Cell Dev. Biol.* 8:197. doi: 10.3389/fcell.2020.00197

Corvera, S., and Gealekman, O. (2014). Adipose tissue angiogenesis: impact on obesity and type-2 diabetes. *Biochim. Biophys. Acta* 1842, 463–472. doi: 10.1016/j.bbadis.2013.06.003

Crewe, C., An, Y. A., and Scherer, P. E. (2017). The ominous triad of adipose tissue dysfunction: inflammation, fibrosis, and impaired angiogenesis. *J. Clin. Invest.* 127, 74–82. doi: 10.1172/jci88883

Dahl, C., and Guldberg, P. (2007). A ligation assay for multiplex analysis of CpG methylation using bisulfite-treated DNA. *Nucleic Acids Res.* 35:e144. doi: 10.1093/nar/gkm984

Despres, J. P. (2006). Intra-abdominal obesity: an untreated risk factor for Type 2 diabetes and cardiovascular disease. *J. Endocrinol. Invest.* 29(3 Suppl.), 77–82.

Despres, J. P., and Lemieux, I. (2006). Abdominal obesity and metabolic syndrome. *Nature* 444, 881–887.

Dobrian, A. D. (2012). A tale with a twist: a developmental gene with potential relevance for metabolic dysfunction and inflammation in adipose tissue. *Front. Endocrinol.* 3:108. doi: 10.3389/fendo.2012.00108

Dong, L., Yuan, Y., Opansky, C., Chen, Y., Aguilera-Barrantes, I., Wu, S., et al. (2017). Diet-induced obesity links to ER positive breast cancer progression via LPA/PKD-1-CD36 signaling-mediated microvascular remodeling. *Oncotarget* 8, 22550–22562. doi: 10.18632/oncotarget.15123

Fan, W., and Evans, R. (2015). PPARs and ERRs: molecular mediators of mitochondrial metabolism. *Curr. Opin. Cell Biol.* 33, 49–54. doi: 10.1016/j.ceb.2014.11.002

Fattet, L., Jung, H. Y., Matsumoto, M. W., Aubol, B. E., Kumar, A., Adams, J. A., et al. (2020). Matrix rigidity controls epithelial-mesenchymal plasticity and tumor metastasis via a mechanoresponsive EPHA2/LYN complex. *Dev. Cell* 54, 302–316.e7.

Finck, B. N., and Kelly, D. P. (2006). PGC-1 coactivators: inducible regulators of energy metabolism in health and disease. *J. Clin. Invest.* 116, 615–622. doi: 10.1172/jci27794

Friedman, J. M. (2000). Obesity in the new millennium. *Nature* 404, 632–634. doi: 10.1038/35007504

Fuster, J. J., Ouchi, N., Gokce, N., and Walsh, K. (2016). Obesity-induced changes in adipose tissue microenvironment and their impact on cardiovascular disease. *Circ. Res.* 118, 1786–1807. doi: 10.1161/circresaha.115.306885

Galic, S., Oakhill, J. S., and Steinberg, G. R. (2010). Adipose tissue as an endocrine organ. *Mol. Cell Endocrinol.* 316, 129–139.

Gavin, T. P., Stallings, H. W. III, Zwetsloot, K. A., Westerkamp, L. M., Ryan, N. A., Moore, R. A., et al. (2005). Lower capillary density but no difference in VEGF expression in obese vs. lean young skeletal muscle in humans. *J. Appl. Physiol.* 98, 315–321. doi: 10.1152/japplphysiol.00353.2004

GBD 2015 Mortality and Causes of Death Collaborators (2016). Global, regional, and national life expectancy, all-cause mortality, and cause-specific mortality for 249 causes of death, 1980-2015: a systematic analysis for the global burden of disease study 2015. *Lancet* 388, 1459–1544.

Gealekman, O., Guseva, N., Hartigan, C., Apotheker, S., Gorgoglione, M., Gurav, K., et al. (2011). Depot-specific differences and insufficient subcutaneous adipose tissue angiogenesis in human obesity. *Circulation* 123, 186–194. doi: 10.1161/circulationaha.110.970145

Genet, G., Boye, K., Mathivet, T., Ola, R., Zhang, F., Dubrac, A., et al. (2019). Endophilin-A2 dependent VEGFR2 endocytosis promotes sprouting angiogenesis. *Nat. Commun.* 10:2350.

Guijarro-Munoz, I., Cuesta, A. M., Alvarez-Cienfuegos, A., Geng, J. G., Alvarez-Vallina, L., and Sanz, L. (2012). The axonal repellent Slit2 inhibits pericyte migration: potential implications in angiogenesis. *Exp. Cell Res.* 318, 371–378. doi: 10.1016/j.yexcr.2011.12.005

Guilherme, A., Virbasius, J. V., Puri, V., and Czech, M. P. (2008). Adipocyte dysfunctions linking obesity to insulin resistance and type 2 diabetes. *Nat. Rev. Mol. Cell Biol.* 9, 367–377. doi: 10.1038/nrm2391

Guo, Y., Zi, X., Koontz, Z., Kim, A., Xie, J., Gorlick, R., et al. (2007). Blocking Wnt/LRP5 signaling by a soluble receptor modulates the epithelial to mesenchymal transition and suppresses met and metalloproteinases in osteosarcoma Saos-2 cells. *J. Orthop. Res.* 25, 964–971. doi: 10.1002/jor.20356

Gustafson, B., Gogg, S., Hedjazifar, S., Jenndahl, L., Hammarstedt, A., and Smith, U. (2009). Inflammation and impaired adipogenesis in hypertrophic obesity in man. *Am. J. Physiol. Endocrinol. Metab.* 297, E999–E1003.

Gustafson, B., Nerstedt, A., and Smith, U. (2019). Reduced subcutaneous adipogenesis in human hypertrophic obesity is linked to senescent precursor cells. *Nat. Commun.* 10:2757.

Guzman-Ruiz, R., Tercero-Alcazar, C., Rabanal-Ruiz, Y., Diaz-Ruiz, A., El Bekay, R., Rangel-Zuniga, O. A., et al. (2020). Adipose tissue depot-specific intracellular and extracellular cues contributing to insulin resistance in obese individuals. *FASEB J.* 34, 7520–7539. doi: 10.1096/fj.201902703r

Halberg, N., Khan, T., Trujillo, M. E., Wernstedt-Asterholm, I., Attie, A. D., Sherwani, S., et al. (2009). Hypoxia-inducible factor 1alpha induces fibrosis and insulin resistance in white adipose tissue. *Mol. Cell. Biol.* 29, 4467–4483. doi: 10.1128/mcb.00192-09

Hammarstedt, A., Gogg, S., Hedjazifar, S., Nerstedt, A., and Smith, U. (2018). Impaired adipogenesis and dysfunctional adipose tissue in human hypertrophic obesity. *Physiol. Rev.* 98, 1911–1941. doi: 10.1152/physrev.00034.2017

Hendee, K., Hunyenyiwa, T., Matus, K., Toledo, M., Mammoto, A., and Mammoto, T. (2021). Twist1 signaling in age-dependent decline in angiogenesis and lung regeneration. *Aging* 13, 7781–7799. doi: 10.18632/aging.202875

Herbert, S. P., and Stainier, D. Y. (2011). Molecular control of endothelial cell behaviour during blood vessel morphogenesis. *Nat. Rev. Mol. Cell Biol.* 12, 551–564. doi: 10.1038/nrm3176

Hosogai, N., Fukuhara, A., Oshima, K., Miyata, Y., Tanaka, S., Segawa, K., et al. (2007). Adipose tissue hypoxia in obesity and its impact on adipocytokine dysregulation. *Diabetes* 56, 901–911. doi: 10.2337/db06-0911

Hradilkova, K., Maschmeyer, P., Westendorf, K., Schliemann, H., Husak, O., von Stuckrad, A. S. L., et al. (2019). Regulation of fatty acid oxidation by twist 1 in the metabolic adaptation of T helper lymphocytes to chronic inflammation. *Arthritis Rheumatol.* 71, 1756–1765. doi: 10.1002/art.40939

Huang, H., Yan, Z., Chen, Y., and Liu, F. (2016). A social contagious model of the obesity epidemic. *Sci. Rep.* 6:37961.

Jeffery, E., Wing, A., Holtrup, B., Sebo, Z., Kaplan, J. L., Saavedra-Pena, R., et al. (2016). The adipose tissue microenvironment regulates depot-specific adipogenesis in obesity. *Cell Metab.* 24, 142–150. doi: 10.1016/j.cmet.2016.05.012

Kim, J. Y., van de Wall, E., Laplante, M., Azzara, A., Trujillo, M. E., Hofmann, S. M., et al. (2007). Obesity-associated improvements in metabolic profile through expansion of adipose tissue. *J. Clin. Invest.* 117, 2621–2637. doi: 10.1172/jci31021

Kluge, M. A., Fetterman, J. L., and Vita, J. A. (2013). Mitochondria and endothelial function. *Circ. Res.* 112, 1171–1188. doi: 10.1161/circresaha.111.300233

Li, J., Liu, C. H., Sun, Y., Gong, Y., Fu, Z., Evans, L. P., et al. (2014). Endothelial TWIST1 promotes pathological ocular angiogenesis. *Invest. Ophthalmol. Vis. Sci.* 55, 8267–8277. doi: 10.1167/iovs.14-15623

Liu, J., Hou, W., Guan, T., Tang, L., Zhu, X., Li, Y., et al. (2018). Slit2/Robo1 signaling is involved in angiogenesis of glomerular endothelial cells exposed to a diabetic-like environment. *Angiogenesis* 21, 237–249. doi: 10.1007/s10456-017-9592-3

Mahmoud, M. M., Kim, H. R., Xing, R., Hsiao, S., Mammoto, A., Chen, J., et al. (2016). TWIST1 integrates endothelial responses to flow in vascular dysfunction and atherosclerosis. *Circ. Res.* 119, 450–462. doi: 10.1161/circresaha.116.308870

Mahmoud, M. M., Serbanovic-Canic, J., Feng, S., Souilhol, C., Xing, R., Hsiao, S., et al. (2017). Shear stress induces endothelial-to-mesenchymal transition via the transcription factor Snail. *Sci. Rep.* 7:3375.

Mahmoud, M., Souilhol, C., Serbanovic-Canic, J., and Evans, P. (2019). GATA4-Twist1 signalling in disturbed flow-induced atherosclerosis. *Cardiovasc. Drugs Ther.* 33, 231–237. doi: 10.1007/s10557-019-06863-3

Mammoto, A., and Mammoto, T. (2019). Vascular niche in lung alveolar development, homeostasis, and regeneration. *Front. Bioeng. Biotechnol.* 7:318. doi: 10.3389/fbioe.2019.00318

Mammoto, A., Connor, K. M., Mammoto, T., Yung, C. W., Huh, D., Aderman, C. M., et al. (2009). A mechanosensitive transcriptional mechanism that controls angiogenesis. *Nature* 457, 1103–1108. doi: 10.1038/nature07765

Mammoto, A., Hendee, K., Muyleart, M., and Mammoto, T. (2020). Endothelial Twist1-PDGFB signaling mediates hypoxia-induced proliferation and migration of αSMA-positive cells. *Sci. Rep.* 10:7563.

Mammoto, A., Muyleart, M., and Mammoto, T. (2019a). LRP5 in age-related changes in vascular and alveolar morphogenesis in the lung. *Aging* 11, 89–103. doi: 10.18632/aging.101722

Mammoto, T., Jiang, A., Jiang, E., and Mammoto, A. (2016). The role of Twist1 phosphorylation in angiogenesis and pulmonary fibrosis. *Am. J. Respir. Cell Mol. Biol.* 55, 633–644. doi: 10.1165/rcmb.2016-0012oc

Mammoto, T., Jiang, E., Jiang, A., Lu, Y., Juan, A. M., Chen, J., et al. (2013). Twist1 controls lung vascular permeability and endotoxin-induced pulmonary edema by altering tie2 expression. *PLoS One* 8:e73407. doi: 10.1371/journal.pone.0073407

Mammoto, T., Muyleart, M., and Mammoto, A. (2019b). Endothelial YAP1 in regenerative lung growth through the angiopoietin-Tie2 pathway. *Am. J. Respir. Cell Mol. Biol.* 60, 117–127. doi: 10.1165/rcmb.2018-0105oc

Mammoto, T., Muyleart, M., Konduri, G. G., and Mammoto, A. (2018). Twist1 in hypoxia-induced pulmonary hypertension through TGFβ-Smad signaling. *Am. J. Respir. Cell Mol. Biol.* 58, 194–207. doi: 10.1165/rcmb.2016-0323oc

Mammoto, T., Torisawa, Y. S., Muyleart, M., Hendee, K., Anugwom, C., Gutterman, D., et al. (2019c). Effects of age-dependent changes in cell size on endothelial cell proliferation and senescence through YAP1. *Aging* 11, 7051–7069. doi: 10.18632/aging.102236

McCullough, L. E., Chen, J., Cho, Y. H., Khankari, N. K., Bradshaw, P. T., White, A. J., et al. (2016). DNA methylation modifies the association between obesity and survival after breast cancer diagnosis. *Breast Cancer Res. Treat.* 156, 183–194. doi: 10.1007/s10549-016-3724-0

Nguyen Ba-Charvet, K. T., Brose, K., Marillat, V., Kidd, T., Goodman, C. S., Tessier-Lavigne, M., et al. (1999). Slit2-Mediated chemorepulsion and collapse of developing forebrain axons. *Neuron* 22, 463–473. doi: 10.1016/s0896-6273(00)80702-3

Nishioka, M., Venkatesan, N., Dessalle, K., Mogas, A., Kyoh, S., Lin, T. Y., et al. (2015). Fibroblast-epithelial cell interactions drive epithelial-mesenchymal transition differently in cells from normal and COPD patients. *Respir. Res.* 16:72.

O'Sullivan, J., Lysaght, J., Donohoe, C. L., and Reynolds, J. V. (2018). Obesity and gastrointestinal cancer: the interrelationship of adipose and tumour microenvironments. *Nat. Rev. Gastroenterol. Hepatol.* 15, 699–714. doi: 10.1038/s41575-018-0069-7

Pan, D., Fujimoto, M., Lopes, A., and Wang, Y. X. (2009). Twist-1 is a PPARdelta-inducible, negative-feedback regulator of PGC-1alpha in brown fat metabolism. *Cell* 137, 73–86. doi: 10.1016/j.cell.2009.01.051

Pasarica, M., Sereda, O. R., Redman, L. M., Albarado, D. C., Hymel, D. T., Roan, L. E., et al. (2009). Reduced adipose tissue oxygenation in human obesity: evidence for rarefaction, macrophage chemotaxis, and inflammation without an angiogenic response. *Diabetes* 58, 718–725. doi: 10.2337/db08-1098

Patten, I. S., and Arany, Z. (2012). PGC-1 coactivators in the cardiovascular system. *Trends Endocrinol. Metab.* 23, 90–97. doi: 10.1016/j.tem.2011.09.007

Pettersson, A. T., Laurencikiene, J., Mejhert, N., Naslund, E., Bouloumie, A., Dahlman, I., et al. (2010). A possible inflammatory role of twist1 in human white adipocytes. *Diabetes* 59, 564–571. doi: 10.2337/db09-0997

Pettersson, A. T., Mejhert, N., Jernas, M., Carlsson, L. M., Dahlman, I., Laurencikiene, J., et al. (2011). Twist1 in human white adipose tissue and obesity. *J. Clin. Endocrinol. Metab.* 96, 133–141.

Pozharskaya, V., Torres-Gonzalez, E., Rojas, M., Gal, A., Amin, M., Dollard, S., et al. (2009). Twist: a regulator of epithelial-mesenchymal transition in lung fibrosis. *PLoS One* 4:e7559.

Rama, N., Dubrac, A., Mathivet, T., Ni Charthaigh, R. A., Genet, G., Cristofaro, B., et al. (2015). Slit2 signaling through Robo1 and Robo2 is required for retinal neovascularization. *Nat. Med.* 21, 483–491. doi: 10.1038/nm.3849

Ren, B., Rose, J. B., Liu, Y., Jaskular-Sztul, R., Contreras, C., Beck, A., et al. (2019). Heterogeneity of vascular endothelial cells, de novo arteriogenesis and therapeutic implications in pancreatic neuroendocrine tumors. *J. Clin. Med.* 8:1980. doi: 10.3390/jcm8111980

Ren, J., Rudemiller, N. P., Wen, Y., Lu, X., Privratsky, J. R., and Crowley, S. D. (2020). The transcription factor Twist1 in the distal nephron but not in macrophages propagates aristolochic acid nephropathy. *Kidney Int.* 97, 119–129. doi: 10.1016/j.kint.2019.07.016

Robciuc, M. R., Kivela, R., Williams, I. M., de Boer, J. F., van Dijk, T. H., Elamaa, H., et al. (2016). VEGFB/VEGFR1-induced expansion of adipose vasculature counteracts obesity and related metabolic complications. *Cell Metab.* 23, 712–724. doi: 10.1016/j.cmet.2016.03.004

Rowe, G. C., Raghuram, S., Jang, C., Nagy, J. A., Patten, I. S., Goyal, A., et al. (2014). PGC-1alpha induces SPP1 to activate macrophages and orchestrate functional angiogenesis in skeletal muscle. *Circ. Res.* 115, 504–517. doi: 10.1161/circresaha.115.303829

Rudnicki, M., Abdifarkosh, G., Nwadozi, E., Ramos, S. V., Makki, A., Sepa-Kishi, D. M., et al. (2018). Endothelial-specific FoxO1 depletion prevents obesity-related disorders by increasing vascular metabolism and growth. *Elife* 7:e39780.

Salerno, P., Garcia-Rostan, G., Piccinin, S., Bencivenga, T. C., Di Maro, G., Doglioni, C., et al. (2011). TWIST1 plays a pleiotropic role in determining the anaplastic thyroid cancer phenotype. *J. Clin. Endocrinol. Metab.* 96, E772–E781.

Savage, D. B. (2009). Mouse models of inherited lipodystrophy. *Dis. Model. Mech.* 2, 554–562. doi: 10.1242/dmm.002907

Seki, T., Hosaka, K., Fischer, C., Lim, S., Andersson, P., Abe, M., et al. (2018). Ablation of endothelial VEGFR1 improves metabolic dysfunction by inducing adipose tissue browning. *J. Exp. Med.* 215, 611–626. doi: 10.1084/jem.20171012

Shibata, R., Ouchi, N., Kihara, S., Sato, K., Funahashi, T., and Walsh, K. (2004). Adiponectin stimulates angiogenesis in response to tissue ischemia through stimulation of amp-activated protein kinase signaling. *J. Biol. Chem.* 279, 28670–28674. doi: 10.1074/jbc.m402558200

Shimizu, I., Aprahamian, T., Kikuchi, R., Shimizu, A., Papanicolaou, K. N., MacLauchlan, S., et al. (2014). Vascular rarefaction mediates whitening of brown fat in obesity. *J. Clin. Invest.* 124, 2099–2112. doi: 10.1172/jci71643

Smith, U., Li, Q., Ryden, M., and Spalding, K. L. (2021). Cellular senescence and its role in white adipose tissue. *Int. J. Obes.* 45, 934–943. doi: 10.1038/s41366-021-00757-x

Spencer, M., Unal, R., Zhu, B., Rasouli, N., McGehee, R. E. Jr., Peterson, C. A., et al. (2011). Adipose tissue extracellular matrix and vascular abnormalities in obesity and insulin resistance. *J. Clin. Endocrinol. Metab.* 96, E1990–E1998.

Sun, K., Tordjman, J., Clement, K., and Scherer, P. E. (2013). Fibrosis and adipose tissue dysfunction. *Cell Metab.* 18, 470–477. doi: 10.1016/j.cmet.2013.06.016

Sun, K., Wernstedt Asterholm, I., Kusminski, C. M., Bueno, A. C., Wang, Z. V., Pollard, J. W., et al. (2012). Dichotomous effects of VEGF-A on adipose tissue dysfunction. *Proc. Natl. Acad. Sci. U.S.A.* 109, 5874–5879. doi: 10.1073/pnas.1200447109

Sung, H. K., Doh, K. O., Son, J. E., Park, J. G., Bae, Y., Choi, S., et al. (2013). Adipose vascular endothelial growth factor regulates metabolic homeostasis through angiogenesis. *Cell Metab.* 17, 61–72. doi: 10.1016/j.cmet.2012.12.010

Svensson, K. J., Long, J. Z., Jedrychowski, M. P., Cohen, P., Lo, J. C., Serag, S., et al. (2016). A secreted slit2 fragment regulates adipose tissue thermogenesis and metabolic function. *Cell Metab.* 23, 454–466.

Tan, J., Tedrow, J. R., Nouraie, M., Dutta, J. A., Miller, D. T., Li, X., et al. (2017). Loss of Twist1 in the mesenchymal compartment promotes increased fibrosis in experimental lung injury by enhanced expression of CXCL12. *J. Immunol.* 198, 2269–2285.

Tavora, B., Mederer, T., Wessel, K. J., Ruffing, S., Sadjadi, M., Missmahl, M., et al. (2020). Tumoural activation of TLR3-SLIT2 axis in endothelium drives metastasis. *Nature* 586, 299–304. doi: 10.1038/s41586-020-2774-y

Tilg, H., and Moschen, A. R. (2006). Adipocytokines: mediators linking adipose tissue, inflammation and immunity. *Nat. Rev. Immunol.* 6, 772–783. doi: 10.1038/nri1937

Urbich, C., Rossig, L., Kaluza, D., Potente, M., Boeckel, J. N., Knau, A., et al. (2009). HDAC5 is a repressor of angiogenesis and determines the angiogenic gene expression pattern of endothelial cells. *Blood* 113, 5669–5679.

Vazquez-Vela, M. E., Torres, N., and Tovar, A. R. (2008). White adipose tissue as endocrine organ and its role in obesity. *Arch. Med. Res.* 39, 715–728. doi: 10.1016/j.arcmed.2008.09.005

Verboven, K., Wouters, K., Gaens, K., Hansen, D., Bijnen, M., Wetzels, S., et al. (2018). Abdominal subcutaneous and visceral adipocyte size, lipolysis and inflammation relate to insulin resistance in male obese humans. *Sci. Rep.* 8:4677.

Virtue, S., and Vidal-Puig, A. (2010). Adipose tissue expandability, lipotoxicity and the metabolic syndrome–an allostatic perspective. *Biochim. Biophys. Acta* 1801, 338–349. doi: 10.1016/j.bbalip.2009.12.006

Wang, G., Dong, W., Shen, H., Mu, X., Li, Z., Lin, X., et al. (2011). A comparison of Twist and E-cadherin protein expression in primary non-small-cell lung carcinoma and corresponding metastases. *Eur. J. Cardiothorac. Surg.* 39, 1028–1032. doi: 10.1016/j.ejcts.2011.01.023

Wang, K. H., Brose, K., Arnott, D., Kidd, T., Goodman, C. S., Henzel, W., et al. (1999). Biochemical purification of a mammalian slit protein as a positive regulator of sensory axon elongation and branching. *Cell* 96, 771–784. doi: 10.1016/s0092-8674(00)80588-7

Wang, L., Zheng, J., Pathak, J. L., Chen, Y., Liang, D., Yang, L., et al. (2020). SLIT2 overexpression in periodontitis intensifies inflammation and alveolar bone loss, possibly via the activation of MAPK pathway. *Front. Cell Dev. Biol.* 8:593. doi: 10.3389/fcell.2020.00593

Wirrig, E. E., and Yutzey, K. E. (2014). Conserved transcriptional regulatory mechanisms in aortic valve development and disease. *Arterioscler. Thromb. Vasc. Biol.* 34, 737–741. doi: 10.1161/atvbaha.113.302071

Xiao, L., Yan, K., Yang, Y., Chen, N., Li, Y., Deng, X., et al. (2016). Anti-vascular endothelial growth factor treatment induces blood flow recovery through vascular remodeling in high-fat diet induced diabetic mice. *Microvasc. Res.* 105, 70–76.

Xue, G., Restuccia, D. F., Lan, Q., Hynx, D., Dirnhofer, S., Hess, D., et al. (2012). Akt/PKB-mediated phosphorylation of Twist1 promotes tumor metastasis via mediating cross-talk between PI3K/Akt and TGF-beta signaling axes. *Cancer Discov.* 2, 248–259. doi: 10.1158/2159-8290.cd-11-0270

Yang, M. H., and Wu, K. J. (2008). TWIST activation by hypoxia inducible factor-1 (HIF-1): implications in metastasis and development. *Cell Cycle* 7, 2090–2096. doi: 10.4161/cc.7.14.6324

Yeo, S. Y., Lee, K. W., Shin, D., An, S., Cho, K. H., and Kim, S. H. (2018). A positive feedback loop bi-stably activates fibroblasts. *Nat. Commun.* 9:3016.

Yokoyama, M., Okada, S., Nakagomi, A., Moriya, J., Shimizu, I., Nojima, A., et al. (2014). Inhibition of endothelial p53 improves metabolic abnormalities related to dietary obesity. *Cell Rep.* 7, 1691–1703. doi: 10.1016/j.celrep.2014.04.046

Zhao, H., Anand, A. R., and Ganju, R. K. (2014). Slit2-Robo4 pathway modulates lipopolysaccharide-induced endothelial inflammation and its expression is dysregulated during endotoxemia. *J. Immunol.* 192, 385–393. doi: 10.4049/jimmunol.1302021

Conflict of Interest: The authors declare that the research was conducted in the absence of any commercial or financial relationships that could be construed as a potential conflict of interest.

Publisher's Note: All claims expressed in this article are solely those of the authors and do not necessarily represent those of their affiliated organizations, or those of the publisher, the editors and the reviewers. Any product that may be evaluated in this article, or claim that may be made by its manufacturer, is not guaranteed or endorsed by the publisher.

Copyright © 2021 Hunyenyiwa, Hendee, Matus, Kyi, Mammoto and Mammoto. This is an open-access article distributed under the terms of the Creative Commons Attribution License (CC BY). The use, distribution or reproduction in other forums is permitted, provided the original author(s) and the copyright owner(s) are credited and that the original publication in this journal is cited, in accordance with accepted academic practice. No use, distribution or reproduction is permitted which does not comply with these terms.

frontiers in Cell and Developmental Biology

HYPOTHESIS AND THEORY
published: 07 October 2021
doi: 10.3389/fcell.2021.702021

Regulation of Partial and Reversible Endothelial-to-Mesenchymal Transition in Angiogenesis

*Jennifer S. Fang[1†], Nan W. Hultgren[2†] and Christopher C. W. Hughes[1,3]**

[1] Department of Molecular Biology and Biochemistry, University of California, Irvine, Irvine, CA, United States, [2] Department of Ophthalmology, Stein Eye Institute, David Geffen School of Medicine at University of California, Los Angeles, Los Angeles, CA, United States, [3] Department of Biomedical Engineering, University of California, Irvine, Irvine, CA, United States

OPEN ACCESS

Edited by:
Bin Ren,
University of Alabama at Birmingham,
United States

Reviewed by:
MIchael Simons,
Yale University, United States
Berta Casar,
Instituto de Biomedicina y Biotecnología de Cantabria, Consejo Superior de Investigaciones Científicas, Spain
Yi Fan,
University of Pennsylvania,
United States

***Correspondence:**
Christopher C. W. Hughes
cchughes@uci.edu

[†] These authors have contributed equally to this work and share first authorship

Specialty section:
This article was submitted to Signaling,
a section of the journal Frontiers in Cell and Developmental Biology

Received: 28 April 2021
Accepted: 22 June 2021
Published: 07 October 2021

Citation:
Fang JS, Hultgren NW and Hughes CCW (2021) Regulation of Partial and Reversible Endothelial-to-Mesenchymal Transition in Angiogenesis. Front. Cell Dev. Biol. 9:702021. doi: 10.3389/fcell.2021.702021

During development and in several diseases, endothelial cells (EC) can undergo complete endothelial-to-mesenchymal transition (EndoMT or EndMT) to generate endothelial-derived mesenchymal cells. Emerging evidence suggests that ECs can also undergo a partial EndoMT to generate cells with intermediate endothelial- and mesenchymal-character. This partial EndoMT event is transient, reversible, and supports both developmental and pathological angiogenesis. Here, we discuss possible regulatory mechanisms that may control the EndoMT program to dictate whether cells undergo complete or partial mesenchymal transition, and we further consider how these pathways might be targeted therapeutically in cancer.

Keywords: EndoMT, EndMT, endothelial, mesenchymal, cell identity, cell plasticity, angiogenesis, partial EndoMT

INTRODUCTION

Endothelial cells (EC) that line the various blood vessels of the body share numerous structural characteristics and gene expression programs, yet are also remarkably heterogeneous (Aird, 2012; Kalucka et al., 2020; Paik et al., 2020) and plastic (Paruchuri et al., 2006; van Meeteren and ten Dijke, 2012; Dejana et al., 2017; Andueza et al., 2020). Blood vessel development is a multi-step process involving dynamic changes in EC morphology and gene expression to drive coalescence of primitive ECs into a primordial network (vasculogenesis), followed by EC proliferation and network expansion (angiogenesis). Lastly, blood vessels reorganize and mature into a hierarchal network architecture (remodeling and specification). During these processes as well as in the context of certain diseases, ECs undergo diversification, and some even take on a new non-EC identity (Welch-Reardon et al., 2015; Gritz and Hirschi, 2016; Piera-Velazquez and Jimenez, 2019; Qiu and Hirschi, 2019; Kenswil et al., 2021). In complete endothelial-to-mesenchymal transition (EndoMT), for example, activation of a central EndoMT program – similar to the program that drives epithelial-to-mesenchymal transition (EMT) in epithelial cells – induces a subpopulation of ECs to fully abandon their EC identity and transition to a mesenchymal cell phenotype (Welch-Reardon et al., 2015; Piera-Velazquez and Jimenez, 2019). This process generates several mesenchymal cell types (Tran et al., 2012; Yao et al., 2013) including endothelial-derived fibroblasts (Zeisberg et al., 2007b; Li et al., 2009; Hashimoto et al., 2010; Aisagbonhi et al., 2011; Moore-Morris et al., 2014; Chen et al., 2016) critical for embryonic tissue development (Timmerman et al., 2004) and disease progression in atherosclerosis (Souilhol et al., 2018), vascular fibrosis (Chen et al., 2012), and cancer (Zeisberg et al., 2007a).

In addition to supporting complete mesenchymal transition, the EndoMT program can also proceed only partially resulting in the temporary and reversible appearance of intermediate cells that exhibit both endothelial and mesenchymal characteristics (Tombor et al., 2021). Tombor et al. (2021), for example, recently used single-cell transcriptomic analysis to show that a subpopulation of ECs transiently adopt a mesenchymal signature within 7 days following myocardial infarction, but that they return to baseline EC identity by 14 days post-infarction rather than fully committing to a mesenchymal fate. While there are several possible explanations for the transient EndoMT signature in this study, one possibility is that partial EndoMT activation following myocardial infarction supports the robust injury-induced activation of acute new vessel growth (i.e., angiogenesis) typically observed in such models (Manavski et al., 2018; Li et al., 2019; Zou et al., 2019). Indeed, we and others have proposed, based on a growing body of evidence, that angiogenic EC undergo partial EndoMT during healthy and pathological angiogenesis to support new vessel formation (Welch-Reardon et al., 2014, 2015; Hultgren et al., 2020). Consistent with this hypothesis, both Manavski et al. (2018) and Li et al. (2019) recently observed in separate lineage-tracing studies that clonal expansion of ECs is enhanced in myocardial infarction-induced neovascularization. Using transcriptomic analysis, Manavski et al. (2018) further found enrichment of EndoMT genes in regions of clonally expanded vessels. By contrast, although Li et al. (2019) also observed enhancement of some mesenchymal genes in single-cell RNA-Seq study of post-infarction EC, they failed to note significant differences in overall EndoMT signature at their assessed timepoint, potentially due to the generally shallower sequencing depth of scRNAseq which may miss key transcription factors.

Activation of the EndoMT program in EC during angiogenesis must be partial and reversible to support the formation of perfused and functional blood vessels. This implies the existence of essential regulatory mechanisms that act on the EndoMT program to determine whether it will proceed completely in some tissues, but only partially in other contexts such as angiogenesis. Here, we revisit the argument for sprouting angiogenesis as a partial EndoMT event and explore possible regulatory mechanisms that might limit complete progression through the EndoMT program during angiogenesis, thereby preventing excessive mesenchymal transition and ensuring organized and controlled new vessel growth.

SPROUTING ANGIOGENESIS AS A PARTIAL EndoMT EVENT

Sprouting angiogenesis is a complex developmental program wherein specialized endothelial "tip" cells migrate away from the parent vessel wall toward pro-angiogenic stimuli, while bringing with them endothelial "stalk" cells, thereby establishing a new blood vessel sprout (Gerhardt et al., 2003). Endothelial tip and stalk cells are dynamic and transient states (Jakobsson et al., 2010) determined by each cell's relative Dll4-activated Notch signaling (Hellstrom et al., 2007; Suchting et al., 2007) and downstream VEGFR1/2 expression levels (Williams et al., 2006). Cells that successfully outcompete adjacent cells for the tip cell position do so through classical Notch-mediated lateral inhibition. Specifically, tip cells strongly express Dll4 to activate high levels of Notch signaling in their neighbors, which are thereby activated to take on the phenotype of stalk cells (Blanco and Gerhardt, 2013) allowing for sprout elongation.

Given the heterogeneous outcomes associated with EMT program activation, identification of an EMT event can be difficult and requires the combined observation of several cellular and molecular hallmarks, including the upregulated expression of at least one of several EMT-associated transcription factors, induced expression of mesenchymal markers, and alterations in functional properties such as cytoskeletal rearrangement, reduced cell-cell adhesions, and increased cell motility (Yang et al., 2020). Furthermore, cells with epithelial-mesenchymal plasticity – that is, with mixed epithelial and mesenchymal character indicating partial EMT – must in addition to the above hallmarks also retain cellular and molecular aspects of epithelial identity such as persistent expression of some epithelial markers and/or residual cell-cell junctions (Yang et al., 2020).

When compared to this standard, the cellular and molecular changes that occur in sprouting angiogenesis are highly suggestive of partial EndoMT (Potenta et al., 2008; Welch-Reardon et al., 2014, 2015; Piera-Velazquez and Jimenez, 2019; Hultgren et al., 2020). During angiogenesis, tip cells retain EC marker expression even while they undergo a dramatic loss of typical EC morphology and function. These changes include altered cell shape and polarity, extension of numerous filopodia that guide cell migration (Gerhardt et al., 2003), destabilization of cell-cell junctions (del Toro et al., 2010; Bentley et al., 2014; Hultgren et al., 2020) as well as increased cell motility (Jakobsson et al., 2010; Welch-Reardon et al., 2014) and upregulated expression of mesenchymal markers [e.g., Smooth Muscle α-actin, or αSMA (Li et al., 2009; Mendoza et al., 2016)] and extracellular matrix degradation proteases (del Toro et al., 2010; Welch-Reardon et al., 2014). Furthermore, tip cells and trailing stalk cells migrate as a train toward external VEGF, a process reminiscent of the collective migration that occurs when epithelial cells undergo EMT during organogenesis as well as in invasive tumors. In a sense, one end of a tip cell – specifically, the leading edge – acquires a mesenchymal-like phenotype, while the trailing edge retains some endothelial characteristics including maintenance of junctional contacts to trailing stalk EC.

In further support of angiogenesis as a partial EndoMT event, we have found that the master transcription factors Snail and Slug are induced in ECs during sprouting angiogenesis, both developmentally (Hultgren et al., 2020) and in the malformed vasculature of growing tumors (Parker et al., 2004; Lu et al., 2007). More recently, our group reported that Slug, although only transiently required for developmental angiogenesis, is critical for pathological angiogenesis, such that absence of Slug leads to a striking lack of tumor vasculature which profoundly limits tumor expansion (Hultgren et al., 2020). We further showed that EC Slug overexpression downregulates adhesion and cell-cell junction proteins, and upregulates pathways associated with cell cycle, cell shape changes, and motility (Hultgren et al., 2020).

Other master transcription factors are likely also involved in partial EndoMT during angiogenesis. For example, Ma W. et al. (2020) recently identified PAK4-induced Zeb1 as a driver of mesenchymal gene expression in glioblastoma EC. Taken together, these recent data strongly support the hypothesis that during sprouting angiogenesis, an EndoMT program is partially and reversibly activated in angiogenic ECs to support acquisition of the subset of mesenchymal characteristics necessary to form new vessel sprouts. This model further implies that tight regulatory mechanisms must govern partial EndoMT events in normal angiogenesis to control the degree of mesenchymal transition, thereby maintaining an organized program of new vessel growth.

REGULATORY MECHANISMS THAT GOVERN THE EndoMT PROGRAM

Signaling Pathways Regulating EndoMT

Similar to its role in EMT, TGF-β superfamily signaling is a potent activator of the EndoMT program, both in developmental and pathological settings (Arciniegas et al., 1992; van Meeteren and ten Dijke, 2012; Xiao et al., 2015; Pardali et al., 2017). This process is mediated by both canonical and non-canonical Smad-dependent downstream pathways (Medici et al., 2011; Piera-Velazquez and Jimenez, 2019) and necessary for organogenesis in many developmental contexts (Niessen et al., 2008; Piera-Velazquez and Jimenez, 2019). Other ligands, including Wnt (Liebner et al., 2004; Aisagbonhi et al., 2011), FGF (Correia et al., 2016; Paik et al., 2020), NFKB (Mahler et al., 2013; Cho et al., 2018), and ET-1 (Widyantoro et al., 2010) also regulate EndoMT, with many of these signals appearing to act in parallel with or converging upon TGF-β and BMP signaling (Arciniegas et al., 1992; Hopper et al., 2016) to drive full mesenchymal transition.

Pro-angiogenic signaling pathways modulate the EndoMT program in many ways. VEGF/VEGFR2 signaling is a potent pro-angiogenic signal critical for healthy vascular development, and is abnormally upregulated in tumor vasculature of many cancer types in association with aggressive blood vessel growth (Shibuya, 2013). VEGF/VEGFR2 signaling regulates numerous cellular functions in EC such as cell survival, proliferation, migration, and junctional integrity via a constellation of downstream signaling modules including PI3K/Akt, PLC-γ/PKC, p38MAPK, ERK, RAC, FAK, JNK, and RhoA pathways (Abhinand et al., 2016). TGF-β signaling can influence VEGF/VEGFR2 signaling directly via canonical activation of intracellular Smads that target several downstream genes, including VEGFR2 (Mandriota et al., 1996) and (in the presence of hypoxia) VEGF (Sanchez-Elsner et al., 2001). TGF-β can also indirectly affect VEGF/VEGFR2 signaling via non-canonical effects on many of the same modules activated by VEGF/VEGFR2, including PI3K/Akt, p38MAPK, ERK, and JNK (Ma J. et al., 2020). VEGF also exerts positive feedback on TGF-β1 expression via PI3K/Akt activation (Li et al., 2005). Taken together, these findings underscore the potential for complex crosstalk between VEGF and TGF-β signaling. We have previously described the interrelationship between the VEGF, Notch, and TGF-β pathways and how this lays the foundation for the sprouting phenotype (Holderfield and Hughes, 2008) and thereby the ensuing EndoMT program. In general, VEGF and TGF-β act synergistically (Holderfield and Hughes, 2008) and VEGF is required for TGF-β-induced angiogenesis *in vivo* (Ferrari et al., 2009). However, TGF-β can also antagonize VEGF/VEGFR2 signaling either directly by inhibiting VEGFR2 expression (Mandriota et al., 1996) or indirectly by antagonizing its cellular effects (Holderfield and Hughes, 2008). For example, VEGF is typically a pro-survival signal, but in the context of co-stimulation with TGF-β it becomes pro-apoptotic (Ferrari et al., 2006, 2009). This suggests that while VEGF plays a crucial role (including downstream of TGF-β) in initiating and driving angiogenesis, VEGF and TGF-β may also antagonize one another to determine the extent of EndoMT progression within the context of angiogenic EC. In support of this idea, exogenous VEGF treatment prevents TGF-β-induced EndoMT during cardiac fibrosis (Illigens et al., 2017) and VEGFR2 expression is reduced in glioblastoma vessels alongside EndoMT program activation and acquired mesenchymal marker expression (Liu et al., 2018).

In contrast to VEGF/VEGFR2, pro-angiogenic HIF-1α (Xu et al., 2015b) and TNFα (Sainson et al., 2008; Yoshimatsu et al., 2020) promote (rather than antagonize) complete EndoMT. Still other pro-angiogenic signals exert a context-dependent effect on the EndoMT program. HGF/c-Met signaling, for example, prevents TGF-β1-induced EndoMT in cardiac fibrosis (Okayama et al., 2012; Wang et al., 2018) but c-Met signaling activates EndoMT and abnormal vessel growth in glioblastoma (Huang et al., 2016) potentially compensating for the loss of VEGFR2 in these tumor vessels described by Liu et al. (2018). CXCL12 (SDF-1α)/CXCR4 signaling is upregulated in radiation-induced EndoMT in tumor vasculature where it is required for tumor-associated macrophage recruitment (Choi et al., 2018), and knockdown of either of CXCL12's receptors, CXCR4 and CXCR7, disrupts angiogenic sprouting *in vitro* (Hultgren et al., 2020). Consistent with this, we found that CXCL12 activation of CXCR4 – but, interestingly, not CXCR7 – is required for CXCL12-induced upregulation of master transcription factor, Slug, which drives partial EndoMT during angiogenesis (Hultgren et al., 2020). By contrast, others have reported that CXCL12 activation of CXCR7 induces Wnt signaling to inhibit EndoMT-associated fibrosis (Shen et al., 2020).

Master Transcription Factors of EndoMT

Perhaps the key determinant for EndoMT is not any specific receptor pathway activation, but the extent to which the combined and integrated signaling through these pathways converge at the level of the EndoMT master transcription factors. These include members of the Snail family of zinc-finger transcription factors, Slug and Snail, as well as zinc-finger transcription factors, Zeb1 and Zeb2, and the basic helix-loop-helix transcription factor, Twist1 (Piera-Velazquez and Jimenez, 2019). These transcription factors were originally described as potent drivers of EMT (Lamouille et al., 2014) with more recent studies finding that their expression in ECs induces EndoMT (Piera-Velazquez and Jimenez, 2019) suggesting a common mesenchymal transition program in both cell types.

In epithelial cells there is significant cross-talk between Slug, Snail, Zeb1, Zeb2, and Twist1 to regulate EMT progression (Peinado et al., 2007). In ECs, the interrelationship between these transcription factors is less well understood, but likely similarly complex (Weinstein et al., 2020). Some studies propose that Snail is the primary driver of the EndoMT program, with other transcription factors playing a largely ancillary role to Snail. Global (Carver et al., 2001), epiblast- (Lomeli et al., 2009) and endothelial-specific Snail (Wu et al., 2014) knockout is embryonic lethal due to profound defects in cardiovascular development (although this may or may not be due to an EndoMT defect), whereas animals lacking Slug survive embryogenesis with comparatively subtle defects in blood vessel development (Hultgren et al., 2020). In cultured ECs, TGF-β2 induces Snail expression via Smad-mediated MEK/ERK, PI3K, and p38MAPK (Medici et al., 2011) but does not significantly upregulate Slug and Twist1 (Kokudo et al., 2008). Snail is also strongly upregulated by hypoxia, and is directly targeted by HIF-1α during induction of EndoMT in corneal ECs (Xu et al., 2015b). Gene silencing approaches show that Snail is necessary for both TGF-β2- (Kokudo et al., 2008) and low shear stress-activated (Mahmoud et al., 2017) EndoMT. Furthermore, in several of these models, Slug expression is at least partially dependent on Snail (Xu et al., 2015b; Mahmoud et al., 2017) indicating cross-talk between Snail- and Slug-mediated EndoMT signaling.

Our studies as well as others, on the other hand, suggest that Slug and Snail both play important and non-redundant (if over-lapping) roles in EndoMT (Welch-Reardon et al., 2014; Hultgren et al., 2020; Weinstein et al., 2020). Slug and Snail negatively regulate one another's expression (Chen and Gridley, 2013a,b) and both participate in distinct (as well as shared) signaling circuits that govern partial and full EndoMT (Weinstein et al., 2020). Further supporting the hypothesis that Slug and Snail function independently in EndoMT, endothelial Snail expression is unaffected by transgenic ablation of Slug in the retinal microvasculature (Hultgren et al., 2020) although it can compensate for Slug during heart formation in embryogenesis (Niessen et al., 2008). Instead, transcriptomic analysis indicates that Slug regulates a distinct suite of genes during early angiogenesis consistent with induction of partial EndoMT, including upregulation of mesenchymal markers (e.g., αSMA) as well as pro-proliferative and pro-migratory genes, and destabilization of endothelial junction genes (e.g., Occludin) without concurrent suppression of endothelial markers such as PECAM-1 (Hultgren et al., 2020).

Aside from Slug and Snail, endothelial expression of Zeb1 (Singh et al., 2019; Fu et al., 2020), Zeb2 (Chen et al., 2010), and Twist1 (Mahmoud et al., 2016) also promote EndoMT and angiogenesis. Endothelial expression of Twist1 induces a partial EndoMT program in ECs in response to TGF-β2 stimulation, resulting in increased EC proliferation and migration, a more mesenchymal-like cell morphology, and downregulation of endothelial junction proteins (Mammoto et al., 2018). Similarly, endothelial Twist1 overexpression drives mesenchymal marker expression in pulmonary ECs, and is necessary for the development of vascular structures in an implanted fibrin gel model of blood vessel network formation (Mammoto et al., 2020). Fu et al. (2020) also found that endothelial deletion of Zeb1 leads to improved vascular normalization and reduced cancer progression in various tumor models by reducing tumor vessel density and permeability, mainly by reducing TGF-β signaling in ECs and associated tumor stroma. More recently, Ma W. et al. (2020) found that PAK4 drives mesenchymal gene expression in the EC of glioblastoma blood vessels, and that in this setting, Zeb1 (but not Slug) is required for PAK4 suppression of cellular adhesion proteins leading to increased vascular permeability.

Experimental studies as well as *in silico* analysis suggest that Twist1 may operate upstream of Slug and Snail (Sanchez-Elsner et al., 2001; Okayama et al., 2012; Huang et al., 2016). For example, Mammoto et al. (2018) found that Twist1 upregulates Slug expression, which the authors propose is a necessary intermediate step for EndoMT to proceed in these cells. Yet, our transcriptomic analysis of Slug overexpressing ECs also indicate positive feedback by Slug onto Twist1 expression (Hultgren et al., 2020). By contrast, Zeb1 and Zeb2 appear to function primarily downstream of these transcription factors (Lee et al., 2018; Weinstein et al., 2020). In corneal ECs, Zeb1 is required for Snail upregulation of cell cycle and extracellular matrix proteins during EndoMT (Lee et al., 2018). Thus, while the sequential as well as lateral relationships between Snail transcription factors, Zeb transcription factors, and Twist1 suggest significant cross-talk, it currently remains unclear exactly how these signals coordinately regulate EndoMT progression. Further studies are necessary to fully elucidate the (clearly complex) relationship between their expression patterns and functions in EndoMT.

Notch

Notch signaling appears to play a central – and still largely unclear – function during EndoMT. Signaling via Notch requires cell-cell contact between membrane-bound Notch ligands (e.g., Dll4 and Jag1) and cell surface Notch receptor expressed on adjacent cells. Thus, Notch signaling necessarily requires that at least some cell-cell junctions be intact, suggesting an initiating role in EMT and presumably an early role also in EndoMT. Indeed, Notch drives EndoMT in development (Niessen et al., 2008; Chang et al., 2011) and during disease (Noseda et al., 2004; Liu et al., 2014). Yet, we and others have also found that Notch limits sprouting angiogenesis (Hellstrom et al., 2007; Suchting et al., 2007) and that small molecule inhibition of Notch signaling exacerbates EndoMT (Chen et al., 2015; Hultgren et al., 2020). Specifically, in our hands, Notch signaling inhibition combined with Slug overexpression leads to complete fragmentation of sprouts during *in vitro* angiogenesis, indicative of cells undergoing more aggressive or complete mesenchymal transition (Hultgren et al., 2020).

The solution to this conundrum likely lies in the way we have traditionally approached Notch signaling, which has thus far been presumed to be an *instructive* signal. More consistent with its multiple and differing roles in numerous developmental programs, however, would be if Notch signaling instead plays a *permissive* role to open a "window of opportunity" for other pathways to be active. Thus, for any process – whether positively or negatively acting pathways – both could each be dependent on Notch signaling, such that neither is able to operate

without a permissive signal from Notch. In EC, Notch may thus control whether pro- or anti-mesenchymal transition signals gain the upper hand. Similar processes have been suggested for Notch during arteriovenous specification (Fang et al., 2017) hemogenesis (Gama-Norton et al., 2015) and endocrine cell specification (Dutta et al., 2008).

MicroRNA

MicroRNAs (miRNA) are short single-stranded, non-coding RNA sequences that regulate post-transcriptional gene expression at the mRNA level. Several miRNAs are involved in EMT (Nicoloso et al., 2009), both through regulation by – and feedback onto – Snail (Gill et al., 2011; Chen D. D. et al., 2019) Slug (Chen D. D. et al., 2019) and Zeb genes (Burk et al., 2008). Multiple miRNA species have recently been identified as positive and negative regulators of TGF-β-induced EndoMT (Kim, 2018; Glover et al., 2019) – including miR-630 which inhibits EndoMT by directly targeting Slug (Sun et al., 2016) – suggesting that the dynamic and integrated signal from multiple miRNAs acting in concert may also determine the extent of EndoMT and other EC fate changes. Furthermore, FGF signaling has been shown to promote TGF-β mediated EndoMT via regulation of let-7 miRNA expression (Chen et al., 2012) but to limit it via miR-20 (Correia et al., 2016). Consistent with this hypothesis, endothelial expression of Dicer – the protein responsible for miRNA pre-processing – is required for angiogenesis (Suárez et al., 2008) and miRNAs have also recently been reported to regulate endothelial-to-hematopoietic transition (Kasper et al., 2020). Thus, the interrelationship between miRNA species in ECs and their combined effect on EndoMT progression warrant further study.

Epigenetic Modifications

Both complete and partial EndoMT depend upon the availability of key inducers to activate core DNA-binding transcription factors that regulate the expression of downstream mesenchymal transition genes. Given this, epigenetic changes that alter access to individual genes (or chromatin, more broadly) play a significant role at multiple levels of the EndoMT program, such as to regulate the availability of EndoMT inducers and effectors (Turunen and Yla-Herttuala, 2011; Lewandowski et al., 2015; Schwanbeck, 2015). For example, during normal heart development, HDAC3-mediated recruitment of EZH2 leads to transcriptional silencing of TGF-β1 to prevent aberrant EndoMT (Lewandowski et al., 2015). Other angiogenic signals that influence the EndoMT pathway – including VEGF and Notch pathway effectors – are also sensitive to DNA modifications (Turunen and Yla-Herttuala, 2011; Schwanbeck, 2015). Lastly, DNA methylation status can also regulate the levels of EMT-associated master transcription factors in epithelial cells (Lee and Kong, 2016) suggesting that similar regulation might occur in ECs to influence EndoMT.

Endothelial-to-mesenchymal transition progression is also sensitive to epigenetic changes that alter access to mesenchymal genes acted upon by EndoMT master transcription factors (Maleszewska et al., 2015). Under both developmental and pathological settings, TGF-β alters the methylation of EndoMT-related genes (Maleszewska et al., 2015; Xu et al., 2015a), and can (either alone or alongside Notch co-stimulation) induce histone acetylation (Fu et al., 2009). More fundamentally, the comparative difference in EndoMT transcription factor importance in physiological versus pathological angiogenesis (Hultgren et al., 2020; Ma W. et al., 2020) may be due to differences in chromatin architecture during development versus under inflammatory and other disease settings, such as in cancer. Alternatively, inflammation-induced epigenetic changes may also explain why the EndoMT program proceeds to completion in some disease contexts such as atherosclerosis or cancer, but not in angiogenesis. Indeed, the complexity and heterogeneity in cell type-specific responses to common inflammatory signals such as NFKB is established by the epigenetic landscape that uniquely determines enhancer region accessibility across distinct tissues (Natoli, 2009; Natoli et al., 2011). Epigenetic changes also occur during carcinogenesis to drive tumor growth and vascularization (Baylin and Jones, 2016). How chromatin remodeling under these and other pathological settings influence the accessibility of mesenchymal transition genes in EC, thereby altering the outcome of EndoMT program activation, remains unclear.

MODEL OF PARTIAL EndoMT REGULATION

Early studies of EMT and EndoMT proposed that mesenchymal transition is a binary, on/off switch between two distinct cell states. However, more sophisticated studies have now refuted that idea, and instead support an alternative model wherein most cell fate changes – including both EMT and EndoMT – involve progressive transition from one cell identity to another via a fluid spectrum of intermediate cell states (Lamouille et al., 2014; Sha et al., 2019). In support of this latter model, initiation of EMT in pluripotent epithelial stem cells through downregulation of the adherens junction protein E-cadherin triggers expression of Slug and related transcription factors, leading to the acquisition of some mesenchymal characteristics; yet, these cells still retain expression of epithelial stem cell markers indicating only a partial EMT (Aban et al., 2021).

Similarly, complete EndoMT also involves fluid transition through intermediate endothelial and mesenchymal substates with characteristics of both cell types. Cell subpopulations that co-express endothelial- and mesenchymal- markers – indicating cells in an intermediate state of EndoMT – have been reported in cardiac (Widyantoro et al., 2010), pulmonary (Mendoza et al., 2016), and dermal (Manetti et al., 2017) fibrosis, as well as in fetal valve endothelial progenitor cells (Paruchuri et al., 2006). Furthermore, pseudotime analysis of single cell transcriptomic and epigenomic data shows a spectrum of intermediate EndoMT cells, as well as ECs undergoing apparent transition to other non-mesenchymal cell types (Andueza et al., 2020; Kenswil et al., 2021). Given this, partial EndoMT is most likely not its own distinct process. Instead, we propose that partial EndoMT is best described as an incomplete activation and/or progression of the core EndoMT program, wherein regulatory signals are activated to limit the EndoMT process and prevent EC from fully transitioning into a mesenchymal endpoint. Clearly,

in some contexts such as atherosclerosis and tumorigenesis, EndoMT program activation proceeds fully to completion. This may be due to chronic activation of the EndoMT program in this setting which (perhaps further augmented by the initiation of positive feedback mechanisms) drives cells rapidly through intermediate endothelial-mesenchymal states to promote robust transition into fibroblasts (Schwartz et al., 2018). Yet, in angiogenesis, we propose that the EndoMT program is only weakly or incompletely activated, or that regulatory "brakes" may inhibit EndoMT program progression to suppress complete mesenchymal transition. Together, this may ensure that cells proceed only partially through the endothelial-to-mesenchymal identity spectrum, enabling temporary and reversible adoption of a hybrid endothelial-mesenchymal cell state (**Figure 1**). To achieve such context-dependent nuance, the EndoMT program must be under strict regulatory control. We propose two layers of regulation on this process: (1) regulation of endothelial and mesenchymal identity signaling; and (2) regulation of cell plasticity to determine target cell sensitivity to those identity cues.

Regulation of Endothelial and Mesenchymal Identity Signaling

Cell identity – even among committed cells – is dynamically established and maintained by the moment-to-moment balance of competing cell fate signals (Lee et al., 2014; Watanabe et al., 2014; Dejana et al., 2017). Indeed, ECs can respond rapidly to changes in local cell fate signals (Dejana et al., 2017) which suggests that EC identity maintenance remains a largely active process involving continuous input from local endothelial identity cues that include ligand-receptor signaling (i.e., VEGF, FGF, BMP, etc.), cell-matrix signaling, perivascular cell signaling, fluid shear stress, and microenvironmental oxygen content (Dejana et al., 2017). EC fate change programs (such as EndoMT) must overcome these signals to release cells from their EC commitment and redirect them toward other cell lineages. Thus, in the context of complete EndoMT, activation of the EndoMT program in ECs must generate mesenchymal fate cues with sufficient magnitude to outcompete endothelial identity signals and drive cells fully through the endothelial-to-mesenchymal identity spectrum to adopt a mesenchymal identity. By contrast, partial EndoMT occurs when the "push" and "pull" of endothelial and mesenchymal cues are momentarily balanced, thereby resulting in cells situated in an intermediate, uncommitted equilibrium state mid-way between endothelial and mesenchymal identities (**Figure 1**). Thus, we might imagine endothelial and mesenchymal identity signals functioning as two competing rheostats to establish target cell identity: fully "turning up" mesenchymal identity signals will successfully drive mesenchymal transition toward completion, especially if endothelial identity signals are simultaneously "turned down." However, if mesenchymal identity signaling are only weakly "turned up" – as would occur if regulatory mechanisms limit or antagonize activation of the EndoMT program – cells would only undergo partial EndoMT.

Several EndoMT signaling pathways likely regulate EndoMT progression by modulating the relative strength of endothelial vs. mesenchymal fate signals. Classic EndoMT activators that drive complete EndoMT to generate endothelial-derived fibroblasts (such as TGF-β, hypoxia, and inflammatory signals, etc.) likely do so by strongly inducing pro-mesenchymal cues that overpower endothelial commitment signals, perhaps through the initiation of positive feedback loops. Others, however, may only modestly activate mesenchymal transition, either alone or in combination with the maintenance of endothelial identity signals, to limit the EndoMT program and ensure it proceeds only partially. VEGF, for example, is a classic pro-angiogenic factor that may promote (controlled and healthy) vessel growth by activating the EndoMT program to induce sprouting angiogenesis, while simultaneously preserving endothelial identity cues to prevent excessive mesenchymal transition in resulting tip and stalk cells. Underscoring its role in promoting new vessel growth, we found that VEGF signaling blocking prevents overaggressive sprouting in the context of Slug overexpression (Hultgren et al., 2020) suggesting that VEGF synergizes with Slug in driving EndoMT. Furthermore, VEGF is strongly overexpressed in cancer, where it is linked to appearance of the disorganized, aggressive hypersprouting typical of the tumor vasculature. Yet, in support of a secondary role for VEGF in securing endothelial identity in angiogenesis, some studies have found VEGF to antagonize TGF-β signaling in EndoMT (Paruchuri et al., 2006). For example, fetal valve progenitors are bipotential cells that co-express endothelial and mesenchymal markers suggesting an intermediate EndoMT state; this plasticity is lost in adult cells (Paruchuri et al., 2006). Using these cells, Paruchuri et al. (2006) found that VEGF promotes (reversible) transition toward greater EC identity, in part by antagonizing TGF-β-induced mesenchymal transition. VEGF similarly limits TGF-β-mediated fibrosis in cardiac tissue (Illigens et al., 2017). Taken together, these data suggest that the distinction between controlled vs. uncontrolled angiogenesis is determined by the precise level of local VEGF signaling such that the EndoMT program is activated only partially, and in a limited and regulated way.

Another possible regulatory mechanism that might prevent complete EndoMT may involve the relative levels of master transcription factors, Slug and Snail. Slug and Snail negatively regulate one another's expression (Chen and Gridley, 2013a,b), and both participate in distinct (as well as shared) signaling circuits that govern partial and full EndoMT (Weinstein et al., 2020). Using an *in vitro* sprouting angiogenesis assay, we found that Slug upregulation precedes that of Snail by several days, suggesting that Slug activation is independent of Snail. Moreover, Slug dominates during the early proliferative phase of angiogenesis, whereas in later stages of angiogenesis, its expression decreases as Snail expression increases (Welch-Reardon et al., 2014). Consistent with this finding, Snail upregulation is also delayed following TGF-β activation of complete EndoMT in cultured ECs (Sobierajska et al., 2020). Thus, the dynamic balance of Slug vs. Snail levels appears to modulate the EndoMT response to dictate the extent of (partial vs. complete) mesenchymal transition. Whereas physiologic levels of Slug support early sprouting angiogenesis

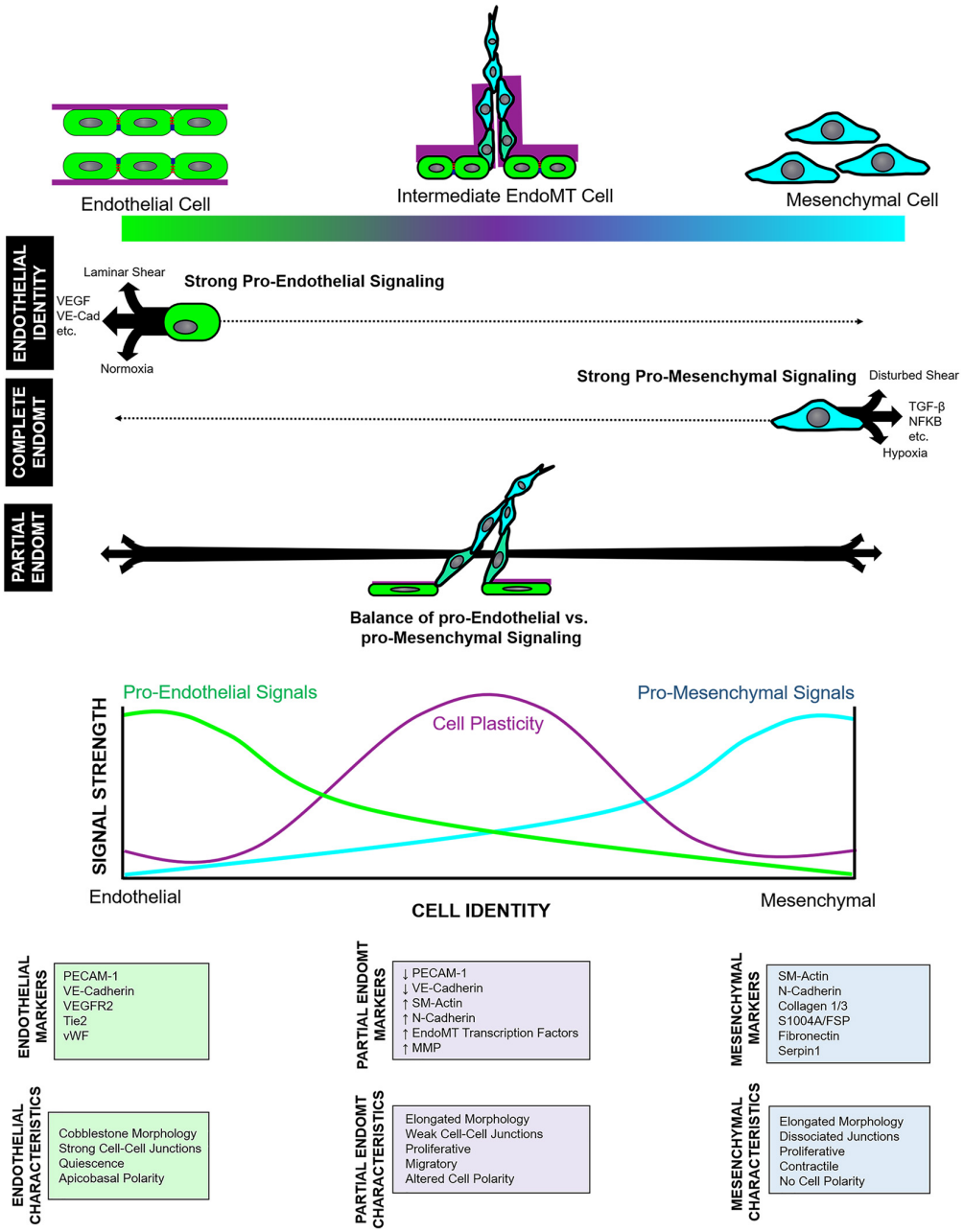

FIGURE 1 | Model of endothelial-to-mesenchymal transition (EndoMT) regulation. EndoMT describes fluid transition between endothelial and mesenchymal identities and involving a spectrum of intermediate states wherein cells acquire a mixture of endothelial and mesenchymal character and marker expression. Complete vs. partial EndoMT is established by both the relative level of pro-endothelial and pro-mesenchymal signals that "push" or "pull" cells toward either endpoint of the endothelial-mesenchymal spectrum, as well as by the extent of cell plasticity.

via induction of a partial EndoMT gene signature, high and prolonged overexpression of Slug – particularly in combination with Notch signaling inhibition – drives full dissociation of ECs from angiogenic sprouts, suggesting that Slug levels tightly regulate the extent of EC response to EndoMT signals (Hultgren et al., 2020). Meanwhile, delayed Snail upregulation during angiogenesis (Welch-Reardon et al., 2014) and in response to exogenous TGF-β-mediated EndoMT activation (Sobierajska et al., 2020) suggests that Snail functions later than Slug, perhaps to support a more robust EndoMT activation signal that pushes cells more aggressively down the EndoMT pathway. Consistent with this possibility, Snail has a higher affinity for target DNA binding sites than does Slug, suggesting that when expressed, Snail may exert a more potent effect to transactivate mesenchymal genes (Bolos et al., 2003).

Regulation of Cell Plasticity

The extent of EndoMT progression likely also depends upon cell plasticity, which acts as a permissive signal to determine the extent to which cells are sensitive to any sort of fate change signal (**Figure 1**). Although EC identity is mostly actively maintained, EC commitment is also controlled in progenitor cells by epigenetic modification to more stably alter accessibility of endothelial lineage genes (Ohtani et al., 2011). Highly committed EC may thus be relatively insensitive to cell identity transition cues. By contrast, cell plasticity signals that "loosen" cell commitment will enhance cell stemness, which may create a necessary window of opportunity that enables EndoMT signals to act upon the target cell. In support of this idea, transcriptomic analysis finds that cells in intermediate EMT states are more stem-like than cells on either end of the epithelial or mesenchymal identity spectrum (Jolly et al., 2014). In other words, cells in partial mesenchymal transition (whether by EMT or EndoMT) may be situated at a cell fate inflection point, wherein they are less committed and therefore especially responsive to external identity cues that might push them either fully toward distinct mesenchymal programs or reverse the transition back toward their original cell identity.

This model may further explain why ECs are heterogeneous in their response to EndoMT program activation, despite being exposed to the same EndoMT activation signal. For example, Xiao et al. (2015) found that TGF-β-induced EndoMT yields subpopulations of both SMA-expressing myofibroblasts as well as SMA-negative fibroblasts, suggesting that EndoMT intermediate states differ in their responsiveness to mesenchymal identity cues. Further, Pinto et al. (2018) recently reported that the extent of EndoMT induction via TGF-β/Snail overexpression differs according to the tissue-specific identity of cultured primary ECs. EC commitment may differ according to EC tissue origin, which may underlie their distinct responsiveness to EndoMT activation. In other words, while some ECs exposed to EndoMT cues may transition fully toward a mesenchymal fate, others in the same population may be more resistant to EndoMT activation and may transition only partially through the EndoMT program, pause in an intermediate EndoMT state, or even reverse course and return to an EC identity.

Although the signaling pathways that regulate cell plasticity in EndoMT remain unidentified, one possibility is that Notch signaling serves this function to prime, or permit, ECs to respond to EndoMT cues (and other cell fate signals) by creating a window of opportunity, as suggested above (Dejana et al., 2017). Notch is critically involved in a context- and tissue-dependent manner throughout embryonic development, including for its well-established role in maintaining stem and progenitor cell pluripotency to regulate the outcome of cell fate decisions (Koch et al., 2013). In ECs, Notch signaling is associated with acquisition and/or maintenance of arteriovenous (Fang et al., 2017; Fang and Hirschi, 2019), lymphatic (Murtomaki et al., 2014), and hemogenic (Gama-Norton et al., 2015; Gritz and Hirschi, 2016) identity, and is also required for EndoMT (Timmerman et al., 2004). The outcome of Notch signaling in ECs is also ligand-dependent: Dll4 and Jagged activation of Notch have opposing roles on angiogenesis, where Dll4-Notch signaling induces EC quiescence but Jagged-Notch signaling is both pro-angiogenic and pro-proliferative (Benedito et al., 2009). As mentioned, high levels of Dll4-Notch signaling by tip cells laterally inhibits adjacent stalk cells, preventing them from similarly adopting the mesenchymal-like tip cell phenotype. More recently, *in silico* modeling suggests that cancer cells undergoing EMT are associated with high Jagged-Notch signaling levels that establish a "window of stemness" wherein hybrid epithelial-mesenchymal cells transiently adopt a more stem-like state (Bocci et al., 2018). Thus, in the context of angiogenesis, Dll4-Notch may normally preserve EC identity, and suppression of this signal through direct repression of Dll4 by Slug (Hultgren et al., 2020) may loosen EC commitment to permit cells to respond to mesenchymal transition cues, thereby enabling EndoMT to (at least partially) proceed. Consistent with this possibility, *in silico* modeling finds that perturbations that downregulate Dll4 are associated with partial EndoMT in modeled ECs (Weinstein et al., 2020). Subsequent regulation of Notch activation levels (perhaps via Jagged) may then determine whether cells remain in an intermediate stage of EndoMT, reverse course back to a committed EC identity, or transition fully toward a mesenchymal state, either by exerting further effects on cell plasticity alone and/or through cross-talk with TGF-β, VEGF or other EndoMT regulatory pathways (Holderfield and Hughes, 2008). Further studies are necessary to test these possibilities.

DYSREGULATED EndoMT IN PATHOLOGICAL ANGIOGENESIS

Mature blood vessels are highly stable, and sprouting angiogenesis is a tightly regulated process that involves the temporary adoption by angiogenic ECs of pro-proliferative and migratory states (via stringent regulation of the EndoMT program). This enables the formation of new vessel sprouts, but also the return of EC to a quiescent and stable state (Schwartz et al., 2018). However, in hypervascular diseases such as diabetic retinopathy and cancer, ECs are persistently destabilized and developmental angiogenic pathways (including the EndoMT program) are reactivated in an aberrant and dysregulated fashion, leading to unrestrained and pathological growth of abnormal and disorganized blood vessels (Schwartz et al., 2018). This suggests that pathological and hyperaggressive angiogenesis may represent a loss of regulatory control over the EndoMT program. In cancer, for example, uncontrolled EndoMT may result in angiogenic ECs that acquire excessive mesenchymal character, leading to aggressive, uncontrolled, and disorganized sprouting to produce the highly aberrant and leaky vasculature characteristic of tumors.

Consistent with this hypothesis, we recently reported that beyond its developmental role in angiogenesis, Slug is critically required to support the pathological hypersprouting of blood vessels into tumor explants. In the absence of endothelial Slug expression, tumor angiogenesis was almost completely abolished (Hultgren et al., 2020) underscoring the importance of Slug-mediated partial EndoMT signaling to enable sprouting angiogenesis in cancer. Indeed, both our group and others

have found that individual EndoMT transcription factors may be largely dispensable during development, but still play a central and indispensable role in the context of pathological angiogenesis, suggesting that regulatory mechanisms that ordinarily compensate for their loss are no longer intact (Hultgren et al., 2020; Ma W. et al., 2020). For example key developmental genes often have multiple (shadow) promoters driven by different transcription factors. Epigenetic shut-down of one of these promoters may then render expression of the gene susceptible to loss of a previously redundant transcription factor. Thus, therapies designed to limit pathological angiogenesis in a variety of diseases may be more effective if they also target Slug, Snail, or other master EndoMT transcription factors or their downstream signaling pathways.

THERAPEUTIC POTENTIAL OF TARGETING EndoMT REGULATORY MECHANISMS FOR PATHOLOGICAL ANGIOGENESIS

Endothelial-to-mesenchymal transition is associated with several disease settings, including atherosclerosis, where activation of the EndoMT program drives robust EC transformation into EC-derived fibroblasts that are critical for plaque formation and progression (Souilhol et al., 2018). Studies of mouse atherosclerotic models have shown that EC in atheroprone regions are induced to express EndoMT transcription factors (Mahmoud et al., 2016, 2017) suggesting that EndoMT is a significant contributor to the fibroblast population in this setting. Consistent with this, Chen et al. (2012) found, somewhat surprisingly, that the TGF-β pathway is required for EC inflammation and atherosclerotic plaque development. Furthermore, they found that genetic knockout or silencing-RNA knockdown of this pathway reduced inflammation, and both prevented and rescued atherosclerotic plaque formation, making the EndoMT pathway, and specifically the TGF-β component, an attractive target for therapeutic treatment of this disease (Chen et al., 2012). Similarly, several drugs with anti-EndoMT properties are already approved for treatment of other diseases such as pulmonary fibrosis (Tsutsumi et al., 2019) and diabetes (Yao et al., 2018) and are further being considered as candidates for the treatment of cancer (Choi et al., 2020). Thus, anti-EndoMT approaches may also be effective in controlling pathological angiogenesis, including in cancer where angiogenic invasion into tumor masses drives further cancer growth and metastasis. However, since several clinically approved anti-EndoMT therapies are aimed at (and have been studied in the context of) preventing complete EndoMT – that is, the appearance of EC-derived fibroblasts to prevent fibrosis – it is unclear how effective existing treatment strategies will be in the context of pathological angiogenesis in which even a partial EndoMT program is sufficient to drive pathology. It is possible that additional, new strategies may be required to halt or reverse this process, potentially by acting early in the cascade of transcriptional events.

Existing anti-angiogenic approaches in cancer treatment have largely focused on inhibiting pro-angiogenic signals. When pathological angiogenesis is reconceptualized as a problem of dysregulated EndoMT – and not merely an issue of over-active pro-angiogenic (e.g., VEGF) signaling – it becomes clearer why anti-VEGF therapy [which has been a standard of care in cancer treatment for the last two decades (Welti et al., 2013)] largely fails to provide long-term control of tumor angiogenesis and cancer progression (Ferrara, 2010). Simply blocking VEGF signaling is not enough since the hypoxic and pro-inflammatory tumor microenvironment as well as the heightened mutation rate of cancer cells allows for rapid adaptation to anti-VEGF treatment through the activation of alternative pro-EndoMT "escape pathways" that rescue pathological angiogenesis in a VEGF-independent manner. Attempting to target and inhibit each pro-mesenchymal pathway individually would result in an inefficient game of "whack-a-mole."

Most pro-EndoMT pathways appear to converge at the level of the master EndoMT transcription factors. Indeed, as mentioned above, several EndoMT transcription factors are abnormally expressed in tumor-associated ECs where they drive abnormal tumor vessel formation. Therefore, therapies that target master EndoMT transcription factors are likely to be more effective than treatments that inhibit EndoMT program activators, particularly in the context of cancer, because of the following properties of these transcription factors: (1) they serve as a common signaling nexus for most upstream pro-EndoMT activators and could therefore alleviate the issue of "escape pathway" activation; (2) they are transcription factors that directly drive expression of suites of cell identity genes, thus ensuring broad effects on target cells; and (3) their abnormal activation is often specific to the tumor environment (Welch-Reardon et al., 2014) which suggests that healthy vessels would be relatively protected from off-target effects.

One concern in this approach might be the challenge of targeting intracellular proteins. However, recent developments in antibody-mimicry and antibody-fusion peptides, as well as advances in viral- and nanoparticle-based delivery methods, have shown great promise for cell-type specific delivery of antibodies that target intracellular antigens (Slastnikova et al., 2018) and should allow for drug delivery specifically to tumor blood vessels that express unique markers relative to healthy vasculature. Recent advances in delivery of RNA-based therapeutic molecules also offer new possibilities for acute, temporary, and efficient knockdown of intracellular protein expression (Nature Medicine, 2019; Dammes and Peer, 2020). This latter approach may be especially feasible when targeting transcription factors like Slug, which have a short half-life and are only transiently expressed. Nonetheless, approaches that target Slug, Snail, Zeb1, Zeb2, and Twist1 – individually or collectively – to limit pathological angiogenesis must consider the likely complex (and still largely unclear) interrelationship between these transcription factors during angiogenesis. More work is therefore needed to better elucidate the cross-talk between master EndoMT transcription factors to enable more precise control of their function as an emerging therapeutic strategy.

Another possible avenue for therapeutic intervention in the EndoMT program may involve targeting regulatory mechanisms that govern EC plasticity. Therapies that selectively promote EC commitment and limit sensitivity to local pro-EndoMT signals may prevent overaggressive and pathological angiogenesis in the tumor mass, particularly when applied in combination with other chemotherapeutic or anti-angiogenic treatments. Such an approach might be used to either normalize tumor vessels, or to block tumor angiogenesis altogether. If, as we propose, Dll4-Notch signaling promotes EC commitment to limit (partial or complete) EndoMT, therapies that activate Notch signaling specifically in tumor vasculature may help suppress pathological angiogenesis. Yet, application of Notch inhibitors have produced mixed outcomes on tumor blood vessels (Bridges et al., 2011) likely due to the fact that Notch's effect on cell plasticity appears to be both ligand- and context-dependent (Benedito et al., 2009). Currently available small molecule Notch inhibitors are overly broad in their suppression of all Notch activation. Blocking antibodies to the Dll4 or Jagged1 Notch ligand are more suitable for specific Notch signaling inhibition, although outcomes have thus far been surprising. Dll4 blockade, for example, promotes excessive tumor vessel growth consistent with a role for Dll4-Notch signaling in promoting EC commitment. However, vessels that result from Dll4-Notch inhibition are excessively disorganized and poorly perfused, which (somewhat unexpectedly) reduces tumor size (Bridges et al., 2011). Thus, further studies are needed to determine precisely what kind of Notch inhibition might be most effective to limit pathological angiogenesis in tumors; or, alternatively, whether targeting other pathways that regulate EC plasticity might be more suitable. Finally, to reiterate our earlier discussion on Notch signaling, activation or inhibition of Notch must always be considered in the context of what other signaling pathways may be active in the local environment that Notch signaling is now permitting or blocking.

DISCUSSION

Complete EndoMT serves as a critical source of endothelial-derived mesenchymal cells during organogenesis and is a significant contributor to fibrosis in disease. It is also increasingly clear that partial EndoMT also plays an essential function during angiogenesis (and likely other processes), and that dysregulation of the EndoMT program may contribute to abnormal and pathological blood vessel growth. Specifically, we propose that tight regulation of a core EndoMT program dictates the extent of mesenchymal transition in a context-appropriate manner by manipulating the strength of identity and transition cues, as well as the extent of target cell plasticity, and that loss of this control contributes to blood vessel disorganization in diseases such as cancer.

However, several questions remain outstanding: What are the contexts aside from angiogenesis under which partial EndoMT occurs? What specific regulatory mechanisms determine the extent of EndoMT progression, and how are they dynamically regulated during angiogenesis to maintain partial endothelial identity during sprouting? What are the regulatory mechanisms that govern cell plasticity during EndoMT, and how do they modulate progression of the EndoMT program? How stable and discrete are intermediate stages of partial EndoMT and, in addition to mesenchymal transition signals, are these cells sensitive to other cell lineage signals? Why do EndoMT transcription factors appear to be more essential in pathological angiogenesis compared to during development, and what aspects of the tumor microenvironment and other disease states lead to dysregulation of EndoMT regulatory mechanisms? And finally, how can EndoMT be targeted therapeutically in these diseases? An improved understanding of EndoMT, and specifically the regulatory mechanisms that dictate complete vs. partial mesenchymal transition in a context-dependent manner, warrant further study and are likely to reveal important insights into these and other crucial questions.

AUTHOR CONTRIBUTIONS

JF and NH wrote the manuscript. CH provided edits and additional scientific insights. All authors contributed to the article and approved the submitted version.

FUNDING

This work was supported by US National Institutes of Health (RO1HL60067, to CH). JF was supported by the Department of Defense (W81XWH2110108). NH was supported by an American Heart Association Predoctoral Fellowship (16PRE27530026), a Ruth L. Kirschstein National Research Service Award Individual Predoctoral Fellowship from the US National Institutes of Health (F31HL131381), and the ARCS Foundation. CH also receives support from the Chao Family Comprehensive Cancer Center (CFCCC) through an NCI Center Grant (P30A062203).

ACKNOWLEDGMENTS

The authors would like to acknowledge members of the Hughes lab for scientific discussions.

REFERENCES

Aban, C. E., Lombardi, A., Neiman, G., Biani, M. C., La Greca, A., Waisman, A., et al. (2021). Downregulation of E-cadherin in pluripotent stem cells triggers partial EMT. *Sci. Rep.* 11:2048.

Abhinand, C. S., Raju, R., Soumya, S. J., Arya, P. S., and Sudhakaran, P. R. (2016). VEGF-A/VEGFR2 signaling network in endothelial cells relevant to angiogenesis. *J. Cell Commun. Signal.* 10, 347–354. doi: 10.1007/s12079-016-0352-8

Aird, W. C. (2012). Endothelial cell heterogeneity. *Cold Spring Harb. Perspect. Med.* 2:a006429.

Aisagbonhi, O., Rai, M., Ryzhov, S., Atria, N., Feoktistov, I., and Hatzopoulos, A. K. (2011). Experimental myocardial infarction triggers canonical Wnt signaling, and endothelial-to-mesenchymal

transition. *Dis. Model Mech.* 4, 469–483. doi: 10.1242/dmm.006510

Andueza, A., Kumar, S., Kim, J., Kang, D. W., Mumme, H. L., Perez, J. I., et al. (2020). Endothelial Reprogramming by Disturbed Flow Revealed by Single-Cell RNA, and Chromatin Accessibility Study. *Cell Rep.* 33:108491. doi: 10.1016/j.celrep.2020.108491

Arciniegas, E., Sutton, A. B., Allen, T. D., and Schor, A. M. (1992). Transforming growth factor beta 1 promotes the differentiation of endothelial cells into smooth muscle-like cells in vitro. *J. Cell Sci.* 103, 521–529. doi: 10.1242/jcs.103.2.521

Baylin, S. B., and Jones, P. A. (2016). Epigenetic Determinants of Cancer. *Cold Spring Harb. Perspect. Biol.* 8:a019505. doi: 10.1101/cshperspect.a019505

Benedito, R., Roca, C., Sorensen, I., Adams, S., Gossler, A., Fruttiger, M., et al. (2009). The notch ligands Dll4, and Jagged1 have opposing effects on angiogenesis. *Cell* 137, 1124–1135. doi: 10.1016/j.cell.2009.03.025

Bentley, K., Franco, C. A., Philippides, A., Blanco, R., Dierkes, M., Gebala, V., et al. (2014). The role of differential VE-cadherin dynamics in cell rearrangement during angiogenesis. *Nat. Cell Biol.* 16, 309–321. doi: 10.1038/ncb2926

Blanco, R., and Gerhardt, H. (2013). VEGF, and Notch in tip, and stalk cell selection. *Cold Spring Harb. Perspect. Med.* 3, a006569. doi: 10.1101/cshperspect.a006569

Bocci, F., Jolly, M. K., George, J. T., Levine, H., and Onuchic, J. N. (2018). A mechanism-based computational model to capture the interconnections among epithelial-mesenchymal transition, cancer stem cells, and Notch-Jagged signaling. *Oncotarget* 9, 29906–29920. doi: 10.18632/oncotarget.25692

Bolos, V., Peinado, H., Perez-Moreno, M. A., Fraga, M. F., Esteller, M., and Cano, A. (2003). The transcription factor Slug represses E-cadherin expression, and induces epithelial to mesenchymal transitions: a comparison with Snail, and E47 repressors. *J. Cell Sci.* 116, 499–511. doi: 10.1242/jcs.00224

Bridges, E., Oon, C. E., and Harris, A. (2011). Notch regulation of tumor angiogenesis. *Future Oncol.* 7, 569–588. doi: 10.2217/fon.11.20

Burk, U., Schubert, J., Wellner, U., Schmalhofer, O., Vincan, E., Spaderna, S., et al. (2008). A reciprocal repression between ZEB1, and members of the miR-200 family promotes EMT, and invasion in cancer cells. *EMBO Rep.* 9, 582–589. doi: 10.1038/embor.2008.74

Carver, E. A., Jiang, R., Lan, Y., Oram, K. F., and Gridley, T. (2001). The mouse snail gene encodes a key regulator of the epithelial-mesenchymal transition. *Mol. Cell Biol.* 21, 8184–8188. doi: 10.1128/mcb.21.23.8184-8188.2001

Chang, A. C., Fu, Y., Garside, V. C., Niessen, K., Chang, L., Fuller, M., et al. (2011). Notch initiates the endothelial-to-mesenchymal transition in the atrioventricular canal through autocrine activation of soluble guanylyl cyclase. *Dev. Cell* 21, 288–300. doi: 10.1016/j.devcel.2011.06.022

Chen, D. D., Cheng, J. T., Chandoo, A., Sun, X. W., Zhang, L., Lu, M. D., et al. (2019). microRNA-33a prevents epithelial-mesenchymal transition, invasion, and metastasis of gastric cancer cells through the Snail/Slug pathway. *Am. J. Physiol. Gastrointest. Liver Physiol.* 317, G147–G160.

Chen, P. Y., Qin, L., Barnes, C., Charisse, K., Yi, T., Zhang, X., et al. (2012). FGF regulates TGF-beta signaling, and endothelial-to-mesenchymal transition via control of let-7 miRNA expression. *Cell Rep.* 2, 1684–1696. doi: 10.1016/j.celrep.2012.10.021

Chen, P. Y., Qin, L., Li, G., Wang, Z., Dahlman, J. E., Malagon-Lopez, J., et al. (2019). Endothelial TGF-beta signalling drives vascular inflammation, and atherosclerosis. *Nat. Metab.* 1, 912–926.

Chen, Q., Zhang, H., Liu, Y., Adams, S., Eilken, H., Stehling, M., et al. (2016). Endothelial cells are progenitors of cardiac pericytes, and vascular smooth muscle cells. *Nat. Commun.* 7:12422.

Chen, X., Cai, J., Zhou, X., Chen, L., Gong, Y., Gao, Z., et al. (2015). Protective Effect of Spironolactone on Endothelial-to-Mesenchymal Transition in HUVECs via Notch Pathway. *Cell Physiol. Biochem.* 36, 191–200. doi: 10.1159/000374063

Chen, Y., Banda, M., Speyer, C. L., Smith, J. S., Rabson, A. B., and Gorski, D. H. (2010). Regulation of the expression, and activity of the antiangiogenic homeobox gene GAX/MEOX2 by ZEB2, and microRNA-221. *Mol. Cell Biol.* 30, 3902–3913. doi: 10.1128/mcb.01237-09

Chen, Y., and Gridley, T. (2013a). Compensatory regulation of the Snai1, and Snai2 genes during chondrogenesis. *J. Bone Miner. Res.* 28, 1412–1421. doi: 10.1002/jbmr.1871

Chen, Y., and Gridley, T. (2013b). The SNAI1, and SNAI2 proteins occupy their own, and each other's promoter during chondrogenesis. *Biochem. Biophys. Res. Commun.* 435, 356–360. doi: 10.1016/j.bbrc.2013.04.086

Cho, J. G., Lee, A., Chang, W., Lee, M. S., and Kim, J. (2018). Endothelial to mesenchymal transition represents a key link in the interaction between inflammation, and endothelial dysfunction. *Front. Immunol.* 9:294. doi: 10.3389/fimmu.2018.00294

Choi, K. J., Nam, J. K., Kim, J. H., Choi, S. H., and Lee, Y. J. (2020). Endothelial-to-mesenchymal transition in anticancer therapy, and normal tissue damage. *Exp. Mol. Med.* 52, 781–792. doi: 10.1038/s12276-020-0439-4

Choi, S. H., Kim, A. R., Nam, J. K., Kim, J. M., Kim, J. Y., Seo, H. R., et al. (2018). Tumour-vasculature development via endothelial-to-mesenchymal transition after radiotherapy controls CD44v6(+) cancer cell, and macrophage polarization. *Nat. Commun.* 9:5108.

Correia, A. C., Moonen, J. R., Brinker, M. G., and Krenning, G. (2016). FGF2 inhibits endothelial-mesenchymal transition through microRNA-20a-mediated repression of canonical TGF-beta signaling. *J. Cell Sci.* 129, 569–579.

Dammes, N., and Peer, D. (2020). Paving the road for RNA therapeutics. *Trends Pharmacol. Sci.* 41, 755–775. doi: 10.1016/j.tips.2020.08.004

Dejana, E., Hirschi, K. K., and Simons, M. (2017). The molecular basis of endothelial cell plasticity. *Nat. Commun.* 8:14361.

del Toro, R., Prahst, C., Mathivet, T., Siegfried, G., Kaminker, J. S., Larrivee, B., et al. (2010). Identification, and functional analysis of endothelial tip cell-enriched genes. *Blood* 116, 4025–4033. doi: 10.1182/blood-2010-02-270819

Dutta, S., Dietrich, J. E., Westerfield, M., and Varga, Z. M. (2008). Notch signaling regulates endocrine cell specification in the zebrafish anterior pituitary. *Dev. Biol.* 319, 248–257. doi: 10.1016/j.ydbio.2008.04.019

Fang, J. S., and Hirschi, K. K. (2019). Molecular regulation of arteriovenous endothelial cell specification. *F1000Res* 8, F1000 FacultyRev-1208.

Fang, J. S., Coon, B. G., Gillis, N., Chen, Z., Qiu, J., Chittenden, T. W., et al. (2017). Shear-induced Notch-Cx37-p27 axis arrests endothelial cell cycle to enable arterial specification. *Nat. Commun.* 8:2149.

Ferrara, N. (2010). Pathways mediating VEGF-independent tumor angiogenesis. *Cytokine Growth Factor Rev.* 21, 21–26. doi: 10.1016/j.cytogfr.2009.11.003

Ferrari, G., Cook, B. D., Terushkin, V., Pintucci, G., and Mignatti, P. (2009). Transforming growth factor-beta 1 (TGF-beta1) induces angiogenesis through vascular endothelial growth factor (VEGF)-mediated apoptosis. *J. Cell Physiol.* 219, 449–458. doi: 10.1002/jcp.21706

Ferrari, G., Pintucci, G., Seghezzi, G., Hyman, K., Galloway, A. C., and Mignatti, P. (2006). VEGF, a prosurvival factor, acts in concert with TGF-beta1 to induce endothelial cell apoptosis. *Proc. Natl. Acad. Sci. U S A.* 103, 17260–17265. doi: 10.1073/pnas.0605556103

Fu, R., Li, Y., Jiang, N., Ren, B. X., Zang, C. Z., Liu, L. J., et al. (2020). Inactivation of endothelial ZEB1 impedes tumor progression, and sensitizes tumors to conventional therapies. *J. Clin Invest.* 130, 1252–1270. doi: 10.1172/jci131507

Fu, Y., Chang, A., Chang, L., Niessen, K., Eapen, S., Setiadi, A., et al. (2009). Differential regulation of transforming growth factor beta signaling pathways by notch in human endothelial cells. *J. Biol. Chem.* 284, 19452–19462. doi: 10.1074/jbc.m109.011833

Gama-Norton, L., Ferrando, E., Ruiz-Herguido, C., Liu, Z., Guiu, J., Islam, A. B., et al. (2015). Notch signal strength controls cell fate in the haemogenic endothelium. *Nat. Commun.* 6:8510.

Gerhardt, H., Golding, M., Fruttiger, M., Ruhrberg, C., Lundkvist, A., Abramsson, A., et al. (2003). VEGF guides angiogenic sprouting utilizing endothelial tip cell filopodia. *J. Cell Biol.* 161, 1163–1177. doi: 10.1083/jcb.200302047

Gill, J. G., Langer, E. M., Lindsley, R. C., Cai, M., Murphy, T. L., Kyba, M., et al. (2011). Snail, and the microRNA-200 family act in opposition to regulate epithelial-to-mesenchymal transition, and germ layer fate restriction in differentiating ESCs. *Stem Cells.* 29, 764–776. doi: 10.1002/stem.628

Glover, E. K., Jordan, N., Sheerin, N. S., and Ali, S. (2019). Regulation of endothelial-to-mesenchymal transition by MicroRNAs in chronic allograft dysfunction. *Transplantation* 103, e64–e73.

Gritz, E., and Hirschi, K. K. (2016). Specification, and function of hemogenic endothelium during embryogenesis. *Cell Mol. Life Sci.* 73, 1547–1567. doi: 10.1007/s00018-016-2134-0

Hashimoto, N., Phan, S. H., Imaizumi, K., Matsuo, M., Nakashima, H., Kawabe, T., et al. (2010). Endothelial-mesenchymal transition in bleomycin-induced pulmonary fibrosis. *Am. J. Respir. Cell Mol. Biol.* 43, 161–172.

Hellstrom, M., Phng, L. K., Hofmann, J. J., Wallgard, E., Coultas, L., Lindblom, P., et al. (2007). Dll4 signalling through Notch1 regulates formation of tip cells during angiogenesis. *Nature* 445, 776–780. doi: 10.1038/nature05571

Holderfield, M. T., and Hughes, C. C. (2008). Crosstalk between vascular endothelial growth factor, notch, and transforming growth factor-beta in vascular morphogenesis. *Circ. Res.* 102, 637–652. doi: 10.1161/circresaha.107.167171

Hopper, R. K., Moonen, J. R., Diebold, I., Cao, A., Rhodes, C. J., Tojais, N. F., et al. (2016). In pulmonary arterial hypertension, reduced BMPR2 promotes endothelial-to-mesenchymal transition via HMGA1, and its target slug. *Circulation* 133, 1783–1794. doi: 10.1161/circulationaha.115.020617

Huang, M., Liu, T., Ma, P., Mitteer, R. A. Jr., Zhang, Z., Kim, H. J., et al. (2016). c-Met-mediated endothelial plasticity drives aberrant vascularization, and chemoresistance in glioblastoma. *J. Clin. Invest.* 126, 1801–1814. doi: 10.1172/jci84876

Hultgren, N. W., Fang, J. S., Ziegler, M. E., Ramirez, R. N., Phan, D. T. T., Hatch, M. M. S., et al. (2020). Slug regulates the Dll4-Notch-VEGFR2 axis to control endothelial cell activation, and angiogenesis. *Nat. Commun.* 11:5400.

Illigens, B. M., Casar Berazaluce, A., Poutias, D., Gasser, R., Del Nido, P. J., and Friehs, I. (2017). Vascular endothelial growth factor prevents endothelial-to-mesenchymal transition in hypertrophy. *Ann. Thorac. Surg.* 104, 932–939. doi: 10.1016/j.athoracsur.2017.01.112

Jakobsson, L., Franco, C. A., Bentley, K., Collins, R. T., Ponsioen, B., Aspalter, I. M., et al. (2010). Endothelial cells dynamically compete for the tip cell position during angiogenic sprouting. *Nat. Cell Biol.* 12, 943–953. doi: 10.1038/ncb2103

Jolly, M. K., Huang, B., Lu, M., Mani, S. A., Levine, H., and Ben-Jacob, E. (2014). Towards elucidating the connection between epithelial-mesenchymal transitions, and stemness. *J. R. Soc. Interface* 11, 20140962. doi: 10.1098/rsif.2014.0962

Kalucka, J., de Rooij, L., Goveia, J., Rohlenova, K., Dumas, S. J., Meta, E., et al. (2020). Single-Cell transcriptome atlas of murine endothelial cells. *Cell* 180, 764–779.e20.

Kasper, D. M., Hintzen, J., Wu, Y., Ghersi, J. J., Mandl, H. K., Salinas, K. E., et al. (2020). The N-glycome regulates the endothelial-to-hematopoietic transition. *Science* 370, 1186–1191. doi: 10.1126/science.aaz2121

Kenswil, K. J. G., Pisterzi, P., Sánchez-Duffhues, G., van Dijk, C., Lolli, A., Knuth, C., et al. (2021). Endothelium-derived stromal cells contribute to hematopoietic bone marrow niche formation. *Cell Stem Cell* 28, 653–670.e11.

Kim, J. (2018). MicroRNAs as critical regulators of the endothelial to mesenchymal transition in vascular biology. *BMB Rep.* 51, 65–72. doi: 10.5483/bmbrep.2018.51.2.011

Koch, U., Lehal, R., and Radtke, F. (2013). Stem cells living with a notch. *Development* 140, 689–704. doi: 10.1242/dev.080614

Kokudo, T., Suzuki, Y., Yoshimatsu, Y., Yamazaki, T., Watabe, T., and Miyazono, K. (2008). Snail is required for TGFbeta-induced endothelial-mesenchymal transition of embryonic stem cell-derived endothelial cells. *J. Cell Sci.* 121, 3317–3324. doi: 10.1242/jcs.028282

Lamouille, S., Xu, J., and Derynck, R. (2014). Molecular mechanisms of epithelial-mesenchymal transition. *Nat. Rev. Mol. Cell Biol.* 15, 178–196.

Lee, B., Villarreal-Ponce, A., Fallahi, M., Ovadia, J., Sun, P., Yu, Q. C., et al. (2014). Transcriptional mechanisms link epithelial plasticity to adhesion, and differentiation of epidermal progenitor cells. *Dev. Cell* 29, 47–58. doi: 10.1016/j.devcel.2014.03.005

Lee, J. G., Jung, E., and Heur, M. (2018). Fibroblast growth factor 2 induces proliferation, and fibrosis via SNAI1-mediated activation of CDK2, and ZEB1 in corneal endothelium. *J. Biol. Chem.* 293, 3758–3769.

Lee, J. Y., and Kong, G. (2016). Roles, and epigenetic regulation of epithelial-mesenchymal transition, and its transcription factors in cancer initiation, and progression. *Cell Mol. Life Sci.* 73, 4643–4660. doi: 10.1007/s00018-016-2313-z

Lewandowski, S. L., Janardhan, H. P., and Trivedi, C. M. (2015). Histone deacetylase 3 Coordinates deacetylase-independent epigenetic silencing of transforming growth Factor-beta1 (TGF-beta1) to orchestrate second heart field development. *J. Biol. Chem.* 290, 27067–27089. doi: 10.1074/jbc.m115.684753

Li, J., Qu, X., and Bertram, J. F. (2009). Endothelial-myofibroblast transition contributes to the early development of diabetic renal interstitial fibrosis in streptozotocin-induced diabetic mice. *Am. J. Pathol.* 175, 1380–1388. doi: 10.2353/ajpath.2009.090096

Li, Z., Solomonidis, E. G., Meloni, M., Taylor, R. S., Duffin, R., Dobie, R., et al. (2019). Single-cell transcriptome analyses reveal novel targets modulating cardiac neovascularization by resident endothelial cells following myocardial infarction. *Eur. Heart J.* 40, 2507–2520. doi: 10.1093/eurheartj/ehz305

Li, Z. D., Bork, J. P., Krueger, B., Patsenker, E., Schulze-Krebs, A., Hahn, E. G., et al. (2005). VEGF induces proliferation, migration, and TGF-beta1 expression in mouse glomerular endothelial cells via mitogen-activated protein kinase, and phosphatidylinositol 3-kinase. *Biochem. Biophys. Res. Commun.* 334, 1049–1060. doi: 10.1016/j.bbrc.2005.07.005

Liebner, S., Cattelino, A., Gallini, R., Rudini, N., Iurlaro, M., Piccolo, S., et al. (2004). Beta-catenin is required for endothelial-mesenchymal transformation during heart cushion development in the mouse. *J. Cell Biol.* 166, 359–367. doi: 10.1083/jcb.200403050

Liu, J., Dong, F., Jeong, J., Masuda, T., and Lobe, C. G. (2014). Constitutively active Notch1 signaling promotes endothelialmesenchymal transition in a conditional transgenic mouse model. *Int. J. Mol. Med.* 34, 669–676. doi: 10.3892/ijmm.2014.1818

Liu, T., Ma, W., Xu, H., Huang, M., Zhang, D., He, Z., et al. (2018). PDGF-mediated mesenchymal transformation renders endothelial resistance to anti-VEGF treatment in glioblastoma. *Nat. Commun.* 9:3439.

Lomeli, H., Starling, C., and Gridley, T. (2009). Epiblast-specific Snai1 deletion results in embryonic lethality due to multiple vascular defects. *BMC Res Notes* 2:22. doi: 10.1186/1756-0500-2-22

Lu, C., Bonome, T., Li, Y., Kamat, A. A., Han, L. Y., Schmandt, R., et al. (2007). Gene alterations identified by expression profiling in tumor-associated endothelial cells from invasive ovarian carcinoma. *Cancer Res.* 67, 1757–1768. doi: 10.1158/0008-5472.can-06-3700

Ma, J., Sanchez-Duffhues, G., Goumans, M. J., and Ten Dijke, P. (2020). TGF-beta-Induced endothelial to mesenchymal transition in disease, and tissue engineering. *Front. Cell Dev. Biol.* 8:260. doi: 10.3389/fcell.2020.00260

Ma, W., Wang, Y., Zhang, R., Yang, F., Zhang, D., Huang, M., et al. (2020). Targeting PAK4 to reprogram the vascular microenvironment, and improve CAR-T immunotherapy for glioblastoma. *Nat. Cancer* 2, 83–97. doi: 10.1038/s43018-020-00147-8

Mahler, G. J., Farrar, E. J., and Butcher, J. T. (2013). Inflammatory cytokines promote mesenchymal transformation in embryonic, and adult valve endothelial cells. *Arterioscler Thromb. Vasc. Biol.* 33, 121–130. doi: 10.1161/atvbaha.112.300504

Mahmoud, M. M., Kim, H. R., Xing, R., Hsiao, S., Mammoto, A., Chen, J., et al. (2016). TWIST1 integrates endothelial responses to flow in vascular dysfunction, and atherosclerosis. *Circ. Res.* 119, 450–462. doi: 10.1161/circresaha.116.308870

Mahmoud, M. M., Serbanovic-Canic, J., Feng, S., Souilhol, C., Xing, R., Hsiao, S., et al. (2017). Shear stress induces endothelial-to-mesenchymal transition via the transcription factor Snail. *Sci. Rep.* 7:3375.

Maleszewska, M., Gjaltema, R. A., Krenning, G., and Harmsen, M. C. (2015). Enhancer of zeste homolog-2 (EZH2) methyltransferase regulates transgelin/smooth muscle-22alpha expression in endothelial cells in response to interleukin-1beta, and transforming growth factor-beta2. *Cell Signal.* 27, 1589–1596. doi: 10.1016/j.cellsig.2015.04.008

Mammoto, A., Hendee, K., Muyleart, M., and Mammoto, T. (2020). Endothelial Twist1-PDGFB signaling mediates hypoxia-induced proliferation, and migration of alphaSMA-positive cells. *Sci. Rep.* 10:7563.

Mammoto, T., Muyleart, M., Konduri, G. G., and Mammoto, A. (2018). Twist1 in Hypoxia-induced pulmonary hypertension through transforming growth factor-beta-smad signaling. *Am. J. Respir. Cell Mol. Biol.* 58, 194–207. doi: 10.1165/rcmb.2016-0323oc

Manavski, Y., Lucas, T., Glaser, S. F., Dorsheimer, L., Gunther, S., Braun, T., et al. (2018). Clonal expansion of endothelial cells contributes to ischemia-induced neovascularization. *Circ. Res.* 122, 670–677. doi: 10.1161/circresaha.117.312310

Mandriota, S. J., Menoud, P. A., and Pepper, M. S. (1996). Transforming growth factor beta 1 down-regulates vascular endothelial growth factor receptor 2/flk-1 expression in vascular endothelial cells. *J. Biol. Chem.* 271, 11500–11505. doi: 10.1074/jbc.271.19.11500

Manetti, M., Romano, E., Rosa, I., Guiducci, S., Bellando-Randone, S., De Paulis, A., et al. (2017). Endothelial-to-mesenchymal transition contributes to

endothelial dysfunction, and dermal fibrosis in systemic sclerosis. *Ann. Rheum. Dis.* 76, 924–934. doi: 10.1136/annrheumdis-2016-210229

Medici, D., Potenta, S., and Kalluri, R. (2011). Transforming growth factor-beta2 promotes Snail-mediated endothelial-mesenchymal transition through convergence of Smad-dependent, and Smad-independent signalling. *Biochem. J.* 437, 515–520. doi: 10.1042/bj20101500

Mendoza, F. A., Piera-Velazquez, S., Farber, J. L., Feghali-Bostwick, C., and Jimenez, S. A. (2016). Endothelial cells expressing endothelial, and mesenchymal cell gene products in lung tissue from patients with systemic sclerosis-associated interstitial lung disease. *Arthritis Rheumatol.* 68, 210–217. doi: 10.1002/art.39421

Moore-Morris, T., Guimaraes-Camboa, N., Banerjee, I., Zambon, A. C., Kisseleva, T., Velayoudon, A., et al. (2014). Resident fibroblast lineages mediate pressure overload-induced cardiac fibrosis. *J. Clin. Invest.* 124, 2921–2934. doi: 10.1172/jci74783

Murtomaki, A., Uh, M. K., Kitajewski, C., Zhao, J., Nagasaki, T., Shawber, C. J., et al. (2014). Notch signaling functions in lymphatic valve formation. *Development* 141, 2446–2451. doi: 10.1242/dev.101188

Natoli, G. (2009). Control of NF-kappaB-dependent transcriptional responses by chromatin organization. *Cold Spring Harb. Perspect. Biol.* 1:a000224. doi: 10.1101/cshperspect.a000224

Natoli, G., Ghisletti, S., and Barozzi, I. (2011). The genomic landscapes of inflammation. *Genes Dev.* 25, 101–106. doi: 10.1101/gad.2018811

Nature Medicine (2019). Delivering the promise of RNA therapeutics. *Nat. Med.* 25:1321. doi: 10.1038/s41591-019-0580-6

Nicoloso, M. S., Spizzo, R., Shimizu, M., Rossi, S., and Calin, G. A. (2009). MicroRNAs–the micro steering wheel of tumour metastases. *Nat. Rev. Cancer* 9, 293–302. doi: 10.1038/nrc2619

Niessen, K., Fu, Y., Chang, L., Hoodless, P. A., McFadden, D., and Karsan, A. (2008). Slug is a direct Notch target required for initiation of cardiac cushion cellularization. *J. Cell Biol.* 182, 315–325. doi: 10.1083/jcb.200710067

Noseda, M., McLean, G., Niessen, K., Chang, L., Pollet, I., Montpetit, R., et al. (2004). Notch activation results in phenotypic, and functional changes consistent with endothelial-to-mesenchymal transformation. *Circ. Res.* 94, 910–917. doi: 10.1161/01.res.0000124300.76171.c9

Ohtani, K., Vlachojannis, G. J., Koyanagi, M., Boeckel, J. N., Urbich, C., Farcas, R., et al. (2011). Epigenetic regulation of endothelial lineage committed genes in pro-angiogenic hematopoietic, and endothelial progenitor cells. *Circ. Res.* 109, 1219–1229. doi: 10.1161/circresaha.111.247304

Okayama, K., Azuma, J., Dosaka, N., Iekushi, K., Sanada, F., Kusunoki, H., et al. (2012). Hepatocyte growth factor reduces cardiac fibrosis by inhibiting endothelial-mesenchymal transition. *Hypertension* 59, 958–965.

Paik, D. T., Tian, L., Williams, I. M., Rhee, S., Zhang, H., Liu, C., et al. (2020). Single-Cell RNA sequencing unveils unique transcriptomic signatures of organ-specific endothelial cells. *Circulation* 142, 1848–1862. doi: 10.1161/circulationaha.119.041433

Pardali, E., Sanchez-Duffhues, G., Gomez-Puerto, M. C., and Ten Dijke, P. (2017). TGF-beta-Induced endothelial-mesenchymal transition in fibrotic diseases. *Int. J. Mol. Sci.* 18:2157. doi: 10.3390/ijms18102157

Parker, B. W., Argani, P., Cook, B. P., Liangfeng, H., Chartrand, S. D., Zhang, M., et al. (2004). Alterations in vascular gene expression in invasive breast carcinoma. *Cancer Res.* 64, 7857–7866. doi: 10.1158/0008-5472.can-04-1976

Paruchuri, S., Yang, J. H., Aikawa, E., Melero-Martin, J. M., Khan, Z. A., Loukogeorgakis, S., et al. (2006). Human pulmonary valve progenitor cells exhibit endothelial/mesenchymal plasticity in response to vascular endothelial growth factor-A, and transforming growth factor-beta2. *Circ. Res.* 99, 861–869. doi: 10.1161/01.res.0000245188.41002.2c

Peinado, H., Olmeda, D., and Cano, A. (2007). Snail, Zeb, and bHLH factors in tumour progression: an alliance against the epithelial phenotype? *Nat. Rev. Cancer* 7, 415–428. doi: 10.1038/nrc2131

Piera-Velazquez, S., and Jimenez, S. A. (2019). Endothelial to mesenchymal transition: role in physiology, and in the pathogenesis of human diseases. *Physiol. Rev.* 99, 1281–1324. doi: 10.1152/physrev.00021.2018

Pinto, M. T., Ferreira Melo, F. U., Malta, T. M., Rodrigues, E. S., Plaça, J. R., Silva, W. A. Jr., et al. (2018). Endothelial cells from different anatomical origin have distinct responses during SNAIL/TGF-β2-mediated endothelial-mesenchymal transition. *Am. J. Transl. Res.* 10, 4065–4081.

Potenta, S., Zeisberg, E., and Kalluri, R. (2008). The role of endothelial-to-mesenchymal transition in cancer progression. *Br. J. Cancer* 99, 1375–1379. doi: 10.1038/sj.bjc.6604662

Qiu, J., and Hirschi, K. K. (2019). Endothelial cell development, and its application to regenerative medicine. *Circ. Res.* 125, 489–501. doi: 10.1161/circresaha.119.311405

Sainson, R. C., Johnston, D. A., Chu, H. C., Holderfield, M. T., Nakatsu, M. N., Crampton, S. P., et al. (2008). TNF primes endothelial cells for angiogenic sprouting by inducing a tip cell phenotype. *Blood* 111, 4997–5007. doi: 10.1182/blood-2007-08-108597

Sanchez-Elsner, T., Botella, L. M., Velasco, B., Corbi, A., Attisano, L., and Bernabeu, C. (2001). Synergistic cooperation between hypoxia, and transforming growth factor-beta pathways on human vascular endothelial growth factor gene expression. *J. Biol. Chem.* 276, 38527–38535. doi: 10.1074/jbc.m104536200

Schwanbeck, R. (2015). The role of epigenetic mechanisms in Notch signaling during development. *J. Cell Physiol.* 230, 969–981. doi: 10.1002/jcp.24851

Schwartz, M. A., Vestweber, D., and Simons, M. (2018). A unifying concept in vascular health, and disease. *Science* 360, 270–271. doi: 10.1126/science.aat3470

Sha, Y., Haensel, D., Gutierrez, G., Du, H., Dai, X., and Nie, Q. (2019). Intermediate cell states in epithelial-to-mesenchymal transition. *Phys. Biol.* 16:021001. doi: 10.1088/1478-3975/aaf928

Shen, M., Feng, Y., Wang, J., Yuan, Y., and Yuan, F. (2020). CXCR7 inhibits fibrosis via Wnt/β-Catenin pathways during the process of angiogenesis in human umbilical vein endothelial cells. *Biomed. Res. Int.* 2020:1216926.

Shibuya, M. (2013). Vascular endothelial growth factor, and its receptor system: physiological functions in angiogenesis, and pathological roles in various diseases. *J. Biochem.* 153, 13–19. doi: 10.1093/jb/mvs136

Singh, K., Sinha, M., Pal, D., Tabasum, S., Gnyawali, S. C., Khona, D., et al. (2019). Cutaneous epithelial to mesenchymal transition activator ZEB1 regulates wound angiogenesis, and closure in a glycemic status-dependent manner. *Diabetes* 68, 2175–2190. doi: 10.2337/db19-0202

Slastnikova, T. A., Ulasov, A. V., Rosenkranz, A. A., and Sobolev, A. S. (2018). Targeted intracellular delivery of antibodies: the state of the art. *Front. Pharmacol.* 9:1208. doi: 10.3389/fphar.2018.01208

Sobierajska, K., Ciszewski, W. M., Macierzynska-Piotrowska, E., Klopocka, W., Przygodzka, P., Karakula, M., et al. (2020). The new model of snail expression regulation: the role of MRTFs in fast, and slow endothelial-mesenchymal transition. *Int. J. Mol. Sci.* 21:5875. doi: 10.3390/ijms21165875

Souilhol, C., Harmsen, M. C., Evans, P. C., and Krenning, G. (2018). Endothelial-mesenchymal transition in atherosclerosis. *Cardiovasc. Res.* 114, 565–577. doi: 10.1093/cvr/cvx253

Suárez, Y., Fernández-Hernando, C., Yu, J., Gerber, S. A., Harrison, K. D., Pober, J. S., et al. (2008). Dicer-dependent endothelial microRNAs are necessary for postnatal angiogenesis. *Proc. Natl. Acad. Sci. U S A.* 105, 14082–14087.

Suchting, S., Freitas, C., le Noble, F., Benedito, R., Breant, C., Duarte, A., et al. (2007). The Notch ligand Delta-like 4 negatively regulates endothelial tip cell formation, and vessel branching. *Proc. Natl. Acad. Sci. U S A.* 104, 3225–3230. doi: 10.1073/pnas.0611177104

Sun, Y., Cai, J., Yu, S., Chen, S., Li, F., and Fan, C. (2016). MiR-630 inhibits endothelial-mesenchymal transition by targeting slug in traumatic heterotopic ossification. *Sci. Rep.* 6:22729.

Timmerman, L. A., Grego-Bessa, J., Raya, A., Bertran, E., Perez-Pomares, J. M., Diez, J., et al. (2004). Notch promotes epithelial-mesenchymal transition during cardiac development, and oncogenic transformation. *Genes Dev.* 18, 99–115. doi: 10.1101/gad.276304

Tombor, L. S., John, D., Glaser, S. F., Luxan, G., Forte, E., Furtado, M., et al. (2021). Single cell sequencing reveals endothelial plasticity with transient mesenchymal activation after myocardial infarction. *Nat. Commun.* 12:681.

Tran, K. V., Gealekman, O., Frontini, A., Zingaretti, M. C., Morroni, M., Giordano, A., et al. (2012). The vascular endothelium of the adipose tissue gives rise to both white, and brown fat cells. *Cell Metab.* 15, 222–229. doi: 10.1016/j.cmet.2012.01.008

Tsutsumi, T., Nagaoka, T., Yoshida, T., Wang, L., Kuriyama, S., Suzuki, Y., et al. (2019). Nintedanib ameliorates experimental pulmonary arterial hypertension via inhibition of endothelial mesenchymal transition, and smooth muscle cell proliferation. *PLoS One* 14:e0214697. doi: 10.1371/journal.pone.0214697

Turunen, M. P., and Yla-Herttuala, S. (2011). Epigenetic regulation of key vascular genes, and growth factors. *Cardiovasc. Res.* 90, 441–446. doi: 10.1093/cvr/cvr109

van Meeteren, L. A., and ten Dijke, P. (2012). Regulation of endothelial cell plasticity by TGF-beta. *Cell Tissue Res.* 347, 177–186. doi: 10.1007/s00441-011-1222-6

Wang, Z., Fei, S., Suo, C., Han, Z., Tao, J., Xu, Z., et al. (2018). Antifibrotic effects of hepatocyte growth factor on endothelial-to-mesenchymal transition via transforming growth Factor-Beta1 (TGF-beta1)/Smad, and Akt/mTOR/P70S6K signaling pathways. *Ann. Trans.* 23, 1–10. doi: 10.12659/aot.906700

Watanabe, K., Villarreal-Ponce, A., Sun, P., Salmans, M. L., Fallahi, M., Andersen, B., et al. (2014). Mammary morphogenesis, and regeneration require the inhibition of EMT at terminal end buds by Ovol2 transcriptional repressor. *Dev. Cell* 29, 59–74. doi: 10.1016/j.devcel.2014.03.006

Weinstein, N., Mendoza, L., and Alvarez-Buylla, E. R. (2020). A computational model of the endothelial to mesenchymal transition. *Front. Genet.* 11:40. doi: 10.3389/fgene.2020.00040

Welch-Reardon, K. M., Ehsan, S. M., Wang, K., Wu, N., Newman, A. C., Romero-Lopez, M., et al. (2014). Angiogenic sprouting is regulated by endothelial cell expression of Slug. *J. Cell Sci.* 127, 2017–2028.

Welch-Reardon, K. M., Wu, N., and Hughes, C. C. (2015). A role for partial endothelial-mesenchymal transitions in angiogenesis? *Arterioscler Thromb. Vasc. Biol.* 35, 303–308. doi: 10.1161/atvbaha.114.303220

Welti, J., Loges, S., Dimmeler, S., and Carmeliet, P. (2013). Recent molecular discoveries in angiogenesis, and antiangiogenic therapies in cancer. *J. Clin. Invest.* 123, 3190–3200. doi: 10.1172/jci70212

Widyantoro, B., Emoto, N., Nakayama, K., Anggrahini, D. W., Adiarto, S., Iwasa, N., et al. (2010). Endothelial cell-derived endothelin-1 promotes cardiac fibrosis in diabetic hearts through stimulation of endothelial-to-mesenchymal transition. *Circulation* 121, 2407–2418. doi: 10.1161/circulationaha.110.938217

Williams, C. K., Li, J. L., Murga, M., Harris, A. L., and Tosato, G. (2006). Up-regulation of the Notch ligand Delta-like 4 inhibits VEGF-induced endothelial cell function. *Blood* 107, 931–939. doi: 10.1182/blood-2005-03-1000

Wu, Z. Q., Rowe, R. G., Lim, K. C., Lin, Y., Willis, A., Tang, Y., et al. (2014). A Snail1/Notch1 signalling axis controls embryonic vascular development. *Nat. Commun.* 5:3998.

Xiao, L., Kim, D. J., Davis, C. L., McCann, J. V., Dunleavey, J. M., Vanderlinden, A. K., et al. (2015). Tumor endothelial cells with distinct patterns of TGFbeta-Driven endothelial-to-mesenchymal transition. *Cancer Res.* 75, 1244–1254. doi: 10.1158/0008-5472.can-14-1616

Xu, X., Tan, X., Tampe, B., Nyamsuren, G., Liu, X., Maier, L. S., et al. (2015a). Epigenetic balance of aberrant Rasal1 promoter methylation, and hydroxymethylation regulates cardiac fibrosis. *Cardiovasc Res.* 105, 279–291. doi: 10.1093/cvr/cvv015

Xu, X., Tan, X., Tampe, B., Sanchez, E., Zeisberg, M., and Zeisberg, E. M. (2015b). Snail is a direct target of hypoxia-inducible factor 1alpha (HIF1alpha) in hypoxia-induced endothelial to mesenchymal transition of human coronary endothelial cells. *J. Biol. Chem.* 290, 16653–16664. doi: 10.1074/jbc.m115.636944

Yang, J., Antin, P., Berx, G., Blanpain, C., Brabletz, T., Bronner, M., et al. (2020). Guidelines, and definitions for research on epithelial-mesenchymal transition. *Nat. Rev. Mol. Cell Biol.* 21, 341–352.

Yao, Y., Jumabay, M., Ly, A., Radparvar, M., Cubberly, M. R., and Bostrom, K. I. (2013). A role for the endothelium in vascular calcification. *Circ. Res.* 113, 495–504. doi: 10.1161/circresaha.113.301792

Yao, Y., Li, Y., Zeng, X., Ye, Z., Li, X., and Zhang, L. (2018). Losartan alleviates renal fibrosis, and inhibits Endothelial-to-Mesenchymal Transition (EMT) under high-fat diet-induced hyperglycemia. *Front. Pharmacol.* 9:1213. doi: 10.3389/fphar.2018.01213

Yoshimatsu, Y., Wakabayashi, I., Kimuro, S., Takahashi, N., Takahashi, K., Kobayashi, M., et al. (2020). TNF-alpha enhances TGF-beta-induced endothelial-to-mesenchymal transition via TGF-beta signal augmentation. *Cancer Sci.* 111, 2385–2399. doi: 10.1111/cas.14455

Zeisberg, E. M., Potenta, S., Xie, L., Zeisberg, M., and Kalluri, R. (2007a). Discovery of endothelial to mesenchymal transition as a source for carcinoma-associated fibroblasts. *Cancer Res.* 67, 10123–10128. doi: 10.1158/0008-5472.can-07-3127

Zeisberg, E. M., Tarnavski, O., Zeisberg, M., Dorfman, A. L., McMullen, J. R., Gustafsson, E., et al. (2007b). Endothelial-to-mesenchymal transition contributes to cardiac fibrosis. *Nat. Med.* 13, 952–961.

Zou, J., Fei, Q., Xiao, H., Wang, H., Liu, K., Liu, M., et al. (2019). VEGF-A promotes angiogenesis after acute myocardial infarction through increasing ROS production, and enhancing ER stress-mediated autophagy. *J. Cell Physiol.* 234, 17690–17703.

Conflict of Interest: The authors declare that the research was conducted in the absence of any commercial or financial relationships that could be construed as a potential conflict of interest.

Publisher's Note: All claims expressed in this article are solely those of the authors and do not necessarily represent those of their affiliated organizations, or those of the publisher, the editors and the reviewers. Any product that may be evaluated in this article, or claim that may be made by its manufacturer, is not guaranteed or endorsed by the publisher.

Copyright © 2021 Fang, Hultgren and Hughes. This is an open-access article distributed under the terms of the Creative Commons Attribution License (CC BY). The use, distribution or reproduction in other forums is permitted, provided the original author(s) and the copyright owner(s) are credited and that the original publication in this journal is cited, in accordance with accepted academic practice. No use, distribution or reproduction is permitted which does not comply with these terms.

frontiers in Cell and Developmental Biology

REVIEW
published: 11 October 2021
doi: 10.3389/fcell.2021.747842

Mechanism-Based Cardiac Regeneration Strategies in Mammals

Nawazish Naqvi[1], Siiri E. Iismaa[2], Robert M. Graham[2] and Ahsan Husain[1]**

[1] Division of Cardiology, Department of Medicine, Emory University School of Medicine, Atlanta, GA, United States, [2] Victor Chang Cardiac Research Institute, Darlinghurst, NSW, Australia

Heart failure in adults is a leading cause of morbidity and mortality worldwide. It can arise from a variety of diseases, with most resulting in a loss of cardiomyocytes that cannot be replaced due to their inability to replicate, as well as to a lack of resident cardiomyocyte progenitor cells in the adult heart. Identifying and exploiting mechanisms underlying loss of developmental cardiomyocyte replicative capacity has proved to be useful in developing therapeutics to effect adult cardiac regeneration. Of course, effective regeneration of myocardium after injury requires not just expansion of cardiomyocytes, but also neovascularization to allow appropriate perfusion and resolution of injury-induced inflammation and interstitial fibrosis, but also reversal of adverse left ventricular remodeling. In addition to overcoming these challenges, a regenerative therapy needs to be safe and easily translatable. Failure to address these critical issues will delay the translation of regenerative approaches. This review critically analyzes current regenerative approaches while also providing a framework for future experimental studies aimed at enhancing success in regenerating the injured heart.

Keywords: heart failure, ischemic injury, cardiomyocyte proliferation, cardioprotection, cardiac regeneration

OPEN ACCESS

Edited by:
Jesus Chimal-Monroy, Universidad Nacional Autónoma de México, Mexico

Reviewed by:
Lu Han, University of Pittsburgh, United States
Katherine Yutzey, Cincinnati Children's Hospital Medical Center, United States
Sean Palecek, University of Wisconsin-Madison, United States

****Correspondence:***
Nawazish Naqvi
nnaqvi@emory.edu
Ahsan Husain
ahusai2@emory.edu

Specialty section:
This article was submitted to Signaling, a section of the journal Frontiers in Cell and Developmental Biology

Received: *26 July 2021*
Accepted: *06 September 2021*
Published: *11 October 2021*

Citation:
Naqvi N, Iismaa SE, Graham RM and Husain A (2021) Mechanism-Based Cardiac Regeneration Strategies in Mammals. Front. Cell Dev. Biol. 9:747842. doi: 10.3389/fcell.2021.747842

INTRODUCTION

About seven million Americans are currently living with heart failure; a number expected to increase to ∼8.5 million by 2030 (Urbich et al., 2020). The total healthcare cost for heart failure was ∼$43 billion in 2020 and, in the absence of a breakthrough in therapy that significantly improves outcomes, is expected to increase to ∼$70 billion by over the next decade (Urbich et al., 2020). This situation is further compounded by an aging population. Treatment for heart failure generally consists of afterload reduction with one or more of several different classes of antihypertensive drugs, diuretics, or both, which generally need to be continued long-term. Despite this therapy, ∼50% of the patients who develop heart failure die within 5 years of diagnosis (Taylor et al., 2017; Jones et al., 2019), a death rate higher than some cancers. In addition, heart failure is associated with a marked deterioration in quality-of-life as it not infrequently leads to depression, hostility and impaired physical activity (Dracup et al., 1992; Bennet et al., 2002; Hobbs et al., 2002; Cai et al., 2019). At present the only definitive therapy for severe heart failure is heart transplantation. However, this requires major expensive surgery and life-long medical management including immunosuppressive therapy with attendant risks of infection and the development of malignancies. Moreover, the number of patients eligible for a heart transplant far exceeds donor organ availability.

Thus, heart failure represents a huge unmet need for the development of next generation therapies that can definitively address the loss of cardiomyocytes associated with ischemic and many other types of heart disease that result in impaired contractile function. Cardiac regeneration

as a strategy for reversing heart failure offers promise because it will allow the myocardium to be rebuilt with attendant improvements in left ventricular (LV) contractility and reversal of adverse LV remodeling.

Initial (first generation) approaches to induce cardiac regeneration focused mainly on cell-based therapies, such as bone marrow derived stem cells or resident cardiac stem cells (Orlic et al., 2001; Chugh et al., 2012; Ellison et al., 2013). These studies assumed that exogenous cells delivered into the heart would engraft and transdifferentiate into functional cardiomyocytes, or that endogenous cardiac stem cells would mature and functionally couple with existing cardiomyocytes. It is now clear that success with these approaches has been limited because engraftment and survival of exogenous stem cells is poor, so benefits are likely largely restricted to short term paracrine effects or immune response triggered by the injected cells (Vagnozzi et al., 2020), rather than conversion into functional, electrically coupled cardiomyocytes. In addition, the adult heart contains few if any endogenous stem cells that can differentiate into cardiomyocytes (van Berlo et al., 2014; Kanisicak et al., 2017).

Another approach to cardiomyocyte regeneration involved differentiation of embryonic stem cells (ESCs) and induced pluripotent stem cells (iPSCs) to cardiomyocytes *in vitro* and then injecting these pluripotent stem cell-derived cardiomyocytes (ESC-CMs or iPSC-CMs) directly into the heart after an ischemic injury (Caspi et al., 2007; Fernandes et al., 2010). Studies by Murry and co-investigators showed the feasibility of producing human ESC-CMs in large scale with good viability; a requisite first step in the potential translation of this technology (Chong et al., 2014). In this study, intramyocardial injection of ∼1 billion ESC-CMs into the infarct border zone 2 weeks after myocardial ischemia–reperfusion (IR) injury in pigtail macaque monkeys resulted in reduced infarct size—these ESC-CMs showed progressive but incomplete maturation over the following 3 months. Despite retention of these ESC-CMs, LV contractile function did not improve. Importantly, Chong et al. (2014) reported arrhythmias in monkeys injected with ESC-CMs, which may be related to imperfect electrical coupling to preexisting cardiomyocytes. Thus, arrhythmogenesis and the need for long-term immunosuppression continue to present significant hurdles for the clinical application of this regenerative approach (Laflamme and Murry, 2011). Although, this field has progressed considerably from these initial studies, significant challenges and limitations of the technique remain (this topic has recently been reviewed by Gao and Pu, 2021).

An alternate approach to cardiac regeneration is to induce gene transcription programs *in situ* in non-myocytes to convert them into induced cardiac-like myocytes (iCLMs). Because cardiac fibroblasts are abundant in the heart and can be reprogrammed after activation in response to injurious stimuli such as ischemia, they have been targeted to form iCLMs. To this end, intramyocardial injection of cardiac fibroblasts in mice, one day after their transduction with three transcription factors (*Gata4*, *Mef2c* and *Tbx5*) *in vitro*, showed reprogramming into iCLMs *in vivo* (Ieda et al., 2010). In mice, intramyocardial injection of retroviral vectors encoding four transcription factors (*Gata4*, *Hand2*, *Mef2c* and *Tbx5* designated as GHMT) also resulted in iCLMs *in vivo* (Song et al., 2012). However, additional factors were required for reprogramming human cells (see Yamakawa and Ieda, 2021 for a detailed review). Importantly, in mice, this therapy improved LV contractility (ejection fraction (EF) at 24 h post-myocardial infarction (post-MI) and reduced subsequent infarct extension (Song et al., 2012). Given that GHMT was administered immediately after MI injury and the efficiency of fibroblast reprogramming to iCLMs is quite low, it is unclear if improvements in contractile function and scar size were due to iCLM formation or to paracrine effects of the transduced fibroblasts. Such effects could include reduced death of endogenous cardiomyocytes, decreased replacement fibrosis, modulation of profibrotic and scar-maturing immune cells or myofibroblasts numbers. While this approach is innovative, the low efficiency of reprogramming vectors remains a challenge (Sadahiro et al., 2015). The need to directly inject reprogramming factors into the myocardium is also a significant hurdle for the clinical application of this approach.

Mechanism-based regenerative therapies have been developed by studying when and how cardiomyocytes lose their ability to proliferate after birth with the hope of identifying molecular targets that could be manipulated to regain adult cardiomyocyte proliferation in order to regenerate cardiac muscle that has been lost due to a myocardial injury. Diverse signaling pathways are involved, but as **Figure 1** and the discussion below show, mitogenic signaling by ERK1/2 (extracellular signal-regulated protein kinase1/2) is central to most of the regenerative therapies that demonstrate functional benefit in preclinical research. The focus of this review is on such mechanism-based approaches with an emphasis on their therapeutic potential in regenerating the adult heart after myocardial injury.

LOSS OF PROLIFERATIVE POTENTIAL IN POSTNATAL HEARTS

An early study suggested that cardiomyocytes in the murine heart cease to divide from birth onwards (Soonpaa et al., 1996). However, many other studies have shown substantial cardiomyocyte proliferation during the early neonatal period (Li et al., 1996; Naqvi et al., 2014; Alkass et al., 2015). The finding that markedly injured postnatal day (P)1 (Porrello et al., 2011) or P2 (Naqvi et al., 2014) murine hearts undergo complete regenerative repair, by cardiomyocyte replication over the subsequent 21 days, indicates that loss of cardiomyocyte replicative potential in mice cannot occur at or before birth.

The finding that efficient post-injury cardiac regeneration, in mice, is lost after P7 could mean that cardiomyocytes lose proliferative capacity immediately after the end of the neonatal period, as suggested by Porrello et al. (2011). This view has support from the findings of Alkass et al. (2015) and Soonpaa et al. (2015) which show no evidence of cardiomyocyte number expansion or cardiomyocyte S-phase entry, respectively, after P7. However, quantitation of cardiomyocyte numbers in healthy hearts of multiple species has questioned this conclusion. For example: Mollova et al. (2013) reported a 3.4-fold increase in cardiomyocyte numbers between the first year and 20 years

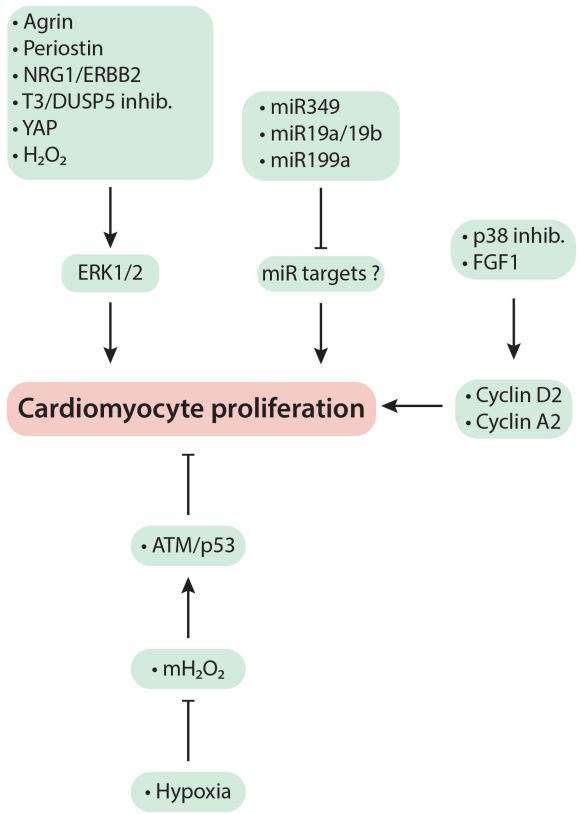

FIGURE 1 | Mechanism-based cardiac regeneration strategies in mammals. See text for a detailed discussion of the mechanisms exploited by each regenerative therapy.

of life in humans; Chen et al. (2007) reported a 12% increase during early adolescence in feline hearts; and Naqvi et al. (2014) and Puente et al. (2014) reported ∼40% (P10→P18) and ∼30% (P7→P21) increases, respectively, during preadolescence in murine hearts. This level of cardiomyocyte number expansion suggests that substantial number of cardiomyocytes should be entering S-phase and mitosis during preadolescence. As a corollary to Naqvi et al. (2014), a blinded analysis of preadolescent heart sections by Harvey's laboratory confirmed extensive cardiomyocyte mitosis using aurora B labeling (Naqvi et al., 2015). For mitosis to occur, S-phase must have successfully completed. However, Soonpaa et al. (2015) using BrdU labeling could not find cardiomyocytes entering S-phase during preadolescence. By contrast, findings from Shah and Brewer's laboratories indicated that a single injection of BrdU given to mice on P14 labeled 2.8% of cardiomyocytes over the following 16 h (Murray et al., 2015). Naqvi et al. (2014) also reported an ∼10% labeling of cardiomyocytes following a BrdU pulse in P14 mice. While these percentages are less than the level of cardiomyocyte number expansion observed during preadolescence/early adolescence in mice, cat and humans (Chen et al., 2007; Mollova et al., 2013; Naqvi et al., 2014; Puente et al., 2014), it is important to note that the ∼2 h half-life of BrdU in circulation (Kriss and Revesz, 1962) is unlikely to label all cardiomyocytes that enter the cell cycle during this developmental period.

Methodological differences between laboratories in estimating cardiomyocyte proliferation could be a source of these conflicting reports as discussed in detail below in "ASSESSMENT OF EXTANT PRECLINICAL CARDIAC REGENERATION RESEARCH." Alternatively, these divergent findings may also be reconciled if ventricular cardiomyocytes in the immediate post-neonatal period are heterogeneous in relation to their proliferative potential, with a sub-population retaining responsiveness to mitogenic stimuli. Bogush et al. (2020) tested this hypothesis and, using genetic lineage tracing, showed that P8 cardiomyocytes of the LV apex proliferate in response to a mitogenic stimulus, but those of the LV base do not (Bogush et al., 2020). After P16, LV cardiomyocytes uniformly become mitotically quiescent. Thus, spatiotemporal heterogeneity in cardiomyocyte proliferative capacity, coupled with methodological differences between laboratories, might explain the divergent findings between laboratories that have evaluated post-neonatal cardiomyocyte proliferative potential (Naqvi et al., 2014; Alkass et al., 2015; Naqvi et al., 2015; Soonpaa et al., 2015; Hirai et al., 2016).

Binucleation and Increased Ploidy as a Gauge of Proliferative Incompetence in Cardiomyocytes

Cardiomyocyte cell cycle entry may not always result in cell division. If progression through the cell cycle is aborted after S-phase but before karyokinesis (nuclear division), each cardiomyocyte nucleus ends up with twice the genetic material (*4c*, or higher, DNA content than normal diploid *2c* DNA content). This phenomenon may be defined as nuclear polyploidy. If cell cycle progression is aborted after karyokinesis, but before cytokinesis (cell division), the cell ends up with two nuclei (a binuclear cardiomyocyte). In mice, cardiomyocyte nuclear polyploidy ($\geq$ *4n*) (Patterson et al., 2017) and binucleation (Soonpaa et al., 1996) increase during the fetal to neonatal transition. Several investigators have noted an association between a diminished regenerative potential of a heart and the presence of nuclear polyploidy and/or multinucleation of its constituent cardiomyocytes and have concluded that cardiomyocytes with increased nuclear ploidy or those that have multiple nuclei are terminally differentiated (Patterson et al., 2017); that is, these cells have permanently exited the cell cycle (Derks and Bergmann, 2020).

Increased nuclear polyploidy or multinucleation are indicators of stalled cell cycle progression. But, are these cells incapable of subsequent proliferation? In the liver, binucleated tetraploid hepatocytes arise due to a failure in cytokinesis (Celton-Morizur et al., 2009). However, after hepatic injury they rapidly divide to effect complete liver regeneration (Miyaoka et al., 2012).

In vitro studies indicate that binuclear cardiomyocytes are capable of proliferation. Engel et al. (2005), D'Uva et al. (2015), and Wang et al. (2017) reported several examples and modes of division of large adult binuclear murine cardiomyocytes. However, it is unknown if mitogen-induced

cardiomyocyte proliferation *in vivo* predominantly stimulates cytokinesis of mononuclear or binuclear cardiomyocytes. This may depend not only on the stimulus threshold that must be overcome to stimulate proliferation of mono- or binuclear cardiomyocytes, but also the percentage of mono- and binuclear cardiomyocytes that populate individual hearts. These issues may be important in the translation of regenerative therapies to humans because unlike mice, human cardiomyocytes are predominantly mononuclear but polyploid (Botting et al., 2012; Derks and Bergmann, 2020).

Role of Early Developmental Shift in Metabolism in Inducing Cardiomyocyte Cell Cycle Arrest

Sadek and co-investigators (Puente et al., 2014) proposed that anaerobic glycolysis is the primary source of energy for mammalian cardiomyocytes in the hypoxic fetal environment and that, after birth, a switch from hypoxia to normoxia triggers a change from glycolysis to mitochondrial oxidative phosphorylation (OXPHOS) as the energy source. Mitochondrial OXPHOS generates hydrogen peroxide (mH_2O_2) as a byproduct of OXPHOS reactions. If the levels become sufficiently high, mH_2O_2 could activate DNA damage response (DDR) signaling and result in cell cycle arrest in murine cardiomyocytes after P6 (Puente et al., 2014). This hypothesis predicts that, after P6, cardiomyocytes are perpetually subjected to heightened DDR signaling. A key DDR effector is the tumor suppressor protein p53, actions of which include cell-cycle arrest and apoptosis. Teleologically, heightened DDR signaling in adult cardiomyocytes is inconsistent with the extraordinarily long life of mammalian cardiomyocytes—in humans, some of these cells survive for more than half a century.

A major controversy surrounds the hypothesis presented by Puente et al. (2014). We briefly present some of the opposing studies. Triiodothyronine (T3; a thyroid hormone) is the key regulator of mitochondrial biosynthesis and OXPHOS in mammalian cardiomyocytes (Turrens, 2003; Marín-García, 2010; Li et al., 2014). Hirose et al. (2019) proposed that, during the fetal to neonatal transition, a developmental increase in circulating T3 at ∼P4, rather than normoxia, induces murine cardiomyocyte cell cycle arrest because T3, by enhancing mitochondrial OXPHOS, would be primarily responsible for increases in mH_2O_2 and DDR signaling. These ideas have been explored by others through studies on the *in vivo* actions of both H_2O_2 and T3. Overexpression of the H_2O_2-generating enzyme NADPH oxidase 4 (Nox4) in murine cardiomyocytes demonstrated that, in P14 hearts, H_2O_2-activates ERK1/2 signaling, which results in c-myc-mediated cyclin D2 expression and BrdU incorporation in cardiomyocytes (Murray et al., 2015). In neonatal mice, exogenous T3 increases *in vivo* cardiomyocyte proliferation without nuclear polyploidization or multinucleation (Tan et al., 2019). Overexpression of mitochondria-localized catalase, which scavenges mH_2O_2, inhibits the proliferative response to exogenous T3. A mechanistic study further revealed that mH_2O_2, which was increased after T3 treatment, mediated the T3 proliferative response. Bogush et al. (2020) showed that exogenous T3 increases the cardiomyocyte endowment of P8 hearts, but the proliferative response—as assessed by cyclin A2 expression, phosphohistone-3 (H3P) labeling and lineage tracing studies—is confined to cardiomyocytes of the LV apex.

How does T3/mH_2O_2 signaling promote cardiomyocyte proliferation? Using *in vitro* and *in vivo* approaches, Tan et al. (2019) showed that T3-induced H_2O_2 stimulates insulin-like growth factor-1 (IGF-1) production. In turn, IGF-1 signaling increases the expression of wild-type p53-induced phosphatase 1 (WIP1), a checkpoint adaptor protein, which inhibits DDR signaling and inactivates p53. IGF-1 signaling simultaneously promotes ERK1/2 phosphorylation and the expression of cyclins that promote cell cycle entry and mitosis. Thus, T3/mH_2O_2-stimulated IGF-1 production not only inactivates cell cycle checkpoints by inhibiting DDR signaling, but simultaneously induces mitotic entry in cardiomyocytes through ERK1/2 activation.

MECHANISM-BASED REGENERATION STRATEGIES

Thyroid Hormone Signaling

T3 signaling through its receptors, TRα and TRβ, is usually associated with cardiomyocyte maturation. These effects of T3 prominently include: an increase in the α/β MHC ratio (Haddad et al., 2008); cardiomyocyte lengthening (Pantos et al., 2007); and, as discussed above, an increase in mitochondrial biosynthesis (Turrens, 2003; Marín-García, 2010), which transforms cardiomyocyte metabolism from glycolysis to OXPHOS (Puente et al., 2014; Hirose et al., 2019). More recently, however, T3 has been shown to induce cardiomyocyte proliferation (Naqvi et al., 2014; **Figure 1**). As detailed below, this effect is cell and context driven.

In neonatal (P1–P5) murine cardiomyocytes, *in vivo*, exogenous T3 increases the amount of cell cycle-promoting cyclins (e.g., D1, A2 and B1) and cardiomyocyte replication. The mechanism involves transcriptional induction of IGF-1 and IGF-1 receptor (IGF-1R) by TRα that leads to a robust increase in ERK phosphorylation (Tan et al., 2019).

In mice older than 2-weeks-of-age, exogenous T3 does not stimulate *in vivo* cardiomyocyte proliferation. This negative effect was surprising because T3 increases IGF-1 and IGF-R accumulation in adult cardiomyocytes as it does in neonatal cardiomyocytes. An important clue to explain this apparent paradox came from the finding that despite increased IGF-1/IGF-1R signaling by exogenous T3, increases in phospho-ERK were markedly attenuated. An in-depth analysis of this apparent discrepancy led to the discovery that after the neonatal period, cardiomyocytes begin to express dual specificity phosphatase-5 (DUSP5). DUSP5 is a phosphatase that differentially dephosphorylates phospho-ERK1/2 in the nucleus. When coupled with T3 administration, *in vivo* DUSP5 depletion, using siRNA, increases cardiomyocyte proliferation in adult mice (Bogush et al., 2020).

In the second week of life, DUSP5 levels in the LV increase in a distinct spatiotemporal fashion. In mice younger than P6, LV

cardiomyocytes do not express DUSP5. After this period, DUSP5 expression increases gradually from the LV base to its apex over the next 7 days. Exogenous T3 stimulates cardiomyocyte cell cycle activation and replication in LV regions that are devoid of DUSP5 (Bogush et al., 2020).

After birth, developmental increases in circulating T3, in mice, occur at 2 distinct periods. First, there is a relatively small increase in circulating T3 that occurs at P4–P5 (Hirose et al., 2019). Then, at about P10–P12, there is a major increase in T3 biosynthesis that causes circulating T3 to increase to levels found in adults (Naqvi et al., 2014). Hirose et al. (2019) propose that a developmental increase in circulating T3 at ∼P4 causes neonatal cardiomyocytes to lose their proliferative capacity. In contrast, Naqvi et al. (2014) propose that the increase in circulating T3 at ∼P12 triggers the second wave of cardiomyocyte proliferation. The role of endogenous T3 in regulation of postnatal cardiomyocyte proliferation, therefore, remains controversial.

Naqvi et al. (2014) reported that cardiomyocyte numbers increase (by about 40%) during the first as well as the second week of life. Blocking endogenous T3 biosynthesis using short-term propylthiouracil (PTU) treatment (between P7 and P18) inhibited the second developmental increase in cardiomyocyte numbers. Hirose et al. (2019) reached an opposite conclusion. Long-term PTU treatment, starting from E13.5 to P14, caused an increase in ventricular cardiomyocyte numbers by P14. Maternal thyroid hormones have an important role in fetal heart development in rodents where placental transfer of maternal thyroid hormones has been shown to occur (Forhead and Fowden, 2014). Hirose et al. (2019) also used a genetic model. Here they inactivated TRα through expression of a dominant negative TRα mutant (*Myh6*-Cre;*Thraa*$^{DN/+}$) in cardiomyocytes and found that it increased cardiomyocyte numbers in P14 hearts. The use of the *Myh6* promoter for these studies would suggest that such inactivation of TRα also occurs during the fetal period. The consequence on postnatal cardiomyocyte proliferative capacity of blocking T3 biosynthesis or TRα during the fetal period, is uncertain, but its understanding should be informative.

The effect of non-conditional genetic inactivation of cardiomyocyte TRα (*Myh6*-Cre;*Thra*$^{DN/+}$) and exogenous T3 administration on cardiac regeneration has also been studied, but in distinct models of cardiac injury. Hirose et al. (2019) studied the role of TRα inactivation in ischemia-reperfusion (IR)-injured mice. At baseline, *Myh6*-Cre;*Thra*$^{DN/+}$ mice had ∼40% larger hearts with 2-fold more cardiomyocytes compared to control mice (*Thra*$^{DN/+}$ mice) and their LV posterior walls were thicker. IR injury resulted in similar-sized infarcts. At 4-week post-IR, *Myh6*-Cre;*Thra*$^{DN/+}$ mice had reduced fibrosis and their LVEFs were ∼40-units higher than those of IR-injured controls (*Thra*$^{DN/+}$). It is uncertain if the post-IR injury differences observed between *Myh6*-Cre;*Thra*$^{DN/+}$ and *Thra*$^{DN/+}$ mice are due to cardiomyocyte TRα inactivation or simply baseline differences in the LV geometry between these mice. Indeed, posterior wall thickness favorably affects myocardial energetics (Iismaa et al., 2018) and thus may have contributed to post-IR recovery between *Myh6*-Cre;*Thra*$^{DN/+}$ and *Thra*$^{DN/+}$ mice.

As discussed above, Bogush et al. (2020) showed that DUSP5 suppression, using siRNA, coupled with T3 treatment results in increased cardiomyocyte proliferation. Tan et al. (2021) studied DUSP5 siRNA + T3-induced cardiac regeneration in mice using the doxorubicin (cancer chemotherapeutic) injury model that is characterized by cardiomyocyte loss (Shi et al., 2010). Repeated doxorubicin administration results in cardiac injury leading to a ∼40 unit decrease in LVEF and an ∼45% increase in LV dilatation (LV volume at end-diastole). In a 3-week follow-up study, Tan et al. (2021) found that parenteral DUSP5 siRNA + T3 therapy rebuilt LV muscle by increasing cardiomyocyte numbers, which reversed LV dysfunction and prevented progressive chamber dilatation. Thus controlled ERK1/2 activation through transient DUSP5 siRNA + T3 therapy (**Figure 1**) induces preexisting cardiomyocyte proliferation to effect cardiac regeneration.

MicroRNAs

MicroRNAs belong to a class of small (21–23 base pair size) non-coding RNAs that regulate expression of many genes, which can cause phenotype changes in cells, including cardiomyocytes. For example, if a microRNA inhibits cardiomyocyte proliferation through suppression of cell cycle activity, its blockade using an anti-miR might induce cardiomyocyte proliferation. Conversely, if a microRNA is known to induce cell cycle entry, administration of a mimic of this microRNA might induce cardiomyocyte proliferation (**Figure 1**).

MicroRNA-34a (miR-34a) levels are low during the first week of life in mouse hearts (Yang et al., 2015); a time when cardiomyocytes can still proliferate (Porrello et al., 2011; Naqvi et al., 2014). However, miR-34a levels increase after the neonatal period when cardiomyocyte replication is lost and remain high in adulthood. This suggested that miR-34a suppresses cardiomyocyte proliferation after the neonatal period and its blockade after MI injury might enhance regenerative repair through cardiomyocyte proliferation. To test this hypothesis, miR-34a was inhibited by administration of an anti-miR 6-h post-MI injury. Inhibition of miR-34a reduced cardiomyocyte apoptosis as measured by TUNEL staining and increased mitosis as measured by H3P labeling. Inhibition of miR-34a also reduced fibrotic scar area 3 days post-MI injury and improved cardiac function 7 days post-MI (Yang et al., 2015). In this study, cardiomyocyte replication was not established using unambiguous techniques such as genetic linage tracing or measurement of cardiomyocyte number. Furthermore, a substantial reduction in cardiomyocyte apoptosis by anti-miR therapy suggests that functional benefits of inhibiting miR-34a might be due to cardioprotection rather than cardiac regeneration.

In another study, Gao et al. (2019) injected miR-19a/19b mimics directly adjacent to the ligation site after coronary artery ligation and determined its impact on cardiac function over a 12-month follow-up period. Cardiac function measured at 2-weeks after injury was improved in miR-19a/19b treated hearts, which persisted for 12-months. The authors showed increased indices of cardiomyocyte mitosis in miR19a/19b treated hearts. However, the findings of a substantial reduction in cardiomyocyte and non-myocyte apoptosis as well as a reduction in inflammatory cells suggests that cardioprotection,

rather than cardiomyocyte replication, accounts for the observed improvements in function.

Gabisonia et al. (2019) induced myocardial injury in pigs by subjecting them to 90 min of ischemia followed by reperfusion. This resulted in an ∼10 unit reduction in EF—that is, a mild injury. Intramyocardial injection of AAV6 viral vector carrying miR-199a at the time of reperfusion prevented further deterioration of EF and reduced infarct size compared to empty vector-injected control animals at 28-days post-IR injury. Cardiomyocyte proliferation was estimated using BrdU, Ki67, H3P and aurora kinase B labeling of cardiomyocytes. These markers showed substantially increased cell cycle activity in miR-199a-expressing hearts. However, miR-199a treatment resulted in increased mortality long-term due to uncontrolled cardiomyocyte proliferation (Gabisonia et al., 2019).

Overexpression of Cell-Cycle Promoting Cyclins

Cell cycle-promoting cyclins such as D1, D2, A2 and B1 are expressed at high levels in cardiomyocytes during fetal life but decrease after birth. The adult mouse heart has undetectable levels of these cyclins and is also considered mitotically quiescent (Ikenishi et al., 2012). Based on these observations, some investigators hypothesized that a decrease in the levels of these cyclins in cardiomyocytes causes postnatal cell cycle arrest. They have, therefore, overexpressed cyclins to force proliferation of adult cardiomyocytes (**Figure 1**). Transgenic overexpression of cyclins D1, D2, D3 and A2 in cardiomyocytes from birth increased cardiomyocyte cell cycle entry (Soonpaa et al., 1997; Chaudhry et al., 2004; Pasumarthi et al., 2005). In addition, cyclin A2 overexpression by intramyocardial injection of an adenoviral vector at the time of MI improved cardiac output by ∼15% at 6-weeks follow-up (Woo et al., 2006). However, neither LVEF nor infarct size was determined immediately after MI to confirm that the treated and control groups had sustained the same degree of injury. While cell cycle activity was determined (by H3P labeling), the report provided no definitive evidence for meaningful cardiomyocyte replication (such as genetic lineage tracing or measuring cardiomyocyte numbers). Cyclin D2-overexpressing mice also had smaller infarcts after MI injury (Pasumarthi et al., 2005). However, ventricular muscle thickness is increased in these mice compared to wildtype littermates, even before MI surgery, due to continued cardiomyocyte proliferation from birth. Increased muscle thickness favorably affects myocardial energetics (Iismaa et al., 2018) and could have accounted for the reduced infarct size observed in cyclin D2 overexpressing mice. These studies also revealed that cyclin overexpression leads to enlarged hearts that are initially hypercontractile but then progress to become hypocontractile (Chaudhry et al., 2004), which could mean that this regenerative strategy might not be safe long-term.

Extracellular Matrix Proteins

Non-myocytes in the cardiac interstitium secrete proteins that form a dynamic three-dimensional network called the ECM, which provides a structural scaffold that offers mechanical support to preserve cardiac geometry. The ECM also functions as a reservoir for growth factors and proteins secreted by cardiomyocytes and non-myocytes. ECM also plays a critical role in cardiac homeostasis by facilitating intercellular communication and signal transduction to modulate cellular responses, both physiologically and in response to injury. Although growth factors and proteins released by cardiomyocytes, endothelial cells and inflammatory cells become part of the matrix, the cardiac ECM is primarily formed and modified during health and after a myocardial injury by the proteins released by cardiac fibroblasts (Fan et al., 2012). These proteins include, but are not limited to, collagens, growth factors, proteases, periostin, agrin, fibronectin, osteopontin, thrombospondins, and laminins. Thus, ECM composition is continually regulated by synthesis and degradation by proteases in the cardiac interstitium. These proteins also impact the structural properties of the matrix. For example, stiffness of the matrix may alter cell movement, survival and proliferation (Wells, 2008). Manipulation of ECM proteins can impact cell phenotype by altering signal transduction by integrins; receptors for these ECM proteins. For example, the RGD motif and amino acids surrounding this motif that are present in most of ECM proteins determine binding of the ECM proteins to integrins, which activates intracellular signal transduction (Ruoslahti, 1996; Chen et al., 1997). ECM proteins are also implicated in cell cycle pathways impacting cardiac regeneration from lower vertebrates to mammals.

In a zebrafish cardiac regeneration model, Poss and co-investigators used a proteomics approach to show that fibronectin (an ECM protein) is associated with zebrafish heart regeneration and further, that regeneration was abolished with fibronectin loss-of-function mutations (Wang et al., 2013).

Periostin is an ECM protein that promotes cell survival through AKT signaling (Bao et al., 2004). Importantly, in mice, its expression increases after acute MI injury where it promotes cardiac healing through its interaction with fibroblasts to modulate collagen fibril formation to prevent cardiac rupture (Shimazaki et al., 2008). Kühn et al. (2007) showed that treatment of cardiomyocytes with periostin induces proliferation of adult cardiomyocytes *in vitro* and *in vivo* in healthy mouse hearts. Furthermore, while MI injury reduced LVEF by ∼12%, periostin applied as a cardiac patch at the time of MI injury increased LVEF by ∼13-units). Post-MI cardiomyocyte cell cycle activity was measured using BrdU and H3P immunohistochemistry while cardiomyocyte replication was indirectly estimated from counting cardiomyocyte nuclei.

Tzahor's group used proteomics to identify agrin as an ECM component present in regenerating mouse neonatal ECM but absent from post-neonatal non-regenerative ECM. They showed that agrin promotes cardiomyocyte proliferation through YAP-ERK signaling (**Figure 1**). Importantly, intramyocardial injection of agrin at the time of MI or IR injury improved LVEF over 4-week follow-up in mouse and pig infarction models (Bassat et al., 2017; Baehr et al., 2020). However, in pigs,

an important functional benefit of agrin therapy was reduced apoptosis (Baehr et al., 2020).

Neuregulin

NRG1 is a member of the epidermal growth factor family that activates membrane-bound tyrosine kinase receptors, ErbB4 or ErbB3, when they heterodimerize with ErbB2. A recombinant NRG1 peptide improves cardiac function and survival in ischemic, dilated and viral cardiomyopathies (Liu et al., 2006). However, the mechanism for these beneficial effects remained unclear. It was of interest, therefore, when Bersell et al. (2009) showed that administration of recombinant NRG1 stimulates neonatal cardiomyocyte proliferation *in vitro*. In healthy young adult mice, overexpression of ErbB4 induced S-phase entry in mononuclear cardiomyocytes. They also showed that recombinant NRG1 administration increased cardiomyocyte cell cycle entry as well as the number of cardiomyocytes. Using genetic fate mapping, the source of new cardiomyocytes was found not to be stem cells but replication of preexisting cardiomyocytes. Importantly, daily injections of recombinant NRG1 for 12-weeks, starting 1-week post-MI, reduced scar size, improved cardiac function, and blunted cardiomyocyte hypertrophy. However, subsequently Field and co-investigators reported that recombinant NRG1 therapy does not stimulate cardiomyocyte proliferation in healthy or MI-injured mouse hearts (Reuter et al., 2014). Nevertheless, Poss and co-investigators showed that NRG1 is induced in the injured zebrafish heart and that blocking ErbB2 impairs regenerative repair of the heart. Furthermore, Tzahor and co-investigators found that ErbB2 expression falls rapidly after birth and is undetectable by the end of first week of mouse life. Overexpression of a constitutively active form of the ErbB2 receptor (caERBB2) in young adult mice resulted in robust cardiomyocyte proliferation. Importantly, ERK1/2 activation was necessary for this robust proliferative response. Overt proliferation was associated with the development of abnormally large hearts, which led to increased mortality (D'Uva et al., 2015). Thus, activation of NRG1/ERBB2/ERK1/2 signaling pathway potently induces cardiomyocyte proliferation (**Figure 1**) and it needs to be controlled to avoid cardiomegaly.

Polizzotti et al. (2015) administered recombinant NRG1 to mouse pups at birth (1 day before cryoinjury, performed on P1 and continued daily for the next 34 days. This protocol resulted in a sustained improvement in heart function up to one-month after cessation of therapy. However, consistent with the downregulation of the receptor for NRG1 (ErbB2) immediately after birth, this benefit was lost if NRG1 therapy was started at P5 (D'Uva et al., 2015). This suggests a narrow therapeutic window for recombinant NRG1 therapy. Tzahor and colleagues overcame this problem by overexpression of a mutated form of the ErbB2 receptor (CaERBB2). CaERBB2 is constitutively active and thus does not require its ligand, NRG1 and also induces cardiomyocyte proliferation also through ERK1/2 activation (D'Uva et al., 2015; Aharonov et al., 2020; **Figure 1**). Overexpressing caERBB2 in mice from 3-6-weeks post-MI initially transiently reduced stroke volume and cardiac output for 3-weeks. This depression in cardiac function was ascribed to cardiomyocyte dedifferentiation and hypertrophy. Cardiac contractile function then improved over the next 3-weeks associated with redifferentiation and reversal of cardiomyocyte hypertrophy. Scar size was also reduced (Aharonov et al., 2020) demonstrating the regenerative potential of NRG1/ErbB2 signaling pathway.

p38 and Meis1

Mechanistic studies of heart development have identified additional molecular pathways/targets regulating the postnatal cardiomyocyte cell cycle activity. Mitogen-activated protein (MAP) kinases comprise a large family of proteins and act as a hub for diverse signal transduction pathways and play a key role in several biological processes. Fibroblast growth factor (FGF) family members are also involved in numerous biological processes possess such as being a mitogen and antiapoptotic. Pharmacological inhibition of p38 MAP kinase using a p38 inhibitor (SB203580HCl) together with FGF1 administration induces proliferation of large adult binuclear cardiomyocytes *in vitro* (Engel et al., 2005). Importantly, intramyocardial injection of FGF1 combined with intraperitoneal injection of SB203580HCl at the time of MI injury prevented LV contractile dysfunction 24 h after MI injury. This therapy also reduced scar size and prevented LV dilatation when treatment was continued for 1-month post-MI injury (Engel et al., 2006). FGF1 stimulation or p38 inhibition has been shown to be cardioprotective post-MI injury by promoting cardiomyocyte survival (Palmen et al., 2004; Kaiser et al., 2004). Given that treatment of mice with FGF1 or SB203580HCl monotherapy similarly attenuated LV dysfunction to that observed in animals treated with FGF1 plus the p38 inhibitor, these benefits may be attributed to antiapoptotic effects of FGF1 signaling and/or p38 inhibition as suggested by Engel et al. (2006).

Meis1 is a member of the TALE (three amino acid loop extension) family of homeodomain transcription factors with an essential role in heart development (Paige et al., 2012; Wamstad et al., 2012). In the mouse heart, Meis1 expression increases after birth around P7, the time of cardiomyocyte cell cycle arrest. Thereafter, Meis1 expression remains high and has been suggested to maintain adult cardiomyocytes in a state of cell cycle arrest (Mahmoud et al., 2013). Genetic knockdown of Meis1 during adulthood increases cardiomyocyte cell cycle entry (Mahmoud et al., 2013). Based on these findings, targeting Meis1 was proposed as a therapeutic approach for regenerating injured adult hearts (Mahmoud et al., 2013) but, as yet, has not been tested.

Hypoxia

Placing the MI-injured hearts in a low oxygen environment was recently proposed as a therapeutic strategy to stimulate cardiomyocyte regeneration for myocardial repair post-MI (Nakada et al., 2017). Mice subjected to either hypoxia or normoxia for 2 weeks after MI injury, were gradually returned over 1 week to normoxia, and then cardiac function determined. While EF in the normoxia group did not improve, mice treated with hypoxia had an ∼15 unit increase in EF. However, because

hypoxia was started within 1 week of MI-injury (before scar maturation and remodeling of heart), the impact of hypoxia on adverse LV remodeling, such as infarct expansion and LV dilatation is not known. Also, because the study was terminated immediately after the hypoxia treatment, it is unknown if 2 weeks of hypoxia therapy has a long-term impact on reverse LV remodeling. This study is based on the concept that immediately after birth transition from the fetal hypoxic to a normoxic environment causes cardiomyocyte cell cycle arrest due to reactive oxygen species (ROS) generated by mitochondrial OXPHOS (Puente et al., 2014). Therefore, use of NAC (a non-specific antioxidant), increases cardiomyocyte proliferation by inhibiting ROS-induced DNA damage (Puente et al., 2014). However, it is not clear how hypoxia therapy will be translated to ischemic heart patients. One way of translating this concept would be to give antioxidants to patients with MI injury, but studies using antioxidants in the setting of MI injury have not shown any benefit (Yellon and Hausenloy, 2007).

Hippo-YAP Pathway

Hippo kinases were first discovered in the fruit fly, *Drosophila melanogaster,* where an inactivating mutation in the gene encoding Hippo, the Drosophila Ste20 family kinase (dMST), showed that Hippo functions as a tumor suppressor by restricting cell proliferation and promoting apoptosis (Jia et al., 2003). The Hippo kinase pathway is evolutionary conserved in mammals, with Hippo orthologs, the Ste20-like protein kinases (Mst1/2) interacting with the Salvador homolog 1, Salv1, to phosphorylate and activate large tumor suppressor homologs (Lats1/2). Lats1/2 in turn phosphorylates the transcriptional co-activator, yes-associated protein 1 (YAP1). YAP1 works in collaboration with the transcription coactivator PDZ-binding motif (TAZ) to mediate gene transcription programs including but not limited to cell proliferation. This phosphorylation of YAP by Lats1/2 inactivates Hippo/YAP signaling by preventing translocation of the YAP/TAZ complex into the nucleus. Phosphorylation of YAP by Hippo kinases during early heart development restricted its transcriptional activity to preclude heart overgrowth (Heallen et al., 2011). Also, many studies have shown that YAP1 has an obligatory role in cardiomyocyte replication, involving distinct proliferative pathways, such as Wnt/β-catenin, IGF-1R/β-catenin, Pi3kcb or epigenetic reprogramming (Xin et al., 2011; von Gise et al., 2012; Lin et al., 2015; Monroe et al., 2019).

Cardiomyocytes become mitotically quiescent during the early postnatal period. However, reactivation of YAP signaling through genetic approaches induces cardiomyocyte proliferation in adults. Mutating YAP at serine 127 to alanine produces a gain-of-function phenotype. Overexpression of YAP^{S127A} protein by intramyocardial injection of a viral vector encoding YAP^{S127A}, at the time of MI injury, improved cardiac function and survival. Cardiomyocyte proliferation was confirmed by genetic lineage tracing (Lin et al., 2014).

There are five serine residues in YAP that can potentially be phosphorylated by Hippo kinases to inhibit YAP transcriptional activity (Monroe et al., 2019). Mutating all five serine residues to alanine generates a highly active form of YAP, designated as YAP^{5SA}. Conditional overexpression of YAP^{5SA} in adult cardiomyocytes produced overt proliferation of these cells resulting in LV chamber occlusion and lethality within 4 days (Monroe et al., 2019).

Hippo pathway component, Salv1, cooperates with Hippo kinases to inactivate YAP. Conditional inactivation of Salv1 in adult cardiomyocytes using αMHC-mcm;$Salv^{f/f}$ (SalvCKO) mouse prevents YAP inactivation through its phosphorylation by Hippo kinases (Leach et al., 2017). Preclinical studies with SalvCKO mice then tested the hypothesis if MI injury-induced LV dysfunction could be reversed by inactivation of the negative regulator of YAP. LVEF before MI injury was about 64%. After MI injury, EF decreased to about 36%. Three weeks post-MI, mice were either treated with tamoxifen to conditionally delete the Salv1 gene from cardiomyocytes. This deletion reversed MI-induced LV dysfunction. Genetic lineage tracing confirmed cardiac regeneration through replication of preexisting cardiomyocytes. Recently, the efficacy of viral vector-mediated *Salv1* knockdown has been tested in pig hearts subjected to MI (Liu et al., 2021). After MI injury, LVEF was reduced from ∼60% to low 40%. Following intramyocardial injection of AAV9-Sav-shRNA 2-weeks after MI-injury, LVEF improved only marginally (by ∼10 units).

ASSESSMENT OF EXTANT PRECLINICAL CARDIAC REGENERATION RESEARCH

Extant studies have examined regenerative therapies in small animal (mainly rodent) models as discussed above (**Table 1**). However, rodent model has its strengths and limitations. Preclinical testing in a small animal model has the advantage of being cost effective and rapid. Importantly, it is easier to manage larger cohorts of animals to have ample statistical power for the study and thus the conclusions drawn from the study will be well supported. However, rodents have differences in cardiac physiology than humans such as higher heart rate. Furthermore, preclinical studies in small animals show larger functional benefits than in large animals which could be related to differences in the cardiac physiology between rodents and large animals. In this respect larger animals (especially the pig) are considered to have higher physiological relevance to humans (Lindsey et al., 2018) and have consistently shown similar drug responses as in human clinical trials (Zwetsloot et al., 2016). However, studies in pigs are expensive. Moreover, most studies in large animals are carried out in an acute MI model with mild to moderate MI injury. Large animal models with chronic severe LV dysfunction are not well established. These challenges need to be addressed for effective translation of these therapies in humans.

Importantly, it remains unclear if the functional benefits that are observed with several regenerative therapy protocols targeting the various molecular pathways, discussed above, are due to *bona fide* cardiac regeneration resulting from induced proliferation of preexisting cardiomyocytes or to other mechanisms, such as decreased cardiomyocyte apoptosis or improved cardiac energetics. Here we provide a perspective on

TABLE 1 | Summary of mechanism-based regenerative strategies in preclinical studies.

Target pathway	Species	Age at MI	Heart failure severity	Time therapy started	Follow-up duration	CM proliferation estimation	References
Cell cycle (Cyclin D2)	Mouse	Young adult	Not known	Embryonic life	5-months	CM density in histological sections	Pasumarthi et al., 2005
Cell cycle (Cyclin A2)	Rat	Young adult	Non-known	At the time of MI	6-weeks	BrdU, PCNA and H3P labeling	Woo et al., 2006
ECM (Periostin)	Mouse	Young adult	Mild	At the time of MI	12-weeks	BrdU, H3P labeling, CM nuclei count	Kühn et al., 2007
ECM (Agrin)	Mouse	Young adult	Mild to moderate	At the time of MI	4-weeks	BrdU, Ki67 and Aurkb B labeling	Bassat et al., 2017
ECM (Agrin)	Pig	Young adult	Moderate	At the time of MI	4-weeks	BrdU labeling	Baehr et al., 2020
miR-34a	Mouse	Young adult	Moderate	6-h post-MI	1-week	H3P labeling	Yang et al., 2015
miR-19a/19b	Mouse	Young adult	Not known	At the time of MI	12-months	Direct CM counting, EdU, H3P and Aurkb labeling	Gao et al., 2019
miR-199a	Pig	Young adult	Mild	At the time of MI	4-weeks	BrdU, H3P labeling, CM number by CM nuclei	Gabisonia et al., 2019
TRα	Mouse	Young adult	Mild	Embryonic life	4-weeks	EdU, H3P and Aurkb labeling	Hirose et al., 2019
Neuregulin 1	Mouse	Young adult	Moderate	1-week post-MI	12-weeks	BrdU, H3P, Aurkb labeling, CM number by CM nuclei	Bersell et al., 2009
ERBB2	Mouse	Young adult	Mild	At the time of MI	2-weeks	Ki67 and Aurkb B labeling	D'Uva et al., 2015
ERBB2	Mouse	Young adult	Moderate	3-weeks post-MI	3-weeks	RNAseq–Cyclin D1, ERK, YAP	Aharonov et al., 2020
p38/FGF1	Rat	Young adult	Moderate	At the time of MI	8-weeks	Cyclin A2 and H3P labeling	Engel et al., 2006
Hypoxia/DDR	Mouse	Young adult	Moderate	1-week post-MI	2-weeks	CM density, BrdU, H3P and Aurkb labeling	Nakada et al., 2017
Hippo/Yap (Salv1)	Mouse	Young adult	Mild to Moderate	3-week post-MI	6-weeks	EdU and H3P labeling, Lineage tracing	Leach et al., 2017
Hippo/Yap (YAP^{S127A})	Mouse	Young adult	Not known	1-week post-MI	4-weeks	EdU and H3P labeling, Lineage tracing	Lin et al., 2014
Hippo/Yap (Salv1)	Pig	Juvenile	Moderate	2-week post-MI	12-weeks	CM density, EdU, H3P and Aurkb labeling	Liu et al., 2021
DUSP5 and T3/IGF-1	Mouse	Young adult	Severe	6-weeks after first doxorubicin exposure	3-weeks	Lineage tracing, CM counting and CM density	Tan et al., 2021

Heart failure severity is binned in 3 groups–Mild (injury induces a reduction in LVEF of 10–20 percentage points), Moderate (LVEF is reduced between 20–35 percentage points) and Severe (LVEF reduction > 35 percentage points with LV dilatation). According to the guidelines by the American College of Cardiology, severe LV dysfunction for patients in heart failure is defined as a decrease in LVEF of > 30-units. This is based on a normal LVEF of 60% in adult humans (American College of Cardiology: https://www.acc.org/tools-and-practice-support/clinical-toolkits/heart-failure-practice-solutions/left-ventricular-ejection-fraction-lvef-assessment-outpatient-setting). MI: myocardial infarction injury, LVEF: left ventricular ejection fraction, CM: cardiomyocyte, BrdU: 5-bromodeoxyuridine, EdU: 5-ethynyl-2′-deoxyuridine, H3P: phosphohistone H3, Aurkb: aurora kinase B, PCNA: proliferating cell nuclear antigen.

extant preclinical research using mechanism-based regenerative strategies (**Table 1**).

Estimation of Post-therapy Cardiomyocyte Proliferation

MI-injury results in substantial loss of functional cardiomyocytes triggering heart failure. Therefore, proliferation of spared cardiomyocytes is the key objective of mechanism-based strategies to effect regenerative repair of infarcted hearts. Assessment of cell cycle markers such as BrdU and EdU-labeling provides evidence of S-phase entry of cardiomyocytes. Aurora kinase B and H3P are widely used markers of mitosis. However, these markers do not provide evidence for cardiomyocyte replication because after cardiomyocytes enter the cell cycle, they can follow distinct trajectories. For example, the cell cycle can terminate prematurely leading to increased ploidy or multinucleation. Labeling efficiency of these markers is uncertain and immunohistochemical assessments of cell cycle markers merely provide a snapshot of cell cycle activity at the time of tissue procurement.

Genetic lineage tracing, by contrast, shows unambiguous replication of preexisting cardiomyocytes (Porrello et al., 2011; Lin et al., 2014; Leach et al., 2017; Tan et al., 2021). However, this technique does not quantify the extent of cardiomyocyte number expansion. Design-based stereology provides an estimate of cardiomyocyte number. The term design-based describes a technique in stereology in which sampling is independent of the size, shape, spatial orientation, and spatial distribution of the geometrical features to be investigated. Random sampling assumes that cardiomyocyte proliferation occurs homogeneously in the LV and that there are no location-based differences in cardiomyocyte morphology. In adult hearts, cardiomyocytes adopt a variety of shapes: simple elongated cylinders or branched. Importantly, cardiomyocytes in different anatomical locations of the heart may not respond uniformly to therapeutic stimuli. For example, cardiomyocytes in the infarct border-zone might respond differently to those in remote zone. Moreover, post-neonatal cardiomyocytes from the LV apex were recently shown to be differentially sensitive to a mitogenic stimulus (Bogush et al., 2020). A further consideration with respect to stereology is that tissue shrinkage, if not studied directly, has the potential to variably impact total cardiomyocyte number calculation between hearts and between different LV regions. Such differences in random tissue sampling might explain why, using the same collection of human hearts, two laboratories reported divergent findings. Mollova et al. (2013) showed a 3.4-fold increase in cardiomyocyte number in humans between birth and late adolescence, while Bergmann et al. (2015) reported no change in cardiomyocyte numbers. This difference occurred even though both laboratories provide evidence for robust cardiomyocyte proliferation during this developmental period.

Another technique to indirectly estimate the number of cardiomyocytes involves measuring the total number of cardiomyocyte nuclei after a regenerative therapy (Kühn et al., 2007; Bersell et al., 2009). However, induced multinucleation in cardiomyocytes would make this technique problematic. For example, cyclin D1 overexpression in cardiomyocytes causes profound multinucleation (Soonpaa et al., 1997). Direct measurement of absolute cardiomyocyte number by disaggregating the ventricular myocardium is the most widely used technique to show definitive cardiomyocyte proliferation (Mahmoud et al., 2013; Naqvi et al., 2014; Puente et al., 2014; Nakada et al., 2017; Tan et al., 2021). This technique requires optimization to achieve a high level of digestion efficiency > 97% (e.g., Bogush et al., 2020). Because enzymatic heart disaggregation requires a patent coronary artery for perfusion with collagenase, it cannot easily be used to determine cardiomyocytes numbers in post-MI hearts where a major branch of the coronary tree has been permanently ligated. However, in other forms of injury that do not involve coronary artery occlusion (e.g., anthracycline induced heart failure) post-therapy changes in cardiomyocyte number have been reported (Tan et al., 2021).

It is important, therefore, that preclinical studies evaluating bona fide cardiomyocyte replication be conducted using techniques, such as genetic lineage tracing and direct cardiomyocyte number quantification, wherever possible, as reported by some investigators (e.g., Lin et al., 2014; Leach et al., 2017; Tan et al., 2021) (**Table 1**).

Cardioprotection Versus Cardiac Regeneration

Both, ischemia (Sutton and Sharpe, 2000) and reperfusion injury (Wu et al., 2018) trigger cardiomyocyte death. Therefore, cardioprotective therapies are usually given immediately after MI or IR injury to reduce cardiomyocyte death with the aim of limiting infarct size, LV dysfunction and adverse LV remodeling (e.g., Piot et al., 2008; Dong et al., 2009; Mewton et al., 2010). Regenerative pathways often intersect with cardioprotective pathways. YAP signaling simultaneously promotes cardiomyocyte proliferation and survival *in vivo* (Lin et al., 2015). To ensure that a therapy is not merely cardioprotective, regenerative therapies must be given after the initial phase of cardiomyocyte apoptosis has ceased, which may not occur until about 3 or 4 days after the ischemic injury (Tejada et al., 2016). However, many cardiac regenerative therapies tested have been given either at the time of, or immediately after MI (**Table 1**). For example, Gao et al. (2019) showed that miR-19a/19b therapy given at the time of MI increased cardiomyocyte mitosis along with a substantial reduction in apoptosis. In this situation, cardioprotection might be an important component of the improvement in LV contractile function. Similarly, the finding that agrin therapy given at the time of IR injury reduced apoptosis (Baehr et al., 2020), reiterates the need to study the contribution of cardioprotective mechanisms toward the overall improvement in LV contractile function, if the therapy is given before or within the first week after MI injury.

Preinjury Differences in Cardiac Phenotypes

Some preclinical studies, involving genetic models, show that, at baseline, the heart has more cardiomyocytes and

TABLE 2 | Potential translation strategies based on preclinical research.

Preclinical therapy	Preclinical safety (test time)	References	Potential therapeutic drug and delivery route in humans
Cyclin D2	Not tested	Pasumarthi et al., 2005	Cyclin D2 viral vector/intramyocardial injection
p38 inhibition	Not tested	Engel et al., 2006	p38 inhibitor/intramyocardial injection
Cyclin A2	Not tested	Woo et al., 2006	Cyclin A2 viral vector/intramyocardial injection
Periostin	Not tested	Kühn et al., 2007	Recombinant periostin/epicardial patch
Neuregulin 1	Not tested	Bersell et al., 2009	Recombinant neuregulin 1/subcutaneous
YAP^{S127A}	Not tested	Lin et al., 2014	YAP^{S127A} viral vector/intramyocardial injection
miR-34a	Not tested	Yang et al., 2015	miR-34a/intravenous
CaERBB2		D'Uva et al., 2015	CaERBB2 viral vector/intramyocardial injection
Hypoxia	Not tested	Nakada et al., 2017	Antioxidant/oral
Salv1	Not tested	Leach et al., 2017	Salv1 viral vector/intramyocardial injection
Agrin	Not tested	Bassat et al., 2017	Recombinant agrin/intramyocardial injection
miR-19a/19b	Safe (12 months)	Gao et al., 2019	miR-19a/19b/intramyocardial injection
miR-199a	Unsafe	Gabisonia et al., 2019	—
TRα inhibition	Not tested	Hirose et al., 2019	T3 biosynthesis inhibitor/oral
Salv1	Not tested	Liu et al., 2021	Salv1 viral vector/intramyocardial injection
DUSP5 inhibition + T3	Not tested	Tan et al., 2021	T3 + DUSP5 inhibitor/oral-intravenous

a thicker LV posterior wall (e.g., Pasumarthi et al., 2005; Hirose et al., 2019). It is not surprising that these mice fair better after MI injury because these mice have increased muscle thickness, which favorably affects myocardial energetics (Iismaa et al., 2018). Such differences between phenotypes must be considered before drawing conclusions about the mechanism of regenerative therapies in genetically modified mice.

CONCLUSION

Long-Term Safety and Efficacy

Most preclinical reports based on induction of cardiomyocyte proliferation have not conducted long-term follow-up studies after regenerative therapy (**Table 2**). This is especially important because regenerative therapies have the potential to change the phenotype of the cardiomyocytes. For example, stimulation of cardiomyocytes to proliferate cause them to dedifferentiate resulting in sarcomeric disassembly (Bersell et al., 2009) and reversion to a fetal-like state characterized by repression of the fast-contractile myosin isoform, αMHC (Monroe et al., 2019). Dedifferentiation is also linked to adverse cardiac remodeling (Kubin et al., 2011). Furthermore, dedifferentiation blunts ATP production by switching from energy-efficient OXPHOS to glycolysis. This could be detrimental for an organ like the heart which has a high energy demand. Indeed, energy starvation is a feature of heart failure (Ventura-Clapier et al., 2004) and a decrease in the α/β - MHC ratio depresses LV contractility and increases disease severity (Krenz and Robbins, 2004). Furthermore, dedifferentiated cardiomyocytes might be a substrate for arrhythmias if these cardiomyocytes do not electrically couple to existing cardiomyocytes. Thus, in preclinical follow-up studies, it is important to show that long-term regenerative repair does not cause electrical conduction dysfunction and arrhythmias. A recent report underscored these concerns by showing that substantial decreases in LV contractile function occurred after genetic overexpression of caERBB2 post-MI injury (Aharonov et al., 2020). This decrease in LV function was ascribed to cardiomyocyte dedifferentiation and hypertrophy, which could be a reason why this therapy is ineffective in repairing severely injured hearts (Aharonov et al., 2020). In severe heart failure patients, further deterioration of LV contractile function, even if it is transient, may be fatal. Thus, there is a need for strategies that either do not or only minimally repress OXPHOS or induce cardiomyocyte dedifferentiation and hypertrophy.

Importantly, undesirable effects of regenerative therapy, such as uncontrolled cardiomyocyte proliferation, could adversely impact LV remodeling long term. For example, overexpression of cyclins can produce overt cardiomyocyte proliferation causing cardiomegaly; these hearts initially show hypercontractility but eventually deteriorate to become hypocontractile (Chaudhry et al., 2004). Recently, Monroe et al. (2019) overexpressed a mitogenic protein and showed that uncontrolled cardiomyocyte proliferation caused overgrowth of the LV free wall, leading to outflow tract obstruction with consequent reductions in cardiac output and increased mortality. Using a microRNA approach, Gabisonia et al. (2019) showed that regenerative therapy worked well in the short term; in the long term it increased mortality, which was ascribed to uncontrolled cardiomyocyte proliferation. Thus, it is important that regenerative therapies be evaluated over several months, rather than weeks, to ensure that they have long-term efficacy and safety.

Translatability

Current regenerative approaches have limited or complicated paths towards effective translation. Some use a genetic approach to overexpress a protein from embryonic life onwards, others use viral vectors for delivery of genes into cardiomyocytes, while others still inject proteins (e.g., FGF1, agrin) directly into the LV wall (**Table 2**). In contrast to these approaches,

development of small molecule(s) that when given parenterally can stably build LV muscle through controlled cardiomyocyte proliferation, would greatly enhance the translational potential of regenerative therapies.

Efficacy of Regenerative Therapy in Reversing Chronic Severe Heart Failure

Post-MI wound healing can be divided into 3 stages: inflammation/necrosis, fibrosis/proliferation, and long-term remodeling/maturation (Richardson et al., 2015). The inflammatory phase occurs over the first few days. In the second phase, fibroblasts proliferate, and collagen accumulation begins by 7–14 days post-MI. Scar formation is complete at 21 days post-MI (Yang et al., 2002). In the final phase, which lasts several weeks, the scar matures via a steady increase in collagen crosslinking (Richardson et al., 2015). In this final phase, also, the LV continues to dilate, causing infarct expansion because of LV wall thinning. Thus, chronic ($\geq$ 1-month) post-MI hearts are very different from acute (1-day-to-1-week) post-MI hearts in that the injury-initiated immune response, which is a critical component of the early regenerative process (Epelman et al., 2015), is no longer operative. Extant cardiac regenerative therapies have been given either at the time of, or soon after MI (**Table 1**). In a few cases, regenerative therapy has been given in a more chronically-injured heart (about 3 to 6 weeks after injury) (Leach et al., 2017; Aharonov et al., 2020; Tan et al., 2021).

LVEF and LV end-systolic volume have been shown to be the strongest predictors of cardiac death following a MI (White et al., 1987; Roes et al., 2007); LV infarct size negatively correlates with LVEF. This correlation is only observed after MI injury that increases infarct size by > 15% (Pride et al., 2010); a finding that highlights the importance of the injury severity for the development of post-MI LV dysfunction. Severe MI injury with larger loss of myocardial muscle results in severe adverse remodeling (e.g., LV dilatation), which determines heart failure severity (Gaudron et al., 1993). A review of the existing preclinical studies suggest that most regenerative therapies have been tested following mild to moderate MI injury as assessed by post-MI LVEF and LV dilatation (**Table 1**). For example, in the study by Leach et al. (2017), the MI injury was moderate; it only resulted in a 28-unti decrease in LVEF without LV dilatation. Similarly, Aharonov et al. (2020) showed that their cardiac regenerative therapy worked within a threshold of functional loss that did not lead to severe heart failure. Gabisonia et al. (2019) also used a large animal model where MI resulted in a decrease in EF of only ∼10 units. Thus, future preclinical studies need to adequately address the applicability of the therapy for treating patients with chronic severe heart failure.

Ability of a Regenerative Therapy to Impact Quality-of-Life

From a patient's perspective, shortness of breath and fatigue are worrisome symptoms of heart failure and a cause for panic in many such patients; these symptoms increase hospitalizations (McDermott et al., 2017). Consequently, patients with a severely remodeled heart avoid physical activity and experience significant deterioration in quality-of-life, as a result of depression, the feeling of hostility toward others and difficulty in performing daily activities (Dracup et al., 1992; Bennet et al., 2002; Hobbs et al., 2002; Cai et al., 2019). There is no therapy currently available to reverse the trajectory of such patients. Regenerative repair by improving contractile function needs to enhance quality-of-life. However, in extant preclinical animal studies that have tested regenerative therapies, quality-of-life assessments are rarely undertaken. In small animal studies, measures of quality-of-life include assessments of grooming status, movement, and ability to perform exercise, including endurance testing.

Aging

Almost all preclinical studies are performed in young adult mice (between 5 to 12 weeks old) (**Table 1**) but, in humans, heart failure mostly afflicts older adults. Furthermore, aging is associated with an increase in the number of heart disease deaths (Sidney et al., 2018). Given that older adults in the US are projected to increase by > 40% in the next 10 years, heart failure therapies must be effective for all age groups. Thus, it is important to know if a regenerative therapy is as effective in triggering cardiomyogenesis in older mice as it does in young adults. Cardiomyogenesis requires cardiomyocyte proliferation concurrent with effective neovascularization (Marín-Juez et al., 2016; Ingason et al., 2018). However, aging impairs neovascularization (Lähteenvuo and Rosenzweig, 2012; Ungvari et al., 2018). Thus, it is important to understand if a regenerative therapy can induce effective cardiomyogenesis by not only inducing cardiomyocyte proliferation but also neovascularization in aged mice. Recently, microRNA-130a therapy was shown to rescue aging-related impaired neovascularization in ischemic muscle by suppressing MEOX2 and HOXA5 gene expression (Dhahri et al., 2020). Thus microRNA-130a co-administration with a regenerative therapy may enhance the regenerative repair in aged mice.

In summary, although initial proof-of-concept cardiac regenerative studies show promise, critical barriers, apart from stimulating cardiomyogenesis, must also be addressed. A therapy that regenerates mildly injured hearts (e.g., Leach et al., 2017; Aharonov et al., 2020) might not be effective in severely injured hearts with marked LV remodeling. It is possible that regenerative therapy approaches to treating severely injured hearts might need to combinatorically target pathways that remodel scar, as well as limit inflammation and enhance neovascularization as well as inducing cardiomyocyte proliferation.

AUTHOR CONTRIBUTIONS

NN and AH researched the literature and wrote the manuscript with input from RG and SI. All authors contributed to the article and approved the submitted version.

FUNDING

This work was supported by grants from the Department of Medicine, Emory University, the NIH (HL127726 and T32 HL007745), The American Heart Association (13SDG16460006 and 17GRNT33670975), the Fondation Leducq Transatlantic Network, National Health and Medical Research Council, Australia (APP1074386), R.T. Hall estate, and the Australian Research Council Stem Cells Australia Special Initiative in Stem Cell Science grant (SR1101002).

REFERENCES

Aharonov, A., Shakked, A., Umansky, K. B., Savidor, A., Genzelinakh, A., Kain, D., et al. (2020). ERBB2 drives YAP activation and EMT-like processes during cardiac regeneration. *Nat. Cell Biol.* 22, 1346–1356. doi: 10.1038/s41556-020-00588-4

Alkass, K., Panula, J., Westman, M., Wu, T. D., Guerquin-Kern, J. L., and Bergmann, O. (2015). No evidence for cardiomyocyte number expansion in preadolescent mice. *Cell* 163, 1026–1036. doi: 10.1016/j.cell.2015.10.035

Baehr, A., Umansky, K. B., Bassat, E., Jurisch, V., Klett, K., Bozoglu, T., et al. (2020). Agrin promotes coordinated therapeutic processes leading to improved cardiac repair in pigs. *Circulation* 142, 868–881. doi: 10.1161/CIRCULATIONAHA.119.045116

Bao, S., Ouyang, G., Bai, X., Huang, Z., Ma, C., Liu, M., et al. (2004). Periostin potently promotes metastatic growth of colon cancer by augmenting cell survival via the Akt/PKB pathway. *Cancer Cell* 5, 329–339. doi: 10.1016/s1535-6108(04)00081-9

Bassat, E., Mutlak, Y. E., Genzelinakh, A., Shadrin, I. Y., Umansky, K. B., Yifa, O., et al. (2017). The extracellular matrix protein agrin promotes heart regeneration in mice. *Nature* 547, 179–184. doi: 10.1038/nature22978

Bennet, S. J., Oldridge, N. B., Eckert, G. J., Embree, J. L., Browning, S., Hou, N., et al. (2002). Discriminant properties of commonly used quality of life measures in heart failure. *Qual. Life Res.* 11, 349–359. doi: 10.1023/a:1015547713061

Bergmann, O., Zdunek, S., Felker, A., Salehpour, M., Alkass, K., Bernard, S., et al. (2015). Dynamics of cell generation and turnover in the human heart. *Cell* 161, 1566–1575. doi: 10.1016/j.cell.2015.05.026

Bersell, K., Arab, S., Haring, B., and Kühn, B. (2009). Neuregulin1/ErbB4 signaling induces cardiomyocyte proliferation and repair of heart injury. *Cell* 138, 257–270. doi: 10.1016/j.cell.2009.04.060

Bogush, N., Tan, L., Naib, H., Faizullabhoy, E., Calvert, J. W., Iismaa, S. E., et al. (2020). DUSP5 expression in left ventricular cardiomyocytes of young hearts regulates thyroid hormone (T3)-induced proliferative ERK1/2 signaling. *Sci. Rep.* 10:21918. doi: 10.1038/s41598-020-78825-x

Botting, K. J., Wang, K. C., Padhee, M., McMillen, I. C., Summers-Pearce, B., Rattanatray, L., et al. (2012). Early origins of heart disease: low birth weight and determinants of cardiomyocyte endowment. *Clin. Exp. Pharmaco.l Physiol.* 39, 814–823. doi: 10.1111/j.1440-1681.2011.05649.x

Cai, F., Luis, M. A. F., Lin, X., Wang, M., Cai, L., Cen, C., et al. (2019). Anthracycline-induced cardiotoxicity in the chemotherapy treatment of breast cancer: preventive strategies and treatment. *Mol. Clin. Oncol.* 11, 15–23. doi: 10.3892/mco.2019.1854

Caspi, O., Lesman, A., Basevitch, Y., Gepstein, A., Arbel, G., Habib, I. H., et al. (2007). Tissue engineering of vascularized cardiac muscle from human embryonic stem cells. *Circ. Res.* 100, 263–272. doi: 10.1161/01.RES.0000257776.05673.ff

Celton-Morizur, S., Merlen, G., Couton, D., Margall-Ducos, G., and Desdouets, C. (2009). The insulin/Akt pathway controls a specific cell division program that leads to generation of binucleated tetraploid liver cells in rodents. *J. Clin. Invest.* 119, 1880–1887. doi: 10.1172/jci38677

Chaudhry, H. W., Dashoush, N. H., Tang, H., Zhang, L., Wang, X., Wu, E. X., et al. (2004). Cyclin A2 mediates cardiomyocyte mitosis in the postmitotic myocardium. *J. Biol. Chem.* 279, 35858–33866. doi: 10.1074/jbc.M404975200

Chen, C. S., Mrksich, M., Huang, S., Whitesides, G. M., and Ingber, D. E. (1997). Geometric control of cell life and death. *Science* 276, 1425–1428. doi: 10.1126/science.276.5317.1425

Chen, X., Wilson, R. M., Kubo, H., Berretta, R. M., Harris, D. M., Zhang, X., et al. (2007). Adolescent feline heart contains a population of small, proliferative ventricular myocytes with immature physiological properties. *Circ. Res.* 100, 536–544. doi: 10.1161/01.RES.0000259560.39234.99

Chong, J. J., Yang, X., Don, C. W., Minami, E., Liu, Y. W., Weyers, J. J., et al. (2014). Human embryonic-stem-cell-derived cardiomyocytes regenerate non-human primate hearts. *Nature* 510, 273–277. doi: 10.1038/nature13233

Chugh, A. R., Beache, G. M., Loughran, J. H., Mewton, N., Elmore, J. B., Kajstura, J., et al. (2012). Administration of cardiac stem cells in patients with ischemic cardiomyopathy: the SCIPIO trial: surgical aspects and interim analysis of myocardial function and viability by magnetic resonance. *Circulation* 126, S54–S64. doi: 10.1161/CIRCULATIONAHA.112.092627

Derks, W., and Bergmann, O. (2020). Polyploidy in cardiomyocytes: roadblock to heart regeneration? *Circ. Res.* 126, 552–565. doi: 10.1161/CIRCRESAHA.119.315408

Dhahri, W., Dussault, S., Légaré, É, Rivard, F., Desjarlais, M., Mathieu, R., et al. (2020). Reduced expression of microRNA-130a promotes endothelial cell senescence and age-dependent impairment of neovascularization. *Aging (Albany NY)* 12, 10180–10193. doi: 10.18632/aging.103340

Dong, S., Cheng, Y., Yang, J., Li, J., Liu, X., Wang, X., et al. (2009). MicroRNA expression signature and the role of microRNA-21 in the early phase of acute myocardial infarction. *J. Biol. Chem.* 284, 29514–29525. doi: 10.1074/jbc.M109.027896

Dracup, K., Walden, J. A., Stevenson, L. W., and Brecht, M. L. (1992). Quality of life in patients with advanced heart failure. *J. Heart Lung Transplant.* 11, 273–279.

D'Uva, G., Aharonov, A., Lauriola, M., Kain, D., Yahalom-Ronen, Y., Carvalho, S., et al. (2015). ERBB2 triggers mammalian heart regeneration by promoting cardiomyocyte dedifferentiation and proliferation. *Nat. Cell Biol.* 17, 627–638. doi: 10.1038/ncb3149

Ellison, G. M., Vicinanza, C., Smith, A. J., Aquila, I., Leone, A., Waring, C. D., et al. (2013). Adult c-kit(pos) cardiac stem cells are necessary and sufficient for functional cardiac regeneration and repair. *Cell* 154, 827–842. doi: 10.1016/j.cell.2013.07.039

Engel, F. B., Hsieh, P. C., Lee, R. T., and Keating, M. T. (2006). FGF1/p38 MAP kinase inhibitor therapy induces cardiomyocyte mitosis, reduces scarring, and rescues function after myocardial infarction. *Proc. Natl. Acad. Sci. U S A.* 103, 15546–15551. doi: 10.1073/pnas.0607382103

Engel, F. B., Schebesta, M., Duong, M. T., Lu, G., Ren, S., Madwed, J. B., et al. (2005). p38 MAP kinase inhibition enables proliferation of adult mammalian cardiomyocytes. *Genes Dev.* 19, 1175–1187. doi: 10.1101/gad.1306705

Epelman, S., Liu, P. P., and Mann, D. L. (2015). Role of innate and adaptive immune mechanisms in cardiac injury and repair. *Nat. Rev. Immunol.* 15, 117–129. doi: 10.1038/nri3800

Fan, D., Takawale, A., Lee, J., and Kassiri, Z. (2012). Cardiac fibroblasts, fibrosis and extracellular matrix remodeling in heart disease. *Fibrogenesis Tissue Repair.* 5:15. doi: 10.1186/1755-1536-5-15

Fernandes, S., Naumova, A. V., Zhu, W. Z., Laflamme, M. A., Gold, J., and Murry, C. E. (2010). Human embryonic stem cell-derived cardiomyocytes engraft but do not alter cardiac remodeling after chronic infarction in rats. *J. Mol. Cell Cardiol.* 49, 941–949. doi: 10.1016/j.yjmcc.2010.09.008

Forhead, A. J., and Fowden, A. L. (2014). Thyroid hormones in fetal growth and prepartum maturation. *J. Endocrinol.* 221, R87–R103. doi: 10.1530/JOE-14-0025

Gabisonia, K., Prosdocimo, G., Aquaro, G. D., Carlucci, L., Zentilin, L., Secco, I., et al. (2019). MicroRNA therapy stimulates uncontrolled cardiac repair after myocardial infarction in pigs. *Nature* 569, 418–422. doi: 10.1038/s41586-019-1191-6

Gao, F., Kataoka, M., Liu, N., Liang, T., Huang, Z. P., Gu, F., et al. (2019). Therapeutic role of miR-19a/19b in cardiac regeneration and protection from myocardial infarction. *Nat. Commun.* 10:1802. doi: 10.1038/s41467-019-09530-1

Gao, Y., and Pu, J. (2021). Differentiation and application of human pluripotent stem cells derived cardiovascular cells for treatment of heart diseases: promises

and challenges. *Front. Cell Dev. Biol.* 9:658088. doi: 10.3389/fcell.2021.658088

Gaudron, P., Eilles, C., Kugler, I., and Ertl, G. (1993). Progressive left ventricular dysfunction and remodeling after myocardial infarction. Potential mechanisms and early predictors. *Circulation* 87, 755–763. doi: 10.1161/01.cir.87.3.755

Haddad, F., Qin, A. X., Bodell, P. W., Jiang, W., Giger, J. M., and Baldwin, K. M. (2008). Intergenic transcription and developmental regulation of cardiac myosin heavy chain genes. *Am. J. Physiol. Heart Circ. Physiol.* 294, H29–H40. doi: 10.1152/ajpheart.01125.2007

Heallen, T., Zhang, M., Wang, J., Bonilla-Claudio, M., Klysik, E., Johnson, R. L., et al. (2011). Hippo pathway inhibits Wnt signaling to restrain cardiomyocyte proliferation and heart size. *Science* 332, 458–461. doi: 10.1126/science.1199010

Hirai, M., Chen, J., and Evans, S. M. (2016). Tissue-Specific cell cycle indicator reveals unexpected findings for cardiac myocyte proliferation. *Circ. Res.* 118, 20–28. doi: 10.1161/CIRCRESAHA.115.307697

Hirose, K., Payumo, A. Y., Cutie, S., Hoang, A., Zhang, H., Guyot, R., et al. (2019). Evidence for hormonal control of heart regenerative capacity during endothermy acquisition. *Science* 364, 184–188. doi: 10.1126/science.aar2038

Hobbs, F. D., Kenkre, J. E., Roalfe, A. K., Davis, R. C., Hare, R., and Davies, M. K. (2002). Impact of heart failure and left ventricular systolic dysfunction on quality of life: a cross-sectional study comparing common chronic cardiac and medical disorders and a representative adult population. *Eur. Heart J.* 23, 1867–1876. doi: 10.1053/euhj.2002.3255

Ieda, M., Fu, J. D., Delgado-Olguin, P., Vedantham, V., Hayashi, Y., Bruneau, B. G., et al. (2010). Direct reprogramming of fibroblasts into functional cardiomyocytes by defined factors. *Cell* 142, 375–386. doi: 10.1016/j.cell.2010.07.002

Iismaa, S. E., Li, M., Kesteven, S., Wu, J., Chan, A. Y., Holman, S. R., et al. (2018). Cardiac hypertrophy limits infarct expansion after myocardial infarction in mice. *Sci. Rep.* 8:6114. doi: 10.1038/s41598-018-24525-6

Ikenishi, A., Okayama, H., Iwamoto, N., Yoshitome, S., Tane, S., Nakamura, K., et al. (2012). Cell cycle regulation in mouse heart during embryonic and postnatal stages. *Dev. Growth Differ.* 54, 731–738. doi: 10.1111/j.1440-169X.2012.01373.x

Ingason, A. B., Goldstone, A. B., Paulsen, M. J., Thakore, A. D., Truong, V. N., Edwards, B. B., et al. (2018). Angiogenesis precedes cardiomyocyte migration in regenerating mammalian hearts. *J. Thorac. Cardiovasc. Surg.* 155, 1118–1127.e1. doi: 10.1016/j.jtcvs.2017.08.127

Jia, J., Zhang, W., Wang, B., Trinko, R., and Jiang, J. (2003). The Drosophila Ste20 family kinase dMST functions as a tumor suppressor by restricting cell proliferation and promoting apoptosis. *Genes Dev.* 17, 2514–2519. doi: 10.1101/gad.1134003

Jones, N. R., Roalfe, A. K., Adoki, I., Hobbs, F. D. R., and Taylor, C. J. (2019). Survival of patients with chronic heart failure in the community: a systematic review and meta-analysis. *Eur. J. Heart Fail.* 21, 1306–1325. doi: 10.1002/ejhf.1594

Kaiser, R. A., Bueno, O. F., Lips, D. J., Doevendans, P. A., Jones, F., Kimball, T. F., et al. (2004). Targeted inhibition of p38 mitogen-activated protein kinase antagonizes cardiac injury and cell death following ischemia-reperfusion in vivo. *J. Biol. Chem.* 279, 15524–15530. doi: 10.1074/jbc.M313717200

Kanisicak, O., Vagnozzi, R. J., and Molkentin, J. D. (2017). Identity crisis for regenerative cardiac cKit+ cells. *Circ. Res.* 121, 1130–1132. doi: 10.1161/CIRCRESAHA.117.311921

Krenz, M., and Robbins, J. (2004). Impact of beta-myosin heavy chain expression on cardiac function during stress. *J. Am. Coll. Cardiol.* 44, 2390–2397. doi: 10.1016/j.jacc.2004.09.044

Kriss, J. P., and Revesz, L. (1962). The distribution and fate of bromodeoxyuridine and bromodeoxycytidine in the mouse and rat. *Cancer Res.* 22, 254–265.

Kubin, T., Pöling, J., Kostin, S., Gajawada, P., Hein, S., Rees, W., et al. (2011). Oncostatin M is a major mediator of cardiomyocyte dedifferentiation and remodeling. *Cell Stem Cell* 9, 420–432. doi: 10.1016/j.stem.2011.08.013

Kühn, B., del Monte, F., Hajjar, R. J., Chang, Y. S., Lebeche, D., Arab, S., et al. (2007). Periostin induces proliferation of differentiated cardiomyocytes and promotes cardiac repair. *Nat. Med.* 13, 962–969. doi: 10.1038/nm1619

Laflamme, M. A., and Murry, C. E. (2011). Heart regeneration. *Nature* 473, 326–335. doi: 10.1038/nature10147

Lähteenvuo, J., and Rosenzweig, A. (2012). Effects of aging on angiogenesis. *Circ. Res.* 110, 1252–1264. doi: 10.1161/CIRCRESAHA.111.246116

Leach, J. P., Heallen, T., Zhang, M., Rahmani, M., Morikawa, Y., Hill, M. C., et al. (2017). Hippo pathway deficiency reverses systolic heart failure after infarction. *Nature* 550, 260–264. doi: 10.1038/nature24045

Li, F., Wang, X., Capasso, J. M., and Gerdes, A. M. (1996). Rapid transition of cardiac myocytes from hyperplasia to hypertrophy during postnatal development. *J. Mol. Cell Cardiol.* 28, 1737–1746. doi: 10.1006/jmcc.1996.0163

Li, M., Iismaa, S. E., Naqvi, N., Nicks, A., Husain, A., and Graham, R. M. (2014). Thyroid hormone action in postnatal heart development. *Stem Cell Res.* 13, 582–591. doi: 10.1016/j.scr.2014.07.001

Lin, Z., von Gise, A., Zhou, P., Gu, F., Ma, Q., Jiang, J., et al. (2014). Cardiac-specific YAP activation improves cardiac function and survival in an experimental murine MI model. *Circ. Res.* 115, 354–363. doi: 10.1161/CIRCRESAHA.115.303632

Lin, Z., Zhou, P., von Gise, A., Gu, F., Ma, Q., Chen, J., et al. (2015). Pi3kcb links Hippo-YAP and PI3K-AKT signaling pathways to promote cardiomyocyte proliferation and survival. *Circ. Res.* 116, 35–45. doi: 10.1161/CIRCRESAHA.115.304457

Lindsey, M. L., Bolli, R., Canty, J. M. Jr., Du, X. J., Frangogiannis, N. G., Frantz, S., et al. (2018). Guidelines for experimental models of myocardial ischemia and infarction. *Am. J. Physiol. Heart Circ. Physiol.* 314, H812–H838. doi: 10.1152/ajpheart.00335.2017

Liu, S., Li, K., Wagner Florencio, L., Tang, L., Heallen, T. R., Leach, J. P., et al. (2021). Gene therapy knockdown of Hippo signaling induces cardiomyocyte renewal in pigs after myocardial infarction. *Sci. Transl. Med.* 13:eabd6892. doi: 10.1126/scitranslmed.abd6892

Liu, X., Gu, X., Li, Z., Li, X., Li, H., Chang, J., et al. (2006). Neuregulin-1/erbB-activation improves cardiac function and survival in models of ischemic, dilated, and viral cardiomyopathy. *J. Am. Coll. Cardiol.* 48, 1438–1447. doi: 10.1016/j.jacc.2006.05.057

Mahmoud, A. I., Kocabas, F., Muralidhar, S. A., Kimura, W., Koura, A. S., Thet, S., et al. (2013). Meis1 regulates postnatal cardiomyocyte cell cycle arrest. *Nature* 497, 249–253. doi: 10.1038/nature12054

Marín-García, J. (2010). Thyroid hormone and myocardial mitochondrial biogenesis. *Vascul. Pharmacol.* 52, 120–130. doi: 10.1016/j.vph.2009.10.008

Marín-Juez, R., Marass, M., Gauvrit, S., Rossi, A., Lai, S. L., Materna, S. C., et al. (2016). Fast revascularization of the injured area is essential to support zebrafish heart regeneration. *Proc. Natl. Acad. Sci. U S A.* 113, 11237–11242. doi: 10.1073/pnas.1605431113

McDermott, K., Elixhauser, A., and Sun, R. (2017). *Trends in Hospital Inpatient Stays in the United Sates, 2005-2014 HCUP*. Rockville, MD: Agency for Healthcare Research and Quality.

Mewton, N., Croisille, P., Gahide, G., Rioufol, G., Bonnefoy, E., Sanchez, I., et al. (2010). Effect of cyclosporine on left ventricular remodeling after reperfused myocardial infarction. *J. Am. Coll. Cardiol.* 55, 1200–1205. doi: 10.1016/j.jacc.2009.10.052

Miyaoka, Y., Ebato, K., Kato, H., Arakawa, S., Shimizu, S., and Miyajima, A. (2012). Hypertrophy and unconventional cell division of hepatocytes underlie liver regeneration. *Curr. Biol.* 22, 1166–1175. doi: 10.1016/j.cub.2012.05.016

Mollova, M., Bersell, K., Walsh, S., Savla, J., Das, L. T., Park, S. Y., et al. (2013). Cardiomyocyte proliferation contributes to heart growth in young humans. *Proc. Natl. Acad. Sci. U S A.* 110, 1446–1451. doi: 10.1073/pnas.1214608110

Monroe, T. O., Hill, M. C., Morikawa, Y., Leach, J. P., Heallen, T., Cao, S., et al. (2019). YAP partially reprograms chromatin accessibility to directly induce adult cardiogenesis in vivo. *Dev. Cell* 48, 765–779.e7. doi: 10.1016/j.devcel.2019.01.017

Murray, T. V., Smyrnias, I., Schnelle, M., Mistry, R. K., Zhang, M., Beretta, M., et al. (2015). Redox regulation of cardiomyocyte cell cycling via an ERK1/2 and c-Myc-dependent activation of cyclin D2 transcription. *J. Mol. Cell Cardiol.* 79, 54–68. doi: 10.1016/j.yjmcc.2014.10.017

Nakada, Y., Canseco, D. C., Thet, S., Abdisalaam, S., Asaithamby, A., Santos, C. X., et al. (2017). Hypoxia induces heart regeneration in adult mice. *Nature* 541, 222–227. doi: 10.1038/nature20173

Naqvi, N., Li, M., Calvert, J. W., Tejada, T., Lambert, J. P., Wu, J., et al. (2014). A proliferative burst during preadolescence establishes the final cardiomyocyte number. *Cell* 157, 795–807. doi: 10.1016/j.cell.2014.03.035

Naqvi, N., Singh, R., Iismaa, S. E., Li, M., Calvert, J. W., Martin, D. I., et al. (2015). Cardiomyocytes replicate and their numbers increase in young hearts. *Cell* 163, 783–784. doi: 10.1016/j.cell.2015.10.038

Orlic, D., Kajstura, J., Chimenti, S., Jakoniuk, I., Anderson, S. M., Li, B., et al. (2001). Bone marrow cells regenerate infarcted myocardium. *Nature* 410, 701–705. doi: 10.1038/35070587

Paige, S. L., Thomas, S., Stoick-Cooper, C. L., Wang, H., Maves, L., Sandstrom, R., et al. (2012). A temporal chromatin signature in human embryonic stem cells identifies regulators of cardiac development. *Cell* 151, 221–232. doi: 10.1016/j.cell.2012.08.027

Palmen, M., Daemen, M. J., De Windt, L. J., Willems, J., Dassen, W. R., Heeneman, S., et al. (2004). Fibroblast growth factor-1 improves cardiac functional recovery and enhances cell survival after ischemia and reperfusion: a fibroblast growth factor receptor, protein kinase C, and tyrosine kinase-dependent mechanism. *J. Am. Coll. Cardiol.* 44, 1113–1123. doi: 10.1016/j.jacc.2004.05.067

Pantos, C., Xinaris, C., Mourouzis, I., Malliopoulou, V., Kardami, E., and Cokkinos, D. V. (2007). Thyroid hormone changes cardiomyocyte shape and geometry via ERK signaling pathway: potential therapeutic implications in reversing cardiac remodeling? *Mol. Cell Biochem.* 297, 65–72. doi: 10.1007/s11010-006-9323-3

Pasumarthi, K. B., Nakajima, H., Nakajima, H. O., Soonpaa, M. H., and Field, L. J. (2005). Targeted expression of cyclin D2 results in cardiomyocyte DNA synthesis and infarct regression in transgenic mice. *Circ. Res.* 96, 110–118. doi: 10.1161/01.RES.0000152326.91223.4F

Patterson, M., Barske, L., Van Handel, B., Rau, C. D., Gan, P., Sharma, A., et al. (2017). Frequency of mononuclear diploid cardiomyocytes underlies natural variation in heart regeneration. *Nat. Genet.* 49, 1346–1353. doi: 10.1038/ng.3929

Piot, C., Croisille, P., Staat, P., Thibault, H., Rioufol, G., Mewton, N., et al. (2008). Effect of cyclosporine on reperfusion injury in acute myocardial infarction. *N. Engl. J. Med.* 359, 473–481. doi: 10.1056/NEJMoa071142

Polizzotti, B. D., Ganapathy, B., Walsh, S., Choudhury, S., Ammanamanchi, N., Bennett, D. G., et al. (2015). Neuregulin stimulation of cardiomyocyte regeneration in mice and human myocardium reveals a therapeutic window. *Sci. Transl. Med.* 7:281ra45. doi: 10.1126/scitranslmed.aaa5171

Porrello, E. R., Mahmoud, A. I., Simpson, E., Hill, J. A., Richardson, J. A., Olson, E. N., et al. (2011). Transient regenerative potential of the neonatal mouse heart. *Science* 331, 1078–1080. doi: 10.1126/science.1200708

Pride, Y. B., Giuseffi, J. L., Mohanavelu, S., Harrigan, C. J., Manning, W. J., Gibson, C. M., et al. (2010). Relation between infarct size in ST-segment elevation myocardial infarction treated successfully by percutaneous coronary intervention and left ventricular ejection fraction three months after the infarct. *Am. J. Cardiol.* 106, 635–640. doi: 10.1016/j.amjcard.2010.04.012

Puente, B. N., Kimura, W., Muralidhar, S. A., Moon, J., Amatruda, J. F., Phelps, K. L., et al. (2014). The oxygen-rich postnatal environment induces cardiomyocyte cell-cycle arrest through DNA damage response. *Cell* 157, 565–579. doi: 10.1016/j.cell.2014.03.032

Reuter, S., Soonpaa, M. H., Firulli, A. B., Chang, A. N., and Field, L. J. (2014). Recombinant neuregulin 1 does not activate cardiomyocyte DNA synthesis in normal or infarcted adult mice. *PLoS One* 9:e115871. doi: 10.1371/journal.pone.0115871

Richardson, W. J., Clarke, S. A., Quinn, T. A., and Holme, S. J. W. (2015). Physiological implications of myocardial scar structure. *Compr. Physiol.* 5, 1877–1909. doi: 10.1002/cphy.c140067

Roes, S. D., Kelle, S., Kaandorp, T. A., Kokocinski, T., Poldermans, D., Lamb, H. J., et al. (2007). Comparison of myocardial infarct size assessed with contrast-enhanced magnetic resonance imaging and left ventricular function and volumes to predict mortality in patients with healed myocardial infarction. *Am. J. Cardiol.* 100, 930–936. doi: 10.1016/j.amjcard.2007.04.029

Ruoslahti, E. (1996). RGD and other recognition sequences for integrins. *Annu. Rev. Cell Dev. Biol.* 12, 697–715. doi: 10.1146/annurev.cellbio.12.1.697

Sadahiro, T., Yamanaka, S., and Ieda, M. (2015). Direct cardiac reprogramming: progress and challenges in basic biology and clinical applications. *Circ. Res.* 116, 1378–1391. doi: 10.1161/CIRCRESAHA.116.305374

Shi, Y., Moon, M., Dawood, S., McManus, B., and Liu, P. P. (2010). Mechanisms and management of doxorubicin cardiotoxicity. *Herz* 36, 296–305. doi: 10.1007/s00059-011-3470-3

Shimazaki, M., Nakamura, K., Kii, I., Kashima, T., Amizuka, N., Li, M., et al. (2008). Periostin is essential for cardiac healing after acute myocardial infarction. *J. Exp. Med.* 205, 295–303. doi: 10.1084/jem.20071297

Sidney, S., Sorel, M. E., Quesenberry, C. P., Jaffe, M. G., Solomon, M. D., Nguyen-Huynh, M. N., et al. (2018). Comparative trends in heart disease, stroke, and all-cause mortality in the united states and a large integrated healthcare delivery system. *Am. J. Med.* 131, 829–836.e1. doi: 10.1016/j.amjmed.2018.02.014

Song, K., Nam, Y. J., Luo, X., Qi, X., Tan, W., Huang, G. N., et al. (2012). Heart repair by reprogramming non-myocytes with cardiac transcription factors. *Nature* 485, 599–604. doi: 10.1038/nature11139

Soonpaa, M. H., Kim, K. K., Pajak, L., Franklin, M., and Field, L. J. (1996). Cardiomyocyte DNA synthesis and binucleation during murine development. *Am. J. Physiol.* 271, H2183–H2189. doi: 10.1152/ajpheart.1996.271.5.H2183

Soonpaa, M. H., Koh, G. Y., Pajak, L., Jing, S., Wang, H., Franklin, M. T., et al. (1997). Cyclin D1 overexpression promotes cardiomyocyte DNA synthesis and multinucleation in transgenic mice. *J. Clin. Invest.* 99, 2644–2654. doi: 10.1172/JCI119453

Soonpaa, M. H., Zebrowski, D. C., Platt, C., Rosenzweig, A., Engel, F. B., and Field, L. J. (2015). Cardiomyocyte cell-cycle activity during preadolescence. *Cell* 163, 781–792. doi: 10.1016/j.cell.2015.10.037

Sutton, M. G., and Sharpe, N. (2000). Left ventricular remodeling after myocardial infarction: pathophysiology and therapy. *Circulation* 101, 2981–2988. doi: 10.1161/01.cir.101.25.2981

Tan, L., Bogush, N., Naib, H., Perry, J., Calvert, J. W., Martin, D. I. K., et al. (2019). Redox activation of JNK2α2 mediates thyroid hormone-stimulated proliferation of neonatal murine cardiomyocytes. *Sci. Rep.* 9:17731. doi: 10.1038/s41598-019-53705-1

Tan, L., Bogush, N., Naqvi, E., Calvert, J. W., Graham, R. M., Taylor, W. R., et al. (2021). Thyroid hormone plus dual-specificity phosphatase-5 siRNA increases the number of cardiac muscle cells and improves left ventricular contractile function in chronic doxorubicin-injured hearts. *Theranostics* 11, 4790–4808. doi: 10.7150/thno.57456

Taylor, C. J., Ryan, R., Nichols, L., Gale, N., Hobbs, F. R., and Marshall, T. (2017). Survival following a diagnosis of heart failure in primary care. *Fam. Pract.* 34, 161–168. doi: 10.1093/fampra/cmw145

Tejada, T., Tan, L., Torres, R. A., Calvert, J. W., Lambert, J. P., Zaidi, M., et al. (2016). IGF-1 degradation by mouse mast cell protease 4 promotes cell death and adverse cardiac remodeling days after a myocardial infarction. *Proc. Natl. Acad. Sci. U S A.* 113, 6949–6954. doi: 10.1073/pnas.1603127113

Turrens, J. F. (2003). Mitochondrial formation of reactive oxygen species. *J. Physiol.* 552, 335–344. doi: 10.1113/jphysiol.2003.049478

Ungvari, Z., Tarantini, S., Donato, A. J., Galvan, V., and Csiszar, A. (2018). Mechanisms of vascular aging. *Circ. Res.* 123, 849–867. doi: 10.1161/CIRCRESAHA.118.311378

Urbich, M., Globe, G., Pantiri, K., Heisen, M., Bennison, C., Wirtz, H. S., et al. (2020). A systematic review of medical costs associated with heart failure in the USA (2014-2020). *Pharmacoeconomics* 38, 1219–1236. doi: 10.1007/s40273-020-00952-0

Vagnozzi, R. J., Maillet, M., Sargent, M. A., Khalil, H., Johansen, A. K. Z., Schwanekamp, J. A., et al. (2020). An acute immune response underlies the benefit of cardiac stem cell therapy. *Nature* 577, 405–409. doi: 10.1038/s41586-019-1802-2

van Berlo, J. H., Kanisicak, O., Maillet, M., Vagnozzi, R. J., Karch, J., Lin, S. C., et al. (2014). c-kit+ cells minimally contribute cardiomyocytes to the heart. *Nature* 509, 337–341. doi: 10.1038/nature13309

Ventura-Clapier, R., Garnier, A., and Veksler, V. (2004). Energy metabolism in heart failure. *J. Physiol.* 555, 1–13. doi: 10.1113/jphysiol.2003.055095

von Gise, A., Lin, Z., Schlegelmilch, K., Honor, L. B., Pan, G. M., Buck, J. N., et al. (2012). YAP1, the nuclear target of Hippo signaling, stimulates heart growth through cardiomyocyte proliferation but not hypertrophy. *Proc. Natl. Acad. Sci. U S A.* 109, 2394–2399. doi: 10.1073/pnas.1116136109

Wamstad, J. A., Alexander, J. M., Truty, R. M., Shrikumar, A., Li, F., Eilertson, K. E., et al. (2012). Dynamic and coordinated epigenetic regulation of developmental transitions in the cardiac lineage. *Cell* 151, 206–220. doi: 10.1016/j.cell.2012.07.035

Wang, J., Karra, R., Dickson, A. L., and Poss, K. D. (2013). Fibronectin is deposited by injury-activated epicardial cells and is necessary for zebrafish heart regeneration. *Dev. Biol.* 382, 427–435. doi: 10.1016/j.ydbio.2013.08.012

Wang, W. E., Li, L., Xia, X., Fu, W., Liao, Q., Lan, C., et al. (2017). Dedifferentiation, proliferation, and redifferentiation of adult mammalian cardiomyocytes after ischemic injury. *Circulation* 136, 834–848. doi: 10.1161/CIRCULATIONAHA.116.024307

Wells, R. G. (2008). The role of matrix stiffness in regulating cell behavior. *Hepatology* 7, 1394–1400. doi: 10.1002/hep.22193

White, H. D., Norris, R. M., Brown, M. A., Brandt, P. W., Whitlock, R. M., and Wild, C. J. (1987). Left ventricular end-systolic volume as the major determinant of survival after recovery from myocardial infarction. *Circulation* 76, 44–51. doi: 10.1161/01.cir.76.1.44

Woo, Y. J., Panlilio, C. M., Cheng, R. K., Liao, G. P., Atluri, P., Hsu, V. M., et al. (2006). Therapeutic delivery of cyclin A2 induces myocardial regeneration and enhances cardiac function in ischemic heart failure. *Circulation* 114, I206–I1213. doi: 10.1161/CIRCULATIONAHA.105.000455

Wu, M. Y., Yiang, G. T., Liao, W. T., Tsai, A. P., Cheng, Y. L., Cheng, P. W., et al. (2018). Current mechanistic concepts in ischemia and reperfusion injury. *Cell Physiol. Biochem.* 46, 1650–1667. doi: 10.1159/000489241

Xin, M., Kim, Y., Sutherland, L. B., Qi, X., McAnally, J., Schwartz, R. J., et al. (2011). Regulation of insulin-like growth factor signaling by Yap governs cardiomyocyte proliferation and embryonic heart size. *Sci. Signal.* 4:ra70. doi: 10.1126/scisignal.2002278

Yamakawa, H., and Ieda, M. (2021). Cardiac regeneration by direct reprogramming in this decade and beyond. *Inflamm. Regen.* 41:20. doi: 10.1186/s41232-021-00168-5

Yang, F., Liu, Y. H., Yang, X. P., Xu, J., Kapke, A., and Carretero, O. A. (2002). Myocardial infarction and cardiac remodelling in mice. *Exp. Physiol.* 87, 547–555. doi: 10.1113/eph8702385

Yang, Y., Cheng, H. W., Qiu, Y., Dupee, D., Noonan, M., Lin, Y. D., et al. (2015). MicroRNA-34a plays a key role in cardiac repair and regeneration following myocardial infarction. *Circ. Res.* 117, 450–459. doi: 10.1161/CIRCRESAHA.117.305962

Yellon, D. M., and Hausenloy, D. J. (2007). Myocardial reperfusion injury. *N. Engl. J. Med.* 357, 1121–1135. doi: 10.1056/NEJMra071667

Zwetsloot, P. P., Végh, A. M., Jansen of Lorkeers, S. J., van Hout, G. P., Currie, G. L., Sena, E. S., et al. (2016). Cardiac stem cell treatment in myocardial infarction: a systematic review and meta-analysis of preclinical studies. *Circ. Res.* 118, 1223–1232. doi: 10.1161/CIRCRESAHA.115.307676

Conflict of Interest: The authors declare that the research was conducted in the absence of any commercial or financial relationships that could be construed as a potential conflict of interest.

Publisher's Note: All claims expressed in this article are solely those of the authors and do not necessarily represent those of their affiliated organizations, or those of the publisher, the editors and the reviewers. Any product that may be evaluated in this article, or claim that may be made by its manufacturer, is not guaranteed or endorsed by the publisher.

Copyright © 2021 Naqvi, Iismaa, Graham and Husain. This is an open-access article distributed under the terms of the Creative Commons Attribution License (CC BY). The use, distribution or reproduction in other forums is permitted, provided the original author(s) and the copyright owner(s) are credited and that the original publication in this journal is cited, in accordance with accepted academic practice. No use, distribution or reproduction is permitted which does not comply with these terms.

Advantages of publishing in Frontiers

OPEN ACCESS
Articles are free to read for greatest visibility and readership

FAST PUBLICATION
Around 90 days from submission to decision

HIGH QUALITY PEER-REVIEW
Rigorous, collaborative, and constructive peer-review

TRANSPARENT PEER-REVIEW
Editors and reviewers acknowledged by name on published articles

Frontiers
Avenue du Tribunal-Fédéral 34
1005 Lausanne | Switzerland

Visit us: www.frontiersin.org
Contact us: frontiersin.org/about/contact

REPRODUCIBILITY OF RESEARCH
Support open data and methods to enhance research reproducibility

DIGITAL PUBLISHING
Articles designed for optimal readership across devices

FOLLOW US
@frontiersin

IMPACT METRICS
Advanced article metrics track visibility across digital media

EXTENSIVE PROMOTION
Marketing and promotion of impactful research

LOOP RESEARCH NETWORK
Our network increases your article's readership